

年報 Annual Report 2018

近畿大学医学部消化器内科学教室

目 次

1. 2018年 Annual Report の発刊にあたって	1
2. 消化器内科学業績抜粋	21
3. 消化器内科診療実績	23
4. 近畿大学消化器内科学教室医局員	28
5. 消化器内科学教室業績一覧（2018年）	32
英文論文	32
和文論文	35
招待講演・特別講演（海外）	37
招待講演・特別講演（国内）	38
学会発表（海外シンポジウム）	41
学会発表・抄録（米国及び国際学会）	41
学会発表（国内シンポジウム・パネルディスカッション・ワークショップ）	48
学会発表（国内一般演題）	52
6. 別刷	66

2018 年 Annual Report の発刊にあたって

近畿大学消化器内科学教室主任教授 工藤正俊

1. 診療活動

診療活動においては平成 29 年度の実績として総稼働額 38 億 4800 万円（附属病院第 2 位）、在院日数は 6.9 日（附属病院第 1 位）、稼働率 89.3%、限界利益は外科に肉薄する 20 億 8700 万円で附属病院第 2 位（1 位は外科全体で 24 億円）、DPC II 以内の退院率は 80% で附属病院第 1 位の成績をあげ大変な診療実績を収めている。一日当たり入院患者は 88.7 人（附属病院第 1 位）、入院延患者数 30,919 人（附属病院第 1 位）、外来延患者数 49,143 人（附属病院第 1 位）、紹介患者数 3,259 件（附属病院第 2 位）、診療所以外の病院からの紹介患者数 1,363 件（附属病院第 1 位）。また 2019 年 1 月からは病床数 101 床に増床になったにも関わらず稼働率 93.5%、在院日数 7.5 日と以前と同様の数字をキープしている。このようなことから消化器内科の病院収入への貢献は大変に大きいものがある。引き続きこのような高度で active な診療活動を継続していただきたいと考えている。

2. 教育活動

教育は当然のことながら大学医学部の役割の極めて根幹を占める重要な部分であります。消化器内科学は消化器コースの内の肝臓の責任科であり、肝臓のユニットを 1 週間担当している他、上部消化管、下部消化管、胆膵のユニットや臨床腫瘍コースならびに画像診断のコースでも講義を担当しております。更には病因・病態のコースの 3 週間のうち 1 週間の責任科として大変多忙な教育活動を行っております。5 年生 6 年生のクリニカルクラークシップも例年 6 年生を常時 6 人程度受け入れており、講義や総括など充実した bed side 教育となるよう全力を尽くしております。国家試験の成績も是非とも向上させなければなりません。

平成 20 年 10 月から病院長に任ぜられ、3 期目となりましたが無事平成 26 年 9 月には任期満了により退任いたしました。その間は公務のために教育活動の多くの部分を渡邊准教授、松井講師はじめ多くの先生方にご負担をおかけすることになってしまい、申し訳なく思っております。消化器コース及び病因・病態コースあるいは日々のクリニカルクラークシップ等の教育活動では決して手を抜かず積極的に行っていくつもりですので何卒ご容赦下さい。この紙面をお借りして感謝とお詫びを申し上げます。

3. 教育活動

(1) 論文業績

英文論文の発表は 1999 年消化器内科の設立当初は一桁台でありましたが、年と共に確実に増

加し、3年目からは平均20編以上の英文論文がコンスタントに出るようになりました。2010年の英文論文数は51編に達しました。残念ながら2011年は48編、2012年は44編にとどまりました。しかし、2014年からは再び57編と50編の大台に回復しました。また19年間の総インパクトファクターは4331.358点であり英文総論文数は800編ですので、近畿大学消化器内科のような小さな所帯の教室としてはまずまずの結果を残せているのではないかと考えております。来年以降は最低、英文原著論文は60編以上を目標に頑張っていきたいと考えておりますので教室員の皆様の自覚と更なる奮闘を期待致しております。

また今年は近畿大学医学部にとってもまた私自身にとっても初めてとなる世界の臨床医学雑誌の中でも最高峰の雑誌であるLancet (Impact Factor 60.392点)に論文が掲載されたことは大変喜ばしい出来事であった。私自身Lancet Gastroenterology and Hepatologyを含めると2018年だけでLancet系の雑誌に4本First authorで論文が掲載された。

また2018年1月にサンフランシスコで開催されたASCO-GIでは当教室が中心になって行った医師主導型臨床試験であるTACTICSのオーラル発表が採択された。TACEとsorafenibの併用効果を示した世界初のエビデンスである。この発表は現在、New England Journal of Medicine (IF=74.699)に投稿中で現在レビューに回っている。NEJMは投稿論文の3-4%しかレビューに回らないといわれているため、レビューに回っただけでも光栄であると考えている。

(2) 厚生労働省科学研究費補助金事業研究班の活動

平成22年度に採択された厚労科研(がん臨床部門)「**進行・再発肝細胞癌に対する動注化学療法と分子標的薬併用による新規治療法の確立を目指した臨床試験(Phase III)ならびに効果を予測するbiomarkerの探索研究**」(工藤班)の主任研究者として日本発のエビデンスを創出すべく、努力してまいりました(平成22-24年)。また平成23年度には厚労科研(難病・がん等の疾患分野の医療の実用化部門)「**慢性ウイルス性肝疾患の非侵襲的線化評価法の開発と臨床的有用性の確立**」(工藤班)の主任研究者としても採択され、多くの大学との協同研究を行いました(平成23-25年)。平成26年度には厚生労働科学研究委託費(肝炎等克服実用化研究事業(肝炎等克服緊急対策研究事業))「**慢性ウイルス性肝炎の病態把握(重症度・治療介入時期・治療効果判定・予後予測)のための非侵襲的病態診断アルゴリズムの確立**」という課題が採択され、平成26年度には平成27年度日本医療研究開発機構(AMED)の委託費となりました。平成30年度、令和元年度からは(臨床研究等ICT基盤構築・人工知能実装研究事業)「**人工知能の利活用を見据えた超音波デジタル画像のナショナルデータベース構築基盤整備に関する研究**」(平成30年度)と平成31年度からは「**超音波デジタル画像のナショナルデータベース構築と人工知能支援型超音波診断システム開発に関する研究**」が採択され、日本超音波医学会理事長としてAI開発の研究が進行中です。

またその他にも下記の厚労科研の分担研究者として教室の先生方に実務を担当して頂いております。この場をお借りして感謝申し上げます。

(3) Research Conference

English Research Conference 出席状況

	2012		2013		2014		2015		2016		2017		2018	
	出席数	出席率	出席数	出席率	出席数	出席率	出席数	出席率	出席数	出席率	出席数	出席率	出席数	出席率
工藤	32/32	100%	25/25	100%	22/22	100%	21/21	100%	28/28	100%	26/26	100%	23/23	100%
檜田	27/32	84%	19/25	76%	20/22	91%	16/21	76%	20/28	71%	22/26	84%	21/23	91%
辻	-	-	-	-	-	-	-	-	-	-	-	-	21/23	91%
西田	24/32	75%	10/25	40%	4/22	18%	13/21	62%	9/28	32%	7/26	26%	2/23	8%
渡邊	-	-	-	-	-	-	-	-	-	-	12/26	46%	2/23	8%
北野	25/32	78%	21/25	84%	12/22	55%	9/21	43%	2/28	7%	-	-	-	-
松井	30/32	94%	23/25	92%	20/22	91%	21/21	100%	25/28	89%	26/26	100%	23/23	100%
上嶋	9/32	28%	6/25	24%	5/22	23%	9/21	43%	15/28	43%	5/26	19%	2/23	8%
櫻井	25/32	78%	15/25	60%	15/22	68%	14/21	67%	20/28	71%	22/26	84%	11/23	47%
依田	-	-	-	-	-	-	-	-	-	-	26/26	100%	22/23	95%
南(康)	31/32	97%	22/25	88%	19/22	86%	20/21	95%	15/28	54%	22/26	84%	22/23	95%
萩原	10/32	31%	9/25	36%	4/22	18%	12/21	57%	8/28	29%	6/26	23%	5/23	21%
竹中	-	-	-	-	-	-	-	-	20/28	71%	14/26	53%	13/23	56%
米田	-	-	-	-	22/22	100%	17/21	81%	23/28	82%	21/26	80%	21/23	91%
田北	9/23	39%	12/25	48%	4/22	18%	8/21	38%	13/28	46%	8/26	30%	8/23	34%
永井	23/32	72%	14/25	56%	-	-	14/21	67%	16/28	57%	17/26	65%	14/23	60%
今井	13/32	41%	7/25	28%	8/22	36%	16/21	76%	-	-	17/26	65%	-	-
山雄	-	-	14/25	56%	19/22	86%	16/21	76%	22/28	79%	22/26	84%	13/23	56%
山田	23/25	92%	15/25	60%	6/22	27%	8/21	38%	-	-	11/26	42%	20/23	86%
鎌田	16/32	50%	9/25	36%	6/22	27%	15/21	71%	27/27	96%	7/26	26%	11/23	47%
高山	16/32	50%	16/25	64%	4/22	18%	-	-	-	-	-	-	-	-
宮田	22/32	69%	15/25	60%	17/22	77%	11/21	52%	18/28	64%	13/26	50%	-	-
松田	-	-	-	-	-	-	9/21	43%	-	-	-	-	-	-
三長	-	-	-	-	-	-	11/21	52%	19/28	68%	12/26	46%	8/23	34%
河野(匡)	-	-	-	-	20/22	91%	8/21	38%	12/28	43%	16/26	61%	8/13	61%
中井	-	-	-	-	-	-	-	-	-	-	12/26	46%	4/23	17%
山崎	-	-	-	-	-	-	-	-	-	-	-	-	16/23	69%
大本	29/32	91%	19/25	76%	18/22	82%	15/21	71%	13/28	46%	14/26	53%	13/23	56%

千品	29/32	91%	22/25	88%	17/22	77%	10/21	48%	10/28	48%	13/26	50%	8/13	61%
南(知)	-	-	21/25	84%	19/22	86%	16/21	76%	18/28	64%	13/26	50%	3/10	30%
正木	-	-	-	-	-	-	-	-	-	-	-	-	12/23	52%
岡本	-	-	-	-	-	-	-	-	15/28	54%	24/26	92%	18/23	78%
岡元	-	-	12/25	48%	18/22	82%	14/21	67%	19/28	68%	22/26	84%	15/23	65%
石川	-	-	-	-	-	-	-	-	-	-	19/26	73%	8/23	34%
橋本	-	-	-	-	-	-	-	-	-	-	-	-	6/10	60%
木下	-	-	-	-	-	-	-	-	-	-	21/26	80%	-	-
高田	-	-	-	-	-	-	-	-	-	-	13/26	50%	6/23	26%
吉川	-	-	-	-	-	-	-	-	-	-	-	-	12/23	52%
河野(辰)	-	-	-	-	-	-	-	-	-	-	16/26	61%	7/23	30%
高島	-	-	-	-	-	-	-	-	-	-	19/26	73%	20/23	86%
田中	-	-	-	-	-	-	-	-	-	-	19/26	73%	9/23	39%
半田	-	-	-	-	-	-	-	-	-	-	21/26	80%	-	-
福永	-	-	-	-	-	-	-	-	-	-	17/26	65%	9/23	39%
吉田	-	-	-	-	-	-	-	-	-	-	16/26	61%	-	-
大塚	-	-	-	-	-	-	-	-	-	-	-	-	9/23	39%
益田	-	-	-	-	-	-	-	-	-	-	-	-	17/23	73%
松村	-	-	-	-	-	-	-	-	-	-	-	-	18/19	94%

4. 学会活動および海外における活動

2018年における国内の学会発表については38演題、国際学会（米国及び国際学会＋シンポ・パネル）の発表については59演題、海外特別講演は17、国内特別講演は15でありました。自身の海外出張は2018年は20回となりました。

1. 2月17日
第5回 Myanmar GI & Liver, International Scientific Meeting and ASEAN Perspective in Liver Diseasesにて招待講演 (APLD) (Yangon, Myanmar)
2. 4月10日
Next Symposium, National Cancer Hospitalにて招待講演 (Vietnam)
3. 4月11日－13日
欧州肝臓会議に参加 (EASL2018) (Paris, France)

4. 4月28日
HCC Advisory Board Meeting に参加 (Singapore, Singapore)
5. 5月5日－6日
5th Asia-Pacific Gastroenterology Cancer Summit 2018 にて特別講演 (APGCS) (Singapore) (Taiwan)
6. 5月10日
Next Symposium, Bach Mai Hospital にて招待講演 (Vietnam)
7. 5月23日－26日
The 13th Congress of the Asian Federation of Societies for Ultrasound in Medicine and Biology にて招待講演 (AFSUMB 2018) (Seoul, Korea)
8. 6月1日－6月5日
米国臨床腫瘍学会にて発表 (ASCO) (Chicago, America)
9. 6月10日
“Current best practice and future perspective of systemic therapies for unresectable hepatocellular carcinoma”. Next Symposium にて招待講演 (Ho Chi Minh, Vietnam)
10. 6月24日－25日
中日肝癌エリートフォーラムにて講演 (Guangzhou, China)
11. 6月30日
2018年中国医学会年次総会にて講演 (Taipei, Taiwan)
12. 7月5日－8日
第9回アジア太平洋肝臓専門家会議にて招待講演 (APPLE) (Seoul, South Korea)
13. 8月9日－10日
肝細胞癌アドバイザーミーティングにて招待講演 (New Jersey, USA)
14. 9月13日－16日
第12回国際肝臓学会にて講演 (ILCA2018) (London, UK)
15. 10月13日－14日
台湾超音波医学会にて招待講演 (TSUM) (Taipei, Taiwan)
16. 10月19日
第3回アジア太平洋肝臓イメージングシンポジウムにて講演 (Shanghai, China)
17. 10月19日－10月23日
ヨーロッパ臨床腫瘍学会にて共同発表 (ESMO 2018) (Munich, Germany)
18. 11月9日－13日
米国肝臓学会にて発表 (AASLD) (San Francisco, America)
19. 11月22日－25日
ヨーロッパ臨床腫瘍学会アジアに参加 (ESMO Asisa) (Singapore)
20. 12月16日
Hot Topics at 米国肝臓学会にて講演 (AASLD 2018) (Hyderabad, India)

5. 留学生受け入れ

ベトナムからの留学生（日本消化器病学会のFellowship 留学制度による）の Dr. Phunc Vihn La が 2018年8月2日から12月10日の約4カ月間消化器内科に在籍し、この他にも6月16日～

7月7日まではタイから Dr. Thanawat Luangsukrererk が約1カ月、7月9日～10月5日までは台湾から Dr. Cheng-Yu Ho が約3カ月、7月27日～9月4日まではカザフスタンから Dr. Elvira Assadova が約1カ月、10月31日～11月30日までは台湾から Dr. Yoen Young Chuah が1カ月間消化器内視鏡を中心に当教室において留学生として在籍した。

6. 人事について

2017年7月には矢田典久先生が「やだ消化器内視鏡クリニック」開設のため、9月には有住忠晃先生が「辻健太郎クリニック」赴任のため、2018年3月には今井元先生が「南和歌山医療センター」赴任のため、宮田剛先生が「山本病院」赴任のため、退職された。結果的に2017年度には4名が退職された。

それに代わる新入局者であるが2018年4月には新進気鋭の計6名の若者（正木 翔先生が兵庫県立尼崎総合医療センターより、山崎 友裕先生が兵庫県立尼崎総合医療センターより、吉川 智恵先生が日本赤十字社和歌山医療センターより、松村 まり子先生が市立札幌病院の研修医より、大塚 康夫先生と益田 康弘先生は近畿大学医学部にて研修修了）に加えて堺病院閉院とともに辻直子教授が加わり計7名の新入局者が新しく消化器内科に加わって頂いた。

来年度も新しい大学院生・後期レジデントとして数名の新人を迎える予定である。これら若く活気あるニューフェイスと一緒に、消化器内科を益々、充実・発展させたいと考えている。

7. 受賞

教室の受賞者としては私（工藤正俊）が2018年6月15日日本肝臓学会から織田賞を受賞、また2018年10月14日には台湾超音波医学会名誉会員賞を、そして2018年12月1日にはSGH特別大賞を受賞した。また2018年11月1日には萩原 智講師が日本肝臓学会冠 GILEAD SCIENCES AWARDを受賞した。萩原講師の受賞研究課題は「Contribution of C1485T mutation in the HBx gene to human and murine hepatocarcinogenesis.」でありB型の肝細胞癌の発癌様式を解明する上で大変重要な研究成果である。この研究課題はScientific Report（2017;7:10440）に掲載されたものである。

8. 新専門医制度

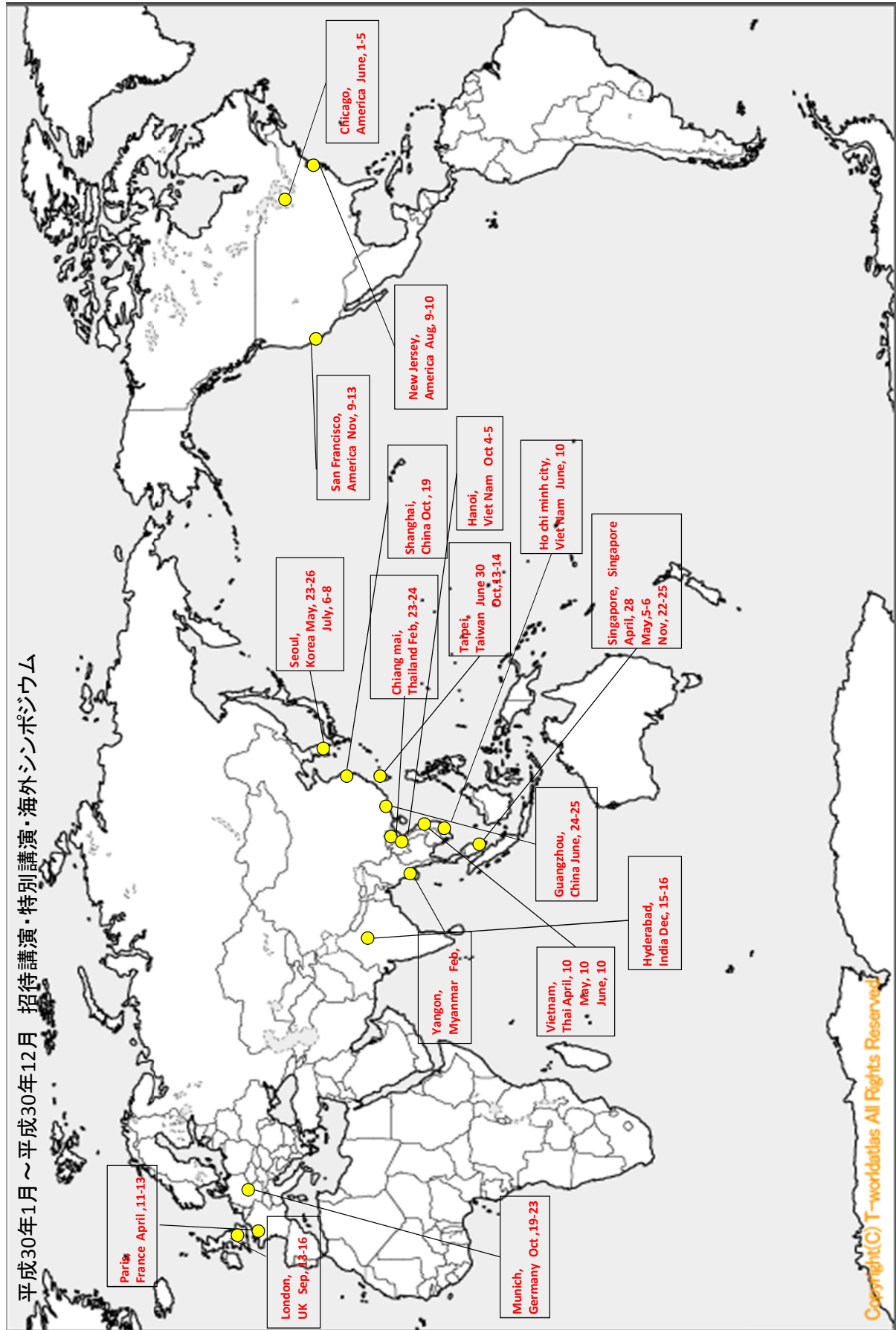
泉が丘の新病院もいよいよ開院まであと4年強となり基本設計部分はほぼ終了した。内視鏡室やエコー室も大幅に拡充されこれまで狭く不便な状態で行われていた内視鏡検査も日本有数の検査室になることが期待される。そのためには質・量ともに益々今後努力が必要である。

9. おわりに

この半世紀、各医学分野における専門の細分化は例外なく進められてきている。内科学から消化器内科学が分離・独立し、さらに上部消化管、下部消化管、肝臓、胆膵と細分化の傾向が顕著である。しかし内科学を包括的学問分野と捉えた場合、知識の連携・統合が本質であり、極く狭い領域しか知らない医師は新の消化器内科医とは言えない。信頼される医師とは広い知識を持ちつつ、ある領域については特に深い見識と技術を持つ organ specialist であり、かつ総合消化器内科医でもあるべきである。内科学全体の広い知識 (generalist) に裏打ちされた organ specialist としての消化器内科医という医師像を目指して医局員の皆様には日夜努力して頂きたいと考えている。今後とも教室員が一丸となって日本だけでなく世界に発信できる今の教室の高いアクティビティを維持し続け更に発展させて頂けるよう医局員一同には引き続き粉骨砕身、刻苦勉励を切にお願いする次第である。

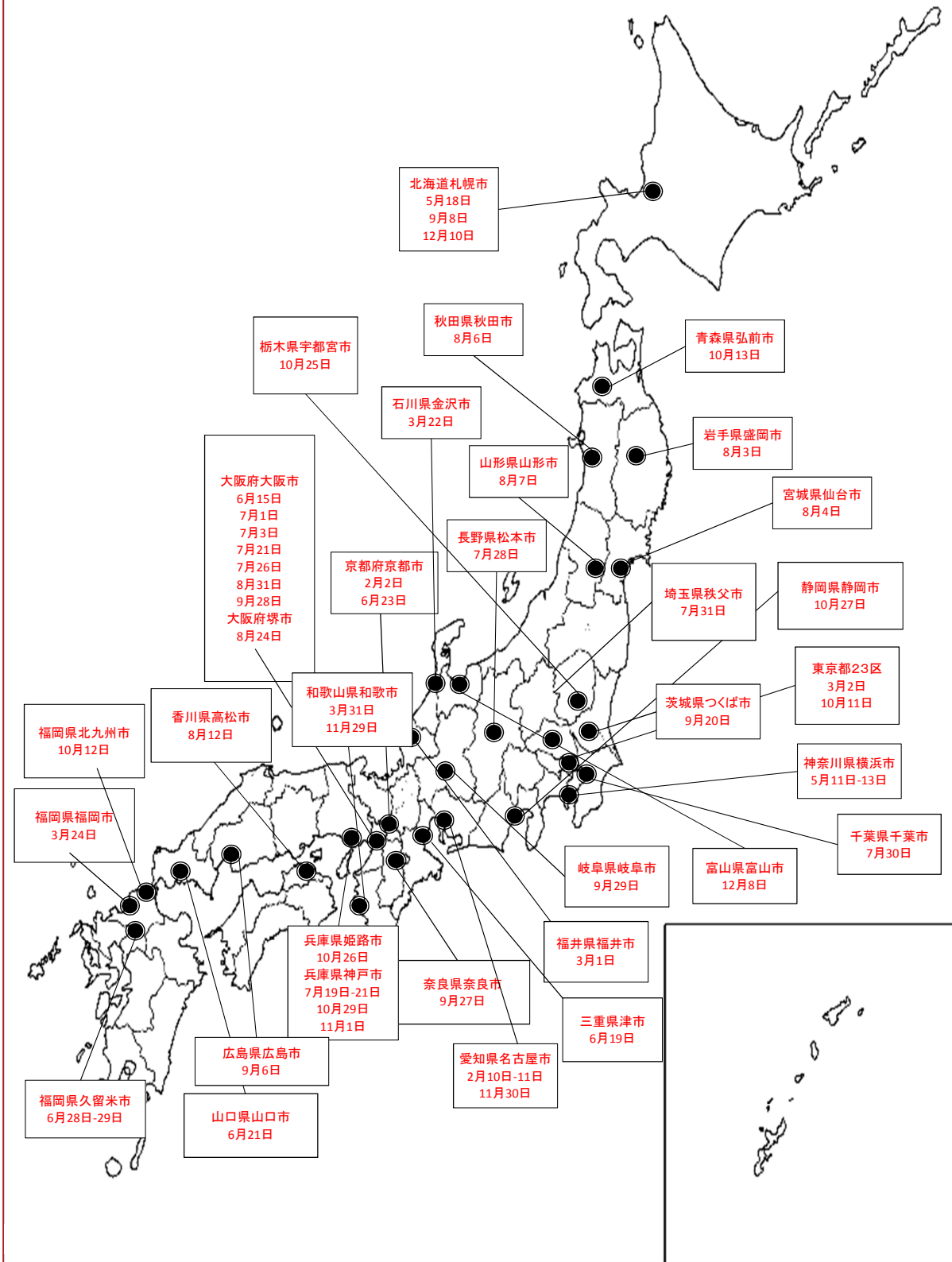
2018年3月 大阪狭山にて

平成30年1月～平成30年12月 招待講演・特別講演・海外シンポジウム



Copyright(C) T-world All Rights Reserved

平成30年1月～平成30年12月 招待講演・特別講演



工藤正俊（くどうまさとし）

（平成31年2月更新）



昭和29年	愛媛県西条市生まれ
昭和53年	京都大学医学部 卒業
同	京都大学医学部附属病院 勤務（研修医）
昭和54年	神戸市立中央市民病院内科 勤務（研修医）
昭和55年	同 消化器内科 医員
昭和60年	同 消化器内科 副医長
昭和62年	カリフォルニア大学留学（デービスメディカルセンター）
平成元年	神戸市立中央市民病院消化器内科 副医長 復職
平成4年	同 消化器内科 医長
平成9年	近畿大学医学部第2内科学 助教授
平成11年	近畿大学医学部消化器内科学 主任教授 現在に至る

（その他大学内役職）

平成19年-20年	近畿大学医学部附属病院副病院長
平成20年-26年	近畿大学医学部附属病院病院長
平成27年-現在	学校法人近畿大学理事（医学部・附属病院担当理事）

（現在の併任）

近畿大学医学部奈良病院消化器内科 教授（兼務）
神戸市立中央市民病院消化器内科 顧問（兼務）

主な所属学会等

日本消化器関連学会機構(JDDW)(理事・国際委員会委員)、日本消化器病学会(執行評議員・指導医・専門医)、日本肝臓学会(理事・国際委員会委員長・指導医・専門医)、日本消化器内視鏡学会(社団評議員・指導医・専門医)、日本超音波医学会(理事長・国際交流委員会委員長・指導医・専門医)、日本内科学会(評議員・認定内科医)、日本高齢消化器病学会(理事)、日本癌学会(評議員)、日本臨床腫瘍学会(協議員)、日本核医学会(評議員・専門医)、日本肝臓学会(常任幹事・事務局代表・追跡調査委員長)、日本肝がん分子標的治療研究会(代表世話人・事務局代表)、日本肝移植研究会(世話人)、肝血流動態イメージ研究会(世話人)、日本腹部造影エコー・ドプラ診断研究会(代表世話人・事務局)、肝臓治療シミュレーション研究会(副代表幹事)、超音波治療研究会(常任世話人)、日本消化器内視鏡財団(評議員)、米国肝臓学会(AASLD)(肝臓部門企画運営委員: Steering Committee of hepatobiliary malignancy)、米国消化器病学会(AGA)、米国消化器内視鏡学会(ASGE)、世界肝臓学会(IASL)、欧州肝臓学会(EASL)、など

委員・資格など

- ・ 世界超音波医学会(WFUMB) Immediate Past President(前理事長)
- ・ アジア超音波医学会(AFSUMB) Immediate Past President(前理事長)
- ・ アジア太平洋肝臓学会(APPLE) President(理事長)
- ・ 国際肝臓学会(ILCA) 理事(Founding Board Member, Governing Board Council Member)
- ・ 米国肝臓学会(AASLD) 肝臓部門運営委員会委員(Steering Committee Member)
- ・ 日本肝がん臨床研究機構(JLOG) (理事長)
- ・ 世界保健機構(WHO) Blue Book「Classification of the Tumor」改訂委員(平成21年5月1日)
- ・ ウイルス肝炎研究財団 日米医学協力研究会肝炎専門部会研究員
- ・ International Liver Thought Leadership Study (ILCS), Council member
- ・ 全国医学部長病院長会議 理事(平成26年5月17日 - 平成28年)
- ・ IASGO 癌分子標的治療国際委員長 (Executive Board President of International IASGO Molecular Targeting Therapy Section)(平成26年12月6日 - 現在)
- ・ ILCA School of Liver Cancer Committee Member(平成27年4月30日 - 現在)
- ・ Editor-in-Chief「Liver Cancer」(Karger, Basel)(2012年 - 現在)

受賞

- ・ 米国核医学会 Berson-Yalow Award 受賞(平成元年6月)
- ・ 日本対がん協会がん研究助成奨励賞 受賞(平成4年3月)
- ・ 日本消化器病学会奨励賞 受賞(平成4年4月)
- ・ 日本超音波医学会優秀論文賞「菊池賞」受賞(平成4年5月21日)
- ・ 日本核医学会賞 受賞(平成5年10月)
- ・ 米国超音波医学会(AIUM) 学会賞受賞(平成15年6月4日)
- ・ ボローニャ大学医学部医学会名誉会員賞(平成18年9月15日)

- ・ フィリピン超音波医学会名誉会員(Honorary Member of PSUCMI)(平成20年3月19日)
- ・ アジア太平洋消化器病学会(APDW)OKUDA Award受賞(平成20年9月13日)
- ・ 北米放射線学会 Certificate of Merit受賞(平成20年)
- ・ インド肝臓学会Madangopalan Award受賞(平成21年3月28日)
- ・ 北米放射線学会 Cum Laude 賞受賞(平成21年12月)(7000編の論文中上位10編に採択)
- ・ 日本肝臓学会「日本肝臓学会機関誌 Highest Citation 賞」受賞(平成22年6月)
- ・ JISAN Lecture Award Presented by Korean Society of Ultrasound in Medicine(平成22年5月)
- ・ 米国超音波医学会名誉会員賞(AIUM Honorary Member Award)受賞(平成23年4月)
- ・ 日本肝臓学会「日本肝臓学会機関誌 Highest Citation 賞」受賞(平成23年6月)(2回目)
- ・ Romanian Society of Ultrasound in Medicine and Biology (SRUMB) Honorary Award受賞(平成23年6月)
- ・ 北米放射線学会 Certificate of Merit受賞(平成23年11月)(2回目)
- ・ USE 論文賞(応用物理学会論文賞)受賞(平成24年11月)
- ・ Lorenzo Capussotti Award受賞(from IASGO)(平成26年12月)
- ・ 韓国超音波医学会名誉会員賞(KSUM honorary Award)受賞(平成30年5月25日)
- ・ 日本肝臓学会 織田賞受賞(平成30年6月13日)
- ・ 台湾超音波医学会名誉会員賞(TSUM Honorary Member Award)受賞(平成30年10月13日)
- ・ SGHがん特別賞受賞(平成30年12月1日)
- ・ Desai Memorial Lecture Award from Education Universe and Care Foundation(平成30年12月16日)
- ・ Highly Cited Researcher 2019 受賞(Clarivate Analytics)(令和元年11月19日)(日本人唯一の選出)

著書 (単著)

- ・ Contrast Harmonic Imaging in the Diagnosis and Treatment of Liver Tumors(Springer-Verlag 2003)
- ・ 肝腫瘍における造影ハーモニックイメージング(医学書院 2001)

編集

- ・ 松井 修, 工藤正俊, 編集: 消化器疾患の造影エコーUp Date. 南江堂, 東京, 2003.
- ・ 工藤正俊, 編集: 肝細胞癌治療の最近の進歩, 消化器病セミナー97, へるす出版, 東京, 2004.
- ・ 河田純男, 白鳥康史, 工藤正俊, 榎本信幸, 編集, 小俣政男, 監修: 肝疾患Review 2004, 日本メディカルセンター, 東京, 2004.
- ・ 河田純男, 白鳥康史, 工藤正俊, 榎本信幸, 編集, 小俣政男, 監修: 肝疾患Review 2006-2007, 日本メディカルセンター, 東京, 2006.

- 河田純男, 横須賀收, 工藤正俊, 榎本信幸, 編集, 小俣政男, 監修: 肝疾患Review 2008-2009, 日本メディカルセンター, 東京, 2008.
- 河田純男, 横須賀收, 工藤正俊, 榎本信幸, 編集, 小俣政男, 監修: 肝疾患Review 2010-2011, 日本メディカルセンター, 東京, 2010.
- 幕内雅敏, 菅野健太郎, 工藤正俊, 編集: 今日の消化器疾患治療指針 第3版, 医学書院, 東京, 2010.
- 工藤正俊, 泉 並木, 編集: 症例から学ぶ ウイルス肝炎の治療戦略. (株)診断と治療社, 東京, 2010.
- 工藤正俊, 編集: 肝細胞癌の分子標的治療, アークメディア, 東京, 2010.
- 山雄健次, 工藤正俊, 編集: 見逃し、誤りを防ぐ!肝・胆・膵癌画像診断アトラス, 羊土社, 東京, 2010.
- 工藤正俊, 編集: 医学のあゆみ「肝癌の分子標的治療」, 医歯薬出版株式会社, 東京, 2011.
- 工藤正俊, 編集: 「肝細胞がん診療の進歩: Up-To-Data」, 最新医学社, 大阪, 2011.
- 工藤正俊, 編集: 朝倉内科学, 矢崎義雄, 「総編集」, 朝倉書店, 東京, 2013.
- 工藤正俊, 國分茂博, 編集: EOB-MRI/ソナゾイド造影超音波による肝癌の診断と治療, 医学書院, 東京, 2013.
- 工藤正俊, 編集: 日本臨床増刊号 最新肝癌学, 日本臨床社, 大阪, 2015.
- 工藤正俊, 編集: 最新医学 別冊「診断と治療のABC103 肝がん」, 最新医学社, 大阪, 2015.
- 千葉 勉, 日比紀文, 東 健, 榎本信幸, 金子周一, 工藤正俊, 坂井田 功, 下瀬川 徹, 茶山一彰, 三輪洋人, 本郷道夫, 渡辺 守, 編集: An International Journal of Gastroenterology and Hepatology「GUT」日本語版 Vol. 7, No. 4, 2015.
- 工藤正俊, 企画: 肝胆膵 75巻2号 特集企画. 特集「肝細胞癌の化学療法が変わる」, 肝胆膵, 2017.
- 工藤正俊, 監修: 肝細胞癌に対するレゴラフェニブ治療. アークメディア, 東京, 2017.
- 工藤正俊, 編集: 消化器内科診療レジデントマニュアル. 医学書院, 東京, 2018.
- 工藤正俊, 総監修: レンバチニブによる肝細胞癌治療. アークメディア, 東京, 2019.
- 工藤正俊, 総監修: ラムシルマブによる肝細胞癌治療. アークメディア, 東京, 2020.
- 工藤正俊, 企画: 医学のあゆみ 273巻13号「肝細胞癌治療のパラダイムシフト～分子標的薬、免疫チェックポイント阻害薬の登場を受けて～」. 医学のあゆみ, 2020.

Editor-in-Chief:

- Liver Cancer (Basel) (5.944)

Associate Editor:

- Journal of Oncology (Germany), 肝胆膵(アークメディア))

EDITORIAL BOARD:

国際学術雑誌：International Journal of Clinical Oncology (Tokyo) Ultrasound in
Medicine and Biology (ELSEVIER, New York) Hepatology International
(Springer, New York) Liver International (Blackwell, UK) World Journal
of Gastroenterology Liver Cancer Review Letters

国内学術雑誌：肝胆膵、その他の学会誌 (3)

論文査読委員

J Clin Oncol(28.245) , Lancet Oncol(35.386), Gastroenterology(19.233),
Hepatology(14.971) , J Hepatol(18.946), Oncologist(5.252), Am J Gastroenterol(10.241),
Endoscopy(6.381), Clin Exp Metastasis(2.513), Cancer Sci(4.751) , Expert Rev Mol
Diagn(2.347) , Eur Radiol(3.962) , Liver Int(5.542), J Gastroenterol(5.130) , Eur
J Clin Invest(2.784), J Nucl Med(7.354), J Gastroen Hepatol(3.632), Oncology-Basel
(International Journal of Cancer Research and Treatment)(2.278), Ultrasound Med
Biol(2.205) , Acta Paediatr(2.265), Hepatol Int(5.490) , Eur J Gastroen Hepat(2.198),
J Hepato-Bil-Pan Scu (2.353), Hepatol Res(3.440), Int J Clin Oncol(2.503), Jpn J
Clin Oncol(2.183), Internal Med(0.956), J Clin Ultrasound(0.820), Biomark Med(2.268),
Hepato-Gastroenterol(0.792), Ann Nucl Med(1.648), Expert Review of Anticancer
Treatment(2.347), J Cancer Res Ther (1.392), CSR National Registry(0), J Gastrointest
Liver (2.063), Cancer Informatics(0), Expert Review of Proteomics and Future
Oncology(0)

SCIENTIFIC PAPER PUBLICATION:

学術論文等：

英文論文：959(IF：5430.285,H-Index 83)

和文論文：948

教科書(単著) 英文：2 和文：6

分担執筆 英文：21 和文：270

特別講演・招待講演・教育講演：

国際学会：415

国内学会：768

文部科学省科学研究費補助金

「肝細胞癌の発生・進展における腫瘍血管構築の分子機構と血流画像-基盤研究(B)」

(主任研究者：工藤正俊)

平成10年度(1998年度) 研究費総額：3,700,000円

平成11年度(1999年度) 研究費総額：2,300,000円

平成12年度(2000年度) 研究費総額：2,000,000円

「肝細胞癌の発癌・進展における腫瘍血管構築の精密血流画像解析とその分子機構の解明-基盤研究(C)」(主任研究者：工藤正俊)

平成14年度(2002年度) 研究費総額：1,800,000円

平成15年度(2003年度) 研究費総額：1,200,000円

「肝発癌の進展と血流動態および肝類洞細胞機能変化：造影ハーモニック法による病態解明-基盤研究(C)」(主任研究者：工藤正俊)

平成16年度(2004年度) 研究費総額：2,300,000円

平成17年度(2005年度) 研究費総額：1,400,000円

「精密血流画像解析法の新規開発による動・門脈血流の分離定量評価と肝発癌研究への応用-基盤研究(B)」(主任研究者：工藤正俊)

平成18年度(2006年度) 研究費総額：10,300,000円

平成19年度(2007年度) 研究費総額：2,860,000円

平成20年度(2008年度) 研究費総額：1,950,000円

「高分解能超音波内視鏡造影による膵微小循環動態の検討—診断および治療への応用-基盤研究(C)」(主任研究者：北野雅之)

分担研究者 工藤正俊

平成15年度(2003年度) 研究費総額：1,900,000円

平成16年度(2004年度) 研究費総額：1,100,000円

平成17年度(2005年度) 研究費総額：600,000円

「超音波内視鏡下バイオセンサー穿刺法の開発—膵疾患局所情報入手と評価-基盤研究(C)」(主任研究者：北野雅之)

分担研究者 工藤正俊

平成18年度(2006年度) 研究費総額：1,600,000円

平成19年度(2007年度) 研究費総額：1,560,000円

平成20年度(2008年度) 研究費総額：910,000円

「肝細胞癌の発癌・進展の分子機序：造影超音波クーパー相と遺伝子発現を用いた融合解析-挑戦的萌芽研究」(主任研究者：工藤正俊)

平成23年度(2011年度) 研究費総額：2,340,000円

平成24年度(2012年度) 研究費総額：1,430,000円

「肝細胞癌のソラフェニブ著効例における感受性規定遺伝子変異の探索-挑戦的萌芽研究」(主任研究者：西尾和人)

分担研究者 工藤正俊

平成23年度 (2011年度) 研究費総額： 4,030,000円 / 配分額： 500,000円

「超音波内視鏡を用いた胆膵疾患診断・治療システムの開発-基盤研究 (C)」

(主任研究者：北野雅之)

分担研究者 工藤正俊

平成22年度 (2010年度) 研究費総額： 1,950,000円 / 配分額： 100,000円

平成23年度 (2011年度) 研究費総額： 1,430,000円 / 配分額： 100,000円

平成24年度 (2012年度) 研究費総額： 1,040,000円 / 配分額： 100,000円

「ガンキリンのプロテアソーム制御機構を利用した展開医療研究-基盤研究 (C)」

(主任研究者：櫻井俊治)

分担研究者 工藤正俊

平成23年度 (2011年度) 研究費総額： 2,080,000円 / 配分額： 200,000円

平成24年度 (2012年度) 研究費総額： 1,950,000円 / 配分額： 200,000円

平成25年度 (2013年度) 研究費総額： 2,080,000円 / 配分額： 200,000円

「FGF3遺伝子増幅による肝細胞癌ソラフェニブ治療の効果予測-基盤研究 (A)」

(主任研究者：西尾和人)

分担研究者 工藤正俊

平成24年度 (2012年度) 研究費総額： 17,420,000円 / 配分額： 1,000,000円

平成25年度 (2013年度) 研究費総額： 17,490,000円 / 配分額： 1,000,000円

平成26年度 (2014年度) 研究費総額： 9,100,000円 / 配分額： 600,000円

「超音波ビスコエラストグラフィ：複合励振による組織粘弾性の定量的可視化技術の開発-基盤研究 (A)」(主任研究者：椎名毅)

分担研究者 工藤正俊

平成25年度 (2013年度) 研究費総額： 26,780,000円 / 配分額： 1,040,000円

平成26年度 (2014年度) 研究費総額： 11,960,000円 / 配分額： 650,000円

平成27年度 (2015年度) 研究費総額： 7,800,000円 / 配分額： 400,000円

「大腸癌、炎症性腸疾患における新規治療標的分子およびバイオマーカーの探索-基盤研究 (C)」

(主任研究者：櫻井俊治)

分担研究者 工藤正俊

平成26年度 (2014年度) 研究費総額： 1,170,000円 / 配分額： 200,000円

平成27年度 (2015年度) 研究費総額： 1,820,000円 / 配分額： 100,000円

平成28年度 (2016年度) 研究費総額： 1,820,000円 / 配分額： 100,000円

「膵疾患の診断能・予後の向上を目指した超音波内視鏡技術の開発-基盤研究(C)」

(主任研究者：北野雅之)

分担研究者 工藤正俊

平成25年度(2013年度) 研究費総額：2,080,000円 / 配分額：150,000円

平成26年度(2014年度) 研究費総額：1,820,000円 / 配分額：150,000円

平成27年度(2015年度) 研究費総額：1,700,000円 / 配分額：100,000円

「血清分泌型マイクロRNAを用いたソラフェニブ治療効果予測マーカーの開発-基盤研究(C)」

(主任研究者：工藤正俊)

平成27年度(2015年度) 研究費総額：1,950,000円

平成28年度(2016年度) 研究費総額：1,950,000円

平成29年度(2017年度) 研究費総額：780,000円

「剪断波伝搬モデルに基づく定量的組織粘・弾性影像法の開発と肝線維化早期診断法の研究-新学術領域研究(研究領域提案型)」(主任研究者：椎名毅)

分担研究者 工藤正俊

平成27年度(2015年度) 研究費総額：2,210,000円 / 配分額：0円

平成28年度(2016年度) 研究費総額：2,600,000円 / 配分額：400,000円

「超音波・光伝播モデルに基づく組織脂肪化・線維化の定量的評価と肝疾患診断への応用-新学術領域研究(研究領域提案型)」(主任研究者：椎名毅)

分担研究者 工藤正俊

平成29年度(2017年度) 研究費総額：2,210,000円 / 配分額：100,000円

平成30年度(2018年度) 研究費総額：2,210,000円 / 配分額：100,000円

「革新的超音波内視鏡技術の開発:膵癌の早期診断・予後改善を目指して-基盤研究(C)」

(主任研究者：北野雅之)

分担研究者 工藤正俊

平成28年度(2016年度) 研究費総額：1,820,000円 / 配分額：100,000円

平成29年度(2017年度) 研究費総額：1,560,000円 / 配分額：100,000円

平成30年度(2018年度) 研究費総額：1,300,000円 / 配分額：100,000円

「発癌とストレス応答の分子基盤解明とその臨床応用」(主任研究者：櫻井俊治)

分担研究者 工藤正俊

平成29年度(2017年度) 研究費総額：1,690,000円 / 配分額：200,000円

平成30年度(2018年度) 研究費総額：1,170,000円 / 配分額：200,000円

平成31年度(2019年度) 研究費総額：1,430,000円 / 配分額：100,000円

「肝癌惹起性HBx変異の存在下で形成される腫瘍微小免疫環境の解析-基盤研究(C)」

(主任研究者：萩原智)

分担研究者 工藤正俊

平成30年度(2018年度) 研究費総額：1,430,000円 / 配分額：100,000円

平成31年度(2019年度) 研究費総額：1,170,000円 / 配分額：100,000円

令和2年度(2020年度) 研究費総額：1,690,000円 / 配分額：100,000円

「肝細胞癌におけるチロシンキナーゼ阻害剤の免疫微小環境への影響に関する研究-基盤研究(C)」

(主任研究者：工藤正俊)

平成30年度(2018年度) 研究費総額：1,690,000円

平成31年度(2019年度) 研究費総額：2,210,000円

令和2年度(2020年度) 研究費総額：520,000円

「自然免疫担当分子RIP2を標的とする炎症性腸疾患の新規治療法の開発-基盤研究(C)」

(主任研究者：渡邊 智裕)

分担研究者 工藤正俊

平成31年度(2019年度) 研究費総額：1,430,000円 / 配分額：100,000円

令和2年度(2020年度) 研究費総額：1,430,000円 / 配分額：100,000円

令和3年度(2021年度) 研究費総額：1,430,000円 / 配分額：100,000円(予定)

「免疫制御機構に注目した難病新規治療戦略の開発-基盤研究(C)」

(主任研究者：櫻井 俊治)

分担研究者 工藤正俊

令和2年度(2020年度) 研究費総額：1,950,000円 / 配分額：50,000円

令和3年度(2021年度) 研究費総額：1,430,000円 / 配分額：50,000円(予定)

令和4年度(2022年度) 研究費総額：1,040,000円 / 配分額：50,000円(予定)

「消化器疾患領域の透視化医療処置における被ばく線量測定(全国多施設前向き観察研究)-基盤研究(C)」(主任研究者：竹中 完)

分担研究者 工藤正俊

令和2年度(2020年度) 研究費総額：2,470,000円 / 配分額：100,000円

令和3年度(2021年度) 研究費総額：780,000円 / 配分額：100,000円(予定)

令和4年度(2022年度) 研究費総額：390,000円 / 配分額：100,000円(予定)

厚生科学研究費補助金

厚生科学研究費補助金(肝炎等克服緊急対策研究事業)

「肝がん患者のQOL向上に関する研究」(班長：藤原研司)

分担研究者 工藤正俊

平成14年度 (2002年度) 研究費総額: 18,700,000円 / 配分額: 1,500,000円

平成15年度 (2003年度) 研究費総額: 14,000,000円 / 配分額: 1,000,000円

平成16年度 (2004年度) 研究費総額: 13,700,000円 / 配分額: 2,500,000円

厚生科学研究費補助金(肝炎等克服緊急対策研究事業)

「肝がん患者のQOL向上に関する研究」(班長: 藤原研司)

分担研究者 工藤正俊

平成18年度 (2006年度) 研究費総額: 22,000,000円 / 配分額: 2,000,000円

平成19年度 (2007年度) 研究費総額: 14,000,000円 / 配分額: 1,300,000円

平成20年度 (2008年度) 研究費総額: 13,230,000円 / 配分額: 1,250,000円

厚生科学研究費補助金(肝炎等克服緊急対策研究事業)

「血小板低値例へのインターフェロン治療法の確立を目指した基礎および臨床的研究」(班長: 西口修平)

分担研究者 工藤正俊

平成21年度 (2009年度) 研究費総額: 20,000,000円 / 配分額: 700,000円

平成22年度 (2010年度) 研究費総額: 20,000,000円 / 配分額: 800,000円

平成23年度 (2011年度) 研究費総額: 17,000,000円 / 配分額: 800,000円

厚生科学研究費補助金(がん臨床研究事業)

「初発肝細胞癌に対する肝切除とラジオ波焼灼両方の有効性に関する多施設共同研究」(班長: 國土典宏)

分担研究者 工藤正俊

平成21年度 (2009年度) 研究費総額: 25,500,000円 / 配分額: 200,000円

平成22年度 (2010年度) 研究費総額: 25,895,000円 / 配分額: 200,000円

平成23年度 (2011年度) 研究費総額: 20,082,000円 / 配分額: 150,000円

厚生科学研究費補助金(肝炎等克服緊急対策研究事業)

「肝がんの新規治療法に関する研究」(班長: 本多政夫)

分担研究者 工藤正俊

平成21年度 (2009年度) 研究費総額: 52,800,000円 / 配分額: 2,000,000円

平成22年度 (2010年度) 研究費総額: 52,800,000円 / 配分額: 2,000,000円

平成23年度 (2011年度) 研究費総額: 55,277,000円 / 配分額: 2,000,000円

厚生科学研究費補助金(がん臨床研究事業)

「進行・再発肝細胞癌に対する動注化学療法と分子標的薬併用による新規治療法の確立を目指した

臨床試験(Phase III)ならびに効果を予測するbiomarkerの探索研究」

(班長：工藤正俊)

平成22年度(2010年度) 研究費総額：45,750,000円

平成23年度(2011年度) 研究費総額：32,500,000円

平成24年度(2012年度) 研究費総額：30,000,000円

厚生科学研究費補助金(難治性疾患克服研究事業)

「多発肝のう胞症に対する治療ガイドライン作成と試料バンクの構築」

(班長：大河内信弘)

分担研究者 工藤正俊

平成22年度(2010年度) 研究費総額：12,285,000円 / 配分額：700,000円

平成23年度(2011年度) 研究費総額：10,000,000円 / 配分額：700,000円

平成24年度(2012年度) 研究費総額：11,700,000円 / 配分額：0円

厚生科学研究費補助金(難病・がん等の疾患分野の医療の実用化研究事業)

「慢性ウイルス性肝疾患の非侵襲的線維化評価法の開発と臨床的有用性の確立」

(班長：工藤正俊)

平成23年度(2011年度) 研究費総額：58,500,000円

平成24年度(2012年度) 研究費総額：57,000,000円

平成25年度(2013年度) 研究費総額：50,000,000円

厚生科学研究費補助金(難病・がん等の疾患分野の医療の実用化研究事業)

「慢性ウイルス性肝疾患患者の情報収集の在り方等に関する研究」(班長：相崎英樹)

分担研究者 工藤正俊

平成23年度(2011年度) 研究費総額：40,000,000円 / 配分額：1,500,000円

平成24年度(2012年度) 研究費総額：35,500,000円 / 配分額：1,500,000円

平成25年度(2013年度) 研究費総額：35,500,000円 / 配分額：1,500,000円

厚生科学研究費補助金(肝炎等克服実用化研究事業)

「肝がん研究の推進及び肝がん患者等への支援のための最適な仕組みの構築を目指した研究」

(班長：小池和彦)

分担研究者 工藤正俊

平成29年度(2017年度) 研究費総額：2,000,000円 / 配分額：0円

「肝がん・重度肝硬変の治療に係るガイドラインの作成等に資する研究」

(班長：小池和彦)

分担研究者 工藤正俊

平成30年度（2018年度） 研究費総額：70,000,000円 / 配分額：2,000,000円
令和 1年度（2019年度） 研究費総額：70,000,000円 / 配分額：2,000,000円
令和 2年度（2020年度） 研究費総額：70,000,000円 / 配分額：2,000,000円
令和 3年度（2021年度） 研究費総額：— 円 / 配分額：— 円
令和 4年度（2022年度） 研究費総額：— 円 / 配分額：— 円

厚生科学研究委託事業(肝炎等克服実用化研究事業(肝炎等克服緊急対策研究事業))

「慢性ウイルス性肝炎の病態把握(重症度・治療介入時期・治療効果判定・予後予測)のための非侵襲的
病態診断アルゴリズムの確立」(班長：工藤正俊)

平成26年度（2014年度） 研究費総額：40,300,000円

国立研究開発法人日本医療研究開発機構（AMED）

(肝炎等克服実用化研究事業(肝炎等克服緊急対策研究事業))

「慢性ウイルス性肝炎の病態把握(重症度・治療介入時期・治療効果判定・予後予測)のための非侵襲
的病態診断アルゴリズムの確立」

主任研究者 工藤正俊

平成27年度（2015年度） 研究費総額：44,220,000円

平成28年度（2016年度） 研究費総額：33,800,000円

(臨床研究等 ICT 基盤構築・人工知能実装研究事業)

「人工知能の利活用を見据えた超音波デジタル画像のナショナルデータベース構築基盤整備に関
する研究」

主任研究者 工藤正俊

平成30年度（2018年度） 研究費総額：190,000,000円

「超音波デジタル画像のナショナルデータベース構築と人工知能支援型超音波診断システム開発
に関する研究」

主任研究者 工藤正俊

平成31年度（2019年度） 研究費総額：61,990,900円

令和 2年度（2020年度） 研究費総額：50,030,759円

「医療ビッグデータ利活用を促進するクラウド基盤・AI画像解析に関する研究」(主任研究者：合田
憲人)(分担課題名:人工知能の開発に資する超音波画像データとアノテーションに関する研究)

分担研究者 工藤正俊

平成31年度（2019年度） 研究費総額：82,999,982円 / 配分額：0円

令和 2年度（2020年度） 研究費総額：124,879,298円 / 配分額：0円

ガイドライン策定委員会委員

- ・ 「科学的根拠に基づく肝臓診療ガイドライン」(日本肝臓学会編), 金原出版
- ・ 「慢性肝炎の治療ガイドライン」(日本肝臓学会編), 文光堂
- ・ 「肝臓診療マニュアル」(日本肝臓学会編), 医学書院
- ・ 「肝臓治療効果判定基準」(日本肝臓学会編), 肝臓
- ・ 臨床病理「肝臓取り扱い規約」(日本肝臓学会編)
- ・ Clinical Practice Guidelines for Hepatocellular Carcinoma, Japan Society of Hepatology, Hepatology Research
- ・ General Rules for the Clinical and Pathological Study of Primary Liver Cancer, 3rd English Version, Liver Cancer Study Group of Japan, Kanehara, Tokyo, 2010
- ・ Response Evaluation criteria in the Cancer of the Liver (RECICL), Liver Cancer Study Group of Japan, Hepatology Research
- ・ 「多発肝のう胞症に対する治療ガイドライン」
- ・ RECICL 2014 update版, Hepatology Research

ガイドライン策定

- ・ 日本肝臓学会 肝臓診療ガイドライン作成委員 (2009年, 2013年, 2017年, 2021年)
- ・ 日本肝臓学会 肝臓診療マニュアル作成委員会委員 (2010年, 2015年, 2020年)
- ・ 日本肝臓学会 慢性肝炎治療ガイドライン作成委員会委員
- ・ 日本肝臓学会 多発性肝嚢胞治療ガイドライン作成委員会委員
- ・ 日本超音波医学会 肝臓のエラストグラフィ作成委員会委員長
- ・ 世界超音波医学会 エラストグラフィガイドライン作成委員会委員長

特許取得

発明の名称: ソラフェニブの効果予測方法

出願番号: 特願2011-104275

出願日: 2011年5月9日

発明者: 荒尾徳三、松本和子、西尾和人、工藤正俊

出願人: 学校法人近畿大学

発明の名称: N型糖鎖を利用した膵臓癌の診断方法

公開番号: 特許公開2009-270996

公開日: 2009年11月19日

発明者: 荒尾徳三、松本和子、西尾和人、坂本洋城、北野雅之、工藤正俊

出願人: 住友ベークライト株式会社

全国規模の学会・研究会事務局

- ・ 日本肝臓学会(事務局・追跡調査委員長・常任幹事)

- ・ 日本腹部造影エコー・ドプラ診断研究会(代表世話人・事務局)
- ・ NPO法人日本肝がん臨床研究機構(理事長・事務局)
- ・ 日本肝がん分子標的治療研究会(代表世話人・事務局)

全国規模の研究会世話人・役員

平成 6年 4月- 8年 3月	日本超音波医学会腹部造影エコー研究部会幹事
平成 7年11月-現在	肝血流動態イメージ研究会世話人
平成 8年 4月-現在	日本腹部造影エコー・ドプラ造影研究会世話人（事務局兼務） (平成25年より <u>代表世話人</u>)
平成 9年 7月-現在	肝動脈塞栓療法研究会世話人
平成10年-現在	国際造影超音波研究会 (現、Asia Contrast Ultrasound Imaging Society)世話人
平成11年10月-現在	臨床消化器病研究会世話人
平成11年 7月-現在	西日本肝臓研究会世話人
平成13年 5月-現在	肝疾患フォーラム世話人
平成14年 4月-現在	犬山シンポジウム会員
平成14年 9月-現在	日本消化器画像診断研究会世話人
平成16年-現在	Liver Forum in Kyoto世話人
平成18年-現在	肝癌治療シミュレーション研究会副代表幹事
平成19年11月-現在	日本超音波治療研究会常任世話人
平成20年-現在	日本肝がん分子標的治療研究会(<u>代表世話人</u>)

関西地区研究会代表世話人

- ・ 平成11年-平成19年 関西造影超音波研究会(代表世話人)
- ・ 平成13年-現在 関西B型肝炎研究会(代表世話人)
- ・ 平成14年-現在 肝癌局所治療研究会(代表世話人)
- ・ 平成14年-現在 大阪消化器化学療法懇話会(代表世話人)
- ・ 平成15年-現在 臨床消化器病フォーラム(代表世話人)
- ・ 平成18年-平成22年 Bay Area Gut Club(代表世話人)
- ・ 平成18年-平成22年 South Osaka Liver Club(代表世話人)
- ・ 平成19年-現在 関西肝血流動態イメージ研究会(代表世話人)
- ・ 平成20年-現在 Kinki Liver Club(代表世話人)
- ・ 平成21年-現在 南大阪肝疾患研究会(代表世話人)
- ・ 平成21年-現在 南大阪肝胆膵疾患研究会(代表世話人)

関西地区研究会世話人

- ・ 平成 2年-現在 大阪肝穿刺生検治療研究会世話人

- ・ 平成 6年-現在 兵庫インターベンショナルラディオロジー研究会世話人
- ・ 平成 8年-現在 肝胆膵治療フォーラム・神戸世話人
- ・ 平成 9年-現在 京都肝疾患懇話会世話人
- ・ 平成 9年-現在 肝臓分子生物学研究会
- ・ 平成11年-平成18年 肝代謝コロキウム世話人
- ・ 平成11年-現在 大阪肝胆膵懇話会世話人
- ・ 平成11年-現在 南大阪肝胆膵疾患研究会世話人
- ・ 平成11年-現在 南大阪消化器病懇話会世話人
- ・ 平成11年-現在 南大阪肝疾患研究会世話人
- ・ 平成11年-平成24年 消化器ラウンドテーブルディスカッション世話人
- ・ 平成11年-平成18年 泉州肝臓病研究会世話人
- ・ 平成11年-平成18年 大阪肝炎ミーティング世話人
- ・ 平成12年-現在 大阪肝臓病談話会世話人
- ・ 平成12年-現在 関西経皮内視鏡的胃瘻造設術研究会世話人
- ・ 平成12年-現在 肝疾患座談会 in Kyoto世話人
- ・ 平成12年-現在 近畿肝癌談話会常任幹事
- ・ 平成13年-現在 関西肝血流動態イメージ研究会世話人
- ・ 平成16年-平成23年 あおい肝臓研究会世話人
- ・ 平成18年-現在 大阪肝臓ミーティング世話人
- ・ 平成19年-現在 近畿・超音波内視鏡研究会顧問

全国規模の国内研究会主催（会長）

- ・ 1997年 2月 第3回肝血流動態イメージ研究会(神戸)
- ・ 1996年10月 第1回日本造影エコー・ドプラ診断研究会(神戸)
- ・ 2005年 2月 第11回肝血流動態イメージ研究会(横浜)
- ・ 2007年 9月 第2回肝癌治療シミュレーション研究会(大阪)
- ・ 2008年 9月 第49回日本消化器画像診断研究会(大阪)
- ・ 2010年 1月 第1回日本肝癌分子標的治療研究会(神戸)
- ・ 2014年 2月 第20回肝血流動態・機能イメージ研究会(大阪)

国内学会主催（会長）

- ・ 第45回日本肝臓学会総会(2009年6月), 神戸
- ・ 第83回日本超音波医学会学術集会(2010年5月), 京都
- ・ 第50回日本肝癌研究会(2014年6月), 京都
- ・ 第89回日本超音波医学会学術集会(2016年5月), 京都

近畿地区学会主催（会長）

- 第82回日本消化器内視鏡学会近畿支部例会(2009年8月)
- 第95回日本消化器病学会近畿支部例会(2011年8月)

近畿地区学会主催（会長）

- 第82回日本消化器内視鏡学会近畿支部例会(2009年8月)
- 第95回日本消化器病学会近畿支部例会(2011年8月)
- 第214回日本内科学会近畿地方会(2016年12月)

国際学会主催（会長）

- JSH Single Topic Conference on HCC (2005年), Awaji-shima
- The 3rd International Kobe Liver Cancer Symposium on HCC(IKLS)(2009年6月), Kobe
- The 2nd Asia Pacific Primary Liver Cancer Expert Meeting (APPLE)(2011年7月), Osaka
- The 14th WFUMB 2013(世界超音波医学会)(2013年5月), Sao Paulo(Co-President with Leandro Fernandez and Giovanni Guido Cerri)
- The 4th International Kyoto Liver Cancer Symposium(IKLS) (2014年6月6-7日), Kyoto
- the 8th International Liver Cancer Association(ILCA)(国際肝癌学会)(2014年9月5日-7日), Kyoto(Co-President with Peter Galle)
- The 6th Asia Pacific Primary Liver Cancer Expert Meeting (APPLE)(2015年7月), Osaka
- AFSUMB 2016(アジア超音波医学会)(2016年5月), Kyoto
- ACUCI(アジア造影超音波医学会)(2016年5月), Kyoto

2018年度表彰式一覧

➤ Highest Impact Factor Award 2018 (最高インパクトファクター賞)

- 1位 渡邊智裕 14.188 (Trends Immunol)
2位 松井繁長 10.231 (Am J Gastroenterol)
- ※ 3位 鎌田 研 7.204 (Gastrointest Endosc)
3位 山雄健太郎 7.204 (Gastrointest Endosc)
※ 工藤正俊 53.254 (Lancet)

➤ Most Numbers of Paper Award 2018 (最多英文論文発表賞)

- 1位 三長孝輔 6本 (J Med Ultrason × 2, Dig Liver Dis × 1, World J Gastroenterol × 1, Endoscopy × 1, Cancers(Basel) × 1)
2位 鎌田 研 5本 (Gastrointest Endosc × 1, Dig Endosc × 1, Endosc Ultrasound × 1, Digest Endosc × 1, Curr Protoc Immunol × 1)
- ※ 3位 竹中 完 3本 (Endoscopy × 1, Dig Endosc × 2)
※ 工藤正俊 13本

➤ Total Highest Impact Factor Award 2018 (累積最高インパクトファクター賞)

- 1位 三長孝輔 19.452 (6本)
2位 鎌田 研 17.003 (5本)
- ※ 3位 渡邊智裕 14.188 (1本)
※ 工藤正俊 124.863 (13本)

➤ 最多入院受持患者賞

- 1位 田中秀和 709人
2位 高島耕太 664人
- ※ 3位 河野辰哉 658人

➤ 最多緊急内視鏡賞

- 1位 田中秀和 49件
2位 高島耕太 34件
- ※ 3位 益田康弘 29件

➤ 最多外来患者診療賞

- 1位 上嶋一臣 2,793人
2位 萩原 智 2,771人
- ※ 3位 松井繁長 2,698人
※ 工藤正俊 1,177人

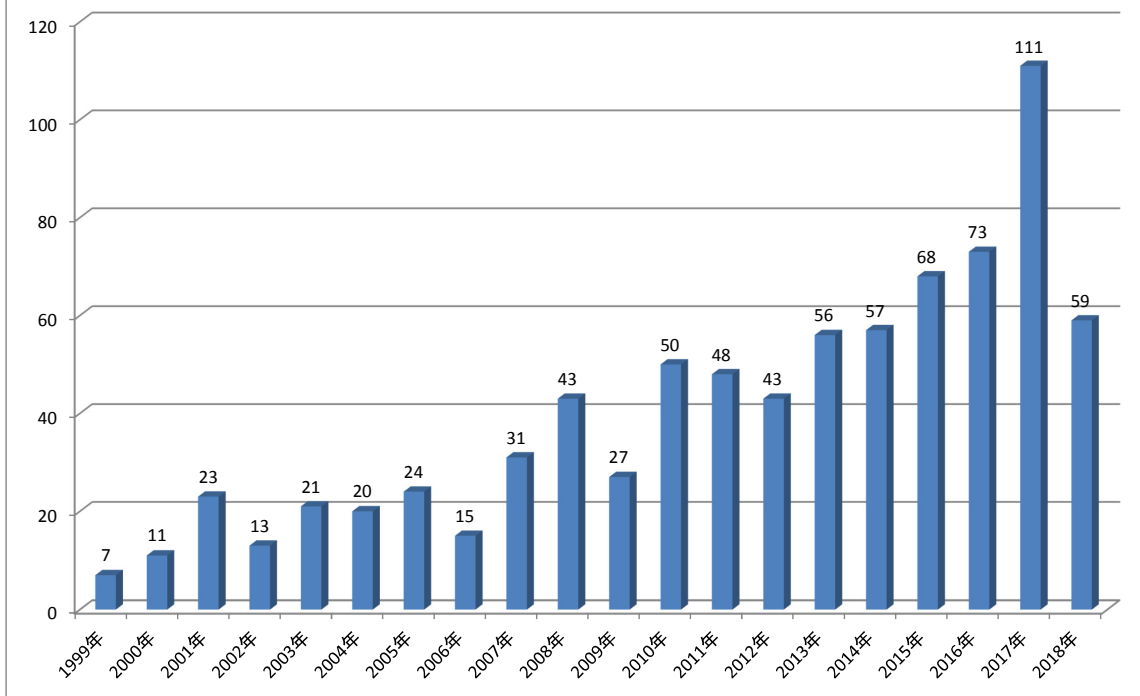
消化器内科学教室業績抜粋

	1999	2000	2001	2002	2003	2004	2005	2006	2007
英文論文 (Impact Factor)	7 57.1	11 61.526	23 80.163	13 29.11	21 75.988	20 99.181	24 92.954	15 59.849	31 127.014
和文論文 (著書・分担執筆を含む)	37	41	43	34	31	54	45	39	45
海外学会発表	2	9	4	6	24	23	14	14	17
国内学会発表	46	56	71	113	105	79	69	52	79
海外特別講演	0	11	4	11	8	18	16	25	18
国内特別講演	37	40	40	52	37	38	39	27	36
単著教科書			1		1 (英文)				

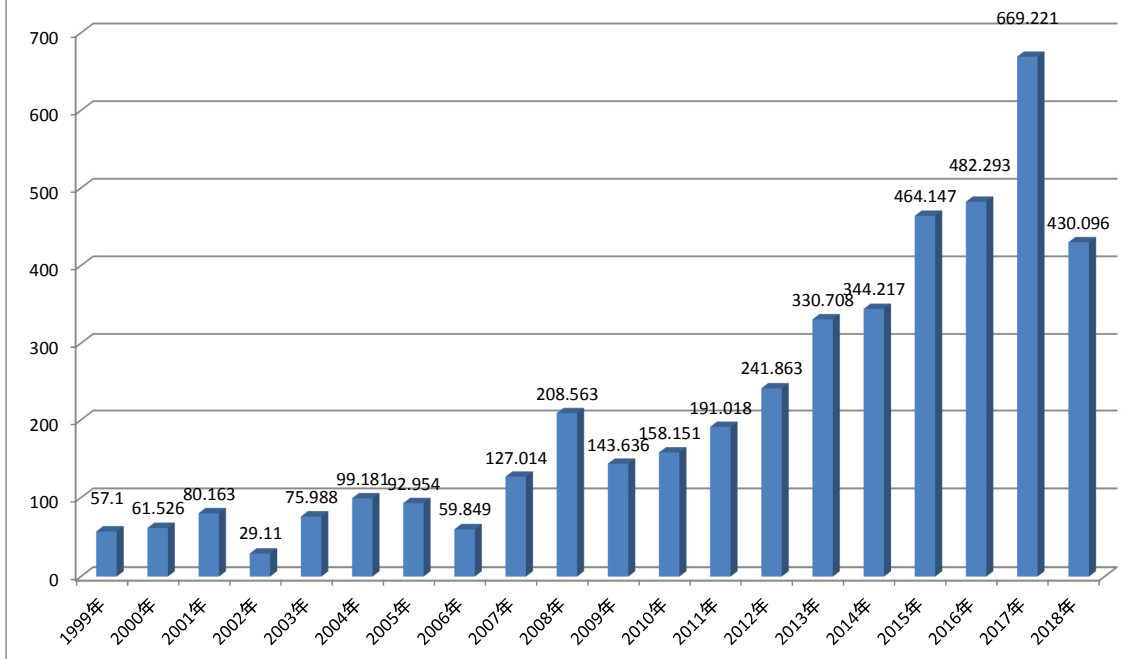
令和2年10月現在

2008	2009	2010	2011	2012	2013	2014	2015	2016	2017	2018	計
43 208.563	27 143.636	50 158.151	48 191.018	43 241.863	56 330.708	57 344.217	68 464.147	73 482.293	111 669.221	59 430.096	800 4346.798
74	81	126	59	54	17	21	55	15	43	41	955
26	20	34	64	52	35	37	32	47	37	63	560
87	65	96	100	118	117	105	98	69	93	63	1681
36	34	42	28	34	33	16	19	16	7	15	391
39	62	94	75	59	43	28	40	34	35	60	818
											2

近畿大学医学部消化器内科 英文論文総数(800編)



近畿大学医学部消化器内科 英文論文 Impact Factor総数 (IF=4346.798)

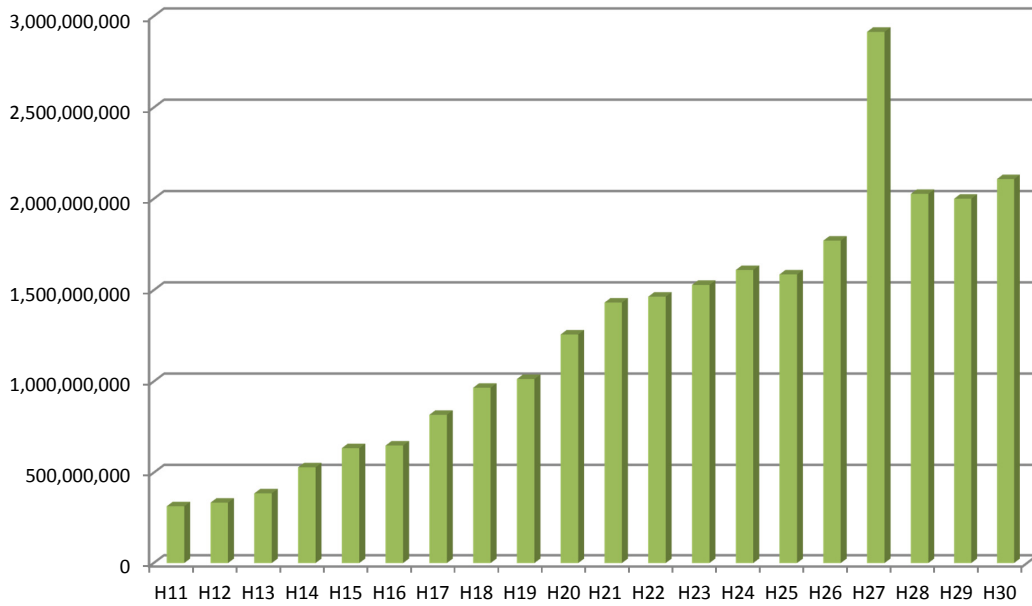


消化器内科年度別診療実績

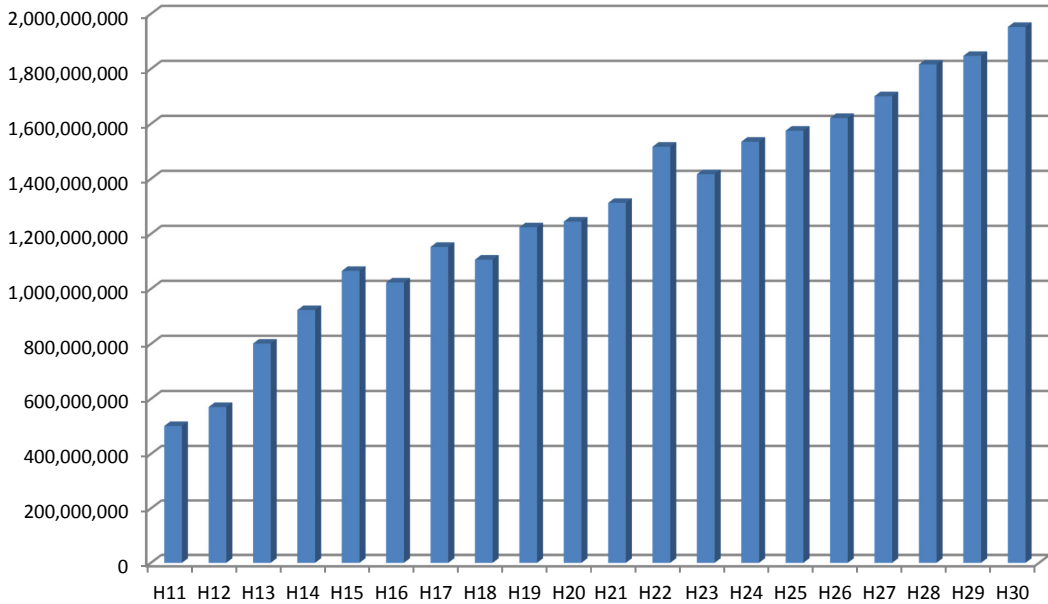
	H11	H12	H13	H14	H15	H16	H17	H18	H19	H20
稼働床	40	44	44	44	60	78	78	77	76	73
稼働率	107.2%	98.5%	126.7%	148.2%	121.0%	89.5%	95.3%	89.2%	94.7%	96.3%
日平均入院患者数	40.0	43.3	55.8	65.2	72.6	69.8	74.4	68.7	72.0	70.3
平均在院日数	31.1	25.6	21.4	18.6	15.4	14.7	12.8	10.7	10.5	9.6
年間入院収入	501,570,188	570,616,464	801,199,124	923,171,333	1,065,481,449	1,023,271,279	1,152,778,111	1,106,484,453	1,224,122,968	1,244,806,271
年間外来収入	314,641,639	334,517,979	386,084,329	530,035,297	635,562,806	649,876,475	818,049,485	966,247,389	1,013,910,559	1,257,804,553
消化器内科年間収入	816,211,827	905,134,443	1,187,283,453	1,453,206,630	1,701,044,255	1,673,147,754	1,970,827,596	2,072,731,842	2,238,033,527	2,502,610,824

	H21	H22	H23	H24	H25	H26	H27	H28	H29年	H30(1-11)
稼働床	85	84	84	84	80	80	80	95	101	101
稼働率	91.8%	89.9%	85.8%	89.0%	91.0%	93.9%	98.7%	96.8%	89.3%	93.5%
日平均入院患者数	70.3	76.1	72.0	74.7	77.0	75.1	78.9	84.7	88.7	94.4
平均在院日数	9	8.6	7.9	7.2	7.2	6.7	7.0	7.6	6.9	7.5
年間入院収入	1,312,812,506	1,516,925,835	1,417,104,402	1,535,069,456	1,575,321,748	1,621,531,082	1,700,694,167	1,816,140,190	1,847,155,829	1,952,570,995
年間外来収入	1,432,350,698	1,464,645,183	1,529,385,181	1,610,826,432	1,586,645,573	1,771,578,798	2,914,910,768	2,027,534,890	2,001,226,787	2,108,778,984
消化器内科年間収入	2,745,163,204	2,981,571,018	2,946,489,583	3,145,895,888	3,161,967,321	3,393,109,880	4,615,604,935	3,843,675,080	3,848,382,616	4,061,349,979

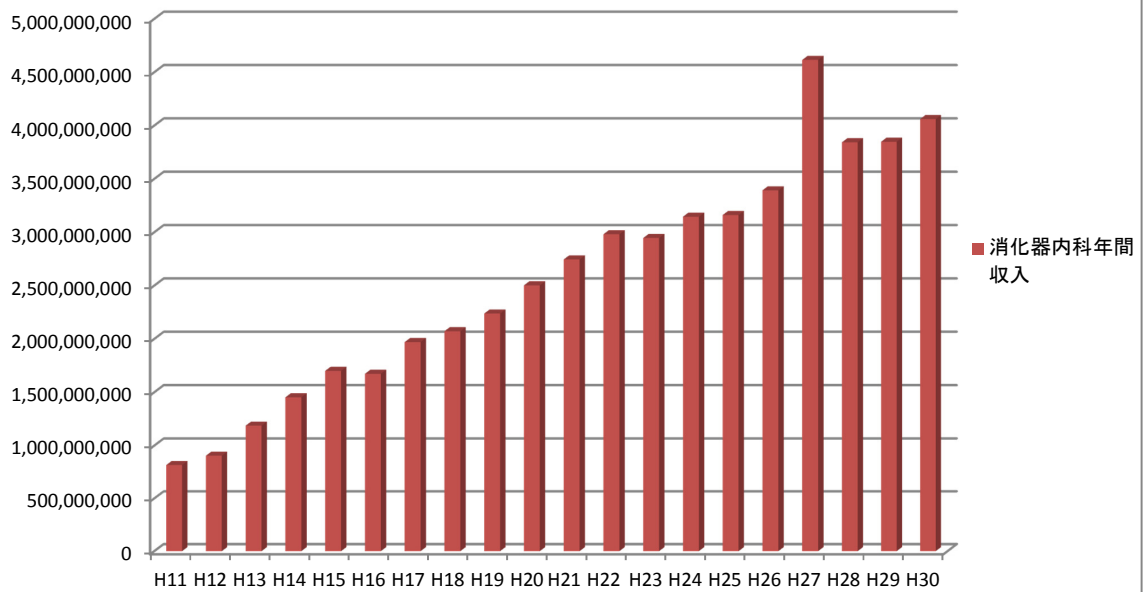
消化器内科年間外来収入



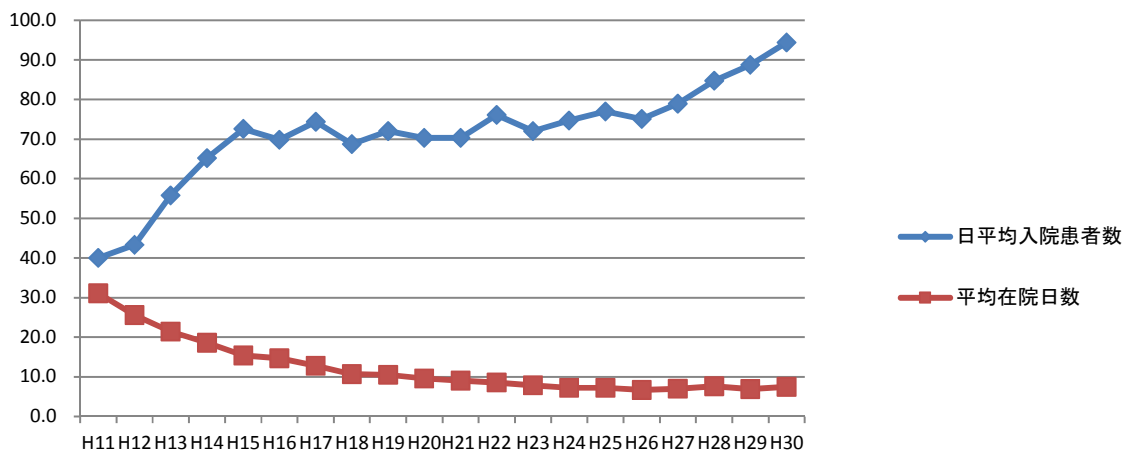
消化器内科年間入院収入



消化器内科年間総収入



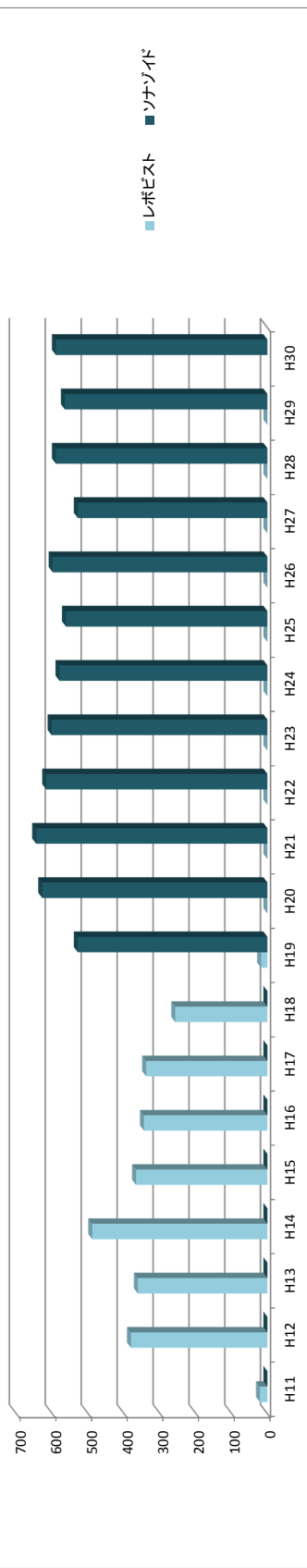
消化器内科入院診療実績



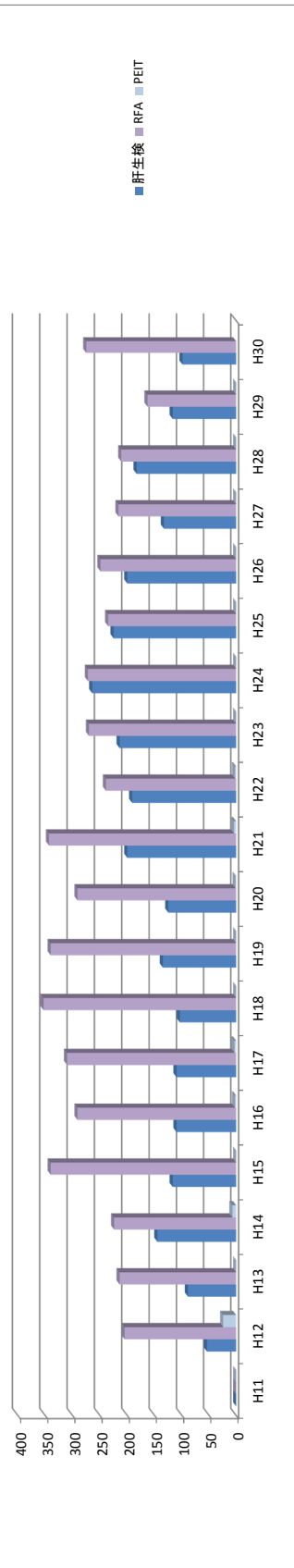
エコー室件数

1月-12月	H11	H12	H13	H14	H15	H16	H17	H18	H19	H20	H21	H22	H23	H24	H25	H26	H27	H28	H29	H30
肝生検		54	89	145	117	110	110	104	135	125	200	191	214	264	225	200	133	183	117	99
RFA		205	214	224	340	291	310	353	340	291	343	239	270	272	235	249	216	211	163	275
PEIT		24	0	7	0	2	3	0	0	1	4	2	0	0	0	0	0	0	0	0
レボピスト	21	381	362	489	367	345	339	258	18	0	0	0	0	0	0	0	0	0	0	0
ソナゾイド	0	0	0	0	0	0	0	0	529	628	645	617	602	580	562	599	529	590	565	590

腹部造影エコー検査



経皮的局所治療・肝生検総件数



平成29年11月現在

内視鏡部年報

検 査	H26	H27	H28	H29	H30
胃・十二指腸 球部(EUS含む)	9003	8993	8487	8422	5228
超音波内視鏡 (胃)	42	53	72	82	111
超音波内視鏡 (胆膵)	1603	1817	1609	1599	1472
胃・十二指腸 ポリペク	4	40	3	6	3
胃・十二指腸 EMR	206	236	224	227	212
止血・上部	125	158	165	160	172
食道静脈瘤結紮術 (EVL)	51	63	56	62	52
硬化療法 (EIS)	0	7	9	10	14
EISL	29	25	28	37	28
食道ブジー	163	153	69	83	82
経皮内視鏡的胃瘻造設術 (PEG)	73	68	59	65	68
ステント留置 (食道)	10	11	16	14	13
ステント留置 (胃・十二指腸)	33	38	24	40	32
イレウス管 (経口)	45	54	64	69	58
トロピン撒布	30	25	24	33	86
異物除去	371	405	415	203	23
大腸ファイバースコピー(EUS含む)	3903	3928	3813	3938	2936
超音波内視鏡 (大腸)	12	10	14	21	12
大腸ポリペク・EMR (大腸ESD含む)	769	729	760	846	873
止血 大腸	50	42	40	37	40
異物除去	30	25	24	0	0
大腸ブジー	6	8	7	7	4
(経肛門) イレウス管	45	54	64	2	1
小腸ファイバースコピーのみ	97	125	95	104	120
小腸 ポリペク	0	0	1	0	4
小腸EMR	4	1	4	4	1
止血 小腸	5	5	3	6	6
小腸ブジー	0	0	7	0	3
小腸カプセル内視鏡	34	17	34	47	41
胆道ドレナージ	278	349	382	304	269
乳頭切開	120	127	127	130	94
乳頭バルーン拡張術	2	1	1	1	6
結石除去	125	106	129	127	78
気管支ファイバースコピー	495	542	544	521	500
胸腔鏡	—	—	17	20	16
予約外内視鏡検査	1117	1101	846	677	618

近畿大学 消化器内科学教室医局員

(令和2年7月現在)

主任教授	工藤正俊	S53	肝臓・消化器・肝癌の診断と治療	
教授（内視鏡部）	樫田博史	S58	下部消化管	
	辻 直子	S60	上部消化管	
准教授	汐見幹夫	S55	上部・胆膵内視鏡（関空クリニック所長・教授兼務）	
	西田直生志	S60	肝臓病学・肝癌の分子生物学	
講師 医学部講師	渡邊智裕	H 5	消化管全般	
	松井繁長	H 3	食道静脈瘤止血・上部消化管	
	上嶋一臣	H 7	慢性肝炎・肝癌の治療	
	櫻井俊治 (病棟医長)	H 7	上部消化管・分子生物学	
	依田 広 (外来医長)	H 8	肝疾患・消化器一般	
	南 康範 (医局長)	H 9	肝疾患・消化器一般	
	萩原 智	H10	肝疾患・消化器一般	
	竹中 完	H13	胆膵疾患・消化器一般	
	米田頼晃	H13	消化器一般	
	田北雅弘	H15	肝疾患・消化器一般	
	永井知行	H16	消化器一般	
	山雄健太郎	H18	胆膵疾患・消化器一般	
	医学部助教	鎌田 研	H19	胆膵疾患・消化器一般
		三長孝輔	H19	胆膵疾患・消化器一般
		山田光成	H19	消化器一般
		大本俊介	H21	消化器一般
千品寛和 (串本病院出向中)		H22	消化器一般	
河野匡志 (富田林病院)		H22	消化器一般	
中井敦史		H22	胆膵疾患・消化器一般	
山崎友裕		H22	胆膵疾患・消化器一般	
南 知宏		H23	消化器一般	
正木 翔		H23	消化器一般	
岡本彩那		H23	胆膵疾患・消化器一般	
橋本有人		H25	消化器一般	
高田隆太郎		H26	肝疾患・消化器一般	
福永明洋		H27	胆膵疾患・消化器一般	
河野辰哉		H27	消化器一般	
半田康平 (府中病院出向中)		H27	消化器一般	
高島耕太	H27	消化器一般		

	吉田晃浩 (府中病院出向中)	H27	消化器一般
	田中秀和	H27	消化器一般
	松村まり子	H25	消化器一般
	大塚康生	H25	消化器一般
	益田康弘	H25	肝疾患・消化器一般
大学院生	山田光成 (4年)	H19	消化器一般
	岡元寿樹 (4年)	H23	消化器一般
	石川 嶺 (2年)	H24	胆膵疾患・消化器一般
	山崎友祐 (1年)	H26	胆膵疾患・消化器一般
実験助手	升本知子		
	小崎秀人		
臨床研究補助	児玉美由紀		
教授秘書	田中真紀		
	本廣佳香		
	上野由紀子		
日本肝癌研究会	田村利恵		
	上妻智子		
医局秘書	胡桃由佳		
	朝隈 智		
	市井由紀		
近大奈良病院	川崎俊彦、水野成人、川崎正憲、高山政樹、茂山朋広、奥田英之		
部門別医師構成			
	○消化管グループ		
	檜田博史、辻 直子、渡邊智裕、松井繁長、櫻井俊治、 米田頼晃、永井知行、山田光成、河野匡志、橋本有人、岡元寿樹、 正木 翔		
	○胆膵グループ		
	汐見幹生、竹中 完、山雄健太郎、鎌田 研、三長孝輔、大本俊介、 中井敦史、石川 嶺、岡本彩那、山崎友裕		
	○肝グループ		
	工藤正俊、西田直生志、上嶋一臣、依田 広、南 康範、萩原 智、 田北雅弘、南 知宏、千品寛和		

消化器内科学教室業績一覽
(2018年)

I. 英文論文

1. 2018 Harding JJ, Watanabe T, El-Dika I, Nishida N, Abou-Alfa GK, **Kudo M**: 2.5 “Gastrointestinal Malignancies” ; 2.5.3 Hepatocellular carcinoma. In “ESMO Handbook of Immuno-Oncology” , Haanen J, Lugowska I, Garassino MC, Califano R, ed., 2018, pp191-202.
2. 2018 Kamata K, Takenaka M, Omoto S, Miyata T, Minaga K, Yamao K, Imai H, Sakurai T, Nishida N, Chikugo T, Chiba Y, Matsumoto I, Takeyama Y, **Kudo M**: Impact of avascular areas, as measured by contrast-enhanced harmonic EUS, on the accuracy of FNA for pancreatic adenocarcinoma. **Gastrointest Endosc**, 87:158-163, 2018. (IF=7.204)
3. 2018 **Kudo M***, Cheng AL, Park JW, Park JH, Liang PC, Hidaka H, Izumi N, Heo J, Lee YJ, Sheen IS, Chiu CF, Arioka H, Morita S, Arai Y: Orantinib versus placebo combined with transcatheter arterial chemoembolisation in patients with unresectable hepatocellular carcinoma (ORIENTAL): a randomised, double-blind, placebo-controlled, multicentre, phase 3 study. **Lancet Gastroenterol Hepatol** 3:37-46, 2018. (IF=0.000)
4. 2018 Nishiyama H, Nagai T, **Kudo M**, Okazaki Y, Azuma Y, Watanabe T, Goto S, Ogata H, Sakurai T: Supplementation of pancreatic digestive enzymes alters the composition of intestinal microbiota in mice. **Biochem Biophys Res Commun** 459:273-279, 2018. (IF=2.466)
5. 2018 Minaga K, Takenaka M, Omoto S, Miyata T, Kamata K, Yamao K, Imai H, Watanabe T, Kitano M, **Kudo M**: A case of successful transluminal drainage of walled-off necrosis under contrast-enhanced harmonic endoscopic ultrasonography guidance. **J Med Ultrason** 45:161-165, 2018. (IF=0.455)
6. 2018 Kamata K, Takenaka M, Kitano M, Omoto S, Miyata T, Minaga K, Yamao K, Imai H, Sakurai T, Nishida N, Kashida H, Chikugo T, Chiba Y, Nakai T, Takeyama Y, Lisotti A, Fusaroli P, **Kudo M**: Contrast-enhanced harmonic endoscopic ultrasonography for differential diagnosis of localized gallbladder lesions. **Dig Endosc** 30:98-106, 2018. (IF=3.238)
7. 2018 Takayasu K, Arii S, Sakamoto M, Matsuyama Y, **Kudo M**, Kaneko S, Nakashima O, Kadoya M, Izumi N, Takayama T, Ku Y, Kumada T, Kubo S, Kokudo T, Hagiwara Y, Kokudo N; Liver Cancer Study Group of Japan: Impact of resection and ablation for single hypovascular hepatocellular carcinoma ≤ 2 cm analysed with propensity score weighting. **Liver Int** 38:484-493, 2018. (IF=4.500)
8. 2018 **Kudo M***: Lenvatinib may drastically change the treatment landscape of hepatocellular carcinoma. **Liver Cancer** 7:1-19, 2018. (IF=7.854)
9. 2018 **Kudo M***: Combination cancer immunotherapy in hepatocellular carcinoma. **Liver Cancer** 7:20-27, 2018. (IF=7.854)
10. 2018 **Kudo M***, Finn RS, Qin S, Han KH, Ikeda K, Piscaglia F, Baron A, Park JW, Han G, Jassem J, Blanc JF, Vogel A, Komov D, Evans TRJ, Lopez C, Dutcus C, Guo M, Saito K, Kraljevic S, Tamai T, Ren M, Cheng AL: Lenvatinib versus sorafenib in first-line treatment of patients with unresectable hepatocellular carcinoma: a randomised phase 3 non-inferiority trial. **Lancet** 391:1163-1173, 2018. (IF=53.254)
11. 2018 Matsui S, Kashida H, **Kudo M**: Gastric inverted hyperplastic polyp mimicking a papilla. **Am J Gastroenterol** 113:462, 2018. (IF=10.231)
12. 2018 Ikeda M, **Kudo M**, Aikata H, Nagamatsu H, Ishii H, Yokosuka O, Torimura T, Morimoto M, Ikeda K, Kumada H, Sato T, Kawai I, Yamashita T, Horio H, Okusaka T, Miriplatin TACE Study Group: Transarterial chemoembolization with miriplatin vs. epirubicin for unresectable hepatocellular carcinoma: a phase III randomized

- trial. *J Gastroenterol* 53:281-290, 2018. (IF=5.561)
13. 2018 Minami Y, Minami T, Hagiwara S, Ida H, Ueshima K, Nishida N, Murakami T, **Kudo M**: Ultrasound-ultrasound image overlay fusion improves real-time control of radiofrequency ablation margin in the treatment of hepatocellular carcinoma. *Eur Radiol* 28:1986-1993, 2018. (IF=4.027)
 14. 2018 Minaga K, Takenaka M, Kamata K, **Kudo M**: Transrectal endoscopic ultrasound-guided paracentesis for diagnosis of malignant ascites in the pelvis. *Dig Liver Dis* 50:311, 2018. (IF=3.287)
 15. 2018 Kono M, Komeda Y, Sakurai T, Okamoto A, Minaga K, Kamata K, Hagiwara S, Inoue H, Enoki E, Matsumura I, Watanabe T, **Kudo M**: Induction of complete remission by azacitidine in a patient with myelodysplastic syndrome-associated inflammatory bowel disease. *J Crohns Colitis* 12:499-502, 2018. (IF=6.637)
 16. 2018 **Kudo M***, Kang YK, Park JW, Qin S, Inaba Y, Assenat E, Umeyama Y, Lechuga MJ, Valota O, Fujii Y, Martini JF, Williams JA, Obi S: Regional differences in efficacy, safety and biomarkers for second-line axitinib in patients with advanced hepatocellular carcinoma: from a randomized phase II study. *Liver Cancer*, 7:148-164, 2018. (IF=7.854)
 17. 2018 **Kudo M***, Ueshima K, Yokosuka O, Ogasawara S, Obi S, Izumi N, Aikata H, Nagano H, Hatano E, Sasaki Y, Hino K, Kumada T, Yamamoto K, Imai Y, Iwadou S, Ogawa C, Okusaka T, Kanai F, Akazawa K, Yoshimura KI, Johnson P, Arai Y; SILIUS study group: Sorafenib plus low-dose cisplatin and fluorouracil hepatic arterial infusion chemotherapy versus sorafenib alone in patients with advanced hepatocellular carcinoma (SILIUS): a randomised, open label, phase 3 trial. *Lancet Gastroenterol Hepatol* 3:424-432, 2018. (IF=0.000)
 18. 2018 Minaga K, Watanabe T, Kamata K, Asano N, **Kudo M**: Nucleotide-binding oligomerization domain 1 and Helicobacter pylori infection: A review. *World J Gastroenterol* 24:1725-1733, 2018. (IF=3.300)
 19. 2018 Raoul JL, **Kudo M**, Finn RS, Edeline J, Reig M, Galle PR: Systemic therapy for intermediate and advanced hepatocellular carcinoma: Sorafenib and beyond. *Cancer Treat Rev* 68:16-24, 2018. (IF=8.122)
 20. 2018 **Kudo M***: Cabozantinib as a second-line agent in advanced hepatocellular carcinoma. *Liver Cancer* 7:123-133, 2018. (IF=7.854)
 21. 2018 **Kudo M***: Management of hepatocellular carcinoma in Japan as a world-leading model. *Liver Cancer* 7:134-147, 2018. (IF=7.854)
 22. 2018 Matsui S, Kashida H, **Kudo M**: Utility of endoscopic ultrasound in hemorrhage from recurrent duodenal varices. *Ann Gastroenterol* 31:636, 2018. (IF=1.250)
 23. 2018 Minaga K, Takenaka M, Okamoto A, Omoto S, Miyata T, Imai H, **Kudo M**: Reintervention for stent occlusion after endoscopic ultrasound-guided hepaticogastrostomy with novel use of a precut needle-knife. *Endoscopy* 50: E153-154, 2018. (IF=6.629)
 24. 2018 Minaga K, Takenaka M, Kamata K, Yoshikawa T, Nakai A, Omoto S, Miyata T, Yamao K, Imai H, Sakamoto H, Kitano M, **Kudo M**: Alleviating pancreatic cancer-associated pain using endoscopic ultrasound-guided neurolysis. *Cancers (Basel)* 10:E50, 2018. (IF=5.326)
 25. 2018 Chau I, Park JO, Ryoo BY, Yen CJ, Poon R, Pastorelli D, Blanc JF, **Kudo M**, Pfiffer T, Hatano E, Chung HC, Kopeckova K, Phelip JM, Brandi G, Ohkawa S, Li CP, Okusaka T, Hsu Y, Abada PB, Zhu AX: Alpha-fetoprotein kinetics in patients with hepatocellular carcinoma receiving ramucirumab or placebo: an analysis of the phase 3 REACH study. *Brit J Cancer* 119:19-26, 2018. (IF=5.922)

26. 2018 Yen CJ, Muro K, Kim TW, **Kudo M**, Shih JY, Lee KW, Chao Y, Kim SW, Yamazaki K, Sohn J, Cheng R, Zhang Y, Binder P, Mi G, Orlando M, Chung HC: Ramucirumab safety in East Asian patients: A meta-analysis of six global, randomized, double-blind, placebo-controlled, phase III clinical trials. **J Glob Oncol**:1-12, 2018. (IF=0.000)
27. 2018 Zhu AX, Finn RS, Edeline J, Cattan S, Ogasawara S, Palmer D, Verslype C, Zagonel V, Fartoux L, Vogel A, Sarker D, Verset G, Chan SL, Knox J, Daniele B, Webber AL, Ebbinghaus, SW, Ma J, Siegel AB, Cheng AL, **Kudo M**, for the KEYNOTE-224 investigators: Pembrolizumab in patients with advanced hepatocellular carcinoma previously treated with sorafenib (KEYNOTE-224): a non-randomised, open-label phase 2 trial. **Lancet Oncol** 19:940-952, 2018. (IF=36.418)
28. 2018 Okamoto K, Watanabe T, Komeda Y, Okamoto A, Minaga K, Kamata K, Yamao K, Takenaka M, Hagiwara S, Sakurai T, Tanaka T, Sakamoto H, Fujimoto K, Nishida N, **Kudo M**: Dysbiosis-associated polyposis of the colon-cap polyposis. **Front Immunol** 9:918, 2018. (IF=5.511)
29. 2018 Nishida N, **Kudo M**: Immune checkpoint blockade for the treatment of human hepatocellular carcinoma. **Hepatol Res** 48:622-634, 2018. (IF=3.415)
30. 2018 Dietrich CF, Averkiou M, Nielsen MB, Barr RG, Burns PN, Calliada F, Cantisani V, Choi B, Chammas MC, Clevert DA, Claudon M, Correas JM, Cui XW, Cosgrove D, D'Onofrio M, Dong Y, Eisenbrey J, Fontanilla T, Gilja OH, Ignee A, Jenssen C, Kono Y, **Kudo M**, Lassau N, Lyschik A, Franca Meloni M, Moriyasu F, Nolsøe C, Piscaglia F, Radzina M, Saftoiu A, Sidhu PS, Sporea I, Schreiber-Dietrich D, Sirlin CB, Stanczak M, Weskott HP, Wilson SR, Willmann JK, Kim TK, Jang HJ, Vezeridis A, Westerway S: How to perform contrast-enhanced ultrasound (CEUS). **Ultrasound Int Open** 4:E2-15, 2018. (IF=0.000)
31. 2018 Yamao K, Kitano M, Takenaka M, Minaga K, Sakurai T, Watanabe T, Kayahara T, Yoshikawa T, Yamashita Y, Asada M, Okabe Y, Hanada K, Chiba Y, **Kudo M**: Outcomes of endoscopic biliary drainage in pancreatic cancer patients with an indwelling gastroduodenal stent: a multicenter cohort study in west Japan. **Gastrointest Endosc** 88:66-75, 2018. (IF=7.204)
32. 2018 Takenaka M, Arisaka Y, Sakai A, Kobayashi T, Shiomi H, Masuda A, **Kudo M**: A novel biliary cannulation method for difficult cannulation cases using a unique, uneven, double-lumen cannula (Uneven method). **Endoscopy** 50:E229-230, 2018. (IF=6.629)
33. 2018 Takenaka M, Yamao K, **Kudo M**: Novel method of biliary cannulation for patients with Roux-en-Y anastomosis using a unique, uneven, double lumen cannula (Uneven method). **Dig Endosc** 30:808-809, 2018. (IF=3.238)
34. 2018 Yoshida A, Hagiwara S, Watanabe T, Nishida N, Ida H, Sakurai T, Komeda Y, Yamao K, Takenaka M, Enoki E, Kimura M, Miyake M, Kawada A, **Kudo M**: Erythropoietic Protoporphyrin-related Hepatopathy Successfully Treated with Phlebotomy. **Intern Med** 57:2505-2509, 2018. (IF=0.817)
35. 2018 Watanabe T, Minaga K, Kamata K, **Kudo M**, Strober W: Mechanistic insights into autoimmune pancreatitis and IgG4-related disease. **Trends Immunol** 39:874-889, 2018. (IF=14.188)
36. 2018 **Kudo M***: Proposal of primary endpoints for TACE combination trials with systemic therapy: Lessons learned from 5 negative trials and the positive TACTICS trial. **Liver Cancer** 7:225-234, 2018. (IF=7.854)
37. 2018 **Kudo M***: Extremely high objective response rate of Lenvatinib: Its clinical relevance and changing the treatment paradigm in hepatocellular carcinoma. **Liver Cancer** 7:215-224, 2018. (IF=7.854)

38. 2018 Takenaka M, Minaga K, **Kudo M**: Cannulation method for intra-diverticular papilla with long oral protrusion using biopsy forceps for axis alignment. *Dig Endosc* 30:700-701, 2018. (IF=3.238)
39. 2018 Kamata K, Takenaka M, Minaga K, Nakai A, Omoto S, Miyata T, Yamao K, Imai H, Sakurai T, Watanabe T, Nishida N, **Kudo M**: Cystic duct antegrade stenting for cholangitis after the long-term deployment of lumen-apposing metal stents for calculous cholecystitis. *Endosc Ultrasound* 7:349-350, 2018. (IF=3.323)
40. 2018 Tanaka H, Kamata K, Takenaka M, **Kudo M**: Contrast-enhanced harmonic EUS imaging of pancreatic mucinous cystadenocarcinoma. *Internal Med* 57:3051-3052, 2018. (IF=0.817)
41. 2018 Tamaki N, Koizumi Y, Hirooka M, Yada N, Takada H, Nakashima O, **Kudo M**, Hiasa Y, Izumi N: Novel quantitative assessment system of liver steatosis using a newly developed attenuation measurement method. *Hepatol Res* 48:821-828, 2018. (IF=3.415)
42. 2018 Kamata K, Takenaka M, Minaga K, Omoto S, Miyata T, Yamao K, Imai H, Nakai A, Tanaka H, Chiba Y, Watanabe T, Sakurai T, Nishida N, Chikugo T, Matsumoto I, Takeyama Y, Kitano M, **Kudo M**: Value of additional endoscopic ultrasonography for surveillance after surgical removal of intraductal papillary mucinous neoplasms. *Digest Endosc* 30:659-666, 2018. (IF=3.238)
43. 2018 Minaga K, Kitano M, Itonaga M, Imai H, Miyata T, Yamao K, Tamura T, Nuta J, Warigaya K, **Kudo M**: Endoscopic ultrasound-guided biliary drainage using a newly designed metal stent with a thin delivery system: A preclinical study in phantom and porcine models. *J Med Ultrason* 45:391-397, 2018. (IF=0.455)
44. 2018 **Kudo M***: Ramucirumab as second-line systemic therapy in hepatocellular carcinoma. *Liver Cancer* 7:305-311, 2018. (IF=7.854)
45. 2018 **Kudo M***: Systemic therapy for hepatocellular carcinoma: Latest advances. *Cancers* 10:E412, 2018. (IF=5.326)
46. 2018 **Kudo M***: Cabozantinib for advanced hepatocellular carcinoma. *Hepatobil Surg Nutr*, 2018 (doi:10.21037/hbsn.2018.11.22). (IF=3.451)
47. 2018 Kamata K, Watanabe T, Minaga K, Strober W, **Kudo M**: Autoimmune pancreatitis mouse model. *Curr Protoc Immunol*, 2018 (doi: 10.1002/cpim.41). (IF=0.000)
48. 2018 Otsuka Y, Kamata K, Minaga K, Takenaka M, Watanabe T, **Kudo M**: Acute pancreatitis with disturbed consciousness caused by hyperparathyroidism. *Internal Med* 57:3075-3078, 2018. (IF=0.817)
49. 2018 Chan AWH, Zhong J, Berhane S, Toyoda H, Cucchetti A, Shi K, Tada T, Chong CCN, Xiang BD, Li LQ, Lai PBS, Mazzaferro V, García-Fiñana M, **Kudo M**, Kumada T, Roayaie S, Johnson PJ: Development of pre and post-operative models to predict early recurrence of hepatocellular carcinoma after surgical resection. *J Hepatol* 69:1284-1293, 2018. (IF=15.040)
50. 2018 Minaga K, Kitano M: Recent advances in endoscopic ultrasound-guided biliary drainage. *Dig Endosc* 30:38-47, 2018. (IF=3.238)
51. 2018 Hagiwara S, Nishida N, Watanabe T, Ida H, Sakurai T, Ueshima K, Takita M, Komeda Y, Nishijima N, Osaki Y, **Kudo M**: Sustained antiviral effects and clearance of hepatitis surface antigen after combination therapy with entecavir and pegylated interferon in chronic hepatitis B. *Antivir Ther* 23:513-521, 2018. (IF=2.594)
52. 2018 Kamata K, Watanabe T, Minaga K, Strober W, **Kudo M**: Autoimmune pancreatitis mouse model. *Curr Protoc Immunol* 120, 2018, DOI: 10.1002/cpim.41. (IF=0.000)
53. 2018 Sofue K, Tsurusaki M, Mileto A, Hyodo T, Sasaki K, Nishii T, Chikugo T, Yada N, **Kudo M**, Sugimura K, Murakami T: Dual-energy computed tomography for non-invasive

- staging of liver fibrosis: Accuracy of iodine density measurements from contrast-enhanced data. *Hepatol Res* 48:1008-1019, 2018. (IF=3.415)
54. 2018 Kato R, Hayashi H, Sano K, Handa K, Kumode T, Ueda H, Okuno T, Kawakami H, Matsumura I, Kudo M, Nakagawa K: Nivolumab-induced hemophilia A presenting as gastric ulcer bleeding in a patient with non-small cell lung cancer. *J Thorac Oncol* 13:e239-e241, 2018. (IF=10.336)
55. 2018 Yoshida A, Yamao K, Takenaka M, Nakai A, Omoto S, Kamata K, Minaga K, Miyata T, Imai H, Matsumoto I, Takeyama Y, Chikugo T, Kudo M: Neurilemmoma mimicking a multilocular cystic lesion of the liver. *Intern Med* 57:3377-3380, 2018. (IF=0.817)
56. 2018 Chau I, Peck-Radosavljevic M, Borg C, Malfertheiner P, Seitz JF, Park JO, Ryoo BY, Yen CJ, Kudo M, Poon R, Pastorelli D, Blanc JF, Chung HC, Baron AD, Okusaka T, Bowman L, Cui ZL, Girvan AC, Abada PB, Yang L, Zhu AX: Corrigendum to “Ramucirumab as second-line treatment in patients with advanced hepatocellular carcinoma following first-line therapy with sorafenib: Patient-focused outcome results from the randomised phase III REACH study”. *Eur J Cancer* 100:135-136, 2018. (IF=2.843)
57. 2018 Ferraioli G, Wong VW, Castera L, Berzigotti A, Sporea I, Dietrich CF, Choi BI, Wilson SR, Kudo M, Barr RG: Liver ultrasound elastography: An update to the World Federation for Ultrasound in Medicine and Biology guidelines and recommendations. *Ultrasound Med Biol* 44:2419-2440, 2018. (IF=2.645)
58. 2018 Tak WY, Ryoo BY, Lim HY, Kim DY, Okusaka T, Ikeda M, Hidaka H, Yeon JE, Mizukoshi E, Morimoto M, Lee MA, Yasui K, Kawaguchi Y, Heo J, Morita S, Kim TY, Furuse J, Katayama K, Aramaki T, Hara R, Kimura T, Nakamura O, Kudo M: Phase I/II study of first-line combination therapy with sorafenib plus resminostat, an oral HDAC inhibitor, versus sorafenib monotherapy for advanced hepatocellular carcinoma in east Asian patients. *Invest New Drugs* 36:1072-1084, 2018. (IF=3.484)
59. 2018 Nishida N, Nishimura T, Kaido T, Minaga K, Yamao K, Kamata K, Takenaka M, Ida H, Hagiwara S, Minami Y, Sakurai T, Watanabe T, Kudo M: Molecular scoring of hepatocellular carcinoma for predicting metastatic recurrence and requirements of systemic chemotherapy. *Cancers* 10: E367, 2018 (doi: 10.3390/cancers10100367). (IF=5.326)

II. 和文論文

- 2018 工藤正俊: 開発中の肝癌治療薬 特集: 肝癌—診断・治療の最新知見— V. 特論. 日本臨床76:343-352, 2018.
- 2018 南 知宏, 南 康範, 千品寛和, 有住忠晃, 田北雅弘, 矢田典久, 萩原 智, 依田 広, 上嶋一臣, 西田直生志, 工藤正俊: 肝細胞癌に対するUS-US overlay fusionを用いたラジオ波焼灼術の有用性. 肝臓 59:142-144, 2018.
- 2018 工藤正俊, 池田公史, 古瀬純司, 北野滋久: 特別座談会「肝細胞癌薬物療法のパラダイムシフトを語る」, 特集「急速に変貌する肝細胞癌の薬物療法2018 update」, 肝胆膵 77:183-210, 2018.
- 2018 平岡 淳, 道堯浩二郎, 熊田 卓, 工藤正俊: TACEによる肝予備能低下 - ALBI score/gradeによる評価—. 肝胆膵 77:224-230, 2018.
- 2018 工藤正俊: TACEとソラフェニブ併用試験 (TACTICS) の概要と成功要因—過去の失敗試験との比較からTACE併用試験のendpointを考える—. 肝胆膵 77:231-240, 2018.
- 2018 工藤正俊: REFLECT試験の結果を振り返る、レンバチニブの高い奏効率の臨床的意義. 肝胆膵 77:263-270, 2018.
- 2018 上嶋一臣, 工藤正俊: レンバチニブとソラフェニブの有効性および肝機能の変化—

- REFLECT試験への登録症例の経験からー. 肝胆膵 77:278-283, 2018.
8. 2018 上嶋一臣, 工藤正俊: レンバチニブのQOLと費用対効果. 肝胆膵 77:306-309, 2018.
 9. 2018 小川 力, 工藤正俊: ラムシルマブの第III相臨床試験結果. 肝胆膵 77:398-408, 2018.
 10. 2018 平岡 淳, 道堯浩二郎, 工藤正俊: ニボルマブの臨床試験のアップデート. 肝胆膵 77:419-424, 2018.
 11. 2018 工藤正俊: どのようにしてcold tumorをhot tumorに変えるか. 肝胆膵 77:449-455, 2018.
 12. 2018 上嶋一臣, 工藤正俊: その他のI0+I0の臨床試験の可能性. 肝胆膵 77:473-475, 2018.
 13. 2018 西田直生志, 工藤正俊: 腫瘍免疫抑制環境の成立とチロシンキナーゼ阻害剤の作用ーチロシンキナーゼ阻害剤と免疫チェックポイント阻害剤併用のコンセプトー. 肝胆膵 77:499-505, 2018.
 14. 2018 工藤正俊: 肝細胞癌の切除・RFA後のアジュバント・ネオアジュバント療法. 肝胆膵 77:506-511, 2018.
 15. 2018 工藤正俊: 学会レポート「第54回米国臨床腫瘍学会 (ASCO)」. 肝胆膵 77:522-532, 2018.
 16. 2018 工藤正俊: 肝がんの新しい薬「消化器病の薬」. 消化器のひろば第13号: 8, 2018.
 17. 2018 工藤正俊: 肝細胞癌における免疫チェックポイント阻害剤とのその他の治療法との組み合わせ治療. The Liver Cancer Journal 10: 49-55, 2018.
 18. 2018 工藤正俊: [レンビマで変わる肝細胞癌の診断と治療]レンビマ徹底解剖, Phase 3 REFLECT試験. クリニシアン 65:593-612, 2018.
 19. 2018 宮田 剛, 竹中 完, 工藤正俊: 【膵癌update】 トピックス 膵癌の癌性疼痛に対するEUSガイド下神経叢ブロック(融解)術の有用性. 臨床消化器内科 33:950-957, 2018.
 20. 2018 幕谷悠介, 松本 逸平, 大本 俊介, 筑後 孝章, 川口 晃平, 松本 正孝, 村瀬 貴昭, 亀井 敬子, 里井 俊平, 中居 卓也, 竹中 完, 工藤 正俊, 竹山 宣典: 膵・胆管合流異常に合併した共通管内乳頭状腫瘍の1例. 日本消化器外科学会雑誌 51:114-121, 2018.
 21. 2018 南 康範, 工藤正俊: 肝癌治療の実際 (2) 穿刺局所療法. 特集「ガイドラインに基づいた肝癌診療」. 臨床消化器内科 33:619-625, 2018.
 22. 2018 鎌田 研, 竹中完, 中井敦史, 大本俊介, 宮田剛, 三長孝輔, 山雄健太郎, 今井元, 樫田博史, 工藤正俊: IPMNの経過観察におけるEUSの今後. 消化器内視鏡30:606-610, 2018.
 23. 2018 工藤正俊: 肝癌診療の最前線. 日本内科学会雑誌 107:1934-1943, 2018.
 24. 2018 南 康範, 工藤正俊: [知っておきたい神経感染症] C型肝炎ウイルス関連クリオグロブリン血管炎. BRAIN and NERVE: 神経研究の進歩 70-133-137, 2018.
 25. 2018 工藤正俊, 山下竜也, 森口理久, 池田公史, 上嶋一臣, 鳥村拓司: 座談会; 肝細胞癌の薬物療法の最先端. 肝臓 59:517-544, 2018.
 26. 2018 工藤正俊: 原発性肝癌(肝細胞癌). 特集「外科医が知っておきたい化学放射線療法・癌免疫療法」. 消化器外科 41:1537-1546, 2018.
 27. 2018 吉川智恵, 鎌田 研, 竹中 完, 大本俊介, 三長孝輔, 山雄健太郎, 今井 元, 榎木英介, 木村雅友, 松本逸平, 竹山宣典, 工藤正俊: 興味深い造影ハーモニックEUS像を呈した胆嚢癌の1例. 胆道 324:775-781, 2018.
 28. 2018 渡邊智裕, 鎌田 研, 三長孝輔, 工藤正俊: IgG4関連疾患の最近の知見 IgG4関連疾患の病因と自然免疫. 月刊リウマチ科 604:347-352, 2018.
 29. 2018 竹中 完, 筑後孝章, 工藤正俊: 充実性 特殊型膵癌-腺扁平上皮癌, 退形成性膵管癌, 腺房細胞癌-, 胆膵疾患内視鏡アトラス I. 膵臓. 消化器内視鏡 30:54-57, 2018.
 30. 2018 南 康範, 工藤正俊: ここまで“見える”最新超音波診断装置[Part2]今“超音波”に求められるものとは 肝癌に対するPrecision RFAと超音波による早期治療効果判定 US-US overlay fusionの有用性. 月刊新医療 459:114-117. 2018.
 31. 2018 田北雅弘, 南 知宏, 千品寛和, 河野匡志, 萩原 智, 南 康範, 依田 広, 上嶋一臣, 西田直生志, 工藤正俊: 常染色体優性多嚢胞性肝疾患 (Autosomal dominant polycystic liver disease: ADPLD). 特集「知っておこう! 遺伝性消化器疾患」. 消化器内視鏡

308:1086-1089, 2018.

32. 2018 工藤正俊: 総説: 肝細胞癌薬物療法の最新の進歩. 肝臓 59:587-603, 2018.
33. 2018 南 康範, 南 知宏, 千品寛和, 田北雅弘, 萩原 智, 依田 広, 上嶋一臣, 西田直生志, 工藤正俊: US-US fusion imagingとUS-US overlay fusion. 特集「肝癌治療のイノベーション-シミュレーション・ナビゲーション技術の新展開-」. 肝胆膵 77:1139-1144, 2018.
34. 2018 南 知宏, 南 康範, 工藤正俊, 鶴崎正勝, 柳生行伸, 村上卓道: Hepatic Guideの有用性. 特集「肝癌治療のイノベーション-シミュレーション・ナビゲーション技術の新展開-」. 肝胆膵 77:1161-1165, 2018.
35. 2018 工藤正俊, 大城幸雄, 小川 力, 宮山士朗: 座談会「肝癌治療のシミュレーション・ナビゲーションを語る」. 特集「肝癌治療のイノベーション-シミュレーション・ナビゲーション技術の新展開-」. 肝胆膵 77:1241-1263, 2018.
36. 2018 工藤正俊: 消化器内科診療レジデントマニュアル. 医学書院, 東京, pp2-431, 2018.
37. 2018 鎌田 研, 竹中 完, 石川 嶺, 吉川智恵, 岡本彩那, 山崎友裕, 中井敦史, 大本俊介, 三長孝輔, 山雄健太郎, 櫻井俊治, 松井繁長, 渡邊智裕, 西田直生志, 樫田博史, 工藤正俊: EUSによる消化管疾患の診断—現状と最新の話— 造影ハーモニックEUSによる消化管粘膜下腫瘍の診断. 胃と腸 53:1795-1799, 2018.
38. 2018 竹中 完, 三長孝輔, 鎌田 研, 山雄健太郎, 工藤正俊: 胆膵ドレナージupdate [3. 困難例とトラブルシューティング] 胆管・膵管プラスチックステント迷入への対処. 消化器内視鏡 30:1605-1611, 2018.
39. 2018 竹中 完, 吉川智恵, 石川 嶺, 岡本彩那, 山崎友祐, 中井敦史, 大本俊介, 三長孝輔, 鎌田 研, 山雄健太郎, 有坂好史, 工藤正俊: Biliary access大辞典 III. 経乳頭のbiliary access~salvage technique~Uneven Double Lumen Cannulaを用いた胆管カニューレーションテクニック(Uneven method)【動画付】. 胆と膵 39:1013-1020, 2018.
40. 2018 上嶋一臣: 肝細胞癌に対する分子標的治療の今後の展望. The Liver Cancer Journal 5 (suppl 1):25-27, 2018.
41. 2018 汐見幹夫: 経管栄養 - 胃瘻を中心に - . 病院と在宅をつなぐ 脳神経内科の摂食嚥下障害 - 病態理解と専門職の視点 -, pp77-83, 2018.

Ⅲ. 招待講演・特別講演 (海外)

1. Kudo M: Invited Lecture “Systemic therapy for hepatocellular carcinoma: 2018 update”. The 33rd Nagoya International Cancer Treatment Symposium, Aichi Cancer Center, February 10-11, 2018.
2. Kudo M: Invited Lecture “Novel management of advanced HCC”. 5th Myanmar GI & Liver, International Scientific Meeting and ASEAN Perspective in Liver Diseases (APLD), Yangon, Myanmar, February 17, 2018.
3. Kudo M: Invited Lecture “Current best practice and future perspective of systemic therapies for unresectable hepatocellular carcinoma”. Next Symposium, National Cancer Hospital, Vietnam, April 10, 2018.
4. Kudo M: Keynote Lecture “The role of TKI in HCC in an immunotherapy world”. 5th Asia-Pacific Gastroenterology Cancer Summit 2018, Singapore, May 5-6, 2018.
5. Kudo M: Invited Lecture “Current best practice and future perspective of systemic therapies for unresectable hepatocellular carcinoma”. Next Symposium, Bach Mai Hospital, Vietnam, May 10, 2018.
6. Kudo M: Invited Lecture “Molecular targeted therapy”, Symposium 6 “Aging society and HCC: up to what age do we consider treating patients with HCC in general?”. Asian Pacific Association for the Study of the Liver (APASL) Single Topic Conference, Yokohama, Japan, May 11-13, 2018.
7. Kudo M: Invited Lecture “Small HCCs”, Hot Issues: ACUCI “CEUS: how to make it

- clear” . The 13th Congress of the Asian Federation of Societies for Ultrasound in Medicine and Biology (AFSUMB 2018), Seoul, Korea, May 23-26, 2018.
8. **Kudo M**: Invited Lecture “Current best practice and future perspective of systemic therapies for unresectable hepatocellular carcinoma” . Next Symposium, Ho Chi Minh, Vietnam, June 10, 2018.
 9. **Kudo M**: Invited Lecture “Role of contrast-enhanced ultrasound in diagnosis of early-stage HCC” . The 9th Asia-Pacific Primary Liver Cancer Expert Meeting (APPLE), Grand Hyatt Seoul, South Korea, July 6-8, 2018.
 10. **Kudo M**: Invited Lecture “TACE refractoriness: definition and treatment options” . The 9th Asia-Pacific Primary Liver Cancer Expert Meeting (APPLE), Grand Hyatt Seoul, South Korea, July 6-8, 2018.
 11. **Kudo M**: Invited Lecture “TKI-Based combination therapy: the more the better?” The 9th Asia-Pacific Primary Liver Cancer Expert Meeting (APPLE), Grand Hyatt Seoul, South Korea, July 6-8, 2018.
 12. **Kudo M**: Educational Lecture “Phase 3 study of ramucirumab versus placebo in 2nd-line advanced HCC patients with high baseline AFP (REACH-2)” , 16th Annual Meeting of the Japanese Society of Medical Oncology, Kobe Convention Center/Kobe Portopia hotel, Kobe, Japan, July 19-21, 2018.
 13. **Kudo M**: Invited Lecture “Eastern perspective” . Hepatocellular Carcinoma (HCC) Scientific Input Engagement, Hoboken, New Jersey, USA, August 9-10, 2018.
 14. **Kudo M**: Invited Lecture “The Role of CEUS in the Detection and Diagnosis of FLL” . The 2018 Convention of Taiwan Society of Ultrasound in Medicine (TSUM), Taipei, Taiwan, October 13-14, 2018.
 15. **Kudo M**: Invited Lecture “HCC Meet the Expert” , European Society for Medical Oncology (ESMO 2018), Munich, Germany, October 19-23, 2018.

IV. 招待講演・特別講演 (国内)

1. **工藤正俊**: 特別講演「急激に変貌する肝癌の薬物療法—免疫療法を含めて—」, 第67回かもがわ肝臓カンファレンス, 平成30年2月2日, 京都タワーホテル, 京都.
2. **工藤正俊**: 特別講演「新たなステージにはいった肝炎・肝癌の治療」, 第29回肝疾患診療従事者研修会, 平成30年3月1日, 福井商工会議所, 福井.
3. **工藤正俊**: 特別講演「新たなステージに入った肝細胞癌治療～薬物療法が変わる～」, 第14回肝胆膵臨床腫瘍カンファレンス, 平成30年3月2日, 慶應義塾大学病院, 東京.
4. **工藤正俊**: 特別講演「旧瘦軀に変貌する肝細胞癌の薬物療法」, 『肝疾患とアミノ酸』学術講演会, 平成30年3月22日, ホテル日航金沢, 石川.
5. **工藤正俊**: 特別講演「肝細胞癌の薬物治療が大きく変わる」, Liver Cancer Forum in FUKUOKA, 平成30年3月24日, ホテルセントラーザ博多, 福岡.
6. **工藤正俊**: 特別講演「新たなステージに入った肝細胞癌治療～薬物療法が変わる～」, Surgical oncology meeting 2018 -HCC treatment-, 平成30年5月18日, ホテルモントレエーデルホフ札幌, 北海道.
7. **工藤正俊**: 特別講演「これからの肝細胞癌診療」, 特別企画2「肝臓研究の過去から未来への潮流②」, 第54回日本肝臓学会総会, 平成30年6月15日, 大阪国際会議場, 大阪.
8. **工藤正俊**: 特別講演「肝細胞癌の治療アルゴリズム—穿刺局所療法・TACE・化学療法」, 特別企画5「日本肝臓学会ガイドラインup to date」, 第54回日本肝臓学会総会, 平成30年6月15日, 大阪国際会議場, 大阪.
9. **工藤正俊**: 特別講演「肝細胞癌の薬物治療が大きく変わる」, Lenvatinib-Meet the Expert in 三重, 平成30年6月19日, 三重県総合文化センター, 三重.
10. **工藤正俊**: 特別講演「肝細胞癌診療のブレイクスルー～薬物療法が変わる～」, 第2回山口県肝臓癌セミナー, レンビマ®効能・効果追加記念講演会, 平成30年6月21日, ANAクラウンプラザホテ

ル, 山口.

11. 工藤正俊: 特別講演「新たなステージに入った肝臓の薬物治療」, 第49回京都肝臓セミナー, 平成30年6月23日, 京都ホテルオークラ, 京都.
12. 工藤正俊: 基調講演「Keynote Lecture」, 第54回日本肝臓研究会, 平成30年6月28日, 久留米シティプラザ, 福岡.
13. 工藤正俊: ランチョンセミナー7「レンビマによる肝臓治療のブレイクスルー」, 第54回日本肝臓研究会, 平成30年6月29日, 久留米シティプラザ, 福岡.
14. 工藤正俊: 教育講演「肝細胞癌の薬物療法: 最近の進歩と将来展望」, 日本内科学会第58回近畿支部生涯教育講演会, 平成30年7月1日, 大阪国際交流センター, 大阪.
15. 工藤正俊: 特別講演「新たなステージに入った肝細胞癌治療～薬物療法が変わる～」, HCC Sorafenib-Regorafenib講演会, 平成30年7月3日, 大阪マリオット都ホテル, 大阪.
16. 工藤正俊: 特別講演「肝細胞癌診療のブレイクスルー」, 第18回関西肝血流動態・機能イメージ研究会, 平成30年7月21日, ユーザイ株式会社大阪コミュニケーションオフィス33階, 大阪.
17. 工藤正俊: 特別講演「肝臓病学の新潮流」, 南大阪Liver Forum, 平成30年7月26日, セントレジスホテル大阪, 大阪.
18. 工藤正俊: 特別講演「新たなステージに入った肝細胞癌診療～薬物療法が変わる～」, LENVIMA-HCC適応拡大記念講演会, 平成30年7月28日, 深志神社, 長野.
19. 工藤正俊: 特別講演「新たなステージに入った肝細胞癌診療～薬物療法が変わる～」, 第1回千葉肝がんフォーラム～適応追加記念講演会～, 平成30年7月30日, 京成ホテルミラマーレ, 千葉.
20. 工藤正俊: 特別講演「肝臓診療のブレイクスルー薬物療法が変わる」, LENVIMA-HCC埼玉適応追加記念講演会, 平成30年7月31日, パレスホテル大宮, 埼玉.
21. 工藤正俊: 特別講演「新たなステージに入った肝細胞癌治療～薬物療法が変わる～」, 肝細胞癌 Meet The Experts in 岩手, 平成30年8月3日, ホテルメトロポリタン盛岡, 岩手.
22. 工藤正俊: 特別講演「急速に変貌する肝細胞癌の薬物療法」, 第171回東北腹部画像診断検討会, 平成30年8月4日, 江陽グランドホテル, 宮城.
23. 工藤正俊: 特別講演「急速に変貌する肝細胞癌の薬物療法」, HCC Meet the Expert in AKITA LENVIMA「肝細胞癌」適応追加記念講演会, 平成30年8月6日, ホテルメトロポリタン秋田, 秋田.
24. 工藤正俊: 特別講演「新たなステージに入った肝細胞癌の薬物療法」, LENVIMA適応追加記念講演会 日本で生まれた新薬・レンビマの登場, 平成30年8月7日, ホテルメトロポリタン山形, 山形.
25. 工藤正俊: 特別講演「肝臓診療のブレイクスルー～薬物療法が変わる～」, 中四国エリアレンビマHCC講演会in香川, 平成30年8月12日, JRホテルクレメント高松, 香川.
26. 工藤正俊: 特別講演「肝細胞癌診療のブレイクスルー～薬物療法が変わる～」, LENVIMA Meet The Expert南大阪, 平成30年8月24日, ホテルアゴーラリージェンシー堺, 大阪.
27. 工藤正俊: 特別講演「新たなステージに入った肝細胞癌診療～薬物療法が変わる～」, 新たな肝臓治療を考える会, 平成30年8月31日, リーガロイヤルホテル大阪, 大阪.
28. 工藤正俊: 特別講演「急速に変貌する肝細胞癌の薬物療法」, Lenvima適応追加記念講演会in 広島, 平成30年9月6日, リーガロイヤルホテル広島, 広島.
29. 工藤正俊: 特別講演「急速に変貌する肝細胞癌の薬物療法」, Lenvima-Meet the Expert 効能・効果追加記念講演会, 平成30年9月8日, 札幌グランドホテル, 北海道.
30. 工藤正俊: 特別講演「新たなステージに入った肝細胞癌診療 - 薬物療法が変わる -」, レンバチニブ適応追加講演会, 平成30年9月20日, オークラフロンティアホテルつくば, 茨城.
31. 工藤正俊: 特別講演「急速に変貌する肝細胞癌の薬物療法」, 第38回奈良消化器代謝セミナー, 平成30年9月27日, 奈良ホテル, 奈良.
32. 工藤正俊: 特別講演「急速に変貌する肝細胞癌の薬物療法」, 肝胆膵の分子標的治療セミナー, 平成30年9月28日, ラグナヴェールプレミア, 大阪.
33. 工藤正俊: 特別講演「肝細胞癌治療のブレイクスルー～薬物療法が変わる～」, 第33回岐阜肝画像研究会, 平成30年9月29日, じゅうろくプラザ, 岐阜.
34. 工藤正俊: 特別講演「新たなステージに入った肝細胞癌治療～薬物療法が変わる～」, 首都圏肝臓交流セミナー, 平成30年10月11日, 八芳園, 東京.

35. 工藤正俊：特別講演「新たなステージに入った肝細胞癌治療－薬物療法が変わる－」，第100回北九州肝腫瘍研究会特別記念講演会，平成30年10月12日，ホテルクラウンパレス小倉，福岡。
36. 工藤正俊：特別講演「肝細胞癌治療のブレイクスルー～薬物療法が変わる～」，第45回青森県肝胆膵研究会，平成30年10月13日，弘前大学医学部コミュニケーションセンター，青森。
37. 工藤正俊：特別講演「急速に変貌する肝細胞癌の薬物療法」，LENVIMA適応追加講演会 日本で生まれた新薬・レンビマの登場，平成30年10月25日，ホテル東日本宇都宮，栃木。
38. 工藤正俊：特別講演「肝細胞癌の薬物治療が大きく変わる」，LENVIMA適応追加講演会，平成30年10月26日，ホテル日航姫路，兵庫。
39. 工藤正俊：特別講演「急速に変貌する肝細胞癌の薬物療法」，The HCC Summit in Shizuoka，平成30年10月27日，ホテルセンチュリー静岡，静岡。
40. 工藤正俊：特別講演「急速に変貌する肝細胞癌の薬物療法-ESMOの最新情報を含めて-」，NEXT Web Conference，平成30年10月29日。
41. 工藤正俊：ランチョンセミナー38「急速に変貌する肝細胞癌の薬物療法」，第26回日本消化器関連学会週間JDDW 2018（第22回日本肝臓学会大会，第96回日本消化器内視鏡学会総会，第60回日本消化器病学会大会），平成30年11月1日，神戸コンベンションセンター，兵庫5。
42. 工藤正俊：特別講演「新たなステージに入った肝細胞癌治療 - 薬物療法のもたらす新たなパラダイム」，LENVIMA HCC Seminar，平成30年11月29日，ホテルグランヴィア和歌山，和歌山。
43. 工藤正俊：特別講演「新たなステージに入った肝細胞癌治療 - 薬物療法のもたらす新たなパラダイム」，LENVIMA-Meet the Expert，平成30年11月30日，JRタワー名古屋，愛知。
44. 工藤正俊：特別講演「新たなステージに入った肝細胞癌治療－薬物療法のもたらす新たなパラダイム」，富山LENVIMA-HCC Expert 治療最前線 - 臨床へどう反映すべきか-，平成30年12月8日，富山大学附属病院，富山。
45. 工藤正俊：特別講演「急速に変貌する肝細胞癌の薬物療法」，LENVIMA-Meet the Expert 効能・効果追加記念講演会，平成30年12月10日，札幌プリンスホテル，北海道。
46. 松井繁長：特別講演「食堂静脈瘤の内視鏡治療：Up Date EIS，EVLから集学的治療まで」．第33回日本消化器内視鏡学会近畿セミナー，平成30年1月14日，大阪国際交流センター，大阪。
47. 松井繁長：特別講演「抗血栓薬服用時の内視鏡診療のマネジメントー消化器内科の立場から」．Next Lecture Meeting in 南河内，平成30年1月27日，すばるホール，大阪。
48. 萩原 智：特別講演「ウイルス性肝炎治療 up to date」．第5回住吉消化器ネットワークセミナー，平成30年3月10日，シェラトン都ホテル大阪，大阪。
49. 松井繁長：特別講演「抗血栓薬による消化管粘膜傷害について」．Daiichi-Sankyo Oral Anti Coagulant Web Seminar，平成30年3月22日，第一三共株式会社，大阪。
50. 高島耕太，松井繁長：症例提示「食道」．第457回大阪胃研究会，平成30年5月16日，エーザイ株式会社，大阪。
51. 松井繁長：特別講演「GERDの現状と今後の展望」．タケキャブ発売3周年記念Web Conference in Osaka，平成30年5月28日，大阪。
52. 松井繁長：特別講演「抗血栓薬による消化管粘膜傷害について」．OMMC循環器病診療連携の会 2018初夏，平成30年6月2日，すばるホール，大阪。
53. 松井繁長：特別講演「上部消化管がんのESD～これから始める先生方への手技の基本と述語管理～」．木曜サロン，平成30年7月26日，三重。
54. 松井繁長：特別講演「NSAIDs潰瘍やGERDに対する対策とPPIの課題」．第8回整形外科連携フォーラム，平成30年8月16日，ホテル・アゴーラリージェンシー堺，大阪。
55. 松井繁長：特別講演「酸関連疾患における現状と対策について」．消化器疾患Update，平成30年9月1日，LICはびきの，大阪。
56. 松井繁長：特別講演「H. pylori陰性時代の逆流性食道炎治療」．富田林医師会学術講演会，平成30年9月13日，富田林医師会，大阪。
57. 松井繁長：特別講演「早期胃癌の内視鏡診断～鑑別から診断、H. Pylori未感染胃がんまで～」．GI Rising Star Seminar，平成30年10月13日，アストラゼネカ株式会社大阪支店，大阪。
58. 松井繁長：特別講演「H. pylori陰性時代のGERD診療」．羽曳野市医師会学術講演会，平成30年10

月25日, LICはびきの, 大阪.

59. 松井繁長: 特別講演「H. pylori陰性時代のGERD診療」. 有田医師会学術講演会, 平成11月8日, 橋家, 和歌山.
60. 田中秀和, 松井繁長: 症例提示「十二指腸」. 第46回大阪胃研究会, 平成30年11月14日, エーザイ株式会社, 大阪.

V. 学会発表 (海外シンポジウム)

1. **Kudo M**: Special Remarks, International Session (Symposium) 2 “Hepatitis towards the control of HCC—the remaining issues and future directions in Japan and the world”. Japan Digestive Disease Week 2018 (JDDW 2018) (the 60th Annual Meeting of the Japanese Society of Gastroenterology, the 96th Congress of the Japan Gastroenterological Endoscopy Society, the 22nd General Meeting of the Japan Society of Hepatology), Kobe Convention Center, Hyogo, November 1-4, 2018.
2. Ueshima K: Second-line chemotherapy for HCC (exclude immunotherapy), Symposium 6 “Current status and future direction of systemic therapies for advanced HCC”. Asian Pacific Association for the Study of the Liver (APASL) Single Topic Conference, Yokohama, Japan, May 11-13, 2018.

VI. 学会発表・抄録 (米国及び国際学会)

1. **Kudo M**, Raoul JL, Lee HC, Cheng AL, Nakajima K, Peck-Radosavljevic M: Deterioration of liver function after transarterial chemoembolization (TACE) in hepatocellular carcinoma (HCC): An exploratory analysis of OPTIMIS—An international observational study assessing the use of sorafenib after TACE. Gastrointestinal Cancers Symposium (ASCO-GI 2018), San Francisco, USA, January 18-20, 2018.
2. **Kudo M**, Ueshima K, Ikeda M, Torimura T, Tanabe N, Aikata H, Izumi N, Yamasaki T, Nojiri S, Hino K, Tsumura H, Kuzuya T, Isoda N, Yasui K, Yoshimura K, Okusaka T, Furuse J, Kokudo N, Okita K, Arai Y, for the TACTICS Trial Group: Randomized, open label, multicenter, phase II trial comparing transarterial chemoembolization (TACE) plus sorafenib with TACE alone in patients with hepatocellular carcinoma (HCC): TACTICS trial. Gastrointestinal Cancers Symposium (ASCO-GI 2018), San Francisco, USA, January 18-20, 2018.
3. **Kudo M**, Ueshima K, Ikeda M, Torimura T, Tanabe N, Aikata H, Izumi N, Yamasaki T, Nojiri S, Hino K, Tsumura H, Kuzuya T, Isoda N, Yasui K, Yoshimura K, Okusaka T, Furuse J, Kokudo N, Okita K, Arai Y, for the TACTICS Trial Group: Randomized, open label, multicenter, phase II trial comparing transarterial chemoembolization (TACE) plus sorafenib with TACE alone in patients with hepatocellular carcinoma (HCC): TACTICS trial. Gastrointestinal Cancers Symposium (ASCO-GI 2018), San Francisco, USA, January 18-20, 2018.
4. El-Khoueiry AB, Merero I, Yau TC, Crocenzi TS, **Kudo M**, Hsu C, Choo S, Trojan J, Welling T, Meyer T, Kang YK, Yeo W, Chopra A, Zhao H, Baakili A, dela Cruz CM, Sangro B: Impact of antitumor activity on survival outcomes, and nonconventional benefit, with nivolumab (NIVO) in patients with advanced hepatocellular carcinoma (aHCC): Subanalyses of CheckMate-040. Gastrointestinal Cancers Symposium (ASCO-GI 2018), San Francisco, USA, January 18-20, 2018.
5. Zhu AX, Galle PR, **Kudo M**, Finn RS, Qin S, Xu Y, Abada P, Llovet J: Deterioration of liver function after transarterial chemoembolization (TACE) in hepatocellular carcinoma (HCC): A study of ramucirumab (LY3009806) versus placebo in patients with hepatocellular carcinoma and elevated baseline alpha-fetoprotein (REACH-2).

- Gastrointestinal Cancers Symposium (ASCO-GI 2018), San Francisco, USA, January 18-20, 2018.
6. Zhu AX, Finn RS, Cattan S, Edeline J, Ogasawara S, Palmer DH, Verslype C, Zagonel V, Rosmorduc O, Vogel A, Sarker D, Verset G, Chan SL, Knox JJ, Daniele B, Ebbinghaus S, Ma J, Siegel AB, Cheng AL, **Kudo M**: KEYNOTE-224: Pembrolizumab in patients with advanced hepatocellular carcinoma previously treated with sorafenib. Gastrointestinal Cancers Symposium (ASCO-GI 2018), San Francisco, USA, January 18-20, 2018.
 7. Zhu AX, Finn RS, Cattan S, Edeline J, Ogasawara S, Palmer DH, Verslype C, Zagonel V, Rosmorduc O, Vogel A, Sarker D, Verset G, Chan SL, Knox JJ, Daniele B, Ebbinghaus S, Ma J, Siegel AB, Cheng AL, **Kudo M**: KEYNOTE-224: Pembrolizumab in patients with advanced hepatocellular carcinoma previously treated with sorafenib. Gastrointestinal Cancers Symposium (ASCO-GI 2018), San Francisco, USA, January 18-20, 2018.
 8. Lencioni R, **Kudo M**, Finn RS, Qin S, Han KH, Ikeda K, Cheng AL, Piscaglia F, Han G, Ikeda M, Simon K, Komov D, OuYang X, Evans TRJ, Sung MW, Binder TA, Damon A, Kraljevic S, Ren M, Ryoo BY: Independent imaging review (IIR) results in a phase 3 trial of lenvatinib (LEN) versus sorafenib (SOR) in first-line treatment of patients (pts) with unresectable hepatocellular carcinoma (uHCC). Gastrointestinal Cancers Symposium (ASCO-GI 2018), San Francisco, USA, January 18-20, 2018.
 9. Bruix J, Merle P, Granito A, Huang YH, Bodoky G, Yokosuka O, Rosmorduc O, Breder VV, Gerolami R, Masi G, Ross PJ, Qin S, Song T, Bronowicki JP, Ollivier-Hourmand I, **Kudo M**, Xu L, Baumhauer A, Meinhardt G, Han G, on behalf of the RESORCE Investigators: Hand-foot skin reaction (HFSR) and overall survival (OS) in the phase 3 RESORCE trial of regorafenib for treatment of hepatocellular carcinoma (HCC) progressing on sorafenib. Gastrointestinal Cancers Symposium (ASCO-GI 2018), San Francisco, USA, January 18-20, 2018.
 10. Bruix J, Merle P, Granito A, Huang Y-H, Bodoky G, Yokosuka O, Rosmorduc O, Breder V, Gerolami R, Masi G, Paul JR, Qin S, Song T, Bronowicki J-P, Ollivier-Hourmand I, **Kudo M**, LeBerre M, Baumhauer A, Meinhardt G, Han G on behalf of the Resorce Investigators: Updated overall survival (OS) analysis from the international, phase 3, randomized, placebo-controlled RESORCE trial of regorafenib for patients with hepatocellular carcinoma (HCC) who progressed on sorafenib treatment. SIR 2018 congress in Los Angeles, CA, USA, March 17-22, 2018.
 11. Komeda Y, Kashida H, **Kudo M**: Appropriate intervals to detect local recurrence after endoscopic treatment of colorectal neoplasms. The 9th Asian Pacific Topic Conference (APTC) Poster Session, The 104th General Meeting of the Japanese Society of Gastroenterology, April 19-21, 2018, Keio Plaza Hotel, Tokyo.
 12. Kono M, Nishida N, **Kudo M**: Studies on AFP, ALT abnormalities and hepatocarcinogenesis after SVR in chronic hepatitis C patients treated with direct acting antivirals. Asian Pacific Association for the Study of the Liver (APASL) Single Topic Conference, Yokohama, Japan, May 11-13, 2018.
 13. Ogawa C, Morita M, Shibatoge M, Takaguchi K, Tani J, Masaki T, Moriya A, Deguchi A, **Kudo M**: Hand-foot syndrome as predictor of survival in advanced HCC treated with sorafenib. Asian Pacific Association for the Study of the Liver (APASL) Single Topic Conference, Yokohama, Japan, May 11-13, 2018.
 14. **Kudo M**, Zhu AX, Finn RS, Cattan S, Edeline J, Palmer D, Verslype C, Zagonel V, Fartoux L, Vogel A, Sarker D, Verset G, Chan S, Knox J, Daniele B: Keynote-224: Pembrolizumab in patients with advanced HCC previously treated with sorafenib. Asian Pacific Association for the Study of the Liver (APASL) Single Topic Conference, Yokohama, Japan, May 11-13, 2018.

15. Ogawa C, Morita M, Shibatoge M, **Kudo M**: Expansion of color fusion outside the liver. The 13th Congress of the Asian Federation of Societies for Ultrasound in Medicine and Biology (AFSUMB 2018), Seoul, Korea, May 23–26, 2018.
16. Zhu AX, Finn RS, Edeline J, Cattan S, Ogasawara S, Palmer D, Verslype C, Zagonel V, Fartoux L, Vogel A, Sarker D, Verset G, Chan S, Knox J, Daniele B, Ebbinghaus S, Ma J, Siegel AB, Cheng AL, **Kudo M**: Pembrolizumab (pembro) in patients with advanced hepatocellular carcinoma (HCC): KEYNOTE-224 update. American Society of Clinical Oncology Annual Meeting (ASCO 2018), Chicago, USA, June 2–6, 2018.
17. Qin S, Finn RS, **Kudo M**, Meyer T, Vogel A, Ducreux M, Mercade TM, Tomasello G, Boisserie F, Hou J, Li C, Song J, Zhu AX: A phase 3, randomized, open-label, multicenter study to compare the efficacy and safety of tislelizumab, an anti-PD-1 antibody, versus sorafenib as first-line treatment in patients with advanced hepatocellular carcinoma. American Society of Clinical Oncology Annual Meeting (ASCO 2018), Chicago, USA, June 2–6, 2018.
18. Zhu AX, Kang YK, Yen CJ, Finn RS, Galle PR, Llovet JM, Assenat E, Brandi G, Lim HY, Pracht M, Rau KM, Merle P, Motomura K, Ohno I, Daniele B, Shin D, Gerken G, Abada P, Hsu Y, **Kudo M**: REACH-2: A randomized, double-blind, placebo-controlled phase 3 study of ramucirumab versus placebo as second-line treatment in patients with advanced hepatocellular carcinoma (HCC) and elevated baseline alpha-fetoprotein (AFP) following first-line sorafenib. American Society of Clinical Oncology Annual Meeting (ASCO 2018), Chicago, USA, June 2–6, 2018.
19. Ikeda M, Sung MW, **Kudo M**, Kobayashi M, Baron AD, Finn RS, Kaneko S, Zhu AX, Kubota T, Kraljevic S, Ishikawa K, Siegel AB, Kumada H, Okusaka T: A phase 1b trial of lenvatinib (LEN) plus pembrolizumab (PEM) in patients (pts) with unresectable hepatocellular carcinoma (uHCC). American Society of Clinical Oncology Annual Meeting (ASCO 2018), Chicago, USA, June 2–6, 2018.
20. Peck-Radosavljevic M, **Kudo M**, Raoul JL, Lee HC, Decaens T, Heo J, Lin SM, Shan H, Yang Y, Bayh I, Nakajima K, Cheng AL: Outcomes of patients (pts) with hepatocellular carcinoma (HCC) treated with transarterial chemoembolization (TACE): Global OPTIMIS final analysis. American Society of Clinical Oncology Annual Meeting (ASCO 2018), Chicago, USA, June 2–6, 2018.
21. **Kudo M**, Ueshima K, Torimura T, Tanabe N, Ikeda M, Aikata H, Izumi N, Yamasaki T, Nojiri S, Hino K, Tsumura H, Isoda N, Yasui K, Kuzuya T, Okusaka T, Furuse J, Kokudo N, Okita K, Yoshimura K, Arai Y, TACTICS Trial Group: Randomized, open label, multicenter, phase II trial of transcatheter arterial chemoembolization (TACE) therapy in combination with sorafenib as compared with TACE alone in patients with hepatocellular carcinoma: TACTICS trial. American Society of Clinical Oncology Annual Meeting (ASCO 2018), Chicago, USA, June 2–6, 2018.
22. Minaga K, Kitano M, Ogura, T, Shiomi H, Hoki N, Nishikiori H, Yamashita Y, Hisa Takeshi, Kato H, Kamada H, Takenaka, M, Higuchi, K, Chiba Y, **Kudo M**: Similar efficacy and safety of endoscopic ultrasound-guided biliary drainage via hepaticogastrostomy and choledochoduodenostomy approaches for malignant distal obstruction: a multicenter, prospective randomized trial. Topic Forum “Exploring Newer Indications for EUS”, Digestive Disease Week (DDW 2018), Washington DC, USA, June 2–5, 2018.
23. **Kudo M**: Practice patterns and deterioration of liver function after transarterial chemoembolization (TACE): final analysis of OPTIMIS in Asian regions. The 9th Asia-Pacific Primary Liver Cancer Expert Meeting (APPLE), Grand Hyatt Seoul, South Korea, July 6–8, 2018.
24. Lim HY, Finn RS, Frenette C, Granito A, Ikeda M, Merle P, Ozgurdal K, **Kudo M**: Safety and Effectiveness of Regorafenib in Patients with Unresectable Hepatocellular Carcinoma

- in Routine Clinical Practice: REFINE, a Prospective, Observational Study. The 9th Asia-Pacific Primary Liver Cancer Expert Meeting (APPLE), Grand Hyatt Seoul, South Korea, July 6-8, 2018.
25. Qin S, Finn RS, **Kudo M**, Meyer T, Vogel A, Ducreux M, Macarulla TM, Tomasello G, Boisserie F, Hou J, Li C, Song J, Zhu AX: Efficacy and safety of Tislelizumab, an anti-PD-1 antibody, versus sorafenib as a potential first-line treatment in patients with advanced hepatocellular carcinoma in a phase 3, randomized, multicenter study: A Trial-in-Progress. 12th Annual Conference International Liver Cancer Association (ILCA), London, United Kingdom, September 14-16, 2018.
 26. Galle PR, **Kudo M**, Kang YK, Yen CJ, Finn R, Llovet JM, Assenat E, Brandi G, Lim HY, Pracht M, Rau KM, Merle P, Motomura K, Ohno I, Daniele B, Shin DB, Gerken G, Abada P, Hsu Y, Zhu AX: Ramucirumab versus placebo as second-line treatment in patients with advanced hepatocellular carcinoma and elevated baseline alpha-fetoprotein following first-line sorafenib (REACH-2): a phase 3, randomized, double-blind, placebo-controlled trial. 12th Annual Conference International Liver Cancer Association (ILCA), London, United Kingdom, September 14-16, 2018.
 27. Finn R, Frenette C, Granito A, Ikeda M, Lim HY, Merle P, Ozgurdal K, **Kudo M**: A prospective, observational study to assess the safety and effectiveness of regorafenib in patients with unresectable hepatocellular carcinoma (uHCC) in routine clinical practice (REFINE). 12th Annual Conference International Liver Cancer Association (ILCA), London, United Kingdom, September 14-16, 2018.
 28. Peck-Radosavljevic M, **Kudo M**, Raoul JL, Lee HC, Decaens T, Heo J, Lin SM, Shan H, Yang Y, Bayh I, Nakajima K, Cheng AL: Outcomes of patients (PTS) with hepatocellular carcinoma (HCC) treated with transarterial chemoembolization (TACE): Global optimistic final analysis. 12th Annual Conference International Liver Cancer Association (ILCA), London, United Kingdom, September 14-16, 2018.
 29. Ueshima K, **Kudo M**, Ikeda M, Torimura T, Tanabe N, Aikata H, Izumi N, Yamasaki T, Nojiri S, Hino K, Tsumura H, Kuzuya T, Isoda N, Yasui K, Yoshimura K, Okusaka T, Furuse J, Kokudo N, Okita K, Arai Y, and TACTICS study group: Randomized, open label, multicenter, phase II trial of transcatheter arterial chemoembolization (TACE) therapy in combination with sorafenib as compared with TACE alone in patients with hepatocellular carcinoma: TACTICS trial. 12th Annual Conference International Liver Cancer Association (ILCA), London, United Kingdom, September 14-16, 2018.
 30. **Kudo M**, Izumi N, Kaneko S, Kobayashi M, Azuma MK, Copher R, Meier G, Ishii M, Ikeda S: A cost-effectiveness analysis of Lenvatinib compared with sorafenib in unresectable hepatocellular carcinoma allowing for AFP adjustment in overall survival in Japan from the REFLECT phase 3 clinical trial. 12th Annual Conference International Liver Cancer Association (ILCA), London, United Kingdom, September 14-16, 2018.
 31. Bruix J, Merle P, Granito A, Huang YH, Bodoky G, Yokosuka O, Rosmorduc O, Breder V, Gerolami R, Masi G, Ross PJ, Qin S, Song T, Bronowicki JP, Ollivier-Houmand I, **Kudo M**, LeBerre MA, Baumhauer A, Meinhardt G, Han G and on behalf of the RESORCE Investigators: Overall survival (OS) update: 2-year follow-up from the phase 3 RESORCE trial of regorafenib for patients with hepatocellular carcinoma (HCC) progressing on sorafenib. 12th Annual Conference International Liver Cancer Association (ILCA), London, United Kingdom, September 14-16, 2018.
 32. Lencioni R, **Kudo M**, Finn RS, Qin S, Han KH, Ikeda K, Cheng AL, Piscaglia F, Han G, Ikeda M, Simon K, Komov D, OuYang X, Evans TR, Sung M, Binder T, Damon A, Kraljevic S, Ren M, Ryoo BY: Independent imaging review (IIR) results in a phase 3 trial of lenvatinib (LEN) vs sorafenib (SOR) in first-line treatment of patients (PTS) with unresectable

- hepatocellular carcinoma (UHCC). 12th Annual Conference International Liver Cancer Association (ILCA), London, United Kingdom, September 14–16, 2018.
33. Izumoto H, Hiraoka A, Kumada T, Hirooka M, Tsuji K, Itobayashi E, Kariyama K, Ishikawa T, Tajiri K, Ochi H, Tada T, Toyoda H, Nouse K, Joko K, Hiasa Y, Ninomiya T, Michitaka K, **Kudo M**: Newly proposed tools for assessment of hepatic function for hepatocellular carcinoma staging and treatment planning—usefulness of modified ALBI grade. 12th Annual Conference International Liver Cancer Association (ILCA), London, United Kingdom, September 14–16, 2018.
 34. Cheng AL, Raoul JL, Lee HC, Bayh I, Nakajima K, Peck-Radosavljevic M, **Kudo M**: Acute and chronic deterioration in liver function after transarterial chemoembolization (TACE) in patients with hepatocellular carcinoma (HCC): the final analysis of OPTIMIS. 12th Annual Conference International Liver Cancer Association (ILCA), London, United Kingdom, September 14–16, 2018.
 35. Evans TR, **Kudo M**, Finn RS, Han KH, Cheng AL, Kraljevic S, Ren M, Dutcus CE, Piscaglia F, Sung MW: Urine protein: creatinine ratio (UPCR) vs 24-h urine protein for the management of proteinuria: results from a phase 3 study of lenvatinib (LEN) vs sorafenib (SOR) in hepatocellular carcinoma (HCC). 12th Annual Conference International Liver Cancer Association (ILCA), London, United Kingdom, September 14–16, 2018.
 36. Ogawa C, Shibato M, Takaguchi K, Tani J, Morishita A, Yoneyama H, Masaki T, Moriya A, Ando M, Deguchi A, **Kudo M**: Hand-foot syndrome as a predictor of survival in advanced hepatocellular carcinoma treated with sorafenib: a multicenter study. 12th Annual Conference International Liver Cancer Association (ILCA), London, United Kingdom, September 14–16, 2018.
 37. Silva M, Carrilho FJ, Merle P, Granito A, Huang YH, Bodoky G, Yokosuka O, Rosmorduc O, Breder V, Gerolami R, Masi G, Ross PJ, Qin S, Song T, Bronowicki JP, Ollivier-Hourmand I, **Kudo M**, Xu L, Baumhauer A, Meinhardt G, Han G, Bruix J, on behalf of the RESORCE Investigators: Hand-foot skin reaction (HFSR) and overall survival (OS) in the phase 3 RESORCE trial of regorafenib for treatment of hepatocellular carcinoma (HCC) progressing on sorafenib. ALEH 2018, International Convention Center, Punta Cana, Dominican Republic, September 20–23, 2018.
 38. Ladron de Guevara L, Dagher L, Miguel Viana Arruda V, Nakajima K, **Kudo M**: Practice patterns in the treatment of unresectable hepatocellular carcinoma with sorafenib in Latin America according to Child-Pugh score: Subgroup analysis of the GIDEON study. ALEH 2018, International Convention Center, Punta Cana, Dominican Republic, September 20–23, 2018.
 39. Sakurai T, **Kudo M**: Stress response protein RBM3 promotes the development of colitis-associated cancer. The 77th Annual Meeting of the Japanese Cancer Association, Osaka International Convention Center, Osaka, September 27–29, 2018.
 40. Finn RS, **Kudo M**, Cheng AL, Wyrwicz L, Ngan R, Blanc JF, Baron A, Vogel A, Ikeda M, Piscaglia F, Han KH, Qin S, Minoshima Y, Kanekiyo M, Ren M, Dairiki R, Tamai T, Dutcus C, Funahashi Y, Evans TRJ: Final analysis of serum biomarkers in patients (pts) from the phase 3 study of lenvatinib (LEN) vs sorafenib (SOR) in unresectable hepatocellular carcinoma (uHCC) [REFLECT]. European Society for Medical Oncology (ESMO 2018), Munich, Germany, October 19–23, 2018.
 41. Cheng AL, Yen CJ, Okusaka T, Ikeda M, Hsu CH, Wu SY, Morizane C, Hashimoto Y, Ueshima K, Ohtomo T, Tanaka T, **Kudo M**: A phase I, open-label, multi-center, dose-escalation study of codrituzumab, an anti-glypican-3 monoclonal antibody, in combination with atezolizumab in patients with locally advanced or metastatic hepatocellular carcinoma. European Society for Medical Oncology (ESMO 2018), Munich, Germany, October 19–23,

- 2018.
42. Raoul JL, Decaens T, Burak K, Koskinas J, Villadsen GE, Heurgue-Berlot A, Bayh I, Cheng AL, Kudo M, Lee HC, Nakajima K, Peck-Radosavljevic M: Practice patterns and deterioration of liver function after transarterial chemoembolization (TACE) in hepatocellular carcinoma (HCC): Final analysis of OPTIMIS in Europe and Canada. European Society for Medical Oncology (ESMO 2018), Munich, Germany, October 19-23, 2018.
 43. Qin S, Finn R, Kudo M, Meyer T, Vogel A, Ducreux M, Macarulla T, Tomasello G, Boisserie F, Hou J, Li C, Song J, Zhu A: Global phase 3 study of tislelizumab versus sorafenib as first-line treatment in patients with advanced hepatocellular carcinoma (HCC): A trial-in-progress. European Society for Medical Oncology (ESMO 2018), Munich, Germany, October 19-23, 2018.
 44. Zhu AX, Finn R, Galle P, Llovet JM, Blanc JF, Okusaka T, Chau I, Cella D, Girvan A, Gable J, Bowman L, Hsu Y, Abada P, Kudo M: Ramucirumab as second-line treatment in patients with advanced hepatocellular carcinoma (HCC) and elevated alpha-fetoprotein (AFP) following first-line sorafenib: patient reported outcome results across two phase 3 studies (REACH-2 and REACH). European Society for Medical Oncology (ESMO 2018), Munich, Germany, October 19-23, 2018.
 45. Yoo C, Oh DY, Choi HJ, Kudo M, Ueno M, Kondo S, Chen LT, Osada M, Helwig C, Dussault I, Ikeda M: M7824 (MSB0011359C), a bifunctional fusion protein targeting PD-L1 and TGF- β , in Asian patients with pretreated biliary tract cancer: Preliminary results from a phase I trial. European Society for Medical Oncology (ESMO 2018), Munich, Germany, October 19-23, 2018.
 46. Zhu A, Finn R, Galle P, Llovet J, Nipp R, Cella D, Girvan A, Gable J, Bowman L, Abada P, Hsu Y, Kudo M: Ramucirumab as second-line treatment in patients with advanced hepatocellular carcinoma (HCC) and elevated baseline alpha-fetoprotein (AFP) following first-line sorafenib (REACH-2): efficacy, safety, and patient-reported outcome results. Gastrointestinal Oncology Conference 2018 (ISGIO), Arlington, VA, USA, November 1-2, 2018.
 47. Ladron de Guevara L, Dagher L, Miguel Viana Arruda V, Nakajima K, Kudo M: Practice patterns in the treatment of unresectable hepatocellular carcinoma with sorafenib in Latin America according to Child-Pugh score: Subgroup analysis of the GIDEON study. Mexican Society of Oncology 36th National Congress 2018 (SMEO 2018), Guardalajara, Mexico, November 7-10, 2018.
 48. Llovet JM, Kudo M, Finn R, Galle PR, Blanc JF, Okusaka T, Chau I, Abada PB, Hsu Y, Zhu AX: Ramucirumab as second-line treatment in patients with hepatocellular carcinoma (HCC) and elevated alpha-fetoprotein (AFP) following sorafenib: pooled results from two global phase 3 studies (REACH-2 and REACH). American Association for the study of liver diseases (AASLD 2018), San Francisco, USA, November 9-13, 2018.
 49. Peck-Radosavljevic, Kudo M, Raoul JL, Lee HC, Decaens T, Heo J, Lin SM, Shan H, Yang Y, Bayh I, Nakajima K, Cheng AL: Outcomes of patients (pts) with hepatocellular carcinoma (HCC) treated with transarterial chemoembolization (TACE): Global OPTIMIS final analysis. American Association for the study of liver diseases (AASLD 2018), San Francisco, USA, November 9-13, 2018.
 50. Hiraoka A, Kumada T, Tsuji K, Takaguchi K, Itobayashi E, Kariyama K, Ochi H, Tajiri K, Hirooka M, Shimada N, Ishikawa T, Tachi Y, Tada T, Toyoda H, Nouse K, Joko K, Hiasa Y, Michitaka K, Kudo M: Validation of modified ALBI grade for more detailed assessment of hepatic function in hepatocellular carcinoma patients: multicenter analysis. American Association for the study of liver diseases (AASLD 2018), San Francisco, USA, November

- 9-13, 2018.
51. Nishida N, Kudo M: Stem cell feature and immune-suppressive microenvironment in human hepatocellular carcinoma. American Association for the study of liver diseases (AASLD 2018), San Francisco, USA, November 9-13, 2018.
 52. Koizumi Y, Hirooka M, Yada N, Tamaki N, Izumi N, Kudo M, Hiasa Y: New diagnostic method for hepatic steatosis using attenuation measurement by ultrasound B mode: comparison with controlled attenuation parameter. American Association for the study of liver diseases (AASLD 2018), San Francisco, USA, November 9-13, 2018.
 53. Kudo M, Matilla A, Santoro A, Melero I, Gracian AC, Acosta MR, Choo SP, El-Khoueiry AB, Kuromatsu R, El-Rayes B, Numata K, Itoh Y, Di Costanzo F, Crysler O, Reig M, Shen Y, Neely J, dela Cruz C, Baccan C, Sangro B: Nivolumab in patients with Child-Pugh B advanced hepatocellular carcinoma (aHCC) in the CheckMate-040 study. American Association for the study of liver diseases (AASLD 2018), San Francisco, USA, November 9-13, 2018.
 54. Minaga K, Yamashita Y, Ogura T, Takenaka M, Shimokawa Y, Hisa T, Itonaga M, Kato H, Nishikiori H, Okuda A, Matsumoto H, Uenoyama Y, Watanabe T, Chiba Y, Higuchi K, Kudo M, Kitano M: Clinical efficacy and safety of EUS-guided gallbladder drainage replacement of percutaneous drainage: A multicenter retrospective study in Japan. Asian Pacific Digestive Week (APDW 2018), Seoul, Korea, November 15-18, 2018.
 55. Heo J, Cheng AL, Raoul JL, Peck-Radosavljevic M, Kudo M, Nakajima K, Bayh I, Lin SM, Lee HC: Practice patterns, radiologic tumor response, and deterioration of liver function after transarterial chemoembolization (TACE): Final analysis of OPTIMIS in Korea and other regions. European Society for Medical Oncology Congress (ESMO-Asia 2018), Singapore, November 23-25, 2018.
 56. Yoo C, Oh DY, Choi HJ, Kudo M, Ueno M, Kondo S, Chen LT, Osada M, Helwig C, Dussault I, Ikeda M: M7824 (MSB0011359C), a bifunctional fusion protein targeting transforming growth factor β (TGF- β) and PD-L1, in Asian patients with pretreated biliary tract cancer (BTC): Efficacy by BTC subtype. European Society for Medical Oncology Congress (ESMO-Asia 2018), Singapore, November 23-25, 2018.
 57. Kang YK, Kudo M, Lim HY, Hsu CH, Vogel A, Brandi G, Cheng R, Carton I, Abada P, Hsu Y, Zhu A, Yen CJ: Efficacy and safety of ramucirumab (RAM) in Asian and non-Asian patients with advanced hepatocellular carcinoma (HCC) and elevated alpha-fetoprotein (AFP): Subgroup analysis from two randomized studies. European Society for Medical Oncology Congress (ESMO-Asia 2018), Singapore,
 58. Kashida H: Detailed diagnosis of early colorectal cancer. The 9th Asian Pacific Topic Conference(APTC) 3” Diagnosis(endoscopy, screening, CT colonography, capsule endoscopy)”, 第104回日本消化器病学会総会, 平成30年4月19-21日, 京王プラザホテル, 東京.
 59. Ueshima K: Second-line chemotherapy for HCC (exclude immunotherapy), Symposium 6 “Current status and future direction of systemic therapies for advanced HCC”. Asian Pacific Association for the Study of the Liver (APASL) Single Topic Conference, Yokohama, Japan, May 11-13, 2018.
 60. Kamata K: Characterization of subepithelial tumors and lymph nodes. The 13th Congress of the Asian Federation of Societies for Ultrasound in Medicine and Biology (AFSUMB 2018), Seoul, Korea, May 23-26, 2018.
 61. Ogura T, Kitano M, Takenaka M, Minaga K, Yamao K, Yamashita Y, Hatamaru K, Noguchi C, Kuroda T, Nishikiori H, Higuchi K, Chiba Y: A multicenter prospective study of EUS-guided hepaticogastrostomy combined with antegrade stent placement. Topic Forum “Exploring Newer Indications for EUS”, Digestive Disease Week (DDW 2018), Washington DC, USA, June 2-5, 2018.

62. Ueshima K: Randomized, open label, multicenter, phase II trial of transcatheter arterial chemoembolization (TACE) therapy in combination with sorafenib as compared with TACE alone in patients with hepatocellular carcinoma: TACTICS trial. The 9th Asia-Pacific Primary Liver Cancer Expert Meeting (APPLE), Grand Hyatt Seoul, South Korea, July 6-8, 2018.
63. Minaga K, Ogura T, Kitano M: Similar efficacy and safety of EUS-guided biliary drainage via hepaticogastrostomy and choledochoduodenostomy approaches for malignant distal biliary stenosis: a multicenter prospective randomized trial. International Session (Workshop) 2 “The current state and problem of endoscopic treatments for the malignant biliary stenosis”, 第26回日本消化器関連学会週間JDDW 2018 (第22回日本肝臓学会大会, 第96回日本消化器内視鏡学会総会, 第60回日本消化器病学会大会), 平成30年11月1-4日, 神戸コンベンションセンター, 兵庫.

VII. 学会発表 (国内シンポジウム・パネルディスカッション・ワークショップ)

1. 山雄健太郎, 竹中 完, 工藤正俊, 竹山宜典: mFOLFIRINOX療法に対するPegfilgrastim 2次予防療法の安全性・有効性の検討. ワークショップ3「外科手術、化学療法を含めた膵癌治療の最前線」, 日本消化器病学会近畿支部第108回例会, 平成30年3月17日, 京都テルサ, 京都.
2. 福永朋洋, 岡元寿樹, 櫻井俊治, 半田康平, 高田隆太郎, 木下 淳, 石川 嶺, 河野匡志, 山田光成, 永井知行, 米田頼晃, 松井繁長, 渡邊智裕, 汐見幹夫, 檜田博史, 工藤正俊: セツキシマブを含む抗がん剤にて肺胞出血を来した一例. Young Investigator Session 6 大腸(1), 日本消化器病学会近畿支部第108回例会, 平成30年3月17日, 京都テルサ, 京都.
3. 河野匡志, 櫻井俊治, 工藤正俊, 檜田博史: ステロイド抵抗性潰瘍性大腸炎に対するシクロスポリンの使用経験. シンポジウム1「生物学的製剤時代におけるIBD治療の現状と課題」, 日本消化器病学会近畿支部第108回例会, 平成30年3月17日, 京都テルサ, 京都.
4. 伊藤智彦, 奥田英之, 秦 康倫, 木下大輔, 高山政樹, 川崎正憲, 岡崎能久, 川崎俊彦, 水野成人, 朝戸信行, 工藤正俊: TACE治療時にEmboGuideが有用であった肝細胞癌の1例. Freshman Session 1 肝臓(1), 日本消化器病学会近畿支部第108回例会, 平成30年3月17日, 京都テルサ, 京都.
5. 藤井佳奈子, 岡本彩名, 半田康平, 高田隆太郎, 福永朋洋, 南 知宏, 河野匡志, 千品寛和, 有住忠晃, 田北雅弘, 南 康範, 依田 広, 上嶋一臣, 西田直生志, 工藤正俊: 動注リザーバーシステム留置時に腫瘍の広範な壊死を呈した進行肝細胞癌の一例. Freshman Session 1 肝臓(1), 日本消化器病学会近畿支部第108回例会, 平成30年3月17日, 京都テルサ, 京都.
6. 大塚康生, 永井知行, 櫻井俊治, 福永明洋, 半田康平, 高田隆太郎, 岡元寿樹, 木下淳, 河野匡志, 山田光成, 米田頼晃, 松井繁長, 渡邊智裕, 汐見幹夫, 檜田博史, 工藤正俊: mFOLFOX6+Cetuximab併用療法により画的にComplete Responseが得られた切除不能肝転移を伴うS状結腸癌の1例. Freshman Session 4 大腸, 日本消化器病学会近畿支部第108回例会, 平成30年3月17日, 京都テルサ, 京都.
7. 吉田早希, 三長孝輔, 竹中 完, 石川 嶺, 岡本彩那, 中井敦史, 大本俊介, 宮田 剛, 鎌田 研, 山雄健太郎, 今井 元, 工藤正俊, 井上宏昭, 松村 到, 清水重喜, 佐藤隆夫: 興味深いEUS像を呈した膵多発Myeloif Sarcomaの1例. Freshman Session 11 膵臓, 日本消化器病学会近畿支部第108回例会, 平成30年3月17日, 京都テルサ, 京都.
8. 中井敦史, 大本俊介, 三長孝輔, 宮田 剛, 鎌田 研, 山雄健太郎, 今井 元, 竹中 完, 工藤正俊: リンパ節転移診断における造影ハーモニックEUS(CH-EUS)の有用性. 主題演題2「肝臓以外の領域」, 第31回日本腹部造影エコー・ドプラ診断研究会, 平成30年3月31日, ホテルアバローム 紀の国, 和歌山.
9. 平岡 淳, 熊田 卓, 工藤正俊: 肝癌診療における新しい肝予備能評価法ALBI-gradeの有用性と可能性: nationwide survey. シンポジウム6「肝癌診療up to date」, 第104回日本消化器病学会総会, 平成30年4月19-21日, 京王プラザホテル, 東京.
10. 三長孝輔, 竹中 完, 工藤正俊: 膵癌に伴う疼痛に対するEUSガイド下神経ブロックの有用性. シ

- ンポジウム11「超音波内視鏡ガイド下治療の現状と問題点」，第104回日本消化器病学会総会，平成30年4月19-21日，京王プラザホテル，東京。
11. 中井敦史，宮田 剛，工藤正俊：膵胆道腫瘍のリンパ節転移診断における造影ハーモニックEUSの有用性. プレナリーセッション「膵」，第104回日本消化器病学会総会，平成30年4月19-21日，京王プラザホテル，東京。
 12. 三長孝輔，竹中 完，鎌田 研，山雄健太郎，工藤正俊：経乳頭的re-intervention困難例の悪性肝門部胆道閉塞に対するEUS下胆道ドレナージの有用性. シンポジウム 1「アンメットメディカルニーズに対する内視鏡の役割-胆膵疾患の診断・治療-」，第100回日本消化器内視鏡学会近畿支部例会，平成30年5月26日，大阪国際交流センター，大阪。
 13. 米田頼晃，榎田博史，櫻井俊治，工藤正俊，奥野清隆：早期直腸癌に対する治療法の選択. パネルディスカッション「アンメットメディカルニーズに対する内視鏡の役割-下部消化管疾患の診断・治療-」，第100回日本消化器内視鏡学会近畿支部例会，平成30年5月26日，大阪国際交流センター，大阪。
 14. 大本俊介，竹中 完，工藤正俊：Chasing methodを用いた安全なEUSスクリーニングの標準化、教育の取り組み. ビデオワークショップ「胆膵内視鏡診療におけるdo and don't」，第100回日本消化器内視鏡学会近畿支部例会，平成30年5月26日，大阪国際交流センター，大阪。
 15. 辻本智之，秦 康倫，木下大輔，高山政樹，奥田英之，川崎俊彦，水野成人，工藤正俊：迷入膵が原因と思われる胃壁内膿瘍の1例. Fresh Endoscopist Session 1 胃，第100回日本消化器内視鏡学会近畿支部例会，平成30年5月26日，大阪国際交流センター，大阪。
 16. 東原久美，三長孝輔，岡本彩那，竹中 完，石川 嶺，中井敦史，大本俊介，鎌田 研，山雄健太郎，工藤正俊，榎木英介：閉塞性黄疸が診断の契機となった低分化型食道胃接合部癌の1例. Fresh Endoscopist Session 2 食道・十二指腸，第100回日本消化器内視鏡学会近畿支部例会，平成30年5月26日，大阪国際交流センター，大阪。
 17. 益田康弘，松井繁長，河野匡志，岡元寿樹，山田光成，米田頼晃，永井知行，櫻井俊治，渡邊智裕，榎田博史，工藤正俊：タビガトランによる薬剤性食道潰瘍の検討. Young Endoscopist Session 3 食道，第100回日本消化器内視鏡学会近畿支部例会，平成30年5月26日，大阪国際交流センター，大阪。
 18. 玉城信治，泉 並木，小泉洋平，廣岡昌史，日浅陽一，中島 収，矢田典久，工藤正俊：超音波エラストグラフィ併用による肝線維化・炎症評価. シンポジウム消化器5「肝臓 エラストグラフィは何を見ている？」，日本超音波医学会第91回学術集会，平成30年6月8-10日，神戸国際会議場，神戸ポートピアホテル，兵庫。
 19. 盛田真弘，小川 力，大村亜紀奈，野田晃世，久保敦司，松中寿浩，玉置敬之，柴峠光成，大西宏明，工藤正俊：肝膿瘍治療指針におけるソナゾイド造影の有用性. シンポジウム消化器6「肝臓 診断 肝膿瘍の悪性度診断～Bモード・エラスト・Sonazoid造影～」，日本超音波医学会第91回学術集会，平成30年6月8-10日，神戸国際会議場，神戸ポートピアホテル，兵庫。
 20. 小川 力，盛田真弘，野田晃世，大村亜紀奈，久保敦司，石川哲朗，松中寿浩，玉置敬之，柴峠光成，工藤正俊：新しい造影法導入後の問題点. シンポジウム消化器7「肝臓 診断 肝腫瘍の診療ガイドラインを考える」，日本超音波医学会第91回学術集会，平成30年6月8-10日，神戸国際会議場，神戸ポートピアホテル，兵庫。
 21. 南 康範，河野匡志，工藤正俊：肝膿瘍の視認性に関する低音圧造影tissue harmonic imagingの有用性. シンポジウム消化器7「肝臓 診断 肝腫瘍の診療ガイドラインを考える」，日本超音波医学会第91回学術集会，平成30年6月8-10日，神戸国際会議場，神戸ポートピアホテル，兵庫。
 22. 南 康範，南 知宏，千品寛和，田北雅弘，萩原 智，依田 広，上嶋一臣，西田直生志，工藤正俊：US-US image overlay fusionを用いたラジオ波焼灼術の有用性：従来治療との比較. パネルディスカッション消化器3「肝臓 治療 安全かつ確実なRFA治療を目指した超音波技術の工夫」，日本超音波医学会第91回学術集会，平成30年6月8-10日，神戸国際会議場，神戸ポートピアホテル，兵庫。
 23. 西田直生志，海道利実，工藤正俊：遺伝子変化に基づいた肝細胞癌の分子スコアリングと転移再発，シンポジウム1「肝癌治療の新展開」，第54回日本肝臓学会総会，平成30年6月14日，大阪国

際会議場，大阪。

24. 南 知宏，村上卓道，工藤正俊：RFA治療の効果判定：Hepatic Guideの有用性，パネルディスカッション5「画像診断の新展開」，第54回日本肝臓学会総会，平成30年6月15日，大阪国際会議場，大阪。
25. 上嶋一臣，池田公史，工藤正俊：切除不能肝細胞癌に対する肝動脈化学塞栓療法（TACE）とソラフェニブの併用療法第II相臨床試験TACTICS Trial，シンポジウム1「肝臓治療の新展開」，第54回日本肝臓学会総会，平成30年6月14日，大阪国際会議場，大阪。
26. 河野匡志，西田直生志，工藤正俊：慢性C型肝炎のDAA投与例におけるSVR後のAFP、ALT異常及び肝発癌に関する検討，ワークショップ11「肝炎ウイルスの制御が肝臓診療に及ぼす影響」，第54回日本肝臓学会総会，平成30年6月15日，大阪国際会議場，大阪。
27. 南 康範，工藤正俊：ラジオ波焼灼術の早期治療効果判定：US-US image overlay fusionの有用性。ワークショップ5-10「医用工学の肝臓治療への応用」，第54回日本肝臓学会，平成30年6月28日，久留米シティプラザ，福岡。
28. 小川 力，盛田真弘，大村亜紀奈，久保敦司，松中寿浩，玉置敬之，柴峠光成，工藤正俊：汎用型Workstationを用いたHCCの診断、治療の試み。ワークショップ5-13「医用工学の肝臓治療への応用」，第54回日本肝臓学会，平成30年6月28日，久留米シティプラザ，福岡。
29. 上嶋一臣，池田公史，工藤正俊：切除不能肝細胞癌に対する肝動脈化学塞栓療法とソラフェニブの併用療法第2相臨床試験（TACTICS）。シンポジウム1-3「肝臓における分子標的薬の新たな治療展開」，第54回日本肝臓学会，平成30年6月28日，久留米シティプラザ，福岡。
30. 工藤正俊，中島圭子：TACE施行後のソラフェニブ投与の有無ならびに開始時期が予後へ与える影響を検討した国際共同観察研究，シンポジウム1「肝臓における分子標的薬の新たな治療展開」，第54回日本肝臓学会，平成30年6月28日，久留米シティプラザ，福岡。
31. 盛田真弘，小川 力，大村亜紀奈，久保敦司，松中寿浩，玉置敬之，柴峠光成，工藤正俊：汎用型Workstationを用いたTACE治療とその問題点，ワークショップ3「TACE治療の新たな進歩」，第54回日本肝臓学会，平成30年6月28日，久留米シティプラザ，福岡。
32. 工藤正俊，角谷眞澄，村上卓道，糸井隆夫，海野倫明：肝内胆管癌：臨床診断，パネルディスカッション5「肝内胆管癌の診断と治療」，第54回日本肝臓学会，平成30年6月29日，久留米シティプラザ，福岡。
33. 平岡 淳，道堯浩二郎，熊田 卓，泉 並木，角谷眞澄，國土典宏，久保正二，松山 裕，中島 収，坂元亨宇，高山忠利，國土貴嗣，柏原康佑，工藤正俊：腫瘍マーカースコアによる肝予備能良好なBCLC-B肝細胞癌に対するTACE予後予測：肝臓学会データベース解析，ワークショップ6「診断技術（画像、腫瘍マーカー、ゲノム解析など）のイノベーション」，第54回日本肝臓学会，平成30年6月29日，久留米シティプラザ，福岡。
34. 海堀昌樹，吉井健悟，長谷川 潔，小川朝生，久保正二，建石良介，泉 並木，角谷眞澄，工藤正俊，熊田 卓，坂元亨宇，中島 収，松山 裕，高山忠利，國土典宏：肝臓学会追跡調査よりみた高齢肝細胞癌に対する至適治療法の検討，ワークショップ7「高齢化時代の肝臓診療」，第54回日本肝臓学会，平成30年6月29日，久留米シティプラザ，福岡。
35. 石川 嶺，鎌田 研，竹中 完，田中秀和，中井敦史，大本俊介，宮田 剛，三長孝輔，山雄健太郎，今井 元，工藤正俊：造影ハーモニックEUSによる膵神経内分泌腫瘍の悪性度評価。ワークショップ1「膵NETの最新の画像診断と治療」，第49回日本膵臓学会大会，平成30年6月29日，和歌山県民文化会館，ホテルアバローム紀の国，和歌山。
36. 平岡 淳，道堯浩二郎，熊田 卓，泉 並木，角谷眞澄，國土典宏，久保正二，松山 裕，中島 収，坂元亨宇，高山忠利，國土貴嗣，柏原康佑，江口 晋，山下達也，工藤正俊：肝予備能良好なBCLC-B肝細胞癌に対するTACE予後予測・腫瘍マーカースコアの有用性；肝臓学会データベース解析。プレナリーセッション1，第18回日本肝がん分子標的治療研究会，平成30年7月14日，東京大学伊藤国際学術研究センター，東京。
37. 西田直生志，工藤正俊：PD-L1陽性肝臓の特徴と腫瘍免疫環境に関する解析。プレナリーセッション2，第18回日本肝がん分子標的治療研究会，平成30年7月14日，東京大学伊藤国際学術研究センター，東京。

38. 南 康範, 依田 広, 工藤正俊: 肝癌に対するラジオ波焼灼術の支援画像: US-US overlay fusionの有用性. シンポジウム2「シミュレーションからナビゲーションへ 内科領域」, 第13回肝癌治療シミュレーション研究会, 平成30年9月29日, 京王プラザホテル, 東京.
39. 鶴崎正勝, 工藤正俊, 村上卓道: シミュレーションからナビゲーション: 放射線科領域での技術の到達点と今後の展望. シンポジウム3「シミュレーションからナビゲーションへ 放射線科領域」, 第13回肝癌治療シミュレーション研究会, 平成30年9月29日, 京王プラザホテル, 東京.
40. 萩原 智, 上嶋一臣, 工藤正俊: 進行肝細胞癌に対するレゴラフェニブの治療成績. パネルディスカッション「消化器癌治療の現状と未来」, 日本消化器病学会近畿支部第109回例会, 平成30年9月29日, 大阪国際交流センター, 大阪.
41. 南 康範, 依田 広, 工藤正俊: 肝癌に対するラジオ波焼灼術の支援画像: US-US overlay fusionの有用性. シンポジウム2「Interventional US」, 日本超音波医学会第45回関西地方会学術集会, 平成30年10月20日, 神戸国際会議場, 兵庫.
42. 相方 浩, 工藤正俊, 池田健次: Independent imaging review analysis of REFLECT trial of lenvatinib in HCC. ワークショップ5「生存期間延長を目指す分子機構に立脚した肝癌診療の基礎と臨床」, 第26回日本消化器関連学会週間JDDW 2018 (第22回日本肝臓学会大会, 第96回日本消化器内視鏡学会総会, 第60回日本消化器病学会大会), 平成30年11月1-4日, 神戸コンベンションセンター, 兵庫.
43. 竹中 完, 山雄健太郎, 工藤正俊: 良性胆道狭窄 (慢性膵炎) に対するfully covered metallic stentの有用性. ワークショップ14「Innovative therapeutic endoscopy良性胆管・膵管狭窄に対する内視鏡治療」, 第26回日本消化器関連学会週間JDDW 2018 (第22回日本肝臓学会大会, 第96回日本消化器内視鏡学会総会, 第60回日本消化器病学会大会), 平成30年11月1-4日, 神戸コンベンションセンター, 兵庫.
44. 鎌田 研, 渡邊智裕, 工藤正俊: 腸内細菌叢からみたIgG4関連疾患の発症機序の解明. ワークショップ21「胆膵領域におけるIgG4関連疾患の研究と診療の進歩」, 第26回日本消化器関連学会週刊JDDW 2018 (第60回日本消化器病学会大会, 第22回日本肝臓学会大会, 第96回日本消化器内視鏡学会総会), 平成30年11月1-4日, 神戸コンベンションセンター, 兵庫.
45. 大本俊介, 竹中 完, 工藤正俊: EUSガイド下膵管ドレナージのトラブルシューティングにおいて Re-puncture techniqueが有用であった一例. シンポジウム1「胆膵内視鏡治療の工夫」, 第101回日本消化器内視鏡学会近畿支部例会, 平成30年11月10日, 大阪国際交流センター, 大阪.
46. 吉川智恵, 三長孝輔, 竹中 完, 工藤正俊: 当院におけるソナゾイド造影下interventional EUSの検討. シンポジウム1「胆膵内視鏡治療の工夫」, 第101回日本消化器内視鏡学会近畿支部例会, 平成30年11月10日, 大阪国際交流センター, 大阪.
47. 大塚康生, 鎌田 研, 竹中 完, 工藤正俊: 肝外胆管癌のT-stagingにおける造影ハーモニックEUSと造影CT検査の有用性についての検討. パネルディスカッション2「膵胆道癌早期診断への内視鏡的アプローチ」, 第101回日本消化器内視鏡学会近畿支部例会, 平成30年11月10日, 大阪国際交流センター, 大阪.
48. 西田直生志: 人工知能の利活用を見据えた超音波デジタル画像のビッグデータベース構築基盤整備—AI支援型超音波診断システムの開発に向けて—, 特別シンポジウム「超音波デジタル画像のナショナルデータベース構築とAI診断開発」, 第30回関東甲信越地方会学術集会, 平成30年10月28日, 都市センターホテル, 東京.

VIII. 学会発表 (国内一般演題)

1. 岡本彩那, 樫田博史, 米田頼晃, 岡元寿樹, 河野匡志, 足立哲平, 永井知行, 朝隈 豊, 櫻井俊治, 松井繁長, 渡邊智裕, 工藤正俊: 腸管症型T細胞リンパ腫の一例. 一般演題 小腸, 第106回日本消化器病学会近畿支部例会, 平成29年2月25日, 大阪国際交流センター, 大阪.
2. 工藤正俊: 肝細胞癌診療と造影エコー法. ランチョンセミナー. 第31回日本腹部造影エコー・ドプラ診断研究会, 平成30年3月31日, ホテルアバローム紀の国, 和歌山
3. 工藤正俊: 肝癌診療の最前線. 教育講演17, 第115回日本内科学会総会・講演会, 平成30年4月

- 13-15日, 京都市観業館 (みやこめっせ) ロームシアター京都, 京都.
4. 工藤正俊: 肝細胞癌診療のブレークスルー: レンビマによる治療革新. LENVIMA-HCC Web Seminar 日本で生まれた新薬・レンビマの登場, 平成30年4月17日, 木村情報技術株式会社 第2スタジオ, 東京.
 5. 南 知宏, 南 康範, 工藤正俊, 鶴崎正勝, 村上桌道: RFA治療の効果判定: Hepatic Guideの有用性. 第24回肝血流動態・機能イメージ研究会. 平成30年2月3-4日, 都久志会館, 福岡.
 6. 盛田真弘, 小川 力, 大村亜紀奈, 野田晃世, 久保敦司, 松中寿浩, 玉置敬之, 柴峠光成, 小森淳二, 石川順英, 香月奈穂美, 荻野哲郎, 隈部 力, 中島 収, 工藤正俊: 診断に難渋した肝細胞腺腫の1例. 第24回肝血流動態・機能イメージ研究会, 平成30年2月3-4日, 都久志会館, 福岡.
 7. 吉田晃浩, 萩原 智, 南 知宏, 千品寛和, 河野匡志, 田北雅弘, 依田 広, 上嶋一臣, 南 康範, 西田直生志, 工藤正俊: C型肝炎に対する初回インターフェロンフリー治療不成功例の臨床的特徴. 一般演題「C型肝炎」, 第104回日本消化器病学会総会, 平成30年4月19-21日, 京王プラザホテル, 東京.
 8. 田中秀和, 萩原 智, 南 知宏, 千品寛和, 河野匡志, 田北雅弘, 南 康範, 依田 広, 上嶋一臣, 西田直生志, 工藤正俊: C型肝炎に対するダクラタスビル・アスナプレビル治療奏効後肝発癌についての臨床的特徴. 一般演題「C型肝炎5」, 第104回日本消化器病学会総会, 平成30年4月19-21日, 京王プラザホテル, 東京.
 9. 永井知行, 櫻井俊治, 工藤正俊, 西山拓輝, 岡崎義久, 東 慶直, 渡邊智裕, 五斗 進, 緒方博之: 一般演題ポスター「大腸基礎」, 第104回日本消化器病学会総会, 平成30年4月19-21日, 京王プラザホテル, 東京.
 10. 高島耕太, 大本俊介, 三長孝輔, 竹中 完, 中井敦史, 宮田 剛, 鎌田 研, 山雄健太郎, 今井 元, 米田頼晃, 松井繁長, 工藤正俊: 十二指腸穿破をきたした正中球状靭帯症候群による膵十二指腸動脈瘤の一例. 一般演題ポスター「消化管出血2」, 第104回日本消化器病学会総会, 平成30年4月19-21日, 京王プラザホテル, 東京.
 11. 河野辰哉, 山雄健太郎, 中井敦史, 大本俊介, 鎌田 研, 三長孝輔, 宮田 剛, 今井 元, 松本逸平, 竹山宜典, 田中伴典, 筑後孝章, 林 暁洋, 工藤正俊: 膵体部の膵神経内分泌腫瘍に合併した膵性胸水の一例. 一般演題ポスター「膵 症例2」, 第104回日本消化器病学会総会, 平成30年4月19-21日, 京王プラザホテル, 東京.
 12. 岡本彩那, 三長孝輔, 竹中 完, 石川 嶺, 中井敦史, 大本俊介, 鎌田 研, 宮田 剛, 山雄健太郎, 今井 元, 工藤正俊, 木村雅友: 経口デジタル胆道鏡(SpyGlass DS)が胆管癌の進展度診断に有用であった一例. 一般演題「肝胆膵」, 第100回日本消化器内視鏡学会近畿支部例会, 平成30年5月26日, 大阪国際交流センター, 大阪.
 13. 中井敦史, 竹中 完, 山雄健太郎, 松本逸平, 竹山宜典, 工藤正俊: 術後膵液瘻(POPF)に対するEUSドレナージの有用性. 第49回日本膵臓学会大会, 平成30年6月29日, 和歌山県民文化会館, ホテルアバローム紀の国, 和歌山.
 14. 大本俊介, 竹中 完, 松本逸平, 竹山宜典, 工藤正俊: 重症急性膵炎の予後不良予測因子および被包化壊死(WON)合併予測因子の検討. 第49回日本膵臓学会大会, 平成30年6月29日, 和歌山県民文化会館, ホテルアバローム紀の国, 和歌山.
 15. 田中秀和, 鎌田 研, 竹中 完, 石川 嶺, 中井敦史, 大本俊介, 三長孝輔, 宮田 剛, 山雄健太郎, 今井 元, 工藤正俊: 造影ハーモニックEUSは膵癌の術前治療の効果判定に有用か? 第49回日本膵臓学会大会, 平成30年6月30日, 和歌山県民文化会館, ホテルアバローム紀の国, 和歌山.
 16. 萩原 智, 西田直生志, 工藤正俊: テノホビルアラフェナミドの初期使用経験について. 第60回京都肝疾患懇話会, 平成30年7月21日, 京都ホテルオークラ, 京都.
 17. 松井繁長, 樫田博史, 工藤正俊: 内視鏡治療後の再発十二指腸静脈瘤に対するEUSの有用性. 第25回日本門脈圧亢進症学会総会, 第20回肝不全治療研究会, 第21回B-RT0研究会, 平成30年9月20-21日, グランキューブ大阪, 大阪.
 18. 大塚康生, 鎌田 研, 竹中 完, 石川 嶺, 岡本彩那, 中井敦史, 大本俊介, 三長孝輔, 山雄健太郎, 筑後孝章, 兵頭朋子, 中居卓也, 竹山宜典, 工藤正俊: 肝外胆管癌における造影ハーモ

- ニックEUSの有用性についての検討. 第54回日本胆道学会学術集会, 平成30年9月27-28日, 幕張メッセ, 千葉.
19. 田中秀和, 永井知行, 櫻井俊治, 河野辰哉, 高島耕太, 正木 翔, 岡元寿樹, 河野匡志, 山田光成, 米田頼晃, 渡邊智裕, 松井繁長, 辻 直子, 檜田博史, 工藤正俊: 慢性偽性腸閉塞に対し、胃瘻造設が有効であった一例. 日本消化器病学会近畿支部第109回例会, 平成30年9月29日, 大阪国際交流センター, 大阪.
 20. 岡本彩那, 三長孝輔, 大塚康生, 高田龍太郎, 吉川智恵, 石川 嶺, 山崎友裕, 中井敦史, 大本俊介, 鎌田 研, 山雄健太郎, 竹中 完, 工藤正俊, 大谷知之: 術前診断が困難であった臍頭部、尾部重複癌の一例. 日本消化器病学会近畿支部第109回例会, 平成30年9月29日, 大阪国際交流センター, 大阪.
 21. 大丸直哉, 永谷奈央, 秦 康倫, 木下大輔, 奥田英之, 高山政樹, 川崎俊彦, 水野成人, 眞鍋弘暢, 辻江正徳, 井上雅智, 若狭朋子, 太田善夫, 工藤正俊, 大谷知之: FNH類似の造影エコー像を示した肝細胞癌の一切除例. 日本消化器病学会近畿支部第109回例会, 平成30年9月29日, 大阪国際交流センター, 大阪.
 22. 永谷奈央, 木下大輔, 秦 康倫, 高山政樹, 奥田英之, 川崎俊彦, 水野成人, 若狭朋子, 太田善夫, 明石雄策, 田村孝雄, 工藤正俊: 胃、十二指腸への転移を来した悪性中皮腫の一例. 日本消化器病学会近畿支部第109回例会, 平成30年9月29日, 大阪国際交流センター, 大阪.
 23. 原 茜, 石川 嶺, 鎌田 研, 大塚康生, 吉川智恵, 山崎友裕, 高田龍太郎, 岡本彩那, 中井敦史, 大本俊介, 三長孝輔, 山雄健太郎, 竹中 完, 工藤正俊, 筑後孝章, 木村雅友, 吉田雄太, 中居卓也, 竹山宜典: セルブブロック法を用いた内視鏡的経鼻胆嚢ドレナージチューブ下細胞診にて診断し得たIntracystic papillary neoplasmの一例. 日本消化器病学会近畿支部第109回例会, 平成30年9月29日, 大阪国際交流センター, 大阪.
 24. 石川 嶺, 鎌田 研, 竹中 完, 大本俊介, 筑後孝章, 松本逸平, 竹山宜典, 工藤正俊: 臍神経内分泌腫瘍における超音波内視鏡下ソナゾイド造影による悪性度診断の有用性. 日本超音波医学会第45回関西地方会学術集会, 平成30年10月20日, 神戸国際会議場, 兵庫.
 25. 横川美加, 南 雅人, 桑口 愛, 市島真由美, 塩見香織, 前川 清, 南 康範, 依田 広, 檜田博史, 工藤正俊: 診断に難渋したNeurilemmomaの一例. 日本超音波医学会第45回関西地方会学術集会, 平成30年10月20日, 神戸国際会議場, 兵庫.
 26. 中井敦史, 鎌田 研, 竹中 完, 松本逸平, 竹山宜典, 兵頭朋子, 筑後孝章, 工藤正俊: 臍癌の門脈浸潤に対する造影ハーモニックEUS (CH-EUS)と造影multidetector CT (MDCT)の診断能の比較検討. 日本超音波医学会第45回関西地方会学術集会, 平成30年10月20日, 神戸国際会議場, 兵庫.
 27. 櫻井俊治, 川上尚人, 工藤正俊: 当院でのirAE大腸炎の臨床的特徴. 第26回日本消化器関連学会週刊JDDW 2018 (第60回日本消化器病学会大会, 第22回日本肝臓学会大会, 第96回日本消化器内視鏡学会総会), 平成30年11月1-4日, 神戸コンベンションセンター, 兵庫.
 28. 中井敦史, 鎌田 研, 竹中 完, 石川 嶺, 岡本彩那, 大本俊介, 三長孝輔, 山雄健太郎, 兵頭朋子, 松本逸平, 竹山宜典, 工藤正俊: 臍癌の門脈浸潤診断における造影ハーモニックEUSと造影CTの診断能の比較検討. 第26回日本消化器関連学会週刊JDDW 2018 (第60回日本消化器病学会大会, 第22回日本肝臓学会大会, 第96回日本消化器内視鏡学会総会), 平成30年11月1-4日, 神戸コンベンションセンター, 兵庫.
 29. 岡本彩那, 鎌田 研, 竹中 完, 石川 嶺, 中井敦史, 大本俊介, 三長孝輔, 山雄健太郎, 工藤正俊: EUS施行時の鎮静に対するBISモニターの有用性の検討. 第26回日本消化器関連学会週刊JDDW 2018 (第60回日本消化器病学会大会, 第22回日本肝臓学会大会, 第96回日本消化器内視鏡学会総会), 平成30年11月1-4日, 神戸コンベンションセンター, 兵庫.
 30. 岡元寿樹, 渡邊智裕, 工藤正俊: Cap polyposisにおける腸内細菌叢の解析. 第26回日本消化器関連学会週刊JDDW 2018 (第60回日本消化器病学会大会, 第22回日本肝臓学会大会, 第96回日本消化器内視鏡学会総会), 平成30年11月1-4日, 神戸コンベンションセンター, 兵庫.
 31. 東原久美, 三長孝輔, 岡本彩那, 榎木英介, 石川 嶺, 中井敦史, 大本俊介, 鎌田 研, 山雄健太郎, 竹中 完, 工藤正俊: 術前水平方向進展度診断にSpyGlass DSが有用であった遠位胆管癌の2例. 第26回日本消化器関連学会週刊JDDW 2018 (第60回日本消化器病学会大会, 第22回日本肝臓

- 学会大会，第96回日本消化器内視鏡学会総会），平成30年11月1-4日，神戸コンベンションセンター，兵庫。
32. 辻 直子，梅原康湖，谷池聡子，工藤正俊：クラリスロマイシン耐性とH. pylori除菌法の選択。第101回日本消化器内視鏡学会近畿支部例会，平成30年11月10日，大阪国際交流センター，大阪。
 33. 秦 康倫，木下大輔，高山政樹，奥田英之，川崎俊彦，水野成人，工藤正俊，渡辺敏彦，若狭朋子，岩渕三哉：Russell body gastritisの一例。第101回日本消化器内視鏡学会近畿支部例会，平成30年11月10日，大阪国際交流センター，大阪。
 34. 久家沙希那，大本俊介，竹中 完，石川 嶺，岡本彩那，中井敦史，鎌田 研，三長孝輔，山雄健太郎，工藤正俊：急性膵炎を発症した肺腺癌膵転移の一例。第101回日本消化器内視鏡学会近畿支部例会，平成30年11月10日，大阪国際交流センター，大阪。
 35. 高島耕太，松井繁長，岡元寿樹，山田光成，正木 翔，河野匡志，米田頼晃，永井知行，櫻井俊治，渡邊智裕，辻 直子，樫田博史，工藤正俊：表在型食道神経内分泌癌の一例。第101回日本消化器内視鏡学会近畿支部例会，平成30年11月10日，大阪国際交流センター，大阪。
 36. 河野辰哉，松井繁長，工藤正俊，樫田博史，渡邊智裕，米田頼晃，山田光成，河野匡志，櫻井俊治，永井知行，辻 直子，安田卓司，白石 治，木村 豊：若年性ポリポーシスにより胃切除を施行した2症例。第101回日本消化器内視鏡学会近畿支部例会，平成30年11月10日，大阪国際交流センター，大阪。
 37. 河野辰哉，松井繁長，工藤正俊，樫田博史，渡邊智裕，米田頼晃，山田光成，河野匡志，櫻井俊治，永井知行，辻 直子，安田卓司，白石 治，木村 豊：若年性ポリポーシスにより胃切除を施行した2症例。第101回日本消化器内視鏡学会近畿支部例会，平成30年11月10日，大阪国際交流センター，大阪。
 38. 岡本彩那，三長孝輔，竹中 完，吉川智恵，石川 嶺，山崎友裕，中井敦史，大本俊介，鎌田 研，山雄健太郎，工藤正俊，岩崎寿光，松本逸平，鶴崎正勝：胆管損傷後のBiloma内でランデブー法にて胆管ステントを留置し得た一例。第101回日本消化器内視鏡学会近畿支部例会，平成30年11月10日，大阪国際交流センター，大阪。
 39. 山崎友裕，大本俊介，竹中 完，吉川智恵，岡本彩那，石川 嶺，中井敦史，鎌田 研，三長孝輔，山雄健太郎，工藤正俊：IPMN切除例からみた新ガイドラインの検証と、造影ハーモニックEUSの有用性について。第101回日本消化器内視鏡学会近畿支部例会，平成30年11月10日，大阪国際交流センター，大阪。
 40. 上嶋一臣：肝細胞癌に対する分子標的治療の今後の展望。シンポジウム「レゴラフェニブ登場によるパラダイムシフト」。第17回日本肝がん分子標的治療研究会，平成30年1月13日，パシフィコ横浜，神奈川。
 41. 松井繁長：食道胃静脈瘤の内視鏡治療：Up Date EIS，EVLから集学的治療まで。第33回日本消化器内視鏡学会近畿セミナー，平成30年1月14日，大阪。
 42. 依田 広：ウイルス性肝炎の最新治療。第2回医療従事者のための肝炎対策セミナー，平成30年3月3日，ビッグ・アイ，大阪。
 43. 上嶋一臣：肝細胞癌診療のパラダイムシフト～進化する肝細胞癌化学療法～。第2回医療従事者のための肝炎対策セミナー，平成30年3月3日，ビッグ・アイ，大阪。
 44. 萩原 智：ウイルス性肝炎治療 up to date。第5回住吉消化器ネットワークセミナー，平成30年3月10日，シェラトン都ホテル大阪，大阪。
 45. 萩原 智：当院におけるC型肝炎治療の成績。第14回Kinki Liver Club，平成30年3月15日，スイスホテル南海大阪，大阪。
 46. 上嶋一臣：肝細胞癌は薬で治せるのか？～化学療法の最近の進歩について～。第14回Kinki Liver Club，平成30年3月15日，スイスホテル南海大阪，大阪。
 47. 千品寛和：肝臓病と採血データの見方。第1部 肝臓の病気。平成29年度「肝がん撲滅運動市民公開講座」，平成30年3月25日，ビッグ・アイ，大阪。
 48. 依田 広：B型肝炎：治療の現在。第1部 肝臓の病気。平成29年度「肝がん撲滅運動市民公開講座」，平成30年3月25日，ビッグ・アイ，大阪。
 49. 萩原 智：飲み薬で治るC型肝炎。第1部 肝臓の病気。平成29年度「肝がん撲滅運動市民公開講

- 座」，平成30年3月25日，ビッグ・アイ，大阪。
50. 河野匡志：肝硬変の治療と肝がんの予防. 第2部 肝硬変と肝がんの治療. 平成29年度「肝がん撲滅運動市民公開講座」，平成30年3月25日，ビッグ・アイ，大阪.
 51. 南 知宏：内科治療～ラジオ波焼灼術と冠動脈塞栓術～. 第2部 肝硬変と肝がんの治療. 平成29年度「肝がん撲滅運動市民公開講座」，平成30年3月25日，ビッグ・アイ，大阪.
 52. 上嶋一臣：肝がん治療薬の最新動向. 第2部 肝硬変と肝がんの治療. 平成29年度「肝がん撲滅運動市民公開講座」，平成30年3月25日，ビッグ・アイ，大阪.
 53. 萩原 智：B型肝炎治療のup-to-date. Hepatitis Forum～肝疾患の新たな治療戦略～，平成30年3月31日，ホテルモントレ グラスミア大阪，大阪.
 54. 上嶋一臣：ここまできた！肝細胞癌の化学療法. Hepatitis Forum～肝疾患の新たな治療戦略～，平成30年3月31日，ホテルモントレ グラスミア大阪，大阪.
 55. 萩原 智：肝癌の分子分類に基づいたスコアリングシステムの確立と根治療法後の転移再発. Kansai Liver Club 2018（肝疾患・肝病態学術研究会/ 若手研究者セミナー） ，平成30年4月7日，太閤園，大阪.
 56. 萩原 智：ベムリディ(TAF)の臨床的意義—自験例を踏まえて—. ランチョンセミナー15，第104回日本消化器病学会総会，平成30年4月19-21日，京王プラザホテル，東京.
 57. 萩原 智：テノホビルアラフェナミドの初期使用経験について. 一般演題 演題II，第3階関西肝疾患フォーラム，平成30年5月19日，帝国ホテル大阪，大阪.
 58. 玉井 結，河野孝一朗，新井 優，増田重人，小島寛子，正木幸作，荒木康宏，河野玲子，伏見洋子，加藤隆夫，西 勝久，加島志朗，竹中 完：SpyglassTMDSを用いたボーリング生検で診断し得た胆管断端神経腫の一例. 一般演題「肝胆膵」，第100回日本消化器内視鏡学会近畿支部例会，平成30年5月26日，大阪国際交流センター，大阪.
 59. 新井 優，増田重人，小島寛子，正木幸作，荒木康宏，伏見洋子，河野孝一朗，加藤隆夫，西 勝久，竹中 完：ENBD留置中に出血性十二指腸潰瘍を発症した2例. Fresh Endoscopist Session 4 胆膵，第100回日本消化器内視鏡学会近畿支部例会，平成30年5月26日，大阪国際交流センター，大阪.
 60. 萩原 智：B型肝炎治療のup-to-date. 肝炎診療連携セミナー，平成30年5月31日，ホテルモントレグラスミア大阪，大阪.
 61. 上嶋一臣：分子標的薬の効果を最大限に引き出すためのknow-how. ランチョンセミナー6「全身化学療法の副作用マネジメント/肝臓専門医が知っておくべき蛋白尿とその管理」，第54回日本肝臓学会総会，平成30年6月14日，大阪国際会議場，大阪.
 62. 萩原 智：IFNフリー治療を臨床で活かす～有効性と忍容性を考慮に入れた治療～. ランチョンセミナー1「実臨床データから紐解くC型肝炎治療と新たな課題」，第54回日本肝臓学会総会，平成30年6月15日，リーガロイヤルNCB，大阪.
 63. 萩原 智：ウイルス型肝炎の最新情報. 肝炎・消化器疾患連携セミナー，平成30年6月20日，市立岸和田市民病院，大阪.
 64. 上嶋一臣：ランチョンセミナー8「分子標的薬の使いどころ、選びどころ」，第54回日本肝癌研究会，平成30年6月29日，久留米シティプラザ，福岡.
 65. 竹中 完：EUSにおける画像強調機能活用法. ランチョンセミナー11「動画で見るEUS～スクリーニングから画像強調機能活用まで～」，第49回日本膵臓学会大会，平成30年6月29日，和歌山県民文化会館，ホテルアバローム紀の国，和歌山.
 66. 上嶋一臣：multi TKI時代のTACE不応判断と分子標的薬への切り替え時期，共催シンポジウム1「レゴラフェニブ登場により何が変わったのか？」，第18回日本肝がん分子標的治療研究会，平成30年7月14日，東京大学伊藤国際学術研究センター，東京.
 67. 南 康範：ラジオ波焼灼術における治療ガイドと早期治療効果判定：US-US overlay fusionの有用性. 第18回関西肝血流動態・機能イメージ研究会，平成30年7月21日，エーザイ株式会社大阪コミュニケーションオフィス33階，大阪
 68. 南 康範：当院でのアミノレバンの治療経験. 南大阪Liver Forum，平成30年7月26日，セントレジスホテル大阪，大阪.

69. 山雄健太郎：胆膵；胆膵疾患診療における超音波内視鏡の役割. 講習会「超音波の未来を切り拓く」, 日本超音波医学会第45回関西地方会学術集会, 平成30年10月20日, 神戸国際会議場, 兵庫.
70. 石川 嶺, 鎌田 研, 竹中 完: 膵神経内分泌腫瘍の悪性度評価における造影ハーモニックEUSの有用性. ワークショップ15「膵神経内分泌腫瘍の治療戦略」, 第26回日本消化器関連学会週間JDDW 2018 (第22回日本肝臓学会大会, 第96回日本消化器内視鏡学会総会, 第60回日本消化器病学会大会), 平成30年11月2日, 神戸コンベンションセンター, 兵庫.
71. 三長孝輔, 竹中 完, 山下幸孝: PTGBDからEUS-GBDへのconversionの有用性・安全性に関する検討: 多施設後ろ向き研究. ワークショップ27「Interventional EUSのトラブルシューティング」, 第26回日本消化器関連学会週間JDDW 2018 (第22回日本肝臓学会大会, 第96回日本消化器内視鏡学会総会, 第60回日本消化器病学会大会), 平成30年11月1-4日, 神戸コンベンションセンター, 兵庫.
72. 原田宜幸, 松本久和, 三長孝輔, 上野山義人, 山下幸孝: 当院の胆管カニューレションにおけるMagicTomeの使用経験. シンポジウム1「胆膵内視鏡治療の工夫」, 第101回日本消化器内視鏡学会近畿支部例会, 平成30年11月10日, 大阪国際交流センター, 大阪.
73. 我妻信和, 三長孝輔, 松本久和, 上野山義人: 胆管生検における10Fr胆道ブジーダイレータを用いた工夫. ビデオワークショップ2「胆膵内視鏡のトラブルシューティング」, 第101回日本消化器内視鏡学会近畿支部例会, 平成30年11月10日, 大阪国際交流センター, 大阪.
74. 脇田 碧, 谷 泰弘, 三長孝輔, 重里徳子, 中野省吾, 枝川剛也, 我妻信和, 原田宜幸, 岡田圭次郎, 池ノ内真衣子, 梅村壮一郎, 林 佑樹, 中井智己, 松本久和, 中谷泰樹, 赤松拓司, 瀬田剛史, 浦井俊二, 上野山義人, 山下幸孝, 小野一雄: 胃粘膜下腫瘍様形態を呈した抗酸菌感染症の一例. 第101回日本消化器内視鏡学会近畿支部例会, 平成30年11月10日, 大阪国際交流センター, 大阪.
75. 竹中 完: コーヒーブレイクセミナー1「肝門部胆管狭窄に対する胆道ドレナージ〜新型ブレイデッドステントの可能性〜」, 第101回日本消化器内視鏡学会近畿支部例会, 平成30年11月10日, 大阪国際交流センター, 大阪.

別刷

2.5 Gastrointestinal Malignancies

2.5.3 Hepatocellular Carcinoma

J.J. Harding¹

T.Watanabe²

I. El-Dika¹

N. Nishida²

G. K. Abou-Alfa¹

M. Kudo²

¹*Department of Medicine, Memorial Sloan Kettering Cancer Center, Weill Cornell School of Medicine, New York, NY, USA*

²*Department of Gastroenterology and Hepatology, Kindai University Faculty of Medicine, Osaka, Japan*

Introduction

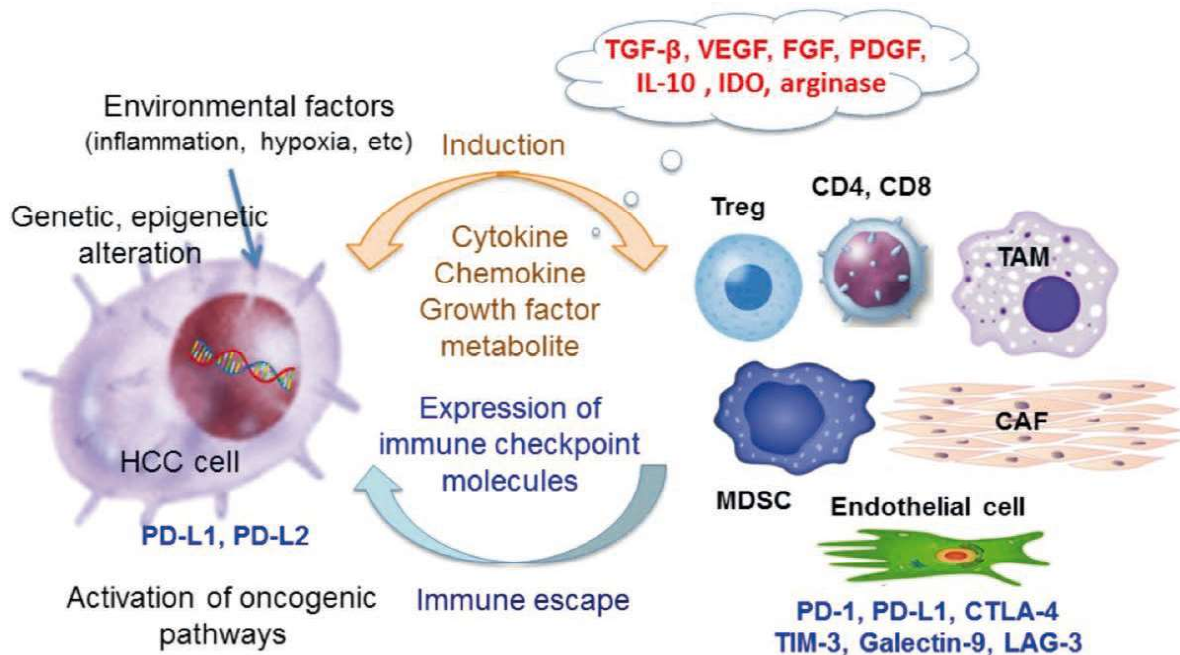
Hepatocellular carcinoma (HCC) originates from chronic fibro-inflammatory disorders of the liver such as chronic viral hepatitis, alcohol-induced hepatitis and non-alcoholic steatohepatitis. In most cases of hepatocarcinogenesis, HCC develops as a result of sustained viral infection or chronic inflammation, leading to the accumulation of genetic mutations and selection of hepatocytes with potent growth ability. In addition to genetic alterations in hepatocytes, recent studies highlight the importance of immune responses that impair cancer immunosurveillance by tissue immune cells. It is now generally accepted that a wide variety of immunosuppressive mechanisms operating in HCC tissue play a critical role in the generation of cancer microenvironment, and interference with these immunological pathways leads to therapeutic benefit in advanced HCC patients. Herein, we will focus on the current understanding of HCC immunobiology and the state of the art in HCC immunotherapies.

HCC Immunobiology

An immunosuppressive tumour milieu is created by cross-talk between tumour cells and immune cells. Cancer cells express tumour-associated antigens (TAAs), such as alpha-foetoprotein (AFP), New York-oesophageal squamous cell carcinoma-1 (NY-ESO-1), telomerase reverse transcriptase (TERT) and melanoma-associated antigen genes A (MAGE-A). In addition to these typical TAAs, HCCs also express neoantigens specific to individual tumours. HCCs evade the immune system even though classical TAAs and neoantigens can be detected by immune cells. Several mechanisms have been proposed for the explanation of such immune escape (Figure 1).

First, failure to process TAAs into antigenic peptide results in ineffective presentation of TAAs in HCCs. Second, HCC cells and immune cells in the tumour microenvironment (TME) produce a large amount of immunosuppressive soluble factors such as transforming growth factor (TGF)- β , interleukin (IL)-10, indoleamine 2,3-dioxygenase (IDO) and arginase. These immunosuppressive mediators inhibit activation of both innate and adaptive immunity cells. Third, HCC cells and immune cells in the TME express immune checkpoint molecules. Immune checkpoint molecules are fail-safe mechanisms to prevent excessive activation of T cells and are reviewed in Chapter 1.1. Immune checkpoint molecules include cytotoxic T-lymphocyte antigen 4 (CTLA-4), programmed cell death protein 1 (PD-1), T cell immunoglobulin and mucin domain-3 (TIM-3) and lymphocyte-activation gene 3 (LAG-3). Programmed death-ligand 1 (PD-L1) and PD-1 are preferentially expressed on HCC cells and T cells, respectively. The interaction between PD-L1 and PD-1 results in T cell exhaustion, and then, as a result, HCC development is accelerated by escape from T cell-mediated cancer immune surveillance. In preclinical models, blockade of these immune checkpoint pathways leads to HCC eradication and, in clinical samples, markers of T cell exhaustion in tumoural tissue often portend worse disease-specific survival outcomes. Finally, alterations in the cellular compartment of the TME, such as the presence of myeloid-derived suppressor cells (MDSCs), tumour-associated macrophages (TAMs) and T regulatory cells (T_{regs}), serve to further suppress an effective immune response in HCC. Interaction between effector T cells and these immunosuppressive cells contributes to the generation of tolerogenic immune responses in HCC.

Figure 1 Establishment of immunosuppressive environment in HCC.



Abbreviations: CAF, cancer-associated fibroblast; CTLA-4, cytotoxic T-lymphocyte antigen 4; FGF, fibroblast growth factor; HCC, hepatocellular carcinoma; IDO, indoleamine 2,3-dioxygenase; IL-10, interleukin-10; LAG-3, lymphocyte-activation gene 3; MDSC, myeloid-derived suppressor cell; PD-1, programmed cell death protein 1; PD-L1/2, programmed death-ligand 1/2; PDGF, platelet-derived growth factor; TAM, tumour-associated macrophage; TGF-β, transforming growth factor-β; TIM-3, T cell immunoglobulin and mucin domain-3; T_{reg}, T regulatory cell; VEGF, vascular endothelial growth factor.

Current Landscape of Immune Checkpoint Inhibition in HCC

CTLA-4 Blockade

Tremelimumab, a fully human immunoglobulin (Ig)G2 monoclonal antibody (mAb), is an antagonist of CTLA-4 on activated T cells and was recently evaluated in 20 patients with hepatitis C virus (HCV)-related HCC (Table 1). The study population included patients who failed prior treatment with sorafenib and had a large burden of disease with impaired liver function (57% Barcelona Clinic Liver Cancer [BCLC] C, 43% Child Pugh B, 29% portal vein invasion, 29% AFP >400 UI/mL). Notably, three of 17 (17.6%) evaluable patients attained a confirmed partial response (PR). These data are provocative and suggest that a patient subset might attain durable disease control with this treatment modality. The relatively high proportion of grade 3 and 4 transaminitis (45%) observed with CTLA-4 blockade was concerning, although impairments in liver func-

tion were reversible and did not progress to liver failure. Another critical observation from this study was that CTLA-4 blockade did not worsen hepatitis C virus (HCV) viraemia. Three patients achieved a transient complete virological response, and a patient subset had a transient decrease in HCV viral load. Given these results, continued development of CTLA-4 blockade in HCC is warranted and, currently, areas of exploration include CTLA-4 blockade in combination with other immune checkpoint blockers (namely with anti-PD-1/PD-L1 mAbs), pairing with regional therapy and, importantly, attempts to mitigate CTLA-4-based toxicity.

Table 1 Reported Results from Completed and Ongoing Clinical Trials Using Immune Checkpoint Blockade in Patients with Advanced HCC Who Failed, Declined or Were Intolerant to Prior Sorafenib

Clinical trial number	Agent	Design and size	ORR % (95% CI)	mDOR months (95% CI)	mOS months (95% CI)
NCT01008358	Tremelimumab	II (N=20)	17.6 (not reported)	not reported	8.2 (4.6–21.3)
NCT01853618	Tremelimumab + TACE/RFA	I (N=32)	26.3 (9.1–51.2)	not reported	12.3 (9.3–15.4)
NCT01658878	Nivolumab	I (N=48) II (N=214)	Phase I: 15 (6–28) Phase II: 20 (15–26)	17 (6–24) 9.9 (8.3–NE)	15 (9.6–20) not reported
NCT02702414	Pembrolizumab	II (N=104)	16.3 (9.8–24.9)	8.2 (2.3–8.3)	not reported
NCT01693562	Durvalumab	II (N=40)	10.3 (2.9–24.2)	not reported	13.2 (6.3–21.1)
NCT02519348	Durvalumab + tremelimumab	I (N=40)	15 (not reported)	not reported	not reported

Abbreviations: CI, confidence interval; HCC, hepatocellular carcinoma; mDOR, median duration of response; mOS, median overall survival; NE, non-evaluable; ORR, overall response rate; TACE/RFA, trans-arterial chemoembolisation/radiofrequency ablation.

PD-1 and PD-L1 Blockade

Several mAbs blocking PD-1 and PD-L1 are in development as monotherapy for HCC (Tables 1 and 2). Nivolumab, a human IgG4 mAb to PD-1, has been extensively tested in HCC. Based on the results from a large phase I/II study, nivolumab received expedited Food and Drug Administration (FDA) approval in 2017 for advanced HCC after failure or intolerance to sorafenib. In the study, 262 patients with advanced HCC and intact hepatic function were treated with nivolumab every 2 weeks in a dose escalation (n=48, 0.1 mg to 10 mg/kg) and a dose expansion (n=214, 3 mg/kg). Importantly, the agent was well tolerated

– 25% of patients experienced grade 3/4 toxicity in dose escalation; the most common events of any grade included transaminitis (31%), increases in amylase (15%) and lipase (15%), rash (31%) as well as pruritus (23%). Low frequencies of immune-related adverse events (irAEs) typical of this class of compound were also observed, such as hepatitis, adrenal insufficiency and diarrhoea. Hepatitis B virus (HBV) reactivation or seroconversion was not reported, and some patients had a transient decrease in HCV viraemia. The objective response rate (ORR) was 15% in the dose-escalation arm with a median duration of response (DOR) of 17 months and median overall survival (OS) of 15 months. The dose expansion confirmed these findings – safety was comparable and the ORR was 20% (95% confidence interval [CI]: 15–26). Responses were seen across HCC aetiologies and in patients who were treatment-naïve or heavily pretreated. As a condition of accelerated approval, further trials will be required to verify the clinical benefit of nivolumab.

Table 2 Status of Late-stage Clinical Trials of Immune Checkpoint Inhibitors in Patients with HCC

Clinical trial number	Agent	Target	Design	Endpoint	Status
Advanced HCC: Not surgical or transplant candidates; ineligible or failed prior embolisation					
NCT02576509	Nivolumab vs sorafenib	PD-I	Phase III	TTP/OS	Accrual complete
NCT02702401	Pembrolizumab vs BSC	PD-I	Phase III	PFS/OS	Accrual complete
NCT03062358	Pembrolizumab vs BSC-Asia	PD-I	Phase III	OS	Active accrual
NCT03298451	Durvalumab ± tremelimumab vs sorafenib	PD-L1 CTLA-4	Phase III	OS	Active accrual
NCT03434379	Atezolizumab + bevacizumab vs sorafenib	PD-L1 VEGF	Phase III	ORR/OS	Active accrual
Early-stage HCC: candidates for surgery					
NCT03383458	Nivolumab vs observation	PD-I	Phase III	RFS	Active accrual

Abbreviations: BSC, best supportive care; CTLA-4, cytotoxic T-lymphocyte antigen 4; HCC, hepatocellular carcinoma; ORR, objective response rate; OS, overall survival; PD-I, programmed cell death protein I; PD-L1, programmed death-ligand 1; PFS, progression-free survival; RFS, recurrence-free survival; TTP, time to progression; VEGF, vascular endothelial growth factor.

An open-label, multicentre, randomised phase III study of nivolumab versus sorafenib in patients with advanced HCC has completed recruitment, and results are currently pending (NCT02576509). Patients with unresectable or metastatic HCC who were treatment-naïve and with Child Pugh A liver function were randomised 1:1 to receive nivolumab at 240 mg intravenously every 2 weeks or sorafenib at 400 mg orally twice a day. Stratification factors included HCC aetiology, vascular invasion, extrahepatic spread and geography. The primary endpoint of the study is OS. With an expected sample size of 726 patients, the study has a 90% power to detect a hazard ratio (HR) of 0.74 with a two-sided error of 0.04 for OS.

Durvalumab, a human IgG1 κ mAb to PD-L1, has also been tested in a small phase I/II study of advanced HCC patients who failed prior treatment with sorafenib (93% of patients). Of 39 evaluable patients, four attained a confirmed PR (ORR 10.3%; 95% CI: 2.9–24.2). The median OS was 13.2 months with 56.4% of patients alive at one year. The anti-PD-1 mAb pembrolizumab is currently being evaluated in sorafenib-pretreated patients in a single-arm, phase II trial and in two randomised phase III studies against placebo in the second-line setting (NCT02702414, NCT02702401 and NCT03062358).

Finally, other agents targeting PD-1/PD-L1, such as PDR001, are studied in HCC-specific trials (NCT02795429), while several other agents are being evaluated for safety and efficacy in basket studies.

Combination Immune Checkpoint Blockade

Although these data are promising, it is important to acknowledge that the majority of HCC patients will progress or will not attain durable disease control with either CTLA-4 or PD-1/PD-L1 monotherapy, due to innate and acquired resistance to each of these treatments. To improve efficacy, biomarker and patient strategies will be of critical importance and are reviewed later in this chapter under ‘Future directions and issues specific to HCC’. Alternatively, combination immune checkpoint therapies may improve anti-tumour efficacy (Tables 1 and 2).

The most relevant example is combination blockade with CTLA-4 and PD-1/PD-L1 mAbs. The scientific rationale is that immune checkpoint

molecules function at different times in the lifecycle of effector T cells – CTLA-4 regulates naïve T cell priming and anergy, while PD-1/PD-L1 functions to blunt the immune response of effector T cells in the periphery. Thus, blocking these two pathways is proposed to stimulate T cell activation further, leading to enhanced tumour eradication. Preclinical data indicate that dual blockade is synergistic and, in the clinic, combination therapy results in statistically higher response rates and improved outcomes over monotherapy in a number of solid tumours. In HCC, both durvalumab and tremelimumab (NCT02519348), and nivolumab and ipilimumab (NCT01658878, NCT03222076), are being evaluated in phase I/II clinical trials, and planning for pivotal phase III studies is expected or ongoing. For example, a randomised, open-label, multicentre phase III study of durvalumab with or without tremelimumab versus sorafenib in advanced HCC patients opened to accrual late 2017 (NCT03298451). This 4-arm study will enrol about 1200 patients and explore two dose schedules of durvalumab and tremelimumab combination therapy. The primary endpoint is OS.

A critical question, of course, is whether the added toxicity of combination therapy will be offset by improved efficacy and outcomes. Another important question is whether sequential or combination checkpoint blockade might prevent resistance. For example, a recent clinical report indicates that TIM-3, a checkpoint protein, may mediate resistance to PD-1 monotherapy, and an antagonist of TIM-3 in combination or in sequence with PD-1 therapy *in vivo* improves anti-tumour efficacy. As more data become available, it is expected that multiple immune checkpoint inhibitor (ICI) doublets, and perhaps triplets, will be assessed in HCC. Presently, anti-PD-1/PD-L1 therapy is being paired with agents targeting TIM-3 (NCT03099109), LAG-3 (NCT03005782, NCT01968109) and KIR (NCT01714739) in HCC patients.

Combination Tyrosine Kinase Inhibitors and Immune Checkpoint Blockade

Hepatomas are sensitive to tyrosine kinase inhibition, and clinically several multitargeted tyrosine kinase inhibitors (TKIs) have demonstrated a survival benefit in advanced HCC, including sorafenib, lenvatinib,

regorafenib and cabozantinib. These agents collectively block vascular endothelial growth factor receptor (VEGFR) and platelet-derived growth factor receptor (PDGFR) with varying potency and each agent preferentially blocks distinct signalling cascades (i.e. cabozantinib/MET and lenvatinib/fibroblast growth factor receptor [FGFR] 1-4). From a purely empirical and practical standpoint, pairing each of these agents with anti-PD-1 therapy might be warranted, although emerging biological data indicate that TKIs clearly affect immune effectors, antigen presentation, the TME and the vasculature, and may serve to blunt or augment the immune response to cancer. In HCC, several preclinical studies have suggested that certain TKIs might act synergistically with anti-PD-1 therapy and, as such, several early phase studies are underway exploring the safety and tolerability of anti-PD-1 therapy with many agents, not limited to sorafenib (NCT03211416, NCT01658878, NCT02988440), lenvatinib (NCT03006926), cabozantinib (NCT03299946, NCT01658878) and axitinib (NCT03289533). In addition, selective inhibitors of VEGF, MET and FGFR4 are currently being evaluated with studies using bevacizumab (NCT03434379), capmatinib (NCT02795429) and FGF401 (NCT02325739), respectively.

Alternative Immunotherapeutic Strategies

Oncolytic Viruses

Oncolytic viruses function by two major mechanisms: direct viral replication within tumour cells leading to tumoural lysis, and activation of cell-mediated tumour specific immunity. Pexa-Vec (pexastimogene devacirepvec), an oncolytic virus derived from vaccinia, has been evaluated in a randomised phase II study of high-dose versus low-dose intratumoural injection in advanced HCC patients (n=30). OS was significantly longer in the high-dose arm compared with the low-dose arm (median: 14.1 months versus 6.7 months, *p*-value 0.02). In contrast, a phase IIb clinical trial of 129 HCC patients who failed sorafenib therapy did not achieve the primary endpoint of prolonging OS in Pexa-Vec-treated patients compared with best supportive care. Importantly, the study population included patients with impaired hepatic function (Child Pugh-B7), large vessel involvement and allowed a heavy burden of disease. A phase III

study of Pexa-Vec in combination with sorafenib versus sorafenib alone (NCT02562755) and a phase I/II study of Pexa-Vec in combination with nivolumab (NCT03071094) in first-line HCC patients are ongoing at the time of writing, with more refined inclusion and exclusion criteria.

Adoptive Cellular Therapy

Adoptive cellular therapies use tumour infiltrating lymphocytes (TILs), modified T cell receptors (TCRs) and chimeric antigen receptors (CARs), and these approaches are all being investigated in HCC. However, all three modalities call for extensive clinical infrastructure since TCRs and CARs require genetic modification to target specific tumour antigens, the former in a major histocompatibility complex (MHC)-restricted manner and the latter in a non-MHC restricted manner. Common antigens studied to date include AFP and glypican 3 (GPC3), as both are abundantly expressed in HCC with limited expression in normal tissues. Several studies are underway to evaluate GPC3-CAR in patients with advanced and refractory HCC (NCT03146234, NCT02715362, NCT03130712, NCT03198546), as well as AFP-specific TCRs (NCT03132792). Future success of these approaches will depend on safe antigen selection, common MHC haplotypes for TCR-based research (especially given the wide ethnic variability observed with HCC) and careful patient selection given the need for cytoreductive treatments prior to adoptive transfer.

Future Directions and Issues Specific to HCC

Application of Immunotherapy to Earlier Stages of Disease

Clinical trials of immunotherapy have mostly enrolled patients with advanced-stage HCCs that are refractory to conventional treatments, such as radiofrequency ablation (RFA) and trans-arterial chemoembolisation (TACE). However, these procedures clearly affect the immune response and may release TAAs and/or contribute to the induction of an anti-tumour immune reaction. Intriguingly, tremelimumab in combination with RFA or TACE in advanced HCC (BCLC-C) patients was found to be safe and led to a 26.3% ORR. Median OS was favourable at 12.3 months for a heavily pretreated population. However, the effect of immune checkpoint blockade at earlier stages of HCC has not been

confirmed, and several pilot studies are ongoing to assess safety and efficacy (NCT03033446, NCT03143270, NCT03099564, NCT02821754). Furthermore, ICIs are also being tested in the surgical setting, and several adjuvant and neoadjuvant studies are in planning or ongoing (NCT03222076, NCT03383458).

Biomarkers and Patient Selection

Specific biomarkers that predict the effect of immunotherapy, including ICIs, have not been clarified for HCC. The largest clinical effort to date has been the analysis of tumoural PD-L1 expression in the phase I/II study of nivolumab – no correlation between response and PD-L1 level was observed. Several other tumoural markers are currently being evaluated, including viral markers, TILs, immune effector composition, cytolytic score by proteomic analysis and tumoural genomics. Several studies indicated that mutational load and inactivation of mismatch repair genes are strongly associated with efficacy of PD-1/PD-L1 inhibitors. However, mutations in mismatch repair genes, microsatellite instability and hypermutation are rare in HCC. HCC as a field has also been at the forefront of imaging, and investigation here will no doubt continue to include novel magnetic resonance imaging (MRI) modalities, texture and vasculature analyses, as well as functional T cell imaging (e.g. ⁸⁹Zr-Df-IAB22M2C, NCT03107663).

Issues Specific to HCC

As nearly 90% of HCC patients have cirrhosis and most patients have viral hepatitis, several issues specific to HCC and immune-based therapy must be addressed. First, transaminitis related to checkpoint blockade must be evaluated carefully to include an assessment of viral reactivation, cross-sectional imaging to rule out progression and hepatic/portal vein involvement, and history to exclude other potential confounders such as toxin-induced injury (i.e. alcohol). In the event of immune-mediated hepatic dysfunction, prompt treatment with corticosteroids or other immunosuppressive medications may be required to prevent liver failure. Second, a subset of HCC patients progress after prior liver allograft; in these cases immune-based therapy is contraindicated and case reports

have shown acute rejection following anti-PD-1 therapy. Third, procurement of fresh tumour tissue for biomarker analysis may be inappropriate, specifically in cases of poor hepatic function and/or severe hepatic dysfunction. Thus, functional imaging, as noted above, must be explored in HCC. Finally, specifically to HCV-related HCC, it is unclear if treatment of the virus will affect immune-based treatment.

Conclusions

The field of HCC treatment is rapidly evolving and, at present, nivolumab is the first immunotherapy approved for the treatment of advanced HCC. The immediate and critical questions for this field are whether this new modality improves OS in the metastatic setting or not, and at what point during the course of the disease should anti-PD-1 therapy be applied (i.e. first or second line). Several groups are actively evaluating combination therapies as well as enrichment strategies to improve anti-PD-1 therapy. Immune checkpoint blockade is rapidly moving to earlier stages of disease and is being evaluated in the context of a variety of regional therapies. Novel treatments, such as oncolytic viruses and cellular therapy, are under active investigation. These collaborative and global efforts will undoubtedly lead to progress and to a new armamentarium of treatments for patients with this devastating disease.

Declaration of Interest:

Dr Harding has received research funding and has consulted for AstraZeneca and Bristol-Myers Squibb.

Dr Watanabe has reported no potential conflicts of interest.

Dr El-Dika has reported no potential conflicts of interest.

Dr Nishida has reported no potential conflicts of interest.

Dr Abou-Alfa has received research funding and has consulted for AstraZeneca and Bristol-Myers Squibb.

Dr Kudo has received research funding from Bristol-Myers Squibb.

Further Reading

- Budhu A, Forgues M, Ye QH, et al. Prediction of venous metastases, recurrence, and prognosis in hepatocellular carcinoma based on a unique immune response signature of the liver microenvironment. *Cancer Cell* 2006; 10:99–111.
- Duffy AG, Ulahannan SV, Makorova-Rusher O, et al. Tremelimumab in combination with ablation in patients with advanced hepatocellular carcinoma. *J Hepatol* 2017; 66:545–551.
- El-Khoueiry AB, Sangro B, Yau T, et al. Nivolumab in patients with advanced hepatocellular carcinoma (CheckMate 040): an open-label, non-comparative, phase 1/2 dose escalation and expansion trial. *Lancet* 2017; 389:2492–2502.
- Harding JJ, El Dika I, Abou-Alfa GK. Immunotherapy in hepatocellular carcinoma: Primed to make a difference? *Cancer* 2016; 122:367–377.
- Heo J, Reid T, Ruo L, et al. Randomized dose-finding clinical trial of oncolytic immunotherapeutic vaccinia JX-594 in liver cancer. *Nat Med* 2013; 19:329–336.
- Park BH, Hwang T, Liu TC, et al. Use of a targeted oncolytic poxvirus, JX-594, in patients with refractory primary or metastatic liver cancer: a phase I trial. *Lancet Oncol* 2008; 9:533–542.
- Sangro B, Gomez-Martin C, de la Mata M, et al. A clinical trial of CTLA-4 blockade with tremelimumab in patients with hepatocellular carcinoma and chronic hepatitis C. *J Hepatol* 2013; 59:81–88.
- Thomson AW, Knolle PA. Antigen-presenting cell function in the tolerogenic liver environment. *Nat Rev Immunol* 2010; 10:753–766.
- Zheng C, Zheng L, Yoo JK, et al. Landscape of infiltrating T cells in liver cancer revealed by single-cell sequencing. *Cell* 2017; 169:1342–1356.e16.

Impact of avascular areas, as measured by contrast-enhanced harmonic EUS, on the accuracy of FNA for pancreatic adenocarcinoma



Ken Kamata, MD, PhD,¹ Mamoru Takenaka, MD, PhD,¹ Shunsuke Omoto, MD,¹ Takeshi Miyata, MD, PhD,¹ Kosuke Minaga, MD,¹ Kentaro Yamao, MD,¹ Hajime Imai, MD,¹ Toshiharu Sakurai, MD, PhD,¹ Naoshi Nishida, MD, PhD,¹ Takaaki Chikugo, MD, PhD,² Yasutaka Chiba, MD, PhD,³ Ippei Matsumoto, MD, PhD,⁴ Yoshifumi Takeyama, MD, PhD,⁴ Masatoshi Kudo, MD, PhD¹

Osaka-sayama, Japan

Background and Aims: EUS-guided FNA (EUS-FNA) is used for the diagnosis of pancreatic adenocarcinoma, but sometimes the method results in a false negative. Occasionally, an avascular area may be observed within the pancreatic adenocarcinoma tumor during contrast-enhanced harmonic EUS (CH-EUS). The aim of this study was to evaluate whether the diagnostic sensitivity of EUS-FNA for pancreatic adenocarcinoma was affected by the presence of avascularity on CH-EUS.

Methods: Two hundred ninety-two patients with pancreatic adenocarcinoma who presented at Kindai University Hospital for EUS-FNA and CH-EUS between June 2009 and August 2013 were retrospectively evaluated. This was a single-center retrospective analysis of prospectively collected data held in a registry. The overall sensitivity of EUS-FNA for the diagnosis of pancreatic adenocarcinoma was calculated. The sensitivities of cytology, histology, and the combination of cytology and histology were also evaluated. These variables were individually evaluated according to the presence or absence of an avascular area on CH-EUS to assess whether the diagnostic sensitivity of EUS-FNA for pancreatic adenocarcinoma was related to the presence of an avascular area within the tumors.

Results: The overall sensitivity of EUS-FNA was 90.8% (265/292). The sensitivities of EUS-FNA for lesions with and without an avascular area were 72.9% (35/48) and 94.3% (230/244), respectively, with the difference being statistically significant ($P < .001$).

Conclusions: EUS-FNA has lower sensitivity for pancreatic adenocarcinoma with avascular areas on CH-EUS. (Gastrointest Endosc 2018;87:158-63.)

EUS-guided FNA (EUS-FNA) is routinely used for the pathologic diagnosis of pancreatic adenocarcinoma, with the pooled sensitivity of EUS-FNA using a 22-gauge needle shown to be 85%.¹ Contrast-enhanced harmonic EUS (CH-EUS) is of assistance during EUS-FNA of pancreatic adenocarcinoma for

detecting and/or selecting the target and avoiding necrotic tissue and/or vascular structures within the lesions.²⁻⁶

Seicean et al³ evaluated the diagnostic accuracy of EUS-FNA with CH-EUS for solid pancreatic tumors and compared it with that of EUS-FNA without CH-EUS,

Abbreviations: CH-EUS, contrast-enhanced harmonic EUS; EUS-FNA, EUS-guided FNA.

DISCLOSURE: All authors disclosed no financial relationships relevant to this publication. Research support for this study was provided to Dr Kudo by grants from the Japan Society for the Promotion of Science (nos. 22590764 and 25461035).



Use your mobile device to scan this QR code and watch the author interview. Download a free QR code scanner by searching "QR Scanner" in your mobile device's app store.

Copyright © 2018 by the American Society for Gastrointestinal Endoscopy 0016-5107/\$36.00

<http://dx.doi.org/10.1016/j.gie.2017.05.052>

Received February 13, 2017. Accepted May 24, 2017.

Current affiliations: Department of Gastroenterology and Hepatology (1), Department of Pathology (2), Department of Surgery (4), Kindai University Faculty of Medicine, Osaka-sayama, Japan; Clinical Research Center (3), Kindai University Hospital, Osaka-sayama, Japan.

Reprint requests: Mamoru Takenaka, MD, PhD, Department of Gastroenterology and Hepatology, Kindai University Faculty of Medicine, 377-2 Ohno-higashi, Osaka-sayama 589-8511, Japan.

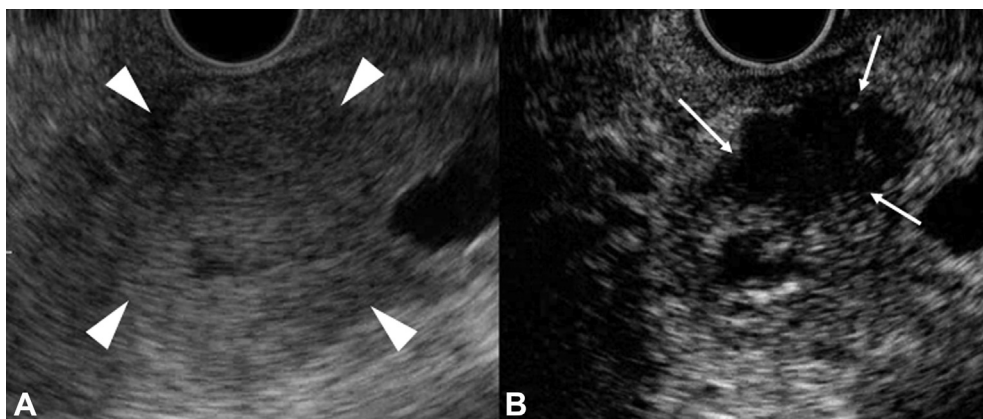


Figure 1. EUS image of pancreatic adenocarcinoma with an avascular area. **A**, Conventional EUS shows a low-echoic mass in the pancreatic head (*arrowheads*). **B**, The CH-EUS image shows an avascular area larger than 10 mm within the tumor (*arrows*). CH-EUS, Contrast-enhanced harmonic EUS.

although both EUS-FNA and surgical findings were used for the final diagnosis. They were able to use CH-EUS to avoid choosing avascular areas for the target during EUS-FNA. The diagnostic accuracy of EUS-FNA with CH-EUS was higher than that of EUS-FNA without CH-EUS (86.5% vs 78.4%), although the difference did not reach the threshold required for statistical significance. This study demonstrated that avoiding avascular areas during EUS-FNA improved the diagnostic accuracy of EUS-FNA for pancreatic masses. However, whether the diagnostic accuracy of EUS-FNA for pancreatic adenocarcinoma with an avascular area is lower than that for pancreatic adenocarcinoma without an avascular area is unknown.

In this study the findings of CH-EUS examinations performed before EUS-FNA in patients with pancreatic adenocarcinoma were retrospectively evaluated in terms of the presence of an avascular area within the lesion. Thereafter, we assessed whether the diagnostic sensitivity of EUS-FNA for pancreatic adenocarcinoma was affected by the presence of avascularity on CH-EUS.

METHODS

Study design

This was a single-center retrospective analysis of prospectively collected data held in a registry. The final diagnoses were retrospectively made according to histologic specimens obtained from surgical resection and/or follow-up until a patient's time of death.

Patients

Three hundred thirty-nine patients with pancreatic masses presented at Kindai University Hospital and underwent CH-EUS and EUS-FNA with a 22-gauge needle between June 2009 and August 2013. Among these, 292 patients with pancreatic adenocarcinoma were retrospectively evaluated. Thirty-six patients with benign pancreatic masses (3 serous cyst neoplasms and 33 inflammatory tumors) and 11 with nonadenocarcinoma masses (3 metastases

and 8 neuroendocrine tumors) were excluded. CH-EUS was performed before EUS-FNA in the same session and in all cases. This study was approved by the ethics committee of the Kindai University School of Medicine.

CH-EUS

The echoendoscope used for CH-EUS was developed specifically for CH-EUS (GF-UCT260; Olympus Medical Systems Co Ltd, Tokyo, Japan), and the EUS images were analyzed using an Aloka ProSound SSD α -10 system (Aloka Co Ltd, Tokyo, Japan). An extended pure harmonic detection mode was used; this synthesized the filtered second-harmonic components with signals obtained from the phase shift to provide contrast-enhanced harmonic imaging.

A conventional EUS examination was initially performed with the patient sedated with midazolam and propofol. When conventional EUS depicted a solid lesion (a hypoechoic nodule or heterogeneous region), the imaging mode was changed to the extended pure harmonic detection mode. The transmitting frequency and mechanical index were 4.7 MHz and .3, respectively. Sonazoid (Daiichi-Sankyo, Tokyo, Japan), which consists of perfluorobutane microbubbles surrounded by a lipid membrane, was used as an ultrasound contrast agent for CH-EUS. The contrast agent was reconstituted with 2 mL of sterile water for injection, and a dose of 15 μ L/kg body weight was prepared in a 2-mL syringe.

The CH-EUS examinations lasted for 60 seconds from injection of the contrast agent. Video sequences of 60 seconds were stored and then independently reviewed by 2 readers (K.M. and K.Y.), who have each performed more than 1000 CH-EUS procedures. For this retrospective review of the stored data, the readers were blinded to the clinical findings.

Definition of the presence of an avascular area on CH-EUS

CH-EUS findings of avascular areas were classified into 3 groups (<5 mm, 5-10 mm, and >10 mm) according to the

TABLE 1. Baseline characteristics of the 292 patients with pancreatic adenocarcinomas

	Total (n = 292)	Without avascular area (n = 244)	With avascular area (n = 48)	P value*
Median age, y (range)	68.5 (41-85)	68.6 (41-85)	68.1 (44-86)	.673
Male/female, n/N	163/129	136/108	27/21	.948
Mean tumor size, mm	31.0	31.2	29.8	.604
Tumor location, head/body and tail, n/N	165/127	137/107	28/20	.780
Puncture site, stomach/duodenum, n/N	138/154	115/129	23/25	.921
No. of passes, n/N				
2 or less	51	46/244	5/48	.163
3	220	179/244	41/48	.076
4 or more	21	19/244	2/48	.561

*P values are for the differences between tumors with or without an avascular area.

size of the nonenhancing area of the tumor (Fig. 1A and B). The enhancement patterns were assessed after the blood-pool phase of the perfusion image (40 seconds after the infusion of Sonazoid). CH-EUS data were stored in a recording system, and the sizes of the nonenhancing areas were measured afterward, while the images were being reviewed for the study. Two reviewers (K.M. and K.Y.) assessed the size of the maximum avascular area of the tumor during the CH-EUS video; this was accomplished by pausing the video at the time when the maximum avascular area was depicted and then measuring the avascular area on the still CH-EUS image. If the independent classifications of the 2 reviewers were discordant, they re-evaluated the videos together until agreement was reached.

The numbers of patients in the 3 groups with avascular areas of <5 mm, 5 to 10 mm, and >10 mm were 244, 44, and 4, respectively. Therefore, tumors with an avascular area were defined as those with a nonenhancing area of 5 mm or larger on CH-EUS.

EUS-FNA technique

After the CH-EUS examination, the imaging mode was changed to conventional mode, and EUS-FNA was performed using a linear array echoendoscope (GF-UCT 240 or GF-UCT 260; Olympus Optical, Tokyo, Japan). A 22-gauge FNA needle (EchoTip Ultra [Cook Medical, Bloomington, Ind, USA] or Expect [Boston Scientific, Marlborough, Mass, USA]) was used for all 292 cases. After the tumor had been punctured, the central stylet was removed and a 20-mL syringe with extension tubing was attached to the hub of the needle. Suction was then applied while moving the needle to and fro within the lesion 20 times. EUS-FNA was performed under conventional EUS imaging, using a fanning technique, which resulted in the whole area of the tumor being punctured, regardless of the evaluation of vascularity on CH-EUS. Thus, avoidance of the avascular area detected by CH-EUS was not enforced during EUS-FNA. Samples were processed for cytologic and histologic analysis; onsite evaluation was not performed.

Cytologic and histologic analysis

The samples obtained by EUS-FNA were subjected to cytologic and histologic analysis. Cell block was not performed for histologic analysis. The cytologic and histologic diagnoses were categorized as either malignant or inadequate for a diagnosis of malignancy. Malignancy was defined as the presence of numerous clusters of cells with a loss of polarity, enlarged (twice the normal) size, irregular nuclear membrane, small nucleoli, or single large cells. Inadequate was defined as an insufficient quantity of collected tissue.

Final diagnosis

In patients who underwent surgical resection of the mass, the final diagnosis was based on surgical pathology. In patients who did not undergo surgical resection, the final diagnosis was based on pathologic diagnosis obtained by EUS-FNA, pancreatic juice cytology under ERCP, and/or biopsy sampling of liver metastases, including during follow-up until the patients' time of death. Patients were diagnosed with malignancy if there were signs of disease progression. Thus, no patients were diagnosed with pancreatic adenocarcinoma without pathologic evidence.

Outcome measures

The overall sensitivity of EUS-FNA for the diagnosis of pancreatic adenocarcinoma was calculated. The sensitivities of cytology, histology, and the combination of cytology and histology were also evaluated. These variables were then individually evaluated according to 2 enhancement patterns (with or without an avascular area) to assess whether the diagnostic sensitivity of EUS-FNA for pancreatic adenocarcinoma was related to the presence of an avascular area within the tumors.

Statistical analysis

The sensitivity of EUS-FNA in the group without an avascular area on CH-EUS was compared with the sensitivity of EUS-FNA in the group with an avascular area. Categorical

TABLE 2. Results of EUS-FNA in the 292 patients with pancreatic adenocarcinomas

Results of EUS-FNA		Total % (n) (n = 292)	Without avascular area % (n) (n = 244)	With avascular area % (n) (n = 48)	P value*
Cytologic analysis	Histologic analysis†				
Malignant	Malignant	70.2 (205)	72.5 (177)	58.3 (28)	.049
Malignant	Inadequate	17.8 (52)	18.4 (45)	14.6 (7)	.523
Inadequate	Malignant	2.7 (8)	3.3 (8)	0 (0)	.430
Inadequate	Inadequate	9.2 (27)	5.7 (14)	27.1 (13)	<.001

EUS-FNA, EUS-guided FNA.

*P values are for the differences between tumors with or without an avascular area.

†Core biopsy samples (cell block was not performed for histologic analysis).

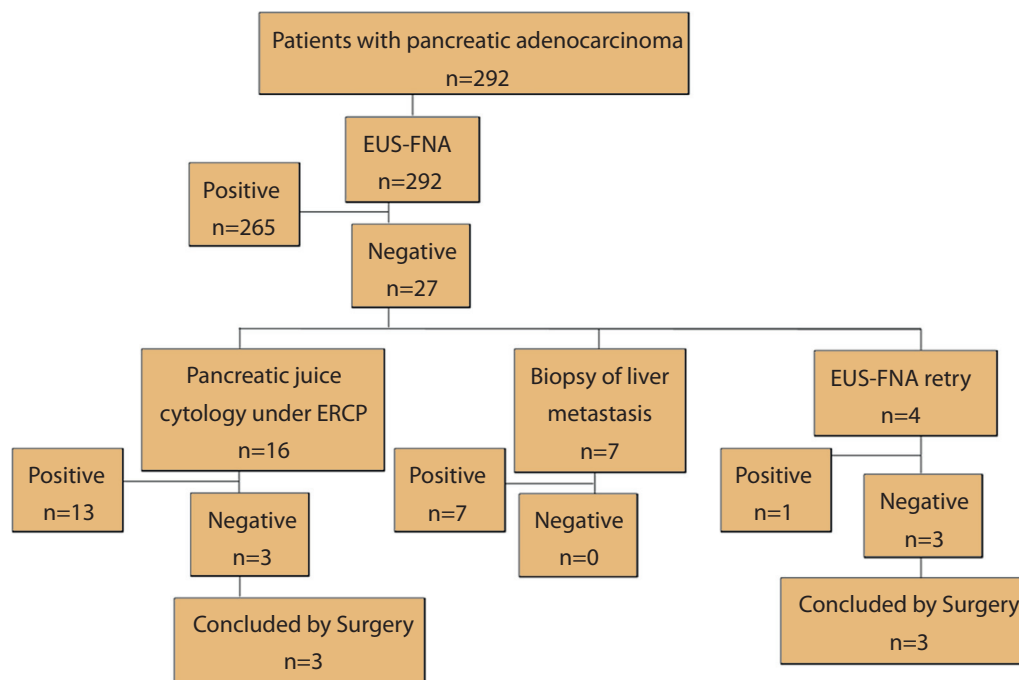


Figure 2. A flowchart demonstrating the routes by which the 292 patients were pathologically diagnosed. EUS-FNA, EUS-guided FNA.

and continuous variables were analyzed using χ^2 and *t* tests, respectively. All statistical analyses were performed using SAS software version 9.1 (SAS Institute, Cary, NC). A κ coefficient $>.8$ was considered to indicate very good interobserver agreement.

RESULTS

Avascular areas as defined above were present in 48 tumors and absent from 244. Analysis of the interobserver reproducibility on the avascular area status of tumors resulted in a κ coefficient of .89. The 2 groups (with and without avascular area) did not differ significantly in terms of their demographic characteristics, mean tumor size, location of the tumor, puncture site, and the number of passes (Table 1). For 89 patients the final diagnoses were

made on the basis of the histologic examination of resected specimens, whereas for 203 patients final diagnoses were made according to the clinical course/imaging analyses undertaken during follow-up.

The overall sensitivity of EUS-FNA was 90.8% (265/292; Table 2). The CH-EUS results for pancreatic adenocarcinoma were classified into 2 patterns according to the presence of an avascular area in the tumor. The sensitivities for lesions with and without an avascular area were 72.9% (35/48) and 94.3% (230/244), respectively, with this difference being statistically significant ($P < .001$).

The flowchart in Figure 2 demonstrates the routes by which the pathologic diagnoses were made in the 292 patients. Twenty-one of 27 EUS-FNA-negative cases were diagnosed with pancreatic adenocarcinoma, 13 by pancreatic juice cytology under ERCP, 7 by biopsy sampling of liver metastases, and 1 by a repeated EUS-FNA procedure.

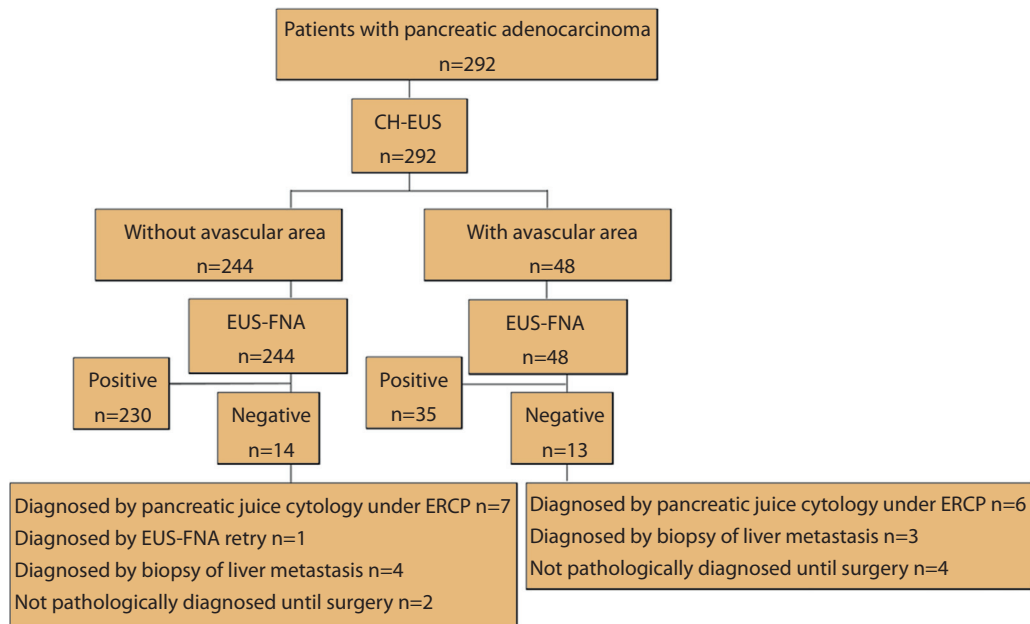


Figure 3. A flowchart demonstrating the routes by which the 292 patients were pathologically diagnosed, with further division according to the 2 groups with or without an avascular area on CH-EUS. CH-EUS, Contrast-enhanced harmonic EUS; EUS-FNA, EUS-guided FNA.

The remaining 6 cases that were not pathologically diagnosed before surgery were diagnosed after surgical resection.

The flowchart in [Figure 3](#) demonstrates the paths for pathologic diagnoses with the patients divided into 2 groups (with or without an avascular area on CH-EUS). An avascular area was present in 13 EUS-FNA–negative cases. Six of these cases were diagnosed by pancreatic cytology under ERCP, 3 cases were diagnosed by biopsy sampling of liver metastases, and 4 cases were diagnosed after surgical resection. Three of these 4 patients underwent a second EUS-FNA; however, this did not result in a firm diagnosis.

DISCUSSION

This study demonstrates that pancreatic adenocarcinoma with an avascular area on CH-EUS resulted in high rates of false-negative findings on EUS-FNA. Moreover, in such cases a diagnosis was not obtained, even when the EUS-FNA procedure was repeated. This indicates that the diagnostic accuracy of EUS-FNA for pancreatic adenocarcinoma with an avascular area may be low and that pancreatic juice cytology under ERCP and biopsy sampling of liver metastases should be considered as alternatives.

Kitano et al⁷ evaluated the enhancement of pancreatic tumors on CH-EUS and divided them into 3 patterns; hyper-, hypo-, and iso-enhancement. Hypoenhancement on CH-EUS was demonstrated to have a high sensitivity and specificity for the presence of ductal carcinomas. When EUS-FNA evaluation was combined with CH-EUS, the

combined diagnostic sensitivity for ductal carcinomas was raised from 92.2% to 100%. However, the purpose of this previous study was not to obtain more specific histologic evidence before patients underwent an operation. The evaluation of the 3 enhancement patterns reported by Kitano et al and the presence of an avascular area could present a new histologic diagnostic strategy for pancreatic adenocarcinoma.

D’Onofrio et al⁸ evaluated the enhancement of pancreatic adenocarcinomas on contrast-enhanced US and divided them into 4 patterns: markedly hypoechoic/hypovascular with an avascular intralesional area; hypoechoic/hypovascular; isoechoic/isovascular; and hyperechoic/hypervascular. They demonstrated the presence of a poorly vascularized tumor on contrast-enhanced US to be a predictor of high mortality. Moreover, they also used an image analysis technique to evaluate the mean vascular density and verify the qualitative data and found a positive correlation between contrast-enhanced US and mean vascular density; therefore, qualitative image analysis for the avascular area was demonstrated as reliable. This study also found very good interobserver agreement, with the κ coefficient for whether the tumor contained an avascular area or not being .89.

We believe that this is the first study to report that the presence of an avascular area on CH-EUS is related to a false-negative finding for pancreatic adenocarcinoma on EUS-FNA. Numata et al⁹ reported that avascular areas in pancreatic adenocarcinoma were related to severe fibrosis and necrosis within the lesion. This may be a reason for the high rates of false-negative findings on EUS-FNA in the group with an avascular area in this study. Seicean et al³ reported that avoidance of avascular areas

during EUS-FNA improved the diagnostic accuracy of EUS-FNA for pancreatic masses. By contrast, we used a fanning technique during EUS-FNA in all cases; in terms of decreasing the necessary passes required to obtain the pathologic diagnosis, a fanning technique during EUS-FNA is superior to the standard method without a fanning technique.¹⁰ Therefore, we were able to evaluate the influence of avascular area on the false-negative rate of EUS-FNA, because in this study the EUS-FNA technique was standardized. In the present study, only pancreatic adenocarcinomas diagnosed by pathologic findings were analyzed, and the sensitivity of EUS-FNA for the diagnosis of pancreatic adenocarcinoma was 90.8% overall. However, in the subgroup analysis the sensitivities for lesions with or without an avascular area were 72.9% and 94.3%, respectively, with the difference being statistically significant, even though the fanning technique was used in both groups. This indicates that in pancreatic adenocarcinoma with an avascular area, there may be difficulties in obtaining a sufficient sample by EUS-FNA, even if CH-EUS is used to avoid the avascular area during the EUS-FNA.

This study has several limitations. First, the study was retrospective, although the data used for analysis were derived from prospectively collected databases. Second, verification bias cannot be excluded, because the CH-EUS results may have influenced decisions on whether to perform EUS-FNA and/or surgery. Third, the presence of an avascular area on CH-EUS was analyzed in a subjective manner, and the number of patients with an avascular area was relatively small. Fourth, the study did not include a control group (patients who underwent EUS-FNA without CH-EUS). Finally, Kandel et al¹¹ recently reported the utility of a novel fork-tip needle for EUS-guided fine-needle biopsy sampling that showed excellent histologic yields. To investigate whether or not the avascular area should be avoided during EUS-guided fine-needle biopsy sampling as well as EUS-FNA, a further prospective randomized study of a large number of cases (eg, avoiding avascular areas vs the fanning technique), even using the novel EUS-guided fine-needle biopsy needle, is warranted.

In conclusion, EUS-FNA shows lower sensitivity for pancreatic adenocarcinoma with avascular areas on CH-EUS. If an avascular area is detected within a pancreatic

tumor on CH-EUS and the EUS-FNA results are inadequate for pathologic diagnosis, then alternative pathologic diagnostic methods such as pancreatic juice cytology under ERCP or biopsy sampling of liver metastases should be considered. Thus, the evaluation of the presence of an avascular area within a pancreatic tumor by CH-EUS may be useful for establishing the appropriate pathologic diagnostic strategy.

REFERENCES

1. Madhoun MF, Wani SB, Rastogi A, et al. The diagnostic accuracy of 22-gauge and 25-gauge needles in endoscopic ultrasound-guided fine needle aspiration of solid pancreatic lesions: a meta-analysis. *Endoscopy* 2013;45:86-92.
2. Fusaroli P, Spada A, Mancino MG, et al. Contrast harmonic echoendoscopic ultrasound improves accuracy in diagnosis of solid pancreatic masses. *Clin Gastroenterol Hepatol* 2010;8:629-34.
3. Seicean A, Badea R, Moldovan-Pop A, et al. Harmonic contrast-enhanced endoscopic ultrasonography for the guidance of fine-needle aspiration in solid pancreatic masses. *Ultraschall Med* 2017;38:174-82.
4. Sugimoto M, Takagi T, Hikichi T, et al. Conventional versus contrast-enhanced harmonic endoscopic ultrasonography-guided fine-needle aspiration for diagnosis of solid pancreatic lesions: a prospective randomized trial. *Pancreatol* 2015;15:538-41.
5. Romagnuolo J, Hoffman B, Vela S, et al. Accuracy of contrast-enhanced harmonic EUS with a second-generation perflutren lipid microsphere contrast agent (with video). *Gastrointest Endosc* 2010;73:52-63.
6. Miyata T, Kitano M, Omoto S, et al. Contrast-enhanced harmonic endoscopic ultrasonography for assessment of lymph node metastases in pancreaticobiliary carcinoma. *World J Gastroenterol* 2016;22:3381-91.
7. Kitano M, Kudo M, Yamao K, et al. Characterization of small solid tumors in the pancreas: the value of contrast-enhanced harmonic endoscopic ultrasonography. *Am J Gastroenterol* 2012;107:303-10.
8. D'Onofrio M, Zamboni GA, Malagò R, et al. Resectable pancreatic adenocarcinoma: is the enhancement pattern at contrast-enhanced ultrasonography a pre-operative prognostic factor? *Ultraschall Med Biol* 2009;35:1929-37.
9. Numata K, Ozawa Y, Kobayashi N, et al. Contrast-enhanced sonography of pancreatic carcinoma: correlations with pathological findings. *J Gastroenterol* 2005;40:631-40.
10. Bang JY, Magee SH, Ramesh J, et al. Randomized trial comparing fanning with standard technique for endoscopic ultrasound-guided fine-needle aspiration of solid pancreatic mass lesions. *Endoscopy* 2013;45:445-50.
11. Kandel P, Tranesh G, Nassar A, et al. EUS-guided fine needle biopsy sampling using a novel fork-tip needle: a case-control study. *Gastrointest Endosc* 2016;84:1034-9.



Orantinib versus placebo combined with transcatheter arterial chemoembolisation in patients with unresectable hepatocellular carcinoma (ORIENTAL): a randomised, double-blind, placebo-controlled, multicentre, phase 3 study

Masatoshi Kudo, Ann-Lii Cheng, Joong-Won Park, Jae Hyung Park, Po-Chin Liang, Hisashi Hidaka, Namiki Izumi, Jeong Heo, Youn Jae Lee, I-Shyan Sheen, Chang-Fang Chiu, Hitoshi Arioka, Satoshi Morita, Yasuaki Arai

Summary

Background Orantinib is an oral multi-kinase inhibitor. This study was done to evaluate the efficacy of orantinib combined with conventional transcatheter arterial chemoembolisation (cTACE) in patients with unresectable hepatocellular carcinoma.

Methods This randomised, double-blind, placebo-controlled, phase 3 study was done at 75 sites in Japan, South Korea, and Taiwan. Patients with unresectable hepatocellular carcinoma, no extra-hepatic tumour spread, and Child-Pugh score of 6 or less were randomly assigned (1:1) by interactive web response system using a computer-generated sequence to receive orantinib or placebo, within 28 days of cTACE. Randomisation was stratified by region, Child-Pugh score (5 vs 6), alpha fetoprotein concentrations (<400 ng/mL vs ≥400 ng/mL), and size of the largest lesion (≤50 mm vs >50 mm). Orantinib at 200 mg, twice per day, or placebo was given orally until TACE failure or unacceptable toxicity. The patients, investigators, and study personnel were masked to treatment assignment. The primary endpoint was overall survival, analysed in the full analysis set (patients who had received at least one dose of study drug). This study is registered at ClinicalTrials.gov, number NCT01465464, and has been terminated.

Findings Between Dec 10, 2010, and Nov 21, 2013, 889 patients were randomly assigned to receive either orantinib (445 patients; 444 treated) or placebo (444 patients; all treated). The study was ended at interim analysis for futility evaluation. Median follow-up was 17·3 months (IQR 11·3–26·4). There was no improvement in overall survival with orantinib compared with placebo (median 31·1 months [95% CI 26·5–34·5] vs 32·3 months [28·4–not reached]; hazard ratio 1·090, 95% CI 0·878–1·352; p=0·435). The main adverse events in the orantinib group were oedema, ascites, and elevation of aspartate and alanine aminotransferases. The most frequent adverse events of grade 3 or worse in the orantinib group included elevated aspartate aminotransferase (189 [43%] patients in the orantinib group, 161 [36%] patients in the placebo group), elevated alanine aminotransferase (150 [34%] patients in the orantinib group, 132 [30%] patients in the placebo group), and hypertension (47 [11%] patients in the orantinib group, 39 [9%] patients in the placebo group). Serious adverse events were reported in 200 (45%) patients in the orantinib group and 134 (30%) patients in the placebo group.

Interpretation Orantinib combined with cTACE did not improve overall survival in patients with unresectable hepatocellular carcinoma.

Funding Taiho Pharmaceutical.

Introduction

Hepatocellular carcinoma is the fifth most common cancer in men and the seventh in women worldwide.¹ Standard treatments for hepatocellular carcinoma include surgical therapies (resection and liver transplantation), locoregional therapies (radiofrequency ablation and transcatheter arterial chemoembolisation [TACE]), and systemic chemotherapy. However, systemic therapy, except sorafenib and regorafenib, has failed to improve survival in patients with advanced hepatocellular carcinoma.^{2–5}

Conventional TACE (cTACE) is the most widely used primary treatment for intermediate hepatocellular carcinoma and has been shown to improve survival.^{6,7} However, it is not a curative treatment, and its

disadvantages include liver function deterioration, incomplete tumour necrosis, and the potential risk of extra-hepatic metastasis. Therefore, new techniques and embolisation agents for TACE are being developed.^{8,9}

In hepatocellular carcinoma, angiogenesis is important for tumour growth, and the process is regulated by angiogenic factors.¹⁰ Expression of VEGF has been associated with aggressive tumour behaviour, early metastatic spread, and poor prognosis.^{11–14} In particular, TACE promotes angiogenesis in the residual tumours through VEGF upregulation resulting from the hypoxic insult.¹⁵ Consequently, several randomised trials have been done to evaluate TACE combined with molecularly targeted agents to improve the efficacy of TACE.¹⁶

Lancet Gastroenterol Hepatol 2018; 3: 37–46

Published Online

October 4, 2017

[http://dx.doi.org/10.1016/S2468-1253\(17\)30290-X](http://dx.doi.org/10.1016/S2468-1253(17)30290-X)

S2468-1253(17)30290-X

See [Comment](#) page 5

Department of Gastroenterology and Hepatology, Kindai University Faculty of Medicine, Osaka, Japan (Prof M Kudo MD); Department of Oncology (Prof A-L Cheng MD) and Division of Abdomen Radiology (P-C Liang MD), National Taiwan University Hospital, Taipei City, Taiwan; Center for Liver Cancer, National Cancer Center Korea, Gyeonggi-do, South Korea (J-W Park MD); Department of Radiology, Seoul National University Hospital, Seoul and Department of Radiology, Myongji Hospital, Gyeonggi-do, South Korea (J H Park MD); Department of Gastroenterology, Internal Medicine, Kitasato University School of Medicine, Kanagawa, Japan (H Hidaka MD); Department of Gastroenterology and Hepatology, Musashino Red Cross Hospital, Tokyo, Japan (N Izumi MD); Department of Internal Medicine, College of Medicine, Pusan National University and Medical Research Institute, Pusan National University Hospital, Busan, South Korea (Y Heo MD); Division of Gastroenterology, Inje University Busan Paik Hospital, Busan, South Korea (Y J Lee MD); Department of Hepato-gastroenterology, Chang Gung Memorial Hospital—Linkou, Taoyuan County, Taiwan (I-S Sheen MD); Division of Hematology/Oncology, China Medical University Hospital, Taichung

City, Taiwan (C-F Chiu MD);
Department of Medical
Oncology, Yokohama Rosai
Hospital, Kanagawa, Japan
(H Arioka MD); Department of
Biomedical Statistics and
Bioinformatics, Kyoto
University Graduate School of
Medicine, Kyoto, Japan
(S Morita PhD); and
Department of Diagnostic
Radiology, National Cancer
Center Hospital, Tokyo, Japan
(Y Arai MD)

Correspondence to:
Prof Masatoshi Kudo,
Department of Gastroenterology
and Hepatology, Kindai University
Faculty of Medicine 377-2,
Ohno-Higashi, Osaka-Sayama,
Osaka 589-8511, Japan
m-kudo@med.kindai.ac.jp

Research in context

Evidence before this study

We searched PubMed and abstracts of major oncology congresses with keywords including “hepatocellular carcinoma”, “HCC”, “molecular targeted therapies”, and “TACE” for papers published between Jan 1, 2008, and Dec 31, 2014. The search was restricted to articles published in English. We found no evidence that molecularly targeted therapies in combination with transcatheter arterial chemoembolisation (TACE) have shown clinical benefit in intermediate hepatocellular carcinoma.

Added value of this study

In patients with unresectable intermediate hepatocellular carcinoma, combination therapy of orantinib and TACE was not superior to placebo and TACE in terms of overall survival.

Implications of all the available evidence

TACE is the most widely used primary treatment for intermediate hepatocellular carcinoma and has been shown to improve survival. However, TACE is not a curative treatment, its efficacy is limited, and there is a potential risk of extra-hepatic metastasis. More refined trial designs, more applicable endpoints, and concomitant use of more potent and less toxic molecularly targeted agents should be explored in future TACE combination trials.

The results from three such trials (SPACE, Brisk TA, and TACE 2) have been reported.^{17–19} Although there were differences in trial design, agent used (sorafenib in SPACE and TACE 2, or brivanib in BRISK TA), location (the USA and Asia in SPACE, global in BRISK TA, or the UK in TACE 2), and primary endpoint (time to progression in SPACE, overall survival in BRISK TA, progression-free survival in TACE2), the results of those trials were all negative.

Orantinib (TSU-68; Taiho Pharmaceutical, Tokyo, Japan) is a small-molecule, orally administered, multiple-receptor tyrosine kinase inhibitor of VEGF receptor-2 and platelet-derived growth factor (PDGF) receptor- β .^{20–22} Orantinib has shown preliminary efficacy and a good safety profile in advanced hepatocellular carcinoma.^{23,24} A phase 2 study showed that orantinib combined with a single TACE seemed to prolong progression-free survival, but this observation was not statistically significant, and overall survival did not improve.²⁵ The adverse event profile of orantinib is different to other molecularly targeted agents; hand–foot syndrome and hypertension, which are frequently observed with sorafenib and brivanib, are rarely recorded with orantinib. Therefore, we did a randomised, double-blind, placebo-controlled phase 3 trial to evaluate the efficacy of orantinib combined with cTACE in patients with advanced hepatocellular carcinoma.

Methods

Study design and participants

The present study was designed as a randomised, multicentre, double-blind, placebo-controlled phase 3 study (ORIENTAL) at 75 sites in Japan, South Korea, and Taiwan. Eligibility criteria included: histologically confirmed hepatocellular carcinoma or confirmed based on a typical imaging profile with at least one contrast enhanced CT or MRI (a malignant lesion that has a higher density or intensity than the surrounding hepatic parenchyma in the arterial phase, and a lower density or intensity than the surrounding hepatic parenchyma in

the portal venous or equilibrium phase), and presented without advanced vascular invasion to the portal vein (Vp3, Vp4), hepatic vein (Vv3), or bile duct (B3, B4); and no extra-hepatic spread but four or more viable intra-hepatic lesions (with at least one lesion >1 cm diameter), two to three viable intra-hepatic lesions (with at least one lesion >3 cm diameter), or one viable intra-hepatic lesion measuring more than 5 cm diameter. Other inclusion criteria were no local therapy during the 120 days before the first TACE, no indications for treatment with curative hepatic resection or percutaneous local therapy, Child-Pugh score of 6 or less, Eastern Cooperative Oncology Group (ECOG) performance status of 0 or 1, age of 20 years or older, and sufficient organ function (white blood cell count ≥ 3000 cells per μL or neutrophil count ≥ 1500 cells per μL ; platelet count ≥ 50000 per μL ; haemoglobin ≥ 8.0 g/dL; aspartate aminotransferase [AST] and alanine aminotransferase [ALT] ≤ 5 times the upper limit of normal [ULN]; total bilirubin < 2.0 mg/dL; serum albumin ≥ 3.0 g/dL; serum creatinine < 1.5 mg/dL; prothrombin time-international normalised ratio < 2.0). Both patients who had no history of TACE and those who were previously treated with TACE were eligible because the prognosis of patients with hepatocellular carcinoma who are eligible for TACE is considered to be almost the same regardless of the history of TACE if tumour characteristics met inclusion criteria (largest diameter, number of lesions, and the 120-day wash-out period from previous treatment for hepatocellular carcinoma including TACE).

Patients were excluded only if they had a diffuse type of hepatocellular carcinoma, a history of liver transplantation, were receiving an anti-angiogenic agent, had ascites, pleural effusion, or pericardial fluid uncontrollable with diuretic therapy, clinical symptoms of hepatic encephalopathy, active infection, or uncontrolled serious infection (excluding chronic hepatitis). All patients provided written informed consent before the initiation of any study-specific procedures.

The study was approved by the institutional review board of each participating hospital and was done in accordance with the principles of the Declaration of Helsinki and Good Clinical Practice Guidelines.

Randomisation and masking

Patients were randomly assigned in a 1:1 ratio to receive either cTACE combined with 200 mg of orantinib twice daily or cTACE with placebo. Randomisation was stratified by region, Child-Pugh score (5 vs 6), alpha fetoprotein concentrations (<400 ng/mL vs ≥400 ng/mL), and size of the largest lesion (≤50 mm vs >50 mm). Treatment assignment was done centrally via an interactive web response system using a computer-generated sequence, generated by EPS (Tokyo, Japan). A minimisation method was used, which included a random component, with 80% probability of assigning a patient to the preferred group. During the study, the treatment assignment was unknown to all patients, investigators, and ancillary study personnel. To maintain masking, orantinib and placebo tablets were identical in appearance.

Procedures

Study drugs were initiated when patients met treatment initiation criteria (AST or ALT ≤5 times the ULN, total bilirubin ≤2.5 mg/dL, serum albumin ≥2.8 g/dL) between days 3 and 28 after the first (and any subsequent) cTACE, and patients who were unable to receive study drugs within 28 days after the first (and any subsequent) cTACE were withdrawn from the study. Interruption of drug administration and up to two dose reductions (first to 200 mg once daily and second to 200 mg every 2 days) were permitted in cases of adverse events such as elevation of AST or ALT concentrations to more than ten times the ULN, grade 3 or worse total bilirubin, oedema, and effusion, or other adverse events, at the investigator's discretion. Treatment continued until the occurrence of radiological progression or unacceptable adverse events.

cTACE involved the concurrent use of lipiodol, embolisation materials (eg, gelatin sponges, porous gelatin particles, polyvinyl alcohol sponges, drug-eluting beads, etc), and anti-tumour drugs (only approved drugs could be used) as mandatory. To chemoembolise all arteries feeding viable lesions and prevent impairment of non-cancerous liver tissues, super selective cTACE was recommended. Subsequent cTACE could be done on demand as necessary when the treating physician suspected unsatisfactory tumour necrosis, local recurrence of tumour in previously treated areas, or new intra-hepatic lesions based on any of the imaging studies done during the treatment period, and the interval of subsequent cTACE was not defined. cTACE was discontinued in cases of an uncontrollable intra-hepatic lesion, damage to the hepatic artery that prevented treatment for hepatocellular carcinoma, severe vascular invasion that made additional cTACE impossible, extra-hepatic spread that could affect a patient's life

expectancy and thus required other hepatocellular carcinoma treatment modalities, or liver function at Child-Pugh class C lasting for 28 days.

Assessment for vital signs, bodyweight, ECOG performance status, Child-Pugh score, and clinical laboratory analyses were done at screening, 14, 28, and 42 days after the first (and any subsequent) cTACE, every 28 days thereafter, and 30 days after the final dose of the study drug. Tumour was assessed via CT or MRI within 28 days before the first cTACE, 42 days after the first (and any subsequent) cTACE, and every 56 days thereafter. Blood samples for measuring endothelial cell markers were collected within 14 days before the first cTACE. The concentrations of PDGF-BB and VEGF-C were determined using an enzyme-linked immunosorbent assays kit (R&D Systems, Minneapolis, MN, USA). No restrictions were placed on use of post-treatment therapies.

Outcomes

The primary endpoint was overall survival. Secondary endpoints were time to TACE failure (originally described in the protocol as time to TACE discontinuation; the two are identical in nature), time to treatment failure, time to progression, time to appearance of extra-hepatic spread or vascular invasion, safety, and biomarker analysis. Overall survival was defined as the period from the date of enrolment to that of death. Time to TACE failure was defined as the period from the date of enrolment to that of meeting TACE discontinuation criteria. Time to treatment failure was defined as the period from the date of enrolment to that of completion of the study medication. Time to progression was defined as the period from the date of enrolment to that of the first observation of progressive disease. Time to appearance of extra-hepatic spread or vascular invasion was defined as the period from the date of enrolment to that of appearance of extra-hepatic spread or advanced vascular invasion. Adverse events were graded according to the National Cancer Institute Common Terminology Criteria for Adverse Events version 4.02.

Statistical analysis

Efficacy was analysed in the full analysis set, defined as all patients with hepatocellular carcinoma who received at least one dose of the study drug. Safety was analysed for the patients who received at least one dose of the study drug. We expected the median time to event would be 19 months in the placebo group and 23.6 months in the experimental group with a minimum 3 years of follow-up; the study was designed to detect a hazard ratio (HR) of 0.8 for overall survival in favour of orantinib, assuming 2.5 years of enrolment and 3 years of follow-up plus the assumed median times to event in each arm, requiring 668 patient deaths. On the basis of a two-sided significance α level of 5% and 80% power, we calculated that approximately 880 patients would need to be randomly assigned. Two interim analyses for safety evaluation and a

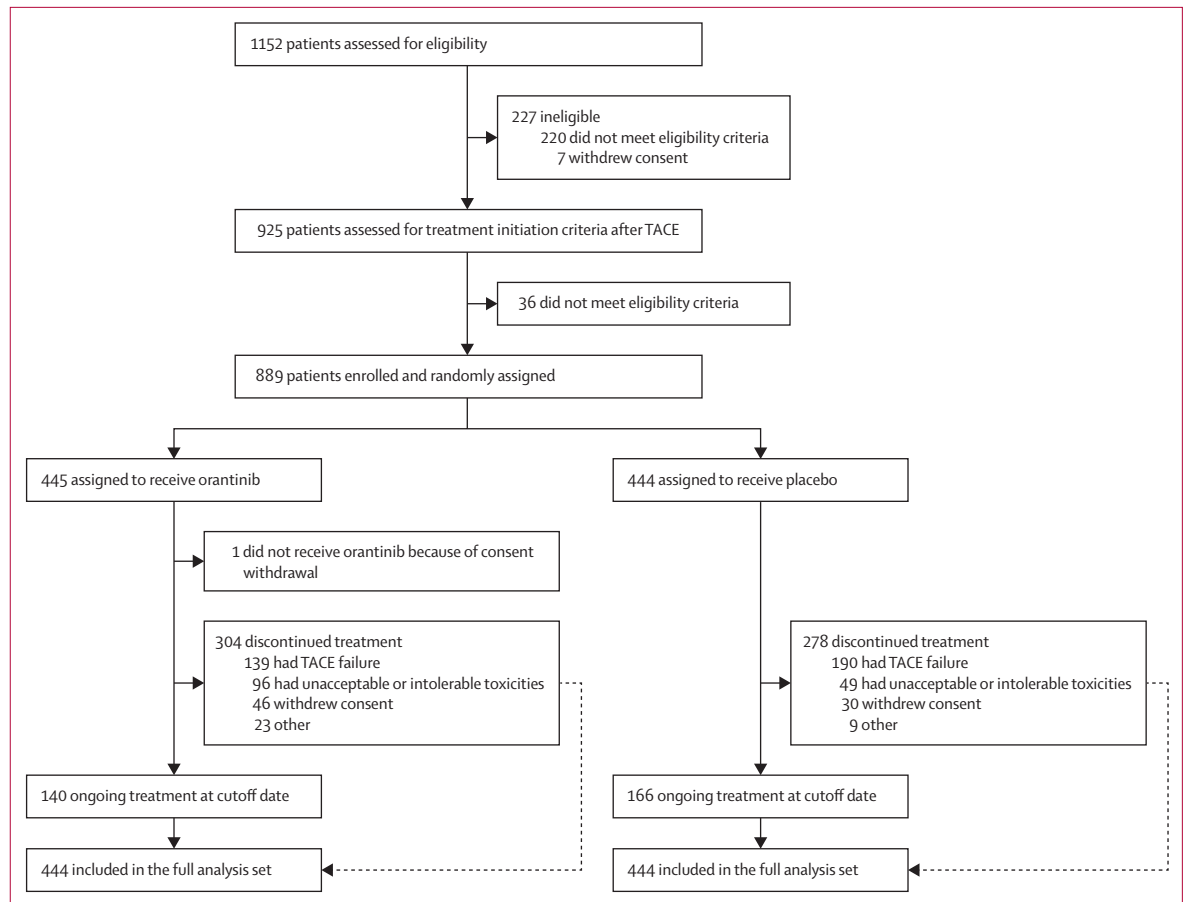


Figure 1: Trial profile

TACE=transcatheter arterial chemoembolisation.

third analysis for futility evaluation of the orantinib group relative to the placebo group were done by an independent data monitoring committee in an open-label fashion as originally planned.

Median overall survival and time to TACE failure were assessed using the Kaplan-Meier method, and 95% CIs were calculated. Groups were compared with a stratified log-rank test. The HRs of the treatment group and its 95% CIs were calculated by Cox's proportional hazard model using the treatment group only as a covariate.

The HRs and 95% CIs of overall survival and time to TACE failure were determined for different trial regions, Child-Pugh score, Barcelona Clinic Liver Cancer (BCLC) staging,^{26,27} sex, age, ECOG performance status, and aetiology, comparing the orantinib group with the placebo group, and a forest plot was prepared for such an analysis.

Subgroup analysis of the median overall survival and time to TACE failure according to biomarker concentrations was also done. To assess the association of PDGF-BB or VEGF-C expression with overall survival and time to TACE failure, the concentrations of each factor were categorised as low or high according to the respective median values. Median overall survival and time to TACE

failure was calculated from patient subgroups with baseline concentrations of each biomarker that were less than or greater than the median baseline values.

All reported p values are two sided, and p values of less than 0.05 were deemed significant. All analyses were done with SAS version 9.2. This study is registered with ClinicalTrials.gov, number NCT01465464.

Role of funding source

The funder of the study was involved in study design, data collection, data analysis, data interpretation, writing of the report, and the decision to submit the report for publication. The corresponding author had full access to all the data in the study and had final responsibility for the decision to submit.

Results

Between Dec 10, 2010, and Nov 21, 2013, 889 patients were randomly assigned to receive either orantinib (n=445) or placebo (n=444) at 41 sites in Japan, 21 sites in South Korea, and 13 sites in Taiwan. One patient in the orantinib group was excluded from the efficacy and safety analysis because the patient did not take the study drug due to withdrawal

of consent (figure 1). 444 patients in the orantinib group and all 444 patients in the placebo group received at least one dose of either orantinib or placebo, respectively, and were used for the analysis of efficacy and safety.

In this study, we did the planned third interim analysis using March 31, 2014, as the cutoff date. The independent data monitoring committee recommended early trial termination for futility. Thus, efficacy and safety were analysed using June 6, 2014, as the cutoff date. Median follow-up was 17.3 months (IQR 11.3–26.4).

There were no differences between the two groups with respect to demographic characteristics (table 1). About half of patients were categorised with BCLC stage B; around a third of patients were BCLC stage A. In each treatment group, the median age of patients from South Korea and Taiwan was about 10 years younger than that of patients from Japan. The major aetiology was hepatitis C virus infection in Japan, hepatitis B virus infection in South Korea, and either infection in almost equal proportion in Taiwan. The number of patients with previous TACE was greater in Japan than in South Korea or Taiwan (appendix p 3).

By the cutoff date, 582 patients had discontinued study treatment, including 304 in the orantinib group and 278 in the placebo group (figure 1). The median duration of treatment was 10.9 months (IQR 5.7–18.2) in the orantinib group and 12.3 months (7.0–19.9) in the placebo group. Dose reduction occurred in 172 (39%) of 444 patients in the orantinib group and 47 (11%) of 444 patients in the placebo group; dose reduction according to region is shown in the appendix (p 5). Mean treatment compliance was 81.1% (SD 22.6) in the orantinib group and 94.7% (10.6) in the placebo group. Post-study treatments, such as systemic chemotherapy, TACE, radiation therapy, and radiofrequency ablation were given to 174 (57%) of 304 patients who discontinued study treatment in the orantinib group and 184 (66%) of 278 patients who discontinued study treatment in the placebo group (appendix p 9). However, because the study was terminated early, the data were not mature and 306 (35%) of 888 patients remained on the study treatment at the time of termination.

Given that around 35% of patients who were randomly assigned were still receiving protocol treatment and over 60% were alive at study termination, and only four patients had been lost to follow-up, many patients were censored on the event of overall survival. Median overall survival was 31.1 months (95% CI 26.5–34.5) in the orantinib group and 32.3 months (28.4–not reached) in the placebo group. Orantinib did not improve overall survival (HR 1.090, 95% CI 0.878–1.352; $p=0.435$; figure 2A). Median time to TACE failure was 23.9 months (95% CI 19.8–26.7) in the orantinib group and 19.8 months (17.7–23.8) in the placebo group (HR 0.887, 95% CI 0.725–1.086; $p=0.245$; figure 2B). Median time to treatment failure was 10.9 months (95% CI 9.8–12.1) in the orantinib group and 12.3 months (10.9–13.4) in the

	Orantinib (n=444)	Placebo (n=444)
Sex		
Male	363 (82%)	364 (82%)
Female	81 (18%)	80 (18%)
Age (years)		
Mean (SD)	66.2 (10.2)	65.4 (10)
Median (IQR)	67 (59–75)	66 (59–73)
Range (min–max)	28–86	29–87
ECOG PS		
0	401 (90%)	406 (91%)
1	43 (10%)	38 (9%)
HCC stage		
I	5 (1%)	3 (1%)
II	141 (32%)	139 (31%)
III	272 (61%)	271 (61%)
IV A	26 (6%)	31 (7%)
BCLC stage*		
O	10 (2%)	13 (3%)
A	148 (33%)	122 (27%)
B	209 (47%)	229 (52%)
C	74 (17%)	72 (16%)
Vascular invasion to the portal vein	34 (8%)	37 (8%)
Child-Pugh score		
5	326 (73%)	328 (74%)
6	118 (27%)	116 (26%)
Previous TACE	173 (39%)	186 (42%)
HBsAg		
Positive	170 (38%)	202 (45%)
Negative	274 (62%)	242 (55%)
HBsAb*		
Positive	108 (24%)	90 (20%)
Negative	336 (76%)	353 (79%)
HBcAb*		
Positive	313 (70%)	304 (68%)
Negative	130 (29%)	139 (31%)
HCV*		
Positive	193 (43%)	165 (37%)
Negative	251 (57%)	275 (62%)

Data are n (%) unless otherwise stated. ECOG PS=Eastern Cooperative Oncology Group performance status. HCC=hepatocellular carcinoma. BCLC=Barcelona Clinic Liver Cancer. TACE=transcatheter arterial chemoembolisation. HBsAg=surface antigen of the hepatitis B virus. HBsAb=hepatitis B surface antibody. HBcAb=hepatitis B core antibody. HCV=hepatitis C virus. *Data were not available for all patients.

Table 1: Baseline patient characteristics

See Online for appendix

placebo group (HR 1.194, 95% CI 1.046–1.363; $p=0.0086$; figure 2C). Median time to progression was 2.9 months (95% CI 2.8–3.0) in the orantinib group and 2.5 months (1.4–2.9) in the placebo group (HR 0.858, 95% CI 0.744–0.990; $p=0.0356$; figure 2D). Median times to appearance of extra-hepatic spread or vascular invasion in the orantinib and placebo groups were not reached (HR 0.959, 95% CI 0.728–1.265; $p=0.7674$; figure 2E).

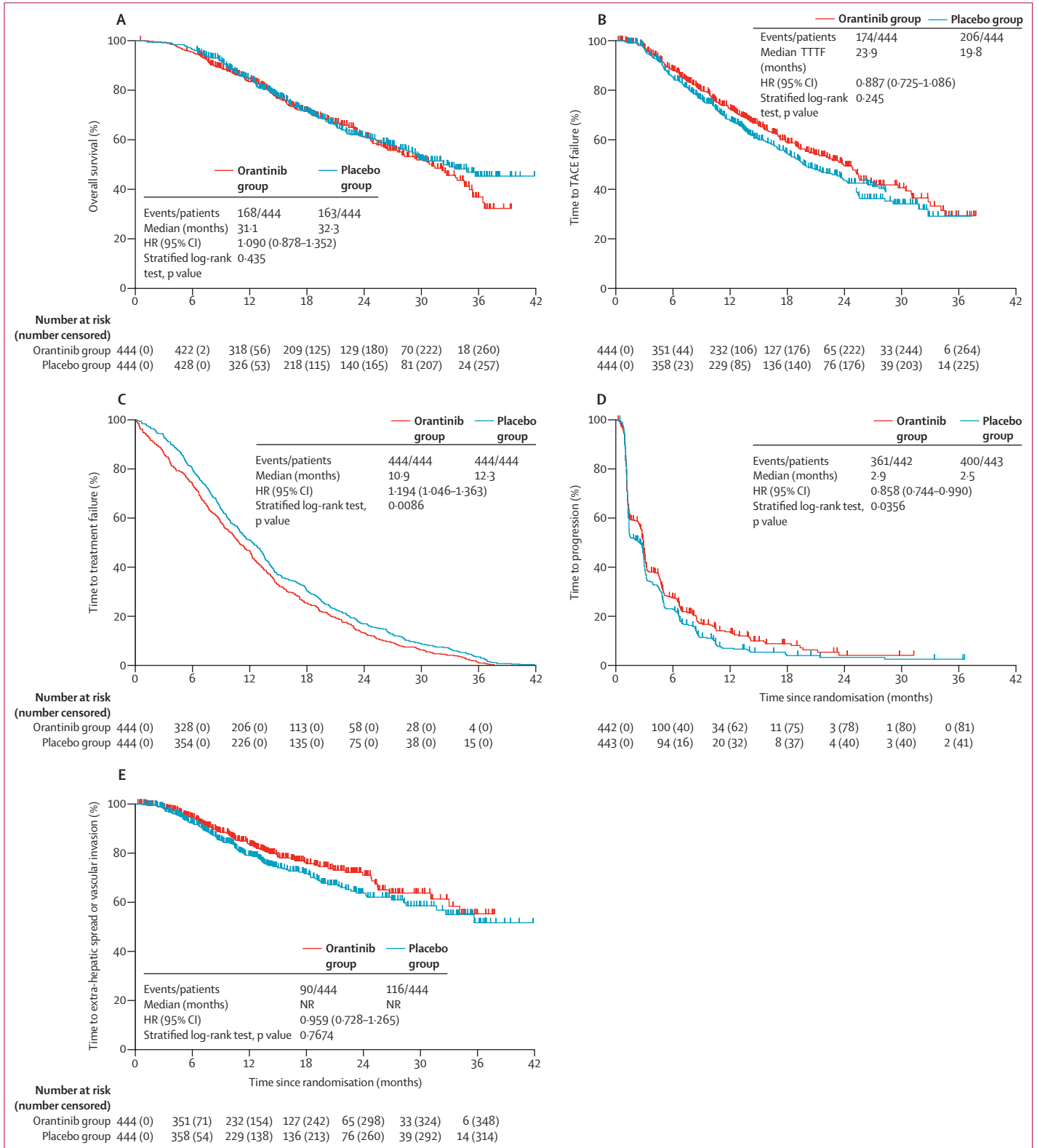


Figure 2: Kaplan-Meier curves

Overall survival (A), time to TACE failure (B), time to treatment failure (C), time to progression (D), and time to appearance of extra-hepatic spread or vascular invasion (E) for all three regions. HR=hazard ratio. NR=not reached. TACE=transcatheter arterial chemoembolisation. TTF=time to TACE failure.

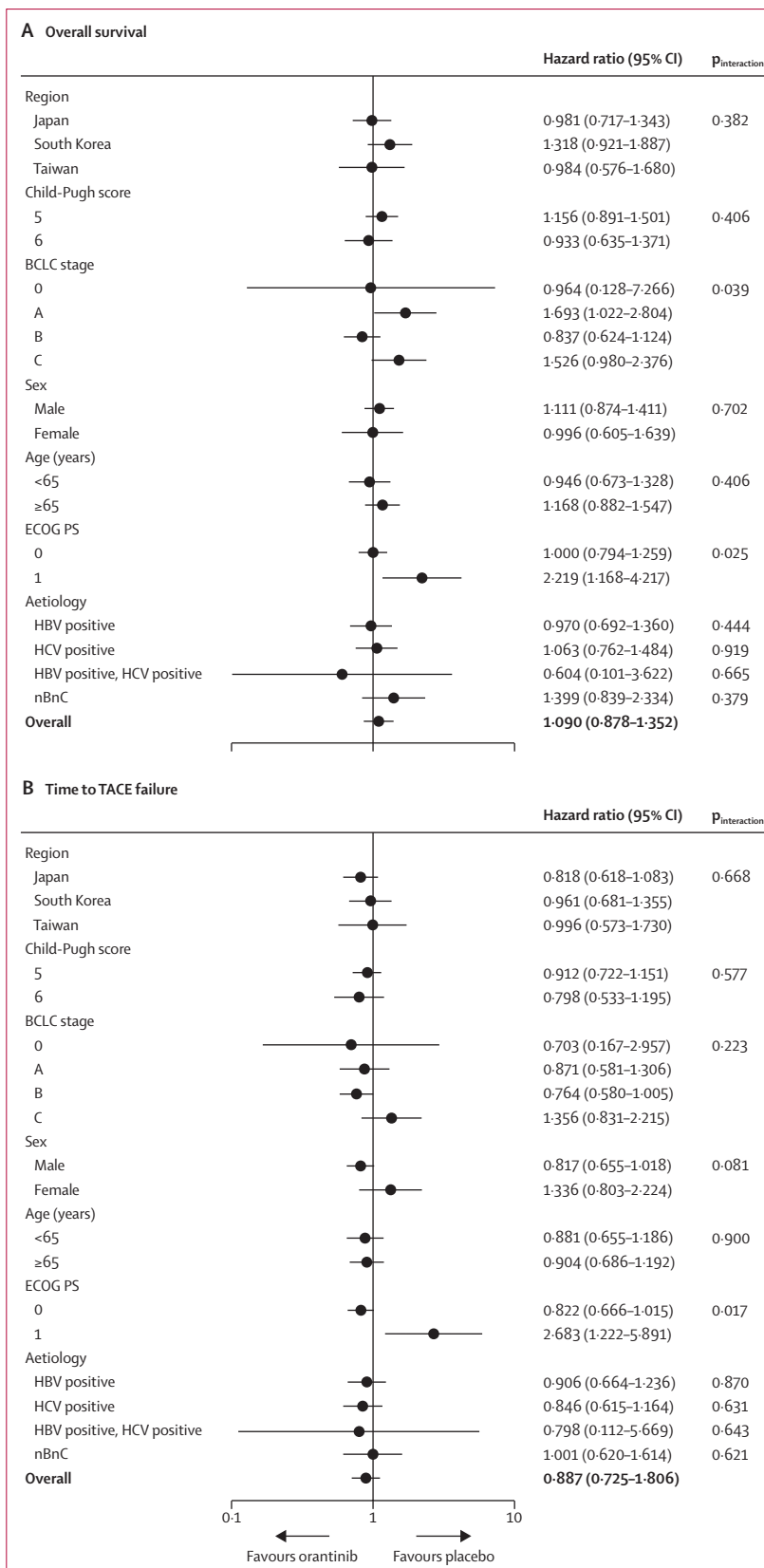
We did a post-hoc subgroup analysis for overall survival comparing patients with or without vascular invasion (V_0 vs V_p). In patients with vascular invasion, median overall survival was 13.0 months (95% CI 8.9–35.1) in the orantinib group and 16.0 months (12.6–32.3) in the placebo group (HR 1.328, 95% CI 0.727–2.428). In patients without vascular invasion, median overall survival was 31.4 months (95% CI 28.0–34.5) in the orantinib group and 34.8 months (29.1–not reached) in the placebo group (HR 1.081, 0.858–1.363; appendix p 21). When stratified by region, the HR for overall survival in Japan was 0.981 (95% CI 0.717–1.343; $p=0.906$), for South Korea it was 1.318 (0.921–1.887; $p=0.129$), and for Taiwan it was 0.984 (0.576–1.680; $p=0.953$; appendix pp 22, 23). The HR for time to TACE failure in Japan was 0.818 (95% CI 0.618–1.083; $p=0.160$), in South Korea it was 0.961 (0.681–1.355; $p=0.819$), and in Taiwan it was 0.996 (0.573–1.730; $p=0.988$; appendix pp 24, 25).

The number of cTACE procedures after randomisation including first TACE was 3.2 (SD 2.4) in the orantinib group and 3.7 (2.4) in the placebo group. The median interval between the first and second TACE was 98.0 days (IQR 59.0–170.5) in the orantinib group and 91.0 days (60.0–175.0) in the placebo group; median times to repeated TACE are shown in the appendix (p 6); the interval to subsequent TACE was longer in Japan than in South Korea and Taiwan (appendix p 6).

Figure 3 presents subgroup analyses of overall survival and time to TACE failure according to seven baseline characteristics identified by a Cox's proportional hazard model as being associated with overall survival and time to TACE failure. Median overall survival and time to TACE failure stratified by plasma concentrations of VEGF-C and PDGF-BB were also evaluated. In patients with PDGF-BB at or above the median, median overall survival was 30.8 months (95% CI 23.2–34.5) in the orantinib group and 33.0 months (27.2–not reached) in the placebo group (HR 1.259, 95% CI 0.925–1.713; $p=0.1432$); the corresponding median time to TACE failure was 20.8 months (17.2–25.2) in the orantinib group and 18.8 months (15.9–27.6) in the placebo group (HR 0.974, 0.736–1.289; $p=0.8549$). In patients with PDGF-BB less than the median, the median overall survival was 32.7 months (95% CI 26.1–36.5) in the orantinib group and 30.2 months (25.6–not reached) in the placebo group (HR 0.950, 95% CI 0.702–1.286; $p=0.7396$); the corresponding median time to TACE failure was 25.5 months (22.1–34.5) in the orantinib group and 20.2 months (17.7–24.3) in the placebo group (HR 0.800, 0.597–1.072; $p=0.1350$). In patients with VEGF-C at or

Figure 3: Subgroup analyses

Forest plot of hazard ratios for overall survival (A) and time to TACE failure (B) according to demographic and disease characteristics. BCLC=Barcelona Clinic Liver Cancer. ECOG PS=Eastern Cooperative Oncology Group performance status. HBV=hepatitis B virus. HCV=hepatitis C virus. nBnC=non-B non-C hepatitis. TACE=transcatheter arterial chemoembolisation.



	All grades		Grade ≥ 3	
	Orantinib group (n=444)	Placebo group (n=444)	Orantinib group (n=444)	Placebo group (n=444)
Abdominal pain	317 (71%)	292 (66%)	27 (6%)	10 (2%)
Pyrexia	264 (59%)	284 (64%)	2 (<1%)	3 (1%)
Aspartate aminotransferase increased	223 (50%)	189 (43%)	189 (43%)	161 (36%)
Decreased appetite	209 (47%)	149 (34%)	16 (4%)	11 (2%)
Alanine aminotransferase increased	200 (45%)	170 (38%)	150 (34%)	132 (30%)
Constipation	179 (40%)	147 (33%)	1 (<1%)	..
Nausea	173 (39%)	179 (40%)	2 (<1%)	2 (<1%)
Ascites	140 (32%)	73 (16%)	18 (4%)	17 (4%)
Facial oedema	138 (31%)	8 (2%)	4 (1%)	1 (<1%)
Peripheral oedema	130 (29%)	59 (13%)	2 (<1%)	..
Vomiting	126 (28%)	116 (26%)	6 (1%)	2 (<1%)
Diarrhoea	123 (28%)	70 (16%)	12 (3%)	10 (2%)
Fatigue	101 (23%)	92 (21%)	2 (<1%)	3 (1%)
Malaise	101 (23%)	86 (19%)	5 (1%)	..
Hypoalbuminaemia	98 (22%)	85 (19%)	7 (2%)	3 (1%)
Back pain	90 (20%)	94 (21%)	3 (1%)	1 (<1%)

Data are n (%).

Table 2: Adverse events that occurred in at least 20% of patients in either group

above the median, the median overall survival in patients was 26.5 months (95% CI 24.0–33.7) in the orantinib group but was not reached (29.7–not reached) in the placebo group (HR 1.397, 95% CI 1.039–1.879; $p=0.0270$); the corresponding median time to TACE failure was 20.3 months (17.0–25.5) in the orantinib group and 22.1 months (17.0–28.2) in the placebo group (HR 1.079, 0.823–1.414; $p=0.5829$). In patients with VEGF-C less than the median, the median overall survival was 33.6 months (95% CI 29.5–not reached) in the orantinib group and 28.4 months (22.0–35.6) in the placebo group (HR 0.812, 95% CI 0.590–1.117; $p=0.2000$); the corresponding median time to TACE failure was 25.5 months (21.4–not reached) in the orantinib group and 18.4 months (16.1–23.3) in the placebo group (HR 0.695, 0.512–0.943; $p=0.0196$; appendix pp 7, 8).

Adverse events were recorded in 443 (>99%) of 444 patients in the orantinib group and 436 (98%) of 444 patients in the placebo group (table 2; appendix pp 10–18). Most adverse events were of grade 1 or 2. The most frequently reported adverse events in the orantinib group were abdominal pain (317 [71%] in the orantinib group vs 292 [66%] in the placebo group), pyrexia (264 [59%] vs 284 [64%]), and elevated AST (223 [50%] vs 189 [43%]). The most frequent grade 3–5 adverse events were elevated AST (189 [43%] in the orantinib group vs 161 [36%] in the placebo group), elevated ALT (150 [34%] vs 132 [30%]), and hypertension (47 [11%] vs 39 [9%]). Other adverse events that were more often reported in the orantinib group were ascites, facial oedema, peripheral oedema, and diarrhoea (table 2).

The overall incidence of serious adverse events from any cause was higher in the orantinib group (200 [45%] of 444 patients) than in the placebo group (134 [30%] of 444 patients). The incidence of infection and infestation was 60 (14%) of 444 patients in the orantinib group and 17 (4%) of 444 patients in the placebo group; 58 (13%) of 444 patients in the orantinib group and 48 (11%) of 444 patients in the placebo group had gastrointestinal disorders, 49 (11%) in the orantinib group and 38 (9%) in the placebo group had hepatobiliary disorders, and 24 (5%) in the orantinib group and 26 (6%) in the placebo group had complications related to the primary hepatocellular carcinoma. 33 deaths (7%) in the orantinib group and 24 deaths (5%) in the placebo group were reported within 30 days after the final dose of the study drug. Only one patient in the orantinib group was evaluated as having a treatment-related death by hepatic failure. No significant difference in fatal events was observed between the two groups.

Discontinuation of study treatment due to adverse events was more common in the orantinib group than in the placebo group (96 [22%] of 444 patients vs 49 [11%] of 444 patients). Dose reduction due to adverse events was needed in 160 (36%) of 444 patients in the orantinib group and 37 (8%) of 444 patients in the placebo group.

Discussion

In the present study, orantinib combined with cTACE did not prolong overall survival in patients with unresectable hepatocellular carcinoma compared with placebo. Of the secondary outcomes, only time to progression was significantly longer in the orantinib group than in the placebo group. Although the trial was terminated earlier than planned, it is the largest randomised controlled trial done of a combination of TACE and a molecularly targeted agent. In that sense, overall survival in the placebo group might represent the world's standard of TACE treatment in this patient group.

The study had limitations. The main limitation was early termination. To be adequately powered to assess overall survival, we calculated we would need to observe 668 deaths, which would require enrolment and random allocation of 880. However, because the study was terminated early for futility, we observed only 263 deaths (39% of the required events). Early termination thus compromised study power, warranting caution in interpreting the data. Additionally, heterogeneity in baseline characteristics (eg, age, hepatocellular carcinoma stage, number of previous TACE sessions, or aetiology) was observed across the three regions from which patients were enrolled, as were differences in the length of the interval between consecutive TACE sessions. Before starting the study we expected the patient population for TACE and the TACE technique to be similar in Japan, South Korea, and Taiwan, but there were several differences which resulted in differences in clinical outcomes in each region.

Although TACE is recommended for patients with hepatocellular carcinoma BCLC stage B in Europe and North America,^{26,27} the procedure tends to be indicated for a broader range of patients in Asia:²⁸ in Asia, TACE is preferred over ablation in patients who have one intra-hepatic lesion over 5 cm, even in those with BCLC stage A. However, since definition of BCLC stage A is vague, some physicians from Europe and North America consider that patients with a single nodule over 5 cm are categorised as BCLC stage B. This is a problem of BCLC staging itself. Our subgroup analyses of overall survival and time to TACE failure suggest more favourable clinical outcomes for patients with BCLC stage B in the orantinib group, although differences were not significant. cTACE often causes liver function deterioration, abdominal pain, and pyrexia, and patients with ECOG performance status 1, BCLC stage C, or vascular invasion at baseline might be unable to tolerate the study drug in combination with cTACE. Nonetheless, the outcome of patients with BCLC stage A in the orantinib group was unfavourable in this study and we are unable to speculate the reasons for such results based on the data available.

Since the dose reduction criteria depended on the investigators' judgment in this study, the frequency of dose reduction in the orantinib group varied by study region, with 50% of patients having a dose reduction in Japan and 25% in South Korea and Taiwan. In general, more than three-quarters of the dose reductions were due to adverse events. However, more South Korean and Taiwanese patients experienced adverse events without any dose reduction than their Japanese counterparts, which might have negatively affected the time to TACE failure and overall survival outcomes.

The interval between two consecutive TACE sessions tended to be shorter in South Korea and Taiwan than in Japan. Raoul and colleagues²⁹ reported an increased incidence of liver deterioration and aggravated quality of life by cTACE. Additionally, Marelli and colleagues³⁰ suggested that since repeated TACE sessions might cause progressive liver atrophy and vascular damage, repeated TACE should be planned based on tumour response and patient tolerance; such a strategy has not been prospectively evaluated. Since the present study was discontinued prematurely, the available data were not sufficient for any conclusion on the effect of the number of TACE sessions and their intervals on efficacy. However, our experience indicates that repeated TACE sessions and their intervals should be more clearly defined in future trials of cTACE combined with a molecularly targeted agent. We also need to recognise that the results of all trials of a molecularly targeted agent and TACE have been negative. More refined trial designs, more applicable endpoints, and concomitant use of more potent and less toxic molecularly targeted agents should be explored in future TACE combination trials.

The adverse events that occurred at an incidence of at least 20% in the orantinib group and more frequently than in the placebo group by at least 10% were oedema, ascites, diarrhoea, and anorexia. These were similar to the major adverse drug reactions observed in the orantinib group of previous trials.^{23–25} Abdominal pain, pyrexia, and AST elevation, which were observed in more than 50% of all patients receiving orantinib, might be attributable to TACE, and there was no tendency for a marked increase of adverse drug reactions following orantinib administration. Furthermore, orantinib treatment could be continued for over 10 months, which is longer than the duration of treatment in other trials of molecularly targeted agents and TACE. Thus, the safety of orantinib in combination with cTACE was confirmed.

Plasma concentrations of two biomarkers, VEGF-C and PDGF-BB, were evaluated in this study. Significantly prolonged time to TACE failures were observed in patients with a VEGF-C concentration below the median value before orantinib administration. This result was consistent with the finding of prolonged progression-free survival in patients with low VEGF-C in a clinical trial of sunitinib for the treatment of bevacizumab-refractory renal cell carcinoma.³¹ VEGF-C is a ligand of VEGF receptor 3, and is thought to be related to the formation of new lymphatic vessels and lymph node metastasis. Although orantinib most strongly inhibits PDGF receptor signalling, it also inhibits VEGF receptor 3.^{20–22} However, overall survival in patients with VEGF-C above the median value in the orantinib group was shorter than for those in the placebo group. We consider that toxic effects might be greater than efficacy in patients with VEGF-C concentrations above the median value. Because of a lack of clinical and preclinical data, further research is necessary to determine whether VEGF-C concentrations are predictive of orantinib efficacy. Although our results on PDGF-BB in Japanese patients were similar to those of previous phase 1–2 and phase 2 studies done in Japan,^{23–25} no particular tendency was observed for PDGF-BB when the data from the three participating countries in this study were combined. Therefore, further study is needed to investigate the usefulness of PDGF-BB as a marker for efficacy.

Contributors

The study was designed and done according to the protocol by the sponsor (Taiho Pharmaceutical) in collaboration with the study coordinating committee (MK, YA, J-WP, JHP, A-LC, and P-CL), a medical expert (HA), and a trial statistician (SM). MK, A-LC, J-WP, HH, NI, JH, YJL, I-SS, C-FC, and YA were involved in data acquisition. SM contributed to analysis and interpretation of the data. All authors contributed to drafting the manuscript and critical revision of the manuscript with regard to important intellectual content. All authors approved the final version of the manuscript before submission.

Declaration of interests

MK reports grants and personal fees from Taiho Pharmaceutical, during the conduct of the study; grants and personal fees from Taiho Pharmaceutical, grants from Chugai, Otsuka, Takeda, Sumitomo Dainippon, Daiichisankyo, MSD, and Eisai, outside the submitted work. A-LC reports grants and personal fees from Taiho Pharmaceutical, during the conduct of the study; personal fees from Eisai, Bayer, Merck, Astellas, Sanofi, and Novartis, outside the submitted

work. J-WP reports grants and personal fees from Taiho Pharmaceutical, during the conduct of the study; personal fees from Bristol-Myers Squibb, Bayer, and Hanmi, outside the submitted work. JHP reports personal fees from Taiho Pharmaceutical, during the conduct of the study. P-CL reports personal fees from Taiho Pharmaceutical, during the conduct of the study. HH reports grants and personal fees from Taiho Pharmaceutical, during the conduct of the study; personal fees from Ajinomoto and Otsuka, outside the submitted work. NI reports grants from Taiho Pharmaceutical, during the conduct of the study. JH reports grants from Taiho Pharmaceutical, during the conduct of the study. YJL reports grants from Taiho Pharmaceutical, during the conduct of the study. I-SS reports grants from Taiho Pharmaceutical, during the conduct of the study. HA reports personal fees from Taiho Pharmaceutical, during the conduct of the study; grants and personal fees from Taiho Pharmaceutical, personal fees from Chugai, Ono, Sanofi, and Kyowa Hakko Kirin, outside the submitted work. SM reports personal fees from Taiho Pharmaceutical, during the conduct of the study; personal fees from Taiho Pharmaceutical, outside the submitted work. YA reports grants and personal fees from Taiho Pharmaceutical, during the conduct of the study; personal fees from Taiho Pharmaceutical, outside the submitted work. C-FC declares no competing interests.

Acknowledgments

This study was sponsored by Taiho Pharmaceutical. We thank all the patients, their families, and the investigators who participated in the study. We thank the independent data monitoring committee members (Hiroshi Ariyoshi, Yuh Sakata, Tomohide Tamura, and Satoshi Teramukai) for their contributions, and Taizo Hasegawa (Taiho Pharmaceutical) for his support in compiling and writing this report. Data collection was done by EPS (Tokyo, Japan), a contract research organisation. BSR corporation (Tokyo, Japan) did the statistical analysis of the collected data. Data were managed in parallel by the study's sponsor and its principal investigator.

References

- Jemal A, Bray F, Center MM, Ferlay J, Ward E, Forman D. Global cancer statistics. *CA Cancer J Clin* 2011; **61**: 69–90.
- Llovet JM, Ricci S, Mazzaferro V, et al. Sorafenib in advanced hepatocellular carcinoma. *N Engl J Med* 2008; **359**: 378–90.
- Cheng AL, Kang YK, Chen Z, et al. Efficacy and safety of sorafenib in patients in the Asia-Pacific region with advanced hepatocellular carcinoma: a phase III randomised, double-blind, placebo-controlled trial. *Lancet Oncol* 2009; **10**: 25–34.
- Llovet JM, Hernandez-Gea V. Hepatocellular carcinoma: reasons for phase III failure and novel perspectives on trial design. *Clin Cancer Res* 2014; **20**: 2072–79.
- Bruix J, Qin S, Merle P, et al. Regorafenib for patients with hepatocellular carcinoma who progressed on sorafenib treatment (RESORCE): a randomised, double-blind, placebo-controlled, phase 3 trial. *Lancet* 2017; **389**: 56–66.
- Llovet JM, Real MI, Montaña X, et al. Arterial embolisation or chemoembolisation versus symptomatic treatment in patients with unresectable hepatocellular carcinoma: a randomised controlled trial. *Lancet* 2002; **359**: 1734–39.
- Lo CM, Ngan H, Tso WK, et al. Randomized controlled trial of transarterial lipiodol chemoembolization for unresectable hepatocellular carcinoma. *Hepatology* 2002; **35**: 1164–71.
- Takayasu K, Arii S, Kudo M, et al. Superselective transarterial chemoembolization for hepatocellular carcinoma. Validation of treatment algorithm proposed by Japanese guidelines. *J Hepatol* 2012; **56**: 886–92.
- Lammer J, Malagari K, Vogl T, et al. Prospective randomized study of doxorubicin-eluting-bead embolization in the treatment of hepatocellular carcinoma: results of the PRECISION V study. *Cardiovasc Intervent Radiol* 2010; **33**: 41–52.
- El-Assal ON, Yamanoi A, Soda Y, et al. Clinical significance of microvessel density and vascular endothelial growth factor expression in hepatocellular carcinoma and surrounding liver: possible involvement of vascular endothelial growth factor in the angiogenesis of cirrhotic liver. *Hepatology* 1998; **27**: 1554–62.
- Yamaguchi R, Yano H, Iemura A, Ogasawara S, Haramaki M, Kojiro M. Expression of vascular endothelial growth factor in human hepatocellular carcinoma. *Hepatology* 1998; **28**: 68–77.
- Miura H, Miyazaki T, Kuroda M, et al. Increased expression of vascular endothelial growth factor in human hepatocellular carcinoma. *J Hepatol* 1997; **27**: 854–61.
- Poon RT, Lau CP, Ho JW, Yu WC, Fan ST, Wong J. Tissue factor expression correlates with tumor angiogenesis and invasiveness in human hepatocellular carcinoma. *Clin Cancer Res* 2003; **9**: 5339–45.
- Schmitt M, Horbach A, Kubitz R, Frilling A, Häussinger D. Disruption of hepatocellular tight junctions by vascular endothelial growth factor (VEGF): a novel mechanism for tumor invasion. *J Hepatol* 2004; **41**: 274–83.
- Suzuki H, Mori M, Kawaguchi C, Adachi M, Miura S, Ishii H. Serum vascular endothelial growth factor in the course of transcatheter arterial embolization of hepatocellular carcinoma. *Int J Oncol* 1999; **14**: 1087–90.
- Hsu C, Liang PC, Morita S, Hu FC, Cheng AL. Perspectives on the design of clinical trials combining transarterial chemoembolization and molecular targeted therapy. *Liver Cancer* 2012; **1**: 168–76.
- Lencioni R, Llovet JM, Han G, et al. Sorafenib or placebo plus TACE with doxorubicin-eluting beads for intermediate stage HCC: the SPACE trial. *J Hepatol* 2016; **64**: 1090–98.
- Kudo M, Han G, Finn RS, et al. Brivanib as adjuvant therapy to transarterial chemoembolization in patients with hepatocellular carcinoma: a randomized phase III trial. *Hepatology* 2014; **60**: 1697–707.
- Meyer T, Fox R, Ma YT, et al. Sorafenib in combination with transarterial chemoembolisation in patients with unresectable hepatocellular carcinoma (TACE 2): a randomised placebo-controlled, double-blind, phase 3 trial. *Lancet Gastroenterol Hepatol* 2017; **2**: 565–75.
- Laird AD, Vajkoczy P, Shawver LK, et al. SU6668 is a potent antiangiogenic and antitumor agent that induces regression of established tumors. *Cancer Res* 2000; **60**: 4152–60.
- Solorzano CC, Jung YD, Bucana CD, et al. In vivo intracellular signaling as a marker of antiangiogenic activity. *Cancer Res* 2001; **61**: 7048–51.
- Kuonen BC, Giaccone G, Ruijter R, et al. Dose-finding study of the multitargeted tyrosine kinase inhibitor SU6668 in patients with advanced malignancies. *Clin Cancer Res* 2005; **11**: 6240–46.
- Kanai F, Yoshida H, Tateishi R, et al. A phase I/II trial of the oral antiangiogenic agent TSU-68 in patients with advanced hepatocellular carcinoma. *Cancer Chemother Pharmacol* 2011; **67**: 315–24.
- Ikeda M, Shiina S, Nakachi K, et al. Phase I study on the safety, pharmacokinetic profile, and efficacy of the combination of TSU-68, an oral antiangiogenic agent, and S-1 in patients with advanced hepatocellular carcinoma. *Invest New Drugs* 2014; **32**: 928–36.
- Inaba Y, Kanai F, Aramaki T, et al. A randomised phase II study of TSU-68 in patients with hepatocellular carcinoma treated by transarterial chemoembolisation. *Eur J Cancer* 2013; **49**: 2832–40.
- European Association for the Study of the Liver; European Organisation for Research and Treatment of Cancer. EASL-EORTC Clinical Practice Guidelines: management of hepatocellular carcinoma. *J Hepatol* 2012; **56**: 908–43.
- Bruix J, Sherman M, American Association for the Study of Liver Diseases. Management of hepatocellular carcinoma: an update. *Hepatology* 2011; **53**: 1020–22.
- Cheng AL, Amarapurkar D, Chao Y, et al. Re-evaluating transarterial chemoembolization for the treatment of hepatocellular carcinoma: consensus recommendations and review by an International Expert Panel. *Liver Int* 2014; **34**: 174–83.
- Raoul JL, Sangro B, Forner A, et al. Evolving strategies for the management of intermediate-stage hepatocellular carcinoma: available evidence and expert opinion on the use of transarterial chemoembolization. *Cancer Treat Rev* 2011; **37**: 212–20.
- Marelli L, Stigliano R, Triantos C, et al. Transarterial therapy for hepatocellular carcinoma: which technique is more effective? A systematic review of cohort and randomized studies. *Cardiovasc Intervent Radiol* 2007; **30**: 6–25.
- Rini BI, Michaelson MD, Rosenberg JE, et al. Antitumor activity and biomarker analysis of sunitinib in patients with bevacizumab-refractory metastatic renal cell carcinoma. *J Clin Oncol* 2008; **26**: 3743–48.



Supplementation of pancreatic digestive enzymes alters the composition of intestinal microbiota in mice



Hiroki Nishiyama^{a,1}, Tomoyuki Nagai^{b,1}, Masatoshi Kudo^b, Yoshihisa Okazaki^b,
Yoshinao Azuma^c, Tomohiro Watanabe^b, Susumu Goto^d, Hiroyuki Ogata^{a,*},
Toshiharu Sakurai^{b,**}

^a Institute for Chemical Research, Kyoto University, Gokasho, Uji, Kyoto 611-0011, Japan

^b Department of Gastroenterology and Hepatology, Kindai University Faculty of Medicine, 377-2 Ohno-Higashi, Osaka-Sayama, Osaka 589-8511, Japan

^c Biology-Oriented Science and Technology, Kindai University, 930 Nishimitani, Kinokawa, Wakayama 649-6493, Japan

^d Database Center for Life Science, Joint Support-Center for Data Science Research, Research Organization of Information and Systems, 178-4-4 Wakashiba, Kashiwa, Chiba 277-0871, Japan

ARTICLE INFO

Article history:

Received 22 September 2017

Accepted 25 October 2017

Available online 26 October 2017

Keywords:

Chronic pancreatitis

Pancreatic exocrine insufficiency

Pancreatic enzyme replacement therapy

Pancrelipase

Intestinal microbiota

Akkermansia muciniphila

ABSTRACT

Although pancreatic enzyme replacement therapy (PERT) is effective in the alleviation of pancreatic exocrine insufficiency (PEI)-related symptoms in patients with chronic pancreatitis, its mechanism of action is poorly understood. Recent studies suggest that the intestinal microbiota is associated with the pathogenesis of chronic pancreatitis. Therefore, we hypothesized that PERT exerts its effect by modifying the intestinal microbiota in addition to its presumed role in promoting fat and protein absorption. To explore the mechanism of action of PERT, we analyzed the intestinal microbiotas of two groups of mice treated with either pancrelipase or tap water by using 16S rRNA amplicon sequencing. The results revealed that the bacterial compositions of the pancrelipase-treated mice were significantly different from those of the control samples. *Akkermansia muciniphila*, a key beneficial bacterium in the intestinal tract, showed a higher relative abundance in the pancrelipase-treated samples than in the control samples. *Lactobacillus reuteri*, a widely used probiotic bacterium known to relieve intestinal inflammation, also showed a higher relative abundance in the pancrelipase-treated samples. These results suggested that PERT induces the colonization of beneficial bacteria, thereby contributing to the attenuation of PEI-associated symptoms in addition to improvement of the nutritional state.

© 2017 Elsevier Inc. All rights reserved.

1. Introduction

Chronic pancreatitis is a persistent inflammation of the pancreas with pathological findings of the infiltration of immune cells and the development of fibrosis [1]. Clinical courses of patients with chronic pancreatitis are characterized by acute exacerbation and remission phases. Repeated episodes of acute exacerbation cause reduction of the functional pancreatic parenchymal mass through the destruction of the acinar architecture, which leads to the development of fibrosis [1]. Such loss of functional pancreatic

parenchymal mass results in impaired functions of both the exocrine and the endocrine pancreas. In fact, patients with advanced stages of chronic pancreatitis exhibit symptoms associated with pancreatic exocrine insufficiency (PEI), such as diarrhea, malabsorption, and steatorrhea [1]. PEI, caused by impaired secretion of pancreatic digestive enzymes due to loss of intact pancreatic acinar cells [1], represents one of the most frequent complications of chronic pancreatitis [2].

Pancreatic enzyme replacement therapy (PERT) is widely used in the treatment of chronic pancreatitis patients exhibiting PEI-associated symptoms and improves fat and protein absorption and serum nutritional parameters in a significant population of these patients [3,4]. Recent clinical trials have shown that PERT results in relief and improvement of PEI-associated symptoms in patients with chronic pancreatitis [5]. PERT is generally assumed to alleviate PEI-associated symptoms by restoring pancreatic digestive

* Corresponding author.

** Corresponding author.

E-mail addresses: ogata@kuicr.kyoto-u.ac.jp (H. Ogata), sakurai@med.kindai.ac.jp (T. Sakurai).

¹ These authors equally contributed to this work.

activity in the gastrointestinal tract. However, the mechanism by which PERT ameliorates PEI-associated symptoms is still poorly defined.

Recent studies have highlighted the involvement of immune responses against intestinal microbiota in the development of chronic pancreatitis [6]. For example, the activation of pattern recognition receptors (i.e., Toll-like receptors and nucleotide-binding oligomerization-like receptors), that detect microbe-associated molecular patterns derived from the intestinal microbiota, have been reported to play a critical role in the development of experimental chronic pancreatitis [7,8]. Significant alterations in the intestinal microbiota in patients with chronic pancreatitis have also been reported [9,10]. Furthermore, changes in nutritional content within the gastrointestinal tract have been known to be able to alter the homeostatic colonization of commensal microbiota [11]. These studies suggest that nutrient mal-digestion caused by PEI leads to a significant alteration in the intestinal microbiota, which may further worsen chronic pancreatitis through the development of excessive innate immune responses. Therefore, we hypothesized that PERT improves PEI-associated symptoms in chronic pancreatitis not only by restoring pancreatic digestive activity, but also by altering the intestinal microbiota. To test this hypothesis, we used male C57BL/6J mice treated with pancrelipase and performed 16S ribosomal RNA gene amplicon analyses of the microbiotas sampled from their cecum, transverse colon, and stool with an aim to understand the effect of PERT on intestinal microbiota. Our findings provide evidence supporting our hypothesis that PERT alleviates PEI-associated symptoms not only by improving digestive activity, but also by altering the composition of the intestinal microbiota in mice.

2. Materials and methods

2.1. Mice

We used 8–9-weeks-old male C57BL/6J mice (25.0 ± 0.5 g; SLC JAPAN, Inc., Shizuoka, Japan) and divided them into 2 groups: control and pancrelipase-treated groups. The control group was given tap water at the dose of 0.75 mL/day divided into 3 parts for 21 days. The pancrelipase-treated group was treated with pancrelipase—a commercial mixture of pancreas amylase, lipase, and protease (chymotrypsin) (Lipacreon, EA pharma, Japan)—at a dose of 1.2 mg/day divided into 3 parts for 21 days. After 21 days, the mice were killed, and their cecum, transverse colon, and stool were collected, frozen, and stored at -20 °C. All animal experiments were conducted according to the ethical guidelines of the review boards of Kindai University Faculty of Medicine, and the animal experiments were approved by the same review boards.

2.2. DNA extraction and sequencing

The frozen cecum, transverse colon, and stool samples were thawed and homogenized using Zirconia/Silica Beads (BioSpec Products) in a MagNAlzyer (Roche Diagnostics). Following homogenization, DNA was extracted using the QIAamp DNA Stool Mini Kit and the QIAamp DNA Mini Kit according to the manufacturer's instructions (Qiagen GmbH, Hilden Germany). The extracted DNA samples were used as the template in PCR for amplification of the variable V3–V4 16S rRNA gene regions with 16S Amplicon PCR Forward primer 5'-TCGTCGGCAGCGTCAGATGTGTATAAGAGACAG-MID-GT-CCTACGGGNGGCWGCAG-3' and 16S Amplicon PCR Reverse primer 5'-GTCTCGTGGGCTCGGAGATGTGTATAAGAGACAG-MID-GT-GACTACHVGGGTATCTAATCC-3'.

Sequencing libraries were prepared using the '16S Metagenomic Sequencing Library Preparation: Preparing 16S Ribosomal RNA

Gene Amplicons for the Illumina MiSeq System' protocol [12] with the use of the Nextera XT Index Kit (Illumina). Sequencings were performed using the MiSeq Reagent Kit v2 (300 cycles) and MiSeq (Illumina, San Diego, CA, USA) device according to the manufacturer's recommendations.

2.3. Preprocessing of sequence data

Low-quality sequence regions were trimmed from each paired-end read using Trimmomatic (version 0.35) (SLIDINGWINDOW:40:15, MINLEN:50) [13]. Primer sequences were trimmed from paired-end reads using Cutadapt (version 1.11) (-e 0.06, -pair-filter = both) [14]. The resulting trimmed paired-end reads were merged using FLASH (version 1.2.1) (-m 30, -M 271, -x 0.25) [15]. These merged reads are referred to as the "reads" in the rest of the manuscript. Raw sequence data were submitted to DDBJ/DRA under the accession number DRA006124. The reads are available from ftp://ftp.genome.jp/pub/db/community/microbiome_kindai.

2.4. Generation of operational taxonomy units

The following analyses were conducted using programs included in the Quantitative Insights Into Microbial Ecology (QIIME version 1.9.1) software [16], unless stated otherwise. The analyses used the representatives of 16S rRNA sequences from the Greengenes database (version 13_5) pre-clustered at 97% sequence identity threshold [17]. These representative sequences are referred to as the "reference sequences" in the rest of the manuscript.

The reads were each clustered against the reference sequences at 97% sequence identity threshold to form operational taxonomic units (OTUs) using `parallel_pick_otus_uclust_ref.py`. Reads that did not match with the reference sequences at the 97% sequence identity threshold were excluded from the analysis. A taxonomic classification was assigned to each OTU by referring to the taxonomy of the reference sequence included in the OTU. The resulting OTU table represents OTU identifiers, assigned taxonomic classifications, and read counts for each sample.

2.5. Assessment of alpha diversity

Alpha diversity, the diversity within a community, was assessed by rarefaction curves as well as by Shannon's diversity index, the latter of which considers both the richness and evenness of the community structure [18]. Rarefaction curves were generated by averaging the OTU counts from 10 times of random re-sampling of reads at different depths with intervals of 5000 sequences using `parallel_multiple_rarefactions.py`. For calculating Shannon's diversity index, each set of reads was rarefied down to 57,762 reads (i.e., the number of reads for the smallest sample) using `single_rarefaction.py`. Statistical significances of the differences in Shannon's index values between the samples were tested using Welch's *t*-test (with a significance level of 0.05 without correction for multiple test) implemented in SciPy [19].

2.6. Assessment of beta diversity

Beta diversity, the dissimilarity between communities, was measured using the weighted UniFrac distance [20], which takes into account the relative abundances of each OTU and their phylogenetic relationships. The reference sequences corresponding to each OTU were first aligned against `97_otus.fasta`, a template alignment provided by Greengenes database, using PyNAST [21] implemented in `align_seqs.py`. The resulting alignment was then used to create a phylogenetic tree using FastTree [22] implemented

in `make_phylogeny.py` (`-r tree_method_default`). Each set of reads was rarefied down to 57,762 reads using `single_rarefaction.py`. The weighted UniFrac distances between samples were calculated using `parallel_beta_diversity.py`, together with the phylogenetic tree and the rarefied set of reads.

2.7. Identification of over-/under-represented bacterial taxa

To identify bacterial taxa that are differentially abundant (i.e., either over- or under-represented) in a set of samples relative to another set of samples, we first grouped OTUs at the species level according to their assigned taxa and generated a taxonomy table, which records the read counts for each taxon across samples, using `summarize_taxa.py`. OTUs with taxonomic assignments at only genus or higher taxonomic levels were grouped at the lowest level of taxonomy that they received. Bacterial taxa with the assignment of less than 10 reads were omitted from analysis using `filter_otus_from_otu_table.py`. Statistical significance of the difference in the relative abundance of a taxon between groups of samples (i.e., differential abundance between control vs. pancrelipase-treated samples) was assessed using the DESeq2 negative binomial Wald test [23] implemented in `differential_abundance.py`. False discovery rate (q-value) was controlled at 0.1 based on the obtained p-values with the use of the Benjamini-Hochberg correction as implemented in DESeq2. For each bacterial taxon showing a significant difference in its relative abundance between two sample groups (i.e., q-value < 0.1), we further examined the sample group showing the higher average relative abundance. If one or more of the samples in this group contained no reads, we did not consider the taxon over- or under-represented.

3. Results

3.1. Generation of OTUs

After quality control, we obtained a total of 5,167,710 merged reads (Table S1). Of these, 3,572,866 reads (69.14%) matched with reference sequences in the Greengenes database and formed 2692 OTUs (corresponding to 31 orders, 54 families, 62 genera, and 19 species of bacteria). These results were organized into an OTU table used for the following analyses.

3.2. Pancrelipase treatment did not induce significant alpha diversity changes

There were no systematic differences in the bacterial community richness (i.e., the number of OTUs in a sequencing depth normalized sample) between the control and the pancrelipase-treated group in any of the cecum, transverse colon, and stool samples (Fig. S1A). Furthermore, there were no statistically significant differences in Shannon's diversity index between the control and pancrelipase-treated samples (Welch's *t*-test, Fig. S1B). Pancrelipase treatment thus had no considerable influence on the alpha diversity of the tested intestinal microbiotas.

3.3. Pancrelipase treatment induced alterations in bacterial community composition

The bacterial composition of the pancrelipase-treated samples at the phylum level were clearly different from those of the control samples (Fig. 1). A major difference was the increased relative abundances of Verrucomicrobia in the pancrelipase-treated samples. This phylum showed extensive increase in the pancrelipase-treated samples (control vs. pancrelipase, 0.13% vs. 7.58% on average). All the OTUs assigned to Verrucomicrobia corresponded

to *Akkermansia muciniphila*. Another subtle difference was the lower Firmicutes to Bacteroidetes ratio in the transverse colon samples compared with that in the controls, although the difference was not statistically significant (Welch's *t*-test, $p = 0.0623$). Principal coordinate analysis was further used to visualize compositional differences at a finer scale (i.e., at the OTU level) based on the weighted UniFrac distance (Fig. 2). The resulting three-dimensional plot showed that the spatial distribution of the pancrelipase-treated samples was distinct from that of the control samples.

3.4. Bacterial taxa showing significant changes in their relative abundances

By re-grouping the 2692 OTUs according to their taxonomic classifications, we obtained a taxonomy table recording read counts for 106 bacterial taxa for each samples. Of these, 51 bacterial taxa represented by less than 10 reads were excluded from the analysis. Comparison between the control and pancrelipase-treated samples revealed 17 instances that had satisfied our criteria (see Materials and Methods) (Fig. 3). In eight of these instances, the bacterial taxa were over-represented (i.e., higher relative abundance) in the pancrelipase-treated samples. These corresponded to *Akkermansia muciniphila* (cecum, transverse colon, and stool), Alcaligenaceae *Sutterella* (transverse colon), *Lactobacillus reuteri* (cecum), Clostridiaceae *Clostridium* (transverse colon), and Erysipelotrichaceae *Coprobacillus* (cecum and stool). In the remaining nine instances, the bacterial taxa were under-represented (i.e., lower relative abundance) in the pancrelipase-treated samples than in the control samples. These taxa were Desulfovibrionales Desulfovibrionaceae (transverse colon), Desulfovibrionaceae *Desulfovibrio* (transverse colon), Desulfovibrionaceae *Bilophila* (transverse colon, stool), Clostridiales Lachnospiraceae (transverse colon and stool), Lachnospiraceae *Dorea* (transverse colon and stool) and Clostridiales Mogibacteriaceae (transverse colon). Collectively, these results suggested that pancrelipase treatment induced a statistically significant compositional shift in the mouse intestinal microbiota.

4. Discussion

PERT has been established as an effective treatment for PEI in chronic pancreatitis. However, the mechanism by which PERT ameliorates PEI-associated symptoms is still poorly defined. We hypothesized that PERT exerts its effect by modifying the intestinal microbiota, and showed that there were significant differences in the compositions of mouse intestinal microbiotas between pancrelipase-treated and control samples.

Of the significant differences in the relative abundances of bacterial taxa between the pancrelipase-treated and control samples, the difference in the relative abundance of *Akkermansia muciniphila* (belonging to Verrucomicrobia) was the most striking. Indeed, the average relative abundance of *A. muciniphila* was 58-fold higher in the pancrelipase-treated samples than in the control samples. One of the biggest risk factors for chronic pancreatitis is alcohol drinking, which impairs intestinal barrier function, followed by translocation of intestinal bacteria [24]. *A. muciniphila* is known to degrade intestinal mucin into propionic and acetic acids, which promote beneficial microbe interactions in the intestinal tract [25]. In line with this, Garnder et al. previously reported that ethanol-induced intestinal barrier dysfunction is associated with a prominent decline of *A. muciniphila* [26]. Furthermore, supplementation of *A. muciniphila* was reported to enhance intestinal barrier function by promoting mucus thickness and tight junction protein expression [26]. Therefore, it is possible that pancrelipase attenuates PEI-associated symptoms by inducing colonization of

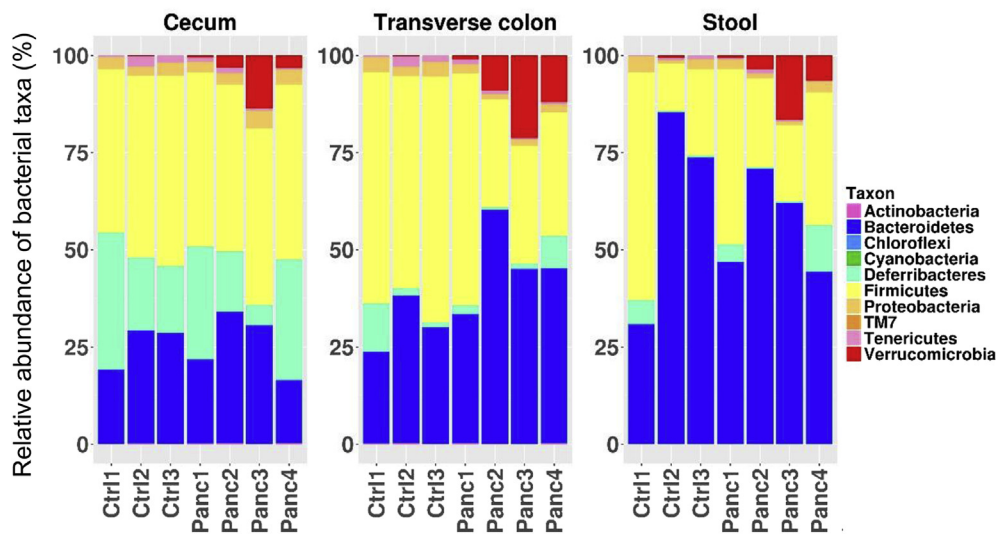


Fig. 1. Relative abundances of different bacterial taxa at the phylum level in the control (Ctrl) and pancrelipase-treated (Panc).

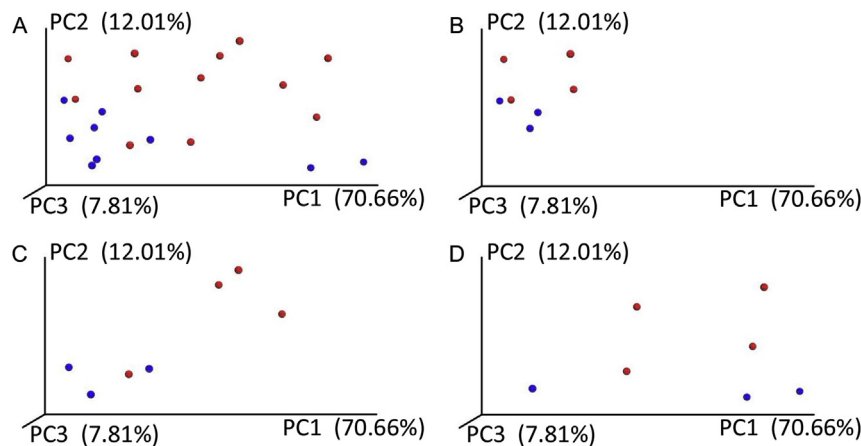


Fig. 2. Comparison of bacterial communities across samples. (A) OTU-level comparisons were performed for all control (blue) and pancrelipase-treated (red) samples by using principal coordinate analysis based on the weighted UniFrac distance. Results for the cecum (B), transverse colon (C), and stool (D) samples were plotted separately for better visualization. (For interpretation of the references to colour in this figure legend, the reader is referred to the web version of this article.)

A. muciniphila, followed by normalization of intestinal barrier function. However, it should be noted that whether pancrelipase treatment induces the colonization of this bacterium in chronic pancreatitis patients and beneficial effects remains to be determined.

Four other bacteria were also over-represented in the pancrelipase-treated samples. One of these bacteria was *Lactobacillus reuteri*, a well-known probiotic bacterium. In fact, *L. reuteri* has been proven to relieve intestinal inflammation by converting ι -histidine to histamine, which suppresses the host immune system by activating the H2 receptor [27]. The ability of *L. reuteri* to prevent or alleviate colitis in mice has also been reported [28,29]. Thus, it is possible that pancrelipase-induced colonization of *L. reuteri* contributes to the maintenance of intestinal immune homeostasis. Alcaligenaceae *Sutterella*, Clostridiaceae *Clostridium*, and Erysipelotrichaceae *Coprobacillus* also showed elevated relative abundances in the pancrelipase-treated samples, but the effect of colonization of these bacteria on host intestinal functions has not been clarified [30,31]. With regard to Clostridiaceae *Clostridium*, the genus contains both pro-inflammatory bacteria (*Clostridium difficile* [32]) and anti-inflammatory bacteria (e.g., *Clostridium butyricum*

MIYARI 588 [33]). Together, these results indicated that *A. muciniphila*, with its ability to promote intestinal barrier function, and *L. reuteri*, with its ability to regulate inflammation, showed increased relative abundances in the colon and stool samples of the pancrelipase-treated mice. The colonization of such beneficial bacteria induced by pancrelipase treatment may partially explain the mechanisms by which PERT attenuates PEI-associated symptoms.

We also identified six bacterial taxa under-represented in the pancrelipase-treated mice. Species belonging to the *Bilophila* and *Desulfovibrio* genera of the family Desulfovibrionaceae might have colitogenic functions, since they produce hydrogen sulfide, which promotes intestinal inflammation in rats when administered at amounts exceeding the capacity of colonocytes to detoxify it [34–36]. Lachnospiraceae *Dorea* also showed lower relative abundance in the pancrelipase-treated samples. Certain members of the Lachnospiraceae family are known to produce butyric acid, which promotes intestinal epithelial barrier function [37]. Clostridiales Mogibacteriaceae also showed decreased relative abundances in the pancrelipase-treated mice, but the effect of colonization of these bacteria on host intestinal functions has not been clarified.

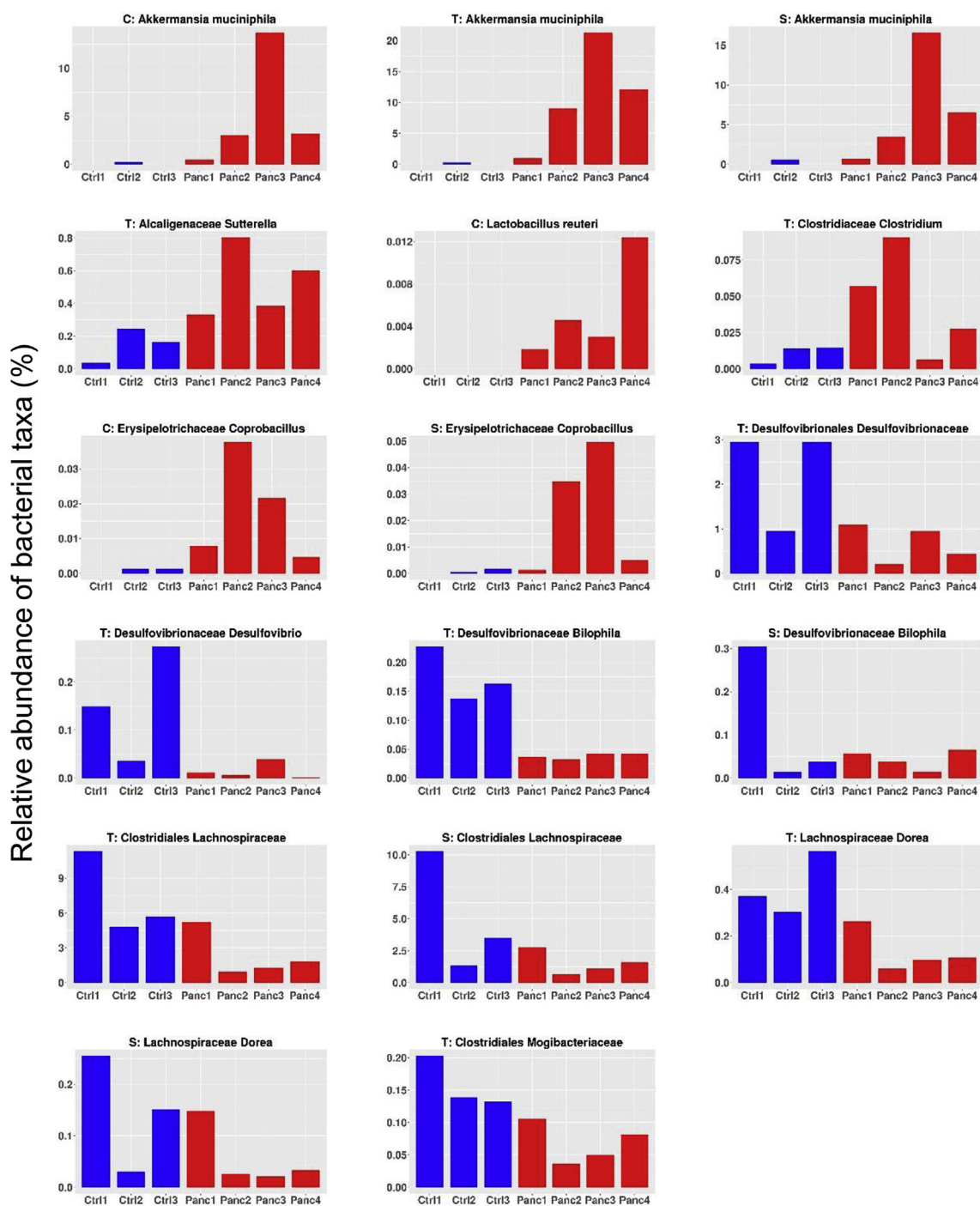


Fig. 3. Bacterial taxa showing significantly different relative abundances between the control and pancrelipase-treated samples collected from the cecum (C), transverse colon (T), or stool (S). Relative abundances in the control (Ctrl) and pancrelipase-treated (Panc) samples are represented by blue and red bars, respectively. (For interpretation of the references to colour in this figure legend, the reader is referred to the web version of this article.)

A few studies have previously investigated the composition of intestinal microbiotas in chronic pancreatitis patients or in chronic pancreatitis model mice [9,38,39]. Jandhyala et al. observed significant decreases in the abundances of *Faecalibacterium prausnitzii* and *Ruminococcus bromii* and an increase in the Firmicutes to Bacteroidetes ratio in the intestinal microbiomes of chronic pancreatitis patients compared with that in healthy subjects. However, in our study, we could not find any significant pancrelipase-induced changes in these species or in the Firmicutes

to Bacteroidetes ratio between the two groups of mice. *Helicobacter pylori* is a suspected pathogen of autoimmune pancreatitis (i.e., a rare form of chronic pancreatitis) [40]. In our study, the relative abundance of *H. pylori* was found to be very low (<0.0035%) in the intestinal microbiotas of the mice and showed no significant changes upon pancrelipase treatment.

Furthermore, several previous studies using chronic pancreatitis model mice have reported increases and decreases in the relative abundance of several bacterial taxa in the model mice relative to

that in the control mice [38,39]. In contrast, most of these taxa did not show any significant changes in their relative abundance upon pancrelipase treatment in our study, except for *Lactobacillus* and *Lachnospiraceae*. These bacteria have been previously reported to show decreased relative abundances in chronic pancreatitis model mice; however, the relative abundance of *Lactobacillus reuteri* was over-represented in the cecum samples of the pancrelipase-treated mice and that of *Lachnospiraceae* was under-represented in the transverse colon and stool samples of the pancrelipase-treated mice. Overall, the administration of pancrelipase did not induce microbial changes akin to those observed in chronic pancreatitis patients or its model mice, with the sole exception of the under-representation of *Lachnospiraceae*.

Future studies on intestinal microbiotas derived from chronic pancreatitis model mice and patients with or without PEI need to be conducted to better understand the mechanism by which pancrelipase ameliorates the symptoms of chronic pancreatitis.

To the best of our knowledge, our study is the first to reveal that oral supplementation of pancrelipase significantly alters the intestinal microbiota in mice. Our findings support the idea that pancrelipase exerts its effect in PERT by modifying the gut microbiota, in addition to its presumed effect of improving the nutritional state of patients. Furthermore, the fact that the relative abundances of *A. muciniphila* and *L. reuteri*—two microorganisms that are known to be beneficial to the maintenance of the intestinal barrier—increased upon pancrelipase administration in the intestinal microbiota of the mice suggests that new possibilities for the treatment of chronic pancreatitis, such as probiotics and fecal transplantation, should be considered.

Conflict of interest

Pancrelipase was provided by EA Pharma Co., Ltd.

Acknowledgements

This work was in part supported by JSPS/KAKENHI (17K09396), JSPS/KAKENHI (No. 16KT0020), the Naito Foundation, the SENSHIN Medical Foundation, the Yakult Bioscience Foundation, the Smoking Research Foundation, and by Japan Agency for Medical Research and Development Grants for Research on Intractable Diseases. Computational work was completed at the Super Computer System, Institute for Chemical Research, Kyoto University.

Transparency document

Transparency document related to this article can be found online at <https://doi.org/10.1016/j.bbrc.2017.10.130>.

Appendix A. Supplementary data

Supplementary data related to this article can be found at <https://doi.org/10.1016/j.bbrc.2017.10.130>.

References

- [1] J.M. Braganza, S.H. Lee, R.F. McCoy, et al., Chronic pancreatitis, *Lancet* 377 (2011) 1184–1197.
- [2] T.C. Hall, G. Garcea, M.A. Webb, et al., The socio-economic impact of chronic pancreatitis: a systematic review, *J. Eval. Clin. Pract.* 20 (2014) 203–207.
- [3] D.C. Whitcomb, A. Bodhani, K. Beckmann, et al., Efficacy and safety of pancrelipase/pancreatin in patients with exocrine pancreatic insufficiency and a medical history of diabetes mellitus, *Pancreas* 45 (2016) 679–686.
- [4] J.G. D'Haese, G.O. Ceyhan, I.E. Demir, et al., Pancreatic enzyme replacement therapy in patients with exocrine pancreatic insufficiency due to chronic pancreatitis: a 1-year disease management study on symptom control and quality of life, *Pancreas* 43 (2014) 834–841.
- [5] D. de la Iglesia-García, W. Huang, P. Szatmary, Efficacy of pancreatic enzyme replacement therapy in chronic pancreatitis: systematic review and meta-analysis, *Gut* 66 (2017) 1354–1355.
- [6] T. Watanabe, M. Kudo, W. Strober, Immunopathogenesis of pancreatitis, *Mucosal Immunol.* 10 (2017) 283–298.
- [7] A. Ochi, A.H. Nguyen, A.S. Bedrosian, et al., MyD88 inhibition amplifies dendritic cell capacity to promote pancreatic carcinogenesis via Th2 cells, *J. Exp. Med.* 209 (2012) 1671–1687.
- [8] T. Watanabe, Y. Sadakane, N. Yagama, et al., Nucleotide-binding oligomerization domain 1 acts in concert with the cholecystokinin receptor agonist, cerulein, to induce IL-33-dependent chronic pancreatitis, *Mucosal Immunol.* 9 (2016) 1234–1249.
- [9] S.M. Jandhyala, A. Madhulika, G. Deepika, et al., Altered intestinal microbiota in patients with chronic pancreatitis: implications in diabetes and metabolic abnormalities, *Sci. Rep.* 7 (2017) 43640.
- [10] M. Signoretti, R. Roggiolani, C. Stornello, et al., Gut microbiota and pancreatic diseases, *Minerva Gastroenterol. Dietol.* 63 (2017) 399–410.
- [11] M. Levy, A.A. Kolodziejczyk, C.A. Thaiss, Dysbiosis and the immune system, *Nat. Rev. Immunol.* 17 (2017) 219–232.
- [12] Illumina, 16S Metagenomic Sequencing Library Preparation, 2013. http://jpp.support.illumina.com/downloads/16s_metagenomic_sequencing_library_preparation.html (accessed 15/July/2015).
- [13] A.M. Bolger, M. Lohse, B. Usadel, Trimmomatic: a flexible trimmer for Illumina sequence data, *Bioinformatics* 30 (2014) 2114–2120.
- [14] M. Martin, Cutadapt removes adapter sequences from high-throughput sequencing reads, *EMBnet.J.* 17 (2011) 10–12.
- [15] T. Magoč, S.L. Salzberg, FLASH: fast length adjustment of short reads to improve genome assemblies, *Bioinformatics* 27 (2011) 2957–2963.
- [16] J.G. Caporaso, J. Kuczynski, J. Stombaugh, et al., QIIME allows analysis of high-throughput community sequencing data, *Nat. Methods* 7 (2010) 355–356.
- [17] D. McDonald, M.N. Price, J. Goodrich, et al., An improved Greengenes taxonomy with explicit ranks for ecological and evolutionary analyses of bacteria and archaea, *ISME J.* 6 (2012) 610–618.
- [18] C.E. Shannon, A mathematical theory of communication, *Bell Syst. Tech. J.* 27 (1948) 379–423.
- [19] E. Jones, E. Oliphant, P. Peterson, et al., SciPy: Open Source Scientific Tools for Python, 0.16.1, 2001. <http://www.scipy.org/>.
- [20] C. Lozupone, R. Knight, UniFrac: a new phylogenetic method for comparing microbial communities, *Appl. Environ. Microbiol.* 71 (2005) 8228–8235.
- [21] J.G. Caporaso, K. Bittinger, F.D. Bushman, et al., PyNAST: a flexible tool for aligning sequences to a template alignment, *Bioinformatics* 26 (2010) 266–267.
- [22] M.N. Price, P.S. Dehal, A.P. Arkin, FastTree 2 – approximately maximum-likelihood trees for large alignments, *PLoS One* 5 (2010), e9490.
- [23] M.I. Love, W. Huber, S. Anders, Moderated estimation of fold change and dispersion for RNA-seq data with DESeq2, *Genome Biol.* 15 (2014) 550.
- [24] A. Vonlaufen, L. Spahr, M.V. Apte, et al., Alcoholic pancreatitis: a tale of spirits and bacteria, *World J. Gastrointest. Pathophysiol.* 5 (2014) 82–90.
- [25] W.M. de Vos, Microbe Profile: *Akkermansia muciniphila*: a conserved intestinal symbiont that acts as the gatekeeper of our mucosa, *Microbiology* 163 (2017) 646–648.
- [26] C. Grander, T.E. Adolph, V. Wieser, et al., Recovery of ethanol-induced *Akkermansia muciniphila* depletion ameliorates alcoholic liver disease, *Gut* (2017), <https://doi.org/10.1136/gutjnl-2016-313432>.
- [27] C. Gao, A. Major, D. Rendon, et al., Histamine H2 receptor-mediated suppression of intestinal inflammation by probiotic *Lactobacillus reuteri*, *mBio* 6 (2015) e01358–15.
- [28] A.R. Mackos, T.D. Eubank, N.M.A. Parry, et al., Probiotic *Lactobacillus reuteri* attenuates the stressor-enhanced severity of *Citrobacter rodentium* infection, *Infect. Immun.* 81 (2013) 3253–3263.
- [29] A.R. Mackos, J.D. Galley, T.D. Eubank, et al., Social stress-enhanced severity of *Citrobacter rodentium*-induced colitis is CCL2-dependent and attenuated by probiotic *Lactobacillus reuteri*, *Mucosal Immunol.* 9 (2016) 515–526.
- [30] A. Labbé, J.G. Ganopoulos, C.J. Martoni, et al., Bacterial bile metabolising gene abundance in Crohn's, ulcerative colitis and type 2 diabetes metagenomes, *PLoS One* 9 (2014), e115175.
- [31] P. Palvidis, N. Powell, R.P. Vincent, et al., Systematic review: bile acids and intestinal inflammation-luminal aggressors or regulators of mucosal defence, *Aliment. Pharmacol. Ther.* 42 (2015) 802–817.
- [32] M.C. Abt, P.T. McKenney, E.G. Pamer, *Clostridium difficile* colitis: pathogenesis and host defence, *Nat. Rev. Microbiol.* 14 (2016) 609–620.
- [33] A. Hayashi, T. Sato, N. Kamada, et al., A single strain of *Clostridium butyricum* induces intestinal IL-10-producing macrophages to suppress acute experimental colitis in mice, *Cell Host Microbe* 13 (2013) 711–722.
- [34] Y.A. Warren, D.M. Citron, C.Y. Merriam, et al., Biochemical differentiation and comparison of *Desulfovibrio* species and other phenotypically similar genera, *J. Clin. Microbiol.* 43 (2005) 4041–4045.
- [35] S.B. Singh, H.C. Lin, Hydrogen sulfide in physiology and diseases of the digestive tract, *Microorganisms* 3 (2015) 866–889.
- [36] M. Beaumont, M. Andriamihaja, A. Lan, et al., Detrimental effects for colonocytes of an increased exposure to luminal hydrogen sulfide: the adaptive response, *Free Radic. Biol. Med.* 93 (2016) 155–164.
- [37] C.J. Meehan, R.G. Beiko, A phylogenomic view of ecological specialization in the Lachnospiraceae, a family of digestive tract-associated bacteria, *Genome Biol. Evol.* 6 (2014) 703–713.

- [38] Y. Hu, C. Teng, S. Yu, et al., Inonotus obliquus polysaccharide regulates gut microbiota of chronic pancreatitis in mice, *A.M.B. Express* 7 (2017), <https://doi.org/10.1186/s13568-017-0341-1>.
- [39] K. Li, C. Zhuo, C. Teng, et al., Effects of *Ganoderma lucidum* polysaccharides on chronic pancreatitis and intestinal microbiota in mice, *Int. J. Biol. Macromol.* 93 (2016) 904–912.
- [40] F. Guarneri, C. Guarneri, S. Benvenega, *Helicobacter pylori* and autoimmune pancreatitis: role of carbonic anhydrase via molecular mimicry? *J. Cell Mol. Med.* 9 (2005) 741–744.

CASE REPORT

A case of successful transluminal drainage of walled-off necrosis under contrast-enhanced harmonic endoscopic ultrasonography guidance

Kosuke Minaga¹ · Mamoru Takenaka¹ · Shunsuke Omoto¹ · Takeshi Miyata¹ · Ken Kamata¹ · Kentaro Yamao¹ · Hajime Imai¹ · Tomohiro Watanabe¹ · Masayuki Kitano² · Masatoshi Kudo¹

Received: 31 January 2017 / Accepted: 1 March 2017 / Published online: 28 March 2017
© The Japan Society of Ultrasonics in Medicine 2017

Abstract We report a case of successful transluminal drainage of walled-off necrosis (WON) under contrast-enhanced harmonic endoscopic ultrasonography (CH-EUS) guidance. Recently, EUS-guided transluminal drainage (EUS-TD) of WON has been increasingly used as a minimally invasive treatment option with reportedly high technical and clinical success rates; however, B-mode EUS occasionally fails to depict the target lesion and its margins, particularly in cases where the target shows a heterogeneous echogenicity. In our case, EUS-TD was attempted for infected WON, but visualization using B-mode EUS imaging was poor. Thus, CH-EUS was performed to enhance the contrast between the targeted WON and its surrounding tissues. Immediately after injecting a sonographic contrast agent, WON and its margins were clearly identified as an avascular area and were punctured under CH-EUS guidance. CH-EUS enables the assessment of the microvasculature and hemodynamics of the target lesion in real time. It may also provide valuable information and could be a useful modality for EUS-TD to clearly visualize target lesions and their margins and to decisively puncture them, even when they could not be identified using B-mode EUS.

Keywords Acute necrotizing pancreatitis · Bile ducts · Endoscopic retrograde cholangiopancreatography · Endoscopic ultrasonography · Sonazoid

Introduction

According to the revised Atlanta classification of acute pancreatitis [1], walled-off necrosis (WON) is defined as an encapsulated fluid collection that includes necrotic tissues formed after acute necrotizing pancreatitis. Since first reported in 1996 by Baron et al., endoscopic ultrasonography (EUS)-guided transluminal drainage (EUS-TD) of WON has played a pivotal role and spread worldwide as a minimally invasive treatment option [2–4]. Previous studies showed that the procedure had high technical and clinical success rates [3–5]; however, B-mode EUS sometimes fails to depict the target lesion or its margins, because it presents as a heterogeneous echogenicity, reflecting solid necrotic components. To address the limitations of B-mode EUS, contrast-enhanced harmonic EUS (CH-EUS) technology was developed, which greatly increased the diagnostic capabilities of B-mode EUS [6–9]. CH-EUS may identify vague lesions and their margins because it provides detailed information regarding the tissue structure and enhances the contrast between necrotic components and their surrounding tissues. Here, we report a case wherein EUS-TD was successfully performed for WON under CH-EUS guidance. To the best of our knowledge, this is the first report on CH-EUS-guided drainage of pancreatic fluid collections.

Case presentation

A male in his fifties had acute pancreatitis and was referred to Kindai University Hospital. Laboratory test results revealed an elevated inflammatory reaction and elevated serum amylase levels. Serum liver function parameters and bilirubin levels were also elevated. Abdominal computed

✉ Mamoru Takenaka
mamoxyo45@gmail.com

¹ Department of Gastroenterology and Hepatology, Kindai University Faculty of Medicine, 377-2 Ohno-Higashi, Osaka-Sayama 589-8511, Japan

² Second Department of Internal Medicine, Wakayama Medical University School of Medicine, Wakayama, Japan

tomography (CT) showed an enlarged head and body of the pancreas with peripancreatic fat stranding. The patient's CT severity index score for acute pancreatitis grading [10] was 5; this was classified as moderate acute pancreatitis. On the basis of the laboratory tests, gallstone-induced acute pancreatitis was suspected; however, bile duct stones were undetectable on CT. B-mode EUS was subsequently performed, and a bile duct stone, measuring 5 × 3 mm in size, was clearly visualized. Next, endoscopic sphincterotomy was performed under endoscopic retrograde cholangiopancreatography (ERCP) guidance for biliary decompression, and a 7-Fr biliary plastic stent was placed. After ERCP, liver function parameters and bilirubin levels immediately decreased; however, elevated inflammatory reaction remained. Abdominal CT obtained 2 weeks later revealed pancreatic fluid collection around the pancreas. Thus, ERCP was reattempted to confirm the presence of a pancreatic fistula. Pancreatography revealed extravasation of the contrast medium injected into the main pancreatic duct, and a 7-Fr pancreatic plastic stent was deployed to cover the pancreatic fistula. After stent placement, high fever and increased inflammatory reactions temporarily improved. Follow-up abdominal CT performed 4 weeks after admission showed 73 × 47-mm WON that contained gas bubbles (Fig. 1). On extracorporeal ultrasonography, the lesion was observed to have a mixed hypo- and hyper-echogenicity around the head of the pancreas (Fig. 2). Furthermore, high fever recurred (Fig. 3), suggesting that WON was clinically infected. According to the 2012 IAP/APA guidelines [11], we decided to perform EUS-TD of WON. As abdominal CT showed that WON was located adjacent to the gastric antrum, an echoendoscope (GF-UCT260; Olympus Medical Systems, Tokyo, Japan) was inserted around the gastric antrum. However, the presence



Fig. 1 Abdominal computed tomography image (portal vein phase) depicting large walled-off necrosis containing a few gas bubbles (white arrows)

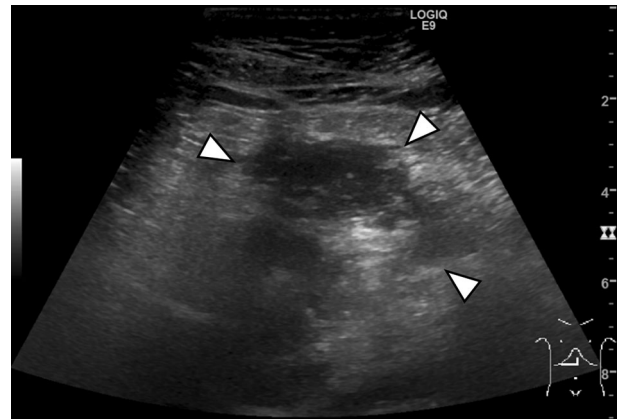


Fig. 2 Extracorporeal sonographic image showing a mixed hypo- and hyper-echoic lesion around the head of the pancreas (white arrowheads). Parts of the border were indistinct

of an echo-free space suggested that WON could not be well recognized. Thus, CH-EUS was performed to enhance the contrast between WON and its surrounding tissues (e.g., pancreatic parenchyma). Immediately after intravenously infusing 0.015 ml/kg of the sonographic contrast agent Sonazoid (perflubutane; Daiichi-Sankyo, Tokyo, Japan), WON and its margins were clearly identifiable as an avascular area (Fig. 4) and could be decisively punctured under CH-EUS guidance with a 19-gauge needle (EZ Shot 3 Plus, Olympus) (Fig. 5). Contrast medium (Iodixanol, Daiichi-Sankyo) was injected to confirm that WON had been correctly punctured, and a 0.025-inch guidewire (VisiGlide2, Olympus) was inserted in the cavity. After dilating the fistulous tract using a 6-mm balloon dilator (REN; Kaneka Medix, Osaka, Japan), a 7-Fr plastic stent and 6-Fr nasocystic drainage catheter were successfully deployed (Fig. 6). Subsequently, the patient's recurring high fever resolved within a few days (Fig. 3). CT performed 1 week later revealed a well-drained WON. The patient completely recovered and was discharged after 7 weeks of hospitalization. ERCP was performed 2 months after discharge. The pancreatic plastic stent was removed, and pancreatography revealed no extravasation of contrast medium injected into the main pancreatic duct.

Discussion

Acute necrotizing pancreatitis has a high mortality rate of 15%. When WON that is formed after acute necrotizing pancreatitis becomes infected, the mortality rate increases to 39% [12], necessitating intervention to achieve sepsis control. Recent evidence suggests that a minimally invasive step-up approach is superior to conventional open necrosectomy, with decreased rates of the composite

Fig. 3 Fever chart including laboratory data (WBC and CRP), imaging modality, and treatments. *BT* body temperature, *CT* computed tomography, *ERCP* endoscopic retrograde cholangiopancreatography, *EUS-TD* endoscopic ultrasonography-guided transluminal drainage

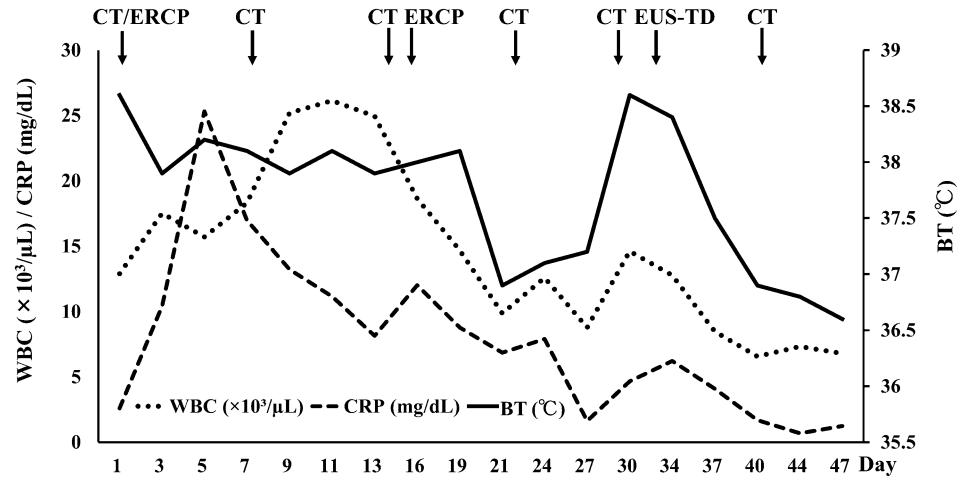


Fig. 4 Contrast-enhanced harmonic endoscopic ultrasonography (CH-EUS) image showing the walled-off necrosis as an avascular area with clear margins (*white arrowheads*), immediately after intravenously infusing Sonazoid (*left* B-mode image, *right* CH-EUS image)

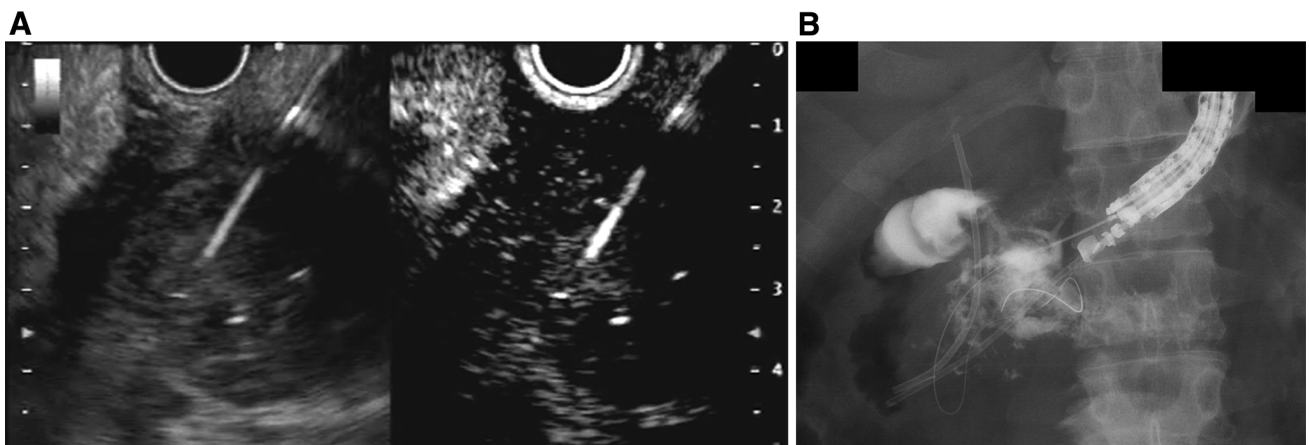
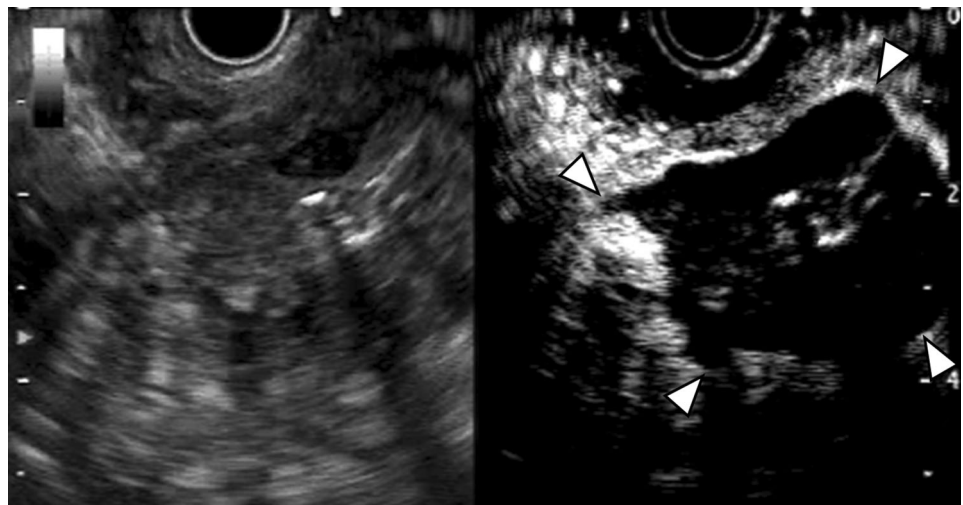


Fig. 5 Transluminal drainage of walled-off necrosis (WON) under contrast-enhanced harmonic endoscopic ultrasonography (CH-EUS) guidance. **a** Under CH-EUS guidance, the WON was punctured using

a 19-gauge aspiration needle (endosonographic view). **b** After puncturing the WON, a small amount of contrast medium was injected, and a guidewire was inserted (fluoroscopic view)

endpoint of major complications or death among patients with necrotizing pancreatitis and infected necrotic tissue [11, 13].

Endoscopic transluminal drainage is a minimally invasive approach. Endoscopic drainage for pancreatic fluid collection is reported to be superior to percutaneous



Fig. 6 Fluoroscopic image showing a successfully deployed 7-Fr plastic stent and 6-Fr nasocystic drainage catheter

drainage or surgery in terms of hospital stay and cost [14, 15]. EUS-TD has recently become important and widely accepted as a treatment option for WON, enabling safe puncture using a visualized approach. A prospective randomized trial comparing EUS-TD and conventional endoscopic drainage without EUS for pancreatic pseudocysts revealed that the technical success associated with EUS-TD was significantly higher than that of conventional endoscopic drainage [16]. Thus, when available, EUS should be considered as the first-line treatment modality for endoscopic drainage of pancreatic pseudocysts. Mean clinical success rates of 81–88% have been reported in systematic reviews of endoscopic approaches for WON using EUS-TD followed by endoscopic necrosectomy [17, 18]. In some cases, however, WON could not be well visualized on B-mode EUS, particularly in cases where WON contained a large amount of solid necrotic components with few liquids. CH-EUS may help identify these vague lesions.

CH-EUS has recently emerged as a powerful imaging modality to assess the microvasculature and hemodynamics of target lesions in real time [6–9]. CH-EUS is useful for characterizing pancreatic tumors [19, 20], diagnosing gallbladder lesions [21, 22], estimating the malignant potential of gastrointestinal stromal tumors [23, 24], and assessing lymph node metastases in pancreatobiliary carcinoma [25]. We recently reported a case in which EUS-guided biliary drainage was successfully performed under CH-EUS guidance [26]. In that case, the bile duct was filled with sludge and debris, which might have impaired the visibility of the bile duct on B-mode EUS. Thus, CH-EUS could be applied for diagnosis and therapeutic intervention.

Conclusion

In conclusion, CH-EUS enabled the visualization of WON and its margins as an avascular area, which facilitated safe puncturing of the target lesion. When B-mode EUS fails to depict the target lesion and its margins for EUS-TD of WON, CH-EUS may provide valuable information.

Compliance with ethical standards

Conflict of interest Kosuke Minaga, Mamoru Takenaka, Shunsuke Omoto, Takeshi Miyata, Ken Kamata, Kentaro Yamao, Hajime Imai, Tomohiro Watanabe, Masayuki Kitano, and Masatoshi Kudo declare that they have no conflict of interest.

Ethical statements All procedures followed were in accordance with the ethical standards of the responsible committee on human experimentation (institutional and national) and with the Helsinki Declaration of 1964 and later versions. Informed consent was obtained from the patient for being included in the study.

References

1. Banks PA, Bollen TL, Dervenis C, et al. Classification of acute pancreatitis—2012: revision of the Atlanta classification and definitions by international consensus. *Gut*. 2013;62:102–11.
2. Baron TH, Thaggard WG, Morgan DE, et al. Endoscopic therapy for organized pancreatic necrosis. *Gastroenterology*. 1996;111:755–64.
3. Varadarajulu S, Phadnis MA, Christein JD, et al. Multiple transluminal gateway technique for EUS-guided drainage of symptomatic walled-off pancreatic necrosis. *Gastrointest Endosc*. 2011;74:74–80.
4. Bapaye A, Dubale NA, Sheth KA, et al. Endoscopic ultrasonography-guided transmural drainage of walled-off pancreatic necrosis: comparison between a specially designed fully covered bi-flanged metal stent and multiple plastic stents. *Dig Endosc*. 2017;29:104–10.
5. Papachristou GI, Takahashi N, Chahal P, et al. Peroral endoscopic drainage/debridement of walled-off pancreatic necrosis. *Ann Surg*. 2007;245:943–51.
6. Dietrich CF, Ignee A, Frey H. Contrast-enhanced endoscopic ultrasound with low mechanical index: a new technique. *Z Gastroenterol*. 2005;43:1219–23.
7. Kitano M, Kudo M, Sakamoto H, et al. Preliminary study of contrast enhanced harmonic endosonography with second-generation contrast agents. *J Med Ultrasonics*. 2008;35:11–8.
8. Alvarez-Sánchez MV, Napoléon B. Contrast-enhanced harmonic endoscopic ultrasound imaging: basic principles, present situation and future perspectives. *World J Gastroenterol*. 2014;20:15549–63.
9. Kitano M, Kamata K. Contrast-enhanced harmonic endoscopic ultrasound: future perspectives. *Endosc Ultrasound*. 2016;5:351–4.
10. Balthazar EJ, Robinson DL, Megibow AJ, et al. Acute pancreatitis: value of CT in establishing prognosis. *Radiology*. 1990;174:331–6.
11. Working Group IAP/APA Acute Pancreatitis Guidelines. IAP/APA evidence-based guidelines for the management of acute pancreatitis. *Pancreatology*. 2013;13:e1–15.
12. Trikudanathan G, Attam R, Arain MA, et al. Endoscopic interventions for necrotizing pancreatitis. *Am J Gastroenterol*. 2014;109:969–81.

13. van Santvoort HC, Besselink MG, Bakker OJ, et al. A step-up approach or open necrosectomy for necrotizing pancreatitis. *N Engl J Med*. 2010;362:1491–502.
14. Akshintala VS, Saxena P, Zaheer A, et al. A comparative evaluation of outcomes of endoscopic versus percutaneous drainage for symptomatic pancreatic pseudocysts. *Gastrointest Endosc*. 2014;79:921–8.
15. Varadarajulu S, Bang JY, Sutton BS, et al. Equal efficacy of endoscopic and surgical cystogastrostomy for pancreatic pseudocyst drainage in a randomized trial. *Gastroenterology*. 2013;145:583–90.
16. Varadarajulu S, Christein JD, Tamhane A, et al. Prospective randomized trial comparing EUS and EGD for transmural drainage of pancreatic pseudocysts (with videos). *Gastrointest Endosc*. 2008;68:1102–11.
17. Fabbri C, Luigiano C, Lisotti A, et al. Endoscopic ultrasound-guided treatments: are we getting evidence based: a systematic review. *World J Gastroenterol*. 2014;20:8424–48.
18. van Brunshot S, Fockens P, Bakker OJ, et al. Endoscopic transluminal necrosectomy in necrotising pancreatitis: a systematic review. *Surg Endosc*. 2014;28:1425–38.
19. Kitano M, Sakamoto H, Matsui U, et al. A novel perfusion imaging technique of the pancreas: contrast-enhanced harmonic EUS (with video). *Gastrointest Endosc*. 2008;67:141–50.
20. Fusaroli P, Spada A, Mancino MG, et al. Contrast harmonic endoscopic ultrasound improves accuracy in diagnosis of solid pancreatic masses. *Clin Gastroenterol Hepatol*. 2010;8:629–34.
21. Imazu H, Mori N, Kanazawa K, et al. Contrast-enhanced harmonic endoscopic ultrasonography in the differential diagnosis of gallbladder wall thickening. *Dig Dis Sci*. 2014;59:1909–16.
22. Choi JH, Seo DW, Choi JH, et al. Utility of contrast-enhanced harmonic EUS in the diagnosis of malignant gallbladder polyps (with videos). *Gastrointest Endosc*. 2013;78:484–93.
23. Sakamoto H, Kitano M, Matsui S, et al. Estimation of malignant potential of GI stromal tumors by contrast-enhanced harmonic EUS (with videos). *Gastrointest Endosc*. 2011;73:227–37.
24. Yamashita Y, Kato J, Ueda K, et al. Contrast-enhanced endoscopic ultrasonography can predict a higher malignant potential of gastrointestinal stromal tumors by visualizing large newly formed vessels. *J Clin Ultrasound*. 2015;43:89–97.
25. Miyata T, Kitano M, Omoto S, et al. Contrast-enhanced harmonic endoscopic ultrasonography for assessment of lymph node metastases in pancreaticobiliary carcinoma. *World J Gastroenterol*. 2016;28:3381–91.
26. Minaga K, Kitano M, Yoshikawa T, et al. Hepaticogastrostomy guided by real-time contrast-enhanced harmonic endoscopic ultrasonography: a novel technique. *Endoscopy*. 2016;48:E228–9.

Original Article

Contrast-enhanced harmonic endoscopic ultrasonography for differential diagnosis of localized gallbladder lesions

Ken Kamata,¹ Mamoru Takenaka,¹ Masayuki Kitano,¹ Shunsuke Omoto,¹ Takeshi Miyata,¹ Kosuke Minaga,¹ Kentaro Yamao,¹ Hajime Imai,¹ Tosiharu Sakurai,¹ Naoshi Nishida,¹ Hiroshi Kashida,¹ Takaaki Chikugo,² Yasutaka Chiba,⁴ Takuya Nakai,³ Yoshifumi Takeyama,³ Andrea Lisotti,⁵ Pietro Fusaroli⁵ and Masatoshi Kudo¹

Departments of ¹Gastroenterology and Hepatology, ²Pathology, and ³Surgery, Kindai University Faculty of Medicine, ⁴Clinical Research Center, Kindai University Hospital, Osaka-Sayama, Japan and ⁵Gastroenterology Unit, Hospital of Imola, University of Bologna, Bologna, Italy

Background and Aim: Differential diagnosis of localized gallbladder lesions is challenging. The aim of the present study was to evaluate the utility of contrast-enhanced harmonic endoscopic ultrasonography (CH-EUS) for diagnosis of localized gallbladder lesions.

Methods: One hundred and twenty-five patients with localized gallbladder lesions were evaluated by CH-EUS between March 2007 and February 2014. This was a single-center retrospective study. Utilities of fundamental B-mode EUS (FB-EUS) and CH-EUS in the differentiation of gallbladder lesions and sludge plug were initially compared. Thereafter, these two examinations were compared with respect to their accuracy in the diagnosis of malignant lesions. Five reviewers blinded to the clinicopathological results evaluated microcirculation patterns in the vascular and perfusion images.

Results: In the differentiation between gallbladder lesions and sludge plug, FB-EUS had a sensitivity, specificity, and accuracy

of 82%, 100%, and 95%, respectively, whereas CH-EUS had a sensitivity, specificity, and accuracy of 100%, 99%, and 99%, respectively. FB-EUS-based diagnosis of carcinomas based on tumor size and/or shape had a sensitivity, specificity, and accuracy of 61–87%, 71–88%, and 74–86%, respectively. Additional information regarding irregular vessel patterns in the vascular image and/or heterogeneous enhancement in the perfusion image on CH-EUS increased the sensitivity, specificity, and accuracy for the diagnosis of carcinomas to 90%, 98%, and 96%, respectively. There was a significant difference between FB-EUS and CH-EUS in terms of carcinoma diagnosis.

Conclusion: CH-EUS was useful for the evaluation of localized gallbladder lesions.

Key words: adenomyomatosis, contrast-enhanced harmonic endoscopic ultrasonography, endoscopic ultrasonography, gallbladder, gallbladder carcinoma

INTRODUCTION

ACCURACY OF DIFFERENTIAL diagnosis of gallbladder diseases by radiological imaging has recently improved, especially in the field of ultrasonography (US), where it has sometimes been difficult to differentiate benign disease from gallbladder carcinoma.^{1–3} The majority of gallbladder carcinomas have a typical appearance on gray-scale sonography, with either a solid mass that occupies the whole gallbladder, or a focal polypoid mass.⁴ A previous report suggested that all patients with gallbladder polyps

larger than 10 mm in diameter should undergo resection.⁵ This size criteria is insufficient to distinguish non-neoplastic from neoplastic polyps.⁶ It has been proposed that color Doppler sonography and contrast-enhanced power Doppler US are useful techniques for the differential diagnosis of malignant and benign gallbladder disease.^{7–11} However, such vascular imaging techniques carry a number of inherent limitations, including blooming or overpainting artifacts.^{12–22} Recently, contrast-enhanced harmonic US (CE-US), has been recognized as a useful method for the diagnosis of gallbladder disease.^{23–26} Additionally, endoscopic ultrasonography (EUS) is considered to be superior to US for depiction of the gallbladder, and provides high-resolution images.^{27–29} As a combination of these techniques, known as contrast-enhanced harmonic EUS (CH-EUS), should be a powerful diagnostic approach,^{30–32}

Corresponding: Mamoru Takenaka, Department of Gastroenterology and Hepatology, Kindai University Faculty of Medicine, 377-2 Ohno-higashi, Osaka-Sayama 589-8511, Japan. Email: mamoxyo45@gmail.com

Received 8 March 2017; accepted 4 June 2017.

we used CH-EUS for the differential diagnosis of gallbladder diseases, and evaluated its utility for their characterization.

METHODS

Patients

BETWEEN MARCH 2007 and February 2014, patients suspected of having localized gallbladder lesions according to conventional EUS at Kindai University Hospital underwent CH-EUS. This retrospective cohort study included retrospective review of imaging, clinical, and pathological data, with additional independent review of the CH-EUS videos. This study was carried out with the approval of the ethics committee of the Kindai University Faculty of Medicine.

Endoscopic ultrasonography

A GF-UCT260 echoendoscope (Olympus Medical Systems Co. Ltd, Tokyo, Japan) specifically developed for CH-EUS was used. EUS images were analyzed using an ALOKA ProSound SSD α -10 system (ALOKA Co. Ltd, Tokyo, Japan). If lesions were detected on fundamental B-mode EUS (FB-EUS) images of the gallbladder (an echogenic structure, polypoid lesion, wall thickening, or heterogeneous region), images of the ideal scanning plane were displayed to portray the whole extent of the lesion. Thereafter, the imaging mode was changed to extended pure harmonic detection (ExPHD), which synthesized the filtered second-harmonic components with signals obtained from the phase shift for contrast-enhanced harmonic imaging. Transmitting frequency and mechanical index were 4.7 MHz and 0.3, respectively. Sonazoid (Daiichi-Sankyo, Tokyo, Japan), which consists of perfluorobutane microbubbles surrounded by a lipid membrane, was used as the US contrast agent for CH-EUS. A bolus injection of the US contrast agent (15 μ L/kg bodyweight) was given. After US contrast infusion, vascular and enhancement patterns were assessed in real time by examination of continuous 0–15 s (vascular images) and 40–60 s (perfusion images) images, respectively.

Imaging analysis

FB-EUS

A localized gallbladder lesion was defined as a solitary gallbladder lesion (i.e. multiple lesions in the gallbladder were excluded for analysis regardless of invasion or metastasis to other organs). If the echogenic gallbladder structure moved in response to tapping on the right hypochondriac region of the body surface, or changed in shape when there was postural change from left lateral to

supine position, the lesion was defined as biliary sludge. Any findings of gallbladder lesions, except for sludge plug, were classified into two categories: pedunculated lesions and sessile lesions. Sessile lesions were defined as those where the base of the lesion was wider than the protuberance of the lesion on FB-EUS.

CH-EUS

Vascular images were categorized according to three patterns: spotty vessels ('spotty vessels', flowing in the lesion), irregular vessels ('linear vessels', flowing from the periphery to the center of the lesion), or no vessels. Perfusion images were categorized into four patterns: homogeneous, homogeneous with clear perfusion defects, heterogeneous, and the absence of an enhancement pattern. These patterns in the vascular and perfusion images were modifications of the gallbladder lesion classifications for contrast-enhanced transabdominal US reported by Inoue *et al.*²³ All data were stored in a recording system and reviewed by five readers (S. Omoto, T. Miyata, K. Minaga, K. Yamao, and M. Takenaka) who were absent during the examination and unaware of the clinicopathological results. Interobserver variations in the CH-EUS vascular and enhancement patterns were assessed by calculating the κ -coefficient. When the independent conclusions of the five reviewers differed, the saved images were reviewed together, and re-evaluated until agreement was reached.

Final diagnosis of gallbladder lesions

Final diagnoses were made on the basis of surgical specimens. Inoperable cases of gallbladder carcinoma were diagnosed according to the histology or cytology of samples of metastatic lesions obtained by EUS-guided fine-needle aspiration (EUS-FNA). In other cases, the final diagnosis was confirmed by follow-up examinations for at least 24 months. If the lesions remained unchanged in appearance, they were diagnosed as benign. When lesions were not found in either the resected gallbladder, or in follow-up EUS examinations of the gallbladder, the observed abnormality was defined as biliary sludge.

Statistical analysis

First, the sensitivities and specificities of FB-EUS and CH-EUS for distinguishing between gallbladder lesions and sludge plug were evaluated. Second, the sensitivities and specificities of FB-EUS were evaluated for cases of gallbladder carcinoma defined according to a size of 1 cm or more (diagnosis by tumor size) and the presence of a

sessile lesion (diagnosis by tumor shape). The sensitivity, specificity, and accuracy of CH-EUS in the diagnosis of gallbladder carcinoma were calculated when the carcinoma was defined as the presence of irregular vessels or heterogeneous enhancement. McNemar's test was applied to evaluate differences between FB-EUS and CH-EUS in terms of the diagnosis of gallbladder lesions from sludge plug and the diagnosis of malignancy versus no malignancy. All analyses were carried out using the statistical software SAS 9.1.3 (SAS Institute Inc., Cary, NC, USA). Differences were considered to be statistically significant when P -value <0.05 .

RESULTS

ONE HUNDRED AND twenty-five consecutive patients were recruited to this study (Table 1). Of the 125 patients, 75 subsequently underwent surgery. For the remaining 50 patients, a final diagnosis was confirmed by follow-up examinations or by EUS-FNA. EUS-FNA confirmed the diagnosis in 15 patients with gallbladder carcinoma, whereas 35 patients with benign gallbladder lesions were diagnosed at a follow-up examination. These follow-up analyses or pathological examinations revealed that 31 patients had a carcinoma (Table 1). All gallbladder carcinomas were diagnosed histologically as adenocarcinoma. In all 31 cases, median size of the gallbladder carcinoma was 19.6 mm (range, 4–50 mm); median size in 16 resected cases was 12.3 mm (range, 4–24 mm). Union for International Cancer Control (UICC) classification (7th edition) of the 16 resected cases revealed that two cases

were stage 0, 10 were stage I, three were stage II, and one case was stage IIIB. CH-EUS detected a polypoid lesion hidden within the biliary sludge in one case (Fig. 1). In this case, FB-EUS resulted in a diagnosis of sludge plug, without detection of the polypoid lesion within the biliary sludge.

CH-EUS vascular and perfusion images analysis

Table 2 shows the results of CH-EUS vascular and perfusion images according to gallbladder lesion type. Reproducibility measures of interobserver assessments showed that the κ -coefficient for the three vascular and four perfusion images categories were 0.915 and 0.928,

Table 1 Characteristics of patients in the present study

Total no. patients	125
Mean age (years)	61 (19–82)
Sex, male : female	67:58
Acquisition of final diagnosis, n (surgically resected)	125 (75)
Sludge plug	29 (20)
Non-neoplastic polyp	31 (9)
Chronic cholecystitis	18 (14)
Adenomyomatosis	16 (16)
Carcinoma	31 (16)
UICC classification [†] (stage)	
0	2
I	10
II	3
IIIA	0
IIIB	1

[†]Resected cases only.

UICC, Union for International Cancer Control.

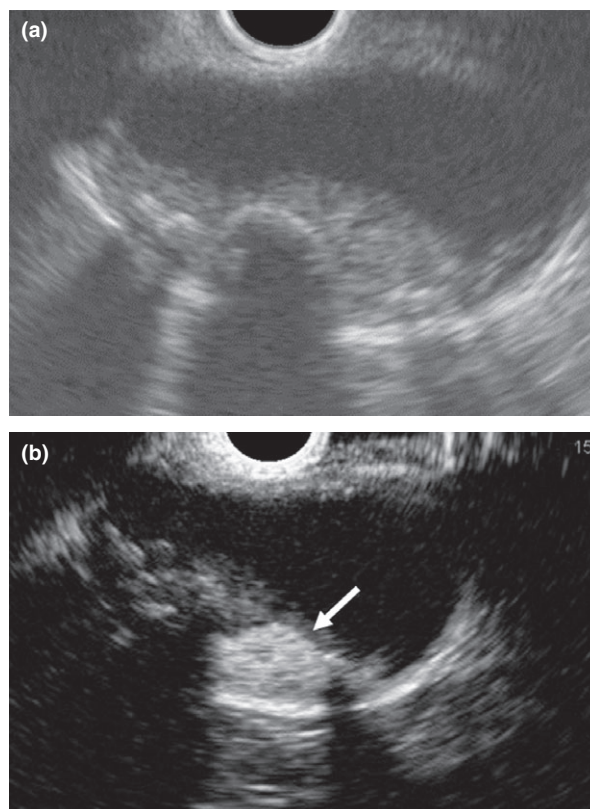


Figure 1 Case with a cholesterol polyp hidden by biliary sludge. (a) Fundamental B-mode endoscopic ultrasonography (monitor mode). A high echoic structure with acoustic shadow can be seen in the gallbladder. (b) Contrast-enhanced harmonic endoscopic ultrasonography (CH-EUS). The majority of the lesion is not enhanced by CH-EUS, but the polypoid lesion is incidentally detected in the center of the lesion as a homogeneous enhancement with spotty vessels (arrow).

Table 2 CH-EUS vascular and perfusion image diagnostic results for gallbladder lesions

Gallbladder lesion (total, <i>n</i> = 125)	Vascular image (%)			Perfusion image (%)			
	Spotty	Irregular	None	Homogeneous	Clear perfusion defects	Heterogeneous	Absent
Sludge plug (<i>n</i> = 29)	0	0	100	0	0	0	100
Non-neoplastic polyp (<i>n</i> = 31)	97	0	3	97	0	0	3
Chronic cholecystitis (<i>n</i> = 18)	100	0	0	100	0	0	0
Adenomyomatosis (<i>n</i> = 16)	87	13	0	0	87	13	0
Carcinoma (<i>n</i> = 31)	32	68	0	10	0	90	0

CH-EUS, contrast-enhanced harmonic endoscopic ultrasonography.

respectively. Vascular images showed that almost all gallbladder lesions, with the exception of the sludge plugs, contained spotty or irregular vessels, whereas no vessels were observed in any of the sludge plugs, or one of the 31 cases with polyps (3%). These lesions also showed no enhancement in the perfusion images (classified as ‘absence of enhancement’).

Classification of gallbladder lesions according to the combination of CH-EUS vascular and perfusion images

Gallbladder lesions were categorized into five types according to the combination of the CH-EUS vascular and perfusion images. The five categories and the classification results for the gallbladder pathology are shown in Figure 2. Type 1 lesions were characterized by no signs of blood flow (Fig. 3). Type 2 lesions were characterized by spotty vessels in the vascular image and a homogeneous enhancement pattern in the perfusion image (Fig. 4). Type 3 lesions were characterized by spotty vessels in the vascular image and a homogeneous pattern with clear perfusion defects in the perfusion image, suggestive of

Rokitansky-Aschoff sinus (Fig. 5). Type 4 lesions were characterized by spotty vessels in the vascular image and heterogeneous enhancement in the perfusion image. Type 5 lesions were characterized by irregular vessels in the vascular image and heterogeneous enhancement in the perfusion image (Fig. 6).

Differentiation of solid lesions from sludge plug in FB-EUS and CH-EUS

For the differential diagnosis of gallbladder lesions from sludge plug, there was no significant difference between FB-EUS and CH-EUS although sensitivity and accuracy of CH-EUS were higher than those of FB-EUS (Table 3). Clinical characteristics of the five cases where biliary sludge in the gallbladder was misdiagnosed by FB-EUS, but correctly diagnosed by CH-EUS, are shown in Table 4.

Diagnosis of gallbladder carcinoma in FB-EUS and CH-EUS

Sensitivity, specificity, and accuracy of FB-EUS and CH-EUS in the diagnosis of gallbladder carcinoma are shown in






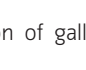
Type (Total, <i>n</i> = 125)	Enhancement pattern (Vascular image/perfusion image)		Final diagnosis
1 (<i>n</i> = 30)	No vessel/absent		Sludge plug <i>n</i> = 29 Non-neoplastic polyp <i>n</i> = 1
2 (<i>n</i> = 51)	Spotty vessel/homogeneous		Non-neoplastic polyp <i>n</i> = 30 Cholecystitis <i>n</i> = 18 Carcinoma <i>n</i> = 3
3 (<i>n</i> = 14)	Spotty vessel/clear perfusion defects		Adenomyomatosis <i>n</i> = 14
4 (<i>n</i> = 7)	Spotty vessel/heterogeneous		Carcinoma <i>n</i> = 7
5 (<i>n</i> = 23)	Irregular vessel/ heterogeneous		Carcinoma <i>n</i> = 21 Adenomyomatosis <i>n</i> = 2

Figure 2 The five types of enhancement pattern and classification of gallbladder disease by contrast-enhanced harmonic endoscopic ultrasonography.

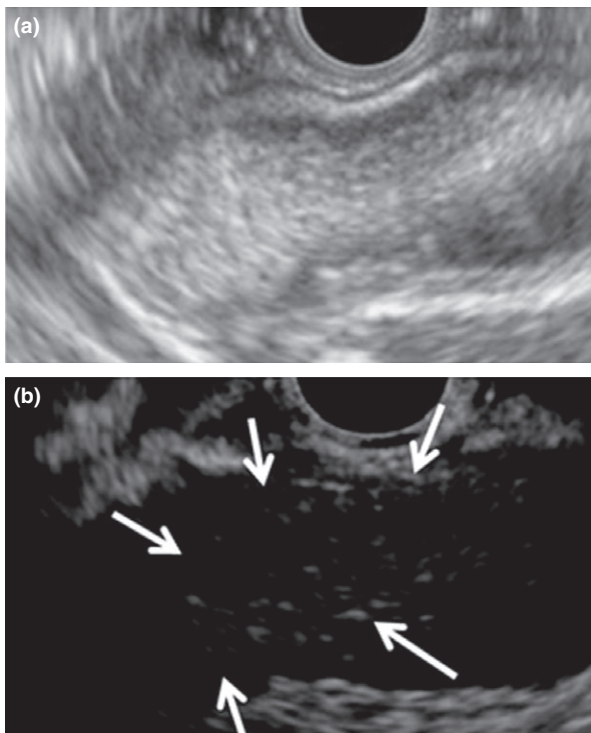


Figure 3 Typical case of gallbladder sludge plug. (a) Fundamental B-mode endoscopic ultrasonography (monitor mode). A high echoic structure can be seen in the gallbladder. (b) Contrast-enhanced harmonic endoscopic ultrasonography. The lesion is not enhanced (arrows).

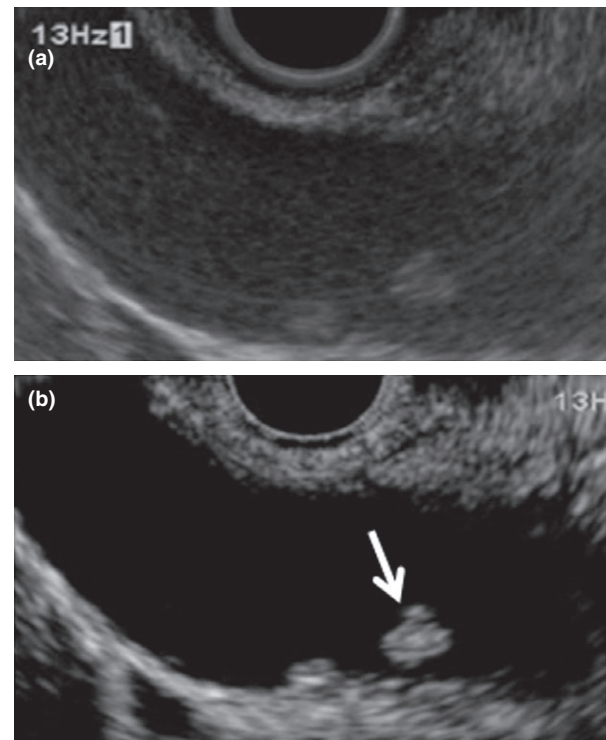


Figure 4 Typical case of a cholesterol polyp. (a) Fundamental B-mode endoscopic ultrasonography (monitor mode). An echogenic mass can be seen in the body of the gallbladder. (b) Contrast-enhanced harmonic endoscopic ultrasonography. The lesion (arrow) demonstrates homogeneous enhancement.

Table 5. When the tumor size classification was used for the diagnosis of gallbladder carcinoma, sensitivity, specificity, and accuracy were 77%, 88%, and 86%, respectively; thus, this diagnosis was more accurate than diagnosis based on tumor shape. Even when a diagnosis based on a combination of tumor size and shape was taken into consideration, the accuracy of FB-EUS did not improve.

Heterogeneous enhancement (equivalent to Type 4 and/or 5 diagnosed by CH-EUS) had a sensitivity, specificity, and accuracy for the diagnosis of the carcinoma of 90%, 98%, and 96%, respectively. There was a significant difference between a FB-EUS diagnosis based on tumor size, tumor shape, and their combination and a CH-EUS diagnosis based on heterogeneous enhancement ($P < 0.001$). Diagnosis of gallbladder carcinoma, based on interpretation of vascular and perfusion images by five independent observers, was also subject to receiver operating characteristic analyses. Area under the curve (AUC) was 0.880 for vascular images, 0.964 for perfusion images, and 0.966 for the combined images.

DISCUSSION

CONTRAST-ENHANCED HARMONIC US has been recognized as a useful tool for evaluation of the vascularity of gallbladder lesions.²³ Moreover, this technique is useful for both characterization of the lesion and observation of gallbladder wall integrity.³³ EUS enabled us to obtain more detailed images of the internal structure of gallbladder lesions;³⁴ therefore, in the present study we used CH-EUS using the ExPHD mode for the diagnosis and characterization of gallbladder lesions through evaluation of their vascularity and enhancement patterns. Doppler EUS with and without contrast enhancement allows the differentiation of gallbladder lesions from sludge plug by evaluation of their vascularity.³⁰ However, the Doppler mode cannot produce parenchymal perfusion images. When used with sonographic contrast agents, power or color Doppler EUS fails to depict signals from microbubbles in very slowly flowing microscopic vessels.^{30,31} Power Doppler used with sonographic contrast agents is also prone to artifacts such as

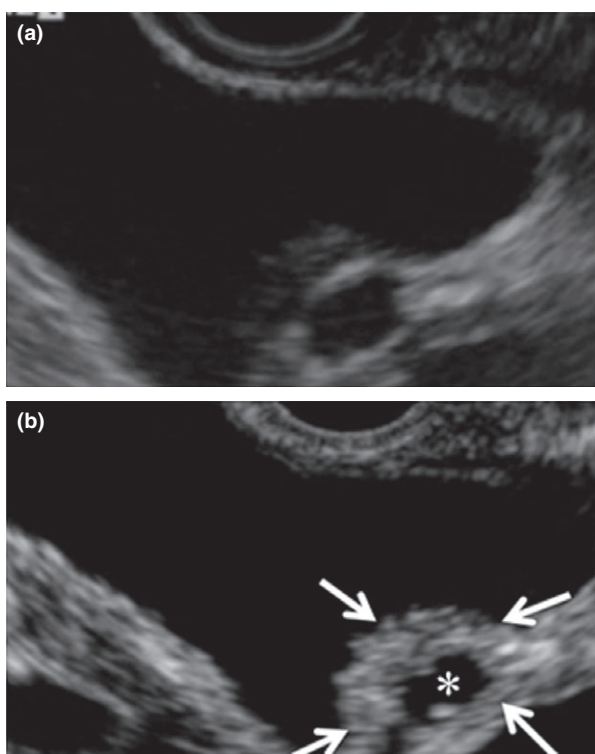


Figure 5 Typical case of adenomyomatosis. (a) Fundamental B-mode endoscopic ultrasonography (monitor mode). Localized wall thickening with an anechoic area is detected in the gallbladder. (b) Contrast-enhanced harmonic endoscopic ultrasonography. The lesion (arrows) is homogeneous, with a clear perfusion enhancement defect (*).

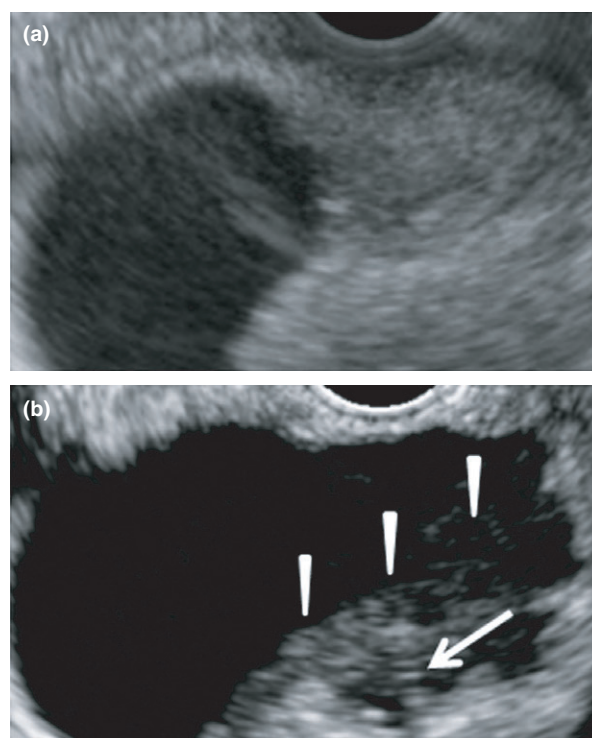


Figure 6 Typical case of gallbladder carcinoma. (a) Fundamental B-mode endoscopic ultrasonography (monitor mode). An echogenic structure is detected in the body of the gallbladder. (b) Contrast-enhanced harmonic endoscopic ultrasonography. The lesion (arrowheads) demonstrates irregular vessels with heterogeneous enhancement (arrow).

Table 3 Sensitivity, specificity, and accuracy of FB-EUS and CH-EUS for differentiating of solid lesions from sludge plugs

Examination	Sensitivity (%)	Specificity (%)	Accuracy (%)	P-value [†]
FB-EUS	82	100	95	0.221
CH-EUS (Type 1) [‡]	100	99	99	

[†]McNemar’s test was used for comparing CH-EUS with FB-EUS.
[‡]No vessels and no enhancement observed on vascular and perfusion images.

CH-EUS, contrast-enhanced harmonic endoscopic ultrasonography; EUS, endoscopic ultrasonography; FB-EUS, fundamental B-mode EUS.

blooming, which makes the visualized blood vessels appear wider than in fundamental B-mode imaging.^{30,31} By contrast, contrast harmonic imaging successfully provided images demonstrating parenchymal perfusion and microcirculation in gallbladder lesions.

Table 4 Clinical characteristics of the five cases of biliary sludge in the gallbladder that were misdiagnosed as gallbladder lesions (except sludge plug) with FB-EUS

Patient no.	FB-EUS diagnosis	CH-EUS diagnosis [†]	Final diagnosis
1	Carcinoma	Type 1	Sludge
2	Carcinoma	Type 1	Sludge
3	Carcinoma	Type 1	Sludge
4	Benign lesion	Type 1	Sludge
5	Benign lesion	Type 1	Sludge

[†]Type 1, no vessel and absent enhancement observed on vascular and perfusion images.

CH-EUS, contrast-enhanced harmonic EUS; EUS, endoscopic ultrasonography; FB-EUS, fundamental B-mode EUS.

There have been several reports on the differential diagnosis of gallbladder lesions, and these have described the use of a variety of imaging methods using contrast media. Xie *et al.*³³ reported that, in 90.9% of malignant

Table 5 Sensitivity, specificity, and accuracy of FB-EUS and CH-EUS for the diagnosis of gallbladder carcinoma

Examination	Sensitivity (95% CI)	Specificity (95% CI)	Accuracy (95% CI)	P-value [†]
FB-EUS(1) Diameter >1 cm	77% (24/31)(0.64–0.87)	88% (83/94)(0.84–0.92)	86% (107/125)(0.70–0.90)	
(2) Sessile lesion	71% (22/31)(0.56–0.83)	79% (74/94)(0.74–0.83)	77% (96/125)(0.70–0.83)	
(3) (1) and/or (2)	87% (27/31)(0.73–0.95)	71% (67/94)(0.67–0.74)	75% (94/125)(0.68–0.80)	
(4) (1) and (2)	61% (19/31)(0.47–0.74)	79% (74/94)(0.74–0.83)	74% (93/125)(0.67–0.81)	
CH-EUS [‡] (5) Type 4	23% (7/31)(0.18–0.26)	100% (94/94)(0.97–1.00)	81% (101/125)(0.78–0.82)	
(6) Type 5	68% (21/31) (0.53–0.69)	98% (92/94) (0.94–0.99)	90% (113/125) (0.84–0.92)	
(7) Type 4 and/or 5	90% (28/31) (0.81–0.95)	98% (92/94) (0.95–0.99)	96% (120/125) (0.91–0.98)	
(1) vs (7)				<0.001
(2) vs (7)				<0.001
(3) vs (7)				<0.001
(4) vs (7)				<0.001

[†]McNemar's test was used to compare CH-EUS with FB-EUS. For this analysis, (1) and (7), (2) and (7), (3) and (7), and (4) and (7) were compared.

[‡]Type 4, spotty vessel and heterogeneous enhancement observed on vascular and perfusion images; Type 5, irregular vessel and heterogeneous enhancement observed on vascular and perfusion images.

CH-EUS, contrast-enhanced harmonic endoscopic ultrasonography; EUS, endoscopic ultrasonography; FB-EUS, fundamental B-mode EUS.

lesions and in 17.0% of benign lesions, a pattern of hyper-enhancement or iso-enhancement was found in the early phase of contrast agent administration, which then faded out to hypo-enhancement within 35 s. They observed the washout of contrast from gallbladder lesions. One study reported on the utility of contrast-enhanced EUS for the diagnosis of gallbladder diseases; however, the authors used conventional EUS, which was not equipped with a specific mode for contrast enhancement.³⁵ According to their report, gallbladder carcinoma showed enhancement, whereas benign gallbladder polyps did not show enhancement. Intensity of contrast enhancement on conventional B-mode imaging was insufficient to permit visualization of the vascular structures. In our study, using Sonazoid and ExPHD mode, which emphasizes the microcirculation imaging effect due to the contrast agent, all gallbladder lesions showed vascularity, with the exception of 29 cases with sludge and one case with a non-neoplastic polyp (2 mm or less in diameter). Choi *et al.*³⁶ reported on the utility of CH-EUS using ExPHD mode. However, 14 of 59 benign polyps (24%) demonstrated no vascularity. This difference might be attributed to their use of SonoVue (Bracco, Milan, Italy) as a contrast agent.

On either transabdominal US or EUS, neoplastic gallbladder lesions sometimes exhibit similar features to other gallbladder lesions, such as cholecystitis, adenomyomatosis, and even biliary sludge.^{1–3} We therefore evaluated the wall thickening of lesions in the gallbladder, as well as polypoid lesions. CE-US using coded phase inversion harmonic US with Levovist (Schering AG, Berlin, Germany) allowed more effective differential diagnosis between gallbladder sludge and gallbladder lesions (except for sludge plug) than

conventional US.²³ In the present study, CH-EUS allowed differentiation of biliary sludge from neoplastic lesions according to the presence of vascularity. This EUS-based result was consistent with that of transabdominal US. CH-EUS demonstrated that adenomyomatosis was indicated by clear perfusion defects in the perfusion image, which may represent Rokitansky-Aschoff sinuses. Gallbladder carcinoma appears as an echogenic or echopenic mass without aggregation of echogenic spots, with the internal echo pattern of carcinoma often being heterogeneous.³⁷ Choi *et al.*²⁸ reported that an EUS-based scoring system aided the identification of malignant gallbladder polypoid lesions, and reported the sensitivity and specificity for differentiation of benign and malignant gallbladder polypoid lesions as 81% and 86%, respectively. In this study, we used a combination of tumor size and tumor shape for diagnosing gallbladder carcinoma, and similar results were observed for the diagnoses made on the basis of tumor size.

CH-EUS showed heterogeneous enhancement in 28 of 31 cases of carcinoma (Type 4 and/or 5). With the exception of two cases of adenomyomatosis, heterogeneous enhancement was not found in benign gallbladder lesions. These results reveal that perfusion image on CH-EUS has a high sensitivity and specificity for the diagnosis of gallbladder carcinoma. The combination of vascular and perfusion image improved the AUC in comparison with vascular image only. However, we cannot conclude that combining images improved the AUC over that obtained for perfusion images only; this is because, when the level of interobserver agreement about vascular and perfusion images is taken into account, the perfusion images alone appear to yield a more definitive diagnosis than combined images.

The present study has several limitations. Study weaknesses include the retrospective nature of the study and the lack of a control group. Endosonographers were not blinded to the sonography techniques; therefore, there may have been bias when carrying out EUS, such as focusing on certain characteristics according to the pretest probability of malignancy. Verification bias cannot be completely excluded, as three cases were affected by the CH-EUS results in terms of surgery.

In conclusion, CH-EUS was useful for depicting micro-circulation, and for differential diagnosis of biliary sludge from other gallbladder lesions. Gallbladder carcinoma was characterized by irregular vessels in the vascular image, and heterogeneous enhancement in the perfusion image. Although this study examined a limited number of patients, and further studies with larger patient numbers are needed to confirm these conclusions, it can be concluded that CH-EUS provided significant improvements over conventional EUS with respect to the quality of diagnoses.

ACKNOWLEDGMENTS

THE PRESENT STUDY was supported by grants from the Japan Society for the Promotion of Science.

CONFLICTS OF INTEREST


AUTHORS DECLARE NO conflicts of interest for this article.

REFERENCES:

- Soiva M, Aro K, Pamilo M, Päivänsalo M, Suramo I, Taavitsainen M. Ultrasonography in carcinoma of the gallbladder. *Acta Radiol.* 1987; **28**: 711–4.
- Demidov VN, Iantovskii IuR, Arkhipov SN. Ultrasonographic diagnosis of tumors of the gallbladder. *Klin Med (Mosk).* 1992;**70**:44–9.
- Anastasi B, Sutherland GR. Biliary sludge-ultrasonic appearance simulating neoplasm. *Br. J. Radiol.* 1981; **54**: 679–81.
- Sauerbrei EE, Nguyen KT, Nolan RL. The gallbladder. In: Sauerbrei EE, Nguyen KT, Nolan RL (eds). *Abdominal Sonography*. New York: Raven Press, 1992; 25–50.
- Boulton RA, Adams DH. Gallbladder polyps: When to wait and when to act. *Lancet* 1997; **349**: 817.
- Terzi C, Sökmen S, Seçkin S, Albayrak L, Uğurlu M. Polypoid lesions of gallbladder: Report of 100 cases with special reference to operative indication. *Surgery* 2000; **127**: 622–7.
- Hirooka Y, Naitoh Y, Goto H, Furukawa T, Ito A, Hayakawa T. Differential diagnosis of gallbladder masses using colour doppler ultrasonography. *J. Gastroenterol. Hepatol.* 1996; **11**: 840–6.
- Ueno N, Tomiyama T, Tano S, Wada S, Kimura K. Diagnosis of gallbladder carcinoma with color doppler ultrasonography. *Am. J. Gastroenterol.* 1996; **91**: 1647–9.
- Taylor KJW, Ramos I, Carter D, Morse SS, Snower D, Fortune K. Correlation of Doppler US tumor signals with neovascular morphologic features. *Radiology* 1988; **166**: 57–62.
- Tanaka S, Kitamura T, Fujita M, Kasugai H, Inoue A, Ishiguro S. Small hepatocellular carcinoma: Differentiation from adenomatous hyperplastic nodule with colour Doppler flow imaging. *Radiology* 1992; **182**: 161–5.
- Shimamoto K, Sakuma S, Ishigaki T, Ishiguchi T, Itoh SM, Fukatsu H. Hepatocellular carcinoma: Evaluation with colour Doppler US and MR imaging. *Radiology* 1992; **182**: 149–53.
- Burns PN. Harmonic imaging with ultrasound contrast agents. *Clin. Radiol.* 1996; **51**(Suppl): 50–5.
- Kim TK, Choi BI, Han JK, Hong HS, Park SH, Moon SG. Hepatic tumors: Contrast agent-enhancement patterns with pulse-inversion harmonic US. *Radiology* 2000; **21**: 411–7.
- Numata K, Tanaka K, Kiba T *et al.* Contrast-enhanced, wide-band harmonic gray scale imaging of hepatocellular carcinoma: correlation with helical computed tomographic findings. *J. Ultrasound Med.* 2001; **20**: 89–98.
- Numata K, Tanaka K, Kiba T *et al.* Using contrast-enhanced sonography to assess the effectiveness of transcatheter arterial embolization for hepatocellular carcinoma. *AJR* 2001; **176**: 1199–205.
- Ding H, Kudo M, Maekawa K, Suetomi Y, Minami Y, Onda H. Detection of tumor parenchymal blood flow in hepatic tumors: Value of second harmonic imaging with a galactose based contrast agent. *Hepatol. Res.* 2001; **21**: 242–51.
- Ding H, Kudo M, Onda H, Nomura H, Haji S. Sonographic diagnosis of pancreatic islet cell tumor: Value of intermittent harmonic imaging. *J. Clin. Ultrasound* 2001; **29**: 411–6.
- Ding H, Kudo M, Onda H, Suetomi Y, Minami Y, Maekawa K. Contrast-enhanced subtraction harmonic sonography for evaluating treatment response in patients with hepatocellular carcinoma. *AJR* 2001; **176**: 661–6.
- Ding H, Kudo M, Onda H *et al.* Evaluation of post treatment response for hepatocellular carcinoma with contrast-enhanced coded phase-inversion harmonic US: comparison with dynamic CT. *Radiology* 2001; **221**: 721–30.
- Jang HJ, Lim HK, Lee WJ, Kim SH, Kim KA, Kim EY. Ultrasonographic evaluation of focal hepatic lesions: Comparison of pulse inversion harmonic, tissue harmonic, conventional imaging techniques. *J. Ultrasound Med.* 2000; **19**: 293–9.
- Burn PN, Wilson SR, Simpson DH. Pulse inversion imaging of liver blood flow: Improved method for characterizing focal masses with microbubble contrast. *Invest. Radiol.* 2000; **35**: 58–71.
- Meloni MF, Goldberg SN, Livraghi T *et al.* Hepatocellular carcinoma treated with radiofrequency ablation: Comparison of pulse inversion contrast-enhanced harmonic sonography, contrast-enhanced power Doppler sonography, and helical CT. *AJR* 2001; **177**: 375–380.

- 23 Inoue T, Kitano M, Kudo M *et al.* Diagnosis of gallbladder diseases by contrast-enhanced phase-inversion harmonic ultrasonography. *Ultrasound Med. Biol.* 2007; **33**: 353–61.
- 24 Adamietz B, Wenkel E, Uder M *et al.* Contrast enhanced sonography of the gallbladder. A tool in the diagnosis of cholecystitis? *Eur. J. Radiol.* 2007; **61**: 262–6.
- 25 Numata K, Oka H, Morimoto M *et al.* Differential diagnosis of gallbladder diseases with contrast-enhanced harmonic gray scale ultrasonography. *J. Ultrasound Med.* 2007; **26**: 763–74.
- 26 Kim KA, Park CM, Park SW *et al.* Contrast-enhanced power Doppler US: Is it useful in differentiation of gallbladder diseases? *Clin. Imaging* 2002; **26**: 319–24.
- 27 Azuma T, Yoshizawa T, Araida T, Takasaki K. Differential diagnosis of polypoid lesions of the gallbladder by endoscopic ultrasonography. *Am. J. Surg.* 2001; **181**: 65–70.
- 28 Choi WB, Lee SK, Kim MH *et al.* A new strategy to predict the neoplastic polyps of the gallbladder based on a scoring system using EUS. *Gastrointest. Endosc.* 2000; **52**: 372–9.
- 29 Sadamoto Y, Oda S, Tanaka M *et al.* A useful approach to the differential diagnosis of small polypoid lesions of the gallbladder, utilizing an endoscopic ultrasound scoring system. *Endoscopy* 2002; **34**: 959–65.
- 30 Sakamoto H, Kitano M, Suetomi Y, Maekawa K, Takeyama Y, Kudo M. Utility of contrast enhanced endoscopic ultrasonography for diagnosis of small pancreatic carcinomas. *Ultrasound Med. Biol.* 2008; **34**: 525–32.
- 31 Kitano M, Sakamoto H, Matsui U *et al.* A novel perfusion imaging technique of the pancreas: Contrast-enhanced harmonic EUS (with video). *Gastrointest. Endosc.* 2008; **67**: 141–50.
- 32 Kitano M, Kudo M, Sakamoto H *et al.* Preliminary study of contrast-enhanced harmonic endosonography with second generation contrast agents. *J. Med. Ultrasonics* 2008; **35**: 11–8.
- 33 Xie XH, Xu HX, Xie XY *et al.* Differential diagnosis between benign and malignant gallbladder diseases with real time contrast-enhanced ultrasound. *Eur. Radiol.* 2010; **20**: 239–48.
- 34 Jang JY, Kim SW, Lee SE *et al.* Differential diagnostic and staging accuracies of high resolution ultrasonography, endoscopic ultrasonography, multidetector computed tomography for gallbladder polypoid lesions and gallbladder cancer. *Ann. Surg.* 2009; **250**: 943–9.
- 35 Hirooka Y, Naitoh Y, Goto H *et al.* Contrast-enhanced endoscopic ultrasonography in gallbladder diseases. *Gastrointest. Endosc.* 1998; **48**: 406–10.
- 36 Choi JH, Seo DW, Choi JH *et al.* Utility of contrast-enhanced harmonic EUS in the diagnosis of malignant gallbladder polyps (with videos). *Gastrointest. Endosc.* 2013; **78**: 484–93.
- 37 Shah T, Wong T. Management of gallbladder polyps. *Minerva Gastroenterol. Dietol.* 2003; **49**: 23.

Impact of resection and ablation for single hypovascular hepatocellular carcinoma ≤ 2 cm analysed with propensity score weighting

Kenichi Takayasu¹  | Shigeki Arii² | Michiie Sakamoto³ | Yutaka Matsuyama⁴ | Masatoshi Kudo⁵ | Shuichi Kaneko⁶ | Osamu Nakashima⁷ | Masumi Kadoya⁸ | Namiki Izumi⁹ | Tadatoshi Takayama¹⁰ | Yonson Ku¹¹ | Takashi Kumada¹² | Shoji Kubo¹³ | Takashi Kokudo¹⁴ | Yasuhiro Hagiwara⁴ | Norihiro Kokudo¹⁵ | for the Liver Cancer Study Group of Japan

¹Department of Diagnostic Radiology, National Cancer Center Hospital, Tokyo, Japan

²Department of Hepato-Biliary-Pancreatic Surgery, Hamamatsu Rosai Hospital, Japan Labor Health and Welfare Organization, Hamamatsu, Japan

³Department of Pathology, Keio University School of Medicine, Tokyo, Japan

⁴Department of Biostatistics, School of Public Health, University of Tokyo, Tokyo, Japan

⁵Department of Gastroenterology and Hepatology, Kinki University School of Medicine, Sayama, Japan

⁶Department of Gastroenterology, Kanazawa University School of Medical Science, Kanazawa, Japan

⁷Department of Clinical Laboratory Medicine, Kurume University Hospital, Kurume, Japan

⁸Department of Radiology, Shinshu University School of Medicine, Matsumoto, Japan

⁹Department of Gastroenterology and Hepatology, Musashino Red Cross Hospital, Musashino, Japan

¹⁰Department of Digestive Surgery, Nihon University School of Medicine, Tokyo, Japan

¹¹Department of Surgery, Kobe University Graduate School of Medicine, Kobe, Japan

¹²Department of Gastroenterology, Ogaki Municipal Hospital, Ogaki, Japan

¹³Department of Hepato-Biliary-Pancreatic Surgery, Osaka City University Graduate School of Medicine, Osaka, Japan

¹⁴Hepato-Biliary-Pancreatic Surgery Division, Artificial Organ and Transplantation Division, Department of Surgery, Graduate School of Medicine, University of Tokyo, Tokyo, Japan

¹⁵National Center for Global Health and Medicine, Tokyo, Japan

Correspondence

Kenichi Takayasu, Department of Diagnostic Radiology, National Cancer Center Hospital, Tokyo, Japan.
Email: ktakayas@ya2.so-net.ne.jp

Handling Editor: Alejandro Forner

Abstract

Background and Aims: Small hypovascular hepatocellular carcinoma (HCC) ≤ 2 cm is biologically less aggressive than hypervascular one, however, the optimal treatment is still undetermined. The efficacy of surgical resection (SR), radiofrequency ablation (RFA) and percutaneous ethanol injection (PEI) was evaluated.

Methods: The 853 (SR, 176; RFA, 491; PEI, 186) patients were enrolled who met Child-Pugh A/B, single hypovascular HCC ≤ 2 cm pathologically proven, available tumour differentiation and absence of macrovascular invasion and extrahepatic metastasis. Overall and recurrence-free survivals were compared in original and a propensity score weighted pseudo-population with 732 patients.

Abbreviations: AFP, α -foetoprotein; BCLC, Barcelona Clinic Liver Cancer; CI, confidence interval; CT, computed tomography; DCP, des- γ -carboxy prothrombin; Gd-EOB-DTPA, gadolinium-ethoxybenzyl-diethylene-triamine pentaacetic acid; HCC, hepatocellular carcinoma; HR, hazard ratio; IPTW, inverse-probability-of-treatment weighting; MRI, magnetic resonance imaging; PEI, percutaneous ethanol injection; RFA, radiofrequency ablation; SR, surgical resection; US, ultrasonography.

Results: The median follow-up time and tumour size were 2.8 years and 1.47 cm respectively. In original population, multivariate Cox regression showed no significant difference for overall survival among three groups. In pseudo-population, Cox regression also revealed no significant difference for overall survival among them, although SR (HR, 0.56; 95% CI, 0.36-0.86) and RFA (HR, 0.75; 95% CI, 0.57-1.00) groups had significantly lower recurrence than PEI group. The overall survival rates at 3 and 5 years for the SR, RFA and PEI groups were 94%/70%, 90%/75% and 94%/73% respectively. Corresponding recurrence-free survival rates were 64%/54%, 59%/41% 48%/33% respectively. Subgroup analysis revealed no significant survival benefit of SR compared with non-SR. No treatment-related death occurred.

Conclusions: For patients with single hypovascular HCC ≤ 2 cm, no significant difference for overall survival was first identified among 3 treatment groups. The SR or RFA could be recommended, and PEI would be alternative to RFA.

KEYWORDS

barcelona clinic liver cancer stage 0, hypovascular hepatocellular carcinoma, inverse-probability-of-treatment weighting, percutaneous ethanol, injection, radiofrequency ablation, surgical resection

See Editorial on Page 415

1 | INTRODUCTION

Hepatocellular carcinoma (HCC) is the fifth most common malignant neoplasm and the third leading cause of cancer-related death worldwide.¹ The establishment of a surveillance system to detect small HCC has improved the incidences of single tumour from 55.2% to 58.9% and small tumour ≤ 2 cm from 24.7% to 33.4% between 1996² and 2007.³ Consequently, we have often encountered patients with single HCC ≤ 2 cm with Child-Pugh class A corresponding to very-early-stage (stage 0) disease in the Barcelona Clinic Liver Cancer (BCLC) staging system.⁴ However, universal consensus of treatment for these patients has not been determined, ie ablation is recommended by the recent BCLC staging and treatment strategy,⁵ whereas surgical resection (SR) is provided by the European Association for the Study of the Liver and the European Organization for Research and Treatment of Cancer.⁶ To date, several comparative studies of SR vs radiofrequency ablation (RFA) for patients with stage 0 disease have been reported.⁷⁻¹² However, their results varied, and consensus is still unclear. In addition, these studies were carried out on patients with arterial "hypervascular-dominant HCC" mainly based on diagnostic criteria of BCLC staging and treatment guidelines,⁴ whereas the study with patients with "hypovascular" HCC was very rare.¹³

Very-early-stage HCC includes 2 types: one is progressed HCC, most of which are hypervascular, and another is early HCC/carcinoma in situ, defined as well-differentiated vaguely nodular tumour,¹⁴ which is commonly hypovascular in the arterial phase on dynamic computed tomography (CT),¹⁵ magnetic resonance imaging (MRI) and combination study of CT and angiography.¹⁶ Multistep hepatocarcinogenesis developed from high-grade dysplastic nodule to early HCC, followed by nodule-in-nodule type, and finally to classic hypervascular HCC,

Key points

- Largest 853 patients with single hypovascular HCC ≤ 2 cm histopathologically proven were enrolled.
- To minimize potential confounders, the inverse-probability-of-treatment weighting (IPTW) method was used in pseudo-population with 732 patients.
- IPTW Cox regression disclosed no significant difference for death among SR, RFA and PEI groups despite superiority of SR and RFA to PEI for recurrence.
- SR or RFA could be recommended as first treatment of choice, and PEI would be alternative to RFA.

has been confirmed by pathological^{14,17} and radiological studies.^{18,19} Recently gadolinium-ethoxybenzyl-diethylene-triamine pentaacetic acid (Gd-EOB-DTPA)-enhanced MRI demonstrated that 1-year cumulative malignant transformation rate from hypovascular nodule to hypervascular HCC was 14.9%-15.6%.^{20,21}

Therefore, we hypothesized that hypovascular HCCs ≤ 2 cm significantly associated with well-differentiated cells and low levels of α -foetoprotein (AFP, normal < 15 ng/mL) and des- γ -carboxy prothrombin (DCP, normal < 40 mAU/mL) as well as less frequency of microvascular invasion and metastasis²² would be locally well controlled by RFA and even percutaneous ethanol injection (PEI), similar to SR and the overall survivals might not be different.

We conducted this study to identify the survival benefit of SR, RFA and PEI for patients with single hypovascular HCC ≤ 2 cm using a large prospective cohort based on nationwide surveillance data.

2 | PATIENTS AND METHODS

Patients were prospectively registered and followed biannually through 645 institutions by the Liver Cancer Study Group of Japan and retrospectively analysed. Although this study protocol was not submitted to the institutional review board of each institution, collection of data and registration of patients with HCC were conducted with the approval of each institution. Informed consent was obtained from all patients before treatment at respective institutions. Overall ethics approval was got from the Liver Cancer Study Group of Japan. The inclusion criteria were (i) treatment-naïve patients with single HCC ≤ 2 cm histologically proven who underwent SR, RFA or PEI; (ii) Child-Pugh class A or B; (iii) arterial hypovascular tumour on dynamic CT/MRI and optional imaging modalities, if necessary; (iv) histological grade of tumour differentiation and (v) absence of macrovascular invasion and extrahepatic metastasis. In this cohort, hypovascular HCC was defined as arterial hypo- or iso-vascular (non-hypervascular) tumour, and it was histologically diagnosed as HCC via needle biopsy and/or resected specimens. Grade of cellular differentiation was based on the Edmondson-Steiner classification.²³ Finally, we failed to extract the patients with early HCC because of lack of items documenting pathological findings of this entity in our questionnaire.

We set the study period from January 2000 to December 2007 (the latest data) to exclude preliminary experience with RFA because it became available for clinical use since 1999 in Japan. During 8 years, a total of 38 532 patients with clinically diagnosed HCC(s) underwent SR, RFA or PEI as initial treatment with curative intent. Of these, 28 899 patients were excluded owing to at least one of three; Child-Pugh C or unknown, tumour >2 cm in diameter or unknown and multiple tumours or unknown and 9633 patients met Child-Pugh A or B and single HCC ≤ 2 cm. Then, 8040 patients with hypervascular tumour or unknown were excluded, and 1593 patients with hypovascular tumour remained. Of these, 662 patients were excluded because of absence of pathological examination, and 931 patients with histologically diagnosed HCC remained. Moreover, 78 patients were excluded because of lack of tumour differentiation, macroscopic portal or hepatic vein invasion, or extrahepatic metastasis and lost to follow-up. Finally, 853 patients were enrolled in this cohort, consisting of 176 with SR, 491 with RFA and 186 with PEI. Then, 732 patients without a missing value were referred to analysis with Cox regression and inverse-probability-of-treatment weighting (IPTW), including 146 with SR, 439 with RFA and 147 with PEI (Figure 1).

The surveillance and treatment algorithms for HCC were based on the Japanese Guidelines for Diagnosis and Treatment of HCC.²⁴ Namely, periodical surveillance for patient with chronic liver disease were recommended using ultrasonography (US) and measurements of AFP,

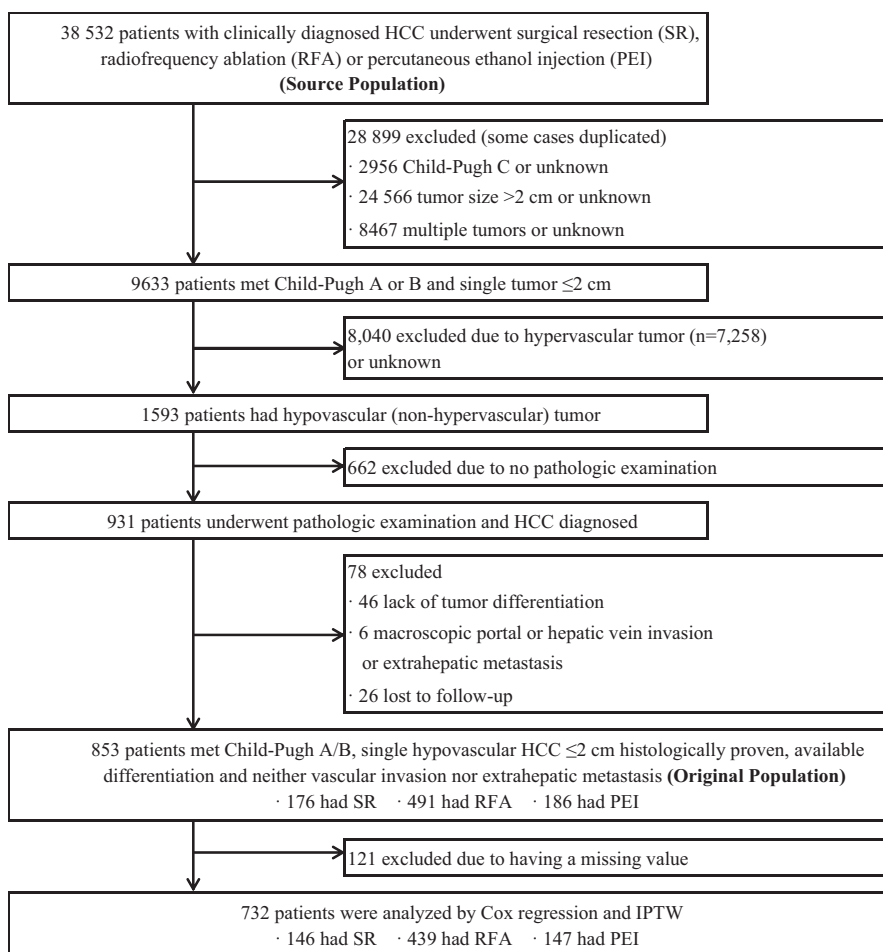


FIGURE 1 Patient flow diagram

TABLE 1 Clinical characteristics of patients before and after inverse-probability-of-treatment weighting (IPTW)

Variables	Study population before IPTW (n = 853)			P	After IPIW			P
	SR n = 176	RFA n = 491	PEI n=186		SR (%)	RFA (%)	PEI (%)	
Age (y) ^a				.922 ^a				.966 ^c
<60	33 (18.8%)	91 (18.5%)	32 (17.2%)		17.4	18.4	17.7	
≥60	139 (79.0%)	397 (80.9%)	150 (80.6%)		82.6	81.6	82.3	
unknown	4 (2.3%)	3 (0.6%)	4 (2.2%)					
Sex ^a				.410 ^a				.786 ^c
Male	104 (59.1%)	297 (60.5%)	102 (54.8%)		60.0	57.3	60.1	
Female	72 (40.9%)	194 (39.5%)	84 (45.2%)		40.0	42.7	39.9	
Child-Pugh class ^a				.193 ^a				.864 ^c
A	151 (85.8%)	394 (80.2%)	147 (79.0%)		83.3	81.0	80.9	
B	25 (14.2%)	97 (19.8%)	39 (21.0%)		16.7	19.0	19.1	
HBV and HCV				.003 ^a				.353
HBs Ag+ & HCV Ab-	21 (11.9%)	41 (8.4%)	14 (7.5%)		7.8	7.9	8.1	
HBs Ag- & HCV Ab+	113 (64.2%)	396 (80.7%)	147 (79.0%)		70.8	81.3	78.7	
HBs Ag+ & HCV Ab+	3 (1.7%)	5 (1.0%)	4 (2.2%)		1.8	1.0	1.4	
HBs Ag- & HCV Ab-	25 (14.2%)	29 (5.9%)	13 (7.0%)		11.9	6.4	6.6	
unknown	14 (8.0%)	20 (4.1%)	8 (4.3%)		7.7	3.4	5.0	
Tumor size (cm) ^a				.030 ^a				.986 ^c
≤1	24 (13.6%)	77 (15.7%)	43 (23.1%)		15.6	16.3	16.3	
1-2	152 (86.4%)	414 (84.3%)	143 (76.9%)		84.4	83.7	83.7	
Differentiation ^a				<.001 ^b				.913 ^d
Well	103 (58.5%)	437 (89.0%)	161 (86.6%)		82.2	82.2	84.0	
Moderate	65 (36.9%)	49 (10.0%)	22 (11.8%)		15.8	15.9	13.7	
Poor	8 (4.5%)	5 (1.0%)	2 (1.1%)		2.0	1.9	1.6	
Undifferentiated	0 (0.0%)	0 (0.0%)	1 (0.5%)		0.0	0.0	0.7	
unknown								
Alpha-fetoprotein (ng/mL) ^a				.693 ^b				.987 ^d
<15	88 (50.0%)	230 (46.8%)	78 (41.9%)		47.4	47.6	47.9	
15-199	67 (38.1%)	229 (46.6%)	95 (51.1%)		47.8	46.8	47.6	
≥200	15 (8.5%)	20 (4.1%)	7 (3.8%)		4.8	5.6	4.5	
unknown	6 (3.4%)	12 (2.4%)	6 (3.2%)					
DCP (mAU/mL) ^a				.018 ^b				.853 ^d
<40	123 (69.9%)	395 (80.4%)	132 (71.0%)		88.2	86.7	85.6	
40-99	8 (4.5%)	28 (5.7%)	12 (6.5%)		3.8	5.7	6.5	
≥100	20 (11.4%)	24 (4.9%)	10 (5.4%)		8.0	7.6	7.9	
Unknown	25 (14.2%)	44(9.0%)	32 (17.2%)					
Image portal thrombus				.021 ^a				.248 ^c
V _p 0	167 (94.9%)	484 (98.6%)	179 (96.2%)		95.6	98.5	98.7	
Unknown	9 (5.1%)	7 (1.4%)	7 (3.8%)		4.4	1.5	1.3	

HBs Ag, hepatitis B surface antigen, HCV, hepatitis C virus antibody. DCP, des-γ-carboxy prothrombin. V_p0, no portal tumor thrombus.

Bold values mean statistical significance.

^aChi-square test.

^bMantel trend test.

^cLogistic model with robust variances.

^dCumulative logit model with robust variances.

*These variables are included in a propensity score model. Patients with a missing value in these variables were excluded from IPTW analysis. Only percentage of patients is shown in pseudo-population.

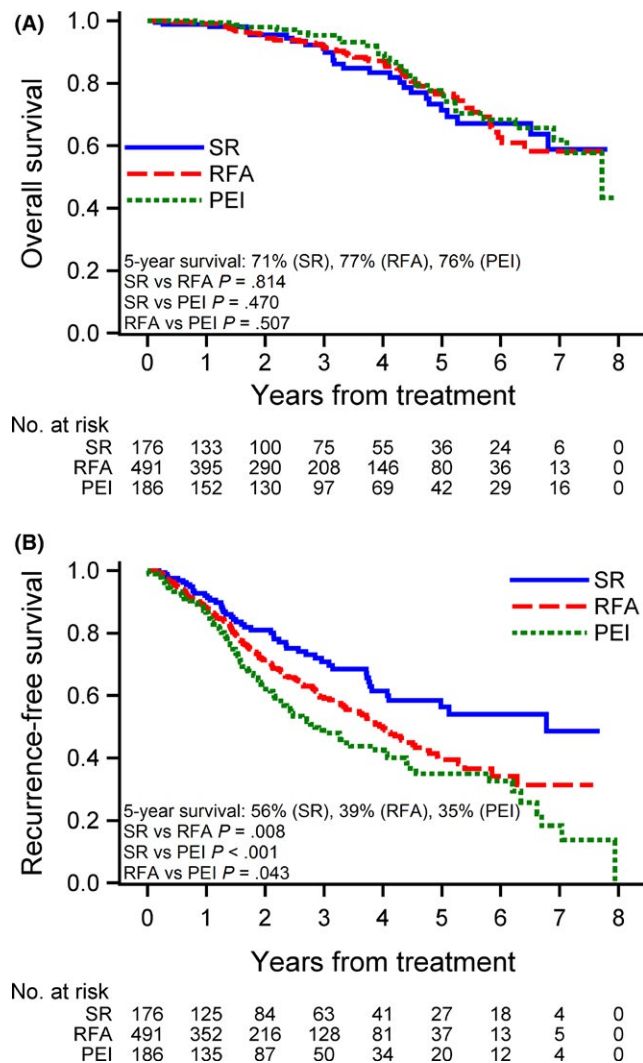


FIGURE 2 Crude Kaplan-Meier curves for overall and recurrence-free survival among surgical resection (SR), radiofrequency ablation (RFA) and percutaneous ethanol injection (PEI) groups evaluated by log-rank test. A, For overall survival, no significant difference was shown between any 2 groups. B, For recurrence-free survival, significant difference was recognized between SR and RFA ($P = .008$), between SR and PEI ($P < .001$), and between RFA and PEI ($P = .043$)

AFP-lectin fraction and DCP every 3-4 months and dynamic CT/MRI every 6 or 12 months. The typical HCC was defined with high density/intensity tumour in the arterial phase (arterial hypervascularity) followed by low density/intensity in the venous phase (washout) on dynamic CT/MRI. For tumours <2 cm, 3-month-interval follow-up with US was offered. The patients were followed after treatment with dynamic CT/MRI every 3-4 months and chest x-ray if necessary, and repeated SR, RFA, PEI, and/or transarterial chemoembolization were performed for recurrent foci depending on the tumour burden and hepatic functional reserve. Gd-EOB-DTPA-enhanced MRI was available after 2008 in Japan.

2.1 | Statistical analysis

The overall survival as primary endpoint was defined as the interval from treatment to death of any cause, and the recurrence-free survival

was designated from treatment to the first recurrence, including local recurrence, intrahepatic distant recurrence and extrahepatic metastasis. Death without recurrence was defined as a censor. Recurrence was diagnosed with imaging studies, clinical data, and/or histology at each institution. Treatment-related death was defined as death within 30 days after initial treatment. Follow-up ended on December 31, 2007. Follow-up time was calculated by reverse Kaplan-Meier method.

Background factors of 3 treatment groups were compared and evaluated using Chi-square or Mantel-trend tests for categorical variables in original population. The background differences were adjusted by the multivariate Cox regression and the hazard ratios were estimated. Then, to minimize the impact of treatment selection bias and other potential confounders, pseudo-population was created by rigorous adjustment using IPTW of propensity scores.^{25,26} Propensity scores were estimated by the polytomous logistic regression to predict the probability of a patient undergoing each treatment using 7 covariates; age, sex, Child-Pugh class, tumour size, differentiation, AFP and DCP levels. In the IPTW analysis, stabilized weights were applied,^{26,27} but weight truncation was not carried out because of no patient showing extremely high value (≥ 5) of stabilized weight.²⁷ The following methods were employed to estimate overall and recurrence-free survival; IPTW Kaplan-Meier estimator^{26,28,29} for estimate of survival curves, IPTW log-rank test^{28,29} for group comparison of survival curves and IPTW Cox regression^{26,29} for estimate of hazard ratio. The 95% confidence intervals were estimated using the robust variances.^{26,28,29} For the study using Cox regression and IPTW, 121 patients with a missing value were excluded (Figure 1). All significance tests were two-tailed, and P values <.05 were considered statistically significant. Statistical analyses were performed with Statistic Analysis System version 9.1 (SAS Inc., Cary, NC, USA).

3 | RESULTS

In this study, 1593 hypovascular HCC patients accounted for 18.0% of 8851 hypo- plus hypervascular HCC patients (Figure 1). Median (25%-75%) follow-up period was 2.8 (1.4-5.0), 2.8 (1.2-5.5), 2.7 (1.4-4.7) and 3.3 (1.5-5.8) years in entire population, SR, RFA and PEI groups respectively. Mean (standard deviation) age and tumour size were 67.0 (8.47) years and 1.47 (0.36) cm respectively.

3.1 | Original population

Demographic and characteristics of 853 enrolled patients are listed in Table 1. Among the 3 treatment groups, significant difference was recognized for HBV and HCV ($P = .003$), tumour size ($P = .03$), tumour differentiation ($P < .001$), DCP level ($P = .018$) and image portal thrombus ($P = .021$). In addition, the SR group had better liver function, lower infection of hepatitis C virus, less differentiation and higher AFP ≥ 200 ng/mL and DCP ≥ 100 mAU/mL levels than the ablation groups. Both the SR and RFA groups had larger tumour size than the PEI group. The RFA and PEI groups had similar proportion of all variables except for tumour size.

TABLE 2 Hazard ratios for death and recurrence in original population analyzed by multivariate Coxregression

	Death		Recurrence	
	HR (95% CI)	P	HR (95% CI)	P
Treatment				
SR vs. RFA	0.82 (0.46-1.45)	.495	0.52 (0.35-0.77)	.001
SR vs. PEI	0.81 (0.43-1.54)	.523	0.38 (0.25-0.59)	<.001
RFA vs. PEI	0.99 (0.61-1.62)	.975	0.74 (0.56-0.98)	.039
Age (year)				
≥60 vs. <60	3.26 (1.63-6.51)	.001	1.70 (1.21-2.38)	.002
Sex				
Male vs. female	1.20 (0.79-1.81)	.388	1.33 (1.03-1.72)	.029
Child-Pugh class				
B vs. A	2.33 (1.49-3.63)	<.001	0.97 (0.71-1.32)	.846
Tumor size (cm)				
1-2 vs. ≤1	0.71 (0.42-1.19)	.191	1.18 (0.84-1.67)	.339
Differentiation				
Moderate, poor & undifferentiated vs. well	1.76 (1.00-3.10)	.052	1.63 (1.14-2.32)	.007
alpha-fetoprotein (ng/mL)				
15-199 vs. <15	1.00 (0.66-1.51)	.989	1.34 (1.04-1.73)	.021
≥200 vs. <15	0.72 (0.29-1.75)	.464	1.27 (0.71-2.26)	.423
DCP mAU/mL				
40-99 vs. <40	0.79 (0.34-1.85)	.582	2.26 (1.50-3.41)	<.001
≥100 vs. <40	2.27 (1.15-4.49)	.018	1.39 (0.85-2.27)	.192

HR, Hazard Ratio. CI, Confidence Interval.

*undifferentiated.

Bold values mean statistical significance.

3.2 | Survival and recurrence

The following number of patients died; 27 (15.8%) in SR, 63 (12.8%) in RFA and 28 (15.1%) in PEI group. The corresponding number of the first overall recurrence was 48 (27.3%), 178 (36.3%) and 93 (50.0%) in the SR, RFA and PEI groups respectively. The extrahepatic metastasis happened in 5 patients with RFA (bone in 4 and lung in one) with a mean interval of 1260 days (range, 568-1968) after initial treatment. No treatment-related death occurred.

The overall survival rates at 3 and 5 years were 91%/71% in the SR group, 92%/77% in the RFA group and 95%/76% in the PEI group respectively (Figure 2A). Corresponding median survival times were not calculated in both RS and RFA groups and 7.7 years in the PEI group. Multivariate Cox regression revealed no significant difference among 3 groups (Table 2). In addition, 3 variables were independent risk factor for death: age ≥ 60 years (HR, 3.26; 95% CI, 1.63-6.51; $P = .001$), Child-Pugh B (HR, 2.33; 95% CI, 1.49-3.63; $P < .001$) and DCP level ≥100 mAU/mL (HR, 2.27; 95% CI, 1.15-4.49; $P = .018$).

While recurrence-free survival rates at 3 and 5 years were 71%/56% in the SR group, 59%/39% in the RFA group and 48%/35% in the PEI group respectively (Figure 2B). Multivariate Cox regression revealed the SR group was superior to both RFA (HR, 0.52; 95% CI, 0.35-0.77; $P = .001$) and PEI groups (HR, 0.38; 95% CI, 0.25-0.59;

$P < .001$), and the RFA group was superior to PEI group (HR, 0.74; 95% CI, 0.56-0.98; $P = .039$) for recurrence. Following 5 factors were independent adverse predictors for recurrence: DCP level 40-99 mAU/mL (HR, 2.26; 95% CI, 1.50-3.41; $P < .001$), age ≥60 years (HR, 1.70; 95% CI, 1.21-2.38; $P = .002$), less differentiation (HR, 1.63; 95% CI, 1.14-2.32; $P = .007$), AFP level 15-199 ng/mL (HR, 1.34; 95% CI, 1.04-1.73; $P = .021$) and male (HR, 1.33; 95% CI, 1.03-1.72; $P = .029$) (Table 2). Tumour size was not significant predictor for death or recurrence.

3.3 | Survival and recurrence in pseudo-population

Seven hundred thirty-two patients were selected for analysis with IPTW, which consisted of 146 patients with SR, 439 with RFA and 147 with PEI (Figure 1). They were well balanced across the 3 groups (Table 1). The overall survival rates at 3 and 5 years were 94%/70% in the SR group, 90%/75% in the RFA group and 94%/73% in the PEI group respectively (Figure 3A). Corresponding median survival times were not calculated in all 3 groups. Cox regression demonstrated no significant difference for death among 3 groups (Table 3). Recurrence-free survival rates at 3 and 5 years were 64%/54% in the SR group, 59%/41% in the RFA group and 48%/33% in the PEI group respectively (Figure 3B). Cox regression revealed that both SR (HR, 0.56; 95% CI, 0.36-0.86; $P = .008$) and RFA (HR, 0.75; 95% CI,

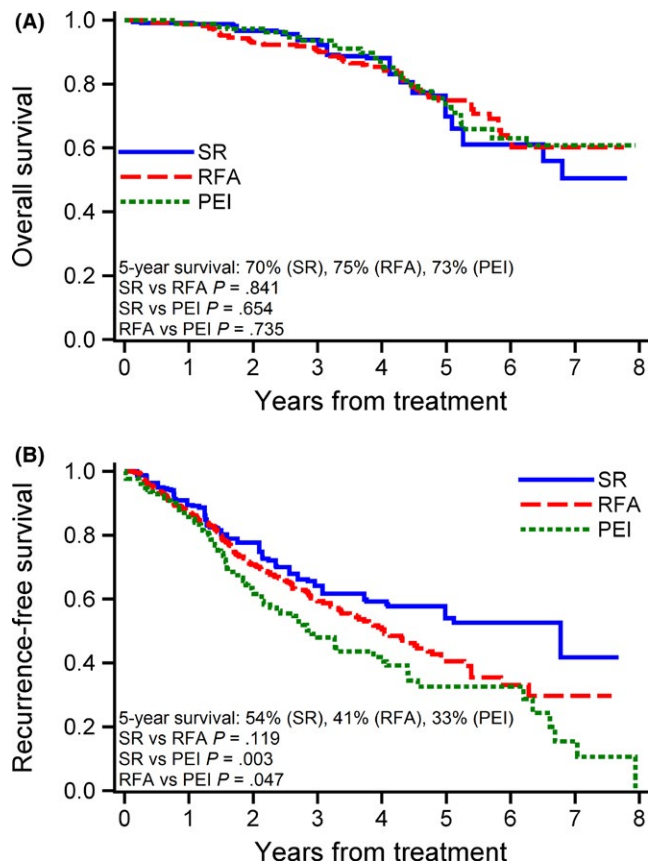


FIGURE 3 Inverse-probability-of-treatment weighting (IPTW) Kaplan-Meier curves for overall and recurrence-free survival among surgical resection (SR), radiofrequency ablation (RFA) and percutaneous ethanol injection (PEI) groups evaluated by log-rank test. A, For overall survival, no significant difference was shown between any 2 groups. B, For recurrence-free survival, significant difference was recognized between SR and PEI ($P = .003$) and between RFA and PEI ($P = .047$). Number of at risk patient was not shown to prevent unnecessary questions on the different number of patients between original and pseudo-populations

0.57-1.00; $P = .048$) groups were superior to the PEI group for recurrence (Table 3).

A subgroup analysis was done to clarify the survival benefit of SR compared with non-SR in IPTW weighted patients (Figure 4). The SR group did not affect significant survival benefit to the non-SR group in any subgroups; age, Child-Pugh, tumour differentiation, AFP and DCP levels.

TABLE 3 Hazard ratios for death and recurrence in pseudo-population analyzed by IPTW Coxregression

	Death		Recurrence	
	HR (95% CI) [*]	P [*]	HR (95% CI) [*]	P [*]
SR vs. RFA	1.06 (0.62-1.79)	.835	0.74 (0.49-1.11)	.146
SR vs. PEI	1.16 (0.63-2.15)	.633	0.56 (0.36-0.86)	.008
RFA vs. PEI	1.10 (0.67-1.81)	.711	0.75 (0.57-1.00)	.048

^{*}95% CIs and P values are based on robust variances.

Bold values mean statistical significance.

4 | DISCUSSION

With the advance of imaging techniques, we have often encountered small hypovascular HCC, ie 35% of HCCs 1-2 cm on both multidetector CT and MRI³⁰ and 15% of HCCs ≤ 2 cm on MRI.³¹ Our incidence of 18% was consistent with prior ones. Moreover, the wide introduction of Gd-EOB-DTPA-enhanced MRI has enabled us to detect small hypovascular hypointense nodules, suggesting early HCC³² even though the differentiation from dysplastic nodule is not feasible.³³ Therefore the consensus of optimal management for patients with stage 0 disease with hypovascular HCC is urgently needed.

In original population, there was no treatment-related death through 3 groups in spite of 0.8%-1.4% reported in SR group of other studies.^{8,9} No significant difference was identified for death among 3 groups, but the SR group was superior to RFA group and the RFA group outperformed the PEI group for recurrence. Between SR and RFA groups, similar results were reported for death^{7,9,11} and for recurrence.⁹ Older age and high DCP level were independent poor predictors for both death and recurrence. It was presumed that the former was frequently associated with comorbidities of cardiovascular and diabetic diseases and the latter was correlated with microvascular invasion.^{34,35} Less differentiated cells, especially poor differentiation were high risk for recurrence owing to association of microsatellites in distant sites from tumour.^{36,37} Interestingly, tumour size was not significant predictor for survival or recurrence.

In the pseudo-population, no significant difference was also clarified for death among 3 groups, although both SR and RFA groups were superior to the PEI group for recurrence. Between SR and RFA groups, our results for death and recurrence were in accordance with those of a prior matched study⁹ and a recent meta-analysis.³⁸ However, limiting the death alone, the outcomes varied; SR group was comparable with RFA group,^{7,12} outperformed RFA group,^{10,11} and was inferior to RFA group.⁸ Our 5-year survival rate of 70% in SR group ranged within 62.1%-91.5% in previous studies with hypervascular-dominant HCC patients.^{7,8,10-12,39} Whereas, 5-year survival rate of 75% in RFA group was also within 66%-85.9% in prior studies.^{7,8,11,12,40}

On the other hand, the SR and PEI groups showed no significant difference for death, even though the PEI group was inferior to the SR group for recurrence. The reason of different recurrence rate could be explained, ie PEI has low local control ability because of inhomogeneous distribution of ethanol, whereas SR completely removes tumour and surrounding micro-metastases *en bloc*. The cause of equivalent overall survival between PEI and SR groups is presumed to be achieved by repeated ablations for local recurrent foci. Our 5-year overall survival rate of 73% in the PEI group was similar to 71.9% studied in hypovascular HCC patients¹³ and ranged within 72.8%-78.3% in hypervascular-dominant HCC patients.^{10,41,42}

The similar outcomes for death between RFA and PEI groups are not surprising because they were noted by a randomized controlled trial using subgroup patients with HCC ≤ 2 cm.⁴³ Whereas our RFA group overtopped the PEI group for recurrence suggesting the inferiority of the PEI group to the RFA group for local control, however, no significant difference was reported for local recurrence between two.⁴³

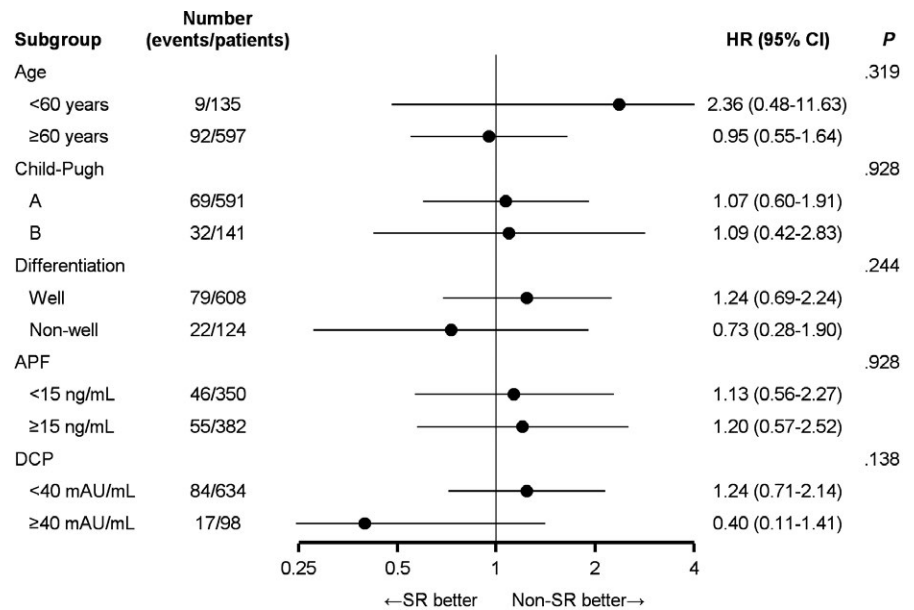


FIGURE 4 Subgroup analysis of overall survival using inverse-probability-of-treatment weighting (IPTW) Cox regression. Interaction *P* values were displayed

In light of our results, following strategies could be proposed for individual patients. The SR and RFA could be recommended as the first treatment of choice because both were superior to PEI for recurrence. The RFA could be offered for patients who are unresectable and/or do not desire SR, and PEI is recommended as an alternative to RFA, eg in patients with tumour close to large vessels and bile ducts, and/or neighbouring organs. To our knowledge, the patients with poorly differentiated tumour and/or DCP level >100 mAU/mL were recommended to SR rather than ablation because these factors are often associated with microvascular invasion and recently SR revealed equivalent survival for patients with solitary HCC ≤2 cm irrespective of microvascular invasion.⁴⁴ However, our subgroup analysis disclosed no significant survival benefit for SR group compared with non-SR group in any subgroups including differentiation and DCP level.

As limitation of this study, first the possibility exists that some hypovascular HCCs were misclassified because of unfit timing for acquisition of optimal arterial phase images. In near future, these flaws would be improved by newly introduced imaging techniques with Gd-EOB-DTPA-enhanced MRI and contrast enhanced US with perflubutane (Sonazoid™; Daiichi Sankyo, Tokyo, Japan).⁴⁵ Second, although the IPTW method was used to minimize the confounding factors, the selection bias would still remain because 662 (41.6%) of 1593 patients with hypovascular HCC were excluded from inclusion criteria because of absence of pretreatment pathological examination (Figure 1). Third, our treatment outcomes do not always apply equally to patients with a hypovascular tumour ≤2 cm diagnosed only by imaging modalities (ie without pathological study) because intrahepatic cholangiocarcinoma and combined hepatocellular-cholangiocarcinoma are possibly mixed in this group.

5 | CONCLUSIONS

This study first clarified no significant difference for death in patients with single hypovascular HCC ≤2 cm pathologically proven among SR,

RFA and PEI groups using propensity score weighting model. For recurrence, SR and RFA groups were superior to PEI group. These outcomes could encourage the patients to choose the best personalized management considering tumour location, association of comorbidities, cost-effectiveness,⁴⁶ etc. Moreover, we believe that these results will contribute to build a consensus on optimal treatment in patients with BCLC stage 0 hypovascular HCC.

CONFLICT OF INTEREST

Authors declared they do not have anything to disclose concerning this manuscript.

ORCID

Kenichi Takayasu  <http://orcid.org/0000-0003-4155-0247>

REFERENCES

1. El-Serag HB. Epidemiology of viral hepatitis and hepatocellular carcinoma. *Gastroenterology*. 2012;142:e1261.
2. The Liver Cancer Study Group of Japan. *Report of the 14th Follow-up Survey of Primary Liver Cancer*. Kyoto, Japan: Shinkou-insatsu Press; 2000. (in Japanese).
3. Kudo M, Izumi N, Ichida T, et al. Report of the 19th follow-up survey of primary liver cancer in Japan. *Hepatol Res*. 2016;46:372-390.
4. Bruix J, Sherman M. Management of hepatocellular carcinoma. *Hepatology*. 2005;42:1208-1236.
5. Forner A, Llovet JM, Bruix J. Hepatocellular carcinoma. *Lancet*. 2012;379:1245-1255.
6. EASL-EORTC. EASL-EORTC clinical practice guidelines: management of hepatocellular carcinoma. *J Hepatol* 2012;56:908-943.
7. Wang JH, Wang CC, Hung CH, Chen CL, Lu SN. Survival comparison between surgical resection and radiofrequency ablation for patients in BCLC very early/early stage hepatocellular carcinoma. *J Hepatol*. 2012;56:412-418.

8. Peng ZW, Lin XJ, Zhang YJ, et al. Radiofrequency ablation versus hepatic resection for the treatment of hepatocellular carcinomas 2 cm or smaller: a retrospective comparative study. *Radiology*. 2012;262:1022-1033.
9. Pompili M, Saviano A, de Matthaeis N, et al. Long-term effectiveness of resection and radiofrequency ablation for single hepatocellular carcinoma 3 cm. Results of a multicenter Italian survey. *J Hepatol*. 2013;59:89-97.
10. Hasegawa K, Kokudo N, Makuuchi M, et al. Comparison of resection and ablation for hepatocellular carcinoma: a cohort study based on a Japanese nationwide survey. *J Hepatol*. 2013;58:724-729.
11. Liu PH, Hsu CY, Hsia CY, et al. Surgical resection versus radiofrequency ablation for single hepatocellular carcinoma ≤ 2 cm in a propensity score model. *Ann Surg*. 2016;263:538-545.
12. Kim GA, Shim JH, Kim MJ, et al. Radiofrequency ablation as an alternative to hepatic resection for single small hepatocellular carcinomas. *Br J Surg*. 2016;103:126-135.
13. Sakamoto M, Hirohashi S. Natural history and prognosis of adenomatous hyperplasia and early hepatocellular carcinoma: multi-institutional analysis of 53 nodules followed up for more than 6 months and 141 patients with single early hepatocellular carcinoma treated by surgical resection or percutaneous ethanol injection. *Jpn J Clin Oncol*. 1998;28:604-608.
14. International Consensus Group for Hepatocellular Neoplasia. Pathologic diagnosis of early hepatocellular carcinoma: a report of the international consensus group for hepatocellular neoplasia. *Hepatology*. 2009;49:658-664.
15. Takayasu K, Furukawa H, Wakao F, et al. CT diagnosis of early hepatocellular carcinoma: sensitivity, findings, and CT-pathologic correlation. *AJR Am J Roentgenol*. 1995;164:885-890.
16. Takayasu K, Muramatsu Y, Furukawa H, et al. Early hepatocellular carcinoma: appearance at CT during arterial portography and CT arteriography with pathologic correlation. *Radiology*. 1995;194:101-105.
17. Sakamoto M, Hirohashi S, Shimamoto Y. Early stages of multistep hepatocarcinogenesis: adenomatous hyperplasia and early hepatocellular carcinoma. *Hum Pathol*. 1991;22:172-178.
18. Hayashi M, Matsui O, Ueda K, et al. Correlation between the blood supply and grade of malignancy of hepatocellular nodules associated with liver cirrhosis: evaluation by CT during intraarterial injection of contrast medium. *AJR Am J Roentgenol*. 1999;172:969-976.
19. Kitao A, Matsui O, Yoneda N, et al. The uptake transporter OATP8 expression decreases during multistep hepatocarcinogenesis: correlation with gadoteric acid enhanced MR imaging. *Eur Radiol*. 2011;21:2056-2066.
20. Inoue T, Hyodo T, Murakami T, et al. Hypovascular hepatic nodules showing hypointense on the hepatobiliary-phase image of Gd-EOB-DTPA-enhanced MRI to develop a hypervascular hepatocellular carcinoma: a nationwide retrospective study on their natural course and risk factors. *Dig Dis*. 2013;31:472-479.
21. Motosugi U, Ichikawa T, Sano K, et al. Outcome of hypovascular hepatic nodules revealing no gadoteric acid uptake in patients with chronic liver disease. *J Magn Reson Imaging*. 2011;34:88-94.
22. Takayasu K, Arii S, Sakamoto M, et al. Clinical implication of hypovascular hepatocellular carcinoma studied in 4,474 patients with solitary tumour equal or less than 3 cm. *Liver Int*. 2013;33:762-770.
23. Edmondson HA, Steiner PE. Primary carcinoma of the liver: a study of 100 cases among 48,900 necropsies. *Cancer*. 1954;7:462-503.
24. Makuuchi M, Kokudo N, Arii S, et al. Development of evidence-based clinical guidelines for the diagnosis and treatment of hepatocellular carcinoma in Japan. *Hepatol Res*. 2008;38:37-51.
25. Robins JM, Hernan MA, Brumback B. Marginal structural models and causal inference in epidemiology. *Epidemiology*. 2000;11:550-560.
26. Cole SR, Hernan MA. Adjusted survival curves with inverse probability weights. *Comput Methods Programs Biomed*. 2004;75:45-49.
27. Cole SR, Hernan MA. Constructing inverse probability weights for marginal structural models. *Am J Epidemiol*. 2008;168:656-664.
28. Xie J, Liu C. Adjusted Kaplan-Meier estimator and log-rank test with inverse probability of treatment weighting for survival data. *Stat Med*. 2005;24:3089-3110.
29. Austin PC. The use of propensity score methods with survival or time-to-event outcomes: reporting measures of effect similar to those used in randomized experiments. *Stat Med*. 2014;33:1242-1258.
30. Sangiovanni A, Manini MA, Iavarone M, et al. The diagnostic and economic impact of contrast imaging techniques in the diagnosis of small hepatocellular carcinoma in cirrhosis. *Gut*. 2010;59:638-644.
31. Forner A, Vilana R, Ayuso C, et al. Diagnosis of hepatic nodules 20 mm or smaller in cirrhosis: prospective validation of the noninvasive diagnostic criteria for hepatocellular carcinoma. *Hepatology*. 2008;47:97-104.
32. Sano K, Ichikawa T, Motosugi U, et al. Imaging study of early hepatocellular carcinoma: usefulness of gadoteric acid-enhanced MR imaging. *Radiology*. 2011;261:834-844.
33. Kogita S, Imai Y, Okada M, et al. Gd-EOB-DTPA-enhanced magnetic resonance images of hepatocellular carcinoma: correlation with histological grading and portal blood flow. *Eur Radiol*. 2010;20:2405-2413.
34. Yamashita Y, Tsujita E, Takeishi K, et al. Predictors for microinvasion of small hepatocellular carcinoma ≤ 2 cm. *Ann Surg Oncol*. 2012;19:2027-2034.
35. Pote N, Cauchy F, Albuquerque M, et al. Performance of PIVKA-II for early hepatocellular carcinoma diagnosis and prediction of microvascular invasion. *J Hepatol*. 2015;62:848-854.
36. Okusaka T, Okada S, Ueno H, et al. Satellite lesions in patients with small hepatocellular carcinoma with reference to clinicopathologic features. *Cancer*. 2002;95:1931-1937.
37. Sasaki A, Kai S, Iwashita Y, Hirano S, Ohta M, Kitano S. Microsatellite distribution and indication for locoregional therapy in small hepatocellular carcinoma. *Cancer*. 2005;103:299-306.
38. Xu Q, Kobayashi S, Ye X, Meng X. Comparison of hepatic resection and radiofrequency ablation for small hepatocellular carcinoma: a meta-analysis of 16,103 patients. *Sci Rep*. 2014;4:7252.
39. Roayaie S, Obeidat K, Sposito C, et al. Resection of hepatocellular cancer ≤ 2 cm: results from two Western centers. *Hepatology*. 2013;57:1426-1435.
40. Livraghi T, Meloni F, Di Stasi M, et al. Sustained complete response and complications rates after radiofrequency ablation of very early hepatocellular carcinoma in cirrhosis: is resection still the treatment of choice? *Hepatology*. 2008;47:82-89.
41. Shiina S, Tateishi R, Imamura M, et al. Percutaneous ethanol injection for hepatocellular carcinoma: 20-year outcome and prognostic factors. *Liver Int*. 2012;32:1434-1442.
42. Ebara M, Okabe S, Kita K, et al. Percutaneous ethanol injection for small hepatocellular carcinoma: therapeutic efficacy based on 20-year observation. *J Hepatol*. 2005;43:458-464.
43. Lin SM, Lin CJ, Lin CC, Hsu CW, Chen YC. Randomised controlled trial comparing percutaneous radiofrequency thermal ablation, percutaneous ethanol injection, and percutaneous acetic acid injection to treat hepatocellular carcinoma of 3 cm or less. *Gut*. 2005;54:1151-1156.
44. Shindoh J, Andreou A, Aloia TA, et al. Microvascular invasion does not predict long-term survival in hepatocellular carcinoma up to 2 cm: reappraisal of the staging system for solitary tumors. *Ann Surg Oncol*. 2013;20:1223-1229.

45. Kudo M, Matsui O, Izumi N, Iijima H, Kadoya M, Imai Y. Surveillance and diagnostic algorithm for hepatocellular carcinoma proposed by the Liver Cancer Study Group of Japan: 2014 update. *Oncology*. 2014;87(suppl 1):7-21.
46. Cucchetti A, Piscaglia F, Cescon M, et al. Cost-effectiveness of hepatic resection versus percutaneous radiofrequency ablation for early hepatocellular carcinoma. *J Hepatol*. 2013;59: 300-307.

How to cite this article: Takayasu K, Arai S, Sakamoto M, et al. ; for the Liver Cancer Study Group of Japan. Impact of resection and ablation for single hypovascular hepatocellular carcinoma ≤ 2 cm analysed with propensity score weighting. *Liver Int*. 2018;38:484–493. <https://doi.org/10.1111/liv.13670>

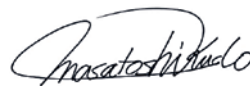
Editorial

Lenvatinib May Drastically Change the Treatment Landscape of Hepatocellular Carcinoma

Masatoshi Kudo

Department of Gastroenterology and Hepatology, Kindai University Faculty of Medicine, Osaka-Sayama, Japan

Prof. M. Kudo

Editor *Liver Cancer***Introduction**

Sorafenib, which was shown to improve survival in the SHARP [1] and Asia-Pacific [2] trials, has been the standard therapy for unresectable hepatocellular carcinoma (HCC) since 2007.

Since then, several first-line clinical trials have been conducted with the aim of developing molecular targeted agents showing better efficacy or safety than sorafenib [3] (Table 1). A superiority trial comparing sorafenib with sunitinib (SUN1170 trial) showed that sunitinib is not superior but rather significantly inferior to sorafenib regarding the primary endpoint of overall survival (OS) [4]. The BRISK-FL and LiGHT trials showed that brivanib and linifanib are not superior and, moreover, not noninferior, despite the fact that the trial designs allowed for assessment of noninferiority [5, 6]. A superiority trial of sorafenib plus erlotinib (SEARCH trial) [7], a superiority trial of sorafenib plus doxorubicin (CALGB808028 trial), and a trial investigating sorafenib plus hepatic arterial infusion chemotherapy (HAIC) (SILIUS trial) [8] all failed. The results of two superiority trials comparing sorafenib with radioembolization called SARA (Sorafenib versus Radioembolization in Advanced Hepatocellular carcinoma) [9] and SIRveNIB (Study to Compare Selective Internal Radiation Therapy [SIRT] Versus Sorafenib in Locally Advanced Hepatocellular Carcinoma [HCC]) were also reported at EASL 2017 and ASCO 2017, although these trials failed as well [10]. These results highlight the diffi-

Masatoshi Kudo, MD, PhD
Department of Gastroenterology and Hepatology
Kindai University Faculty of Medicine
377-2 Ohno-Higashi, Osaka-Sayama 589-8511 (Japan)
E-Mail m-kudo@med.kindai.ac.jp

Kudo: Lenvatinib May Drastically Change the Treatment Landscape of Hepatocellular Carcinoma

Table 1. Phase III clinical trials of advanced-stage HCC

Target population	Design	Trial name	Result	Presentation	Publication	1st author
Advanced	1. Sorafenib vs. sunitinib 2. Sorafenib ± erlotinib 3. Sorafenib vs. brivanib 4. Sorafenib vs. lenvatinib 5. Sorafenib ± doxorubicin 6. Sorafenib ± HAIC ^a 7. Sorafenib ± Y90 8. Sorafenib ± Y90 9. Sorafenib vs. lenvatinib 10. Sorafenib vs. nivolumab 11. Sorafenib vs. durvalumab vs. durvalumab + tremelimumab	SUN1170	Negative	ASCO 2011	J Clin Oncol 2013	Cheng A.L.
		SEARCH	Negative	ESMO 2012	J Clin Oncol 2015	Zhu A.X.
		BRISK-FL	Negative	AASLD 2012	J Clin Oncol 2013	Johnson P.J.
		LIGHT	Negative	ASCO-GI 2013	J Clin Oncol 2015	Cainap C.
		CALGB 80802	Negative	ASCO-GI 2016	Lancet Gastroenterol Hepatol 2018	Kudo M.
		SILIUS	Negative	EASL 2016	Lancet Oncol 2017	Vilgrain V.
		SARAH	Negative	EASL 2017		
		SIRveNIB	Negative	ASCO 2017		
		REFLECT	Positive	ASCO 2017	Lancet 2018	Kudo M.
		CheckMate-459	Ongoing			
		HIMALAYA	Ongoing			
Second line	1. Brivanib vs. placebo 2. Everolimus vs. placebo 3. Ramucirumab vs. placebo 4. S-1 vs. placebo 5. ADI-PEG 20 vs. placebo 6. Regorafenib vs. placebo 7. Tivantinib vs. placebo 8. Tivantinib vs. placebo 9. DT ^b vs. placebo 10. Cabozantinib vs. placebo 11. Ramucirumab vs. placebo 12. Pembrolizumab vs. placebo	BRISK-PS	Negative	EASL 2012	J Clin Oncol 2013	Llovet J.M.
		EYOLIVE-1	Negative	ASCO-GI 2014	JAMA 2014	Zhu A.X.
		REACH	Negative	ESMO 2014	Lancet Oncol 2015	Zhu A.X.
		S-CUBE	Negative	ASCO 2015	Lancet Gastroenterol Hepatol 2017	Kudo M.
		NA	Negative	ASCO 2016		
		RESORCE	Positive	WCGC 2016	Lancet 2017	Bruix J.
		METIV-HCC	Negative	ASCO 2017		
		JET-HCC	Negative	ESMO 2017		
		ReLive	Negative	ILCA 2017		
		CELESTIAL	Positive	ASCO-GI 2018		
		REACH-2	Ongoing			
		KEYNOTE-240	Ongoing			

Red, positive trials; Blue, ongoing trials; Black, negative trials. ^a HAIC, hepatic arterial infusion chemotherapy. ^b DT; doxorubicin-loaded nanoparticles.

Table 2. Randomized phase II and phase III clinical trials of early/intermediate-stage HCC

Target population	Design	Trial name	Result	Presentation	Publication	1st author
Early	Adjuvant (prevention of recurrence)	1. Vitamin K ₂ vs. placebo	Negative	ASCO 2010	Hepatology 2011	Yoshida H.
		2. Peritoin vs. placebo	Negative	ASCO 2014	J Gastroenterol 2014	Okita K.
		3. Sorafenib vs. placebo	Negative		Lancet Oncol 2015	Bruix J.
		4. Peritoin vs. placebo	Ongoing			
Improvement of RFA	1. RFA ± LTLD ^a 2. RFA ± LTLD ^a	HEAT	Negative	ILCA 2013	Clin Cancer Res 2017	Tak W.Y.
		OPTIMA				
Intermediate	Improvement of TACE	1. TACE ± sorafenib	Negative	ASCO-GI 2010	Eur J Cancer 2011	Kudo M.
		2. TACE ± sorafenib	Negative	ASCO-GI 2012	J Hepatol 2016	Lencioni R.
		3. TACE ± brivanib	Negative	ILCA 2013	Hepatology 2014	Kudo M.
		4. TACE ± orantinib	Negative	EASL 2015	Lancet Gastroenterol Hepatol 2017	Kudo M.
		5. TACE ± sorafenib	Negative	ASCO 2016	Lancet Gastroenterol Hepatol 2017	Meyer T.
		6. TACE ± sorafenib	Positive	ASCO-GI 2018		Kudo M.

Red, positive trial; Blue, ongoing trial; Black, negative trials. ^a LTLD, lyso-thermosensitive liposomal doxorubicin.

Kudo: Lenvatinib May Drastically Change the Treatment Landscape of Hepatocellular Carcinoma

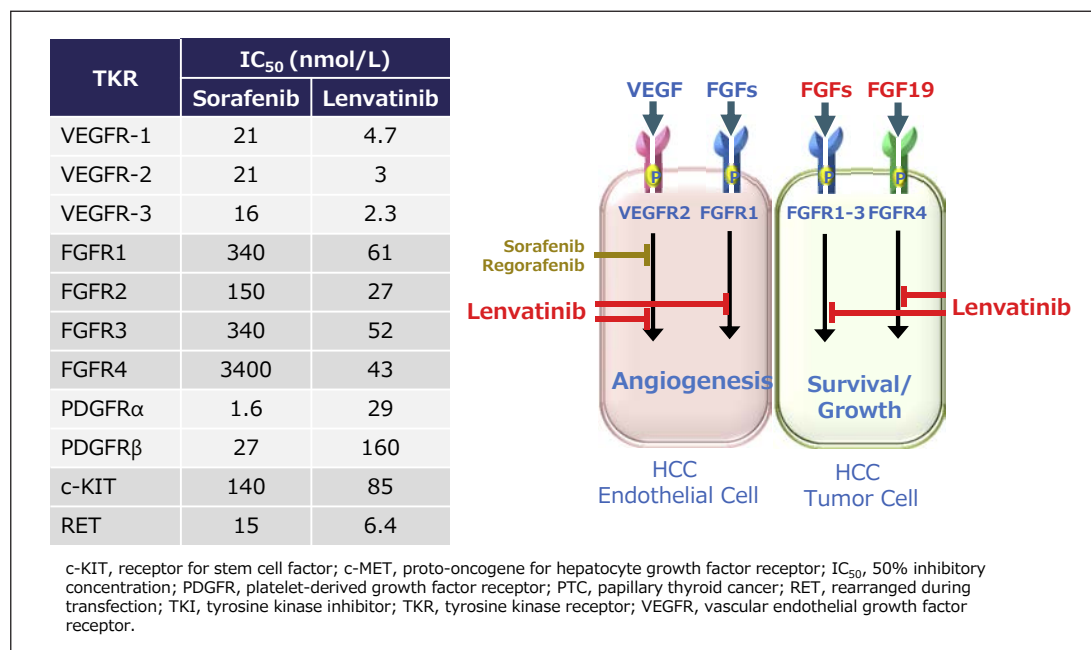


Fig. 1. Dual inhibition of VEGF and FGF pathways by lenvatinib (cited from Tohyama et al. [13]).

culties associated with conducting clinical trials of first-line HCC drugs using OS as the endpoint, and demonstrate the superiority of sorafenib for improving survival compared with other drugs.

Amid these failed trials, the results of a phase III trial of lenvatinib and sorafenib were presented at ASCO 2017. The trial met the primary endpoint of noninferiority, a shocking result that produced the greatest breakthrough in 10 years, suggesting a new option for first-line molecular targeted therapy [11]. Another recent development was the improvement in progression-free survival (PFS) achieved with sorafenib plus transcatheter arterial chemoembolization (TACE), as this approach was extremely challenging to develop (Table 2) [12].

Development History of Lenvatinib

Lenvatinib was discovered at Tsukuba Research Laboratory in Japan as a result of exploratory research on angiogenesis inhibitors. It primarily inhibits vascular endothelial growth factor (VEGF) receptors (VEGFR1–3), fibroblast growth factor (FGF) receptors (FGFR1–4), KIT, and RET [13]. Lenvatinib simultaneously suppresses the activity of factors involved in tumor angiogenesis while also suppressing proliferation signals from VEGFR and FGFR, which are strongly expressed in cancer cells. Because of these properties, lenvatinib is an extremely effective inhibitor of angiogenesis (Fig. 1) [14]. Inhibition of FGFR4 in particular is considered a critical and important factor in the antitumor effects of lenvatinib [15–19].

The recommended dose is 24 mg/day based on the results of phase I trials in solid cancers and subsequent trials in other cancers. However, a recommended dose had to be established specifically for patients with HCC, because lenvatinib is primarily metabolized by cytochrome P450 3A in the liver, and could potentially have a different adverse event (AE) profile in patients with HCC associated with liver cirrhosis than in patients with other solid cancers. A phase I trial in patients with Child-Pugh A and B HCC was conducted for that purpose. Based

Table 3. REFLECT: investigator assessment according to mRECIST

	Lenvatinib (n = 478)	Sorafenib (n = 476)	HR/OR	p value
OS, months	13.6 (12.1–14.9)	12.3 (10.4–13.9)	HR 0.92 (0.79–1.06)	–
PFS, months	7.4 (6.9–8.8)	3.7 (3.6–4.6)	HR 0.66 (0.57–0.77)	<0.0001
TTP, months	8.9 (7.4–9.2)	3.7 (3.6–5.4)	HR 0.63 (0.53–0.73)	<0.0001
ORR, %	24.1 (20.2–27.9)	9.2 (6.6–11.8)	OR 3.13 (2.15–4.56)	<0.0001

Values in parentheses are 95% CI. OS, overall survival; PFS, progression-free survival; TTP, time to progression; ORR, objective response rate; HR, hazard ratio; OR, odds ratio. Cited and modified from Kudo et al. [11].

on the results, the recommended dose was set at 12 mg/day for Child-Pugh A patients and 8 mg/day for Child-Pugh B patients [20].

A phase II trial in patients with HCC conducted in Japan and South Korea confirmed the potent antitumor effect of lenvatinib and the feasibility of managing AEs in patients with HCC [21]. A later detailed analysis of the pharmacokinetics of lenvatinib in patients with HCC determined that the optimal dose was 8 mg/day for patients weighing less than 60 kg and 12 mg/day for patients weighing 60 kg or more. These findings sparked the planning of a phase III trial comparing lenvatinib with sorafenib (REFLECT trial).

Overview of the REFLECT Trial Results

The REFLECT trial was a global, randomized, open-label, phase III noninferiority trial. The trial enrolled patients with unresectable HCC with no history of systemic chemotherapy, and they were randomized 1:1 to lenvatinib and sorafenib arms. Patients were stratified by region (Asia or non-Asia), macroscopic portal vein involvement and/or extrahepatic spread, ECOG performance status (0 or 1), and body weight (<60 kg or ≥60 kg). Treatment was continued until disease progression or onset of an intolerable AE. Noninferiority of OS was set as the primary endpoint, and the noninferiority margin was set at 1.08. Time to progression (TTP), PFS, objective response rate (ORR), and safety were evaluated as secondary endpoints.

Of the 954 patients enrolled, 478 were assigned to the lenvatinib arm and 476 to the sorafenib arm. In the lenvatinib arm, 67% of enrolled patients were from the Asia-Pacific region and 33% were from Western countries. Body weight was <60 kg in 32% and ≥60 kg in 68% of patients. Macroscopic vein involvement and/or extrahepatic spread was detected in 69% of patients, and 78% were Barcelona clinic liver cancer stage C. The proportion of patients with HCC caused by hepatitis C was favorably imbalanced toward sorafenib (26 vs. 19% in the lenvatinib arm) [11]. Conversely, the proportion of patients with HCC caused by hepatitis B was 53% in the lenvatinib arm and 48% in the sorafenib arm. The proportion of patients with an α-fetoprotein (AFP) level of ≥200 ng/mL was also favorably imbalanced toward sorafenib (39 vs. 46% in the lenvatinib arm).

The primary endpoint of OS was 13.6 months in the lenvatinib arm and 12.3 months in the sorafenib arm. The upper limit of the 95% confidence interval (CI) of the hazard ratio (HR), which was 0.92 (0.79–1.06), was below the predetermined noninferiority margin of 1.08, which demonstrated the statistically significant noninferiority of lenvatinib with respect to OS [11]. PFS, TTP, and ORR (lenvatinib arm/sorafenib arm) per investigator assessment using the modified RECIST criteria (mRECIST) were 7.4/3.7 months, 8.9/3.7 months, and 24.1/9.2%, respectively. These results demonstrate that lenvatinib had a statistically signifi-

Table 4. REFLECT: masked independent imaging review according to mRECIST

	Lenvatinib (n = 478)	Sorafenib (n = 476)	HR/OR	p value
PFS, months	7.3 (5.6–7.5)	3.7 (3.6–3.7)	HR 0.64 (0.55–0.75)	<0.0001
TTP, months	7.4 (7.2–9.1)	3.7 (3.6–3.9)	HR 0.60 (0.51–0.71)	<0.0001
ORR, %	40.6 (36.2–45.0)	12.4 (9.4–15.4)	OR 5.01 (3.59–7.01)	<0.0001

Values in parentheses are 95% CI. PFS, progression-free survival; TTP, time to progression; ORR, objective response rate; HR, hazard ratio; OR, odds ratio. Cited and modified from Kudo et al. [11].

Table 5. REFLECT: masked independent imaging review according to RECIST1.1

	Lenvatinib (n = 478)	Sorafenib (n = 476)	HR/OR	p value
PFS, months	7.3 (5.6–7.5)	3.6 (3.6–3.9)	HR 0.65 (0.56–0.77)	<0.0001
TTP, months	7.4 (7.3–9.1)	3.7 (3.6–5.4)	HR 0.61 (0.51–0.72)	<0.0001
ORR, %	18.8 (15.3–22.3)	6.5 (4.3–8.7)	OR 3.34 (2.17–5.14)	<0.0001

Values in parentheses are 95% CI. PFS, progression-free survival; TTP, time to progression; ORR, objective response rate; HR, hazard ratio; OR, odds ratio. Cited and modified from Kudo et al. [11].

cantly better antitumor effect than sorafenib (Table 3) [11]. Another surprising finding was that tumor shrinkage according to the masked independent imaging review using mRECIST was considerably greater in the lenvatinib arm than in the sorafenib arm (ORR: 40.6 vs. 12.4%) (Table 4) [11]. This favorable antitumor effect indicated by the PFS, TTP, and ORR rates was reproduced exactly in a masked independent imaging review using RECIST 1.1 (Table 5) [11].

Since patients were not stratified by AFP in this trial, the lenvatinib arm had a higher proportion of patients with AFP of ≥ 200 ng/mL. When this AFP imbalance was corrected by analysis of covariance in the OS analysis, lenvatinib demonstrated a statistically significant superior effect over sorafenib with respect to OS (HR = 0.856, 95% CI = 0.736–0.995, nominal $p = 0.0342$) (Fig. 2) [11]. This result indicates that the trial may have demonstrated superiority if patients had been stratified by AFP.

In the OS subanalysis, lenvatinib was superior to sorafenib for improving OS in almost all groups. One particularly noteworthy finding was that lenvatinib was more effective than sorafenib for improving OS even in patients weighing < 60 kg who received a dose of only 8 mg, and the HR was even better than that in patients weighing ≥ 60 kg who received 12 mg (< 60 kg: HR = 0.85 vs. ≥ 60 kg: HR = 0.95). This indicated that weight-based dosing is successful. Lenvatinib also yielded a good improvement in OS in patients with high AFP, a poor prognostic factor, as indicated by the HR of 0.78 (95% CI = 0.63–0.98) (Fig. 2). The only subgroup in which the numerical values indicated that sorafenib yielded better OS was that of patients enrolled in Western countries. This can be attributed to the fact that patients in the sorafenib arm in those countries frequently received post-study systemic anticancer treatment (38.9 vs. 26.1% in the lenvatinib arm), and patients in the sorafenib arm more frequently underwent anticancer procedures such as TACE (11.5 vs. 7.0% in the lenvatinib arm) (Table 6) [11]. In the Asia-Pacific region, the percentage of patients who received post-study therapy was well balanced; however, in the Western region, 45.2% of patients in the sorafenib arm received

Table 6. Post-study anticancer therapy during survival follow-up

	Lenvatinib			Sorafenib		
	Asia-Pacific subgroup (n = 321)	Western subgroup (n = 157)	total (n = 478)	Asia-Pacific subgroup (n = 319)	Western subgroup (n = 157)	total (n = 476)
Received any anticancer therapy during survival follow-up, n (%)	162 (50.5)	44 (28.0)	206 (43.1)	172 (53.9)	71 (45.2)	243 (51.1)
Received any anticancer medication (not given for any procedure) during survival follow-up, n (%)	115 (35.8)	41 (26.1)	156 (32.6)	123 (38.6)	61 (38.9)	184 (38.7)
Underwent any anticancer procedure during survival follow-up, n (%)	111 (34.6)	11 (7.0)	122 (25.5)	112 (35.1)	18 (11.5)	130 (27.3)

Anticancer therapy includes anticancer medication and anticancer procedure. Cited from Kudo et al. [11].

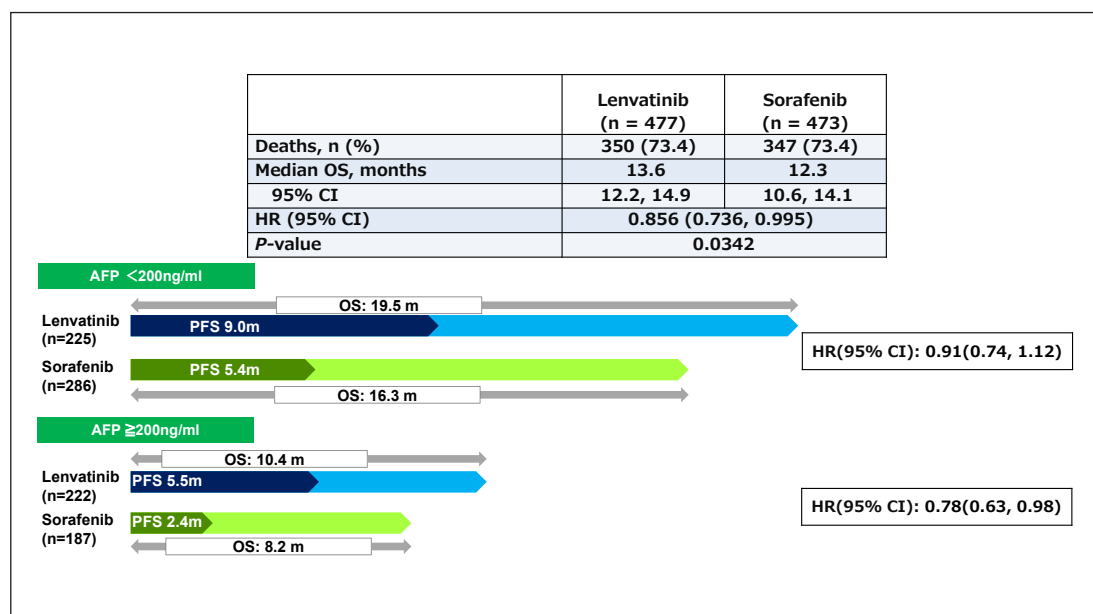


Fig. 2. Overall survival adjusted by baseline AFP (<200 ng/mL and ≥200 ng/mL). AFP, α-fetoprotein; HR, hazard ratio.

post-study treatment versus 28.0% in the lenvatinib arm. An imbalance between the treatment arms was observed in the proportion of patients who received post-anticancer therapy during the survival follow-up, which was higher in the sorafenib than in the lenvatinib arm: 51.1% (243/476) versus 43.1% (206/478), respectively. In post-study treatment, new agents were used in 17.0% of patients in the sorafenib arm compared with 5.9% in the lenvatinib arm. In the lenvatinib arm, 25.3% of patients received sorafenib after progression, and 11.8% of patients in the sorafenib arm were rechallenged with sorafenib (Table 7) [22].

Table 7. Subsequent anticancer therapy during survival follow-up

	Lenvatinib (n = 478), n (%)	Sorafenib (n = 476), n (%)
Subjects with any anticancer medication ^a	156 (32.6)	184 (38.7)
Post-study treatment with new agents	28 (5.9)	81 (17.0)
Investigational drugs ^b	20 (4.2)	73 (15.3)
Checkpoint inhibitors	9 (1.9)	9 (1.9)
Cytotoxic chemotherapy	44 (9.2)	77 (16.2)
Sorafenib	121 (25.3)	56 (11.8)
Other	25 (5.2)	31 (6.5)

^a Anticancer medication: not given for any procedure. ^b Investigational drugs including drugs coded as investigational drugs, tivantinib, regorafenib, cabozantinib, and the other VEGF inhibitors.

Treatment duration was 5.7 months in the lenvatinib arm and 3.7 months in the sorafenib arm, indicating that treatment with lenvatinib was better tolerated. Dose intensity of the planned starting dose was also slightly better in the lenvatinib arm than in the sorafenib arm (88 vs. 83%).

The above results demonstrate the statistically significant noninferiority of lenvatinib over sorafenib with respect to OS, and statistically and clinically meaningful improvements were also observed in the secondary endpoints (PFS, TTP, and ORR). These findings indicate that lenvatinib is an effective first-line drug for unresectable HCC.

Factors Contributing to the Success of the REFLECT Trial

Several critical factors contributed to the first successful demonstration of noninferiority of a first-line drug in 10 years. The REFLECT trial was the first noninferiority trial of a molecular targeted agent with dose selection by body weight (12 vs. 8 mg). In the GIDEON observational study, only 45.5% of Japanese patients started sorafenib at 800 mg, and there was no clear evidence to support reducing doses based on patients' body weight [23]. In the lenvatinib arm, the same level of efficacy was obtained across weight groups (<60 kg and ≥60 kg), and toxicity was within an acceptable range. The incidence of hand-foot skin reaction and diarrhea was lower, enabling longer treatment duration in the lenvatinib than in the sorafenib arm. The antitumor effect was surprisingly better (ORR: 40.6%), and no other molecular targeted drug has yielded such good response rates (Fig. 3, 4) [24–27]. PFS and TTP were also better for lenvatinib than for sorafenib, supporting that its antitumor effect is more potent than that of sorafenib. Another factor contributing to the success of the trial was that patients could receive an additional 2 months of treatment with lenvatinib because of its acceptable AE profile and slightly greater tolerability than sorafenib in some respects.

The REFLECT trial did not demonstrate superiority over sorafenib likely because of the unfavorably high proportion of high-AFP patients in the lenvatinib arm, which was due to the lack of stratification by AFP and macroscopic vein involvement, as well as the higher proportion of patients with hepatitis C (a favorable prognostic factor for sorafenib) in the sorafenib arm [28]. Another possible reason was that both arms consisted of patients with favorable prognosis who were good candidates for post-study treatment because of the exclusion of patients with tumor thrombus at the main portal vein (VP4) and ≥50% tumor occupancy in the liver [29, 30]. The longer post-progression survival associated with post-study treatment in both arms may have diluted the OS benefit, as observed in previous failed trials [31–33]. In fact,

Kudo: Lenvatinib May Drastically Change the Treatment Landscape of Hepatocellular Carcinoma

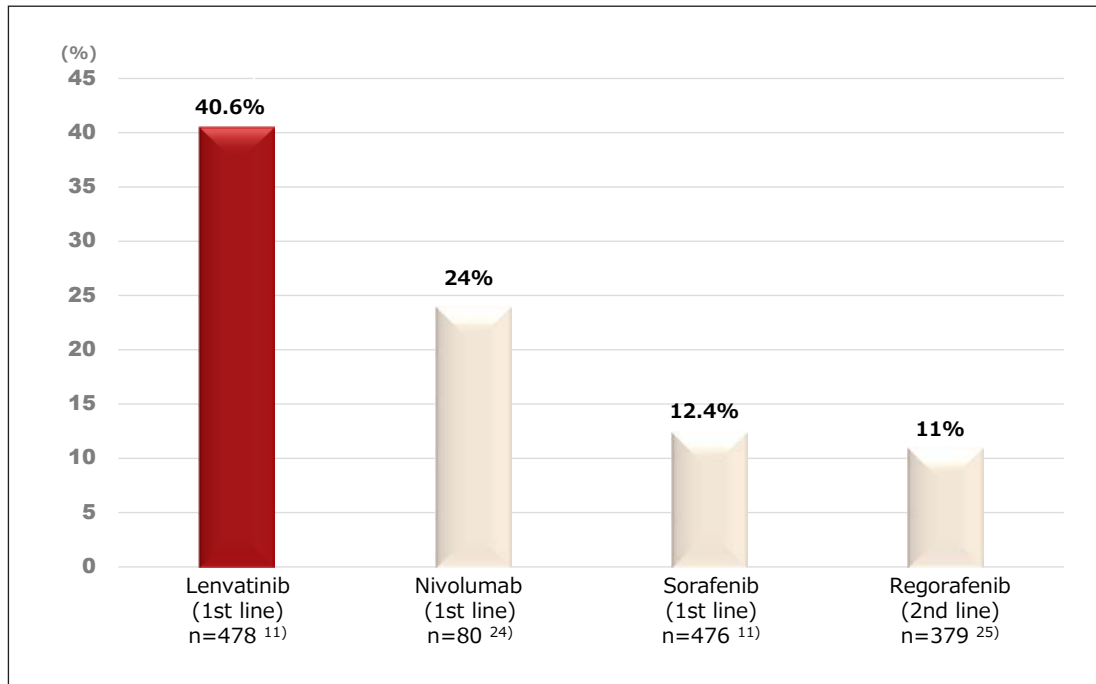


Fig. 3. Objective response rate by mRECIST in systemic therapy [11, 24, 25].

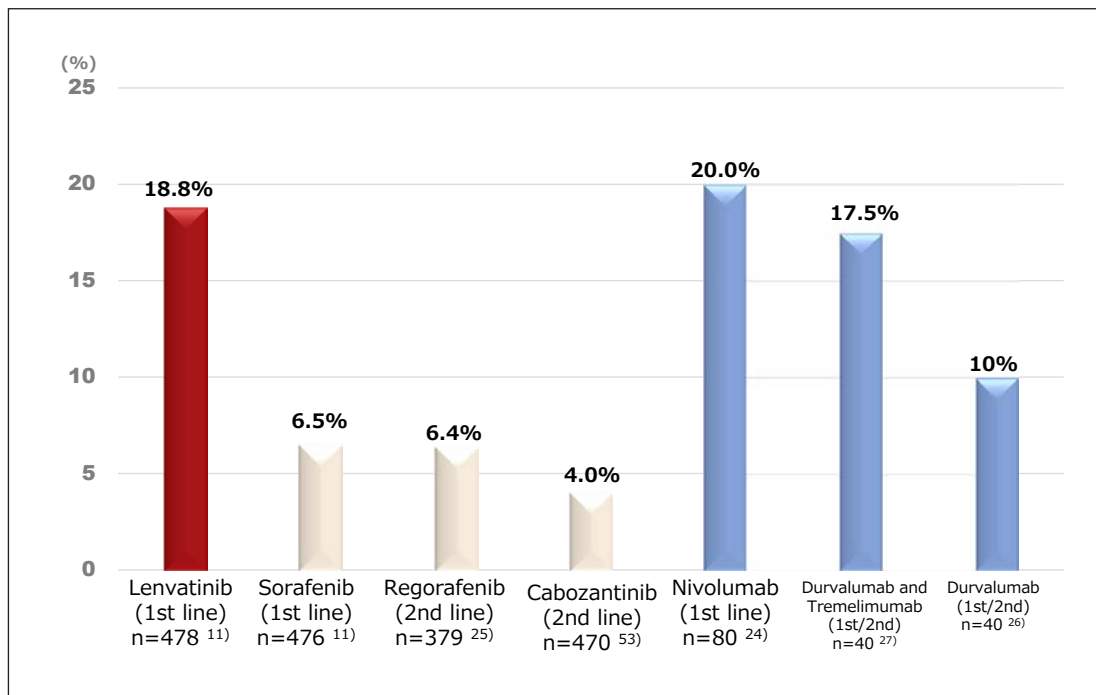


Fig. 4. Objective response rate by RECIST1.1 in systemic therapy [11, 24–27, 53].

Table 8. Stratification factors in phase III clinical trials in first-line agents for HCC

Study arm vs. sorafenib arm	SUN1170 (sunitinib)	BRISK-FL (brivanib)	LiGHT (linifanib)	SEARCH (+ erlotinib)	CheckMate-459 (nivolumab)	REFLECT (lenvatinib)
Stratification factor	Region Vascular invasion and/or extrahepatic spread Prior TACE	Region ECOG-PS score Extrahepatic spread and/or vascular invasion	Region ECOG-PS score Vascular invasion and/or extrahepatic spread Hepatitis B virus infection	Region ECOG-PS score Vascular invasion and/or extrahepatic spread Smoking status	Region Vascular invasion and/or extrahepatic spread Etiology	Region ECOG-PS score Vascular invasion and/or extrahepatic spread Body weight

Cited and modified from previously published studies [4–7, 11, 56].

patients in both the lenvatinib and sorafenib arms of the REFLECT trial received a significant amount of post-study treatment (Tables 6, 7), which resulted in extremely long OS in the sorafenib arm (12.3 months), the longest ever observed in clinical trials of first-line agents (SHARP: 10.7 months, Asia-Pacific: 6.5 months, SUN1170: 10.2 months, Brisk-FL: 9.9 months, LiGHT: 9.8 months) [1, 2, 4–6].

The imbalance in AFP was a critical issue. This was an accidental imbalance resulting from the lack of inclusion of AFP as a stratification factor. However, AFP was not commonly used as a stratification factor when the REFLECT trial was started, and it was not included in any past or current first-line trials [4–7, 11] (Table 8). In their review, Llovet et al. [34] do not recommend using AFP as a stratification factor in first-line trials. Nevertheless, as noted above, lenvatinib demonstrated statistically significant superiority over sorafenib with respect to OS when the AFP imbalance was corrected by analysis of covariance, indicating that AFP should be used as a stratification factor in future first-line trials.

AE Profile

Certain AEs were slightly more frequent in the lenvatinib arm than in the sorafenib arm, including hypertension, proteinuria, dysphonia, and hypothyroidism. Hand-foot skin reaction, diarrhea, and hair loss were slightly more frequent in the sorafenib arm than in the lenvatinib arm. The low incidence of hand-foot skin reaction, diarrhea, and other events that directly impact compliance is one reason that patients continued lenvatinib for a longer period than sorafenib. However, treatment-emergent AEs (TEAEs) of all grades were more frequent in the lenvatinib arm; the incidence of TEAEs of grade 3 or higher in particular was higher in the lenvatinib arm than in the sorafenib arm (57 vs. 49%), and the incidence of serious TEAEs was also slightly higher in the lenvatinib arm than in the sorafenib arm (18 vs. 10%) [11]. However, this can be attributed to the longer duration of treatment with lenvatinib (+2 months). The incidence of AEs of all grades, grade 3 or higher, as well as SAEs was either comparable between the two arms or lower in the lenvatinib arm after correction by actual treatment duration (Table 9) [35].

Significance of Body Weight-Based Dosing

In the phase II trial, a uniform daily dose of 12 mg irrespective of body weight and surface area led to dose reduction in a large proportion of patients: dose adjustment occurred in 34 of 46 patients (74%) because of treatment-related AEs, and withdrawal occurred in 10 patients (22%) because of toxicity. Close examination of the patients' background suggested

Table 9. Treatment-emergent adverse events (TEAEs) adjusted by treatment duration

	Lenvatinib (n = 476), AE rate	Sorafenib (n = 475), AE rate
TEAEs		
TEAE episodes	18.89%	19.73%
Related TEAE episodes	10.94%	11.98%
TEAE episodes of grade ≥3	3.16%	3.33%
Related TEAE episodes of grade ≥3	1.59%	1.80%
Serious TEAE episodes	1.26%	0.97%
Serious related TEAE episodes	0.41%	0.28%
Related episodes of TEAE leading to study drug:		
Dose reduction	0.84%	0.97%
Reductions or interruption	1.59%	1.77%
Withdrawal	0.15%	0.18%

Lenvatinib, total duration 324.2 years; sorafenib, total duration 239.1 years.

that body weight and serum lenvatinib levels were associated with dose reduction or early treatment withdrawal. More precisely, patients who had dose reduction or early withdrawal within 30 days of lenvatinib treatment were significantly lighter (median weight, 54.1 vs. 67.6 kg) and had a significantly higher minimum plasma concentration of lenvatinib (trough concentration [$C_{1D15C_{trough}}$], 62.4 vs. 33.9 ng/mL) [36, 37].

Relationship between Body Weight and Plasma Level of Lenvatinib in HCC Patients

Following the phase I and II trials, population pharmacokinetics were analyzed in 65 HCC patients enrolled in those trials, and in 155 patients with solid cancer and 232 healthy individuals enrolled in other clinical trials [36]. A relationship was observed between body weight and plasma lenvatinib level (represented by the area under the blood concentration time curve [AUC]), indicating that exposure to lenvatinib increased as body weight decreased [36, 37]. This trend was more prominent in HCC patients than in patients with other types of solid cancers, suggesting that the relationship has an especially strong impact in HCC patients.

Relationship between Pharmacokinetics of Lenvatinib and Dose Reduction or Withdrawal in HCC Patients

Forty-five patients who participated in trials for HCC treatment were divided into a low AUC group (<2,051.1 ng•h/mL), an intermediate AUC group (>2,051.1 to ≤2,747.1 ng•h/mL), and a high AUC group (>2,747.1 ng•h/mL) to examine the relationship between AUC and time to dose reduction or withdrawal of lenvatinib. Kaplan-Meier plots showed a reduction in the time to dose reduction or withdrawal with increasing AUC [36, 37]. A similar relationship was observed between body weight and time to dose reduction or withdrawal; time to dose reduction or withdrawal became shorter as body weight decreased, demonstrating that dose reduction or withdrawal may be required earlier in lighter patients than in heavier patients [36, 37].

Optimal Cutoff Values for Body Weight and AUC in HCC Patients Treated with Lenvatinib

Strong correlations between lenvatinib withdrawal, blood concentration (AUC), and body weight indicated that dose adjustment by body weight and AUC may improve the safety of lenvatinib for the treatment of patients with HCC. The sensitivity and specificity of different

body weight cutoff values for predicting the early occurrence (within 30 days after the start of therapy) of dose reduction and withdrawal were calculated to draw receiver operating characteristic (ROC) curves [36, 37]. The optimal body weight cutoff (the point at which the distance between the top left corner of the graph and the ROC is smallest) that most effectively distinguished the high-risk group for early withdrawal or dose reduction of lenvatinib was 57.8 kg, showing a sensitivity of 0.77 and specificity of 0.67 (false-positive rate, 0.33). Similarly, the optimal AUC cutoff was 2,430 ng•h/mL, with a sensitivity of 0.71 and specificity of 0.71 (false-positive rate, 0.29) [36, 37].

Significance of Maintaining the AUC within a Certain Range and Lenvatinib Dose Adjustment in HCC

Regarding the prediction of early withdrawal or dose reduction of lenvatinib, the AUC was more effective than other factors such as sex, body weight, age, liver function, platelet count, ECOG performance status, Child-Pugh class, hepatitis viral status, portal vein tumor thrombus, prior chemotherapy, prior antihypertensive therapy, and prior surgery. An AUC probability curve [36, 37] can predict early withdrawal or dose reduction of lenvatinib. Consequently, the AUC needs to be maintained below a certain level to reduce the occurrence of early withdrawal or dose reduction; for example, lenvatinib dosing may be adjusted to obtain an AUC value that is below the optimal cutoff (2,430 ng•h/mL).

Based on the findings that the optimal body weight cutoff for a similar prediction was 57.8 kg, the predicted AUC values for weight-based dosing (daily dose of 12 or 8 mg in patients with body weight ≥ 60 kg or < 60 kg, respectively) were calculated and plotted against body weight [36, 37]. The predicted AUC values were in the range of 1,540–2,050 ng•h/mL in patients with body weight < 60 kg, and 1,410–2,310 ng•h/mL in those with body weight ≥ 60 kg. These AUC ranges were similar and lower than 2,430 ng•h/mL in both body weight categories, indicating that the weight-based dose adjustment might efficiently reduce early withdrawal and dose reduction of lenvatinib.

Relationship between the AUC and the Efficacy of Lenvatinib in the Treatment of HCC

A major concern is that lenvatinib dose adjustment to reduce the AUC could impair efficacy. To test this, patients enrolled in the phase II trial that tested an initial daily dose of 12 mg were divided into the low AUC group ($< 2,051.1$ ng•h/mL), the intermediate AUC group ($> 2,051.1$ to $\leq 2,747.1$ ng•h/mL), and the high AUC group ($> 2,747.1$ ng•h/mL) to examine the relationship between AUC and efficacy. There was no trend in TTP in the three groups [36, 37], suggesting that a certain level of efficacy can be maintained even when the AUC is small.

Because of the lack of data on reduced-dose sorafenib, the recommended dose remains at 400 mg twice daily even in patients with lower body weight. However, a dose of 200 mg twice daily yields a satisfactory effect in patients with lower body weight, as in Japanese patients. The REFLECT trial showed that the 8 mg dose used in patients weighing 60 kg or less was comparable or better regarding safety and efficacy than the full 12 mg dose. These results are valuable data supporting the feasibility of determining proper dosing by weight.

Quality of Life Assessment

In the REFLECT trial, quality of life (QOL) was evaluated using two health questionnaires, the EORTC QLQ-C30 and the EORTC QLQ-HCC18 (Table 10). Baseline scores were comparable between the lenvatinib and sorafenib arms, although the scores in both arms decreased after the start of treatment [11].

Table 10. QOL Questionnaire

<i>EORTC QLQ-C30</i>	
Role functioning	Were you limited in doing either your work or other daily activities? Were you limited in pursuing hobbies or other leisure activities?
Pain	Did pain interfere with your daily activities?
Diarrhea	Have you had pain? Have you had diarrhea?
<i>EORTC QLQ-HCC18</i>	
Nutrition	Have you had problems with sense of taste? Have you felt full up to quickly after beginning to eat? Have you worried about getting enough nourishment? Have you worried about your weight being too low?
Body image	Have you lost muscle from your arms or legs? Have you been concerned by the appearance of your abdomen?

However, analysis of time to clinically meaningful deterioration showed that role functioning (nominal $p = 0.0193$), pain (nominal $p = 0.0105$), and diarrhea (nominal $p < 0.0001$) in the EORTC QLQ-C30, and nutrition (nominal $p = 0.0113$) and body image (nominal $p = 0.0051$) deterioration in the EORTC QLQ-HCC18, occurred earlier in patients treated with sorafenib than in those treated with lenvatinib. QLQ-C30 summary scores were also better for lenvatinib than sorafenib (HR = 0.87).

Maintaining good QOL in patients taking medications is critically important to improve compliance. Therefore, the detection of clinically meaningful differences between lenvatinib and sorafenib in these five critical items explains why treatment with lenvatinib could continue for longer and produce such a potent antitumor effect. These high QOL measures should be reproduced in clinical practice, and will most certainly make lenvatinib a highly tolerable and effective first-line drug for patients with HCC.

Results of Exploratory Research on Blood Biomarkers

The results of blood biomarker testing were presented at the Congress of the European Society of Medical Oncology in 2017 [38]. Blood VEGF, FGF19, and FGF23 were elevated in the lenvatinib arm but not in the sorafenib arm. Angiopoietin 2 (Ang2) was decreased in the lenvatinib arm but not in the sorafenib arm. The increase in VEGF indicates that lenvatinib is a more potent inhibitor of VEGFR1–3 activity than sorafenib. The increase in FGF19 indicates that lenvatinib is a potent inhibitor of the activity of the FGF19 receptor, FGFR4. FGF23 is secreted by osteocytes and plays a key role in phosphorus homeostasis and vitamin D metabolism [39]. Increased FGF23 is a surrogate marker of FGFR1 inhibition [40], and is part of the FGF pathway escape mechanism in response to VEGF-targeted antiangiogenic therapies [41]. Therefore, increase of FGF 23 suggests that lenvatinib is a potent inhibitor of FGFR1.

Ang2 and its receptor Tie2 are regulators of angiogenesis [42], and the role of Ang2 in adaptive tumor resistance to anti-VEGF therapy was recently identified [43], suggesting that lenvatinib is a potent agent in the adaptive tumor resistance to anti-VEGF therapy. The blood concentration of PIVKA-II was lower in the lenvatinib arm than in the sorafenib arm, which reflects the potent antitumor effect of lenvatinib.

These results provide important data to explain how the effects of lenvatinib at and above the IC50 calculated from in vitro studies, particularly its suppression of VEGF and FGF receptor activity, can be reproduced in vivo (Fig. 1).

Table 11. Objective response rate of TACE and lenvatinib (mRECIST)

Placebo arm of BRISK-TA trial [49] (n = 253) (cTACE)	Placebo arm of SPACE trial [50] (n = 153) (DEB-TACE)	Placebo arm of TACE-2 trial [51] (n = 156) (DEB-TACE)	Lenvatinib arm of REFLECT trial [11] (n = 478) (systemic)
42%	28.1%	52%	40.6%

cTACE, conventional lipiodol transcatheter arterial chemoembolization. DEB-TACE, drug-eluting beads TACE.

Clinical Significance of High Response Rates

Sorafenib is a molecular targeted agent that does not yield a very high response rate, although it improves survival by maintaining stable disease for a long duration. Several drugs show significantly higher response rates than sorafenib in clinical trials; however, these trials all failed because the high response rates never led to an OS benefit (linifanib: 10.1% per RECIST 1.1; sorafenib plus HAIC: 36.3% vs. sorafenib: 17.5% per mRECIST). In a clinical trial of second-line brivanib, the drug yielded a significantly higher ORR per mRECIST than the placebo (10 vs. 2%), although it did not show OS benefit. The same outcomes were obtained with ramucirumab, which yielded a higher response rate per RECIST 1.1 than the placebo (7 vs. <1%), but could not show OS benefit. However, it would be premature to conclude from these findings that the ORR has absolutely no positive impact on survival. Measures such as disease control rate, PFS, TTP, and ORR are inherently critical factors in the antitumor effect of a drug. However, in clinical trials in HCC, other sources of “noise” overwhelm these signals, and a complex web of various factors determines whether the trial will succeed or fail. In fact, even in the RESORCE trial, which succeeded because of its excellent study design, regorafenib had a greater antitumor effect (TTP or PFS) than the placebo and a significantly greater ORR per mRECIST (11 vs. 4%) [25]. Not only the response rate but also a clinical trial design is an important factor for the success to the OS endpoint trial of systemic therapy. However, when it comes to clinical practice, once approved a better response rate is an extremely favorable feature. Indeed, necrotic effect assessed by mRECIST in systemic therapy correlates well with OS [44–47].

A high response rate is extremely important for drugs that have moved from successful clinical trials into clinical use as mentioned above. Drugs with good response rates are not only highly effective, but also increase the motivation of physicians and patients to continue the treatment, as well as increasing compliance; in addition, they have the potential for curative conversion (e.g., surgical resection or ablation or TACE) through downstaging.

For example, TACE, the standard therapy for intermediate-stage HCC, generally has an excellent necrotic effect on tumors and is associated with a good prognosis in responders [48]. Indeed, TACE has made treatment effectiveness feasible for both physicians and patients, increasing their motivation to continue treatment. To describe TACE as the global standard for response rate, the most trustworthy source of data would be the control arms of well-designed prospective randomized trials investigating combination therapy with TACE.

ORRs in the BRISK-TA [49], SPACE [50], and TACE-2 [51] trials were 42, 28.1, and 52%, respectively (Table 11; Fig. 5), and the BRISK-TA results could be considered the global standard because the study had the largest enrollment and was conducted on a global scale. The ORR for TACE in the control arm of the BRISK-TA trial was 42%, which was comparable to the 40.6% ORR for lenvatinib. This indicates that systemic therapy with lenvatinib can

Kudo: Lenvatinib May Drastically Change the Treatment Landscape of Hepatocellular Carcinoma

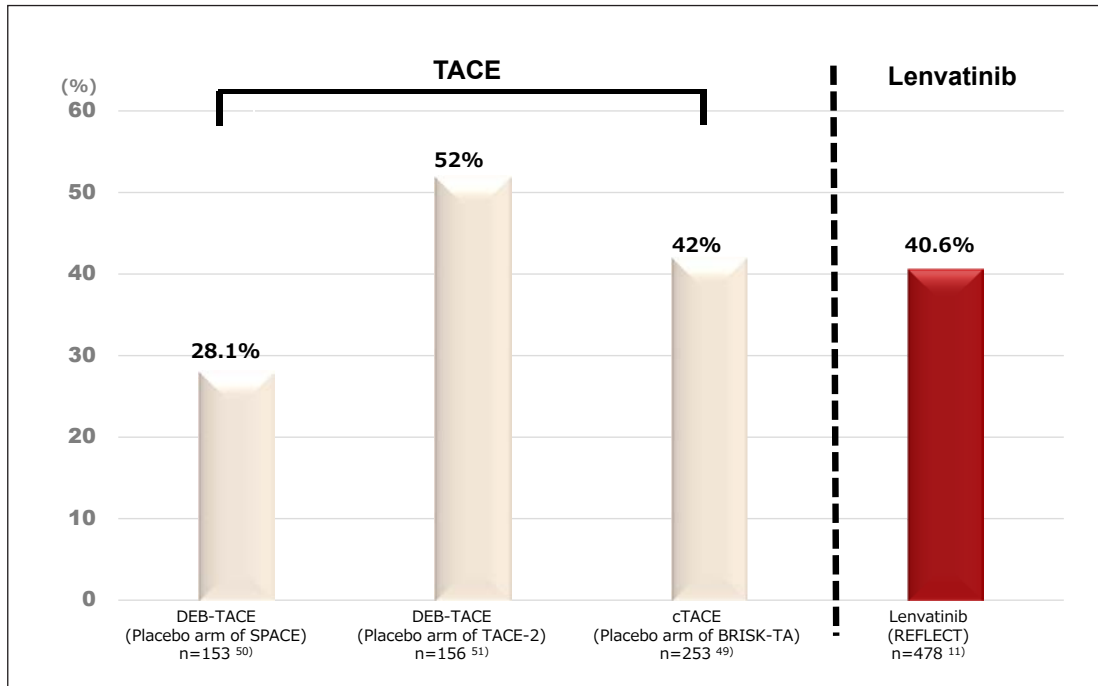


Fig. 5. Objective response rate by mRECIST TACE and lenvatinib [11, 49-51].

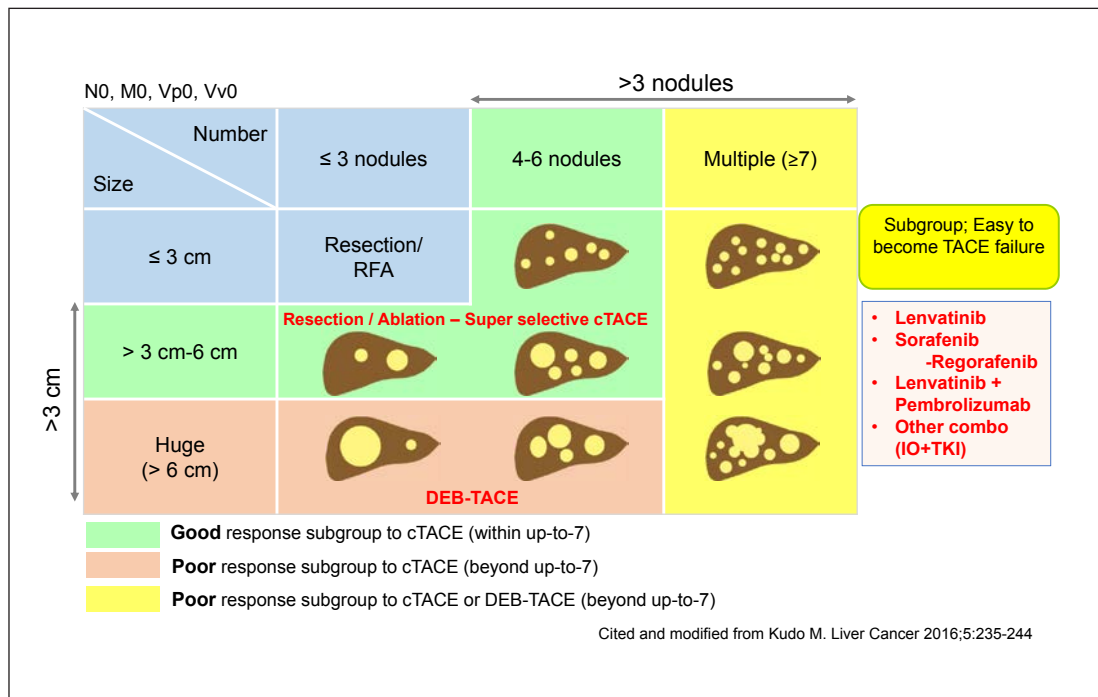


Fig. 6. Heterogeneity and treatment strategy of intermediate-stage HCC [52, 54].

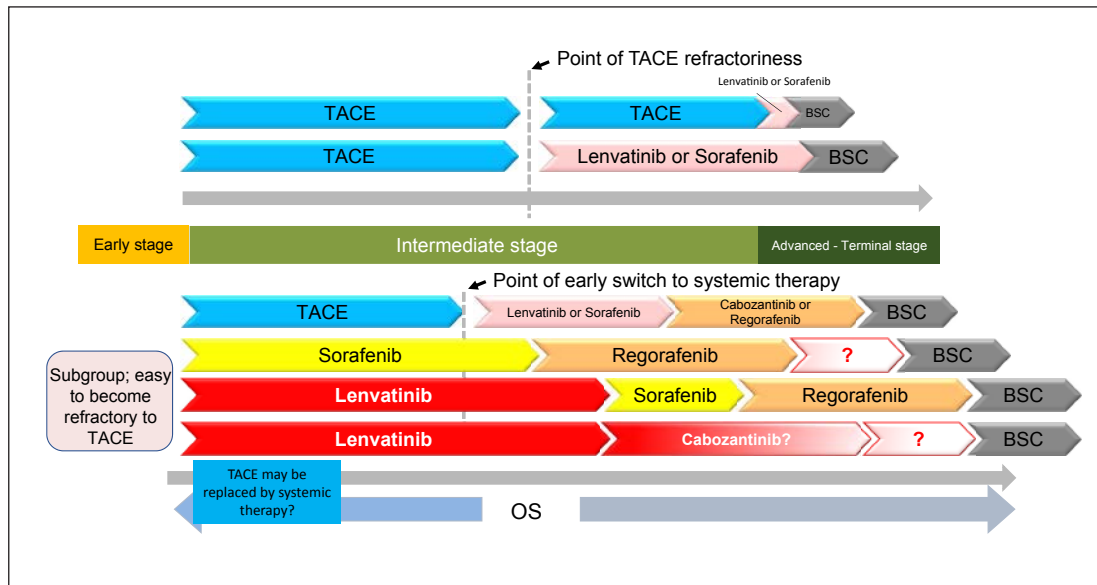


Fig. 7. Treatment strategy for systemic therapy for HCC. Identification of the subgroup that easily develops to TACE failure/refractoriness may be important.

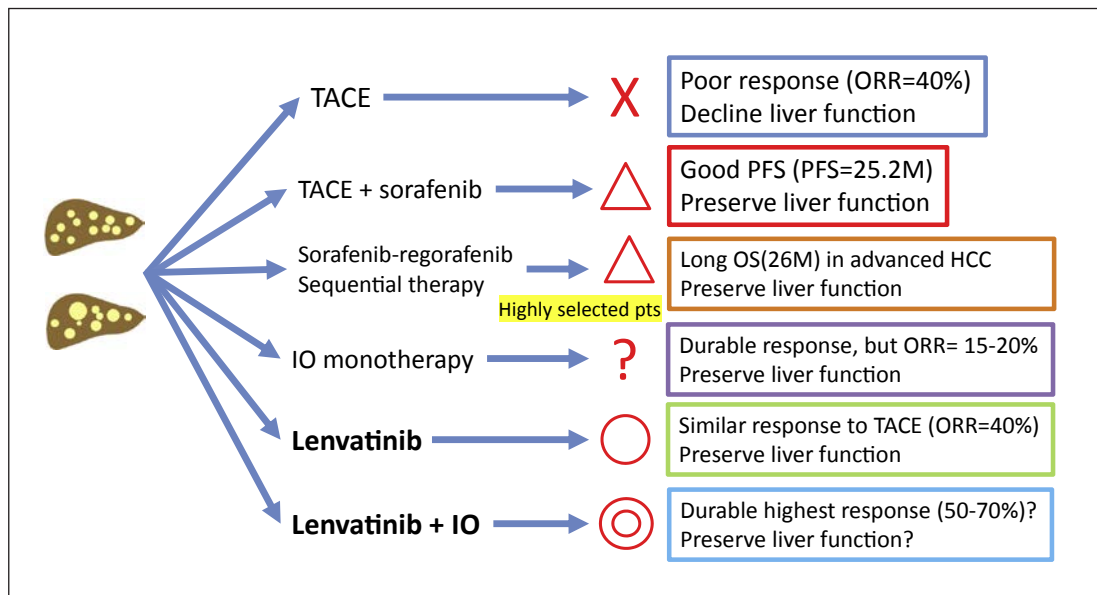


Fig. 8. Future treatment strategy of bilobar multinodular intermediate-stage HCC.

yield a comparable response to that of TACE without impairing hepatic functional reserve in patients with intermediate-stage HCC. Therefore, systemic therapy may be more effective than TACE for improving survival in a subgroup of patients with intermediate-stage HCC (Fig. 6). However, properly designed prospective clinical trials are necessary to confirm this hypothesis. The favorable properties of lenvatinib could result in a paradigm shift in the treatment of not only advanced-stage HCC, but also intermediate-stage HCC.

Kudo: Lenvatinib May Drastically Change the Treatment Landscape of Hepatocellular Carcinoma

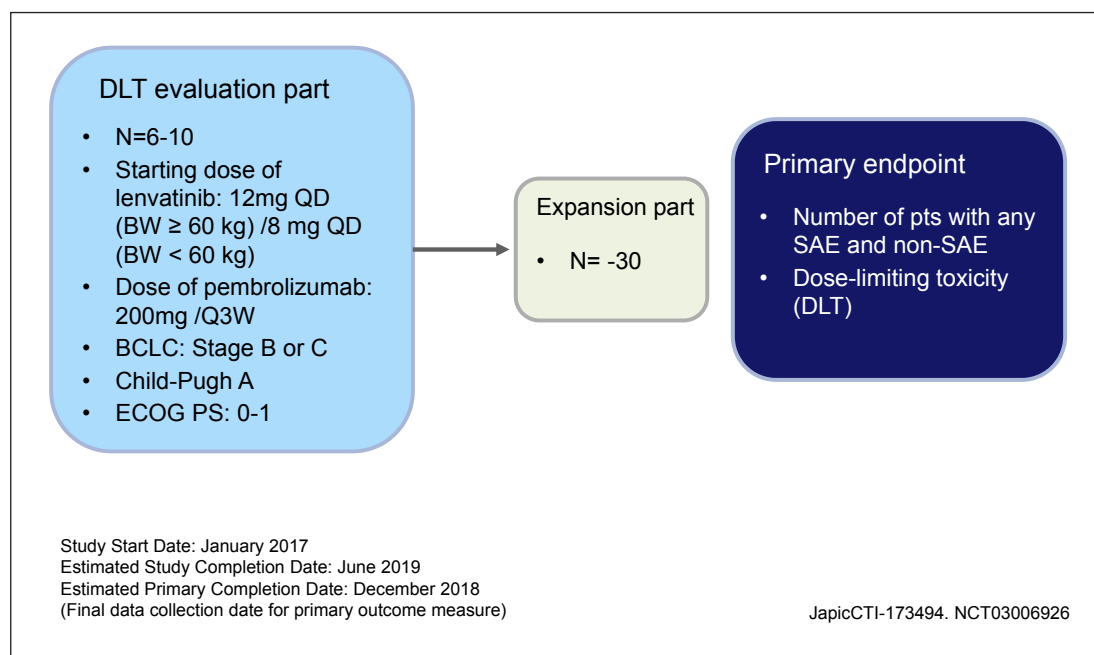


Fig. 9. Phase Ib lenvatinib plus pembrolizumab in unresectable HCC.

Future Perspectives of HCC Treatment with the Introduction of Lenvatinib

The success of the REFLECT trial will drastically change the future treatment landscape of HCC. Approval of lenvatinib would provide physicians with a first-line drug of greater potency than that of current drugs and high tolerability. Questions that remain to be answered include when to use lenvatinib rather than the other first-line drug, sorafenib, and which second-line drug should be used in patients who do not respond to lenvatinib. Regorafenib is currently the only available effective second-line agent [25, 52]; however, cabozantinib will soon become available as well [53]. In this era of multimolecular targeted agents, it may be necessary to rapidly identify the subgroup of intermediate-stage HCC patients who do not respond to TACE besides advanced-stage HCC patients. TACE plus a molecular targeted agent [12] is another optional treatment to improve the clinical outcome; furthermore, systemic therapy is currently a better first choice of treatment for improving survival than TACE for certain subgroups (bilobar multinodular HCC or Kinki criteria B2 substage) of intermediate-stage HCC patients who are conventionally candidates for TACE [54] (Fig. 7, 8).

Conclusion

The emergence of lenvatinib will change the treatment landscape of HCC. Most notably, the ability of lenvatinib to yield response rates as high as those of TACE indicates that systemic therapy may soon replace TACE as the standard therapy in certain subgroups of patients with intermediate-stage HCC (Fig. 6–8). Trials in other cancers show that combination therapy with immune checkpoint inhibitors such as pembrolizumab or nivolumab [55–57] yields extremely high response rates of 50–70%, and it is an ideal treatment with a response that is both long-lasting and durable [58–60]. If this approach is applied as adjuvant or neoadjuvant therapy for curatively treated early-stage HCC or as an addition to or replacement for TACE

in intermediate-stage HCC, a real cure for HCC may cease to be a dream. In fact, clinical trials of combination therapy with lenvatinib and pembrolizumab for HCC have already started (Fig. 9), leaving little doubt that the landscape of HCC treatment will undergo drastic changes in years to come.

References

- 1 Llovet JM, Ricci S, Mazzaferro V, Hilgard P, Gane E, Blanc JF, de Oliveira AC, et al: Sorafenib in advanced hepatocellular carcinoma. *N Engl J Med* 2008;359:378–390.
- 2 Cheng AL, Kang YK, Chen Z, Tsao CJ, Qin S, Kim JS, Luo R, et al: Efficacy and safety of sorafenib in patients in the Asia-Pacific region with advanced hepatocellular carcinoma: a phase III randomised, double-blind, placebo-controlled trial. *Lancet Oncol* 2009;10:25–34.
- 3 Kudo M: Molecular targeted agents for hepatocellular carcinoma: current status and future perspectives. *Liver Cancer* 2017;6:101–112.
- 4 Cheng AL, Kang YK, Lin DY, Park JW, Kudo M, Qin S, Chung HC, et al: Sunitinib versus sorafenib in advanced hepatocellular cancer: results of a randomized phase III trial. *J Clin Oncol* 2013;31:4067–4075.
- 5 Johnson PJ, Qin S, Park JW, Poon RT, Raoul JL, Philip PA, Hsu CH, et al: Brivanib versus sorafenib as first-line therapy in patients with unresectable, advanced hepatocellular carcinoma: results from the randomized phase III BRISK-FL study. *J Clin Oncol* 2013;31:3517–3524.
- 6 Cainap C, Qin S, Huang WT, Chung IJ, Pan H, Cheng Y, Kudo M, et al: Lenvatinib versus Sorafenib in patients with advanced hepatocellular carcinoma: results of a randomized phase III trial. *J Clin Oncol* 2015;33:172–179.
- 7 Zhu AX, Rosmorduc O, Evans TR, Ross PJ, Santoro A, Carrilho FJ, Bruix J, et al: SEARCH: a phase III, randomized, double-blind, placebo-controlled trial of sorafenib plus erlotinib in patients with advanced hepatocellular carcinoma. *J Clin Oncol* 2015;33:559–566.
- 8 Kudo M, Ueshima K, Yokosuka O, Ogasawara S, Obi S, Izumi N, Aikata H, et al: Randomized, open label, multi-center phase III trial comparing sorafenib plus low-dose cisplatin/fluorouracil hepatic arterial infusion chemotherapy with sorafenib alone in patients with advanced hepatocellular carcinoma: SILIUS trial. *Lancet Gastroenterol Hepatol* 2018, in press.
- 9 Vilgrain V, Pereira H, Assenat E, Guiu B, Ilonca AD, Pageaux GP, Sibert A, et al: Efficacy and safety of selective internal radiotherapy with yttrium-90 resin microspheres compared with sorafenib in locally advanced and inoperable hepatocellular carcinoma (SARAH): an open-label randomised controlled phase 3 trial. *Lancet Oncol* 2017;18:1624–1636.
- 10 Chow PK, et al: Phase III multi-centre open-label randomized controlled trial of selective internal radiation therapy (SIRT) versus sorafenib in locally advanced hepatocellular carcinoma: The SIRveNIB study. *J Clin Oncol* 2017;35(suppl):A4002.
- 11 Kudo M, Finn RS, Qin S, Han KH, Ikeda K, Piscaglia F, Baron A, et al: Lenvatinib versus sorafenib in first-line treatment of patients with unresectable hepatocellular carcinoma: a randomised phase 3 non-inferiority trial. *Lancet* 2018, Epub ahead of print.
- 12 Kudo M, Ueshima K, Torimura T, Tanabe N, Ikeda M, Aikata H, Izumi N, et al: Randomized, open label, multi-center, phase II trial comparing transcatheter arterial chemoembolization (TACE) plus sorafenib with TACE alone in patients with hepatocellular carcinoma (HCC): TACTICS trial (abstract). *J Clin Oncol* 2018;36(suppl 4S):206.
- 13 Tohyama O, Matsui J, Kodama K, Hata-Sugi N, Kimura T, Okamoto K, Minoshima Y, et al: Antitumor activity of lenvatinib (e7080): an angiogenesis inhibitor that targets multiple receptor tyrosine kinases in preclinical human thyroid cancer models. *J Thyroid Res* 2014;2014:638747.
- 14 Yamamoto Y, Matsui J, Matsushima T, Obaishi H, Miyazaki K, Nakamura K, Tohyama O, et al: Lenvatinib, an angiogenesis inhibitor targeting VEGFR/FGFR, shows broad antitumor activity in human tumor xenograft models associated with microvessel density and pericyte coverage. *Vasc Cell* 2014;6:18.
- 15 Gao L, Wang X, Tang Y, Huang S, Hu CA, Teng Y: FGF19/FGFR4 signaling contributes to the resistance of hepatocellular carcinoma to sorafenib. *J Exp Clin Cancer Res* 2017;36:8.
- 16 Sawey ET, Chanrion M, Cai C, Wu G, Zhang J, Zender L, Zhao A, et al: Identification of a therapeutic strategy targeting amplified FGF19 in liver cancer by oncogenomic screening. *Cancer Cell* 2011;19:347–358.
- 17 Miura S, Mitsuhashi N, Shimizu H, Kimura F, Yoshidome H, Otsuka M, Kato A, et al: Fibroblast growth factor 19 expression correlates with tumor progression and poorer prognosis of hepatocellular carcinoma. *BMC Cancer* 2012;12:56.
- 18 Chen Z, Xie B, Zhu Q, Xia Q, Jiang S, Cao R, Shi L, et al: FGFR4 and TGF- β 1 expression in hepatocellular carcinoma: correlation with clinicopathological features and prognosis. *Int J Med Sci* 2013;10:1868–1875.
- 19 Wang K, Lim HY, Shi S, Lee J, Deng S, Xie T, Zhu Z, et al: Genomic landscape of copy number aberrations enables the identification of oncogenic drivers in hepatocellular carcinoma. *Hepatology* 2013;58:706–717.
- 20 Ikeda M, Okusaka T, Mitsunaga S, Ueno H, Tamai T, Suzuki T, Hayato S, et al: Safety and pharmacokinetics of lenvatinib in patients with advanced hepatocellular carcinoma. *Clin Cancer Res* 2016;22:1385–1394.

Kudo: Lenvatinib May Drastically Change the Treatment Landscape of Hepatocellular Carcinoma

- 21 Ikeda K, Kudo M, Kawazoe S, Osaki Y, Ikeda M, Okusaka T, Tamai T, et al: Phase 2 study of lenvatinib in patients with advanced hepatocellular carcinoma. *J Gastroenterol* 2017;52:512–519.
- 22 Cheng AL, Finn RS, Qin S, Han KH, Ikeda K, Piscaglia F, Baron A, et al: Phase 3 trial of lenvatinib (LEN) vs sorafenib (SOR) in first-line treatment of patients (PTS) with unresectable hepatocellular carcinoma (UHCC). ILCA Annual Conference, 2017, Abstract O-001.
- 23 Kudo M, Lencioni R, Marrero JA, Venook AP, Bronowicki JP, Chen XP, Dagher L, et al: Regional differences in sorafenib-treated patients with hepatocellular carcinoma: GIDEON observational study. *Liver Int* 2016;36:1196–1205.
- 24 Crocenzi TS, El-Khoueiry AB, Yau T, Melero I, Sangro B, Kudo M, Hsu C, et al: Nivolumab (nivo) in sorafenib (sor)-naive and -experienced pts with advanced hepatocellular carcinoma (HCC): CheckMate 040 study. *J Clin Oncol* 2017;35(suppl):A4013.
- 25 Bruix J, Qin S, Merle P, Granito A, Huang YH, Bodoky G, Pracht M, et al: Regorafenib for patients with hepatocellular carcinoma who progressed on sorafenib treatment (RESORCE): a randomised, double-blind, placebo-controlled, phase 3 trial. *Lancet* 2017;389:56–66.
- 26 Wainberg ZA, Segal NH, Jaeger D, Lee KH, Marshall J, Antonia SJ, Butler M, et al: Safety and clinical activity of durvalumab monotherapy in patients with hepatocellular carcinoma (HCC). *J Clin Oncol* 2017;35(suppl):A4071.
- 27 Kelley RK, Abou-Alfa GK, Bendell JC, Kim TY, Borad MJ, Yong WP, Morse M, et al: Phase I/II study of durvalumab and tremelimumab in patients with unresectable hepatocellular carcinoma (HCC): phase I safety and efficacy analyses. *J Clin Oncol* 2017;35(suppl):A4073.
- 28 Jackson R, Psarelli EE, Berhane S, Khan H, Johnson P: Impact of viral status on survival in patients receiving sorafenib for advanced hepatocellular cancer: a meta-analysis of randomized phase III trials. *J Clin Oncol* 2017;35:622–628.
- 29 Nagahama H, Okada S, Okusaka T, Ishii H, Ikeda M, Nakasuka H, Yoshimori M: Predictive factors for tumor response to systemic chemotherapy in patients with hepatocellular carcinoma. *Jpn J Clin Oncol* 1997;27:321–324.
- 30 Chung GE, Lee JH, Kim HY, Hwang SY, Kim JS, Chung JW, Yoon JH, et al: Transarterial chemoembolization can be safely performed in patients with hepatocellular carcinoma invading the main portal vein and may improve the overall survival. *Radiology* 2011;258:627–634.
- 31 Kudo M: Molecular targeted therapy for hepatocellular carcinoma: where are we now? *Liver Cancer* 2015;4:1–VII.
- 32 Kudo M: Why does every hepatocellular carcinoma clinical trial using molecular targeted agents fail? *Liver Cancer* 2012;1:59–60.
- 33 Llovet JM, Hernandez-Gea V: Hepatocellular carcinoma: reasons for phase III failure and novel perspectives on trial design. *Clin Cancer Res* 2014;20:2072–2079.
- 34 Llovet JM, Zucman-Rossi J, Pikarsky E, Sangro B, Schwartz M, Sherman M, Gores G: Hepatocellular carcinoma. *Nat Rev Dis Primers* 2016;2:16018.
- 35 Ikeda M, Kudo M, Ikeda K, Izumi N, Okusaka T, Okita K, Tamai T, et al: Subanalysis of Japanese patients in a phase 3 study of lenvatinib vs sorafenib for unresectable hepatocellular carcinoma. JSMO Annual Meeting, 2017, Abstract PS-2.
- 36 Tamai T, Hayato S, Hojo S, Suzuki T, Okusaka T, Ikeda K, Kumada H: Dose finding of lenvatinib in subjects with advanced hepatocellular carcinoma based on population pharmacokinetic and exposure-response analyses. *J Clin Pharmacol* 2017;57:1138–1147.
- 37 Kudo M: Lenvatinib in advanced hepatocellular carcinoma. *Liver Cancer* 2017;6:253–263.
- 38 Finn RS, Kudo M, Cheng AL, Wyrwicz L, Ngan R, Blanc JF, Baron AD, et al: Analysis of serum biomarkers (BM) in patients (pts) from a phase 3 study of lenvatinib (LEN) vs sorafenib (SOR) as first-line treatment for unresectable hepatocellular carcinoma (uHCC). *Ann Oncol* 2017;28(suppl 5):LBA30.
- 39 Wohrle S, Henninger C, Bonny O, Thuery A, Beluch N, Hynes NE, Guagnano V, et al: Pharmacological inhibition of fibroblast growth factor (FGF) receptor signaling ameliorates FGF23-mediated hypophosphatemic rickets. *J Bone Miner Res* 2013;28:899–911.
- 40 Kim KB, Chesney J, Robinson D, Gardner H, Shi MM, Kirkwood JM: Phase I/II and pharmacodynamic study of dovitinib (TKI258), an inhibitor of fibroblast growth factor receptors and VEGF receptors, in patients with advanced melanoma. *Clin Cancer Res* 2011;17:7451–7461.
- 41 Bergers G, Hanahan D: Modes of resistance to anti-angiogenic therapy. *Nat Rev Cancer* 2008;8:592–603.
- 42 Gerald D, Chintharlapalli S, Augustin HG, Benjamin LE: Angiopoietin-2: an attractive target for improved anti-angiogenic tumor therapy. *Cancer Res* 2013;73:1649–1657.
- 43 Rigamonti N, Kadioglu E, Keklikoglou I, Wyser Rmili C, Leow CC, De Palma M: Role of angiopoietin-2 in adaptive tumor resistance to VEGF signaling blockade. *Cell Rep* 2014;8:696–706.
- 44 Lencioni R, Montal R, Torres F, Park JW, Decaens T, Raoul JL, Kudo M, et al: Objective response by mRECIST as a predictor and potential surrogate end-point of overall survival in advanced HCC. *J Hepatol* 2017;66:1166–1172.
- 45 Arizumi T, Ueshima K, Takeda H, Osaki Y, Takita M, Inoue T, Kitai S, et al: Comparison of systems for assessment of post-therapeutic response to sorafenib for hepatocellular carcinoma. *J Gastroenterol* 2014;49:1578–1587.
- 46 Meyer T, Palmer DH, Cheng AL, Hocke J, Loembe AB, Yen CJ: mRECIST to predict survival in advanced hepatocellular carcinoma: Analysis of two randomised phase II trials comparing nintedanib vs sorafenib. *Liver Int* 2017;37:1047–1055.

- 47 Takada J, Hidaka H, Nakazawa T, Kondo M, Numata K, Tanaka K, Matsunaga K, et al: Modified response evaluation criteria in solid tumors is superior to response evaluation criteria in solid tumors for assessment of responses to sorafenib in patients with advanced hepatocellular carcinoma. *BMC Res Notes* 2015;8:609.
- 48 Llovet JM, Real MI, Montana X, Planas R, Coll S, Aponte J, Ayuso C, et al: Arterial embolisation or chemoembolisation versus symptomatic treatment in patients with unresectable hepatocellular carcinoma: a randomised controlled trial. *Lancet* 2002;359:1734–1739.
- 49 Kudo M, Han G, Finn RS, Poon RT, Blanc JF, Yan L, Yang J, et al: Brivanib as adjuvant therapy to transarterial chemoembolization in patients with hepatocellular carcinoma: a randomized phase III trial. *Hepatology* 2014;60:1697–1707.
- 50 Lencioni R, Llovet JM, Han G, Tak WY, Yang J, Guglielmi A, Paik SW, et al: Sorafenib or placebo plus TACE with doxorubicin-eluting beads for intermediate stage HCC: the SPACE trial. *J Hepatol* 2016;64:1090–1098.
- 51 Meyer T, Fox R, Ma YT, Ross PJ, James MW, Sturgess R, Stubbs C, et al: Sorafenib in combination with transarterial chemoembolisation in patients with unresectable hepatocellular carcinoma (TACE 2): a randomised placebo-controlled, double-blind, phase 3 trial. *Lancet Gastroenterol Hepatol* 2017;2:565–575.
- 52 Kudo M: Regorafenib as second-line systemic therapy may change the treatment strategy and management paradigm for hepatocellular carcinoma. *Liver Cancer* 2016;5:235–244.
- 53 Abou-Alfa GK, Meyer T, Cheng AL, Anthony B, Khoueiry EI, Rimassa L, et al: Cabozantinib (C) versus placebo (P) in patients (pts) with advanced hepatocellular carcinoma (HCC) who have received prior sorafenib: results from the randomized phase III CELESTIAL trial. *J Clin Oncol* 2018;36(suppl 4S):A207.
- 54 Kudo M, Arizumi T, Ueshima K, Sakurai T, Kitano M, Nishida N: Subclassification of BCLC B stage hepatocellular carcinoma and treatment strategies: proposal of modified Bolondi's subclassification (Kinki criteria). *Dig Dis* 2015;33:751–758.
- 55 Finn RS, Chan SL, Zhu AX, Knox JJ, Cheng AL, Siegel AB, et al: KEYNOTE-240: randomized phase III study of pembrolizumab versus best supportive care for second-line advanced hepatocellular carcinoma (abstract). *J Clin Oncol* 2017;35(suppl 4S):TPS503.
- 56 Sangro B, Park JW, Dela Cruz C, Anderson J, Lang L, Neely J, Shaw JW, et al: A randomized, multicenter, phase 3 study of nivolumab vs sorafenib as first-line treatment in patients (pts) with advanced hepatocellular carcinoma (HCC): CheckMate-459 (abstract). *J Clin Oncol* 2016;34(suppl):TPS4147.
- 57 El-Khoueiry AB, Sangro B, Yau T, Crocenzi TS, Kudo M, Hsu C, Kim TY, et al: Nivolumab in patients with advanced hepatocellular carcinoma (CheckMate 040): an open-label, non-comparative, phase 1/2 dose escalation and expansion trial. *Lancet* 2017;389:2492–2502.
- 58 Taylor M, Dutcus C, Schmidt E, Bagulho T, Li D, Shumaker R, Rasco D: A phase 1b trial of lenvatinib (LEN) plus pembrolizumab (PEM) in patients with selected solid tumors. *Ann Oncol* 2016;27(suppl 6):776PD.
- 59 Makker V, Rasco DW, Dutcus CE: A phase Ib/II trial of lenvatinib (LEN) plus pembrolizumab (Pembro) in patients (Pts) with endometrial carcinoma. *J Clin Oncol* 2017;35(suppl):A5598.
- 60 Lee C-H, Makker V, Rasco D, Taylor M, Dutcus C, Shumaker R, Schmidt EV, et al: A phase 1b/2 trial of lenvatinib plus pembrolizumab in patients with renal cell carcinoma. *Ann Oncol* 2017;28(suppl 5):8470.

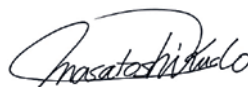
Editorial

Combination Cancer Immunotherapy in Hepatocellular Carcinoma

Masatoshi Kudo

Department of Gastroenterology and Hepatology, Kindai University Faculty of Medicine,
Osaka-Sayama, Japan

Prof. M. Kudo

Editor *Liver Cancer***Introduction**

Combination cancer immunotherapy is becoming a major topic in cancer therapy research including in hepatocellular carcinoma (HCC). Well-known combinations include two types of immune checkpoint inhibitors (anti-PD-1/PD-L1 and anti-CTLA-4 antibodies), anti-PD-1/PD-L1 antibody with a molecular targeted agent, and anti-PD-1/PD-L1 or -CTLA-4 antibody with existing locoregional therapies (Fig. 1).

Immunotherapy for the treatment of various types of cancer has advanced rapidly in recent years. The Federal Drug Administration (FDA) designated nivolumab, an anti-PD-1 antibody, as a breakthrough therapy in 2014, and pembrolizumab, another anti-PD-1 antibody, also received this designation. Nivolumab was approved as a highly effective agent for the treatment of certain malignancies, including malignant melanoma, non-small cell lung cancer, kidney cancer, Hodgkin lymphoma, head and neck cancer, and gastric cancer [1–6]. Promising clinical trials evaluating this agent for the treatment of many other types of cancer are currently ongoing. HCC is more heterogeneous than other types of solid cancer and hematological malignancies, and is not associated with a specific driver mutation. HCC cannot be treated with agents that impair liver function, and thus requires different therapeutic strategies than those used for other cancers. Despite this limitation, the CheckMate 040 study revealed that nivolumab is a promising therapy for HCC [7]. Many pharmaceutical companies started phase III or earlier-phase trials of anti-PD-1/PD-L1 antibodies for HCC treatment (Table 1). In addition, the FDA approved nivolumab for second-line therapy after sorafenib in September 2017.

Masatoshi Kudo, MD, PhD
Department of Gastroenterology and Hepatology
Kindai University Faculty of Medicine
377-2 Ohno-Higashi, Osaka-Sayama 589-8511 (Japan)
E-Mail m-kudo@med.kindai.ac.jp

Table 1. Immune checkpoint inhibitors in hepatocellular carcinoma clinical trials

Target cell	Target molecule	Development code	Drug name	Commercial name	Antibody	Company
T lymphocyte	PD-1	BMS-36558 ONO-4538	Nivolumab	Optivo	Fully human IgG4 antibody	ONO/BMS
	PD-1	MK-4375	Pembrolizumab	Keytruda	Humanized IgG4 antibody	Merck
Tumor cell	PD-L1	MPDL3280A	Atezolizumab	Tecentriq	Fully humanized IgG1 antibody	Roche
	PD-L1	MEDI4736	Durvalumab	Imfinzi	Humanized IgG1 antibody	AstraZeneca
	PD-L1	MSB-0010718C	Avelumab	Bavencio	Humanized IgG1 antibody	Merck Serono
T lymphocyte	CTLA-4	BMS-734016	Ipilimumab	Yervoy	Fully humanized IgG1 antibody	BMS Medarex
	CTLA-4	MEDI1123	Tremelimumab	Not yet approved	Fully humanized IgG2 antibody	AstraZeneca MedImmune

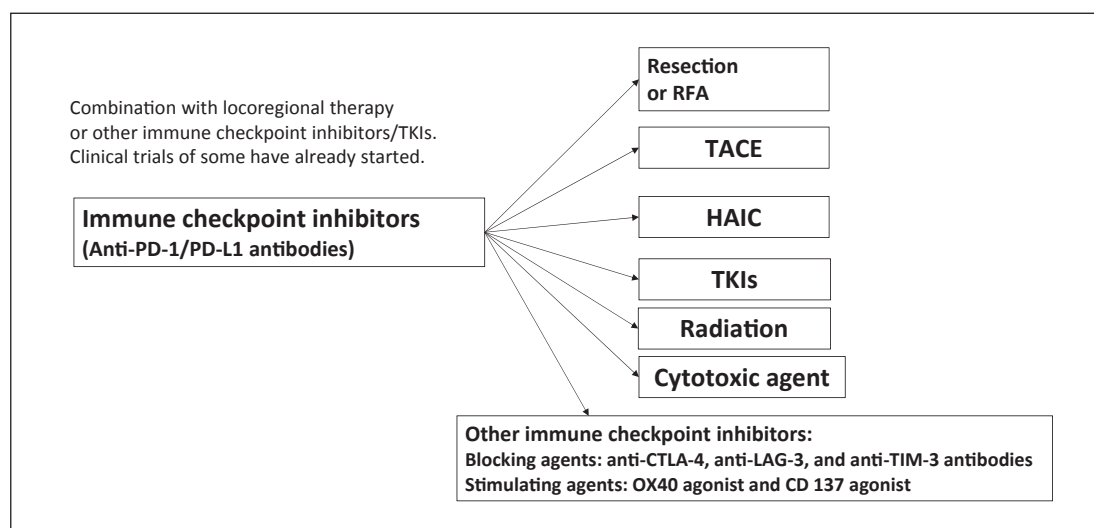


Fig. 1. Treatment strategy using immune checkpoint inhibitors. Future direction: combination therapy. RFA, radiofrequency ablation; TACE, transarterial chemoembolization; HAIC, hepatic arterial infusion chemotherapy; TKIs, tyrosine kinase inhibitors.

Combination of Immune Checkpoint Inhibitors

Anti-PD-1/PD-L1 and anti-CTLA-4 antibodies are expected to be promising agents in HCC immunotherapy, and clinical trials evaluating the simultaneous blockade of multiple immune checkpoints are currently ongoing (Fig. 1; Table 2). The high efficacy of combination therapy was demonstrated in malignant melanoma [6], and a trial of the same combination for the treatment of HCC is currently ongoing [8]. Inhibition of the PD-1/PD-L1 pathway will not activate tumor immunity as expected if the required CD8⁺ T cells are not present in the cancer tissue. However, simultaneous inhibition of the B7-CTLA-4 pathway by an anti-CTLA-4 antibody can increase the number of activated CD8⁺ T cells in lymph nodes, followed by an

Table 2. Immune checkpoint inhibitors: ongoing trials

Drug	Trial name	ClinicalTrials.gov No.	Company	Phase	Subjects, n	Line of therapy	Design	Endpoint	Status
<i>Nivolumab</i>									
Nivolumab (PD-1 Ab)/ ipilimumab (CTLA-4 Ab)	CheckMate 040	NCT01658878	BMS/ONO	I/II	42	1L/2L	Cohort 1: dose escalation	DLT/MTD	Completed
	CheckMate 040	NCT01658878	BMS/ONO	I/II	214	1L/2L	Cohort 2: dose expansion	ORR	Completed
	CheckMate 040	NCT01658878	BMS/ONO	I/II	200	1L	Cohort 3: nivolumab vs. sorafenib	ORR	Completed
	CheckMate 040	NCT01658878	BMS/ONO	I/II	120	2L	Cohort 4: nivolumab + ipilimumab	Safety/ tolerability	Completed
	CheckMate 040	NCT01658878	BMS/ONO	I/II	-	1L	Cohort 5: nivolumab (Child-Pugh B)	ORR	Completed
	CheckMate 040	NCT01658878	BMS/ONO	I/II	-	1L	Cohort 6: nivolumab + cabozantinib	ORR	Recruiting
	CheckMate 040	NCT01658878	BMS/ONO	I/II	-	1L	Cohort 7: nivolumab + ipilimumab + cabozantinib	ORR	Recruiting
	CheckMate 459	NCT02576509	ONO	III	726	1L	Nivolumab vs. sorafenib	TTP/OS	Completed
<i>Pembrolizumab</i>									
Pembrolizumab (PD-1 Ab)	KEYNOTE-224	NCT02702414	MSD	II	100	2L	Pembrolizumab (1 arm)	ORR	Completed
Pembrolizumab (PD-1 Ab)	KETNOTE-240	NCT02702401	MSD	III	408	2L	Pembrolizumab vs. placebo	PFS/OS	Recruiting
<i>Durvalumab</i>									
Durvalumab (PD-L1 Ab)/ tremelimumab (CTLA-4 Ab)	-	NCT02519348	AstraZeneca	II	144	1L/2L	Durvalumab (arm A) tremelimumab (arm B) durvalumab + tremelimumab (arm C)	Safety/ tolerability	Recruiting
Durvalumab + tremelimumab	-	NCT028211754	AstraZeneca	I/II	-	TACE/RFA	1 arm	Safety/ tolerability	Recruiting
Durvalumab ± tremelimumab vs. Sorafenib	-	NCT03298451	AstraZeneca	III	-	1L	Durvalumab ± tremelimumab vs. sorafenib	OS	Recruiting
<i>MSB0011359C</i>									
(PD-L1 Ab + TGFB Trap)	-	NCT02699515	Merk Serono	I	-	1L	1 arm	Safety/ tolerability	Recruiting
<i>PDR001 + INC280</i>									
PDR001 + INC280	-	NCT02795429	Novartis	I/II	-	1L/2L	PDR001 + INC280	Safety/OS	Active accrual
LY3300054 + LY3321367	-	NCT03099109	Eli Lilly	I/II	-	1L/2L	LY3300054 + LY3321367	Safety/OS	Active accrual

TACE, transarterial chemoembolization; RFA, radiofrequency ablation; DLT, dose-limiting toxicity; MTD, median survival time; ORR, overall response rate; TTP, time to progression; OS, overall survival.

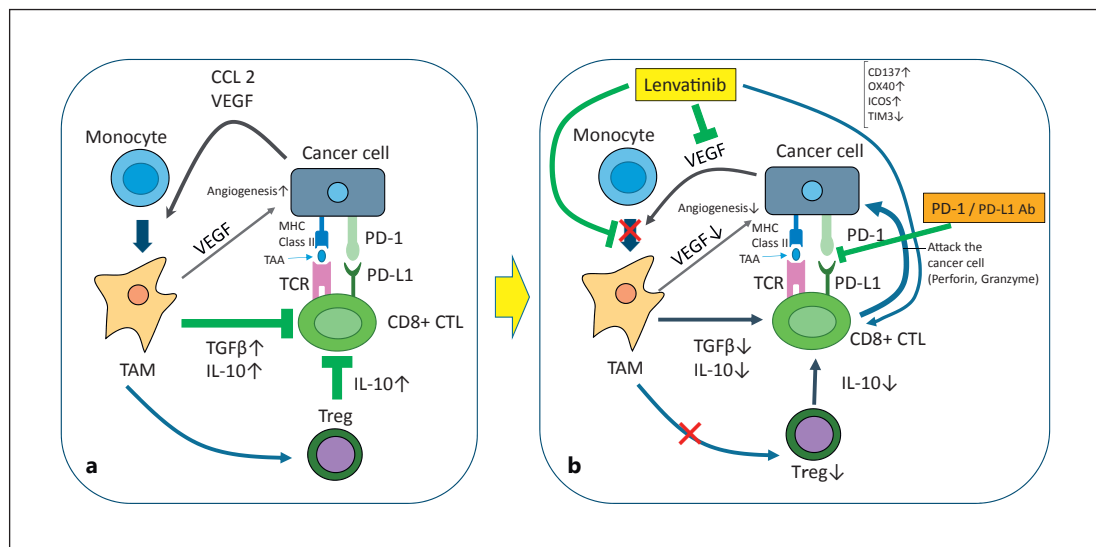


Fig. 2. Mechanism of synergistic effects of lenvatinib and anti-PD-1/PD-L1 antibodies. **a** Immunosuppressive microenvironment + PD-1/PD-L1 immunosuppression. **b** Lenvatinib + anti-PD-1/PD-L1 antibodies synergistically induce PD-1/PD-L1 blockade and inhibit the immunosuppressive microenvironment.

increase in the number of activated CD8⁺ T cells infiltrating into tumor tissues, thereby enhancing the antitumor effects. In addition, anti-CTLA-4 antibody therapy may be effective against regulatory T cells in the cancer immunosuppressive microenvironment.

This is the rationale for the use of combination therapy with an anti-PD-1/PD-L1 antibody and an anti-CTLA-4 antibody, and several trials evaluating these combinations for the treatment of HCC are currently ongoing (Table 2). The CheckMate 040 study tested the efficacy of nivolumab in combination with ipilimumab at varying doses and dose intervals. Another trial comparing the efficacy and safety of combination therapy with durvalumab (anti-PD-L1 antibody) plus tremelimumab (anti-CTLA-4 antibody) to those of monotherapy is currently ongoing. The results of phase I of this phase I/II study were reported at the ASCO 2017 with favorable outcomes (ORR of 25.0% in 40 cases) [9]; the eagerly awaited phase II is expected to be completed in April 2018.

Combination of Immune Checkpoint Inhibitors and Molecular Targeted Therapy

The therapeutic outcomes of nivolumab plus ipilimumab are superior to those of monotherapy in melanoma [6, 10]. Therapy involving an immune checkpoint inhibitor plus a molecular targeted agent was suggested as a promising strategy in recent years. In HCC, interstitial cells (Kupffer cells, dendritic cells, liver endothelial cells, and liver stellate cells) and immunosuppressive cytokines (e.g., IL-10 or TGF-β) may contribute to the immunosuppressive environment, and the PD-1/PD-L1 pathway plays an important role in the development of the immunosuppressive microenvironment in HCC. Combining a molecular targeted agent and an immune checkpoint inhibitor is expected to improve this immunosuppressive microenvironment [11] (Fig. 2).

Table 3 shows the currently ongoing trials evaluating combination therapy involving immune checkpoint inhibition with molecular targeted therapy. A trial evaluating the combination of pembrolizumab and lenvatinib for the treatment of HCC was started in Japan and

Table 3. Immune checkpoint inhibitors in combination with tyrosine kinase inhibitors in hepatocellular carcinoma

Phase	Target	Agent	Company	Trial #
1–2	PD-1 + TGF- β receptor I	Nivolumab + galunisertib (LY2157299)	Eli Lilly	NCT02423343
1	PD-L1 + VEGFR-2	Ramucirumab + durvalumab (MEDI4736)	Eli Lilly	NCT02572687
1	PD-1 + multikinase	Pembrolizumab + lenvatinib	Eisai	NCT03006926
1	PD-1 + multikinase	Pembrolizumab + nintedanib	Gustave Roussy	NCT02856425
1	PD-1 + multikinase	PDR001 + sorafenib	Novartis	NCT02988440
1–2	PD-1 + c-Met	PDR001 + capmatinib (INC280)	Novartis	NCT02795429
1–2	PD-1 + CTLA-4 + MET/VEGFR2	Nivolumab + ipilimumab + cabozantinib	BMS	NCT01658878
1	PD-1 + multikinase	Nivolumab + lenvatinib	Ono	
1–2	PD-L1 + multikinase	Avelumab + axitinib	Pfizer	NCT03289533
1–2	PD-L1 + multikinase	Atezolizumab + bevacizumab	Roche	

then will be expanded to the rest of the world. High response rates (50–70%) and the long-lasting durable response of this combination therapy in other types of solid cancer (e.g., kidney cancer and endometrial cancer) were presented at the ESMO 2016 and ASCO 2017. Therefore, similar high response rates and long-lasting durable responses are highly expected in HCC as well.

The mechanism underlying the synergistic effect of an immune checkpoint inhibitor plus a molecular targeted agent, unlike that of the combination of two immune checkpoint inhibitors, needs to be thoroughly clarified. Regarding the mechanism of action of pembrolizumab-levatinib combination therapy [12], a preclinical study including in vitro and in vivo studies showed that suppression of tumor-associated macrophages, regulatory T cells, and other constituents of the tumor-suppressive microenvironment resulted in decreases in TGF- β and IL-10, the downregulation of PD-1 and Tim3, and the upregulation of ICOS and OX40, thereby inducing tumor immunity through IL-12 [13] (Fig. 2). It is anticipated that similar future studies on HCC will identify the best combination between a specific immune checkpoint inhibitor and molecular targeted agent. In addition to pembrolizumab-levatinib combination therapy (Fig. 3), many similar combination therapies for HCC are currently being evaluated in early-phase clinical trials (Table 3).

Combination of Immune Checkpoint Inhibitors with an Existing Locoregional Therapy

A different approach, namely, combining an immune checkpoint inhibitor with an existing locoregional therapy for HCC, is currently under evaluation. Transcatheter arterial chemoembolization (TACE), radiofrequency ablation (RFA), or radiation therapy is expected to enhance the effects of immunotherapy by inducing local inflammation. This would lead to the release of neoantigens that activate antigen presentation and the relevant immune system activation. These locoregional therapies are particularly beneficial when the levels of cancer antigens are negligible because of poor antigen release. The results of combination therapy with an anti-CTLA-4 antibody and locoregional therapy in advanced HCC were recently published [14]. The NCT01853618 study evaluated the efficacy of adjuvant therapy with tremelimumab (anti-CTLA-4 antibody) after RFA or TACE in several, but not all, HCC nodules, with favorable outcomes, including a partial response rate of 26%, time to tumor progression of 7.4 months, and overall survival of 12.3 months. Increases in CD3⁺ and CD8⁺ cells in untreated nodules were clearly confirmed and attributed to the abscopal effect.

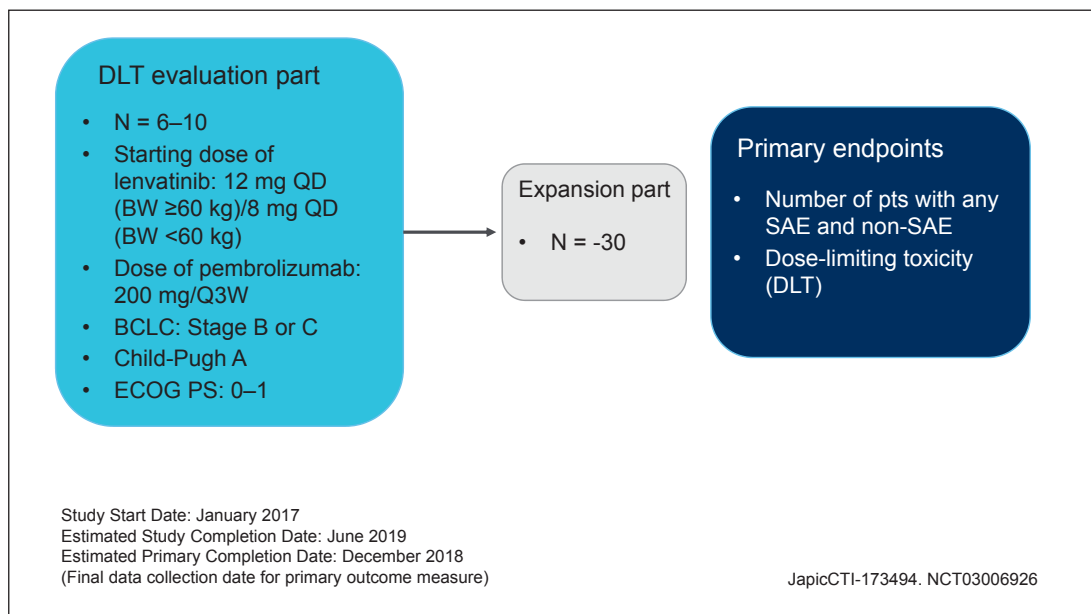


Fig. 3. Phase Ib study of lenvatinib plus pembrolizumab in hepatocellular carcinoma.

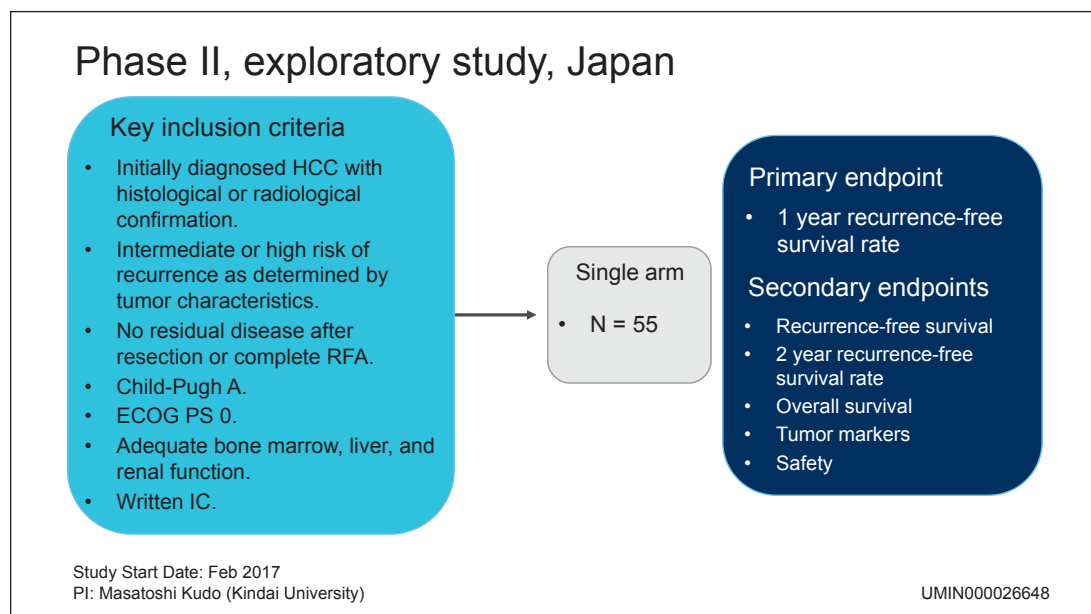


Fig. 4. Adjuvant treatment with anti-PD-1 antibody to prevent recurrence after curative treatment of HCC. HCC, hepatocellular carcinoma; RFA, radiofrequency ablation; ECOG PS, Eastern Cooperative Oncology Group Performance Status; IC, informed consent.

Immune checkpoint inhibitors (antibodies to PD-1, PD-L1, and CTLA-4) are potentially beneficial in all forms of neoadjuvant therapy, adjuvant therapy after resection or ablation, and in combination with TACE, cytotoxic chemotherapy, or radiotherapy (Fig. 1).

HCC recurrence rates after curative therapy (resection or ablation) are particularly high, and its management remains an unmet need. This is mainly because of the presence of

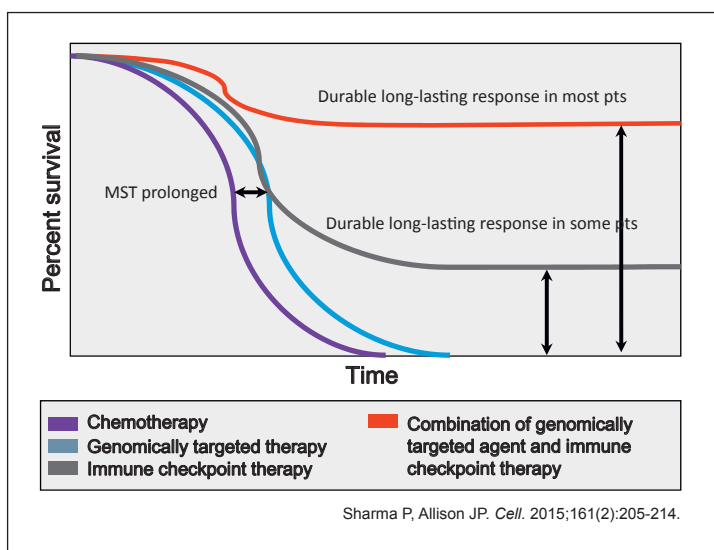


Fig. 5. Improved overall survival as a result of combination therapy: very near future. MST, median survival time.

extremely small microsatellite metastatic lesions that are undetectable by imaging even at the time of resection or ablation. To address this issue, various agents (e.g., IFN, peretinoin, vitamin K, and sorafenib) were tested for their efficacy as an adjuvant therapy in clinical trials, although all showed negative results [15–18].

Theoretically, microsatellite lesions and intrahepatic metastases may be suppressed by administration of anti-PD-1 antibody after recruitment of cytotoxic T lymphocytes to the microsatellite lesions upon release of tumor antigens by TACE or RFA [19]. Mizukoshi et al. [20] observed a significant increase in tumor-specific T cells, which is indicative of post-treatment tumor antigen release, after RFA in 62% of patients, and a significant correlation between tumor-specific T cells and recurrence-free survival.

A clinical trial of nivolumab in the adjuvant setting after curative treatment was started in February 2017 in Japan (Fig. 4). The combination strategy of an immune checkpoint inhibitor in the adjuvant setting with curative therapy (resection or RFA) is anticipated to prevent HCC recurrence effectively.

Conclusion

Padmanee Sharma and James P. Allison predicted the possibility of long-term survival and real cure in patients who responded to combination treatment with immune checkpoint inhibitors and molecular targeted agents because its high efficacy can lead to “cure in a real sense” [21, 22] (Fig. 5). Indeed, immune checkpoint inhibitors will extend the overall survival of HCC patients, and, further, combination therapy with molecular targeted agents may result in real cure, which might lead to a paradigm shift in the treatment of HCC.

Emerging therapeutic strategies involving immune checkpoint inhibition combined with other treatment modalities will definitely change the future landscape of HCC treatment.

References

- 1 Wolchok JD, Kluger H, Callahan MK, Postow MA, Rizvi NA, Lesokhin AM, Segal NH, et al: Nivolumab plus ipilimumab in advanced melanoma. *N Engl J Med* 2013;369:122–133.
- 2 Ansell SM, Lesokhin AM, Borrello I, Halwani A, Scott EC, Gutierrez M, Schuster SJ, et al: PD-1 blockade with nivolumab in relapsed or refractory Hodgkin's lymphoma. *N Engl J Med* 2015;372:311–319.
- 3 Robert C, Schachter J, Long GV, Arance A, Grob JJ, Mortier L, Daud A, et al: Pembrolizumab versus ipilimumab in advanced melanoma. *N Engl J Med* 2015;372:2521–2532.
- 4 Garon EB, Rizvi NA, Hui R, Leigh N, Balmanoukian AS, Eder JP, Patnaik A, et al: Pembrolizumab for the treatment of non-small-cell lung cancer. *N Engl J Med* 2015;372:2018–2028.
- 5 Brahmer J, Reckamp KL, Baas P, Crino L, Eberhardt WE, Poddubskeya E, Antonia S, et al: Nivolumab versus docetaxel in advanced squamous-cell non-small-cell lung cancer. *N Engl J Med* 2015;373:123–135.
- 6 Larkin J, Chiarion-Sileni V, Gonzalez R, Grob JJ, Cowey CL, Lao CD, Schadendorf D, et al: Combined nivolumab and ipilimumab or monotherapy in untreated melanoma. *N Engl J Med* 2015;373:23–34.
- 7 El-Khoueiry AB, Sangro B, Yau T, Crocenzi TS, Kudo M, Hsu C, Kim TY, et al: Nivolumab in patients with advanced hepatocellular carcinoma (CheckMate 040): an open-label, non-comparative, phase 1/2 dose escalation and expansion trial. *Lancet* 2017;389:2492–2502.
- 8 Kudo M: Molecular targeted agents for hepatocellular carcinoma: current status and future perspectives. *Liver Cancer* 2017;6:101–112.
- 9 Kelley RK, Abou-Alfa GK, Bendell JC, Kim TY, Borad MJ, Yong WP, Morse M, et al: Phase I/II study of durvalumab and tremelimumab in patients with unresectable hepatocellular carcinoma (HCC): phase I safety and efficacy analyses. *J Clin Oncol* 2017;35(suppl);abstract 4073.
- 10 Postow MA, Chesney J, Pavlick AC, Robert C, Grossmann K, McDermott D, Linette GP, et al: Nivolumab and ipilimumab versus ipilimumab in untreated melanoma. *N Engl J Med* 2015;372:2006–2017.
- 11 Tiegs G, Lohse AW: Immune tolerance: what is unique about the liver. *J Autoimmun* 2010;34:1–6.
- 12 Kudo M, Finn RS, Qin S, Han KH, Ikeda K, Piscaglia F, Baron A, et al: A randomised phase 3 trial of lenvatinib vs sorafenib in first-line treatment of patients with unresectable hepatocellular carcinoma. *Lancet* 2017, in press.
- 13 Kato T, Bao X, Macgrath S, Tabata K, Hori Y, Tachino S, Matijevici M, et al: Lenvatinib mesilate (LEN) enhanced antitumor activity of a PD-1 blockade agent by potentiating Th1 immune response. *Ann Oncol* 2016;27:1–14.
- 14 Duffy AG, Ulahannan SV, Makorova-Rusher O, Rahma O, Wedemeyer H, Pratt D, Davis JL, et al: Tremelimumab in combination with ablation in patients with advanced hepatocellular carcinoma. *J Hepatol* 2017;66:545–551.
- 15 Yoshida H, Shiratori Y, Kudo M, Shiina S, Mizuta T, Kojiro M, Yamamoto K, et al: Effect of vitamin K2 on the recurrence of hepatocellular carcinoma. *Hepatology* 2011;54:532–540.
- 16 Bruix J, Takayama T, Mazzaferro V, Chau GY, Yang J, Kudo M, Cai J, et al: Adjuvant sorafenib for hepatocellular carcinoma after resection or ablation (STORM): a phase 3, randomised, double-blind, placebo-controlled trial. *Lancet Oncol* 2015;16:1344–1354.
- 17 Mazzaferro V, Romito R, Schiavo M, Mariani L, Camerini T, Bhoori S, Capussotti L, et al: Prevention of hepatocellular carcinoma recurrence with alpha-interferon after liver resection in HCV cirrhosis. *Hepatology* 2006;44:1543–1554.
- 18 Okita K, Izumi N, Matsui O, Tanaka K, Kaneko S, Moriwaki H, Ikeda K, et al: Peretinoin after curative therapy of hepatitis C-related hepatocellular carcinoma: a randomized double-blind placebo-controlled study. *J Gastroenterol* 2015;50:191–202.
- 19 Kudo M: Immune checkpoint inhibition in hepatocellular carcinoma: basics and ongoing clinical trials. *Oncology* 2017;92(suppl 1):50–62.
- 20 Mizukoshi E, Yamashita T, Arai K, Sunagozaka H, Ueda T, Arihara F, Kagaya T, et al: Enhancement of tumor-associated antigen-specific T cell responses by radiofrequency ablation of hepatocellular carcinoma. *Hepatology* 2013;57:1448–1457.
- 21 Sharma P, Allison JP: Immune checkpoint targeting in cancer therapy: toward combination strategies with curative potential. *Cell* 2015;161:205–214.
- 22 Sharma P, Allison JP: The future of immune checkpoint therapy. *Science* 2015;348:56–61.



Lenvatinib versus sorafenib in first-line treatment of patients with unresectable hepatocellular carcinoma: a randomised phase 3 non-inferiority trial

Masatoshi Kudo, Richard S Finn, Shukui Qin, Kwang-Hyub Han, Kenji Ikeda, Fabio Piscaglia, Ari Baron*, Joong-Won Park*, Guohong Han*, Jacek Jassem, Jean Frederic Blanc, Arndt Vogel, Dmitry Komov, T R Jeffrey Evans, Carlos Lopez, Corina Dutcus, Matthew Guo, Kenichi Saito, Silvija Kraljevic, Toshiyuki Tamai, Min Ren, Ann-Lii Cheng

Summary

Background In a phase 2 trial, lenvatinib, an inhibitor of VEGF receptors 1–3, FGF receptors 1–4, PDGF receptor α , RET, and KIT, showed activity in hepatocellular carcinoma. We aimed to compare overall survival in patients treated with lenvatinib versus sorafenib as a first-line treatment for unresectable hepatocellular carcinoma.

Methods This was an open-label, phase 3, multicentre, non-inferiority trial that recruited patients with unresectable hepatocellular carcinoma, who had not received treatment for advanced disease, at 154 sites in 20 countries throughout the Asia-Pacific, European, and North American regions. Patients were randomly assigned (1:1) via an interactive voice–web response system—with region; macroscopic portal vein invasion, extrahepatic spread, or both; Eastern Cooperative Oncology Group performance status; and bodyweight as stratification factors—to receive oral lenvatinib (12 mg/day for bodyweight ≥ 60 kg or 8 mg/day for bodyweight < 60 kg) or sorafenib 400 mg twice-daily in 28-day cycles. The primary endpoint was overall survival, measured from the date of randomisation until the date of death from any cause. The efficacy analysis followed the intention-to-treat principle, and only patients who received treatment were included in the safety analysis. The non-inferiority margin was set at 1·08. The trial is registered with ClinicalTrials.gov, number NCT01761266.

Findings Between March 1, 2013 and July 30, 2015, 1492 patients were recruited. 954 eligible patients were randomly assigned to lenvatinib (n=478) or sorafenib (n=476). Median survival time for lenvatinib of 13·6 months (95% CI 12·1–14·9) was non-inferior to sorafenib (12·3 months, 10·4–13·9; hazard ratio 0·92, 95% CI 0·79–1·06), meeting criteria for non-inferiority. The most common any-grade adverse events were hypertension (201 [42%]), diarrhoea (184 [39%]), decreased appetite (162 [34%]), and decreased weight (147 [31%]) for lenvatinib, and palmar-plantar erythrodysesthesia (249 [52%]), diarrhoea (220 [46%]), hypertension (144 [30%]), and decreased appetite (127 [27%]) for sorafenib.

Interpretation Lenvatinib was non-inferior to sorafenib in overall survival in untreated advanced hepatocellular carcinoma. The safety and tolerability profiles of lenvatinib were consistent with those previously observed.

Funding Eisai Inc.

Introduction

Hepatocellular carcinoma is the most common type of liver cancer, which is the third leading cause of cancer deaths worldwide, causing nearly 745 000 deaths each year.¹ The disease usually occurs in people with chronic liver disease, particularly cirrhosis, which limits the feasibility of surgical resection.^{2,3} Sorafenib, an oral multikinase inhibitor, is the only systemic therapy proven to extend overall survival when used as a first-line treatment, showing a median improvement of 2·8 months compared with placebo (10·7 months vs 7·9 months; hazard ratio [HR] 0·69; $p < 0\cdot001$), despite a low response rate of 2%.⁴ In patients from the Asia-Pacific region taking sorafenib, the median improvement in overall survival compared with placebo was 2·3 months (6·5 months vs 4·2 months; HR 0·68; $p = 0\cdot014$).⁵

Drug development for hepatocellular carcinoma in the past 10 years has been marked by four failed global

phase 3 trials (of sunitinib, brivanib, linifanib, and erlotinib plus sorafenib) that did not show non-inferiority^{6–8} or superiority⁹ to sorafenib in terms of overall survival in first-line treatment of hepatocellular carcinoma. No approved first-line systemic treatments are available for advanced unresectable hepatocellular carcinoma other than sorafenib. Only regorafenib and nivolumab are approved as second-line systemic treatments for patients who do not respond to sorafenib.¹⁰ Otherwise, best supportive care or participation in clinical trials is recommended in the second-line setting by treatment guidelines.¹¹ Therefore, because of the paucity of systemic treatment options for patients with advanced hepatocellular carcinoma, a need exists to develop new drugs for effective management of this disease.

Lenvatinib is an oral multikinase inhibitor that targets VEGF receptors 1–3, FGF receptors 1–4, PDGF receptor α , RET, and KIT.^{12–15} Lenvatinib monotherapy is approved for

Lancet 2018; 391: 1163–73

Published Online

February 9, 2018

[http://dx.doi.org/10.1016/S0140-6736\(18\)30207-1](http://dx.doi.org/10.1016/S0140-6736(18)30207-1)

See [Comment](#) page 1123

*Contributed equally

Department of Gastroenterology and Hepatology, Kindai University Faculty of Medicine, Osaka, Japan (Prof M Kudo MD); Toranomon Hospital, Tokyo, Japan (K Ikeda MD); University of Bologna, Bologna, Italy (Prof F Piscaglia MD); California Pacific Medical Center, San Francisco, CA, USA (A Baron MD); National Cancer Center Korea, Goyang-si, South Korea (Prof J-W Park MD); Xijing Hospital, Fourth Military Medical University, Xi'an, China (Prof G Han MD); Medical University of Gdansk, Gdansk, Poland (Prof J Jassem MD); University of Bordeaux, Bordeaux, France (Prof J F Blanc MD); Hannover Medical School, Hannover, Germany (Prof A Vogel MD); N N Blokhin Cancer Research Center, Moscow, Russia (Prof D Komov MD); University of Glasgow, Beatson West of Scotland Cancer Centre, Glasgow, UK (Prof T R J Evans MD); Marqués de Valdecilla University Hospital, Santander, Spain (C Lopez PhD); Eisai, Woodcliff Lake, NJ, USA (C Dutcus MD, M Guo PhD, K Saito MS, T Tamai MS, M Ren PhD); Eisai, Hatfield, UK (S Kraljevic MD); and National Taiwan University Hospital, Taipei, Taiwan (Prof A-L Cheng MD)

Correspondence to:
Prof Masatoshi Kudo,
Department of Gastroenterology
and Hepatology,
Kindai University Faculty of
Medicine, 337-2 Ohno-Higashi,
Osaka, Japan
m-kudo@med.kindai.ac.jp

Research in context

Evidence before this study

We searched PubMed from inception up to March 16, 2017 using the search terms “phase 3” [Title/Abstract] OR “phase III” [Title/Abstract] AND “hepatocellular carcinoma” [MeSH Terms]. The search was restricted to clinical trials in English language only and yielded 65 reports. Of these publications, 21 described the use of targeted drugs for treatment of hepatocellular carcinoma, 11 were studies of single-drug sorafenib treatment, and three were studies of sorafenib in combination with another drug. Five trials investigated targeted agents following treatment with sorafenib and four trials investigated first-line treatment of hepatocellular carcinoma with sorafenib as the comparator. None of these four trials met their primary endpoints of non-inferiority or superiority over sorafenib in terms of overall survival.

Added value of this study

To our knowledge, this is the first global phase 3 trial in 10 years to meet its primary endpoint of non-inferiority in terms of overall survival against sorafenib as a first-line treatment for hepatocellular carcinoma. Furthermore, lenvatinib showed statistically significant and clinically meaningful improvement in terms of all secondary endpoints (progression-free survival, time to progression, and objective response rate) with a reasonable safety profile.

Implications of all the available evidence

The results of this study support lenvatinib as a first-line treatment option for patients with unresectable hepatocellular carcinoma.

treatment of radioiodine-refractory differentiated thyroid cancer.¹⁶ Lenvatinib and everolimus are approved as a combined treatment for advanced renal cell carcinoma following one previous antiangiogenic therapy.¹⁷ In a phase 2 study of patients with advanced hepatocellular carcinoma, 12 mg lenvatinib once-daily showed clinical activity and had an acceptable safety profile.¹⁸ Based on dose adjustments depending on bodyweight and pharmacokinetic modelling data,¹⁹ a starting dose of lenvatinib was adopted (12 mg for patients ≥ 60 kg and 8 mg for patients < 60 kg once-daily) for further clinical development in hepatocellular carcinoma. Given the efficacy signal observed in this phase 2 study,¹⁸ we did a phase 3 randomised, open-label, non-inferiority study to compare the efficacy and safety of lenvatinib versus sorafenib as a first-line treatment for unresectable hepatocellular carcinoma.

Methods

Study design and participants

This multicentre, phase 3, randomised, open-label, non-inferiority study was done at 154 sites in 20 countries throughout the Asia-Pacific, European, and North American regions (China, Hong Kong, Japan, South Korea, Malaysia, Philippines, Singapore, Taiwan, Thailand, Belgium, Canada, France, Germany, Israel, Italy, Poland, Russia, Spain, UK, and USA).

Eligible patients had unresectable hepatocellular carcinoma, with diagnoses confirmed histologically or cytologically, or confirmed clinically in accordance with American Association for the Study of Liver Diseases criteria. Included patients also had one or more measurable target lesions (lesions previously treated with radiotherapy or locoregional therapy had to show radiographic evidence of disease progression to be deemed target lesions) based on modified Response Evaluation Criteria in Solid Tumours (mRECIST),²⁰ Barcelona Clinic Liver Cancer stage B or C categorisation,²¹ Child-Pugh class A, and an Eastern Cooperative Oncology Group performance status

score of 0 or 1. All eligible patients had controlled blood pressure ($\leq 150/90$ mm Hg), adequate liver function (albumin ≥ 2.8 g/dL, bilirubin ≤ 3.0 mg/dL, and aspartate aminotransferase, alkaline phosphatase, and alanine aminotransferase ≤ 5 times the upper limit of normal), and adequate bone marrow (haemoglobin ≥ 8.5 g/dL, platelet count $\geq 75 \times 10^9$ per L, and absolute neutrophil count $\geq 1.5 \times 10^9$ per L), blood (international normalised ratio ≤ 2.3), renal, and pancreatic function (see appendix for a full list of inclusion criteria). Patients with 50% or higher liver occupation, obvious invasion of the bile duct, or invasion at the main portal vein were excluded from the study. Patients were also excluded if they had received previous systemic therapy for hepatocellular carcinoma (see appendix for a full list of exclusion criteria).

All patients provided written informed consent before undergoing any study-specific procedures. All relevant institutional review boards approved the study, which was done in accordance with the Declaration of Helsinki and local laws.

Randomisation and masking

Patients were randomly assigned in a 1:1 ratio to receive either lenvatinib or sorafenib. Allocation of treatment group was done with an interactive voice-web response system, which also functioned as the allocation concealment method, with region (Asia-Pacific [defined as China, Hong Kong, Japan, South Korea, Malaysia, Philippines, Singapore, Taiwan, and Thailand] or western [defined as Belgium, UK, Spain, Germany, Italy, Poland, France, USA, Canada, Israel, and Russia]), macroscopic portal vein invasion, extrahepatic spread, or both (yes or no), Eastern Cooperative Oncology Group performance status (0 or 1), and bodyweight (< 60 kg or ≥ 60 kg) as stratification factors. A randomisation block size of 2 was used. The randomisation sequence was generated by an independent statistician by the system vendor, and the investigators obtained the randomisation assignments from the system directly. Because the study was open

See Online for appendix

label, the treatments were not masked to the patients or investigators.

Procedures

Patients received oral lenvatinib (Eisai Inc., Woodcliff Lake, NJ, USA) 12 mg/day (for bodyweight ≥ 60 kg) or 8 mg/day (for bodyweight < 60 kg) or sorafenib (Bayer, Leverkusen, Germany) 400 mg twice-daily in 28-day cycles. Dose interruptions followed by reductions for lenvatinib-related toxicities (to 8 mg and 4 mg/day, or 4 mg every other day) were permitted. Modifications to sorafenib doses were implemented according to prescribing information in each region (all patients in the sorafenib arm received a starting dose of 400 mg orally twice-daily).

Local investigators evaluated tumours in each treatment arm in accordance with mRECIST.^{20,22} The liver was examined with CT or MRI by use of a triphasic scanning technique. Tumour assessments were done every 8 weeks (irrespective of dose interruptions) until radiological disease progression. Patients who discontinued study treatment without disease progression had tumour assessments every 8 weeks or until disease progression or the start of another anticancer treatment. Safety assessments were done throughout the study. Quality-of-life questionnaires were administered at baseline, on day 1 of each subsequent treatment cycle, and at the off-treatment visit, which occurred within 30 days of the final administration of study drug. Quality of life was assessed with the European Organisation for Research and Treatment of Cancer Quality of Life Questionnaire C30 (EORTC QLQ-C30)^{23,24} and the hepatocellular carcinoma-specific EORTC QLQ-HCC18²⁵ health questionnaires.

The follow-up period began immediately after the off-treatment visit and was planned to continue if the patient was alive or until the sponsor terminated the study, or the patient withdrew consent. Patients were planned to be followed up for survival every 12 weeks, and all anticancer treatments received were reported.

Outcomes

The primary endpoint was overall survival, measured from the date of randomisation until the date of death from any cause. Patients who were lost to follow-up were censored at the last date they were known to be alive, and patients who remained alive were censored at the time of data cutoff.

Secondary endpoints were progression-free survival, time to progression, objective response rate, quality-of-life measurements, and plasma pharmacokinetics lenvatinib exposure parameters. All efficacy evaluations were based on the full analysis set (all randomised patients).

Safety assessments included recording of vital signs, haematological and biochemical laboratory testing, urinalysis, and electrocardiography. Adverse events were graded according to the National Cancer Institute Common Terminology Criteria for Adverse Events version 4.0.²⁶ All safety evaluations were based on

the safety analysis set (all patients who received at least one dose of study treatment). Post-hoc exploratory tumour assessments using mRECIST and RECIST version 1.1 were done by masked central independent imaging review.

A population pharmacokinetic analysis for lenvatinib was done to derive individual pharmacokinetic parameters and lenvatinib exposure for this study. The dataset used in the analysis included lenvatinib plasma concentrations from 468 patients with hepatocellular carcinoma in this study, and lenvatinib plasma concentration pooled from 12 additional studies (phase 1–3) in healthy people and patients with other tumour types (eg, differentiated thyroid cancer).

Statistical analysis

The primary endpoint of overall survival was first tested for non-inferiority, then for superiority. Using a non-inferiority test by the 95% CI lower-limit method on log HR for overall survival with assumed true HR of 0.80 and a non-inferiority margin of 1.08 (corresponding to

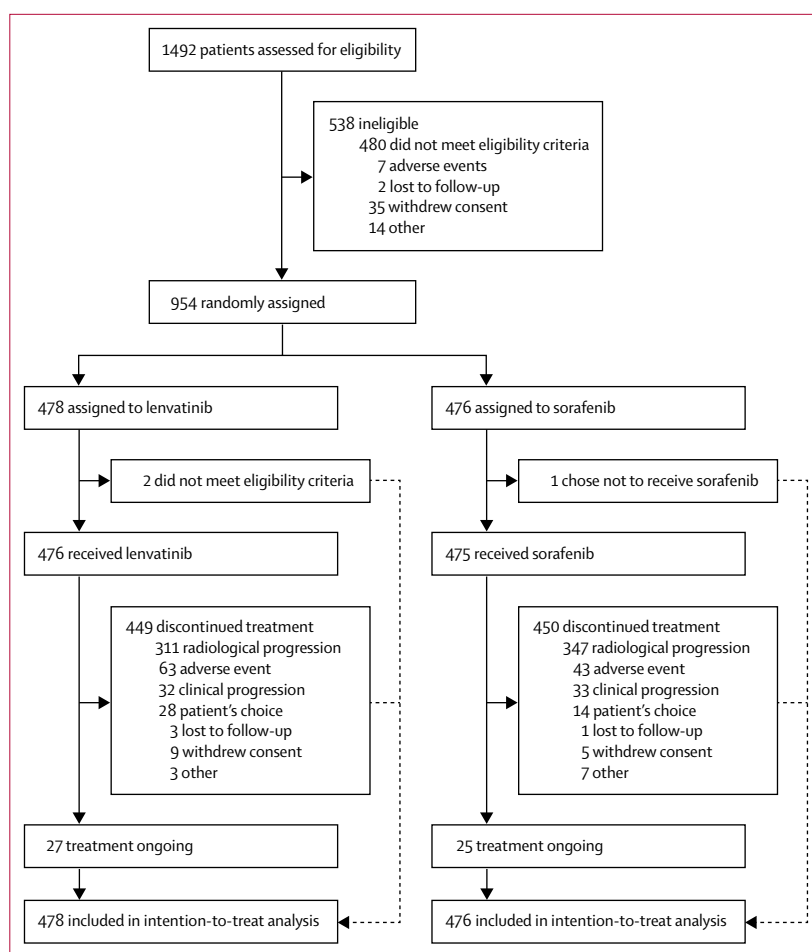


Figure 1: Trial profile

At the time of data cutoff (Nov 13, 2016; for the required 700 death events), 701 deaths had occurred (351 in the lenvatinib arm, 350 in the sorafenib arm).

60% retention of sorafenib effect vs placebo, and set based on previous phase 3 trials of sorafenib^{4,5}), the power of the study to declare non-inferiority was approximately 97%. The power of the study to declare superiority of lenvatinib to sorafenib was approximately

82% using a superiority test with assumed true HR of 0.80. The overall false positive rate was set at 0.05 (two-sided). Non-inferiority was declared if the upper limit of the two-sided 95% CI for HR was less than 1.08. The required number of events for the primary analysis was 700 deaths, assuming 5% dropout. HR and 95% CI were estimated from a Cox proportional hazard model with treatment group as a factor, and with the analysis stratified according to the same factors applied for randomisation for primary and subgroup analyses where appropriate. For the subgroup analysis, analyses were done within each subgroup.

A fixed sequence procedure was used to control the overall type I error rate of analyses for both the primary and secondary efficacy endpoints at $\alpha=0.05$ (two-sided). After non-inferiority was declared, secondary efficacy endpoints were tested. Differences in progression-free survival and time to progression were evaluated using a stratified log-rank test with randomisation stratification factors, with the associated HR and 95% CI. The same method was used to evaluate differences in progression-free survival and time to progression in the subgroup analyses. A difference in the objective response rate was evaluated using the Cochran-Mantel-Haenszel χ^2 test with randomisation stratification factors as strata, with associated odds ratio (OR) and 95% CI. To assess futility, two interim analyses (at 30% and 70% of the target number of events) were done using Bayesian predictive probability in a non-inferiority design.

The efficacy analysis followed the intention-to-treat principle. Only patients who received treatment were included in the safety analysis.

Programming and statistical analyses were done with SAS version 9 or higher. The study was overseen by an independent data monitoring committee. The study is registered with ClinicalTrials.gov, number NCT01761266.

Role of the funding source

The study was funded by Eisai Inc, (Woodcliff Lake, NJ, USA) and designed in collaboration with the principal investigators. The funder employed CD, MG, KS, SK, TT, and MR, who played a significant part in study design, data collection, data analysis, data interpretation, and writing of the report. The corresponding author had full access to all data in the study and had final responsibility for the decision to submit for publication.

Results

Between March 1, 2013, and July 30, 2015, 1492 patients were recruited. 954 eligible patients from 20 countries were randomly assigned to receive lenvatinib (n=478) or sorafenib (n=476, figure 1).

Patient baseline characteristics were similar between treatment groups, except for baseline hepatitis C aetiology and α -fetoprotein concentrations (table 1). At the time of data cutoff (Nov 13, 2016, at 701 deaths), the median duration of follow-up was 27.7 months

	Lenvatinib (n=478)	Sorafenib (n=476)	Total (n=954)
Age (years), median (range)	63.0 (20–88)	62.0 (22–88)	62.0 (20–88)
Age group (years)			
<65	270 (56%)	283 (59%)	553 (58%)
≥65 to <75	150 (31%)	126 (26%)	276 (30%)
≥75	58 (12%)	67 (14%)	125 (13%)
Sex			
Male	405 (85%)	401 (84%)	806 (84%)
Female	73 (15%)	75 (16%)	148 (16%)
Region			
Western	157 (33%)	157 (33%)	314 (33%)
Asia-Pacific	321 (67%)	319 (67%)	640 (67%)
Race			
White	135 (28%)	141 (30%)	276 (29%)
Asian	334 (70%)	326 (68%)	660 (69%)
Other	9 (2%)	9 (2%)	18 (2%)
Bodyweight (kg)			
<60	153 (32%)	146 (31%)	299 (31%)
≥60	325 (68%)	330 (69%)	655 (69%)
Eastern Cooperative Oncology Group performance status			
0	304 (64%)	301 (63%)	605 (63%)
1	174 (36%)	175 (37%)	349 (37%)
Child-Pugh class			
A	475 (99%)	471 (99%)	946 (99%)
B	3 (1%)	5 (1%)	8 (1%)
Macroscopic portal vein invasion			
Yes	109 (23%)	90 (19%)	199 (21%)
No	369 (77%)	386 (81%)	755 (79%)
Extrahepatic spread			
Yes	291 (61%)	295 (62%)	586 (61%)
No	187 (39%)	181 (38%)	368 (39%)
Macroscopic portal vein invasion, extrahepatic spread, or both			
Yes	329 (69%)	336 (71%)	665 (70%)
No	149 (31%)	140 (29%)	289 (30%)
Underlying cirrhosis based on masked independent imaging review			
Yes	356 (74%)	364 (76%)	720 (75%)
No	122 (26%)	112 (24%)	234 (25%)
Barcelona Clinic Liver Cancer stage			
B (intermediate stage)	104 (22%)	92 (19%)	196 (21%)
C (advanced stage)	374 (78%)	384 (81%)	758 (79%)
Involved disease sites			
Liver	441 (92%)	430 (90%)	871 (91%)
Lung	163 (34%)	144 (30%)	307 (32%)
Involved disease sites per patient*			
1	207 (43%)	207 (43%)	414 (43%)
2	167 (35%)	183 (38%)	350 (37%)
≥3	103 (22%)	86 (18%)	189 (20%)

(Table 1 continues on next page)

(IQR 23.3–32.8) in the lenvatinib group and 27.2 months (22.6–31.3) in the sorafenib group.

Lenvatinib showed non-inferiority in terms of overall survival compared with sorafenib (figure 2). Median overall survival duration was 13.6 months (95% CI 12.1–14.9) for 478 patients in the lenvatinib group, compared with 12.3 months (10.4–13.9) for 476 patients in the sorafenib group (HR 0.92, 95% CI 0.79–1.06, figure 2, table 2; results from the per-protocol analysis set are shown in the appendix). Overall survival superiority over sorafenib was not achieved. The effect of lenvatinib and sorafenib on median overall survival was consistent across subgroups based on baseline characteristics (figure 3). Although baseline α -fetoprotein concentration was not a prespecified stratum, patients with baseline α -fetoprotein concentrations less than 200 ng/mL had longer overall survival than did those with α -fetoprotein concentration of at least 200 ng/mL in both treatment groups (figure 3). More patients had baseline α -fetoprotein levels less than 200 ng/mL in the sorafenib arm compared with the lenvatinib arm (table 1).

Lenvatinib showed a statistically significant improvement compared with sorafenib for all secondary efficacy endpoints as determined by investigator tumour assessments based on mRECIST. Median progression-free survival for lenvatinib was longer than that for sorafenib (table 2, figure 4). Median time to progression was 8.9 months (95% CI 7.4–9.2) for patients in the lenvatinib group compared to 3.7 months (3.6–5.4) for patients in the sorafenib group (table 2, appendix). Lenvatinib also showed a greater objective response rate than did sorafenib (table 2, appendix). Improvements in all secondary efficacy endpoints (progression-free survival, time to progression, and objective response) with lenvatinib compared to sorafenib were consistent across all predefined subgroups (figure 3, appendix). Analysis for overall survival with predefined subgroups supports the robustness of the non-inferiority result (appendix). Masked independent imaging review confirmed progression-free survival and time to progression based on investigator assessments according to mRECIST (table 2, figure 4). Similar progression-free survival and time-to-progression results were observed for mRECIST and RECIST 1.1 based on masked independent imaging review. Masked independent imaging review confirmed a significantly higher objective response rate in the lenvatinib arm than in the sorafenib arm by mRECIST and RECIST 1.1 (table 2).

156 (33%) patients in the lenvatinib arm and 184 (39%) in the sorafenib arm received post-study anticancer medication (including investigational therapy). Of these patients, 121 (25%) in the lenvatinib arm and 56 (12%) in the sorafenib arm received sorafenib during survival follow-up. In the western region, 41 (26%) patients in the lenvatinib arm received anticancer medication during survival follow-up versus 61 (39%) patients in the

	Lenvatinib (n=478)	Sorafenib (n=476)	Total (n=954)
(Continued from previous page)			
Aetiology of chronic liver disease			
Hepatitis B	251 (53%)	228 (48%)	479 (50%)
Hepatitis C	91 (19%)	126 (26%)	217 (23%)
Alcohol	36 (8%)	21 (4%)	57 (6%)
Other	38 (8%)	32 (7%)	70 (7%)
Unknown	62 (13%)	69 (14%)	131 (14%)
Baseline α -fetoprotein concentration (ng/mL)			
Number of patients	471 (99%)	463 (97%)	934 (98%)
Mean (SD)	17507.5 (105137.4)	16678.5 (94789.5)	17096.5 (100088.8)
Median (IQR)	133.1 (8.0–3730.6)	71.2 (5.2–1081.8)	89.0 (6.3–2120.2)
Baseline α -fetoprotein concentration group (ng/mL)			
<200	255 (53%)	286 (60%)	541 (57%)
\geq 200	222 (46%)	187 (39%)	409 (43%)
Missing	1 (<1%)	3 (1%)	4 (<1%)
Concomitant systemic antiviral therapy for hepatitis B or C			
Previous therapy			
Previous anticancer procedures	327 (68%)	344 (72%)	671 (70%)
Radiotherapy	49 (10%)	60 (13%)	109 (11%)

Data are mean (SD) or n (%) unless otherwise specified. *One patient had no baseline target lesion.

Table 1: Demographic and disease characteristics at baseline

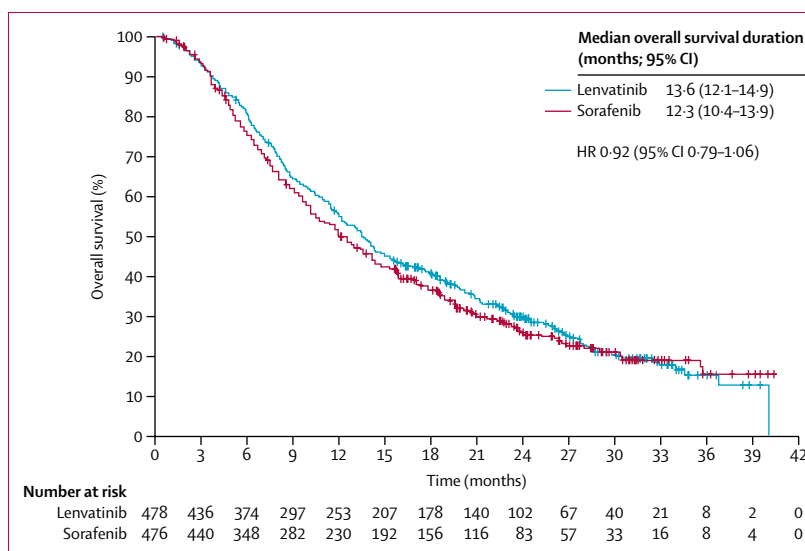


Figure 2: Overall survival outcomes

Kaplan-Meier estimates of overall survival by treatment group. HR=hazard ratio.

sorafenib arm. In the lenvatinib arm, 11 (7%) patients in the western region had an anticancer procedure during follow-up compared with 18 (11%) patients in the sorafenib arm in this region (appendix).

The median duration of study treatment for patients in the lenvatinib group was 5.7 months (IQR 2.9–11.1), compared with 3.7 months (1.8–7.4) in the sorafenib

	Lenvatinib (n=478)	Sorafenib (n=476)	Effect size (95% CI)	p value
Investigator review according to mRECIST				
Overall survival (months)	13.6 (12.1-14.9)	12.3 (10.4-13.9)	HR 0.92 (0.79-1.06)	..
Progression-free survival (months)	7.4 (6.9-8.8)	3.7 (3.6-4.6)	HR 0.66 (0.57-0.77)	<0.0001
Time to progression (months)	8.9 (7.4-9.2)	3.7 (3.6-5.4)	HR 0.63 (0.53-0.73)	<0.0001
Objective response (%; 95% CI)	115 (24.1%, 20.2-27.9)	44 (9.2%, 6.6-11.8)	OR 3.13 (2.15-4.56)	<0.0001
Complete response	6 (1%)	2 (<1%)
Partial response	109 (23%)	42 (9%)
Stable disease	246 (51%)	244 (51%)
Durable stable disease lasting ≥23 weeks	167 (35%)	139 (29%)
Progressive disease	71 (15%)	147 (31%)
Unknown or not evaluable	46 (10%)	41 (9%)
Disease control rate (%; 95% CI)	361 (75.5%, 71.7-79.4)	288 (60.5%, 56.1-64.9)
Masked independent imaging review according to mRECIST				
Progression-free survival (months)	7.3 (5.6-7.5)	3.6 (3.6-3.7)	HR 0.64 (0.55-0.75)	<0.0001
Time to progression (months)	7.4 (7.2-9.1)	3.7 (3.6-3.9)	HR 0.60 (0.51-0.71)	<0.0001
Objective response (%; 95% CI)	194 (40.6%, 36.2-45.0)	59 (12.4%, 9.4-15.4)	OR 5.01 (3.59-7.01)	<0.0001
Complete response	10 (2%)	4 (1%)
Partial response	184 (38%)	55 (12%)
Stable disease	159 (33%)	219 (46%)
Durable stable disease lasting ≥23 weeks	84 (18%)	90 (19%)
Progressive disease	79 (17%)	152 (32%)
Unknown or not evaluable	46 (10%)	46 (10%)
Disease control rate (%; 95% CI)	353 (73.8%, 69.9-77.8)	278 (58.4%, 54.0-62.8)
Masked independent imaging review according to RECIST 1.1				
Progression-free survival (months)	7.3 (5.6-7.5)	3.6 (3.6-3.9)	HR 0.65 (0.56-0.77)	<0.0001
Time to progression (months)	7.4 (7.3-9.1)	3.7 (3.6-5.4)	HR 0.61 (0.51-0.72)	<0.0001
Objective response (%; 95% CI)	90 (18.8%, 15.3-22.3)	31 (6.5%, 4.3-8.7)	OR 3.34 (2.17-5.14)	<0.0001
Complete response	2 (<1%)	1 (<1%)
Partial response	88 (18%)	30 (6%)
Stable disease	258 (54%)	250 (53%)
Durable stable disease lasting ≥23 weeks	163 (34%)	118 (25%)
Progressive disease	84 (18%)	152 (32%)
Unknown or not evaluable	46 (10%)	43 (9%)
Disease control rate (%; 95% CI)	348 (72.8%, 68.8-76.8)	281 (59.0%, 54.6-63.5)

Data are presented as median (95% CI) or n (%) unless otherwise indicated. mRECIST=modified Response Evaluation Criteria in Solid Tumours. HR=hazard ratio. OR=odds ratio.

Table 2: Efficacy measures

group. Treatment-emergent adverse events occurred in most patients who received lenvatinib or sorafenib (table 3). Adjusted by patient-years, the adverse event rate was 18.9 episodes per patient-year in the lenvatinib group and 19.7 episodes per patient-year in the sorafenib group. Treatment-emergent adverse events of grade 3 or higher occurred at similar rates in the lenvatinib and sorafenib arms (episodes per patient-year 3.2 vs 3.3). The most common treatment-emergent adverse events among patients who received lenvatinib were hypertension, diarrhoea, decreased appetite, and decreased weight. In the sorafenib arm, the most common treatment-emergent adverse events were palmar-plantar erythrodysesthesia, diarrhoea, hypertension, and decreased appetite (table 3). Fatal adverse events occurred throughout treatment and appeared to occur at similar rates in both arms. Fatal

adverse events determined by the investigator to be related to lenvatinib treatment occurred in 11 (2%) patients and included hepatic failure (three patients), cerebral haemorrhage (three patients), and respiratory failure (two patients). In the sorafenib group, treatment-related fatal adverse events occurred in four (1%) patients and included tumour haemorrhage, ischaemic stroke, respiratory failure, and sudden death (one each). Treatment-related treatment-emergent adverse events led to lenvatinib drug interruption in 190 (40%) patients, dose reduction in 176 (37%) patients, and drug withdrawal in 42 (9%) patients. In the sorafenib arm, treatment-related treatment-emergent adverse events led to drug interruption in 153 (32%) patients, dose reduction in 181 (38%), and drug withdrawal in 34 (7%) patients. The mean lenvatinib dose intensity was 7.0 mg in the

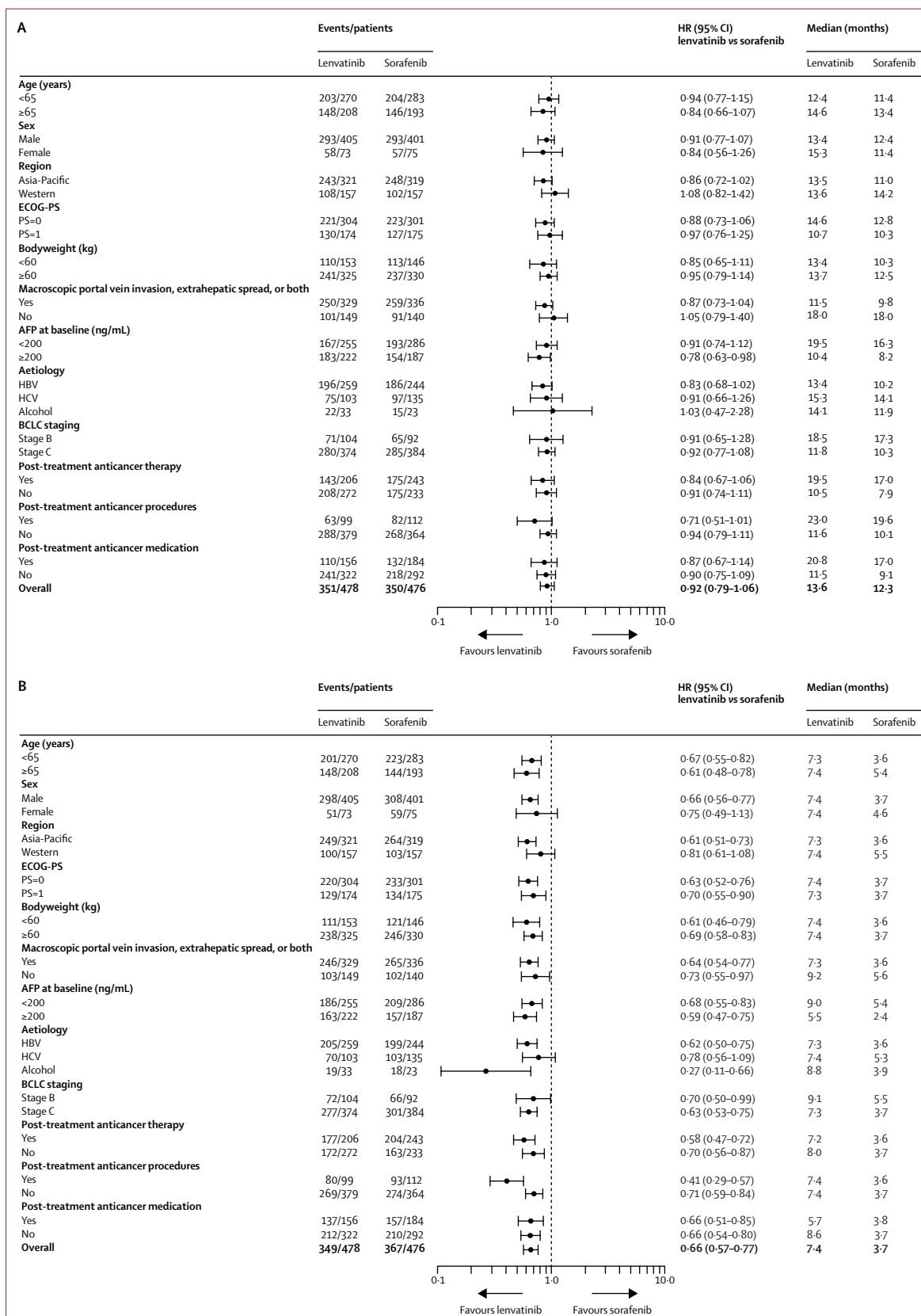


Figure 3: Forest plots of overall and progression-free survival in patient subgroups
Subgroup analyses for overall survival (A) and progression-free survival (B). HR=hazard ratio. ECOG-PS=Eastern Cooperative Oncology Group performance status. AFP=α-fetoprotein. HBV=hepatitis B virus. HCV=hepatitis C virus. BCLC=Barcelona Clinic Liver Cancer.

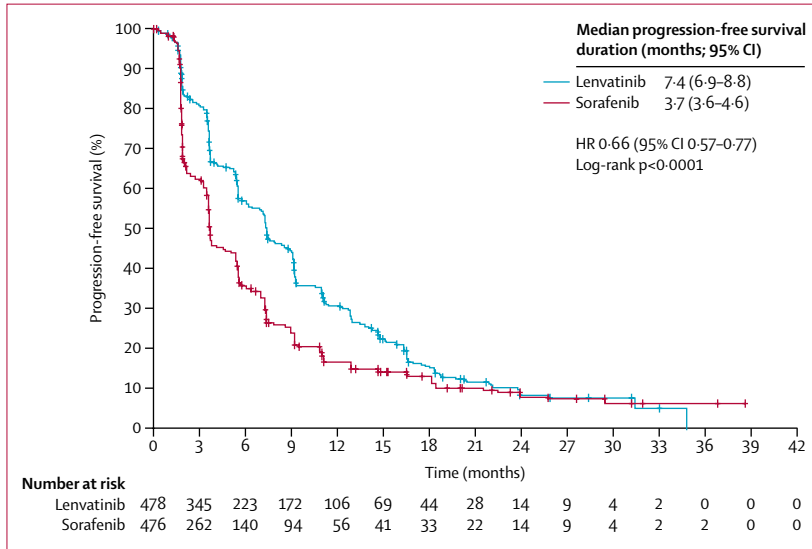


Figure 4: Progression-free survival outcomes
Kaplan-Meier estimates of progression-free survival by modified Response Evaluation Criteria in Solid Tumours. HR=hazard ratio.

	Lenvatinib (n=476)	Sorafenib (n=475)
Total treatment-emergent adverse events	470 (99%)	472 (99%)
Total treatment-related treatment-emergent adverse events	447 (94%)	452 (95%)
Treatment-emergent adverse events of grade ≥3	357 (75%)	316 (67%)
Treatment-related treatment-emergent adverse events of grade ≥3	270 (57%)	231 (49%)
Serious treatment-emergent adverse events	205 (43%)	144 (30%)
Serious treatment-related treatment-emergent adverse events	84 (18%)	48 (10%)
Treatment-emergent adverse events occurring in ≥15% of patients in either treatment group		
Palmar-plantar erythrodysesthesia		
Any grade	128 (27%)	249 (52%)
Grade ≥3	14 (3%)	54 (11%)
Diarrhoea		
Any grade	184 (39%)	220 (46%)
Grade ≥3	20 (4%)	20 (4%)
Hypertension		
Any grade	201 (42%)	144 (30%)
Grade ≥3	111 (23%)	68 (14%)
Decreased appetite		
Any grade	162 (34%)	127 (27%)
Grade ≥3	22 (5%)	6 (1%)
Decreased weight		
Any grade	147 (31%)	106 (22%)
Grade ≥3	36 (8%)	14 (3%)
Fatigue		
Any grade	141 (30%)	119 (25%)
Grade ≥3	18 (4%)	17 (4%)

(Table 3 continues in next column)

	Lenvatinib (n=476)	Sorafenib (n=475)
(Continued from previous column)		
Alopecia		
Any grade	14 (3%)	119 (25%)
Grade ≥3	0	0
Proteinuria		
Any grade	117 (25%)	54 (11%)
Grade ≥3	27 (6%)	8 (2%)
Dysphonia		
Any grade	113 (24%)	57 (12%)
Grade ≥3	1 (<1%)	0
Nausea		
Any grade	93 (20%)	68 (14%)
Grade ≥3	4 (1%)	4 (1%)
Abdominal pain		
Any grade	81 (17%)	87 (18%)
Grade ≥3	8 (2%)	13 (3%)
Decreased platelet count		
Any grade	87 (18%)	58 (12%)
Grade ≥3	26 (5%)	16 (3%)
Elevated aspartate aminotransferase		
Any grade	65 (14%)	80 (17%)
Grade ≥3	24 (5%)	38 (8%)
Hypothyroidism		
Any grade	78 (16%)	8 (2%)
Grade ≥3	0	0
Vomiting		
Any grade	77 (16%)	36 (8%)
Grade ≥3	6 (1%)	5 (1%)
Constipation		
Any grade	76 (16%)	52 (11%)
Grade ≥3	3 (1%)	0
Rash		
Any grade	46 (10%)	76 (16%)
Grade ≥3	0	2 (<1%)
Increased blood bilirubin		
Any grade	71 (15%)	63 (13%)
Grade ≥3	31 (7%)	23 (5%)

Data are presented as n (%).

Table 3: Adverse events

8 mg/day group and 10.5 mg in the 12 mg/day group, corresponding to 88% of the planned starting dose in both cases. The mean sorafenib dose intensity was 663.8 mg, or 83% of the planned starting dose.

Baseline scores on the EORTC QLQ-C30 and EORTC QLQ-HCC18 health questionnaires were similar in the lenvatinib and sorafenib treatment groups. Following treatment, scores declined in both groups. Analysis of time to clinically meaningful deterioration showed that role functioning (nominal p=0.0193), pain (nominal p=0.0105), and diarrhoea (nominal p<0.0001) from EORTC QLQ-C30, and nutrition (nominal p=0.0113) and body image

(nominal $p=0.0051$) from EORTC QLQ-HCC18 were observed earlier in patients treated with sorafenib than in those treated with lenvatinib. For between-group comparison, the summary score was not significantly different between the treatment arms (HR 0.87, 95% CI 0.754–1.013, appendix).

Based on individual model-derived predicted lenvatinib area under the curve (AUC) values at steady state for patients with hepatocellular carcinoma in our study, the median values and ranges of AUC between the group with a starting dose of 8 mg for bodyweight less than 60 kg (median 1820.2 ng·h/mL, range 704.8–4980.7) and the group with a 12 mg starting dose for bodyweight of at least 60 kg (1996.0 ng·h/mL, 925.5–5427.9) are comparable, which supports a starting dose of 8 mg for bodyweights less than 60 kg, and confirms the weight-based dosing reported in pharmacokinetic analyses from a previous study.¹⁹ There were no differences in lenvatinib oral clearance or in AUC at steady state among Western, Asian, Chinese, and Japanese populations in our study.

Discussion

To our knowledge, our study is the first global phase 3 trial in 10 years to show a treatment effect on overall survival, and the first ever positive trial against an active control. Our study showed lenvatinib to be non-inferior to sorafenib—the current standard of care in hepatocellular carcinoma—for overall survival. Lenvatinib showed statistically significant clinically meaningful improvement for all secondary efficacy endpoints (progression-free survival, time to progression, and objective response) across subgroups, and in quality-of-life assessments. Together, these data support the overall survival result of our study.

The median overall survival time of patients who received sorafenib in our study is longer than that reported in any previous large randomised phase 3 study.^{4–9} A possible explanation for this result is the high proportion of post-sorafenib anticancer therapy in our study. For example, in a previous phase 3 study⁷ of brivanib versus sorafenib, 21% of patients who received sorafenib underwent systemic post-sorafenib treatments and 17% had non-systemic post-sorafenib treatments, compared with 39% of patients receiving systemic post-sorafenib treatments and 27% of patients receiving non-systemic post-sorafenib treatments in our study. Continuous improvements in care for unresectable hepatocellular carcinoma have been made, and multimodality therapies, including locoregional treatment approaches, are often used after disease progression because they might be efficacious, even after systemic therapies such as sorafenib treatment.^{27,28} If post-progression survival is prolonged by such post-study treatments, this could lead to dilution of the observed overall survival treatment benefit. Hence, although still representing the gold standard, overall survival as an endpoint alone for trials in first-line

hepatocellular carcinoma treatment might no longer capture the full extent of antitumour efficacy. The substantial improvement in progression-free survival, time to progression, and objective response with lenvatinib in our study might indicate, as in some other tumours, the emergence of a broader framework in drug assessment and treatment in advanced hepatocellular carcinoma.

Our study did not enrol patients with more than 50% liver involvement and main portal vein invasion because this exclusion criterion was used in the preceding phase 2 proof-of-concept study in Japan, as mandated by Japan Society of Hepatology consensus-based clinical practice guidelines.^{17,29} This decision resulted in only 4.2% screen failures in the phase 3 study. Although this exclusion criterion could have slightly changed the overall prognosis of the patient population, it did not affect the distribution of patients between the study arms because this was controlled for by the randomisation.

The safety profile of lenvatinib was consistent with that observed in previous studies.^{16,18,30} Patients who received lenvatinib experienced fewer instances of palmar-plantar erythrodysesthesia, diarrhoea, and alopecia, and more instances of hypertension, proteinuria, dysphonia, and hypothyroidism than did patients who received sorafenib. Although quality-of-life scores declined in both groups after treatment, a clinically meaningful delay in deterioration for multiple domains was observed with lenvatinib compared with sorafenib.

The median duration of lenvatinib treatment was 1.5 times longer than that of sorafenib treatment, which might have contributed to the higher incidence of adverse events. When adjusted for treatment duration, almost all adverse event episodes were comparable for the lenvatinib and sorafenib arms. Doses of lenvatinib for hepatocellular carcinoma are lower than the dosage for radioiodine-refractory differentiated thyroid cancer (24 mg/day). In a phase 1 study of lenvatinib in hepatocellular carcinoma,³¹ patients with hepatocellular carcinoma who received 12 mg of lenvatinib per day and patients with solid tumours who received 25 mg of lenvatinib per day had similar lenvatinib plasma concentrations at 24 h, possibly because lenvatinib is metabolised in the liver. In our study, similar clinical activities and safety profiles were observed for both the 8 mg/day and 12 mg/day lenvatinib starting doses.

Unlike other cancer types, including differentiated thyroid cancer and renal cell carcinoma, lenvatinib pharmacokinetics were affected by bodyweight to a clinically significant degree. The final pharmacokinetic model for lenvatinib included bodyweight effect as an allometric constant on both clearance and volume parameters, whereby both parameters increased with increasing bodyweight. The clinical relevance of this finding is that, when administered equivalent doses, patients with hepatocellular carcinoma with low bodyweight will have clinically significantly higher

exposures than will patients with high bodyweight, supporting bodyweight-based dosing.

Our study was potentially limited by its open-label design. However, because of the distinct toxicities and dose management requirements, this design was essential to ensure patient safety. Major protocol deviations were few and balanced, the percentage of patients having clinical progression and drug discontinuations were similar in both arms, and results were confirmed by masked independent imaging review. Therefore, we believe any bias introduced by the open-label design was minimal. The full analysis set was used as the primary analysis set as opposed to the per-protocol set. However, the sample size calculation for our study was such that any factor introducing bias toward the null hypothesis would reduce the power of the study. Therefore, use of the full analysis set as the primary analysis set for non-inferiority testing is a conservative approach, and, in fact, overall survival analysis based on the per-protocol set was completely consistent with that based on the full analysis set.

Use of mRECIST could also be considered as a limitation of this study. However, mRECIST is an established tool in hepatocellular carcinoma.^{32,33} Furthermore, exploratory post-hoc analysis confirmed that progression-free survival and time to progression based on investigator assessment using mRECIST were similar to those observed based on independent imaging review using both mRECIST and RECIST 1.1.

In conclusion, this study showed non-inferiority of lenvatinib versus sorafenib in terms of overall survival, as well as statistically significant and clinically meaningful improvement in progression-free survival, time to progression, and objective response rate. The safety profiles of lenvatinib and sorafenib in our study appear consistent with the known safety profiles of these drugs in hepatocellular carcinoma, and no new safety signals were identified. Based on our results, lenvatinib might be a potential new treatment option for advanced hepatocellular carcinoma.

Contributors

MK, RSF, SQ, K-HH, KI, FP, and A-LC were protocol steering committee members and made substantial contributions in all aspects of ICMJE criteria. Equal contributions were made by AB, J-WP, and GH (non-protocol steering committee member investigators). AB and J-WP contributed to helpful communications in study management and acquisition of good quality data, and GH contributed to substantial good quality data acquisition and critical data interpretation of the Chinese patient population. JJ, JFB, AV, DK, TRJE, and CL were national coordinating or representing investigators in European countries, and particularly contributed to study coordination and acquisition of good quality data. CD, MG, KS, SK, TT, and MR are Eisai employees primarily involved in the study, and played a significant role in study design, data collection, data analysis, data interpretation, and writing of the report. MK, RSF, SQ, K-HH, KI, FP, CD, MG, KS, TT, and A-LC contributed to the study design. MG, KS, and MR did the statistical analysis.

Declaration of interests

MK reports honoraria from Bayer, Eisai, MSD, and EA Pharma. RSF reports grants, personal fees and non-financial support from Eisai, Bayer, Pfizer, Novartis, Bristol Myers Squibb (BMS), and Merck outside

the submitted work. K-HH reports grants and consultant fees from Eisai and KOWA, and consultant fees from Bayer, all outside the submitted work. KI reports honoraria from Eisai and Dainippon Sumitomo Pharma. FP reports personal fees from Eisai during the conduct of the study, and grants and personal fees from Bayer, and personal fees from Bracco, both outside the submitted work. AB reports research funding from Eisai. JJ reports personal fees from AstraZeneca, Roche, Pfizer, G1 Therapeutics, Pierre Fabre, Celgene, Merck, and BMS outside the submitted work. JFB reports personal fees from Bayer SP, Eli Lilly Oncology, Novartis, and BMS outside the submitted work. TRJE reports other fees (reimbursement of study costs of this clinical trial [to the institution]; advisory board honorarium [payable to the institution]) from Eisai during the conduct of the study, and other fees from BMS (financial support for clinical trials of novel anti-cancer drugs, honoraria for consultancies or speaker's fees, and support to attend international conferences), Clovis (support for clinical trials [to institution] and honorarium for advisory board), Karus Therapeutics (scientific advisory board [payable to the institution]), Baxalta (advisory board honorarium [payable to the institution]), Bayer (support for clinical trials and advisory board honorarium [payable to the institution]), Celgene (support for clinical trials and advisory board honorarium [payable to the institution]), GlaxoSmithKline (support for clinical trials and advisory board honorarium [payable to the institution]), Otsuka (support for clinical trials and advisory board honorarium [payable to the institution]), Roche/Genentech (support for clinical trials and advisory board honorarium [payable to the institution]), TC Biopharm (support for clinical trials), Immunova (advisory board honorarium [payable to the institution]), Basilea (support for clinical trials), e-Therapeutics (support for clinical trials), Immunocore (support for clinical trials), Vertex (support for clinical trials), Verastem (support for clinical trials), Daiichi (support for clinical trials), and Merck (support for clinical trials) outside the submitted work. CL reports grants, personal fees, non-financial support and advisory board fees from Eisai, Bayer, Lilly, and Daiichi Sankyo during the conduct of the study. CD, MG, KS, SK, TT, and MR are employees of Eisai. A-LC reports personal fees from BMS, Ono, Novartis, Bayer, Merck, and MSD during the conduct of the study. SQ, J-WP, GH, AV, and DK declare no competing interests.

Acknowledgments

We thank the patients, their families, the investigators, and the teams who participated in this trial, and Terri Binder (Eisai Inc., Woodcliff Lake, NJ, USA) for overseeing the independent image review. Editorial assistance was provided by Nicolette Belletier of Oxford PharmaGenesis (funded by Eisai Inc).

References

- 1 Ferlay J, Soerjomataram I, Dikshit R, et al. Cancer incidence and mortality worldwide: sources, methods and major patterns in GLOBOCAN 2012. *Int J Cancer* 2015; **136**: E359–86.
- 2 El-Serag HB, Rudolph KL. Hepatocellular carcinoma: epidemiology and molecular carcinogenesis. *Gastroenterology* 2007; **132**: 2557–76.
- 3 Balogh J, Victor D 3rd, Asham EH, et al. Hepatocellular carcinoma: a review. *J Hepatocell Carcinoma* 2016; **3**: 41–53.
- 4 Llovet JM, Ricci S, Mazzaferro V, et al. Sorafenib in advanced hepatocellular carcinoma. *N Engl J Med* 2008; **359**: 378–90.
- 5 Cheng AL, Kang YK, Chen Z, et al. Efficacy and safety of sorafenib in patients in the Asia-Pacific region with advanced hepatocellular carcinoma: a phase III randomised, double-blind, placebo-controlled trial. *Lancet Oncol* 2009; **10**: 25–34.
- 6 Cheng AL, Kang YK, Lin DY, et al. Sunitinib versus sorafenib in advanced hepatocellular cancer: results of a randomized phase III trial. *J Clin Oncol* 2013; **31**: 4067–75.
- 7 Johnson PJ, Qin S, Park JW, et al. Brivanib versus sorafenib as first-line therapy in patients with unresectable, advanced hepatocellular carcinoma: results from the randomized phase III BRISK-FL study. *J Clin Oncol* 2013; **31**: 3517–24.
- 8 Cainap C, Qin S, Huang WT, et al. Linifanib versus sorafenib in patients with advanced hepatocellular carcinoma: results of a randomized phase III trial. *J Clin Oncol* 2015; **33**: 172–79.
- 9 Zhu AX, Rosmorduc O, Evans TR, et al. SEARCH: a phase III, randomized, double-blind, placebo-controlled trial of sorafenib plus erlotinib in patients with advanced hepatocellular carcinoma. *J Clin Oncol* 2015; **33**: 559–66.

- 10 Bruix J, Qin S, Merle P, et al. Regorafenib for patients with hepatocellular carcinoma who progressed on sorafenib treatment (RESORCE): a randomised, double-blind, placebo-controlled, phase 3 trial. *Lancet* 2017; **389**: 55–66.
- 11 NCCN. Clinical practice guidelines in oncology, version 1: hepatobiliary cancers. Fort Washington, PA: National Comprehensive Cancer Network, 2017.
- 12 Matsui J, Yamamoto Y, Funahashi Y, et al. E7080, a novel inhibitor that targets multiple kinases, has potent antitumor activities against stem cell factor producing human small cell lung cancer H146, based on angiogenesis inhibition. *Int J Cancer* 2008; **122**: 664–71.
- 13 Matsui J, Funahashi Y, Uenaka T, Watanabe T, Tsuruoka A, Asada M. Multi-kinase inhibitor E7080 suppresses lymph node and lung metastases of human mammary breast tumor MDA-MB-231 via inhibition of vascular endothelial growth factor-receptor (VEGF-R) 2 and VEGF-R3 kinase. *Clin Cancer Res* 2008; **14**: 5459–65.
- 14 Tohyama O, Matsui J, Kodama K, et al. Antitumor activity of lenvatinib (e7080): an angiogenesis inhibitor that targets multiple receptor tyrosine kinases in preclinical human thyroid cancer models. *J Thyroid Res* 2014; **2014**: 638747.
- 15 Yamamoto Y, Matsui J, Matsushima T, et al. Lenvatinib, an angiogenesis inhibitor targeting VEGFR/FGFR, shows broad antitumor activity in human tumor xenograft models associated with microvessel density and pericyte coverage. *Vasc Cell* 2014; **6**: 18.
- 16 Schlumberger M, Tahara M, Wirth LJ, et al. Lenvatinib versus placebo in radioiodine-refractory thyroid cancer. *N Engl J Med* 2015; **372**: 621–30.
- 17 Motzer RJ, Hutson TE, Glen H, et al. Lenvatinib, everolimus, and the combination in patients with metastatic renal cell carcinoma: a randomised, phase 2, open-label, multicentre trial. *Lancet Oncol* 2015; **16**: 1473–82.
- 18 Ikeda K, Kudo M, Kawazoe S, et al. Phase 2 study of lenvatinib in patients with advanced hepatocellular carcinoma. *J Gastroenterol* 2017; **52**: 512–19.
- 19 Tamai T, Hayato S, Hojo S, et al. Dose finding of lenvatinib in subjects with advanced hepatocellular carcinoma based on population pharmacokinetic and exposure-response analyses. *J Clin Pharmacol* 2017; **57**: 1138–47.
- 20 Lencioni R, Llovet JM. Modified RECIST (mRECIST) assessment for hepatocellular carcinoma. *Semin Liver Dis* 2010; **30**: 52–60.
- 21 Bruix J, Sherman M. Management of hepatocellular carcinoma: an update. *Hepatology* 2011; **53**: 1020–22.
- 22 Eisenhauer EA, Therasse P, Bogaerts J, et al. New response evaluation criteria in solid tumours: revised RECIST guideline (version 1.1). *Eur J Cancer* 2009; **45**: 228–47.
- 23 Cocks K, King MT, Velikova G, Martyn St-James M, Fayers PM, Brown JM. Evidence-based guidelines for determination of sample size and interpretation of the European Organisation for the Research and Treatment of Cancer Quality of Life Questionnaire Core 30. *J Clin Oncol* 2011; **29**: 89–96.
- 24 Giesinger JM, Kieffer JM, Fayers PM, et al. Replication and validation of higher order models demonstrated that a summary score for the EORTC QLQ-C30 is robust. *J Clin Epidemiol* 2016; **69**: 79–88.
- 25 Chie WC, Blazeby JM, Hsiao CF, et al. International cross-cultural field validation of an European Organization for Research and Treatment of Cancer questionnaire module for patients with primary liver cancer, the European Organization for Research and Treatment of Cancer quality-of-life questionnaire HCC18. *Hepatology* 2012; **55**: 1122–29.
- 26 National Cancer Institute. Protocol development. Cancer therapy evaluation program. https://ctep.cancer.gov/protocolDevelopment/electronic_applications/ctc.htm (accessed March 21, 2017).
- 27 Terashima T, Yamashita T, Arai K, et al. Feasibility and efficacy of hepatic arterial infusion chemotherapy for advanced hepatocellular carcinoma after sorafenib. *Hepatol Res* 2014; **44**: 1179–85.
- 28 Shao YY, Liang PC, Wu YM, et al. A pilot study of hepatic arterial infusion of chemotherapy for patients with advanced hepatocellular carcinoma who have failed anti-angiogenic therapy. *Liver Int* 2013; **33**: 1413–19.
- 29 Kudo M, Matsui O, Izumi N, et al. JSH consensus-based clinical practice guidelines for the management of hepatocellular carcinoma: 2014 update by the Liver Cancer Study Group of Japan. *Liver Cancer* 2014; **3**: 458–68.
- 30 Boss DS, Glen H, Beijnen JH, et al. A phase I study of E7080, a multitargeted tyrosine kinase inhibitor, in patients with advanced solid tumours. *Br J Cancer* 2012; **106**: 1598–604.
- 31 Ikeda M, Okusaka T, Mitsunaga S, et al. Safety and pharmacokinetics of lenvatinib in patients with advanced hepatocellular carcinoma. *Clin Cancer Res* 2016; **22**: 1385–94.
- 32 Lencioni R, Montal R, Torres F, et al. Objective response by mRECIST as a predictor and potential surrogate end-point of overall survival in advanced HCC. *J Hepatol* 2017; **66**: 1166–72.
- 33 Meyer T, Palmer DH, Cheng AL, Hocke J, Loembé AB, Yen CJ. mRECIST to predict survival in advanced hepatocellular carcinoma: analysis of two randomised phase II trials comparing nintedanib vs sorafenib. *Liver Int* 2017; **37**: 1047–55.

Images of the Month

Gastric Inverted Hyperplastic Polyp Mimicking a Papilla

Shigenaga Matsui¹, Hiroshi Kashida¹ and Masatoshi Kudo¹

Am J Gastroenterol 2018;113:327; doi:10.1038/ajg.2017.498

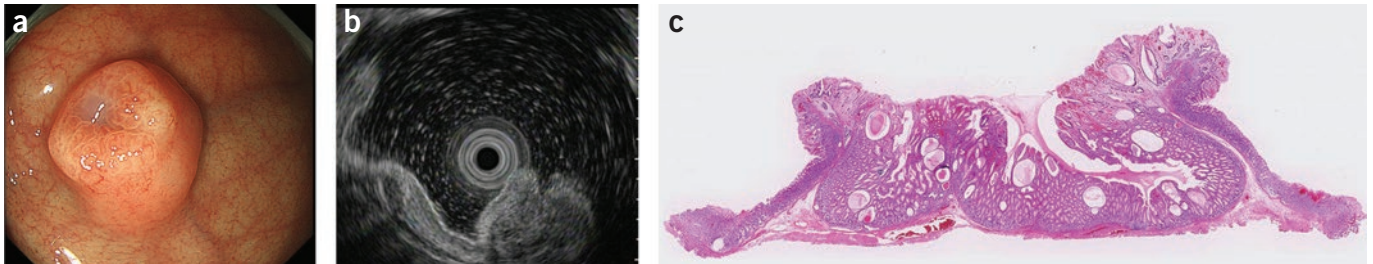


Figure 1. A 37-year-old woman was admitted to our hospital with a gastric submucosal tumor that had been detected in gastrointestinal endoscopy screening. The lesion, 10 mm in diameter, was located at the fornix of the stomach. Milky mucus flowed from a small orifice at the top of the lesion, making it look like a papilla (a). Endoscopic ultrasound revealed a heterogeneous lesion containing small cystic areas, located in the third layer of the gastric wall (b). Endoscopic submucosal dissection (ESD) was performed to remove the lesion en bloc. Pathologically, the lesion was covered with invertedly proliferating columnar epithelium and was composed primarily of hyperplastic foveolar-type glands with focal dilatation of the cystic duct (c). Therefore, the final diagnosis was gastric inverted hyperplastic polyp (GIHP) without adenocarcinoma. A GIHP is a rare entity characterized by the downward growth of hyperplastic mucosal components into the submucosal layer. It is usually asymptomatic and found incidentally. Endoscopic ultrasound is useful for the diagnosis of GIHP. Although basically benign, GIHPs tend to harbor foci of adenocarcinoma. Therefore, en bloc resection with ESD is the treatment of choice, enabling adequate pathological assessment. (Informed consent was obtained from the patient to publish these images.)

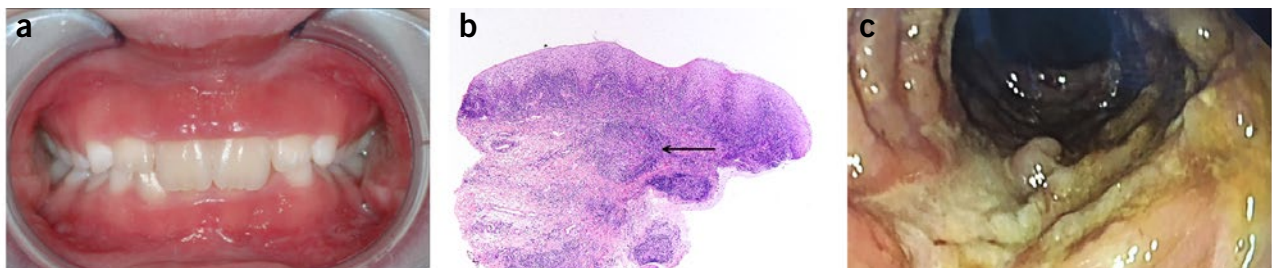
¹Department of Gastroenterology and Hepatology, Kindai University Faculty of Medicine, Osaka-Sayama, Osaka, Japan

Gingival Hyperplasia as a Presenting Symptom of Crohn's Disease in a Teenager

N. Hoogenes¹, S.C. Kommers², K.H.N. de Boer³, A.L. Görts⁴, E.A.J.M. Schulten² and T.G.J. de Meij¹

Am J Gastroenterol 2018;113:328; doi:10.1038/ajg.2017.472

Figure 1. A 10-year-old girl without relevant medical history was referred to an oral and maxillofacial surgeon for evaluation of progressive



gingival hyperplasia. On physical examination, hyperplastic and hyperemic gingiva of the maxilla and mandible was observed (a). Histopathologic examination of a gingival biopsy showed extensive inflammation and granulomas (b; the arrow indicates a granuloma). The patient was referred to a pediatric gastroenterologist for suspicion of inflammatory bowel disease. She reported having had abdominal pain for several weeks and passage of soft stools without blood up to three times per day, without weight loss. Laboratory analysis revealed iron-deficiency anemia (hemoglobin level 8.0 mmol/l, mean cellular volume 72 fl, serum iron 6.8 mol/l, ferritin 22 µg/l) with elevated levels of C-reactive protein (58 mg/l) and fecal calprotectin (>3000 µg/g). Ileocolonoscopy revealed inflammation with longitudinal ulcers and skip lesions throughout the colon, including ileal involvement (c); esophagogastroduodenoscopy was normal. A diagnosis of Crohn's disease was based on macroscopic and histopathologic (chronic active inflammation) features. Exclusive enteral nutrition and azathioprine were initiated for induction of remission and maintenance therapy, respectively. Gastrointestinal and oral symptoms resolved completely within several months. This case illustrates that gingival hyperplasia can be the presenting symptom of Crohn's disease. (Informed consent was obtained from the patient's guardians to publish these images.)

¹Department of Pediatric Gastroenterology, VU University Medical Center, Amsterdam, The Netherlands; ²Department of Oral and Maxillofacial Surgery, VU University Medical Center/Academic Center for Dentistry Amsterdam (ACTA), Amsterdam, The Netherlands; ³Department of Gastroenterology, VU University Medical Center, Amsterdam, The Netherlands; ⁴Department of Pathology, VU University Medical Center, Amsterdam, The Netherlands

Transarterial chemoembolization with miriplatin vs. epirubicin for unresectable hepatocellular carcinoma: a phase III randomized trial

Masafumi Ikeda¹ · Masatoshi Kudo² · Hiroshi Aikata³ · Hiroaki Nagamatsu⁴ · Hiroshi Ishii⁵ · Osamu Yokosuka⁶ · Takuji Torimura⁷ · Manabu Morimoto⁸ · Kenji Ikeda⁹ · Hiromitsu Kumada⁹ · Tosiya Sato¹⁰ · Ikuko Kawai¹¹ · Toru Yamashita¹¹ · Hiroshi Horio¹¹ · Takuji Okusaka¹² · Miriplatin TACE Study Group

Received: 9 February 2017 / Accepted: 21 July 2017 / Published online: 1 August 2017
© The Author(s) 2017. This article is an open access publication

Abstract

Background This prospective study investigated the superiority of transarterial chemoembolization (TACE) with miriplatin over TACE with epirubicin regarding overall survival (OS) in patients with unresectable hepatocellular carcinoma (HCC).

Methods Patients with unresectable HCC were randomized 1:1 to receive TACE with miriplatin or epirubicin in lipiodol. The primary endpoint was OS; secondary endpoints were percentages of patients who achieved treatment effect (TE) 4 (100% necrotizing effect or tumor reduction), duration of time to TACE failure, and adverse events (AEs). OS was compared using a stratified log-rank test adjusted for clinical stage, Child–Pugh class, and institution.

Results Of 257 patients enrolled from August 2008 to August 2010, 247 were analyzed for efficacy and toxicity

(miriplatin, $n = 124$; epirubicin, $n = 123$). Baseline characteristics were well balanced between the two groups. Median OS times were 1111 days for miriplatin and 1127 days for epirubicin (adjusted hazard ratio 1.01, 95% confidence interval 0.73–1.40, $P = 0.946$). TE4 rates were 44.4% for miriplatin and 37.4% for epirubicin. Median times to TACE failure were 365.5 days for miriplatin and 414.0 days for epirubicin. AEs of grade 3 or higher, including elevated aspartate aminotransferase (miriplatin, 39.5%; epirubicin, 57.7%) and elevated alanine aminotransferase (miriplatin, 31.5%; epirubicin, 53.7%), were less frequent in the miriplatin than the epirubicin group.

Conclusions OS after TACE with miriplatin was not superior to that after TACE with epirubicin; however, hepatic AEs were less frequent with miriplatin.

Clinical Trial Registration: JapicCTI-080632.

Electronic supplementary material The online version of this article (doi:10.1007/s00535-017-1374-6) contains supplementary material, which is available to authorized users.

✉ Masafumi Ikeda
masikeda@east.ncc.go.jp

¹ Department of Hepatobiliary and Pancreatic Oncology, National Cancer Center Hospital East, 6-5-1 Kashiwanoha, Kashiwa, Chiba 277-8577, Japan

² Department of Gastroenterology and Hepatology, Faculty of Medicine, Kindai University, Osaka, Japan

³ Department of Gastroenterology and Metabolism, Hiroshima University, Hiroshima, Japan

⁴ Department of Hepatology, Yame General Hospital, Fukuoka, Japan

⁵ Hepatobiliary and Pancreatic Section, Gastroenterological Division, The Cancer Institute Hospital of JFCR, Tokyo, Japan

⁶ Department of Gastroenterology and Nephrology, Chiba University, Chiba, Japan

⁷ Division of Gastroenterology, Department of Medicine, Kurume University School of Medicine, Fukuoka, Japan

⁸ Gastroenterological Center, Yokohama City University Hospital Medical Center, Kanagawa, Japan

⁹ Department of Hepatology, Toranomon Hospital, Tokyo, Japan

¹⁰ Department of Biostatistics, Kyoto University School of Public Health, Kyoto, Japan

¹¹ Sumitomo Dainippon Pharma Co., Ltd, Osaka, Japan

¹² Department of Hepatobiliary and Pancreatic Oncology, National Cancer Center Hospital, Tokyo, Japan

Keywords Carcinoma · Hepatocellular · Chemoembolization · Therapeutic · Miriplatin · Epirubicin · Randomized controlled trial

Introduction

The strategy for treatment of hepatocellular carcinoma (HCC) is determined by tumor characteristics and liver function, and may include resection, local ablative therapy, transarterial chemoembolization (TACE), chemotherapy, or radiotherapy. TACE is currently the mainstay of unresectable HCC and has been shown to significantly prolong survival in several randomized controlled trials compared with chemotherapy alone [1] or conservative treatment [2, 3]. Meta-analyses have also demonstrated a clear survival benefit of TACE for unresectable HCC [4, 5]. Therefore, TACE has been acknowledged as a palliative treatment for unresectable HCC. Conventional TACE, administered with lipiodol and chemotherapeutic agents followed by an embolic material such as a gelatin sponge particles, is widely used as standard treatment in Asian countries including Japan; TACE with drug-eluting beads is often used in Western countries. Epirubicin, doxorubicin, mitomycin C, and cisplatin are common in conventional TACE, but the effects on overall survival (OS) and complete response rate of these agents in this context are unknown. Epirubicin is currently approved for TACE in Japan, where it is most widely used with lipiodol to treat unresectable HCC [6].

Miriplatin, (SP-4-2)-[(1*R*,2*R*)-cyclohexane-1,2-diamine-*N,N'*]bis(tetradecanoato-*O*)platinum monohydrate, is a third-generation lipophilic platinum derivative developed to treat HCC via hepatic artery administration as a sustained-release suspension with lipiodol [7]. Miriplatin is retained in local tumors with lipiodol and slowly releases an active platinum drug for a persistent antitumor effect; little transfer occurs to the systemic circulation, and systemic adverse events (AEs) are reduced. A phase I study of miriplatin with lipiodol indicated a recommended dose of 20 mg/mL with 6 mL of lipiodol [8], and an early phase II study of miriplatin with lipiodol showed a promising anticancer effect with a mild toxicity profile in patients with unresectable HCC [9]. In a randomized late phase II study, the efficacy of miriplatin with lipiodol was similar to that of zinstatin stimalamer (SMANCS®) [10], another lipophilic anticancer agent used to treat unresectable HCC in Japan [11, 12]. Subsequently, miriplatin was approved as a chemolipiodolization agent in Japan in October 2009. A pilot study of TACE with miriplatin showed no severe AEs and a good antitumor effect in patients with HCC [13]. TACE with miriplatin is anticipated to be more effective and less toxic than conventional TACE with epirubicin.

This study aimed to determine the superiority of TACE with miriplatin over TACE with epirubicin, in terms of OS, in patients with unresectable HCC.

Methods

Study design

This prospective, multicenter, open-label, randomized phase III trial was conducted between August 2008 and August 2010, and compared TACE with miriplatin vs. TACE with epirubicin in patients with unresectable HCC. The primary endpoint was OS. Secondary endpoints were the proportion of patients showing treatment effect (TE) 4 (100% necrosis or reduction of the treated tumor), time to TACE failure, and AEs. This study was registered with the Japanese Pharmaceutical Information Center (JapicCTI-080632) and was conducted in full accordance with the guidelines for Good Clinical Practice and the Declaration of Helsinki. Written informed consent was obtained from each participant; the protocol and any modifications were from an institutional review board for each participating site.

Eligibility criteria

Included in the study were patients aged at least 20 years having histologically or clinically (e.g., angiography and computed tomography [CT]) diagnosed HCC; measurable disease (i.e., a lesion having at least 10 mm as its longest diameter, measurable in two dimensions with dynamic CT); tumor stains on dynamic CT (arterial phase); no indications for hepatectomy, percutaneous ethanol injection, percutaneous microwave coagulation, or radiofrequency ablation; tumor, lymph node, metastases (TNM) stage II or III by the classification of Liver Cancer Study Group of Japan (LCSGJ) (e.g., tumor size greater than 2 cm, multiple tumors, or both) [14, 15]; Child–Pugh class A or B; liver damage grade A or B (classified by ascites, serum bilirubin, albumin, indocyanine green retention at 15 min, and prothrombin time) [14, 15]; sufficient organ function; a white blood cell count of at least 3000/ μ L; a platelet count of at least 5.0×10^4 / μ L; serum total bilirubin of less than 3.0 mg/dL; and an Eastern Cooperative Oncology Group performance status (ECOG PS) of 0–2.

Exclusion criteria were hypersensitivity to iodine-containing drug/contrast medium, gelatin-containing injection product or food, or epirubicin or platinum; thyroid disease requiring any treatments or renal failure requiring dialysis; history of myocardial infarction or arrhythmia requiring treatment; active concomitant cancer; obvious tumor thrombosis in the bile duct, portal vein, or hepatic vein;

history of previous TACE; systemic chemotherapy; and history of treatment within 4 weeks prior to giving informed consent for this study.

Treatment method

Eligible patients were temporarily registered and allocated to the miriplatin and epirubicin groups at a ratio of 1:1 with open-label, dynamic allocation before undergoing angiography. The final registration was completed by each participating investigator after confirmation of the following conditions by angiographic findings: intrahepatic lesions showing tumor staining that were fed by an appropriate artery for catheter insertion; no evidence of tumor thrombosis in the main portal or hepatic vein; and no evidence of severe intrahepatic arterio-venous shunt. Stratification factors were TNM stage of LCSGJ, Child–Pugh class, and institution. TACE was performed using the Seldinger technique. The dose of anticancer agents was determined according to tumor size. Maximum doses were defined as 120 mg/person for miriplatin (MIRIPLA[®]; Sumitomo Dainippon Pharma, Japan) and 60 mg/person for epirubicin (Farmorubicin[®]; Pfizer, USA). Patients allocated to the miriplatin group were given miriplatin suspended in 6 mL of lipiodol (20 mg/mL). Patients allocated to the epirubicin group were given epirubicin in 6 mL of solution suspended with 6 mL of lipiodol (10 mg/mL). Embolization was achieved using 1- or 2-mm porous gelatin particles (Gelpart[®], Nippon Kayaku, Japan) from the feeding artery (both groups) according to the tumor size and vascular diameter (upper limit 80 mg/session). Tumor response was evaluated by dynamic CT at 5 and 12 weeks after each TACE session. TACE was repeated when the accumulation of lipiodol in the treated tumor was insufficient and tumor staining or new lesions were seen by follow-up dynamic CT evaluation. During periods of treatment, TACE was repeated on an as-needed basis until discontinuation criteria were met or a maximum of 3 years after the first session of TACE; TACE was administered repeatedly as indicated at minimum intervals of 4 weeks. The criteria for administration of subsequent treatments were as follows: Child–Pugh class A or B; liver damage grade A or B; sufficient organ function; ECOG PS of 0–2; no hypersensitivity to iodine-containing contrast medium, gelatin, epirubicin, or platinum; and no obvious tumor thrombosis in the bile duct or portal/hepatic veins. Discontinuation of treatment occurred when less than 50% of the necrotizing effect was achieved in the target lesion and enlargement of at least 25% occurred in the treated tumor; or when sufficient recovery from previous TACE to meet the criteria of subsequent TACE could not be expected. Completion of protocol treatments with TACE was defined as not meeting discontinuation criteria or a maximum of 3 years after the

first session of TACE. After termination of protocol treatment, any other anticancer treatments, including hepatic arterial infusion chemotherapy, systemic chemotherapy, and, radiotherapy, could be administered.

Efficacy and safety evaluation

OS time was calculated as the period from the first day of administration until death from any cause or last follow-up. The TE after the first administration was judged using the response criteria proposed by LCSGJ [15], in which lipiodol accumulation in the tumor is regarded as an indication of necrosis. TE was defined as follows: TE4, 100% necrosis or 100% reduction in size of all targeted tumors; TE3, at least 50% or less than 100% of tumor necrotizing effect or tumor size reduction rate, respectively; TE2, effects other than TE3 or TE1; TE1, greater than 25% tumor enlargement, regardless of the necrotizing effect. The tumor responses were evaluated in a blinded manner by an external committee for efficacy evaluation. Time to TACE failure was defined as the period from the first day of TACE administration to the completion or discontinuation of the treatment protocol. If the date of completion or discontinuation could not be confirmed, the date of the final hospital visit was used as the end date of completion or discontinuation. Specified laboratory tests were performed at 3 and 7 days, then 2, 3, 5, and 12 weeks, and AEs were evaluated throughout TACE treatment using the Common Terminology Criteria for Adverse Events (CTCAE) v3.0. OS and time to TACE failure was calculated using the Kaplan–Meier method.

Statistical analysis

The primary analysis compared the OS in the miriplatin group with that of the epirubicin group with a stratified log-rank test adjusted for clinical stage, Child–Pugh class, and institution. A hazard ratio (HR) was generated with a stratified Cox regression model. A subgroup analysis of OS by patient background was also conducted. The study population was defined as the full analysis set (FAS), including any patients who received at least one course of the study treatment. The 2-year survival rate with miriplatin was estimated to be 76–80%, as informed by a 2-year survival rate of 75.9% in a randomized phase II study of miriplatin without embolization [10] and a somewhat expected increase in survival when used in combination with embolization. The 2-year survival rate of patients treated with epirubicin was assumed to be 63%, as informed by results of a study using doxorubicin [3] and a Japanese multicenter prospective cohort study [16]. Assuming a 2-year survival rate of 76–80% in patients treated with miriplatin and 63% in those treated with

epirubicin, a total of 200 patients were needed to verify the superiority of miriplatin over epirubicin using a two-sided significance level of 5% and 80% power. To account for the potential loss of patients to follow-up, the number of planned patients enrolled was set at 220. Statistical Analysis System (SAS Institute Inc., Cary, NC, USA) version 9.2 was used for all statistical analyses.

Results

Patient disposition and characteristics

Of the 257 patients enrolled at 29 participating hospitals, 129 and 128 patients were allocated to the miriplatin and epirubicin groups, respectively. Of these, 124 and 123 patients in the miriplatin and epirubicin groups, respectively, were included in the FAS (Fig. 1). Baseline characteristics were well balanced between the two groups (Table 1).

Mean numbers of TACE sessions following the protocol were 2.1 and 2.2 in the miriplatin group and epirubicin group, respectively. Median total doses of drugs administered were 120.0 mg and 61.6 mg in the miriplatin group

and epirubicin group, respectively. The protocol was discontinued in 103 patients in each group. The need for other treatment for residual or recurrent HCC was the most frequent reason for discontinuation, which was applied to 66 miriplatin patients (53.2%) and 67 epirubicin patients (54.5%) in the epirubicin group.

After termination of protocol treatment, 95 patients in the miriplatin and 96 in the epirubicin group underwent the following treatments: hepatic resection (zero and one patient, respectively), percutaneous ethanol injection (one and one, respectively), TACE with miriplatin (17 and 14, respectively), TACE with epirubicin (38 and 34, respectively), and TACE with another drug (11 and 15, respectively).

Efficacy analysis

At the time of final analysis, 71 and 75 patients had died in the miriplatin and epirubicin groups, respectively. The median survival time and 2-year/3-year survival rates were 1111 days (miriplatin group; 95% confidence interval [CI] 888–1390) vs. 1127 days (epirubicin group; 95% CI 995–1300), 67% (miriplatin group; 95% CI 58–75) vs. 76% (epirubicin group; 95% CI 68–83), and 50% (miriplatin

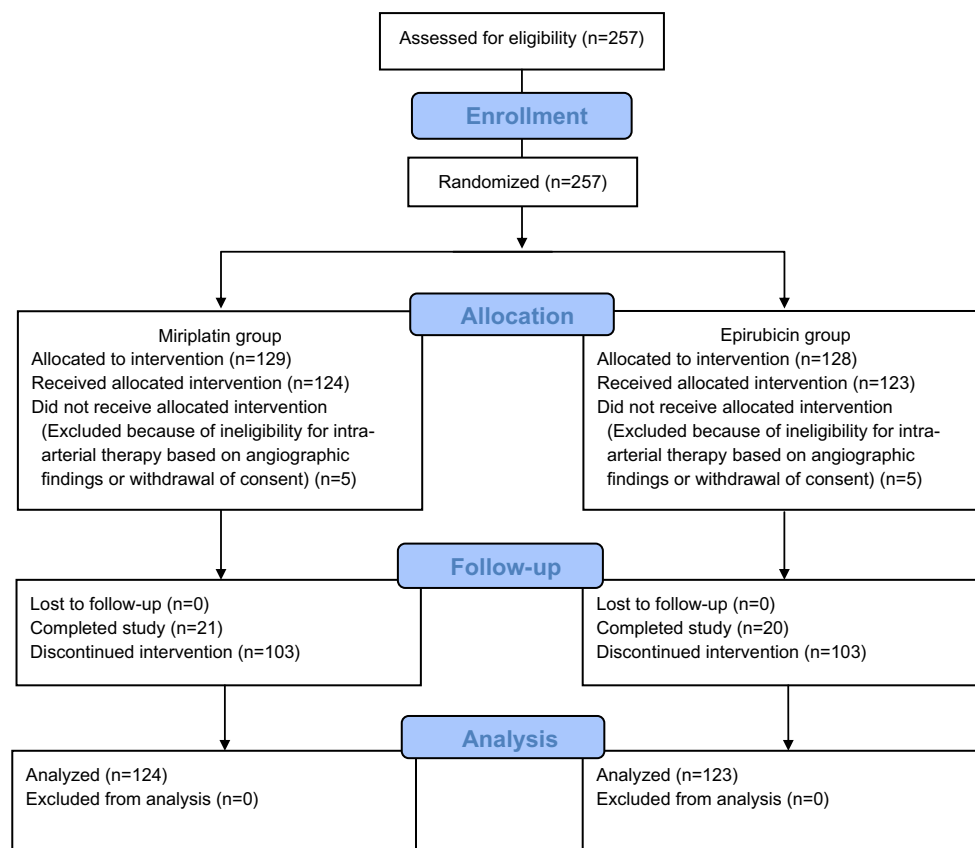


Fig. 1 Patient allocation

Table 1 Patient characteristics

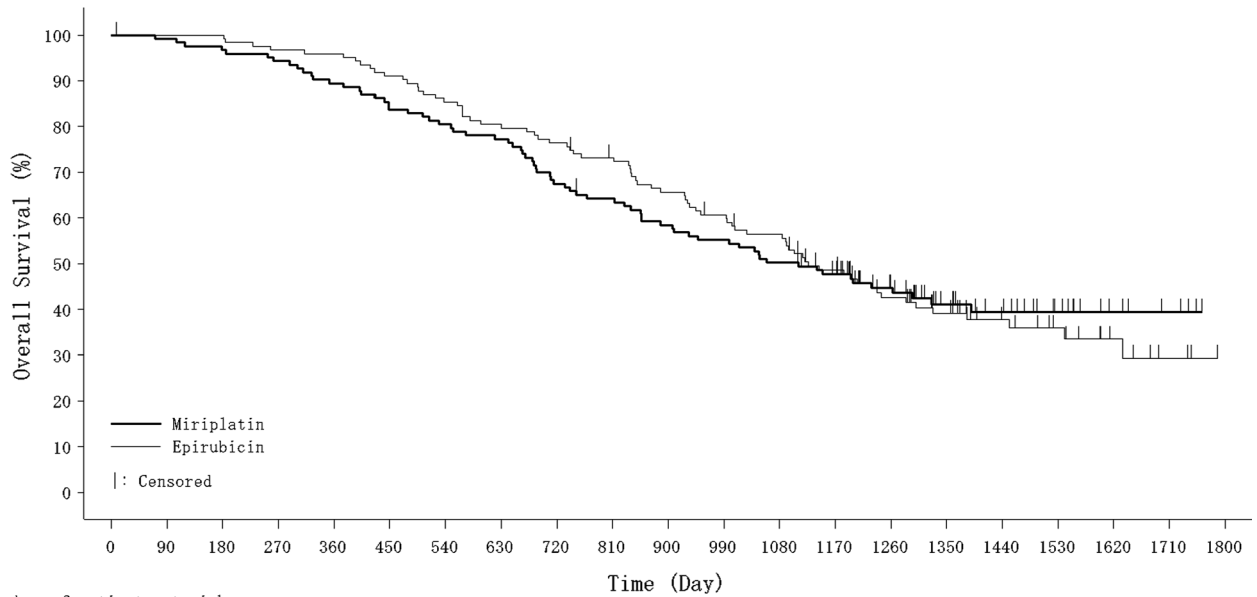
	Miriplatin group (n = 124)		Epirubicin group (n = 123)	
	No.	%	No.	%
Sex				
Male	92	74.2	92	74.8
Female	32	25.8	31	25.2
Age, years				
Median	72		71	
Range	46–86		40–87	
ECOG performance status				
0	116	93.5	114	92.7
1	7	5.6	5	4.1
2	1	0.8	4	3.3
Hepatitis viral infection				
HBs antigen-positive	15	12.1	17	13.8
HCV antibody-positive	71	57.3	77	62.6
Child–Pugh classification				
A	104	83.9	105	85.4
B	20	16.1	18	14.6
Tumor stage				
I	1	0.8	0	0
II	57	46.0	56	45.5
III	66	53.2	67	54.5
Previous treatment before TACE				
Hepatic resection	23	18.5	25	20.3
Local ablation	24	19.5	39	31.5
Other	1	0.8	2	1.6
None	86	69.4	79	64.2
Maximum tumor size (mm)				
Median	30.5		27.0	
Range	10.0–127.0		10.0–137.2	
No. of tumors				
Single	24	19.4	24	19.5
Multiple	100	80.6	99	80.5
Tumor distribution				
Single-segment	42	33.9	46	37.4
Multi-segment	82	66.1	77	62.6
AFP (ng/dL)				
Median	25.1		22.8	
Range	1–71,180		2–82,739	

AFP alpha-fetoprotein, HBs hepatitis B surface, HCV hepatitis C virus, ECOG Eastern Cooperative Oncology Group

group; 95% CI 41–59) vs. 53% (epirubicin group; 95% CI 44–61), respectively (Fig. 2). The predefined stratified HR for OS by the Cox model adjusted for clinical stage and Child–Pugh class for miriplatin to epirubicin was 1.01 (95% CI 0.73–1.40), and the *P* value by log-rank test for the comparison of OS in the two groups gave a two-sided *P* value of 0.946. After the first session of TACE, TE4 was observed in 55 patients (44.4%) in the miriplatin group and

46 patients (37.4%) in the epirubicin group (*P* = 0.184). The median time to TACE failure was 365.5 days (95% CI 258–449) in the miriplatin group and 414.0 days (95% CI 335–507) in the epirubicin group (*P* = 0.250) (Fig. 3).

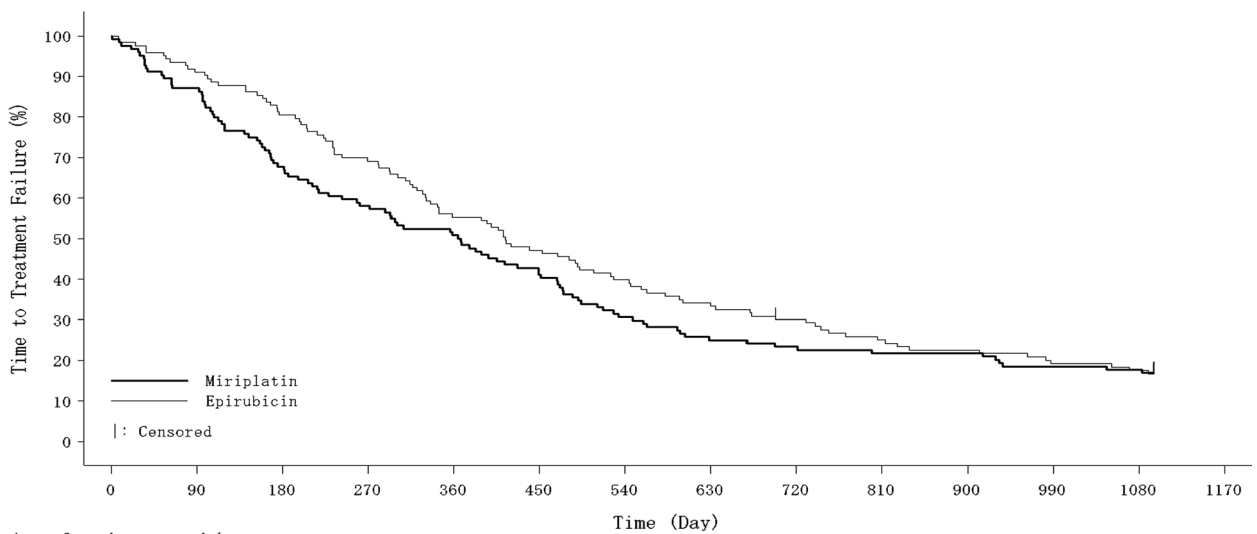
In the prespecified subgroup analysis of OS by patient background, the OS in patients in the epirubicin group who had previous HCC treatment was longer than that of similarly treated patients in the miriplatin group (Fig. 4). No



The number of patients at risk

Treatment	0d	90d	180d	270d	360d	450d	540d	630d	720d	810d	900d	990d	1080d	1170d	1260d	1350d	1440d	1530d	1620d	1710d	1800d
Miriplatin	124	122	119	116	110	103	99	95	83	78	71	67	61	55	41	28	22	14	7	4	0
Epirubicin	123	123	123	119	118	112	105	99	94	88	79	72	66	53	40	32	21	15	8	3	0

Fig. 2 Overall survival rates in the miriplatin and epirubicin groups



The number of patients at risk

Treatment	0d	90d	180d	270d	360d	450d	540d	630d	720d	810d	900d	990d	1080d	1170d
Miriplatin	124	108	84	72	63	51	38	31	29	27	27	23	22	0
Epirubicin	123	112	99	85	68	58	49	42	36	30	27	23	21	0

Fig. 3 Time to TACE failure in the miriplatin and epirubicin groups

significant differences in OS between the groups were seen in the subgroup analysis.

Adverse events

Table 2 shows the AEs in both groups for all protocol sessions of TACE. Symptoms of so-called post-embolization syndrome, such as fever, abdominal pain, and nausea, were frequently observed in both groups (Table 2).

Decreased white blood cell count, fever, and increased alanine aminotransferase (ALT) were observed more frequently in the epirubicin group than the miriplatin group. Severe AEs of grade 3 or higher developed in 94 (75.8%) and 106 (86.2%) patients in the miriplatin and epirubicin groups, respectively; among these, at least grade 3 increased ALT and increased aspartate aminotransferase (AST) were observed less frequently in the miriplatin group (ALT, 31.5%; AST, 39.5%) than in the epirubicin

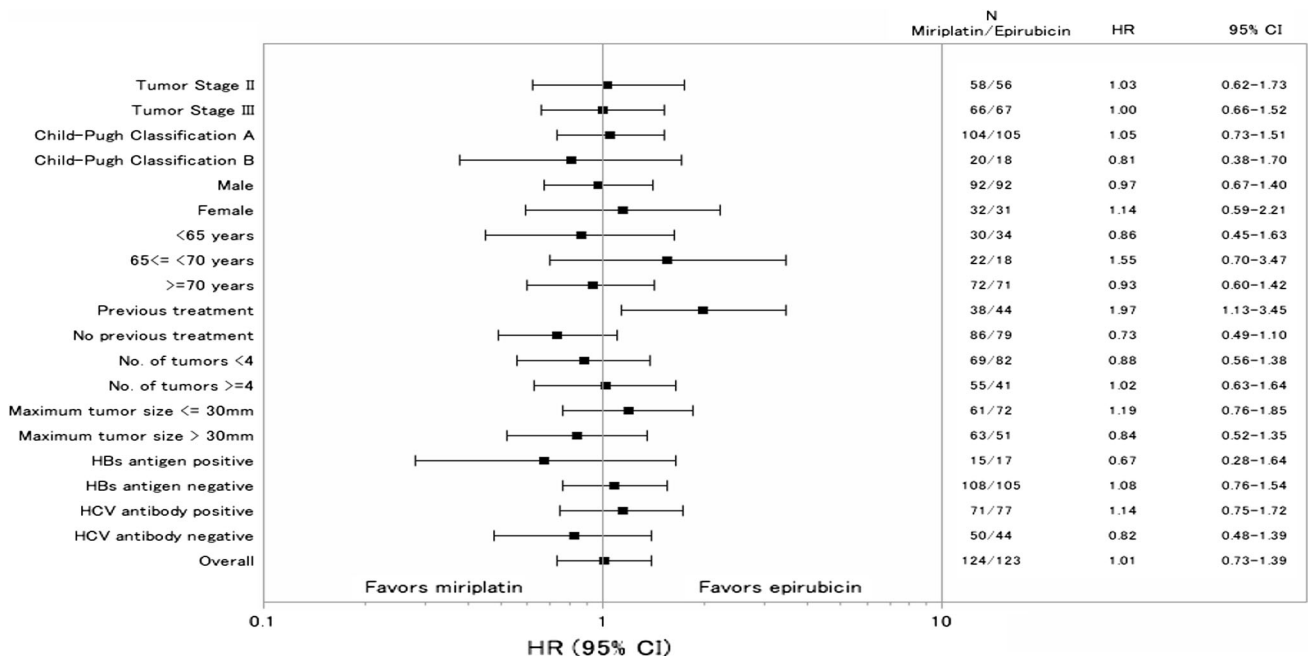


Fig. 4 Subgroup analysis of overall survival rates in the miriplatin and epirubicin groups

Table 2 Adverse events for all protocol sessions of TACE according to treatment group

	Miriplatin group (n = 124)		Epirubicin group (n = 123)		P value*				
	All grades		All grades						
	n	%	n	%					
Hematological toxicity									
Eosinophil count increased	108	87.1	1	0.8	47	38.2	0	0	1.000
Platelet count decreased	76	61.3	14	11.3	85	69.1	20	16.3	0.274
Neutrophil count increased	56	45.2	0	0	58	47.2	0	0	–
White blood cell decreased	55	44.4	1	0.8	76	61.8	10	8.1	0.005
Neutrophil decreased	54	43.5	11	8.9	58	47.2	16	13.0	0.316
Hemoglobin decreased	70	56.5	1	0.8	68	55.3	3	2.4	0.370
White blood cell increased	52	41.9	0	0	45	36.6	0	0	–
Non-hematological toxicity									
Fever	117	94.4	2	1.6	123	100.0	1	0.8	1.000
Abdominal pain	80	64.5	1	0.8	94	76.4	3	2.4	0.370
Nausea	55	44.4	0	0	67	54.5	1	0.8	0.498
ALT increased	103	83.1	39	31.5	114	92.7	66	53.7	<0.001
AST increased	103	83.1	49	39.5	109	88.6	71	57.7	0.005
Glycemia increased	102	82.3	22	17.7	84	68.3	14	11.4	0.207
Hypoalbuminemia	97	78.2	1	0.8	98	79.7	0	0	1.000
Hyponatremia	77	62.1	6	4.8	63	51.2	9	7.3	0.439
Blood bilirubin increased	74	59.7	3	2.4	84	68.3	7	5.7	0.216

Grading according to the Common Terminology Criteria for Adverse Events, v3.0

ALT alanine aminotransferase, AST aspartate aminotransferase

* P values were calculated using two-sided Fisher’s exact test for grade ≥3 adverse events

group (ALT, 53.7%; AST, 57.7%) (AST, P = 0.005; ALT, P < 0.001). Clinically significant treatment-related serious AEs were cholangitis and liver abscess (one patient each)

in the miriplatin group and hemorrhagic gastric ulcer, bacillemia, and septic shock (one patient each) in the epirubicin group. One treatment-related death due to an

HCC rupture with hemorrhagic ascites on day 48 after the sixth TACE session occurred in the epirubicin group; no treatment-related death occurred in the miriplatin group. Almost all severe AEs developed initially following the first session of TACE; no cumulative AEs developed in this series. No hepatic injuries necessitating discontinuation occurred in the miriplatin group, whereas hepatic failure and bile duct stenosis each occurred in one patient in the epirubicin group.

Delayed fever of at least 1 week after treatment was a miriplatin-specific AE (Table S1). After the first session of TACE, the incidence of fever that developed within at most 7 days did not differ significantly between groups (miriplatin, 111 patients, 89.5%; epirubicin, 121 patients, 98.4%), while the incidence of fever that developed at least 8 days was significantly higher in the miriplatin group (80 patients, 64.5%) than in the epirubicin group (49 patients, 39.8%). However, this difference decreased as the number of TACE sessions increased. The incidence of eosinophilia following the first session of TACE was also significantly higher in the miriplatin group (105 patients, 84.7%) than the epirubicin group (28 patients, 22.8%). However, no clinical symptoms developed in patients with eosinophilia, and the incidence of eosinophilia also decreased as the number of TACE sessions increased.

Discussion

Miriplatin is a structurally modified lipophilic platinum complex with improved affinity for lipiodol [7]. Miriplatin suspended in lipiodol showed favorable antitumor activities after hepatic arterial administration [17, 18] in animal models with hepatic tumors. Miriplatin is retained preferentially in liver tumors, which gradually release active platinum [8–10]; its low systemic distribution likely reduces systemic adverse effects. We conducted this study to elucidate the superiority of TACE with miriplatin over TACE with epirubicin as a combination chemotherapeutic regimen in patients with unresectable HCC.

Median survival was similar in the two groups, and superiority of TACE with miriplatin over TACE with epirubicin was not shown for the primary endpoint of OS. There was a crossover of treatments in this series: after termination of protocol treatment, 38 patients in the miriplatin group received TACE with epirubicin and 14 patients in the epirubicin group received TACE with miriplatin. Thus, we cannot exclude the possibility that these and other post-protocol treatments, such as hepatic resection and percutaneous ethanol injection, influenced OS. At the planning of this study, the survival rate of patients treated with miriplatin may have been overestimated and that of patients treated with epirubicin may have been

underestimated. The expected 2-year survival rate of TACE with miriplatin in this phase III study was assumed to be 76–80%; however, the actual rate was only 67%. This discrepancy may be explained by differences in patient characteristics: more patients had multiple tumors or large tumor sizes in this study than in the randomized phase II study (Table S2). Conversely, the observed 2-year survival rate of 76% in the epirubicin group in this study was similar to that found in a prospective study of TACE in 99 unresectable HCC patients in Japan and Korea (75%) [19], and was more favorable than the estimate of 63%. Thus, the OS of patients recently treated with TACE plus epirubicin in Japan seems to be longer than that of patients receiving the same treatment in other countries or in earlier reported studies. In several randomized controlled studies comparing various chemotherapeutic agents combined with TACE for unresectable HCC, no survival benefit of the specific agent was demonstrated [20–22]. The combined use of chemotherapeutic agents may not influence TACE treatment.

In this study, the percentage of patients achieving TE4 following TACE did not differ significantly between the two groups (miriplatin, 44.4%; epirubicin, 37.4%); however, the CT evaluations may not have accurately reflected the extent of tumor necrosis because of the artifacts created by iodized oil. The complete response was reported to be 42% in the Asian TACE study mentioned above using anthracycline agents plus lipiodol with embolization [20]; a similar tumor response was observed in this study. Therefore, miriplatin and epirubicin were found to elicit equivalent antitumor effects after TACE, although an additional effect of embolization was observed compared with the TE4 rate (26.5%) following chemolipiodolization with miriplatin in a randomized phase II trial of miriplatin/lipiodol vs. zinstatin stimalamer/lipiodol [10]. Time to TACE failure tended to be shorter in the miriplatin than in the epirubicin group; however, this difference was not statistically significant. Because the stratified HR by the Cox model adjusted for clinical stage and Child–Pugh class was not calculated, the explanation for this remains unknown.

The tolerability of TACE with miriplatin in patients with liver dysfunction was favorable. Incidences of increased AST, ALT, and total bilirubin were lower in the miriplatin group than the epirubicin group. Most patients with unresectable HCC have liver cirrhosis, which is usually associated with compromised hepatic reserve. Therefore, the mild hepatotoxicity of TACE with miriplatin was beneficial for patients with unresectable HCC, considering that TACE was repeated. However, fever that developed at least 1 week after treatment and eosinophilia were also observed in the miriplatin group, mainly during the first sessions of TACE, and the incidence of these events

decreased after more sessions of TACE with miriplatin. No findings were suggestive of anaphylactic reactions and no clinically serious events occurred, and the cause remains unknown. No other miriplatin-specific AEs occurred. The safety of TACE with miriplatin was consistent with the safety profile of miriplatin alone, and the combination was well tolerated.

This study has some limitations. First, miriplatin is a novel lipophilic platinum agent, and our results cannot be generalized to other platinum-based agents such as cisplatin. Second, miriplatin with TACE for treatment of HCC is currently approved only in Japan; therefore, these results cannot be generalized to populations in other countries. Finally, we did not use drug-eluting beads in this study, although these are often used in Western countries. The efficacy of miriplatin combined with drug-eluting beads has not been clarified in this study.

In conclusion, superiority of miriplatin over epirubicin for the OS endpoint was not demonstrated, although hepatic AEs were less frequent with miriplatin. It remains unclear which chemotherapeutic agent is most suitable for combined use with TACE for unresectable HCC.

Acknowledgements This study was supported by Sumitomo Dainippon Pharma Co., Ltd. The sponsor designed the study and collected the data. An employee of the sponsor analyzed the data. The coordinating investigators gave advice to the sponsor.

Author contributions The sponsor contributed to conception, design, and interpretation of this study, and the coordinating investigators gave advice to the sponsor. The data were collected by the sponsor and analyzed by HH. TS provided guidance on data analysis and interpretation. MI, IK, TY, and HH prepared the initial draft of the manuscript and revised it to the final approval of the version to be published. MI, MK, HA, HN, HI, OY, TT, MM, KI, HK, and TO contributed to registration and patient enrollment, prepared subsequent drafts, and approved the final manuscript draft prior to submission.

Compliance with ethical standards

Conflict of interest MI and TO received research Grants from Sumitomo Dainippon Pharma. MK, OY, and TT received speaker's bureau fees and research Grants from Sumitomo Dainippon Pharma. MM received unrestricted Grants from Sumitomo Dainippon Pharma. KI and HK received speaker's bureau fees from Sumitomo Dainippon Pharma. TS received consultant fees from Sumitomo Dainippon Pharma. IK, TY, and HH are employees of Sumitomo Dainippon Pharma. HA, HN, and HI declare that they have no conflict of interest.

Open Access This article is distributed under the terms of the Creative Commons Attribution 4.0 International License (<http://creativecommons.org/licenses/by/4.0/>), which permits unrestricted use, distribution, and reproduction in any medium, provided you give appropriate credit to the original author(s) and the source, provide a link to the Creative Commons license, and indicate if changes were made.

References

1. Lin DY, Liaw YF, Lee TY, et al. Hepatic arterial embolization in patients with unresectable hepatocellular carcinoma—a randomized controlled trial. *Gastroenterology*. 1988;94(2):453–6.
2. Lo CM, Ngan H, Tso WK, et al. Randomized controlled trial of transarterial lipiodol chemoembolization for unresectable hepatocellular carcinoma. *Hepatology*. 2002;35(5):1164–71.
3. Llovet JM, Real MI, Montana X, et al. Arterial embolisation or chemoembolisation versus symptomatic treatment in patients with unresectable hepatocellular carcinoma: a randomised controlled trial. *Lancet*. 2002;359(9319):1734–9.
4. Camma C, Schepis F, Orlando A, et al. Transarterial chemoembolization for unresectable hepatocellular carcinoma: meta-analysis of randomized controlled trials. *Radiology*. 2002;224(1):47–54.
5. Llovet JM, Bruix J. Systematic review of randomized trials for unresectable hepatocellular carcinoma: chemoembolization improves survival. *Hepatology*. 2003;37(2):429–42.
6. Takayasu K. Transarterial chemoembolization for hepatocellular carcinoma over three decades: current progress and perspective. *Jpn J Clin Oncol*. 2012;42(4):247–55.
7. Maeda M, Uchida NA, Sasaki T. Liposoluble platinum(II) complexes with antitumor activity. *Jpn J Cancer Res*. 1986;77(6):523–5.
8. Fujiyama S, Shibata J, Maeda S, et al. Phase I clinical study of a novel lipophilic platinum complex (SM-11355) in patients with hepatocellular carcinoma refractory to cisplatin/lipiodol. *Br J Cancer*. 2003;89(9):1614–9.
9. Okusaka T, Okada S, Nakanishi T, et al. Phase II trial of intra-arterial chemotherapy using a novel lipophilic platinum derivative (SM-11355) in patients with hepatocellular carcinoma. *Invest New Drugs*. 2004;22(2):169–76.
10. Okusaka T, Kasugai H, Ishii H, et al. A randomized phase II trial of intra-arterial chemotherapy using SM-11355 (Miriplatin) for hepatocellular carcinoma. *Invest New Drugs*. 2012;30(5):2015–25.
11. Maeda H, Sawa T, Konno T. Mechanism of tumor-targeted delivery of macromolecular drugs, including the EPR effect in solid tumor and clinical overview of the prototype polymeric drug SMANCS. *J Control Release*. 2001;74(1–3):47–61.
12. Okusaka T, Kasugai H, Shioyama Y, et al. Transarterial chemotherapy alone versus transarterial chemoembolization for hepatocellular carcinoma: a randomized phase III trial. *J Hepatol*. 2009;51(6):1030–6.
13. Ikeda K, Okusaka T, Ikeda M, et al. Transcatheter arterial chemoembolization with a lipophilic platinum complex SM-11355(miriplatin hydrate)—safety and efficacy in combination with embolizing agents. *Gan To Kagaku Ryoho*. 2010;37(2):271–5.
14. Kudo M, Izumi N, Kokudo N, et al. Management of hepatocellular carcinoma in Japan: consensus-based clinical practice guidelines proposed by the Japan Society of Hepatology (JSH) 2010 updated version. *Dig Dis*. 2011;29(3):339–64.
15. The Liver Cancer Study Group of Japan. The general rules for the clinical and pathological study of primary liver cancer. 2nd ed. Tokyo: Kanehara; 2003.
16. Takayasu K, Arai S, Ikai I, et al. Prospective cohort study of transarterial chemoembolization for unresectable hepatocellular carcinoma in 8510 patients. *Gastroenterology*. 2006;131(2):461–9.
17. Hanada M, Baba A, Tsutsumishita Y, et al. Intra-hepatic arterial administration with miriplatin suspended in an oily lymphographic agent inhibits the growth of human hepatoma cells orthotopically implanted in nude rats. *Cancer Sci*. 2009;100(1):189–94.

18. Kishimoto S, Noguchi T, Yamaoka T, et al. Antitumor effects of a novel lipophilic platinum complex (SM-11355) against a slowly-growing rat hepatic tumor after intra-hepatic arterial administration. *Biol Pharm Bull.* 2000;23(3):344–8.
19. Ikeda M, Arai Y, Park SJ, et al. Prospective study of transcatheter arterial chemoembolization for unresectable hepatocellular carcinoma: an Asian cooperative study between Japan and Korea. *J Vasc Interv Radiol.* 2013;24(4):490–500.
20. Kawai S, Tani M, Okamura J, et al. Prospective and randomized trial of lipiodol-transcatheter arterial chemoembolization for treatment of hepatocellular carcinoma: a comparison of epirubicin and doxorubicin (second cooperative study). The Cooperative Study Group for Liver Cancer Treatment of Japan. *Semin Oncol.* 1997;24(2 Suppl 6):S6-38–S6-45.
21. Bronowicki JP, Vetter D, Dumas F, et al. Transcatheter oily chemoembolization for hepatocellular carcinoma. A 4-year study of 127 French patients. *Cancer.* 1994;74(1):16–24.
22. Kasugai H, Kojima J, Tatsuta M, et al. Treatment of hepatocellular carcinoma by transcatheter arterial embolization combined with intraarterial infusion of a mixture of cisplatin and ethiodized oil. *Gastroenterology.* 1989;97(4):965–71.

Ultrasound-ultrasound image overlay fusion improves real-time control of radiofrequency ablation margin in the treatment of hepatocellular carcinoma

Yasunori Minami¹ · Tomohiro Minami¹ · Satoru Hagiwara¹ · Hiroshi Ida¹ · Kazuomi Ueshima¹ · Naoshi Nishida¹ · Takamichi Murakami² · Masatoshi Kudo¹

Received: 2 August 2017 / Revised: 21 October 2017 / Accepted: 30 October 2017 / Published online: 1 December 2017
© European Society of Radiology 2017

Abstract

Objectives To assess the clinical feasibility of US-US image overlay fusion with evaluation of the ablative margin in radiofrequency ablation (RFA) for hepatocellular carcinoma (HCC).

Methods Fifty-three patients with 68 HCCs measuring 0.9–4.0 cm who underwent RFA guided by US-US overlay image fusion were included in this retrospective study. By an overlay of pre-/postoperative US, the tumor image could be projected onto the ablative hyperechoic zone. Therefore, the ablative margin three-dimensionally could be shown during the RFA procedure. US-US image overlay was compared to dynamic CT a few days after RFA for assessment of early treatment response. Accuracy of graded response was calculated, and the performance of US-US image overlay fusion was compared with that of CT using a Kappa agreement test.

Results Technically effective ablation was achieved in a single session, and 59 HCCs (86.8 %) succeeded in obtaining a 5-mm margin on CT. The response with US-US image overlay correctly predicted early CT evaluation with an accuracy of 92.6 % (63/68) ($k = 0.67$; 95 % CI: 0.39–0.95).

Conclusion US-US image overlay fusion can be proposed as a feasible guidance in RFA with a safety margin and predicts early response of treatment assessment with high accuracy.

Key points

- US-US image overlay fusion visualizes the ablative margin during RFA procedure.
- Visualizing the margin during the procedure can prompt immediate complementary treatment.
- US image fusion correlates with the results of early evaluation CT.

Keywords Ablation techniques · Hepatocellular carcinoma · Liver · Neoplasms · Ultrasonography

Abbreviations

3D	Three-dimensional
BCLC	Barcelona clinic liver cancer
CEUS	Contrast-enhanced ultrasonography
HCC	Hepatocellular carcinoma
MDCT	Multidetector CT
MPR	Multiplanar reconstruction
RFA	Radiofrequency ablation
ROI	Region of interest
SD	Standard deviation
US	Ultrasound

Introduction

The local efficacy of radiofrequency ablation (RFA) for small hepatocellular carcinomas (HCCs; i.e., < 2 cm) has been shown to be comparable to that of surgical outcomes [1–4]. However, many studies have reported a trend towards higher recurrence in patients treated by RFA [5–9]. It has been reported that the local recurrence rates after RFA for HCC ranged from 1.7 % to 41 % over the 2–3 years of follow-up [10]. The local recurrence rate differs markedly depending on

✉ Yasunori Minami
minkun@med.kindai.ac.jp

¹ Department of Gastroenterology and Hepatology, Kindai University Faculty of Medicine, 377-2 Ohno-Higashi Osaka-Sayama, Osaka 589-8511, Japan

² Department of Radiology, Kindai University Faculty of Medicine, 377-2 Ohno-Higashi Osaka-Sayama, Osaka 589-8511, Japan

whether or not a 5-mm ablative margin is secured to eradicate potential microscopic invasion [11]. For the RFA procedure to be considered technically successful, the tumour and a sufficient ablative margin (at least 5 mm) must be included in the ablation zone [12]. Unfortunately, a safety margin is not always obtained in RFA therapy [13, 14]. Sonography is often restricted by the formation of gas bubbles showing strong acoustic scatters within the ablation zone, and then an irregular hyperechoic zone visually obscures the targeted tumour [15]. Blind assessments of an ablative margin on ultrasound (US) could result in an insufficient ablative margin, representing a significant risk factor for residual or recurrent HCC tumours [15, 16].

Advances in computer processing and image display have allowed cross-sectional images of CT or MRI volume data to be displayed in the same plane as US in real-time by multiplanar reconstruction (MPR). It has been reported that US-CT/MRI fusion imaging-guided RFA was useful in the treatment of hepatic malignancies that were inconspicuous on B-mode US [17–20]. Recently, the development of image fusion has made it possible to visualize the ablative margin on US [21]. By an overlay of preoperative and postoperative US, the tumour image could be projected onto the white ablation zone in real-time. Therefore, US-US overlay image fusion could show the ablative margin during the RFA procedure. In a good response case, two concentric circles containing the centred tumour within the ablative hyperechoic zone should be shown by US-US image overlay fusion. We hypothesized that this US-US image overlay fusion guidance in RFA could improve safety margin achievement and reduce the risk of local tumour progression. The purpose of this retrospective study was to assess the usefulness of US-US image overlay fusion with evaluation of the ablative margin in RFA for HCC.

Materials and methods

Patient selection and eligibility

Institutional review board approval and informed patient consent regarding the retrospective analysis of the clinical data were obtained for this single-centre study. Diagnosis of HCC was based on the clinical guidelines of the American Association for the Study of Liver Disease following the observation of arterial hyperenhancement with washout on delayed-phase images [22]. The therapeutic decision regarding RFA was made by consensus of the multidisciplinary tumour board before each treatment.

A total of 53 patients with 68 HCCs were treated with RFA between May 2014 and July 2015. The eligibility criteria were: (1) age 18 years or more; (2) proven HCC; (3) eligible for RFA (≤ 3 nodules with a maximum diameter ≤ 3 cm, Barcelona Clinic liver cancer (BCLC) stage 0 to B1; (4)

patient unwilling to undergo hepatectomy or liver transplantation; (5) well-preserved liver function (Child–Pugh score ≤ 8 , serum total bilirubin level ≤ 3 mg/dl and prothrombin time-international normalized ratio ≤ 1.5) and (6) Eastern Cooperative Oncology Group (ECOG) performance status score ≤ 1 . The exclusion criteria were as follows: (1) tumour invasion of major hepatic vessels or extrahepatic metastases; (2) present or past history of uncontrolled ascites, hepatic encephalopathy or variceal bleeding; (3) severe dysfunction of the heart, kidney or other organs; and (4) active infection (except viral hepatitis).

Equipment

An US machine (LOGIQ E9, GE Healthcare, Chalfont St. Giles, UK) coupled with a low magnetic field generator was used. Two electromagnetic position sensors connected with a position-sensing unit were attached on the probe (4.0 MHz curvilinear C1-6, GE Healthcare) through a bracket. Both the transmitter and the sensors were connected to a position-sensing unit embedded in the ultrasound machine. Volume navigation system (V nav, GE Healthcare) delivers real-time image fusion of US with other modalities such as MRI or CT. The standard of volume navigation can serve a function of US-US image overlay fusion.

Patients were treated by RFA (VIVA RF ablation system; STARMed Co., Goyang, Gyeonggi, South Korea). Twenty 1-cm long, 17-gauge, monopolar internally cooled electrodes (VIVA RF electrode; STARMed) were used to deliver radiofrequency energy, and the active metallic tip could be adjusted in 5-mm intervals up to 3 cm long. A 200-W, 480-kHz monopolar radiofrequency generator regulated by impedance (VIVA RF generator, STARMed) and with three styles of power distribution (General, Auto, Continuance modes) was used as the energy source.

US-US image overlay fusion and RFA procedure

Before inserting the radiofrequency needle, the 3D US volume was obtained by scanning the liver in a manual sweeping manner with the patient in a breath-holding position (Fig. 1). The scanning area had to include not only the tumour but also intrahepatic vessels around the tumour. This 3D volume data contained the spatial information in the generated magnetic field. A cross-section of the 3D US volume was selected based on the largest diameter dimension of the tumour, and two green squares on the screen were arranged to fix a perpendicular line through the centre of the tumour image. Six rotated sections passing through the tumour centre were then automatically displayed. A ROI was drawn along the tumour border in each of the rotated sections using the ellipse ROI method, with the result that the tumour border could be traced

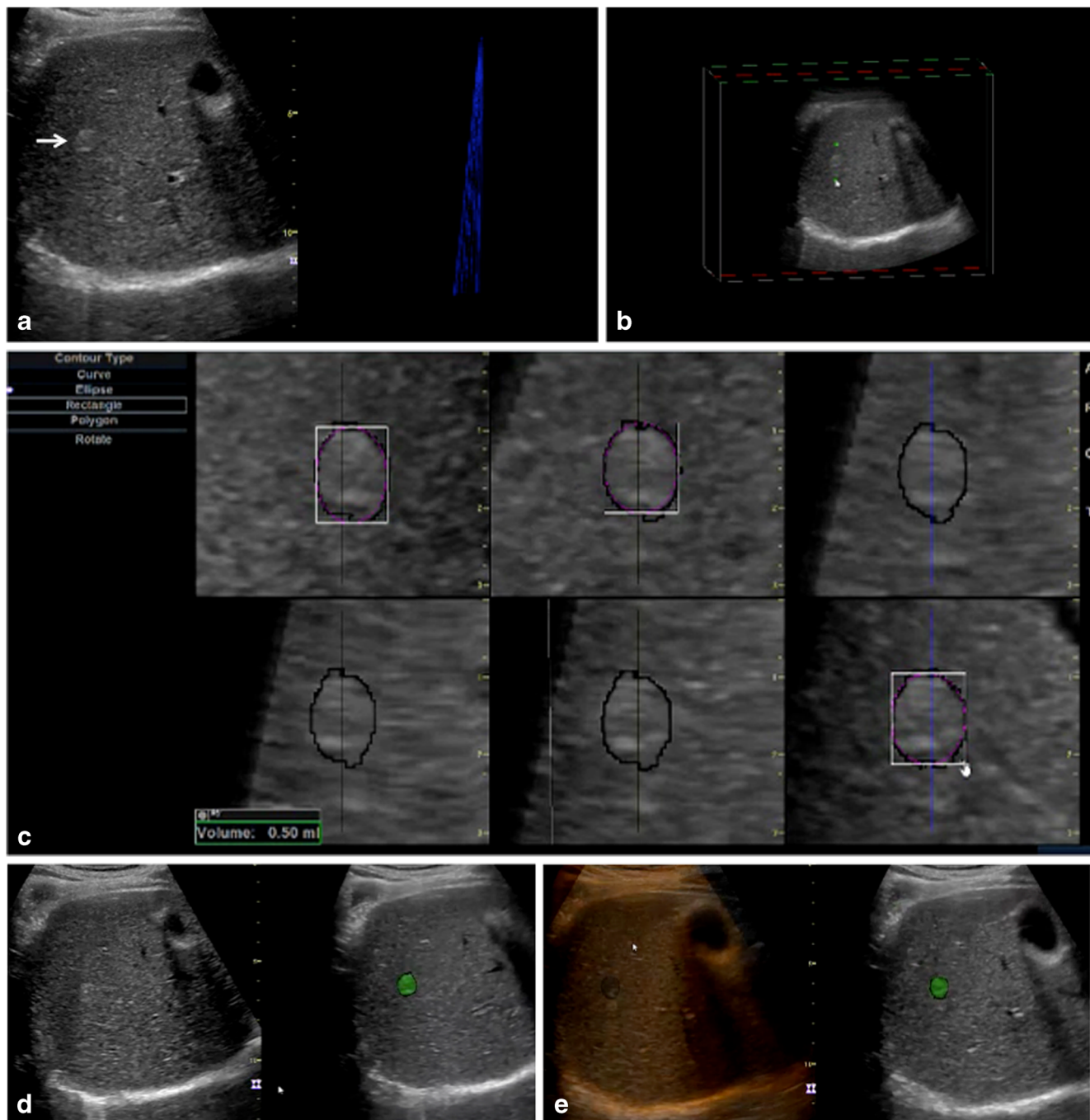


Fig. 1 Image processing of US-US overlay image fusion in a demonstration case. **(A)** The still image during the sweep scanning shows a small hyperechoic nodule (arrow) in the right liver on B-mode (left) and blue cross-sections that depict the trajectory of sweeping the US transducer (right). **(B)** The box image mean 3D volume data of US by sweep scanning. Two green squares are arranged on the perpendicular line through the centre of the hyperechoic nodule. **(C)** The borders of the

hyperechoic nodule are traced in each of six rotated sections using the ellipse region of interest method. **(D)** This US fusion imaging shows the real-time image on B-mode US (left) and the cross-section of 3D US volume data (right). The hyperechoic nodule is shown as green. **(E)** US-US overlay image fusion shows an orange-coloured background image overlaying these two images (left)

three-dimensionally. The interior was colorized, and this 3D US volume data was stored within the US machine.

During and immediately after ablation, the clinical role of US is markedly limited because of the initial hyperechoic ablated zone, the so-called echogenic cloud, and the resultant

acoustic shadowing [23]. When the acoustic shadowing had gradually begun to disappear at the deeper side of the tumour (2–3 min), the 3D US volume data were carefully fused with the real-time 2D US image to the millimetre using a volume navigation system (V nav). The fusion imaging showed the

real-time 2D US image (post-ablation) and MPR US image (pre-ablation) side-by-side. If needed, some landmark markers were marked successively on each image set using a caliper. Thereafter, US-US image overlay could display the ablative hyperechoic zone including the coloured tumour. The image overlay allowed easy visualization of the ablative margin on US. When the ablation zone created with a single ablation was not sufficient to cover the index tumour with an adequate ablative margin, a multiple overlapping ablation technique was applied by replacing the electrode to insufficient ablation sites. After the final ablation, the ablative margin was assessed by US-US image overlay fusion.

All RFA procedures were performed by three experienced hepatologists (M.T, Y.M and H.I, with 6, 20 and 21 years of experience, respectively). The tip length choice for the active RF electrode was 0.5–1.0 cm over the tumour size. Under Auto mode, power was usually begun at 40 W with a 2-cm exposed-tip RF electrode or at 50 W with a 3-cm exposed-RF tip. After a few times of power roll-off, the RFA procedure was terminated if the ablative hyperechoic zone had expanded over the tumour with the safety margin assessed using US-US image overlay fusion.

Imaging data evaluation

A few days after treatment, the technical effectiveness of ablation was assessed with dynamic MDCT using 5-mm slice scans. The patients were classified into four groups as follows: grade A (absolutely curative), a 5-mm or larger ablative margin around the entire tumour; grade B (relatively curative), an ablative margin around the tumour but less than 5 mm in diameter in some places; grade C (relatively non-curative), only an incomplete ablative margin around the tumour although no residual tumour was apparent; grade D (absolutely non-curative), the tumour was not completely ablated [13, 14].

Data are expressed as mean \pm SD. US-US image overlay was compared to dynamic CT a few days after RFA for assessment of early treatment response. The accuracy of graded response was calculated, and the performance of US-US image overlay fusion for the evaluation of early response was compared with that of CT as the gold standard using a Kappa agreement test [24–26]. Statistical analyses were performed by using statistical software (SPSS 12.0; SPSS, Chicago, IL, USA).

Results

Fifty-three patients (39 men, 14 women; age range, 44–91 years; mean age \pm SD, 70.0 \pm 12.0 years) with 68 HCCs were analysed (Table 1). The maximal diameter of the tumours ranged from 0.9 to 4.0 cm (mean \pm SD, 1.8 \pm 0.7 cm) on dynamic CT. Forty-three patients had liver cirrhosis of

Table 1 Baseline clinical characteristics of the patients

Number of patients	53
Sex	
Male	39 (73.6)
Female	14 (26.4)
Age (year)	
Mean \pm SD	70.0 \pm 12.0
Range	44–91
Aetiological cause of HCC	
Hepatitis B	4 (7.5)
Hepatitis C	34 (64.2)
nonBnonC	15 (28.3)
Mean serum albumin level (g/dl)*	3.7 \pm 0.6
Mean serum total bilirubin level (g/dl)*	1.0 \pm 1.0
Child-Pugh class	
A	43 (81.1)
B	10 (18.9)
C	0
Serum AFP level	
< 20 ng/ml	33 (62.2)
20–200 ng/ml	19 (35.8)
> 200 ng/ml	1 (1.9)
Number of HCCs	68
Tumour location	
Left lateral	10 (14.7)
Left medial	8 (11.8)
Right medial	25 (36.8)
Right lateral	22 (45.8)
Segment 1	3 (4.4)
Tumour size (cm)	
Mean \pm SD	1.8 \pm 0.7
Range	0.9–4.0

Unless otherwise stated, data are number of patients or HCCs and data in parentheses are percentages

HCC hepatocellular carcinoma, AFP alpha-fetoprotein

*Data are means \pm standard deviation

Child-Pugh class A and the remaining eight had Child-Pugh class B cirrhosis. Nineteen patients with 26 HCCs had not previously been treated for these hepatic lesions. The remaining 34 patients with 42 HCCs had previously been treated by RFA at other sites in the liver. No patient had shown local tumour progression after various therapies.

Technically effective ablation was achieved in a single session in all patients, and the total number of RF needle insertions for ablation was 1.9 \pm 1.2 (range, 1–8) per tumour. Tumour enhancement completely disappeared in early assessment of treatment response in all patients (Figs. 2 and 3). According to the grading system for early assessment with MDCT, we classified 59 HCCs (86.8 %) as grade A, seven (10.3 %) as grade B, two (2.9 %) as grade C, and none as

grade D. The response category with US-US image overlay correctly predicted the early MDCT response category with an accuracy of 92.6 % (63/68) (Table 2). The kappa coefficient comparing the agreement of dynamic CT and US-US image overlay fusion results was substantial ($k = 0.67$; 95 % confidence interval: 0.39– 0.95).

The mean follow-up was 17.8 ± 7.6 months (median 19 months; range 1–29 months). All procedures were performed successfully without immediate or late complications. During the follow-up period, none of the patients showed local tumour progression. Indeed, we found no local recurrence in patients with nine HCCs presenting grade B or C during the

Fig. 2 Hepatocellular carcinoma in a 57-year-old man in segment VI of the liver. **(A)** Transverse arterial phase CT scan shows a viable hepatocellular carcinoma (HCC) measuring 1.6 cm in diameter (arrow) before radiofrequency ablation (RFA). **(B)** B-mode sonographic image shows a well-circumscribed irregular hyperechoic nodule. **(C)** Right shows a cross-sectional image of 3D US volume before ablation, and the tumour is shown as green. The orange-coloured background indicates real-time overlaying imaging before ablation onto the cross-sectional image after ablation. The overlay image shows the green colorised tumour inside the ablative hyperechoic zone. The ablative margin is then revealed. **(D)** Transverse portal phase CT scan shows that HCC and the surrounding area are not enhanced, indicating complete necrosis of the lesion

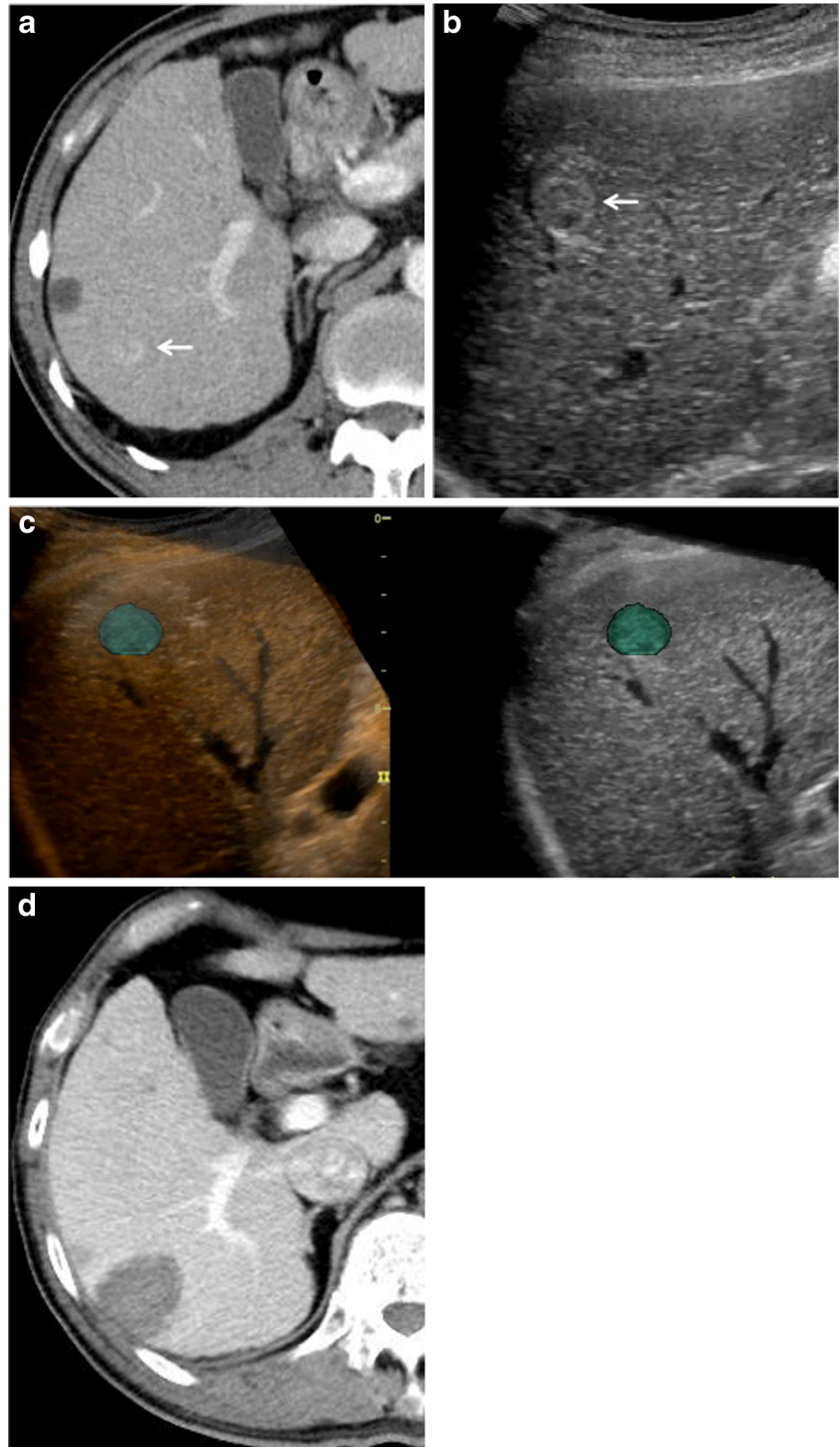
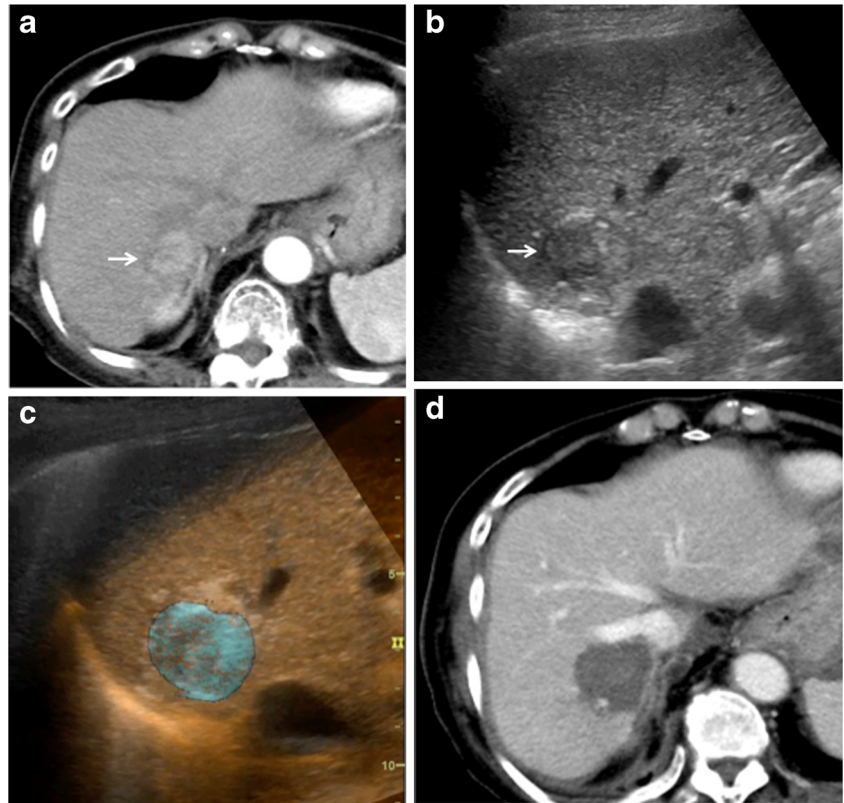


Fig. 3 Hepatocellular carcinoma in an 81-year-old woman in segment VII of the liver. **(A)** Transverse arterial phase CT scan shows a viable hepatocellular carcinoma (HCC) measuring 2.8 cm in diameter (arrow) before radiofrequency ablation (RFA). **(B)** B-mode sonographic image shows a well-circumscribed irregular hypoechoic nodule (arrow). **(C)** US-US overlay image fusion demonstrates the green colorised tumour inside the ablative hyperechoic zone. **(D)** Transverse portal phase CT scan shows that HCC and the surrounding area are not enhanced, indicating complete necrosis of the lesion



follow-up periods of 17–19 months. However, two patients demonstrated distant single metastases in the liver.

Discussion

Usually, the ablative margin cannot be precisely evaluated on B-mode US and/or CEUS immediately after RFA because gas bubbles due to the ablation hide the tumor and the surroundings. Therefore, CT/MRI is commonly used for evaluating the treatment response to local ablation therapy for HCC [11, 22, 27]. However, this US-US image overlay allowed us to evaluate the ablative margin during the RFA procedure. Using a grading system to assess the early response of RFA, Nishikawa et al. reported rates of grades from A (absolutely curative) to D (absolutely non-curative) of 18.2–19.0 %, 42.0–

44.0 %, 27.2–27.5 % and 9.8–12.3 %, respectively [13, 14]. In contrast, our data were classified as 86.8 %, 10.3 %, 2.9 % and 0 %, respectively. The achievement of US-US image overlay fusion guidance supported sufficient margins because we could provide additional ablation more efficiently. We considered the following three features of US-US image overlay fusion as the reasons for our good results: first, the real-time monitoring of the ablating area; second, the effective decision-making regarding additional ablation; third, the confirmation of sufficient ablative margins during the RFA procedure.

Larger HCC had a higher frequency of portal vein invasion and intrahepatic metastases in the surrounding tumour than smaller HCC. Larger tumours require sufficient ablative margins to prevent recurrences by multiple ablations. It is often technically difficult to obtain a sufficient ablative margin over the whole of a large HCC. Many have reported that local

Table 2 Comparison of ultrasound-ultrasound (US-US) overlay image fusion and dynamic CT for early assessment of tumour response after radiofrequency ablation (RFA) for hepatocellular carcinoma (HCC)

US-US overlay image fusion	Dynamic CT				Total
	Grade A	Grade B	Grade C	Grade D	
Grade A	58	2	0	0	60
Grade B	1	5	2	0	8
Grade C	0	0	0	0	0
Grade D	0	0	0	0	0
Total	59	7	2	0	68

recurrence rates increased with larger sizes of tumour in RFA [28–30]. However, we could obtain sufficient ablative margins in HCCs larger than 2 cm, and our data also showed very low rates of local tumour progression.

Many reports indicate that dynamic CT is currently a common technique to assess the early response within one week after RFA [12, 14, 15]. Early detection of residual HCC after RFA is critical and can facilitate successful retreatment. Late diagnosis results in peripheral regrowth and might make retreatment difficult owing to limited access. However, such HCC patients could tend to accumulate radiation exposure.

In addition, MRI for its intrinsic contrast resolution is particularly suitable in ‘identification’ and ‘quantization’ of the necrosis induced by ablative therapies. A further advantage of the combined interpretation of dynamic and hepatobiliary phase MR images was the lower number of false-positive findings compared with those using dynamic MR or CT image sets [31, 32]. However, the use of MRI can be hindered because of the generally high costs, long examination duration and limited availability in this clinical setting.

Furthermore, the diagnostic accuracy of the response category with US-US image overlay fusion was very high, 92.6 %, in this study. If precise image registration adjustment with US-US image overlay fusion can be achieved, contrast-enhanced CT or hepatospecific contrast-enhanced MRI for early response assessment of RFA could potentially be omitted.

The principal limitation of this study was its retrospective design. The second was that this study could suffer from selection bias because the patients were enrolled according to tumour size, number and/or location for RFA indication. Moreover, patients with a poor quality of US image of the liver due to artifacts might have been avoided from enrolling in this study because it was often difficult to adjust the location of intrahepatic vessels between two US images before and after ablation using US-US image overlay. Another limitation was the preliminary nature of the study, with a relatively small number of patients and a short follow-up time. Further prospective studies of this technique with a larger number of patients are warranted.

In conclusion, US-US image overlay fusion could visualize the ablative margin of RFA on US. US-US image overlay fusion guidance can contribute to obtaining sufficient margins for RFA therapy. US-US image overlay fusion could have potential usefulness for predicting the early response of treatment assessment during the RFA procedure.

Funding The authors state that this work has not received any funding.

Compliance with ethical standards

Guarantor The scientific guarantor of this publication is Prof. Masatoshi Kudo.

Conflict of interest The authors of this manuscript declare no relationships with any companies whose products or services may be related to the subject matter of the article.

Statistics and biometry No complex statistical methods were necessary for this paper.

Informed consent Written informed consent was obtained from all subjects (patients) in this study.

Ethical approval Institutional Review Board approval was obtained.

Methodology

- retrospective
- case-control study
- performed at one institution

References

1. Chen MS, Li JQ, Zheng Y et al (2006) A prospective randomized trial comparing percutaneous local ablative therapy and partial hepatectomy for small hepatocellular carcinoma. *Ann Surg* 243:321–328
2. Takayama T, Makuuchi M, Hasegawa K (2010) Single HCC smaller than 2 cm: surgery or ablation? a surgeon's perspective. *J Hepatobiliary Pancreat Sci* 17(4):422–424
3. Wang JH, Wang CC, Hung CH, Chen CL, Lu SN (2012) Survival comparison between surgical resection and radiofrequency ablation for patients in BCLC very early/early stage hepatocellular carcinoma. *J Hepatol* 56(2):412–418
4. Peng ZW, Lin XJ, Zhang YJ et al (2012) Radiofrequency ablation versus hepatic resection for the treatment of hepatocellular carcinomas 2 cm or smaller: a retrospective comparative study. *Radiology* 262(3):1022–1033
5. Huang J, Yan L, Cheng Z et al (2010) A randomized trial comparing radiofrequency ablation and surgical resection for HCC conforming to the Milan criteria. *Ann Surg* 252(6):903–912
6. Feng K, Yan J, Li X et al (2012) A randomized controlled trial of radiofrequency ablation and surgical resection in the treatment of small hepatocellular carcinoma. *J Hepatol* 57(4):794–802
7. Imai K, Beppu T, Chikamoto A et al (2013) Comparison between hepatic resection and radiofrequency ablation as first-line treatment for solitary small-sized hepatocellular carcinoma of 3 cm or less. *Hepatal Res* 43(8):853–864
8. Liu PH, Hsu CY, Hsia CY et al (2016) Surgical Resection Versus Radiofrequency Ablation for Single Hepatocellular Carcinoma \leq 2 cm in a Propensity Score Model. *Ann Surg* 263(3):538–545
9. Liu CH, Arellano RS, Uppot RN, Samir AE, Gervais DA, Mueller PR (2010) Radiofrequency ablation of hepatic tumours: effect of post-ablation margin on local tumour progression. *Eur Radiol* 20(4):877–885
10. Minami Y, Kudo M (2010) Radiofrequency ablation of hepatocellular carcinoma: Current status. *World J Radiol* 2(11):417–424
11. Minami Y, Nishida N, Kudo M (2014) Therapeutic response assessment of RFA for HCC: contrast-enhanced US, CT and MRI. *World J Gastroenterol* 20(15):4160–4166
12. Goldberg SN, Grassi CJ, Cardella JF et al (2005) Image-guided tumor ablation: standardization of terminology and reporting criteria. *J Vasc Interv Radiol* 16:765–778
13. Nishikawa H, Inuzuka T, Takeda H et al (2011) Percutaneous radiofrequency ablation therapy for hepatocellular carcinoma: a proposed new grading system for the ablative margin and prediction of

- local tumor progression and its validation. *J Gastroenterol* 46(12): 1418–1426
14. Nishikawa H, Osaki Y, Iguchi E et al (2013) Radiofrequency ablation for hepatocellular carcinoma: the relationship between a new grading system for the ablative margin and clinical outcomes. *J Gastroenterol* 48(8):951–965
 15. Leyendecker JR, Dodd GD 3rd, Halff GA et al (2002) Sonographically observed echogenic response during intraoperative radiofrequency ablation of cirrhotic livers: pathologic correlation. *AJR Am J Roentgenol* 178(5):1147–1151
 16. Zytoon AA, Ishii H, Murakami K et al (2007) Recurrence-free survival after radiofrequency ablation of hepatocellular carcinoma. A registry report of the impact of risk factors on outcome. *Jpn J Clin Oncol* 37(9):658–672
 17. Minami Y, Chung H, Kudo M, et al. (2008) Radiofrequency ablation of hepatocellular carcinoma: value of virtual CT sonography with magnetic navigation. *AJR Am J Roentgenol* 190(6):W335–W341
 18. Kitada T, Murakami T, Kuzushita N et al (2008) Effectiveness of real-time virtual sonography-guided radiofrequency ablation treatment for patients with hepatocellular carcinomas. *Hepatol Res* 38(6):565–571
 19. Song KD, Lee MW, Rhim H, Cha DI, Chong Y, Lim HK (2013) Fusion imaging-guided radiofrequency ablation for hepatocellular carcinomas not visible on conventional ultrasound. *AJR Am J Roentgenol* 201(5):1141–1147
 20. Makino Y, Imai Y, Igura T et al (2016) Feasibility of Extracted-Overlay Fusion Imaging for Intraoperative Treatment Evaluation of Radiofrequency Ablation for Hepatocellular Carcinoma. *Liver Cancer* 5(4):269–279
 21. Minami Y, Minami T, Chishina H et al (2016) US-US Fusion Imaging in Radiofrequency Ablation for Liver Metastases. *Dig Dis* 34(6):687–691
 22. Bruix J, Sherman M, Practice Guidelines Committee, American Association for the Study of Liver Diseases (2005) Management of hepatocellular carcinoma. *Hepatology* 42(5):1208–1236
 23. Kim YS, Rhim H, Lim HK, Choi D, Lee MW, Park MJ (2011) Coagulation necrosis induced by radiofrequency ablation in the liver: histopathologic and radiologic review of usual to extremely rare changes. *Radiographics* 31(2):377–390
 24. Orth RC, Guillerman RP, Zhang W, Masand P, Bisset GS 3rd (2014) Prospective comparison of MR imaging and US for the diagnosis of pediatric appendicitis. *Radiology* 272(1): 233–240
 25. Martin ML, Tay KH, Flak B et al (2003) Multidetector CT angiography of the aortoiliac system and lower extremities: a prospective comparison with digital subtraction angiography. *AJR Am J Roentgenol* 180(4):1085–1091
 26. Viera AJ, Garrett JM (2005) Understanding interobserver agreement: the kappa statistic. *Fam Med* 37(5):360–363
 27. Costa AF, Kajal D, Pereira A, Atri M (2017) Should fat in the radiofrequency ablation zone of hepatocellular adenomas raise suspicion for residual tumour? *Eur Radiol* 27(4):1704–1712
 28. Germani G, Pleguezuelo M, Gurusamy K et al (2010) Clinical outcomes of radiofrequency ablation, percutaneous alcohol and acetic acid injection for hepatocellular carcinoma: a meta-analysis. *J Hepatol* 52(3):380–388
 29. Tanis E, Nordlinger B, Mauer M et al (2014) Local recurrence rates after radiofrequency ablation or resection of colorectal liver metastases. Analysis of the European Organisation for Research and Treatment of Cancer #40004 and #40983. *Eur J Cancer* 50(5): 912–919
 30. Donadon M, Solbiati L, Dawson L et al (2016) Hepatocellular Carcinoma: The Role of Interventional Oncology. *Liver Cancer* 6(1):34–43
 31. Granata V, Petrillo M, Fusco R et al (2013) Surveillance of HCC Patients after Liver RFA: Role of MRI with Hepatospecific Contrast versus Three-Phase CT Scan-Experience of High Volume Oncologic Institute. *Gastroenterol Res Pract* 2013:469097. <https://doi.org/10.1155/2013/469097>
 32. Kang TW, Rhim H, Lee J et al (2016) Magnetic resonance imaging with gadoteric acid for local tumour progression after radiofrequency ablation in patients with hepatocellular carcinoma. *Eur Radiol* 26(10):3437–3446

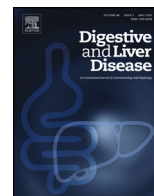


Image of the Month

Transrectal endoscopic ultrasound-guided paracentesis for diagnosis of malignant ascites in the pelvis



Kosuke Minaga, Mamoru Takenaka*, Ken Kamata, Masatoshi Kudo

Department of Gastroenterology and Hepatology, Kindai University, Faculty of Medicine, Osaka-Sayama, Japan

A 67-year-old man was referred to our hospital for weight loss evaluation. He had a history of distal gastrectomy for a poorly differentiated gastric adenocarcinoma (T2N0M0) diagnosed eight years previously. Abdominal computed tomography showed small-volume ascites in the pelvis (Fig. 1). Tumor marker levels were unremarkable. Gastroscopy and colonoscopy revealed no apparent lesions, and ^{18}F -fluorodeoxyglucose positron emission tomography showed no abnormal uptake. A linear-array echoendoscopic examination was performed through the anus, and it identified ascites as an irregular-shaped anechoic region outside the rectal wall. Percutaneous paracentesis presented difficulties; therefore, transrectal endoscopic ultrasound-guided paracentesis (EUS-P) was performed using a 22-gauge needle (Fig. 2A). Using a 10 mL suction syringe, 6 mL of serous yellow fluid was aspirated. Antibiotics were administered before and after the procedure. The post-procedural period was uneventful. The serum-ascites albumin gradient was 0.8 g/dL. Cytopathologic testing of the aspirated fluid

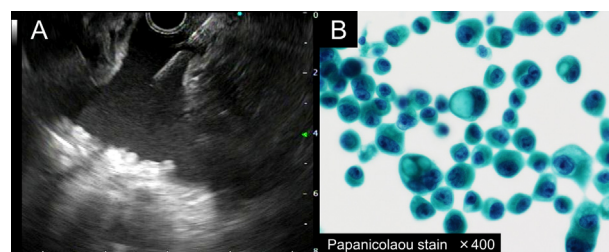


Fig. 2. A. Transrectal endoscopic ultrasound-guided paracentesis was performed using a 22-gauge needle for ascites in the pelvis. B. Cytopathologic testing of the aspirated fluid showing malignant cells characteristic of a poorly differentiated adenocarcinoma.

revealed malignant cells characteristic of a poorly differentiated adenocarcinoma (Fig. 2B), which suggested gastric adenocarcinoma recurrence. The patient received chemotherapy according to EUS-P findings. In a recent retrospective study that evaluated 101 patients who underwent EUS-P via a transgastric or transduodenal approach, the sensitivity, specificity, and diagnostic accuracy were 80%, 100%, and 96%, respectively [1]. When ascites accumulation presents around the rectum, transrectal EUS-P may be useful for the diagnosis of malignant ascites.

Disclosure

All authors disclosed no financial relationships relevant to this publication.

Conflict of interest

None declared.

Reference

- [1] Wardeh R, Lee JG, Gu M. Endoscopic ultrasound-guided paracentesis of ascitic fluid: a morphologic study with ultrasonographic correlation. *Cancer Cytopathol* 2011;119:27–36.



Fig. 1. Abdominal computed tomography showing small-volume ascites in the pelvis around the rectum (arrowheads).

* Corresponding author at: Department of Gastroenterology and Hepatology, Kindai University Faculty of Medicine, 377-2 Ohno-Higashi, Osaka-Sayama 589-8511, Japan.

E-mail address: mamoxyo45@gmail.com (M. Takenaka).



Short report

Induction of Complete Remission by Azacitidine in a Patient with Myelodysplastic Syndrome-Associated Inflammatory Bowel Disease

Masashi Kono^a, Yoriaki Komeda^a, Toshiharu Sakurai^a, Ayana Okamoto^a,
Kosuke Minaga^a, Ken Kamata^a, Satoru Hagiwara^a, Hiroaki Inoue^b,
Eisuke Enoki^c, Itaru Matsumura^b, Tomohiro Watanabe^a, Masatoshi Kudo^a

^aDepartment of Gastroenterology and Hepatology, Kindai University Faculty of Medicine, Osaka, Japan ^bDepartment of Hematology and Rheumatology, Kindai University Faculty of Medicine, Osaka, Japan ^cDepartment of Pathology, Kindai University Faculty of Medicine, Osaka, Japan

Corresponding author: Tomohiro Watanabe MD, PhD, Department of Gastroenterology and Hepatology, Kindai University Faculty of Medicine, 377-2 Ohno-Higashi, Osaka-Sayama, Osaka 589-8511, Japan. Tel: 81-72-366-0221; fax: 81-72-367-2880; e-mail: tomohiro@med.kindai.ac.jp

Abstract

Myelodysplastic syndrome [MDS] is a clonal disorder of bone marrow [BM] cells, caused by acquired chromosomal abnormalities and gene mutations. Pro-inflammatory antigen-presenting cells [APCs] originating from BM cells bearing chromosomal abnormalities and gene mutations can cause immune-mediated disorders including inflammatory bowel disease [IBD]. Here, we report the first case with MDS-associated IBD that was successfully treated with the DNA methyltransferase inhibitor, azacitidine [AZA]. A 75-year-old man with a 5-year history of MDS was admitted for examination of diarrhoea and high fever. Blood examination revealed pancytopenia and a marked elevation of C-reactive protein. Colonoscopy revealed multiple round ulcers from the terminal ileum to the sigmoid colon. Pathological examination of the endoscopic biopsy specimens showed destruction of crypt architecture and infiltration of CD3⁺T cells and CD68⁺ macrophages. Surprisingly, administration of AZA, which has been approved for the treatment of high-risk MDS, improved the symptoms, and the multiple round ulcers disappeared. AZA treatment markedly decreased the expressions of tumour necrosis factor- α , interleukin-12 (IL-12)/23p40 and IL-17 in colonic biopsy samples, as assessed by quantitative reverse transcription polymerase chain reaction. In contrast, AZA treatment did not change the expression of forkhead box P3, a master regulator of regulatory T cells. These data suggest that AZA treatment led to complete remission in MDS-associated IBD through suppression of pro-inflammatory cytokine responses.

Key Words: Azacitidine, inflammatory bowel disease, myelodysplastic syndrome

1. Introduction

Excessive immune responses towards intestinal microflora underlie the immunopathogenesis of inflammatory bowel diseases [IBD] such as Crohn's disease [CD] and ulcerative colitis [UC].¹ Pro-inflammatory cytokines produced by T cells and bone marrow [BM]-derived

antigen-presenting cells [APCs] such as macrophages and dendritic cells play pivotal roles in the development of IBD.^{1,2} Thus, BM-derived myeloid APCs producing pro-inflammatory cytokines are colitogenic populations that cause persistent intestinal inflammation. This idea has been fully supported by clinical trials in which the blockade of

tumour necrosis factor α (TNF- α) and interleukin-12 (IL-12)/23 p40 expressed in APCs results in remarkable success in patients with IBD.³ Moreover, resetting of BM-derived immunological microenvironments by autologous haematopoietic stem cell transplantation [HSCT] has been implicated as an alternative treatment option for patients with severe and treatment-resistant CD.^{4,5} Thus, it is clear that BM-derived APCs with the ability to produce pro-inflammatory cytokines contribute to the development of IBD.

Myelodysplastic syndrome [MDS] is a clonal disorder of haematopoietic cells characterized by impaired haematopoiesis, peripheral blood cytopenia and a pre-condition of acute myeloid leukaemia.⁶ MDS is caused by acquired chromosomal abnormalities and gene mutations that have significant influence on the sequence and function of oncogenes and tumour suppressor genes.^{6,7} These chromosomal abnormalities and gene mutations often alter the function and properties of BM-derived APCs, and pro-inflammatory APCs originating from abnormal BM environments in MDS can cause immune-mediated disorders including IBD.⁸ In fact, several cases with concurrent IBD and MDS have been reported,^{9,10} and trisomy 8, a frequent chromosomal abnormality in patients with MDS, has been identified as a risk factor for intestinal Behcet's disease [BD].^{11,12} Although some cases of MDS-associated IBD have been successfully treated with HSCT,^{13,14} no effective treatment for this condition has

yet been established. Azacitidine [AZA], a DNA methyltransferase inhibitor, has been shown to be safe and effective for the treatment of patients with MDS.¹⁵ However, the therapeutic efficacy of AZA on MDS-associated IBD has not been reported. Here, we report a case of a patient with MDS-associated IBD who was successfully treated with AZA.

2. Case Report

A 75-year-old Japanese man with no past history of gastrointestinal diseases was admitted to our hospital for evaluation of diarrhoea and high fever that had persisted for 3 months. He had been diagnosed with MDS [refractory anaemia with excess blast type 2, RAEB 2] at the age of 70 years. No oral or genital ulceration, uveitis, or skin lesions were observed. Blood tests showed pancytopenia [leukocyte count, $1.55 \times 10^3/\mu\text{l}$; red blood cell count, $2.59 \times 10^6/\mu\text{l}$; haemoglobin, 7.5 g/dl; haematocrit, 22.9%; platelet count, $2.3 \times 10^4/\mu\text{l}$] and a marked elevation of serum C-reactive protein [CRP, 12.3 mg/dl]. Both the human leukocyte antigen B51 and anti-neutrophil cytoplasmic antibody tests showed negative results.

Colonoscopy performed to investigate the cause of diarrhoea revealed multiple round ulcers in the terminal ileum and the entire colon [Figure 1A]. Colonoscopic examination showed no

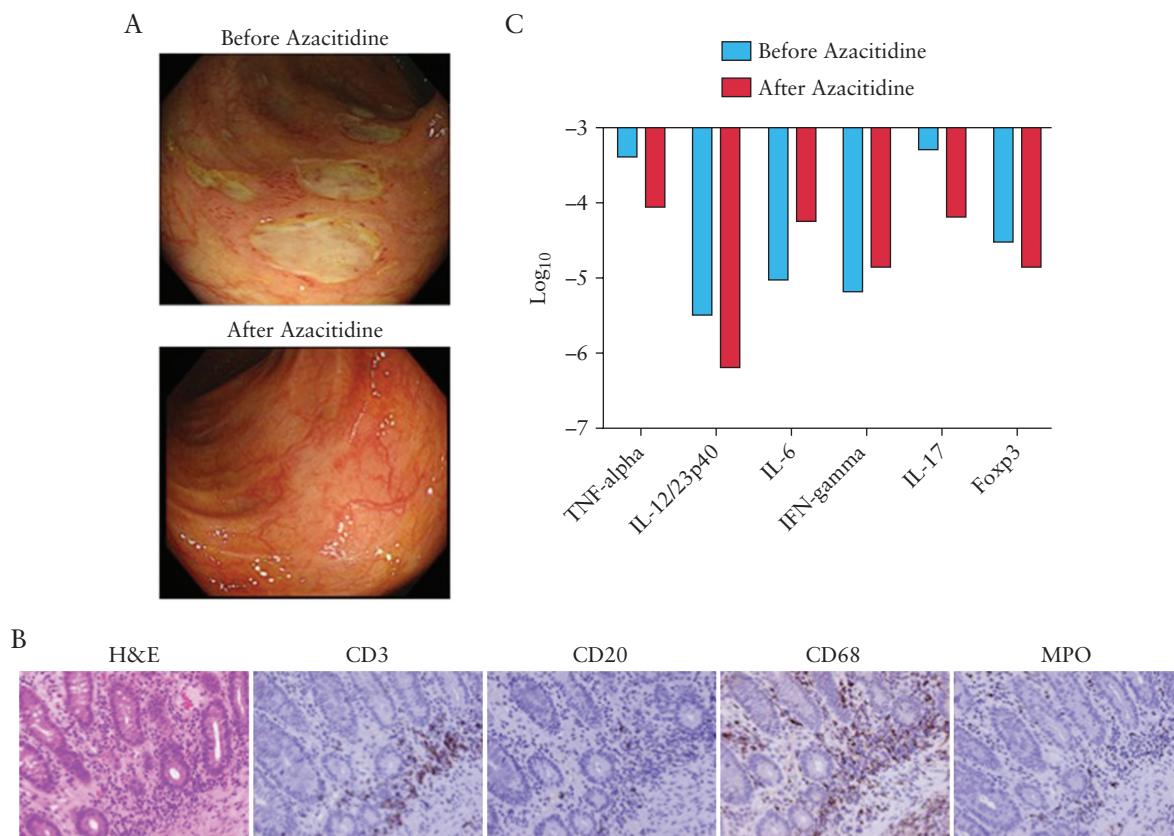


Figure 1. Endoscopic and pathological findings and cytokine profiles of a patient with myelodysplastic syndrome-associated inflammatory bowel disease. [A] Endoscopic images of the patient. Multiple round ulcers were observed in the transverse colon before azacitidine [AZA] treatment, and they disappeared after AZA treatment. [B] Pathological images of the patient. Endoscopic biopsy samples obtained from the transverse colon before AZA treatment were fixed in 10% formalin, followed by haematoxylin & eosin [H&E] staining. H&E staining revealed massive infiltration of immune cells and destruction of crypt architecture. Biopsy samples were also subjected to immunohistochemical analysis by using anti-CD3 antibody [Ab], anti-CD20 Ab, anti-CD68 Ab and anti-myeloperoxidase [MPO] Ab. Infiltration of CD3⁺T cells and CD68⁺ macrophages was observed in the transverse colon [x200]. [C] Cytokine profiles of the patient. mRNA was isolated from endoscopic biopsy specimens of the transverse colon before and after AZA and subjected to quantitative reverse transcription polymerase chain reaction to determine the expression of TNF- α , IL-12/23p40, IL-6, IFN- γ , IL-17 and forkhead box p3 [Foxp3]. Expression of these molecules was normalized by the expression of β -actin.

longitudinal ulcers/cobble stone appearance, continuous lesions, diffuse mucosal oedema or erosion. These findings suggested BD rather than CD or UC. Polymerase chain reaction [PCR] for cytomegalovirus and tuberculosis using colon biopsy specimens showed negative results. No small bowel lesions were detected in contrast-enhanced abdominal computed tomography scans although endoscopic examinations of the small bowel were not performed. Stool and urine cultures for pathogenic micro-organisms were negative and serum level of β -d-glucan was within normal limits. Thus, microbe infection was less likely to cause colitis in this case.

Pathological analysis of the colon biopsy specimen revealed a marked infiltration of inflammatory cells and destruction of crypt architecture [Figure 1B]. Immunohistochemical analysis was performed to determine the type of immune cells accumulated into the lesions, as previously described.¹⁰ Immunohistochemical analysis showed that inflammatory cells were mainly composed of CD68⁺ macrophages and CD3⁺ T cells [Figure 1B]. Infiltration of myeloperoxidase [MPO]⁺ neutrophils or CD20⁺ B cells was barely observed in the intestinal lesions [Figure 1B]. Thus, these pathological examinations suggest that macrophages and T cells, but not neutrophils, played a pathogenic role in this case; these findings were not consistent with those of BD.

BM examination showed that the nucleated cell count was 27 000/ μ l and the megakaryocyte count was 27/ μ l, with dysplastic features of megakaryocyte and myeloid cells. The karyotype of BM cells was 44, XY, add(4)(q11), del(5)(q2), -6, -7, add(11)(q13), add(13)(p11.2)(2 cells)/45, idem, add(3)(q11, 2), add(5)(q13), add(8)(q11, 2), -add(11), +add(11)(q13), -12, -13, -add(13), +mar1, +mar2, +mar3, +mar4(2 cells)/46, XY(12 cells). Trisomy 8, a strong risk factor for BD,^{11,12} was absent in the BM. The patient was again diagnosed with high-risk RAEB2 according to the international prognostic system of MDS.^{6,7}

Because the diagnosis of CD, UC or BD was not supported by physical, endoscopic or pathological examinations, we considered this case as MDS-associated IBD. Administration of colchicine and antibiotics did not improve the symptoms of the patient. AZA [75 mg/m²/day for 5 days of the week] was also started for the treatment of high-risk MDS. Administration of ceftriaxone [2 g/day] was continued during the AZA treatment to prevent systemic bacterial infection due to bacterial translocation. Surprisingly, the diarrhoea and fever of the patient disappeared after administration of AZA. A marked reduction of serum CRP level and increase of blood leukocyte, red blood cell and platelet counts were observed. More importantly, multiple round ulcers observed before AZA treatment became scars and mucosal healing was achieved [Figure 1A]. Thus, AZA treatment successfully induced complete remission of MDS-associated IBD in this case.

We then tried to determine the molecular mechanisms underlying the AZA-induced complete remission in MDS-associated IBD. For this, isolated mRNA from colon biopsy specimens before and after AZA treatment was subjected to quantitative reverse transcription PCR [qPCR] analysis, as previously described.¹⁶ Ethical permission for this study was obtained by the Review Boards of Kindai University Faculty of Medicine. As shown in Figure 1C, expression of pro-inflammatory cytokines such as TNF- α , IL-12/23p40 and IL-17 was markedly reduced after AZA treatment, whereas expression of IL-6 and interferon- γ [IFN- γ] was unchanged. Thus, induction of complete remission by AZA treatment was accompanied by suppression of pro-inflammatory cytokine responses [TNF- α , IL-12/23p40 and IL-17]. One possible mechanism accounting for the

suppression of pro-inflammatory cytokine responses is expansion of regulatory T cells [Tregs] expressing forkhead box p3 [Foxp3].^{17,18} Lal and colleagues have reported that demethylation of CpG sites of the Foxp3 non-intronic upstream enhancer by AZA results in strong and stable expression of Foxp3 and, thereby, differentiation of Tregs.^{19,20} We then assessed the expression of Foxp3 before and after AZA treatment. As shown in Figure 1C, Foxp3 expression was unchanged after AZA treatment. Taken together, these qPCR data suggest strongly that AZA treatment suppressed IBD through down-regulation of pro-inflammatory cytokine responses rather than expansion of Tregs.

3. Discussion

BM-derived APCs are the cellular source of pro-inflammatory cytokines such as TNF- α , IL-12, IL-23 and IL-6, all of which have been implicated as pathogenic mediators in IBD.^{1,2} MDS is caused by acquired chromosomal abnormalities and gene mutations that may have significant influence on the function of BM-derived APCs.^{6,7} Therefore, it is not surprising that pro-inflammatory APCs originating from abnormal BM environments in patients with MDS are involved in the development of immune disorders including IBD.⁸⁻¹⁰ Although the immunopathogenesis of MDS-associated IBD has not been fully clarified, Nakamura *et al.* have provided evidence that chromosomal abnormalities of BM cells set the stage for the development of colitogenic APCs, producing a large amount of pro-inflammatory cytokines and exhibiting resistance to apoptosis upon stimulation with microbial antigens.¹⁰ In line with this finding, a marked elevation of the APC-derived cytokines, TNF- α and IL-12/23p40, was observed in this patient at active phase. Thus, our data support the idea that chromosomal abnormalities and gene mutations in BM cells lead to the development of pathogenic APCs with the ability to cause MDS-associated IBD through the production of pro-inflammatory cytokines.

To our knowledge, this is the first case of MDS-associated IBD successfully treated with AZA. Regarding the molecular mechanisms, treatment with AZA markedly reduced the expression of TNF- α , IL-12/23p40, and IL-17, whereas the expression of IL-6 and IFN- γ remained unchanged. Given that IL-12/23p40 and TNF- α are potent inducers for T helper 17 cells producing IL-17,¹² these cytokine data suggest that the TNF- α -IL-12/23p40-IL-17 axis contributes to the development of MDS-associated IBD. Impaired function of Foxp3-expressing Tregs mediates intestinal inflammation.¹⁸ Although AZA induces the differentiation of naïve CD4⁺ T cells into Foxp3-expressing Tregs,^{19,20} no significant change was observed in Foxp3 expression before and after AZA treatment. Therefore, we speculate that AZA treatment led to complete remission through suppression of pro-inflammatory cytokine responses, but not expansion of Tregs. Consistent with this observation, Sánchez-Abarca *et al.* reported that AZA inhibits the production of pro-inflammatory cytokines including TNF- α .²¹ Collectively, our findings, together with previous reports, support the idea that AZA might suppress MDS-associated IBD through immunomodulatory action against pro-inflammatory cytokine responses.

To the best of our knowledge, this is the first case of MDS-associated IBD successfully treated with AZA. AZA treatment might be recommended for MDS-associated IBD. Confirmation of this idea awaits future studies addressing both the efficacy of AZA treatment and pro-inflammatory cytokine responses in a large number of patients with MDS-associated IBD.

Funding

This work was supported by the Naito Foundation, SENSHIN Medical Research Foundation, Yakult Bio-Science Foundation, Smoking Research Foundation, Kobayashi Foundation for Cancer Research and Takeda Science Foundation.

Conflict of Interest

None to declare.

Author Contributions

M. Kono, YK, TS and HI took care of the patient. M. Kono, TW, YK, AO, KM, KK and SH wrote the manuscript. EE performed pathological examinations. M. Kono and TW performed the experiments. IM and M. Kudo supervised the research.

References

1. Strober W, Fuss IJ. Proinflammatory cytokines in the pathogenesis of inflammatory bowel diseases. *Gastroenterology* 2011;**140**:1756–67.
2. Strober W. The multifaceted influence of the mucosal microflora on mucosal dendritic cell responses. *Immunity* 2009;**31**:377–88.
3. Neurath MF. New targets for mucosal healing and therapy in inflammatory bowel diseases. *Mucosal Immunol* 2014;**7**:6–19.
4. Hommes DW, Duijvestein M, Zelinkova Z, et al. Long-term follow-up of autologous hematopoietic stem cell transplantation for severe refractory Crohn's disease. *J Crohns Colitis* 2011;**5**:543–9.
5. Oyama Y, Craig RM, Traynor AE, et al. Autologous hematopoietic stem cell transplantation in patients with refractory Crohn's disease. *Gastroenterology* 2005;**128**:552–63.
6. Bejar R, Levine R, Ebert BL. Unraveling the molecular pathophysiology of myelodysplastic syndromes. *J Clin Oncol* 2011;**29**:504–15.
7. Tefferi A, Vardiman JW. Myelodysplastic syndromes. *N Engl J Med* 2009;**361**:1872–85.
8. Komrokji RS, Kulasekararaj A, Al Ali NH, et al. Autoimmune diseases and myelodysplastic syndromes. *Am J Hematol* 2016;**91**:E280–3.
9. Harewood GC, Loftus EV Jr, Tefferi A, Tremaine WJ, Sandborn WJ. Concurrent inflammatory bowel disease and myelodysplastic syndromes. *Inflamm Bowel Dis* 1999;**5**:98–103.
10. Nakamura F, Watanabe T, Hori K, et al. Simultaneous occurrence of inflammatory bowel disease and myelodysplastic syndrome due to chromosomal abnormalities in bone marrow cells. *Digestion* 2009;**79**:215–9.
11. Kawabata H, Sawaki T, Kawanami T, et al. Myelodysplastic syndrome complicated with inflammatory intestinal ulcers: significance of trisomy 8. *Intern Med* 2006;**45**:1309–14.
12. Kimura S, Kuroda J, Akaogi T, Hayashi H, Kobayashi Y, Kondo M. Trisomy 8 involved in myelodysplastic syndromes as a risk factor for intestinal ulcers and thrombosis–Behçet's syndrome. *Leuk Lymphoma* 2001;**42**:115–21.
13. Nonami A, Takenaka K, Sumida C, et al. Successful treatment of myelodysplastic syndrome (MDS)-related intestinal Behçet's disease by up-front cord blood transplantation. *Intern Med* 2007;**46**:1753–6.
14. Marmont AM, Gualandi F, Piaggio G, et al. Allogeneic bone marrow transplantation (BMT) for refractory Behçet's disease with severe CNS involvement. *Bone Marrow Transplant* 2006;**37**:1061–3.
15. Bejar R, Steensma DP. Recent developments in myelodysplastic syndromes. *Blood* 2014;**124**:2793–803.
16. Sakurai T, Kashida H, Watanabe T, et al. Stress response protein Cirp links inflammation and tumorigenesis in colitis-associated cancer. *Cancer Res* 2014;**74**:6119–28.
17. Xu L, Kitani A, Strober W. Molecular mechanisms regulating TGF- β -induced *Foxp3* expression. *Mucosal Immunol* 2010;**3**:230–8.
18. Xu L, Kitani A, Stuelten C, McGrady G, Fuss I, Strober W. Positive and negative transcriptional regulation of the *Foxp3* gene is mediated by access and binding of the Smad3 protein to enhancer I. *Immunity* 2010;**33**:313–25.
19. Lal G, Bromberg JS. Epigenetic mechanisms of regulation of *Foxp3* expression. *Blood* 2009;**114**:3727–35.
20. Lal G, Zhang N, van der Touw W, et al. Epigenetic regulation of *Foxp3* expression in regulatory T cells by DNA methylation. *J Immunol* 2009;**182**:259–73.
21. Sánchez-Abarca LI, Gutierrez-Cosío S, Santamaría C, et al. Immunomodulatory effect of 5-azacytidine (5-azaC): potential role in the transplantation setting. *Blood* 2010;**115**:107–21.

Original Paper

Regional Differences in Efficacy, Safety, and Biomarkers for Second-Line Axitinib in Patients with Advanced Hepatocellular Carcinoma: From a Randomized Phase II Study

Masatoshi Kudo^a Yoon-Koo Kang^b Joong-Won Park^c Shukui Qin^d
Yoshitaka Inaba^e Eric Assenat^f Yoshiko Umeyama^g Maria José Lechuga^h
Olga Valota^h Yosuke Fujii^g Jean-Francois Martiniⁱ J. Andrew Williamsⁱ
Shuntaro Obi^j

^aDepartment of Gastroenterology and Hepatology, Kindai University Faculty of Medicine, Osaka-Sayama, Japan; ^bDepartment of Oncology, Asan Medical Center, University of Ulsan College of Medicine, Seoul, and ^cCenter for Liver Cancer, National Cancer Center, Goyang, Republic of Korea; ^dDepartment of Medical Oncology, Nanjing Bayi Hospital, Nanjing, China; ^eDepartment of Diagnostic and Interventional Radiology, Aichi Cancer Center Hospital, Nagoya, Japan; ^fDepartment of Medical Oncology, Hôpital Saint Eloi, Montpellier, France; ^gPfizer Japan Inc., Tokyo, Japan; ^hPfizer Srl, Milan, Italy; ⁱPfizer Inc., San Diego, CA, USA; ^jDepartment of Hepatology, Sasaki Foundation Kyoundo Hospital, Tokyo, Japan

Keywords

Asian · Axitinib · Biomarkers · Hepatocellular carcinoma · MicroRNAs

Abstract

Background: An unmet need exists for treatment of patients with advanced hepatocellular carcinoma (HCC) who progress on or are intolerant to sorafenib. A global randomized phase II trial (ClinicalTrials.gov No. NCT01210495) of axitinib, a vascular endothelial growth factor receptor 1–3 inhibitor, in combination with best supportive care (BSC) did not prolong overall survival (OS) over placebo/BSC, but showed improved progression-free survival in some patients. Subgroup analyses were conducted to identify potential predictive/prognostic factors.

Methods: The data from this phase II study were analyzed for the efficacy and safety of axitinib/BSC in patients from Asia versus non-Asia versus Asian subgroups (Japan, Korea, or mainland China/Hong Kong/Taiwan) and predictive/prognostic values of baseline microRNAs

M.K. and Y.-K.K. equally contributed to the study and share first authorship. J.A.W. was employed at Pfizer at the time of the study.

Yoon-Koo Kang, MD, PhD
Department of Oncology, Asan Medical Center, University of Ulsan
88 Olympic-ro 43-gil
Songpa-gu, Seoul 138-736 (Republic of Korea)
E-Mail ykkang@amc.seoul.kr

and serum soluble proteins, using the Cox proportional hazards model. **Results:** Of 202 patients, 78 were from non-Asia and 124 from Asia (37 Japanese, 36 Korean, and 51 Chinese). No significant differences in OS were found between axitinib/BSC and placebo/BSC in non-Asians, Asians, or Asian subgroups. However, in an exploratory analysis, axitinib/BSC showed favorable OS in Asians, especially Japanese, when patients intolerant to prior antiangiogenic therapy were excluded from the data set. Axitinib/BSC was well tolerated by non-Asians and Asians alike. The presence of 4 circulating microRNAs, including miR-5684 and miR-1224-5p, or a level lower than or equal to the median protein level of stromal cell-derived factor 1 at baseline was significantly associated with longer OS in axitinib/BSC-treated Asians or non-Asians. **Conclusions:** Axitinib/BSC did not prolong survival over placebo/BSC in non-Asians, Asians, or Asian subgroups, but favorable OS with axitinib/BSC was observed in a subset of Japanese patients. A patient population that excludes sorafenib-intolerant patients might potentially be more suitable for clinical trials of new agents in advanced HCC. Since these results are very preliminary, further investigation is warranted. The potential predictive/prognostic value of several baseline microRNAs and soluble proteins identified in this study would require validation in prospective studies on a large cohort of patients. © 2017 S. Karger AG, Basel

Introduction

The incidence of liver cancer varies geographically, with higher incidence rates observed in developing countries in Asia and Africa than in developed countries in Europe and North America [1]. The etiology of hepatocellular carcinoma (HCC), which accounts for the majority of liver cancers, is diverse and complex, with hepatitis B virus being the primary cause of HCC, particularly in Asia (other than Japan) and Africa. For resectable HCC, treatment options include resection, locoregional therapy, ablation, or external-beam radiation therapy, whereas for unresectable, advanced, or metastatic HCC, systemic therapy with sorafenib is one of few treatments recommended by the National Comprehensive Cancer Network [2]. Sorafenib is so far the only targeted agent approved for advanced HCC, but its efficacy is limited and short-lived, which necessitates the evaluation of novel agents and/or new treatment approaches in this setting and later lines of therapy.

Several agents targeting the vascular endothelial growth factor (VEGF)/VEGF receptor (VEGFR) signaling pathway, including the multitargeted tyrosine kinase inhibitor brivanib [3] and the monoclonal antibody ramucirumab [4], or the mechanistic target of rapamycin inhibitor everolimus [5] were investigated in 2009–2013 in patients with sorafenib-refractory and -intolerant HCC in randomized phase III trials with generally disappointing results.

Axitinib is a potent and selective inhibitor of VEGFRs 1–3, approved for treatment of second-line metastatic renal cell carcinoma (RCC) [6]. Based on the antitumor activity of agents inhibiting the VEGF/VEGFR signaling pathway observed in HCC in clinical studies and the nonclinical activity of axitinib in HCC animal models, the efficacy and safety of axitinib in combination with best supportive care (BSC) was compared with placebo plus BSC (placebo/BSC) in patients with locally advanced or metastatic HCC following failure of one prior antiangiogenic therapy in a global randomized phase II study conducted in 2010–2012 [7]. Although the study did not meet its primary endpoint of overall survival (OS), improvements favoring the axitinib/BSC arm were observed in progression-free survival (PFS), time to tumor progression, and the clinical benefit rate, especially among Asian patients. Furthermore, an exploratory analysis indicated a longer OS with axitinib/BSC than with placebo/BSC when patients who were intolerant to prior antiangiogenic therapy were excluded from the data set

[7]. The safety profile in patients with metastatic HCC was as expected based on prior studies of axitinib in RCC, with no new safety signals or unexpected toxicities.

The aims of the current analyses were to explore the efficacy and safety of axitinib/BSC compared with placebo/BSC in patients from non-Asia versus Asia versus Asian subgroups by country of origin (Japan; Korea; and mainland China, Hong Kong, and Taiwan combined [CHT]), and to investigate the potential predictive and/or prognostic value of baseline levels of circulating microRNAs (miRNAs) and serum soluble proteins for OS in the overall population as well as in non-Asian and Asian patients.

Subjects and Methods

Study Design and Patients

The data from the global randomized double-blind phase II trial (ClinicalTrials.gov No. NCT01210495) of axitinib/BSC versus placebo/BSC in patients previously treated with antiangiogenic therapy for locally advanced or metastatic HCC were analyzed in this study. The details of the study design and patient eligibility criteria have been reported previously [7]. In brief, patients with confirmed HCC who progressed on or were intolerant to one prior antiangiogenic therapy, with Child-Pugh class A liver function, and with an Eastern Cooperative Oncology Group performance status (ECOG PS) of 0 or 1 were stratified by tumor invasion (presence vs. absence of extrahepatic spread and/or vascular invasion) and geographic region (non-Asia vs. Asia) and randomly assigned in a 2:1 ratio to axitinib/BSC or placebo/BSC. The primary endpoint was OS, and secondary endpoints included PFS, safety, and assessment of baseline levels of circulating miRNAs and serum soluble proteins for their predictive and/or prognostic potential.

Treatment and Assessments

As described previously [7], the randomized patients received axitinib or placebo orally at a starting dose of 5 mg twice daily in 4-week cycles. The axitinib or placebo dose could be increased to 7 mg twice daily, and then to a maximum of 10 mg twice daily, if patients tolerated the drug without any treatment-related adverse events (AEs) of grade >2 for 2 consecutive weeks and were normotensive. The drug dose could be decreased to 3 mg twice daily, and then to 2 mg twice daily, to manage axitinib-related AEs.

Radiological tumor assessments were performed by the investigators at baseline and every 8 weeks according to the Response Evaluation Criteria in Solid Tumors (RECIST) version 1.1. Safety was monitored throughout the study period, and AEs were graded per the National Cancer Institute Common Terminology Criteria for Adverse Events (NCI-CTCAE) version 3.0.

For evaluation of circulating miRNAs or serum soluble proteins, 5- or 10-mL whole-blood samples were collected from all randomized patients before administration of axitinib or placebo on cycle 1 day 1 and at the end of the study, and 2–3 h after dose administration on cycle 2 day 1. After extraction with Agilent 8 × 60K miRNA arrays (Release 19.0; www.genomics.agilent.com), human miRNAs were assessed using probes based on the latest Sanger miRBase (release 12.0; www.mirbase.org) at ShanghaiBio Corporation, Shanghai, China. The miRNA array data were extracted and processed using Agilent's proprietary Feature Extraction Software version 10.7.1.1 and were further normalized via the quantile method using Bioconductor R software. A total of 2,006 probes were measured from 170 patients. However, 78.8% of these miRNAs were not expressed at detectable levels; hence, the analyses correlating circulating miRNAs with efficacy were restricted to those miRNAs that were detected in at least 10 patients. Serum soluble proteins tested included angiopoietin (Ang)-2, matrix metalloproteinase 2, VEGF-A, VEGF-C, soluble VEGFR (sVEGFR)2, sVEGFR3, hepatocyte growth factor, soluble c-MET, stem cell factor (the ligand for c-KIT), neutrophil gelatinase-associated lipocalin, stromal cell-derived factor 1 (SDF-1), interleukin (IL)-6, IL-8, E-selectin, macrophage migration inhibitory factor (MIF), and chemokine (C-C motif) ligand 5 (also known as RANTES). Serum concentrations of proteins were assessed by Aushon BioSystems (Billerica, MA, USA) using the validated Aushon SearchLight Multiplex Analysis platform or an enzyme-linked immunosorbent assay.

Statistical Analysis

In the subgroup and exploratory analyses of the regional differences, OS and PFS was estimated using the Kaplan-Meier method, and the median and 95% confidence interval (CI) were provided. An unstratified one-sided log-rank test was used to compare OS and PFS between the treatment arms, using a 0.025 signifi-

cance level for interpretation. The hazard ratio (HR) and 95% CI were also estimated. For miRNA predictive and/or prognostic factor analysis, a Cox proportional hazards model was used to estimate the HR and 95% CI. A predictive effect was assessed as the interaction effect in this model, including main effects, and the interaction of treatment stratum with baseline miRNA expression status. A prognostic effect was assessed as the covariate effect in this model, including miRNA expression status stratified by treatment. The *p* value was calculated using the Wald test. In the subgroup analyses of baseline level of soluble proteins, an unstratified two-sided log-rank test was used to compare OS between the treatment arms. In the exploratory analyses of miRNAs and soluble proteins, the Benjamini-Hochberg procedure was used with the false discovery rate (FDR) at the level of 0.2 [8].

Results

Patients

In this multinational study, 78 patients were enrolled from non-Asian countries, whereas the majority ($n = 124$) were from Asian countries (Japan [$n = 37$], Korea [$n = 36$], and CHT [$n = 51$]). Of a total of 202 randomized patients, 134 (51 non-Asians and 83 Asians) were assigned to axitinib/BSC and 68 (27 non-Asians and 41 Asians) to placebo/BSC. The median age was not significantly different between non-Asian and all Asian patients (65.0 vs. 61.0 years). However, the patients in Japan were older (median 74.0 years), whereas the patients in Korea and CHT were younger (median 57.0 and 55.0 years, respectively), than those in non-Asia. The patient demographics and baseline characteristics of the axitinib/BSC and placebo/BSC arms of the non-Asian and Asian groups, as well as of the Asian subgroups, are summarized in Table 1. The percentage of female patients was slightly imbalanced between the axitinib/BSC and placebo/BSC arms, except in CHT (9 and 11%, respectively). It was higher in the axitinib/BSC arm than in the placebo/BSC arm in non-Asia (31 vs. 11%), but it was lower in Asia (10 vs. 22%), Japan (15 vs. 36%), and Korea (4 vs. 27%).

The baseline clinical characteristics, such as ECOG PS, the presence of tumor vascular invasion, or liver cirrhosis, were generally comparable between the two treatment arms, as well as between the non-Asian group, the Asian group, and the Asian subgroups. The majority of the patients in Japan had an ECOG PS of 0. All patients had Child-Pugh class A liver function. However, the percentage of patients with extrahepatic spread or hepatitis B, although similar between the treatment arms in each geographical region, was substantially higher in Asia, particularly in Korea and CHT, than in non-Asia. Based on the Barcelona Clinic Liver Cancer (BCLC) stage classification, a higher percentage of the Asian than of the non-Asian patients had a poorer prognosis of stage C, whereas the percentage of patients with BCLC stage B was higher in non-Asia than in Asia. Of note, the percentage of patients with hepatitis C was highest in Japan compared with Korea, CHT, or non-Asia.

Prior locoregional therapy had been administered more frequently in Asia, especially in Japan and Korea, than in non-Asia. The majority of patients in both the axitinib/BSC and the placebo/BSC arm in each geographical region had previously received systemic therapy with sorafenib. However, the percentage of patients who were intolerant to prior sorafenib treatment (i.e., patients who discontinued prior antiangiogenic therapy due to treatment-related grade 3/4 AEs per NCI-CTCAE version 3.0) was higher in the placebo/BSC arm than in the axitinib/BSC arm in each region except in CHT (Table 1).

Patient Disposition and Drug Exposure

At the time of data cutoff (March 3, 2014), a similar number of patients in the axitinib/BSC and the placebo/BSC arm in the non-Asian and Asian groups and the Asian subgroups discontinued the study, with death as the primary reason; almost all patients discontinued

Table 1. Patient demographics and baseline characteristics

Characteristics	Non-Asia (n = 78)		Asia		Japan (n = 37)		Korea (n = 36)		CHT (n = 51)	
	axitinib/BSC (n = 51)	placebo/BSC (n = 27)	axitinib/BSC (n = 83)	placebo/BSC (n = 41)	axitinib/BSC (n = 26)	placebo/BSC (n = 11)	axitinib/BSC (n = 25)	placebo/BSC (n = 11)	axitinib/BSC (n = 32)	placebo/BSC (n = 19)
Age, years	65.0 (40–84)	65.0 (26–83)	59.0 (25–82)	62.0 (43–83)	74.5 (43–82)	72.0 (47–83)	56.0 (45–75)	57.0 (45–78)	54.0 (25–75)	60.0 (43–74)
Sex										
Male	35 (69)	24 (89)	75 (90)	32 (78)	22 (85)	7 (64)	24 (96)	8 (73)	29 (91)	17 (89)
Female	16 (31)	3 (11)	8 (10)	9 (22)	4 (15)	4 (36)	1 (4)	3 (27)	3 (9)	2 (11)
ECOG PS										
0	29 (57)	16 (59)	49 (59)	23 (56)	22 (85)	10 (91)	9 (36)	5 (45)	18 (56)	8 (42)
1	22 (43)	11 (41)	34 (41)	18 (44)	4 (15)	1 (9)	16 (64)	6 (55)	14 (44)	11 (58)
Tumor invasion ^a present	31 (61)	16 (59)	71 (86)	36 (88)	20 (77)	9 (82)	22 (88)	9 (82)	29 (91)	18 (95)
Tumor vascular invasion present	12 (24)	7 (26)	21 (25)	12 (29)	5 (19)	4 (36)	10 (40)	3 (27)	6 (19)	5 (26)
Extrahepatic spread present	24 (47)	13 (48)	68 (82)	35 (85)	18 (69)	9 (82)	21 (84)	9 (82)	29 (91)	17 (89)
With intrahepatic tumors	20 (39)	11 (41)	49 (59)	30 (73)	13 (50)	9 (82)	14 (56)	6 (55)	22 (69)	15 (79)
Without intrahepatic tumors	4 (8)	2 (7)	19 (23)	5 (12)	5 (19)	0	7 (28)	3 (27)	7 (22)	2 (11)
Child-Pugh class A	51 (100)	27 (100)	83 (100)	41 (100)	26 (100)	11 (100)	25 (100)	11 (100)	32 (100)	19 (100)
BCLC stage ^b										
A	0	1 (4)	5 (6)	2 (5)	4 (15)	2 (18)	0	0	1 (3)	0
B	13 (25)	9 (33)	7 (8)	3 (7)	2 (8)	0	3 (12)	2 (18)	2 (6)	1 (5)
C	37 (73)	17 (63)	71 (86)	36 (88)	20 (77)	9 (82)	22 (88)	9 (82)	29 (91)	18 (95)
Hepatitis B	5 (10)	4 (15)	64 (77)	30 (73)	10 (38)	5 (45)	24 (96)	7 (64)	30 (94)	18 (95)
Hepatitis C	18 (35)	5 (19)	21 (25)	6 (15)	17 (65)	5 (45)	0	0	4 (13)	1 (5)
Liver cirrhosis	32 (63)	16 (59)	57 (69)	25 (61)	18 (69)	7 (64)	19 (76)	7 (64)	20 (63)	11 (58)
Prior locoregional therapy	31 (61)	17 (63)	68 (82)	29 (71)	24 (92)	10 (91)	22 (88)	10 (91)	22 (69)	9 (47)
Prior systemic therapy										
Sorafenib containing	48 (94)	22 (81)	76 (92)	36 (88)	26 (100)	10 (91)	24 (96)	11 (100)	25 (78)	15 (79)
Other ^c	3 (6)	5 (19)	7 (8)	5 (12)	0	1 (9)	1 (4)	0	7 (22)	4 (21)
Intolerant to prior systemic therapy	6 (12)	11 (41)	7 (8)	6 (15)	4 (15)	3 (27)	1 (4)	2 (18)	2 (6)	1 (5)

^a n (%) for all except median (range) years for age. BCLC, Barcelona Clinic Liver Cancer; BSC, best supportive care; CHT, China/Hong Kong/Taiwan; ECOG PS, Eastern Cooperative Oncology Group performance status. ^b Tumor vascular invasion and/or extrahepatic spread. ^c Either does not add up to 100% due to unknown/missing data or exceeds 100% due to rounding off of numbers. ^d Includes brivanib and blind therapy.

Table 2. Drug exposure

Parameters	Non-Asia (n = 78)		Asia		Korea (n = 36)		CHT (n = 51 ^a)	
	axitinib/BSC (n = 51)	placebo/BSC (n = 27)	axitinib/BSC (n = 83)	placebo/BSC (n = 41)	axitinib/BSC (n = 26)	placebo/BSC (n = 11)	axitinib/BSC (n = 25)	placebo/BSC (n = 11)
Days on treatment ^b	110 (4–769)	74 (17–532)	140 (14–741)	56 (11–925)	103 (14–741)	56 (22–189)	262 (30–679)	57 (11–290)
Days on drugs ^c	103 (4–741)	64 (16–532)	139 (14–733)	56 (11–925)	102 (14–733)	56 (22–189)	261 (20–586)	57 (11–286)
Average daily dose, mg	9.9 (3.5–19.1)	13.4 (3.2–19.5)	9.3 (3.0–17.7)	10.0 (7.4–19.4)	6.7 (3.2–10.0)	10.0 (9.4–10.0)	9.5 (6.0–15.1)	9.8 (7.4–18.9)
Relative dose intensity, %	97 (33–188)	129 (15–195)	87 (23–173)	100 (63–194)	57 (24–100)	100 (90–100)	91 (47–141)	98 (63–189)
Dose modification, %								
Increases	39	78	29	37	0	0	44	45
Interruptions	80	74	80	44	92	45	84	45
Reductions	37	4	49	7	69	0	44	9

Values are presented as the median (range) except for dose modification, which shows the percentage of patients with dose increases, interruptions, or reductions. BSC, best supportive care; CHT, China/Hong Kong/Taiwan. ^a One patient in the axitinib/BSC arm from China did not receive treatment. ^b Time from the date of first dose to the date of last dose. ^c Total number of days on which the drug was actually administered.

Table 3. Follow-up therapy

Therapy	Non-Asia (n = 78)		Asia		Japan (n = 37)		Korea (n = 36)		CHT (n = 51)	
	axitinib/BSC (n = 51)	placebo/BSC (n = 27)	axitinib/BSC (n = 83)	placebo/BSC (n = 41)	axitinib/BSC (n = 26)	placebo/BSC (n = 11)	axitinib/BSC (n = 25)	placebo/BSC (n = 11)	axitinib/BSC (n = 32)	placebo/BSC (n = 19)
Locoregional therapy	1 (2)	0	12 (14)	6 (15)	12 (46)	6 (55)	0	0	0	0
Any systemic therapy	13 (25)	13 (48)	30 (36)	23 (56)	16 (62)	10 (91)	10 (40)	4 (36)	4 (13)	9 (47)
Any TKI or mTOR										
Sorafenib	3 (6)	4 (15)	12 (14)	7 (17)	7 (27)	4 (36)	3 (12)	1 (9)	2 (6)	2 (11)
Sunitinib	2 (4)	2 (7)	2 (2)	0	0	0	2 (8)	0	0	0
Everolimus/sirolimus	2 (4)	1 (4)	2 (2)	1 (2)	0	0	0	0	2 (6)	1 (5)

Values are n (%). BSC, best supportive care; CHT, China/Hong Kong/Taiwan; mTOR, mechanistic target of rapamycin; TKI, tyrosine kinase inhibitor.

study treatment, mostly due to objective progression/relapse or AEs (online suppl. Material S1; for all online suppl. material, see www.karger.com/doi/10.1159/000484620).

Within each region, the patients in the axitinib/BSC arm were on treatment for a significantly longer duration than those in the placebo/BSC arm (Table 2). Thus, the median time on the drug (i.e., the total number of days on which the drug was actually administered) in the axitinib/BSC arm was longer than in the placebo/BSC arm, especially among the patients from Korea (261 vs. 57 days). However, more frequent dose interruptions or dose reductions were observed with axitinib/BSC than with placebo/BSC treatment within each region (Table 2). When comparing the different regions, Japan had a higher percentage of patients with axitinib dose reductions than non-Asia, Korea, or CHT (69 vs. 37 vs. 44 vs. 35%), and none of the Japanese patients had an increase in axitinib dose. Consequently, the patients in Japan received a lower axitinib dose than the patients in non-Asia, Korea, or CHT: an average daily axitinib dose of 6.7 mg in Japan compared with 9.9 mg in non-Asia, 9.5 mg in Korea, and 9.8 mg in CHT. The lowest median axitinib relative dose intensity was reported among the patients in Japan (57%), compared with the median relative dose intensities of 91–97% achieved among the patients in non-Asia, Korea, or CHT.

Follow-Up Therapy

Geographical differences were seen in the use of follow-up locoregional or systemic therapies (Table 3). The number of patients in the axitinib/BSC and the placebo/BSC arm, respectively, receiving post-study locoregional therapy was higher in Japan (46 and 55%) than in Korea (0 and 0%), CHT (0 and 0%), or non-Asia (2 and 0%). Also, a higher percentage of patients (70% of all patients) in Japan received follow-up systemic therapy, including hepatic arterial infusion chemotherapy, compared with those in Korea, CHT, or non-Asia (39, 25, and 33%, respectively). Sorafenib was the most frequently used tyrosine kinase inhibitor in follow-up therapy in all regions.

Efficacy

In the subgroup analysis, there was no statistically significant difference in OS between the axitinib/BSC and the placebo/BSC arm observed among the patients from non-Asia, from Asia, or from the Asian subgroups (Fig. 1). Median OS in the axitinib/BSC and the placebo/BSC arm, respectively, was 12.3 months (95% CI 9.5–14.9) and 11.2 months (95% CI 7.9–16.0) in non-Asia (HR 0.977, 95% CI 0.572–1.670; $p = 0.4647$) and 13.5 months (95% CI 9.2–18.1) and 6.3 months (95% CI 3.1–11.6) in Asia (HR 0.832, 95% CI 0.539–1.283; $p = 0.2018$). The HR between the two treatment arms was 0.836 (95% CI 0.378–1.849; $p = 0.3319$) in Japan, 0.925 (95% CI 0.359–2.382; $p = 0.4358$) in Korea, and 0.787 (95% CI 0.419–1.480; $p = 0.2262$) in CHT.

In an exploratory analysis in which patients intolerant to prior antiangiogenic therapy were excluded from the data set, OS favored axitinib/BSC over placebo/BSC in Asia, especially in Japan (Fig. 2). In non-Asia, median OS in the axitinib/BSC and the placebo/BSC arm, respectively, was 12.3 months (95% CI 9.5–14.9) and 9.8 months (95% CI 6.8–13.3) (HR 0.700, 95% CI 0.373–1.316; $p = 0.1318$), whereas in Asia it was 12.4 months (95% CI 7.4–16.4) and 5.2 months (95% CI 3.1–9.9) (HR 0.653, 95% CI 0.415–1.027; $p = 0.0312$). The HR between the axitinib/BSC and the placebo/BSC arm reached statistical significance among the patients from Japan (0.251, 95% CI 0.097–0.650; $p = 0.0011$), but not among the patients from Korea (0.780, 95% CI 0.283–2.150; $p = 0.3150$) or CHT (0.918, 95% CI 0.480–1.756; $p = 0.3954$). In Japan, OS with axitinib/BSC was significantly ($p = 0.0011$) longer than with placebo/BSC (median 13.6 months [95% CI 5.0–19.7] vs. 4.7 months [95% CI 2.8–9.2]).

PFS remained significantly longer in the axitinib/BSC arm than in the placebo/BSC arm in Asia (HR 0.556, 95% CI 0.370–0.835; $p = 0.0023$) but not in non-Asia (HR 0.745, 95% CI

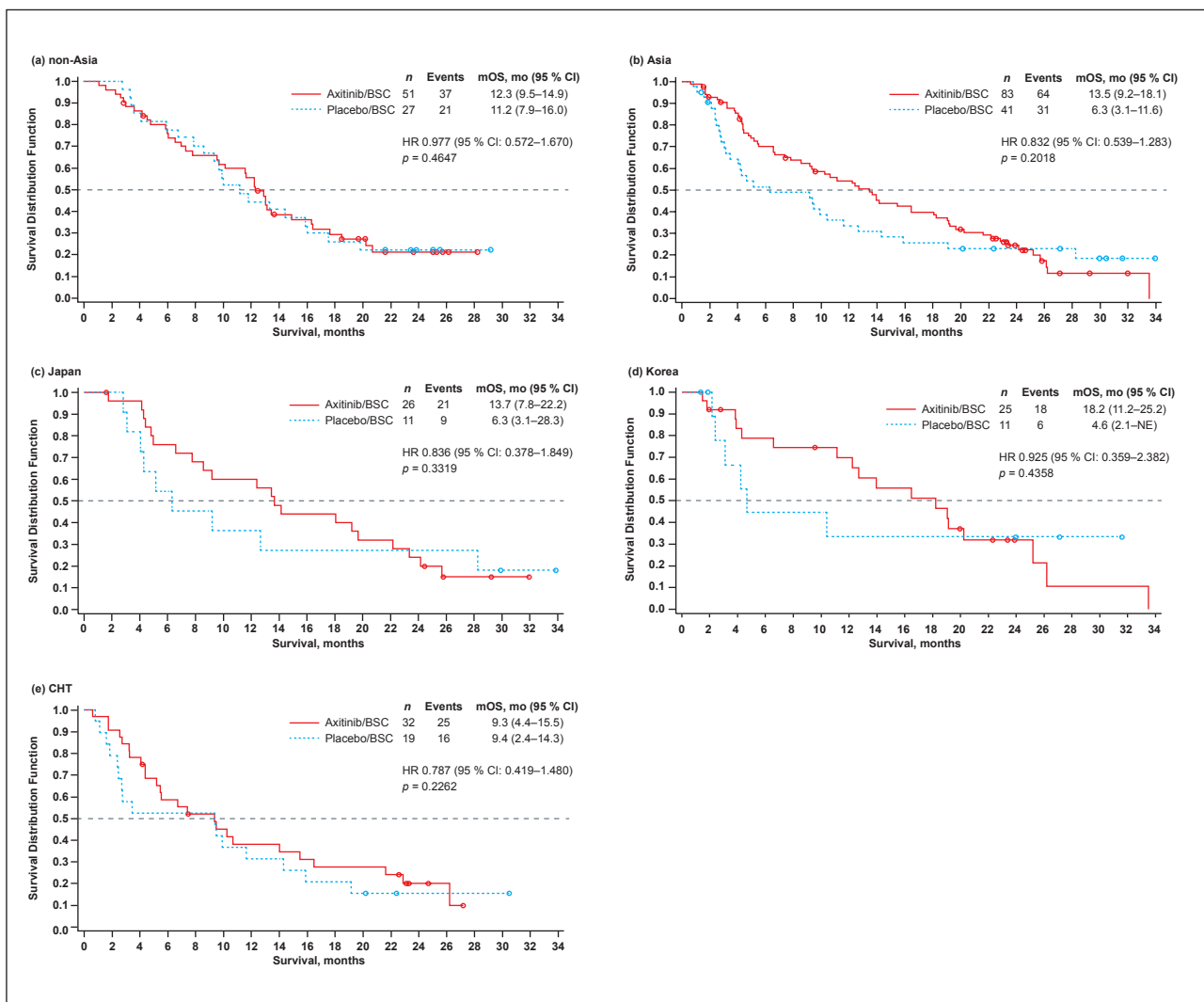


Fig. 1. Kaplan-Meier estimates for OS of patients from non-Asia (a), Asia (b), Japan (c), Korea (d), and CHT (e). *p* values are based on an unstratified one-sided log-rank test. The primary data are available online. BSC, best supportive care; CHT, China/Hong Kong/Taiwan; CI, confidence interval; HR, hazard ratio; mo, months; mOS, median overall survival; NE, not estimable; OS, overall survival.

0.416–1.335; *p* = 0.1590) (online suppl. Material S2). Median PFS among the axitinib/BSC-treated Asian patients was 3.6 months (95% CI 1.9–4.6) as compared with 1.8 months (95% CI 1.7–1.9) among the placebo/BSC-treated Asian patients, whereas among the non-Asian patients, median PFS was 3.7 months (95% CI 1.9–8.8) with axitinib/BSC compared with 3.6 months (95% CI 1.9–3.9) with placebo/BSC. Among the Asian subgroups, the difference in PFS favoring axitinib/BSC over placebo/BSC was statistically significant for Japan (HR 0.325, 95% CI 0.140–0.753; *p* = 0.0032), but not for Korea (HR 0.613, 95% CI 0.277–1.356; *p* = 0.1046) or CHT (HR 0.715, 95% CI 0.389–1.315; *p* = 0.1460) (online suppl. Material S2). Median PFS with axitinib/BSC and with placebo/BSC, respectively, was 3.6 months (95% CI 2.0–7.4) and 1.9 months (95% CI 1.0–1.9) in Japan.

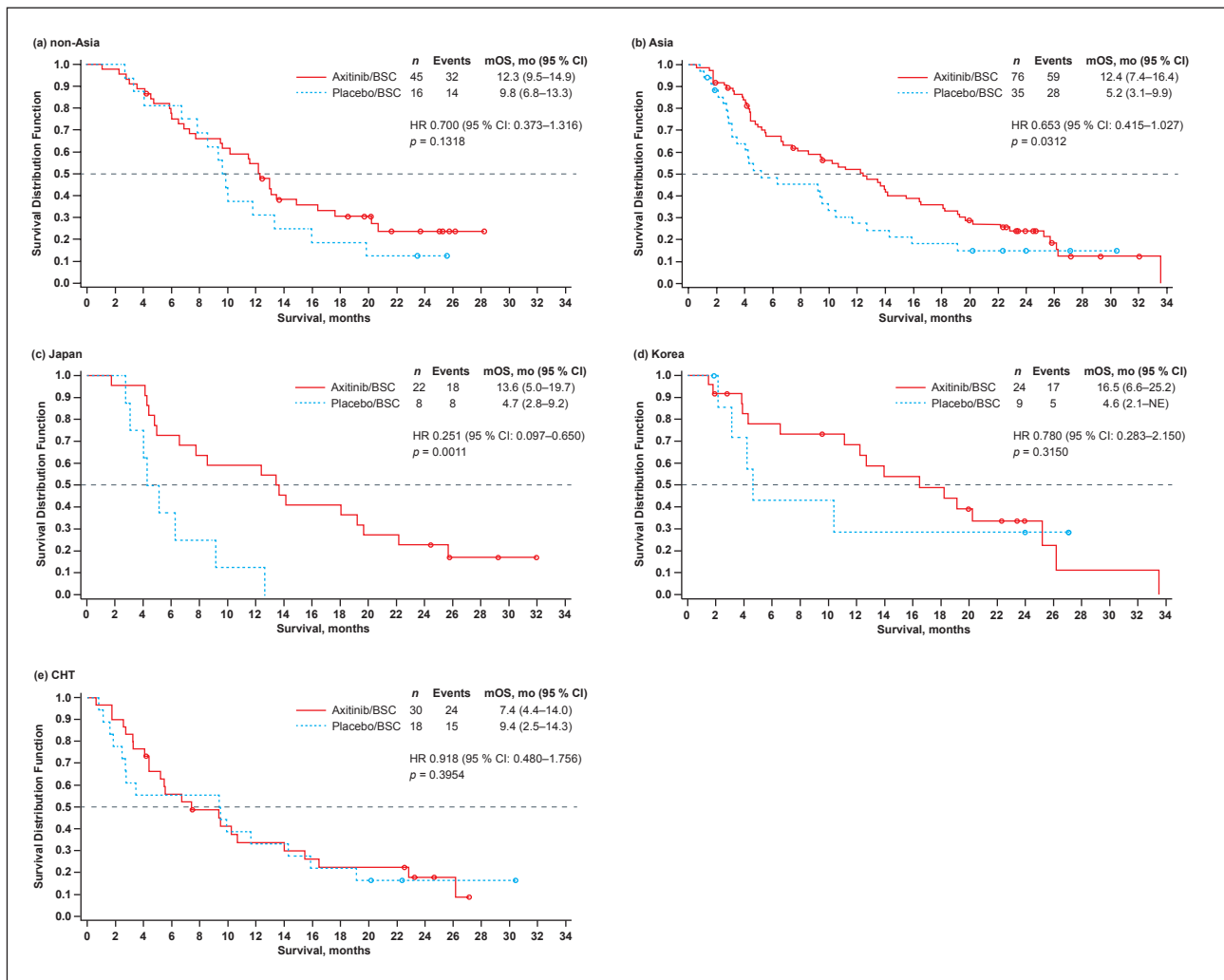


Fig. 2. Kaplan-Meier estimates for OS, excluding patients who were intolerant to prior antiangiogenic therapy, of patients from non-Asia (a), Asia (b), Japan (c), Korea (d), and CHT (e). *p* values are based on an unstratified one-sided log-rank test. BSC, best supportive care; CHT, China/Hong Kong/Taiwan; CI, confidence interval; HR, hazard ratio; mo, months; mOS, median overall survival; NE, not estimable; OS, overall survival.

Safety

Overall, axitinib/BSC was well tolerated by both patients from non-Asia and those from Asia, although the incidence rates for several AEs were elevated compared with placebo/BSC (Table 4). For example, hypertension, diarrhea, and hypothyroidism were >20% higher with axitinib/BSC than with placebo/BSC in both the non-Asian and the Asian patients. Decreased appetite, weight decrease, dysphonia, hand-foot syndrome, and proteinuria were >20% higher with axitinib/BSC than with placebo/BSC only among the Asian patients, whereas asthenia (but not fatigue) and nausea were >20% higher with axitinib/BSC than with placebo/BSC only among the non-Asian patients.

Among the Asian subgroups, the incidence rates of several AEs varied substantially between the axitinib/BSC- and the placebo/BSC-treated patients, as well as between the Asian subgroups. The rate of hypertension was particularly higher (85%) among the axitinib/

Table 4. Common treatment-emergent, all-cause, all-grade adverse events of relevance

Adverse event ^a	Non-Asia (n = 78)		Asia				Japan (n = 37)		Korea (n = 36)		CHT ^b (n = 51)	
	axitinib/BSC (n = 51)	placebo/BSC (n = 27)	axitinib/BSC (n = 83)	placebo/BSC (n = 41)	axitinib/BSC (n = 26)	placebo/BSC (n = 11)	axitinib/BSC (n = 25)	placebo/BSC (n = 11)	axitinib/BSC (n = 32)	placebo/BSC (n = 19)		
Hypertension	28 (55)	5 (19)	44 (54)	4 (10)	22 (85)	0	10 (40)	2 (18)	12 (39)	2 (11)		
Diarrhea	26 (51)	5 (19)	46 (56)	3 (7)	16 (62)	2 (18)	14 (56)	1 (9)	16 (52)	0		
Asthenia	19 (37)	3 (11)	8 (10)	0	0	0	6 (24)	0	2 (6)	0		
Fatigue	17 (33)	8 (30)	29 (35)	10 (24)	7 (27)	2 (18)	8 (32)	4 (36)	14 (45)	4 (21)		
Nausea	17 (33)	3 (11)	18 (22)	4 (10)	9 (35)	1 (9)	6 (24)	2 (18)	3 (10)	1 (5)		
Abdominal pain	16 (31)	7 (26)	29 (35)	7 (17)	7 (27)	1 (9)	12 (48)	2 (18)	10 (32)	4 (21)		
Vomiting	15 (29)	5 (19)	11 (13)	2 (5)	7 (27)	0	4 (16)	1 (9)	0	1 (5)		
Decreased appetite	14 (28)	7 (26)	48 (59)	7 (17)	16 (62)	2 (18)	19 (76)	3 (27)	13 (42)	2 (11)		
Hypothyroidism	12 (24)	0	21 (26)	0	8 (31)	0	6 (24)	0	7 (23)	0		
Weight decrease	10 (20)	1 (4)	26 (32)	1 (2)	8 (31)	0	10 (40)	1 (9)	8 (26)	0		
Dysphonia	8 (16)	0	25 (30)	0	9 (35)	0	10 (40)	0	6 (19)	0		
Constipation	7 (14)	2 (7)	14 (17)	6 (15)	4 (15)	0	6 (24)	1 (9)	4 (13)	5 (26)		
Hand-foot syndrome	6 (12)	2 (7)	39 (48)	2 (5)	12 (46)	0	14 (56)	1 (9)	13 (42)	1 (5)		
Cough	6 (12)	2 (7)	10 (12)	4 (10)	1 (4)	3 (27)	1 (4)	0	8 (26)	1 (5)		
Stomatitis	4 (8)	0	15 (18)	0	4 (15)	0	10 (40)	0	1 (3)	0		
Proteinuria	3 (6)	0	24 (29)	1 (2)	11 (42)	0	5 (20)	0	8 (26)	1 (5)		
Malaise	1 (2)	0	12 (14)	1 (2)	11 (42)	1 (9)	0	0	1 (3)	0		

Values are n (%). BSC, best supportive care; CHT, China/Hong Kong/Taiwan. ^a Adverse event reported by ≥25% of the patients in any group. ^b One patient in the axitinib/BSC arm from CHT did not receive treatment.

BSC-treated Japanese patients than among the placebo/BSC-treated Japanese patients (0%) or the axitinib/BSC-treated patients from Korea (40%) or CHT (39%). Nausea and vomiting were also more frequently reported by the Japanese patients receiving axitinib/BSC compared with those receiving placebo/BSC or the patients from Korea or CHT who received axitinib/BSC, but the reason for the higher incidence of nausea among the Japanese patients is unknown. Decreased appetite and stomatitis were more common in the axitinib/BSC-treated patients from Korea, whereas cough was more common in the axitinib/BSC-treated patients from CHT. Malaise had a higher incidence in the axitinib/BSC-treated Japanese patients than in the axitinib-treated patients from Korea or CHT (42 vs. 0 or 3%). However, a plausible reason for this observation might be the different definition of malaise in these countries, since the incidence rate was lower in Japan than in Korea or CHT for AEs that could have been used interchangeably: asthenia (0, 24, and 6%, respectively) and fatigue (27, 32, and 45%, respectively).

All-cause grade ≥ 3 AEs reported in $\geq 20\%$ of the axitinib/BSC-treated patients in non-Asia versus Asia were hypertension (18 vs. 30%), diarrhea (22 vs. 20%), and hand-foot syndrome (4 vs. 22%). Serious AEs associated with axitinib/BSC were reported in 51% of the patients from non-Asia versus 44% of those from Asia; among the Asian subgroups, 46, 44, and 42% of the patients treated with axitinib/BSC in Japan, Korea, and CHT, respectively, reported serious AEs.

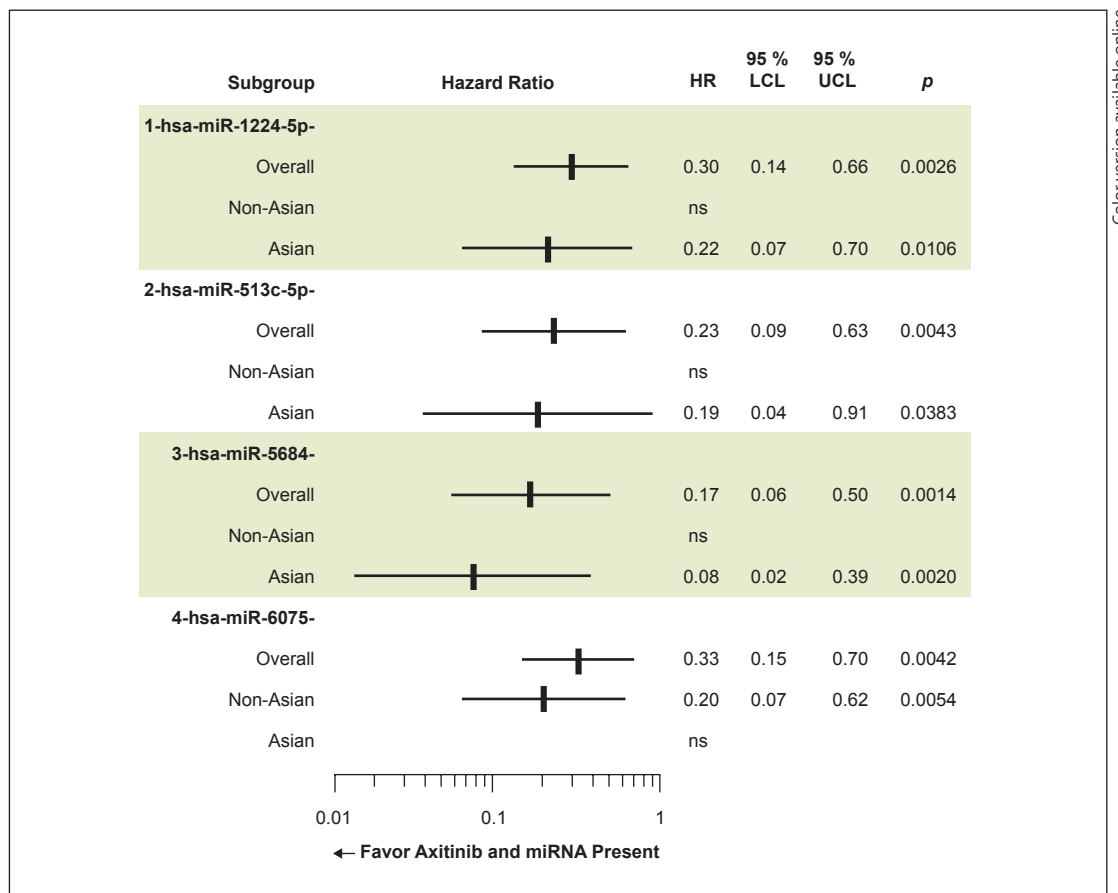
The proportion of patients who had AEs requiring axitinib dose reductions was higher in Asia than in non-Asia (41 vs. 24%), but a lower proportion of patients had AEs leading to treatment discontinuation in Asia than in non-Asia (22 vs. 39%). Among the Asian subgroups, a higher percentage of patients had AEs requiring axitinib dose reductions in Korea than in Japan or CHT (60 vs. 42 or 26%), but fewer patients had AEs leading to treatment discontinuations (8 vs. 23 or 32%).

Predictive and/or Prognostic Factors

From the blood samples collected at baseline, RNA of sufficient quality for Agilent microarray analysis was generated from a majority of the patients (84%, $n = 170$, including 72 non-Asians and 98 Asians). The predictive and/or prognostic potential of baseline levels of 174 circulating miRNAs for OS were evaluated, including those known to be associated with angiogenesis or tumor growth. The baseline characteristics of the patients included in the analyses were found to be balanced between the treatment arms (online suppl. Material S3).

The analysis identified several circulating miRNAs using the Cox proportional hazards model for OS. Positive (FDR = 0.2) predictive effects associated with increased OS were observed for 3 miRNAs (hsa-miR-5684, hsa-miR-1224-5p, and hsa-miR-513c-5p) in the patients from Asia, but not in those from non-Asia. Another miRNA (hsa-miR-6075) was positively (FDR = 0.2) predictive of survival in the patients from non-Asia, but not in those from Asia. A total of 4 circulating miRNAs were found to be statistically significantly (FDR = 0.2) associated with longer OS (HR ranging from 0.08 to 0.33) when present versus absent in the overall, Asian, or non-Asian population (Fig. 3). In the Asian patients treated with axitinib/BSC, median (95% CI) OS was 19.1 months (9.2–25.2) if circulating hsa-miR-1224-5p was present, compared with 8.6 months (5.5–14.1) if absent. In the placebo/BSC arm, median (95% CI) OS was 6.3 months (2.8–12.7) if present, and not estimable (1.8 to not estimable) if absent. Median OS in the presence versus absence of each of these 4 miRNAs is summarized in Table 5.

As reported elsewhere [7], the previous analysis based on the unstratified log-rank test unadjusted for multiple comparisons revealed an association between a low baseline serum level of E-selectin or SDF-1 and longer OS among all axitinib/BSC-treated patients compared with placebo/BSC-treated patients. Furthermore, in that report the Cox proportional hazards



Color version available online

Fig. 3. Predictive circulating microRNA subgroup analysis of overall survival in the overall, non-Asian, and Asian population. HR, hazard ratio; LCL, lower confidence limit; miR, microRNA; ns, not significant; UCL, upper confidence limit.

model showed a lower-than-median baseline level of IL-6, E-selectin, IL-8, Ang-2, MIF, or soluble c-MET to be a potential positive prognostic factor for OS in HCC. In the current subgroup analyses, the significant association between a lower-than- or equal-to-median baseline serum level of SDF-1 ($p_{unadjusted} = 0.0026$) and longer OS was observed in the Asian patients who were treated with axitinib/BSC compared with those treated with placebo/BSC (FDR = 0.2). Among the non-Asian patients, no association was identified between any of the soluble proteins tested and OS.

Discussion

The current exploratory analyses of the efficacy and safety data from the phase II study of axitinib in advanced HCC were conducted in order to identify demographics and baseline characteristics of patients who might best benefit from axitinib treatment and to select more suitable target populations for future trials in advanced HCC. The analyses showed several interesting findings. First, some geographical differences in demographics and baseline characteristics were observed between patients with HCC enrolled in non-Asia and those enrolled in Asia, as well as between different Asian ethnicities. Notably, the percentage of patients with

Table 5. Median OS stratified by select microRNAs in the axitinib/BSC and placebo/BSC arms

miR	Median OS (95% CI), months							
	axitinib/BSC				placebo/BSC			
	<i>n</i>	miR present	<i>n</i>	miR absent	<i>n</i>	miR present	<i>n</i>	miR absent
hsa-miR-1224-5p								
Overall	63	13.9 (10.2–19.1)	48	12.2 (6.7–14.1)	36	8.9 (4.1–11.6)	23	14.4 (7.9–NE)
Non-Asian	31	12.3 (6.9–17.6)	17	13.0 (4.6–20.2)	15	9.3 (3.4–13.3)	11	14.4 (7.9–NE)
Asian	32	19.1 (9.2–25.2)	31	8.6 (5.5–14.1)	21	6.3 (2.8–12.7)	12	NE (1.8–NE)
hsa-miR-513c-5p								
Overall	83	13.5 (11.6–18.2)	28	7.8 (4.6–13.9)	47	9.3 (4.3–11.2)	12	19.8 (1.8–NE)
Non-Asian	39	12.3 (9.7–13.5)	9	14.9 (2.8–20.7)	20	9.5 (4.1–13.3)	6	18.7 (11.8–NE)
Asian	44	18.2 (8.6–23.4)	19	7.8 (3.9–13.7)	27	9.2 (3.1–12.7)	6	NE (1.1–NE)
hsa-miR-5684								
Overall	93	13.5 (11.5–16.5)	18	8.9 (3.9–18.1)	48	9.4 (4.1–12.7)	11	NE (7.9–NE)
Non-Asian	42	12.9 (9.5–14.9)	6	15.4 (3.0–20.7)	21	10.0 (5.9–15.9)	5	11.8 (7.9–NE)
Asian	51	16.4 (8.6–22.2)	12	6.1 (1.7–12.4)	27	4.6 (2.8–12.7)	6	NE (4.3–NE)
hsa-miR-6075								
Overall	62	16.4 (10.2–22.2)	49	12.2 (6.7–13.7)	35	9.2 (4.2–12.7)	24	11.8 (7.9–NE)
Non-Asian	28	12.9 (7.3–NE)	20	12.2 (4.6–14.9)	14	7.7 (3.4–13.3)	12	16.0 (9.3–NE)
Asian	34	18.2 (5.5–25.2)	29	11.2 (6.6–14.1)	21	9.4 (4.2–15.9)	12	4.0 (1.6–NE)

BSC, best supportive care; CI, confidence interval; miR, microRNA; NE, not estimable; OS, overall survival.

hepatitis B, one of the primary causes of HCC, was significantly higher in Asia (excluding Japan) than in non-Asia, especially in CHT, where ~95% of the patients had hepatitis B. Hepatitis C, another potential cause of HCC, was prevalent among Japanese patients. The percentage of patients with baseline extrahepatic spreads with intrahepatic tumors and BCLC stage C, and thus a less favorable prognosis, was also higher among patients in Asia than among those in non-Asia. These results suggest a different etiology of HCC in patients from different regions and ethnicities, which would have confounded the interpretation of the results of the subgroup analyses. Additionally, despite the fact that the randomization of patients was stratified by tumor invasion (i.e., the presence or absence of extrahepatic spread and/or tumor vascular invasion) in the overall population, minor differences in baseline characteristics – such as extrahepatic spread with intrahepatic tumors, tumor vascular invasion, and hepatitis C – were observed between the axitinib/BSC and the placebo/BSC treatment arm in the Asian subgroups, especially in Japan, further making the interpretation of the data more challenging.

Second, there was no statistically significant difference in OS between axitinib/BSC-treated and placebo/BSC-treated patients in non-Asia or in Asia. A lack of clinical benefit from adding axitinib to BSC was also evident in the Asian subgroups. However, in an exploratory analysis in which patients who were intolerant to prior antiangiogenic therapy were excluded, there was a difference in OS between the two treatment arms, favoring axitinib/BSC among Japanese patients. Finally, our analyses suggest that baseline levels of 4 circulating miRNAs, including hsa-miR-5684 and hsa-miR-1224-5p, as well as serum protein SDF-1 might have some predictive value for OS with axitinib and/or prognostic value in HCC patients, which warrants further investigation.

Apart from the geographical differences noted in baseline characteristics of the HCC patients, the analyses revealed an interesting disparity in clinical practice relative to treatment regimens between the Asian group, the non-Asian group, and the Asian subgroups. Patients in CHT had similar treatment schedules and dose modifications to non-Asian patients,

whereas patients from Korea were on axitinib/BSC treatment more than twice as long as patients from other regions. Although Japanese and Korean patients had more axitinib dose reductions due to AEs than Chinese patients, they had fewer axitinib discontinuations due to AEs. Japanese patients had the most axitinib dose reductions and temporary dose interruptions due to any cause, and with none of the Japanese patients receiving dose increases, their axitinib relative dose intensity was the lowest. Based on these observations, it is tempting to postulate that more aggressive axitinib treatment modifications in Japan might have contributed to more favorable efficacy outcomes, including both PFS and OS, than those in Korea, CHT, or non-Asia. However, it is likely that other factors, such as more frequent use of post-study therapies, must also have accounted for the outcome. It is noteworthy that similar regional disparities in treatment practice patterns and patient baseline characteristics have been reported in a subgroup analysis of a randomized phase III trial of ramucirumab in advanced HCC, which the authors saw as some of the likely reasons for achieving survival benefits in Japanese patients ($n = 93$) [9] but not in the total population ($n = 565$) [4]. These findings observed in clinical trials seem to reflect the real-world setting, as seen in a subgroup analysis of a prospective, international, noninterventional study of sorafenib in patients with unresectable HCC [10].

In this analysis, median OS with axitinib/BSC in non-Asian patients was marginally shorter than in Asian patients, although non-Asian patients had better prognostic factors at baseline. Among Asian ethnicities, median OS was longest in axitinib/BSC-treated Korean patients and shortest in Chinese patients. Patients in Korea were on axitinib/BSC treatment for the longest period, and patients in Japan received the most locoregional or systemic follow-up therapies, which might explain, at least in part, the numerically longer median OS of these patients. Interestingly, median OS in the placebo/BSC arm was shorter in patients from Korea (4.6 months) and Japan (6.3 months) than in those from CHT (9.4 months) or non-Asia (11.2 months), especially in light of the fact that a higher percentage of placebo/BSC-treated patients in Japan underwent post-study locoregional and/or systemic therapy. Incidentally, the treatment duration was substantially shorter in the placebo/BSC arm than in the axitinib/BSC arm in all the groups.

It was reported that patients who discontinued prior antiangiogenic therapy due to AEs had a better prognosis than those who discontinued treatment due to disease progression or liver failure [11]. In the current analysis, the placebo/BSC arm had a higher proportion of patients who were intolerant to prior antiangiogenic therapy than the axitinib/BSC arm, except for the CHT subgroup. This might explain, at least in part, the improvement in HR favoring axitinib/BSC observed in all Asian regions except CHT when patients intolerant to prior antiangiogenic therapy were excluded from the analysis. In particular, a potentially better OS favoring axitinib/BSC over placebo/BSC was seen in patients from Japan. It is possible that aggressive post-study treatment with sorafenib and/or locoregional therapy resulted in prolonged postprogression survival (PPS), especially in patients who had discontinued prior sorafenib due to AEs, since those patients were generally in good health. Postprogression survival, defined as the time between the last day of treatment and death or last visit recorded, has been demonstrated to strongly correlate with median OS [11, 12]. Additionally, if there are more patients in the placebo/BSC arm who are intolerant to sorafenib but receive sorafenib rechallenge post-study treatment, those patients may benefit from sorafenib rechallenge after failure of study treatment, as has been reported in another study [13].

The nature of AEs reported by patients treated with axitinib/BSC was similar between non-Asia and Asia. However, some AEs, such as asthenia, were more frequent in non-Asia, whereas decreased appetite, hand-foot syndrome, and proteinuria were more common in Asia. Unexpectedly, the incidence rates for several AEs varied between different Asian ethnicities, which may be attributed not only to some minor genomic variations in drug-metabo-

lizing enzymes and/or transporters [14, 15] but also to differences in clinical practice in monitoring and management of common AEs. It should be mentioned that although axitinib population pharmacokinetic analysis for RCC has indicated that Japanese ethnicity is associated with decreased systemic clearance, the magnitude of the effect was considered such that dose adjustments on the basis of Japanese ethnicity were deemed unnecessary [16, 17].

There has been a growing list of targeted therapies that failed to show improved OS in sorafenib-refractory patients with advanced HCC in multinational, double-blind, randomized phase III trials. For instance, median OS for a selective dual inhibitor of VEGFR and the fibroblast growth factor receptor brivanib in combination with BSC was 9.4 months compared with 8.2 months for placebo/BSC (HR 0.89; $p = 0.3307$), indicating a lack of survival benefit for brivanib in HCC [3]. Targeting VEGFR using the monoclonal antibody ramucirumab did not lead to prolongation of survival compared with placebo in the overall population (HR 0.87; $p = 0.14$) [4], despite findings from subgroup analyses that ramucirumab improved OS and PFS among Japanese patients [9]. Another targeted agent, everolimus – an inhibitor of mechanistic target of rapamycin – failed to improve OS over placebo (HR 1.05; $p = 0.68$) when added to BSC in patients with advanced HCC previously treated with sorafenib [5]. However, recently, a phase III trial of another multitargeted tyrosine kinase inhibitor, regorafenib (ClinicalTrials.gov No. NCT01774344, RESORCE trial), met its primary endpoint of a statistically significant improvement in OS in sorafenib-refractory HCC [18]. In that study, only patients who progressed on sorafenib were enrolled, excluding sorafenib-intolerant patients.

The current study has some limitations, the most critical one being that it was an exploratory analysis, and although the patient baseline characteristics were generally comparable between the two treatment arms, there were some minor differences, including tumor invasion, in the Asian group and the Asian subgroups, which could have impacted the results. There were also differences in the frequency of follow-up therapy, with the highest in Japan, which could have contributed to the outcomes. Another limitation is that confounding factors such as the level of hepatic functionality were not evaluated in the current study, and thus were not taken into account in the analyses. It should also be acknowledged that the sample size for some Asian subgroups (e.g., 11 patients each in the placebo/BSC arms in Japan and Korea) was too small to draw definite conclusions.

As in other similar studies, the lack of validated biomarkers that would predict treatment outcomes in metastatic HCC has prevented the selection of patients who might preferentially achieve better clinical outcomes with axitinib/BSC treatment. This study identified a set of circulating miRNAs (e.g., hsa-miR-5684 and hsa-miR-1224-5p) that may have the potential to serve as predictors of response to axitinib treatment in Asian patients with metastatic HCC. However, target genes for these miRNAs are currently unknown, and because the results are extremely preliminary with a potential imbalance in background characteristics – such as regarding tumor vascular invasion and/or extrahepatic spread – between subgroups consisting of small numbers of patients included in the biomarker analysis, additional investigations are necessary in a large group of patients to validate these results.

The current analyses further provided evidence that a low baseline level of SDF-1 was associated with longer OS in Asian patients receiving axitinib/BSC compared with placebo/BSC, as was observed in the overall population [7]. But this association was not observed in non-Asian patients. Since the pathophysiology of HCC and responses to blocking the VEGF/VEGFR signaling pathway are far more complex, additional studies are required to elucidate why these associations were preferentially observed in Asian patients but not in non-Asian patients.

In conclusion, addition of axitinib to BSC did not prolong survival over placebo/BSC in patients from non-Asia, Asia, or Asian subgroups. However, axitinib/BSC showed favorable OS versus placebo/BSC in patients from Asia, especially Japan, when patients intolerant to prior antiangiogenic therapy were excluded from the data set. The data suggest that patients

who progress on prior systemic therapy might constitute a more suitable population for clinical trials of new agents in advanced HCC. Furthermore, PFS in the axitinib/BSC arm remained significantly longer than in the placebo/BSC arm in Asia, but not in non-Asia. Differences in demographics and baseline characteristics observed in patients from different geographical regions could potentially explain the more favorable OS seen in patients from regions such as Japan. In addition, appropriate axitinib dose modifications may play an important role in maintaining a longer duration of treatment, which could lead to better efficacy outcomes. The potential predictive and/or prognostic value of a set of 4 baseline miRNAs (including hsa-miR-5684 and hsa-miR-1224-5p) and soluble protein SDF-1 identified in this study warrants further investigation in a prospective study.

Acknowledgments

Medical writing support was provided by Mariko Nagashima, PhD, of Engage Scientific Solutions (Southport, CT, USA) and was funded by Pfizer.

Statement of Ethics

The study was conducted in accordance with the Declaration of Helsinki and the International Conference on Harmonization guidelines on Good Clinical Practice. The protocol was approved by an institutional review board or independent ethics committee at each center, and all patients provided written informed consent.

Disclosure Statement

M.K. has served as an adviser for Kowa, MSD, Bristol-Myers Squibb, Bayer, Chugai, and Taiho, has received honoraria from Bayer, Eisai, MSD, and Ajinomoto, and has received research funding from Chugai, Otsuka, Takeda, Taiho, Sumitomo Dainippon, Daiichi Sankyo, MSD, Eisai, Bayer, and AbbVie. Y.-K.K. has received a research grant from Bayer and Sanofi. E.A. has served as a consultant for Sanofi, IPSEN, Novartis, and Bayer, and has received travel/accommodations/expenses from Celgene. Y.U. and Y.F. are employed by Pfizer Japan, and Y.U. owns stock in Pfizer. M.J.L., O.V., and J.-F.M. are employed by and own stock in Pfizer. J.A.W. was employed by Pfizer at the time of the study; he is currently employed by Genentech/Roche. All the other authors declare that they have no conflict of interest.

Funding Source

This study was sponsored by Pfizer.

References

- 1 Ferlay J, Soerjomataram I, Ervik M, Dikshit R, Eser S, Mathers C, Rebelo M, Parkin DM, Forman D, Bray F: GLOBOCAN 2012 v1.0, Cancer Incidence and Mortality Worldwide: IARC CancerBase No. 11. Lyon, International Agency for Research on Cancer. <http://globocan.iarc.fr> (accessed May 18, 2016).
- 2 National Comprehensive Cancer Network: NCCN Clinical Practice Guidelines in Oncology (NCCN Guidelines) Hepatobiliary Cancers version 1. 2016. https://www.nccn.org/professionals/physician_gls/pdf/hepatobiliary.pdf (accessed May 19, 2016).
- 3 Llovet JM, Decaens T, Raoul JL, Boucher E, Kudo M, Chang C, Kang YK, Assenat E, Lim HY, Boige V, Mathurin P, Fartoux L, Lin DY, Bruix J, Poon RT, Sherman M, Blanc JF, Finn RS, Tak WY, Chao Y, Ezzeddine R, Liu D, Walters I, Park JW: Brivanib in patients with advanced hepatocellular carcinoma who were intolerant to sorafenib or for whom sorafenib failed: results from the randomized phase III BRISK-PS study. *J Clin Oncol* 2013;31:3509–3516.

- 4 Zhu AX, Park JO, Ryoo BY, Yen CJ, Poon R, Pastorelli D, Blanc JF, Chung HC, Baron AD, Pfiffer TE, Okusaka T, Kubackova K, Trojan J, Sastre J, Chau I, Chang SC, Abada PB, Yang L, Schwartz JD, Kudo M: Ramucirumab versus placebo as second-line treatment in patients with advanced hepatocellular carcinoma following first-line therapy with sorafenib (REACH): a randomised, double-blind, multicentre, phase 3 trial. *Lancet Oncol* 2015; 16:859–870.
- 5 Zhu AX, Kudo M, Assenat E, Cattani S, Kang YK, Lim HY, Poon RT, Blanc JF, Vogel A, Chen CL, Dorval E, Peck-Radosavljevic M, Santoro A, Daniele B, Furuse J, Jappe A, Perraud K, Anak O, Sellami DB, Chen LT: Effect of everolimus on survival in advanced hepatocellular carcinoma after failure of sorafenib: the EVOLVE-1 randomized clinical trial. *JAMA* 2014;312:57–67.
- 6 INLYTA® (axitinib) prescribing information. Pfizer, 2012. <http://labeling.pfizer.com/ShowLabeling.aspx?id=759>.
- 7 Kang YK, Yau T, Park JW, Lim HY, Lee TY, Obi S, Chan SL, Qin S, Kim RD, Casey M, Chen C, Bhattacharyya H, Williams JA, Valota O, Chakrabarti D, Kudo M: Randomized phase II study of axitinib versus placebo plus best supportive care in second-line treatment of advanced hepatocellular carcinoma. *Ann Oncol* 2015;26:2457–2463.
- 8 Benjamini Y, Hochberg Y: Controlling the false discovery rate: a practical and powerful approach to multiple testing. *JR Stat Soc Series B Methodol* 1995;57:289–300.
- 9 Kudo M, Hatano E, Ohkawa S, Fujii H, Masumoto A, Furuse J, Wada Y, Ishii H, Obi S, Kaneko S, Kawazoe S, Yokosuka O, Ikeda M, Ukai K, Morita S, Tsuji A, Kudo T, Shimada M, Osaki Y, Tateishi R, Sugiyama G, Abada PB, Yang L, Okusaka T, Zhu AX: Ramucirumab as second-line treatment in patients with advanced hepatocellular carcinoma: Japanese subgroup analysis of the REACH trial. *J Gastroenterol* 2017;52:494–503.
- 10 Kudo M, Lencioni R, Marrero JA, Venook AP, Bronowicki JP, Chen XP, Dagher L, Furuse J, Geschwind JF, Ladrón de Guevara L, Papandreou C, Sanyal AJ, Takayama T, Yoon SK, Nakajima K, Lehr R, Heldner S, Ye SL: Regional differences in sorafenib-treated patients with hepatocellular carcinoma: GIDEON observational study. *Liver Int* 2016;36:1196–1205.
- 11 Iavarone M, Cabibbo G, Biolato M, Della Corte C, Maida M, Barbara M, Basso M, Vavassori S, Craxi A, Grieco A, Cammà C, Colombo M: Predictors of survival in patients with advanced hepatocellular carcinoma who permanently discontinued sorafenib. *Hepatology* 2015;62:784–791.
- 12 Terashima T, Yamashita T, Takata N, Nakagawa H, Toyama T, Arai K, Kitamura K, Yamashita T, Sakai Y, Mizukoshi E, Honda M, Kaneko S: Post-progression survival and progression-free survival in patients with advanced hepatocellular carcinoma treated by sorafenib. *Hepatol Res* 2016;46:650–656.
- 13 Nozawa M, Yamamoto Y, Minami T, Shimizu N, Hatanaka Y, Tsuji H, Uemura H: Sorafenib rechallenge in patients with metastatic renal cell carcinoma. *BJU Int* 2012;110(pt B):E228–E234.
- 14 Kurose K, Sugiyama E, Saito Y: Population differences in major functional polymorphisms of pharmacokinetics/pharmacodynamics-related genes in Eastern Asians and Europeans: implications in the clinical trials for novel drug development. *Drug Metab Pharmacokinet* 2012;27:9–54.
- 15 Liu JY, Qu K, Sferruzza AD, Bender RA: Distribution of the *UGT1A1*28* polymorphism in Caucasian and Asian populations in the US: a genomic analysis of 138 healthy individuals. *Anticancer Drugs* 2007;18:693–696.
- 16 Rini BI, Garrett M, Poland B, Dutcher JP, Rixe O, Wilding G, Stadler WM, Pithavala YK, Kim S, Tarazi J, Motzer RJ: Axitinib in metastatic renal cell carcinoma: results of a pharmacokinetic and pharmacodynamic analysis. *J Clin Pharmacol* 2013;53:491–504.
- 17 Chen Y, Suzuki A, Tortorici MA, Garrett M, LaBadie RR, Umeyama Y, Pithavala YK: Axitinib plasma pharmacokinetics and ethnic differences. *Invest New Drugs* 2015;33:521–532.
- 18 Bruix J, Qin S, Merle P, Granito A, Huang Y-H, Bodoky G, Pracht M, Yokosuka O, Rosmorduc O, Breder V, Gerolami R, Masi G, Ross PJ, Song T, Bronowicki JP, Ollivier-Hourmand I, Kudo M, Cheng AL, Llovet JM, Finn RS, LeBerre MA, Baumhauer A, Meinhardt G, Han G; RESORCE Investigators: Regorafenib for patients with hepatocellular carcinoma who progressed on sorafenib treatment (RESORCE): a randomised, double-blind, placebo-controlled, phase 3 trial. *Lancet* 2017;389:56–66.



Sorafenib plus low-dose cisplatin and fluorouracil hepatic arterial infusion chemotherapy versus sorafenib alone in patients with advanced hepatocellular carcinoma (SILIUS): a randomised, open label, phase 3 trial

Masatoshi Kudo*, Kazuomi Ueshima*, Osamu Yokosuka, Sadahisa Ogasawara, Shuntaro Obi, Namiki Izumi, Hiroshi Aikata, Hiroaki Nagano, Etsuro Hatano, Yutaka Sasaki, Keisuke Hino, Takashi Kumada, Kazuhide Yamamoto, Yasuharu Imai, Shouta Iwadou, Chikara Ogawa, Takuji Okusaka, Fumihiko Kanai, Kohei Akazawa, Ken-ichi Yoshimura, Philip Johnson, Yasuaki Arai, for the SILIUS study group†

Summary

Background Hepatic arterial infusion chemotherapy plus sorafenib in phase 2 trials has shown favourable tumour control and a manageable safety profile in patients with advanced, unresectable hepatocellular carcinoma. However, no randomised phase 3 trial has tested the combination of sorafenib with continuous arterial infusion chemotherapy. We aimed to compare continuous hepatic arterial infusion chemotherapy plus sorafenib with sorafenib alone in patients with advanced, unresectable hepatocellular carcinoma.

Methods We did an open-label, randomised, phase 3 trial (SILIUS) at 31 sites in Japan. Eligible patients were aged 20 years or older, with advanced hepatocellular carcinoma not suitable for resection, local ablation, or transarterial chemoembolisation; Eastern Cooperative Oncology Group (ECOG) performance status 0–1; Child-Pugh score 7 or lower; and adequate bone marrow, liver, and renal function. Patients were randomly assigned (1:1) via an interactive web response system with a computer-generated sequence to receive 400 mg sorafenib orally twice daily or 400 mg sorafenib orally twice daily plus hepatic arterial infusion chemotherapy (cisplatin 20 mg/m² on days 1 and 8 and fluorouracil 330 mg/m² continuously on days 1–5 and 8–12 of every 28-day cycle via an implanted catheter system). The primary endpoint was overall survival. The primary efficacy analysis comprised all randomised patients (the intention-to-treat population), and the safety analysis comprised all randomised patients who received at least one dose of study treatment. This trial is registered with ClinicalTrials.gov, number NCT01214343.

Findings Between Nov 4, 2010, and June 10, 2014, 206 patients were randomly assigned (103 to the sorafenib group, 103 to the sorafenib plus hepatic arterial infusion chemotherapy group). One patient in the sorafenib plus hepatic arterial infusion chemotherapy group withdrew after randomisation. Median overall survival was similar in the sorafenib plus hepatic arterial infusion chemotherapy (n=102) and sorafenib monotherapy (n=103) groups (11·8 months [95% CI 9·1–14·5] vs 11·5 months [8·2–14·8]; hazard ratio 1·009 [95% CI 0·743–1·371]; p=0·955). Grade 3–4 adverse events that were more frequent in the sorafenib plus hepatic arterial infusion chemotherapy group than in the sorafenib monotherapy group included anaemia (15 [17%] of 88 vs six [6%] of 102), neutropenia (15 [17%] vs one [1%]), thrombocytopenia (30 [34%] vs 12 [12%]), and anorexia (12 [14%] vs six [6%]).

Interpretation Addition of hepatic arterial infusion chemotherapy to sorafenib did not significantly improve overall survival in patients with advanced hepatocellular carcinoma.

Funding Japanese Ministry of Health, Labour and Welfare.

Copyright © Elsevier Ltd. All rights reserved.

Introduction

Although surgical resection and local ablation therapies, such as percutaneous ethanol injection and percutaneous radiofrequency ablation, are considered curative in patients with hepatocellular carcinoma, most patients worldwide are not diagnosed until the disease is unresectable.^{1–3} Treatment options for patients with unresectable hepatocellular carcinoma include transarterial chemoembolisation, systemic chemotherapy, and hepatic arterial infusion chemotherapy.^{4,5} In hepatic arterial infusion chemotherapy, anticancer drugs are

infused directly into the hepatic artery, resulting in increased local intratumoural drug concentrations.⁶ Drugs infused using this approach include cisplatin monotherapy, with a response rate of 30–40%,^{7,8} and combinations of cisplatin plus fluorouracil, with responses ranging from 7% to 71%.^{9–14}

Hepatic arterial infusion chemotherapy with either low-dose cisplatin plus fluorouracil or fluorouracil plus systemic interferon is widely utilised in Japan, South Korea, and Taiwan. In retrospective comparative cohort studies, hepatic arterial infusion chemotherapy

Lancet Gastroenterol Hepatol 2018

Published Online
April 6, 2018
[http://dx.doi.org/10.1016/S2468-1253\(18\)30078-5](http://dx.doi.org/10.1016/S2468-1253(18)30078-5)

See Online/Comment
[http://dx.doi.org/10.1016/S2468-1253\(18\)30084-0](http://dx.doi.org/10.1016/S2468-1253(18)30084-0)

*Contributed equally

†Members of the SILIUS study group are listed in the appendix

Kindai University Faculty of Medicine, Osaka-Sayama, Japan (Prof M Kudo MD, K Ueshima MD); Chiba University Graduate School of Medicine, Chiba, Japan (O Yokosuka MD, S Ogasawara MD, F Kanai MD); Kyoundo Hospital, Tokyo, Japan (S Obi MD); Japanese Red Cross Musashino Hospital, Musashino, Japan (N Izumi MD); Hiroshima University Hospital, Hiroshima, Japan (H Aikata MD); Osaka University Graduate School of Medicine, Osaka, Japan (H Nagano MD); Kyoto University, Graduate School of Medicine, Kyoto, Japan (E Hatano MD); Kumamoto University Graduate School of Medical Sciences, Kumamoto, Japan (Prof Y Sasaki MD); Kawasaki Medical School, Kurashiki, Japan (Prof K Hino MD); Ogaki Municipal Hospital, Ogaki, Japan (T Kumada MD); Okayama University Medical School, Okayama, Japan (K Yamamoto MD); Ikeda Municipal Hospital, Ikeda, Japan (Y Imai MD); Hiroshima City Hospital, Hiroshima, Japan (S Iwadou MD); Takamatsu Red Cross Hospital, Takamatsu, Japan (C Ogawa MD); National Cancer Center Hospital, Tokyo, Japan (T Okusaka MD, Y Arai MD); Niigata University, Niigata, Japan (K Akazawa PhD);

Kanazawa University,
Kanazawa, Japan
(K-i Yoshimura PhD);
and University of Liverpool,
Liverpool, UK
(Prof P Johnson MD)

Correspondence to:
Dr Masatoshi Kudo, Department
of Gastroenterology and
Hepatology, Kindai University
Faculty of Medicine,
377-2 Ohnohigashi, Osaka-
Sayama, 589-8511, Japan
m-kudo@med.kindai.ac.jp

See Online for appendix

Research in context

Evidence before this study

We searched the PubMed database from January, 2007, to December, 2017, with the keywords “sorafenib” and “hepatic arterial infusion chemotherapy” for studies published in the English language. Studies identified show that sorafenib significantly prolongs overall survival in patients with advanced, unresectable hepatocellular carcinoma. Moreover, retrospective comparative cohort studies have shown that hepatic arterial infusion chemotherapy with low-dose cisplatin plus fluorouracil has survival benefits compared with historical controls in patients with advanced hepatocellular carcinoma, and that, after propensity score matching, hepatic arterial infusion chemotherapy was superior to best supportive care. No phase 3 trials have investigated the safety and efficacy of hepatic arterial infusion chemotherapy, especially that of low-dose cisplatin plus fluorouracil, continually infused via an implanted catheter port system, in patients with advanced hepatocellular carcinoma. Sorafenib and hepatic arterial infusion chemotherapy might have complementary effects in patients with advanced hepatocellular carcinoma, with sorafenib prolonging survival through disease stabilisation and hepatic arterial infusion chemotherapy shrinking tumours. A phase 1/2 trial found that sorafenib plus low-dose cisplatin plus fluorouracil was safe and effective in patients with advanced hepatocellular

carcinoma, suggesting that this combination might benefit patients more than either treatment alone.

Added value of this study

In this randomised phase 3 trial we compared the combination of sorafenib and low-dose cisplatin plus fluorouracil with sorafenib alone in 205 patients with advanced, unresectable hepatocellular carcinoma who were refractory to transarterial chemoembolisation, or had macrovascular invasion, or extrahepatic spread. Although treatment with sorafenib plus hepatic arterial infusion chemotherapy did not increase overall survival, it significantly increased time to progression and the proportion of patients who achieved an overall response.

Implications of all the available evidence

The results of the SILIUS trial suggest that the combination of sorafenib plus hepatic arterial infusion chemotherapy might benefit a selected subgroup of patients, although these results cannot be considered conclusive given the small number of patients. Large-scale trials comparing sorafenib plus hepatic arterial infusion chemotherapy with sorafenib alone in selected patients might be warranted to further investigate this hypothesis. For now, sorafenib monotherapy should remain the standard of care in patients with advanced hepatocellular carcinoma.

showed survival benefits when compared with historical controls.¹⁵ Moreover, after propensity score matching, median survival was longer with hepatic arterial infusion chemotherapy than with best supportive care in a cohort of 476 patients with hepatocellular carcinoma included in a survey by the Liver Cancer Study Group of Japan.¹⁶ Nevertheless, hepatic arterial infusion chemotherapy is not considered standard of care, since no randomised phase 3 trials to date have shown survival benefits in patients with advanced hepatocellular carcinoma.

A phase 2 trial in patients with advanced hepatocellular carcinoma showed better outcomes with single-dose cisplatin arterial infusion chemotherapy plus sorafenib than with sorafenib monotherapy.¹⁷ The arterial infusion technique in that study, however, differed from continuous hepatic arterial infusion chemotherapy using an implanted catheter port system. Thus, prospective trials are needed to assess the safety and efficacy of continuous infusion of low-dose cisplatin plus fluorouracil in patients with advanced hepatocellular carcinoma.

Overall, cytotoxic chemotherapy agents alone have shown little survival benefit in patients with advanced hepatocellular carcinoma.¹⁸ By contrast, sorafenib—an oral inhibitor of serine/threonine kinases—significantly prolonged overall survival in patients with advanced hepatocellular carcinoma, resulting in a key advancement in the treatment of this disease.^{19,20} Sorafenib has since been approved worldwide and has become the standard

treatment for patients with advanced unresectable hepatocellular carcinoma. Other new agents tested in first-line settings, and combinations of sorafenib with other agents, have so far not shown better survival benefits than sorafenib alone.^{21,22}

Two retrospective analyses of propensity score-matched patients showed no significant differences in survival between hepatic arterial infusion chemotherapy and sorafenib monotherapy in patients with advanced hepatocellular carcinoma.^{23,24} However, another retrospective analysis showed better survival with hepatic arterial infusion chemotherapy than with sorafenib monotherapy in patients with advanced portal vein thrombosis (branch and major portal vein invasion).⁶ Therefore, the combination of sorafenib and hepatic arterial infusion chemotherapy might have complementary effects in patients with advanced hepatocellular carcinoma, with sorafenib prolonging survival through disease stabilisation and hepatic arterial infusion chemotherapy shrinking tumours.²⁵ A phase 1/2 study showed that the combination of sorafenib and low-dose cisplatin plus fluorouracil resulted in favourable tumour control and a generally manageable safety profile in patients with advanced hepatocellular carcinoma.²⁵ Combination treatment with sorafenib and hepatic arterial infusion chemotherapy might, therefore, benefit patients with advanced hepatocellular carcinoma more than either treatment alone.

We aimed to compare sorafenib monotherapy with sorafenib plus hepatic arterial infusion chemotherapy in patients with unresectable, advanced hepatocellular carcinoma.

Methods

Study design and patients

The SILIUS trial was a randomised, open-label, active-controlled, parallel-group phase 3 trial done at 31 sites throughout Japan. We recruited patients with advanced hepatocellular carcinoma not suitable for resection, local ablation, or transarterial chemoembolisation. Advanced hepatocellular carcinoma was defined as four or more tumours refractory to transarterial chemoembolisation or tumours with vascular invasion or extrahepatic spread based on histological examination of biopsy samples or findings by dynamic CT, dynamic MRI, or CT scan during hepatic arteriography or arteriportography, according to American Association for the Study of Liver Diseases (AASLD) criteria.

Patients with advanced hepatocellular carcinoma were eligible if they were aged 20 years or older, had a life expectancy of 12 weeks or greater, and were not candidates for hepatectomy, local ablation therapy, or transarterial chemoembolisation. All patients had an Eastern Cooperative Oncology Group (ECOG) performance status of 0–1, a Child-Pugh score of 7 or lower, and adequate bone marrow, liver, and renal function.

Patients were excluded if they had another previous or current malignancy, except for curatively treated intraepithelial cervical cancer, basal cell carcinoma, superficial bladder cancer, early gastric cancer, or other early cancers with a low risk of recurrence. Patients were also excluded if they had renal failure requiring haemodialysis or peritoneal dialysis; congestive heart failure, active coronary artery disease, ischaemic heart disease, or serious cardiac arrhythmia; poorly controlled hypertension; active clinically serious infection (grade ≥ 3); hearing impairment; history of HIV infection; significant gastrointestinal bleeding within 4 weeks of study entry; or were taking a CYP3A4 inhibitor.

All patients provided written informed consent. The study protocol was approved by the ethics committees of all participating institutions, and is available online.

Randomisation and masking

Patients were randomly assigned (1:1) to receive either sorafenib monotherapy or sorafenib plus hepatic arterial infusion chemotherapy (low-dose cisplatin plus fluorouracil). Randomisation was done centrally via an interactive web response system involving a computer-generated sequence and Electric Data Capture System software (Viedoc, Uppsala, Sweden). Masking was not possible because hepatic arterial infusion chemotherapy involved catheter insertion with an implanted reservoir port.

Stratification factors for randomisation by use of the minimisation method included institution; the presence or absence of extrahepatic spread; and macroscopic vascular invasion (Vp0, Vp1–3, or Vp4), where Vp0 indicates no portal vein invasion, Vp1 third branch portal vein invasion, Vp2 second branch portal vein invasion (segmental invasion), Vp3 first branch portal vein invasion (branch invasion), and Vp4 main portal vein invasion, according to Liver Cancer Study Group of Japan criteria.

Procedures

Treatment was divided into 28-day cycles. All patients in both groups were treated with 400 mg sorafenib orally twice daily on days 1–28. In the hepatic arterial infusion chemotherapy combination therapy group, cisplatin was administered at a dose of 20 mg/m² per day on days 1 and 8 and fluorouracil was administered at a dose of 330 mg/m² per day on days 1–5 and 8–12 of every 28-day cycle, followed by 2 weeks off treatment. The first treatment cycle was started within 28 days of randomisation.

Patients in the sorafenib plus hepatic arterial infusion chemotherapy group underwent catheter placement in the hepatic artery for 24 h continuous delivery of low-dose cisplatin and fluorouracil through a subcutaneously implanted port system.²⁶ Both the gastroduodenal artery and the right gastric artery were embolised with a metallic coil to avoid drug flow to the stomach, duodenum, or pancreas. The arterial catheters were placed in a manner allowing for proper drug distribution throughout the liver, with the flow checked by contrast CT through the

For the study protocol see [http://www.med.kindai.ac.jp/shoukaki/research/SILIUS_PhaseIII_Protocol\(3.28\).pdf](http://www.med.kindai.ac.jp/shoukaki/research/SILIUS_PhaseIII_Protocol(3.28).pdf)

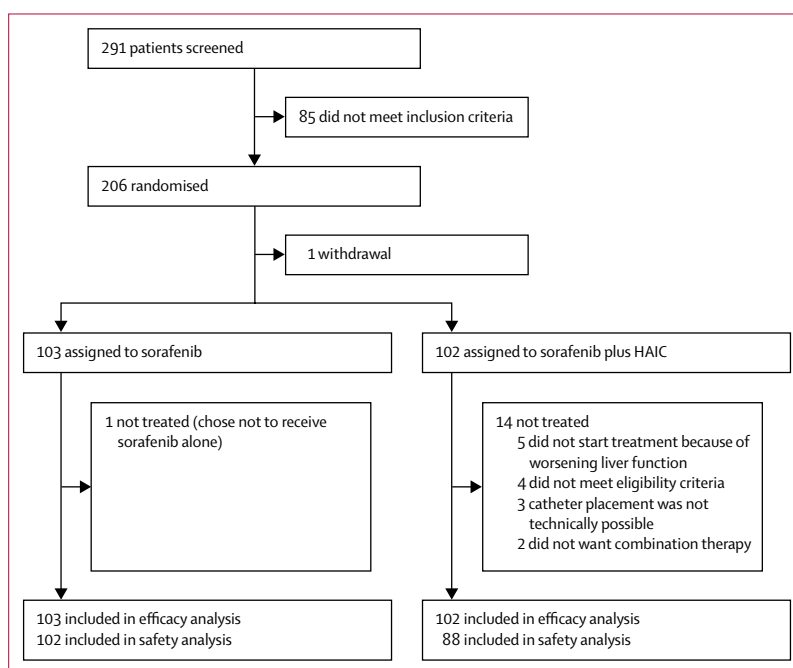


Figure 1: Trial profile
HAIC=hepatic arterial infusion chemotherapy.

	Sorafenib group (n=103)	Sorafenib plus HAIC group (n=102)
Mean age, years	68.1 (9.1)	66.7 (10.2)
Median age, years (IQR)	68 (62–75)	69 (62–75)
Sex		
Men	88 (85%)	89 (87%)
Women	15 (15%)	13 (13%)
ECOG performance status		
0	91 (88%)	89 (87%)
1	12 (12%)	13 (13%)
Child-Pugh score		
5	59 (57%)	61 (60%)
6	34 (33%)	29 (28%)
7	10 (10%)	12 (12%)
Cause		
Hepatitis B virus	22 (21%)	26 (26%)
Hepatitis C virus	46 (45%)	47 (46%)
BCLC stage		
B	27 (26%)	32 (31%)
C	76 (74%)	70 (69%)
Presence of microvascular invasion	64 (62%)	58 (57%)
Presence of extrahepatic spread	26 (25%)	27 (27%)
Presence of microvascular invasion and extrahepatic spread	75 (73%)	73 (72%)
Baseline AFP concentration		
≥400 µg/L	46 (45%)	49 (48%)
<400 µg/L	57 (55%)	46 (45%)
Median baseline AFP, µg/L	195.0	440.5
Median baseline DCP, mAU/mL	1487.0	2780.5
Median baseline AFP-L3, %	24.6	21.6
Data are n (%), mean (SD), or median (IQR). HAIC=hepatic arterial infusion chemotherapy. ECOG=Eastern Cooperative Oncology Group. AFP=α-fetoprotein. AFP-L3=L3 fraction of AFP. BCLC=Barcelona Clinic Liver Cancer. DCP=des-γ-carboxyprotein. Baseline AFP data are missing for seven patients in the sorafenib plus HAIC group.		
Table 1: Baseline demographic and clinical characteristics of the intention-to-treat (efficacy) population		

port or by digital subtraction angiography before starting treatment. All hepatic arterial infusion chemotherapy infusions were done in the outpatient clinic.

Treatment with sorafenib before hepatic arterial infusion chemotherapy was allowed, but patients were required to be off sorafenib for 2 days before and 7 days after reservoir port placement. Treatment was continued until patients had progressive disease, as defined by modified Response Evaluation Criteria in Solid Tumors (mRECIST) and confirmed by imaging, or worsening of general condition. Treatment was also discontinued as a result of adverse events, death, at the patient's request, or if hepatic arterial infusion chemotherapy became technically infeasible due to problems such as occlusion, kinking, or dislocation of the catheter. Patients who achieved a complete response also discontinued treatment.

Criteria for delaying the start of the next cycle of treatment included a neutrophil count of 1000 cells per µL or lower, platelet count of 50 000 cells per µL or lower, total bilirubin 34.2 µmol/L or higher, alanine aminotransferase or aspartate aminotransferase concentrations six or more times the institutional upper limit of normal, serum creatinine up to 1.5 times the institutional upper limit of normal, and amylase up to two times the institutional upper limit of normal. If these criteria were not met, and the start of the next cycle was delayed for 8 weeks or longer, the patient discontinued treatment. Sorafenib doses were adjusted, by interruption or reduction, in patients who had clinically significant haematological or non-haematological toxicities attributed to sorafenib. As defined in the protocol, oral doses of sorafenib were reduced stepwise from 400 mg twice daily to 400 mg once daily to 400 mg every other day to 200 mg every other day. Stepwise increases were allowed after resolution of the adverse event.

Hepatic arterial infusion chemotherapy was interrupted in patients who had haematological and non-haematological toxicities attributed to chemotherapy; sorafenib treatment was continued in these patients. Infusions were resumed at the same dose or a lower dose. Dose was established according to the severity of the toxicities that led to interruption of treatment as well as at the physician's discretion. Two levels of dose reduction of hepatic arterial infusion chemotherapy were allowed: cisplatin 20 mg/m² per day and fluorouracil 170 mg/m² per day; and cisplatin 10 mg/m² per day and fluorouracil 170 mg/m² per day. Cisplatin alone was discontinued without reducing the fluorouracil dose in patients who had adverse events caused by renal dysfunction.

Outcomes

The primary endpoint was overall survival, calculated from the date of randomisation to death from any cause or date of last evaluation. Secondary endpoints were time to progression, calculated from the date of randomisation until documented tumour progression by mRECIST criteria; progression-free survival, calculated from the date of randomisation until documented tumour progression or death from any cause, whichever occurred first; and the proportion of patients with an overall response, calculated as the number of patients who achieved either a complete response or a partial response divided by the total number of patients in the group. In pre-planned subgroup analyses, overall survival was compared in patients without or with varying degrees of portal vascular invasion (Vp0, Vp1–3, or Vp4); and in responders versus non-responders. Responses were assessed by investigators.

Statistical analysis

The sample size was based on the assumptions that median overall survival in patients receiving sorafenib monotherapy would be 10 months and that hepatic arterial

infusion chemotherapy would improve median overall survival to 17 months (hazard ratio [HR] 0.59). Thus, we estimated that 112 events would be required to detect this difference with a power of 80% and a one-sided α of 0.05. We calculated that the required number of events would be observed if 164 patients were enrolled, with an enrolment period of 24 months and a follow-up period of 12 months. Based on an estimated dropout rate of 15%, target enrolment was set at 190 patients (95 per group).

The primary efficacy analysis was done in the intention-to-treat population. The safety analysis comprised all randomised patients who received at least one dose of protocol treatment. Results were reported as mean (SD), number (%), or median (95% CI), and compared by Student's *t* tests or χ^2 tests. Survival outcomes were calculated with the Kaplan-Meier method and compared by log-rank tests. Differences between the two groups were reported as HR and 95% CI. All statistical analyses were done with SPSS, version 23. All *p* values were two sided, with *p* values less than 0.05 considered significant. A data monitoring committee oversaw the study.

This trial is registered with Clinical Trials.gov, number NCT01214343.

Role of the funding source

The funder of the study had no role in study design, data collection, data analysis, data interpretation, or writing of the report. The corresponding author had full access to all the data in the study and had final responsibility for the decision to submit for publication.

Results

Between Nov 4, 2010, and June 10, 2014, 291 patients were screened and 206 were randomly assigned, 103 to receive sorafenib monotherapy and 103 to receive sorafenib plus hepatic arterial infusion chemotherapy. One patient who was randomly assigned to receive sorafenib plus hepatic arterial infusion chemotherapy withdrew after randomisation, leaving 205 patients in the intention-to-treat population. 15 patients (one in the sorafenib group and 14 in the combination therapy group) were not treated, leaving 190 patients in the safety population (figure 1).

Most demographic and clinical characteristics were well balanced between the two groups (table 1). Mean ages of patients in the intention-to-treat population were 68.1 (SD 9.1) years in the sorafenib group and 66.7 (10.2) years in the sorafenib plus hepatic arterial infusion chemotherapy group (median 68 years [IQR 62–75] in the sorafenib group and 69 years [62–75] in the sorafenib plus hepatic arterial infusion chemotherapy group), and more than 80% of patients in both groups were men. The two groups also did not differ significantly in Child-Pugh score, disease cause, Barcelona Clinic Liver Cancer (BCLC) stage, or presence of extrahepatic spread and macroscopic vascular invasion (table 1).

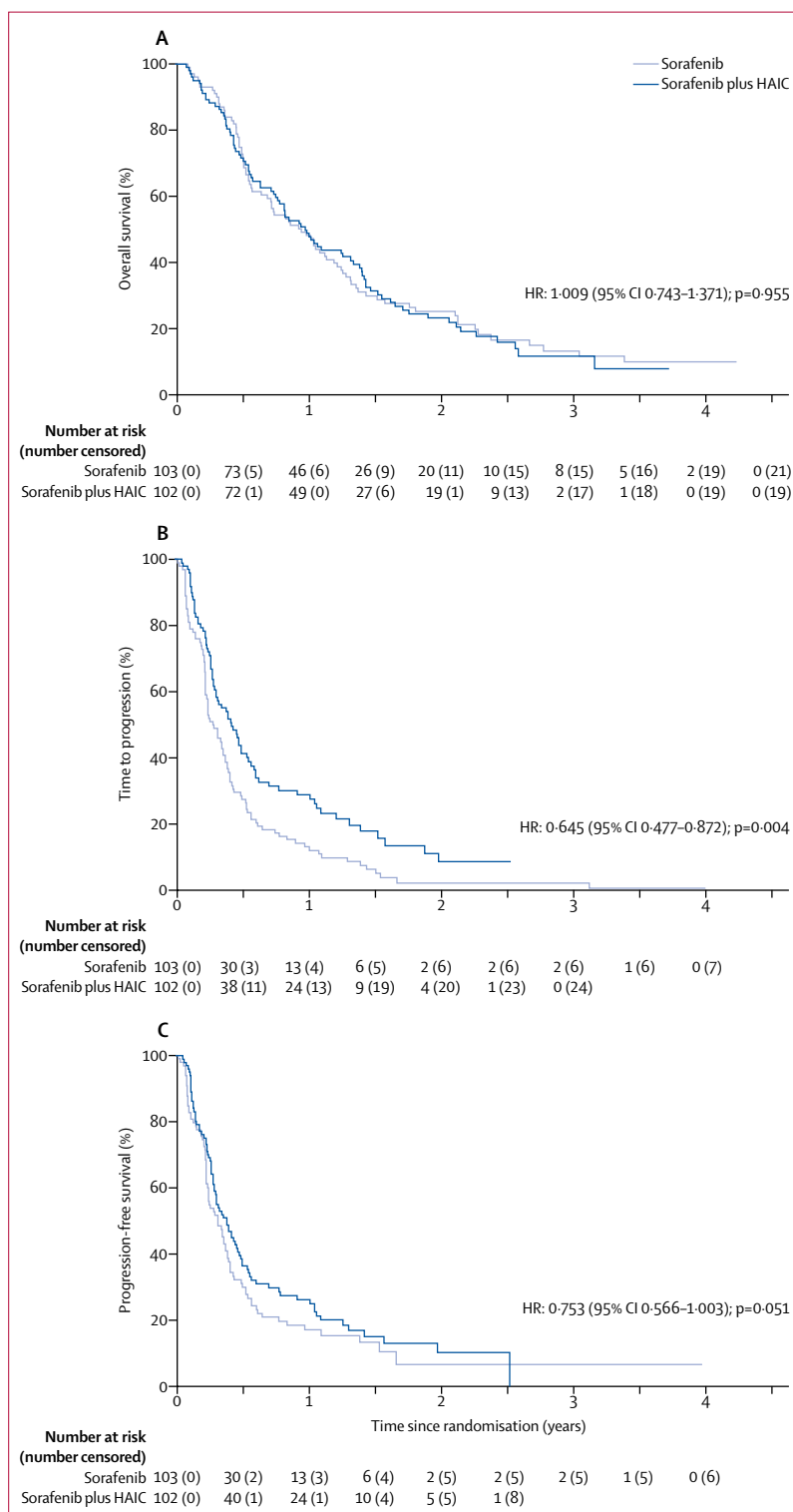


Figure 2: Kaplan-Meier analyses

Overall survival (A), time to progression (B), and progression-free survival (C) in patients treated with sorafenib alone and sorafenib plus hepatic arterial infusion chemotherapy (HAIC).

	Sorafenib group (n=103)	Sorafenib plus HAIC group (n=102)	p value
Best response			
Complete response	2 (2%)	8 (8%)	<0.001
Partial response	16 (16%)	29 (28%)	..
Stable disease	57 (55%)	29 (28%)	..
Progressive disease	21 (20%)	16 (16%)	..
Not evaluable*	7 (7%)	20 (20%)	..
Overall response (complete response and partial response)	18 (18%)	37 (36%)	0.003

Data are n (%). RECIST=Response Evaluation Criteria in Solid Tumors.
 *The seven patients not evaluable in the sorafenib group comprised one who could not start sorafenib treatment and six with vascular invasion alone or irregular vague tumour margins. The 20 patients not evaluable in the hepatic arterial infusion chemotherapy (HAIC) and sorafenib group comprised 14 who could not start HAIC for technical reasons and six with vascular invasion alone or irregular vague tumour margins.

Table 2: Summary of best response by modified RECIST criteria in the randomised population

duration was slightly longer in the sorafenib monotherapy group (appendix). Mean and median relative sorafenib dose intensities were greater in the sorafenib monotherapy group than in the sorafenib plus hepatic arterial infusion chemotherapy treatment group (appendix). The mean number of hepatic arterial infusion chemotherapy cycles in the combination therapy group was 4.0 (SD 4.0) and the median was 2.0 (IQR 1.0–5.0; appendix).

Overall survival was similar in the two treatment groups (figure 2A). Median overall survival was 11.5 months (95% CI 8.2–14.8) in patients treated with sorafenib alone and 11.8 months (9.1–14.5) in those treated with sorafenib plus hepatic arterial infusion chemotherapy (HR 1.009 [95% CI 0.743–1.371], p=0.955).

Median time to progression was significantly longer in patients treated with sorafenib plus hepatic arterial infusion chemotherapy (5.3 months [95% CI 3.9–6.7]) than in those treated with sorafenib alone (3.5 months [2.5–4.6]; HR 0.645 [95% CI 0.477–0.872], p=0.004; figure 2B). The proportion of patients who achieved an overall response was also significantly higher in the combination therapy group than in the sorafenib monotherapy group (37 [36%] of 102 vs 18 [18%] of 103, p=0.003; table 2). Median progression-free survival, however, was similar in both groups (4.8 months [95% CI 3.4–6.2] with sorafenib plus hepatic arterial infusion chemotherapy vs 3.5 months [2.6–4.4] with sorafenib alone; HR 0.753 [95% CI 0.566–1.003], p=0.051; figure 2C).

Median overall survival was similar in patients with no vascular invasion (Vp0) who received sorafenib monotherapy (11.9 months [95% CI 5.4–18.4]) and in those who received sorafenib plus hepatic arterial infusion chemotherapy (11.3 months [6.6–16.0]; HR 1.001 [95% CI 0.623–1.608]; p=0.996; figure 3 and appendix). Median overall survival in patients with Vp1–3 (branch-segmental portal vein invasion) was 14.4 months (95% CI 9.3–19.5) with sorafenib monotherapy versus 12.6 months (4.3–20.9) with sorafenib plus hepatic arterial infusion chemotherapy, but this difference was not significant (HR 1.367 [95% CI 0.829–2.255]; p=0.218; figure 3 and appendix). Median overall survival in patients with main portal vein invasion (Vp4) was 11.4 months (95% CI 7.0–15.9) in those treated with sorafenib plus hepatic arterial infusion chemotherapy versus 6.5 months (4.5–8.4) in those treated with sorafenib alone (HR 0.493 [95% CI 0.240–1.014]; p=0.050; figure 3 and appendix). Cox proportional hazards model analysis of the interaction between treatment and grade of portal vein invasion showed no significant differences between the two groups, both for Vp1–3 (p=0.423) and for Vp4 (p=0.074). Furthermore, when adjusting for the effect of portal vein invasion, no significant difference in overall survival was observed between the two treatment groups (p=0.934).

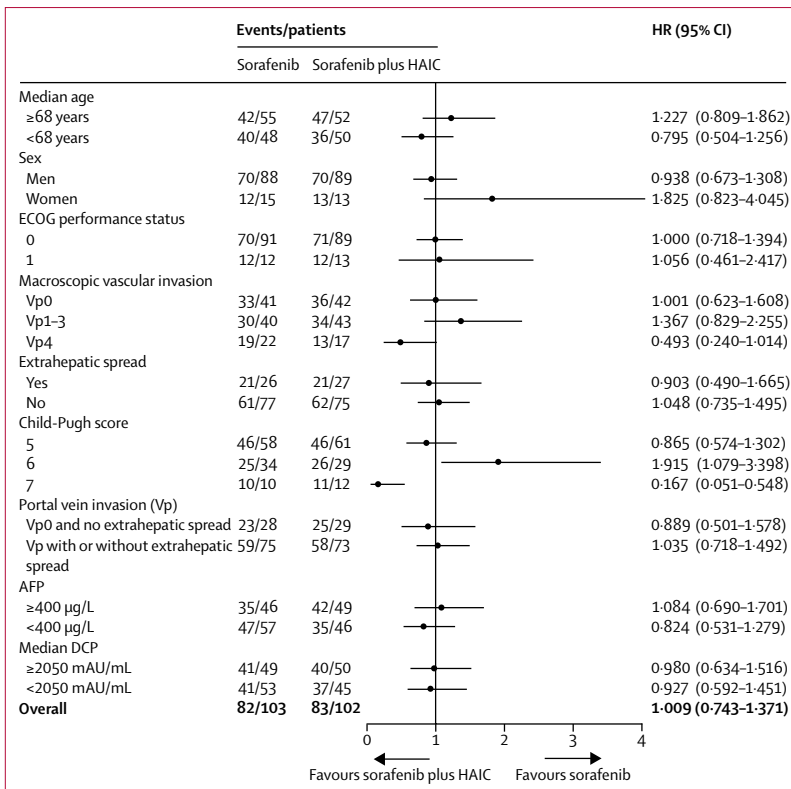


Figure 3: Forest plot of factors associated with overall survival in patients treated with sorafenib alone and with sorafenib plus HAIC
 HAIC=hepatic arterial infusion chemotherapy. HR=hazard ratio. ECOG=Eastern Cooperative Oncology Group. Vp0=no portal vein invasion. Vp1–3=branch-segmental portal vein invasion. Vp4=main portal vein invasion. AFP=α-fetoprotein. DCP=des-γ-carboxyprotein.

Although the mean duration of sorafenib treatment was slightly longer in the combination therapy group than in the sorafenib monotherapy group, the median

Forest plot analysis of factors associated with overall survival showed that, in patients with Child-Pugh score 6, overall survival was longer with sorafenib monotherapy than with sorafenib plus hepatic arterial infusion chemotherapy (figure 3). However, combination therapy resulted in longer overall survival than did sorafenib alone in patients with main portal vein invasion and in those with Child-Pugh score 7, although this outcome was of borderline significance for main portal vein invasion.

Overall survival was significantly longer in patients who achieved a complete or partial response than in those with stable or progressive disease (appendix), but was similar between the two treatment groups in patients who achieved a complete or partial response (appendix).

Overall, 82 (80%) of 103 patients treated with sorafenib alone died, as did 83 (81%) of 102 patients treated with sorafenib plus hepatic arterial infusion chemotherapy. Details of post-progression treatment in the two study groups is shown in the appendix.

The frequency of adverse events was similar in the two groups (table 3). However, the following grade 3–4 adverse events were more frequent in the combination therapy group than in the sorafenib monotherapy group: anaemia (15 [17%] of 88 vs six [6%] of 102), neutropenia (15 [17%] vs one [1%]), thrombocytopenia (30 [34%] vs 12 [12%]), and anorexia (12 [14%] vs six [6%]). The frequency of all-grade alopecia, hoarseness, diarrhoea, and increased alanine aminotransferase was significantly higher in the sorafenib monotherapy than in the combination therapy group, whereas the frequency of all-grade nausea, vomiting, and decreased white blood cell counts was significantly higher in the sorafenib plus hepatic arterial infusion chemotherapy group (table 3). The frequencies of dose reductions, dose interruptions, and treatment discontinuations due to adverse events were similar in both groups (appendix).

Discussion

Results of the phase 3 SILIUS trial show that the addition of low-dose cisplatin plus fluorouracil hepatic arterial infusion chemotherapy to sorafenib did not significantly improve overall survival in patients with advanced hepatocellular carcinoma. However, combination therapy resulted in significantly longer time to progression and a higher proportion of patients achieving an overall response than did sorafenib monotherapy, suggesting that this combination might have additive anticancer effects in certain patients. The longer overall survival achieved in responders with hepatic arterial infusion chemotherapy is similar to findings reported in retrospective cohort studies of patients with advanced hepatocellular carcinoma. For example, a large, nationwide cohort study of patients with advanced hepatocellular carcinoma who were treated with low-dose cisplatin plus fluorouracil hepatic arterial infusion chemotherapy found that median overall survival was significantly longer in those who responded to therapy compared with those with progressive or stable disease

	Sorafenib group (n=102)			Sorafenib plus HAIC group (n=88)		
	Grades 1–2	Grade 3	Grade 4	Grades 1–2	Grade 3	Grade 4
Elevated AST	68 (67%)	29 (28%)	2 (2%)	60 (68%)	24 (27%)	2 (2%)
Elevated ALT	75 (74%)	14 (14%)	1 (1%)	53 (60%)	11 (13%)	2 (2%)
Thrombocytopenia	71 (70%)	12 (12%)	0	51 (58%)	24 (27%)	6 (7%)
Anaemia	73 (72%)	5 (5%)	1 (1%)	63 (72%)	13 (15%)	2 (2%)
Hypertension	52 (51%)	26 (25%)	0	46 (52%)	22 (25%)	0
Elevated lipase	32 (31%)	24 (24%)	11 (11%)	29 (33%)	19 (22%)	7 (8%)
Elevated bilirubin	55 (54%)	10 (10%)	2 (2%)	50 (57%)	6 (7%)	1 (1%)
Hand-foot skin reaction	46 (45%)	15 (15%)	0	37 (42%)	8 (9%)	0
Elevated serum amylase	48 (47%)	10 (10%)	1 (1%)	35 (40%)	10 (11%)	0
Malaise	54 (53%)	0	0	44 (50%)	0	0
Anorexia	48 (47%)	6 (6%)	0	40 (45%)	12 (14%)	0
Diarrhoea	40 (39%)	10 (10%)	0	26 (30%)	4 (5%)	0
Decreased white blood cell count	45 (44%)	5 (5%)	0	50 (57%)	11 (13%)	0
Elevated INR	50 (49%)	0	0	41 (47%)	0	0
Neutropenia	42 (41%)	1 (1%)	0	46 (52%)	14 (16%)	1 (1%)
Fatigue	33 (32%)	8 (8%)	0	21 (24%)	9 (10%)	0
Weight loss	33 (32%)	1 (1%)	0	35 (40%)	0	0
Hoarseness	32 (31%)	1 (1%)	0	14 (16%)	0	0
Alopecia	26 (26%)	0	0	8 (9%)	0	0
Fever	22 (22%)	3 (3%)	0	21 (24%)	0	0
Nausea	15 (15%)	2 (2%)	0	29 (33%)	5 (6%)	0
Vomiting	6 (6%)	1 (1%)	0	15 (17%)	3 (3%)	0
Implanted catheter system trouble	NA	NA	NA	0	10 (11%)	1 (1%)

The safety population comprised all randomised patients who received at least one dose of study treatment. HAIC=hepatic arterial infusion chemotherapy. ALT=alanine aminotransferase. AST=aspartate aminotransferase. INR=international normalised ratio. NA=not applicable.

Table 3: Treatment-emergent adverse events of all grades occurring in more than 15% of patients in the safety population

(25·8 months for complete or partial response vs 6·0 months for progressive disease or 9·5 months for stable disease),¹⁶ with similar findings reported in another trial of hepatic arterial infusion chemotherapy.¹⁵ The finding that a significantly higher proportion of patients achieved an overall response with combination therapy than with sorafenib monotherapy suggests that more patients benefited from combination therapy than from sorafenib alone.

In another study, comparison of low-dose cisplatin plus fluorouracil with sorafenib in patients with advanced hepatocellular carcinoma with severe portal vein invasion (Vp3 and Vp4) showed that, in the low-dose cisplatin plus fluorouracil group, 31·3% of patients achieved an overall response and 56·3% achieved disease control as per RECIST 1.0, whereas the corresponding outcomes for the sorafenib group were 0% and 28·6%.⁶ That study also reported that median overall survival was significantly longer in the low-dose cisplatin plus fluorouracil group than in the sorafenib group (309 days vs 120 days; $p=0\cdot009$). Similar results were observed in studies comparing low-dose cisplatin plus fluorouracil with best

supportive care.¹⁶ The results of the SILIUS study suggest that combination therapy might improve overall survival in patients with hepatocellular carcinoma with main portal vein invasion (Vp4) when compared with sorafenib monotherapy; however, this finding was of borderline significance and was underpowered.

An analysis of patients with advanced hepatocellular carcinoma prospectively registered in the nationwide database of the Liver Cancer Study Group of Japan from 2000 to 2005 compared 476 patients who received low-dose cisplatin plus fluorouracil hepatic arterial infusion chemotherapy via a subcutaneous infusion port with 1466 patients who received best supportive care.¹⁶ Following propensity score matching, median overall survival was significantly longer in the 189 patients with main portal vein invasion who received low-dose cisplatin plus fluorouracil hepatic arterial infusion chemotherapy than in the 189 patients who did not (7.9 months vs 3.1 months). Indeed, the average overall survival in patients with main portal vein invasion is less than 3 months.^{27,28} In the SILIUS study, the median overall survival in patients with main portal vein invasion was 11.4 months in those treated with low-dose cisplatin plus fluorouracil hepatic arterial infusion chemotherapy plus sorafenib, compared with 6.5 months in those treated with sorafenib monotherapy.

The longer time to progression and higher proportion of patients achieving an overall response observed with hepatic arterial infusion chemotherapy plus sorafenib suggest that this combination might be a more potent therapy than sorafenib alone in selected subgroups. Furthermore, a high overall response sometimes leads to conversion therapy; resection or transarterial chemo-embolisation could become feasible in some patients following tumour downstaging resulting from the disappearance of portal vein invasion or shrinkage of intrahepatic nodules, or both.

Although the data suggest the possibility that the combination of low-dose cisplatin plus fluorouracil hepatic arterial infusion chemotherapy and sorafenib might benefit selected patients with advanced hepatocellular carcinoma, including older patients and those with main portal vein invasion (Vp4), these results cannot be considered conclusive and are unlikely to affect clinical practice or clinical guidelines in Japan or elsewhere, because of the small number of patients in the subgroups analysed.

Although patients treated with combination therapy had a significantly higher frequency of grade 3–4 thrombocytopenia and neutropenia, probably due to the cytotoxic agents cisplatin and fluorouracil, these adverse events were not unexpected and were manageable by treatment interruption or dose modification.

The major limitation of this study was the small numbers of patients in the various subgroups, making it difficult to ascertain the significance of outcomes observed in these groups. Other limitations include the

absence of generalisability of these results, the one-sided nature of the power calculation, the use of mRECIST to assess patients' response to treatment, the number of patients who were not evaluable, and the absence of quality-of-life assessments.

Additional studies with larger numbers of patients are required to ascertain whether sorafenib plus low-dose cisplatin plus fluorouracil hepatic arterial infusion chemotherapy is more effective than sorafenib alone in patients with advanced hepatocellular carcinoma, especially in patients with main portal vein invasion. Similarly to previous unsuccessful first-line trials,^{21,22} the SILIUS study also confirmed that overall response and time to progression are not surrogate endpoints for overall survival in treatment of hepatocellular carcinoma.

In conclusion, when compared with sorafenib monotherapy, low-dose cisplatin plus fluorouracil hepatic arterial infusion chemotherapy plus sorafenib did not improve overall survival in patients with advanced hepatocellular carcinoma. However, this combination increased the proportion of patients with an overall response and time to progression, consistent with data from retrospective cohort studies, which found higher response rates in patients treated with low-dose cisplatin plus fluorouracil hepatic arterial infusion chemotherapy plus sorafenib than with sorafenib alone. Prospective trials are needed to assess whether sorafenib plus low-dose cisplatin plus fluorouracil hepatic arterial infusion chemotherapy might benefit selected subgroups of patients with advanced hepatocellular carcinoma.

Contributors

MK and KU contributed to the study design, data collection, study analysis, manuscript writing, critical review of the manuscript, and final approval of the manuscript submission. OY, SOg, SOb, NI, HA, EH, YS, KH, TK, KY, YI, SI, CO, TO, and FK contributed to data collection, critical review of the manuscript, and final approval of the manuscript submission. KA did the statistical analysis and the critical manuscript review. K-iY contributed to the study design, critical review of the manuscript, and statistical analysis. PJ and YA contributed to critical review of the manuscript and final approval of the manuscript submission.

Declaration of interests

MK has received grants from Taiho Pharmaceuticals, Chugai Pharmaceuticals, Otsuka, Takeda, Sumitomo Dainippon-Sumitomo, Daiichi Sankyo, Abbvie, Medico's Hirata, Astellas Pharma, and Bristol-Myers Squibb; grants and personal fees from MSD, Eisai, and Bayer, and is an adviser for Taiho Pharmaceuticals, Chugai Pharmaceuticals, MSD, Eisai, Bayer, Bristol-Myers Squibb, and ONO Pharmaceutical. KU, SOg, and EH have received personal fees and honoraria from Bayer. OY has received grants from Tanabe-Mitsubishi, Otsuka, Eisai, Daiichi Sankyo, MSD, Gilead, Chugai, Astellas, Takeda, and Dainippon-Sumitomo. TO has received grants from Kowa K.K. and Kyowa Hakko Kirin, grants and personal fees from Novartis, Nippon Boehringer Ingelheim, Dainippon-Sumitomo, Pfizer, Jana, Inc, Bayer Yakuhin, Chugai Pharmaceuticals, Eli Lilly, Yakuruto Honsha, Ono Pharmaceuticals, Eisai, AstraZeneca, Merck Serono, Baxter, Nano Carrier, Zeria Pharmaceuticals, NobelPharma, and Taiho Pharmaceuticals, and personal fees from Bristol-Myers Squibb, Nipponchemofa, EA Pharma, Fujifilm RI Pharma, Nippon Kayaku, Daiichi Sankyo, Celgene, and Teijin Pharma. TK has received personal fees from Gilead, Bristol-Myers Squibb, MSD, and AbbVie. All other authors declare no competing interests.

Acknowledgments

This research was supported by a grant from the Japanese Ministry of Health, Labour and Welfare.

References

- 1 Donadon M, Solbiati L, Dawson L, et al. Hepatocellular carcinoma: the role of interventional oncology. *Liver Cancer* 2016; **6**: 34–43.
- 2 Lanza E, Donadon M, Poretti D, et al. Transarterial therapies for hepatocellular carcinoma. *Liver Cancer* 2016; **6**: 27–33.
- 3 Kudo M, Izumi N, Sakamoto M, et al; Liver Cancer Study Group of Japan. Survival analysis over 28 years of 173,378 patients with hepatocellular carcinoma in Japan. *Liver Cancer* 2016; **5**: 190–97.
- 4 Bruix J, Reig M, Sherman M. Evidence-based diagnosis, staging, and treatment of patients with hepatocellular carcinoma. *Gastroenterology* 2016; **150**: 835–53.
- 5 Kudo M, Trevisani F, Abou-Alfa GK, Rimassa L. Hepatocellular carcinoma: therapeutic guidelines and medical treatment. *Liver Cancer* 2016; **6**: 16–26.
- 6 Moriguchi M, Aramaki T, Nishiofuku H, et al. Sorafenib versus hepatic arterial infusion chemotherapy as initial treatment for hepatocellular carcinoma with advanced portal vein tumor thrombosis. *Liver Cancer* 2017; **6**: 275–86.
- 7 Yoshikawa M, Ono N, Yodono H, Ichida T, Nakamura H. Phase II study of hepatic arterial infusion of a fine-powder formulation of cisplatin for advanced hepatocellular carcinoma. *Hepatol Res* 2008; **38**: 474–83.
- 8 Iwasa S, Ikeda M, Okusaka T, et al. Transcatheter arterial infusion chemotherapy with a fine-powder formulation of cisplatin for advanced hepatocellular carcinoma refractory to transcatheter arterial chemoembolization. *Jpn J Clin Oncol* 2011; **41**: 770–75.
- 9 Ueshima K, Kudo M, Takita M, et al. Hepatic arterial infusion chemotherapy using low-dose 5-fluorouracil and cisplatin for advanced hepatocellular carcinoma. *Oncology* 2010; **78** (suppl 1): 148–53.
- 10 Oh MJ, Lee HJ, Lee SH. Efficacy and safety of hepatic arterial infusion chemotherapy for advanced hepatocellular carcinoma as first-line therapy. *Clin Mol Hepatol* 2013; **19**: 288–99.
- 11 Woo HY, Bae SH, Park JY, et al; Korean Liver Cancer Study Group. A randomized comparative study of high-dose and low-dose hepatic arterial infusion chemotherapy for intractable, advanced hepatocellular carcinoma. *Cancer Chemother Pharmacol* 2010; **65**: 373–82.
- 12 Tsai WL, Lai KH, Liang HL, et al. Hepatic arterial infusion chemotherapy for patients with huge unresectable hepatocellular carcinoma. *PLoS One* 2014; **9**: e92784.
- 13 Song MJ, Bae SH, Chun HJ, et al. A randomized study of cisplatin and 5-FU hepatic arterial infusion chemotherapy with or without adriamycin for advanced hepatocellular carcinoma. *Cancer Chemother Pharmacol* 2015; **75**: 739–46.
- 14 Ma MC, Chen YY, Li SH, et al. Intra-arterial chemotherapy with doxorubicin and cisplatin is effective for advanced hepatocellular cell carcinoma. *Sci World J* 2014; **2014**: 160138.
- 15 Obi S, Yoshida H, Toune R, et al. Combination therapy of intraarterial 5-fluorouracil and systemic interferon-alpha for advanced hepatocellular carcinoma with portal venous invasion. *Cancer* 2006; **106**: 1990–97.
- 16 Nouse K, Miyahara K, Uchida D, et al; Liver Cancer Study Group of Japan. Effect of hepatic arterial infusion chemotherapy of 5-fluorouracil and cisplatin for advanced hepatocellular carcinoma in the Nationwide Survey of Primary Liver Cancer in Japan. *Br J Cancer* 2013; **109**: 1904–07.
- 17 Ikeda M, Shimizu S, Sato T, et al. Sorafenib plus hepatic arterial infusion chemotherapy with cisplatin versus sorafenib for advanced hepatocellular carcinoma: randomized phase II trial. *Ann Oncol* 2016; **27**: 2090–96.
- 18 Thomas MB, O'Beirne JP, Furuse J, Chan AT, Abou-Alfa G, Johnson P. Systemic therapy for hepatocellular carcinoma: cytotoxic chemotherapy, targeted therapy and immunotherapy. *Ann Surg Oncol* 2008; **15**: 1008–14.
- 19 Llovet JM, Ricci S, Mazzaferro V, et al; SHARP Investigators Study Group. Sorafenib in advanced hepatocellular carcinoma. *N Engl J Med* 2008; **359**: 378–90.
- 20 Cheng AL, Kang YK, Chen Z, et al. Efficacy and safety of sorafenib in patients in the Asia-Pacific region with advanced hepatocellular carcinoma: a phase III randomised, double-blind, placebo-controlled trial. *Lancet Oncol* 2009; **10**: 25–34.
- 21 Raoul JL, Gilibert M, Adhoue X, Edeline J. An in-depth review of chemical angiogenesis inhibitors for treating hepatocellular carcinoma. *Expert Opin Pharmacother* 2017; **18**: 1467–76.
- 22 Abou-Alfa GK, Johnson P, Knox JJ, et al. Doxorubicin plus sorafenib vs doxorubicin alone in patients with advanced hepatocellular carcinoma: a randomized trial. *JAMA* 2010; **304**: 2154–60.
- 23 Fukubayashi K, Tanaka M, Izumi K, et al. Evaluation of sorafenib treatment and hepatic arterial infusion chemotherapy for advanced hepatocellular carcinoma: a comparative study using the propensity score matching method. *Cancer Med* 2015; **4**: 1214–23.
- 24 Shiozawa K, Watanabe M, Ikehara T, et al. Comparison of sorafenib and hepatic arterial infusion chemotherapy for advanced hepatocellular carcinoma: a propensity score matching study. *Hepatogastroenterology* 2014; **61**: 885–91.
- 25 Ueshima K, Kudo M, Tanaka M, et al. Phase I/II study of sorafenib in combination with hepatic arterial infusion chemotherapy using low-dose cisplatin and 5-fluorouracil. *Liver Cancer* 2015; **4**: 263–73.
- 26 Arai Y, Takeuchi Y, Inaba Y, et al. Percutaneous catheter placement for hepatic arterial infusion chemotherapy. *Tech Vasc Interv Radiol* 2007; **10**: 30–37.
- 27 Woo HY, Heo J. New perspectives on the management of hepatocellular carcinoma with portal vein thrombosis. *Clin Mol Hepatol* 2015; **21**: 115–21.
- 28 Costentin CE, Ferrone CR, Arellano RS, Ganguli S, Hong TS, Zhu AX. Hepatocellular carcinoma with macrovascular invasion: defining the optimal treatment strategy. *Liver Cancer* 2017; **6**: 360–74.

THE LANCET

Gastroenterology & Hepatology

Supplementary appendix

This appendix formed part of the original submission and has been peer reviewed. We post it as supplied by the authors.

Supplement to: Kudo M, Ueshima K, Yokosuka O, et al, for the SILIUS study group. Sorafenib plus low-dose cisplatin and fluorouracil hepatic arterial infusion chemotherapy versus sorafenib alone in patients with advanced hepatocellular carcinoma (SILIUS): a randomised, open label, phase 3 trial. *Lancet Gastroenterol Hepatol* 2018; published online April 6. [http://dx.doi.org/10.1016/S2468-1253\(18\)30078-5](http://dx.doi.org/10.1016/S2468-1253(18)30078-5).

SILIUS study group

First name	Surnames
Masatoshi	Kudo
Kazuto	Nishio
Kohei	Akazawa
Takuji	Okusaka
Takashi	Kumada
Masafumi	Ikeda
Yasuaki	Arai
Hiroaki	Nagano
Etsuro	Hatano
Yutaka	Sasaki
Hiroshi	Aikata
Takahiro	Yamasaki
Namiki	Izumi
Shuntaro	Obi
Kazuhide	Yamamoto
Yasuharu	Imai
Keisuke	Hino
Tetsuji	Takayama
Kazuomi	Ueshima
Toru	Ishikawa
Chikara	Ogawa
Kunihiko	Tsuji
Hidemori	Sakamoto
Takumi	Omura
Junji	Kato
Yukio	Osaki
Shigehiro	Kokubu
Katsuya	Shiraki

Masatoshi	Tanaka
Eiichi	Tomita
Hiromi	Ishibashi
Shunsuke	Nojiri
Junji	Furuse
Shinya	Oooka
Tetsurou	Inokuma
Toyokazu	Fukunaga
Shigeo	Shimose
Sadahisa	Ogasawara
Shouta	Iwadou
Kohei	Akazawa
Takamichi	Murakami
Fumihiko	Kanai
Ken-ichi	Yoshimura
Osamu	Yokosuka
Philip	Johnson

Supplementary Table 1. Dose intensities of sorafenib and number of HAIC cycles in the safety population.

	Sorafenib (n=102)	Sorafenib + HAIC (n=88)
Duration of sorafenib treatment, weeks		
Mean ± SD	23.9 ± 29.0	25.0 ± 31.9
Median (range)	14.4 (159.3)	13.6 (216.0)
Relative sorafenib dose intensity, %		
Mean ± SD	60.0 ± 25.6	53.7 ± 26.6
Median	55.6 (100.0)	53.1 (100.0)
Total number of HAIC cycles (1 cycle = 28 days)		(n=85)
Mean ± SD		4.0 ± 4.0
Median (range)		2.0 (19.0)

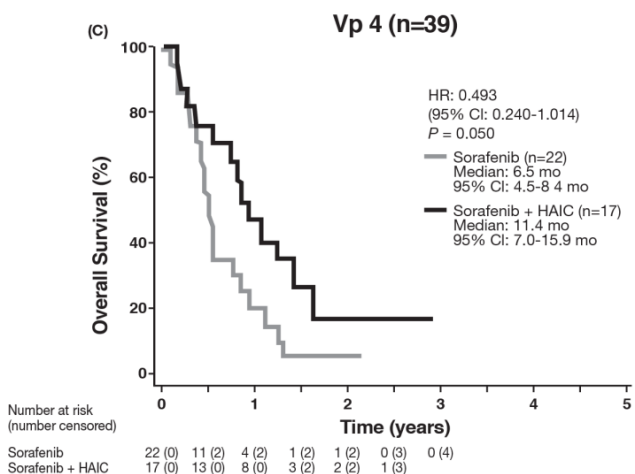
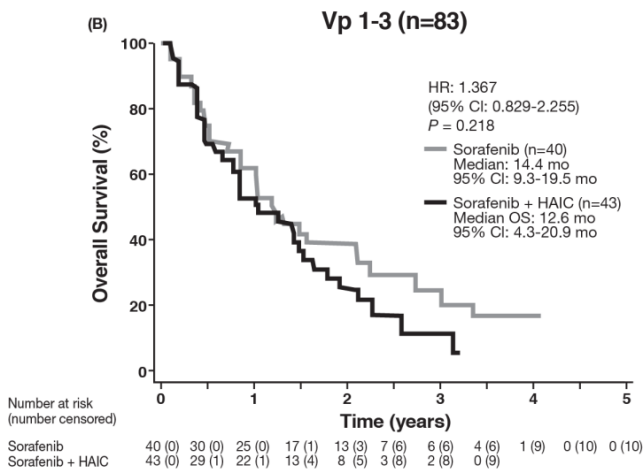
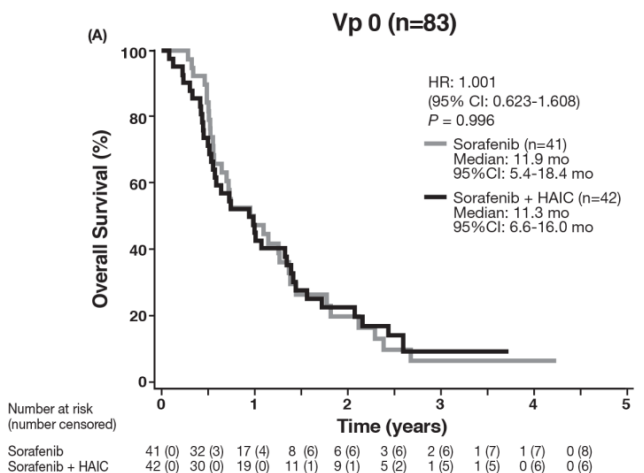
Supplementary Table 2. Post-progression treatment in the two study arms.

	Sorafenib	Sorafenib + HAIC
Sorafenib	25	15
HAIC	16	30
TACE	23	29
Immunotherapy	3	1
Investigational agent	8	11
Systemic therapy	11	12
RFA	3	4
Resection	3	3

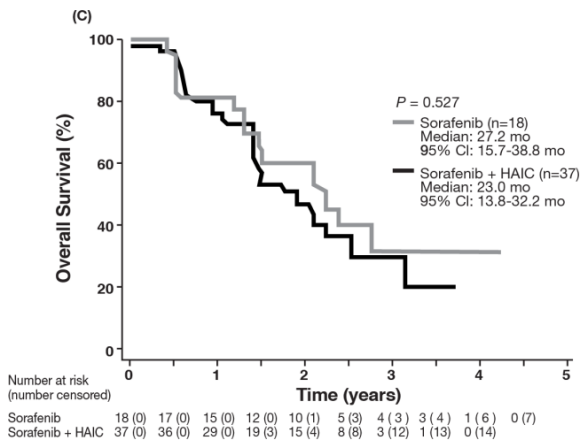
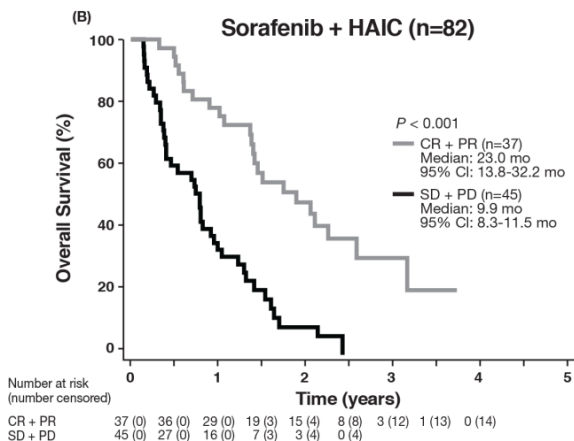
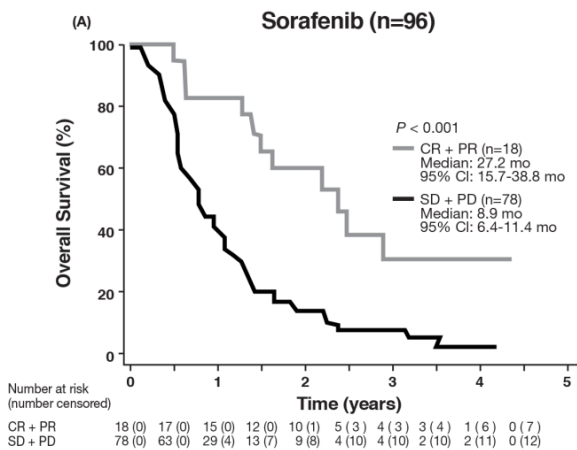
Supplementary Table 3. Summary of dose reductions, dose interruptions, and treatment discontinuations due to adverse events in the sorafenib and sorafenib+HAIC groups

	Sorafenib (n=102)	Sorafenib + HAIC (n=88)
Dose reductions, n (%)	63 (61.8)	54 (61.4)
Dose interruptions, n (%)	76 (74.5)	79 (89.8)
Treatment discontinuations, n (%)	25 (24.5)	26 (29.5)

Supplementary Figure 1. Kaplan-Meier analysis of overall survival in patients treated with sorafenib alone and sorafenib plus HAIC and stratified by MVI. (A) Vp 0, (B) Vp 1–3 and (C) Vp 4.



Supplementary Figure 2. Kaplan-Meier analysis of overall survival in patients stratified by tumour response. (A, B) OS was significantly longer in patients who achieved CR+PR than in those who achieved SD+PD in response to sorafenib alone (A) and sorafenib plus HAIC (B). (C) OS was similar in patients who achieved CR+PR in response to sorafenib alone and sorafenib plus HAIC.



Sorafenib and hepatic arterial infusion chemotherapy: another failed combination



Hepatic arterial infusion chemotherapy has not been shown to improve survival for patients with advanced hepatocellular carcinoma in prospective trials and, for this reason, is not considered a standard of care. Masatoshi Kudo and colleagues,¹ the authors of the SILIUS trial, reported in *The Lancet Gastroenterology & Hepatology*, are therefore to be congratulated for addressing the absence of evidence on the effectiveness of hepatic arterial infusion chemotherapy by doing a randomised trial comparing the standard of care, sorafenib, with sorafenib plus low-dose cisplatin and fluorouracil hepatic arterial infusion chemotherapy.

SILIUS was an open-label, phase 3 trial for which the primary endpoint was overall survival, although the sample size was relatively small, based on the optimistic assumption that combination therapy would improve survival from 10 months to 17 months (hazard ratio [HR] 0.59). However, the results for median overall survival were convincingly negative for the superiority of sorafenib plus hepatic arterial infusion chemotherapy versus sorafenib alone (HR 1.009, 95% CI 0.743–1.371; $p=0.955$) and it is unlikely that a larger trial would have detected a more modest improvement in survival. The result observed appears plausible based on patient selection, matched patient characteristics, and the fact that sorafenib monotherapy achieved a median overall survival of 11.5 months, which is in keeping with expected outcomes. Furthermore, addition of hepatic arterial infusion chemotherapy did not appear to have a major effect on sorafenib dose or duration. Appropriately, the primary endpoint was reported according to intention to treat, but since 14% of patients allocated to the combination therapy group did not receive treatment compared with 1% in the monotherapy group, an exploratory analysis of the per-protocol outcome might have been interesting. Despite the negative result for the primary outcome, the authors are encouraged by some of the secondary outcomes and subgroup analyses. Both time to progression and the proportion of patients with an overall response were reported to be significantly superior in the combination group, which the authors

perceive as beneficial since a high proportion of patients achieving a response might result in downstaging and permit potentially curative therapies. However, upon review of the subsequent therapies received, both groups were equivalent: three patients underwent resection in each group, and three patients had radiofrequency ablation in the monotherapy group versus four in the combination therapy group. Moreover, since this was an open-label trial there was no masked central review of imaging, which makes endpoints based on imaging vulnerable to bias. Interestingly, progression-free survival, which included death and progression, did not significantly differ between the two groups. The investigators also selected modified Response Evaluation Criteria In Solid Tumors (mRECIST) as the method of response assessment, which prevents cross-trial comparisons. mRECIST has not been fully validated in advanced hepatocellular carcinoma and has yet to be proven as a superior endpoint to standard RECIST 1.1.² Until mRECIST is validated as such, both mRECIST and RECIST should be reported. In this case, a higher proportion of patients achieving a response according to mRECIST in the combination group did not translate into an improved median overall survival. In the subgroup analysis, an apparent benefit was reported for the combination group in patients with Child-Pugh score 7 liver disease and those with main portal vein invasion. In fact, overall survival was equivalent for patients with a Child-Pugh score of 5 ($n=119$), superior for sorafenib monotherapy in those with a Child-Pugh score of 6 ($n=63$), and superior for combination therapy in those with a Child-Pugh score of 7 ($n=22$). Similarly, the cohort of patients with Vp4 main portal vein invasion comprised 22 patients in the monotherapy group and 17 in the combination group. The authors are rightly cautious in drawing conclusions from subgroups with such small numbers, and these data should only be considered hypothesis generating.

Ultimately, the conclusion from the SILIUS trial is that the combination of sorafenib and hepatic arterial infusion chemotherapy as delivered in this trial does not improve survival and the additional toxicity and complexity associated with combination therapy

Lancet Gastroenterol Hepatol
2018

Published Online
April 6, 2018

[http://dx.doi.org/10.1016/S2468-1253\(18\)30084-0](http://dx.doi.org/10.1016/S2468-1253(18)30084-0)

See Online/Articles

[http://dx.doi.org/10.1016/S2468-1253\(18\)30078-5](http://dx.doi.org/10.1016/S2468-1253(18)30078-5)

do not appear to be justified by the less clinically relevant and less robust secondary endpoints and subgroup analyses. As such, the results of this trial add to the growing list of unsuccessful sorafenib-based combinations, which include doxorubicin,³ erlotinib,⁴ and transarterial chemoembolisation.^{5,6} For 10 years, sorafenib monotherapy has been the only standard of care for patients with advanced hepatocellular carcinoma; however, the past year has seen some progress. Lenvatinib⁷ has shown non-inferiority in the first-line setting, and both regorafenib⁸ and cabozantinib⁹ have shown survival benefit in placebo-controlled second-line trials. Immunotherapy also seems promising, with two large phase 2 trials showing encouraging responses for both nivolumab¹⁰ and pembrolizumab. These drugs might prove to be better combination partners than sorafenib, but further investigation through well designed and well conducted trials will be required.

Tim Meyer

Department of Oncology, UCL Cancer Institute, University College London, London WC1E 6DD, UK
t.meyer@ucl.ac.uk

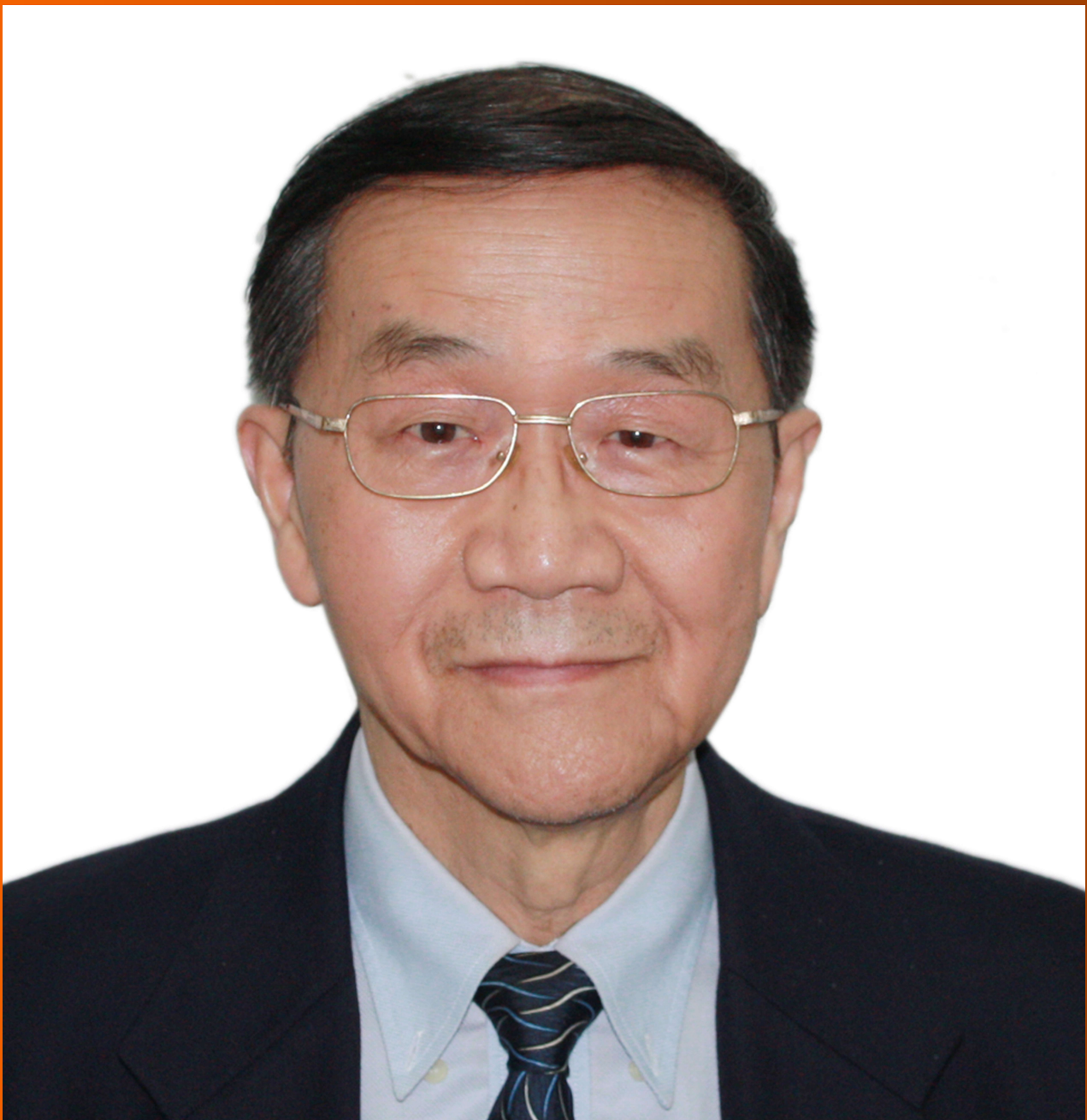
I declare no competing interests.

- 1 Kudo M, Ueshima K, Yokosuka O, et al. Sorafenib plus low-dose cisplatin and fluorouracil hepatic arterial infusion chemotherapy versus sorafenib alone in patients with advanced hepatocellular carcinoma (SILIUS): a randomised, open label, phase 3 trial. *Lancet Gastroenterol Hepatol* 2018; published online April 6. [http://dx.doi.org/10.1016/S2468-1253\(18\)30078-5](http://dx.doi.org/10.1016/S2468-1253(18)30078-5).
- 2 Meyer T, Palmer DH, Cheng AL, Hocke J, Loembé AB, Yen CJ. mRECIST to predict survival in advanced hepatocellular carcinoma: analysis of two randomised phase II trials comparing nintedanib vs sorafenib. *Liver Int* 2017; **37**: 1047–55.
- 3 Abou-Alfa GK, Niedzwieski D, Knox JJ, et al. Phase III randomized study of sorafenib plus doxorubicin versus sorafenib in patients with advanced hepatocellular carcinoma (HCC): CALGB 80802 (Alliance). *Proc Am Soc Clin Oncol* 2016; **34** (suppl 4S): 192 (abstr).
- 4 Zhu AX, Rosmorduc O, Evans TR, et al. SEARCH: a phase III, randomized, double-blind, placebo-controlled trial of sorafenib plus erlotinib in patients with advanced hepatocellular carcinoma. *J Clin Oncol* 2015; **33**: 559–66.
- 5 Meyer T, Fox R, Ma YT, et al. Sorafenib in combination with transarterial chemoembolisation in patients with unresectable hepatocellular carcinoma (TACE 2): a randomised placebo-controlled, double-blind, phase 3 trial. *Lancet Gastroenterol Hepatol* 2017; **2**: 565–75.
- 6 Lencioni R, Llovet JM, Han G, et al. Sorafenib or placebo plus TACE with doxorubicin-eluting beads for intermediate stage HCC: the SPACE trial. *J Hepatol* 2016; **64**: 1090–98.
- 7 Kudo M, Finn RS, Qin S, et al. Lenvatinib versus sorafenib in first-line treatment of patients with unresectable hepatocellular carcinoma: a randomised phase 3 non-inferiority trial. *Lancet* 2018; **391**: 1163–73.
- 8 Bruix J, Qin S, Merle P, et al. Regorafenib for patients with hepatocellular carcinoma who progressed on sorafenib treatment (RESORCE): a randomised, double-blind, placebo-controlled, phase 3 trial. *Lancet* 2017; **389**: 56–66.
- 9 Abou-Alfa GK, Meyer T, Cheng AL et al. Cabozantinib (C) versus placebo (P) in patients (pts) with advanced hepatocellular carcinoma (HCC) who have received prior sorafenib: results from the randomized phase III CELESTIAL trial. *Proc Am Soc Clin Oncol* 2018; **36**: 208 (abstr).
- 10 El-Khoueiry AB, Sangro B, Yau T, et al. Nivolumab in patients with advanced hepatocellular carcinoma (CheckMate 040): an open-label, non-comparative, phase 1/2 dose escalation and expansion trial. *Lancet* 2017; **389**: 2492–502.

ISSN 1007-9327 (print)
ISSN 2219-2840 (online)

World Journal of *Gastroenterology*

World J Gastroenterol 2018 April 28; 24(16): 1679-1824



Published by Baishideng Publishing Group Inc

REVIEW

- 1679 Beneficial effects of naringenin in liver diseases: Molecular mechanisms
Hernández-Aquino E, Muriel P
- 1708 Naturally occurring hepatitis B virus reverse transcriptase mutations related to potential antiviral drug resistance and liver disease progression
Choi YM, Lee SY, Kim BJ

MINIREVIEWS

- 1725 Nucleotide-binding oligomerization domain 1 and *Helicobacter pylori* infection: A review
Minaga K, Watanabe T, Kamata K, Asano N, Kudo M
- 1734 Diversion colitis and pouchitis: A mini-review
Tominaga K, Kamimura K, Takahashi K, Yokoyama J, Yamagiwa S, Terai S

ORIGINAL ARTICLE**Basic Study**

- 1748 Nonalcoholic steatohepatitis severity is defined by a failure in compensatory antioxidant capacity in the setting of mitochondrial dysfunction
Boland ML, Oldham S, Boland BB, Will S, Lapointe JM, Guionaud S, Rhodes CJ, Trevaskis JL
- 1766 Mucosa repair mechanisms of Tong-Xie-Yao-Fang mediated by CRH-R2 in murine, dextran sulfate sodium-induced colitis
Gong SS, Fan YH, Wang SY, Han QQ, Lv B, Xu Y, Chen X, He YE
- 1779 Sodium chloride exacerbates dextran sulfate sodium-induced colitis by tuning proinflammatory and antiinflammatory lamina propria mononuclear cells through p38/MAPK pathway in mice
Guo HX, Ye N, Yan P, Qiu MY, Zhang J, Shen ZG, He HY, Tian ZQ, Li HL, Li JT

Retrospective Cohort Study

- 1795 High tacrolimus intra-patient variability is associated with graft rejection, and *de novo* donor-specific antibodies occurrence after liver transplantation
Del Bello A, Congy-Jolivet N, Danjoux M, Muscarei F, Lavayssière L, Esposito L, Hebral AL, Bellière J, Kamar N

Randomized Clinical Trial

- 1803 Papillary fistulotomy vs conventional cannulation for endoscopic biliary access: A prospective randomized trial
Furuya CK, Sakai P, Marinho FR, Otoch JP, Cheng S, Prudencio LL, de Moura EG, Artifon EL

META-ANALYSIS

- 1812 Compared efficacy of preservation solutions on the outcome of liver transplantation: Meta-analysis
Szilágyi ÁL, Mátrai P, Hegyi P, Tuboly E, Pécz D, Garami A, Solymár M, Pétervári E, Balaskó M, Veres G, Czopf L, Wobbe B, Szabó D, Wagner J, Hartmann P

Contents

World Journal of Gastroenterology
Volume 24 Number 16 April 28, 2018

ABOUT COVER

Editorial board member of *World Journal of Gastroenterology*, Shu-You Peng, FRCS (Gen Surg), FRCS (Hon), MD, Professor, Surgeon, General Surgery, The Second Affiliated Hospital, College of Medicine, Zhejiang University, Hangzhou 310009, Zhejiang Province, China

AIMS AND SCOPE

World Journal of Gastroenterology (*World J Gastroenterol*, *WJG*, print ISSN 1007-9327, online ISSN 2219-2840, DOI: 10.3748) is a peer-reviewed open access journal. *WJG* was established on October 1, 1995. It is published weekly on the 7th, 14th, 21st, and 28th each month. The *WJG* Editorial Board consists of 642 experts in gastroenterology and hepatology from 59 countries.

The primary task of *WJG* is to rapidly publish high-quality original articles, reviews, and commentaries in the fields of gastroenterology, hepatology, gastrointestinal endoscopy, gastrointestinal surgery, hepatobiliary surgery, gastrointestinal oncology, gastrointestinal radiation oncology, gastrointestinal imaging, gastrointestinal interventional therapy, gastrointestinal infectious diseases, gastrointestinal pharmacology, gastrointestinal pathophysiology, gastrointestinal pathology, evidence-based medicine in gastroenterology, pancreatology, gastrointestinal laboratory medicine, gastrointestinal molecular biology, gastrointestinal immunology, gastrointestinal microbiology, gastrointestinal genetics, gastrointestinal translational medicine, gastrointestinal diagnostics, and gastrointestinal therapeutics. *WJG* is dedicated to become an influential and prestigious journal in gastroenterology and hepatology, to promote the development of above disciplines, and to improve the diagnostic and therapeutic skill and expertise of clinicians.

INDEXING/ABSTRACTING

World Journal of Gastroenterology (*WJG*) is now indexed in Current Contents[®]/Clinical Medicine, Science Citation Index Expanded (also known as SciSearch[®]), Journal Citation Reports[®], Index Medicus, MEDLINE, PubMed, PubMed Central and Directory of Open Access Journals. The 2017 edition of Journal Citation Reports[®] cites the 2016 impact factor for *WJG* as 3.365 (5-year impact factor: 3.176), ranking *WJG* as 29th among 79 journals in gastroenterology and hepatology (quartile in category Q2).

EDITORS FOR THIS ISSUE

Responsible Assistant Editor: *Xiang Li*
Responsible Electronic Editor: *Yan Huang*
Proofing Editor-in-Chief: *Lian-Sheng Ma*

Responsible Science Editor: *Xue-Jiao Wang*
Proofing Editorial Office Director: *Ze-Mao Gong*

NAME OF JOURNAL
World Journal of Gastroenterology

ISSN
ISSN 1007-9327 (print)
ISSN 2219-2840 (online)

LAUNCH DATE
October 1, 1995

FREQUENCY
Weekly

EDITORS-IN-CHIEF
Damian Garcia-Olmo, MD, PhD, Doctor, Professor, Surgeon, Department of Surgery, Universidad Autonoma de Madrid; Department of General Surgery, Fundacion Jimenez Diaz University Hospital, Madrid 28040, Spain

Stephen C Strom, PhD, Professor, Department of Laboratory Medicine, Division of Pathology, Karolinska Institutet, Stockholm 141-86, Sweden

Andrzej S Tarnawski, MD, PhD, DSc (Med), Professor of Medicine, Chief Gastroenterology, VA Long Beach Health Care System, University of California, Irvine, CA, 5901 E. Seventh Str., Long Beach,

CA 90822, United States

EDITORIAL BOARD MEMBERS
All editorial board members resources online at <http://www.wjgnet.com/1007-9327/editorialboard.htm>

EDITORIAL OFFICE
Ze-Mao Gong, Director
World Journal of Gastroenterology
Baishideng Publishing Group Inc
7901 Stoneridge Drive, Suite 501,
Pleasanton, CA 94588, USA
Telephone: +1-925-2238242
Fax: +1-925-2238243
E-mail: editorialoffice@wjgnet.com
Help Desk: <http://www.f6publishing.com/helpdesk>
<http://www.wjgnet.com>

PUBLISHER
Baishideng Publishing Group Inc
7901 Stoneridge Drive, Suite 501,
Pleasanton, CA 94588, USA
Telephone: +1-925-2238242
Fax: +1-925-2238243
E-mail: bpgoffice@wjgnet.com
Help Desk: <http://www.f6publishing.com/helpdesk>
<http://www.wjgnet.com>

PUBLICATION DATE
April 28, 2018

COPYRIGHT
© 2018 Baishideng Publishing Group Inc. Articles published by this Open-Access journal are distributed under the terms of the Creative Commons Attribution Non-commercial License, which permits use, distribution, and reproduction in any medium, provided the original work is properly cited, the use is non commercial and is otherwise in compliance with the license.

SPECIAL STATEMENT
All articles published in journals owned by the Baishideng Publishing Group (BPG) represent the views and opinions of their authors, and not the views, opinions or policies of the BPG, except where otherwise explicitly indicated.

INSTRUCTIONS TO AUTHORS
Full instructions are available online at <http://www.wjgnet.com/bpg/geninfo/204>

ONLINE SUBMISSION
<http://www.f6publishing.com>





Nucleotide-binding oligomerization domain 1 and *Helicobacter pylori* infection: A review

Kosuke Minaga, Tomohiro Watanabe, Ken Kamata, Naoki Asano, Masatoshi Kudo

Kosuke Minaga, Tomohiro Watanabe, Ken Kamata, Masatoshi Kudo, Department of Gastroenterology and Hepatology, Kindai University Faculty of Medicine, Osaka 589-8511, Japan

Naoki Asano, Division of Gastroenterology, Tohoku University Graduate School of Medicine, Miyagi 980-8574, Japan

ORCID number: Kosuke Minaga (0000-0001-5407-7925); Tomohiro Watanabe (0000-0001-7781-6305); Ken Kamata (0000-0003-1568-0769); Naoki Asano (0000-0003-4452-8459); Masatoshi Kudo (0000-0002-4102-3474).

Author contributions: Minaga K and Watanabe T wrote the manuscript draft and prepared the figures; Kamata K, Asano N and Kudo M assisted in writing the manuscript and reviewed the final version.

Conflict-of-interest statement: None of the authors has any conflict of interests related to this manuscript.

Open-Access: This article is an open-access article which was selected by an in-house editor and fully peer-reviewed by external reviewers. It is distributed in accordance with the Creative Commons Attribution Non Commercial (CC BY-NC 4.0) license, which permits others to distribute, remix, adapt, build upon this work non-commercially, and license their derivative works on different terms, provided the original work is properly cited and the use is non-commercial. See: <http://creativecommons.org/licenses/by-nc/4.0/>

Manuscript source: Invited manuscript

Correspondence to: Tomohiro Watanabe, MD, PhD, Associate Professor, Department of Gastroenterology and Hepatology, Kindai University Faculty of Medicine, 377-2 Ohno-Higashi, Osaka-Sayama, Osaka 589-8511, Japan. tomohiro@med.kindai.ac.jp
Telephone: +81-72-366-0221
Fax: +81-72-367-2880

Received: March 6, 2018
Peer-review started: March 6, 2018
First decision: March 29, 2018
Revised: April 3, 2018
Accepted: April 9, 2018
Article in press: April 9, 2018

Published online: April 28, 2018

Abstract

Nucleotide-binding oligomerization domain 1 (NOD1) is an intracellular innate immune sensor for small molecules derived from bacterial cell components. NOD1 activation by its ligands leads to robust production of pro-inflammatory cytokines and chemokines by innate immune cells, thereby mediating mucosal host defense systems against microbes. Chronic gastric infection due to *Helicobacter pylori* (*H. pylori*) causes various upper gastrointestinal diseases, including atrophic gastritis, peptic ulcers, and gastric cancer. It is now generally accepted that detection of *H. pylori* by NOD1 expressed in gastric epithelial cells plays an indispensable role in mucosal host defense systems against this organism. Recent studies have revealed the molecular mechanism by which NOD1 activation caused by *H. pylori* infection is involved in the development of chronic gastritis and gastric cancer. In this review, we have discussed and summarized how sensing of *H. pylori* by NOD1 mediates the prevention of chronic gastritis and gastric cancer.

Key words: Nucleotide-binding oligomerization domain 1; *Helicobacter pylori*; Gastritis; Gastric cancer

© The Author(s) 2018. Published by Baishideng Publishing Group Inc. All rights reserved.

Core tip: Nucleotide-binding oligomerization domain 1 (NOD1), an intracellular innate immune sensor, plays a role in mucosal host defense systems against *Helicobacter pylori* (*H. pylori*) infection. NOD1 activation is involved in the generation of T helper type 1 responses against *H. pylori* through activation of type I IFN signaling pathways. NOD1 activation prevents gastric carcinogenesis through negative regulation of caudal-related homeobox 2 expression.

Minaga K, Watanabe T, Kamata K, Asano N, Kudo M. Nucleotide-binding oligomerization domain 1 and *Helicobacter pylori* infection: A review. *World J Gastroenterol* 2018; 24(16): 1725-1733 Available from: URL: <http://www.wjgnet.com/1007-9327/full/v24/i16/1725.htm> DOI: <http://dx.doi.org/10.3748/wjg.v24.i16.1725>

INTRODUCTION

Helicobacter pylori (*H. pylori*) is a Gram negative bacterium that preferentially colonizes the human gastric mucosa^[1,2]. Infection due to this organism is usually established during childhood^[1,2], which then causes various upper gastrointestinal (GI) disorders, including atrophic gastritis, peptic ulcers, gastric mucosa-associated lymphoid tissue lymphoma, and gastric cancer. Thus, it is now generally accepted that persistent *H. pylori* infection in the gastric mucosa is the highest risk factor for the development of the aforementioned diseases^[3]. This notion is supported by recent studies indicating that successful eradication of *H. pylori* prevents the development of gastric cancer^[4,5].

Colonization of the human stomach by *H. pylori* triggers innate and adaptive immune responses. As in the cases of other microbial infections, sensing of *H. pylori* by pattern recognition receptors (PRRs) expressed in innate immune cells, such as epithelial cells (ECs) and antigen-presenting cells (APCs), is an initial step for eradicating this organism. Toll-like receptors (TLRs) and nucleotide-binding oligomerization domain (NOD)-like receptors (NLRs) are the prototypical PRRs and represent the first line of defense against *H. pylori*^[6,7]. Indeed, gastric epithelial cells and APCs express functional TLRs and lipopolysaccharide (LPS)-mediated TLR4 activation is involved in the development of gastric mucosal inflammatory responses^[8]. However, the ability to stimulate TLRs by *H. pylori*-derived antigens is much lower than that by other pathogenic bacteria. For example, *H. pylori*-derived LPS and flagellin exhibit low stimulatory activity toward TLR4 and TLR5^[9,10]. Thus, *H. pylori* might evade the major innate immune system molecules, TLRs, to establish persistent gastric infection. Therefore, it is possible that PRRs other than TLRs might play a major role in mucosal host defense systems against *H. pylori* although roles played by TLRs need to be determined in future studies.

NOD1 is a prototypical innate immune receptor belonging to the NLR protein family, which detects small molecules derived from Gram-negative bacteria^[7,11]. NOD1 activation induced by intestinal microflora is associated with lymphoid tissue genesis^[12] and development of pancreatitis^[13-15]. In 2004, Viala *et al.*^[16] demonstrated that gastric mucosal host defense against *H. pylori* depends on the activation of NOD1 in gastric ECs. Many efforts have been made by gastroenterologists, microbiologists, and immunologists to elucidate the molecular mechanisms by which colonization of the human stomach by *H. pylori*

induces the activation of NOD1 and such NOD1 activation mediates antimicrobial immune responses^[11]. In this review, we have summarized and discussed how sensing of *H. pylori* by NOD1 mediates the prevention of chronic gastritis and gastric cancer.

CYTOKINE AND CHEMOKINE RESPONSES IN THE GASTRIC MUCOSA HARBORING *H. PYLORI* INFECTION

Gastric inflammation caused by chronic *H. pylori* infection is mediated by gastric mucosal T helper type 1 (Th1) and Th17 cells producing IFN- γ and IL-17, respectively^[17]. Initial studies addressing the role of IFN- γ in *H. pylori*-induced gastritis revealed that lack of chronic gastritis in IFN- γ -deficient mice is associated with higher colonization of the gastric mucosa by this organism than in IFN- γ -intact mice^[18]. In addition, gastric mucosal CD4⁺ T cells isolated from *H. pylori*-infected patients have been reported to produce a high level of IFN- γ ^[19]. Thus, gastric mucosa harboring chronic *H. pylori* infection is characterized by Th1 responses that are involved in both eradication and inflammation^[20]. In addition to a well-established role played by Th1 cells, recent studies have highlighted the importance of another type of Th cells, Th17 cells, producing IL-17^[20]. The development of chronic gastritis is significantly attenuated in IL-17-deficient mice in long-term *H. pylori* infection^[20]. Moreover, treatment of mice with a neutralizing anti-IL-17 antibody reduced the *H. pylori* burden and inflammation in the stomach^[21]. In line with these experimental studies, Serrano *et al.*^[22] provided evidence that downregulation of Th17 responses is associated with reduced gastritis in *H. pylori*-infected patients. Therefore, both Th1 and Th17 cells are involved in the development of chronic gastritis caused by persistent *H. pylori* infection in the gastric mucosa.

Differentiation of Th1 and Th17 cells requires cytokines produced by APCs such as dendritic cells and macrophages^[23]. Differentiation of Th1 cells depends on IL-12, whereas that of Th17 cells depends on IL-1 β , IL-6, and IL-23. Expression of IFN- γ and IL-17 in the gastric mucosa of mice challenged with *H. pylori* was accompanied by IL-12 and IL-23 expression, derived from APCs^[21]. Furthermore, the levels of APC-derived pro-inflammatory cytokines in the gastric mucosa, including IL-1 β , IL-6 and TNF- α were significantly higher in *H. pylori*-positive patients than in *H. pylori*-negative patients^[24]. Thus, it is likely that pro-inflammatory cytokines produced by APCs contribute to *H. pylori*-induced gastric pathology through differentiation of Th1 and Th17 cells. Consistent with this idea, the exposure of human APCs to *H. pylori* results in robust production of IL-6, IL-12, and TNF- α ^[25,26].

ECs are an important source of chemokines that attract immune cells to the lesions^[27,28]. Yamaoka *et al.*^[28] assessed chemokine responses in the gastric mucosa

of patients with *H. pylori* infection and found that *H. pylori* infection is associated with increased expression of C-X-C motif chemokine ligand 8 (CXCL8) and chemokine (C-C motif) ligand 5 (CCL5). In addition to CXCL8 and CCL5, the gastric mucosa of *H. pylori*-positive patients exhibited enhanced expression of CXCL9 and CXCL10^[29]. Given the fact that CXCL8 is a strong attractant for neutrophils and that CXCL9 and CXCL10 are strong attractants for Th1 cells^[28,29], these results suggest that EC-derived chemokines are also involved in the development of chronic gastritis caused by persistent *H. pylori* infection. Taken together, these findings suggest that cytokines and chemokines produced by immune cells and ECs play a substantial role in the development of *H. pylori*-induced gastric pathology.

TYPE IV SECRETION SYSTEM OF *H. PYLORI* AND NOD1 ACTIVATION

NOD1 is expressed in the cytosolic regions of innate immune cells, such as APCs and ECs^[7,11]. Peptidoglycan (PGN) is a polymer consisting of sugars and amino acids that constitute the cell wall of both Gram-positive and Gram-negative bacteria^[7]. Small peptides derived from the PGN layer of Gram-negative bacteria activate intracellular NOD1^[7,11]. γ -D-glutamyl-mesodiaminopimelic acid (iE-DAP) is considered as the minimal motif of the NOD1 ligand, and NOD1-deficient mice exhibit impaired responses to iE-DAP^[30]. Two models have been proposed by which *H. pylori* activates intracellular NOD1.

H. pylori is classified into two types according to the expression of cag pathogenicity island (*cagPAI*)^[1]. *cagPAI* is a gene locus necessary to assemble type IV secretion system (T4SS), a syringe and needle-like structure^[1,31]. The primary function of T4SS, encoded by *cagPAI*, is the injection of pathogenic factors, such as cytotoxin-associated gene A (CagA) into the host gastric ECs upon attachment to the epithelium^[1,31]. Thus, *cagPAI*-positive *H. pylori* can cause gastric mucosal injury through injection of CagA mediated by T4SS. Hence, T4SS may enable *H. pylori* to deliver its cell wall components, such as PGN, into the host ECs. Viala *et al.*^[16] addressed this possibility and demonstrated that intracellular NOD1 expressed in gastric ECs sense *H. pylori*-derived PGN delivered to the cytosolic region through T4SS. NOD1 activation is not observed in gastric ECs upon exposure to *H. pylori* harboring non-functional *cagPAI*, which supports the idea that NOD1 functions as an intracellular innate immune sensor for *cagPAI*-positive *H. pylori*. Interestingly, *H. pylori* burden in the stomach was much higher in NOD1-deficient mice than in the NOD1-intact ones, when they were orally challenged with *cagPAI*-positive *H. pylori*^[16]. In contrast, *H. pylori* burden in the stomach was comparable between NOD1-intact and NOD1-deficient mice when mice were orally challenged with *cagPAI*-mutated *H. pylori*. Thus, these studies showed that NOD1 is an

intracellular receptor for *cagPAI*-positive *H. pylori* and that NOD1 activation is necessary for eradication of this organism.

OUTER MEMBRANE VESICLE OF *H. PYLORI* AND NOD1 ACTIVATION

Outer membrane vesicles (OMVs), which are released by Gram-negative bacteria during normal growth, contain bacterial cell components, including PGN^[32]. Kaparakis *et al.*^[33] addressed the possibility that OMVs released from *H. pylori* activate cytosolic NOD1 through intracellular delivery of PGN. OMVs isolated from *H. pylori* activate nuclear factor kappa B (NF- κ B) in AGS cells, a gastric cancer cell line, in a *cagPAI*-independent manner. Importantly, knockdown of NOD1 expression by siRNA abrogated CXCL8 production in AGS cells upon exposure to *H. pylori*-derived OMVs. Furthermore, intragastrically delivered OMVs efficiently induced gastric mucosal expression of CXCL2, a murine chemoattractant for neutrophils, and antibody responses against OMVs. These innate and adaptive responses to OMVs depend on NOD1 activation because NOD1-deficient mice exhibit defective CXCL2 expression and OMV-specific antibody responses. Thus, these data suggest that intracellular delivery of PGN as a form of OMVs activates NOD1 in gastric ECs in a *cagPAI*-independent manner.

A study has highlighted the role of autophagy to address the molecular mechanisms accounting for OMV-mediated NOD1 activation^[34]. Irving *et al.*^[34] first found that *H. pylori*-derived OMVs induce autophagy in ECs. Consistent with autophagy induction, mouse embryonic fibroblasts (MEFs) deficient in *ATG5*, a critical molecule for autophagy, exhibited diminished production of CXCL2 compared with *ATG5*-intact MEFs upon exposure to *H. pylori*-derived OMVs. Autophagosome formation was diminished in NOD1-knockdown AGS cells stimulated with *H. pylori*-derived OMVs, suggesting the involvement of NOD1 activation in autophagy induction. Fluorescent labeling studies clearly demonstrated that EEA1 (early endosome antigen 1)-positive early endosomes containing both OMVs and PGN recruit NOD1 and its downstream kinase, receptor interacting protein 2 (RIP2). Such endosomal interactions between *H. pylori*-derived OMVs, NOD1, and RIP2 are necessary for chemokine production and autophagy induction, as RIP2 inhibitor efficiently blocks these responses. Collectively, these studies provide the evidence that NOD1 recognizes *H. pylori*-derived PGN within EEA1⁺ early endosomes and subsequently activates RIP2 to induce autophagy and pro-inflammatory chemokine responses^[34]. However, it should be noted that involvement of RIP2 in the induction of NOD1-mediated autophagy requires future studies, as it has been previously observed that NOD1 activation induces RIP2-independent autophagy in case of *Shigella flexneri* infection^[35].

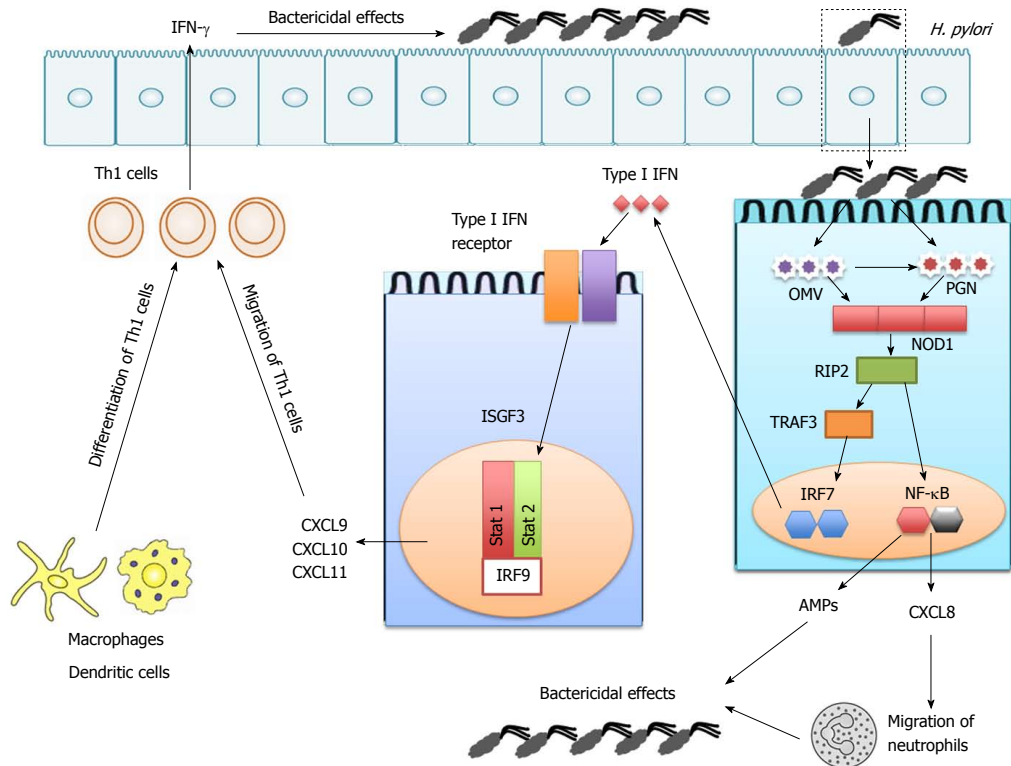


Figure 1 Nucleotide-binding oligomerization domain 1-mediated mucosal host defense against *Helicobacter pylori* infection. Nucleotide-binding oligomerization domain 1 (NOD1) recognizes *Helicobacter pylori* (*H. pylori*)-derived peptidoglycan (PGN) or outer membrane vesicles (OMVs). Sensing of *H. pylori*-derived PGN or OMVs by intracellular NOD1 in the gastric epithelial cells induces production of type I IFN and C-X-C motif chemokine ligand 10 (CXCL10) through the receptor interacting protein 2 (RIP2)-TNF receptor-associated factor 3 (TRAF3)-interferon regulatory factor 7 (IRF7)-IFN-stimulated gene factor 3 (ISGF3) pathway, thereby promoting T helper type 1 (Th1) responses. ISGF3 is a heterotrimeric complex composed of signal transduction and activator of transcription 1 (Stat1), Stat2, and IRF9. NOD1 activation also induces production of anti-microbial peptides (AMPs) through nuclear translocation of nuclear factor-kappa B (NF-κB) subunits. IFN-γ and AMPs exert bactericidal effects.

CYTOKINE AND CHEMOKINE RESPONSES AGAINST *H. PYLORI* BY NOD1 ACTIVATION

NOD1 senses *H. pylori*-derived PGN that is delivered to the cytosolic region of gastric ECs via T4SS and/or OMV transport. The next question is how NOD1 activation leads to the induction of Th1 and Th17 responses, both of which are characteristics of chronic *H. pylori* infection (Figure 1).

NOD1 activation leads to the physical interaction between NOD1 and RIP2, its downstream effector molecule^[7,11]. NOD1-induced RIP2 activation triggers the pro-inflammatory signaling cascade through nuclear translocation of NF-κB subunits^[7,11]. In addition to NF-κB, the interaction between NOD1 and RIP2 leads to the activation of mitogen-activated kinases (MAPKs), including extracellular signal-regulated kinase, c-JUN N-terminal kinase, and p38^[7,11]. Thus, one major outcome of NOD1-mediated signaling pathways is the activation of NF-κB and MAPKs^[7,11]. Activation of NF-κB and MAPKs as well as production of CXCL8 is induced

in gastric ECs, such as AGS cells, upon exposure to *H. pylori*^[36-38]. However, it remains controversial whether activation of NF-κB/MAPKs and production of CXCL8 are dependent upon the recognition of *H. pylori* by NOD1. Grubman *et al.*^[36] established a stable AGS cell line with diminished expression of NOD1 (NOD1 knockdown, NOD1 KD cells), and found that NF-κB activation and CXCL8 production are markedly reduced in NOD1 KD cells than in AGS cells with intact NOD1 expression. Moreover, *H. pylori*-induced CXCL8 production by gastric ECs is partially mediated by MAPK activation following the recognition of this organism by NOD1, as knockdown of NOD1 expression by siRNA results in reduced activation of MAPKs and MAPKs inhibitors efficiently blocks CXCL8 production^[39]. These reports support the idea that activation of NF-κB/MAPK and production of CXCL8 induced by exposure to *H. pylori* are dependent on NOD1. On the other hand, Hirata *et al.*^[38] reported that knockdown of NOD1 or RIP2 expression by specific siRNAs did not affect *H. pylori*-induced NF-κB/MAPK activation or CXCL8 production in AGS cells. Future *in vitro* studies are required to determine the contribution of NOD1 in NF-κB activation

in response to *H. pylori* infection.

Human gastric mucosa with persistent *H. pylori* infection is characterized by Th1 responses. CXCL9, CXCL10, and CXCL11 are EC-derived chemokines that play a pivotal role in the generation of Th1 responses through the attraction of Th1 cells expressing C-X-C chemokine receptor type 3 (CXCR3)^[40]. High expression of CXCL9 and CXCL10 in the human gastric mucosa with chronic *H. pylori* infection strongly suggests that CXCL9 and CXCL10 contribute to the generation of Th1 responses^[29,41]. We discerned from previous studies that stimulation of colon and gastric cancer cell lines (HT-29 and AGS cells) with NOD1 ligands lead to the robust production of CXCL9, CXCL10, and CXCL11^[11,27,42]. Surprisingly, NOD1-induced CXCL10 production by colonic and gastric ECs is not dependent on NF- κ B or MAPK activation, because blockade of these pathways by specific pharmacological inhibitors or siRNA transfection did not alter the production of CXCL10^[11,27,42]. Instead, NOD1-induced CXCL10 production is markedly decreased by the addition of type I IFN receptor antibody, suggesting that type I IFN production is one of the major outcomes following NOD1 activation. Indeed, HT-29 cells produce a large amount of type I IFN upon stimulation with NOD1 ligand.

Next, we focused on identifying the signaling pathways involved in type I IFN production through NOD1 activation. Detailed knockdown and over-expression studies revealed the involvement of TNF receptor-associated factor 3 (TRAF3) in the induction of type I IFN^[11,27,42]. The interaction between NOD1 and RIP2 initiates recruitment of TRAF3 to this complex and leads to the activation of downstream signaling molecules, TANK-binding kinase 1 (TBK1) and I κ B kinase ϵ (IKK ϵ), both of which play an indispensable role in the induction of type I IFN responses through nuclear translocation of interferon regulatory factor 3 (IRF3) and IRF7^[43,44]. Indeed, the RIP2-TRAF3-TBK1-IKK ϵ -IRF7 axis plays a key role in inducing the production of type I IFN by ECs^[27,42]. Furthermore, NOD1-mediated type I IFN production promotes the transcription of CXCL10 through nuclear translocation of the heterotrimeric complex, IFN-stimulated gene factor 3 (ISGF3), composed of signal transduction and activator of transcription 1 (Stat1), Stat2, and IRF9, because gene silencing of Stat1 or Stat2 by siRNA leads to a marked reduction in CXCL10 production. Thus, these data suggest that NOD1 activation induces the production of type I IFN and CXCL10 through activation of the RIP2-TRAF3-TBK1-IKK ϵ -IRF7-ISGF3 pathway^[11,27,42].

The relevance of NOD1-mediated type I IFN responses was examined in animal studies in which NOD1-intact and NOD1-deficient mice were challenged with *H. pylori*. As expected, NOD1-deficient mice exhibited a higher bacterial burden in the stomach two weeks after the infection, and the effects were

accompanied by reduced expression of type I IFN-related factors, such as IFN- β , IFN- γ and CXCL10, rather than NF- κ B-related factors, such as TNF- α and CXCL2^[11,27,42]. Reduced expression of phospho-Stat1 (p-Stat1) and p-Stat2 is observed in the gastric mucosa of NOD1-deficient mice, when compared with that in NOD1-intact mice. However, comparable levels of NF- κ B activation are observed in both mice. Finally, the blockade of type I IFN signaling pathways by Stat1 siRNA increased bacterial burden in the stomach upon oral infection with *H. pylori* in NOD1-intact mice. Its effects were accompanied by reduced expression of IFN- γ and CXCL10 in the stomach. In contrast, blockade of NF- κ B signaling pathways by NF- κ B decoy oligonucleotide did not alter the bacterial burden or expression of IFN- γ or CXCL10 in the stomach, although these treatments reduced the gastric expression of TNF- α and CXCL2. Collectively, these data suggest that sensing of *H. pylori*-derived PGN by intracellular NOD1 in gastric ECs induces production of type I IFN and CXCL10 through the RIP2-TRAF3-TBK1-IKK ϵ -IRF7-ISGF3 pathway and thereby promotes Th1 responses. Because IFN- γ produced by Th1 cells enhances the expression of NOD1^[27,42,45], we propose that the type I IFN-CXCL10-IFN- γ axis induced by NOD1 activation forms a positive feedback loop for the generation of Th1 responses in the gastric mucosa with persistent *H. pylori* infection.

Little is known about the molecular mechanisms accounting for NOD1-mediated Th17 responses in *H. pylori* infection. In this regard, a recent study has highlighted the importance of NOD1 activation in non-hematopoietic cells, *i.e.* ECs, in the generation of Th17 responses^[46]. Therefore, it is possible that the sensing of *H. pylori*-derived PGN or OMVs by intracellular NOD1 in gastric ECs is involved in Th17 responses.

RESPONSE OF ANTI-MICROBIAL PEPTIDES AGAINST *H. PYLORI* BY NOD1 ACTIVATION

Antimicrobial peptides (AMPs) constitute a part of the innate host defense system^[47]. AMPs released by APCs and ECs rapidly act to eradicate invading microorganisms^[47]. Grubman *et al.*^[36] reported that AGS cells release β -defensins upon exposure to *cag*PAI-positive *H. pylori*. Production of β -defensins by AGS cells is dependent on NOD1 activation, because stable NOD1-knockdown AGS cells exhibit reduced production of AMPs. Moreover, AMPs induced by exposure to *H. pylori* exhibit potent *H. pylori* eradicating activity. Consistent with this, the expression of β -defensin 4 in the stomach is markedly decreased in NOD1-deficient mice than in NOD1-intact mice following *H. pylori* infection^[48]. Collectively, these *in vitro* and *in vivo* studies suggest the possible involvement of NOD1-dependent production of AMPs in the mucosal host

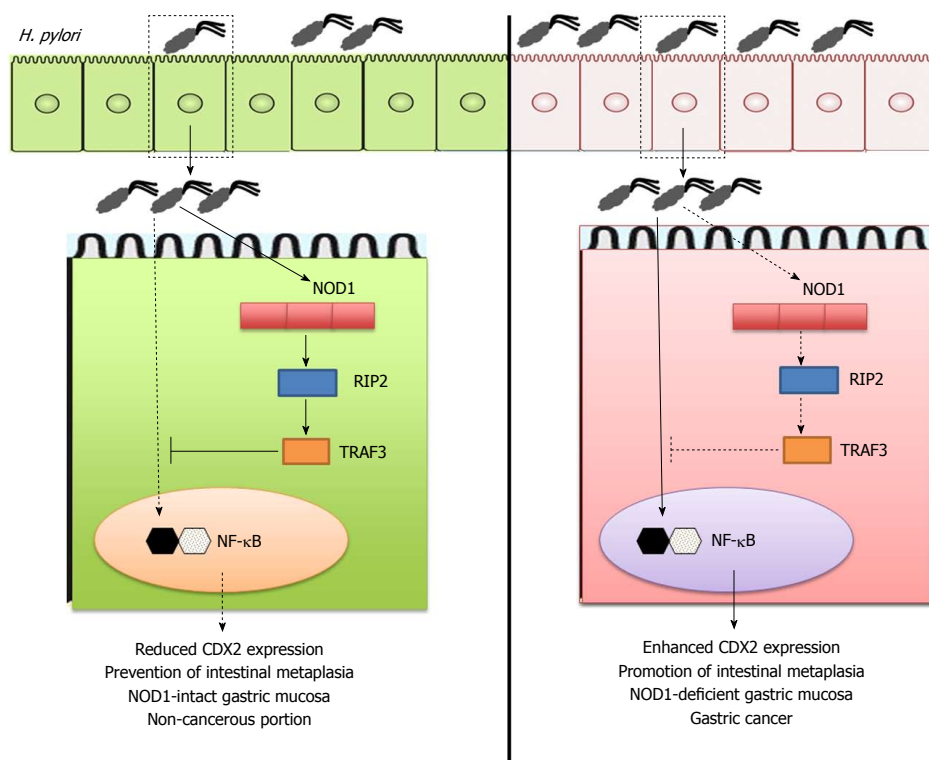


Figure 2 Prevention of gastric cancer development by nucleotide-binding oligomerization domain 1. Sensing of *Helicobacter pylori* (*H. pylori*)-derived peptidoglycan (PGN) by intracellular nucleotide-binding oligomerization domain 1 (NOD1) in gastric epithelial cells induces activation of TNF receptor associated factor 3 (TRAF3) as mentioned in Figure 1. TRAF3 activation by NOD1 negatively regulates expression of caudal-related homeobox 2 (Cdx2) via the inhibition of nuclear factor-kappa B (NF-κB) activation to prevent intestinal metaplasia and gastric cancer (left panel). On the other hand, lack of NOD1-mediated negative regulation on Cdx2 expression promotes the development of gastric cancer (right panel).

defenses against *H. pylori* infection (Figure 1).

NOD1 POLYMORPHISMS AND UPPER GASTROINTESTINAL DISEASES

Several reports have suggested an association between NOD1 gene polymorphisms and upper GI diseases^[49-51]. Wang *et al.*^[51] identified the NOD1 rs7789045 TT genotype as an increased risk for gastric cancer in a Chinese population. Another Chinese cohort study reported that the risk of gastric cancer is high in *H. pylori*-infected subjects carrying the NOD1 rs 2709800 TT genotype^[52]. Moreover, Hofner *et al.*^[53] reported that the G796A NOD1 polymorphism is associated with peptic ulcers in *H. pylori*-infected patients. Although these studies support the correlation between NOD1 polymorphisms and upper GI disorders caused by *H. pylori*, the mechanisms by which NOD1 polymorphisms lead to the development of *H. pylori*-associated diseases remain unknown. Because NOD1 deficiency increases gastric *H. pylori* burden in animals and its expression is lower in the cancerous tissues of the stomach than in the non-cancerous tissues^[54], it would be interesting to study whether NOD1 function is impaired or enhanced

in the presence of such polymorphisms associated with gastric cancer.

PREVENTION OF GASTRIC CANCER BY NOD1 ACTIVATION

NOD1 activation is required for mucosal host defense against *H. pylori* infection. This protective effect is partially mediated by the activation of type I IFN signaling pathways following the molecular interaction between NOD1 and TRAF3^[11,27]. Suarez *et al.*^[54] have addressed the clinical relevance of NOD1-TRAF3 interaction in human *H. pylori*-associated diseases. They reported that expression levels of NOD1 and TRAF3 are much weaker in gastric cancer tissues than in non-cancerous tissues. Thus, these studies utilizing human gastric cancer samples strongly suggest that impaired activation of NOD1 and TRAF3 is involved in the pathogenesis of gastric cancer and that NOD1-TRAF3 interaction may play a protective role in the development of gastric cancer (Figure 2).

Thus, after confirming the possible involvement of NOD1 activation in the development of human gastric cancer, the next question is how NOD1 serves

as a protective factor for gastric cancer development. Intestinal metaplasia, wherein the gastric mucosa exhibits an intestinal phenotype, is a pre-neoplastic lesion of gastric cancer^[55]. Aberrant expression of caudal-related homeobox 2 (Cdx2)^[55], a transdifferentiation factor, in the gastric tissue induces intestinal metaplasia and gastric carcinogenesis. We hypothesized that NOD1 activation inhibits the development of gastric cancer through negative regulation of Cdx2^[37]. To address this question, we performed a long-term infection study in which NOD1-intact and NOD1-deficient mice were challenged with *cagPAI*-positive *H. pylori*. Interestingly, formation of gastric intestinal metaplasia was observed in NOD1-deficient mice, eight months after initial challenge with *H. pylori*, but not in NOD1-intact mice. This effect was accompanied with higher expression of Cdx2 in the gastric mucosa of NOD1-deficient mice than in the NOD1-intact mice. On the contrary, expression of TRAF3 was lower in the gastric mucosa of NOD1-deficient mice than in NOD1-intact mice. Furthermore, development of gastric intestinal metaplasia in the absence of intact NOD1 signaling pathways is associated with enhanced activation of NF- κ B, because most gastric ECs are positive for nuclear p65 staining. Detection of *H. pylori* in gastric mucosa exhibiting intestinal metaplasia is difficult in human samples^[56]. Consistent with this, *H. pylori* burden in the gastric mucosa was much lower in NOD1-deficient mice than in the NOD1-intact mice^[37]. Thus, the results of our long-term *H. pylori* infection study support the data^[54] obtained from human gastric cancer samples, demonstrating that impaired activation of NOD1-TRAF3 signaling pathways is involved in the development of intestinal metaplasia^[37].

Regarding the molecular mechanisms by which NOD1 activation prevents the development of intestinal metaplasia and gastric cancer, we provided evidence that NOD1 activation upon exposure to *H. pylori* negatively regulates Cdx2 expression through activation of TRAF3^[37]. Exposure to *H. pylori* upregulates Cdx2 expression in gastric cancer cell lines, and the effects are enhanced or diminished by gene silencing of NOD1 by siRNA or over-expression of TRAF3, respectively^[37]. Furthermore, promoter gene and gel shift assays revealed that interaction between NOD1 and TRAF3 inhibits the expression of Cdx2 through negative regulation of NF- κ B activation. Thus, these *in vitro* studies have elucidated a part of the molecular mechanisms accounting for the prevention of intestinal metaplasia followed by gastric cancer *via H. pylori*-induced NOD1 activation. Collectively, these two recent studies strongly suggest that NOD1 activation by *H. pylori* infection plays a protective role in the development of gastric cancer.

CONCLUSION

NOD1 contributes to mucosal host defense against *H. pylori* infection through the activation of type I IFN signaling pathways and production of AMPs. In

addition, NOD1 activation negatively regulates Cdx2 expression, and thereby inhibits the development of gastric cancer. Molecules involved in NOD1-mediated signaling pathways might be new therapeutic targets for treating chronic gastric diseases and gastric cancer.

REFERENCES

- Hatakeyama M. Helicobacter pylori CagA and gastric cancer: a paradigm for hit-and-run carcinogenesis. *Cell Host Microbe* 2014; **15**: 306-316 [PMID: 24629337 DOI: 10.1016/j.chom.2014.02.008]
- Amieva M, Peek RM Jr. Pathobiology of Helicobacter pylori-Induced Gastric Cancer. *Gastroenterology* 2016; **150**: 64-78 [PMID: 26385073 DOI: 10.1053/j.gastro.2015.09.004]
- Chiba T, Marusawa H, Ushijima T. Inflammation-associated cancer development in digestive organs: mechanisms and roles for genetic and epigenetic modulation. *Gastroenterology* 2012; **143**: 550-563 [PMID: 22796521 DOI: 10.1053/j.gastro.2012.07.009]
- Fukase K, Kato M, Kikuchi S, Inoue K, Uemura N, Okamoto S, Terao S, Amagai K, Hayashi S, Asaka M; Japan Gast Study Group. Effect of eradication of Helicobacter pylori on incidence of metachronous gastric carcinoma after endoscopic resection of early gastric cancer: an open-label, randomised controlled trial. *Lancet* 2008; **372**: 392-397 [PMID: 18675689 DOI: 10.1016/S0140-6736(08)61159-9]
- Uemura N, Okamoto S, Yamamoto S, Matsumura N, Yamaguchi S, Yamakido M, Taniyama K, Sasaki N, Schlemper RJ. Helicobacter pylori infection and the development of gastric cancer. *N Engl J Med* 2001; **345**: 784-789 [PMID: 11556297 DOI: 10.1056/NEJMoa001999]
- Akira S, Takeda K. Toll-like receptor signalling. *Nat Rev Immunol* 2004; **4**: 499-511 [PMID: 15229469 DOI: 10.1038/nri1391]
- Strober W, Murray PJ, Kitani A, Watanabe T. Signalling pathways and molecular interactions of NOD1 and NOD2. *Nat Rev Immunol* 2006; **6**: 9-20 [PMID: 16493424 DOI: 10.1038/nri1747]
- Slomiany BL, Slomiany A. Role of LPS-elicited signaling in triggering gastric mucosal inflammatory responses to *H. pylori*: modulatory effect of ghrelin. *Inflammopharmacology* 2017; **25**: 415-429 [PMID: 28516374 DOI: 10.1007/s10787-017-0360-1]
- Andersen-Nissen E, Smith KD, Strober KL, Barrett SL, Cookson BT, Logan SM, Aderem A. Evasion of Toll-like receptor 5 by flagellated bacteria. *Proc Natl Acad Sci USA* 2005; **102**: 9247-9252 [PMID: 15956202 DOI: 10.1073/pnas.0502040102]
- Ferrero RL. Innate immune recognition of the extracellular mucosal pathogen, Helicobacter pylori. *Mol Immunol* 2005; **42**: 879-885 [PMID: 15829277 DOI: 10.1016/j.molimm.2004.12.001]
- Watanabe T, Asano N, Kudo M, Strober W. Nucleotide-binding oligomerization domain 1 and gastrointestinal disorders. *Proc Jpn Acad Ser B Phys Biol Sci* 2017; **93**: 578-599 [PMID: 29021509 DOI: 10.2183/pjab.93.037]
- Bouskra D, Brézillon C, Bérard M, Werts C, Varona R, Boneca IG, Eberl G. Lymphoid tissue genesis induced by commensals through NOD1 regulates intestinal homeostasis. *Nature* 2008; **456**: 507-510 [PMID: 18987631 DOI: 10.1038/nature07450]
- Tsuji Y, Watanabe T, Kudo M, Arai H, Strober W, Chiba T. Sensing of commensal organisms by the intracellular sensor NOD1 mediates experimental pancreatitis. *Immunity* 2012; **37**: 326-338 [PMID: 22902233 DOI: 10.1016/j.immuni.2012.05.024]
- Watanabe T, Kudo M, Strober W. Immunopathogenesis of pancreatitis. *Mucosal Immunol* 2017; **10**: 283-298 [PMID: 27848953 DOI: 10.1038/mi.2016.101]
- Watanabe T, Sadakane Y, Yagama N, Sakurai T, Ezoe H, Kudo M, Chiba T, Strober W. Nucleotide-binding oligomerization domain 1 acts in concert with the cholecystokinin receptor agonist, cerulein, to induce IL-33-dependent chronic pancreatitis. *Mucosal Immunol* 2016; **9**: 1234-1249 [PMID: 26813347 DOI: 10.1038/mi.2015.144]
- Viala J, Chaput C, Boneca IG, Cardona A, Girardin SE, Moran AP, Athman R, Mémet S, Huerre MR, Coyle AJ, DiStefano PS, Sansonetti PJ, Labigne A, Bertin J, Philpott DJ, Ferrero RL. Nod1

- responds to peptidoglycan delivered by the *Helicobacter pylori* cag pathogenicity island. *Nat Immunol* 2004; **5**: 1166-1174 [PMID: 15489856 DOI: 10.1038/ni1131]
- 17 **Moyat M**, Velin D. Immune responses to *Helicobacter pylori* infection. *World J Gastroenterol* 2014; **20**: 5583-5593 [PMID: 24914318 DOI: 10.3748/wjg.v20.i19.5583]
 - 18 **Sawai N**, Kita M, Kodama T, Tanahashi T, Yamaoka Y, Tagawa Y, Iwakura Y, Imanishi J. Role of gamma interferon in *Helicobacter pylori*-induced gastric inflammatory responses in a mouse model. *Infect Immun* 1999; **67**: 279-285 [PMID: 9864227]
 - 19 **Itoh T**, Wakatsuki Y, Yoshida M, Usui T, Matsunaga Y, Kaneko S, Chiba T, Kita T. The vast majority of gastric T cells are polarized to produce T helper 1 type cytokines upon antigenic stimulation despite the absence of *Helicobacter pylori* infection. *J Gastroenterol* 1999; **34**: 560-570 [PMID: 10535482]
 - 20 **Gray BM**, Fontaine CA, Poe SA, Eaton KA. Complex T cell interactions contribute to *Helicobacter pylori* gastritis in mice. *Infect Immun* 2013; **81**: 740-752 [PMID: 23264048 DOI: 10.1128/IAI.01269-12]
 - 21 **Shi Y**, Liu XF, Zhuang Y, Zhang JY, Liu T, Yin Z, Wu C, Mao XH, Jia KR, Wang FJ, Guo H, Flavell RA, Zhao Z, Liu KY, Xiao B, Guo Y, Zhang WJ, Zhou WY, Guo G, Zou QM. *Helicobacter pylori*-induced Th17 responses modulate Th1 cell responses, benefit bacterial growth, and contribute to pathology in mice. *J Immunol* 2010; **184**: 5121-5129 [PMID: 20351183 DOI: 10.4049/jimmunol.0901115]
 - 22 **Serrano C**, Wright SW, Bimczok D, Shaffer CL, Cover TL, Venegas A, Salazar MG, Smythies LE, Harris PR, Smith PD. Downregulated Th17 responses are associated with reduced gastritis in *Helicobacter pylori*-infected children. *Mucosal Immunol* 2013; **6**: 950-959 [PMID: 23299619 DOI: 10.1038/mi.2012.133]
 - 23 **Strober W**, Fuss IJ. Proinflammatory cytokines in the pathogenesis of inflammatory bowel diseases. *Gastroenterology* 2011; **140**: 1756-1767 [PMID: 21530742 DOI: 10.1053/j.gastro.2011.02.016]
 - 24 **Yamaoka Y**, Kita M, Kodama T, Sawai N, Kashima K, Imanishi J. Induction of various cytokines and development of severe mucosal inflammation by cagA gene positive *Helicobacter pylori* strains. *Gut* 1997; **41**: 442-451 [PMID: 9391240]
 - 25 **Amedei A**, Cappon A, Codolo G, Cabrelle A, Polenghi A, Benagiano M, Tasca E, Azzurri A, D'Elia MM, Del Prete G, de Bernard M. The neutrophil-activating protein of *Helicobacter pylori* promotes Th1 immune responses. *J Clin Invest* 2006; **116**: 1092-1101 [PMID: 16543949 DOI: 10.1172/JCI27177]
 - 26 **Kranzer K**, Eckhardt A, Aigner M, Knoll G, Deml L, Speth C, Lehn N, Rehli M, Schneider-Brachert W. Induction of maturation and cytokine release of human dendritic cells by *Helicobacter pylori*. *Infect Immun* 2004; **72**: 4416-4423 [PMID: 15271898 DOI: 10.1128/IAI.72.8.4416-4423.2004]
 - 27 **Watanabe T**, Asano N, Fichtner-Feigl S, Gorelick PL, Tsuji Y, Matsumoto Y, Chiba T, Fuss IJ, Kitani A, Strober W. NOD1 contributes to mouse host defense against *Helicobacter pylori* via induction of type I IFN and activation of the ISGF3 signaling pathway. *J Clin Invest* 2010; **120**: 1645-1662 [PMID: 20389019 DOI: 10.1172/JCI39481]
 - 28 **Yamaoka Y**, Kita M, Kodama T, Sawai N, Tanahashi T, Kashima K, Imanishi J. Chemokines in the gastric mucosa in *Helicobacter pylori* infection. *Gut* 1998; **42**: 609-617 [PMID: 9659152]
 - 29 **Eck M**, Schmausser B, Scheller K, Toksoy A, Kraus M, Menzel T, Müller-Hermelink HK, Gillitzer R. CXC chemokines Gro(alpha)/IL-8 and IP-10/MIG in *Helicobacter pylori* gastritis. *Clin Exp Immunol* 2000; **122**: 192-199 [PMID: 11091274]
 - 30 **Chamaillard M**, Hashimoto M, Horie Y, Masumoto J, Qiu S, Saab L, Ogura Y, Kawasaki A, Fukase K, Kusumoto S, Valvano MA, Foster SJ, Mak TW, Nuñez G, Inohara N. An essential role for NOD1 in host recognition of bacterial peptidoglycan containing diaminopimelic acid. *Nat Immunol* 2003; **4**: 702-707 [PMID: 12796777 DOI: 10.1038/ni945]
 - 31 **Varga MG**, Peek RM. DNA Transfer and Toll-like Receptor Modulation by *Helicobacter pylori*. *Curr Top Microbiol Immunol* 2017; **400**: 169-193 [PMID: 28124154 DOI: 10.1007/978-3-319-50520-6_8]
 - 32 **Kuehn MJ**, Kesty NC. Bacterial outer membrane vesicles and the host-pathogen interaction. *Genes Dev* 2005; **19**: 2645-2655 [PMID: 16291643 DOI: 10.1101/gad.1299905]
 - 33 **Kaparakis M**, Turnbull L, Carneiro L, Firth S, Coleman HA, Parkington HC, Le Bourhis L, Karrar A, Viala J, Mak J, Hutton ML, Davies JK, Crack PJ, Hertzog PJ, Philpott DJ, Girardin SE, Whitchurch CB, Ferrero RL. Bacterial membrane vesicles deliver peptidoglycan to NOD1 in epithelial cells. *Cell Microbiol* 2010; **12**: 372-385 [PMID: 19888989 DOI: 10.1111/j.1462-5822.2009.01404.x]
 - 34 **Irving AT**, Mimuro H, Kufer TA, Lo C, Wheeler R, Turner LJ, Thomas BJ, Malosse C, Gantier MP, Casillas LN, Votta BJ, Bertin J, Boneca IG, Sasakawa C, Philpott DJ, Ferrero RL, Kaparakis-Liaskos M. The immune receptor NOD1 and kinase RIP2 interact with bacterial peptidoglycan on early endosomes to promote autophagy and inflammatory signaling. *Cell Host Microbe* 2014; **15**: 623-635 [PMID: 24746552 DOI: 10.1016/j.chom.2014.04.001]
 - 35 **Travassos LH**, Carneiro LA, Ramjeet M, Hussey S, Kim YG, Magalhães JG, Yuan L, Soares F, Chea E, Le Bourhis L, Boneca IG, Allaoui A, Jones NL, Nuñez G, Girardin SE, Philpott DJ. Nod1 and Nod2 direct autophagy by recruiting ATG16L1 to the plasma membrane at the site of bacterial entry. *Nat Immunol* 2010; **11**: 55-62 [PMID: 19898471 DOI: 10.1038/ni.1823]
 - 36 **Grubman A**, Kaparakis M, Viala J, Allison C, Badea L, Karrar A, Boneca IG, Le Bourhis L, Reeve S, Smith IA, Harland EL, Philpott DJ, Ferrero RL. The innate immune molecule, NOD1, regulates direct killing of *Helicobacter pylori* by antimicrobial peptides. *Cell Microbiol* 2010; **12**: 626-639 [PMID: 20039881 DOI: 10.1111/j.1462-5822.2009.01421.x]
 - 37 **Asano N**, Imatani A, Watanabe T, Fushiya J, Kondo Y, Jin X, Ara N, Uno K, Iijima K, Koike T, Strober W, Shimosegawa T. Cdx2 Expression and Intestinal Metaplasia Induced by *H. pylori* Infection of Gastric Cells Is Regulated by NOD1-Mediated Innate Immune Responses. *Cancer Res* 2016; **76**: 1135-1145 [PMID: 26759244 DOI: 10.1158/0008-5472.CAN-15-2272]
 - 38 **Hirata Y**, Ohmae T, Shibata W, Maeda S, Ogura K, Yoshida H, Kawabe T, Omata M. MyD88 and TNF receptor-associated factor 6 are critical signal transducers in *Helicobacter pylori*-infected human epithelial cells. *J Immunol* 2006; **176**: 3796-3803 [PMID: 16517750]
 - 39 **Allison CC**, Kufer TA, Kremmer E, Kaparakis M, Ferrero RL. *Helicobacter pylori* induces MAPK phosphorylation and AP-1 activation via a NOD1-dependent mechanism. *J Immunol* 2009; **183**: 8099-8109 [PMID: 20007577 DOI: 10.4049/jimmunol.0900664]
 - 40 **Antonelli A**, Ferrari SM, Giuggioli D, Ferrannini E, Ferri C, Fallahi P. Chemokine (C-X-C motif) ligand (CXCL)10 in autoimmune diseases. *Autoimmun Rev* 2014; **13**: 272-280 [PMID: 24189283 DOI: 10.1016/j.autrev.2013.10.010]
 - 41 **Allison CC**, Ferrand J, McLeod L, Hassan M, Kaparakis-Liaskos M, Grubman A, Bhathal PS, Dev A, Sievert W, Jenkins BJ, Ferrero RL. Nucleotide oligomerization domain 1 enhances IFN- γ signaling in gastric epithelial cells during *Helicobacter pylori* infection and exacerbates disease severity. *J Immunol* 2013; **190**: 3706-3715 [PMID: 23460743 DOI: 10.4049/jimmunol.1200591]
 - 42 **Watanabe T**, Asano N, Kitani A, Fuss IJ, Chiba T, Strober W. Activation of type I IFN signaling by NOD1 mediates mucosal host defense against *Helicobacter pylori* infection. *Gut Microbes* 2011; **2**: 61-65 [PMID: 21637021 DOI: 10.4161/gmic.2.1.15162]
 - 43 **Kawai T**, Akira S. Signaling to NF-kappaB by Toll-like receptors. *Trends Mol Med* 2007; **13**: 460-469 [PMID: 18029230 DOI: 10.1016/j.molmed.2007.09.002]
 - 44 **Honda K**, Yanai H, Takaoka A, Taniguchi T. Regulation of the type I IFN induction: a current view. *Int Immunol* 2005; **17**: 1367-1378 [PMID: 16214811 DOI: 10.1093/intimm/dxh318]
 - 45 **Hisamatsu T**, Suzuki M, Podolsky DK. Interferon-gamma augments CARD4/NOD1 gene and protein expression through interferon regulatory factor-1 in intestinal epithelial cells. *J Biol Chem* 2003; **278**: 32962-32968 [PMID: 12813035 DOI: 10.1074/

- jbc.M304355200]
- 46 **Fritz JH**, Le Bourhis L, Sellge G, Magalhaes JG, Fsihi H, Kufer TA, Collins C, Viala J, Ferrero RL, Girardin SE, Philpott DJ. Nod1-mediated innate immune recognition of peptidoglycan contributes to the onset of adaptive immunity. *Immunity* 2007; **26**: 445-459 [PMID: 17433730 DOI: 10.1016/j.immuni.2007.03.009]
- 47 **Roudi R**, Syn NL, Roudbary M. Antimicrobial Peptides As Biologic and Immunotherapeutic Agents against Cancer: A Comprehensive Overview. *Front Immunol* 2017; **8**: 1320 [PMID: 29081781 DOI: 10.3389/fimmu.2017.01320]
- 48 **Boughan PK**, Argent RH, Body-Malapel M, Park JH, Ewings KE, Bowie AG, Ong SJ, Cook SJ, Sorensen OE, Manzo BA, Inohara N, Klein NJ, Nuñez G, Atherton JC, Bajaj-Elliott M. Nucleotide-binding oligomerization domain-1 and epidermal growth factor receptor: critical regulators of beta-defensins during *Helicobacter pylori* infection. *J Biol Chem* 2006; **281**: 11637-11648 [PMID: 16513653 DOI: 10.1074/jbc.M510275200]
- 49 **Castaño-Rodríguez N**, Kaakoush NO, Mitchell HM. Pattern-recognition receptors and gastric cancer. *Front Immunol* 2014; **5**: 336 [PMID: 25101079 DOI: 10.3389/fimmu.2014.00336]
- 50 **Rosenstiel P**, Hellmig S, Hampe J, Ott S, Till A, Fischbach W, Sahly H, Lucius R, Fölsch UR, Philpott D, Schreiber S. Influence of polymorphisms in the NOD1/CARD4 and NOD2/CARD15 genes on the clinical outcome of *Helicobacter pylori* infection. *Cell Microbiol* 2006; **8**: 1188-1198 [PMID: 16819970 DOI: 10.1111/j.1462-5822.2006.00701.x]
- 51 **Wang P**, Zhang L, Jiang JM, Ma D, Tao HX, Yuan SL, Wang YC, Wang LC, Liang H, Zhang ZS, Liu CJ. Association of NOD1 and NOD2 genes polymorphisms with *Helicobacter pylori* related gastric cancer in a Chinese population. *World J Gastroenterol* 2012; **18**: 2112-2120 [PMID: 22563200 DOI: 10.3748/wjg.v18.i17.2112]
- 52 **Li ZX**, Wang YM, Tang FB, Zhang L, Zhang Y, Ma JL, Zhou T, You WC, Pan KF. NOD1 and NOD2 Genetic Variants in Association with Risk of Gastric Cancer and Its Precursors in a Chinese Population. *PLoS One* 2015; **10**: e0124949 [PMID: 25933107 DOI: 10.1371/journal.pone.0124949]
- 53 **Hofner P**, Gyulai Z, Kiss ZF, Tiszai A, Tiszlavicz L, Tóth G, Szöke D, Molnár B, Lonovics J, Tulassay Z, Mándi Y. Genetic polymorphisms of NOD1 and IL-8, but not polymorphisms of TLR4 genes, are associated with *Helicobacter pylori*-induced duodenal ulcer and gastritis. *Helicobacter* 2007; **12**: 124-131 [PMID: 17309748 DOI: 10.1111/j.1523-5378.2007.00481.x]
- 54 **Suarez G**, Romero-Gallo J, Piazuolo MB, Wang G, Maier RJ, Forsberg LS, Azadi P, Gomez MA, Correa P, Peek RM Jr. Modification of *Helicobacter pylori* Peptidoglycan Enhances NOD1 Activation and Promotes Cancer of the Stomach. *Cancer Res* 2015; **75**: 1749-1759 [PMID: 25732381 DOI: 10.1158/0008-5472.CAN-14-2291]
- 55 **Camilo V**, Barros R, Sousa S, Magalhães AM, Lopes T, Mário Santos A, Pereira T, Figueiredo C, David L, Almeida R. *Helicobacter pylori* and the BMP pathway regulate CDX2 and SOX2 expression in gastric cells. *Carcinogenesis* 2012; **33**: 1985-1992 [PMID: 22791809 DOI: 10.1093/carcin/bgs233]
- 56 **Yabuki N**, Sasano H, Tobita M, Imatani A, Hoshi T, Kato K, Ohara S, Asaki S, Toyota T, Nagura H. Analysis of cell damage and proliferation in *Helicobacter pylori*-infected human gastric mucosa from patients with gastric adenocarcinoma. *Am J Pathol* 1997; **151**: 821-829 [PMID: 9284831]

P- Reviewer: Day AS, Ozen H, Slomiany BL **S- Editor:** Gong ZM
L- Editor: A **E- Editor:** Huang Y





Published by **Baishideng Publishing Group Inc**
7901 Stoneridge Drive, Suite 501, Pleasanton, CA 94588, USA
Telephone: +1-925-223-8242
Fax: +1-925-223-8243
E-mail: bpgoffice@wjgnet.com
Help Desk: <http://www.f6publishing.com/helpdesk>
<http://www.wjgnet.com>



ISSN 1007-9327



© 2018 Baishideng Publishing Group Inc. All rights reserved.



Anti-Tumour Treatment

Systemic therapy for intermediate and advanced hepatocellular carcinoma: Sorafenib and beyond

Jean-Luc Raoul^{a,*}, Masatoshi Kudo^b, Richard S. Finn^c, Julien Edeline^d, Maria Reig^e, Peter R. Galle^f^a Digestive Oncology, Institut de Cancérologie de l'Ouest, Boulevard Professeur Jacques Monod, 44805 Nantes-Saint Herblain, France^b Department of Gastroenterology and Hepatology, Kindai University Faculty of Medicine, 377-2 Ohno-Higashi, 589-8511 Osaka, Japan^c Division of Hematology/Oncology, David Geffen School of Medicine at UCLA, Le Conte Ave, 90095 Los Angeles, CA, USA^d Medical Oncology, Centre Eugène Marquis, Avenue de la Bataille Flandres-Dunkerque, 35000 Rennes, France^e BCLC Group, Liver Unit, Hospital Clinic, University of Barcelona, IDIBAPS, CIBEREHD, Villarroel 170, 08036 Barcelona, Spain^f I. Medical Department, Mainz University Medical Center, Langenbeckstraße 1, 55131 Mainz, Germany

ARTICLE INFO

Keywords:

Advanced HCC
Systemic therapy
Sorafenib
Regorafenib

ABSTRACT

The hepatocellular carcinoma (HCC) treatment landscape changed a decade ago, with sorafenib demonstrating survival benefit in the first-line setting and becoming the first systemic therapy to be approved for HCC. More recently, regorafenib and nivolumab have received approval in the second-line setting after sorafenib, with further positive phase 3 studies emerging in the first line (lenvatinib non-inferior to sorafenib) and second line versus placebo (cabozantinib and ramucirumab). A key recommendation in the management of patients receiving sorafenib is to promote close communication between the patient and the physician so that adverse events (AEs) are detected early and severe AEs can be prevented. Sorafenib-related AEs have been identified as clinical biomarkers for sorafenib efficacy. Healthcare professionals have become more efficient in managing AEs, identifying patients who are likely to benefit from treatment, and assessing response to treatment, resulting in a trend towards increased overall survival in the sorafenib arms of clinical studies. The rapidly changing treatment landscape due to the emergence of new treatment options (sorafenib and lenvatinib equally effective in first line; regorafenib, cabozantinib, and ramucirumab showing OS benefit in second line with nivolumab approved by the FDA based on response rate) underscores the importance of re-assessing the role of the first approved systemic agent in HCC, sorafenib.

Introduction

Hepatocellular carcinoma (HCC) is the most common primary malignancy of the liver and the second leading cause of cancer-related mortality worldwide [1,2]. Cirrhosis due to chronic hepatitis B, alcoholism, or hepatitis C infection is the main risk factor for HCC, followed by nonalcoholic steatohepatitis [2]. The incidence of HCC is highest in regions where hepatitis B virus (HBV) is endemic, including Southeast Asia and sub-Saharan Africa, whereas in Japan, the United States, and parts of Europe, hepatitis C virus (HCV) is the predominant risk factor for HCC [2–4].

Several treatment options are currently available to patients with HCC. Treatment allocation depends on various factors known to impact prognosis, including tumor burden, liver function, and the performance status of the patient [5,6]. The most widely used HCC staging system,

the Barcelona Clinic Liver Cancer (BCLC) model, takes these variables into account and is currently the only staging system that uses evidence-based medicine to link prognosis with treatment options [7–9]. The BCLC system differentiates patients with very early-/early-stage disease (BCLC stage 0 or A) who are candidates for potentially curative treatment options (resection, transplantation, ablation), and three subgroups of patients with unresectable HCC: intermediate- (BCLC stage B), advanced- (BCLC stage C), and end-stage disease (BCLC stage D). For intermediate- and advanced-stage disease, standard of care includes transarterial chemoembolization (TACE) or systemic therapy while patients with end-stage disease generally receive palliative care only [5,6,10,11].

Sorafenib was the first systemic therapy to be approved for the treatment of HCC after having demonstrated a survival benefit in patients with advanced HCC in the first-line setting [12,13]. Since the

* Corresponding author at: Digestive Oncology, Institut de Cancérologie de l'Ouest, Nantes, France.

E-mail addresses: jean-luc.raoul@ico.unicancer.fr (J.-L. Raoul), m-kudo@med.kindai.ac.jp (M. Kudo), RFinn@mednet.ucla.edu (R.S. Finn), j.edeline@rennes.unicancer.fr (J. Edeline), MRREIG1@clinic.cat (M. Reig), Peter.Galle@unimedizin-mainz.de (P.R. Galle).<https://doi.org/10.1016/j.ctrv.2018.05.006>

Received 23 January 2018; Received in revised form 11 May 2018; Accepted 12 May 2018

0305-7372/ © 2018 The Authors. Published by Elsevier Ltd. This is an open access article under the CC BY-NC-ND license (<http://creativecommons.org/licenses/by-nc-nd/4.0/>).

results with sorafenib were published, multiple phase 3 trials have failed to demonstrate improved outcomes over sorafenib in this setting [14–18]. Only recently, a phase 3 trial of lenvatinib showed non-inferiority to sorafenib [19]. Similarly, a number of trials have failed in the second-line setting [20–23], with two agents recently approved in patients who have received prior sorafenib: regorafenib, which has demonstrated a survival benefit after progression on sorafenib in sorafenib-tolerant patients [24–26]; and nivolumab, which received an accelerated FDA approval based on tumor response rate and durability of response in an uncontrolled, single-arm study [27]. More recently, results from two phase 3 trials reported improved survival with cabozantinib versus placebo and ramucirumab versus placebo in the second line following sorafenib [28,29]. With the advent of new agents, it appears timely to reflect on the role of sorafenib as the gold standard in the first-line setting, its efficacy, and on the progress achieved in managing its side effects as new drugs are emerging in the first line (none of which have demonstrated superiority to sorafenib), and in second line after sorafenib failure. This review will provide an overview of established and novel systemic therapies in development for unresectable HCC and will discuss ways to improve their use to benefit patients.

Sorafenib history: Efficacy and safety

Sorafenib is an oral multikinase inhibitor that inhibits a number of receptor tyrosine kinases (VEGFR1-3, PDGFR, KIT, and RET) and downstream Raf signaling molecules (Raf-1 and B-Raf), affecting multiple tumor-signaling pathways including those involved in angiogenesis, tumor proliferation, and apoptosis [30–34].

Clinical trials

Four phase 1 trials evaluated a range of oral doses of sorafenib in patients with advanced recurrent or refractory solid tumors [35–38]. The optimal regimen was continuous oral administration of 400 mg sorafenib twice daily (bid) [35]. The most common drug-related toxicities were gastrointestinal or dermatologic [39].

A subsequent single-arm, phase 2 trial was carried out in patients with unresectable HCC (N = 137) who had not received prior systemic treatment and had a Child–Pugh score of A (72%) or B (28%) [40]. Treatment with continuous oral sorafenib 400 mg bid was associated with manageable toxicity – grade 3/4 drug-related toxicities included fatigue (9.5%), diarrhea (8.0%), and hand–foot skin reaction (HFSR; 5.1%). Tumor response rate was low, with 2.2% of patients showing a partial response (PR) based on independent assessment. Investigator-assessed median time to progression (TTP) was 4.2 months and median overall survival (OS) was 9.2 months. Independent review reported an interesting median TTP of 5.5 months, which provided the rationale for the continued development of sorafenib as an HCC treatment.

Subsequently, two phase 3 clinical trials were initiated, the results of which led to the approval of sorafenib for the treatment of HCC [41,42] – the Sorafenib HCC Assessment Randomized Protocol (SHARP) trial (N = 602; randomization ratio 1:1 sorafenib 400 mg bid vs placebo) and the sorafenib Asia-Pacific (AP) trial (N = 226; randomization ratio 2:1 sorafenib 400 mg bid vs placebo) [12,13]. These trials, although from geographically different areas, had the same inclusion and exclusion criteria; patients had advanced HCC with a measurable lesion, received no prior systemic therapy, had Child–Pugh class A liver disease, an Eastern Cooperative Oncology Group (ECOG) performance status of 0–2, and adequate hematological, renal, and hepatic function. Sorafenib demonstrated a significant survival benefit of a similar magnitude in both SHARP and AP (Table 1): in SHARP, median OS was 10.7 months with sorafenib versus 7.9 months with placebo (hazard ratio [HR] 0.69, 95% confidence interval [CI] 0.55–0.87, $P < 0.001$); in AP, median OS was 6.5 months with sorafenib and 4.2 months with placebo (HR 0.68, 95% CI 0.50–0.93, $P < 0.014$). Median time to

radiologic progression was significantly longer and the disease control rate (DCR) was significantly higher with sorafenib than with placebo in both studies (Table 1) but no difference in median time to symptomatic progression was observed between study arms. The lower absolute survival observed in the AP study compared with the SHARP study, while maintaining similar relative benefit in both studies (HR 0.69 in SHARP vs 0.68 in AP), may reflect the different patient populations, including more advanced disease in the AP study, and therapeutic options before inclusion in the two studies. The tumor response rates in both studies were low, with no complete responses and low PR rates (Table 1).

Overall, the adverse event (AE) profile of sorafenib was generally comparable in the SHARP and AP phase 3 trials, with the most common grade 3/4 drug-related AEs being HFSR, diarrhea, and fatigue [12,13]. Drug-related AEs of any grade occurring at a higher frequency ($P < 0.001$) in patients treated with sorafenib compared with placebo included diarrhea (39% vs 11%), weight loss (9% vs 1%), HFSR (21% vs 3%), anorexia (14% vs 3%), alopecia (14% vs 2%), and voice changes (6% vs 1%). Grade 3 drug-related AEs that were more common with sorafenib compared with placebo included diarrhea and HFSR ($P < 0.001$). Drug-related AEs resulted in permanent discontinuation of sorafenib in 11% of patients, dose interruptions in 44%, and dose reductions in 26%. The most frequent AEs leading to sorafenib dose reductions were diarrhea (8%), HFSR (5%), and rash or desquamation (3%). A generally similar safety profile has been observed in the sorafenib arms of other phase 3 trials in HCC [14–16].

Real-world evidence: GIDEON

Real-world studies have been instrumental in providing additional information on sorafenib efficacy and safety in a broader population of patients [43–46]. The GIDEON study, a large, prospective, open-label, non-interventional study, evaluated sorafenib safety and HCC treatment practices in 3202 patients in real-world practice across 39 countries, and expanded the patient pool to Child–Pugh B patients (n = 666) [44]. The median OS in patients with Child–Pugh A liver disease was 13.6 months (95% CI 12.8–14.7) compared with 5.2 months (95% CI 4.6–6.3) for Child–Pugh B patients (Table 1). The tolerability profile of sorafenib was comparable between Child–Pugh A and B patients and was consistent with the results of the two pivotal phase 3 trials [12,13,44]. Overall, the incidence of AEs was similar between Child–Pugh A and B patients, except for HFSR which was observed more frequently in Child–Pugh A patients. GIDEON also highlighted regional variation in HCC management, including differences in the prior use of TACE and patient outcomes [47,48]. Other studies have expanded these findings to patients who had become refractory or unresponsive to TACE, showing that survival seemed to be improved in these patients who switched early to sorafenib therapy versus those who continued on TACE [49–51].

Guidelines

Currently, AASLD, EASL, and ESMO-ESDO treatment guidelines, which all use the BCLC staging system, place sorafenib as the standard first-line systemic therapy for patients with advanced HCC (BCLC stage C) [5,6,10,11]. The European guidelines also recommend sorafenib for patients with intermediate-stage HCC (BCLC stage B) who do not respond to TACE (at least two cycles of therapy) [52] or progress following TACE [11]. The Japanese guidelines base their treatment recommendations on different factors (extrahepatic spread [EHS], liver function, macroscopic vascular invasion (MVI), tumor number, and tumor size) and recommend sorafenib as the first choice for patients with EHS and/or MVI and for TACE-refractory patients with Child–Pugh A liver function [53].

Table 1
Summary of key efficacy results of the SHARP and AP phase 3 trials and the GIDEON real-world cohort study.

Study	SHARP [12]		AP [13]		GIDEON [44]
	Sorafenib n = 299	Placebo n = 303	Sorafenib n = 150	Placebo n = 76	Sorafenib n = 2708
<i>Baseline patient characteristics, %</i>					
BCLC stage C	82	83	95	96	69
Child–Pugh A	95	98	97	97	73
Child–Pugh B	5	2	3	3	25
Child–Pugh C	0	0	0	0	3
<i>Efficacy results</i>					
Median OS, months (95% CI)	10.7 (9.4–13.3)	7.9 (6.8–9.1)	6.5 (5.6–7.6)	4.2 (3.8–5.6)	Child–Pugh A: 13.6 (12.8–14.7) Child–Pugh B: 5.2 (4.6–6.3) Child–Pugh C: 2.6 (1.5–4.0)
HR (95% CI), P-value	0.69 (0.55–0.87), < 0.001		0.68 (0.50–0.93), 0.014		
Median TTSP, months (95% CI)	4.1 (3.5–4.8)	4.9 (4.2–6.3)	3.5 (2.8–4.2)	3.4 (2.4–4.1)	
HR (95% CI), P-value	1.08 (0.88–1.31), 0.77		0.9 (0.67–1.22), 0.5		
Median TTP, months (95% CI)	5.5 (4.1–6.9)	2.8 (2.7–3.9)	2.8 (2.6–3.6)	1.4 (1.4–1.6)	
HR (95% CI), P-value	0.58 (0.45–0.74), < 0.001		0.57 (0.42–0.79), = 0.0005		
<i>Tumor response rate, %</i>					
Criteria used	RECIST v1.0		RECIST v1.0		
Complete response	0	0	0	0	
Partial response	2	1	3.3	1.3	
P-value	0.05		NR		
Stable disease	71	67	54.0	27.6	
P-value	0.17		NR		
DCR	43	32	35.3	15.8	
P-value	0.002		0.0019		

AP, Asia-Pacific; BCLC, Barcelona Clinic Liver Cancer; CI, confidence interval; DCR, disease control rate; HR, hazard ratio; OS, overall survival; NR, not reported; RECIST, Response Evaluation Criteria in Solid Tumors; SHARP, Sorafenib HCC Assessment Randomized Protocol; TTSP, time to symptomatic progression; TTP, time to progression.

Sorafenib dosing and patient management

Dose

The recommended sorafenib regimen is 400 mg bid administered orally, regardless of the patient’s characteristics [41,42]. In general, no dose adjustments are required for patients with renal or Child–Pugh B hepatic impairment, or for elderly patients. Dose adjustments to 400 mg once daily can be made to manage possible adverse drug reactions.

Sorafenib, which is primarily metabolized in the liver by cytochrome p450 (CYP3A4)-mediated oxidative metabolism and UGT1A9-mediated glucuronidation, is an inhibitor of CYP2B6, CYP2C8, CYP2C9, UGT1A1, and UGT1A9 [41,42]. Concomitant use of sorafenib with rifampicin and other strong inducers of CYP3A4 (e.g. carbamazepine, dexamethasone, phenobarbital, and plant extracts such as hypericum) should be avoided as these may lower sorafenib exposure. Regular monitoring of patients taking warfarin during sorafenib therapy is recommended and caution is also advised when treating patients with sorafenib in combination with docetaxel or drugs that are substrates of UGT1A1, such as irinotecan.

Side effect management

The management of dermatologic events represents one of the main challenges in the care of patients treated with sorafenib for HCC [54,55]; however, extensive clinical experience with sorafenib has led to the development of several effective strategies for managing dermatologic toxicities. These include the use of topical agents for the relief of symptoms, and sorafenib dose reduction or treatment interruption with the possibility to resume treatment [41,42]. It is important to emphasize that careful clinical monitoring is required during the first 2 months of treatment when HFSR is most likely to appear [55,56]. While most strategies deal with dermatologic toxicities once they arise, the use of urea-based creams has been shown to confer a prophylactic benefit against HFSR in patients receiving sorafenib [57]. Specifically, urea-based (10%) creams reduced HFSR rates, extended the time to first

occurrence of HFSR, and improved patient quality of life compared with best supportive care.

Although current efforts focus on preventing and managing the AEs of anti-tumor agents to increase patient compliance and maximize their clinical benefit, the occurrence of certain sorafenib-related AEs, such as diarrhea, hypertension, and skin toxicities, have been positively correlated with survival and could therefore possibly act as clinical biomarkers for sorafenib efficacy in patients with HCC [58]. Evidence from retrospective and prospective studies shows that developing dermatologic AEs during the first 60 days of treatment (DAE60) is related to better TTP and OS [59,60]. In addition, in a multicenter Spanish study, 11/12 patients who achieved a complete radiologic response with sorafenib treatment had developed DAE60 [61]. The BCLC group suggests that patients who develop DAE60 (HFSR, erythema, edema, rash, folliculitis, or pruritus) should not be considered as ‘intolerant’ to sorafenib, but should stay on treatment and have their sorafenib dose modified if necessary until a tolerated dose is achieved [59,61]. According to BCLC recommendations, dose modifications due to AEs or cirrhosis complications should be based on AE severity: symptomatic treatment without sorafenib dose modification for mild AEs (grade 1), dose reduction for moderate AEs (grade 2), and dose interruption for severe AEs (grade 3/4) [62]. For certain AEs, such as an ischemic event, the dose may need to be modified in all cases [41]. If the AEs return to baseline status, the relationship with sorafenib is confirmed and the tolerated dose for that patient needs to be defined. If the AEs do not return to baseline status, tumor progression, cirrhosis complications, or other causes need to be ruled out [41,62].

Patient selection: Identifying patients who benefit from sorafenib treatment

In order to identify factors that may affect individual responses to sorafenib treatment, a pre-planned subgroup analysis was carried out in the SHARP and AP trials [12,13]. These studies showed similar results across subgroups, with sorafenib providing treatment benefit (OS) in subgroups based on ECOG performance status, tumor burden (EHS,

MVI, MVI and/or EHS), age, and HBV infection. Only in patients with EHS in the SHARP trial was the benefit less prominent. These results were confirmed and expanded in subsequent exploratory subgroup analyses in both studies, which demonstrated that sorafenib efficacy is unaffected by baseline performance status, viral status (HCV, HBV), tumor burden, tumor stage, prior therapy, and hepatic markers [63–65]. A pooled, exploratory analysis of the two studies showed that, although sorafenib benefit was observed in all subgroups, HCV-positive patients (HR 0.47; 95% CI 0.32–0.69), those without EHS (HR 0.55; 95% CI 0.42–0.72), and those with a lower neutrophil:lymphocyte ratio (HR 0.59; 95% CI 0.46–0.77) derived the greatest benefit [66]. This effect, which was particularly clear in HCV-infected patients, has also been observed in head-to-head comparisons of first-line sorafenib versus other drugs [14,15] and could be related to the mechanism of action of sorafenib [67–69]. Unfortunately, at present, none of the biomarkers tested have predicted response to sorafenib [70].

Treatment after progression on sorafenib

Until the approval of regorafenib in 2017, there were no systemic treatment options after progression on sorafenib. Prior to that, several potential second-line treatments were assessed in phase 3 studies but failed [20–22]. Regorafenib was the first agent to show a survival benefit over placebo in patients progressing on sorafenib [24]. Regorafenib, an oral multikinase inhibitor, potently blocks the activity of multiple protein kinases involved in tumor angiogenesis, proliferation, the tumor microenvironment, metastasis, and tumor immunity [71,72]. Regorafenib was initially explored in early-phase HCC studies in pre-treated patients with evidence of tumor control, which supported further development of regorafenib in this patient population [73,74]. RESORCE was a randomized, double-blind, parallel-group, phase 3 trial that enrolled patients with HCC and Child–Pugh A disease who tolerated (≥ 400 mg daily for at least 20 of the 28 days before discontinuation) but progressed on prior sorafenib [24]. Patients were required to have documented radiologic progression during sorafenib treatment. The patients had received prior sorafenib for a median of 7.8 months in both treatment arms. The median OS (primary endpoint) was 10.6 months with regorafenib versus 7.8 months with placebo (HR 0.63, 95% CI 0.50–0.79; $P < 0.0001$). The survival of the control arm in this study was consistent with other phase 3 studies in the second line [20–22]. Regorafenib also improved progression-free survival (PFS; HR 0.46, 95% CI 0.37–0.56; $P < 0.0001$), with a median PFS of 3.1 months versus 1.5 months for placebo, and TTP (HR 0.44, 95% CI 0.36–0.55; $P < 0.0001$) with a median of 3.2 months for regorafenib and 1.5 months for placebo, based on modified Response Evaluation Criteria in Solid Tumors (mRECIST). Patients treated with regorafenib had a significantly higher objective response rate (11% vs 4%; $P = 0.0037$) and DCR (65% vs 36%; $P < 0.0001$) than those receiving placebo. Treatment-emergent AEs (TEAEs) were reported in all patients treated with regorafenib and 93% of patients receiving placebo. The most common clinically relevant grade 3/4 TEAEs (regorafenib vs placebo) were hypertension (15% vs 5%), HFSR (13% vs 1%), fatigue (9% vs 5%), and diarrhea (3% vs 0%) [24]. An exploratory analysis of the RESORCE trial assessing the time from the start of prior sorafenib treatment to death during RESORCE (in patients who tolerated sorafenib and were ECOG performance status 0 or 1) reported a median of 26.0 months (95% CI 22.6–28.1) in the regorafenib group versus 19.2 months (95% CI 16.3–22.8) in the placebo group [75]. This analysis also showed that regorafenib conferred a survival benefit regardless of the last dose of prior sorafenib (HR 0.67 for 800 mg/day; 0.68 for < 800 mg/day).

More recently, the monoclonal antibody nivolumab, which targets the cell surface receptor programmed death-1 (PD-1), received an accelerated FDA approval based on tumor response and durability of response for the treatment of patients with HCC who had previously been treated with sorafenib in the phase 1/2 single-arm CheckMate 040

study [27,76]. The ORR was 15% in the dose-escalation phase ($n = 48$) and 20% in the dose-expansion phase ($n = 214$). Median duration of response was 17 months in the dose-escalation phase. The results from randomized phase 3 trials of immunotherapy (nivolumab and pembrolizumab) in first and second line are pending and will help us to further build on the current treatment strategy for HCC.

Further approvals are on the horizon, with positive results emerging from phase 3 trials evaluating cabozantinib and ramucirumab in the second-line setting. Cabozantinib is a small-molecule multikinase inhibitor which was superior to placebo in the randomized, phase 3 CELESTIAL trial [28]. The trial, which at the time of the analysis had evaluated 707 patients (Child–Pugh A, ECOG performance status 0–1) with advanced HCC who had previously received sorafenib, demonstrated that cabozantinib significantly improved OS over placebo (10.2 vs 8.0 months, respectively; HR 0.76, 95% CI 0.63–0.92; $P = 0.0049$) [28]. The safety profile was as expected, with HFSR, hypertension, increased aspartate aminotransferase, fatigue, and diarrhea the most common grade 3/4 AEs with higher incidence in the cabozantinib arm versus sorafenib. Positive results for the antiangiogenic agent ramucirumab versus placebo in the phase 3 REACH-2 trial were recently announced, with REACH-2 meeting its OS endpoint in patients with high AFP (≥ 400 ng/mL) and who were intolerant to or had progression on sorafenib [29].

With the approval of regorafenib and nivolumab, and the continued search for additional second-line treatment options, the optimal time to stop sorafenib treatment and initiate a new therapy needs to be determined. This decision is complicated by the lack of guidance in treatment guidelines on the frequency of tumor assessments during sorafenib treatment. The EASL-EORTC 2012 guidelines recommend the assessment of tumor progression every 6–8 weeks [52]. In the SHARP trial, tumor measurements were performed every 6 weeks during treatment [12].

Assessing clinical efficacy in HCC

For any cancer treatment, it is essential to use appropriate treatment response measures to ensure that treatment discontinuation decisions are based on an accurate assessment of clinical benefit. Tumor size is a key factor in the decision to stop or continue treatment. However, targeted therapies such as sorafenib and other angiogenesis inhibitors demonstrate improved survival without a significant response rate [12,13,24,77]. Thus, more appropriate measures for assessing the clinical efficacy of systemic therapies in advanced HCC are needed [78].

Tumor size is commonly measured using RECIST [79]. These criteria sum the longest diameters of the tumors, reflecting changes in the size of existing tumors and the appearance of new tumors (Table 2). The revised criteria, RECIST 1.1, were published in 2009 and aimed to improve and further standardize the assessment of tumor size [80]. The contribution of underlying liver cirrhosis and viral hepatitis to the development of some parameters assessed by RECIST 1.1 as tumor-related (ascites, pleural effusion, and lymph nodes < 15 mm still considered non-measurable lesions) make these criteria unreliable when assessing tumor burden in HCC [77]. Nevertheless, RECIST has been widely used to categorize tumor responses and enable the measurement of surrogate endpoints such as TTP in clinical studies of systemic treatments for HCC. However, it is now increasingly recognized in HCC and in other cancers that there is no strong correlation between TTP and survival. For example, a recent pooled analysis of data from the sorafenib phase 3 clinical studies indicated only a weak correlation between TTP and survival [81].

To overcome some of the limitations of the standard RECIST, and specifically to consider the value of tumor necrosis as a marker of response to locoregional ablative or antiangiogenic treatments, mRECIST was developed specifically for the assessment of HCC [82]. These new criteria include the use of contrast-enhanced imaging techniques and

Table 2
Comparison of RECIST (1.0 vs 1.1) and mRECIST.

	RECIST v 1.0 [79]	RECIST v 1.1 [80]	mRECIST for HCC [82]
CR	Disappearance of all target lesions	Disappearance of all target lesions. <u>Any pathological lymph nodes (whether target or non-target) must have a reduction in the short axis to < 10 mm</u>	Disappearance of <u>any intratumoral arterial enhancement</u> in all target lesions
PR	At least a 30% decrease in the sum of the diameters of target lesions, taking as reference the baseline sum diameters	At least a 30% decrease in the sum of the diameters of target lesions, taking as reference the baseline sum diameters	At least a 30% decrease in the sum of diameters of <u>viable (contrast enhancement in the arterial phase)</u> target lesions, taking as reference the baseline sum of the diameters of target lesions
SD	Neither sufficient shrinkage to qualify for PR nor sufficient increase to qualify for PD, taking as reference the smallest sum of the longest diameter recorded since the start of treatment	Neither sufficient shrinkage to qualify for PR nor sufficient increase to qualify for PD, taking as reference the smallest sum of the longest diameters while on study	Any cases that do not qualify as either PR or PD
PD	At least a 20% increase in the sum of the longest diameters of the target lesions, taking as reference the smallest sum of the longest diameter recorded since the treatment started, or the appearance of one or more new lesions	At least a 20% increase in the sum of the diameters of the target lesions, taking as reference the smallest sum on study (this includes the baseline sum if that is the smallest on study). <u>In addition to the relative increase of 20%, the sum must also demonstrate an absolute increase of at least 5 mm.</u> (Note: the appearance of one or more new lesions is also considered progression)	An increase of at least 20% in the sum of the diameters of <u>viable (enhancing)</u> target lesions, taking as reference the smallest sum of the diameters of <u>viable (enhancing)</u> target lesions recorded since the start of treatment

CR, complete response; HCC, hepatocellular carcinoma; mRECIST, modified Response Evaluation Criteria in Solid Tumors; PD, progressive disease; PR, partial response; RECIST, Response Evaluation Criteria in Solid Tumors; SD, stable disease.

consider as target only the enhancing component of the tumor (Table 2). Recently, assessments of response using mRECIST to predict survival with targeted therapies has been reported. Objective response as measured by mRECIST had an independent prognostic value for survival in an analysis of individual patient data from a negative phase 3 randomized trial, BRISK-PS [83], comparing brivanib, a tyrosine kinase inhibitor with antiangiogenic effects, with placebo after sorafenib progression or intolerance [20]. However, recent results of a pooled analysis of the SHARP and AP trials suggested that the response rate by RECIST with SHARP–BCLC amendments (which formed the basis for mRECIST [82]) was not a reliable surrogate endpoint for sorafenib OS in advanced HCC [84]. Another analysis based on data from two trials of nintedanib suggested that, while both mRECIST and RECIST were associated with improved survival, mRECIST might not be a better surrogate of survival than RECIST [85]. This is an important consideration for tyrosine kinase inhibitors with antiangiogenic function because contrast enhancement may be lost due to reduced perfusion rather than necrosis, which can be misleading [78].

While mRECIST provides a step forward in the identification of optimal surrogates for assessing responses to angiogenesis inhibitors in HCC, they do not clearly discriminate between different patterns of progression [86]. HCC progression can be classified into four patterns: intrahepatic growth, extrahepatic growth, new intrahepatic lesion, and new extrahepatic lesion and/or vascular invasion. Survival may depend on the type of progression experienced rather than simply on tumor burden.

A prospective study carried out by the BCLC group showed that the development of a new extrahepatic lesion and/or vascular invasion, regardless of the baseline BCLC stage at the time of starting sorafenib, was an independent predictor of reduced OS and reduced post-progression survival (PPS) during sorafenib treatment [86]. This data was confirmed by Iavarone et al. [87] and Ogasawara et al. [88]. Furthermore, an exploratory analysis of the regorafenib phase 3 trial, RESORCE, confirmed the finding that the pattern of progression influences PPS. Regorafenib provided an OS benefit regardless of the pattern of progression on prior sorafenib; however, in both regorafenib and placebo treatment groups, PPS was reduced for patients who developed new extrahepatic lesions [89]. This suggests that the progression pattern may be a key prognostic parameter and should be considered when designing and analyzing future trials.

Therapeutic agents in development

There is an active search for agents that provide an improved survival benefit over sorafenib in the first-line setting and for additional treatment options in the second-line setting. Several phase 3 trials evaluating multikinase inhibitors such as sunitinib, brivanib, and lenvatinib failed to demonstrate clinical superiority over sorafenib in the first line [14–17]. Candidate first-line therapies face a challenge due to the accumulating clinical experience with sorafenib which is constantly shifting the bar as healthcare professionals become more efficient at preventing and managing sorafenib AEs and identifying patients who are likely to respond to treatment. This is illustrated by the trend toward increased OS in the sorafenib arms of clinical studies (Table 3).

While most of the new agents currently being evaluated are systemic, two recent randomized, controlled phase 3 trials evaluated the efficacy and safety of sorafenib compared to selective internal radiation therapy (SIRT) with yttrium-90 (Y90) resin microspheres in patients with advanced HCC. Neither study demonstrated a statistically significant improvement in OS compared with sorafenib: in the SARAH trial, treatment with SIRT resulted in a median OS of 8.0 months compared with 9.9 months with sorafenib ($P = 0.18$; intent-to-treat (ITT) analysis) [90]; in the SIRveNIB trial, treatment with SIRT resulted in a median OS of 8.8 months compared with 10.0 months with sorafenib ($P = 0.36$; ITT analysis) [91]. Recently, the phase 3 SORAMIC study failed to meet its primary endpoint of improved OS with the addition of Y-90 to sorafenib [92].

Some of the systemic agents which have shown promise and are being evaluated in phase 3 clinical trials are summarized below and in Table 4. Lenvatinib is an oral multikinase inhibitor approved for the treatment of differentiated thyroid cancer [93,94] and renal cell cancer [94]. In a phase 2 trial in patients with HCC carried out in Japan and South Korea, lenvatinib treatment was associated with a 37% objective response rate (by mRECIST), a median TTP of 7.4 months, and an acceptable toxicity profile [95]. This led to further evaluation in the open-label phase 3 REFLECT trial. In this non-inferiority trial, 954 patients (67% from Asia-Pacific) were randomized 1:1 to receive sorafenib or lenvatinib [19]. Inclusion criteria were more restrictive than in the SHARP trial; patients with ECOG performance status 0–1 and less advanced HCC (no invasion of the main portal vein and hepatic involvement less than 50%) were included. Lenvatinib demonstrated non-inferiority to sorafenib with a median OS of 13.6 months versus 12.3 months, respectively (HR 0.92, 95% CI 0.79–1.06), with OS results consistent across subgroups. For HBV-infected patients, and those with

Table 3
Median overall survival with sorafenib in advanced hepatocellular carcinoma.

Enrollment period	Study	Patient population	Median sorafenib, months		Reference
			OS	TTP ^a	
2005–2006	SHARP: sorafenib (n = 299) vs placebo (n = 303); NCT00105443	Western patients	10.7	5.5	[12]
2005–2007	AP: sorafenib (n = 150) vs placebo (n = 76); NCT00492752	Asian patients	6.5	2.8	[13]
2008–2010	Sunitinib (n = 530) vs sorafenib (n = 544); NCT00699374	All patients	10.2	3.8	[14]
2009–2011	Brivanib (n = 577) vs sorafenib (n = 578); NCT00858871	Non-Asian patients (24%)	15.1	6.0	[15]
		Asian patients (76%)	8.8	2.8	
		All patients	9.9	4.1 ^c	
2010–2012	Linifanib (n = 514) vs sorafenib (n = 521); NCT01009593	Non-Asian patients (36%)	11.8	4.0 ^b	[16]
		Asian patients (64%)	8.9		
		All patients	9.8		
		Non-Asian patients (33%)	12.4		
2013–2017	Lenvatinib (n = 478) vs sorafenib (n = 476); NCT01761266	Japanese patients (8%)	9.5	3.7 ^c	[19]
		Rest of Asia patients (59%)	8.5		
		All patients	12.3		
		Asia-Pacific (67%)	11.0		
		Western	14.2	5.6	

AP, Asia-Pacific; OS, overall survival; TTP, time to progression.

^a RECIST v1.0 unless otherwise specified.

^b RECIST v1.1.

^c mRECIST.

certain tumor characteristics (extrahepatic spread, portal vein invasion or both, and AFP blood level ≥ 200 ng/mL) there was also a trend in favor of lenvatinib. Safety was not an endpoint of the REFLECT trial but the lenvatinib safety profile was consistent with that observed in previous trials with lenvatinib with hypertension (42%) and diarrhea (39%) the most frequent lenvatinib-related TEAEs while HFSR was the most frequent for sorafenib (52%).

The receptor tyrosine kinase c-MET has emerged as a possible therapeutic target in HCC and other cancers, with aberrant expression of the receptor promoting cellular proliferation and metastasis observed in numerous cancers [96]. However, tivantinib, a selective oral c-MET inhibitor, failed to meet its primary endpoint of improved OS over placebo in its pivotal phase 3 METIV-HCC trial, in which patients with advanced HCC with high MET expression were evaluated in the second-line setting [97,98]. While reasons for its failure are unclear, it has been speculated that the efficacy of tivantinib may be c-MET independent and therefore the patient selection based on c-MET expression was inappropriate [98]. Cabozantinib is a multikinase inhibitor which targets c-MET but also VEGFRs, AXL, RET, KIT, and FLT3 [99]. In a phase 2 trial, cabozantinib demonstrated signs of clinical activity in patients with HCC in both treatment-naïve and sorafenib-treated patients [100]. The most common grade 3/4 AEs (regardless of causality) were diarrhea, HFSR, and thrombocytopenia, which were effectively managed with dose reductions. As described previously, the cabozantinib data in the phase 3 CELESTIAL trial were positive, with the trial meeting its primary endpoint of superiority in OS for cabozantinib over placebo [28]. However, unlike the phase 3 tivantinib study which selected patients based on elevated c-MET expression, patient selection in the phase 3 cabozantinib study was not based on a specific biomarker.

Ramucirumab is an IgG1 monoclonal antibody to VEGFR2 which has demonstrated improved OS alone and in combination with paclitaxel in patients receiving second-line treatment for metastatic gastric cancer [101,102]. In a phase 3 study (REACH), ramucirumab failed to improve OS compared with placebo in patients with HCC after sorafenib failure (due to progression or intolerance); however, PFS was increased compared with placebo [22]. A prespecified subgroup analysis of this study showed that 250 patients with AFP ≥ 400 ng/mL experienced a clinically meaningful improvement in OS compared with placebo (HR 0.67, 95% CI 0.51–0.90; $P = 0.0059$) [103]. Following on from these results, ramucirumab was investigated in another randomized, double-blind, placebo-controlled phase 3 study REACH-2, which

enrolled patients with elevated AFP levels at baseline (≥ 400 ng/mL). A recent press release announced the trial met its primary OS endpoint, however detailed results are still to be presented [29].

As mentioned previously, the PD-1 blocking antibody nivolumab was recently approved by the FDA in the second-line setting based on results of the single-arm phase 1/2 CheckMate 040 study [27,76]. Nivolumab is being evaluated in the CheckMate 459 phase 3 trial (NCT02576509) which is evaluating nivolumab in comparison with sorafenib as a first-line treatment in patients with advanced HCC. Primary endpoints are OS; secondary endpoints are PFS, ORR, and evaluation of the relationship between PD-L1 expression and efficacy.

Pembrolizumab is another monoclonal antibody targeting the PD-1 interaction with PD-L1, first approved for metastatic melanoma [104]. Results from the single-arm phase 2 KEYNOTE 224 trial in 104 patients with advanced HCC previously treated with sorafenib were recently reported, in which treatment with pembrolizumab resulted in 1 complete response (1%) and 16 partial response (15%) [105]. The placebo-controlled phase 3 (KEYNOTE 240) trial is in progress to assess pembrolizumab safety and efficacy in patients previously treated with sorafenib which is due to complete in February 2019 (NCT02702401).

Future scenario in HCC treatment

With the increasing availability of drugs for first- and second-line treatment for HCC, a prominent question among physicians will be regarding treatment strategy. To date, we do not have results from randomized phase 3 trials evaluating immunotherapy in either first or second line. At present, there are two drugs that are recognized for the treatment of HCC in the first-line setting: sorafenib and lenvatinib which have different safety profiles. Lenvatinib is associated with a higher incidence of hypertension, anorexia, and fatigue while sorafenib is associated with HFSR. Several agents have been evaluated in the second-line setting following sorafenib; regorafenib was only assessed in patients who tolerated prior sorafenib therapy, while the nivolumab population was not limited to those who tolerated prior sorafenib in an uncontrolled phase 1/2 trial. Since then, cabozantinib has also been evaluated in patients with prior sorafenib exposure, and the ramucirumab REACH-2 study was restricted to patients treated in second-line after sorafenib but with elevated AFP. How to integrate new drugs and data into the evolving sequence paradigm needs to be determined. One approach, would be to propose regorafenib as second-line treatment in patients who tolerated sorafenib, whereas for patients

Table 4
Overview of systemic agents in phase 3 development for the treatment of HCC.

Agent	MOA	Phase 2 results	Phase 3 trials Efficacy outcomes	Outcomes
Lenvatinib (first line)	Multiple TKI that targets VEGFR1–3, FGFR1–4, PDGFR α , RET, and KIT [93,94] PD-1 inhibitor [76]	12 mg qd: mTTP 7.4 months; mOS 18.7 months; ORR 37%, DCR 78%; DR 74%; DC 22% [95] ^a CheckMate 040: 3 mg/kg q2w: ORR 15%, DCR 58%; mOS 15 months [76]	REFLECT: non-inferiority of lenvatinib 8 mg/12 mg qd versus sorafenib 400 mg bid (NCT01761266) CheckMate 459: comparison with sorafenib (NCT02576509)	Non-inferior OS Improved PFS, TTP, and ORR [19] Ongoing
Nivolumab (second line)				
Ramucirumab (second line)	VEGFR2 inhibitor [103]	8 mg/kg IV q2w: mTTP 4.2 months; mOS 12.0 months; ORR 9.5%, DCR 69%; DR 7%; DC 1.4% [106]	KEYNOTE-240: pembrolizumab 200 mg IV q3w versus placebo (NCT02702401)	Significant improvement in OS, PFS, and ORR [28]
Pembrolizumab (second line)	PD-1 inhibitor [104]	KEYNOTE 224: Pembrolizumab 200 mg IV q3w: ORR 16%, DCR 61.5%, mPFS 4.8 months [105]	CELESTIAL: 60 mg qd versus placebo in patients who progressed on sorafenib (NCT01908426)	
Cabozantinib (second line)	Multiple TKI that targets TIE-1, TIE-2, FLT3, c-MET, KIT, RET, and VEGFR [99]	100 mg qd: DCR 66%, mPFS 5.2 months; mOS 11.5 months [100]		

AFP, alpha-fetoprotein; bid, twice daily; DC, discontinuation due to adverse event; DCR, disease control rate; DR, dose reduction; HCC, hepatocellular carcinoma; IV, intravenous; MOA, mechanism of action; mRECIST, modified Response Evaluation Criteria in Solid Tumors; (m)OS, (median) overall survival; ORR, objective response rate; (m)PFS, (median) progression-free survival; q2w, every 2 weeks; q3w, every 3 weeks; qd, once daily; TKI, tyrosine kinase inhibitor; (m)TTP, (median) time to progression.
^a mRECIST.

discontinuing sorafenib because of toxicity, cabozantinib and perhaps nivolumab may be more appropriate second-line treatment options, while ramucirumab should be restricted to patients with high AFP levels. However, this treatment strategy may be significantly modified following data from upcoming trials with immunotherapy drugs. Furthermore, the cost of newer drugs will be an important factor in treatment decisions, whereby the cost may fall significantly in the future when generic options become available. Still, patients likely will benefit from treatment at centers that have multi-disciplinary teams to assess and manage patients with HCC.

Conclusions

The HCC treatment landscape changed a decade ago following the approval of sorafenib, the first systemic therapy demonstrating a survival benefit. More recently, lenvatinib, regorafenib, cabozantinib, nivolumab, and ramucirumab have provided additional options in the first- and second-line setting, with regorafenib demonstrating a survival benefit in patients who tolerated, but progressed on, sorafenib. It is imperative that patients eligible for sorafenib treatment receive it in a timely manner (for example early after progression on TACE) and that toxicities are managed prospectively and effectively to ensure that patients could benefit from all currently available therapies. The emergence of novel treatment options is likely to transform the treatment landscape in the near future, placing further emphasis on the value of systemic therapies in HCC treatment and ultimately improving the care of out-patients.

Financial disclaimers

Bayer funded editorial assistance for the development of the review and was allowed to review the manuscript for factual correctness, but did not influence the content or decision to publish.

Author contributions

All authors contributed to the conception, writing, and critically reviewing the content of the article. All authors approved the final version for submission.

Conflicts of interest

Dr. Raoul reports personal fees* from AstraZeneca, Bayer, BMS, BTG, Terumo, Guerbet, and GenoScience, and grants from Celgene.

Dr. Kudo reports speaker fees from Bayer, Eisai, MSD, Ajinomoto, Kowa, and Taiho, grants from Chugai, Otsuka, Takeda, Taiho, Sumitomo Dainippon, and Daiichi Sankyo, advisory board attendance for MSD, Eisai, Bayer, AbbVie, Medico’s Hirata, Astellas Pharma, and BMS, and consultancy fees from Kowa, MSD, BMS, Bayer, Chugai, Taiho, and Eisai.

Dr. Finn reports consultancy fees from Bayer, Eisai, BMS, Novartis, Pfizer, MSD, and Roche.

Dr. Edeline reports personal fees* from Bayer, BMS, and BTG.

Dr. Reig reports personal fees* from Bayer, BMS, and BTG.

Dr. Galle reports personal fees* from Adaptimmune, AstraZeneca, Bayer, Blueprint, BMS, Eli Lilly, MSD, and Sirtex, and grants from Bayer.

*Personal fees as defined by ICMJE as “Monies paid to you for services rendered, generally honoraria, royalties, or fees for consulting, lectures, speakers bureaus, expert testimony, employment, or other affiliation (e.g. advisory boards) etc.”

Acknowledgments

Editorial assistance in the preparation of this article was provided by Esther Race and Katrin Gudmundsdottir of SuccinctChoice Medical Communications (London, UK), with financial support from Bayer.

References

- [1] Ferlay J, Soerjomataram I, Ervik M, Dikshit R, Eser S, Mathers C, et al. GLOBOCAN 2012 v1.0, Cancer Incidence and Mortality Worldwide. IARC Cancer Base No. 11. Lyon, France: International Agency for Research on Cancer (2013) < <http://globocan.iarc.fr/old/FactSheets/cancers/liver-new.asp> > [accessed 4 April 2018].
- [2] Ghouri YA, Mian I, Rowe JH. Review of hepatocellular carcinoma: epidemiology, etiology, and carcinogenesis. *J Carcinog* 2017;16:1.
- [3] Mittal S, El-Serag HB. Epidemiology of hepatocellular carcinoma: consider the population. *J Clin Gastroenterol* 2013;47(Suppl):S2–6.
- [4] Venook AP, Papandreou C, Furuse J, de Guevara LL. The incidence and epidemiology of hepatocellular carcinoma: a global and regional perspective. *Oncologist* 2010;15(Suppl 4):5–13.
- [5] Galle PR, Forner A, Llovet JM, Mazzaferro V, Piscaglia F, Raoul J-L, et al. EASL clinical practice guidelines: management of hepatocellular carcinoma. *J Hepatol*.
- [6] Bruix J, Sherman M. American association for the study of liver diseases. Management of hepatocellular carcinoma: an update. *Hepatology* 2011;53:1020–2.
- [7] Forner A, Reig ME, de Lope CR, Bruix J. Current strategy for staging and treatment: the BCLC update and future prospects. *Semin Liver Dis* 2010;30:61–74.
- [8] Bruix J, Reig M, Sherman M. Evidence-based diagnosis, staging, and treatment of patients with hepatocellular carcinoma. *Gastroenterology* 2016;150:835–53.
- [9] Forner A, Reig M, Bruix J. Hepatocellular carcinoma. *Lancet* 2018;391:1301–14.
- [10] Heimbach JK, Kulik LM, Finn R, Sirlin CB, Abecassis M, Roberts LR, et al. AASLD guidelines for the treatment of hepatocellular carcinoma. *Hepatology* 2017; doi: 10.1002/hep.29086 [Epub ahead of print].
- [11] Verslype C, Rosmorduc O, Rougier P, Group EGW. Hepatocellular carcinoma: ESMO-ESDO Clinical Practice Guidelines for diagnosis, treatment and follow-up. *Ann Oncol* 2012;23 Suppl 7:vii41–8.
- [12] Llovet JM, Ricci S, Mazzaferro V, Hilgard P, Gane E, Blanc JF, et al. Sorafenib in advanced hepatocellular carcinoma. *N Engl J Med* 2008;359:378–90.
- [13] Cheng A, Kang Y, Chen Z, Tsao C, Qin S, Kim J, et al. Efficacy and safety of sorafenib in patients in the Asia-Pacific region with advanced hepatocellular carcinoma: a phase III randomised, double-blind, placebo-controlled trial. *Lancet Oncol* 2009;10:25–34.
- [14] Cheng AL, Kang YK, Lin DY, Park JW, Kudo M, Qin S, et al. Sunitinib versus sorafenib in advanced hepatocellular cancer: results of a randomized phase III trial. *J Clin Oncol* 2013;31:4067–75.
- [15] Johnson PJ, Qin S, Park JW, Poon RT, Raoul JL, Philip PA, et al. Brivanib versus sorafenib as first-line therapy in patients with unresectable, advanced hepatocellular carcinoma: results from the randomized phase III BRISK-FL study. *J Clin Oncol* 2013;31:3517–24.
- [16] Cainap C, Qin S, Huang WT, Chung LJ, Pan H, Cheng Y, et al. Linifanib versus Sorafenib in patients with advanced hepatocellular carcinoma: results of a randomized phase III trial. *J Clin Oncol* 2015;33:172–9.
- [17] Zhu AX, Rosmorduc O, Evans TR, Ross PJ, Santoro A, Carrilho FJ, et al. SEARCH: a phase III, randomized, double-blind, placebo-controlled trial of sorafenib plus erlotinib in patients with advanced hepatocellular carcinoma. *J Clin Oncol* 2015;33:559–66.
- [18] Abou-Alfa GK, Niedzwieski D, Knox JJ, Kaubisch A, Posey J, Tan BR, et al. Phase III randomized study of sorafenib plus doxorubicin versus sorafenib in patients with advanced hepatocellular carcinoma (HCC): CALGB 80802. *J Clin Oncol* 2016;34:4003.
- [19] Kudo M, Finn RS, Qin S, Han KH, Ikeda K, Piscaglia F, et al. Lenvatinib versus sorafenib in first-line treatment of patients with unresectable hepatocellular carcinoma: a randomised phase 3 non-inferiority trial. *Lancet* 2018;391:1163–73.
- [20] Llovet JM, Decaens T, Raoul JL, Boucher E, Kudo M, Chang C, et al. Brivanib in patients with advanced hepatocellular carcinoma who were intolerant to sorafenib or for whom sorafenib failed: results from the randomized phase III BRISK-PS study. *J Clin Oncol* 2013;31:3509–16.
- [21] Zhu AX, Kudo M, Assenat E, Cattani S, Kang YK, Lim HY, et al. Effect of everolimus on survival in advanced hepatocellular carcinoma after failure of sorafenib: the EVOLVE-1 randomized clinical trial. *JAMA* 2014;312:57–67.
- [22] Zhu AX, Park JO, Ryou BY, Yen CJ, Poon R, Pastorelli D, et al. Ramucirumab versus placebo as second-line treatment in patients with advanced hepatocellular carcinoma following first-line therapy with sorafenib (REACH): a randomised, double-blind, multicentre, phase 3 trial. *Lancet Oncol* 2015;16:859–70.
- [23] Abou-Alfa GK, Qin S, Ryou B-Y, Lu S-N, Yen C-J, Feng Y-H, et al. Phase III randomized study of second-line ADI-peg 20 (A) plus best supportive care versus placebo (P) plus best supportive care in patients (pts) with advanced hepatocellular carcinoma (HCC). *J Clin Oncol* 2016;34:4017.
- [24] Bruix J, Qin S, Merle P, Granito A, Huang Y-H, Bodoky G, et al. Regorafenib for patients with hepatocellular carcinoma who progressed on sorafenib treatment (RESORCE): a randomised, double-blind, placebo-controlled, phase 3 trial. *Lancet* 2017;389:56–66.
- [25] Food and Drug Administration. Regorafenib (Stivarga) prescribing information [accessed 4 April 2018].
- [26] European Medicines Agency. Regorafenib (Stivarga). Summary of Product Characteristics [accessed 4 April 2018].
- [27] Food and Drug Administration. Nivolumab (Opdivo) prescribing information [accessed 4 April 2018].
- [28] Abou-Alfa GK, Meyer T, Cheng A-L, El-Khoueiry AB, Rimassa L, Ryou B-Y, et al. Cabozantinib (C) versus placebo (P) in patients (pts) with advanced hepatocellular carcinoma (HCC) who have received prior sorafenib: results from the randomized phase III CELESTIAL trial. *J Clin Oncol* 2018;36:207.
- [29] Lilly Press Release. Lilly announces CYRAMZA® (ramucirumab) phase 3 REACH-2 study in second-line hepatocellular carcinoma patients met overall survival endpoint < <https://investor.lilly.com/news-releases/news-release-details/lilly-announces-cyramzar-ramucirumab-phase-3-reach-2-study> > [accessed 4 April 2018].
- [30] Wilhelm SM, Carter C, Tang L, Wilkie D, McNabola A, Rong H, et al. BAY 43-9006 exhibits broad spectrum oral antitumor activity and targets the RAF/MEK/ERK pathway and receptor tyrosine kinases involved in tumor progression and angiogenesis. *Cancer Res* 2004;64:7099–109.
- [31] Wilhelm S, Carter C, Lynch M, Lowinger T, Dumas J, Smith RA, et al. Discovery and development of sorafenib: a multikinase inhibitor for treating cancer. *Nat Rev Drug Discov* 2006;5:835–44.
- [32] Carlomagno F, Anaganti S, Guida T, Salvatore G, Troncone G, Wilhelm SM, et al. BAY 43-9006 inhibition of oncogenic RET mutants. *J Natl Cancer Inst* 2006;98:326–34.
- [33] Chang YS, Adnane J, Trail PA, Levy J, Henderson A, Xue D, et al. Sorafenib (BAY 43-9006) inhibits tumor growth and vascularization and induces tumor apoptosis and hypoxia in RCC xenograft models. *Cancer Chemother Pharmacol* 2007;59:561–74.
- [34] Liu L, Cao Y, Chen C, Zhang X, McNabola A, Wilkie D, et al. Sorafenib blocks the RAF/MEK/ERK pathway, inhibits tumor angiogenesis, and induces tumor cell apoptosis in hepatocellular carcinoma model PLC/PRF/5. *Cancer Res* 2006;66:11851–8.
- [35] Strumberg D, Richly H, Hilger RA, Schleichner N, Korfee S, Tewes M, et al. Phase I clinical and pharmacokinetic study of the Novel Raf kinase and vascular endothelial growth factor receptor inhibitor BAY 43-9006 in patients with advanced refractory solid tumors. *J Clin Oncol* 2005;23:965–72.
- [36] Clark JW, Eder JP, Ryan D, Lathia C, Lenz HJ. Safety and pharmacokinetics of the dual action Raf kinase and vascular endothelial growth factor receptor inhibitor, BAY 43-9006, in patients with advanced, refractory solid tumors. *Clin Cancer Res* 2005;11:5472–80.
- [37] Awada A, Hendlitz A, Gil T, Bartholomeus S, Mano M, de Valeriola D, et al. Phase I safety and pharmacokinetics of BAY 43-9006 administered for 21 days on/7 days off in patients with advanced, refractory solid tumours. *Br J Cancer* 2005;92:1855–61.
- [38] Moore M, Hirte HW, Siu L, Oza A, Hottel SJ, Petrenciu O, et al. Phase I study to determine the safety and pharmacokinetics of the novel Raf kinase and VEGFR inhibitor BAY 43-9006, administered for 28 days on/7 days off in patients with advanced, refractory solid tumors. *Ann Oncol* 2005;16:1688–94.
- [39] Strumberg D, Awada A, Hirte H, Clark JW, Seeber S, Piccart P, et al. Pooled safety analysis of BAY 43-9006 (sorafenib) monotherapy in patients with advanced solid tumours: is rash associated with treatment outcome? *Eur J Cancer* 2006;42:548–56.
- [40] Abou-Alfa GKSL, Ricci S, Amadori D, Santoro A, Figuer A, De Greve J, et al. Phase II study of sorafenib in patients with advanced hepatocellular carcinoma. *J Clin Oncol* 2006;24:4293–300.
- [41] Food and Drug Administration. Sorafenib (Nexavar) prescribing information [accessed 4 April 2018].
- [42] European Medicines Agency. Sorafenib (NEXAVAR). Summary of Product Characteristics [accessed 4 April 2018].
- [43] Lencioni R, Kudo M, Ye SL, Bronowicki JP, Chen XP, Dagher L, et al. GIDEON (Global Investigation of therapeutic DEcisions in hepatocellular carcinoma and of its treatment with sorafenib): second interim analysis. *Int J Clin Pract* 2014;68:609–17.
- [44] Marrero JA, Kudo M, Venook AP, Ye SL, Bronowicki JP, Chen XP, et al. Observational registry of sorafenib use in clinical practice across Child-Pugh subgroups: the GIDEON study. *J Hepatol* 2016;65:1140–7.
- [45] Hollebecque A, Cattani S, Romano O, Sergeant G, Mourad A, Louvet A, et al. Safety and efficacy of sorafenib in hepatocellular carcinoma: the impact of the Child-Pugh score. *Aliment Pharmacol Ther* 2011;34:1193–201.
- [46] Iavarone M, Cabibbo G, Piscaglia F, Zavaglia C, Grieco A, Villa E, et al. Field-practice study of sorafenib therapy for hepatocellular carcinoma: a prospective multicenter study in Italy. *Hepatology* 2011;54:2055–63.
- [47] Geschwind JF, Kudo M, Marrero JA, Venook AP, Chen XP, Bronowicki JP, et al. TACE treatment in patients with sorafenib-treated unresectable hepatocellular carcinoma in clinical practice: final analysis of GIDEON. *Radiology* 2016;279:630–40.
- [48] Kudo MLR, Marrero JA, et al. Regional differences in sorafenib-treated patients with hepatocellular carcinoma: GIDEON observational study. *Liver Int* 2016;36:1196–205.
- [49] Ogasawara S, Chiba T, Ooka Y, Suzuki E, Inoue M, Wakamatsu T, et al. Analysis of sorafenib outcome: focusing on the clinical course in patients with hepatocellular carcinoma. *PLoS ONE* 2016;11:e0161303.
- [50] Arizumi T, Ueshima K, Minami T, Kono M, Chishina H, Takita M, et al. Effectiveness of sorafenib in patients with transcatheter arterial chemoembolization (TACE) refractory and intermediate-stage hepatocellular carcinoma. *Liver Cancer* 2015;4:253–62.
- [51] Ohki T, Kondo M, Karasawa Y, Kawamura S, Maeshima S, Kojima K, et al. Evaluation of the efficacy of sorafenib on overall survival in patients with hepatocellular carcinoma using FT rate: a devised index. *Adv Ther* 2017;34:1097–108.
- [52] European Association for the Study of the Liver. European organisation for research treatment of cancer. EASL-EORTC clinical practice guidelines: management of hepatocellular carcinoma. *J Hepatol* 2012;56:908–43.
- [53] Kudo M, Matsui O, Izumi N, Iijima H, Kadoya M, Imai Y, et al. JSH consensus-based clinical practice guidelines for the management of hepatocellular carcinoma: 2014 update by the Liver Cancer Study Group of Japan. *Liver Cancer*

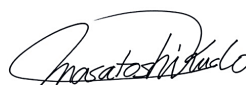
- 2014;3:458–68.
- [54] Porta C, Paglino C, Imarisio I, Bonomi L. Uncovering Pandora's vase: the growing problem of new toxicities from novel anticancer agents. The case of sorafenib and sunitinib. *Clin Exp Med* 2007;7:127–34.
- [55] Bracarda S, Ruggeri EM, Monti M, Merlano M, D'Angelo A, Ferraro F, et al. Early detection, prevention and management of cutaneous adverse events due to sorafenib: recommendations from the Sorafenib Working Group. *Crit Rev Oncol Hematol* 2012;82:378–86.
- [56] Brose MS, Nutting CM, Jarzab B, Elisei R, Siena S, Bastholt L, et al. Sorafenib in radioactive iodine-refractory, locally advanced or metastatic differentiated thyroid cancer: a randomised, double-blind, phase 3 trial. *Lancet* 2014;384:319–28.
- [57] Ren Z, Zhu K, Kang H, Lu M, Qu Z, Lu L, et al. Randomized controlled trial of the prophylactic effect of urea-based cream on sorafenib-associated hand-foot skin reactions in patients with advanced hepatocellular carcinoma. *J Clin Oncol* 2015;33:894–900.
- [58] Abdel-Rahman O, Lamarca A. Development of sorafenib-related side effects in patients diagnosed with advanced hepatocellular carcinoma treated with sorafenib: a systematic-review and meta-analysis of the impact on survival. *Expert Rev Gastroenterol Hepatol* 2017;11:75–83.
- [59] Reig M, Torres F, Rodriguez-Lopez C, Forner A, N LL, Rimola J, et al. Early dermatologic adverse events predict better outcome in HCC patients treated with sorafenib. *J Hepatol* 2014;61:318–24.
- [60] Branco F, Alencar RS, Volt F, Sartori G, Dode A, Kikuchi L, et al. The impact of early dermatologic events in the survival of patients with hepatocellular carcinoma treated with sorafenib. *Ann Hepatol* 2017;16:263–8.
- [61] Rimola J, Diaz-Gonzalez A, Darnell A, Varela M, Pons F, Hernandez-Guerra M, et al. Complete response under sorafenib in patients with hepatocellular carcinoma. Relationship with dermatologic adverse events. *Hepatology* 2017;doi: <http://dx.doi.org/10.1002/hep.29515> [Epub ahead of print].
- [62] Reig M, Gazzola A, Di Donato R, Bruix J. Systemic treatment. *Best Pract Res Clin Gastroenterol* 2014;28:921–35.
- [63] Bruix J, Raoul JL, Sherman M, Mazzaferro V, Bolondi L, Craxi A, et al. Efficacy and safety of sorafenib in patients with advanced hepatocellular carcinoma: sub-analyses of a phase III trial. *J Hepatol* 2012;57:821–9.
- [64] Cheng AL, Guan Z, Chen Z, Tsao CJ, Qin S, Kim JS, et al. Efficacy and safety of sorafenib in patients with advanced hepatocellular carcinoma according to baseline status: subset analyses of the phase III Sorafenib Asia-Pacific trial. *Eur J Cancer* 2012;48:1452–65.
- [65] Raoul JL, Bruix J, Greten TF, Sherman M, Mazzaferro V, Hilgard P, et al. Relationship between baseline hepatic status and outcome, and effect of sorafenib on liver function: SHARP trial subanalyses. *J Hepatol* 2012;56:1080–8.
- [66] Bruix J, Cheng AL, Meinhardt G, Nakajima K, De Sanctis Y, Llovet J. Prognostic factors and predictors of sorafenib benefit in patients with hepatocellular carcinoma: analysis of two phase III studies. *J Hepatol* 2017;67:999–1008.
- [67] Himmelsbach K, Sauter D, Baumert TF, Ludwig L, Blum HE, Hildt E. New aspects of an anti-tumour drug: sorafenib efficiently inhibits HCV replication. *Gut* 2009;58:1644–53.
- [68] Ma W, Tao L, Wang X, Liu Q, Zhang W, Li Q, et al. Sorafenib inhibits renal fibrosis induced by unilateral ureteral obstruction via inhibition of macrophage infiltration. *Cell Physiol Biochem* 2016;39:1837–49.
- [69] Pinter M, Sieghart W, Reiberger T, Rohr-Udilova N, Ferlitsch A, Peck-Radosavljevic M. The effects of sorafenib on the portal hypertensive syndrome in patients with liver cirrhosis and hepatocellular carcinoma – a pilot study. *Aliment Pharmacol Ther* 2012;35:83–91.
- [70] Llovet JM, Pena CE, Lathia CD, Shan M, Meinhardt G, Bruix J. Plasma biomarkers as predictors of outcome in patients with advanced hepatocellular carcinoma. *Clin Cancer Res* 2012;18:2290–300.
- [71] Wilhelm SM, Dumas J, Adnane L, Lynch M, Carter CA, Schutz G, et al. Regorafenib (BAY 73–4506): a new oral multikinase inhibitor of angiogenic, stromal and oncogenic receptor tyrosine kinases with potent preclinical antitumor activity. *Int J Cancer* 2011;129:245–55.
- [72] Abou-Elkacem L, Arns S, Brix G, Gremse F, Zopf D, Kiessling F, et al. Regorafenib inhibits growth, angiogenesis, and metastasis in a highly aggressive, orthotopic colon cancer model. *Mol Cancer Ther* 2013;12:1322–31.
- [73] Bruix J, Tak WY, Gasbarrini A, Santoro A, Colombo M, Lim HY, et al. Regorafenib as second-line therapy for intermediate or advanced hepatocellular carcinoma: multicentre, open-label, phase II safety study. *Eur J Cancer* 2013;49:3412–9.
- [74] Finn RS, Blumenschein GR, Tolcher AW, Leong S, Boix O, Diefenbach K. Continuous-dose regorafenib (REG) in hepatocellular carcinoma (HCC): Phase I safety and pharmacokinetic (PK) study. *J Clin Oncol* 2013;31:300.
- [75] Finn RS, Merle P, Granito A, Huang YH, Bodoky G, Pracht M, et al. Outcomes of sequential treatment with sorafenib followed by regorafenib for HCC: additional analyses from the phase 3 RESORCE trial. *J Hepatol* 2018.
- [76] El-Khoueiry AB, Sangro B, Yau T, Crocenzi TS, Kudo M, Hsu C, et al. Nivolumab in patients with advanced hepatocellular carcinoma (CheckMate 040): an open-label, non-comparative, phase 1/2 dose escalation and expansion trial. *Lancet* 2017;389:2492–502.
- [77] Raoul JL, Adhoute X, Gilabert M, Edeline J. How to assess the efficacy or failure of targeted therapy: deciding when to stop sorafenib in hepatocellular carcinoma. *World J Hepatol* 2016;8:1541–6.
- [78] Bruix J, Reig M, Sangro B. Assessment of treatment efficacy in hepatocellular carcinoma: response rate, delay in progression or none of them. *J Hepatol* 2017;66:1114–7.
- [79] Therasse P, Arbuick S, Eisenhaue rE. New guidelines to evaluate the response to treatment in solid tumors (RECIST Guidelines). *J Natl Cancer Inst* 2000;92:205–16.
- [80] Eisenhauer EA, Therasse P, Bogaerts J, Schwartz LH, Sargent D, Ford R, et al. New response evaluation criteria in solid tumours: revised RECIST guideline (version 1.1). *Eur J Cancer* 2009;45:228–47.
- [81] Huang L, Yorlko D, Minghua S, Bruix J, Llovet J, Cheng A-L. Weak correlation of overall survival and time to progression in advanced hepatocellular carcinoma. *J Clin Oncol* 2017;35:233.
- [82] Lencioni R, Llovet JM. Modified RECIST (mRECIST) assessment for hepatocellular carcinoma. *Semin Liver Dis* 2010;30:52–60.
- [83] Lencioni R, Montal R, Torres F, Park JW, Decaens T, Raoul JL, et al. Objective response by mRECIST as a predictor and potential surrogate end-point of overall survival in advanced HCC. *J Hepatol* 2017;66:1166–72.
- [84] Huang L, Sanctis YD, Shan M, Bruix J, Llovet J, Cheng A-L, et al. Weak correlation of overall survival (OS) and response rate (RR) by RECIST in advanced hepatocellular carcinoma (HCC). Presented at ILCA 2017; abstract P-056 [accessed 4 April 2018].
- [85] Meyer T, Palmer DH, Cheng AL, Hocke J, Loembe AB, Yen CJ. MRECIST to predict survival in advanced hepatocellular carcinoma: analysis of two randomised phase II trials comparing nintedanib vs sorafenib. *Liver Int* 2017;37:1047–55.
- [86] Reig M, Rimola J, Torres F, Darnell A, Rodriguez-Lopez C, Forner A, et al. Postprogression survival of patients with advanced hepatocellular carcinoma: rationale for second-line trial design. *Hepatology* 2013;58:2023–31.
- [87] Iavarone M, Cabibbo G, Biolato M, Della Corte C, Maida M, Barbara M, et al. Predictors of survival in patients with advanced hepatocellular carcinoma who permanently discontinued sorafenib. *Hepatology* 2015;62:784–91.
- [88] Ogasawara S, Chiba T, Ooka Y, Suzuki E, Kanogawa N, Saito T, et al. Post-progression survival in patients with advanced hepatocellular carcinoma resistant to sorafenib. *Invest New Drugs* 2016;34:255–60.
- [89] Bruix J, Merle P, Granito A, Huang Y-H, Bodoky G, Pracht M, et al. Survival by pattern of tumor progression during prior sorafenib (SOR) treatment in patients with hepatocellular carcinoma (HCC) in the phase III RESORCE trial comparing second-line treatment with regorafenib (REG) or placebo. *J Clin Oncol* 2017;35:229.
- [90] Vilgrain V, Pereira H, Assenat E, Guiu B, Ilonca AD, Pageaux GP, et al. Efficacy and safety of selective internal radiotherapy with yttrium-90 resin microspheres compared with sorafenib in locally advanced and inoperable hepatocellular carcinoma (SARAH): an open-label randomised controlled phase 3 trial. *Lancet Oncol* 2017;18:1624–36.
- [91] Chow PKH, Gandhi M, Tan SB, Khin MW, Khasbazar A, Ong J, et al. SIRveNIB: selective internal radiation therapy versus sorafenib in Asia-Pacific patients with hepatocellular carcinoma. *J Clin Oncol* 2018;Jco2017760892.
- [92] Ricke J, Sangro B, Amthauer H, Bargellini I, Bartenstein P, De Toni E, et al. The impact of combining Selective Internal Radiation Therapy (SIRT) with Sorafenib on overall survival in patients with advanced hepatocellular carcinoma: the Soramic trial palliative cohort. *J Hepatol* 2018;68:5102.
- [93] European Medicines Agency. Lenvatinib (LENVIMA). Summary of Product Characteristics [accessed 4 April 2018].
- [94] Food and Drug Administration. Lenvatinib (Lenvima) prescribing information [accessed 4 April 2018].
- [95] Ikeda K, Kudo M, Kawazoe S, Osaki Y, Ikeda M, Okusaka T, et al. Phase 2 study of lenvatinib in patients with advanced hepatocellular carcinoma. *J Gastroenterol* 2017;52:512–9.
- [96] Scagliotti GV, Novello S, von Pawel J. The emerging role of MET/HGF inhibitors in oncology. *Cancer Treat Rev* 2013;39:793–801.
- [97] Rimassa L, Assenat E, Peck-Radosavljevic M, Pracht M, Zagonel V, Mathurin P, et al. Tivantinib for second-line treatment of MET-high, advanced hepatocellular carcinoma (METIV-HCC): a final analysis of a phase 3, randomised, placebo-controlled study. *Lancet Oncol* 2018.
- [98] Best J, Schotten C, Lohmann G, Gerken G, Dechene A. Tivantinib for the treatment of hepatocellular carcinoma. *Expert Opin Pharmacother* 2017;18:727–33.
- [99] Yakes FM, Chen J, Tan J, Yamaguchi K, Shi Y, Yu P, et al. Cabozantinib (XL184), a novel MET and VEGFR2 inhibitor, simultaneously suppresses metastasis, angiogenesis, and tumor growth. *Mol Cancer Ther* 2011;10:2298–308.
- [100] Kelley RK, Verslype C, Cohn AL, Yang TS, Su WC, Burris H, et al. Cabozantinib in hepatocellular carcinoma: results of a phase 2 placebo-controlled randomized discontinuation study. *Ann Oncol* 2017;28:528–34.
- [101] Clarke JM, Hurwitz HI. Targeted inhibition of VEGF receptor 2: an update on ramucirumab. *Expert Opin Biol Ther* 2013;13:1187–96.
- [102] Wilke H, Muro K, Van Cutsem E, Oh SC, Bodoky G, Shimada Y, et al. Ramucirumab plus paclitaxel versus placebo plus paclitaxel in patients with previously treated advanced gastric or gastro-oesophageal junction adenocarcinoma (RAINBOW): a double-blind, randomised phase 3 trial. *Lancet Oncol* 2014;15:1224–35.
- [103] Zhu AX, Ryou B-Y, Yen C-J, Kudo M, Poon RT-P, Pastorelli D, et al. Ramucirumab (RAM) as second-line treatment in patients (pts) with advanced hepatocellular carcinoma (HCC): analysis of patients with elevated α -fetoprotein (AFP) from the randomized phase III REACH study. *J Clin Oncol* 2015;33:232.
- [104] Khoja L, Butler MO, Kang SP, Ebbinghaus S, Joshua AM. Pembrolizumab. *J Immunother Cancer* 2015;3:36.
- [105] Zhu AX, Finn RS, Cattan S, Edeline J, Ogasawara S, Palmer DH, et al. KEYNOTE-224: Pembrolizumab in patients with advanced hepatocellular carcinoma previously treated with sorafenib. *J Clin Oncol* 2018;36:209.
- [106] Zhu AX, Finn RS, Mulcahy M, Gurtler J, Sun W, Schwartz JD, et al. A phase II and biomarker study of ramucirumab, a human monoclonal antibody targeting the VEGF receptor-2, as first-line monotherapy in patients with advanced hepatocellular cancer. *Clin Cancer Res* 2013;19:6614–23.

Editorial

Cabozantinib as a Second-Line Agent in Advanced Hepatocellular Carcinoma

Masatoshi Kudo

Department of Gastroenterology and Hepatology, Kindai University Faculty of Medicine, Osaka-Sayama, Japan

Prof. M. KudoEditor *Liver Cancer***Introduction**

The results of the phase III CELESTIAL trial of cabozantinib were presented by Prof. Ghassan Abou-Alfa at the ASCO Gastrointestinal Cancer Symposium held in San Francisco from January 18 to 20, 2018 [1]. Although most of the previous clinical trials of second-line agents, except regorafenib [2], failed [3–8], the CELESTIAL trial yielded positive results in line with most expectations and produced a fourth molecular-targeted drug option for hepatocellular carcinoma (HCC). Based on this trial, cabozantinib can be added as a second-line option to the first-line drugs sorafenib [9, 10] and lenvatinib [11] and the second-line drug regorafenib [2] (Table 1).

Phase II Trial of Cabozantinib

The structural formula of cabozantinib is relatively similar to that of regorafenib [12, 13] (Fig. 1), although the kinase inhibitory activity (IC_{50}) of cabozantinib is different. Cabozantinib was originally identified as a dual inhibitor of VEGFR-2 and c-MET [14, 15], whereas current data suggest that it is a more potent inhibitor of MET, AXL, RET, FLT3, and TIE-2 than regorafenib (Tables 2, 3). VEGF, MET, and AXL are involved in tumor proliferation and angiogenesis, and MET and AXL are involved in the acquisition of resistance to antiangiogenic drugs [14–18]. VEGF, MET, or AXL expression is considered a poor prognostic factor [14–18].

Masatoshi Kudo
Department of Gastroenterology and Hepatology
Kindai University Faculty of Medicine
377-2 Ohno-Higashi, Osaka-Sayama 589-8511 (Japan)
m-kudo@med.kindai.ac.jp

Table 1. Phase III clinical trials of advanced stage HCC

	Design	Trial name	Result	Presentation	Publication	First author	
First line	1	Sorafenib vs. sunitinib	SUN1170	Negative	ASCO 2011	J Clin Oncol 2013	Cheng
	2	Sorafenib ± erlotinib	SEARCH	Negative	ESMO 2012	J Clin Oncol 2015	Zhu
	3	Sorafenib vs. brivanib	BRISK-FL	Negative	AASLD 2012	J Clin Oncol 2013	Johnson
	4	Sorafenib vs. lenvatinib	LiGHT	Negative	ASCO-GI 2013	J Clin Oncol 2015	Cainap
	5	Sorafenib ± doxorubicin	CALGB 80802	Negative	ASCO-GI 2016		
	6	Sorafenib ± HAIC	SILIUS	Negative	EASL 2016	Lancet Gastroenterol Hepatol 2018	Kudo
	7	Sorafenib ± Y90	SARAH	Negative	EASL 2017	Lancet Oncol 2017	Vilgrain
	8	Sorafenib ± Y90	SIRveNIB	Negative	ASCO 2017	J Clin Oncol 2018	Chow
	9	Sorafenib vs. nivolumab	REFLECT	Positive	ASCO 2017	Lancet 2018	Kudo
	10	Sorafenib vs. durvalumab + tremelimumab vs. durvalumab	CheckMate-459	Ongoing			
	11	Sorafenib vs. durvalumab + tremelimumab vs. durvalumab	HIMALAYA	Ongoing			
Second line	1	Brivanib vs. placebo	BRISK-PS	Negative	EASL 2012	J Clin Oncol 2013	Llovet
	2	Everolimus vs. placebo	EVOLVE-1	Negative	ASCO-GI 2014	JAMA 2014	Zhu
	3	Ramucirumab vs. placebo	REACH	Negative	ESMO 2014	Lancet Oncol 2015	Zhu
	4	S-1 vs. placebo	S-CUBE	Negative	ASCO 2015	Lancet Gastroenterol Hepatol 2017	Kudo
	5	ADI-PEG 20 vs. placebo	NA	Negative	ASCO 2016		
	6	Regorafenib vs. placebo	RESORCE	Positive	WCGC 2016	Lancet 2017	Bruix
	7	Tivantinib vs. placebo	METIV-HCC	Negative	ASCO 2017		
	8	Tivantinib vs. placebo	JET-HCC	Negative	ESMO 2017		
	9	DT vs. placebo	ReLive	Negative	ILCA 2017		
	10	Cabozantinib vs. placebo	CELESTIAL	Positive	ASCO-GI 2018		Ghassan
	11	Ramucirumab vs. placebo	REACH-2	Ongoing			
	12	Pembrolizumab vs. placebo	KEYNOTE-240	Ongoing			

Red, positive trials; blue, ongoing trials; black, negative trials. HCC, hepatocellular carcinoma; HAIC, hepatic arterial infusion chemotherapy; DT, doxorubicin-loaded nanoparticles.

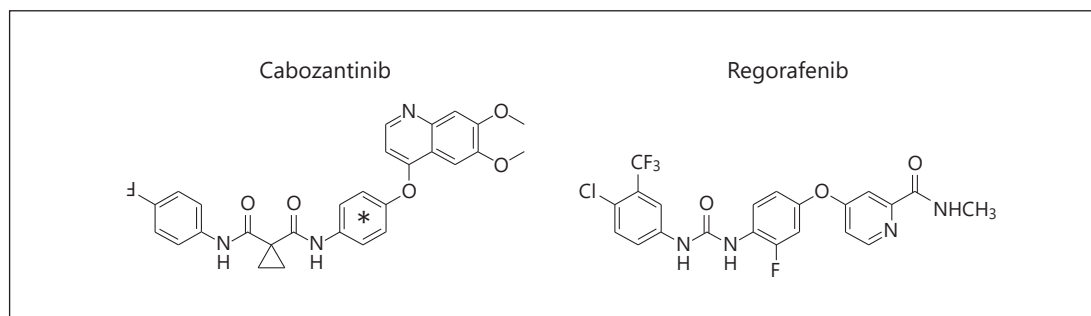


Fig. 1. Chemical structure of cabozantinib and regorafenib.

A waterfall plot from the phase II trial showed tumor shrinkage in a large proportion of patients. Progression-free survival (PFS) was 4.2 months in sorafenib-naïve patients and 5.5 months in sorafenib-pretreated patients, and overall survival (OS) was 11.5 months [15] (Table 4). The overall response rate (ORR) was 5%, the disease control rate was 81%, and PFS was 5.2 months (Table 4). Considering that some patients in the cabozantinib trial received first-line therapy, the results were not very good compared with the results of the phase II trial of regorafenib [19] (Table 4). Cabozantinib was also associated with a higher incidence of adverse events (AEs) than regorafenib (Table 5).

Table 2. Cabozantinib targets VEGFR-2, c-MET, RET, AXL, TIE2, and FLT3

Biochemical activity	IC ₅₀ , nmol/L
VEGFR-2	14
c-MET	2
c-KIT	752
RET	8
AXL	8
TIE2	13
FLT3	21
PDGFR-β	575

Table 3. Mode of action: cabozantinib and regorafenib

Biochemical activity	Cabozantinib IC ₅₀ , nM	Regorafenib IC ₅₀ ± SD, nM
MET	2	NA
AXL	8	NA
VEGFR-2	14	4.2±1.6
VEGFR-1	NA	13±0.4
VEGFR-3	NA	46±10
BRAF	NA	28±10
TIE-2	13	311±46
PDGFR-β	575	22±3
FGFR1	NA	202±18
c-Kit	752	7±2
RET	8	1.5±0.7
Flt-3	21	NA

Modified from [12, 13].

Table 4. Comparison of efficacy (phase II): cabozantinib and regorafenib

	Cabozantinib (n = 41)	Regorafenib (n = 36)
ORR, %	5	3
DCR, %	81	72
PFS/TTP, months	5.2 (5.5)	4.3
OS, months	11.5	13.8

ORR, objective response rate; DCR, disease control rate; PFS, progression-free survival; TTP, time to progression; OS, overall survival.

Phase III CELESTIAL Trial

In light of these results, a phase III trial of cabozantinib was conducted (Fig. 2). The trial design was not as sophisticated as that of the RESORCE trial [2, 20]. For example, vascular invasion and/or extrahepatic spread was included as a stratification factor, which may result in an unfavorable imbalance regarding patients with vascular invasion. In fact, this unfavorable imbalance was present in the BRISK-PS trial and resulted in negative results [3]. The BRISK-PS trial did not include alpha-fetoprotein as a stratification factor, which caused an unfavorable balance against the trial drug similar to that seen in the REFLECT trial [11]. The RESORCE trial led to the inclusion of vascular invasion as an independent stratification factor

Table 5. Cabozantinib vs. regorafenib: comparison of adverse events (phase II)

	Cabozantinib (n = 41)		Regorafenib (n = 36)	
	all grades	grade 3–4	all grades	grade 3–4
Hand foot skin reaction	56	15	53	14
Fatigue	56	2	53	17
Hypertension	24	10	36	3
Appetite loss	29	0	36	0
Nausea	37	2	33	0
Vomiting	37	2	14	0
Diarrhea	63	20	53	6
Body weight loss	22	2	19	0
Constipation	22	0	25	0

Values are shown as percentages. Modified from [15, 19].

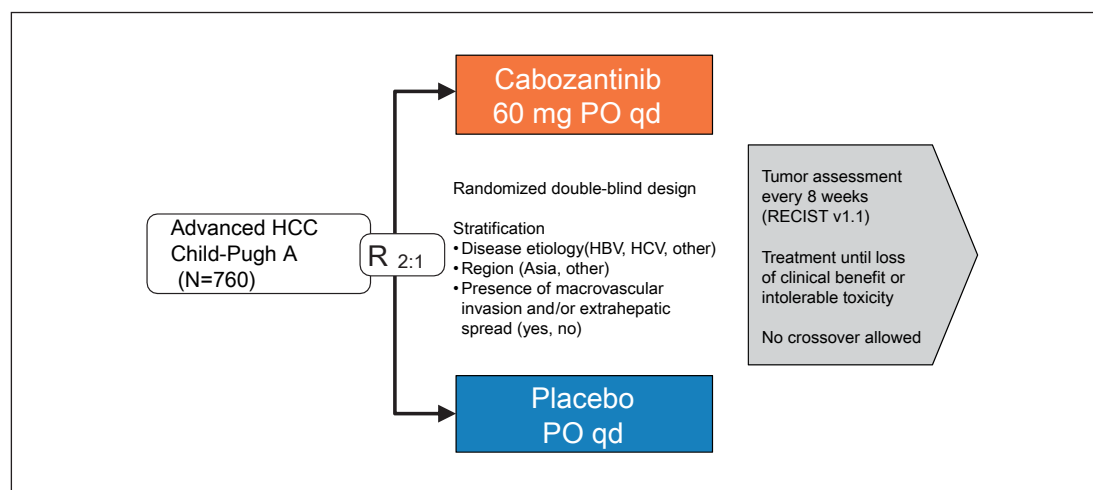


Fig. 2. CELESTIAL trial: study design.

and alpha-fetoprotein as a stratification factor in the design of trials of second-line drugs [21]. However, the CELESTIAL trial had a conventional design with few strategic elements (Table 6) and did not even exclude sorafenib-intolerant patients as in the RESORCE trial [2, 20, 21]. The only inclusion criteria regarding prior treatment were (a) prior sorafenib treatment, (b) progression following at least 1 prior systemic treatment for HCC, and (c) up to 2 prior systemic regimens for advanced HCC; the exact number of sorafenib-intolerant patients enrolled remains unclear.

Between September 2013 and September 2017, the trial enrolled 773 patients with unresectable HCC showing disease progression after at least 1 prior systemic chemotherapy regimen containing sorafenib. The second interim analysis performed in January 2016 demonstrated the superiority of cabozantinib in terms of the primary endpoint of OS. There was an imbalance in baseline patient characteristics between the cabozantinib and placebo groups caused by the failure to include vascular invasion and extrahepatic spread as independent stratification factors; namely, the rate of vascular invasion was only 27% in the cabozantinib group compared with 34% in the placebo group, which favored the cabozantinib

Table 6. Phase III clinical trials: advanced stage second line versus placebo

	BRISK-PS Brivanib	EVOLVE-1 Everolimus	REACH Ramucirumab	S-CUBE S1	RESORCE Regorafenib	METIV-HVV Tivantinib	KEYNOTE-240 Pembrolizumab	CELESTIAL Cabozantinib
Intolerance of sorafenib, %	12–13	18.5–20	13–15	30.6–33.8	0	17–21	–	N/A
Stratification factor	Reason for sorafenib discontinuation ECOG-PS score Extrahepatic spread, and/or vascular invasion	Region MVI	Region Cause of liver disease (HBV, HCV, other)	Medical institutions Extrahepatic metastasis and/or vascular invasion	Region ECOG-PS score Extrahepatic spread Vascular invasion AFP	Extrahepatic spread Vascular invasion AFP	Region Vascular invasion AFP	Region Disease etiology (HBV, HCV, other) Extrahepatic metastasis and/or vascular invasion

After the BRISK-PS trial, where there was an imbalance of AFP and MVI in the testing arm, AFP and MVI started to be included as independent stratification factors in most trials, but not in the CELESTIAL trial. Modified from [1–6]. AFP, alpha-fetoprotein; MVI, macrovascular invasion.

Table 7. Baseline characteristics

	Cabozantinib (n = 470)	Placebo (n=237)
Median (range) age, years	64 (22–86)	64 (24–86)
Male, %	81	85
ECOG performance status 0/1, %	52/48	55/45
AFP ≥400 ng/mL, %	41	43
Enrollment region, %		
Asia/Europe/North America/Pacific	25/49/23/3	25/46/25/5
Etiology of HCC, %		
HBV	38	38
HCV	22	22
Other	40	41
Extrahepatic spread of disease, %	79	77
Macrovascular invasion, %	27	34
Extrahepatic spread and/or macrovascular invasion, %	85	84

Asia: Hong Kong, South Korea, Singapore, Taiwan; Pacific: Australia and New Zealand. Cited from [1]. AFP, alpha-fetoprotein; HCC, hepatocellular carcinoma.

group (Table 7). This resulted in significantly better OS in the cabozantinib group (10.2 months, 95% CI: 9.1–12.0) than in the placebo group (8.2 months, 95% CI: 9.1–12.0) and consequently in a positive result for the clinical trial. PFS, the secondary endpoint, was also better in the cabozantinib group (5.2 months, 95% CI: 4.0–5.5) than in the placebo group (1.9 months, 95% CI: 1.9–1.9) (Table 8). PFS of 1.9 months in the placebo arm in the CELESTIAL trial was similar to that of 1.5 months in the placebo arm in the RESORCE trial (Fig. 3). Moreover, ORR was superior in the cabozantinib group (4 vs. 0.4%; $p = 0.0086$) (Table 9). Post-trial treatment was performed in a comparably low proportion of patients in the cabozantinib and placebo groups (25 vs. 30%), demonstrating the poor condition of the patient population. In summary, although the relative number of sorafenib-intolerant patients in the trial was not reported, it can be inferred from the trial results that the proportion was relatively low (Table 10).

Table 8. Time to event: CELESTIAL (second and third line) versus RESORCE

	CELESTIAL trial (second and third line)		RESORCE trial (SOR → REG)	
	cabozantinib (n = 470)	placebo (n = 237)	regorafenib (n=379)	placebo (n = 194)
TTP, months	N/A	N/A	3.2	1.5
HR		N/A		0.44
p value				<0.0001
PFS, months	5.2	1.9	3.1	1.5
HR		0.44		0.46
p value		<0.0001		<0.0001
OS, months	10.2	8.2	10.6	7.8
HR		0.76		0.63
p value		0.0049		<0.0001

TTP, time to progression; PFS, progression-free survival; OS, overall survival. Modified from [1, 2].

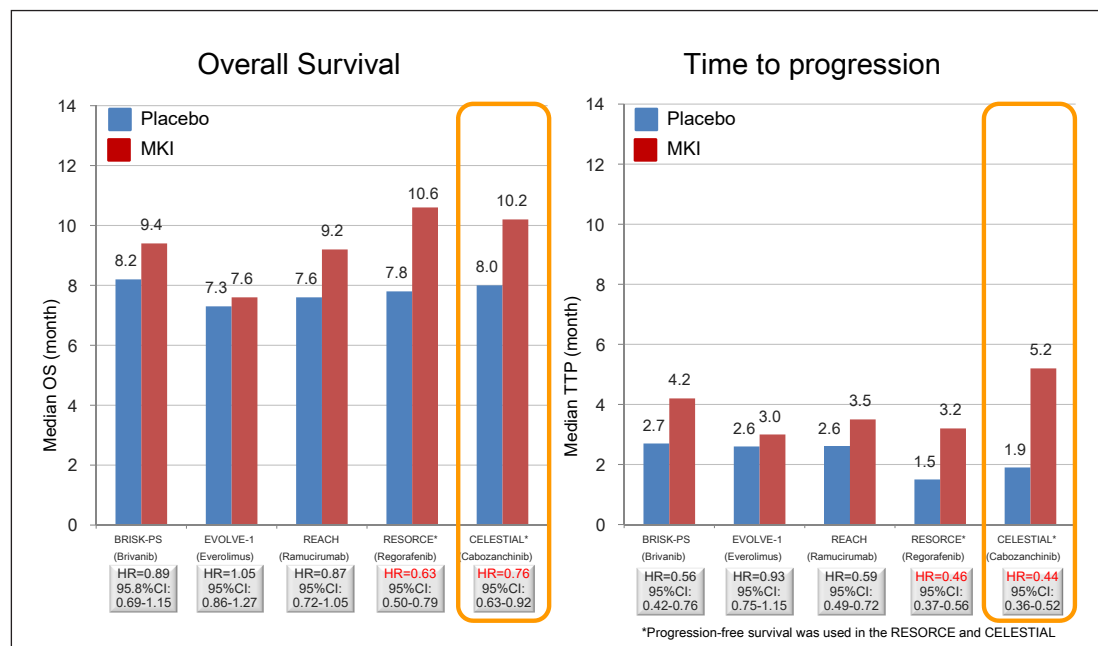


Fig. 3. Phase III trial: second line. Time to progression (TTP) was shorter in the placebo arm in the CELESTIAL trial, similar to placebo arm in the RESORCE trial, suggesting that there were fewer sorafenib-intolerant patients in the CELESTIAL trial. Anticancer activity may be higher than that of other agents, as indicated by the longer TTP. MKI, multikinase inhibitor.

Comparison between Regorafenib and Cabozantinib: Efficacy and Safety

Cabozantinib and regorafenib had comparable efficacy in terms of OS, ORR, and PFS (Tables 8, 9). Patients who received prior treatment with sorafenib alone showed slightly better outcomes (Table 10), which were comparable to those of regorafenib.

The duration of treatment with cabozantinib was 3.8 months, which was comparable to the 3.6 months for regorafenib and indicates acceptable tolerability, similar to that of regorafenib.

Table 9. Tumor response: CELESTIAL vs. RESORCE

	CELESTIAL trial		RESORCE trial	
	cabozantinib (n = 470)	placebo (n = 237)	regorafenib (n = 379)	placebo (n = 194)
Response criteria	RECIST 1.1		RECIST 1.1	
ORR, %	4	0.4	6.6	2.6
p value	0.0086		0.02	
DCR, %	64	33.4	65.7	34.5
p value	N/A		<0.0001	

ORR, objective response rate; DCR, disease control rate. Modified from [1, 2].

Table 10. Time to event: CELESTIAL (SOR → CAB) vs. RESORCE

	CELESTIAL trial (SOR→CAB)		RESORCE trial (SOR → REG)	
	cabozantinib (n = 331)	placebo (n = 164)	regorafenib (n = 379)	placebo (n = 194)
TTP, months	N/A	N/A	3.2	1.5
HR	N/A		0.44	
p value			<0.0001	
PFS, months	5.5	1.9	3.1	1.5
HR			0.46	
p value	0.40		<0.0001	
OS, months	11.3	7.2	10.6	7.8
HR	0.70		0.63	
p value			<0.0001	

TTP, time to progression; PFS, progression-free survival; OS, overall survival. Modified from [1, 2].

Dose reduction or discontinuation because of treatment-related AEs was more common with cabozantinib than with regorafenib. Specific AEs such as palmar-plantar erythrodysesthesia, diarrhea, and asthenia were more common with cabozantinib than with regorafenib, indicating that cabozantinib may have a slightly higher toxicity than regorafenib (Table 11).

Key Factors Contributing to the Success of the CELESTIAL Trial

The following 5 factors may have contributed to the success of the CELESTIAL trial of cabozantinib despite the unsophisticated trial design compared with that of the RESORCE trial and the drug's slightly higher toxicity (Table 12).

1. Cabozantinib has a sufficiently potent antitumor activity.
2. Toxicity and tolerability were clinically acceptable.
3. An imbalance in vascular invasion favored cabozantinib.

Table 11. Safety analysis: CELESTIAL vs. RESORCE

	Cabozantinib (n = 467)	Regorafenib (n = 374)
Treatment duration, months	3.8	3.6
Dose reduction due to adverse event, %	62	48
Discontinuation due to TRAE, %	16	10
<i>Grade 3/4</i>		
Any grade 3 or 4 adverse event, %	68	66
Palmar-plantar erythrodysesthesia, %	17	13
Fatigue, %	10	9
Hypertension, %	16	15
Diarrhea, %	10	3
Asthenia, %	7	NA
Bilirubin increased, %	NA	10
AST increased, %	12	11
Ascites, %	NA	4
Anemia, %	4	5
Hypophosphatemia, %	NA	9

AST, aspartate aminotransferase; NA, not applicable. TRAE, treatment-related adverse event. NCI-CTCAE v4.03.

Table 12. CELESTIAL trial: key factors of the success

- Cabozantinib has good anticancer activity
- Acceptable toxicity and tolerability
- Imbalance of vascular invasion favoring cabozantinib
- Small number of sorafenib-intolerant patients (short time to progression in placebo)
- Extremely high numbers of enrolled patients (n = 470 vs. 379, 362, 283, 263)
→ Higher power to detect the small difference and eliminate the effect of tiny imbalance

4. The short time to progression in the placebo arm and low proportion of patients having post-trial treatment indicate low enrollment of sorafenib-intolerant patients, which was similar to no enrollment of sorafenib-intolerant patients in the RESORCE trial.
5. The sample size of 470 patients was considerably higher than that of other second-line trials and provided sufficient power to eliminate the effect of the small imbalance and detect small differences as significant (Table 13).

Paradigm Shift in the Treatment Strategy for HCC

Sorafenib was the only HCC drug available between 2007 and 2016. Between 2017 and 2018, 5 drugs, sorafenib, lenvatinib, regorafenib, cabozantinib, and nivolumab, became available. Therefore, it is necessary to establish how these drugs should be used in clinical practice (Fig. 4). Combinations of immune checkpoint inhibitors and molecular-targeted drugs or molecular-targeted drugs and established locoregional therapies [22] are particularly likely to produce a paradigm shift in the treatment of HCC. The treatment landscape for

Table 13. Phase III trials in a second line setting

	CELESTIAL cabozantinib arm (n = 470)	RESORCE regorafenib arm (n = 379)	BRISK-PS brivanib arm (n = 263)	EVOLVE-1 everolimus arm (n = 362)	REACH ramucirumab arm (n = 283)
Male, %	81	88	82	84	83
Median age (range), years	64 (22–86)	64 (19–85)	64 (19–89)	67 (21–86)	64 (28–87)
Asian race, %	25	41	48	38	46
ECOG PS 0/1, %	52/48	65/35	57/39	59/36	56/44
Child Pugh A, %	NA	98	92	98	98
BCLC stage, B/C, %	NA	14/86	9/87	14/87	12/88
AFP ≥400 ng/mL, %	41	43	50 ^a	47 ^a	42
MVI, %	27	29	31	33	29
EHS, %	79	70	65	74	73
Etiology, %					
Alcohol	NA	24	23	18	–
HBV	38	38	39	25	35
HCV	22	21	28	26	27
NASH	NA	7	–	4	–
Intolerance of sorafenib, %	–	0	13	19	13
Median total duration of prior sorafenib, months	5.3	7.8	–	–	–
Median time from disease progression to randomization, months	1.6	0.9	–	–	–

AFP, alpha-fetoprotein; MVI, macrovascular invasion; EHS, extrahepatic spread; NASH, non-alcoholic steatohepatitis.

^a AFP ≥200 ng/mL.

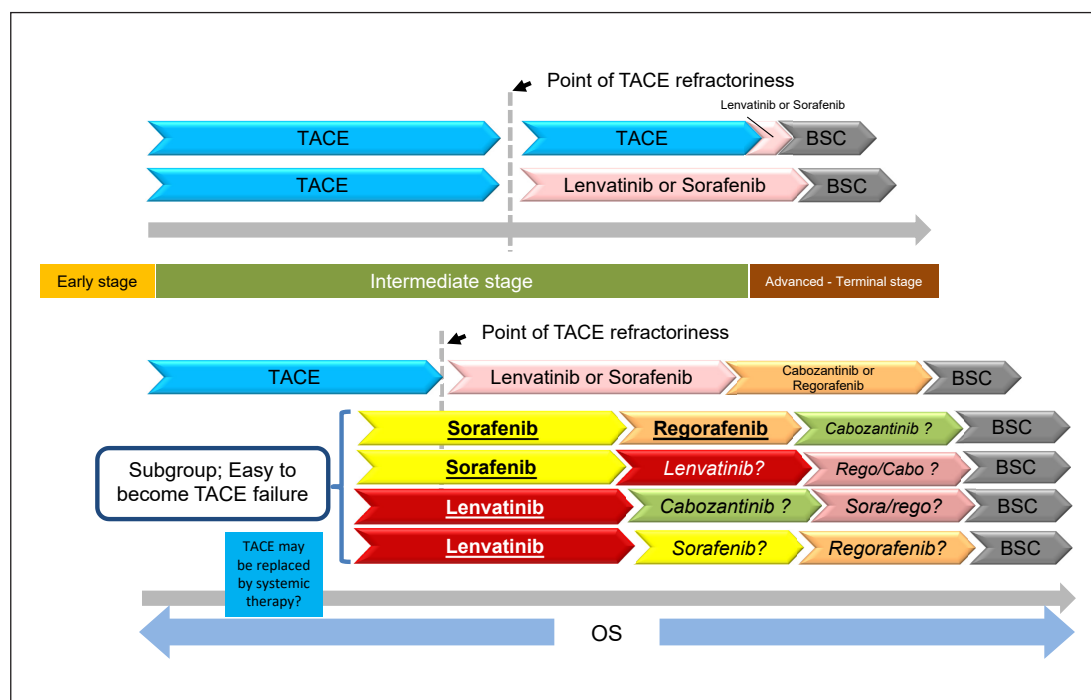


Fig. 4. New treatment landscape in HCC associated with the emergence of multiple molecular-targeted agents. Identification of the subgroup that easily develops to TACE failure/refractoriness may be important. BSC, best supportive care.

HCC will soon undergo major changes as systemic therapy is integrated into the treatment for all stages, from early to intermediate to advanced, which could drastically improve the prognosis of patients with HCC.

Conclusion

The success of the clinical trial of cabozantinib increased the treatment options for HCC, and combination treatment with immunotherapy may soon improve the prognosis of patients with HCC.

References

- 1 Ghassan K, Abou-Alfa GK, Meyer T, Cheng AL, Anthony B, Khoueiry EI, Rimassa L, et al: Cabozantinib (C) versus placebo (P) in patients (pts) with advanced hepatocellular carcinoma (HCC) who have received prior sorafenib: results from the randomized phase III CELESTIAL trial. *J Clin Oncol* 2018;36(suppl 4S);abstr 207.
- ▶ 2 Bruix J, Qin S, Merle P, Granito A, Huang YH, Bodoky G, Pracht M, et al: Regorafenib for patients with hepatocellular carcinoma who progressed on sorafenib treatment (RESORCE): a randomised, double-blind, placebo-controlled, phase 3 trial. *Lancet* 2017;389:56–66.
- ▶ 3 Llovet JM, Decaens T, Raoul JL, Boucher E, Kudo M, Chang C, Kang YK, et al: Brivanib in patients with advanced hepatocellular carcinoma who were intolerant to sorafenib or for whom sorafenib failed: results from the randomized phase III BRISK-PS study. *J Clin Oncol* 2013;31:3509–3516.
- ▶ 4 Zhu AX, Kudo M, Assenat E, Cattani S, Kang YK, Lim HY, Poon RT, et al: Effect of everolimus on survival in advanced hepatocellular carcinoma after failure of sorafenib: the EVOLVE-1 randomized clinical trial. *JAMA* 2014;312:57–67.
- ▶ 5 Zhu AX, Park JO, Ryoo BY, Yen CJ, Poon R, Pastorelli D, Blanc JF, et al: Ramucirumab versus placebo as second-line treatment in patients with advanced hepatocellular carcinoma following first-line therapy with sorafenib (REACH): a randomised, double-blind, multicentre, phase 3 trial. *Lancet Oncol* 2015;16:859–870.
- ▶ 6 Kudo M, Moriguchi M, Numata K, Hidaka H, Tanaka H, Ikeda M, Kawazoe S, et al: S-1 versus placebo in patients with sorafenib-refractory advanced hepatocellular carcinoma (S-CUBE): a randomised, double-blind, multicentre, phase 3 trial. *Lancet Gastroenterol Hepatol* 2017;2:407–417.
- ▶ 7 Kudo M: Molecular targeted agents for hepatocellular carcinoma: current status and future perspectives. *Liver Cancer* 2017;6:101–112.
- ▶ 8 Cucchetti A, Piscaglia F, Pinna AD, Djulbegovic B, Mazzotti F, Bolondi L: Efficacy and safety of systemic therapies for advanced hepatocellular carcinoma: a network meta-analysis of phase III trials. *Liver Cancer* 2017;6:337–348.
- ▶ 9 Llovet JM, Ricci S, Mazzaferro V, Hilgard P, Gane E, Blanc JF, de Oliveira AC, et al: Sorafenib in advanced hepatocellular carcinoma. *N Engl J Med* 2008;359:378–390.
- ▶ 10 Cheng AL, Kang YK, Chen Z, Tsao CJ, Qin S, Kim JS, Luo R, et al: Efficacy and safety of sorafenib in patients in the Asia-Pacific region with advanced hepatocellular carcinoma: a phase III randomised, double-blind, placebo-controlled trial. *Lancet Oncol* 2009;10:25–34.
- ▶ 11 Kudo M, Finn RS, Qin S, Han KH, Ikeda K, Piscaglia F, Baron A, et al: Lenvatinib versus sorafenib in first-line treatment of patients with unresectable hepatocellular carcinoma: a randomised phase 3 non-inferiority trial. *Lancet* 2018:Epub ahead of print.
- ▶ 12 Lacy S, Hsu B, Miles D, Aftab D, Wang R, Nguyen L: Metabolism and disposition of cabozantinib in healthy male volunteers and pharmacologic characterization of its major metabolites. *Drug Metab Dispos* 2015;43:1190–1207.
- ▶ 13 Strumberg D, Schultheis B: Regorafenib for cancer. *Expert Opin Investig Drugs* 2012;21:879–889.
- ▶ 14 Yakes FM, Chen J, Tan J, Yamaguchi K, Shi Y, Yu P, Qian F, et al: Cabozantinib (XL184), a novel MET and VEGFR2 inhibitor, simultaneously suppresses metastasis, angiogenesis, and tumor growth. *Mol Cancer Ther* 2011;10:2298–2308.
- ▶ 15 Kelley RK, Verslype C, Cohn AL, Yang TS, Su WC, Burris H, Braithwaite F, et al: Cabozantinib in hepatocellular carcinoma: results of a phase 2 placebo-controlled randomized discontinuation study. *Ann Oncol* 2017;28:528–534.
- ▶ 16 Gay CM, Balaji K, Byers LA: Giving AXL the axe: targeting AXL in human malignancy. *Br J Cancer* 2017;116:415–423.
- ▶ 17 Zhu AX, Duda DG, Sahani DV, Jain RK: HCC and angiogenesis: possible targets and future directions. *Nat Rev Clin Oncol* 2011;8:292–301.

- ▶18 Ueki T, Fujimoto J, Suzuki T, Yamamoto H, Okamoto E: Expression of hepatocyte growth factor and its receptor, the c-met proto-oncogene, in hepatocellular carcinoma. *Hepatology* 1997;25:619–623.
- ▶19 Bruix J, Tak WY, Gasbarrini A, Santoro A, Colombo M, Lim HY, Mazzaferro V, et al: Regorafenib as second-line therapy for intermediate or advanced hepatocellular carcinoma: multicentre, open-label, phase II safety study. *Eur J Cancer* 2013;49:3412–3419.
- ▶20 Kudo M: Regorafenib as second-line systemic therapy may change the treatment strategy and management paradigm for hepatocellular carcinoma. *Liver Cancer* 2016;5:235–244.
- ▶21 Kudo M: A new era of systemic therapy for hepatocellular carcinoma with regorafenib and lenvatinib. *Liver Cancer* 2017;6:177–184.
- 22 Kudo M, Ueshima K, Torimura T, Tanabe N, Ikeda M, Aikata H, Izumi N, et al: Randomized, open label, multicenter, phase II trial of transcatheter arterial chemoembolization (TACE) therapy in combination with sorafenib as compared with TACE alone in patients with hepatocellular carcinoma: TACTICS trial. ASCO-GI, 2018, Abstract No 206.

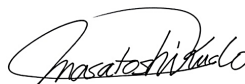
Editorial

Management of Hepatocellular Carcinoma in Japan as a World-Leading Model

Masatoshi Kudo

Department of Gastroenterology and Hepatology, Kindai University Faculty of Medicine, Osaka-Sayama, Japan

Prof. M. Kudo

Editor *Liver Cancer***Introduction**

Japan has achieved highly favorable outcomes in hepatocellular carcinoma (HCC) treatment. Several factors contributed to this achievement as shown in Tables 1 and 2. The establishment of a nationwide liver cancer screening program, which was developed in the 1980s and involves institutes across all over Japan, is one of such factors. For example, Japan was the first country in the world to develop and implement diagnostic ultrasound systems for liver cancer screening. In addition to the already established tumor marker α -fetoprotein (AFP), other markers such as protein induced by vitamin K absence or antagonist-II (PIVKA-II) and *Lens culinaris*-agglutinin-reactive fraction of AFP (AFP-L3) were developed in Japan. These two tumor markers were included among health insurance-covered screening tests in 1989 and 1994, respectively. Japan is the only country in the world in which these three tumor markers are included in routine surveillance under national health insurance without restrictions. Other important achievements in Japan include the invention of transcatheter arterial chemoembolization (TACE) [1], the development and the world's first commercialization of technetium-99m galactosyl human serum albumin liver scintigraphy for the assessment of hepatic functional reserve [2, 3], the world's first hepatectomy [4], the development of anatomic liver resection [5], and the invention of local ablation (percutaneous ethanol injection) [6] and percutaneous microwave coagulation therapy [7]. Japan also has the highest number of cases treated with radiofrequency ablation (RFA). Other methods developed in Japan include contrast-enhanced liver ultrasound (initially by intra-arterial

Masatoshi Kudo, MD, PhD
Department of Gastroenterology and Hepatology
Kindai University Faculty of Medicine
377-2 Ohno-Higashi, Osaka-Sayama 589-8511 (Japan)
E-Mail m-kudo@med.kindai.ac.jp

Table 1. Epoch-making developments, which were established in Japan first in the world

1949	World 1st case of anatomical right liver lobectomy (Prof. Ichio Honjo, Kyoto Univ.)
1950	Development of ultrasound machine (Japan Radio, later ALOKA Company)
1967	Foundation of LCSGJ, started nationwide survey (Dept. Surgery, Kyoto Univ.)
1971	Development of ultrasound electronic scanner (ALOKA company)
1978	Invention of TAE for HCC (Prof. Ryusaku Yamada)
1982	Invention of contrast-enhanced US (arterial) (Yasuo Matsuda, Masatoshi Kudo)
1982	Invention of color Doppler flow imaging (ALOKA Company)
1983	Invention of CTHA/CTAP (Prof. Osamu Matsui)
1983	Invention of PEIT (percutaneous ethanol injection therapy) (Nobuyuki Sugiura)
1985	Establishment of anatomical liver resection (Prof. Masatoshi Makuuchi)
1990	Superselective cTACE (Profs. Hideo Uchida, Hironobu Nakamura, Osamu Matsui)
1990	Invention of microwave coagulation therapy (Prof. Toshihito Seki)
1989	Approval and reimbursement of PIVKA-II (Eisai Company)
1992	Development of asialoglycoprotein receptor scintigraphy, reimbursement (Masatoshi Kudo)
1992	Establishment of pathological concept of early HCC (Prof. Masamichi Kojiro)
1992	Invention of fusion imaging and strain elastography (Hitachi Company)
1992	Discovery of PD-1 molecule (Prof. Tasuku Honjo, Kyoto Univ.)
1994	Approval and reimbursement of AFP-L3 fraction (Wako Company)
1995	Stop HCC campaign for general citizen and general physician started by the Japan Society of Hepatology (JSH)
2004	Establishment of integrated staging system, JIS score (Masatoshi Kudo)
2007	Approval of Sonazoid (Dai-ichi Sankyo) invention of re-injection method (Masatoshi Kudo)
2014	Nivolumab approved for melanoma (Ono Pharma) (under trial in HCC)
2017	Lenvatinib (Eisai) (positive phase 3 global trial in HCC presented at ASCO2017)

Table 2. Reasons why Japan established the world's best HCC practice system, different from other countries

Early HCC detection due to established nationwide surveillance
Free testing for HBsAg and HCV Ab anywhere in the clinic all over in Japan
Establishment of nationwide surveillance system by US and 3 tumor markers every 3 – 6 months for high-risk patients for HCC
Measurement of all 3 tumor markers (AFP, PIVKA-II, AFP-L3) are covered by insurance
MDCT and/or EOB-MRI every 6 – 12 months/year for super high risk is also covered by insurance
Stop the HCC campaign for general citizen and physicians every year by JSH has been established
Antiviral therapy
Interferon treatment, interferon-free DAA treatment for hepatitis C and nucleoside analogue for hepatitis B are specially covered by the Government (100 – 200 USD/month can be paid by patients)
All of the patients only infected to hepatitis B or hepatitis C can receive special reimbursement program
Establishment of precise diagnostic algorithm of HCC
Precise evaluation of intramodular hemodynamics by CTHA/CTAP or CEUS
Accurate pathological diagnosis, establishment of pathological diagnostic criteria of early HCC
Cooperative work between pathologist and clinician, image-pathology correlation
Skill of ultrasound diagnosis is superior to other country, ultrasound surveillance is easy since there are not many obese patients in Japan
Detection of very tiny nodule by extensive use of EOB-MRI and extensive effort on differential diagnosis between dysplastic nodule and early HCC leading to early treatment intervention
Unique US contrast agent, Sonazoid which have Kupffer phase makes it possible to accurate diagnosis and used as an accurate treatment guidance
Precise and accurate treatment selection and high quality treatment technique
Skill of resection, ablation, TACE and HAIC is better than other countries and outcome is best in the world
Multimodal approach together with hepatologist, radiologist, surgeon, and oncologist of these treatments
Especially hepatologist covers ablation, TACE, HAIC and systemic therapy as an organ specialist

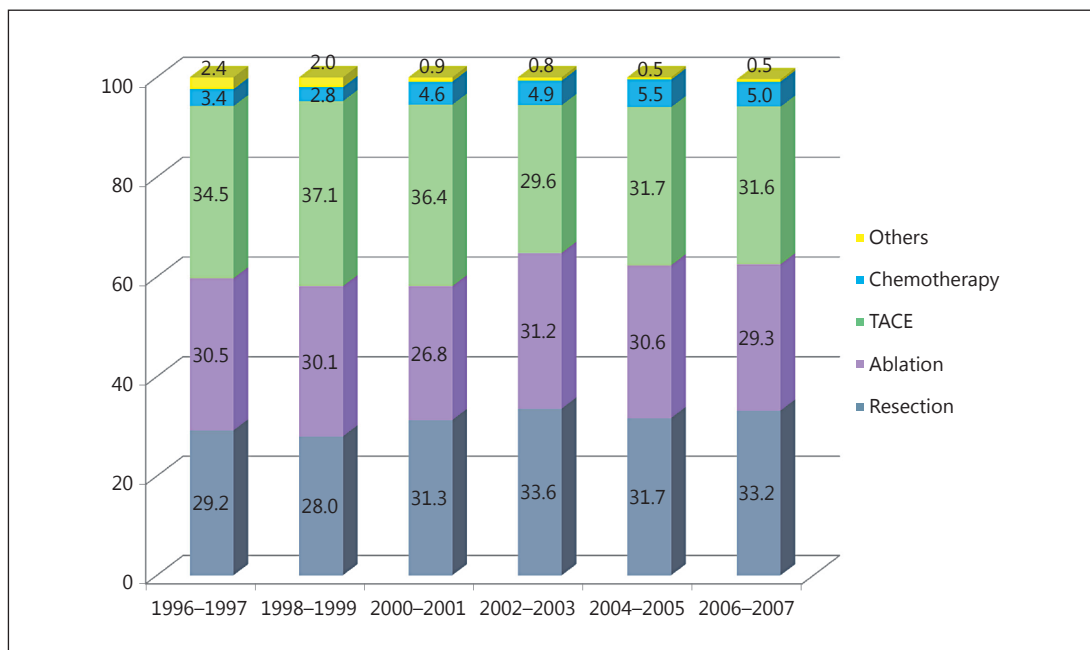


Fig. 1. Treatment modality for initially diagnosed HCC.

infusion of carbon dioxide microbubbles) [8, 9]; fusion imaging; perfluorobutane (Sonazoid), a unique ultrasound contrast agent that enables Kupffer-phase imaging; and defect reperfusion imaging using Sonazoid, which assists in screening, definitive diagnosis, and local ablation therapy [10].

Among several immunotherapies that garnered significant interest in recent years, PD-1 molecule was discovered by Prof. Tasuku Honjo of Kyoto University [11] and commercialized by Ono Pharmaceutical Co., Ltd. in Japan. A study investigating its use in the treatment of liver cancer is currently ongoing. Lenvatinib, a molecular-targeted agent discovered by Eisai Tsukuba Research Institute in Japan, was recently commercialized as an indication for thyroid cancer. The positive results of a trial that tested the efficacy of lenvatinib in liver cancer were reported at the 2017 annual meeting of the American Society of Clinical Oncology [12] followed by publication [13], and approval for this indication is currently pending.

Japan has made remarkable contributions to the screening, diagnosis, and treatment of liver cancer, and these have led to the best liver cancer treatment outcomes in the world. It is fair to say that the management of HCC in Japan sets a good example for the rest of the world, a fact acknowledged by HCC specialists globally.

Results of a Follow-Up Survey of the Nationwide Registry of HCC Patients by the Liver Cancer Study Group of Japan

In Japan, liver cancer screening by ultrasound and measurement of three tumor markers (AFP, PIVKA-II, and AFP-L3) is recommended every 3–4 months for super high-risk patients (cirrhosis caused by hepatitis B or hepatitis C virus) or every 6 months for high-risk patients (hepatitis B, hepatitis C, and nonviral cirrhosis) [14, 15]. For super high-risk patients, multi-detector-row computed tomography (MDCT) or gadolinium ethoxybenzyl diethylenetriamine pentaacetic acid magnetic resonance imaging (EOB-MRI) is recommended 1–2 times

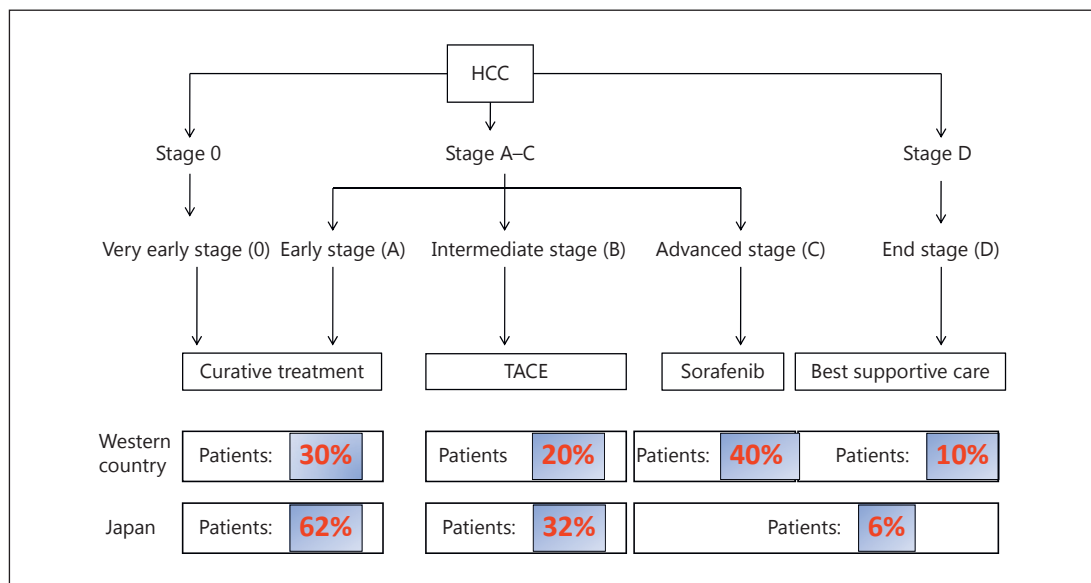


Fig. 2. BCLC stage at the initial detection of HCC: comparison between Western countries and Japan.

Table 3. Rate of BCLC 0 and A in various regions at the initial detection

Western countries	
Spain	10–30%
Italy	10–20%
United States	17%
Latin America	23%
Asian countries	
Japan	60–65%
South Korea	20–30%
Taiwan	10–20%
China	<10%
Other Asian countries	<5%

per year. Because of these comprehensive surveillance programs, of all cases at the initial diagnosis, 62.5% are curatively treatable early-stage HCC (Barcelona Clinic Liver Cancer [BCLC] stage 0 or A) that are treated by resection or RFA, 31.6% are intermediate-stage liver cancer and are treated by TACE (Fig. 1), and only 6% of cases are advanced HCC with vascular invasion or extrahepatic spread (BCLC stage C) or Child-Pugh grade C HCC (BCLC stage D) [16]. This is completely different from the status in Western countries, where 50% of cases are BCLC stage C or D at first detection, which corresponds to the average HCC population based on conventional BCLC staging (Fig. 2). These differences reflect the efficacy and advanced status of the HCC surveillance program in Japan. This system appears to be unique to Japan because the detection rates of curatively treatable HCC (BCLC stages 0–A) do not exceed 30% in other parts of Asia or in Western countries (Table 3), which could be attributed to the lack of established nationwide surveillance programs. This highlights the value of the established HCC surveillance program in Japan.

In the early 1980s, the HCC screening system in Japan was not as effective as the present system because of the limited capabilities of diagnostic imaging tools. Consequently, the 5-year survival rate and median survival time were unsatisfactory. Between 1978 and 1982,

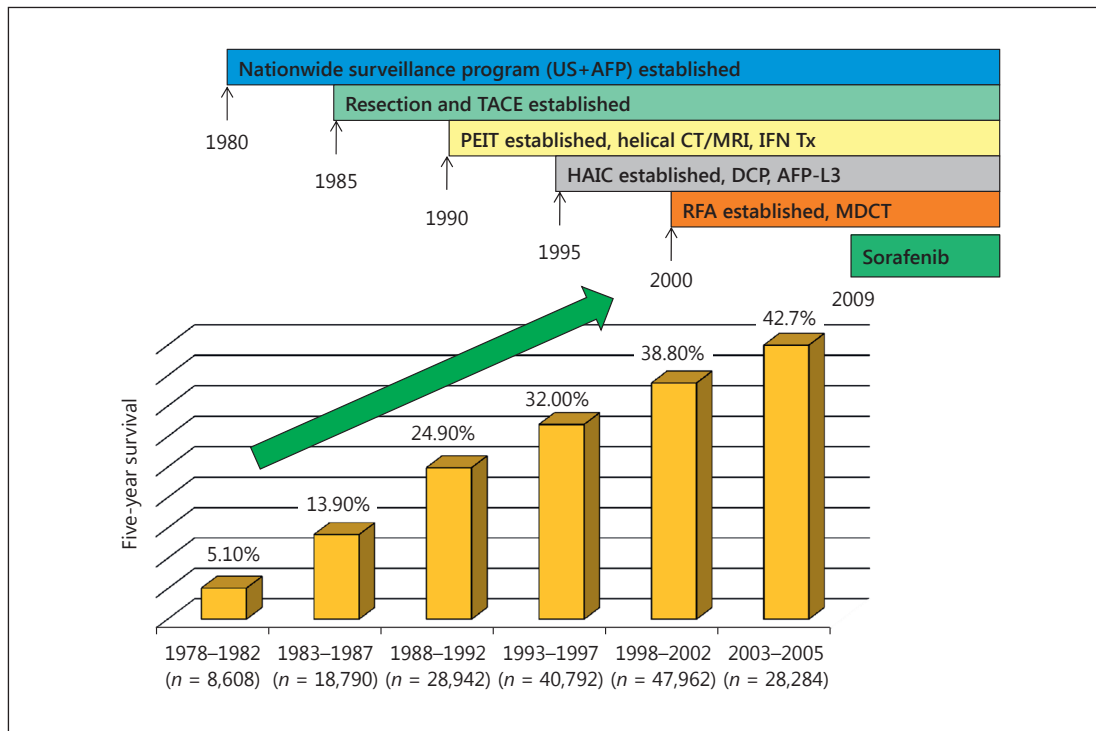


Fig. 3. Improvement of 5-year survival rate in patients with HCC. Results of the nationwide survey of the Liver Cancer Study Group of Japan ($n = 173,378$). MDCT, multidetector-row CT; PEIT, percutaneous ethanol injection therapy; IFN Tx, interferon treatment; DCP, des- γ -carboxy protein.

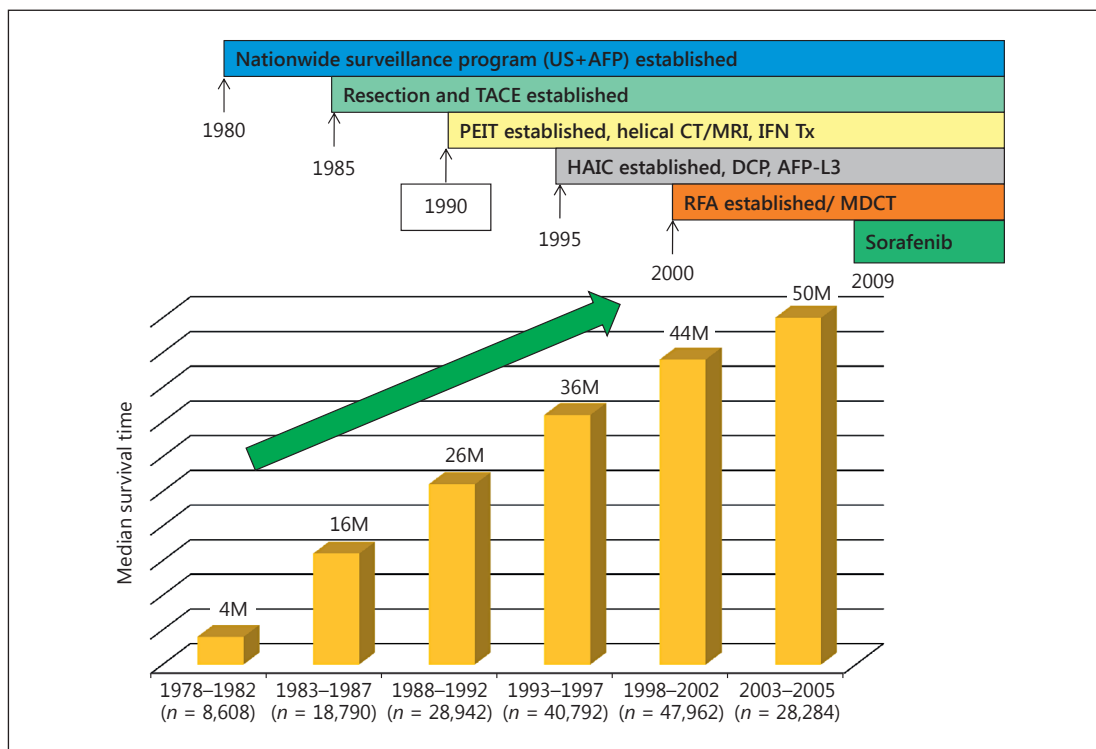


Fig. 4. Improvement of overall survival in patients with HCC. Results of the nationwide survey of the Liver Cancer Study Group of Japan ($n = 173,378$). M, months. For further abbreviations, see Figure 3.

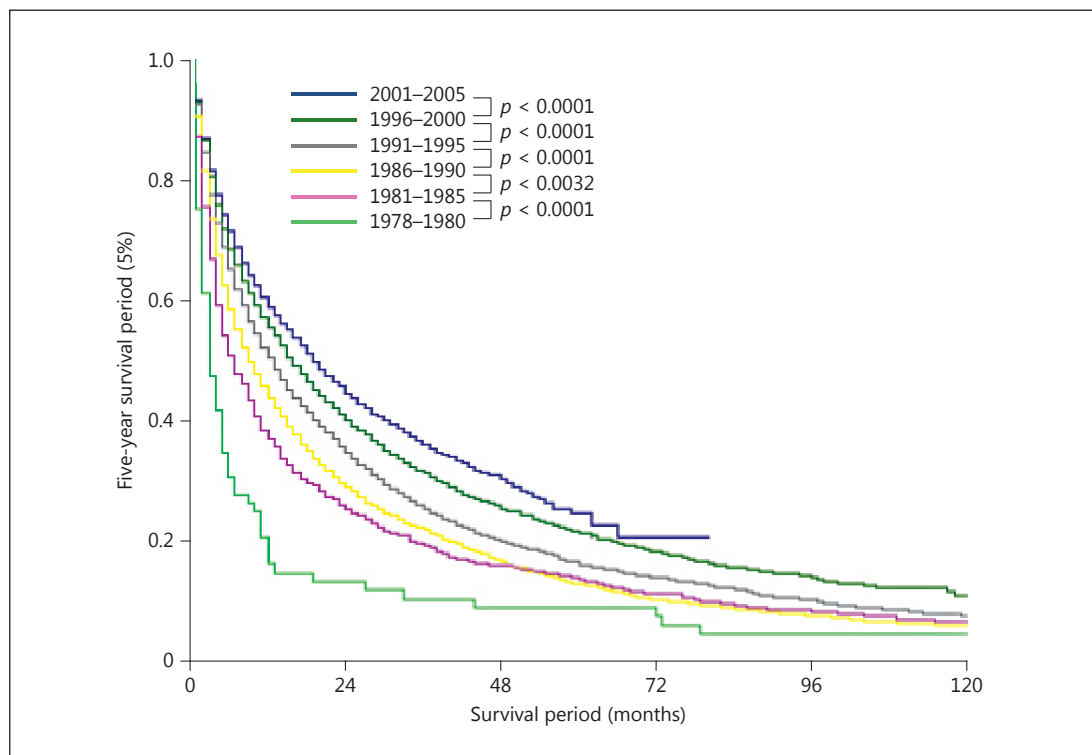


Fig. 5. Improvement of treatment outcome in HCC patients with AFP value ≥ 400 ng/mL.

the 5-year survival rate was 5.1%, and it gradually improved to 42.7% between 2003 and 2005. This increase was buoyed by rapid advances in diagnostic imaging technologies, the development of three tumor markers (AFP, PIVKA-II, and AFP-L3) with health insurance coverage, technological advances in surgery, and the development of local ablation therapy, TACE, and hepatic arterial infusion chemotherapy (HAIC) (Fig. 3). Similarly, the median survival time improved steadily from 4 months in the period of 1978–1982 to 50 months in the period of 2003–2005 (Fig. 4). These improvements were attributed to the establishment of the screening system, advances in diagnostic imaging enabling early detection of small tumors, and advanced therapeutic technologies. Indeed, assessment of the outcomes of resection, ablation, TACE, and HAIC in patients at 5-year intervals over 28 years shows a steady improvement in all modalities [17]. Moreover, the treatment outcomes of patients with poor prognostic indicators (AFP level ≥ 400 ng/mL) are also improving steadily (Fig. 5).

Implications of the Results of the GIDEON Study

A global prospective noninterventional observational study, GIDEON (global investigation of therapeutic decisions in HCC and of its treatment with sorafenib: NCT 00812175), examined HCC patients treated with sorafenib at 378 institutes in 39 countries (including 3,213 patients treated at 40 participating institutes in Japan). Subgroup analysis of a vast amount of GIDEON data detected regional differences in the characteristics of patients at the initial examination for HCC and in treatment outcomes according to BCLC stage in the Asia-Pacific region ($n = 955$), Europe ($n = 1,115$), Latin America ($n = 90$), the United States ($n = 553$), and Japan ($n = 500$) [18] (Table 4).

Table 4. Median time from initial diagnosis to death (in months) by BCLC stage at initial diagnosis

	AP (n = 955)	EU (n = 1,115)	LA n = 90	USA (n = 553)	Japan (n = 500)	Overall (n = 3,213) ^a
BCLC stage A (n = 686)	54.0 (10.3–NA)	49.3 (42.3–58.0)	23.3 (17.2–NA)	24.9 (18.4–53.5)	91.0 (76.6–113.1)	59.2 (51.9–67.5)
BCLC stage B (n = 633)	31.0 (18.4–47.7)	27.3 (23.0–33.1)	22.2 (12.9–NA)	19.7 (11.1–36.8)	47.9 (40.9–86.2)	29.9 (25.6–39.0)
BCLC stage C (n = 973)	10.3 (8.6–14.8)	11.0 (8.9–13.0)	11.2 (3.1–NA)	8.5 (6.2–10.2)	27.7 (16.6–40.8)	10.6 (9.4–12.4)
BCLC stage D (n = 91)	8.9 (8.6–14.8)	11.0 (4.2–21.7)	NA	7.5 (4.5–12.8)	13.1 (NA–NA)	8.9 (6.2–13.1)
Overall	20.9 (17.3–25.2)	25.0 (22.9–28.7)	19.5 (13.5–NA)	14.8 (13.1–17.0)	79.6 (62.1–96.0)	25.5 (23.9–28.3)

Figures in parentheses are 95% CI. AP, Asia-Pacific region; LA, Latin America; NA, not available. ^a Intention-to-treat population.

Notable regional differences were observed in the time between initial diagnosis and death. The median survival of HCC patients in Japan was 79.6 months, which was longer than that of patients in other regions (20.9 months in the Asia-Pacific region, 25.0 months in Europe, 19.5 months in Latin America, and 14.8 months in the United States). Although each BCLC stage group is expected to consist of homogeneous patients in terms of tumor burden and liver function, the median survival of patients with BCLC stage A HCC (curatively treatable early-stage disease) was 91.0 months in Japan, which is considerably longer than that in other regions (54.0 months in the Asia-Pacific region, 49.3 months in Europe, 23.3 months in Latin America, and 24.9 months in the United States) [18, 19].

Similarly, in patients with BCLC stage B HCC (multinodular disease with preserved hepatic functional reserve), the median survival was 47.9 months in Japan, which was markedly longer than that in other regions (31.0 months in the Asia-Pacific region, 27.3 months in Europe, 22.2 months in Latin America, and 19.7 months in the United States). In patients with BCLC stage C HCC (with vascular invasion and/or extrahepatic spread), the median survival was longer in Japan (27.7 months) than in other regions (8.5–11.2 months) (Table 4).

In patients with BCLC stage D HCC (terminal stage: hepatic functional reserve of Child-Pugh C HCC) who would generally receive palliative treatment, the median survival was still the longest in Japan (13.1 months) compared with that in other regions (7.5–11.0 months) [18, 19].

Collectively, treatment outcomes were better in Japan than in any other regions in all BCLC stage categories (A–D), each of which is thought to have a homogeneous patient population. This can be explained by Japan’s well-established nationwide screening system, which enables early detection of small tumors in many cases. Another reason is the accurate and comprehensive diagnostic imaging capabilities available in Japan, which facilitate the appropriate allocation of treatment strategies according to liver function and tumor burden/characteristics. The superior outcomes of patients with BCLC stage A HCC in Japan can be attributed to the technical superiority of resection and locoregional therapies. For example, indications for liver resection are based on stringent assessment of hepatic functional reserve, and in resectable cases, repeated resections are proactively performed even in cases of recurrence after first resection.

Similarly, a standard RFA procedure in Japan includes that post-RFA response evaluation is proactively performed using imaging technique such as MDCT, contrast-enhanced ultrasonography, or EOB-MRI on the same day immediately after RFA procedure or the day after RFA to confirm that a complete tumor necrosis with a sufficient ablative margin is achieved. If the margin is not satisfactory, RFA is repeated until an adequate ablative margin is obtained and complete response is achieved during a single hospital stay. The rate of complete response, either in theory or in practice, is therefore 100% in Japan. However, these procedures are different in Western countries. In Western countries, response evaluation CT is usually performed at approximately 1 month after RFA to assess the therapeutic effect, and intrahepatic microscopic spread originating from the residual tumor or local recurrence might occur during that period. So, achieving complete response at a single hospital stay is a key point to reduce local recurrence as well as intrahepatic spread.

In patients with intermediate-stage (BCLC stage B) HCC who would typically undergo TACE, the number and size of nodules tend to be smaller in Japan than in Western and other Asian countries because of the beneficial effects of early detection of HCC in Japan. Therefore, patients can be treated by superselective conventional TACE (cTACE) with iodized oil (Lipiodol®). During this procedure, a catheter is inserted into a feeding artery in close proximity to the feeding artery of each multinodular tumor. The Lipiodol injection within the feeding artery close to the tumors causes reflux of Lipiodol from the hepatic artery into the portal branches through physiologic arterioportal communications in the peribiliary plexus, thereby temporarily blocking portal flow. The subsequent placement of a gelatin sponge at the arterial side blocks arterial and portal blood flow; the resulting transient liver infarction, albeit on a small scale, can cause complete necrosis of subcapsular viable lesions, extracapsular growth, and even microsattellite lesions, which would not be treated by arterial occlusion alone. Furthermore, superselective embolization minimizes the impairment of hepatic functional reserve, allowing repeated TACE and improving prognosis. Superselective cTACE, in addition to resection, liver transplantation, and ablation, is categorized into one of the curative treatment modalities for patients with HCC included in the up-to-seven criteria in Japan [20]. This technique is not widely used in Europe and North America; however, given that many intermediate-stage HCC patients in these regions present with numerous nodules (≥ 10) in both lobes or with a large tumor, the superselective cTACE procedure cannot be applied.

The BCLC stage C population, comprising patients with advanced HCC characterized by vascular invasion and/or extrahepatic spread, is relatively homogeneous compared with BCLC stage 0, A, and B populations; therefore, patients with the same stage disease are expected to have similar prognoses. Indeed, the median survival of these patients in Europe, Asia, Latin America, and the United States (8.5–11.2 months) is reasonable and similar to that in the sorafenib and placebo groups of the SHARP study. Why then does Japan have such an outstandingly better median survival (27.7 months)? According to Japanese guidelines [15], HCC specialists in Japan opt for resection for the treatment of HCC even in cases with vascular invasion, provided that tumor conditions and liver function meet the requirements in selected patients. Propensity score-matching analysis shows that vascular invasion-positive patients who undergo resection have a better prognosis than those treated with other modalities [21, 22]. Similarly, TACE is preferred over molecular-targeted therapy because of its strong necrotizing effect in many cases of HCC with minor vascular invasion (Vp1, 2) that meet liver function criteria. The benefits of TACE in patients with vascular invasion were demonstrated in a systematic review [23]. Another unique treatment approach for vascular invasion in Japan is HAIC. This modality has not been tested in a prospective study and is not globally recognized as a standard of care.

Although it is only performed in Japan, South Korea, and Taiwan, it showed beneficial effects in the selected HCC patients with vascular invasion [24]. Propensity score-matching

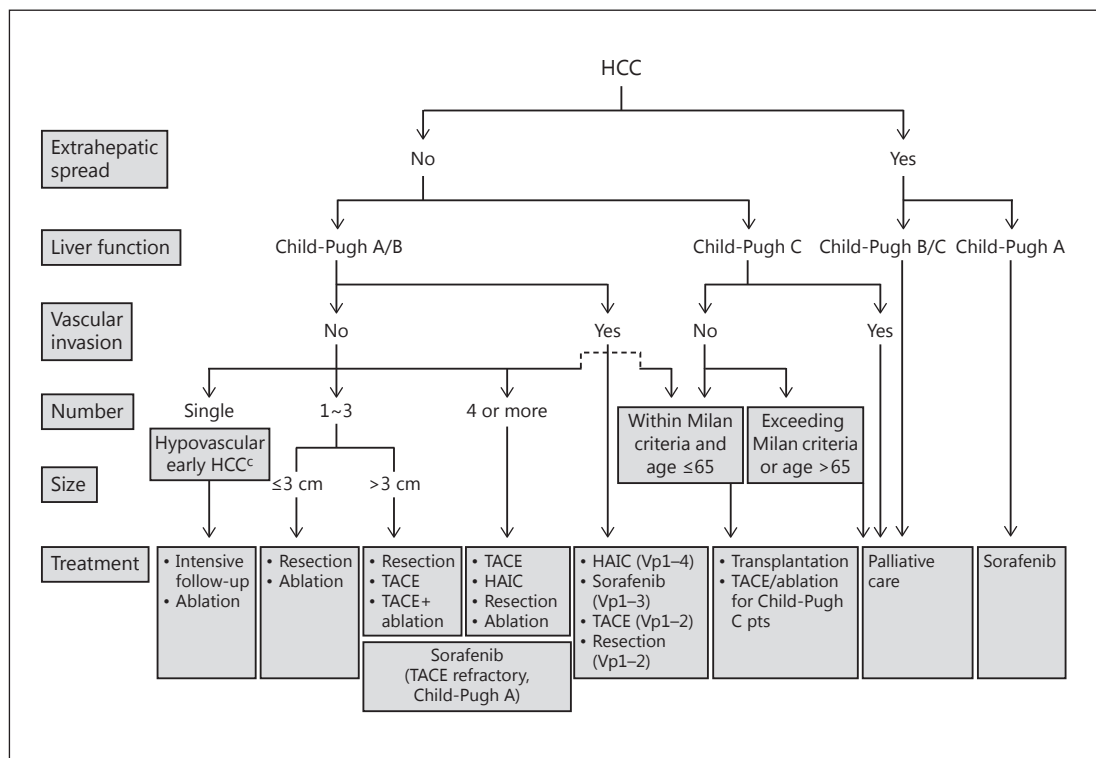


Fig. 6. The Japan Society of Hepatology consensus-based HCC treatment algorithm.

analysis of data collected through a nationwide follow-up survey of primary liver cancer by the Liver Cancer Study Group of Japan showed that patients with HCC with vascular invasion treated with HAIC had a better prognosis than those treated with other therapies [25]. As reported at the European Association for the Study of the Liver (EASL) International Liver Congress 2016, the SILIUS trial, which compared sorafenib alone with sorafenib plus HAIC in patients with a tumor thrombus in the main trunk of the portal vein (Vp4, a stratification factor), showed that additional HAIC extended median survival from 6.5 to 11.4 months (hazard ratio = 0.493, 95% confidence interval = 0.240–1.014, $p = 0.050$) [26]. Given the typical survival of 2–3 months in Vp4 HCC patients [27], these results suggest that HAIC provides additional clinically meaningful benefits to the moderate survival extension by sorafenib alone. Taken together, resection, TACE, and HAIC, in addition to molecular-targeted therapy, are more readily used in the treatment of HCC with vascular invasion in Japan, albeit in selected cases only, than in other regions, which may prolong overall survival in BCLC C HCC patients. Moreover, because intrahepatic lesions are a strong prognostic factor in HCC, even in cases with extrahepatic spread [23], locoregional therapy, such as TACE and HAIC, is frequently performed in these patients, and this may contribute to the favorable treatment outcomes of patients with advanced HCC in Japan. Indeed, a trial of second-line S-1 versus placebo in HCC patients refractory or intolerant to sorafenib conducted only in Japan (S-CUBE trial) showed a survival of 11.3 months in the placebo arm [28], which was longer than the survival times in similar placebo groups in other second-line trials conducted globally (BRISK-PS, 8.2 months; EVOLVE-1, 7.3 months; and REACH, 7.6 months) [29–31]. Furthermore, compared with first-line trials conducted globally, the placebo arm in the S-CUBE trial showed the longest survival, even in comparison with the survival of patients treated with sorafenib (SUN1170, 10.2 months; BRISK-FL, 9.9 months; and LiGHT, 9.8 months) [32–34]. It is likely

Table 5. Overall survival of HCC by country

Country	Period	5-year overall survival, %
Japan [40]	1998–2007	44.1
Korea ^a	2004–2008	23.3
Taiwan ^b	2010–2013	22
United States [41–44]	1992–2008	11–15

^a Ministry of Health & Welfare, The Korean Cancer Registry, 2010. ^b Cancer Registry, Taiwan 2001–2005.

that as the clinical practice guidelines in Japan recommend resection, TACE, and HAIC for the patients with advanced HCC (Fig. 6), these proactive strategies may result in a considerable improvement in the survival of patients with advanced HCC.

The survival of patients with end-stage HCC (BCLC stage D or Child-Pugh class C) is also longer in Japan than in other countries. A follow-up survey by the Liver Cancer Study Group of Japan revealed that approximately half of Child-Pugh class C HCC patients in Japan receive locoregional therapy (resection, ablation, and TACE, or HAIC). Propensity score-matching analysis of data from this follow-up survey showed that local ablation therapies and TACE improve survival in patients with a Child-Pugh score of 10 or 11 [35], consistent with other multicenter or single-center studies [36–39]. In Japan, locoregional therapy is used in routine clinical practice for carefully selected patients with Child-Pugh C HCC within the Milan criteria, and TACE and ablation appear to be beneficial in such patients. This is why the consensus-based clinical practice guidelines of the Japan Society of Hepatology include TACE and ablation as treatment options for Child-Pugh C HCC patients after careful patient selection [15].

Analysis of data from the GIDEON study also showed that survival, even in BCLC stage D HCC patients, was better in Japan than in other regions, reflecting the unique clinical practice pattern for HCC management and the consequent favorable treatment outcomes in Japan.

Comparison of the Outcomes of HCC Treatments among Countries

Only a few countries publish nationwide HCC treatment outcomes. The 5-year survival rate of all HCCs in Japan is 44.1% [40], which is outstanding compared with the rates in other countries that published in the corresponding period (23.3% in South Korea, 22% in Taiwan, and 11–15% in the United States) [41–44] (Table 5).

Total Number of Deaths from HCC in Japan

The total number of deaths from HCC peaked in 2004 (34,510 deaths), and then gradually decreased to a number lower than that of deaths from pancreatic cancer in 2013 (30,175 vs. 30,672 deaths). This trend continued in 2014 and 2015, and the number of HCC deaths fell below 30,000 (28,889 deaths) in 2015 (Fig. 7). Early detection of HCC by established surveillance programs and the resulting high rate of opportunities for receiving curative treatment are clear contributing factors. Another likely reason is that most hepatitis B patients are treated with a nucleoside or nucleotide analogue. Disease progression to HCC is inhibited and liver function is preserved even after progression to HCC in these patients, which increases the therapeutic options and opportunities for repeated treatment. Similarly, the eradication of the hepatitis C virus by interferon-based therapy and interferon-free direct-acting anti-

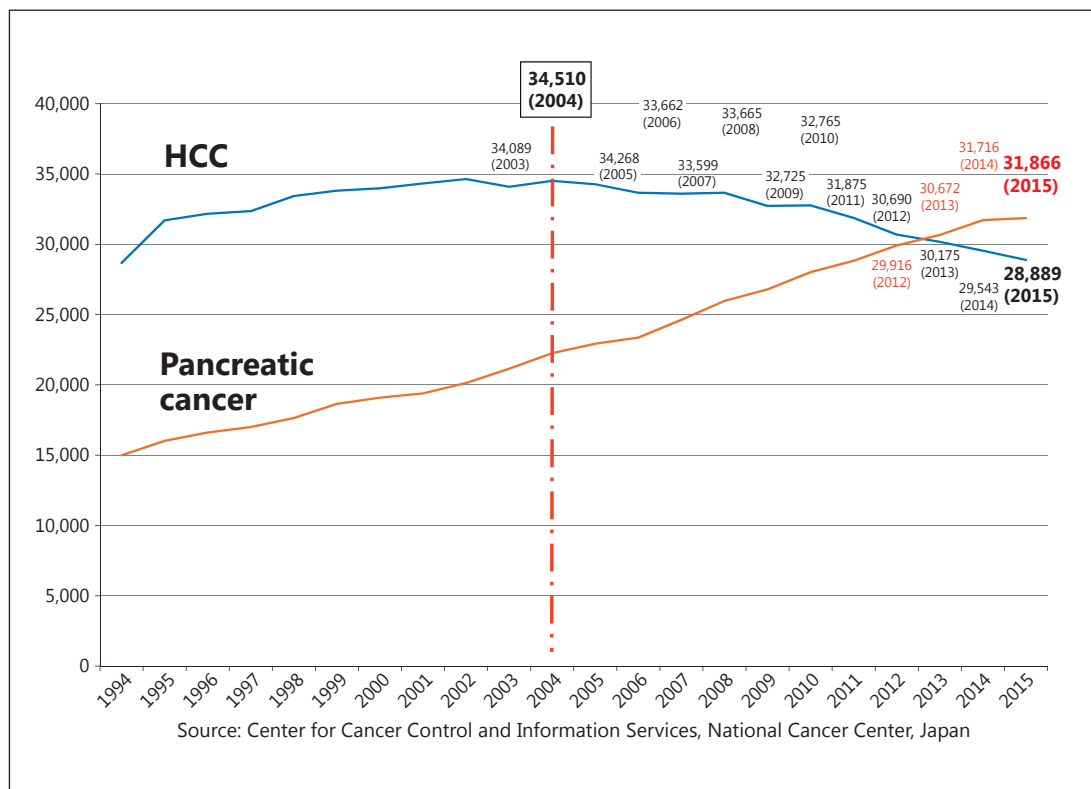


Fig. 7. Trend in HCC mortality in Japan.

virals contributes to suppressing the incidence of HCC. In addition, viral eradication, which is defined by a sustained virologic response, is likely to play a crucial role in inhibiting recurrence and maintaining hepatic functional reserve after curative treatment for HCC. Furthermore, the inclusion of the hepatitis B vaccine in the vaccination program for newborns in 1986 undoubtedly had some impact.

Conclusion

Japan leads the world in HCC treatment outcomes, which can be attributed to numerous achievements by Japanese pioneers in HCC treatment, the establishment of a nationwide surveillance system, precise diagnosis (confirmation, staging, use of contrast-enhanced ultrasound and EOB-MRI, and highly precise pathological diagnosis), and sophisticated treatment strategies (anatomic liver resection, contrast-enhanced ultrasound-assisted or fusion imaging-assisted RFA, RFA techniques that achieve adequate ablation margins, the proactive use of superselective cTACE, and intra-arterial infusion chemotherapy). In this respect, Japan is undoubtedly a suitable model for the world in HCC management [16]. The prognosis of liver cancer patients in Japan will improve further continuously, when additional molecular-targeted agents such as regorafenib [45] or lenvatinib [46], or even immunotherapy [47], become available in clinical practice for the treatment of HCC.

References

- 1 Yamada R, Sato M, Kawabata M, Nakatsuka H, Nakamura K, Takashima S: Hepatic artery embolization in 120 patients with unresectable hepatoma. *Radiology* 1983;148:397–401.
- 2 Kudo M, Vera DR, Trudeau WL, Stadalnik RC: Validation of in vivo receptor measurements via in vitro radioassay: technetium-99m-galactosyl-neoglycoalbumin as prototype model. *J Nucl Med* 1991;32:1177–1182.
- 3 Kudo M, Todo A, Ikekubo K, Yamamoto K, Vera DR, Stadalnik RC: Quantitative assessment of hepatocellular function through in vivo radioreceptor imaging with technetium 99m galactosyl human serum albumin. *Hepatology* 1993;17:814–819.
- 4 Honjo I, Araki C: Total resection of the right lobe of the liver; report of a successful case. *J Int Coll Surg* 1955;23:23–28.
- 5 Makuuchi M, Hasegawa H, Yamazaki S: Ultrasonically guided subsegmentectomy. *Surg Gynecol Obstet* 1985;161:346–350.
- 6 Sugiura NTK, Ohto M, et al: Ultrasound image-guided percutaneous intratumor ethanol injection for small hepatocellular carcinoma. *Acta Hepatol Jpn* 1983;24:920.
- 7 Seki T, Wakabayashi M, Nakagawa T, Itho T, Shiro T, Kunieda K, Sato M, Uchiyama S, Inoue K: Ultrasonically guided percutaneous microwave coagulation therapy for small hepatocellular carcinoma. *Cancer* 1994;74:817–825.
- 8 Kudo M, Tomita S, Tochio H, Mimura J, Okabe Y, Kashida H, Hirasa M, Ibuki Y, Todo A: Sonography with intra-arterial infusion of carbon dioxide microbubbles (sonographic angiography): value in differential diagnosis of hepatic tumors. *AJR Am J Roentgenol* 1992;158:65–74.
- 9 Kudo M, Tomita S, Tochio H, Mimura J, Okabe Y, Kashida H, Hirasa M, Ibuki Y, Todo A: Small hepatocellular carcinoma: diagnosis with US angiography with intraarterial CO₂ microbubbles. *Radiology* 1992;182:155–160.
- 10 Kudo M: Defect reperfusion imaging with Sonazoid®: a breakthrough in hepatocellular carcinoma. *Liver Cancer* 2016;5:1–7.
- 11 Ishida Y, Agata Y, Shibahara K, Honjo T: Induced expression of PD-1, a novel member of the immunoglobulin gene superfamily, upon programmed cell death. *EMBO J* 1992;11:3887–3895.
- 12 Cheng A, Finn R, Qin S, et al: Phase III trial of lenvatinib (LEN) vs sorafenib (SOR) in first-line treatment of patients (pts) with unresectable hepatocellular carcinoma (uHCC). *J Clin Oncol* 2017;35(suppl;abstr 4001).
- 13 Kudo M, Finn RS, Qin S, Han KH, Ikeda K, Piscaglia F, Baron AD, Park JW, Han G, Jassem J, Blanc JF, Vogel A, Komov D, Evans TJ, Lopez C, Dutcus C, Guo M, Saito K, Kraljevic S, Tamai T, Ren M, Cheng AL: A randomised phase 3 trial of lenvatinib vs. sorafenib in first-line treatment of patients with unresectable hepatocellular carcinoma. *Lancet* 2017, in press.
- 14 Kokudo N, Hasegawa K, Akahane M, Igaki H, Izumi N, Ichida T, Uemoto S, Kaneko S, Kawasaki S, Ku Y, Kudo M, Kubo S, Takayama T, Tateishi R, Fukuda T, Matsui O, Matsuyama Y, Murakami T, Arii S, Okazaki M, Makuuchi M: Evidence-Based Clinical Practice Guidelines for Hepatocellular Carcinoma: the Japan Society of Hepatology 2013 update (3rd JSH-HCC Guidelines). *Hepatol Res* 2015;45, DOI: 10.1111/hepr.12464.
- 15 Kudo M, Matsui O, Izumi N, Iijima H, Kadoya M, Imai Y, Okusaka T, Miyayama S, Tsuchiya K, Ueshima K, Hiraoka A, Ikeda M, Ogasawara S, Yamashita T, Minami T, Yamakado K: JSH consensus-based clinical practice guidelines for the management of hepatocellular carcinoma: 2014 update by the Liver Cancer Study Group of Japan. *Liver Cancer* 2014;3:458–468.
- 16 Kudo M: Japan's successful model of nationwide hepatocellular carcinoma surveillance highlighting the urgent need for global surveillance. *Liver Cancer* 2012;1:141–143.
- 17 Kudo M, Izumi N, Sakamoto M, Matsuyama Y, Ichida T, Nakashima O, Matsui O, Ku Y, Kokudo N, Makuuchi M: Survival analysis over 28 years of 173,378 patients with hepatocellular carcinoma in Japan. *Liver Cancer* 2016;5:190–197.
- 18 Kudo M, Lencioni R, Marrero JA, Venook AP, Bronowicki JP, Chen XP, Dagher L, Furuse J, Geschwind JF, Ladron de Guevara L, Papandreou C, Sanyal AJ, Takayama T, Yoon SK, Nakajima K, Lehr R, Heldner S, Ye SL: Regional differences in sorafenib-treated patients with hepatocellular carcinoma: GIDEON observational study. *Liver Int* 2016;36:1196–1205.
- 19 Kudo M, Ikeda M, Takayama T, Numata K, Izumi N, Furuse J, Okusaka T, Kadoya M, Yamashita S, Ito Y, Kokudo N: Safety and efficacy of sorafenib in Japanese patients with hepatocellular carcinoma in clinical practice: a subgroup analysis of GIDEON. *J Gastroenterol* 2016;51:1150–1160.
- 20 Kudo M, Arizumi T, Ueshima K, Sakurai T, Kitano M, Nishida N: Subclassification of BCLC B stage hepatocellular carcinoma and treatment strategies: proposal of modified Bolondi's subclassification (Kinki criteria). *Dig Dis* 2015;33:751–758.
- 21 Kokudo T, Hasegawa K, Matsuyama Y, Takayama T, Izumi N, Kadoya M, Kudo M, Ku Y, Sakamoto M, Nakashima O, Kaneko S, Kokudo N: Survival benefit of liver resection for hepatocellular carcinoma associated with portal vein invasion. *J Hepatol* 2016;65:938–943.
- 22 Kokudo T, Hasegawa K, Matsuyama Y, Takayama T, Izumi N, Kadoya M, Kudo M, Kubo S, Sakamoto M, Nakashima O, Kumada T, Kokudo N: Liver resection for hepatocellular carcinoma associated with hepatic vein invasion: a Japanese nationwide survey. *Hepatology* 2017;66:510–517.

- 23 Zhao Y, Cai G, Zhou L, Liu L, Qi X, Bai M, Li Y, Fan D, Han G: Transarterial chemoembolization in hepatocellular carcinoma with vascular invasion or extrahepatic metastasis: a systematic review. *Asia Pac J Clin Oncol* 2013; 9:357–364.
- 24 Obi S, Yoshida H, Toune R, Unuma T, Kanda M, Sato S, Tateishi R, Teratani T, Shiina S, Omata M: Combination therapy of intraarterial 5-fluorouracil and systemic interferon-alpha for advanced hepatocellular carcinoma with portal venous invasion. *Cancer* 2006;106:1990–1997.
- 25 Nouse K, Miyahara K, Uchida D, Kuwaki K, Izumi N, Omata M, Ichida T, Kudo M, Ku Y, Kokudo N, Sakamoto M, Nakashima O, Takayama T, Matsui O, Matsuyama Y, Yamamoto K: Effect of hepatic arterial infusion chemotherapy of 5-fluorouracil and cisplatin for advanced hepatocellular carcinoma in the Nationwide Survey of Primary Liver Cancer in Japan. *Br J Cancer* 2013;109:1904–1907.
- 26 Kudo M, Ueshima K, Yokosuka O, Obi S, Izumi N, Aikata H, Nagano H, Hatano E, Sasaki Y, Hino K, Kumada T, Yamamoto K, Imai Y, Iwadou S, Ogawa C, Okusaka T, Arai Y, Kanai F, Akazawa K, SILIUS Study Group: Prospective randomized controlled phase III trial comparing the efficacy of sorafenib versus sorafenib in combination with low-dose cisplatin/fluorouracil hepatic arterial infusion chemotherapy in patients with advanced hepatocellular carcinoma. *J Hepatol* 2016;64:S209–S210.
- 27 Chung GE, Lee JH, Kim HY, Hwang SY, Kim JS, Chung JW, Yoon JH, Lee HS, Kim YJ: Transarterial chemoembolization can be safely performed in patients with hepatocellular carcinoma invading the main portal vein and may improve the overall survival. *Radiology* 2011;258:627–634.
- 28 Kudo M, Moriguchi M, Numata K, Hidaka H, Tanaka H, Ikeda M, Kawazoe S, Ohkawa S, Sato Y, Kaneko S, Furuse J, Takeuchi M, Fang X, Date Y, Takeuchi M, Okusaka T: S-1 versus placebo in patients with sorafenib-refractory advanced hepatocellular carcinoma (S-CUBE): a randomised, double-blind, multicentre, phase 3 trial. *Lancet Gastroenterol Hepatol* 2017;2:407–417.
- 29 Llovet JM, Decaens T, Raoul JL, Boucher E, Kudo M, Chang C, Kang YK, Assenat E, Lim HY, Boige V, Mathurin P, Fartoux L, Lin DY, Bruix J, Poon RT, Sherman M, Blanc JF, Finn RS, Tak WY, Chao Y, Ezzeddine R, Liu D, Walters I, Park JW: Brivanib in patients with advanced hepatocellular carcinoma who were intolerant to sorafenib or for whom sorafenib failed: results from the randomized phase III BRISK-PS study. *J Clin Oncol* 2013;31:3509–3516.
- 30 Zhu AX, Kudo M, Assenat E, Cattani S, Kang YK, Lim HY, Poon RT, Blanc JF, Vogel A, Chen CL, Dorval E, Peck-Radosavljevic M, Santoro A, Daniele B, Furuse J, Jappe A, Perraud K, Anak O, Sellami DB, Chen LT: Effect of everolimus on survival in advanced hepatocellular carcinoma after failure of sorafenib: the EVOLVE-1 randomized clinical trial. *JAMA* 2014;312:57–67.
- 31 Zhu AX, Park JO, Ryoo BY, Yen CJ, Poon R, Pastorelli D, Blanc JF, Chung HC, Baron AD, Pfiffer TE, Okusaka T, Kubackova K, Trojan J, Sastre J, Chau I, Chang SC, Abada PB, Yang L, Schwartz JD, Kudo M: Ramucirumab versus placebo as second-line treatment in patients with advanced hepatocellular carcinoma following first-line therapy with sorafenib (REACH): a randomised, double-blind, multicentre, phase 3 trial. *Lancet Oncol* 2015; 16:859–870.
- 32 Cheng AL, Kang YK, Lin DY, Park JW, Kudo M, Qin S, Chung HC, Song X, Xu J, Poggi G, Omata M, Pitman Lowenthal S, Lanzalone S, Yang L, Lechuga MJ, Raymond E: Sunitinib versus sorafenib in advanced hepatocellular cancer: results of a randomized phase III trial. *J Clin Oncol* 2013;31:4067–4075.
- 33 Johnson PJ, Qin S, Park JW, Poon RT, Raoul JL, Philip PA, Hsu CH, Hu TH, Heo J, Xu J, Lu L, Chao Y, Boucher E, Han KH, Paik SW, Robles-Avina J, Kudo M, Yan L, Sobhonslidsuk A, Komov D, Decaens T, Tak WY, Jeng LB, Liu D, Ezzeddine R, Walters I, Cheng AL: Brivanib versus sorafenib as first-line therapy in patients with unresectable, advanced hepatocellular carcinoma: results from the randomized phase III BRISK-FL study. *J Clin Oncol* 2013;31:3517–3524.
- 34 Cainap C, Qin S, Huang WT, Chung IJ, Pan H, Cheng Y, Kudo M, Kang YK, Chen PJ, Toh HC, Gorbunova V, Eskens FA, Qian J, McKee MD, Ricker JL, Carlson DM, El-Nowiem S: Linifanib versus sorafenib in patients with advanced hepatocellular carcinoma: results of a randomized phase III trial. *J Clin Oncol* 2015;33:172–179.
- 35 Kitai S, Kudo M, Nishida N, Izumi N, Sakamoto M, Matsuyama Y, Ichida T, Nakashima O, Matsui O, Ku Y, Kokudo N, Makuuchi M, Liver Cancer Study Group of Japan: Survival benefit of locoregional treatment for hepatocellular carcinoma with advanced liver cirrhosis. *Liver Cancer* 2016;5:175–189.
- 36 Nishikawa H, Kita R, Kimura T, Ohara Y, Takeda H, Sakamoto A, Saito S, Nishijima N, Nasu A, Komekado H, Osaki Y: Clinical efficacy of non-transplant therapies in patients with hepatocellular carcinoma with Child-Pugh C liver cirrhosis. *Anticancer Res* 2014;34:3039–3044.
- 37 Nouse K, Kokudo N, Tanaka M, Kuromatsu R, Nishikawa H, Toyoda H, Oishi N, Kuwaki K, Kusanaga M, Sakaguchi T, Morise Z, Kitai S, Kudo M: Treatment of hepatocellular carcinoma with Child-Pugh C cirrhosis. *Oncology* 2014;87(suppl 1):99–103.
- 38 Nouse K, Ito Y, Kuwaki K, Kobayashi Y, Nakamura S, Ohashi Y, Yamamoto K: Prognostic factors and treatment effects for hepatocellular carcinoma in Child C cirrhosis. *Br J Cancer* 2008;98:1161–1165.
- 39 Kudo M, Osaki Y, Matsunaga T, Kasugai H, Oka H, Seki T: Hepatocellular carcinoma in Child-Pugh C cirrhosis: prognostic factors and survival benefit of nontransplant treatments. *Dig Dis* 2013;31:490–498.
- 40 Kudo M, Izumi N, Ichida T, Ku Y, Kokudo N, Sakamoto M, Takayama T, Nakashima O, Matsui O, Matsuyama Y: Report of the 19th follow-up survey of primary liver cancer in Japan. *Hepatol Res* 2016;46:372–390.
- 41 Altekruse SF, McGlynn KA, Dickie LA, Kleiner DE: Hepatocellular carcinoma confirmation, treatment, and survival in surveillance, epidemiology, and end results registries, 1992–2008. *Hepatology* 2012;55:476–482.

- 42 Ries LAG, Melbert D, Krapcho M, et al (eds): SEER Cancer Statistics Review, 1975–2005, National Cancer Institute, Bethesda, MD. seer.cancer.gov/csr/1975_2005/, seer.cancer.gov/csr/1975_2008/ (accessed February 27, 2012).
- 43 American Cancer Society: Cancer Facts and Figures 2012. <https://www.cancer.org/research/cancer-facts-statistics/all-cancer-facts-figures/cancer-facts-figures-2012.html>.
- 44 El-Serag HB: Hepatocellular carcinoma. *N Engl J Med* 2011;365:1118–1127.
- 45 Bruix J, Qin S, Merle P, Granito A, Huang YH, Bodoky G, Pracht M, Yokosuka O, Rosmorduc O, Breder V, Gerolami R, Masi G, Ross PJ, Song T, Bronowicki JP, Ollivier-Hourmand I, Kudo M, Cheng AL, Llovet JM, Finn RS, LeBerre MA, Baumhauer A, Meinhardt G, Han G: Regorafenib for patients with hepatocellular carcinoma who progressed on sorafenib treatment (RESORCE): a randomised, double-blind, placebo-controlled, phase 3 trial. *Lancet* 2017;389:56–66.
- 46 Kudo M, Finn RS, Qin S, Han KH, Ikeda K, Piscaglia F, Baron A, Park JW, Han G, Jassem J, Blanc JF, Vogel A, Komov D, Evans J, Lopez C, Dutcus C, Guo M, Saito K, Kraljevic S, Tamai T, Ren M, Cheng AL: A randomised Phase 3 trial of lenvatinib vs sorafenib in first-line treatment of patients with unresectable hepatocellular carcinoma. *Lancet* 2017, in press.
- 47 El-Khoueiry AB, Sangro B, Yau T, Crocenzi TS, Kudo M, Hsu C, Kim TY, Choo SP, Trojan J, Welling THR, Meyer T, Kang YK, Yeo W, Chopra A, Anderson J, Dela Cruz C, Lang L, Neely J, Tang H, Dastani HB, Melero I: Nivolumab in patients with advanced hepatocellular carcinoma (CheckMate 040): an open-label, non-comparative, phase 1/2 dose escalation and expansion trial. *Lancet* 2017;389:2492–2502.

Utility of endoscopic ultrasound in hemorrhage from recurrent duodenal varices

Shigenaga Matsui, Hiroshi Kashida, Masatoshi Kudo

Kindai University Faculty of Medicine, Japan

A 69-year-old woman with medical history of endoscopic variceal ligation (EVL) of hemorrhagic duodenal varices at another hospital was transferred to our institution with hematemesis. Gastrointestinal endoscopy revealed a flat, scarred, post-EVL lesion in the second section of the duodenum (Fig. 1A). There were no other hemorrhagic lesions. Endoscopic ultrasound (EUS) revealed duodenal varices in the submucosal layer under the post-EVL lesion (Fig. 1B). Therefore, hemorrhage from recurrent duodenal varices was suspected. We performed endoscopic injection sclerotherapy (EIS) using a mixture of 1.5 mL N-butyl-2-cyanoacrylate (CA) and 0.5 mL Lipiodol at the post-EVL lesion (Fig. 1C). X-ray and computed tomography after EIS showed that the injected CA occupied the duodenal varices (Fig. 2A,B). No rebleeding was observed after EIS.

Management of hemorrhage from duodenal varices can be challenging because of the difficulty of treatment. Endoscopic procedures, such as EIS with CA, EVL and clip, are less invasive compared to surgery or interventional radiology [1,2]. EUS can improve the detection and diagnosis of duodenal varices and collateral veins, and can facilitate the intravariceal injection of duodenal varices by techniques such as EIS. EUS is useful for revealing recurrence and helps in the management of duodenal varices.

Department of Gastroenterology and Hepatology, Kindai University Faculty of Medicine, Japan

Correspondence to: Shigenaga Matsui, MD, PhD, Department of Gastroenterology and Hepatology, Kindai University Faculty of Medicine, Osaka, Japan, e-mail: ma2i@med.kindai.ac.jp

Conflict of Interest: None

Received 29 April 2018; accepted 30 May 2018; published online 12 July 2018

DOI: <https://doi.org/10.20524/aog.2018.0289>

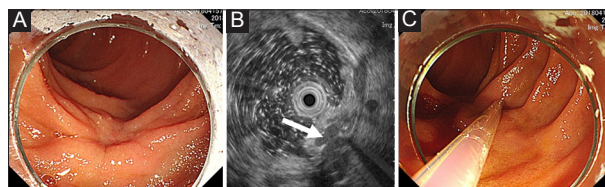


Figure 1 (A) Gastrointestinal endoscopy revealed a flat, scarred, post-endoscopic variceal ligation (EVL) lesion in the second section of the duodenum. (B) Endoscopic ultrasound revealed duodenal varices (arrow) in the submucosal layer under the post-EVL lesion. (C) Intravariceal injection of cyanoacrylate into the duodenum

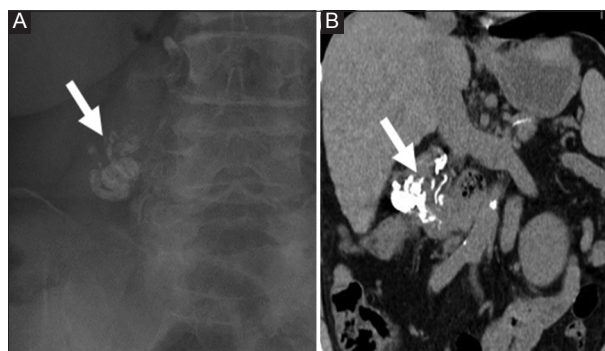


Figure 2 X-ray (A) and computed tomography (B) after endoscopic injection sclerotherapy showed that the injected N-butyl-2-cyanoacrylate occupied the duodenal varices (arrow)

References

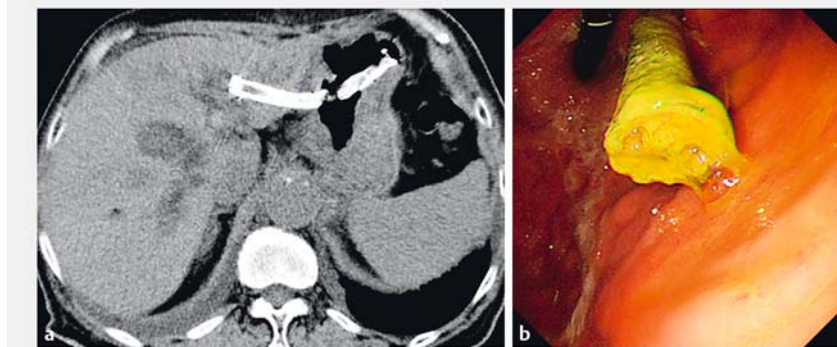
1. Matsui S, Kudo M, Ichikawa T, Okada M, Miyabe Y. The clinical characteristics, endoscopic treatment, and prognosis for patients presenting with duodenal varices. *HepatoGastroenterology* 2008;55:959-962.
2. Kakizaki S, Toyoda M, Ichikawa T, et al. Clinical characteristics and treatment for patients presenting with bleeding duodenal varices. *Dig Endosc* 2010;22:275-281.

Reintervention for stent occlusion after endoscopic ultrasound-guided hepaticogastrostomy with novel use of a precut needle-knife

Endoscopic ultrasound-guided hepaticogastrostomy (EUS-HGS) has gained popularity as an alternative biliary drainage method [1, 2]; however, reintervention after EUS-HGS remains to be elucidated. In EUS-HGS, use of a biliary stent that is longer than 100 mm is recommended in order to prevent stent migration [2, 3]. However, such stent placement occasionally makes reintervention challenging owing to the long length of the stent in the gastric lumen. A few reports have described technical efforts involved in reintervention after EUS-HGS [4, 5]. We describe a patient who underwent successful reintervention via a novel use of a precut needle-knife.

A 74-year-old woman with recurrent pancreatic cancer after pancreaticoduodenectomy presented with recurrent cholangitis. An 8 × 100 mm covered metal stent (Niti-S biliary covered stent; Taewoong Medical, Seoul, South Korea) had been previously deployed during EUS-HGS for biliary obstruction at the hepatic hilum. Stent occlusion occurred 4 months after EUS-HGS. Abdominal computed tomography showed a dilated intrahepatic bile duct, and stent occlusion was confirmed on endoscopy (► Fig. 1). Revisionary stent placement was attempted.

First, the advancement of an endoscopic retrograde cholangiopancreatography (ERCP) catheter was attempted via the proximal end of the HGS stent; however, the long stent length in the gastric lumen rendered catheter insertion impossible. Therefore, reintervention through the stent mesh was attempted. A 0.035-inch guidewire (Jagwire; Boston Scientific, Marlborough, Massachusetts, USA) was successfully passed through the stent mesh (► Fig. 2); however, an ERCP catheter could not be passed. Subsequently, a diathermic dilator was utilized, but it failed to break the stent mesh. Next, the use of a precut needle-knife (NeedleCut3V; Olympus, Tokyo, Japan) was



► Fig. 1 Stent occlusion after endoscopic ultrasound-guided hepaticogastrostomy. **a** Abdominal computed tomography showed a dilated intrahepatic bile duct. **b** Gastroscopy showed an occluded hepaticogastrostomy stent.



► Fig. 2 A 0.035-inch guidewire (Jagwire; Boston Scientific, Marlborough, Massachusetts, USA) was passed successfully through the mesh of the previously deployed hepaticogastrostomy stent (Niti-S biliary covered stent, 8 × 100 mm; Taewoong Medical, Seoul, South Korea).

considered. Using this knife, the stent mesh was broken easily (► Fig. 3), and a 7-Fr plastic stent (Flexima; Boston Scientific) was successfully deployed via the stent mesh into the left intrahepatic bile duct (► Fig. 4, ► Video 1). Cholangitis resolved in a few days.

The use of a precut needle-knife is simple and may be considered as a useful treatment option for reintervention after EUS-HGS.

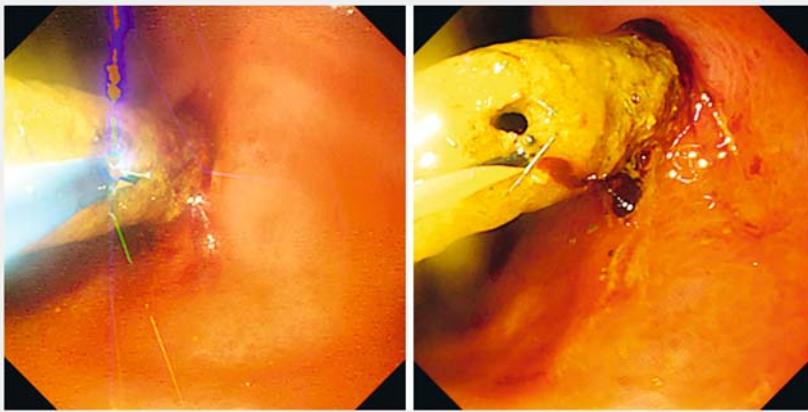
Endoscopy_UCTN_Code_CPL_1AL_2AD

Competing interests

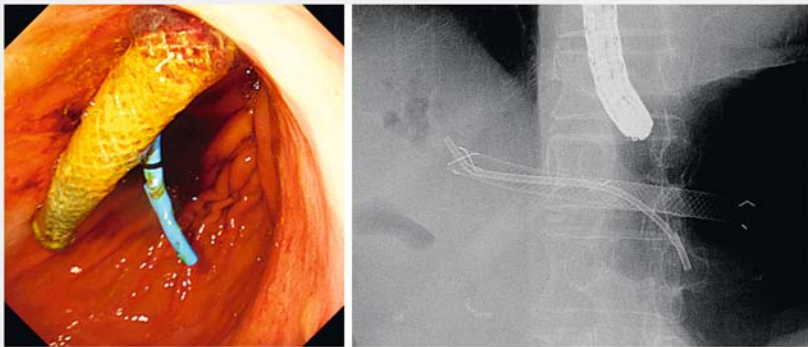
None

The authors

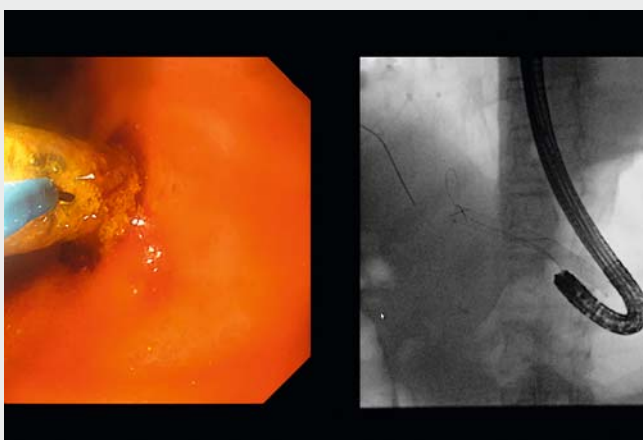
Kosuke Minaga, Mamoru Takenaka, Ayana Okamoto, Shunsuke Omoto, Takeshi Miyata, Hajime Imai, Masatoshi Kudo
Department of Gastroenterology and Hepatology, Kindai University Faculty of Medicine, Osaka-Sayama, Japan



▶ **Fig. 3** A precut needle-knife (NeedleCut3V; Olympus, Tokyo, Japan) was inserted over the guidewire and could break the stent mesh easily.



▶ **Fig. 4** A 7-Fr biliary plastic stent (70 mm long, Flexima; Boston Scientific, Marlborough, Massachusetts, USA) was deployed successfully via the stent mesh into the left intrahepatic bile duct.



▶ **Video 1** Using a precut needle-knife, the mesh of the previously deployed hepaticogastrostomy stent was broken easily. Thereafter, a 7-Fr biliary plastic stent was deployed successfully via the stent mesh into the left intrahepatic bile duct.



Corresponding author

Mamoru Takenaka, MD

Department of Gastroenterology and Hepatology, Kindai University Faculty of Medicine, 377-2 Ohno-Higashi, Osaka-Sayama 589-8511, Japan
 Fax: +81-72-3672880
 mamoxyo45@gmail.com

References

- [1] Wang K, Zhu J, Xing L et al. Assessment of efficacy and safety of EUS-guided biliary drainage: a systematic review. *Gastrointest Endosc* 2016; 83: 1218–1227
- [2] Nakai Y, Isayama H, Yamamoto N et al. Safety and effectiveness of a long, partially covered metal stent for endoscopic ultrasound-guided hepaticogastrostomy in patients with malignant biliary obstruction. *Endoscopy* 2016; 48: 1125–1128
- [3] Okuno N, Hara K, Mizuno N et al. Stent migration into the peritoneal cavity following endoscopic ultrasound-guided hepaticogastrostomy. *Endoscopy* 2015; 47 (Suppl. 01): E311
- [4] Ogura T, Masuda D, Takeuchi T et al. Simplified reintervention method of EUS-guided hepaticogastrostomy stent obstruction. *Gastrointest Endosc* 2016; 83: 831
- [5] Minaga K, Takenaka M, Miyata T et al. Through-the-mesh technique after endoscopic ultrasonography-guided hepaticogastrostomy: a novel re-intervention method. *Endoscopy* 2016; 48: E369–E370

Bibliography

DOI <https://doi.org/10.1055/a-0596-7171>
 Published online: 13.4.2018
Endoscopy 2018; 50: E153–E154
 © Georg Thieme Verlag KG
 Stuttgart · New York
 ISSN 0013-726X

ENDOSCOPY E-VIDEOS

<https://eref.thieme.de/e-videos>




Endoscopy E-Videos is a free access online section, reporting on interesting cases and new techniques in gastroenterological endoscopy. All papers include a high quality video and all contributions are freely accessible online.

This section has its own submission website at
<https://mc.manuscriptcentral.com/e-videos>

Review

Alleviating Pancreatic Cancer-Associated Pain Using Endoscopic Ultrasound-Guided Neurolysis

Kosuke Minaga ^{1,*}, Mamoru Takenaka ¹, Ken Kamata ¹, Tomoe Yoshikawa ¹, Atsushi Nakai ¹, Shunsuke Omoto ¹, Takeshi Miyata ¹, Kentaro Yamao ¹, Hajime Imai ¹, Hiroki Sakamoto ², Masayuki Kitano ³ and Masatoshi Kudo ¹

¹ Department of Gastroenterology and Hepatology, Kindai University Faculty of Medicine, Osaka-Sayama 589-8511, Japan; mamoxyo45@gmail.com (M.T.); ky11@leto.eonet.ne.jp (K.K.); t.yoshikawa113@gmail.com (T.Y.); nakai_agmc@yahoo.co.jp (A.N.); shunsuke.oomoto@gmail.com (S.O.); miyatchi77@yahoo.co.jp (T.M.); yamaken_volvo@yahoo.co.jp (K.Y.); codenamegenchan1023@gmail.com (H.I.); m-kudo@med.kindai.ac.jp (M.K.)

² Department of Gastroenterology, Katsuragi Hospital, Kishiwada 596-0825, Japan; hiroki.sakamoto@nifty.com

³ Second Department of Internal Medicine, Wakayama Medical University, Wakayama 641-8509, Japan; kitano@wakayama-med.ac.jp

* Correspondence: kousukeminaga@yahoo.co.jp; Tel.: +81-72-366-0221 (ext. 3525); Fax: +81-72-367-2880

Received: 14 January 2018; Accepted: 12 February 2018; Published: 15 February 2018

Abstract: The most common symptom in patients with advanced pancreatic cancer is abdominal pain. This has traditionally been treated with nonsteroidal anti-inflammatory drugs and opioid analgesics. However, these treatments result in inadequate pain control or drug-related adverse effects in some patients. An alternative pain-relief modality is celiac plexus neurolysis, in which the celiac plexus is chemically ablated. This procedure was performed percutaneously or intraoperatively until 1996, when endoscopic ultrasound (EUS)-guided celiac plexus neurolysis was first described. In this transgastric anterior approach, a neurolytic agent is injected around the celiac trunk under EUS guidance. The procedure gained popularity as a minimally invasive approach and is currently widely used to treat pancreatic cancer-associated pain. We focus on two relatively new techniques of EUS-guided neurolysis: EUS-guided celiac ganglia neurolysis and EUS-guided broad plexus neurolysis, which have been developed to improve efficacy. Although the techniques are safe and effective in general, some serious adverse events including ischemic and infectious complications have been reported as the procedure has gained widespread popularity. We summarize reported clinical outcomes of EUS-guided neurolysis in pancreatic cancer (from the PubMed and Embase databases) with a goal of providing information useful in developing strategies for pancreatic cancer-associated pain alleviation.

Keywords: endoscopic ultrasound; EUS; EUS-guided neurolysis; neurolysis; interventional EUS; pancreatic cancer; pain

1. Introduction

Pancreatic cancer has one of the worst prognoses among all solid carcinomas. The 5-year overall survival in pancreatic cancer remains dismal, with approximately 5–10% of patients surviving; more than half of the patients do not survive beyond 1 year [1,2]. Up to 80% of patients with pancreatic cancer experience abdominal and back pain, with 50–70% suffering from severe pain [3–5]. Because patients frequently present at an advanced stage, palliative care and not curative intent tends to be the primary goal. Pain control is a major goal of palliative care in advanced pancreatic cancer. Conventionally, pain is alleviated using nonsteroidal anti-inflammatory agents and/or opioid analgesics, following the three-step analgesic ladder pain management strategy recommended by

the World Health Organization [6]. However, pain is difficult to control in some cases presenting a challenge to the physician. Further, some patients experience serious drug-related side effects that can markedly reduce quality of life. Under such circumstances, celiac plexus neurolysis (CPN), in which the celiac plexus (CP) is chemically ablated, has been widely performed as an alternative treatment for alleviating cancer-associated pain [4,7]. For several years, CPN had been performed percutaneously or during open surgery. Anterior or posterior percutaneous CPN can be performed under the guidance of transabdominal ultrasound, fluoroscopy, or computed tomography [7].

Endoscopic ultrasound-guided celiac plexus neurolysis (EUS-CPN) is a relatively new technique first described in 1996 [8]. In EUS-CPN, a neurolytic agent is injected around the celiac trunk using a linear-array echo endoscope. Since the time it was first described, EUS-CPN has been widely applied as a minimally invasive approach in treating pancreatic cancer-associated pain. The current National Comprehensive Cancer Network guidelines (version 3, 2017, National Comprehensive Cancer Network, Fort Washington, PA, USA) recommend EUS-CPN for treatment of severe cancer-associated pain [9]. Other EUS-guided techniques including EUS-guided celiac ganglia neurolysis (EUS-CGN) [10] and EUS-guided broad plexus neurolysis (EUS-BPN) [11] have recently been developed with a goal of improving the efficacy of this endoscopic technique. EUS-guided neurolysis is thought to be safer than the conventional percutaneous approach because EUS, particularly with color Doppler technology, provides detailed real-time imaging of blood vessels around the gastric lumen. However, as these EUS-guided techniques have gained widespread popularity, serious procedure-related adverse effects including ischemic and infectious complications have also been reported [12,13]. The aim of this review is to summarize clinical outcomes of EUS-guided neurolysis in pancreatic cancer with a goal of providing information useful for development of strategies to alleviate pancreatic cancer-associated pain.

2. Literature Review Methodology

This review used electronic literature searches of the PubMed and Embase databases to identify articles focused on EUS-guided neurolysis published during the period from October 1996 to September 2017. Search terms used were “EUS OR endoscopic ultrasound” AND “neurolysis”. Our search was limited to articles published in the English language. Based on the title and abstract, we selected articles for full text review. In addition, bibliographies of the selected articles were manually searched to find additional relevant articles that were also reviewed in detail. Overall, we identified 50 references on EUS-guided neurolysis comprising 34 original articles [8,10,11,14–44], 11 case reports [45–55] and five systematic reviews [5,7,56–58].

3. Indications for EUS-Guided Neurolysis

EUS-guided neurolysis is mainly indicated in patients with chronic abdominal and back pain associated with upper gastrointestinal malignancies including pancreatic cancer. Patients with pancreatic cancer who are candidates for surgery with curative intent usually do not present with pain; on other hand, patients with pancreatic cancer at an unresectable stage who experience pain affecting their quality of life are good candidates for this treatment. Conventional treatment with analgesic drugs alleviates pain at least partially in most patients; however, some patients have inadequate pain control with this approach and some have drug-related side effects including dry mouth, constipation, nausea, vomiting and dependence [4,59]. In such cases, EUS-guided neurolysis is a useful alternative treatment that may reduce risk of drug-related side effects. Regarding timing of EUS-guided neurolysis, Wyse et al. reported that early EUS-CPN performed during diagnostic EUS provided better pain relief than conventional pain management and prevented progressive increases in morphine consumption [27]. Thus, EUS-guided neurolysis may be effective not only during follow-up but also at the time of initial cancer detection. To date, no randomized controlled trials comparing percutaneous and EUS-guided neurolysis have been conducted; therefore, the optimal initial approach remains unclear.

Contraindications to EUS-guided neurolysis include bleeding tendency (prothrombin time international normalized ratio >1.5, platelet count <50,000/ μ L) and cardiorespiratory instability prohibiting adequate sedation. Presence of esophageal or gastric varices may be a relative contraindication due to an increased risk of bleeding. Other relative contraindications include distorted or surgically altered anatomy, making it difficult to clearly visualize anatomic landmarks such as the celiac trunk or celiac ganglia under EUS guidance, direct tumor invasion or congenital anatomic malformations of the celiac or superior mesenteric artery [60].

4. Anatomy Relevant to Pancreatic Cancer Pain

It is speculated that abdominal pain associated with pancreatic cancer results from intra- and extra-pancreatic perineural invasion by cancer cells [3]. Complex neuronal pathways that transmit pain signals arise in the pancreas and travel to higher centers of the central nervous system through thoracic splanchnic nerves. Afferent neurons from the pancreas connect to the CP; electrical signals are then transmitted through dorsal root ganglia at the T12–L2 spinal level [61].

The CP is the largest plexus in the autonomic nervous system, composed of ganglia that surround the celiac trunk with sympathetic, parasympathetic and visceral sensory fibers and extending from the origin of the celiac artery (CA) to the origin of the superior mesenteric artery. The CP consists of right and left celiac ganglia which are located anterior to the aorta, slightly to the left and cephalad to the celiac trunk and medial to the left adrenal gland at the T12–L2 level [7,43,61]. The superior mesenteric plexus and inferior mesenteric plexus are situated on the lateral and anterior aspects of the aorta, respectively, between the origin of the superior mesenteric artery and the inferior mesenteric artery. The CP, superior mesenteric plexus and inferior mesenteric plexus consist of a network of both sympathetic and parasympathetic nerve fibers [43]. These plexuses are believed to play an indispensable role in pain perception in pancreatic cancer patients [62].

5. Endoscopic Procedures in EUS-Guided Neurolysis

5.1. Pretreatment Procedure

Hydration with intravenous saline solution (500–1000 mL) is recommended before the endoscopic procedure to minimize risk of hypotension. Patients are placed in the left lateral position under moderate sedation with various combinations of intravenous midazolam, propofol, and/or fentanyl. Vital signs are continuously monitored during the procedure with an automated noninvasive blood pressure device, electrocardiogram tracing and pulse oximetry. Before the endoscopic procedures, pain scores are evaluated objectively using a visual analog scale, a numeric rating scale, or a 10-point Likert pain score.

5.2. Endoscopic Procedure

5.2.1. EUS-Guided Celiac Plexus Neurolysis (EUS-CPN)

EUS-CPN, first described in 1996 by Wiersema and Wiersema [8], is a relatively new technique in which a local anesthetic (bupivacaine or lidocaine) and a neurolytic agent (absolute alcohol or phenol) are injected around the CP under EUS guidance (Figure 1). EUS-CPN can be performed with either an oblique-viewing or forward-viewing curved linear-array echo endoscope [8,23,24]. Under moderate sedation, the echo endoscope is passed per-orally into the esophagus. Under endoscopic visualization, the echo endoscope is advanced through the gastroesophageal junction into the stomach. EUS imaging from the posterior lesser curvature of the gastric body allows visualization of the longitudinal view of the aorta. The aorta is traced distally to the origin of the CA, which is the first major branch below the diaphragm. The CP per se cannot be identified as a clear structure but is located based on its position around the celiac trunk. A 19- or 22-gauge aspiration needle filled with normal saline solution is prepared, passed through the biopsy channel and affixed to the hub. If a specially designed 20-gauge

“spray needle” with multiple side holes is available [63], it could be used to spread the desired agent across a larger area.

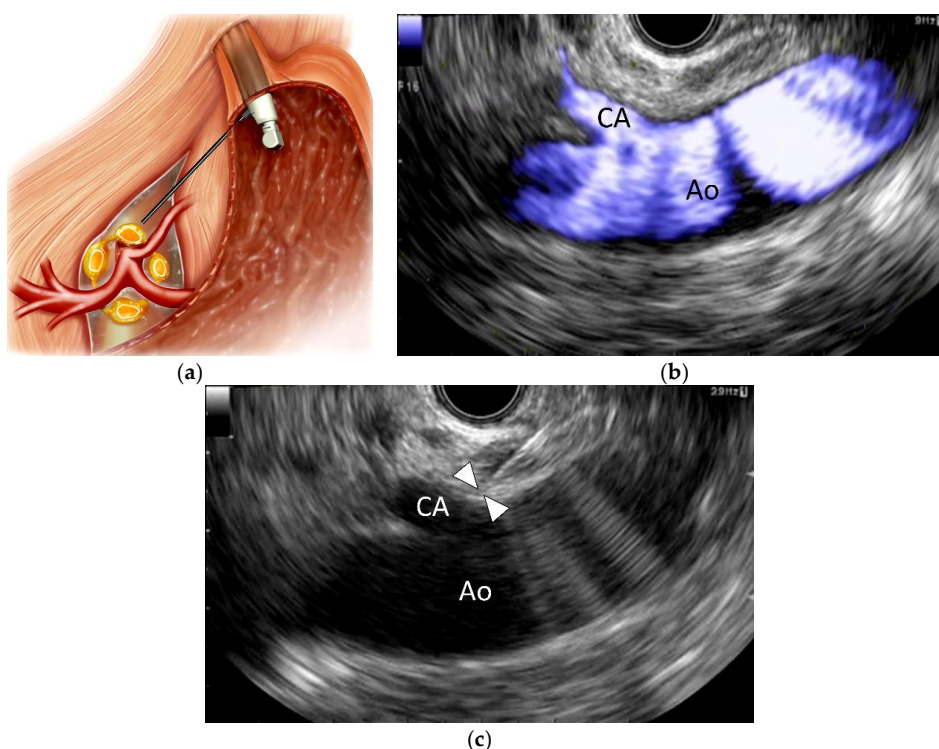


Figure 1. Endoscopic ultrasound-guided celiac plexus neurolysis (EUS-CPN). (a) Schematic of EUS-CPN; (b) Color flow EUS image from the lesser curvature of the stomach showing a longitudinal view of the aorta (Ao) and celiac artery (CA); (c) EUS image of EUS-CPN during needle puncture. A 22-gauge needle was advanced adjacent to the CA origin. Arrowheads indicate the needle tip. Blue: vascular flow.

EUS-CPN can be performed via a unilateral approach or a bilateral approach [19,56]. In the unilateral approach, the neurolytic agent is injected adjacent to a point just above the celiac trunk; in the bilateral approach, the agent is injected on both sides of the celiac trunk. For the unilateral approach, the needle is inserted under EUS guidance adjacent to the CA origin. To avoid transient pain induced by chemical stimulation with a neurolytic agent, 2–3 mL of a local anesthetic (bupivacaine or lidocaine) is initially injected. Then, a mixed solution of absolute alcohol and contrast medium is injected around the celiac trunk. The total volume of alcohol injected is usually 10–20 mL in EUS-CPN. For the bilateral approach, the probe is rotated clockwise toward the patient’s left at the level of the CA until the celiac trunk is no longer visualized but the aorta is still visible. The agent is injected in this region. Subsequently, the same process is carried out on the opposite side of the aorta (with counter-clockwise rotation).

To learn the procedure of Hands-on training using an animal model may be helpful in learning the EUS-guided neurolysis procedure. Bhutani et al. developed a swine model for teaching EUS and successfully performed EUS-CPN using the model. They concluded that the swine model was useful for hands-on training in EUS-guided interventions [14].

5.2.2. EUS-Guided Celiac Ganglia Neurolysis (EUS-CGN)

In EUS-CGN, first described by Levy et al. [10], a neurolytic agent is directly injected into celiac ganglia (Figure 2). Several studies demonstrated that EUS could visualize celiac ganglia in 62.5–89.4% of patients [25,44,64,65]. After visualization of the celiac trunk, the scope is rotated clockwise, enabling

visualization of the left adrenal gland. Most frequently, the celiac ganglia can be visualized on the left of the CA between the aorta and the left adrenal gland, at a level between the CA and the left renal artery. In some cases, celiac ganglia can be visualized cephalad to the CA. Under EUS guidance, hypoechoic round or nodular structures connected by hypoechoic thread-like structures in the periphery of this region are defined as celiac ganglia. Celiac ganglia vary in number (1 to 5), size (diameter 0.5–4.5 cm) and location (T12–L2) [66]. In EUS-CGN, each ganglion is punctured with a 19- or 22-gauge aspiration needle and absolute alcohol is injected until the entire ganglion becomes hyperechoic, reflecting alcohol injection. A volume of 1–2 mL alcohol is injected in each ganglion. An effort is made to puncture as many visualized ganglia as possible, to maximize efficacy.

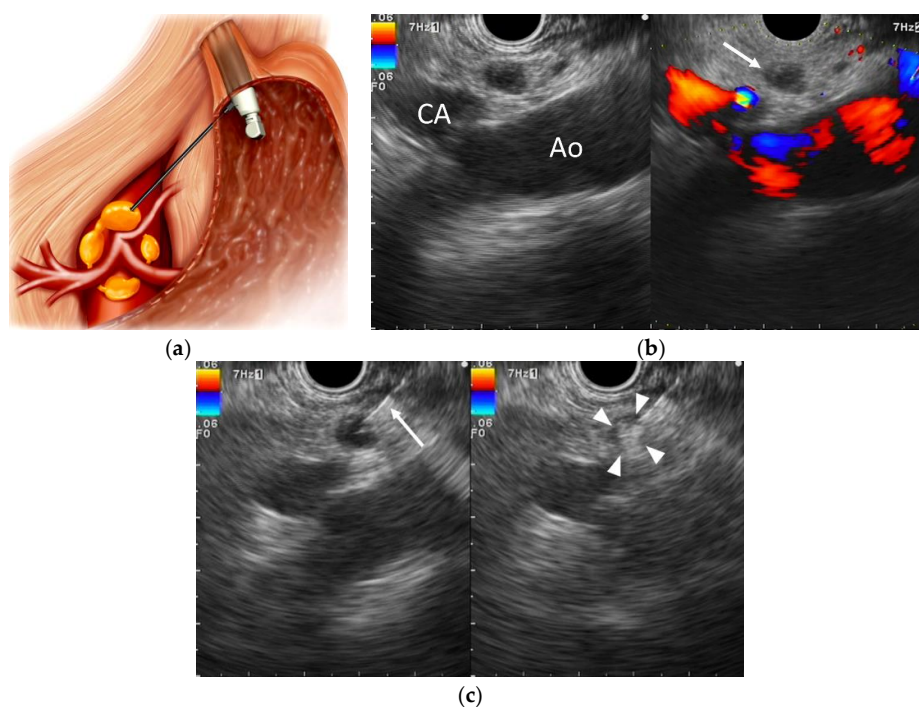


Figure 2. Endoscopic ultrasound-guided celiac ganglia neurolysis (EUS-CGN). (a) Schematic of EUS-CGN; (b) EUS image from the lesser curvature of the stomach showing the celiac ganglion located anterior to the aorta (arrow). Ao: aorta, CA: celiac artery. (c) EUS image of EUS-CGN before and after injection of a neurolytic agent. The ganglion has a hyperechoic appearance (arrowheads). Blue: vascular flow away from the transducer; Red: vascular flow towards the transducer.

5.2.3. EUS-Guided Broad Plexus Neurolysis (EUS-BPN)

EUS-BPN is a recently developed variation of EUS-guided neurolysis, first described in 2010 by Sakamoto et al. [11]. In EUS-BPN, a neurolytic agent is injected around the origin of the superior mesenteric artery to produce a wider distribution of neurolytic agent (Figure 3). In EUS-BPN, the probe is rotated clockwise toward the patient's left at the level of the superior mesenteric artery until the origin of the superior mesenteric artery can no longer be visualized but the aorta is still visible. Because the aspiration needle is advanced deeper in EUS-BPN than in EUS-CPN, use of a 25-gauge needle is preferable to provide safety and flexibility during needle advancement into the target area. A 25-gauge aspiration needle filled with normal saline solution is prepared and introduced through the biopsy channel. Under EUS guidance, the needle is advanced adjacent and anterior to the lateral aspect of the aorta at a level above or next to the superior mesenteric artery. Two or 3 mL of a lidocaine solution is injected to prevent transient pain caused because of neurolytic agent injection. Subsequently, a neurolytic agent (absolute alcohol) is injected up to a maximum volume of 10 mL. Next, the process is repeated on the opposite side of the aorta (with counter-clockwise rotation), if possible.

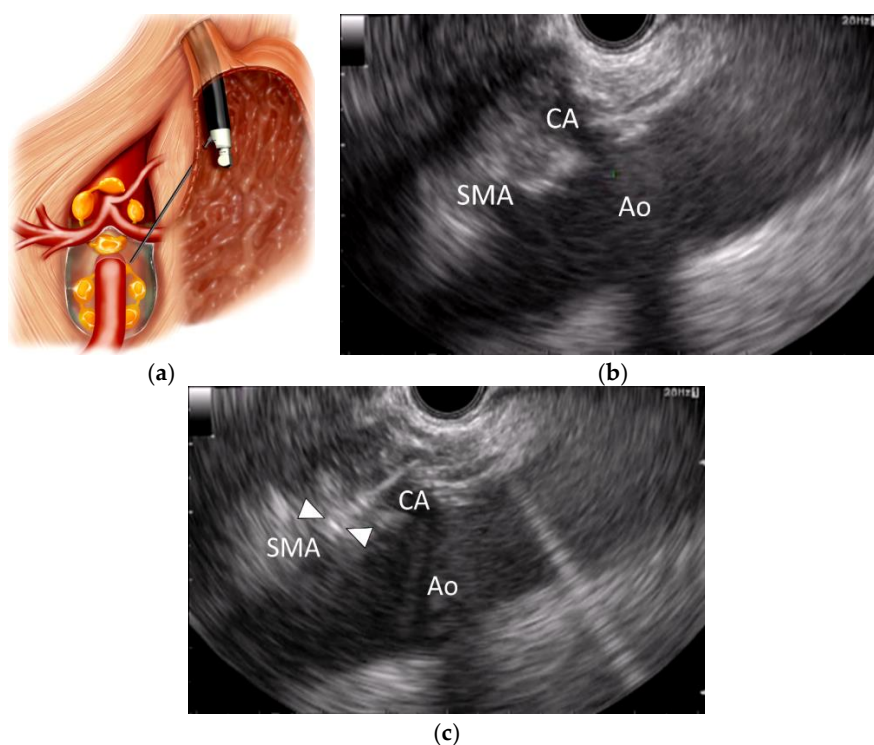


Figure 3. Endoscopic ultrasound-guided broad plexus neurolysis (EUS-BPN). (a) Schematic of EUS-BPN; (b) EUS image from the lesser curvature of the stomach showing a longitudinal view of the aorta (Ao), celiac artery (CA) and superior mesenteric artery (SMA); (c) EUS image of EUS-BPN during needle puncture. A 25-gauge needle was advanced adjacent to the SMA. Arrowheads indicate the needle tip.

6. Efficacy of EUS-Guided Neurolysis

6.1. EUS-CPN

In an initial report of EUS-CPN use, 30 patients with intra-abdominal malignancy-associated pain (with 25 pancreatic cancer patients) underwent EUS-CPN. Pain improvement was achieved at 2, 4, 8 and 12 weeks after EUS-CPN in 79–88% of the patients [8]. Several clinical trials of EUS-CPN have been published since the first report [15–19,22,26–30,33–40,42] (Table 1). Two meta-analyses of the utility of EUS-CPN in unresectable abdominal cancer-associated pain showed an alleviation rate of 73–80% with treatment duration of approximately 1–2 months [57,58]. According to a recent systematic review by Nagels et al., EUS-CPN should be considered in pancreatic cancer patients whose pain is inadequately controlled with systemic analgesics or who suffer from significant drug-related side effects [7]. To date, there has been only one randomized controlled trial which assessed EUS-CPN in comparison with conventional drug-based pain management [27]. According to the trial report by Wyze et al. 96 patients with advanced pancreatic cancer were randomly assigned to early EUS-CPN (i.e., EUS-CPN was performed during diagnosis of pancreatic cancer) or conventional drug-based pain management; early CPN was found to be superior in pain relief at three months compared with conventional pain management [27]. A Cochrane Review of six studies (358 patients) showed that in comparison with control, EUS-CPN afforded pain relief at four and eight weeks (visual analog score -0.42 (-0.70 to -0.13) and -0.44 (-0.89 to -0.01), respectively) and that it was associated with significant reduction in post-procedural analgesic consumption ($p < 0.00001$) [5]. These results indicate that EUS-CPN may be superior to drug-based management for pain relief in advanced pancreatic cancer patients.

Table 1. Clinical studies of efficacy and safety of endoscopic ultrasound (EUS)-guided neurolysis.

First Author (Year) [Reference]	Study Design	No. of Patients	Procedure	Outcomes	Complications
Wiersma (1996) [8]	Prospective? Non-randomized	30	EUS-CPN Bilateral	Pain improvement in 79 to 88% of patients with a median follow-up of 10 weeks	Self-limited complications Diarrhea 13.3% Pain increase 3.3%
Gunaratnam (2001) [15]	Prospective Non-randomized	58	EUS-CPN Bilateral	Decline in pain score after EUS-CPN in 78% of patients	No major complications Pain increase 8.6%
Tran (2006) [16]	Retrospective Non-randomized	8	EUS-CPN Unilateral	Pain improvement in 70% of 10 procedures (8 patients)	Not described
Sakamoto (2006) [17]	Retrospective Non-randomized	13	EUS-CPN Bilateral	Pain improvement in 84.6% of patients	Self-limited complications Inebriation 7.7% Pain increase 7.7% Hypotension 15.4%
Levy (2008) [10]	Retrospective Non-randomized	36 (Malignant 18)	EUS-CGN	Pain improvement in 94% of patients	Pain increase 36.1% Hypotension 33.3% Diarrhea 16.6%
Ramirez-Luna (2008) [18]	Retrospective Non-randomized	11	EUS-CPN Unilateral	Pain improvement in 72% of patients at 4 weeks after CPN	No major complications Transient pain increase 45.4%
Sahai (2009) [19]	Retrospective Non-randomized	160 (Malignant 81)	EUS-CPN Bilateral 89 Unilateral 71	Pain improvement; 70.4% (bilateral) vs 45.9% (unilateral) Bilateral CPN is more effective than unilateral CPN	Retroperitoneal bleeding 1% (bilateral CPN)
Sakamoto (2010) [11]	Retrospective Non-randomized	67	EUS-CPN 34 EUS-BPN 33	Reduction in pain score on days 7 and 30; EUS-BPN > EUS-CPN	No serious complications No cases of prolonged hospitalization
Asuncion (2011) [25]	Retrospective Non-randomized	64	EUS-CGN 40 EUS-CPN 24	Pain improvement at 1 week after neurolysis; 65.0% (CGN) vs. 25.0% (bilateral CPN)	Transient pain increase 1.6%, Diarrhea 23.4%, Hypotension 1.6%
Iwata (2011) [26]	Retrospective Non-randomized	47	EUS-CPN Unilateral	Pain improvement; 68.1% Complete pain relief; 36.2%	Transient hypotension 17.0%, Inebriation 8.5%, Diarrhea 23.4%
Wyse (2011) [27]	Prospective Randomized	48	EUS-CPN Bilateral	Randomized trial; EUS-CPN vs conventional drug-based pain management Pain relief at 3 months; CPN > drug-based pain management	No evidence of early or late complications

Table 1. Cont.

First Author (Year) [Reference]	Study Design	No. of Patients	Procedure	Outcomes	Complications
LeBlanc (2011) [28]	Prospective Randomized	50	EUS-CPN Bilateral 21 Unilateral 29	Randomized trial; bilateral CPN vs unilateral CPN Pain relief and survival; no difference between the groups	Transient pain increase 36%, Hypotension 2%
Wiechowska-Kozłowska (2012) [29]	Retrospective Non-randomized	29	EUS-CPN Bilateral	Pain improvement; 86% Complete pain relief; 14%	Transient diarrhea 10.3%, Hypotension 3.4%, Pain increase 6.9%
Wang (2012) [32]	Prospective Non-randomized	23	EUS-guided irradiation	EUS-guided celiac ganglion irradiation (iodine-125 seeds) Pain improvement in 82.6% of patients at 2 weeks	No major complications Constipation 21.7% Nausea 8.7%
Leblanc (2013) [33]	Prospective Randomized	20	EUS-CPN Unilateral (+EUS-CGN)	Randomized trial; EUS-CPN using 10 mL vs. 20 mL alcohol Similar clinical outcomes between the groups	Self-limited complications Lightheadedness 5% Diarrhea 10% Nausea 15%
Seicean (2013) [34]	Retrospective Non-randomized	32	EUS-CPN Unilateral	Pain improvement in 75% of patients	No complications
Doi (2013) [35]	Prospective Randomized	68	EUS-CGN 34 EUS-CPN 34	Randomized trial; EUS-CGN vs. EUS-CPN (unilateral) Pain improvement; 73.5% (CGN) vs. 45.5% (CPN) Complete pain relief; 50% (CGN) vs. 18.2% (CPN)	Transient hypotension 4.5%, Inebriation 3.0%, Pain increase 25.4%, Diarrhea 7.5%
Tellez-Ávila (2013) [37]	Retrospective Non-randomized	53	EUS-CPN Unilateral 21 Bilateral 32	Bilateral vs. unilateral CPN No significant difference between the groups	No major complications Transient pain increase 1.9%
Si-Jie (2014) [36]	Retrospective Non-randomized	41	EUS-CGN 26 EUS-CPN 15	Pain improvement in 90.2% and 61.0% of patients at 1 week and at 3 months, respectively	Transient hypotension 4.9%
Ishiwatari (2014) [38]	Retrospective Non-randomized	22	EUS-CPN Phenol 6 Ethanol 16	Pain improvement in 83% and 69% of patients in the phenol and ethanol groups, respectively	Minor complications Phenol group 16.7%, ethanol group 37.5% Inebriation 12.5% (ethanol group)

Table 1. Cont.

First Author (Year) [Reference]	Study Design	No. of Patients	Procedure	Outcomes	Complications
Ishiwatani (2015) [39]	Prospective Non-randomized	9	EUS-CPN Phenol-glycerol	Complete, partial and no pain relief in 44.4%, 44.4% and 11.1% of patients at 7 days after the procedure	Minor complications 33.3%
Fuji-Lau (2015) [40]	Retrospective Non-randomized	230	EUS-CPN or EUS-CCN	EUS-guided celiac neurolysis was associated with longer survival compared with non-EUS approaches	Mild adverse events; 7 patients (1.7%) Moderate to severe adverse events; 5 patients (1.2%)
Bang (2016) [41]	Prospective Non-randomized	51	EUS-CPN Unilateral	Heart rate change during CPN in 49.0% of patients Better pain relief in the heart rate change cohort	Diarrhea 33.3%
Minaga (2016) [43]	Retrospective Non-randomized	112	EUS-BPN 65 EUS-BPN + EUS-CCN 47	Pain improvement in 78% of patient at 1 week EUS-BPN in combination with EUS-CCN is a predictor of a good pain response	Major: Paraplegia 1% Minor: Inebriation 8.0%, Hypotension 4.5%, Pain increase 3.6%, Diarrhea 3.6%
Facciorusso (2017) [42]	Retrospective Non-randomized	123	EUS-CPN 58 EUS-CPN + ablation 65	EUS-guided tumor ethanol ablation combined with EUS-CPN increased pain relief and complete pain response rate	No severe treatment-related complications

CPN, celiac plexus neurolysis; CCN, celiac ganglia neurolysis; BPN, broad plexus neurolysis.

Differences between the two major approaches of EUS-CPN were evaluated by LeBlanc et al. in a randomized study comprising 50 pancreatic cancer patients comparing efficacy of unilateral and bilateral CPN; pain relief was reported in 69% patients who underwent unilateral injection and in 81% patients who underwent bilateral injection, with no statistically significant differences [28]. Sahai et al. evaluated efficacy of the two approaches in 160 patients and found that bilateral CPN was the only determinant of >50% pain relief by day seven [19]. The most recent meta-analysis comparing the two approaches, by Lu et al. included six studies (437 patients); no significant difference was found between the approaches in short-term pain relief or response to treatment. However, EUS-guided bilateral CPN was associated with significantly lesser analgesic consumption than unilateral CPN [56].

Another new technique is EUS-guided ethanol tumor ablation combined with CPN. A recent study by Facciorusso et al. compared the efficacy and safety of EUS-guided ethanol tumor ablation combined with CPN ($n = 65$) with those of CPN alone ($n = 58$) for pain management in advanced pancreatic cancer patients ($n = 123$). The study found that EUS-guided tumor ablation combined with CPN appeared to be superior to CPN alone with respect to pain relief and overall survival [42,53].

There is insufficient evidence to evaluate the impact of EUS-CPN on overall survival in pancreatic cancer. A retrospective case-control study of 417 patients by Fujii-Lau et al. suggested that celiac neurolysis (including EUS-CPN and EUS-CGN) was an independent determinant of shortened survival in pancreatic cancer [40]. According to a meta-analysis by Yan et al. comprising five randomized controlled trials on the effect of non-EUS-guided CPN in pain management in advanced pancreatic cancer, CPN use was associated with a significant reduction in pain intensity and analgesic consumption; however, CPN did not affect survival [67]. In contrast, in a study by Fujii-Lau, EUS-guided neurolysis was associated with longer survival than non-EUS-guided approaches [40]. Further prospective studies are needed to evaluate impact of EUS-guided neurolysis on patient survival.

6.2. EUS-CGN

As previously described, EUS allows visualization of celiac ganglia in 62.5–89.4% of patients [25,44,64,65]. Kappelle et al. reported that a total of 204 ganglia in 83 patients were detected during 97 consecutive EUS procedures and that the mean length of the major axis of the ganglia was 8.1 mm [44]. The ganglia were visualized anterior to the aorta and/or to the left of the CA in 94% of patients [44]. A retrospective study by Ascunce et al. suggested that visualization of celiac ganglia with direct CGN was the best determinant of pain-relief response following EUS-guided celiac neurolysis [25]. In a randomized multicenter trial by Doi et al. EUS-CGN was more effective than EUS-CPN in providing pain relief (pain-relief response of 73.5% vs. 45.5%, respectively, $p = 0.02$) [35]. Considering these findings, EUS-CGN may be more effective than EUS-CPN for pain relief in advanced pancreatic cancer. Most recently, Kappelle et al. successfully visualized the area of alcohol spread following various EUS-guided neurolysis approaches and alcohol doses in a human cadaver model [44]. In their study, EUS-CGN was performed with 1 mL (low volume) or 4 mL (high volume) alcohol injection per ganglion. Neurolytic-spread area was assessed by visualizing spread of an orange dye mixed with the alcohol. After low-volume EUS-CGN in cadavers, the neurolytic agent spread well beyond the targeted ganglion. High-volume EUS-CGN resulted in wider ethanol spread, also reaching undefined ganglia. The authors concluded that high-volume EUS-CGN is preferable to low-volume EUS-CGN because it is likely to achieve more thorough neurolysis [44].

In a pilot study by Wang et al. EUS-guided implantation of iodine-125 (^{125}I) around the celiac ganglia was performed in 23 advanced pancreatic cancer patients. The authors found that EUS-guided celiac ganglia irradiation with ^{125}I seeds was effective for pain relief and reduced analgesic consumption at two weeks following the procedure, with no major procedure-related complications [32].

6.3. EUS-BPN

An initial retrospective study by Sakamoto et al. compared efficacy and safety of EUS-CPN and EUS-BPN in pancreatic cancer pain management. The results of the study suggested that EUS-BPN was more effective, especially in patients with extensive spread of cancer within the abdominal cavity beyond the distribution of the CP and that the procedure did not result in serious complications [11]. In several studies, EUS-CPN, EUS-CGN and EUS-BPN have shown satisfactory results and excellent safety profiles, indicating that they are all promising methods; however, the efficacy of these techniques is not assured. Therefore, we conducted a study to explore determinants of pain-relief response in 112 patients undergoing EUS-guided neurolysis for pancreatic cancer-associated abdominal pain. Multivariable analysis revealed that EUS-BPN in combination with EUS-CGN was a significant determinant of pain-relief response [43]. In our study, the neurolytic-spread area was divided into six sections and assessed using post-procedural computed tomography. The number of sections with neurolytic spread was higher in patients who underwent EUS-BPN in combination with EUS-CGN than in patients who underwent EUS-BPN alone. This finding suggests that wider distribution of neurolytic agent may be associated with better pain relief. Because EUS-BPN has been reported only at a single institution currently, a multicenter study with a larger number of patients is required to confirm efficacy and safety of this technique.

7. Complications of EUS-Guided Neurolysis

Although EUS-guided neurolysis has been shown to be a safe procedure, side effects and complications can occur during and after the procedure. A recent review on interventional EUS-related safety and complications comprising 15 studies found that complications occurred in 21% of 661 patients [68]. Most of the reported complications were minor and self-limiting, usually lasting less than two days and were attributed to disruption of sympathetic activity [20]. According to a systematic review by Nagels et al. frequent complications related to EUS-CPN were diarrhea (18%) and hypotension (20%) resulting from sympatholytic reactions [7]. A transient increase in pain occurred in 1.5–8% of patients after EUS-CPN [7]. Signs of alcohol intoxication resulting from the procedure were reported only in Japan [11].

Serious complications have been reported to be uncommon, occurring in only 0.2% of EUS-guided neurolysis cases [68]. Table 2 shows all major complications reported following EUS-guided neurolysis in pancreatic cancer patients [46,48–52,54,55]. Among these, ischemic complications, which can be fatal, are considered the most serious adverse events. Four cases of acute paraplegia have been reported; in all four cases, the paraplegia was permanent [48,49,52,55]. Paraplegia following EUS-guided neurolysis is thought to be caused by acute spinal cord ischemia resulting from injury to the anterior radicular artery (artery of Adamkiewicz) or from vasospasm associated with neurolytic agent injection. A recent case report first described acute respiratory failure resulting from bilateral diaphragmatic paralysis following EUS-CPN [54]. In that case, paralysis involved cranial spread of neurolytic agent from the CP toward the diaphragm; the neurolytic agent made contact with both phrenic nerves which innervate the diaphragm from below. Hepatic and splenic infarction and bowel ischemia occurred in two patients, both of whom died due to multiorgan failure and sepsis [50,51]. Possible mechanisms of injury include diffusion of neurolytic agent adjacent to the CA resulting in arterial vasospasm reflecting the sclerosing effect of absolute ethanol and arterial embolization following injection of neurolytic agent. Because serious and even fatal complications can occur, endosonographers should bear the risk of ischemic complications in mind when considering EUS-guided neurolysis and all patients should be informed about these serious complications before the procedure.

Table 2. Major complications of EUS-guided neurolysis in pancreatic cancer.

First Author (Year) [Reference]	Complications	Procedure	Neurolytic Agents/Anesthetic Agents	Outcomes
Muscatiello (2006) [46]	Retroperitoneal abscess	CPN	Alcohol/Bupivacaine	EUS-guided puncture, complete resolution
Mittal (2012) [48]	Paraplegia	CGN + CPN	Alcohol/Bupivacaine	No improvement
Fujii-Lau (2012) [49]	Paraplegia	CGN + CPN	Alcohol/Bupivacaine	No improvement
Gimeno-García (2012) [50]	Celiac artery thrombosis, hepatic, kidney, splenic infarction, bowel ischemia	CPN Bilateral	Alcohol/Bupivacaine	Conservative treatment, died 8 days later
Jang (2013) [51]	Hepatic, splenic infarction, bowel ischemia	CPN Unilateral	Alcohol, triamcinolone acetonide/Bupivacaine	Conservative treatment, died 27 days later
Minaga (2016) [52]	Paraplegia	CPN Bilateral	Alcohol/Lidocaine	No improvement
Mulhall (2016) [54]	Bilateral diaphragmatic paralysis	CPN	No description	Mechanical ventilation, no improvement
Köker (2017) [55]	Paraplegia	CPN Bilateral	Alcohol/Bupivacaine	No improvement

8. Determinants of Pain-Relief Response

Several studies have investigated determinants of pain-relief response following EUS-guided neurolysis. Several studies have reported that a wider distribution of neurolytic agent is associated with better pain-relief response. In a retrospective study by Iwata et al. including 47 patients who underwent EUS-CPN, multivariable analysis revealed that direct tumor invasion of the celiac axis and distribution of alcohol on only the left side of the CA were significant factors associated with negative pain-relief response to EUS-CPN [26]. Our retrospective study of 112 patients with advanced pancreatic cancer who underwent EUS-guided neurolysis showed that EUS-BPN in combination with EUS-CGN (combination method) was a significant predictor of good pain-relief response. The results of our study also showed that the number of neurolytic-spread areas in post-procedural CT was significantly higher in patients who received the combination method than in those treated with EUS-BPN alone. This result suggests that larger spread of neurolytic agent might contribute to improved efficacy of the combination method.

Most recently, Bang et al. prospectively analyzed data from 51 patients who underwent EUS-CPN for abdominal pain caused by advanced pancreatic cancer to examine whether a correlation existed between increased heart rate and treatment outcomes. The authors found that heart rate change (increase of ≥ 15 beats/min for 30 s) during alcohol injection was associated with improved pain-relief response and quality of life [41].

One explanation for the reduction in EUS-CPN pain improvement after 2–3 months following the procedure is that the neurolytic agent does not remain in the targeted anatomic location but flows away from the injection site because of its high fluidity [21]. This suggests that neurolytic agent delivery in a solid or gel form may result in enhanced efficacy and safety. A study by Obstein et al. described the use of EUS-CPN with a reverse-phase polymer in a porcine model. The study found that formation of a gel plug at the exact location of the celiac ganglia prevented diffusion of the injected agent and prolonged the duration of analgesic effect [21].

9. Conclusions and Future Directions

EUS-guided neurolysis has been increasingly used as minimally invasive intervention for pain relief in patients with advanced pancreatic cancer. Recent systematic reviews on the procedure have reported an efficacy of approximately 80% with few serious complications. Three different neurolytic approaches exist, comprising EUS-CPN, EUS-CGN and EUS-BPN. A bilateral approach in EUS-CPN is

associated with lower analgesic consumption although efficacy of bilateral and unilateral EUS-CPN appears similar. EUS-CGN may be more effective than unilateral EUS-CPN without an increase in complications. EUS-BPN in combination with EUS-CGN may provide better pain relief than either approach alone, although the combination approach may be technically challenging. In several small studies, EUS-CPN, EUS-CGN and EUS-BPN have been reported to show satisfactory results and excellent safety profiles; however, efficacy of these techniques is not assured. Moreover, no studies comparing conventional percutaneous and EUS-guided neurolysis can be found. Drug-based pain management has improved with recent development of new analgesic agents. Future prospective, well-designed studies comparing the CPN techniques and analgesic pain management using new drugs are essential to establish the role of EUS-guided neurolysis as a pain-management modality in pancreatic cancer. Comparison with other interventional procedures including radiotherapy and intrathecal therapy may also be warranted. Further, to achieve lasting pain relief, neurolytic agents and the associated delivery methods may need improvement. As the use of EUS-guided neurolysis has become widespread, serious adverse events including ischemic and infectious complications have been described increasingly frequently. Endosonographers should bear the possibility of serious complications in mind when considering EUS-guided neurolysis.

Acknowledgments: This study was supported by grants from the Japan Society for the Promotion of Science.

Author Contributions: Kosuke Minaga and Masayuki Kitano developed the initial concept and designed the structure of the review. Kosuke Minaga and Ken Kamata performed the literature search. Tomoe Yoshikawa corrected the manuscript. Mamoru Takenaka, Ken Kamata, Tomoe Yoshikawa, Atsushi Nakai, Shunsuke Omoto, Tekeshi Miyata, Kentarō Yamao, Hajime Imai, Hiroki Sakamoto, Masayuki Kitano and Masatoshi Kudo contributed to editing and final approval.

Conflicts of Interest: The authors declare no conflict of interest.

References

1. Bilimoria, K.Y.; Bentrem, D.J.; Ko, C.Y.; Ritchey, J.; Stewart, A.K.; Winchester, D.P.; Talamonti, M.S. Validation of the 6th edition AJCC Pancreatic Cancer Staging System: Report from the National Cancer Database. *Cancer* **2007**, *110*, 738–744. [[CrossRef](#)] [[PubMed](#)]
2. Sirri, E.; Castro, F.A.; Kieschke, J.; Jansen, L.; Emrich, K.; Gondos, A.; Holleczeck, B.; Katalinic, A.; Urbschat, I.; Vohmann, C.; et al. Recent trends in survival of patients with pancreatic cancer in Germany and the United States. *Pancreas* **2016**, *45*, 908–914. [[CrossRef](#)] [[PubMed](#)]
3. Mekaroonkamol, P.; Willingham, F.F.; Chawla, S. Endoscopic management of pain in pancreatic cancer. *J. Oncol. Pract.* **2015**, *16*, 33–40.
4. Caraceni, A.; Portenoy, R.K. Pain management in patients with pancreatic carcinoma. *Cancer* **1996**, *78*, 639–653. [[CrossRef](#)]
5. Arcidiacono, P.G.; Calori, G.; Carrara, S.; McNicol, E.D.; Testoni, P.A. Celiac plexus block for pancreatic cancer pain in adults. *Cochrane Database Syst. Rev.* **2011**, CD007519. [[CrossRef](#)] [[PubMed](#)]
6. World Health Organization. *Cancer Pain Relief*, 2nd ed.; WHO: Geneva, Switzerland, 2006.
7. Nagels, W.; Pease, N.; Bekkering, G.; Cools, F.; Dobbels, P. Celiac plexus neurolysis for abdominal cancer pain: A systematic review. *Pain Med.* **2013**, *14*, 1140–1163. [[CrossRef](#)] [[PubMed](#)]
8. Wiersema, M.J.; Wiersema, L.M. Endosonography-guided celiac plexus neurolysis. *Gastrointest. Endosc.* **1996**, *44*, 656–662. [[CrossRef](#)]
9. NCCN Guidelines for Pancreatic Adenocarcinoma. Version 3. 2017. Available online: <http://jaxelection.altervista.org/pancreatic/NCCN3.2017Pancreatic.pdf> (accessed on 21 December 2017).
10. Levy, M.J.; Topazian, M.D.; Wiersema, M.J.; Clain, J.E.; Rajan, E.; Wang, K.K.; de la Mora, J.G.; Gleeson, F.C.; Pearson, R.K.; Pelaez, M.C.; et al. Initial evaluation of the efficacy and safety of endoscopic ultrasound-guided direct ganglia neurolysis and block. *Am. J. Gastroenterol.* **2008**, *103*, 98–103. [[CrossRef](#)] [[PubMed](#)]
11. Sakamoto, H.; Kitano, M.; Kamata, K.; Komaki, T.; Imai, H.; Chikugo, T.; Takeyama, Y.; Kudo, M. EUS-guided broad plexus neurolysis over the superior mesenteric artery using a 25-gauge needle. *Am. J. Gastroenterol.* **2010**, *105*, 2599–2606. [[CrossRef](#)] [[PubMed](#)]

12. Yasuda, I.; Wang, H.P. Endoscopic ultrasound-guided celiac plexus block and neurolysis. *Dig. Endosc.* **2017**, *29*, 455–462. [[CrossRef](#)] [[PubMed](#)]
13. Gohil, V.B.; Klapman, J.B. Endoscopic palliation of pancreatic cancer. *Curr. Treat. Options Gastroenterol.* **2017**, *15*, 333–348. [[CrossRef](#)] [[PubMed](#)]
14. Bhutani, M.S.; Hoffman, B.J.; Hawes, R.H. A swine model for teaching endoscopic ultrasound (EUS) imaging and intervention under EUS guidance. *Endoscopy* **1998**, *30*, 605–609. [[CrossRef](#)] [[PubMed](#)]
15. Gunaratnam, N.T.; Sarma, A.V.; Norton, I.D.; Wiersema, M.J. A prospective study of EUS-guided celiac plexus neurolysis for pancreatic cancer pain. *Gastrointest. Endosc.* **2001**, *54*, 316–324. [[CrossRef](#)] [[PubMed](#)]
16. Tran, Q.N.; Urayama, S.; Meyers, F.J. Endoscopic ultrasound-guided celiac plexus neurolysis for pancreatic cancer pain: A single-institution experience and review of the literature. *J. Support. Oncol.* **2006**, *4*, 460–464. [[PubMed](#)]
17. Sakamoto, H.; Kitano, M.; Nishio, T.; Takeyama, Y.; Yasuda, C.; Kudo, M. Value of computed tomography for evaluating the injection site in endosonography-guided celiac plexus neurolysis for pancreatic cancer pain. *Dig. Endosc.* **2006**, *18*, 206–211. [[CrossRef](#)]
18. Ramirez-Luna, M.A.; Chavez-Tapia, N.C.; Franco-Guzman, A.M.; Garcia-Saenz-de-Sicilia, M.; Tellez-Avila, F.I. Endoscopic ultrasound-guided celiac plexus neurolysis in patients with unresectable pancreatic cancer. *Rev. Gastroenterol. Mex.* **2008**, *73*, 63–67. [[PubMed](#)]
19. Sahai, A.V.; Lemelin, V.; Lam, E.; Paquin, S.C. Central vs. bilateral endoscopic ultrasound-guided celiac plexus block or neurolysis: A comparative study of short-term effectiveness. *Am. J. Gastroenterol.* **2009**, *104*, 326–329. [[CrossRef](#)] [[PubMed](#)]
20. O'Toole, T.M.; Schmulewitz, N. Complication rates of EUS-guided celiac plexus blockade and neurolysis: Results of a large case series. *Endoscopy* **2009**, *41*, 593–597. [[CrossRef](#)] [[PubMed](#)]
21. Obstein, K.L.; Martins, F.P.; Fernández-Esparrach, G.; Thompson, C.C. Endoscopic ultrasound-guided celiac plexus neurolysis using a reverse phase polymer. *World J. Gastroenterol.* **2010**, *16*, 728–731. [[CrossRef](#)] [[PubMed](#)]
22. Soweid, A.M.; Azar, C. Endoscopic ultrasound-guided celiac plexus neurolysis. *World J. Gastrointest. Endosc.* **2010**, *2*, 228–231. [[CrossRef](#)] [[PubMed](#)]
23. Eloubeidi, M.A. Initial evaluation of the forward-viewing echoendoscope prototype for performing fine-needle aspiration, Tru-cut biopsy and celiac plexus neurolysis. *J. Gastroenterol. Hepatol.* **2011**, *26*, 63–67. [[CrossRef](#)] [[PubMed](#)]
24. Kida, M.; Araki, M.; Miyazawa, S.; Ikeda, H.; Kikuchi, H.; Watanabe, M.; Imaizumi, H.; Koizumi, W. Fine needle aspiration using forward-viewing endoscopic ultrasonography. *Endoscopy* **2011**, *43*, 796–801. [[CrossRef](#)] [[PubMed](#)]
25. Ascunce, G.; Ribeiro, A.; Reis, I.; Rocha-Lima, C.; Sleeman, D.; Merchan, J.; Levi, J. EUS visualization and direct celiac ganglia neurolysis predicts better pain relief in patients with pancreatic malignancy (with video). *Gastrointest. Endosc.* **2011**, *73*, 267–274. [[CrossRef](#)] [[PubMed](#)]
26. Iwata, K.; Yasuda, I.; Enya, M.; Mukai, T.; Nakashima, M.; Doi, S.; Iwashita, T.; Tomita, E.; Moriwaki, H. Predictive factors for pain relief after endoscopic ultrasound-guided celiac plexus neurolysis. *Dig. Endosc.* **2011**, *23*, 140–145. [[CrossRef](#)] [[PubMed](#)]
27. Wyse, J.M.; Carone, M.; Paquin, S.C.; Usatii, M.; Sahai, A.V. Randomized, double-blind, controlled trial of early endoscopic ultrasound-guided celiac plexus neurolysis to prevent pain progression in patients with newly diagnosed, painful, inoperable pancreatic cancer. *J. Clin. Oncol.* **2011**, *29*, 3541–3546. [[CrossRef](#)] [[PubMed](#)]
28. LeBlanc, J.K.; Al-Haddad, M.; McHenry, L.; Sherman, S.; Juan, M.; McGreevy, K.; Johnson, C.; Howard, T.J.; Lillemoe, K.D.; DeWitt, J. A prospective, randomized study of EUS-guided celiac plexus neurolysis for pancreatic cancer: one injection or two? *Gastrointest. Endosc.* **2011**, *74*, 1300–1307. [[CrossRef](#)] [[PubMed](#)]
29. Wiechowska-Kozłowska, A.; Boer, K.; Wójcicki, M.; Milkiewicz, P. The efficacy and safety of endoscopic ultrasound-guided celiac plexus neurolysis for treatment of pain in patients with pancreatic cancer. *Gastroenterol. Res. Pract.* **2012**, *2012*, 503098. [[CrossRef](#)] [[PubMed](#)]
30. Zou, X.P.; Chen, S.Y.; Lv, Y.; Li, W.; Zhang, X.Q. Endoscopic ultrasound-guided celiac plexus neurolysis for pain management in patients with pancreatic carcinoma reasons to fight a losing battle. *Pancreas* **2012**, *41*, 655–657. [[CrossRef](#)] [[PubMed](#)]

31. Varadarajulu, S.; Bang, J.Y.; Hebert-Magee, S. Assessment of the technical performance of the flexible 19-gauge EUS-FNA needle. *Gastrointest. Endosc.* **2012**, *76*, 336–343. [[CrossRef](#)] [[PubMed](#)]
32. Wang, K.X.; Jin, Z.D.; Du, Y.Q.; Zhan, X.B.; Zou, D.W.; Liu, Y.; Wang, D.; Chen, J.; Xu, C.; Li, Z.S. EUS-guided celiac ganglion irradiation with iodine-125 seeds for pain control in pancreatic carcinoma: A prospective pilot study. *Gastrointest. Endosc.* **2012**, *76*, 945–952. [[CrossRef](#)] [[PubMed](#)]
33. Leblanc, J.K.; Rawl, S.; Juan, M.; Johnson, C.; Kroenke, K.; McHenry, L.; Sherman, S.; McGreevy, K.; Al-Haddad, M.; Dewitt, J. Endoscopic ultrasound-guided celiac plexus neurolysis in pancreatic cancer: A prospective pilot study of safety using 10 mL versus 20 mL alcohol. *Diagn. Ther. Endosc.* **2013**, *2013*, 327036. [[CrossRef](#)] [[PubMed](#)]
34. Seicean, A.; Cainap, C.; Gulei, I.; Tantau, M.; Seicean, R. Pain palliation by endoscopic ultrasound-guided celiac plexus neurolysis in patients with unresectable pancreatic cancer. *J. Gastrointestin. Liver Dis.* **2013**, *22*, 59–64. [[PubMed](#)]
35. Doi, S.; Yasuda, I.; Kawakami, H.; Hayashi, T.; Hisai, H.; Irisawa, A.; Mukai, T.; Katanuma, A.; Kubota, K.; Ohnishi, T.; et al. Endoscopic ultrasound-guided celiac ganglia neurolysis vs. celiac plexus neurolysis: A randomized multicenter trial. *Endoscopy* **2013**, *45*, 362–369. [[CrossRef](#)] [[PubMed](#)]
36. Si-Jie, H.; Wei-Jia, X.; Yang, D.; Lie, Y.; Feng, Y.; Yong-Jian, J.; Ji, L.; Chen, J.; Liang, Z.; De-Liang, F. How to improve the efficacy of endoscopic ultrasound-guided celiac plexus neurolysis in pain management in patients with pancreatic cancer: Analysis in a single center. *Surg. Laparosc. Endosc. Percutan. Tech.* **2014**, *24*, 31–35. [[CrossRef](#)] [[PubMed](#)]
37. Téllez-Ávila, F.I.; Romano-Munive, A.F.; Herrera-Esquivel, J.J.; Ramírez-Luna, M.A. Central is as effective as bilateral endoscopic ultrasound-guided celiac plexus neurolysis in patients with unresectable pancreatic cancer. *Endosc. Ultrasound* **2013**, *2*, 153–156. [[CrossRef](#)] [[PubMed](#)]
38. Ishiwatari, H.; Hayashi, T.; Yoshida, M.; Ono, M.; Masuko, H.; Sato, T.; Miyanishi, K.; Sato, Y.; Takimoto, R.; Kobune, M.; et al. Phenol-based endoscopic ultrasound-guided celiac plexus neurolysis for East Asian alcohol-intolerant upper gastrointestinal cancer patients: A pilot study. *World J. Gastroenterol.* **2014**, *20*, 10512–10517. [[CrossRef](#)] [[PubMed](#)]
39. Ishiwatari, H.; Hayashi, T.; Yoshida, M.; Ono, M.; Sato, T.; Miyanishi, K.; Sato, Y.; Takimoto, R.; Kobune, M.; Masuko, H.; et al. EUS-guided celiac plexus neurolysis by using highly viscous phenol-glycerol as a neurolytic agent (with video). *Gastrointest. Endosc.* **2015**, *81*, 479–483. [[CrossRef](#)] [[PubMed](#)]
40. Fujii-Lau, L.L.; Bamlet, W.R.; Eldrige, J.S.; Chari, S.T.; Gleeson, F.C.; Abu Dayyeh, B.K.; Clain, J.E.; Pearson, R.K.; Petersen, B.T.; Rajan, E.; et al. Impact of celiac neurolysis on survival in patients with pancreatic cancer. *Gastrointest. Endosc.* **2015**, *82*, 46–56. [[CrossRef](#)] [[PubMed](#)]
41. Bang, J.Y.; Hasan, M.K.; Sutton, B.; Holt, B.A.; Navaneethan, U.; Hawes, R.; Varadarajulu, S. Intraprocedural increase in heart rate during EUS-guided celiac plexus neurolysis: Clinically relevant or just a physiologic change? *Gastrointest. Endosc.* **2016**, *84*, 773–779. [[CrossRef](#)] [[PubMed](#)]
42. Facciorusso, A.; Di Maso, M.; Serviddio, G.; Larghi, A.; Costamagna, G.; Muscatiello, N. Echoendoscopic ethanol ablation of tumor combined with celiac plexus neurolysis in patients with pancreatic adenocarcinoma. *J. Gastroenterol. Hepatol.* **2017**, *32*, 439–445. [[CrossRef](#)] [[PubMed](#)]
43. Minaga, K.; Kitano, M.; Sakamoto, H.; Miyata, T.; Imai, H.; Yamao, K.; Kamata, K.; Omoto, S.; Kadosaka, K.; Sakurai, T.; et al. Predictors of pain response in patients undergoing endoscopic ultrasound-guided neurolysis for abdominal pain caused by pancreatic cancer. *Therap. Adv. Gastroenterol.* **2016**, *9*, 483–494. [[CrossRef](#)] [[PubMed](#)]
44. Kappelle, W.F.W.; Bleys, R.L.A.W.; van Wijck, A.J.M.; Siersema, P.D.; Vleggaar, F.P. EUS-guided celiac ganglia neurolysis: A clinical and human cadaver study (with video). *Gastrointest. Endosc.* **2017**, *86*, 655–663. [[CrossRef](#)] [[PubMed](#)]
45. Soetikno, R.M.; Nguyen, P.T.; Chang, K.J. EUS in combination with fine-needle injection celiac plexus neurolysis from within a Wallstent stent. *Gastrointest. Endosc.* **2002**, *56*, 136–139. [[CrossRef](#)] [[PubMed](#)]
46. Muscatiello, N.; Panella, C.; Pietrini, L.; Tonti, P.; Ierardi, E. Complication of endoscopic ultrasound-guided celiac plexus neurolysis. *Endoscopy* **2006**, *38*, 858. [[CrossRef](#)] [[PubMed](#)]
47. Ahmed, H.M.; Friedman, S.E.; Henriques, H.F.; Berk, B.S. End-organ ischemia as an unforeseen complication of endoscopic-ultrasound-guided celiac plexus neurolysis. *Endoscopy* **2009**, *41*, E218–E219. [[CrossRef](#)] [[PubMed](#)]

48. Mittal, M.K.; Rabinstein, A.A.; Wijdicks, E.F. Acute spinal cord infarction following endoscopic ultrasound-guided celiac plexus neurolysis. *Neurology* **2012**, *78*, e57–e59. [[CrossRef](#)] [[PubMed](#)]
49. Fujii, L.; Clain, J.E.; Morris, J.M.; Levy, M.J. Anterior spinal cord infarction with permanent paralysis following endoscopic ultrasound celiac plexus neurolysis. *Endoscopy* **2012**, *44*, E265–E266. [[CrossRef](#)] [[PubMed](#)]
50. Gimeno-García, A.Z.; Elwassief, A.; Paquin, S.C.; Sahai, A.V. Fatal complication after endoscopic ultrasound-guided celiac plexus neurolysis. *Endoscopy* **2012**, *44*, E267. [[CrossRef](#)] [[PubMed](#)]
51. Jang, H.Y.; Cha, S.W.; Lee, B.H.; Jung, H.E.; Choo, J.W.; Cho, Y.J.; Ju, H.Y.; Cho, Y.D. Hepatic and splenic infarction and bowel ischemia following endoscopic ultrasound-guided celiac plexus neurolysis. *Clin. Endosc.* **2013**, *46*, 306–309. [[CrossRef](#)] [[PubMed](#)]
52. Minaga, K.; Kitano, M.; Imai, H.; Miyata, T.; Kudo, M. Acute spinal cord infarction after EUS-guided celiac plexus neurolysis. *Gastrointest. Endosc.* **2016**, *83*, 1039–1040. [[CrossRef](#)] [[PubMed](#)]
53. Facciorusso, A.; Maso, M.D.; Barone, M.; Muscatiello, N. Echoendoscopic ethanol ablation of tumor combined to celiac plexus neurolysis improved pain control in a patient with pancreatic adenocarcinoma. *Endosc. Ultrasound* **2015**, *4*, 342–344. [[CrossRef](#)] [[PubMed](#)]
54. Mulhall, A.M.; Rashkin, M.C.; Pina, E.M. Bilateral diaphragmatic paralysis: A rare complication related to endoscopic ultrasound-guided celiac plexus neurolysis. *Ann. Am. Thorac. Soc.* **2016**, *13*, 1660–1662. [[CrossRef](#)] [[PubMed](#)]
55. Köker, I.H.; Aralaşmak, A.; Ünver, N.; Asil, T.; Şentürk, H. Spinal cord ischemia after endoscopic ultrasound guided celiac plexus neurolysis: Case report and review of the literature. *Scand. J. Gastroenterol.* **2017**, *52*, 1158–1161. [[CrossRef](#)] [[PubMed](#)]
56. Lu, F.; Dong, J.; Tang, Y.; Huang, H.; Liu, H.; Song, L.; Zhang, K. Bilateral vs. unilateral endoscopic ultrasound-guided celiac plexus neurolysis for abdominal pain management in patients with pancreatic malignancy: A systematic review and meta-analysis. *Support. Care Cancer* **2017**. [[CrossRef](#)]
57. Kaufman, M.; Singh, G.; Das, S.; Concha-Parra, R.; Erber, J.; Micames, C.; Gress, F. Efficacy of endoscopic ultrasound-guided celiac plexus block and celiac plexus neurolysis for managing abdominal pain associated with chronic pancreatitis and pancreatic cancer. *J. Clin. Gastroenterol.* **2010**, *44*, 127–134. [[CrossRef](#)] [[PubMed](#)]
58. Puli, S.R.; Reddy, J.B.; Bechtold, M.L.; Antillon, M.R.; Brugge, W.R. EUS-guided celiac plexus neurolysis for pain due to chronic pancreatitis or pancreatic cancer pain: A meta-analysis and systematic review. *Dig. Dis. Sci.* **2009**, *54*, 2330–2337. [[CrossRef](#)] [[PubMed](#)]
59. Michaels, A.J.; Draganov, P.V. Endoscopic ultrasonography guided celiac plexus neurolysis and celiac plexus block in the management of pain due to pancreatic cancer and chronic pancreatitis. *World J. Gastroenterol.* **2007**, *13*, 3575–3580. [[CrossRef](#)] [[PubMed](#)]
60. Penman, I.D. State of the art: Putting EUS-guided block/neurolysis into perspective. *Gastrointest. Endosc.* **2009**, *69*, S174–S175. [[CrossRef](#)] [[PubMed](#)]
61. Barreto, S.G.; Saccone, G.T. Pancreatic nociception—Revisiting the physiology and pathophysiology. *Pancreatology* **2012**, *12*, 104–112. [[CrossRef](#)] [[PubMed](#)]
62. Kitoh, T.; Tanaka, S.; Ono, K.; Ohfusa, Y.; Ina, H.; Otagiri, T. Combined neurolytic block of celiac, inferior mesenteric and superior hypogastric plexuses for incapacitating abdominal and/or pelvic cancer pain. *J. Anesth.* **2005**, *19*, 328–332. [[CrossRef](#)] [[PubMed](#)]
63. Adler, D.G.; Conway, J.D.; Coffie, J.M.; Disario, J.A.; Mishkin, D.S.; Shah, R.J.; Somogyi, L.; Tierney, W.M.; Wong Kee Song, L.M.; Petersen, B.T.; et al. EUS accessories. *Gastrointest. Endosc.* **2007**, *66*, 1076–1081. [[CrossRef](#)] [[PubMed](#)]
64. Gleeson, F.C.; Levy, M.J.; Papachristou, G.I.; Pelaez-Luna, M.; Rajan, E.; Clain, J.E.; Topazian, M.D. Frequency of visualization of presumed celiac ganglia by endoscopic ultrasound. *Endoscopy* **2007**, *39*, 620–624. [[CrossRef](#)] [[PubMed](#)]
65. Ha, T.; Kim, G.; Kang, D.; Song, G.; Kim, S.; Lee, J. Detection of celiac ganglia with radial scanning endoscopic ultrasonography. *Korean J. Intern. Med.* **2008**, *23*, 5–8. [[CrossRef](#)] [[PubMed](#)]
66. Levy, M.J.; Wiersema, M.J. EUS-guided celiac plexus neurolysis and celiac plexus block. *Gastrointest. Endosc.* **2003**, *57*, 923–930. [[CrossRef](#)]

67. Yan, B.M.; Myers, R.P. Neurolytic celiac plexus block for pain control in unresectable pancreatic cancer. *Am. J. Gastroenterol.* **2007**, *102*, 430–438. [[CrossRef](#)] [[PubMed](#)]
68. Alvarez-Sánchez, M.V.; Jenssen, C.; Faiss, S.; Napoléon, B. Interventional endoscopic ultrasonography: An overview of safety and complications. *Surg. Endosc.* **2014**, *28*, 712–734. [[CrossRef](#)] [[PubMed](#)]



© 2018 by the authors. Licensee MDPI, Basel, Switzerland. This article is an open access article distributed under the terms and conditions of the Creative Commons Attribution (CC BY) license (<http://creativecommons.org/licenses/by/4.0/>).



ARTICLE

Clinical Study

Alpha-fetoprotein kinetics in patients with hepatocellular carcinoma receiving ramucirumab or placebo: an analysis of the phase 3 REACH study

Ian Chau¹, Joon Oh Park², Baek-Yeol Ryoo³, Chia-Jui Yen⁴, Ronnie Poon⁵, Davide Pastorelli⁶, Jean-Frédéric Blanc⁷, Masatoshi Kudo⁸, Tullio Pfiffer⁹, Etsuro Hatano¹⁰, Hyun Cheol Chung¹¹, Katerina Kopeckova¹², Jean-Marc Phelip¹³, Giovanni Brandi¹⁴, Shinichi Ohkawa¹⁵, Chung-Pin Li^{16,17}, Takuji Okusaka¹⁸, Yanzhi Hsu¹⁹, Paolo B. Abada²⁰ and Andrew X. Zhu²¹

BACKGROUND: Post-hoc analyses of AFP response and progression and their relationship with objective measures of response and survival were performed in patients from REACH.

METHODS: Serum AFP was measured at baseline and every 3 cycles (2 weeks/cycle). Associations between AFP and radiographic progression and efficacy end points were analysed.

RESULTS: Median percent AFP increase from baseline was smaller in the ramucirumab than in the placebo arm throughout treatment. Time to AFP progression (HR 0.621; $P < 0.0001$) and to radiographic progression (HR 0.613; $P < 0.0001$) favoured ramucirumab. Association between AFP and radiographic progression was shown at 6 (OR 6.44, 95% CI 4.03, 10.29; $P < 0.0001$) and 12 weeks (OR 2.28, 95% CI 1.47, 3.53; $P = 0.0002$). AFP response was higher with ramucirumab compared with placebo ($P < 0.0001$). More patients in the ramucirumab arm experienced tumour shrinkage and AFP response compared with placebo. Survival was longer in patients with AFP response (13.6 months) than in patients without (6.2 months), irrespective of treatment (HR 0.457, $P < 0.0001$).

CONCLUSIONS: Treatment with ramucirumab prolonged time to AFP progression, slowed AFP increase and was more likely to induce AFP response. Similar benefits in radiographic progression and response correlated with AFP changes.

British Journal of Cancer <https://doi.org/10.1038/s41416-018-0103-0>

INTRODUCTION

Liver cancer is the sixth most commonly diagnosed cancer worldwide and the second most common cause of cancer death.¹ Hepatocellular carcinoma (HCC) represents approximately 90% of primary liver cancers and occurs most frequently in patients with cirrhosis from chronic hepatitis B or C virus infection or alcohol abuse.²

Alpha-fetoprotein (AFP) level has long been known to correlate with HCC prognosis and has historically played a role in diagnosis. Elevated AFP levels are associated with larger tumours, bilobar involvement, portal vein invasion, poorly differentiated histology

and decreased median survival.³ Measurement of AFP level has been incorporated into some HCC prognostic scoring systems.^{4,5} While high levels of AFP are recognised as a poor prognostic factor, the utility of AFP response or progression during anticancer treatment is still unclear. There are limited studies in patients with HCC correlating AFP kinetics with treatment response during locoregional therapy or while on sorafenib and no published results of patients on second-line treatment.

Vascular endothelial growth factor (VEGF) is overexpressed in HCC and associated with poorer clinical outcomes, suggesting VEGF-mediated signalling is important in HCC pathogenesis and is

¹Department of Medicine, Royal Marsden Hospital, Sutton, Surrey SM2 5PT, UK; ²Division of Hematology-Oncology, Department of Medicine, Samsung Medical Center, Sungkyunkwan University School of Medicine, Seoul 135-710, Korea; ³Department of Oncology, Asan Medical Center, University of Ulsan College of Medicine, Seoul 05505, Korea; ⁴Department of Internal Medicine, National Cheng Kung University Hospital, College of Medicine, National Cheng Kung University, Tainan 701, Taiwan; ⁵Department of Surgery, The University of Hong Kong, Pokfulam, Hong Kong; ⁶Department of Oncology, Santa Maria del Prato Hospital, Feltre (Belluno) 32032, Italy; ⁷Department of Hepato-Gastroenterology and Medical Oncology, CHU de Bordeaux, Hôpital Haut-Lévêque, 33604 Pessac, France; ⁸Department of Gastroenterology and Hepatology, Kindai University Faculty of Medicine, Osaka-Sayama 589-8511, Japan; ⁹Department of Medical Oncology, Instituto do Câncer do Estado de São Paulo, São Paulo 01246-000, Brazil; ¹⁰Department of Surgery, Graduate School of Medicine, Kyoto University, Kyoto 606-8507, Japan; ¹¹Department of Medical Oncology, Yonsei Cancer Center, Yonsei University College of Medicine, Seoul 03722, Korea; ¹²Department of Oncology, University Hospital Motol, 2nd Faculty of Medicine of Charles University, 150 00 Praha, Czech Republic; ¹³Department of Gastroenterology and Digestive Oncology, University Hospital of St Etienne, 42100 Saint Etienne, France; ¹⁴Department of Experimental, Diagnostic and Specialty Medicine, University Hospital S. Orsola, 40138 Bologna, Italy; ¹⁵Division of Hepatobiliary and Pancreatic Oncology, Kanagawa Cancer Center, Yokohama 241-0815, Japan; ¹⁶Division of Gastroenterology and Hepatology, Department of Medicine, Taipei Veterans General Hospital, Taipei 112, Taiwan; ¹⁷National Yang-Ming University School of Medicine, Taipei 112, Taiwan; ¹⁸Department of Hepatobiliary and Pancreatic Oncology, National Cancer Center Hospital, Tokyo 104-0045, Japan; ¹⁹Eli Lilly and Company, New York, NY 10016, USA; ²⁰Eli Lilly and Company, Indianapolis, IN 46285, USA and ²¹Department of Medicine, Harvard Medical School, Massachusetts General Hospital, Boston, MA 02114, USA

Correspondence: Ian Chau (Ian.Chau@rmh.nhs.uk)

These authors contributed equally: Ian Chau, Andrew X. Zhu.

Received: 25 October 2017 Revised: 4 April 2018 Accepted: 11 April 2018

Published online: 29 May 2018

a therapeutic target.^{6–8} Ramucirumab is a recombinant immunoglobulin G, subclass 1 monoclonal antibody that specifically binds to the extracellular domain of VEGFR-2 with high affinity, preventing binding of VEGF ligands and receptor activation.⁹ REACH, a global, randomised, double-blinded placebo-controlled Phase 3 study, evaluated the efficacy and safety of single-agent ramucirumab for patients with advanced HCC after prior treatment with sorafenib ($N = 565$).¹⁰ Significant improvement in overall survival (OS) in the intent-to-treat (ITT) population was not achieved. However, a clinically meaningful improvement in OS was observed in patients with elevated baseline AFP levels (≥ 400 ng/mL [$n = 250$]) treated with ramucirumab vs placebo (OS 7.8 vs 4.2 months, respectively; hazard ratio (HR) 0.67, $P = 0.006$).

In the REACH study, AFP values were collected at baseline and during treatment. Post-hoc analyses of AFP response and progression, and correlations with other measures of efficacy including time to progression (TTP), objective response rate (ORR), and OS, were performed.

PATIENTS AND METHODS

Patient selection, randomisation and masking

The details of eligibility for inclusion in the REACH trial were previously described.¹⁰

Procedures

Patients received either ramucirumab 8 mg/kg (ImClone Systems Corporation, Branchburg, NJ, USA) ($n = 283$) or placebo ($n = 282$) intravenously every 2 weeks until disease progression, unacceptable toxicity or withdrawal of consent. All patients received supportive care. Predefined dose modifications were allowed to manage treatment-related toxicity.¹⁰ Local radiological imaging was performed at baseline, every 6 weeks over the first 6 months of treatment and every 9 weeks thereafter. In the event of ramucirumab/placebo dose delays or missed doses, disease assessment and imaging studies were to be undertaken according to the original study schedule (i.e. every 6 weeks after first dose for the first 6 months and every 9 weeks thereafter), regardless of the actual number of on-study treatments received.

Statistical definitions

TTP was defined as the time from randomisation to radiographic progression; radiographic response was assessed by protocol-defined criteria based on Response Evaluation Criteria in Solid Tumors 1.1 (appendix); ORR was defined as the proportion of patients who achieved complete response (CR) or partial response (PR) as their best overall response (BOR).

OS was defined as the time from randomisation to death from any cause.

Serum AFP levels were measured locally at baseline (within 2 weeks prior to randomisation), and every 3 cycles, i.e. every 6 weeks until treatment discontinuation, and at short-term follow-up. AFP progression was defined as $\geq 20\%$ increase from non-zero baseline and absolute increase ≥ 10 ng/mL. For the small number of patients ($n = 4$; 2 in the ramucirumab arm, 2 in the placebo arm) with a true baseline AFP of zero, AFP progression was defined as absolute increase AFP ≥ 10 ng/mL from zero baseline. These definitions were chosen to limit the risk of non-significant variations in AFP levels being considered AFP progression. AFP response was assessed in the population subset with baseline AFP ≥ 1.5 upper limit of normal (ULN) and was defined as $\geq 20\%$ decrease from baseline. This threshold of a minimum level of baseline AFP was selected to allow for a meaningful analysis since patients with very low levels of baseline AFP experiencing non-significant variations in AFP levels during treatment could result in large percent changes. Changes of 20 and 50% from baseline have been examined in previous studies.^{11–13}

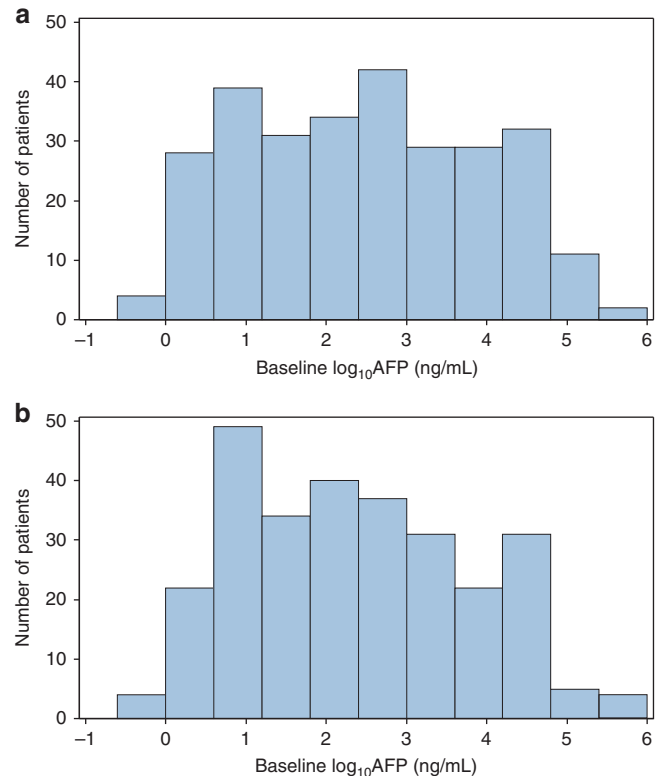


Fig. 1 Distribution of patients by baseline AFP level in each arm. **a** Patients treated with placebo and best standard of care. **b** Patients treated with ramucirumab and best standard of care. AFP alpha-fetoprotein

Statistical analysis

This post hoc analysis was conducted within the ITT population of REACH. The baseline distribution of patients by AFP level was plotted for comparison between arms. After taking log₁₀ of baseline AFP values, the frequency (patient count) was plotted for each arm. AFP response rate is presented with 95% confidence interval (CI) and was compared using the Cochran–Mantel–Haenszel test. Percent change in AFP from baseline was analysed for each arm at each time point up to Cycle 12. Analyses evaluated the association between the events of AFP progression and radiographic progression in each AFP level measurement time interval (Fisher’s exact test and odds ratio [OR]).

Time to AFP progression and time to radiographic progression between treatment arms were evaluated by the Kaplan–Meier method and tested by a stratified log-rank test. HR was generated using a stratified Cox proportional hazard model. AFP response rate is presented with 95% CI and compared using Cochran–Mantel–Haenszel test. The statistical analysis was done using the SAS® software Version 9.2.

AFP percent changes observed in patients in the ramucirumab arm were compared to those in the placebo arm at Cycles 3, 6, 9 and 12 by non-parametric Wilcoxon rank-sum tests.

RESULTS

Baseline patient and disease characteristics in the ITT population were well balanced between treatment groups.¹⁰ Baseline characteristics of patients in whom AFP response was assessed (with baseline AFP above 1.5 ULN, $n = 417$) were also well balanced and, apart from baseline, AFP showed no meaningful differences from the baseline characteristics of the ITT population

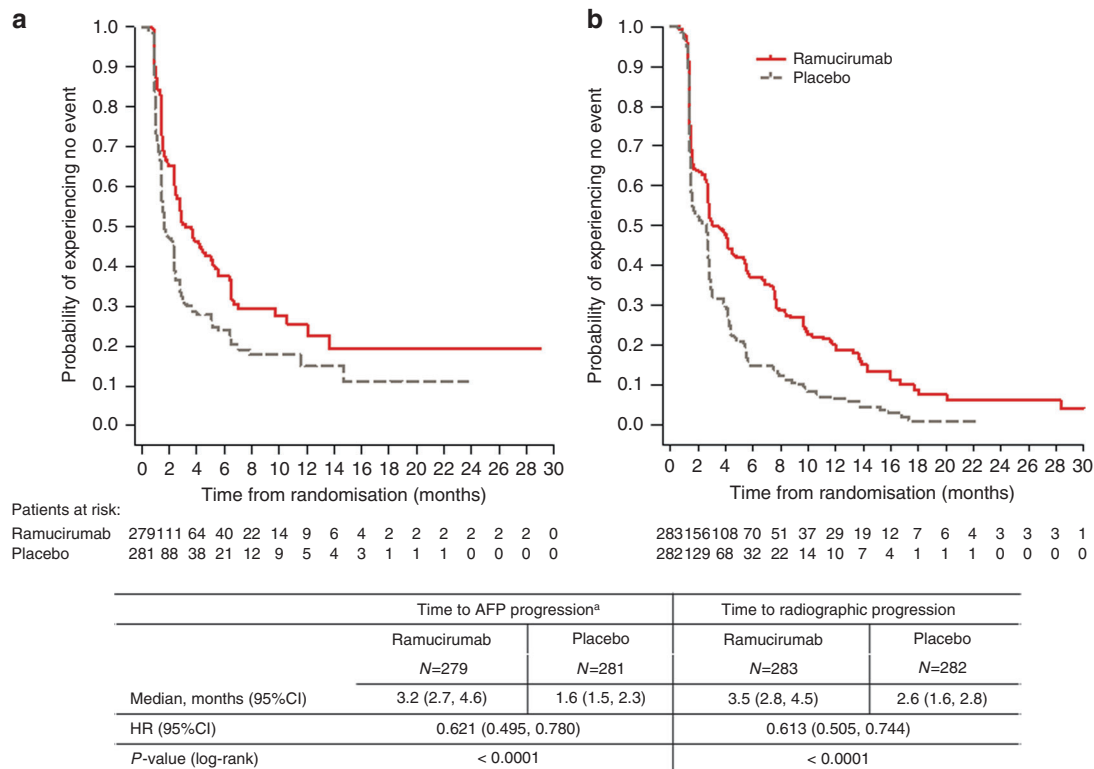


Fig. 2 Kaplan–Meier plots of **a** time to AFP progression^a and **b** time to radiographic progression in the ITT population. AFP alpha-fetoprotein, CI confidence interval, HR hazard ratio, ITT intention to treat. ^aFive patients were not included because of missing baseline AFP level

(Table S1). Additional details on the REACH study population have been disclosed previously.¹⁰ After log transformation of baseline AFP, the distribution of patients by log AFP for each treatment arm appeared similar in both treatment arms. A *t*-test on the log-transformed baseline AFP levels did not show any significant difference in baseline AFP levels between two arms (Fig. 1).

Changes in AFP relative to baseline were analysed and defined as either AFP progression or response, or neither, as per the Patients and methods section. A Kaplan–Meier plot of time to AFP progression for patients treated with ramucirumab vs placebo is shown in Fig. 2. The median time to AFP progression was 3.2 months in the ramucirumab arm (95% CI 2.7, 4.6, *n* = 279) and 1.6 months in the placebo arm (95% CI 1.5, 2.3, *n* = 281) with an HR of 0.621 (*P* < 0.0001).

Consistent with the results on time to AFP progression, patients treated with ramucirumab were more likely to experience an AFP response (decrease) at any time post-baseline compared to patients treated with placebo (ramucirumab: 27.8% vs placebo: 10.8%; *P* < 0.0001) and less likely to experience AFP progression (increase) at any time post-baseline compared to those treated with placebo (ramucirumab: 62.4% vs placebo: 75.9%; *P* = 0.0033). The difference in the percentage of patients with AFP response or progression between arms was significant when AFP response and progression were defined as a 20% (*P* < 0.0001) or 50% (*P* = 0.0004) change from baseline. No meaningful differences in the rates of AFP response were observed for patients with baseline ≥ 400 ng/mL compared to those with AFP < 400 ng/mL, suggesting that AFP response was independent of the magnitude of baseline AFP (data not shown).

Waterfall plots of best percent change in AFP from baseline for patients treated with ramucirumab or placebo also support the results of the analyses on AFP response and progression (Fig. 3a). The proportion of patients who experienced an increase in AFP was not only lower in the ramucirumab arm but the magnitude of

the increase also appeared smaller when compared with the placebo arm. Of note, 23 patients on the placebo arm also experienced an AFP response. An assessment of baseline characteristics for these patients did not identify any meaningful differences from the rest of the cohort, and other definitions of AFP response would not eliminate the presence of patients with AFP response in the placebo arm and likely represent true spontaneous responses.

To further assess the kinetics of AFP during treatment, AFP percent changes from baseline were calculated, and the median percent change from baseline evaluated by treatment arm (Fig. 4a). At each AFP assessment time point following baseline at Cycles 3, 6, 9 and 12, the median percent increase in AFP level from baseline was smaller in the ramucirumab arm (4, 0, 3, 33%) than in the placebo arm (37, 50, 99, 78%), respectively, and AFP percent change was significantly smaller in the ramucirumab arm at Cycles 3, 6 and 9.

Correlation of AFP changes with measures of radiographic response or progression

Kaplan–Meier plots of time to AFP progression and time to radiographic progression were similar in appearance (Fig. 2). The median time to radiographic progression was 3.5 months on the ramucirumab arm (95% CI 2.8, 4.5, *n* = 283) and 2.6 months in the placebo arm (95% CI 1.6, 2.8, *n* = 282, HR 0.613, *P* < 0.0001). A high association between AFP progression and radiographic progression occurring within each tumour assessment period was also observed (OR 6.4, 95% CI 4.0, 10.3, *P* < 0.0001 for up to Week 6, OR 2.3, 95% CI 1.5, 3.5, *P* = 0.0002 for Weeks 6–12) (Table 1).

Median percent change in AFP was further assessed in subgroups of patients defined by their best overall radiographic response (objective response [complete response/partial response (CR/PR)], disease control [CR/PR/stable disease (SD)] and progressive disease [PD]). For patients with a best overall radiographic

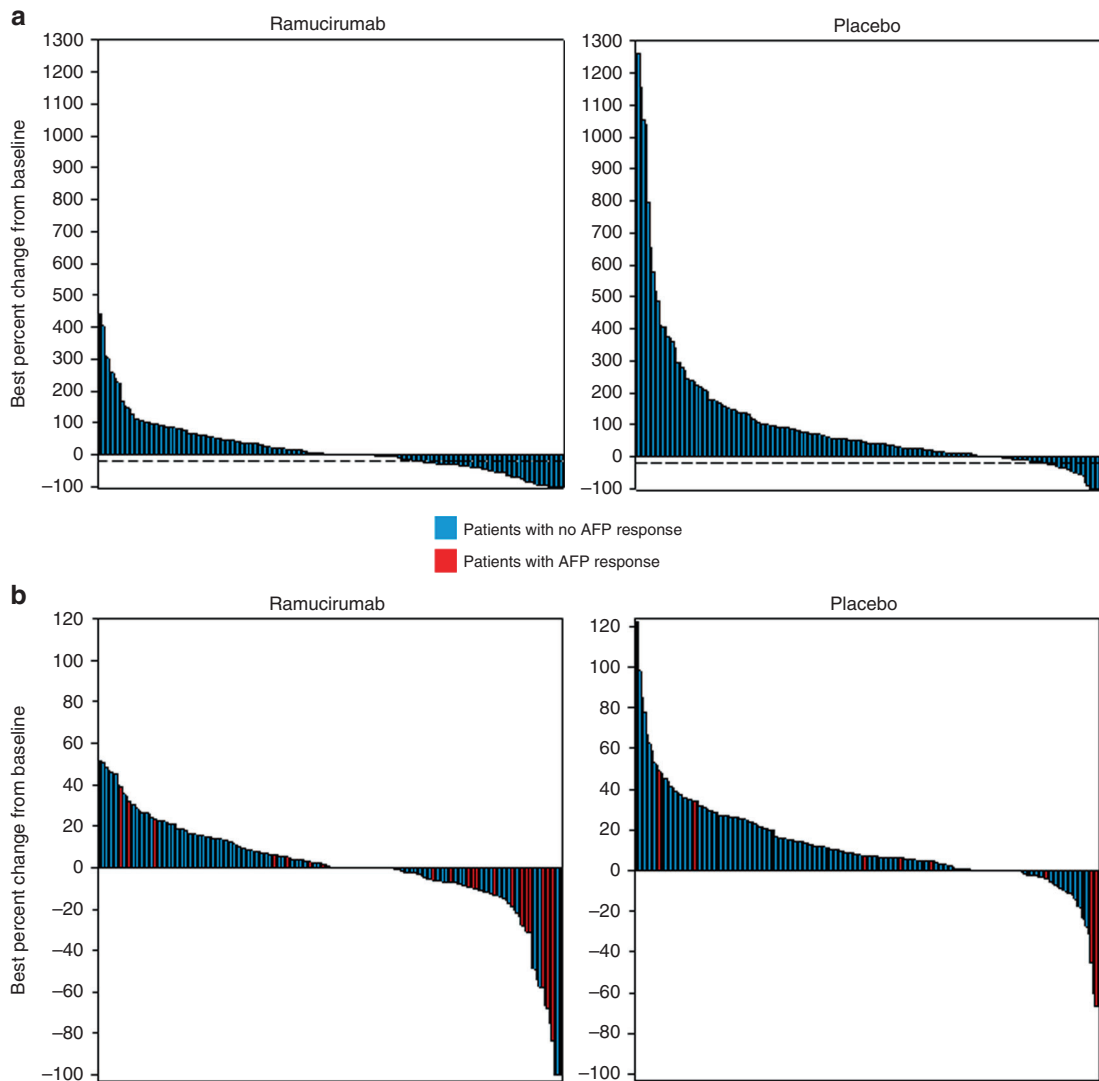


Fig. 3 Waterfall plots of response for patients by treatment arm. **a** Best percent change in AFP from baseline measurements by treatment arm. **b** Best percent change in radiographic tumour response, and relationship with AFP response. AFP alpha fetoprotein

response of CR/PR, the observed median percent change in AFP was a decrease in both treatment arms, with more patients in the ramucirumab arm experiencing an objective response compared to placebo (Fig. 4b). However, this should be interpreted with caution given the small number of patients with best response of CR/PR and the differences between the groups were not statistically significant (Fig. 4b). For patients with a BOR of disease control (CR/PR/SD), the median percent AFP increase from baseline for patients in the ramucirumab arm was lower than what was observed in the placebo arm at each cycle (Fig. 4c), with AFP percent changes being statistically different for the two arms at Cycles 6 and 9. In patients experiencing a best response of PD defined by radiographic progression, AFP increase from baseline for patients on the ramucirumab arm was significantly lower than what was observed on the placebo arm at Cycle 3 (Fig. 4d). There was no data available at Cycle 9 or 12 for this subgroup of patients as most patients with a best response of progression had already discontinued treatment.

Waterfall plots of radiographic tumour response by treatment arm and the relationship with AFP response (yes vs no) are shown in Fig. 3b. A higher proportion of patients experienced a radiographic response in the ramucirumab arm compared with the placebo arm. Most patients with a radiographic response (14

on RAM, 4 on PBO) also experienced an AFP response (10 on RAM, 3 on PBO).

Overall survival by AFP response

Additional analyses on the relationship between AFP response and OS were performed. A Kaplan–Meier plot of OS for patients (baseline AFP $> 1.5 \times$ ULN), irrespective of treatment arm, with either an AFP response ($n = 80$) or no AFP response ($n = 337$) is shown in Fig. 5a. The median OS for patients with an AFP response was significantly longer than that for patients without AFP response (13.6 vs 6.2 months, HR = 0.457, 95% CI 0.338, .616; $P < 0.0001$).

Kaplan–Meier plots of OS by treatment arm in patients with either an AFP response (Fig. 5b) or no AFP response (Fig. 5c) are shown in Fig. 5. In patients with an AFP response, there was no statistically significant survival benefit of ramucirumab treatment over placebo over the course of treatment (up to 28 months). Notably, in patients without an AFP response, a potentially significant survival benefit was observed for patients treated with ramucirumab compared to placebo (7.2 vs 5.2 months, HR = 0.758, 95% CI 0.600, 0.958; $P = 0.020$), suggesting that even patients with elevated AFP ($> 1.5 \times$ ULN) who do not have an AFP response may derive a benefit from ramucirumab treatment.

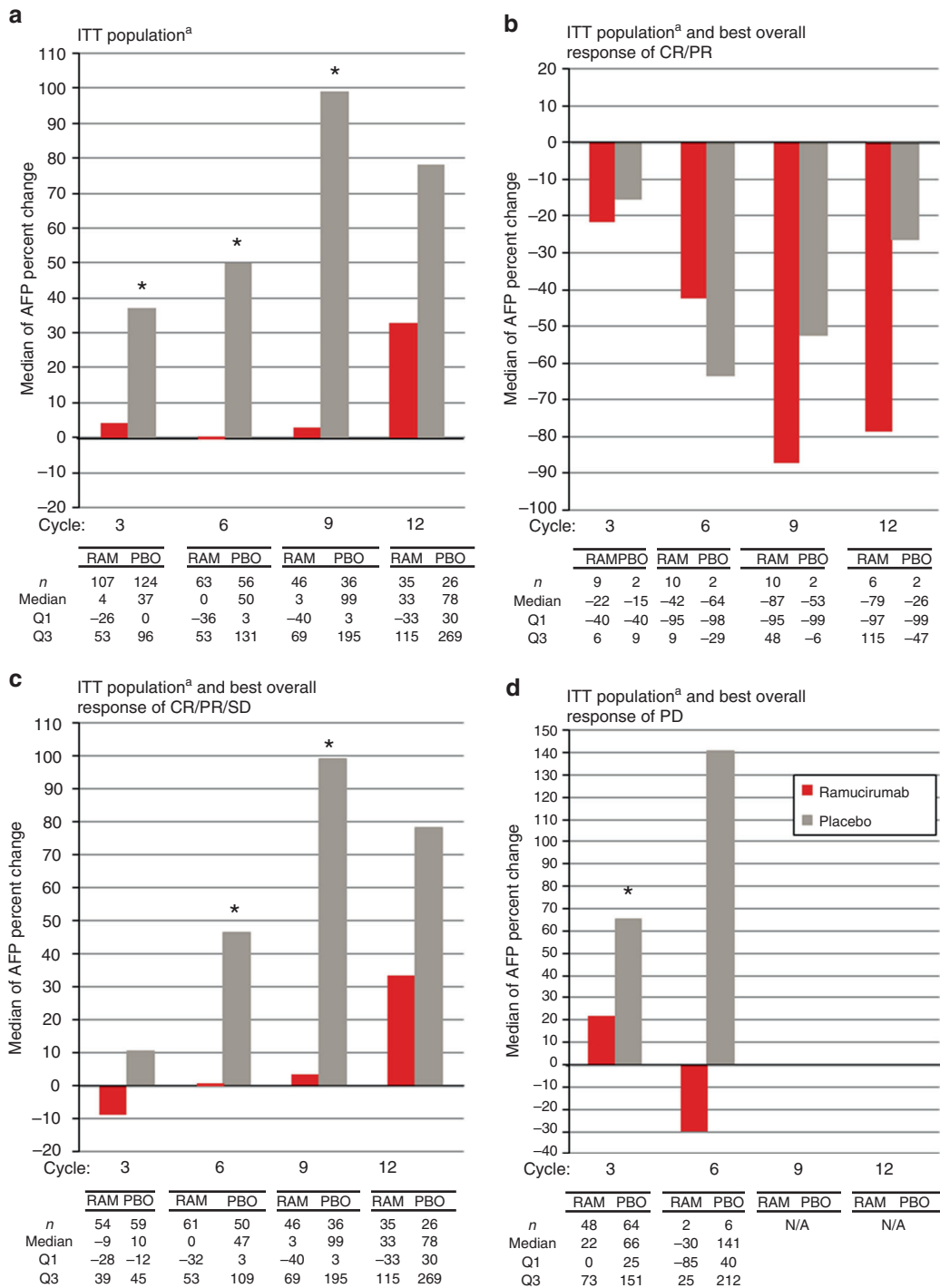


Fig. 4 AFP percent change from baseline by cycle. Medians of AFP percent changes from baseline were plotted every three cycles for patients from the ITT population with baseline AFP ≥ 1.5 ULN by treatment arm. **a** for all patients; **b** for patients with best overall response of CR/PR; **c** for patients with best overall response of CR/PR/SD; **d** for patients with best overall response of PD. ^aITT population with baseline AFP ≥ 1.5 ULN. *Indicates a statistical difference between the two groups by non-parametric Wilcoxon rank-sum tests. AFP alpha-fetoprotein, CR complete response, ITT intention to treat, NA not available, PD progressive disease, PR partial response, SD stable disease, Q1 lower quartile, Q3 upper quartile

Further analyses showed that 11 patients completely normalised their AFP level, 8 from the ramucirumab arm, and 3 from the placebo arm. The OS for these 11 patients who completely normalised their AFP level was significantly longer than the OS for patients who had AFP response without completely normalising their AFP level ($n = 111$) (25.6 vs 10.6 months, respectively, HR = 0.147, $P = 0.0019$).

DISCUSSION

Serum AFP has long been recognised as both a diagnostic and prognostic marker.^{14–17} However, assessing AFP kinetics during treatment has been limited. Some retrospective studies have been performed in patients undergoing locoregional therapy, where an AFP response has been associated with a longer survival following transarterial chemoembolisation.^{12,18,19} In the more advanced

Table 1. Radiographic progression and AFP progression by tumour measurement period

	Radiographic progression event	No radiographic progression event	<i>P</i> -value	Odds ratio (95% CI)
Up to 6 weeks, <i>N</i>	97	463		
AFP progression, <i>n</i> (%)	56 (58)	81 (18)		
No AFP progression, <i>n</i> (%)	41 (42)	382 (83)		
			<0.0001	6.4 (4.0, 10.3)
6–12 weeks, <i>N</i>	159	246		
AFP progression, <i>n</i> (%)	63 (40)	55 (22)		
No AFP progression, <i>n</i> (%)	96 (60)	191 (78)		
			0.0002	2.3 (1.5, 3.5)

AFP alpha-fetoprotein, CI confidence interval

AFP progression was defined as ≥20% increase from non-zero baseline and absolute increase ≥10 ng/mL, or absolute increase AFP ≥ 10 ng/mL from zero baseline, within 2 weeks.

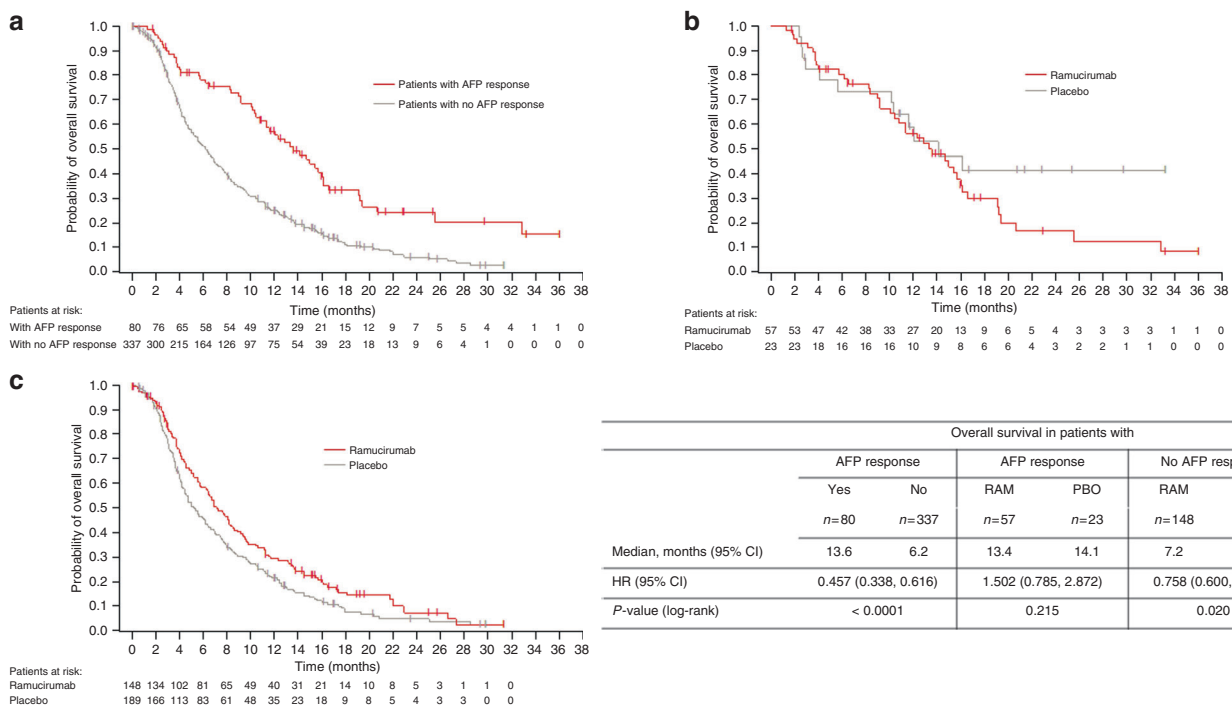


Fig. 5 Kaplan–Meier plots of overall survival. **a** By AFP response, both arms combined. **b** By arm, in patients with AFP response. **c** By arm, in patients with no AFP response. AFP alpha-fetoprotein, CI confidence interval, HR hazard ratio, RAM ramucirumab, PBO placebo

setting, AFP response has been evaluated in patients being treated with chemotherapy as well as sorafenib where a response is often associated with a survival advantage.^{13,20,21} In these previously published studies, there were fewer than 200 patients evaluated, only one of them derived data from a randomised study and none was placebo-controlled. Here we report post-hoc analyses of AFP response and progression in 565 patients enrolled in the REACH study. Five hundred and sixty patients with assessable changes in AFP were included in our analysis. An additional advantage of having a placebo arm in our REACH study was to allow assessment of AFP kinetics due to underlying HCC rather than treatment-related. However, in most studies examining systemic therapy, including REACH, the number of patients who experience an AFP response has been quite low. Molecularly targeted agents more commonly result in disease stability, and restricting treatment to patients experiencing an AFP response would exclude a large proportion of patients with stable or slowed progression of AFP levels, who would also derive survival benefit from continued treatment.

In the current analysis of REACH, there was an observed benefit with ramucirumab in delaying time to AFP progression, inducing more frequent and deeper AFP response and lesser AFP progression. AFP changes also correlated with radiographic response and progression. The phase 2 biomarker study of ramucirumab as first-line monotherapy in patients with advanced HCC showed that an AFP decrease was more likely in patients who experienced a radiographic response and an AFP increase more likely in patients with radiographically progressive or non-evaluable disease.²² Similar correlations have been made between AFP and other radiographic measures of response with other systemic treatments including sorafenib.^{13,23–26} The observations of changes in AFP and measures of objective response in REACH continue to support a correlation between AFP and objective radiographic measures of tumour assessment.

The results presented here support the notion that the ramucirumab antitumour effect is not restricted to patients with AFP or objective tumour response but rather has some activity in all tumours with varying degree. In the ramucirumab arm, more

patients experienced both an AFP and a radiographic response compared to placebo. We also observed a shift in the rest of the treated population favouring ramucirumab compared to placebo. More patients in the ramucirumab arm experienced stable AFP or SD compared to placebo. Even in patients who only experienced AFP or radiographic progression, the amplitude of the observed AFP or tumour increase was generally lower.

However, while changes in AFP may correlate with other measures of tumour assessment, neither changes in AFP nor other objective measures of tumour response have been good surrogates to predict OS.²⁷ In REACH, while an AFP response was associated with significantly longer OS, analyses support that OS benefit extends to a larger population. Notably, in patients with an elevated baseline AFP ($>1.5 \times \text{ULN}$) a potential OS benefit was still observed in ramucirumab-treated patients compared to placebo, even when AFP responders were excluded; this is likely driven by the much larger proportion of patients who experience disease stability rather than regression. While this re-demonstrates that an elevated baseline AFP can identify the subset of patients most likely to derive an OS benefit, the finding also shows that AFP response is inadequate to select patients most likely to derive a survival benefit. Based on the studies presented here, the lack of an AFP response for a patient should not be used in isolation to judge clinical benefit of systemic treatments like ramucirumab.

Of note, a number of patients on placebo also experienced an AFP response. While the reasons for spontaneous AFP response in the placebo arm are unknown, we note that a similar proportion of patients on the placebo arm also experienced a radiographic response. Other limitations of the results presented here are due to the fact that these were post-hoc analyses performed on a phase 3 study that did not meet its primary end point.

In conclusion, exploratory analyses of REACH show that changes in AFP over time appear to correlate with other measures of objective progression and may help predict patient response, but the utility of AFP to make treatment decisions needs to be validated through a prospective study. Further assessment of the potential benefit of ramucirumab in patients with elevated baseline AFP is being validated in the ongoing REACH-2 study.

ACKNOWLEDGEMENTS

This study was funded by Eli Lilly and Company. We thank the patients, their families and the study personnel across all sites for participating in this study. Yihuan Xu of Eli Lilly and Company (Bridgewater, NJ) provided statistical expertise. Nathalie Godinot of Eli Lilly and Company (Indianapolis, IN) provided writing assistance. I.C. would like to thank the National Health Service for funding to the National Institute for Health Research Biomedical Research Centre at the Royal Marsden NHS Foundation Trust and The Institute of Cancer Research.

ADDITIONAL INFORMATION

Supplementary information is available for this paper at <https://doi.org/10.1038/s41416-018-0103-0>.

Ethical Approval: Each centre's institutional review board or ethics committee approved the study. The trial followed the principles of the Declaration of Helsinki and the Good Clinical Practice Guidelines of the International Conference on Harmonisation. All patients provided written informed consent.

Competing interests: I.C. reports advisory board roles at Sanofi Oncology, Eli Lilly and Company, Bristol Meyers Squibb, MSD, Bayer, Roche, Five Prime Therapeutics; honoraria from Taiho, Pfizer, Amgen, Eli-Lilly, Gilead Science; research funding from Janssen-Cilag, Sanofi Oncology, Merck-Serono, Novartis. J.O.P. reports receiving clinical research grants, honoraria from Celgene and research grant from AstraZeneca. He reports a role on the advisory board for Celgene. J.-F.B. reports payments from Lilly Oncology, Bayer SP, BMS and Novartis outside the submitted work. M.K. received research grants from Chugai, Otsuka, Takeda, Taiho, Sumitomo Dainippon, Daiichi Sankyo, MSD, Eisai, Bayer, Abbvie, Medico's Hirata, Astellas Pharma

and Bristol-Myers Squibb; lecture fees from Bayer, Eisai, MSD, Ajinomoto, Kowa and Taiho; and consulting fees from Kowa, MSD, BMS, Bayer, Chugai, Taiho and Eisai. H.C. C. is a consultant for Eli Lilly and Company, MSD, Merck-Serono, Taiho, BMS, Celltrion, he has received research grants from Eli Lilly and Company, GSK and MSD. J.-M.P. reports receiving research grants from Roche and Merck and payments from Eli Lilly and Company, Bayer, Sanofi, Roche and Merck. T.O. reports research grants, advisory role and honoraria from Eli Lilly, during the conduct of the study; he also reports research grants advisory role and/or honoraria from Novartis Pharma K.K., Kowa K.K., Takeda Bio Development Center Limited, Nippon Boehringer Ingelheim Co., Ltd., Dainippon Simitomo Pharma Co., Ltd., Pfizer Jana Inc, Taiho Pharmaceutical Co., Ltd., Bayer Yakuhin, Ltd., Chugai Pharmaceutical Co., Ltd., Yakuruto Honsha Co., Ltd., Ono Pharmaceutical Co., Ltd., Eisai Co., Ltd., AstraZeneca K.K., Merck Serono Co., Ltd., OncoTherapy Science Inc., Kyowa Hakko Kirin Co., Ltd., Shizuoka Industry, Baxter, Nano Carrier Co., Ltd., Zeria Pharmaceutical Co., Ltd., Glaxo Smith Kline K.K., Nobelpharma Co., Ltd., burisutoru, Nipponchemofa, EA Pharma Co., Ltd., FUJIFILM RI Pharma Co., Ltd., Astellas Pharma Inc., Nippon Kayaku Co., Ltd., Daiichi Sankyo Co., Ltd., J-CRSU CO., LTD., outside the submitted work. P.A. and Y.H. are employees of Eli Lilly and Company and own stock from Eli Lilly and Company. A.X.Z. reports that his institution received research support from Eli Lilly and Company. The other authors declare no competing interests.

Note: This work is published under the standard license to publish agreement. After 12 months the work will become freely available and the license terms will switch to a Creative Commons Attribution 4.0 International licence (CC BY 4.0).

Funding: This work was supported by Eli Lilly and Company.

REFERENCES

1. Ferlay, J. et al. Cancer incidence and mortality worldwide: sources, methods and major patterns in GLOBOCAN 2012. *Int. J. Cancer* **136**, E359–386 (2015).
2. Jelic, S., Sotiropoulos, G. C. & Group, E. G. W. Hepatocellular carcinoma: ESMO Clinical Practice Guidelines for diagnosis, treatment and follow-up. *Ann. Oncol.* **21**, v59–64 (2010).
3. Gooma, A. I., Khan, S. A., Leen, E. L., Waked, I. & Taylor-Robinson, S. D. Diagnosis of hepatocellular carcinoma. *World J. Gastroenterol.* **15**, 1301–1314 (2009).
4. Pons, F., Varela, M. & Llovet, J. M. Staging systems in hepatocellular carcinoma. *HPB (Oxf.)* **7**, 35–41 (2005).
5. Borzio, M. et al. External validation of the ITA.LI.CA prognostic system for patients with hepatocellular carcinoma: a multicenter cohort study. (HEP-17-0903). *Hepatology* <https://doi.org/10.1002/hep.29662> (2017).
6. Tugues, S., Koch, S., Gualandi, L., Li, X. & Claesson-Welsh, L. Vascular endothelial growth factors and receptors: anti-angiogenic therapy in the treatment of cancer. *Mol. Asp. Med.* **32**, 88–111 (2011).
7. Amini, A., Masoumi Moghaddam, S., Morris, D. L. & Pourgholami, M. H. The critical role of vascular endothelial growth factor in tumor angiogenesis. *Curr. Cancer Drug Targets* **12**, 23–43 (2012).
8. Zhu, A. X., Duda, D. G., Sahani, D. V. & Jain, R. K. HCC and angiogenesis: possible targets and future directions. *Nat. Rev. Clin. Oncol.* **8**, 292–301 (2011).
9. Sprattlin, J. L. et al. Phase I pharmacologic and biologic study of ramucirumab (IMC-1121B), a fully human immunoglobulin G1 monoclonal antibody targeting the vascular endothelial growth factor receptor-2. *J. Clin. Oncol.* **28**, 780–787 (2010).
10. Zhu, A. X. et al. Ramucirumab versus placebo as second-line treatment in patients with advanced hepatocellular carcinoma following first-line therapy with sorafenib (REACH): a randomised, double-blind, multicentre, phase 3 trial. *Lancet Oncol.* **16**, 859–870 (2015).
11. Personeni, N. et al. Usefulness of alpha-fetoprotein response in patients treated with sorafenib for advanced hepatocellular carcinoma. *J. Hepatol.* **57**, 101–107 (2012).
12. Memon, K. et al. Alpha-fetoprotein response correlates with EASL response and survival in solitary hepatocellular carcinoma treated with transarterial therapies: a subgroup analysis. *J. Hepatol.* **56**, 1112–1120 (2012).
13. Chan, S. L. et al. New utility of an old marker: serial alpha-fetoprotein measurement in predicting radiologic response and survival of patients with hepatocellular carcinoma undergoing systemic chemotherapy. *J. Clin. Oncol.* **27**, 446–452 (2009).
14. CLIP Investigators. A new prognostic system for hepatocellular carcinoma: a retrospective study of 435 patients: the Cancer of the Liver Italian Program (CLIP) investigators. *Hepatology* **28**, 751–755 (1998).
15. Tangkijvanich, P. et al. Clinical characteristics and prognosis of hepatocellular carcinoma: analysis based on serum alpha-fetoprotein levels. *J. Clin. Gastroenterol.* **31**, 302–308 (2000).

16. Zhang, X. F. et al. Prognostic factors after liver resection for hepatocellular carcinoma with hepatitis B virus-related cirrhosis: surgeon's role in survival. *Eur. J. Surg. Oncol.* **35**, 622–628 (2009).
17. Wang, N. Y. et al. Prognostic value of serum AFP, AFP-L3, and GP73 in monitoring short-term treatment response and recurrence of hepatocellular carcinoma after radiofrequency ablation. *Asian Pac. J. Cancer Prev.* **15**, 1539–1544 (2014).
18. Riaz, A. et al. Alpha-fetoprotein response after locoregional therapy for hepatocellular carcinoma: oncologic marker of radiologic response, progression, and survival. *J. Clin. Oncol.* **27**, 5734–5742 (2009).
19. Liu, L. et al. The prognostic value of alpha-fetoprotein response for advanced-stage hepatocellular carcinoma treated with sorafenib combined with transarterial chemoembolization. *Sci. Rep.* **6**, 19851 (2016).
20. Vora, S. R., Zheng, H., Stadler, Z. K., Fuchs, C. S. & Zhu, A. X. Serum alpha-fetoprotein response as a surrogate for clinical outcome in patients receiving systemic therapy for advanced hepatocellular carcinoma. *Oncologist* **14**, 717–725 (2009).
21. Kim, B. et al. Early a-fetoprotein response as a predictor for clinical outcome after localized concurrent chemoradiotherapy for advanced hepatocellular carcinoma. *Liver Int.* **31**, 369–376 (2011).
22. Zhu, A. X. et al. A phase II and biomarker study of ramucirumab, a human monoclonal antibody targeting the VEGF receptor-2, as first-line monotherapy in patients with advanced hepatocellular cancer. *Clin. Cancer Res.* **19**, 6614–6623 (2013).
23. Matsumoto, Y., Suzuki, T., Ono, H., Nakase, A. & Honjo, I. Evaluation of hepatoma chemotherapy by alpha-fetoprotein determination. *Am. J. Surg.* **132**, 325–328 (1976).
24. Choi, T. K., Lee, N. W. & Wong, J. Chemotherapy for advanced hepatocellular carcinoma. Adriamycin versus quadruple chemotherapy. *Cancer* **53**, 401–405 (1984).
25. Chen, L. T. et al. Alpha-fetoprotein response predicts survival benefits of thalidomide in advanced hepatocellular carcinoma. *Aliment. Pharmacol. Ther.* **22**, 217–226 (2005).
26. Lee, S. et al. Early alpha-fetoprotein response predicts survival in patients with advanced hepatocellular carcinoma treated with sorafenib. *J. Hepatocell. Carcinoma* **2**, 39–47 (2015).
27. Llovet, J. M., Villanueva, A., Lachenmayer, A. & Finn, R. S. Advances in targeted therapies for hepatocellular carcinoma in the genomic era. *Nat. Rev. Clin. Oncol.* **12**, 408–424 (2015). 436.

Ramucirumab Safety in East Asian Patients: A Meta-Analysis of Six Global, Randomized, Double-Blind, Placebo-Controlled, Phase III Clinical Trials

abstract

Purpose Several ramucirumab trials have reported a higher incidence of selected adverse events (AEs) in East Asian (EA) patients with cancer versus non-EA patients. A meta-analysis was conducted across six completed phase III trials to establish the safety parameters of ramucirumab in EA compared with non-EA patients.

Materials and Methods Six global, randomized, double-blind, placebo-controlled, phase III registration trials investigating ramucirumab were assessed. Relative risks (RRs) and 95% CIs were calculated for selected all-grade and grade ≥ 3 AEs using fixed-effects and mixed-effects models. Ratio of RR and number needed to harm were calculated for AEs (all grade and grade ≥ 3) between EA and non-EA patients.

Results Of 4,996 randomly assigned patients receiving ramucirumab or placebo, 802 (16.1%) were EA (ramucirumab, $n = 411$; placebo, $n = 391$) and 4,194 were non-EA (ramucirumab, $n = 2,337$; placebo, $n = 1,857$). Patient baseline characteristics were generally balanced between treatment arms in EA and non-EA patients, excluding sex and body weight. Grade ≥ 3 AEs possibly associated with ramucirumab, which were increased in EA versus non-EA patients, included neutropenia (42.1% v 25.5%, respectively) and proteinuria (3.9% v 0.6%, respectively). There was an increase in the RR of several grade ≥ 3 AEs, including hypertension and proteinuria, in ramucirumab-treated EA and non-EA patients compared with placebo. The ratio of RR revealed no significant differences between EA and non-EA patients for all-grade and grade ≥ 3 AEs.

Conclusion Despite the enhanced propensity of selected AEs in EA patients relative to non-EA patients, there were no substantial differences in the RR for AEs possibly associated with ramucirumab in these phase III trials.

© 2018 by American Society of Clinical Oncology Licensed under the Creative Commons Attribution 4.0 License

INTRODUCTION

Ramucirumab is a human immunoglobulin G1 monoclonal antibody targeting vascular endothelial growth factor (VEGF) receptor-2,¹ a key mediator of VEGF-induced angiogenesis.² Six global, randomized, double-blind, placebo-controlled, phase III clinical trials have been completed, investigating ramucirumab in breast (ROSE),³ gastric (REGARD, RAINBOW),^{4,5} lung (REVEL),⁶ hepatocellular (REACH),⁷ and colorectal (RAISE)⁸ carcinomas.

Subsequently, ramucirumab (Cyramza; Eli Lilly, Indianapolis, IN) received worldwide and US Food and Drug Administration approval for gastric, lung, and colorectal cancers in the

second-line setting.⁹ The safety parameters of ramucirumab across these six, global, phase III clinical trials have recently been investigated.¹⁰ This study, comprising a large patient population of 4,996, demonstrated a higher percentage of proteinuria, hypertension, low-grade bleeding, GI perforation, and wound-healing complications in ramucirumab-treated patients, consistent with antiangiogenic treatment. Notably, ramucirumab may be distinct among antiangiogenic agents in terms of no apparent increased risk of arterial thromboembolic events, venous thromboembolic events, high-grade bleeding, or high-grade GI bleeding.¹⁰

Subgroup analyses have been performed in selected phase III trials examining the efficacy

Chia-Jui Yen
Kei Muro
Tae-Won Kim
Masatoshi Kudo
Jin-Yuan Shih
Keun-Wook Lee
Yee Chao
Sang-We Kim
Kentaro Yamazaki
JooHyuk Sohn
Rebecca Cheng
Yawei Zhang
Polina Binder
Gu Mi
Mauro Orlando
Hyun Cheol Chung

Author affiliations and support information (if applicable) appear at the end of this article.

Corresponding author:
Hyun Cheol Chung,
MD, PhD, Yonsei
Cancer Center, Yonsei
University College of
Medicine, Seoul, South
Korea 03722; e-mail:
Unchung8@yuhs.ac.

Table 1. Six Global Phase III Trials Investigating Ramucirumab

Trial	Dosing Regimen	No. of Patients (Safety Population)	
		EA	Non-EA
Breast cancer			
ROSE	First line (n = 1,144); docetaxel (75 mg/m ²) ± RAM (10 mg/kg) once every 3 weeks; randomization ratio, 2:1	27	1,107
Gastric/GEJ cancer			
REGARD	Second line (n = 355); RAM + BSC (8 mg/kg) once every 2 weeks v placebo + BSC; randomization ratio, 2:1	26	325
RAINBOW	Second line (n = 655); paclitaxel (80 mg/m ²) on days 1, 8, and 15 of a 28-day cycle ± RAM (8 mg/kg) once every 2 weeks	220	436
Hepatocellular carcinoma			
REACH	Second line (n = 565); RAM + BSC (8 mg/kg) once every 2 weeks v placebo + BSC	246	307
Lung cancer			
REVEL	Second line (n = 1,253); docetaxel (75 mg/m ² ; 60 mg/m ² Korea and Taiwan) ± RAM (10 mg/kg) once every 3 weeks	89	1,156
Colorectal carcinoma			
RAISE	Second line (n = 1,072); RAM (8 mg/kg) ± FOLFIRI/placebo once every 2 weeks	194	863

Abbreviations: BSC, best supportive care; EA, East Asian; FOLFIRI, leucovorin (folinic acid), fluorouracil, and irinotecan; GEJ, gastroesophageal junction; RAINBOW, Ramucirumab Plus Paclitaxel Versus Placebo Plus Paclitaxel in Patients With Previously Treated Advanced Gastric or Gastroesophageal Junction Adenocarcinoma; RAISE, Ramucirumab Versus Placebo in Combination With Second-Line FOLFIRI in Patients With Metastatic Colorectal Carcinoma That Progressed During or After First-Line Therapy With Bevacizumab, Oxaliplatin, and a Fluoropyrimidine; RAM, ramucirumab; REACH, Ramucirumab Versus Placebo as Second-Line Treatment in Patients With Advanced Hepatocellular Carcinoma Following First-Line Therapy With Sorafenib; REGARD, Ramucirumab Monotherapy for Previously Treated Advanced Gastric or Gastroesophageal Junction Adenocarcinoma; REVEL, Ramucirumab Plus Docetaxel Versus Placebo Plus Docetaxel for Second-Line Treatment of Stage IV Non–Small-Cell Lung Cancer After Disease Progression on Platinum-Based Therapy; ROSE, Ramucirumab Overall Survival Evaluation.

and safety of ramucirumab in East Asian (EA) patients compared with non-EA patients.¹¹⁻¹⁴ Overall, ramucirumab treatment conferred benefits to EA patients in terms of prolonging median survival times, improving progression-free survival, and increasing response rate.¹¹⁻¹³ As for safety, EA patients have been reported to exhibit a higher incidence of certain adverse events (AEs) compared with non-EA patients.³⁻⁸ For instance, subgroup analyses from the RAINBOW and REVEL trials indicated higher incidence rates of any-grade neutropenia in ramucirumab-treated EA patients compared with those in the non-EA population (RAINBOW, 78% EA v 43% non-EA; REVEL, 84.4% EA v 53.4% non-EA).^{5,6}

To further examine the safety of ramucirumab among EA patients, we conducted a meta-analysis examining the incidence of AEs possibly associated with VEGF-pathway inhibition in EA compared with non-EA patients across the six completed phase III trials. This analysis may assist and guide clinicians to optimize the treatment of EA patients with cancer with ramucirumab by

maximizing efficacy while minimizing potential treatment-related toxicities.

MATERIALS AND METHODS

Details of the study design and patients for each of the six randomized, double-blind, phase III ramucirumab trials have been published.³⁻⁸ A meta-analysis was conducted to review AEs in EA patients and non-EA patients across these six trials. The EA population was defined based on the geographic region in which patients enrolled at each study site. Each trial followed the guiding principles of the Declaration of Helsinki and the Good Clinical Practice Guidelines of the International Conference on Harmonization. All patients provided written informed consent. An overview of these trials is presented in [Table 1](#).

AEs, identified via literature review to be possibly related to VEGF inhibition,¹⁵ were evaluated in the safety population for each trial. In addition, we report results for neutropenia, a common AE among EA patients. The safety population

Table 2. Baseline Patient Characteristics in EA and Non-EA Patients

Characteristics	EA Patients		Non-EA Patients	
	Ramucirumab (n = 411)	Placebo (n = 391)	Ramucirumab (n = 2,337)	Placebo (n = 1,857)
Age, years, median (range)	61.0 (27.0-85.0)	61.3 (25.5-84.0)	59.7 (21.5-87.0)	60.4 (24.0-88.0)
< 65	264 (64.2)	245 (62.7)	1,575 (67.4)	1,230 (66.2)
≥ 65	147 (35.8)	146 (37.3)	762 (32.6)	627 (33.8)
Sex				
Male	275 (66.9)	293 (74.9)	1053 (45.1)	989 (53.3)
Female	136 (33.1)	98 (25.1)	1284 (54.9)	868 (46.7)
Body weight, kg				
Median (range)	58.9 (31.9-97.7)	59.9 (31.0-91.5)	71.0 (35.4-144.4)	71.0 (30.0-149.0)
Mean (SD)	59.1 (10.3)	60.4 (10.8)	72.8 (16.2)	73.1 (16.7)
ECOG PS				
0	199 (48.4)	187 (47.8)	1,051 (45.0)	834 (44.9)
1	212 (51.6)	204 (52.2)	1,283 (54.9)	1,019 (54.9)
2	0	0	2 (0.1)	3 (0.2)
Missing	0	0	1 (0.0)	1 (0.1)
Extent of disease, metastasis	126 (30.7)	120 (30.7)	936 (40.1)	573 (30.9)

NOTE. Data given as No. (%) unless otherwise indicated.

Abbreviations: EA, East Asian; ECOG PS, Eastern Cooperative Oncology Group performance status; SD, standard deviation.

included all randomly assigned patients who received any dose of an investigational product (ie, ramucirumab or placebo). Grading of the AEs was based on Common Terminology Criteria for Adverse Events versions 3.0 to 4.02.

A key aspect of meta-analyses is to quantify the heterogeneity among a collection of studies.¹⁶ When there was no evidence of significant inter-study heterogeneity (Cochran’s *Q* test *P* > .05),¹⁷ the estimates of the relative risks (RRs) for each study were reported with 95% CIs using the fixed-effects (Mantel-Haenszel) method; otherwise, the random effects meta-analysis was adopted.¹⁸ The *rmeta* R package was used for computation (<https://cran.r-project.org/web/packages/rmeta/index.html>).¹⁹

The ratio of relative risk (RRR)²⁰ was calculated to compare the two estimated RRs for each AE between EA and non-EA patients. An estimated RRR and the associated 95% CI were reported for each AE. There is no evidence of a difference in RRs if the 95% CI for the RRR contains 1.0. It should be noted that this test for interactions has limited power. The number needed to harm (NNH) was calculated for all-grade and grade ≥ 3 AEs using the following formula: 1/(risk of ramucirumab – risk of placebo).

RESULTS

The safety population consisted of 4,996 patients randomly assigned to receive at least one dose of ramucirumab (n = 2,748) or placebo (n = 2,248). There were a total of 802 (16.1%) EA patients (ramucirumab, n = 411; placebo, n = 391) and 4,194 (83.9%) non-EA patients (ramucirumab, n = 2,337; placebo, n = 1,857). Patient baseline characteristics for EA and non-EA patients are summarized in Table 2. Baseline characteristics between EA and non-EA patients were generally comparable, with the exception of sex and body weight. Among EA patients, there was a higher percentage of male patients in both the ramucirumab and placebo treatment arms in comparison with non-EA patients (ramucirumab, 66.9% EA v 45.1% non-EA patients; placebo, 74.9% EA v 53.3% non-EA patients). In addition, the mean body weight of EA patients was less than that of non-EA patients (ramucirumab, 59.1 kg EA v 72.8 kg non-EA patients; placebo, 60.4 kg EA v 73.1 kg non-EA patients; Table 2).

The extent of treatment exposure for each of the six completed trials in EA and non-EA patients, including median duration of treatment and cumulative dose, is presented in Table 3. Median relative dose intensity of ramucirumab exposure was mostly similar between EA and

non-EA patients with the exception of the RAISE study (79.7% EA v 89.2% non-EA patients).

The incidence of AEs in EA and non-EA patients in completed phase III trials is listed in [Table 4](#). In EA patients, AEs occurring in $\geq 10\%$ of patients, regardless of grade, and at a higher rate in the ramucirumab-treated group versus the placebo-controlled counterpart, respectively, were hypertension (23.4% v 6.1%), proteinuria (24.6% v 7.7%), bleeding (41.8% v 18.9%), and neutropenia (53.0% v 36.6%). In non-EA patients, all-grade AEs occurring in $\geq 10\%$ of patients and at a higher rate in the ramucirumab-treated group than the control group, respectively, included hypertension (20.9% v 7.7%), bleeding (36.8% v 19.0%), and neutropenia (33.2% v 29.6%). Among the grade ≥ 3 AEs in [Table 4](#), only neutropenia occurred in $\geq 10\%$ of patients and at a higher rate in the ramucirumab-treated group than the control group, respectively, in EA patients (42.1% v 26.6%) and non-EA patients (25.5% v 20.5%).

In ramucirumab-treated patients, AEs occurring with at least a 5% incidence difference between EA and non-EA patients were all-grade proteinuria (24.6% EA v 6.8% non-EA patients), bleeding (41.8% EA v 36.8% non-EA patients), and neutropenia (53.0% EA v 33.2% non-EA patients). Neutropenia was the only grade ≥ 3 AE with a $\geq 5\%$ incidence difference between EA and non-EA patients (42.1% EA v 25.5% non-EA patients).

The RR and corresponding RRR of AEs in EA and non-EA patients are listed in [Table 5](#). In cases where the Cochran's *Q* test $P < .05$, a random-effects model was adopted (instead of a fixed-effects model) to accommodate for the interstudy variability; in [Table 5](#), the RR is marked with a '#' for such cases. In EA patients, adding ramucirumab was associated with increased risk of all-grade hypertension (RR, 3.6; 95% CI, 2.4 to 5.5), proteinuria (RR, 3.1; 95% CI, 2.2 to 4.5), bleeding (RR, 2.2; 95% CI, 1.8 to 2.8), GI bleeding (RR, 1.9; 95% CI, 1.1 to 3.2), and neutropenia (RR, 1.5; 95% CI, 1.3 to 1.7). In non-EA patients, adding ramucirumab was associated with an increased risk of all-grade hypertension (RR, 2.6; 95% CI, 2.2 to 3.1), proteinuria (RR, 3.4; 95% CI, 2.4 to 4.7), bleeding (RR, 1.9; 95% CI, 1.7 to 2.1), GI bleeding (RR, 1.5; 95% CI, 1.2 to 2.0), GI perforation (RR, 3.0; 95% CI, 1.3 to 6.9), neutropenia (RR, 1.3; 95% CI, 1.1 to 1.6),

and febrile neutropenia (RR, 1.6; 95% CI, 1.2 to 2.1). For several AEs, the NNH differed between EA and non-EA patients ([Table 5](#)). According to our NNH calculations, EA patients exhibited an absolute increased risk of all-grade proteinuria (one in six EA v one in 22 non-EA patients), GI bleeding (one in 24 EA v one in 54 non-EA patients), GI perforation (one in 104 EA v one in 134 non-EA patients), and neutropenia (one in six EA v one in 28 non-EA patients).

There was an increase in the RR of several grade ≥ 3 AEs in EA patients, including hypertension (RR, 5.6; 95% CI, 2.4 to 13.0), proteinuria (RR, 5.5; 95% CI, 1.7 to 17.7), and neutropenia (RR, 1.6; 95% CI, 1.4 to 1.9); and an increase in RR for hypertension (3.4; 95% CI, 2.5 to 4.6), proteinuria (RR, 4.1; 95% CI, 1.3 to 12.8), GI perforation (RR, 3.0; 95% CI, 1.3 to 7.2), neutropenia (RR, 1.5; 95% CI, 1.2 to 1.9), and febrile neutropenia (RR, 1.6; 95% CI, 1.2 to 2.1) in non-EA patients ([Table 5](#)). EA patients also exhibited an absolute increased risk in the NNH of grade ≥ 3 AEs, including proteinuria (one in 26 EA v one in 170 non-EA patients), GI bleeding (one in 696 EA v one in 3,065 non-EA patients), GI perforation (one in 104 EA v one in 140 non-EA patients), and neutropenia (one in six EA v one in 20 non-EA patients; [Table 5](#)). No substantial differences in the NNH were observed between EA and non-EA patients in terms of grade ≥ 3 febrile neutropenia (one in 40 EA v one in 41 non-EA patients) and hypertension (one in 13 EA v one in 16 non-EA patients). The RRR revealed no significant differences between EA and non-EA patients for all-grade and grade ≥ 3 AEs ([Table 5](#); Data Supplement).

Analysis of RRs in ramucirumab plus chemotherapy combination trials (ie, ROSE, RAINBOW, RAISE, REVEL) revealed an increase in the risk of developing all-grade and grade ≥ 3 proteinuria and GI perforation (Data Supplement). Equivalent analysis of ramucirumab monotherapy trials (ie, REGARD, REACH) indicates an increased risk of all-grade hypertension, proteinuria, bleeding, and neutropenia, as well as increased risk of grade ≥ 3 hypertension (Data Supplement). Overall, the RR of selected AEs was mostly comparable between EA and non-EA patients in both ramucirumab combination and monotherapy cohorts (Data Supplement).

Table 3. Ramucirumab Exposure in EA and non-EA Patients Across Six Phase III Trials

Clinical Trial	EA RAM Exposure (n = 411)				Non-EA RAM Exposure (n = 2,337)			
	Total No. of Cycles	Duration of Treatment, Weeks	Cumulative Dose, mg/kg	Relative Dose Intensity, %	Total No. of Cycles	Duration of Treatment, Weeks	Cumulative Dose, mg/kg	Relative Dose Intensity, %
ROSE (n = 752)	8 (2-16)	24.0 (6-51)	78.5 (19.8-156.9)	95.38 (81.9-103.9)	9 (0-58)	29.0 (3-181)	88.3 (3.0-561.3)	97.22 (30.0-114.0)
REGARD (n = 236)	6 (1-25)	10.9 (2-50)	44.8 (8.0-208.4)	101.61 (67.5-106.9)	4 (1-34)	7.9 (2-72)	29.5 (7.6-279.2)	99.36 (59.8-114.5)
RAINBOW (n = 327)	5 (1-22)	19.9 (2-96)	81.0 (8.0-420.0)	98.90 (65.9-113.9)	4 (1-22)	15.0 (2-102)	57.0 (8.0-326.0)	98.40 (63.5-112.4)
REACH (n = 277)	4 (1-62)	8.0 (2-128)	31.9 (7.7-499.6)	98.38 (66.3-108.7)	7 (1-45)	14.0 (2-98)	55.3 (4.9-362.5)	98.83 (38.5-105.7)
REVEL (n = 627)	6 (1-25)	18.0 (3-77)	50.8 (10.0-261.5)	96.41 (67.3-101.9)	4 (1-38)	14.6 (3-118)	42.1 (0.3-388.3)	98.29 (1.2-162.7)
RAISE (n = 529)	8 (1-49)	19.0 (2-106)	64.0 (7.6-384.9)	79.73 (46.6-103.7)	8 (1-68)	19.0 (2-167)	66.3 (3.8-514.7)	89.24 (37.3-108.3)

NOTE. Data given as median (range).

Abbreviations: EA, East Asian; RAINBOW, Ramucirumab Plus Paclitaxel Versus Placebo Plus Paclitaxel in Patients With Previously Treated Advanced Gastric or Gastroesophageal Junction Adenocarcinoma; RAISE, Ramucirumab Versus Placebo in Combination With Second-Line FOLFIRI in Patients With Metastatic Colorectal Carcinoma That Progressed During or After First-Line Therapy With Bevacizumab, Oxaliplatin, and a Fluoropyrimidine; RAM, ramucirumab; REACH, Ramucirumab Versus Placebo as Second-Line Treatment in Patients With Advanced Hepatocellular Carcinoma Following First-Line Therapy With Sorafenib; REGARD, Ramucirumab Monotherapy for Previously Treated Advanced Gastric or Gastroesophageal Junction Adenocarcinoma; REVEL, Ramucirumab Plus Docetaxel Versus Placebo Plus Docetaxel for Second-Line Treatment of Stage IV Non-Small-Cell Lung Cancer After Disease Progression on Platinum-Based Therapy; ROSE, Ramucirumab Overall Survival Evaluation.

Table 4. Incidence of All-Grade and Grade ≥ 3 AEs in EA and Non-EA Patients in Completed Phase III Ramucirumab Trials

Adverse Event	EA Patients (n = 802)			Non-EA Patients (n = 4,194)		
	Ramucirumab (n = 411)	Placebo (n = 391)	Placebo (n = 1,857)	Ramucirumab (n = 2,337)	Placebo (n = 1,857)	Placebo (n = 1,857)
	All Grades	Grade ≥ 3	All Grades	All Grades	Grade ≥ 3	Grade ≥ 3
Hypertension*	96 (23.4)	36 (8.8)	24 (6.1)	489 (20.9)	210 (9.0)	143 (7.7)
Proteinuria*	101 (24.6)	16 (3.9)	30 (7.7)	158 (6.8)	15 (0.6)	40 (2.2)
Bleeding*	172 (41.8)	13 (3.2)	74 (18.9)	859 (36.8)	61 (2.6)	352 (19.0)
GI bleeding*	36 (8.8)	9 (2.2)	18 (4.6)	150 (6.4)	36 (1.5)	85 (4.6)
GI perforation*	5 (1.2)	5 (1.2)	1 (0.3)	25 (1.1)	23 (1.0)	6 (0.3)
ATE*	3 (0.7)	1 (0.2)	7 (1.8)	35 (1.5)	20 (0.9)	33 (1.8)
VTE*	11 (2.7)	3 (0.7)	7 (1.8)	95 (4.1)	53 (2.3)	109 (5.9)
IRR*	17 (4.1)	0 (0.0)	18 (4.6)	163 (7.0)	28 (1.2)	86 (4.6)
WHC*	0 (0.0)	0 (0.0)	0 (0.0)	12 (0.5)	5 (0.2)	4 (0.2)
Neutropenia†	218 (53.0)	173 (42.1)	143 (36.6)	775 (33.2)	596 (25.5)	550 (29.6)
Febrile neutropenia	25 (6.1)	25 (6.1)	15 (3.8)	166 (7.1)	163 (7.0)	85 (4.6)

NOTE. Data given as No. (%).

Abbreviations: AE, adverse event; ATE, arterial thromboembolism; EA, East Asian; IRR, infusion-related reaction; VTE, venous thromboembolism; WHC, wound-healing complication.

*AE of special interest.

†Consolidated AE.

Table 5. RR, RRR, and NNH[†] in AEs in EA and Non-EA Patients

Adverse Event	All Grades									
	EA RR (95% CI)	Non-EA RR (95% CI)	RRR (95% CI)	EA NNH [†]	Non-EA NNH [†]	EA RR (95% CI)	Non-EA RR (95% CI)	RRR (95% CI)	EA NNH [†]	Non-EA NNH [†]
Hypertension [†]	3.6 (2.4 to 5.5)	2.6 (2.2 to 3.1)	1.385 (0.884 to 2.169)	6	8	5.6 (2.4 to 13.0)	3.4 (2.5 to 4.6)	1.647 (0.671 to 4.043)	13	16
Proteinuria [†]	3.1 (2.2 to 4.5)	3.4 (2.4 to 4.7)	0.912 (0.558 to 1.49)	6	22	5.5 (1.7 to 17.7)	4.1 (1.3 to 12.8)	1.341 (0.261 to 6.895)	26	170
Bleeding [†]	2.2 (1.8 to 2.8)	1.9 (1.7 to 2.1)	1.158 (0.906 to 1.479)	4	6	0.8 (0.4 to 1.6)	1.1 (0.8 to 1.6)	0.727 (0.335 to 1.579)	-149	1,262
GI bleeding [†]	1.9 (1.1 to 3.2)	1.5 (1.2 to 2.0)	1.267 (0.701 to 2.289)	24	54	1.0 (0.4 to 2.3)	1.1 (0.7 to 1.8)	0.909 (0.336 to 2.456)	696	3,065
GI perforation [†]	1.9 (0.6 to 6.3)	3.0 (1.3 to 6.9)	0.633 (0.15 to 2.678)	104	134	1.9 (0.6 to 6.3)	3.0 (1.3 to 7.2)	0.633 (0.148 to 2.711)	104	140
ATE [†]	0.5 (0.2 to 1.5)	0.9 (0.5 to 1.4)	0.556 (0.179 to 1.722)	-94	-358	0.5 (0.1 to 2.1)	1.0 (0.5 to 2.0)	0.500 (0.094 to 2.663)	-191	-17,222
VTE [†]	1.4 (0.6 to 3.2)	0.7 (0.6 to 1.0)	2.000 (0.834 to 4.798)	113	-55	0.8 (0.2 to 2.3)	0.8 (0.5 to 1.1)	1.000 (0.277 to 3.608)	-341	-125
IRR [†]	0.9 (0.5 to 1.7)	1.5 [‡] (0.9 to 2.6)	0.600 (0.267 to 1.348)	-214	43	0.6 (0.1 to 2.8)	1.5 (0.8 to 2.9)	0.400 (0.067 to 2.387)	-391	181
WHC [†]	0.8 (0.2 to 3.8)	1.7 (0.6 to 4.5)	0.824 (0.14 to 4.831)	0	335	0.8 (0.2 to 3.8)	1.9 (0.5 to 7.5)	0.421 (0.057 to 3.112)	0	467
Neutropenia [§]	1.5 (1.3 to 1.7)	1.3 [‡] (1.1 to 1.6)	1.154 (0.916 to 1.453)	6	28	1.6 (1.4 to 1.9)	1.5 [‡] (1.2 to 1.9)	1.067 (0.81 to 1.406)	6	20
Febrile neutropenia	1.5 (0.9 to 2.7)	1.6 (1.2 to 2.1)	0.937 (0.506 to 1.737)	45	40	1.6 (0.9 to 3.0)	1.6 (1.2 to 2.1)	1.000 (0.515 to 1.942)	40	41

Abbreviations: AE, adverse event; ATE, arterial thromboembolism; EA, East Asian; IRR, infusion-related reaction; NNH[†], number needed to harm; RR, relative risk; RRR, ratio of relative risk; VTE, venous thromboembolism; WHC, wound healing complications.

[†]NNH calculated using the following formula: 1/(risk of ramucirumab - risk of placebo). Negative values indicate that the incidence rate was higher in the placebo arm in comparison with the ramucirumab arm. †AE of special interest.

[‡]Given the Cochran's Q test P value for evaluating heterogeneity is less than .05, the RR and 95% CI are based on the random-effects model.

[§]Consolidated AE.

DISCUSSION

Ramucirumab, like other VEGF-targeted treatments, is associated with several “classes” of AEs. These AEs have been well documented and encompass hematologic and cardiovascular toxicities.^{3-6,8,21,22} It has been increasingly reported that EA patients may have greater toxicity to chemotherapy and targeted therapies compared with Western patients.^{23,24} For this reason, sub-analyses are often conducted in EA patients with the aim of confirming that a regimen with a positive risk-benefit profile in a global population also confers meaningful efficacy with an acceptable safety profile in the EA subpopulation. We describe a meta-analysis of six completed phase III ramucirumab trials to explore whether EA patients are at increased risk of AEs associated with ramucirumab therapy. Differences were noted in the incidence rates of selected AEs between EA and non-EA patients; however, based on comparative exposure data, these differences did not jeopardize ramucirumab treatment and patients were able to continue therapy.

The EA patient cohort across all six phase III ramucirumab trials exhibited comparable baseline characteristics in comparison with non-EA patients, with the exception of sex (more male patients in the EA patient cohort) and body weight (EA patients weighed less). The sex imbalance may be due to the relatively low number of EA patients enrolled in the ROSE breast cancer trial ($n = 27$). Despite EA patients having a lower body weight compared with non-EA patients, ramucirumab exposure was mostly comparable between these patient cohorts. Although we observed variations in the number of ramucirumab treatment cycles and in median cumulative doses between trials, which may affect the frequency and grade of AEs, the overall dose intensity was mostly comparable between EA and non-EA patients.

Hypertension is a frequently observed AE associated with VEGF inhibitors²¹ and is commonly reported in ramucirumab clinical trials.⁴⁻⁸ Our analysis revealed no obvious differences in the risk of hypertension in the ramucirumab arm between EA and non-EA patients (23% EA *v* 21% non-EA patients). Although there was an increased trend in RR for grade ≥ 3 hypertension (5.6 EA *v* 3.4 non-EA patients), our findings suggest that the risk of grade ≥ 3 hypertension

is low under antihypertensive intervention and comparable between EA and non-EA patients.

Proteinuria is a known AE occurring frequently in patients receiving anti-VEGF therapy, because of the suppression of nephrin, an important protein for the maintenance of the glomerular slit diaphragm.²⁵ Our findings indicate that treatment with ramucirumab increases the risk of proteinuria in EA patients with cancer; however, proteinuria overall was of low-grade severity and did not lead to treatment discontinuation. Notably, the incidence of proteinuria in placebo-treated EA patients was also higher relative to their non-EA counterparts; therefore, the RRs were similar between EA and non-EA patients and the RRR was not significant. Some studies have reported that Asian patients are more vulnerable to developing proteinuria in comparison with Western patients.^{11,26,27} Given that we did not evaluate confounding factors, such as concomitant use of nephrotoxic agents or previous cisplatin exposure in GI cancers, the reasons behind ethnic differences in absolute incidence of proteinuria are far from being understood. Because proteinuria is a risk factor for cardiovascular disease and loss of renal function, periodic monitoring of urinary protein and appropriate intervention should be recommended for all ramucirumab-treated patients.

Neutropenia incidence was increased in EA patients in comparison with non-EA patients, but the incidence of febrile neutropenia was low and similar between EA and non-EA patients. Given that the increase in neutropenia incidence in EA patients was mainly noted in ramucirumab-chemotherapy combination trials, it is possible that this observed increase was driven by chemotherapies. Support for this conclusion comes from the improvement in the safety profile among EA patients accompanied by a dose reduction of docetaxel in the REVEL trial.⁶ The decrement of docetaxel starting dose from 75 mg/m² to 60 mg/m² in EA patients reduced the incidence of neutropenia and febrile neutropenia to a rate similar to that observed for non-EA patients.¹³

Consistent with the intent-to-treat populations, all-grade bleeding was increased in ramucirumab-treated patients in comparison with placebo-treated patients, and this was observed in EA and non-EA patients. Importantly, the incidence of grade ≥ 3 bleeding was low and similar in both treatment arms and between EA and non-EA

patients. The incidences of additional grade ≥ 3 AEs associated with VEGF-targeted treatments were also low and comparable between EA and non-EA patients. These include GI bleeding and GI perforation, arterial and venous thromboembolism, and wound-healing complications. Our meta-analysis suggests that ramucirumab is well tolerated in EA patients using the dosage and regimen outlined in the six completed phase III trials under investigation.

The NNH provides a useful indication to clinicians and patients of the absolute risks involved with treatment. Although no substantial differences were observed in the RR of AEs between EA and non-EA patients, the incidence rates (and rate differences) of selected AEs were increased in EA patients, including proteinuria, neutropenia, and bleeding. The NNH supports this finding, providing clinicians with an evidence-based tool to assist with treatment decisions regarding optimal supportive care and dose modification concerning EA patients with cancer.

To the best of our knowledge, this is the first and largest individual-patient meta-analysis to evaluate the safety profile of ramucirumab among East Asian patients with cancer. In this meta-analysis, we found an increased RR in certain AEs in EA patients. However, the results of this analysis should be interpreted with caution: there were limited numbers of EA patients in some trials, and patients were categorized by their geographic location, and limited ethnicity data were available. In addition, heterogeneity between studies should be noted in terms of cancer types, treatment regimens including the trial chemotherapy backbone, and patient

characteristics. Furthermore, wide confidence intervals were observed, which reflect substantial uncertainty in the point estimation of RR for some AEs. No obvious differences in RRR were noted between EA and non-EA patients; however, this interaction test may not be powerful enough to detect a significant difference.²⁰ As with many clinical trials, patients enrolled in ramucirumab clinical trials may not represent patients in the general population, because trial patients are screened for adequate organ function and concurrent morbidities and medications.

Benefit versus risk is an important factor for clinicians and patients when making decisions concerning cancer treatments. Collectively, results from our meta-analysis were consistent with the overall ramucirumab safety profile¹⁰ as well as demonstrating that ramucirumab has a similar risk profile in EA patients compared with non-EA patients enrolled in clinical trials. In addition to routine clinical practices, clinicians should monitor patients for potential ramucirumab-related AEs, including hypertension and proteinuria. The risks associated with ramucirumab may be increased by other factors, including patient comorbidities and concomitant medications, prior therapies, and tumor characteristics.

Across these six completed phase III ramucirumab trials, the majority of AEs discussed here in EA patients were manageable and did not jeopardize EA patients' cancer therapy. Patients were able to continue to receive ramucirumab therapy to achieve maximum clinical benefits.

DOI: <https://doi.org/10.1200/JGO.17.00227>

Published online on [jgo.org](https://www.jgo.org) on June 8, 2018.

AUTHOR CONTRIBUTIONS

Conception and design: Jin-Yuan Shih, Rebecca Cheng, Polina Binder, Gu Mi, Mauro Orlando

Provision of study material or patients: Chia-Jui Yen, Kei Muro, Masatoshi Kudo, Yee Chao, Sang-We Kim, JooHyuk Sohn, Hyun Cheol Chung

Collection and assembly of data: Chia-Jui Yen, Kei Muro, Masatoshi Kudo, Jin-Yuan Shih, Keun-Wook Lee, Yee Chao, Sang-We Kim, Rebecca Cheng, JooHyuk Sohn, Mauro Orlando, Hyun Cheol Chung

Data analysis and interpretation: Chia-Jui Yen, Tae-Won Kim, Jin-Yuan Shih, Keun-Wook, Sang-We Kim, Lee Kentaro Yamazaki, Rebecca Cheng, Yawei Zhang, Polina Binder, Gu Mi, Mauro Orlando, Hyun Cheol Chung

Manuscript writing: All authors

Final approval of manuscript: All authors

Accountable for all aspects of the work: All authors

AUTHORS' DISCLOSURES OF POTENTIAL CONFLICTS OF INTEREST

The following represents disclosure information provided by authors of this manuscript. All relationships are considered compensated. Relationships are self-held unless noted. I = Immediate Family Member, Inst = My Institution. Relationships may not relate to the subject matter of this manuscript. For more information about ASCO's conflict of interest policy, please refer to www.asco.org/rwc or ascopubs.org/jco/site/ifc.

Chia Jui Yen

No relationship to disclose

Kei Muro

Honoraria: Takeda, Chugai Pharma, Yakult Honsha, Merck Serono, Taiho Pharmaceutical, Eli Lilly

Research Funding: Ono Pharmaceutical, MSD, Daiichi Sankyo, Shionogi Pharma, Kyowa Hakko Kirin, Gilead Sciences

Tae Won Kim

Employment: Asan Medical Center

Honoraria: Merck Serono, AstraZeneca

Masatoshi Kudo

Honoraria: Bayer, Eisai, Novartis, MSD, EA Pharma, Bristol-Myers Squibb, Abbvie, Taiho Pharmaceutical, Pfizer, Gilead Sciences, Merck Serono

Consulting or Advisory Role: MSD, Bristol-Myers Squibb, Bayer, Eisai

Research Funding: Chugai Pharma (Inst), Otsuka (Inst), Taiho Pharmaceutical (Inst), Daiichi Sankyo (Inst), Abbvie (Inst), Astellas Pharma (Inst), Bristol-Myers Squibb (Inst)

Jin-Yuan Shih

Honoraria: AstraZeneca, Roche, Boehringer Ingelheim, Eli Lilly, Pfizer, Novartis, Merck Sharp & Dohme, Ono Pharmaceutical, Bristol-Myers Squibb

Consulting or Advisory Role: Chugai Pharma, Boehringer Ingelheim

Keun Wook Lee

Research Funding: Macrogenics (Inst), MSD (Inst), Ono Pharmaceutical (Inst), Green Cross, ASLAN Pharmaceuticals (Inst), AstraZeneca/MedImmune (Inst), Five Prime Therapeutics (Inst), LSK BioPharma (Inst), Merck (Inst), Array BioPharma (Inst), Pharmacyclics (Inst), Pfizer (Inst)

Yee Chao

No relationship to disclose

Sang-We Kim

No relationship to disclose

Kentaro Yamazaki

Honoraria: Chugai Pharma, Daiichi Sankyo, Yakult Honsha, Takeda, Bayer, Merck Serono, Bristol-Myers Squibb, Taiho Pharmaceutical, Eli Lilly, Taiho Pharmaceutical

Research Funding: Taiho Pharmaceutical (Inst)

Joohyuk Sohn

No relationship to disclose

Rebecca Cheng

Employment: Eli Lilly

Stock and Other Ownership Interests: Eli Lilly
Travel, Accommodations, Expenses: Eli Lilly

Yawei Zhang

Stock and Other Ownership Interests: Eli Lilly

Polina Binder

Employment: Eli Lilly

Stock and Other Ownership Interests: Eli Lilly

Gu Mi

Employment: Eli Lilly, Eli Lilly (I)

Stock and Other Ownership Interests: Eli Lilly, Eli Lilly (I)

Mauro Orlando

Employment: Eli Lilly

Stock and Other Ownership Interests: Eli Lilly

Hyun Cheol Chung

Consulting or Advisory Role: Taiho Pharmaceutical, Celltrion, MSD, Eli Lilly, Quintiles, Bristol-Myers Squibb, Merck Serono

Speakers' Bureau: Merck Serono, Eli Lilly, Foundation Medicine, GlaxoSmithKline, MSD

Research Funding: Merck Serono, Bristol-Myers Squibb, Taiho Pharmaceutical

ACKNOWLEDGMENT

We thank the patients, their families, the study sites, and the study personnel who participated in the clinical trials. Project support was provided by Esther Gonzalez of Eli Lilly and Company. Medical writing support was provided by Lisa Cossens, and editorial support by Antonia Baldo, of Syneos Health, and funded by Eli Lilly and Company.

Affiliations

Chia-Jui Yen, National Cheng Kung University Hospital, Tainan; **Jin-Yuan Shih**, National Taiwan University Hospital; **Yee Chao**, National Yang-Ming University and Taipei Veterans General Hospital; **Rebecca Cheng**, Eli Lilly and Company, Taipei, Taiwan; **Kei Muro**, Aichi Cancer Center Hospital, Nagoya; **Masatoshi Kudo**, Kindai University School of Medicine, Osaka-Sayama City, Osaka; **Kentaro Yamazaki**, Shizuoka Cancer Center, Shizuoka, Japan; **Tae-Won Kim** and **Sang-We Kim**, Asan Medical Center; **Joohyuk Sohn** and **Hyun Cheol Chung**, Yonsei University College of Medicine, Seoul; **Keun-Wook Lee**, Seoul National University College of Medicine, Seongnam, South Korea; **Yawei Zhang** and **Polina Binder**, Eli Lilly and Company, Bridgewater, NJ; **Gu Mi**, Eli Lilly and Company, Indianapolis, IN, USA; and **Mauro Orlando**, Eli Lilly and Company, Buenos Aires, Argentina.

Support

This study was funded by Eli Lilly and Company.

Prior Presentation

Presented in part at European Society for Medical Oncology (ESMO) Asia, December 16-19, 2016, Singapore.

REFERENCES

1. Spratlin JL, Cohen RB, Eadens M, et al: Phase I pharmacologic and biologic study of ramucirumab (IMC-1121B), a fully human immunoglobulin G1 monoclonal antibody targeting the vascular endothelial growth factor receptor-2. *J Clin Oncol* 28:780-787, 2010
2. Tian S, Quan H, Xie C, et al: YN968D1 is a novel and selective inhibitor of vascular endothelial growth factor receptor-2 tyrosine kinase with potent activity in vitro and in vivo. *Cancer Sci* 102:1374-1380, 2011

3. Mackey JR, Ramos-Vazquez M, Lipatov O, et al: Primary results of ROSE/TRIO-12, A randomized placebo-controlled phase III trial evaluating the addition of ramucirumab to first-line docetaxel chemotherapy in metastatic breast cancer. *J Clin Oncol* 33:141-148, 2015
4. Fuchs CS, Tomasek J, Yong CJ, et al: Ramucirumab monotherapy for previously treated advanced gastric or gastro-oesophageal junction adenocarcinoma (REGARD): An international, randomised, multicentre, placebo-controlled, phase 3 trial. *Lancet* 383:31-39, 2014
5. Wilke H, Muro K, Van Cutsem E, et al: Ramucirumab plus paclitaxel versus placebo plus paclitaxel in patients with previously treated advanced gastric or gastro-oesophageal junction adenocarcinoma (RAINBOW): A double-blind, randomised phase 3 trial. *Lancet Oncol* 15:1224-1235, 2014
6. Garon EB, Ciuleanu TE, Arrieta O, et al: Ramucirumab plus docetaxel versus placebo plus docetaxel for second-line treatment of stage IV non-small-cell lung cancer after disease progression on platinum-based therapy (REVEL): A multicentre, double-blind, randomised phase 3 trial. *Lancet* 384:665-673, 2014
7. Zhu AX, Park JO, Ryoo BY, et al: Ramucirumab versus placebo as second-line treatment in patients with advanced hepatocellular carcinoma following first-line therapy with sorafenib (REACH): A randomised, double-blind, multicentre, phase 3 trial. *Lancet Oncol* 16:859-870, 2015
8. Tabernero J, Yoshino T, Cohn AL, et al: Ramucirumab versus placebo in combination with second-line FOLFIRI in patients with metastatic colorectal carcinoma that progressed during or after first-line therapy with bevacizumab, oxaliplatin, and a fluoropyrimidine (RAISE): A randomised, double-blind, multicentre, phase 3 study. *Lancet Oncol* 16:499-508, 2015
9. Eli Lilly and Company: Cyramza [product guide]. Indianapolis, IN: Eli Lilly and Company; 2016. http://www.cyramzahcp.com/img/pdf/CYRAMZA_Product_Guide.pdf
10. Arnold D, Fuchs CS, Tabernero J, et al: Meta-analysis of individual patient safety data from six randomized, placebo-controlled trials with the antiangiogenic VEGFR2-binding monoclonal antibody ramucirumab. *Ann Oncol* 28:2932-2942, 2017
11. Muro K, Oh SC, Shimada Y, et al: Subgroup analysis of East Asians in RAINBOW: A phase 3 trial of ramucirumab plus paclitaxel for advanced gastric cancer. *J Gastroenterol Hepatol* 31:581-589, 2016
12. Shitara K, Muro K, Shimada Y, et al: Subgroup analyses of the safety and efficacy of ramucirumab in Japanese and Western patients in RAINBOW: A randomized clinical trial in second-line treatment of gastric cancer. *Gastric Cancer* 19:927-938, 2016
13. Park K, Kim JH, Cho EK, et al: East Asian subgroup analysis of a randomized, double-blind, phase 3 study of docetaxel and ramucirumab versus docetaxel and placebo in the treatment of stage IV non-small cell lung cancer following disease progression after one prior platinum-based therapy (REVEL). *Cancer Res Treat* 48:1177-1186, 2016
14. Park JO, Ryoo BY, Yen CJ, et al: Second-line ramucirumab therapy for advanced hepatocellular carcinoma (REACH): An East Asian and non-East Asian subgroup analysis. *Oncotarget* 7:75482-75491, 2016
15. Chen HX, Cleck JN: Adverse effects of anticancer agents that target the VEGF pathway. *Nat Rev Clin Oncol* 6:465-477, 2009
16. Higgins JP, Thompson SG: Quantifying heterogeneity in a meta-analysis. *Stat Med* 21:1539-1558, 2002
17. Cochran WG: The combination of estimates from different experiments. *Biometrics* 10:101-129, 1954
18. DerSimonian R, Laird N: Meta-analysis in clinical trials. *Control Clin Trials* 7:177-188, 1986
19. Lumley T: rmeta: Meta-analysis. R package version 2.16. 2012. <https://cran.r-project.org/web/packages/rmeta/index.html>

20. Altman DG, Bland JM: Interaction revisited: The difference between two estimates. *BMJ* 326:219, 2003
21. Hamnvik OP, Choueiri TK, Turchin A, et al: Clinical risk factors for the development of hypertension in patients treated with inhibitors of the VEGF signaling pathway. *Cancer* 121:311-319, 2015
22. Wang J, Wang Z, Zhao Y: Incidence and risk of hypertension with ramucirumab in cancer patients: A meta-analysis of published studies. *Clin Drug Investig* 35:221-228, 2015
23. Hasegawa Y, Kawaguchi T, Kubo A, et al: Ethnic difference in hematological toxicity in patients with non-small cell lung cancer treated with chemotherapy: A pooled analysis on Asian versus non-Asian in phase II and III clinical trials. *J Thorac Oncol* 6:1881-1888, 2011
24. Phan VH, Moore MM, McLachlan AJ, et al: Ethnic differences in drug metabolism and toxicity from chemotherapy. *Expert Opin Drug Metab Toxicol* 5:243-257, 2009
25. Izzedine H, Massard C, Spano JP, et al: VEGF signalling inhibition-induced proteinuria: Mechanisms, significance and management. *Eur J Cancer* 46:439-448, 2010
26. Sorich MJ, Rowland A, Kichenadasse G, et al: Risk factors of proteinuria in renal cell carcinoma patients treated with VEGF inhibitors: A secondary analysis of pooled clinical trial data. *Br J Cancer* 114:1313-1317, 2016
27. Chen Z, Zhong B, Lun X, et al: Specific safety profile of bevacizumab in Asian patients with advanced NSCLC: A meta-analysis. *Medicine (Baltimore)* 94:e975, 2015



Pembrolizumab in patients with advanced hepatocellular carcinoma previously treated with sorafenib (KEYNOTE-224): a non-randomised, open-label phase 2 trial

Andrew X Zhu, Richard S Finn, Julien Edeline, Stephane Cattan, Sadahisa Ogasawara, Daniel Palmer, Chris Verslype, Vittorina Zagonel, Laetitia Fartoux, Arndt Vogel, Debashis Sarker, Gontran Verset, Stephen L Chan, Jennifer Knox, Bruno Daniele, Andrea L Webber, Scot W Ebbinghaus, Junshui Ma, Abby B Siegel, Ann-Lii Cheng, Masatoshi Kudo, for the KEYNOTE-224 investigators*

Summary

Background Immune checkpoint blockade therapy has shown promising results in patients with advanced hepatocellular carcinoma. We aimed to assess the efficacy and safety of pembrolizumab in this patient population.

Methods KEYNOTE-224 is a non-randomised, multicentre, open-label, phase 2 trial that is set in 47 medical centres and hospitals across ten countries. Eligible patients had pathologically confirmed hepatocellular carcinoma; had previously been treated with sorafenib and were either intolerant to this treatment or showed radiographic progression of their disease after treatment; an Eastern Cooperative Oncology Group performance status of 0–1; adequate organ function, and were Child-Pugh class A. Participants received 200 mg pembrolizumab intravenously every 3 weeks for about 2 years or until disease progression, unacceptable toxicity, patient withdrawal, or investigator decision. The primary endpoint was objective response, defined as the proportion of patients with complete or partial response in all patients who received at least one dose of pembrolizumab, which was radiologically confirmed by use of the Response Evaluation Criteria in Solid Tumors version 1.1 by central review. Safety was also assessed in all treated patients. This trial is ongoing but closed to enrolment and is registered with ClinicalTrials.gov number NCT02702414.

Findings Between June 7, 2016, and Feb 9, 2017, we screened 169 patients with advanced hepatocellular carcinoma, of whom 104 eligible patients were enrolled and treated. As of data cutoff on Feb 13, 2018, 17 (16%) patients were still receiving pembrolizumab. We recorded an objective response in 18 (17%; 95% CI 11–26) of 104 patients. The best overall responses were one (1%) complete and 17 (16%) partial responses; meanwhile, 46 (44%) patients had stable disease, 34 (33%) had progressive disease, and six (6%) patients who did not have a post-baseline assessment on the cutoff date were considered not to be assessable. Treatment-related adverse events occurred in 76 (73%) of 104 patients, which were serious in 16 (15%) patients. Grade 3 treatment-related events were reported in 25 (24%) of the 104 patients; the most common were increased aspartate aminotransferase concentration in seven (7%) patients, increased alanine aminotransferase concentration in four (4%) patients, and fatigue in four (4%) patients. One (1%) grade 4 treatment-related event of hyperbilirubinaemia occurred. One death associated with ulcerative oesophagitis was attributed to treatment. Immune-mediated hepatitis occurred in three (3%) patients, but there were no reported cases of viral flares.

Interpretation Pembrolizumab was effective and tolerable in patients with advanced hepatocellular carcinoma who had previously been treated with sorafenib. These results indicate that pembrolizumab might be a treatment option for these patients. This drug is undergoing further assessment in two phase 3, randomised trials as a second-line treatment in patients with hepatocellular carcinoma.

Funding Merck & Co, Inc.

Copyright © 2018 Elsevier Ltd. All rights reserved.

Introduction

Hepatocellular carcinoma is one of the most common causes of cancer-related deaths worldwide. In most patients, hepatocellular carcinoma arises in conjunction with liver cirrhosis and is attributed to several risk factors, including infection (usually with hepatitis B or C viruses), excessive alcohol consumption, and non-alcoholic fatty liver disease.^{1,2} Surgical resection, transplantation, and ablation are potentially curative

treatment options for patients with early-stage disease; however, most patients present with advanced, unresectable disease.¹ These patients are typically treated worldwide with locoregional and systemic therapies.

Sorafenib, a multi-kinase inhibitor, remains the standard first-line systemic treatment for advanced hepatocellular carcinoma, and lenvatinib has been shown to be non-inferior to sorafenib in overall

Lancet Oncol 2018; 19: 940–52

Published Online
June 3, 2018

[http://dx.doi.org/10.1016/S1470-2045\(18\)30351-6](http://dx.doi.org/10.1016/S1470-2045(18)30351-6)

This online publication has been corrected. The corrected version first appeared at theLancet.com/oncology on August 30, 2018

See [Comment](#) page 855

*Investigators listed in the appendix, p2

Department of Medicine, Harvard Medical School, Boston, MA, USA (Prof A X Zhu MD);

Massachusetts General Hospital Cancer Center, Boston, MA, USA (Prof A X Zhu);

Department of Medicine, University of California, Los Angeles, Los Angeles, CA, USA (R S Finn MD);

Department of Medical Oncology, Centre Eugène Marquis, Rennes, France (J Edeline MD);

Department of Medical Oncology and Gastroenterology, Hôpital Claude Huriez, Centre Hospitalier Régional Universitaire de Lille, Lille, France (S Cattan MD);

Department of Gastroenterology, Graduate School of Medicine, Chiba University, Chiba, Japan (S Ogasawara MD);

Department of Medical Oncology, University of Liverpool, Liverpool, UK (Prof D Palmer PhD);

Department of Hepatology, University Hospital Gasthuisberg, Leuven, Leuven, Belgium (Prof C Verslype MD);

Istituto Oncologico Veneto-Istituto di Ricovero e Cura a Carattere Scientifico (IOV-IRCCS), Padua, Italy (V Zagonel MD);

Department of Gastroenterology and Hepatology, Hôpital Universitaire Pitié-Salpêtrière, Paris, France (L Fartoux MD);

Department of Gastroenterology and Hepatology, Hôpital Universitaire Pitié-Salpêtrière, Paris, France (L Fartoux MD);

Department of Gastroenterology and Hepatology, Hôpital Universitaire Pitié-Salpêtrière, Paris, France (L Fartoux MD);

Department of Gastroenterology and Hepatology, Hôpital Universitaire Pitié-Salpêtrière, Paris, France (L Fartoux MD);

Department of Gastroenterology and Hepatology, Hôpital Universitaire Pitié-Salpêtrière, Paris, France (L Fartoux MD);

Research in context

Evidence before this study

Few treatment options are available for patients with advanced hepatocellular carcinoma. First-line sorafenib and second-line regorafenib therapies have been approved; however, these treatments have modest efficacy and associated toxicity. Thus, there is an unmet need to develop additional therapeutic strategies and identify biomarkers that are predictive of therapeutic response in these patients. Immunotherapies, including checkpoint blockade therapies, have shown promising preliminary results in patients with hepatocellular carcinoma, and the programmed cell death protein-1 (PD-1) inhibitor nivolumab has received accelerated approval for second-line treatment in the USA. We searched PubMed from Sept 1, 2017, to Feb 22, 2018, with the search terms “advanced hepatocellular carcinoma AND treatment”, “immunotherapy AND hepatocellular carcinoma”, “anti-PD-1 OR pembrolizumab OR MK-3475 OR nivolumab AND hepatocellular carcinoma”, and “biomarkers AND immunotherapy AND hepatocellular carcinoma”. This search was limited to articles and abstracts in English. We found few studies that evaluated immunotherapy in hepatocellular carcinoma; in one study, the cytotoxic T lymphocyte antigen inhibitor, tremelimumab, showed antitumour activity and manageable toxicity in patients with advanced hepatocellular carcinoma. Combination therapy with the programmed death-ligand 1 (PD-L1) inhibitor durvalumab and tremelimumab also showed encouraging preliminary results and no unexpected safety signals in patients with hepatocellular carcinoma. The only study that has described treatment of patients with hepatocellular carcinoma with an anti-PD-1 inhibitor was that of nivolumab, which showed promising outcomes and a safety profile generally consistent with that reported for nivolumab in other tumour types. Apart from the nivolumab study, which suggested that PD-L1 expression in tumour cells was not significantly

associated with a clinical response, no relevant studies have evaluated biomarkers of response to immunotherapy in hepatocellular carcinoma, as was done in our study.

Added value of this study

To our knowledge, the KEYNOTE-224 study is the first to show the clinical efficacy and safety of pembrolizumab in patients with advanced hepatocellular carcinoma who were previously treated with sorafenib. A substantial proportion of patients had objective responses and both median progression-free survival and overall survival were promising after treatment with pembrolizumab. These results are also consistent with findings for nivolumab in these patients, indicating the importance of anti-PD-1 therapy as a potential treatment option for these patients. The study also showed that PD-L1 expression, as shown by combined positive score (a measure of PD-L1-positive immune and tumour cell number), was associated with response to pembrolizumab; however, further study is needed to determine the clinical usefulness of PD-L1 in predicting response to anti-PD-1 therapy in patients with advanced hepatocellular carcinoma.

Implications of all the available evidence

Overall, this study indicated that pembrolizumab could be an additional treatment option for patients with advanced hepatocellular carcinoma whose disease progressed on or were intolerant to previous sorafenib therapy; further assessment is ongoing in the phase 3 KEYNOTE-240 and KEYNOTE-394 trials in patients with second-line advanced hepatocellular carcinoma. PD-L1 expression, as assessed by the combined positive score, appeared to be associated with response to pembrolizumab in these patients; however, additional studies are needed to better understand the associations between biomarkers and response to anti-PD-1 therapy in hepatocellular carcinoma.

survival³⁻⁵ and is approved for treatment in Japan. All other treatments that have been assessed as first-line therapy, and several other drugs that have been evaluated as second-line therapies have not shown improved survival over sorafenib or placebo.⁶ Regorafenib, another anti-angiogenic multi-kinase inhibitor, is the only second-line therapy that has been globally approved for use after treatment with sorafenib in patients with hepatocellular carcinoma.⁷ In 2018, cabozantinib was shown to improve overall survival compared with placebo in patients with advanced hepatocellular carcinoma who were intolerant to or had progressive disease after sorafenib treatment.⁸ A phase 3 study⁹ (REACH-2) that evaluated ramucirumab as a second-line therapy in patients with hepatocellular carcinoma who had blood concentrations of alpha-fetoprotein of at least 400 ng/mL also showed improved overall survival compared with placebo. Although these inhibitors have led to improved survival, the benefits remain modest

and many of these drugs have prohibitive side-effects. Novel treatment strategies for these patients are desperately needed.

The liver maintains a balance between activation of and tolerance by immune cells in response to antigenic hyperstimulation, and dysregulation of this tightly controlled immunological network leads to chronic liver disease and hepatocellular carcinoma.² Hepatocellular carcinoma has been shown to be associated with inflammation and a suppressed immune environment.^{2,10} An inflammatory gene-expression signature was shown to be predictive of lower overall survival in liver tissue adjacent to tumours in patients with hepatocellular carcinoma,¹¹ and high expression of programmed death-ligand 1 (PD-L1) in tumours correlates with a poorer prognosis than lower expression of PD-L1 in patients with resected hepatocellular carcinoma.¹² Upregulation of programmed cell death protein-1 (PD-1) and PD-L1 expression on T cells is also associated with a more

Department of Gastroenterology, Hepatology, and Endocrinology, Medizinische Hochschule, Hannover, Germany (Prof A Vogel MD); Department of Medical Oncology, King's College Hospital, London, UK (D Sarker PhD); Gastrointestinal Oncology Unit, Hôpital Erasme, Brussels, Belgium (G Verset MD); Department of Clinical Oncology, State Key Laboratory of Oncology in South China, The Chinese University of Hong Kong, Shatin, Hong Kong (S L Chan MRCP); Department of Medical Oncology, Princess Margaret Cancer Centre, University of Toronto, Toronto, ON, Canada (J Knox MD); Department of Oncology, Azienda Ospedaliera Gaetano Rummo, Benevento, Italy (B Daniele MD); Department of Global Clinical Development, Merck & Co, Kenilworth, NJ, USA (A L Webber PhD, S W Ebbinghaus MD, J Ma PhD, A B Siegel MD); Department of Medical Oncology, National Taiwan University Hospital, Taipei, Taiwan (Prof A-L Cheng MD); and Department of Gastroenterology and Hepatology, Faculty of Medicine, Kindai University, Osaka, Japan (M Kudo MD)

Correspondence to: Prof Andrew X Zhu, Department of Medicine, Harvard Medical School, Boston, MA 02114, USA azhu@mgh.harvard.edu

See Online for appendix

advanced disease stage and higher recurrence rates in patients with hepatocellular carcinoma.¹³ Signature genes in subsets of infiltrating regulatory T cells and exhausted CD8+ cells of patients with hepatocellular carcinoma have been identified, including layllin (*LAYN*), which might be linked to immune suppression by these cells.¹⁴ These immunological findings suggest that immunotherapy approaches could benefit these patients.

Immunotherapy with checkpoint blockade inhibitors has shown promising preliminary results in patients with advanced hepatocellular carcinoma, either as monotherapy or combination therapy.² The anti-PD-1 inhibitor nivolumab has shown encouraging outcomes and a safety profile that is generally consistent with that reported in other tumour types and, as such, has received accelerated approval in the USA for the treatment of hepatocellular carcinoma that has previously been treated with sorafenib.^{15,16} Pembrolizumab, an anti-PD-1 monoclonal antibody, has shown antitumour activity and a manageable safety profile in several cancers, including melanoma, non-small cell lung cancer, head and neck cancer, squamous cell carcinoma, gastric and urothelial cancers, and classical Hodgkin's lymphoma.^{17,18}

We present the results of KEYNOTE-224, an open-label, phase 2 trial, in which we aim to evaluate the efficacy and safety of pembrolizumab in patients with advanced hepatocellular carcinoma who have been previously treated with sorafenib, and to assess the association between PD-L1 expression and clinical outcomes.

Methods

Study design and participants

KEYNOTE-224 is a non-randomised, multicentre, open-label, phase 2 trial of pembrolizumab in patients with advanced hepatocellular carcinoma who have previously been treated with sorafenib. The trial was done at 47 medical centres and hospitals in ten countries (Australia, Belgium, Canada, France, Germany, Italy, Japan, Sweden, the UK, and the USA; appendix p 2); participants were enrolled at 38 sites (appendix p 3).

Patients who were eligible for the trial were aged at least 18 years; had a histologically or cytologically confirmed diagnosis of hepatocellular carcinoma; and had documented radiographic progression of disease after treatment with sorafenib or intolerance to sorafenib (defined as any grade ≥ 2 drug-related adverse event which, despite supportive therapy, recurred after interruption of treatment with sorafenib for at least 7 days and dose reduction, resulting in the patient requesting or physician recommending discontinuation of sorafenib treatment). Eligible patients also had Barcelona Clinical Liver Cancer Stage (BCLC) C or B disease that was not amenable to, or refractory after, locoregional therapy or to a curative treatment approach (eg, transplantation, surgery, or ablation); had at least one measurable lesion as defined by Response Evaluation Criteria in Solid

Tumors (RECIST)¹⁹ version 1.1 and confirmed by central review at ICON Medical Imaging (North Wales, PA, USA) before enrolment; an Eastern Cooperative Oncology Group (ECOG) performance status of 0–1; a predicted life expectancy greater than 3 months; adequate organ function; and were Child-Pugh class A. Patients with chronic infections with hepatitis C virus (treated or untreated) and patients with hepatitis B virus who were treated with antiviral therapy and who had a viral load less than 100 IU/mL before receiving their first pembrolizumab dose were also included. Provision of a tumour sample for biomarker assessment was optional.

Exclusion criteria included treatment with sorafenib up to 2 weeks before the first study dose, previous immunotherapy (anti-PD-1, anti-PD-L1, or anti-PD-L2), and previous systemic therapy for advanced hepatocellular carcinoma other than sorafenib. Patients who were currently participating in and receiving therapy from another study, and those who had previously participated in a study of an investigational drug and received study therapy within 4 weeks of the first dose of treatment were also excluded. Participants must also have recovered from any associated therapy (ie, to grade ≤ 1 by the NCI Common Terminology Criteria for Adverse Events 4.0 or baseline) and from adverse events associated with any previous therapy. Patients with previous locoregional therapy, major surgery to the liver up to 6 weeks before the first study dose, minor surgery to the liver or other sites up to 1 week before the first study dose, previous solid organ or haematological transplantation, active autoimmune disease that had required systemic treatment in the past 2 years, a diagnosis of immunodeficiency, or those who had received systemic steroid therapy or other immunosuppressive therapy up to 7 days before the first study dose were also excluded. Other exclusion criteria included evidence of metastases to the CNS; carcinomatous meningitis; fibrolamellar and mixed hepatocellular or cholangiocarcinoma subtypes of hepatocellular carcinoma; clinically apparent ascites on physical examination; and clinically diagnosed hepatic encephalopathy or oesophageal or gastric variceal bleeding within the past 6 months. Patients with portal vein invasion at the main portal (Vp4) or the inferior vena cava or cardiac involvement of hepatocellular carcinoma (determined by imaging) were also excluded. Additional eligibility and exclusion criteria are provided in the protocol (appendix p 8).

The trial was done in accordance with the International Conference on Good Clinical Practice Standards and the Declaration of Helsinki. The relevant institutional and ethics committees of participating sites approved the protocol and amendments. All patients provided written informed consent.

Procedures

All participants received 200 mg pembrolizumab intravenously every 3 weeks, on day 1 of each 3-week

cycle, for up to 35 cycles (for about 2 years) or until disease progression, unacceptable toxicity, patient withdrawal of consent, or investigator decision. Response was assessed every 9 weeks, was measured according to RECIST version 1.1, and was assessed both by investigators and by central imaging review. Response was assessed until the first radiological evidence of progressive disease. After the first determination of progressive disease made by the investigator (which was verified at ICON Medical Imaging), assessment of progression was done with immune-related RECIST (irRECIST) guidelines.²⁰ The decision to continue treatment of participants who were clinically stable (with no symptoms or signs indicative of clinically significant disease progression, including laboratory values, no decline in ECOG performance status, and absence of rapid disease progression that required urgent alternative medical intervention) was at the discretion of the site investigator. Treatment could be continued until confirmation of progressive disease by another scan at least 4 weeks after the date at which progression was first seen. If radiological progression was confirmed on the repeat scan, the treatment was discontinued unless, in the opinion of the investigator, the participant was still receiving a clinically meaningful benefit from the treatment; in these participants, an exception for continued treatment was considered following consultation with the funder representative and co-author, ABS.

Participants who were determined to have radiological disease progression by investigator assessment and who were clinically stable could continue to receive treatment at the discretion of the investigator if no other cancer treatment had been administered since the last dose of pembrolizumab and if the trial was ongoing. Participants who discontinued trial treatment for a reason other than disease progression were followed up and assessed every 9 weeks by radiological imaging until the start of new anticancer treatment, disease progression, death, or the end of the study. We monitored all participants every 12 weeks for overall survival until death, withdrawal of consent from participation in the study, or the end of the study, whichever occurred first.

Imaging of the patient's tumour was done by triple phase contrast-enhanced CT scan (preferred) or MRI (when CT was contraindicated or when dictated by local practice standards) at baseline, by 21 days before allocation for initial tumour imaging, and we did the first on-study assessment at 9 weeks. Thereafter, subsequent imaging throughout the trial was done every 9 weeks.

Participants could withdraw consent from study participation at any time for any reason, or they could be removed from the trial at the discretion of the investigator if adverse effects occurred. Additionally, a patient could be withdrawn by the investigator or the sponsor if enrolment into the trial was deemed inappropriate, the trial plan was violated, or for administrative or other safety reasons.

Dose reductions of pembrolizumab were not allowed during this trial. Dose interruptions were permitted in the case of medical or surgical events or for reasons not related to study therapy (such as elective surgery, unrelated medical events, patient vacations, or public holidays); participants were placed back on study therapy within 3 weeks of the scheduled interruption, unless otherwise discussed with the sponsor. Therapy was also interrupted or permanently discontinued if the participant met criteria for hepatic events of clinical interest, including non-overdose related events (appendix p 8).

The duration of previous sorafenib use, the time from stopping sorafenib use, and the time from progressive disease or recurrence after sorafenib use to the first pembrolizumab dose were evaluated. Data related to the pattern of progression (ie, extrahepatic disease) after sorafenib use was not collected.

Adverse events were assessed from the time of treatment allocation until 30 days after treatment cessation (for serious adverse events, 90 days, or 30 days if the patient started a new anticancer therapy, whichever was earlier) and were graded by use of the National Cancer Institute Common Terminology Criteria for Adverse Events version 4.0. After confirmed disease progression or the start of new anticancer therapy, participants were contacted every 12 weeks by phone, to monitor survival. Potential immune-related hepatitis due to pembrolizumab treatment was considered if a patient had increased bilirubin, aspartate aminotransferase, or alanine aminotransferase concentrations, or clinical hepatic decompensation in accordance with the criteria specified in the appendix (p 8). Hepatic events were reviewed by two separate physicians (of Merck & Co, Inc) to determine whether or not the event was immune-mediated. When there was disagreement in the opinions given by these physicians, a third physician (of Merck & Co, Inc) also reviewed the case and finalised the decision. All final assessments were reviewed by an independent data monitoring committee. An immune-related hepatitis diagnosis was made after other possible reasons for these events, including viral flare (if applicable), biliary or vascular obstruction, infection, medications, and alcohol use, were excluded.

Laboratory tests for haematology, blood histochemistry, and urinalysis were done up to 7 days before the first dose of pembrolizumab; an exception was hepatitis and thyroid serologies, which could be done up to 28 days before the first dose. For subsequent doses of pembrolizumab, laboratory safety tests were generally done up to 72 h before administration of doses.

PD-L1 expression was assessed retrospectively by immunohistochemistry of newly obtained or archival pre-treatment tumour samples with an investigational version of the PD-L1 IHC 22C3 pharmDx kit (Agilent Technologies; Santa Clara, CA, USA).²¹ Expression levels were reported by use of the combined positive score, defined as the number of PD-L1-positive cells (tumour

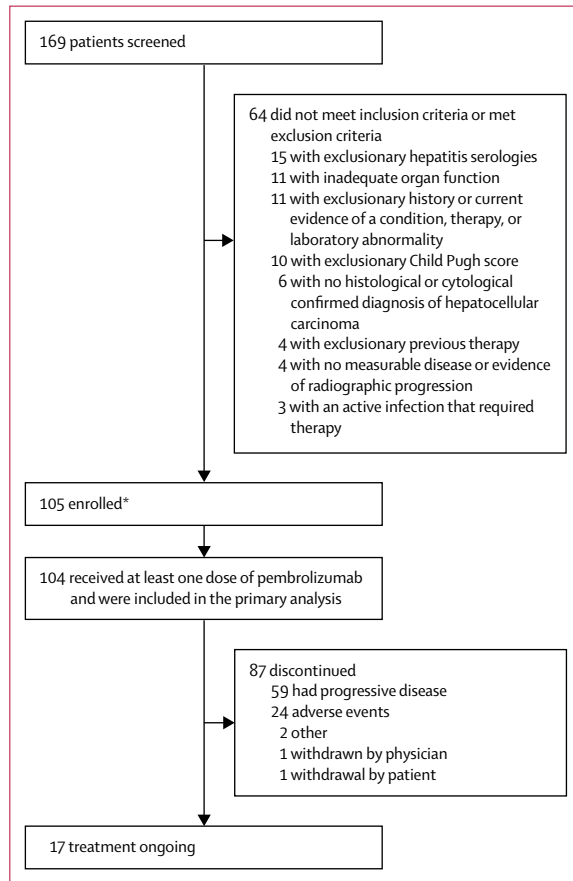


Figure 1: Trial profile

*One patient enrolled in error (not treated due to laboratory values that made them ineligible).

cells, lymphocytes, and macrophages) divided by the total number of viable tumour cells and multiplied by 100. The combined positive score was previously reported as a percentage and is now reported as a measure without units, equivalent to the former combined positive score percentage. This change was made because the cells counted in the numerator are not a percentage of those counted in the denominator, but are the number of PD-L1-positive tumour and immune cells per 100 tumour cells.²² PD-L1 expression was also assessed by use of the tumour proportion score, defined as the percentage of viable tumour cells that showed partial or complete membrane staining of PD-L1 (at least 1%) relative to all viable tumour cells present in the sample.²¹

Outcomes

The primary endpoint was objective response, defined as the proportion of participants with a confirmed complete response or partial response (assessed with RECIST version 1.1 guidelines by central imaging review); responses to pembrolizumab were only assessed until patients received new anticancer therapies so that the results would not be confounded by other treatments.

Secondary endpoints were the duration of response (time from first confirmed complete or partial response to disease progression or death), disease control (the proportion of participants with complete and partial responses plus stable disease with a duration of at least 6 weeks), and time to progression (time from first day of treatment to first documented disease progression), all of which were assessed with RECIST version 1.1 by central imaging review; progression-free survival (time from first day of treatment to first documented disease progression, based on the RECIST version 1.1 guidelines by central review, or death, whichever occurred first); overall survival (time from the first dose of study medication to death from any cause); and safety and tolerability.

Protocol-specified exploratory endpoints included evaluation of objective response, duration of response, disease control, and progression-free survival according to irRECIST and modified RECIST for hepatocellular carcinoma (mRECIST) guidelines²³ by central imaging review. The associations between PD-L1 expression by combined positive score and tumour proportion score and clinical efficacy were also assessed as prespecified exploratory endpoints. A full list of the prespecified exploratory endpoints is available in the protocol (appendix p 30).

Statistical analysis

A sample size of approximately 100 participants was chosen for this study to provide sufficient precision for assessment of the primary endpoint of objective response. Hypothesis testing was not specified in this trial. Objective response, disease control, time to progression, progression-free survival, overall survival, and safety were assessed in all participants who received at least one dose of pembrolizumab. The duration of response was evaluated in responders, who were defined as those who had confirmed partial and complete responses. Objective response and disease control were evaluated with point estimates and 95% CIs.²⁴ Duration of response, time to progression, progression-free survival, and overall survival were estimated by the Kaplan-Meier method for censored data. For duration of response, participants with a confirmed response who were alive and without subsequent radiological disease progression were censored at the time of their last imaging assessment and before the start of new anticancer treatment (if applicable); for time to progression, participants without disease progression were censored at the last imaging assessment, regardless of whether they were alive or not; and, for progression-free survival, participants who were alive and without disease progression or who were lost to follow-up were censored at the last imaging assessment. For overall survival, participants who were alive or who were lost to follow-up were censored at the time of last known survival.

Patient flow through the trial, baseline characteristics, and adverse events were summarised by descriptive

All patients (n=104)	
Sex	
Male	86 (83%)
Female	18 (17%)
Age (years)	
	68 (62–73)
Race	
White	84 (81%)
Asian	14 (13%)
Black	3 (3%)
Other	2 (2%)
Unknown	1 (1%)
Eastern Cooperative Oncology Group performance status	
0	63 (61%)
1	41 (39%)
Child Pugh Class	
A	98 (94%)
B	6 (6%)
Barcelona Clinic Liver Cancer stage	
B	25 (24%)
C	79 (76%)
Reason for previous discontinuation of sorafenib	
Intolerance	21 (20%)
Progressive disease	83 (80%)
Alcohol use	
Current or previous use	80 (77%)
Never used	23 (22%)
Unknown	1 (1%)
Hepatitis B virus status	
Positive	22 (21%)
Negative	81 (78%)
Unknown	1 (1%)
Hepatitis C virus status	
Positive	26 (25%)
Negative	78 (75%)
Extrahepatic disease	
Macrovascular invasion	18 (17%)
Baseline alpha-fetoprotein concentration	
>200 ng/mL	43 (41%)
≤200 ng/mL	59 (57%)
Unknown	2 (2%)

Data are n (%) or median (IQR).

Table 1: Baseline characteristics

statistics. Participants with complete or partial responses who were alive, did not show disease progression, or start a new anticancer treatment, did not miss two or more consecutive disease assessments, were not lost to follow-up, and whose last disease assessment was less than 5 months before the data cutoff date were considered ongoing responders at the time of analysis. Participants without imaging after the baseline disease assessment were considered non-responders for objective response analysis and were not assessable for best overall response. An analysis of objective response in several baseline

All treated participants (n=104)	
Objective response*	18 (17%; 11–26)
Best overall response†	
Complete response	1 (1%)
Partial response	17 (16%)
Stable disease	46 (44%)
Progressive disease	34 (33%)
Not assessable‡	6 (6%)
Disease control§	64 (62%; 52–71)
Median time to response, months (IQR)¶	2.1 (2.1–4.1)
Median duration of response, months (range)¶	Not reached (3.1–14.6+**)
Duration of response ≥9 months¶	12 (77%)

Data are n (%) or n (%; 95% CI), unless otherwise indicated. *Includes complete and partial responses. †Confirmed by independent central review with Response Evaluation Criteria in Solid Tumors. ‡These patients had a baseline assessment by investigator review or central radiology but no assessment after baseline on the data cutoff date, including discontinuation or death before the first scan after baseline. §Includes complete and partial responses and stable disease for at least 6 weeks. ¶Assessed in patients who had confirmed complete or partial responses as their best overall response. ||From product-limit (Kaplan-Meier) method for censored data. **No progressive disease by the time of last disease assessment.

Table 2: Responses to pembrolizumab treatment

factor subgroups was prespecified. Associations of PD-L1 combined positive score and tumour proportion score with objective response and progression-free survival were assessed by logistic regression (objective response) and Cox regression models (progression-free survival). Data were analysed with SAS (version 9.3). This study is registered with ClinicalTrials.gov, number NCT02702414. The data cutoff date was Feb 13, 2018; the study is ongoing for follow-up but is no longer enrolling participants.

Role of the funding source

The authors and the funder of the study collaborated in the design of the study, data collection, data interpretation, data analysis, drafting, critical review, and the decision to submit the article for publication. The corresponding author had full access to all the data and had final responsibility for the decision to submit for publication.

Results

Between June 7, 2016, and Feb 9, 2017, 169 patients were assessed for eligibility. Of these patients, 64 (38%) were deemed ineligible because they did not meet the inclusion criteria or met exclusion criteria (figure 1). We enrolled participants between June 22, 2016, and Feb 20, 2017. One (1%) patient was enrolled in error. 104 enrolled patients were treated with at least one dose of pembrolizumab and were included in the primary analysis. The baseline characteristics of the enrolled participants are shown in table 1. The median size of the baseline target lesions (sum of longest diameters)

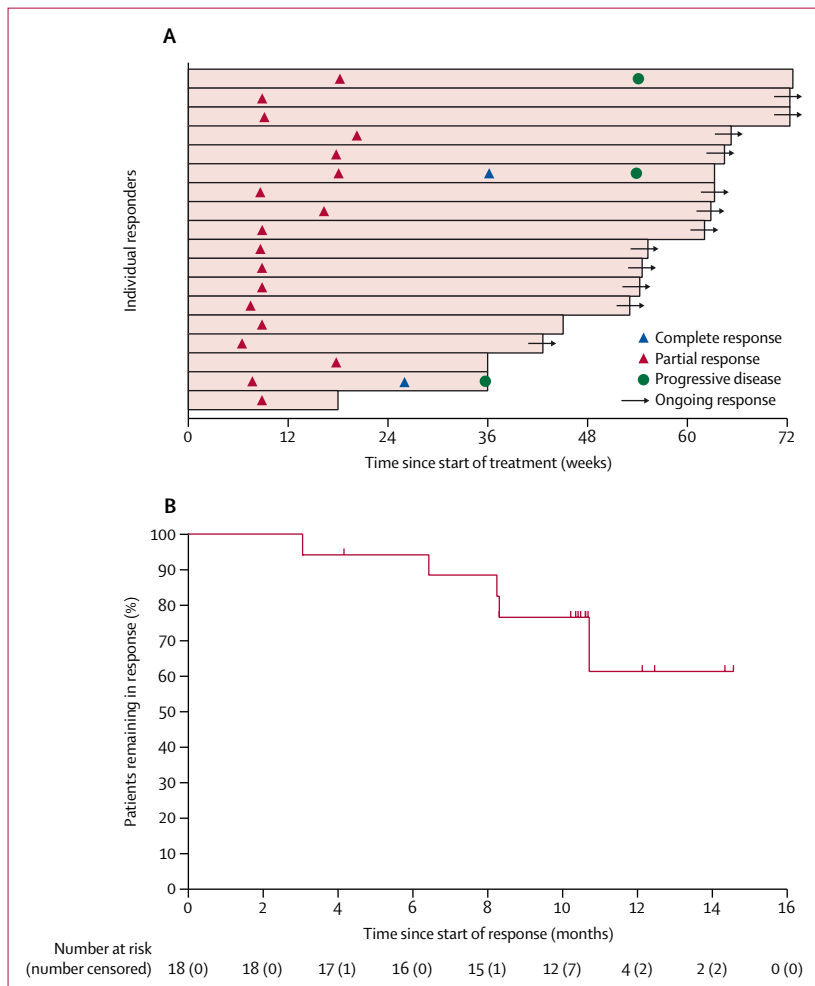


Figure 2: Tumour response, assessed with RECIST guidelines by independent central review

(A) Response and duration for the 18 responders with a best overall response of confirmed complete or partial responses only. Complete responses, partial responses, and progressive disease are the time each response was first reported (not best overall response). Each bar represents an individual patient and the length of each bar represents the time from the start of treatment to the last radiographic assessment and the duration of treatment. (B) Kaplan-Meier estimate of the duration of response in the 18 patients who had a best overall response of complete or partial responses by the Kaplan-Meier method for censored data.

was 105.5 mm (IQR 58.8–170.3, ranging from a minimum of 18 mm to a maximum of 414 mm (appendix p 4). In terms of previous sorafenib therapy, 83 (80%) of the 104 participants had discontinued sorafenib due to progressive disease and 21 (20%) participants had discontinued due to intolerance. The median duration of previous sorafenib therapy was 6.8 months (IQR 3.3–11.2), the median time since stopping sorafenib use was 1.3 months (0.8–2.5), and the median time from progressive disease or recurrence until the first dose of pembrolizumab treatment was 1.7 months (0.9–2.9).

As of data cutoff on Feb 13, 2018, the median duration of follow-up was 12.3 months (IQR 7.6–15.1) and, on this date, 17 (16%) of the 104 participants who had received at least one pembrolizumab dose were still

receiving the treatment. The median duration of pembrolizumab treatment was 4.2 months (2.1–7.7). The most common reasons for treatment discontinuation were progressive disease in 59 (57%) participants and adverse events in 24 (23%) participants (figure 1). 20 participants went on to receive an alternative treatment after disease progression: one participant received cabozantinib and 19 participants received regorafenib.

An objective response was recorded in 18 (17%) of 104 participants (95% CI 11–26; table 2) who had received at least one dose of pembrolizumab. Among the 18 responders, the best overall responses were one (1%) complete response, 17 (16%) partial responses, 46 (44%) participants had stable disease, and 34 (33%) participants had progressive disease. Six patients (6%) could not be assessed because they did not have assessment data after baseline; five (5%) died, and one (1%) stopped receiving scans. Disease control was reported in 64 (62%; 95% CI 52–71) of the 104 treated participants. 12 (77%) responders showed a response for at least 9 months, as estimated by the Kaplan-Meier method, and the median time to response was 2.1 months (IQR 2.1–4.1). 12 (67%) of 18 responders achieved objective responses at the first scheduled scan, within 8–10 weeks after initiation of treatment (figure 2), and the remaining objective responses, including one complete confirmed response and one complete unconfirmed response, occurred during weeks 15–37 of treatment. As of data cutoff, 12 of the 18 responses were ongoing, and the median duration of response was not reached (range 3.1–14.6+ months).

At data cutoff, 84 (81%) of 104 participants had died or had disease progression, as determined by independent central review. The median time to progression was 4.9 months (95% CI 3.9–8.0) and median progression-free survival was 4.9 months (95% CI 3.4–7.2; figure 3). At data cutoff, 60 (58%) of the 104 participants in the study had died, and the median overall survival was 12.9 months (95% CI 9.7–15.5; figure 3). At 12 months, of the 104 patients, 29 were still alive and progression-free, giving a 12-month progression-free survival of 28% (95% CI 19–37), and 56 patients were still alive, giving a 12-month overall survival of 54% (95% CI 44–63).

At least one adverse event was reported in 101 (97%) participants and, of these events, 42 (40%) were deemed serious. 28 (27%) deaths were reported in the study, 12 of which were attributed to adverse events, and one death, due to ulcerative oesophagitis (in a patient with ascites and progressive disease), was considered by the investigator to be possibly treatment related. 26 (25%) of the 104 participants in the study had dose interruptions because of adverse events; the most frequent of these included increased aspartate aminotransferase concentration in four (4%) participants, increased alanine aminotransferase concentration in

three (3%) participants, hypothyroidism in two (2%) participants, and a rash in two (2%) participants.

At least one treatment-related adverse event occurred in 76 (73%) of 104 participants (grade 1–2 in 49 [47%] patients, grade 3 in 25 [24%], grade 4 in one [1%], and grade 5 in one [1%]; table 3), and 16 (15%) had a treatment-related serious adverse event. The most frequent serious adverse events were increased aspartate aminotransferase concentration in four (4%) participants, increased alanine aminotransferase concentration in two (2%) participants, and adrenal insufficiency in two (2%) participants. 18 (17%) patients had dose interruptions that were attributed to drug-related adverse events; the most frequent of these adverse events were increased aspartate aminotransferase concentration in four (4%) participants, increased alanine aminotransferase concentration in three (3%) participants, hypothyroidism in two (2%) participants, and rash in two (2%) participants. Five (5%) participants discontinued study treatment after an adverse event, including one (1%) patient with each of adrenal insufficiency, increased aspartate aminotransferase and alanine aminotransferase concentrations, elevated bilirubin concentration, cholestatic jaundice, and ulcerative oesophagitis (the patient who died). The most common treatment-related events of any grade that occurred in at least 10% of the participants were fatigue (22 [21%] of 104 participants), increased aspartate aminotransferase concentration (14 [13%]), pruritus (12 [12%]), diarrhoea (11 [11%]), and rash (ten [10%]). Treatment-related events of grade 3 or worse severity were reported in 27 (26%) participants. The most common treatment-related grade 3 events were fatigue (four [4%] participants), increased aspartate aminotransferase concentration (seven [7%] participants), and increased alanine aminotransferase concentration (four [4%]). One grade 4 occurrence of hyperbilirubinaemia was reported.

Immune-mediated events of any attribution occurred in 15 (14%) participants, and the most common events of any grade of severity were hypothyroidism (eight [8%] participants) and adrenal insufficiency (three [3%] participants). Four immune-mediated events of grade 3 severity were reported, including two (2%) participants with adrenal insufficiency, one (1%) with severe skin toxicity, and one (1%) with type 1 diabetes mellitus; no immune-mediated events worse than grade 3 severity occurred (table 4). Immune-mediated hepatitis was seen in three (3%) participants. No cases of flares of hepatitis B virus or hepatitis C virus occurred.

In our prespecified exploratory analysis of responses according to irRECIST and mRECIST criteria, similar proportions of patients achieved an objective response as in our primary analysis, with objective responses recorded in 18 (17%; 95% CI 11–26) participants with use of irRECIST and in 16 (15%; 9–24) according to mRECIST (appendix p 5). With use of irRECIST assessment, best overall responses were one (1%) complete response, 17 (16%) partial responses, 54 (52%) participants

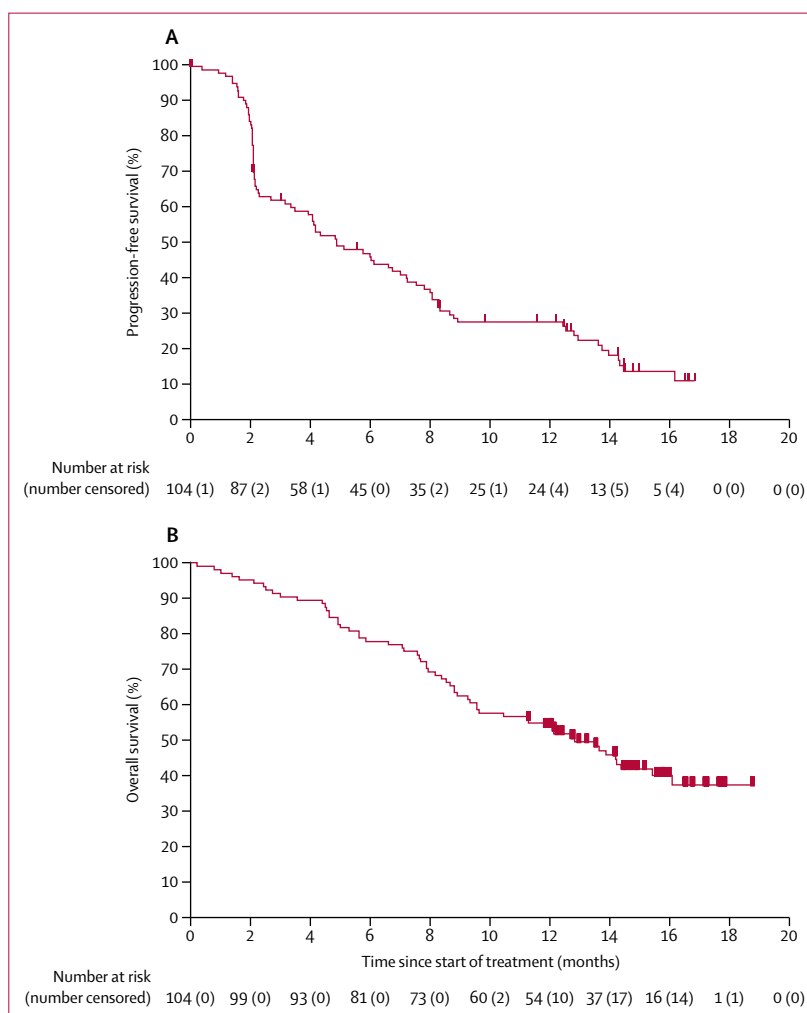


Figure 3: Kaplan-Meier estimates of progression-free and overall survival
(A) Progression-free survival. (B) Overall survival.

with stable disease, and 26 (25%) participants with progressive disease. With the irRECIST assessment, disease control was observed in 72 (69%) participants, median time to response was 2.1 months (IQR 2.1–4.1), median duration of response was not reached (3.1–14.6+ months), and the Kaplan-Meier estimate of participants with a duration of response of at least 9 months was 13 (83%) participants. With use of the mRECIST criteria, there were four (4%) complete responses, 12 (12%) partial responses, 37 (36%) participants with stable disease, and 45 (43%) participants with progressive disease. With the mRECIST assessment, disease control was observed in 53 (51%) participants, median time to response was 2.1 months (IQR 2.1–2.7), median duration of response was not reached (95% CI 3.1–14.6+ months), and the Kaplan-Meier estimate of the participants with a duration of response of at least 9 months was eight (75%) participants. When assessed with irRECIST, median progression-free survival was

	Grade 1-2	Grade 3	Grade 4	Grade 5
Fatigue	18 (17%)	4 (4%)	0	0
Pruritus	12 (12%)	0	0	0
Diarrhoea	11 (11%)	0	0	0
Rash	10 (10%)	0	0	0
Nausea	8 (8%)	0	0	0
Asthenia	7 (7%)	0	0	0
Increased aspartate aminotransferase	7 (7%)	7 (7%)	0	0
Decreased appetite	6 (6%)	1 (1%)	0	0
Myalgia	6 (6%)	1 (1%)	0	0
Hypothyroidism	6 (6%)	0	0	0
Increased alanine aminotransferase	5 (5%)	4 (4%)	0	0
Arthralgia	5 (5%)	0	0	0
Maculopapular rash	5 (5%)	0	0	0
Hyperbilirubinaemia	3 (3%)	1 (1%)	1 (1%)	0
Dyspnoea	4 (4%)	1 (1%)	0	0
Anaemia	2 (2%)	1 (1%)	0	0
Adrenal insufficiency	1 (1%)	2 (2%)	0	0
Cardiac failure	0	1 (1%)	0	0
Diabetic metabolic decompensation	0	1 (1%)	0	0
Increased gamma-glutamyltransferase	0	1 (1%)	0	0
Hepatic vein thrombosis	0	1 (1%)	0	0
Gastric ulcer	0	1 (1%)	0	0
Hyperlipasaemia	0	1 (1%)	0	0
Iron deficiency anaemia	0	1 (1%)	0	0
Cholestatic jaundice	0	1 (1%)	0	0
Lichenoid keratosis	0	1 (1%)	0	0
Lung infection	0	1 (1%)	0	0
Mucosal inflammation	0	1 (1%)	0	0
Type 1 diabetes mellitus	0	1 (1%)	0	0
Generalised rash	0	1 (1%)	0	0
Vena cava thrombosis	0	1 (1%)	0	0
Ulcerative oesophagitis	0	0	0	1 (1%)

Data are n (%) in all treated patients (n=104). The table lists treatment-related adverse events (attributed to treatment by the investigator) experienced by at least 10% of patients (grades 1-2) or by any patient (grades 3-5). Patients are counted once for each applicable specific adverse event and could have more than one treatment-related event.

Table 3: Treatment-related adverse events

7.0 months (95% CI 4.9–8.0), with an estimated 30 (29%; 95% CI 20–38) participants alive and progression-free at 12 months. When assessed with mRECIST, median progression-free survival was 3.2 months (95% CI 2.2–4.1), with an estimated 20 (19%; 95% CI 12–27) participants alive and progression-free at 12 months; appendix p 7). These findings were similar to those in our primary analysis in which we used the RECIST 1.1 guidelines.

In our prespecified subgroup analyses, the proportion of patients with an objective response was generally similar across prespecified subgroups of participants with various risk factors, including macrovascular invasion, viral infections, and reasons for discontinuation of sorafenib (figure 4). We observed reductions from baseline in tumour target lesion size in 52 (50%) of the 104 participants in the overall study cohort, including 33 (58%) of

57 patients who were not infected with hepatitis B virus or hepatitis C virus, 12 (57%) of 21 participants who were infected with hepatitis B virus, and ten (39%) of 26 participants who were infected with hepatitis C virus (figure 5).

In another prespecified exploratory analysis, we evaluated the associations between biomarkers and clinical response to pembrolizumab in subsets of participants with data available for PD-L1 expression by combined positive score and tumour proportion score (n=52; 47 were archival samples and five were newly obtained). The baseline characteristics of these subgroups were similar to those of the overall study cohort, including prognostic factors, such as alpha-fetoprotein concentration, BCLC stage, ECOG status, extrahepatic disease, and macrovascular invasion (appendix p 6). The proportion of patients who achieved an objective response was also similar for the overall cohort (18 [17%] of 104 participants) and the subgroup with available PD-L1 expression data (13 [25%] of 52 participants), as were event rates for progression-free survival (84 [81%] of 104 participants in the overall cohort; 43 [83%] of 52 participants in the PD-L1 subgroup). Associations between biomarkers and clinical response are shown in table 5. The proportion of patients with positive PD-L1 expression according to a combined positive score of at least 1 was 22 (42%) of 52, and the proportion of patients with positive PD-L1 expression according to a PD-L1 tumour proportion score of at least 1% was 7 (13%) of 52. Objective responses for participants with PD-L1-positive and PD-L1-negative expression were recorded in 32% (seven of 22 patients) with combined positive scores of at least 1 versus 20% (six of 30 patients) with combined positive scores less than 1, and 43% (three of seven patients) for tumour proportion scores of at least 1% versus 22% (ten of 45 patients) for tumour proportion scores less than 1%.

Discussion

In this phase 2 trial, pembrolizumab showed promising clinical efficacy and manageable safety in patients with advanced hepatocellular carcinoma who were previously treated with sorafenib. To our knowledge, this trial was the first to evaluate pembrolizumab in this patient population. We found a substantial number of objective responses (17%) that were consistently observed across several risk factors associated with the prognosis of hepatocellular carcinoma, including hepatitis B virus and hepatitis C virus infections, and also in those whose disease progressed with or who were intolerant to sorafenib. Responses seemed to be durable: the median duration of response was not reached, medians of both time to progression and progression-free survival were 4.9 months, and median overall survival was 12.9 months, indicating that pembrolizumab could be an efficacious treatment option in this setting.

The safety and toxicity profile of pembrolizumab in these patients was manageable and generally similar to

that of pembrolizumab in other tumour types.¹⁷ The number of discontinuations due to treatment-related adverse events was low, and the treatment-related events that were observed in more than 10% of participants were fatigue, diarrhoea, pruritis, and rashes, which are events that are typically observed following pembrolizumab treatment. Although underlying liver dysfunction can be anticipated in patients with hepatocellular carcinoma, few participants had immune-mediated hepatitis, no viral flares of hepatitis B virus or hepatitis C virus were observed, and increased concentrations of aspartate aminotransferase were within the expected range in this population. The most common immune-mediated adverse events reported were hypothyroidism, adrenal insufficiency, and thyroiditis at low frequencies, consistent with effects seen with immunotherapy—including pembrolizumab—in other cancer types.

The results of a few studies have suggested that immune-checkpoint blockade therapy provides a clinical benefit for some patients with hepatocellular carcinoma. In a small study²⁵ of patients with hepatitis C virus-associated hepatocellular carcinoma, inhibition of cytotoxic T lymphocyte-associated antigen 4 (CTLA-4) with tremelimumab showed anti-tumour effects and manageable toxicity. Combination therapy with PD-L1 and CTLA-4 inhibitors, durvalumab and tremelimumab, also showed encouraging preliminary results and no unexpected safety signals in patients with hepatocellular carcinoma.²⁶ The PD-1 inhibitor nivolumab showed promising outcomes and a tolerable safety profile in a phase 1–2 trial¹⁵ in patients with advanced hepatocellular carcinoma, both with and without infections with hepatitis B virus and hepatitis C virus. The findings in our study of pembrolizumab are consistent with those observed for nivolumab, including an overall response rate of 14% (according to RECIST version 1.1) and a duration of response of at least 12 months in 55% of participants.^{15,16,27} Taken together, these findings support the potential clinical usefulness of anti-PD-1 therapy in patients with advanced hepatocellular carcinoma.

Given the heterogeneity of hepatocellular carcinoma, identification of biomarkers that are predictive of response to immunotherapy could aid the identification of patients who would derive the greatest benefit from these therapies. Although biomarkers that are predictive of response to immunotherapy have been studied in other cancer types,^{28–33} little is known about biomarkers that are predictive of response to these therapies in hepatocellular carcinoma. Biomarkers that are predictive of response to anti-PD-1 therapy include PD-L1 expression when assessed by immunohistochemistry, which has been shown to be associated with response to anti-PD-1 therapy in several cancers, and is approved as a diagnostic assay for treatment of non-small-cell lung and gastric cancers with pembrolizumab.¹⁷ Preliminary results described in our study showed that PD-L1 expression in immune and tumour cells, as assessed by

	Grade 1–2	Grade 3	Grade 4	Grade 5
At least 1 event	11 (11%)	4 (4%)	0	0
Hypothyroidism	8 (8%)	0	0	0
Adrenal insufficiency	1 (1%)	2 (2%)	0	0
Thyroiditis	2 (2%)	0	0	0
Severe skin reaction	0	1 (1%)	0	0
Autoimmune colitis	1 (1%)	0	0	0
Colitis	1 (1%)	0	0	0
Hyperthyroidism	1 (1%)	0	0	0
Type 1 diabetes mellitus	0	1 (1%)	0	0
At least 1 immune-mediated hepatic event*	0	3 (3%)	0	0

The table shows immune-mediated adverse events of any attribution in all treated patients (n=104), listed in order of decreasing frequency based on presumed immunological mechanism of action. *Based on sponsor assessment; includes three events initially reported as increased aspartate and alanine aminotransferases, which were determined to be immune-mediated hepatitis by the sponsor.

Table 4: Immune-mediated adverse events of any attribution

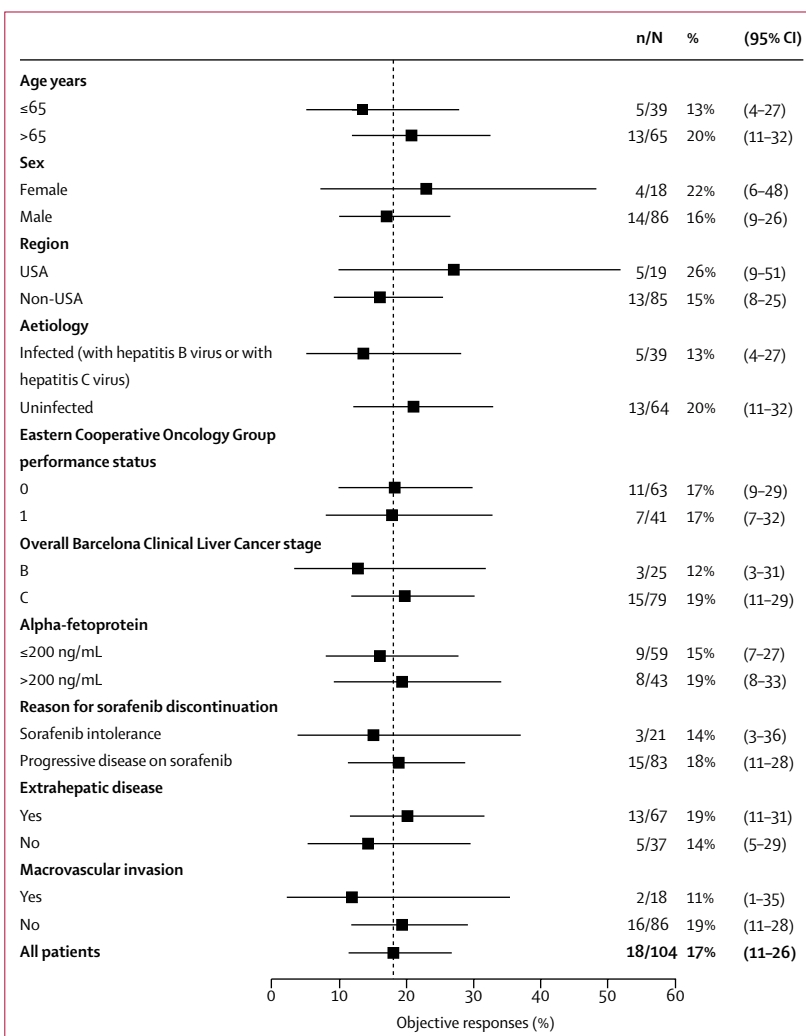


Figure 4: Subgroup analysis of objective responses
Data are for all patients (n=104) in the as-treated population.

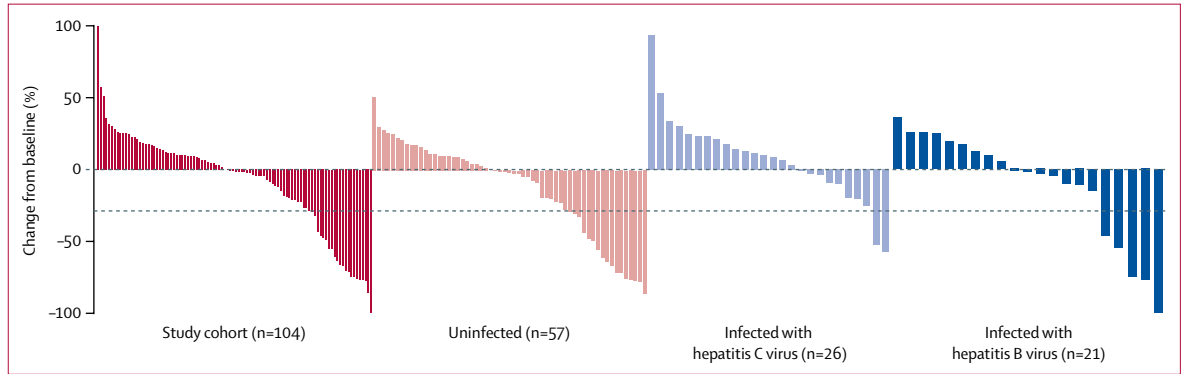


Figure 5: Best percentage changes from baseline in size of target lesions
 Assessed with RECIST by central radiology review in patients with image measurements before and after treatment. The horizontal dashed line represents the threshold for response according to RECIST version 1.1.

	Objective response (confirmed best overall response)		Progression-free survival	
	Number of responders* (%)	p value†	Number of events* (%)	p value†
Combined positive score	13 (25%)	0.021	43 (83%)	0.026
Tumour proportion score	13 (25%)	0.088	43 (83%)	0.096

Combined positive score is the number of PD-L1-positive cells (tumour cells, lymphocytes, and macrophages)/total number of viable tumour cells $\times 100$. Tumour proportion score is the percentage of viable tumour cells with partial or complete membrane staining of PD-L1 ($\geq 1\%$) relative to all viable tumour cells present in the sample. PD-L1=programmed death-ligand 1.*Of 52 patients or 52 events with available data. †p values are for the association of PD-L1 expression with objective responses and progression-free survival by use of a one-sided test from logistic regression for objective response and Cox regression for progression-free survival.

Table 5: Association of biomarkers with clinical outcomes

the combined positive score, was associated with response to anti-PD-1 therapy with pembrolizumab in a subset of patients. The association with tumour proportion score was not significant, suggesting that inclusion of immune cell scoring with tumour cell scoring could improve the predictive value of a PD-L1 immunohistochemistry assay; however, these findings need to be confirmed in larger studies. The tumour proportion score results observed in our study are consistent with preliminary findings from another study¹⁵ wherein PD-L1 tumour proportion score was not associated with response to nivolumab in patients with hepatocellular carcinoma. Determination of the clinical usefulness of PD-L1 expression as a biomarker in these patients will require further study.

Our results show clinical activity of pembrolizumab in patients with advanced hepatocellular carcinoma; however, a limitation of our study is the absence of a randomised, controlled study design. A large randomised, phase 3 trial (KEYNOTE-240; ClinicalTrials.gov, NCT02702401) that will assess pembrolizumab versus placebo as a second-line therapy in advanced hepatocellular carcinoma is ongoing in several countries in the Asia-Pacific region, Europe, and North and South America. There is also a phase 3 trial ongoing in the Asia-Pacific region (KEYNOTE-394;

ClinicalTrials.gov, NCT03062358). The subgroups evaluated in KEYNOTE-224 were of modest size; nonetheless, clinical responses to pembrolizumab were observed irrespective of causation and other baseline characteristics, including BCLC stages B and C, in which a slightly higher proportion of stage B patients were enrolled in this study than in some other second-line trials in patients with hepatocellular carcinoma. Notably, this study was not designed to assess the effect of these factors in relation to survival, and evaluation in larger, randomised controlled studies is required. The low numbers of patients who were infected with hepatitis B and hepatitis C viruses limited the ability to assess these viral groups separately; however, as a combined group, the efficacy of pembrolizumab was similar to that recorded for uninfected patients. Another limitation is that the pattern of progression for patients after sorafenib therapy was not assessed. It should also be noted that provision of a tumour sample for biomarker assessment was not a requirement for patient inclusion in the trial. Thus, the associations between biomarkers and response to pembrolizumab reported here are based on a retrospective evaluation of PD-L1 expression as a continuous variable in this small subset of patients with available biomarker data, and are considered exploratory only. The study also was not designed to statistically compare the clinical usefulness of various PD-L1 expression levels, and further study in larger populations is warranted.

Overall, this study in patients with advanced hepatocellular carcinoma suggests that pembrolizumab provides durable clinical efficacy and a safety profile similar to that of pembrolizumab in other indications, and could be a therapeutic option for patients who progress after treatment with, or are intolerant of, sorafenib. Although these results and those reported in other immunotherapy studies are encouraging, additional treatment strategies for advanced hepatocellular carcinoma, such as combination immunotherapy and targeted therapy approaches, are needed, in addition to improved treatment selection for patients. In this regard, the preliminary results in this

study suggest that expression of PD-L1, as assessed by the combined positive score, might be predictive of response to pembrolizumab. Additional studies are needed to better define biomarkers that are predictive of response to anti-PD-1 and other therapies in advanced hepatocellular carcinoma, which could aid in the selection of patients who might benefit from monotherapy and combination immunotherapy treatments.

Contributors

AXZ, RSF, SLC, JK, SWE, and ABS conceived, designed, or planned the study. AXZ, JE, DP, CV, VZ, AV, DS, GV, ALW, ABS, and MK acquired the data. AXZ, RSF, JK, SWE, JM, and ABS analysed the data. AXZ, RSF, JE, SC, SO, DP, CV, LF, AV, DS, SLC, JK, BD, ALW, SWE, JM, ABS, A-LC, and MK interpreted the results. AXZ, SWE, and ABS drafted the manuscript. All authors critically reviewed or revised the manuscript for intellectual content and approved the final version to be submitted. All authors had access to the data in the study and had the final responsibility for the decision to submit for publication.

Declaration of interests

AXZ has served as a consultant for Eisai, Bristol-Myers Squibb, Merck & Co, Novartis, Sanofi, AstraZeneca, Bayer, Exelixis, and Eli Lilly and Company; and reports research funding to his institution from Eli Lilly and Company, Bayer, Bristol-Myers Squibb, Novartis, and Merck & Co. RSF has served as a consultant for Pfizer, Bayer, Novartis, Bristol-Myers Squibb, and Merck & Co; and reports research funding to his institution from Pfizer. JE has received honoraria from BTG and travel expenses from Amgen and Bristol-Myers Squibb. SO has served as a consultant for Bayer and Eisai; and has received honoraria from Bayer and Eisai. DP has received honoraria from Bayer, Celgene, NuCana, and Bristol-Myers Squibb; has served as a consultant for Bayer, Celgene, NuCana, and Bristol-Myers Squibb; and has received research funding from Bayer and NuCana. CV has served as a consultant for Bayer, Ipsen, and Novartis; and has received research funding from Ipsen and Bayer. VZ has served as a consultant for Merck Sharp & Dohme, Bristol-Myers Squibb, and Celgene; has been on a speakers' bureau for Bayer, Roche, Pfizer, and Janssen; and has received travel fees from Merck Sharp & Dohme, Roche, and Bayer. AV has served as a consultant for Novartis, Delcath Systems, Eli Lilly and Company, Roche, Amgen, Bayer, and Baxalta; has received travel expenses from Bayer, Roche, and Ipsen; has received honoraria from Novartis, Roche, Bayer, Sanofi, Amgen, Delcath Systems, Eli Lilly and Company, Bristol-Myers Squibb, and Merck Sharp & Dohme; and has received research funding from Novartis. DS has served as a consultant for Eisai, Baxalta, Novartis, and Blueprint Medicines; has received travel expenses from Bayer, Ipsen and MiNA Therapeutics; and has received honoraria from Pfizer, Bayer, and Ipsen. SLC has served as a consultant for Novartis, Merck Sharp & Dohme, and MedImmune (AstraZeneca); has received honoraria from Bayer; and has received research funding from Novartis and Sirtex Medical. JK has served as a consultant for Eli Lilly and Company and Merck & Co; has received honoraria from Novartis; and has received research funding from AstraZeneca. BD has served as a consultant for Eisai and Bayer; has received honoraria from Bayer, Merck Sharp & Dohme, Merck Serono, Eli Lilly and Company, and Bristol-Myers Squibb; and has received travel grants from Janssen, Celgene, and Bristol-Myers Squibb. ALW, SWE, JM, and ABS are employees of Merck Sharp & Dohme, a subsidiary of Merck & Co, Kenilworth, NJ, USA; and own stock or stock options in the company. A-LC has served as a consultant for Merck Sharp & Dohme, Exillix, Merck KGaA, Bristol-Myers Squibb, Bayer, BeiGene, and Ono Pharmaceuticals; has served on advisory board for Novartis, and has received honoraria from Bayer and Merck KGaA. MK has served as a consultant for Kowa, Merck Sharp & Dohme, Bristol-Myers Squibb, Bayer, Chugai Pharma, and Taiho Pharmaceuticals; has received honoraria from Bayer, Eisai, Merck Sharp & Dohme, and Ajinomoto; and has received research funding from Chugai Pharma, Otsuka, Takeda Pharmaceuticals, Taiho Pharmaceuticals, Sumitomo Dainippon Pharma, Daiichi Sankyo, Merck Sharp & Dohme, Eisai, Bayer, and AbbVie. SC, LF, and GV declare no competing interests.

Acknowledgments

The study was funded, administered, and sponsored by Merck & Co, Inc (Kenilworth, NJ, USA). We thank the patients and their families and all the investigators and site personnel. We would also like to acknowledge Roger Dansey and Olga Kuznetsova for helpful discussions and study input, Melissa Buckland for clinical study support, Larry Wu for integrated safety analysis, Himanshu Patel for statistical programming support, Robin Mogg and Anran Wang for statistical biomarker analysis, Joanne E Tomassini for medical writing support, and Sheila Erespe for editorial support, who are current or former employees of Merck & Co.

References

- Llovet JM, Villanueva A, Lachenmayer A, Finn RS. Advances in targeted therapies for hepatocellular carcinoma in the genomic era. *Nat Rev Clin Oncol* 2015; **12**: 408–24.
- Ringelhan M, Pfister D, O'Connor T, Pikarsky E, Heikenwalder M. The immunology of hepatocellular carcinoma. *Nat Immunol* 2018; **19**: 222–32.
- Cheng AL, Kang YK, Chen Z, et al. Efficacy and safety of sorafenib in patients in the Asia-Pacific region with advanced hepatocellular carcinoma: a phase III randomised, double-blind, placebo-controlled trial. *Lancet Oncol* 2009; **10**: 25–34.
- Llovet JM, Ricci S, Mazzaferro V, et al. Sorafenib in advanced hepatocellular carcinoma. *N Engl J Med* 2008; **359**: 378–90.
- Kudo M, Finn RS, Qin S, et al. Lenvatinib versus sorafenib in first-line treatment of patients with unresectable hepatocellular carcinoma: a randomised phase 3 non-inferiority trial. *Lancet* 2018; **391**: 1163–73.
- Kudo M. Systemic therapy for hepatocellular carcinoma: 2017 update. *Oncology* 2017; **93** (suppl 1): 135–46.
- Bruix J, Qin S, Merle P, et al. Regorafenib for patients with hepatocellular carcinoma who progressed on sorafenib treatment (RESORCE): a randomised, double-blind, placebo-controlled, phase 3 trial. *Lancet* 2017; **389**: 56–66.
- Abou-Alfa GK, Meyer T, Cheng AL, et al. Cabozantinib (C) versus placebo (P) in patients (pts) with advanced hepatocellular carcinoma (HCC) who have received prior sorafenib: results from the randomized phase III CELESTIAL trial. *Proc Am Soc Clin Oncol* 2018; **36** (suppl 4): 207.
- Eli Lilly and Company. Lilly announces CYRAMZA (ramucirumab) phase 3 REACH-2 Study in second-line hepatocellular carcinoma patients met overall survival endpoint. April 4, 2018. <https://investor.lilly.com/news-releases/news-release-details/lilly-announces-cyramzar-ramucirumab-phase-3-reach-2-study> (accessed April 25, 2018).
- Prieto J, Melero I, Sangro B. Immunological landscape and immunotherapy of hepatocellular carcinoma. *Nat Rev Gastroenterol Hepatol* 2015; **12**: 681–700.
- Hoshida Y, Villanueva A, Kobayashi M, et al. Gene expression in fixed tissues and outcome in hepatocellular carcinoma. *N Engl J Med* 2008; **359**: 1995–2004.
- Gao Q, Wang XY, Qiu SJ, et al. Overexpression of PD-L1 significantly associates with tumor aggressiveness and postoperative recurrence in human hepatocellular carcinoma. *Clin Cancer Res* 2009; **15**: 971–79.
- Shi F, Shi M, Zeng Z, et al. PD-1 and PD-L1 upregulation promotes CD8(+) T-cell apoptosis and postoperative recurrence in hepatocellular carcinoma patients. *Int J Cancer* 2011; **128**: 887–96.
- Zheng C, Zheng L, Yoo JK, et al. Landscape of infiltrating T cells in liver cancer revealed by single-cell sequencing. *Cell* 2017; **169**: 1342–56.
- El-Khoueiry AB, Sangro B, Yau T, et al. Nivolumab in patients with advanced hepatocellular carcinoma (CheckMate 040): an open-label, non-comparative, phase 1/2 dose escalation and expansion trial. *Lancet* 2017; **389**: 2492–502.
- Onclive. FDA approves nivolumab for hepatocellular carcinoma. Sept 22, 2017. <http://www.onclive.com/web-exclusives/fda-approves-nivolumab-for-hepatocellular-carcinoma> (accessed Feb 28, 2018).
- Merck Sharp & Dohme. Keytruda (pembrolizumab) prescribing information. March, 2017. https://www.accessdata.fda.gov/drugsatfda_docs/label/2017/125514s0151bl.pdf (accessed May 17, 2018).
- Sharma P, Allison JP. The future of immune checkpoint therapy. *Science* 2015; **348**: 56–61.
- Eisenhauer EA, Therasse P, Bogaerts J, et al. New response evaluation criteria in solid tumours: revised RECIST guideline (version 1.1). *Eur J Cancer* 2009; **45**: 228–47.

- 20 Nishino M, Giobbie-Hurder A, Gargano M, et al. Developing a common language for tumor response to immunotherapy: immune-related response criteria using unidimensional measurements. *Clin Cancer Res* 2013; **19**: 3936–43.
- 21 Dolled-Filhart M, Roach C, Toland G, et al. Development of a companion diagnostic for pembrolizumab in non-small cell lung cancer using immunohistochemistry for programmed death ligand-1. *Arch Pathol Lab Med* 2016; **140**: 1243–49.
- 22 Kulangara K, Zhang N, Corigliano E, et al. Clinical utility of the combined positive score for programmed death ligand 1 expression and the approval of pembrolizumab in gastric cancer. *Arch Pathol Lab Med* (in press).
- 23 Lencioni R, Llovet JM. Modified RECIST (mRECIST) assessment for hepatocellular carcinoma. *Semin Liver Dis* 2010; **30**: 52–60.
- 24 Clopper CJ, Pearson ES. The use of confidence or fiducial limits illustrated in the case of binomial. *Biometrika* 1934; **26**: 404–13.
- 25 Sangro B, Gomez-Martin C, de la Mata M, et al. A clinical trial of CTLA-4 blockade with tremelimumab in patients with hepatocellular carcinoma and chronic hepatitis C. *J Hepatol* 2013; **59**: 81–88.
- 26 Kelley RK, Abou-Alfa GK, Bendel JC, et al. Phase I/II study of durvalumab and tremelimumab in patients with unresectable hepatocellular carcinoma (HCC): phase I safety and efficacy analyses. *Proc Am Soc Clin Oncol* 2017; **35** (suppl 15): 4073.
- 27 Bristol-Meyers Squibb. Opdivo (nivolumab) prescribing information. May, 2016. https://www.accessdata.fda.gov/drugsatfda_docs/label/2016/125554s019lbl.pdf (accessed May 17, 2018).
- 28 Le DT, Uram JN, Wang H, et al. PD-1 blockade in tumors with mismatch-repair deficiency. *N Engl J Med* 2015; **372**: 2509–20.
- 29 Reck M, Rodríguez-Abreu D, Robinson AG, et al. Pembrolizumab versus chemotherapy for PD-L1-positive non-small-cell lung cancer. *N Engl J Med* 2016; **375**: 1823–33.
- 30 Wainberg ZA, Jalal S, Muro K, et al. KEYNOTE-059 update: efficacy and safety of pembrolizumab alone or in combination with chemotherapy in patients with advanced gastric or gastroesophageal (G/GEJ) cancer. *Ann Oncol* 2017; **28** (suppl 5).
- 31 Carbognin L, Pilotto S, Milella M, et al. Differential activity of nivolumab, pembrolizumab and MPDL3280A according to the tumor expression of programmed death-ligand-1 (PD-L1): sensitivity analysis of trials in melanoma, lung and genitourinary cancers. *PLoS One* 2015; **10**: e0130142.
- 32 Garon EB, Rizvi NA, Hui R, et al. Pembrolizumab for the treatment of non-small-cell lung cancer. *N Engl J Med* 2015; **372**: 2018–28.
- 33 Overman MJ, McDermott R, Leach JL, et al. Nivolumab in patients with metastatic DNA mismatch repair-deficient or microsatellite instability-high colorectal cancer (CheckMate 142): an open-label, multicentre, phase 2 study. *Lancet Oncol* 2017; **18**: 1182–91.



Dysbiosis-Associated Polyposis of the Colon—Cap Polyposis

Kazuki Okamoto¹, Tomohiro Watanabe^{1*}, Yoriaki Komeda¹, Ayana Okamoto¹, Kosuke Minaga¹, Ken Kamata¹, Kentaro Yamao¹, Mamoru Takenaka¹, Satoru Hagiwara¹, Toshiharu Sakurai¹, Tomonori Tanaka², Hiroki Sakamoto³, Kiyoshige Fujimoto³, Naoshi Nishida¹ and Masatoshi Kudo¹

¹Department of Gastroenterology and Hepatology, Kindai University Faculty of Medicine, Osaka-Sayama, Japan,

²Department of Pathology, Kindai University Faculty of Medicine, Osaka-Sayama, Japan, ³Department of Gastroenterology and Hepatology, Katsuragi Hospital, Kishiwada, Japan

Cap polyposis is a rare gastrointestinal disease characterized by multiple inflammatory polyps located between the distal colon and the rectum. Despite the lack of clarity regarding its pathogenesis, mucosal prolapse, chronic inflammatory responses, and *Helicobacter pylori* infection are considered key contributors to the development of this disease entity. Although it is now generally accepted that dysbiosis of gut microbiota is associated with intestinal and extra-intestinal diseases, alterations of intestinal microbiota have been poorly defined in cap polyposis. Here, we report a patient with *H. pylori*-negative cap polyposis who was successfully treated with antibiotics and exhibited dramatic alterations in intestinal microbiota composition after antibiotic treatment. The patient was treated with oral administration of ampicillin and metronidazole and showed regression of cap polyposis 6 months after antibiotic treatment. Fecal microbiota analysis using the next-generation sequencing technology revealed a significant alteration in the intestinal microbiota composition following antibiotic treatment—a marked reduction of *Blautia*, *Dorea*, and *Sutterella* was observed concomitant with a marked increase in *Fusobacterium*. These data suggest that cap polyposis may originate from dysbiosis and that microbiome-targeted therapy may be useful in this disorder.

Keywords: cap polyposis, intestinal microbiota, next-generation sequencing, inflammation, antibiotics

OPEN ACCESS

Edited by:

Ashutosh K. Mangalam,
University of Iowa, United States

Reviewed by:

Anastasia Sobolewski,
University of East Anglia,
United Kingdom
Mohamad Mokadem,
University of Iowa, United States

*Correspondence:

Tomohiro Watanabe
tomohiro@med.kindai.ac.jp

Specialty section:

This article was submitted to Mucosal Immunity, a section of the journal *Frontiers in Immunology*

Received: 18 January 2018

Accepted: 13 April 2018

Published: 07 May 2018

Citation:

Okamoto K, Watanabe T, Komeda Y, Okamoto A, Minaga K, Kamata K, Yamao K, Takenaka M, Hagiwara S, Sakurai T, Tanaka T, Sakamoto H, Fujimoto K, Nishida N and Kudo M (2018) Dysbiosis-Associated Polyposis of the Colon—Cap Polyposis. *Front. Immunol.* 9:918. doi: 10.3389/fimmu.2018.00918

HIGHLIGHTS

- Cap polyposis patient.
- Cap polyposis is considered as multiple inflammatory polyps.
- Regression of colonic polyposis after antibiotic treatment.
- Next-generation sequencing reveals dynamic changes in the intestinal microbiota composition following antibiotic treatment.
- Identification of pathogenic bacteria associated with cap polyposis.

INTRODUCTION

Cap polyposis is a rare disease characterized by multiple inflammatory polyps that are covered by a cap of fibrinopurulent mucus and are located between the distal colon and the rectum (1–3). Patients

Abbreviations: IBD, inflammatory bowel disease; MPS, mucosal prolapse syndrome; NGS, next-generation sequencing; OTU, operational taxonomic unit; rRNA, ribosomal RNA.

usually present with abdominal pain, blood and/or mucus in diarrheal stool, and hypoproteinemia (1–3). Microscopically, the colonic polyps are characterized by a cap of fibrinopurulent exudates, distorted glands, fibromuscular obliteration of the lamina propria with inflammatory cell infiltration (1–3). Although the pathogenesis of cap polyposis remains unknown, the clinical and histopathological features of this disorder resemble those observed in patients with mucosal prolapse syndrome (MPS) (4). Therefore, mucosal prolapse secondary to impaired colonic motility has been considered a possible etiological contributor to cap polyposis (4). Several reports have shown regression of cap polyposis following the use of infliximab (2) or steroid (3), thereby demonstrating the possible involvement of chronic inflammatory responses in the development of cap polyposis. Reportedly, eradication of *Helicobacter pylori* is effective in the management of cap polyposis (5, 6). However, *H. pylori* were not detected in the colonic mucosa in any of these cases. Therefore, it is possible that unidentified intestinal bacteria, sensitive to *H. pylori*-eradication therapy, may contribute to the development of cap polyposis. Considering that eradication of *H. pylori* causes a significant alteration in the intestinal microbiota composition, these case reports suggest that dysbiosis-related immune responses may underlie the pathogenesis of cap polyposis. However, the intestinal microbiota composition has not been determined in this condition.

We report a patient with *H. pylori*-negative cap polyposis who was successfully treated using antibiotics. Fecal microbiota analysis using the next-generation sequencing (NGS) technology revealed a significant alteration in the intestinal microbiota composition pre- and post-antibiotic treatment. The results of our study strongly support the contributory role of dysbiosis in the pathogenesis of cap polyposis.

CASE REPORT

An asymptomatic 45-year-old man without a relevant past or family history of gastrointestinal disease underwent a colonoscopic and esophagogastroduodenoscopic examination for the evaluation of a positive fecal occult blood test. Colonoscopic examination revealed multiple sessile polyps in the descending colon, which showed a reddish surface covered by white mucus (Figure 1A). Esophagogastroduodenoscopic examination revealed multiple fundic gland polyps. Serum anti-*H. pylori* antibody titers were below the detection limit, and serum total protein and albumin levels were within the reference range, as was the complete blood cell count. Endoscopic mucosal resection was performed to determine a histopathological diagnosis of the colonic polyps. The resected specimen showed mucus-containing distorted glands and significant inflammatory cell infiltration with fibrosis in the lamina propria (Figure 1B) and their surface was covered by inflammatory granulation tissue and fibrinopurulent exudate. These endoscopic and histopathological findings were consistent with those typically observed in patients with cap polyposis (1–3). Thus, this patient was diagnosed with cap polyposis without *H. pylori* infection.

Helicobacter pylori infection has been considered a possible etiological contributor to the development of cap polyposis

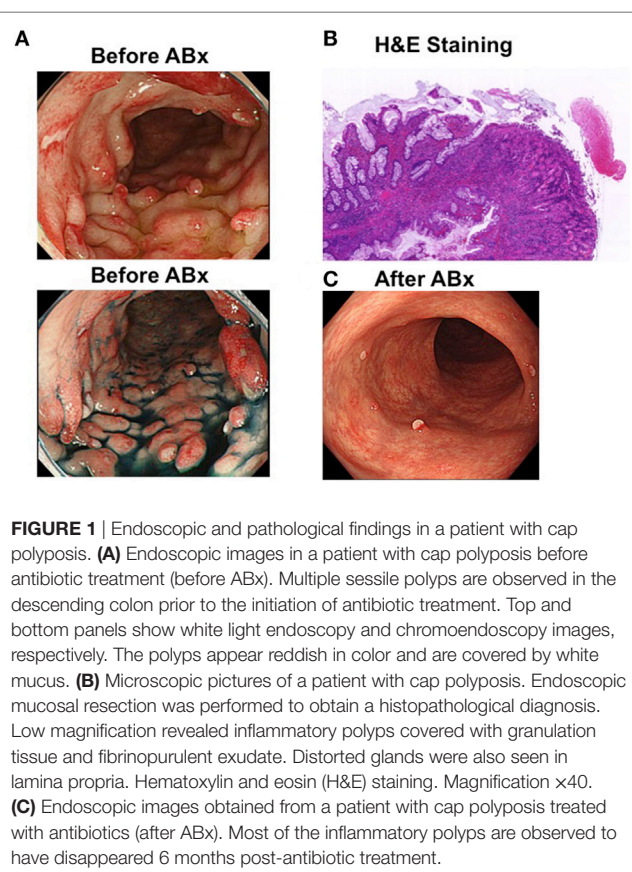


FIGURE 1 | Endoscopic and pathological findings in a patient with cap polyposis. **(A)** Endoscopic images in a patient with cap polyposis before antibiotic treatment (before ABx). Multiple sessile polyps are observed in the descending colon prior to the initiation of antibiotic treatment. Top and bottom panels show white light endoscopy and chromoendoscopy images, respectively. The polyps appear reddish in color and are covered by white mucus. **(B)** Microscopic pictures of a patient with cap polyposis. Endoscopic mucosal resection was performed to obtain a histopathological diagnosis. Low magnification revealed inflammatory polyps covered with granulation tissue and fibrinopurulent exudate. Distorted glands were also seen in lamina propria. Hematoxylin and eosin (H&E) staining. Magnification $\times 40$. **(C)** Endoscopic images obtained from a patient with cap polyposis treated with antibiotics (after ABx). Most of the inflammatory polyps are observed to have disappeared 6 months post-antibiotic treatment.

because eradication of this organism is observed to cause regression of colonic polyps in some patients (5, 6). However, notably, *H. pylori* have not been detected in the colonic mucosa in any patient diagnosed with cap polyposis. Thus, gut bacteria sensitive to the antibiotic component of *H. pylori*-eradication therapy are likely to play a pathogenic role in patients with cap polyposis. Based on this hypothesis, this patient was treated with oral administration of ampicillin (1,500 mg/day) and metronidazole (500 mg/day) for 1 week, and regression of cap polyposis was observed 6 months post-antibiotic treatment (Figure 1C). This clinical course strongly suggests that antibiotic-induced eradication of pathogenic gut bacteria responsible for the development of inflammatory polyps can cause regression of cap polyposis.

FECAL MICROBIOTA ANALYSIS

Stool samples pre- and post-antibiotic treatment were subjected to fecal microbiota analysis, which was performed as previously described (7, 8) to assess any alterations in the intestinal microbiota composition. Ethical approval for this study was granted by a Review Board of the Kindai University Faculty of Medicine. DNA samples extracted from the stool were subjected to polymerase chain reaction for the amplification of the 16S ribosomal RNA (16S rRNA) V3 and V4 regions. Primer sequences are available in our previous report (8). We performed 16S rRNA sequencing using the MiSeq system (Illumina) (7, 8). Trimmomatic, Cutadapt, and Fastq-join programs were used

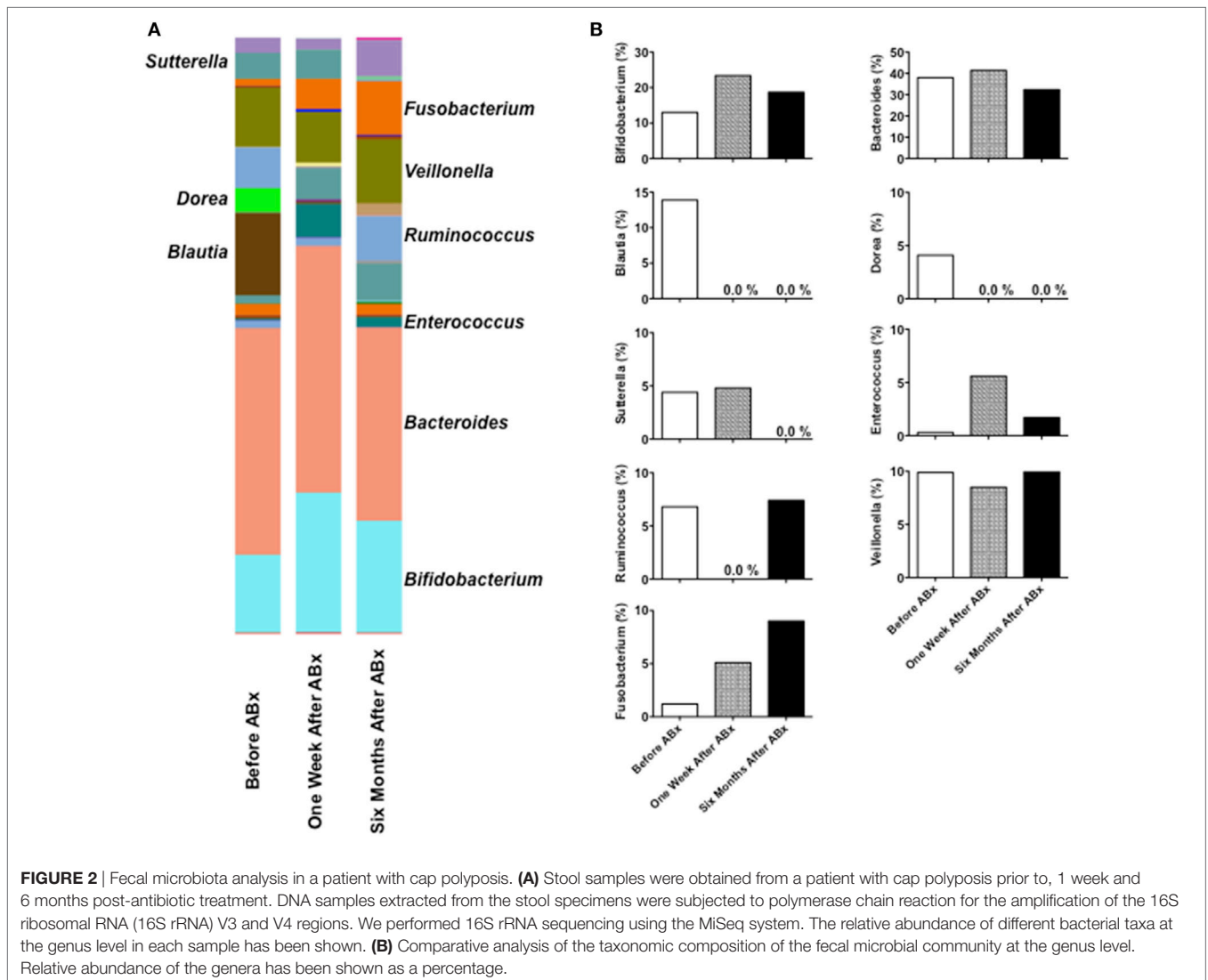
for sequence data processing, and operational taxonomic units (OTUs) were defined using the QIIME program (7, 8). The defined OTUs were subjected to population analysis to identify the bacterial phylum, class, order, family, and genus.

We detected 1,077 OTUs from 3 stool samples obtained pre- and post-antibiotic treatment. No major taxonomic alterations in the microbial communities were observed at the level of the phylum, order, or family (data not shown). Significant changes in the composition of fecal microbiota were noted at the genus level pre- and post-antibiotic treatment (**Figure 2A**). *Blautia* and *Dorea*, which showed a high relative abundance in the feces pre-antibiotic treatment, disappeared 1 week and 6 months post-antibiotic treatment (**Figure 2B**), and *Sutterella* disappeared 6 months post-antibiotic treatment. By contrast, the relative abundance of *Fusobacterium* was observed to have increased post-antibiotic treatment. The relative abundance of *Bifidobacterium*, *Bacteroides*, or *Veillonella* remained largely unchanged pre- and post-antibiotic treatment. This microbiota analysis suggests that regression of cap polyposis following antibiotic treatment

is accompanied by a marked decrease in *Blautia*, *Dorea*, and *Sutterella* and a marked increase in *Fusobacterium*, indicating that cap polyposis might have originated from dysbiosis in this patient.

DISCUSSION

Recent progress in NGS technology has highlighted the role of an altered intestinal microbiome (dysbiosis) in human diseases (9). Inflammatory bowel disease (IBD) is a prototypical dysbiosis-related disorder mediated by abnormal immune responses to altered intestinal microbiota (9). In this study, we report a patient with cap polyposis in whom antibiotic treatment resulted in regression of multiple inflammatory polyps. Interestingly, regression of cap polyposis was associated with significant alterations in the composition of the intestinal microbiota. Thus, we propose that cap polyposis might be a dysbiosis-related intestinal disorder. It should be noted, however, that we cannot exclude two other possibilities in the regression of cap polyposis. First, spontaneous regression might have occurred in antibiotic



treatment-independent manner as previously reported (3). Second, anti-inflammatory responses leading to the regression of cap polyposis might be induced by antibiotic treatment.

Mucosal prolapse syndrome and cap polyposis share endoscopic findings in that reddish elevated mucus-covered lesions are common to both conditions (4). Histopathologically, both disorders are characterized by findings of superficial erosions covered by inflammatory granulation tissue, distorted and elongated glands, and fibromuscular obliteration of the lamina propria—all these being typical findings observed in our patient. These clinical and histopathological similarities lead us to the conclusion that MPS and cap polyposis share common pathogenetic mechanisms—mucosal prolapse secondary to impaired colonic motility noted in MPS has been considered a possible etiological factor in cap polyposis. However, MPS and cap polyposis differ in terms of treatment because suppression of a chronic inflammatory response using steroid or infliximab is often effective only in the latter (2, 3). Moreover, antibiotic-induced eradication of *H. pylori* or as yet unidentified bacteria can lead to regression of cap polyposis (5, 6). These reports strongly indicate the role of chronic immune reactions toward intestinal microflora in the pathogenesis of cap polyposis. Therefore, cap polyposis might be caused by impaired host-bacterial mutualism. We have demonstrated that antibiotic treatment leads to regression of cap polyposis through significant alterations in fecal microbiota composition. Our results strongly support the idea that impaired host-bacterial mutualism caused by dysbiosis underlies the pathogenesis of cap polyposis. Further studies are warranted to assess the intestinal microbiota composition in a larger number of samples with cap polyposis to validate our results.

Significant changes in fecal microbiota composition were observed at the genus levels pre- and post-antibiotic treatment. The relative abundance of *Blautia*, *Dorea*, and *Sutterella* was markedly decreased 6 months post-antibiotic treatment compared to the pre-antibiotic treatment finding, whereas the relative abundance of *Fusobacterium* was markedly increased post-antibiotic treatment. Thus, disappearance of *Blautia*, *Dorea*, and *Sutterella* and colonization of *Fusobacterium* were observed to be associated with regression of cap polyposis. Therefore, *Blautia*, *Dorea*, and *Sutterella*, and *Fusobacterium* might be considered pathogenic and beneficial bacteria, respectively, for cap polyposis. Consistent with these results, Nishino et al. have shown that mucosal microbiota composition in those with ulcerative colitis is characterized by a greater abundance of *Blautia* (10). An increased abundance of *Dorea* has been detected in the normal colonic mucosa in patients with colorectal adenomas (11). However, an increased percentage of *Blautia* and *Dorea* observed in the gut mucosal

microbiota composition is reportedly associated with remission after surgery in IBD patients (12, 13). Mukhopadhyaya et al. have reported that *Sutterella* is unlikely to play a role in the pathogenesis of IBD (14). Moreover, *Fusobacterium*, which demonstrated higher relative abundance post-antibiotic treatment in this patient, has been shown to promote colorectal tumor growth (15). Although the discrepancy between our data and previous reports remains unexplained, it could be attributed to a likely difference between fecal and mucosal microbiota composition. Identification of pathogenic or beneficial bacteria for cap polyposis requires future studies that assess microbiota composition in a larger number of patients with cap polyposis. Fecal microbiota analyses in a large number of patients with cap polyposis are necessary to confirm the involvement of dysbiosis and to determine the sensitivity to antibiotic treatment in this disorder.

CONCLUDING REMARKS

To our knowledge, this is the first report describing intestinal microbiota analysis in a patient with cap polyposis. Our results strongly suggest that cap polyposis may originate from dysbiosis and that microbiome-targeted therapy may be useful in this disorder.

ETHICS STATEMENT

This study was carried out in accordance with the recommendations of a Review Board of the Kindai University Faculty of Medicine with written informed consent from the patient. The patient gave written informed consent in accordance with the Declaration of Helsinki. The protocol was approved by a Review Board of the Kindai University Faculty of Medicine.

AUTHOR CONTRIBUTIONS

KO, TW, YK, AO, HS, and KF took care of the patient. KO, TW, KM, KK, KY, MT, SH, and TS wrote the manuscript. TT performed pathological examinations. KO, TW, and NN performed experiments. MK supervised the research. All the coauthors checked the final version of the manuscript before the submission.

FUNDING

This work was supported by the Naito Foundation, SENSHIN Medical Research Foundation, the Yakult Bio-Science Foundation, the Smoking Research Foundation, the Kobayashi Foundation for Cancer Research, and the Takeda Science Foundation.

REFERENCES

- Kini GP, Murray I, Champion-Young J, Lau M, Katta V, Thorn M, et al. Cap polyposis mistaken for Crohn's disease: case report and review of literature. *J Crohns Colitis* (2013) 7(3):e108–11. doi:10.1016/j.crohns.2012.06.005
- Bookman ID, Redston MS, Greenberg GR. Successful treatment of cap polyposis with infliximab. *Gastroenterology* (2004) 126(7):1868–71. doi:10.1053/j.gastro.2004.03.007
- Chang HS, Yang SK, Kim MJ, Ye BD, Byeon JS, Myung SJ, et al. Long-term outcome of cap polyposis, with special reference to the effects of steroid therapy. *Gastrointest Endosc* (2012) 75(1):211–6. doi:10.1016/j.gie.2011.08.027
- Oriuchi T, Kinouchi Y, Kimura M, Hiwatashi N, Hayakawa T, Watanabe H, et al. Successful treatment of cap polyposis by avoidance of intraluminal trauma: clues to pathogenesis. *Am J Gastroenterol* (2000) 95(8):2095–8. doi:10.1111/j.1572-0241.2000.02277.x

5. Akamatsu T, Nakamura N, Kawamura Y, Shinji A, Tateiwa N, Ochi Y, et al. Possible relationship between *Helicobacter pylori* infection and cap polyposis of the colon. *Helicobacter* (2004) 9(6):651–6. doi:10.1111/j.1083-4389.2004.00273.x
6. Oiya H, Okawa K, Aoki T, Nebiki H, Inoue T. Cap polyposis cured by *Helicobacter pylori* eradication therapy. *J Gastroenterol* (2002) 37(6):463–6. doi:10.1007/s005350200067
7. Caporaso JG, Kuczynski J, Stombaugh J, Bittinger K, Bushman FD, Costello EK, et al. QIIME allows analysis of high-throughput community sequencing data. *Nat Methods* (2010) 7(5):335–6. doi:10.1038/nmeth.f.303
8. Nishiyama H, Nagai T, Kudo M, Okazaki Y, Azuma Y, Watanabe T, et al. Supplementation of pancreatic digestive enzymes alters the composition of intestinal microbiota in mice. *Biochem Biophys Res Commun* (2018) 495(1):273–9. doi:10.1016/j.bbrc.2017.10.130
9. Levy M, Kolodziejczyk AA, Thaiss CA, Elinav E. Dysbiosis and the immune system. *Nat Rev Immunol* (2017) 17(4):219–32. doi:10.1038/nri.2017.7
10. Nishino K, Nishida A, Inoue R, Kawada Y, Ohno M, Sakai S, et al. Analysis of endoscopic brush samples identified mucosa-associated dysbiosis in inflammatory bowel disease. *J Gastroenterol* (2017) 53(1). doi:10.1007/s00535-017-1384-4
11. Shen XJ, Rawls JF, Randall T, Burcal L, Mpande CN, Jenkins N, et al. Molecular characterization of mucosal adherent bacteria and associations with colorectal adenomas. *Gut Microbes* (2010) 1(3):138–47. doi:10.4161/gmic.1.3.12360
12. Mondot S, Lepage P, Seksik P, Allez M, Treton X, Bouhnik Y, et al. Structural robustness of the gut mucosal microbiota is associated with Crohn's disease remission after surgery. *Gut* (2016) 65(6):954–62. doi:10.1136/gutjnl-2015-309184
13. Tyler AD, Knox N, Kabakchiev B, Milgrom R, Kirsch R, Cohen Z, et al. Characterization of the gut-associated microbiome in inflammatory pouch complications following ileal pouch-anal anastomosis. *PLoS One* (2013) 8(9):e66934. doi:10.1371/journal.pone.0066934
14. Mukhopadhyay I, Hansen R, Nicholl CE, Alhaidan YA, Thomson JM, Berry SH, et al. A comprehensive evaluation of colonic mucosal isolates of *Sutterella wadsworthensis* from inflammatory bowel disease. *PLoS One* (2011) 6(10):e27076. doi:10.1371/journal.pone.0027076
15. Mima K, Nishihara R, Qian ZR, Cao Y, Sukawa Y, Nowak JA, et al. *Fusobacterium nucleatum* in colorectal carcinoma tissue and patient prognosis. *Gut* (2016) 65(12):1973–80. doi:10.1136/gutjnl-2015-310101

Conflict of Interest Statement: The authors declare that the research was conducted in the absence of any commercial or financial relationships that could be construed as a potential conflict of interest.

The reviewer MM and handling Editor declared their shared affiliation.

Copyright © 2018 Okamoto, Watanabe, Komeda, Okamoto, Minaga, Kamata, Yamao, Takenaka, Hagiwara, Sakurai, Tanaka, Sakamoto, Fujimoto, Nishida and Kudo. This is an open-access article distributed under the terms of the Creative Commons Attribution License (CC BY). The use, distribution or reproduction in other forums is permitted, provided the original author(s) and the copyright owner are credited and that the original publication in this journal is cited, in accordance with accepted academic practice. No use, distribution or reproduction is permitted which does not comply with these terms.

Review Article

Immune checkpoint blockade for the treatment of human hepatocellular carcinoma

Naoshi Nishida and Masatoshi Kudo

Department of Gastroenterology and Hepatology, Kindai University Faculty of Medicine, Osaka-Sayama, Japan

Hepatocellular carcinoma (HCC) is one of the most common cancers with a high recurrence rate. Currently, tyrosine kinase inhibitors (TKIs) are the first-line treatment for cases refractory to conventional therapies. However, the acquisition of somatic mutations can result in TKI resistance. Clinical evidence suggests that acquired immunity contributes to the suppression of tumor recurrence, indicating the potential of induced antitumor immune reaction for the treatment of HCC. Recently, immune checkpoint inhibitors have become available for the treatment of malignancies. They are effective regardless of the response to prior therapies and a durable effect can be expected, which should be attributed to an adaptive immunity to HCC components. The results of phase I/II trials of nivolumab, an anti-programmed cell death-1 antibody, showed that 20% of patients showed objective response and that nivolumab was effective regardless of prior sorafenib treatment and viral status. Nivolumab received expedited Food

and Drug Administration approval in 2017 for the treatment of advanced HCC after failure or intolerance to sorafenib. However, the majority of the patients remain refractory, likely due to the solid immune suppressive status, which involves many stromal cells, humoral mediators, and suppressive checkpoint molecules. Therefore, current clinical trials are focusing on how immunosuppressive conditions in HCC might be overcome using immune checkpoint inhibitors in combination with different types of immune checkpoint blockades, TKIs, and other conventional treatments. The development of immune checkpoint inhibitors is rapidly progressing and these inhibitors are likely to be key agents for HCC treatment in the near future.

Key words: hepatocellular carcinoma, immunity, immune checkpoint inhibitor, molecular targeted agents, programmed cell death 1, tyrosine kinase inhibitor

INTRODUCTION

HEPATOCELLULAR CARCINOMA (HCC) is the sixth most common cancer and the third most frequent cause of cancer-related death worldwide. For patients with advanced stages of HCC, including those who have progressed following locoregional therapies, sorafenib is recommended as a first-line treatment;¹ however, several novel tyrosine kinase inhibitors (TKIs) are also recently available.^{2,3} For example, regorafenib has been approved for use in patients refractory to sorafenib.⁴ Lenvatinib, which targets receptor-type tyrosine kinases including fibroblast growth factor receptors (FGFRs), has also been

shown to be effective in phase III frontline HCC trials.^{5–7} Targeting the hepatocyte growth factor/c-met pathway could also be promising based on a phase II trial of cabozantinib.⁸ However, the acquisition of somatic mutations could result in resistance to TKIs.⁹

Compared to TKIs, immunotherapy has several advantages for the treatment of HCC, as its effects are not hampered by common mutations or mutational heterogeneity of tumors. Therefore, this type of agent is effective regardless of the response to prior therapies. In addition, a durable response can be expected due to adaptive immunity to the cancer cell components.¹⁰ However, the profile of adverse events (AEs) is completely different from those of other cytotoxic and molecular targeting agents. The tolerability of this class of agents greatly depends on the severity of immune-related AEs (irAEs), although the majority of AEs are mild. Immune checkpoint inhibitors are an essential agent for immunotherapy; thus, we discuss the role of the immune checkpoint blockade in the treatment of HCC, including their combinations with other treatment methods.^{10–12}

Correspondence: Dr Naoshi Nishida, Department of Gastroenterology and Hepatology, Kindai University Faculty of Medicine, 377-2 Ohno-Higashi, Osaka-Sayama 589-8511, Japan. Email: naoshi@med.kindai.ac.jp

Conflict of interest: The authors have no conflict of interest.

Financial support: This work was supported in part by a Grant-in-Aid for Scientific Research (KAKENHI: 16 K09382) from the Japanese Society for the Promotion of Science (N. Nishida) and a grant from the Smoking Research Foundation (N. Nishida).

Received 22 February 2018; revision 30 April 2018; accepted 1 May 2018.

IMPACT OF ANTITUMOR IMMUNITY ON PROGNOSIS OF HCC PATIENTS

SEVERAL REPORTS HAVE shown an association between the infiltration of CD8⁺ T cells in HCC tissue and patient survival.^{13,14} This evidence suggests that CD8⁺ lymphocytes that react to HCC components have antitumor activity. Another report showed that the expression of type 1 helper T (Th1) cytokines was associated with a good prognosis in HCC patients, whereas a predominance of type 2 helper T (Th2) cytokines was a predictor of future recurrence.¹⁵ Collectively, the effective induction of cell-mediated immunity may be critical for an antitumor immune response.

However, a subset of poorly differentiated HCC with significant lymphoid stroma, the so-called lymphoepithelioma-like histological subtype, may present aggressive tumor characteristics.¹⁶ This type of HCC frequently expresses inhibitory checkpoint molecules such as programmed cell death-ligand 1 (PD-L1) on the surface of tumor cells.¹⁷ CD8⁺ cells in HCC tissues cannot effectively produce γ -interferon (IFN- γ), although tumor-specific CD8⁺ cells in the peripheral blood are still able to respond for IFN- γ production.¹⁸ Therefore, T cells that have infiltrated HCC tissues might represent an “exhausted” phenotype that may lead to tumor progression.

The stimulation of IFN- γ can induce PD-L1 expression, and chronic inflammation of the liver might be a source of inflammatory cytokines.^{10,19} A previous study suggested that ectopic lymphoid structure in the background liver of HCC could act as a niche for tumor progenitor cells.²⁰ Taken together, these observations suggest that a considerable number of HCC cases may show T-cell exhaustion during the development of HCC, which could be attributed to an inflamed liver. Indeed, the expression of several inhibitory checkpoint molecules has been reported in HCCs, the majority of which show a negative impact on survival. According to our current understanding, although anti-programmed cell death-1 (PD-1) antibody is a promising agent for the treatment of HCC, the effect of this type of agent remains limited because of the solid immune suppressive microenvironment in tumor cells. Therefore, a number of studies are now focusing on how the immunosuppressive condition could be reversed through interventions affecting HCC immunity.^{10,21}

MALFUNCTION OF IMMUNE SURVEILLANCE TOWARD CANCER-SPECIFIC ANTIGENS

HEPATOCELLULAR CARCINOMA DEVELOPS as a result of chronic liver diseases that cause liver cell

damage and regeneration. This background involves the sustained activation of the immune system by virus antigens as well as tissue debris that contain damage-associated molecular patterns.²² In contrast, chronic inflammation results in the development of HCC through the induction of many genetic/epigenetic alterations.^{23,24} Transformed hepatocytes may emerge and thrive in inflamed liver tissues that could act as microniches for HCC cells.²⁰ Among genetic alterations, passenger mutations, which are generally non-synonymous but not considered to play a major role in carcinogenesis, could be a source of neoantigens unique to HCC cells. Oncofetal and cancer/testis antigens, termed tumor-associated antigens (TAAs), are also produced in cancer. After uptake of antigens by dendritic cells (DCs) and their migration to the regional lymph nodes, processed antigens are presented to CD4⁺ T cells, which enhances the development and expansion of CD8⁺ T cells that exert antitumor immunity (Fig. 1). However, although neoantigens and TAAs should be targets of the immune response to HCC cells, several mechanisms could disturb the immune surveillance. First, the presentation of TAAs and neoantigens might be insufficient because of a failure to process them into antigenic peptides.²⁵ Second, the continuous production of cytokines and chemokines in the inflamed liver could induce the production of inhibitory checkpoint molecules. Finally, the development of HCC is accompanied by the further induction of immunosuppressive cells and soluble factors that enforce the insufficient immune reaction to HCC cells.^{10,22}

IMMUNOSUPPRESSIVE COMPONENTS IN HCC TISSUES

AN IMMUNOSUPPRESSIVE MILIEU in HCC develops due to interactions among cellular components, humoral mediators, and immune checkpoint molecules (Fig. 2). Their cross-talk becomes more complex during tumor progression.

Cellular components

Suppressive stromal cells, including myeloid-derived suppressor cells (MDSCs), tumor-associated macrophages (TAMs), regulatory T cells (Tregs), type 2 helper T (Th2) cells, and cancer-associated fibroblasts (CAFs), may participate in the development of the immune escape of HCC cells.^{10,21}

Myeloid-derived suppressor cells are heterogeneous cell populations from the myeloid lineage in cancer tissues and infiltration in tumors is associated with HCC progression.²⁶ Although the detailed mechanism of their immune

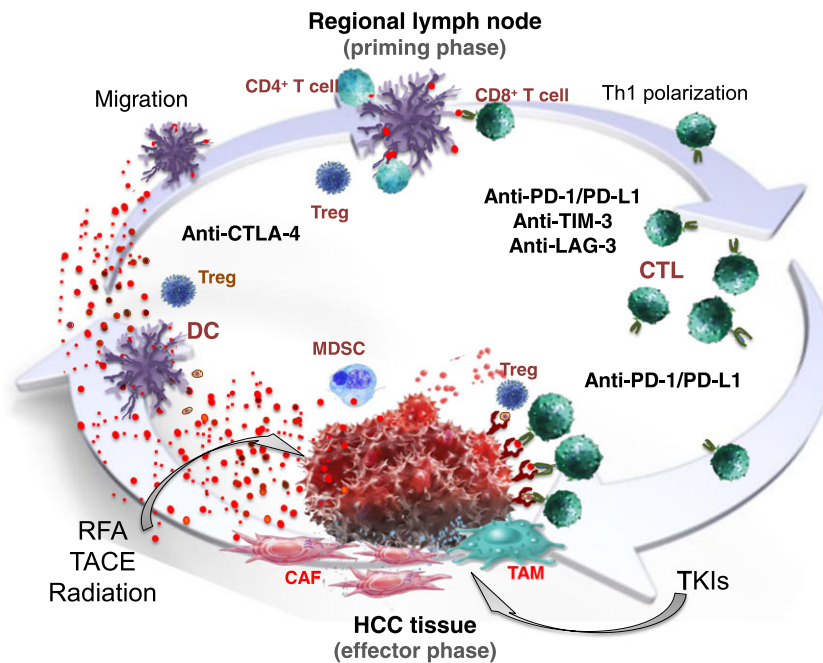


Figure 1 Immune recognitions and escape of hepatocellular carcinoma (HCC) cells, and action of immune checkpoint blockade. HCC cells release several neoantigens that are mainly derived from passenger mutations; dendritic cells (DCs) uptake these antigens unique to cancer cells. Subsequently, the DCs migrate to regional lymph nodes and present the processed antigen to CD4⁺ T cells (priming phase). After the type 1 helper T (Th1) polarization of CD4⁺ and cross-presentation of the antigenic peptide to CD8⁺ T cells, activation of CD8⁺ to cytotoxic T cells (CTLs) and its proliferation take place. CTLs are transported to HCC tissues and exert cytotoxic activity (effector phase). The circular arrow represents the progression of cell-mediated antitumor immunity to HCC. Red dots show neoantigens from HCC cells. Anti-CTL antigen-4 (CTLA-4) antibody should act mainly in the priming phase of immune response, and restore the CD4⁺ T cell function. Anti-programmed cell death-1 (PD-1)/programmed cell death-ligand 1 (PD-L1) antibody induce the immune response of effector T cells in the lymph node and peripheral tumor tissues. Several combination therapies using immune checkpoint inhibitors are in trial. Among them, CTLA-4 and PD-1/PD-L1 blockade is the most relevant combination that affect both in the priming phase and effector phase; several other combinations are also under investigation. Tyrosine kinase inhibitors (TKIs) could interfere with the cellular signaling in HCC and stromal cells that affect the production of immune suppressive cytokines/chemokines, and humoral factors, which result in the improvement of the immune suppressive condition. Conventional procedures, such as radiofrequency ablation (RFA), transarterial chemoembolization (TACE), and radiation should increase the release of neoantigens and facilitate the antigen uptake by DCs (shown by twisted arrows). The trials pairing immune checkpoint blockade and TKIs as well as RFA, TACE, and radiation are also ongoing. CAF, cancer-associated fibroblast; LAG-3, lymphocyte activation gene-3; MDSC, myeloid-derived suppressor cell; TIM-3, T-cell immunoglobulin and mucin containing protein-3; Treg, regulatory T cell. [Color figure can be viewed at wileyonlinelibrary.com]

regulation is unclear, several mechanisms have been proposed, such as arginine depletion due to their arginase activity.²⁷ Myeloid-derived suppressor cells also produce transforming growth factor (TGF)- β and interleukin (IL)-10 that lead to the induction of Tregs and suppression of natural killer (NK) cell functions.²⁸ The induction of IL-10 from MDSCs causes the M2 polarization of macrophages in tumors, so-called TAMs, and downregulates the production of IL-12 in TAMs. High IL-10 and low IL-12 levels further stimulate the differentiation of CD4⁺ T cells into Th2 and the induction of M2 macrophages. In addition, high IL-10 expression leads to the downregulation

of human leukocyte antigen class II on macrophages.²⁹ Transforming growth factor- β from MDSCs induces the expression of T-cell immunoglobulin and mucin-containing protein-3 (TIM-3) on TAMs, which is associated with galectin-9 and further facilitates M2 polarization.³⁰

Regulatory T cells are CD4⁺ T cells characterized by membranous expression of CD25, CD62L, and cytotoxic T-lymphocyte antigen-4 (CTLA-4) with nuclear transcription factor and forkhead box protein 3. Levels of Tregs are increased in HCC tissues and peripheral blood; the degree of Treg increase is associated with worse overall survival (OS) in HCC patients.³¹ Induction of Tregs through

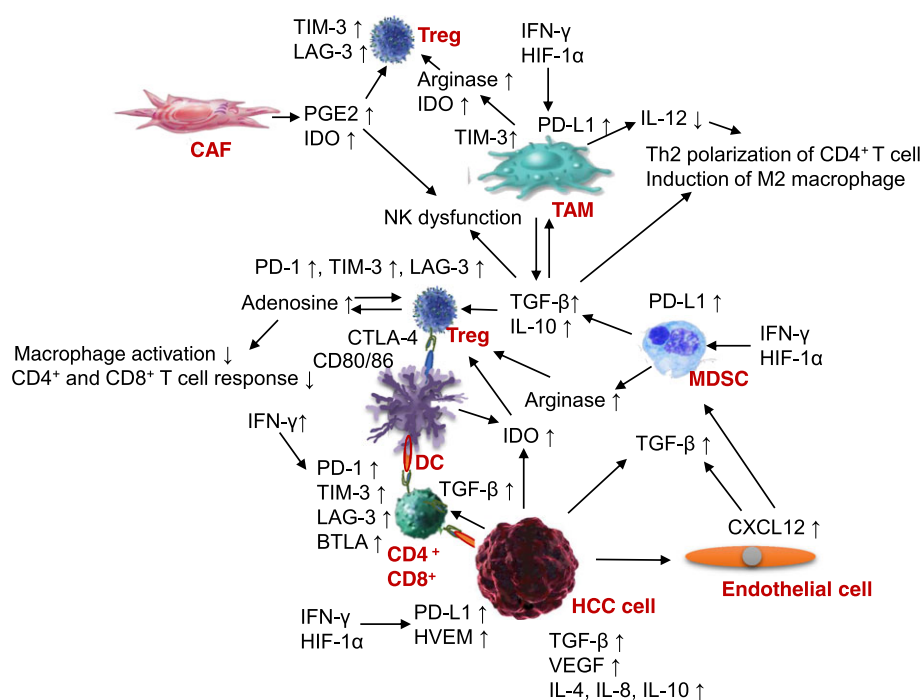


Figure 2 Involvement of cellular and humoral components for establishment of immunosuppressive microenvironment of hepatocellular carcinoma (HCC). Mutual interactions between cellular components and humoral mediators, and expression of the immune checkpoint molecules are shown. BTLA, B and T lymphocyte attenuator; CAF, cancer-associated fibroblast; CTLA-4, cytotoxic T-lymphocyte antigen 4; CXCL12, C-X-C motif chemokine ligand 12; DC, dendritic cell; HIF-1 α , hypoxia inducible factor-1 α ; HVEM, herpes virus entry mediator; IDO, indoleamine 2,3-dioxygenase; IFN- γ , interferon- γ ; IL, interleukin; LAG-3, lymphocyte activation gene-3; MDSC, myeloid-derived suppressor cell; NK, natural killer; PD-1, programmed cell death-1; PD-L1, programmed cell death-ligand 1; PGE2, prostaglandin E2; TAM, tumor-associated macrophage; TGF- β , transforming growth factor- β ; TIM-3, T-cell immunoglobulin and mucin-containing protein-3; Th2, type 2 helper T; Treg, regulatory T cell; VEGF, vascular endothelial growth factor. [Color figure can be viewed at wileyonlinelibrary.com]

the interaction of CTLA-4 with CD80/86 on antigen-presenting cells is one of the suppressive mechanisms for antitumor immunity. Regulatory T cells are further activated through the T cell receptor engagement with antigenic peptide concurrent with TGF- β and IL-10 signaling.³²

Cancer-associated fibroblasts, hepatic stellate cells, and endothelial cells also participate in the formation of the immunosuppressive microenvironment. For example, HCC-associated CAF triggers NK cell dysfunction through the release of prostaglandin E2 and indoleamine 2,3-dioxygenase (IDO) that is a rate-limiting enzyme critical for tryptophan metabolism.³³ Hepatic stellate cells may be activated by the amphiregulin endothelial growth factor ligand from HCC, and might also play a role in the further induction of Tregs.³⁴ Hepatic stellate cells and endothelial cells produce the C-X-C motif chemokine ligand 12 and stimulate the chemoattraction of myeloid cells into HCC.³⁵ Activation of endothelial cells fosters TGF- β -mediated Treg induction.

Humoral mediators

Hepatocellular carcinoma and immune cells in tumor tissue produce a number of soluble factors, which mediate the immune suppressive function of cellular components (Fig. 2).

An increase in IDO results in the suppression of T cell activation and proliferation, and it also induces naïve CD4⁺ T cells to Tregs through tryptophan depletion.³⁶ Several pro-inflammatory cytokines upregulate IDO in DCs, macrophages, CAFs, endothelial cells, and HCC cells.^{33,37–39} Arginase-1, which is involved in the ornithine cycle, is mainly released from MDSCs and TAMs, and also mediates immune suppression through the depletion of L-arginine.²⁷ Adenosine also acts as an immune regulator; signal from adenosine receptor A2a inhibits macrophage activation, CD4⁺ and CD8⁺ T cell response, and induces Tregs.⁴⁰ The galectin protein family binds to β -galactoside sugars on the cell membrane and modulates tumor immunity. Galectin-9 is a ligand of TIM-3; it induces Treg

stimulation and T-cell exhaustion. Galectin-3 interacts with lymphocyte activation gene-3 (LAG-3) and inhibits CD8⁺ T cell and NK cell function; its expression is also associated with a poor prognosis in HCC patients.⁴¹ In addition, growth factors, including TGF- β and vascular endothelial growth factor (VEGF), as well as Th2 cytokines IL-4, IL-8, and IL-10, are also involved in the immune suppression of HCC tissues.^{15,42,43} Because these immune modulators may play a role for refractoriness to immune therapies, some preclinical/early clinical trials that target humoral mediators with immune checkpoint inhibitors have been carried out and are described later.

Immune checkpoint molecules

Immune checkpoint molecules are involved in inhibitory pathways hardwired into the immune system. This type of molecule regulates the T cell reactions to prevent excessive collateral tissue damage. Several inhibitory checkpoint molecules, such as CTLA-4, PD-1, TIM-3, LAG-3, and B and T lymphocyte attenuator (BTLA), play a role in carcinogenesis, including HCC.^{30,44,45}

CTLA-4 is a protein receptor that negatively regulates T cell response by competing with CD28 for the binding of CD80 or CD86 on the surface of antigen-presenting cells. It is expressed on activated T cells as well as Tregs and plays a critical role in the regulation of CD4⁺ T cells in the primary phase of immune response. Compared to CTLA-4, PD-1 is expressed on a variety of immune cells including activated T cells and B cells as well as NK cells, Tregs, MDSCs, and DCs.^{46,47} It also promotes self-tolerance by suppressing T cell activity. The signal from PD-1 could facilitate apoptosis in CD8⁺ and CD4⁺ T cells but could inhibit apoptosis in Tregs. Two kinds of ligands, PD-L1 and PD-L2, have been reported, with the expression of PD-L1 observed in hematopoietic, endothelial, and epithelial cells and PD-L2 exclusively detected in hematopoietic cells. Because the interaction of PD-1 with PD-L1 is critical for the regulation of excessive T cell response in the peripheral tissue, the expression of PD-L1 in cancer cells could result in antitumor immunity evasion. In HCC, the expression of PD-L1 but not PD-L2 in tumors is associated with aggressive tumor behavior, although this observation is controversial.⁴⁸ IFN- γ from antigen-specific T cells induces both PD-1 on T cells and PD-L1 on antigen-presenting and tumor cells.^{19,46} Hypoxia-inducible factor 1 α also induces PD-L1 expression in cancer cells as well as MDSCs and TAMs.⁴⁹

TIM-3 is expressed by a variety of immune cells, such as CD4⁺ and CD8⁺ tumor-infiltrating lymphocytes (TILs), and acts as a receptor for several ligands including

galectin-9; the TIM-3/galectin-9 signaling pathway reportedly mediates T-cell senescence in hepatitis B virus (HBV)-associated HCC.⁵⁰ Clinically, the degree of TIM-3 expressing TILs, TAMs, and monocytes in the peripheral blood are negatively associated with patient survival of HCC.⁵⁰ TGF- β induces TIM-3 expression and mediates the alternative activation of TAMs.³⁰ Expression of LAG-3 on TILs, along with PD-L1 on tumor cells, is also reported in HCC tissues.⁴⁵ Another report also showed up-regulated LAG-3 expression and functional defects in CD8⁺ TILs in HBV-positive HCC patients.⁵¹ Taken together, TIM-3, LAG-3, and PD-1 act synergistically and facilitate the immune evasion that portends a worse prognosis.⁴⁵ B and T lymphocyte attenuator is another co-inhibitory molecule expressed on activated lymphocytes, and its ligand, herpes virus entry mediator (HVEM), is expressed in HCC cells. Hepatocellular carcinoma with HVEM expression is also characterized by aggressive tumor characteristics that lead to poorer survival.⁵²

CURRENT PROGRESS OF IMMUNE CHECKPOINT INHIBITORS IN HCC TREATMENT

CURRENTLY, CLINICAL TRIALS of anti-PD-1 and anti-PD-L1 antibodies for HCC cases, individually or in combination with an anti-CTLA-4 antibody, are ongoing.²¹ Several other trials have also been registered in the clinical trial database.

Monotherapy of immune checkpoint inhibitors

Thus far, two kinds of anti-PD-1 (nivolumab and pembrolizumab) and anti-PD-L1 (durvalumab and avelumab) antibodies have been applied for clinical trials in HCC and nivolumab, pembrolizumab, and avelumab are in development as monotherapy (Table 1).

Nivolumab is a fully human immunoglobulin G4 (IgG4)-type, monoclonal inhibitory antibody for PD-1. In phase I/II trials, 262 patients with advanced HCC were treated with nivolumab every 2 weeks.⁵³ Objective response (OR) was observed in 20% of cases and the disease control rate (DCR) was 64%. In addition, the OR did not differ between the sorafenib progressor and sorafenib untreated or intolerant groups, indicating that nivolumab could be effective, even in cases refractory to TKIs.⁵³ The ORs were similar regardless of viral status, although that of HBV-positive cases was lower (14%) compared to non-HBV cases (20–23%). There was no significant association between PD-L1 expression in HCC and the response to nivolumab. However, the OR tended to be higher in PD-L1-positive HCC cases, with

Table 1 Clinical trials of immune checkpoint monotherapy

Clinical trial number	Title	Agent	Design	Start date
NCT03062358	Study of pembrolizumab (MK-3475) or placebo given with best supportive care in Asian participants with previously treated advanced hepatocellular carcinoma (MK-3475-394/KEYNOTE-394)	PD-1 Ab vs. BSC	Phase III	Apr. 2017
NCT02702401	Study of pembrolizumab (MK-3475) vs. best supportive care in participants with previously systemically treated advanced hepatocellular carcinoma (MK-3475-240/KEYNOTE-240)	PD-1 Ab vs. BSC	Phase III	May 2016
NCT02576509	An investigational immuno-therapy study of nivolumab compared to sorafenib as a first treatment in patients with advanced hepatocellular carcinoma (CheckMate 459)	PD-1 Ab vs. sorafenib	Phase III	Nov. 2015
NCT03163992	Pembrolizumab in advanced hepatocellular carcinoma as second-line treatment after failure of sorafenib	PD-1 Ab	Phase II	Dec. 2017
NCT02940496	Pembrolizumab (MK-3475) in hepatocellular carcinoma	PD-1 Ab	Phase I/II	Dec. 2016
NCT02658019	Pembrolizumab (Keytruda) in advanced hepatocellular carcinoma	PD-1 Ab	Phase II	May 2016
NCT02702414	Study of pembrolizumab (MK-3475) as monotherapy in adults with previously systemically treated advanced hepatocellular carcinoma (MK-3475-224/KEYNOTE-224)	PD-1 Ab	Phase II	May 2016
NCT02828124	A study of the safety and tolerability of BMS-986183 in patients with liver cancer	PD-1 Ab	Phase I/II	Aug. 2016
NCT03389126	Phase II study of avelumab in patients with advanced hepatocellular carcinoma after prior sorafenib treatment	PD-L1 Ab	Phase II	Dec. 2017
NCT01008358	Anti-CTLA-4 human monoclonal antibody CP-675206 in patients with advanced hepatocellular carcinoma	CTLA-4 Ab	Phase II	Dec. 2008
NCT03337841	Pembrolizumab as neoadjuvant treatment in HCC	PD-1 Ab (neoadjuvant)	Phase II	Nov. 2017
NCT03383458	A study of nivolumab in patients with hepatocellular carcinoma who are at high risk of recurrence after curative hepatic resection or ablation	PD-1 Ab vs. placebo (adjuvant)	Phase III	Dec. 2017

Clinical trial information was examined in the public database <http://clinicaltrials.gov>, (accessed January 11, 2018).

Ab, antibody; BSC, best supportive care; CTLA-4, cytotoxic T lymphocyte-associated antigen 4; PD-1, program cell death receptor-1; PD-L1, programmed cell death receptor-1 ligand.

OR frequencies of 27% and 12% among PD-L1-positive and -negative cases in the dose escalation cohort and 26% and 19% in the dose expansion cohort, respectively.⁵³ Importantly, however, a flare of hepatitis B and seroconversion of hepatitis B surface antigen was not observed under treatment with antiviral agents, a transient decrease in hepatitis C virus (HCV) viremia was detected

in some cases, suggesting the potential for a non-severe antiviral immune response. A randomized phase III clinical trial is ongoing, aiming to compare the efficacy of nivolumab to that of sorafenib as a first-line treatment (NCT02576509; Table 1). Pembrolizumab is another humanized IgG4-type PD-1 antibody. Randomized phase III clinical trials in sorafenib-experienced patients are

ongoing to compare the effect of pembrolizumab with that of best supportive care (NCT03062358 and NCT02702401). Furthermore, a clinical trial of monotherapy agents targeting PD-L1, such as avelumab, has also been undertaken in patients with advanced HCC (NCT03389126).

Tremelimumab is an IgG2-type anti-CTLA-4 antibody that was evaluated in a phase II clinical trial including 21 patients with HCV-related HCC. In this trial, the partial response (PR) rate was 17.6% (3/17), the DCR was 76.4%, and the time to progression (TTP) was 6.48 months (NCT01008358).⁵⁴ Notably, a clinical benefit exceeding 12 months was observed in one-third of patients, indicating durable disease control in immune checkpoint therapy. In the CTLA-4 trial, a transient disappearance or decrease of HCV-RNA was also observed in the majority of patients.⁵⁴

Combined blockade of immune checkpoint molecules

Although the efficacy of immune checkpoint inhibitors in HCC is promising, a considerable percentage of HCC patients could not attain satisfactory tumor control in monotherapy. To enhance the antitumor activity, several combined immune checkpoint blockades studies are

ongoing (Table 2). The most relevant combination is a CTLA-4 and PD-1/PD-L1 blockade, in which CTLA-4 acts on naïve T-cells in the priming phase and PD-1/PD-L1 also suppresses the immune response of effector T cells in peripheral tumor tissues (Fig. 1). Preclinical data indicate that the dual blockade is synergistic, with higher rates of antitumor response than that of monotherapy in many kinds of solid tumors.⁵⁵

Durvalumab is a human monoclonal IgG1 κ antibody to PD-L1 that is currently being evaluated in combination with an anti-CTLA-4 antibody (tremelimumab) for sorafenib-experienced HCC patients in a phase II trial (NCT02519348). A randomized phase III trial is also ongoing to assess the efficacy and safety of a durvalumab plus tremelimumab combination and durvalumab monotherapy versus sorafenib as a first-line treatment (NCT03298451). The efficacy of another anti-CTLA-4 antibody, ipilimumab, is also being analyzed in combination with the anti-PD-1 antibody, nivolumab, for evaluation of the safety and OR as a phase I/II clinical trial (NCT01658878 and NCT03222076). However, a recent report indicated that TIM-3 and LAG-3, checkpoint proteins expressed on the effector T cell, could mediate resistance to the PD-1/PD-L1 blockade.^{30,45} Given the fact that there are multiple players in the establishment of

Table 2 Clinical trials of combined blockade of immune checkpoint molecules

Clinical trial number	Title	Agent	Design	Start date
NCT03298451	Study of durvalumab and tremelimumab as first-line treatment in patients with unresectable hepatocellular carcinoma	PD-L1 Ab \pm CTLA-4 Ab vs. sorafenib	Phase III	Oct. 2017
NCT02519348	A study of MEDI4736 with tremelimumab, MEDI4736 or tremelimumab monotherapy in unresectable hepatocellular carcinoma	PD-L1 Ab, CTLA-4 Ab, combination	Phase II	Oct. 2015
NCT03222076	Study evaluating nivolumab (anti-PD-1 antibody) alone versus nivolumab plus ipilimumab (anti-CTLA-4 antibody) in patients with resectable and potentially resectable hepatocellular carcinoma (HCC) (CA209–956)	PD-1 Ab vs. PD-1 Ab + CTLA-4 Ab	Phase II	Sep. 2017
NCT03099109	A study of LY3321367 alone or with LY3300054 in participants with advanced relapsed/refractory solid tumors	TIM-3 Ab \pm PD-L1 Ab	Phase I	Apr. 2017
NCT01968109	An investigational immuno-therapy study to assess the safety, tolerability and effectiveness of anti-LAG-3 with and without anti-PD-1 in the treatment of solid tumors	LAG-3 Ab \pm PD-1 Ab	Phase I/II	Oct. 2013

Ab, antibody; CTLA-4, cytotoxic T lymphocyte-associated antigen 4; LAG-3, lymphocyte activation gene-3; PD-1, program cell death receptor-1; PD-L1, programmed cell death receptor-1 ligand; TIM-3, T-cell immunoglobulin and mucin-containing protein-3.

immune tolerance in HCC, anti-PD-1/PD-L1 therapy is being paired with agents targeting TIM-3 (NCT03099109) and LAG-3 (NCT01968109).

Combination of immune checkpoint inhibitors with TKIs

Activation of oncogenic signaling through driver mutations in cancer could also play a role in the immunosuppressive milieu. In the case of melanoma, a gain-of-function BRAF mutation (BRAF^{V600}) recruits MDSCs and Tregs and suppresses CD8⁺ T and NK cells in addition to downregulating major histocompatibility complex class I through the induction of IL-6, IL-10, and VEGF.^{56,57} In mouse model, targeted inhibition of IL-6 could reportedly enhance the efficacy of anti-PD-L1 antibody, overcoming anti-PD-L1 resistance in HCC.⁵⁸ A combined blockade using extracellular signal-regulated kinase inhibition and anti-PD-L1 antibody should have a synergistic effect on tumor regression; thus, TKIs might enhance the effect of immune checkpoint inhibitors by altering the immune microenvironment of HCC.^{59,60}

Sorafenib and regorafenib are available in the clinical setting for the treatment of advanced HCC; lenvatinib and cabozantinib have also shown a survival benefit.^{4,7,8}

Given the fact that these agents could collectively block the signaling from various growth factors and affect immune effectors and the vasculature, the combination of TKIs and immune checkpoint inhibitors could reactivate the immune response to HCC.⁶⁰ Several early phase studies are currently underway to explore the safety and tolerability of TKIs such as sorafenib (NCT03211416, NCT01658878, and NCT02988440), lenvatinib (NCT03418922 and NCT03006926), cabozantinib (NCT03299946 and NCT01658878), axitinib (NCT03289533), capmatinib (NCT02795429), and FGFR4 inhibitor (NCT02325739) in combination with immune checkpoint inhibitors (Table 3).

Other combinations of immune checkpoint inhibitors

It is conceivable that conventional procedures such as radiofrequency ablation (RFA) and transarterial chemoembolization (TACE) could trigger effector T cell response through the release of TAAs and neoantigens from HCC cells. Therefore, these procedures could enhance the antitumor effects of immune checkpoint inhibitors.

The combination with RFA or TACE improved the antitumor effect of tremelimumab through the induction of CD8⁺ T cells in HCC tissues compared to those of

monotherapy; the PR, median TTP, and OS were 26.3%, 7.4 months, and 12.3 months in combination and 17.6%, 6.48 months, and 8.2 months in monotherapy, respectively.^{54,61} Because tremelimumab is more effective, even at lower doses, in combination with RFA or TACE than in tremelimumab monotherapy, the combination may be promising for the enhancement of the antitumor effects of immune checkpoint inhibitors.⁶¹ Several pilot studies are ongoing to assess their safety and efficacy in combination with locoregional therapies (NCT03033446, NCT03143270, NCT03099564, and NCT02821754; Table 4). In a murine HCC model, the combination of anti-PD-L1 antibody and radiation improved the inhibition of tumor growth and survival, in which radiation activated IFN- γ /transducers and activator of transcription signaling and induced the infiltration of CD8⁺ T cells in HCC tissues.⁶² Several studies are focusing on the combination of immune checkpoint inhibitors with radiation therapy.

In addition, because the activation of antitumor response by immune checkpoint blockade might suppress residual HCCs after curative treatment, clinical trials aimed at adjuvant and neoadjuvant applications of the anti-PD-1 antibody have also been carried out (NCT03337841 and NCT03383458; Table 1).

Combinations of immune checkpoint inhibitors with immunosuppressive humoral mediators are also under preclinical/early clinical trial in other types of cancers. The combination of IDO inhibitors and nivolumab boosts response rates among patients with bladder and cervical cancer.⁶³ A galectin inhibitor, in combination with pembrolizumab and ipilimumab, is also under trial (NCT02575404 for pembrolizumab and NCT02117362 for ipilimumab). Combination with arginase inhibitor and pembrolizumab (NCT02903914), and triple blockade using IDO1 inhibitor, arginase inhibitors, and pembrolizumab have been examined in advanced solid tumors (NCT03361228). These combinations might be applied in HCC cases.

Adverse events with immune checkpoint blockade in HCC cases

Because of the unique action of immune checkpoint inhibitors on the immune system, this type of agent could well generate irAEs that mainly involve the gut, skin, endocrine glands, liver, and lung but can potentially affect any tissue. Based on the previous clinical trials of nivolumab, the agent was well tolerated, with low frequencies of grade 3/4 potential irAEs, such as pemphigoid, adrenal insufficiency, diarrhea, and hepatitis.⁵³ Compared to treatment

Table 3 Clinical trials of combinations of immune checkpoint inhibitors with tyrosine kinase inhibitors

Clinical trial number	Title	Target	Design	Start date
NCT03347292	Regorafenib plus pembrolizumab in first line systemic treatment of HCC	PD-1 Ab + regorafenib	Phase I	May 2018
NCT03382886	Nivolumab and bevacizumab in patients with advanced and or metastatic hepatocellular carcinoma	PD-1 Ab + VEGF Ab	Phase I	Mar. 2018
NCT03418922	A study of lenvatinib plus nivolumab in participants with hepatocellular carcinoma	PD-1 Ab + lenvatinib	Phase I	Jan. 2018
NCT03006926	A trial of lenvatinib plus pembrolizumab in subjects with hepatocellular carcinoma	PD-1 Ab + lenvatinib	Phase I	Feb. 2017
NCT03299946	Feasibility and efficacy of neoadjuvant cabozantinib plus nivolumab (CaboNivo) followed by definitive resection for patients with locally advanced hepatocellular carcinoma (HCC)	PD-1 Ab + cabozantinib (neoadjuvant)	Phase I	Dec. 2017
NCT03211416	Sorafenib tosylate and pembrolizumab in treating patients with advanced or metastatic liver cancer	PD-1 Ab + sorafenib	Phase I/II	Sep. 2017
NCT03289533	A study of avelumab in combination with axitinib in advanced HCC	PD-L1 Ab + Axitinib	Phase I	Sep. 2017
NCT02988440	Study of safety and tolerability of PDR001 in combination with sorafenib and to identify the maximum tolerated dose and/or phase 2 dose for this combination in advanced hepatocellular patients	PD-1 Ab + sorafenib	Phase I	Apr. 2017
NCT02859324	A safety and efficacy study of CC-122 in combination with nivolumab in subjects with unresectable hepatocellular carcinoma (HCC)	PD-1 Ab + E3 ubiquitin ligase	Phase I/II	Sep. 2016
NCT02795429	Phase Ib/II study of INC280 + PDR001 or PDR001 single agent in advanced HCC	PD-1 Ab ± cMet inhibitor	Phase Ib/II	Jun. 2016
NCT02423343	A study of galunisertib (LY2157299) in combination with nivolumab in advanced refractory solid tumors and in recurrent or refractory NSCLC, or hepatocellular carcinoma	PD-1 Ab + TGF-βR1 inhibitor	Phase Ib/II	Oct. 2015
NCT02325739	FGF401 in HCC and solid tumors characterized by positive FGFR4 and KLB expression	PD-1 Ab + FGFR4 inhibitor	Phase I/II	Dec. 2014
NCT01658878	An immuno-therapy study to evaluate the effectiveness, safety and tolerability of nivolumab or nivolumab in combination with other agents in patients with advanced liver cancer	PD-1 Ab ± sorafenib, PD-1 Ab ± CTLA-4 Ab, PD-1 Ab + cabozantinib ± CTLA-4 Ab	Phase I/II	Sep. 2012

Ab, antibody; FGFR4, fibroblast growth factor receptor 4; HCC, hepatocellular carcinoma; KLB, klotho-β; PD-1, program cell death receptor-1; PD-L1, programmed cell death receptor-1 ligand; TGF-βR1, transforming growth factor-β receptor 1; VEGF, vascular endothelial growth factor.

with anti-PD-1 antibody, a relatively high proportion of grade 3 and 4 AEs were observed in patients treated with anti-CTLA-4 antibody, such as increased levels of aspartate

aminotransferase and alanine aminotransferase (45% and 25%, respectively).⁵⁴ As both anti-PD-1 and anti-CTLA-4 trials did not show any treatment-related death, AEs

Table 4 Clinical trials of combinations of immune checkpoint inhibitors with other treatments

Clinical trial number	Title	Target	Design	Start date
NCT03397654	Study of pembrolizumab following TACE in primary liver carcinoma	PD-1 Ab + TACE	Phase I/II	Jan. 2018
NCT03259867	Combination of TATE and PD-1 inhibitor in liver cancer	PD-1 Ab + TATE	Phase II	Jul. 2017
NCT02886897	A study of combinations of D-CIK immunotherapy and anti-PD-1 in refractory solid tumors	PD-1 Ab + D-CIK	Phase I/II	Jul. 2016
NCT03380130	A study of the safety and antitumoral efficacy of nivolumab after SIRT for the treatment of patients with HCC	PD-1 Ab + SIRT	Phase II	Sep. 2017
NCT03143270	A study to test the safety and feasibility of nivolumab with drug eluting bead transarterial chemoembolization in patients with liver cancer	PD-1 Ab + DEB-TACE	Phase I	Apr. 2017
NCT03099564	Pembrolizumab plus Y90 radioembolization in HCC subjects	PD-1 Ab + radioembolization	Phase I	Mar. 2017
NCT03033446	Study of Y90-radioembolization with nivolumab in Asians with hepatocellular carcinoma	PD-1 Ab + radioembolization	Phase II	Dec. 2016
NCT02837029	Nivolumab and yttrium Y 90 glass microspheres in treating patients with advanced liver cancer	PD-1 Ab + radioembolization	Phase I	Jul. 2016
NCT03316872	Study of pembrolizumab and radiotherapy in liver cancer	PD-1 + SBRT	Phase II	Nov. 2017
NCT03203304	Study of stereotactic body radiotherapy (SBRT) followed by nivolumab or ipilimumab with nivolumab in unresectable hepatocellular carcinoma	PD-1 Ab ± CTLA-4 Ab + SBRT	Phase I	Aug. 2017
NCT03071094	A trial to evaluate the safety and efficacy of the combination of the oncolytic immunotherapy Pexa-Vec With the PD-1 receptor blocking antibody nivolumab in the first-line treatment of advanced hepatocellular carcinoma (HCC)	PD-1 Ab + Pexa-Vec	Phase I/II	Jul. 2017
NCT02821754	A pilot study of combined immune checkpoint inhibition in combination with ablative therapies in subjects with hepatocellular carcinoma (HCC) or biliary tract carcinomas (BTC)	PD-L1 Ab + CTLA-4 Ab ± TACE or RFA or cryoablation	Phase I/II	Jun. 2016
NCT01853618	Tremelimumab with chemoembolization or ablation for liver cancer	CTLA-4 Ab + TACE or RFA or SBRT or cryoablation	Phase I	May 2013

Ab, antibody; CTLA-4, cytotoxic T lymphocyte-associated antigen 4; D-CIK, dendritic and cytokine-induced killer cell based adoptive immunotherapy; DEB-TACE, drug eluting bead transarterial chemoembolization; HCC, hepatocellular carcinoma; PD-1, program cell death receptor-1; PD-L1, programmed cell death receptor-1 ligand; Pexa-Vec, pexastimogene devacirepvec; RFA, radiofrequency ablation; SBRT, stereotactic body radiotherapy; SIRT, selective internal radiation therapy; TACE, transarterial chemoembolization; TATE, transarterial tirapazamine embolization.

caused by immune checkpoint monotherapies were manageable under steroid therapy and/or discontinuation of the agent. However, although long-term response could be expected, improved survival might lead to the increase of delayed irAEs. From this point of view, long-term safety remains to be clarified.

Adverse events caused by combination blockade of immune checkpoint molecules could be more severe compared to monotherapy. For example, cases of early lethal myocarditis have been reported under nivolumab–ipilimumab combination in patients with melanoma.⁶⁴ As AEs in particular situations, such as under complex combinations, are currently poorly understood, their characterization is essential to balance their expected benefits with their risks.

CONCLUSIONS

THE APPLICATION OF immune checkpoint blockade is rapidly progressing in the field of HCC treatment. Notably, nivolumab received expedited Food and Drug Administration approval in 2017 for use in cases of advanced HCC after failure or intolerance to sorafenib. Currently, two randomized, multicenter phase III clinical trials, nivolumab versus sorafenib as a first-line treatment and pembrolizumab versus best supportive care as a second-line treatment, are ongoing for immune checkpoint monotherapy. The trials are expected to clarify several critical questions, such as the efficacy and timing of the application of anti-PD-1 therapy during the course of the disease. In addition, the concept of immune checkpoint blockade should be applicable to the treatment of advanced tumors as well as in adjuvant and neoadjuvant settings; thus, the application of this novel modality will certainly expand to earlier stages of the disease.

ACKNOWLEDGMENTS

THIS WORK WAS supported in part by a Grant-in-Aid for Scientific Research (KAKENHI: 16 K09382) from the Japanese Society for the Promotion of Science (N. Nishida) and a grant from the Smoking Research Foundation (N. Nishida).

REFERENCES

- 1 Kudo M, Matsui O, Izumi N *et al.* JSH consensus-based clinical practice guidelines for the management of hepatocellular carcinoma: 2014 update by the Liver Cancer Study Group of Japan. *Liver Cancer*. 2014; 3: 458–68.
- 2 Kudo M, Trevisani F, Abou-Alfa GK, Rimassa L. Hepatocellular carcinoma: therapeutic guidelines and medical treatment. *Liver Cancer*. 2016; 6: 16–26.
- 3 Kudo M. Molecular targeted agents for hepatocellular carcinoma: current status and future perspectives. *Liver Cancer*. 2017; 6: 101–12.
- 4 Bruix J, Qin S, Merle P *et al.* Regorafenib for patients with hepatocellular carcinoma who progressed on sorafenib treatment (RESORCE): a randomised, double-blind, placebo-controlled, phase 3 trial. *Lancet* 2017; 389: 56–66.
- 5 Kudo M. A new era of systemic therapy for hepatocellular carcinoma with regorafenib and lenvatinib. *Liver Cancer* 2017; 6: 177–84.
- 6 Kudo M, Finn RS, Qin S *et al.* Lenvatinib versus sorafenib in first-line treatment of patients with unresectable hepatocellular carcinoma: a randomised phase 3 non-inferiority trial. *Lancet* 2018; 391: 1163–73.
- 7 Ikeda K, Kudo M, Kawazoe S *et al.* Phase 2 study of lenvatinib in patients with advanced hepatocellular carcinoma. *J Gastroenterol* 2017; 52: 512–19.
- 8 Kelley RK, Verslype C, Cohn AL *et al.* Cabozantinib in hepatocellular carcinoma: results of a phase 2 placebo-controlled randomized discontinuation study. *Ann Oncol* 2017; 28: 528–34.
- 9 Rudalska R, Dauch D, Longerich T *et al.* *In vivo* RNAi screening identifies a mechanism of sorafenib resistance in liver cancer. *Nat Med* 2014; 20: 1138–46.
- 10 Prieto J, Melero I, Sangro B. Immunological landscape and immunotherapy of hepatocellular carcinoma. *Nat Rev Gastroenterol Hepatol* 2015; 12: 681–700.
- 11 Nishida N, Kudo M. Role of immune checkpoint blockade in the treatment for human hepatocellular carcinoma. *Dig Dis* 2017; 35: 618–22.
- 12 Kudo M. Immune checkpoint blockade in hepatocellular carcinoma: 2017 update. *Liver Cancer* 2016; 6: 1–2.
- 13 Wada Y, Nakashima O, Kutami R, Yamamoto O, Kojiro M. Clinicopathological study on hepatocellular carcinoma with lymphocytic infiltration. *Hepatology* 1998; 27: 407–14.
- 14 Unitt E, Marshall A, Gelson W *et al.* Tumour lymphocytic infiltrate and recurrence of hepatocellular carcinoma following liver transplantation. *J Hepatol* 2006; 45: 246–53.
- 15 Budhu A, Forgues M, Ye QH *et al.* Prediction of venous metastases, recurrence, and prognosis in hepatocellular carcinoma based on a unique immune response signature of the liver microenvironment. *Cancer Cell* 2006; 10: 99–111.
- 16 Shafizadeh N, Kakar S. Hepatocellular carcinoma: histologic subtypes. *Surg Pathol Clin* 2013; 6: 367–84.
- 17 Calderaro J, Rousseau B, Amaddeo G *et al.* Programmed death ligand 1 expression in hepatocellular carcinoma: relationship with clinical and pathological features. *Hepatology* 2016; 64: 2038–46.
- 18 Flecken T, Schmidt N, Hild S *et al.* Immunodominance and functional alterations of tumor-associated antigen-specific CD8+ T-cell responses in hepatocellular carcinoma. *Hepatology* 2014; 59: 1415–26.

- 19 Zou W, Chen L. Inhibitory B7-family molecules in the tumour microenvironment. *Nat Rev Immunol* 2008; 8: 467–77.
- 20 Finkin S, Yuan D, Stein I *et al*. Ectopic lymphoid structures function as microniches for tumor progenitor cells in hepatocellular carcinoma. *Nat Immunol* 2015; 16: 1235–44.
- 21 Roth GS, Decaens T. Liver immunotolerance and hepatocellular carcinoma: patho-physiological mechanisms and therapeutic perspectives. *Eur J Cancer* 2017; 87: 101–12.
- 22 Ringelhan M, Pfister D, O'Connor T, Pikarsky E, Heikenwalder M. The immunology of hepatocellular carcinoma. *Nat Immunol* 2018; 19: 222–32.
- 23 Nishida N, Kudo M. Recent advancements in comprehensive genetic analyses for human hepatocellular carcinoma. *Oncology* 2013; 84(Suppl 1): 93–7.
- 24 Nishida N, Kudo M. Alteration of epigenetic profile in human hepatocellular carcinoma and its clinical implications. *Liver Cancer* 2014; 3: 417–27.
- 25 Mittal D, Gubin MM, Schreiber RD, Smyth MJ. New insights into cancer immunoediting and its three component phases – elimination, equilibrium and escape. *Curr Opin Immunol* 2014; 27: 16–25.
- 26 Arihara F, Mizukoshi E, Kitahara M *et al*. Increase in CD14+HLA-DR –/low myeloid-derived suppressor cells in hepatocellular carcinoma patients and its impact on prognosis. *Cancer Immunol Immunother* 2013; 62: 1421–30.
- 27 Hoechst B, Ormandy LA, Ballmaier M *et al*. A new population of myeloid-derived suppressor cells in hepatocellular carcinoma induces CD4(+)CD25(+)Foxp3(+) T cells. *Gastroenterology* 2008; 135: 234–43.
- 28 Li H, Han Y, Guo Q, Zhang M, Cao X. Cancer-expanded myeloid-derived suppressor cells induce anergy of NK cells through membrane-bound TGF- β 1. *J Immunol* 2009; 182: 240–9.
- 29 Ostrand-Rosenberg S, Sinha P, Beury DW, Clements VK. Cross-talk between myeloid-derived suppressor cells (MDSC), macrophages, and dendritic cells enhances tumor-induced immune suppression. *Semin Cancer Biol* 2012; 22: 275–81.
- 30 Yan W, Liu X, Ma H *et al*. Tim-3 fosters HCC development by enhancing TGF- β -mediated alternative activation of macrophages. *Gut* 2015; 64: 1593–604.
- 31 Chen KJ, Lin SZ, Zhou L *et al*. Selective recruitment of regulatory T cell through CCR6-CCL20 in hepatocellular carcinoma fosters tumor progression and predicts poor prognosis. *PLoS One* 2011; 6: e24671.
- 32 Quezada SA, Peggs KS, Simpson TR, Allison JP. Shifting the equilibrium in cancer immunoediting: from tumor tolerance to eradication. *Immunol Rev* 2011; 241: 104–18.
- 33 Li T, Yang Y, Hua X *et al*. Hepatocellular carcinoma-associated fibroblasts trigger NK cell dysfunction via PGE2 and IDO. *Cancer Lett* 2012; 318: 154–61.
- 34 Zaiss DM, van Loosdregt J, Gorlani A *et al*. Amphiregulin enhances regulatory T cell-suppressive function via the epidermal growth factor receptor. *Immunity* 2013; 38: 275–84.
- 35 Chen Y, Huang Y, Reiberger T *et al*. Differential effects of sorafenib on liver versus tumor fibrosis mediated by stromal-derived factor 1 α /CX-C receptor type 4 axis and myeloid differentiation antigen-positive myeloid cell infiltration in mice. *Hepatology* 2014; 59: 1435–47.
- 36 Mezrich JD, Fechner JH, Zhang X, Johnson BP, Burlingham WJ, Bradfield CA. An interaction between kynurenine and the aryl hydrocarbon receptor can generate regulatory T cells. *J Immunol* 2010; 185: 3190–8.
- 37 Han Y, Chen Z, Yang Y *et al*. Human CD14+CTLA-4+ regulatory dendritic cells suppress T-cell response by cytotoxic T-lymphocyte antigen-4-dependent IL-10 and indoleamine-2,3-dioxygenase production in hepatocellular carcinoma. *Hepatology* 2014; 59: 567–79.
- 38 Pan K, Wang H, Chen MS *et al*. Expression and prognosis role of indoleamine 2,3-dioxygenase in hepatocellular carcinoma. *J Cancer Res Clin Oncol* 2008; 134: 1247–53.
- 39 Zhao Q, Kuang DM, Wu Y *et al*. Activated CD69+ T cells foster immune privilege by regulating IDO expression in tumor-associated macrophages. *J Immunol* 2012; 188: 1117–24.
- 40 Zarek PE, Huang CT, Lutz ER *et al*. A2A receptor signaling promotes peripheral tolerance by inducing T-cell anergy and the generation of adaptive regulatory T cells. *Blood* 2008; 111: 251–9.
- 41 Matsuda Y, Yamagiwa Y, Fukushima K, Ueno Y, Shimosegawa T. Expression of galectin-3 involved in prognosis of patients with hepatocellular carcinoma. *Hepatol Res* 2008; 38: 1098–111.
- 42 Sprinzl MF, Galle PR. Immune control in hepatocellular carcinoma development and progression: role of stromal cells. *Semin Liver Dis* 2014; 34: 376–88.
- 43 Voron T, Colussi O, Marcheteau E *et al*. VEGF-A modulates expression of inhibitory checkpoints on CD8+ T cells in tumors. *J Exp Med* 2015; 212: 139–48.
- 44 Fourcade J, Sun Z, Pagliano O *et al*. CD8(+) T cells specific for tumor antigens can be rendered dysfunctional by the tumor microenvironment through upregulation of the inhibitory receptors BTLA and PD-1. *Cancer Res* 2012; 72: 887–96.
- 45 Yarchoan M, Xing D, Luan L *et al*. Characterization of the immune microenvironment in hepatocellular carcinoma. *Clin Cancer Res* 2017; 23: 7333–9.
- 46 Hato T, Goyal L, Greten TF, Duda DG, Zhu AX. Immune checkpoint blockade in hepatocellular carcinoma: current progress and future directions. *Hepatology* 2014; 60: 1776–82.
- 47 Nguyen LT, Ohashi PS. Clinical blockade of PD1 and LAG3 – potential mechanisms of action. *Nat Rev Immunol* 2015; 15: 45–56.
- 48 Umemoto Y, Okano S, Matsumoto Y *et al*. Prognostic impact of programmed cell death 1 ligand 1 expression in human leukocyte antigen class I-positive hepatocellular carcinoma after curative hepatectomy. *J Gastroenterol* 2015; 50: 65–75.
- 49 Noman MZ, Desantis G, Janji B *et al*. PD-L1 is a novel direct target of HIF-1 α , and its blockade under hypoxia enhanced MDSC-mediated T cell activation. *J Exp Med* 2014; 211: 781–90.

- 50 Li H, Wu K, Tao K *et al.* Tim-3/galectin-9 signaling pathway mediates T-cell dysfunction and predicts poor prognosis in patients with hepatitis B virus-associated hepatocellular carcinoma. *Hepatology* 2012; 56: 1342–51.
- 51 Li FJ, Zhang Y, Jin GX, Yao L, Wu DQ. Expression of LAG-3 is coincident with the impaired effector function of HBV-specific CD8(+) T cell in HCC patients. *Immunol Lett* 2013; 150: 116–22.
- 52 Hokuto D, Sho M, Yamato I *et al.* Clinical impact of herpesvirus entry mediator expression in human hepatocellular carcinoma. *Eur J Cancer* 2015; 51: 157–65.
- 53 El-Khoueiry AB, Sangro B, Yau T *et al.* Nivolumab in patients with advanced hepatocellular carcinoma (Check-Mate 040): an open-label, non-comparative, phase 1/2 dose escalation and expansion trial. *Lancet* 2017; 389: 2492–502.
- 54 Sangro B, Gomez-Martin C, de la Mata M *et al.* A clinical trial of CTLA-4 blockade with tremelimumab in patients with hepatocellular carcinoma and chronic hepatitis C. *J Hepatol* 2013; 59: 81–8.
- 55 Smyth MJ, Ngjow SF, Ribas A, Teng MW. Combination cancer immunotherapies tailored to the tumour microenvironment. *Nat Rev Clin Oncol* 2016; 13: 143–58.
- 56 Sumimoto H, Imabayashi F, Iwata T, Kawakami Y. The BRAF-MAPK signaling pathway is essential for cancer-immune evasion in human melanoma cells. *J Exp Med* 2006; 203: 1651–6.
- 57 Frederick DT, Piris A, Cogdill AP *et al.* BRAF inhibition is associated with enhanced melanoma antigen expression and a more favorable tumor microenvironment in patients with metastatic melanoma. *Clin Cancer Res* 2013; 19: 1225–31.
- 58 Liu H, Shen J, Lu K. IL-6 and PD-L1 blockade combination inhibits hepatocellular carcinoma cancer development in mouse model. *Biochem Biophys Res Commun* 2017; 486: 239–44.
- 59 Ebert PJR, Cheung J, Yang Y *et al.* MAP kinase inhibition promotes T cell and anti-tumor activity in combination with PD-L1 checkpoint blockade. *Immunity* 2016; 44: 609–21.
- 60 Nishida N, Kudo M. Oncogenic signal and tumor microenvironment in hepatocellular carcinoma. *Oncology* 2017; 93(Suppl 1): 160–4.
- 61 Duffy AG, Ulahannan SV, Makrova-Rusher O *et al.* Tremelimumab in combination with ablation in patients with advanced hepatocellular carcinoma. *J Hepatol* 2017; 66: 545–51.
- 62 Kim KJ, Kim JH, Lee SJ, Lee EJ, Shin EC, Seong J. Radiation improves antitumor effect of immune checkpoint inhibitor in murine hepatocellular carcinoma model. *Oncotarget* 2017; 8: 41242–55.
- 63 Blocking IDO1 helps shrink bladder, cervical tumors. *Cancer Discov* 2018; 8: OF3.
- 64 Johnson DB, Balko JM, Compton ML *et al.* Fulminant myocarditis with combination immune checkpoint blockade. *N Engl J Med* 2016; 375: 1749–55.

How to perform Contrast-Enhanced Ultrasound (CEUS)



Authors

Christoph F. Dietrich¹, Michalakis Averkiou², Michael Bachmann Nielsen³, Richard G. Barr⁴, Peter N. Burns⁵, Fabrizio Calliada⁶, Vito Cantisani⁷, Byung Choi⁸, Maria C. Chammas⁹, Dirk-André Clevert¹⁰, Michel Claudon¹¹, Jean-Michel Correas¹², Xin-Wu Cui¹³, David Cosgrove¹⁴, Mirko D'Onofrio¹⁵, Yi Dong¹⁶, John R. Eisenbrey¹⁷, Teresa Fontanilla¹⁸, Odd Helge Gilja¹⁹, Andre Ignee¹³, Christian Janssen²⁰, Yuko Kono²¹, Masatoshi Kudo²², Nathalie Lassau²³, Andrej Lyshchik¹⁷, Maria Franca Meloni²⁴, Fuminori Moriyasu²⁵, Christian Nolsøe²⁶, Fabio Piscaglia²⁷, Maija Radzina²⁸, Adrian Saftoiu²⁹, Paul S. Sidhu³⁰, Ioan Sporea³¹, Dagmar Schreiber-Dietrich³², Claude B. Sirlin³³, Maria Stanczak¹⁷, Hans-Peter Weskott³⁴, Stephanie R. Wilson³⁵, Juergen Karl Willmann³⁶, Tae Kyong Kim³⁷, Hyun-Jung Jang³⁷, Alexandar Vezeridis³⁸, Sue Westerway³⁹

Affiliations

- 1 Caritas-Krankenhaus, Medizinische Klinik 2, Bad Mergentheim, Germany and Ultrasound Department, The First Affiliated Hospital of Zhengzhou University, Zhengzhou, China
- 2 Bioengineering, University of Washington, Seattle, United States
- 3 Rigshospitalet, Dep. of Radiology, Copenhagen, Denmark
- 4 Radiology, Northeastern Ohio Medical University, Rootstown, United States
- 5 Dept Medical Biophysics, University of Toronto. Sunnybrook Research Institute, Toronto, Canada
- 6 Policlinico San Matteo, University of Pavia, Department of Radiology, Pavia, Italy
- 7 Department of Radiology, "Sapienza" University of Rome, ROME, Italy
- 8 Department of Radiology, Chung-Ang University Hospital, Seoul, Korea (the Republic of)
- 9 Hospital das Clínicas da Faculdade de Medicina da Universidade de São Paulo, Instituto de Radiologia, São Paulo, Brazil
- 10 Department of Clinical Radiology, University of Munich-Grosshadern Campus, Munich, Germany
- 11 Department of Pediatric Radiology, Centre Hospitalier Universitaire de Nancy and Université de Lorraine, Vandoeuvre, France
- 12 Hôpital universitaire Necker-Enfants malades, Service de Radiologie Adultes, Paris, France
- 13 Department of Medical Ultrasound, Tongji Hospital of Tongji Medical college, Huazhong University of Science and Technology, Wuhan, China
- 14 Imperial College London, Imaging, London, United Kingdom of Great Britain and Northern Ireland
- 15 Radiology, University of Verona, Verona, Italy
- 16 Department of Ultrasound, Zhongshan Hospital, Fudan University, 200032 Shanghai, China
- 17 Department of Radiology, Thomas Jefferson University, Philadelphia, United States
- 18 Radiology, Hospital Universitario Puerta del Hierro Majadahonda, Majadahonda, Spain
- 19 National Centre for Ultrasound in Gastroenterology, Haukeland University Hospital, Bergen and Department of Clinical Medicine, University of Bergen, Norway
- 20 Krankenhaus Märkisch Oderland Strausberg/ Wriezen, Klinik für Innere Medizin, Wriezen, Germany
- 21 Department of Medicine and Radiology, University of California, San Diego, United States
- 22 Kinki Daigaku Igakubu, Department Gastroenterology and Hepatology, Osakasayama, Osaka, Japan
- 23 Gustave Roussy and IR4MUMR8081. Université Paris-Sud, Université Paris-Saclay, Radiology, Paris, France
- 24 Radiology Department of Interventional Ultrasound - Casa di cura Igea- Milano, Italy
- 25 Sanno Hospital, International University of Health and Welfare, Center for Cancer Ablation Therapy, Tokyo, Japan
- 26 Ultrasound Section, Division of Surgery, Dep. of Gastroenterology, Herlev Hospital Copenhagen Academy for Medical Education and Simulation (CAMES), University of Copenhagen, Denmark
- 27 Div. Internal Medicine, Dept of Medical and Surgical Sciences, Bologna, Italy
- 28 P.Stradina Clinical University Hospital, Diagnostic Radiology Institute, Riga, Latvia
- 29 Research Center of Gastroenterology and Hepatology, University of Medicine and Pharmacy of Craiova, Craiova, Romania
- 30 King's College London, Radiology, London, United Kingdom of Great Britain and Northern Ireland
- 31 Gastroenterology, University of Medicine and Pharmacy Timisoara, Timisoara, Romania
- 32 Cariats-Krankenhaus Bad Mergentheim, Pediatrics, Bad Mergentheim, Germany
- 33 Liver Imaging Grup, University of California, Department of Radiology, San Diego, United States
- 34 Klinikum Siloah, Ultrasound Outpatient Department, Hannover, Germany
- 35 Department of Radiology, Foothills Medical Centre University of Calgary, Division of Ultrasound, Calgary, Canada
- 36 Department of Radiology, Stanford University, Stanford, United States

37 Department of Medical Imaging, University of Toronto,
Toronto, Canada
38 Radiology, University of California, San Diego, United States
39 Ultrasound, Charles Sturt University NSW Australia, NSW,
Australia

Key words

guidelines, teaching, ultrasonography, cancer

received 25.09.2017

revised 27.11.2017

accepted 29.11.2017

Bibliography

DOI <https://doi.org/10.1055/s-0043-123931>

Ultrasound Int Open 2017; 3: E2–E15

© Georg Thieme Verlag KG Stuttgart · New York

ISSN 2199-7152

Correspondence

Dr. Christoph Dietrich, MD
Caritas-Krankenhaus

Medizinische Klinik 2
Uhlandstr. 7

Bad Mergentheim, 97980

Germany

Tel.: +49/7931/58 2201, Fax: +49/7931/58 2290

Christoph.Dietrich@ckbm.de

ABSTRACT

“How to perform contrast-enhanced ultrasound (CEUS)” provides general advice on the use of ultrasound contrast agents (UCAs) for clinical decision-making and reviews technical parameters for optimal CEUS performance. CEUS techniques vary between centers, therefore, experts from EFSUMB, WFUMB and from the CEUS LI-RADS working group created a discussion forum to standardize the CEUS examination technique according to published evidence and best personal experience. The goal is to standardise the use and administration of UCAs to facilitate correct diagnoses and ultimately to improve the management and outcomes of patients.

Introduction

An introduction to terminology

The acronym CEUS refers to contrast-enhanced ultrasound techniques in general [1–11]. Dynamic contrast enhanced ultrasound (DCE-US) refers to quantitative time intensity curve (TIC) analysis [11–13] using either bolus injection of microbubbles [13–16] or intravenous infusion with disruption-replenishment technique [17] which are used for treatment response evaluation in oncology [18] and for activity assessment in inflammation of the bowel wall in inflammatory bowel disease [19–22]. 3D CEUS refers to image acquisition of data volumes. Introduced in 2002 [9], 3D CEUS is available in certain systems but it is still under investigation [23–26].

CEUS phases

CEUS allows real-time recording and evaluation of the wash-in and wash-out phases of the ultrasound contrast agent (UCA) over several minutes. When examining the liver, this provides dynamic visualisation of different vascular phases. Owing to the specific supply of blood to the liver three different phases have been defined: the arterial (AP), the portal venous (PVP), and the late (sinusoidal) phases (LP) [27, 28].

All clinically approved microbubbles, regardless of whether they are reticuloendothelial or purely blood pool, can easily be destroyed by ultrasound energy. This occurs most often by excessive or continuous scanning in a single plane, though it may also occur if the acoustic power is changed from the recommended value (typically less than 1%) to a higher acoustic power. Once the shell is disrupted, the gas from the microbubbles diffuses, and microbubbles lose their scattering properties and are no longer effective contrast agents. Microbubble destruction, therefore, results in time- and depth-dependent loss of contrast, which not only reduces image quality but can also lead to spurious signal loss that may mimic le-

sion washout. Reducing microbubble destruction is therefore important. Using optimal low MI settings reduces microbubble destruction to a minimal level. A useful sequence is to scan continuously and record a cine loop from the earliest arrival of the microbubbles to include the peak of arterial enhancement, and up to 60 s. Thereafter scanning should be intermittent, with storage of single images or short loops at about 30–60 s intervals to show the presence of washout.

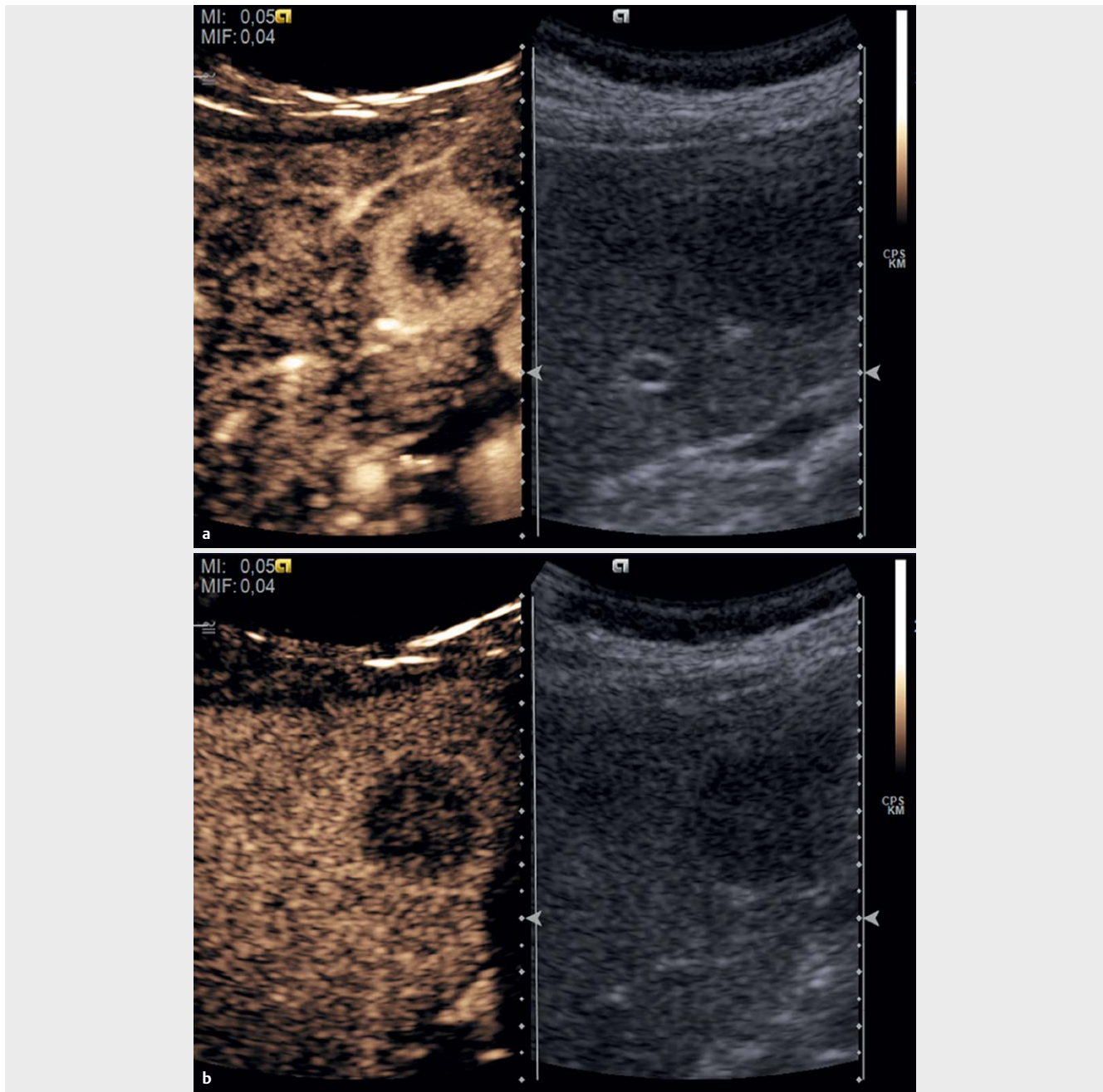
The main diagnostic features are:

1. Vascular architecture (evaluated in the early wash-in phase).
2. Contrast enhancement of the lesion compared to the adjacent tissue (time course of wash-in and wash-out).

The combined evaluation of above diagnostic features makes it possible to characterize focal liver lesions (FLL) in healthy parenchyma [29–32] as malignant ▶ **Fig. 1** or benign ▶ **Fig. 2**.

The combined evaluation of the above diagnostic features makes it possible to characterize focal liver lesions (FLL) in patients with liver cirrhosis as typical for HCC according to the LI-RADS system (see below) [33–36].

Some contrast agents (such as Sonazoid™, BR14, BR38) are phagocytosed by cells of the mononuclear phagocyte system (reticulo-endothelium, e. g., Kupffer cells in the liver). Phagocytosis may start as early as the arterial phase and becomes pronounced in the late phase. This results in accelerated clearance of the agents from the vascular distribution volume [37]. These UCAs persist significantly longer in the liver parenchyma than purely vascular agents so that a fourth phase, the post-vascular phase (also known as the Kupffer cell phase), can be defined. For these reasons, transit times and time intensity curves (TIC) differ for purely blood pool versus reticuloendothelial UCAs. The latter should not be used to evaluate hepatic transit times, as they do not reflect the hepatic kinetics.



► **Fig. 1** Malignant focal liver lesions in healthy liver parenchyma show a variable arterial enhancement pattern according to their etiology (rim enhancement in the case of some metastases **a** and as decisive criteria hypoenhancement in the portal venous (sinusoidal and “liver specific”) phase in comparison to the surrounding liver parenchyma **b**.

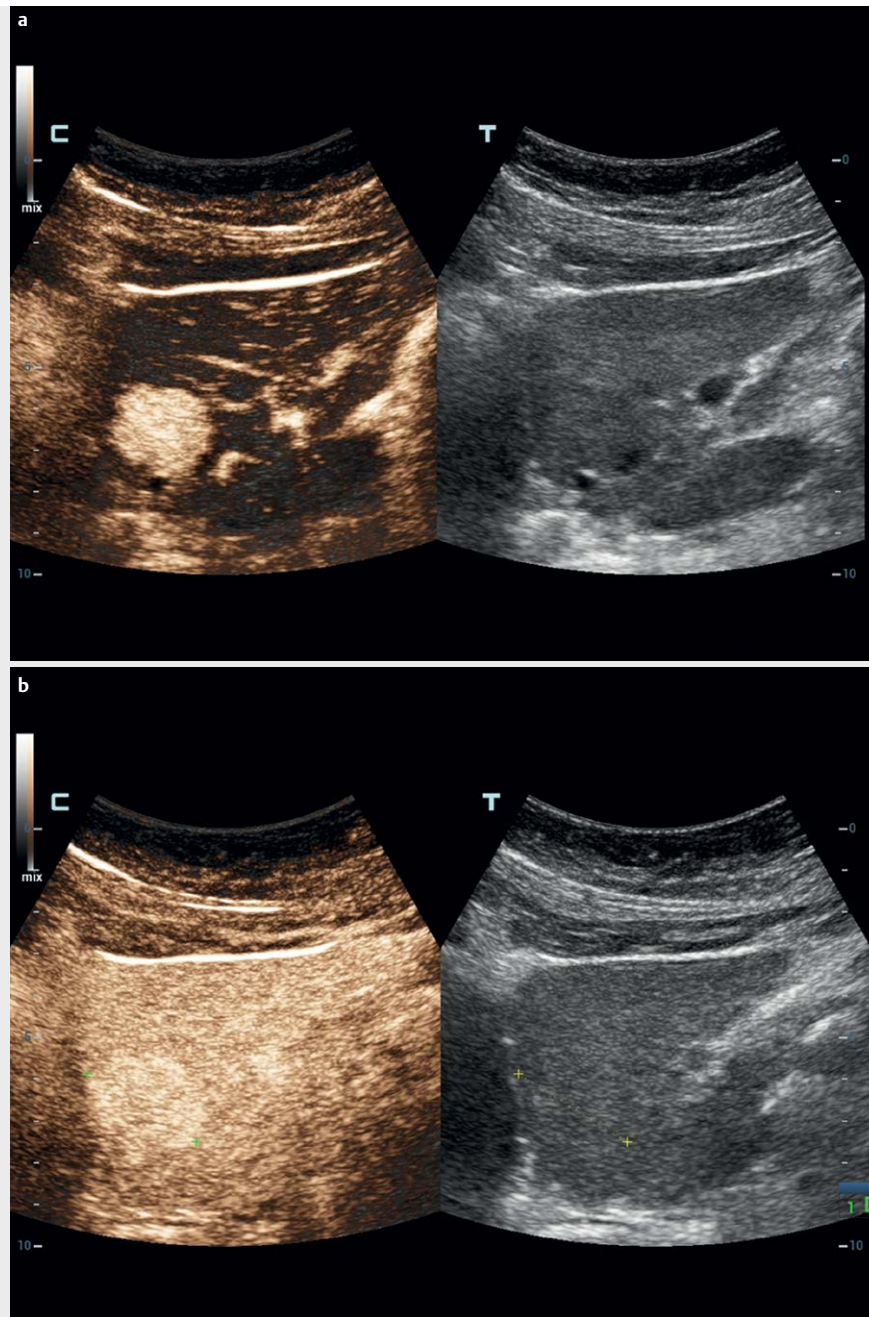
Enhancement (degree and timing)

The contrast behaviour of a lesion or region of interest in the liver described in terms of the degree (relative to the adjacent parenchyma) and timing (phase) of enhancement is discussed in [4, 38]. It is important to know in advance if the liver is healthy or diseased (e.g. liver cirrhosis, fibrosis or steatosis). This may affect the contrast behavior of the lesion and liver parenchyma as well.

Enhancement refers to the intensity of the signal relative to the adjacent parenchyma as iso-enhancing, hyper-enhancing and hypo-enhancing. Sustained enhancement refers to continuation of

the same or greater intensity of enhancement in the lesion relative to the adjacent parenchyma over time. It applies to lesions that are iso- or hyper-enhancing in the arterial phase. Complete absence of enhancement can be described as non-enhancing [4, 38, 39].

Describing the degree of enhancement is preferred although some authors designate the degree of vascularity of a region relative to adjacent liver as hypervascular, iso-vascular, hypovascular. The term “vascular” may be incorrect from a histologic, as well as physiologic, point of view. It should be clarified that imaging major vessels, likewise by Doppler technique, is defined as vascularization.



► **Fig. 2** Benign focal liver lesions in healthy liver parenchyma show a variable arterial enhancement pattern according to their etiology **a** and as decisive criteria iso- or hyper-enhancement in the portal venous (sinusoidal and “liver specific”) phase in comparison to the surrounding liver parenchyma **b**.

The definition of perfusion is “volume of blood per time per mass of tissue” (unit: ml/min/g tissue). To know this is relevant for tissues with volume pulsation (e. g., the myocardium). By using CEUS, both vascularization and relative perfusion can be imaged. Both terms are sometimes used interchangeably without clarification.

The enhancement pattern should be described separately for the different phases discussed above. Conventional, but imprecise time points separate these different phases (see also “contrast phases of enhancement”) [40]. By convention, however, the timing of events on CEUS is routinely recorded by its actual time in seconds as shown on a visible timer on the scanner screen.

“Wash-in” and “wash-out”

“Wash-in”, used for both qualitative and quantitative analyses, refers to the progressive enhancement within a region of interest from the arrival of microbubbles in the field of view, to “peak enhancement”, and “wash-out” to the reduction in enhancement which follows peak enhancement [4, 38]. As explained above, the timing (early versus late onset, fast versus slow), degree (complete, incomplete) and pattern should be described in comparison to the surrounding “normal” parenchyma. The characteristic features of a TIC analysis are shown in ► **Fig. 3** [11, 41]. This model for quantification of tumor vascularization was applied in multicentric studies validating the AUC as predictive marker [42, 43].

Imaging mode

Only machines that offer nonlinear imaging modes designed for contrast imaging should be used. Where there is a choice of modes, those designed for low MI abdominal scanning should be selected. While in these modes, settings like “high resolution” or “penetration” are often available. These change a host of parameters together and can help adjust the scanner when optimizing a particular examination. These settings should be tried before attempting to adjust the MI or the dose of agent (see below). Once in a low MI contrast mode and the agent is in the patient, reverting to a non-contrast mode will immediately raise the MI and destroy the agent. This should therefore be avoided.

Choice of transducer

Transducers that have specific CEUS optimized settings are recommended. For liver imaging, curvilinear arrays are preferred for most cases. Linear probes with higher transmit frequencies may be useful in cases of superficial lesions and when more spatial resolution is necessary. In this case, higher contrast doses may be beneficial (e. g., thyroid, breast, lymph nodes, prostate), as the agents become less efficient nonlinear scatterers at higher frequencies.

Image depth consideration

Typically, at low MI FLL up to 12–15 cm in depth can be imaged. At larger depths (and depending on the system used, and the patient's condition, e. g., cirrhosis) it may be difficult to visualize lesions. Lower transmit frequency can be selected using the same transducer or lower frequency transducers allowing better penetration with the disadvantage of lower spatial resolution, eventually resulting in suboptimal imaging of small superficially located lesions. Increasing the MI may improve penetration but at the expense of microbubble destruction especially in the nearfield. In general, where there is a choice of amplitude or power modulation imaging modes, these will have better depth penetration (though somewhat poorer resolution) than pure pulse inversion modes.

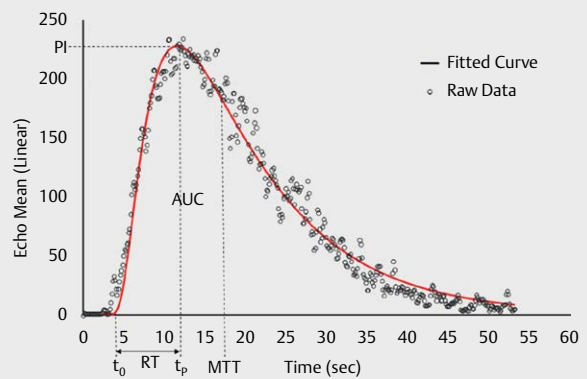
Focus

The focus should be positioned just deep to the target lesion for most ultrasound scanners [44]. Deeper focal zones might be used to achieve a more uniform acoustic field, which improves sensitivity to the agents and lessens the risk of bubble disruption. Other focus positions have been proposed for quantification studies [45].

Gain

Gain refers to the received signal amplification. For CEUS the gain usually is set very slightly above the noise floor so that before microbubbles arrive, the image is dark and with a “hint” (very low level) of noise. If the gain is set too low (image starts out too dark), weak microbubble signals are not detected and only signals from larger vessels are recorded. If the gain is set too high (image starts out bright and grainy even before the microbubbles arrive) the received echoes from the bubbles are clipped after a certain amplitude (signal saturation ▶ Fig. 4).

Acoustic shadowing is the depth-dependent reduction in ultrasound amplitude due to excessive scattering from microbubbles. The nearfield microbubbles obscure and “shadow” the far field ones. Acoustic shadowing is due to excessive dose of UCA or in-



▶ **Fig. 3** Time-intensity curve for a bolus injection in a tissue mimicking flow phantom. A lognormal curve (solid line) is fitted to the data and it is used to calculate the important quantification parameters (44) (PI, RT, MTT, and AUC).

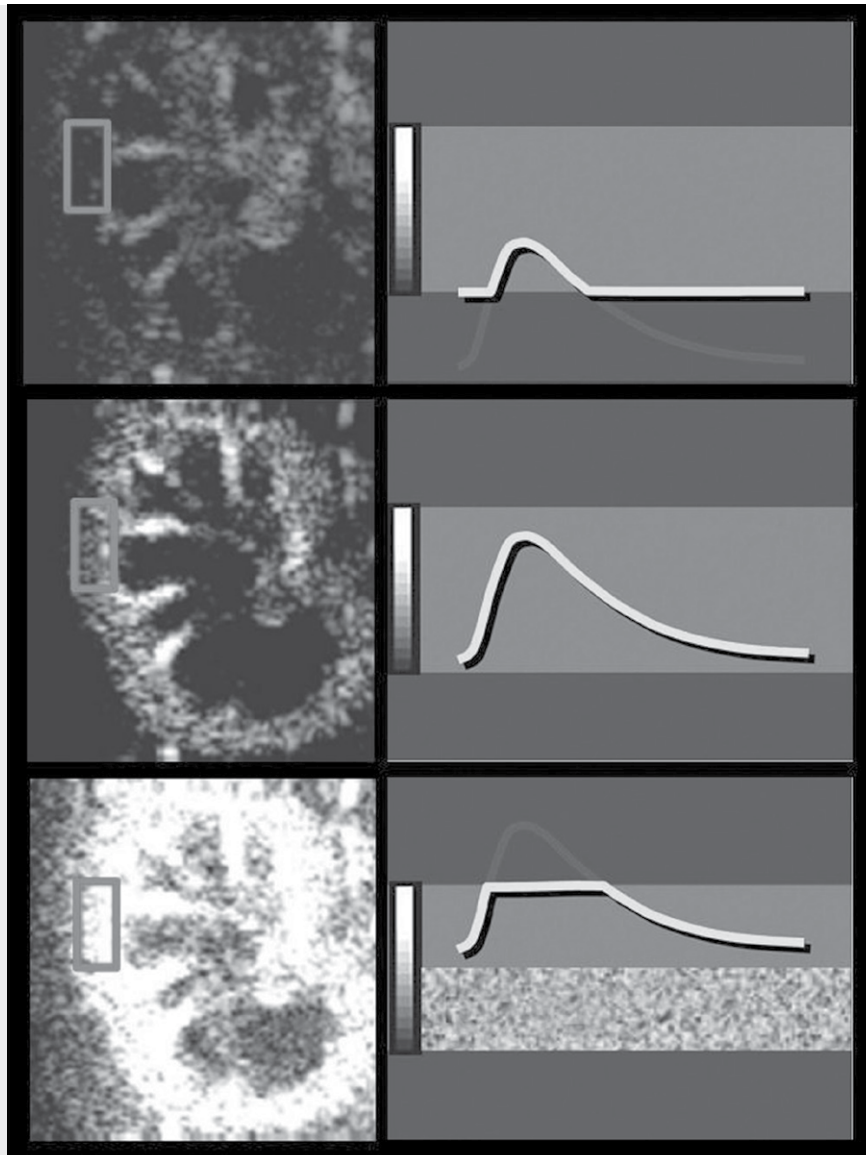
creased microbubble concentration. The UCA dose should be adapted to the patient and the clinical indication. CEUS is always performed with low MI to avoid bubble destruction and harmonic signal generation from tissues. Typically, modern high-end diagnostic ultrasound scanners should effectively suppress tissue signals at low MI's over the entire depth to enhance the visualization of microbubbles.

Background signal (noise)

The use of a dual-image display format is essential in CEUS studies and it is recommended especially in examining small lesions. In this display format, a conventional B-mode low MI fundamental image and a bubble-only contrast image are displayed side-by-side. The reason this is useful is that the nonlinear image is almost completely black (before contrast administration and under ideal conditions) making it difficult to keep the lesion of interest in the image plane. Having the conventional image displayed simultaneously allows the operator to keep the lesion in the imaging plane. Using the B-mode image for guidance, place calipers on the target lesion on both screens simultaneously to facilitate enhancement characterization. It is also possible to overlay the contrast and low MI fundamental B-mode plane image. For quantitative studies, it is critical to maintain the transducer at the same place and avoid motion. Pronounced hyperechoic lesions may still be visible on the contrast image before the arrival of the agent. TIC will help to better define the wash-out characteristics in these cases. It should be noted that in most systems, the quality of the B-mode image in dual-image displays is inferior to that obtained with the same settings in non-contrast mode.

Dynamic range

The compression or dynamic range of the ultrasound system also plays a key role in microbubble visualization. A small dynamic range is preferred in cases of very low signal and a wide dynamic range is preferred when the objective is to perform quantification (to avoid signal saturation). The dynamic range should be set to optimise the expected enhancement pattern. The dynamic range is the range



► **Fig. 4** Low gain setting results in underestimation of the microbubbles located in the microcirculation (a). The proper gain setting results in a correct display of microbubbles in both micro- and macrovessels (b). High gain results in signal oversaturation and the image is too bright making the distinction between macro and micro-vasculature more difficult (c).

of signal intensities to be displayed. A wide dynamic range increases the number of signal levels (“grey levels”), allowing for better differentiation between different degrees of enhancement. A small dynamic range will decrease the number of “colours” in the image and increases visual contrast but can limit the differentiation between areas of variable enhancement. For example, in a vascular metastatic lesion there is often a rim of increased signal surrounding the lesion. If the dynamic range is set too narrow - the rim will be displayed in the same “colour” as the lesion and the increased signal in this area may not be appreciated. Lowering the dynamic range will let the vessels stand out brighter, but it should not be too low that the gray or colorized bubble image suffers in contrast resolution. With a large dynamic range, the increased rim of signal can be better identified.

For visualisation of lesions with low perfusion, a narrow dynamic range is preferred. For perfusion quantification studies, a wide dynamic range should be used to avoid signal saturation. It should be noted that reducing the dynamic range can increase the apparent difference between lesional and parenchymal enhancement. If acquiring a series of cases whose appearances are to be compared, it may be advantageous to keep the dynamic range and other post-processing settings constant.

Frame rate

A frame rate ≥ 10 Hz is recommended for adequate visualization and recording of the wash-in patterns when characterizing focal liver lesions (FLL). The contrast wash-in may only be visualized for about a second in some highly vascularized lesions and is best appreciated using retrospective frame-by-frame cine review. Moreo-

ver, a high frame rate is also important during sweeps of the liver to detect lesions so as to avoid skipping significant regions of the organ [40]. However, increased frame rates can augment bubble destruction, and decreasing the frame rate in the late vascular phases will prolong the enhancement time.

Acoustic amplitude (AA) and mechanical index (MI)

The Acoustic Pressure Amplitude (P) refers to the peak negative amplitude of the ultrasound pulse used for imaging. It is measured in Pa and is used in the calculation of the Mechanical Index (MI). The MI is an estimate of the maximum peak negative acoustic pressure in the tissue within the acoustic field scaled by the square root of the center frequency. MI is related to the likelihood of cavitation and the US Food and Drug Administration (FDA) limits the maximum MI to a value of 1.9 [when P is measured in MPa and frequency in MHz]. In addition to the MI, which refers to the highest value in the acoustic field, some manufacturers also estimate and display the MI at the focus zone or the percentage of maximum acoustic power that allows finer tuning of the acoustic energy delivered [40]. It is important to note that there is a direct linear relationship between P and the MI (within linear acoustics). Choosing the appropriate MI is important for effective CEUS because as summarized in [40] this parameter affects several processes relevant to image quality and microbubble behaviour. These parameters are listed below and discussed in more detail later.

- The degree and rate of microbubble destruction.
- The depth of ultrasound beam penetration.
- The ability to separate signals scattered from background tissue versus those scattered by microbubbles, since tissue scattering is linear at low amplitudes (low MIs) while microbubble scattering is non-linear at all amplitudes.

While the MI on-screen labelling is mandated by the FDA, manufacturers nonetheless use different calculations to arrive at this number. In practice, for contrast imaging, the number is not transferrable between machines. Thus, an optimal MI for a particular patient scanned with one machine may not be the same as for the same patient scanned with another.

Contrast Enhanced Ultrasound

Ultrasound contrast agents (UCA)

UCAs consist of gas microbubbles coated with a shell, usually comprised of phospholipid or albumin. Microbubbles act as resonant scatterers, increasing the backscatter signal by up to 30 dB, and producing echoes with characteristic harmonics. All UCAs are blood pool agents, but – as discussed earlier – some are pure blood pool agents while others are phagocytosed by reticulo-endothelial cells, causing their appearance to differ in the liver-specific late phases.

No need for laboratory tests prior to CEUS

UCAs are extremely safe with low incidence of side effects [46] and no cardio-, hepato- or nephrotoxic effects. Therefore, it is not necessary to perform laboratory tests to assess liver or kidney function prior to their administration [47].

Pre-contrast examination

The pre-contrast examination preparations include the identification of the best position of the patient, the identification of the target lesion and the optimal scan plane along the axis of the respiratory movements (usually longitudinal) to minimize out-of-plane motion from respiration. The optimal patient breathing position is determined and practiced with the patient prior to the contrast injection. Quiet breathing and breath suspension in neutral are preferred over breath hold in full inspiration or expiration.

Catheter

The best position of the patient should be determined during the pre-contrast examination and this may affect which arm is chosen for injection. In most circumstances, the cannula should be inserted in the left arm, preferably the antecubital vein, to avoid interaction of the injector with the right-sided examiner. Be aware of other important influencing factors, e. g., avoid the side of breast (or axillary) surgery to minimise the risk of worsening lymphedema.

Ideally, the diameter of the venous line should be 20 gauge or larger to minimize microbubble destruction during passage through the cannula, with its length as short as possible. Central line and port systems can be used as long as there is no filter requiring a high injection pressure. Their use will shorten contrast arrival time [48].

In cases of difficult venous cannulation, US guided needle placement using a high frequency linear probe is recommended.

The catheter can be removed after exclusion of any kind of pseudoanaphylactic, e. g., 15 min after contrast injection.

3-way stopcock

A three-way stopcock may be valuable, especially if multiple injections are anticipated, as this facilitates sequential administration of the contrast material and then the saline flush, without removal of either syringe.

Injection

The injection bolus for SonoVue™ is given at about 1–2 ml/s. Avoid high pressure (risk of microbubble destruction). Immediately after injecting the contrast agent, a (5-) 10 ml saline bolus should be given to flush the line at about 2 ml/s [4, 38].

Central venous line and “port”

Central venous lines and ports may be used for CEUS if necessary if safety and aseptic requirements are met, but their use is discouraged if a peripheral vein can be accessed. Injecting UCAs through a central venous line or port requires a higher level of expertise to ensure a successful injection. Bubble disruption may also be increased necessitating a dose increase. The use of a central venous line requires a 3-way stopcock. Contrast arrival times are usually significantly shorter in case of a central-venous administration, a fact which might favour starting the timer earlier, at the beginning of the contrast injection.

Contrast agent dose

Using the optimal dose is important. Too high a contrast agent dose results in artefacts, particularly in the early phases of enhancement.

These include acoustic shadowing, over-enhancement of small structures and signal saturation, which is also detrimental for quantification. On the other hand, too low a dose causes the concentration of microbubbles to be subdiagnostic in the late phase, challenging the detection of wash out. If the liver washes out early, the dose was probably too low or inherent significant intrahepatic shunting may prevent a longer enhancement time. Again, it is important to evaluate the status of the liver as being healthy or diseased. In difficult cases, a second (higher) dose may be administered, with no or only limited scanning in the early phases [40] to reduce bubble destruction. The exact dose depends on the UCA, ultrasound equipment (software version, transducer), type of examination, organ and target lesion, size and age of the patient and other factors.

For SonoVue™/Lumason™, 2.4 ml (1/2 vial) is recommended for most indications in the liver (detection, characterisation) but many investigators are now using 1.2 ml (this topic has been controversially discussed with co-authors and the reviewers).

For SonoVue™/Lumason™, 2.4 ml (1/2 vial) is the standard dose for most indications in the pancreas, spleen and kidney. For the pancreas, spleen and kidney, 1.2 ml often suffices. Depending on scanning conditions and depth of the lesion (organ) even lower doses can be used. For high frequency applications 4.8 ml is suggested. In particular, endoscopic ultrasound usually requires the complete vial of 4.8 ml [51–53]. For the extravascular (intraluminal) use only few drops diluted in normal saline solution are necessary. For Definity™ and Optison™ a standard dose is 0.2–0.3 ml for an adult. For Sonazoid™ a dose of 0.015 ml/kg (e. g., 0.5–1.0 ml) of the reconstituted suspension is recommended.

Repeated injection

Multiple injections of UCA are variably indicated and influenced mainly by the manufacturing of the different solutions and the volume needed to provide good visualization of the liver and a focal liver mass. SonoVue™/Lumason™, supplied in a 4.8 ml aliquot may allow for two or possibly three or four injections per vial, whereas Definity™, supplied in a 1.3 ml vial, which expands to 1.8 ml in solution may allow for multiple injections as needed (easily 6 or 7) as a standard bolus would generally be only 0.2–0.3 ml. For Sonazoid™ supplied in a 2 ml vial, a dose of 0.5–1.0 ml per injection (0.015 ml/kg) is recommended.

Repeated injection may occur in the following circumstances:

- There are additional nodules or observations, which require characterization.
- The initial injection may not provide the full answer to the characterization of a lesion, requiring a second injection to allow for assessment of missing information.
- A wash-out region may be identified on sweeps of the liver in either the PVP or the LP. Even if a corresponding nodule is not visible on the conventional B-mode images, arterial phase enhancement in the wash-out region can be characterized by re-injecting contrast material while keeping that region in the field of view.

For the first two indications above, the examiner usually should wait before reinjecting until the bubbles from the previous injection have disappeared or least greatly reduced, which usually requires 10 to 15 min for SonoVue™/Lumason™ and Definity™ also

depending on patient age and constitution. The waiting period is much longer for Sonazoid™, the disappearance of bubbles may take longer than one hour. To expedite bubble destruction and reduce the delay for re-injection, continuous scanning at high MI, such as B-mode or colour Doppler can be performed including the heart and kidney. To assess arterial enhancement of a wash-out region that does not have a correlate on B-mode imaging, by comparison, the examiner should re-inject before bubbles have disappeared so as to maintain visibility of the wash-out region.

Continuous Infusion

Dynamic real-time characterization of focal liver masses with CEUS is best performed with a bolus technique. However, measurement of blood flow parameters for assessment of oncologic response to therapy is also possible with an infusion and the destruction-replenishment technique. The agent is, depending on the contrast agent, suspended in saline or other media and intravenously infused with controlled pressure, to avoid bubble destruction and at a constant rate to permit prolonged scanning. This technique provides a steady-state bubble concentration which can be used with the burst and replenish mode (manoeuvre) to generate multiple measurements. For Definity™, where bubble flotation is not usually an issue, the agent can be mixed in a 50 ml saline bag. For SonoVue™, a dedicated infusion pump is recommended. For more details see the EFSUMB guidelines [11].

Contrast timer

All ultrasound scanners must have a visible timer. This timer should be started at the time of the beginning of the UCA injection for SonoVue™/Lumason™. With Definity™, no CA enters the body prior to the flush. The authors controversially discussed when to start the timer. Most (but not all) of the group agreed that the timer should be started at the beginning of the contrast injection. The application via a central venous line with much shorter arrival time is a good reason for this. It should be noted that in special situations (e. g., right heart insufficiency) contrast phases may appear at unusual time points including potential initial retrograde inflow via the liver vein.

Artefacts

Nonlinear propagation artefact

A pseudo-enhancement of tissue has been reported in the literature where targets in tissue are registered as bubble signals [54–56]. It has been suggested that the artefact is the result of nonlinear propagation of ultrasound in tissue perfused with a high concentration of microbubbles. The presence of microbubbles effectively increases the nonlinear coefficient of the “bulk” medium causing some nonlinear propagation to occur despite using low MI to prevent this phenomenon. Thus, when bright targets are encountered in the ultrasound path they produce echoes with nonlinear components caused by nonlinear propagation rather than by microbubble scattering. This pseudo-enhancement can be differentiated from true bubble signals by recognizing their non-physiologic nature, or by comparing the bubble image with the tissue image and identifying the same bright targets in both images. A

way to reduce this artefact is to avoid high doses of contrast agents, and/or avoid having a large vessel in the ultrasound path proximal to the area/lesion of interest. In clinical practice, this is problematic most often in the follow up of treatment sites following ablative therapy for liver tumours [57]. A bright echogenic focus within the treatment zone may show linear artefact which may be mistaken for residual or recurrent tumour. Clues to the correct interpretation include lack of arterial phase enhancement dynamics, when a real tumour would be perfused, and increasing pseudoenhancement in the portal and delayed phases attributed to the nonlinear artefact as bubbles fill the portal system.

How to avoid artefacts?

The ideal is to find a good compromise between the contrast agent dose and the equipment-specific settings. The MI and the transmit frequency (“penetration mode”) play a crucial role here. This balances the signal intensity and penetration on the one hand, and the stability of the microbubbles on the other hand. A higher MI results in a stronger signal and better penetration but also increased destruction of the microbubbles. The contrast agent dose balances the contrast enhancement intensity in the early phase (prevention of the over saturation of structures with shadowing) and the contrast enhancement duration (sufficient contrast agent concentration in the late phase).

The CEUS “circle of disaster” is characterized by the following criteria: Microbubble destruction → increase in contrast agent dose → attenuation (shadowing) → higher mechanical index → additional microbubble destruction [40, 41, 58].

In conclusion, if the MI is too high, an increase of UCA dose to compensate may cause additional attenuation. Further influencing factors are gain, dynamic range, frame rate, transmission frequency, and equipment software [40]. Most often, the default settings on the machine provide an excellent starting point for beginning CEUS studies of the liver. For more details on CEUS artefacts we refer to the current literature [40, 55–59].

Prolonged Liver Enhancement

Prolonged innocuous liver enhancement after the bolus injection of microbubble contrast agents appears as a heterogeneous enhancement in the liver during the performance of the CEUS examination, often beginning at around 2 min and lasting up to 5 h after contrast injection on both B-mode and contrast-specific modes. It is not destroyed by conventional B-mode imaging. The enhanced signals can also be observed in the portal and superior mesenteric veins, though not in the systemic circulation [60]. It is similar in appearance to the US finding of free portal venous gas.

Safety of CEUS

As mentioned earlier, UCAs are safe with a very low incidence of side effects. As there are no cardio-, hepato-, or nephro-toxic effects, it is not necessary to perform laboratory checks to assess liver, renal or thyroid function before administration. The incidence of severe adverse events is lower than with current X-ray contrast agents and is comparable to those encountered with MR contrast

agents. Life-threatening anaphylactic reactions in abdominal applications have been reported with a rate of 0.001 %, with no death in a series of > 23,000 abdominal patients [46]. Further studies have reproduced this very low adverse event rate [61, 62]. Nonetheless, investigators should be trained in resuscitation and have the appropriate facilities available to react in cases of adverse events [4, 38]. In particular, each centre should be prepared with a crash cart and ability to treat anaphylactic shock if it occurs.

Paediatric Patients and Newborns

The use of CEUS in children, first reported in 2002, has been addressed in an EFSUMB position statement discussing the current status of CEUS and its further development in children [63]. Currently sulphur hexafluoride gas microbubbles (SonoVue™/Lumason™, Bracco SpA, Milan) has been approved in the United States by the Food and Drug Administration (FDA) as Lumason™ for characterising focal liver lesions in children [“Lumason is indicated for use with ultrasound of the liver in adult and pediatric patients to characterize focal liver lesions”] and vesico-ureteral reflux. In Europe, CEUS in children is mostly “off-label” use, except for a few indications including vesico-ureteral reflux [64]. The same is true for many drugs, which are used off-label in paediatric practice and the question of “off label use” has been widely discussed [65, 66]. The recent approval of SonoVue™/Lumason™ for use in paediatrics in the United States is a welcome first step towards the acceptance of this technique in the non-ionising imaging of children [67].

CEUS-guided Interventions

CEUS-guided interventions for practical considerations is performed very much like a standard US guided procedure except that two injections of UCAs are used, one to plan the procedure and a second to guide the actual intervention. In some cases, a continuous infusion may be the better choice while in other cases the procedure may be performed without a second contrast injection if the perfusion conditions are adequately demonstrated with the first CEUS to allow for a standard ultrasound guided procedure. CEUS-guided biopsy has been reported to increase the diagnostic accuracy rate by up to 10 % either by directing the biopsy towards contrast-enhanced – and thus viable – tissue inside the tumour and thereby avoiding sampling of necrotic material, or by identifying previously not-visualised lesions more accessible for biopsy [4, 68–72]. Furthermore, CEUS may visualise active bleeding, hemobilia or segmental liver infarction.

CEUS is also helpful in performing and follow-up for radiofrequency ablation or cryotherapy for hepatic and renal masses [37, 73, 74]. CEUS allows evaluation of the extent of the ablated zone at the end of the procedure. If residual tumour is identified, the ablation can be extended after repositioning the needle to the residual tumour using CEUS guidance. On follow-up studies, CEUS is able to identify - immediately following treatment - small amounts of residual tumour, which can be too small or too soon to detect with CECT or CTMRI [75, 76].

Extravascular, Intracavitary

Extravascular (intracavitary) CEUS (EV-CEUS) is used for imaging physiological and non-physiological body cavities. Physiological cavities include the peritoneal cavity, pleural cavity, biliary tract, gastrointestinal tract, urinary tract, etc. and pathological cavities include abscesses, cysts, diverticula, etc. [68, 77]. The UCA is given through a needle or catheter, for instance, at cholangiography or nephrostomy. However, UCAs can also be given orally or as an enema for imaging the upper and lower gastrointestinal tract [78, 79].

The following clinical applications of EV-CEUS have been described in case studies: percutaneous nephrostomy [80], biliary tract imaging via percutaneous transhepatic cholangiography and drainage (PTCD) [81], abscess drainage [82], swallow CEUS for imaging Zenker's diverticulum, voiding vesicoureteral reflux sonography [83, 84], salivary gland duct imaging [85], contrast-enhanced hysterosalpingo-sonography (CE-HyCoSy [86], biliary tract imaging via endoscopic retrograde cholangiography (ERCP) [87] and fistula imaging [88].

The transducer used in extravascular CEUS is the same as that used in conventional US. SonoVue™ is currently the most often used UCA for VUR [89] though it is not licensed for other extravascular indications of CEUS. To date, no standard dosage of UCA has been established for extravascular CEUS. The reported range is 0.1 ml–1 ml SonoVue™ (most commonly just a few drops) diluted in 50 ml or more of 0.9% saline. A higher content of SonoVue™ may be needed for high frequency US probes [68]. Compared with X-ray contrast techniques, EV-CEUS does not require exposure to ionizing radiation and can be performed at the bedside.

Education, Qualification

The World Health Organization (WHO) estimates that 2/3 of the world's population lacks access to medical imaging [90]. Ultrasound (US) with CEUS may provide a way forwards. Investigators and clinicians wishing to perform CEUS examinations should gain experience by observing contrast studies performed by experts in the field [91]. The diagnostic performance of CEUS is correlated with the observer's level of experience [58, 92]. The examiner should also verify that his or her equipment is optimized for contrast examination and that the volume and diversity of cases will suffice to maintain skills. Practitioners need to be competent in the intravenous administration of contrast agents, be familiar with contraindications and be able to manage any possible adverse effects within the medical and legal framework of their country [4, 38]. We refer to the educational activities of the collaborating societies of this paper, the World Federation of Ultrasound in Medicine and Biology (WFUMB) [9, 23, 93–102], the European Federation of Societies for Ultrasound in Medicine and Biology (EFSUMB) [1, 3, 4, 11, 37, 38, 49, 50, 74, 79, 103–119] and the CEUS LI-RADS Working Group for Liver Imaging Reporting and Data System (LI-RADS®) [34–36, 120–124].

Conclusion

High-quality performance of CEUS is experience-dependent and requires regular use and understanding of the relevant physics,

technical adjustments and contrast media variability. Each individual case requires detailed analysis of the enhancement patterns in all vascular and post-vascular phases. Despite the regulatory and practice obstacles for the use of UCAs for CEUS, the evidence indicates that CEUS can provide unique and accurate diagnostic information, in many cases also comparable and sometimes superior to the performance of CT and MRI [125–127].

Acknowledgement

We were all saddened by the news of David Cosgrove's death in May 2017 following a gallant battle with cancer. David Cosgrove was an esteemed teacher, prominent researcher and a good friend. He will be missed by all. We express our sincere condolences.

Conflict of Interest

Some authors declare conflicts of interest, which are available by the publisher and as supplementary file.

References

- [1] Albrecht T, Blomley M, Bolondi L, Claudon M, Correas JM, Cosgrove D, Greiner L et al. Guidelines for the use of contrast agents in ultrasound. January 2004. *Ultraschall Med.* 2004; 25: 249–256
- [2] Claudon M, Cosgrove D, Albrecht T, Bolondi L, Bosio M, Calliada F, Correas JM et al. Guidelines and good clinical practice recommendations for contrast enhanced ultrasound (CEUS) - Update 2008. *Ultraschall Med.* 2008; 29: 28–44
- [3] Piscaglia F, Nolsoe C, Dietrich CF, Cosgrove DO, Gilja OH, Bachmann NM, Albrecht T et al. The EFSUMB guidelines and recommendations on the clinical practice of contrast enhanced ultrasound (CEUS): Update 2011 on non-hepatic applications. *Ultraschall Med.* 2012; 33: 33–59
- [4] Claudon M, Dietrich CF, Choi BI, Cosgrove DO, Kudo M, Nolsoe CP, Piscaglia F et al. Guidelines and good clinical practice recommendations for contrast enhanced ultrasound (CEUS) in the liver - update 2012: a WFUMB-EFSUMB initiative in cooperation with representatives of AFSUMB, AIUM, ASUM, FLAUS and ICUS. *Ultraschall Med* 2013; 34: 11–29
- [5] Claudon M, Dietrich CF, Choi BI, Cosgrove DO, Kudo M, Nolsoe CP, Piscaglia F et al. Guidelines and good clinical practice recommendations for Contrast Enhanced Ultrasound (CEUS) in the liver - update 2012: A WFUMB-EFSUMB initiative in cooperation with representatives of AFSUMB, AIUM, ASUM, FLAUS and ICUS. *Ultrasound Med Biol* 2013; 39: 187–210
- [6] Dietrich CF, Ignee A, Trojan J, Fellbaum C, Schuessler G. Improved characterisation of histologically proven liver tumours by contrast enhanced ultrasonography during the portal venous and specific late phase of SHU 508 A. *Gut* 2004; 53: 401–405
- [7] Dietrich CF, Schuessler G, Trojan J, Fellbaum C, Ignee A. Differentiation of focal nodular hyperplasia and hepatocellular adenoma by contrast-enhanced ultrasound. *Br.J.Radiol.* 2005; 78: 704–707
- [8] Dietrich CF. Signalverstärkte Leber-sonographie zur verbesserten Detektion und Charakterisierung von Leber-raumforderungen. *Dt Aertzblatt* 2002; 24: 7
- [9] Dietrich CF. [3D real time contrast enhanced ultrasonography, a new technique]. *Rofo* 2002; 174: 160–163

- [10] Dietrich CF, Brunner V, Braden B, Zeuzem S, Caspary WF. Erste Erfahrungen mit einem neuen Signalverstärker bei der Untersuchung der Leber. *Ultraschall Med* 1998; 19:
- [11] Dietrich CF, Averkiou MA, Correas JM, Lassau N, Leen E, Piscaglia F. An EFSUMB introduction into Dynamic Contrast-Enhanced Ultrasound (DCE-US) for quantification of tumour perfusion. *Ultraschall Med* 2012; 33: 344–351
- [12] Ignee A, Jedrejczyk M, Schuessler G, Jakubowski W, Dietrich CF. Quantitative contrast enhanced ultrasound of the liver for time intensity curves-Reliability and potential sources of errors. *Eur J Radiol* 2010; 73: 153–158
- [13] Lassau N, Cosgrove D, Armand JP. Early evaluation of targeted drugs using dynamic contrast-enhanced ultrasonography for personalized medicine. *Future Oncol* 2012; 8: 1215–1218
- [14] Lassau N, Koscielny S, Chami L, Chebil M, Benatsou B, Roche A, Ducreux M et al. Advanced hepatocellular carcinoma: early evaluation of response to bevacizumab therapy at dynamic contrast-enhanced US with quantification—preliminary results. *Radiology* 2011; 258: 291–300
- [15] Lassau N, Koscielny S, Albiges L, Chami L, Benatsou B, Chebil M, Roche A et al. Metastatic renal cell carcinoma treated with sunitinib: early evaluation of treatment response using dynamic contrast-enhanced ultrasonography. *Clin Cancer Res* 2010; 16: 1216–1225
- [16] Frampas E, Lassau N, Zappa M, Vullierme MP, Koscielny S, Vilgrain V. Advanced Hepatocellular Carcinoma: early evaluation of response to targeted therapy and prognostic value of Perfusion CT and Dynamic Contrast Enhanced-Ultrasound. Preliminary results. *Eur J Radiol* 2013; 82: e205–e211
- [17] Williams R, Hudson JM, Lloyd BA, Sureshkumar AR, Lueck G, Milot L, Atri M et al. Dynamic microbubble contrast-enhanced US to measure tumor response to targeted therapy: A proposed clinical protocol with results from renal cell carcinoma patients receiving antiangiogenic therapy. *Radiology* 2011; 260: 581–590
- [18] Leen E, Averkiou M, Arditi M, Burns P, Bokor D, Gauthier T, Kono Y et al. Dynamic contrast enhanced ultrasound assessment of the vascular effects of novel therapeutics in early stage trials. *Eur Radiol* 2012; 22: 1442–1450
- [19] Serra C, Menozzi G, Labate AM, Giangregorio F, Gionchetti P, Beltrami M, Robotti D et al. Ultrasound assessment of vascularization of the thickened terminal ileum wall in Crohn's disease patients using a low-mechanical index real-time scanning technique with a second generation ultrasound contrast agent. *Eur J Radiol* 2007; 62: 114–121
- [20] Atkinson NS, Bryant RV, Dong Y, Maaser C, Kucharzik T, Maconi G, Asthana AK et al. WFUMB Position Paper. Learning gastrointestinal ultrasound: Theory and practice. *Ultrasound Med Biol* 2016; 42: 2732–2742
- [21] Nylund K, Maconi G, Hollerweger A, Ripolles T, Pallotta N, Higginson A, Serra C et al. EFSUMB recommendations and guidelines for gastrointestinal ultrasound. *Ultraschall Med* 2017; 38: e1–e15
- [22] Nylund K, Maconi G, Hollerweger A, Ripolles T, Pallotta N, Higginson A, Serra C et al. EFSUMB recommendations and guidelines for gastrointestinal ultrasound. *Ultraschall Med* 2017; 38: 273–284
- [23] Hocke M, Dietrich CF. New technology—combined use of 3D contrast enhanced endoscopic ultrasound techniques. *Ultraschall Med* 2011; 32: 317–318
- [24] Hocke M, Ignee A, Dietrich CF. Three-dimensional contrast-enhanced endoscopic ultrasound for the diagnosis of autoimmune pancreatitis. *Endoscopy* 2011; 43: (Suppl 2): UCTN E381–E382
- [25] Fusaroli P, Saftoiu A, Dietrich CF. Contrast-enhanced endoscopic ultrasound: Why do we need it? A foreword. *Endosc Ultrasound* 2016
- [26] Dietrich CF, Sharma M, Hocke M. Contrast-enhanced endoscopic ultrasound. *Endosc Ultrasound* 2012; 1: 130–136
- [27] Solbiati L, Tonolini M, Cova L, Goldberg SN. The role of contrast-enhanced ultrasound in the detection of focal liver lesions. *Eur Radiol* 2001; 11: (Suppl 3): E15–E26
- [28] D'Onofrio M, Martone E, Faccioli N, Zamboni G, Malago R, Mucelli RP. Focal liver lesions: Sinusoidal phase of CEUS. *Abdom Imaging* 2006; 31: 529–536
- [29] Strobel D, Seitz K, Blank W, Schuler A, Dietrich C, von Herbay A, Friedrich-Rust M et al. Contrast-enhanced ultrasound for the characterization of focal liver lesions—diagnostic accuracy in clinical practice (DEGUM multicenter trial). *Ultraschall Med* 2008; 29: 499–505
- [30] Bernatik T, Seitz K, Blank W, Schuler A, Dietrich CF, Strobel D. Unclear focal liver lesions in contrast-enhanced ultrasonography—lessons to be learned from the DEGUM multicenter study for the characterization of liver tumors. *Ultraschall Med* 2010; 31: 577–581
- [31] Seitz K, Greis C, Schuler A, Bernatik T, Blank W, Dietrich CF, Strobel D. Frequency of tumor entities among liver tumors of unclear etiology initially detected by sonography in the noncirrhotic or cirrhotic livers of 1349 patients. Results of the DEGUM multicenter study. *Ultraschall Med* 2011; 32: 598–603
- [32] Strobel D, Bernatik T, Blank W, Schuler A, Greis C, Dietrich CF, Seitz K. Diagnostic accuracy of CEUS in the differential diagnosis of small ($\leq 20\text{ mm}$) and subcentimetric ($\leq 10\text{ mm}$) focal liver lesions in comparison with histology. Results of the DEGUM multicenter trial. *Ultraschall Med* 2011; 32: 593–597
- [33] Jo PC, Jang HJ, Burns PN, Burak KW, Kim TK, Wilson SR. Integration of Contrast-enhanced US into a Multimodality Approach to Imaging of Nodules in a Cirrhotic Liver: How I Do It. *Radiology* 2017; 282: 317–331
- [34] Dietrich CF, Kono Y, DC Jang HJ, Kim TK, Piscaglia F, Sirlin CB et al. Contrast-Enhanced Ultrasound: Liver Imaging Reporting and Data System (CEUS LI-RADS). In. <http://www.solutionsincontrastimaging.com/> 2016;
- [35] Kono Y, Lyshchik A, Cosgrove D, Dietrich CF, Jang HJ, Kim TK, Piscaglia F et al. Contrast Enhanced Ultrasound (CEUS) Liver Imaging Reporting and Data System (LI-RADS(R)): The official version by the American College of Radiology (ACR). *Ultraschall Med* 2017; 38: 85–86
- [36] Piscaglia F, Wilson SR, Lyshchik A, Cosgrove D, Dietrich CF, Jang HJ, Kim TK et al. American College of Radiology Contrast Enhanced Ultrasound Liver Imaging Reporting and Data System (CEUS LI-RADS) for the diagnosis of Hepatocellular Carcinoma: A pictorial essay. *Ultraschall Med* 2017
- [37] Dietrich CF, Lorentzen T, Appelbaum L, Buscarini E, Cantisani V, Correas JM, Cui XW et al. EFSUMB Guidelines on Interventional Ultrasound (INVUS), Part III - Abdominal Treatment Procedures (Long Version). *Ultraschall Med* 2016; 37: E1–E32
- [38] Claudon M, Dietrich CF, Choi BI, Cosgrove DO, Kudo M, Nolsoe CP, Piscaglia F et al. Guidelines and good clinical practice recommendations for Contrast Enhanced Ultrasound (CEUS) in the liver – update 2012: A WFUMB-EFSUMB initiative in cooperation with representatives of AFSUMB, AIUM, ASUM, FLAUS and ICUS. *Ultrasound Med Biol* 2013; 39: 187–210
- [39] Kudo M. Defect Reperfusion Imaging with Sonazoid(R): A Breakthrough in Hepatocellular Carcinoma. *Liver Cancer* 2016; 5: 1–7
- [40] Dietrich CF, Ignee A, Greis C, Cui XW, Schreiber-Dietrich DG, Hocke M. Artifacts and pitfalls in contrast-enhanced ultrasound of the liver. *Ultraschall Med* 2014; 35: 108–125 quiz 126-107
- [41] Dietrich CF, Greis C. [How to perform contrast enhanced ultrasound]. *Dtsch Med Wochenschr* 2016; 141: 1019–1024

- [42] Lassau N, Bonastre J, Kind M, Vilgrain V, Lacroix J, Cuiet M, Taieb S et al. Validation of dynamic contrast-enhanced ultrasound in predicting outcomes of antiangiogenic therapy for solid tumors: The French multicenter support for innovative and expensive techniques study. *Invest Radiol* 2014; 49: 794–800
- [43] O'Connor JP, Aboagye EO, Adams JE, Aerts HJ, Barrington SF, Beer AJ, Boellaard R et al. Imaging biomarker roadmap for cancer studies. *Nat Rev Clin Oncol* 2017; 14: 169–186
- [44] Averkiou M, Lampaskis M, Kyriakopoulou K, Skarlos D, Klouvas G, Strouthos C, Leen E. Quantification of tumor microvasculature with respiratory gated contrast enhanced ultrasound for monitoring therapy. *Ultrasound Med Biol* 2010; 36: 68–77
- [45] Lassau N, Chapotot L, Benatsou B, Vilgrain V, Kind M, Lacroix J, Cuiet M et al. Standardization of dynamic contrast-enhanced ultrasound for the evaluation of antiangiogenic therapies: The French multicenter Support for Innovative and Expensive Techniques Study. *Invest Radiol* 2012; 47: 711–716
- [46] Piscaglia F, Bolondi L. Italian Society for Ultrasound in M, Biology study group on ultrasound contrast A. The safety of Sonovue in abdominal applications: retrospective analysis of 23188 investigations. *Ultrasound Med Biol* 2006; 32: 1369–1375
- [47] Appis AW, Tracy MJ, Feinstein SB. Update on the safety and efficacy of commercial ultrasound contrast agents in cardiac applications. *Echo Res Pract* 2015; 2: R55–R62
- [48] Eisenbrey JR, Daecher A, Kramer MR, Forsberg F. Effects of Needle and catheter size on commercially available ultrasound contrast agents. *J Ultrasound Med* 2015; 34: 1961–1968
- [49] Jenssen C, Brkljacic B, Hocke M, Ignee A, Piscaglia F, Radjina M, Sidhu PS et al. EFSUMB Guidelines on Interventional Ultrasound (INVUS), Part VI - Ultrasound-Guided Vascular Interventions. *Ultraschall Med* 2015
- [50] Dietrich CF, Horn R, Morf S, Chiorean L, Dong Y, Cui XW, Atkinson N et al. US-guided peripheral vascular interventions, comments on the EFSUMB guidelines. *Med Ultrason* 2016; 18: 231–239
- [51] Dietrich CF, Sahai AV, D'Onofrio M, Will U, Arcidiacono PG, Petrone MC, Hocke M et al. Differential diagnosis of small solid pancreatic lesions. *Gastrointest Endosc* 2016; 84: 933–940
- [52] Ignee A, Atkinson NS, Schuessler G, Dietrich CF. Ultrasound contrast agents. *Endosc Ultrasound* 2016
- [53] Ignee A, Jenssen C, Hocke M, Dong Y, Wang WP, Cui XW, Woenckhaus M et al. Contrast-enhanced (endoscopic) ultrasound and endoscopic ultrasound elastography in gastrointestinal stromal tumors. *Endosc Ultrasound* 2017; 6: 55–60
- [54] Yildiz YO, Eckersley RJ, Senior R, Lim AK, Cosgrove D, Tang MX. Correction of Non-Linear Propagation Artifact in Contrast-Enhanced Ultrasound Imaging of Carotid Arteries: Methods and in Vitro Evaluation. *Ultrasound Med Biol* 2015; 41: 1938–1947
- [55] Renaud G, Bosch JG, Ten Kate GL, Shamdasani V, Entekin R, de Jong N, van der Steen AF. Counter-propagating wave interaction for contrast-enhanced ultrasound imaging. *Phys Med Biol* 2012; 57: L9–L18
- [56] Thapar A, Shalhoub J, Averkiou M, Mannaris C, Davies AH, Leen EL. Dose-dependent artifact in the far wall of the carotid artery at dynamic contrast-enhanced US. *Radiology* 2012; 262: 672–679
- [57] Yu H, Jang HJ, Kim TK, Khalili K, Williams R, Lueck G, Hudson J et al. Pseudoenhancement within the local ablation zone of hepatic tumors due to a nonlinear artifact on contrast-enhanced ultrasound. *AJR Am J Roentgenol* 2010; 194: 653–659
- [58] Greis C. Technical aspects of contrast-enhanced ultrasound (CEUS) examinations: Tips and tricks. *Clin Hemorheol Microcirc* 2014; 58: 89–95
- [59] Dietrich CF, Ignee A, Hocke M, Schreiber-Dietrich D, Greis C. Pitfalls and artefacts using contrast enhanced ultrasound. *Z Gastroenterol* 2011; 49: 350–356
- [60] Cui XW, Ignee A, Hocke M, Seitz K, Schrade G, Dietrich CF. Prolonged heterogeneous liver enhancement on contrast-enhanced ultrasound. *Ultraschall Med* 2014; 35: 246–252
- [61] Kusnetzky LL, Khalid A, Khumri TM, Moe TG, Jones PG, Main ML. Acute mortality in hospitalized patients undergoing echocardiography with and without an ultrasound contrast agent: Results in 18,671 consecutive studies. *J Am Coll Cardiol* 2008; 51: 1704–1706
- [62] Main ML, Ryan AC, Davis TE, Albano MP, Kusnetzky LL, Hibberd M. Acute mortality in hospitalized patients undergoing echocardiography with and without an ultrasound contrast agent (multicenter registry results in 4,300,966 consecutive patients). *Am J Cardiol* 2008; 102: 1742–1746
- [63] Sidhu PS, Cantisani V, Deganello A, Dietrich CF, Duran C, Franke D, Harkanyi Z et al. Role of Contrast-Enhanced Ultrasound (CEUS) in Paediatric Practice: An EFSUMB Position Statement. *Ultraschall Med* 2016
- [64] Schreiber-Dietrich DG, Cui XW, Piscaglia F, Gilja OH, Dietrich CF. Contrast enhanced ultrasound in pediatric patients: A real challenge. *Z Gastroenterol* 2014; 52: 1178–1184
- [65] Dietrich CF, Maurer M, Riemer-Hommel P. Challenges for the German Health Care System – Pharmaceuticals. *Endheue* 2014; 27: 45–53
- [66] Esposito F, Di Serafino M, Sgambati P, Mercogliano F, Tarantino L, Vallone G, Oresta P. Ultrasound contrast media in paediatric patients: is it an off-label use? Regulatory requirements and radiologist's liability. *Radiol Med* 2012; 117: 148–159
- [67] Chiorean L, Cui XW, Tannapfel A, Franke D, Stenzel M, Kosiak W, Schreiber-Dietrich D et al. Benign liver tumors in pediatric patients – Review with emphasis on imaging features. *World J Gastroenterol* 2015; 21: 8541–8561
- [68] Piscaglia F, Nolsoe C, Dietrich CF, Cosgrove DO, Gilja OH, Bachmann Nielsen M, Albrecht T et al. The EFSUMB Guidelines and Recommendations on the Clinical Practice of Contrast Enhanced Ultrasound (CEUS): update 2011 on non-hepatic applications. *Ultraschall Med* 2012; 33: 33–59
- [69] Wu W, Chen MH, Yin SS, Yan K, Fan ZH, Yang W, Dai Y et al. The role of contrast-enhanced sonography of focal liver lesions before percutaneous biopsy. *AJR Am J Roentgenol* 2006; 187: 752–761
- [70] Bang N, Bachmann Nielsen M, Vejborg I, Mellon Mogensen A. Clinical report: Contrast enhancement of tumor perfusion as a guidance for biopsy. *Eur J Ultrasound* 2000; 12: 159–161
- [71] Sparchez Z, Radu P, Zaharia T, Kacso G, Grigorescu I, Botis G, Badea R. Usefulness of contrast enhanced ultrasound guidance in percutaneous biopsies of liver tumors. *J Gastrointest Liver Dis* 2011; 20: 191–196
- [72] Yoon SH, Lee KH, Kim SY, Kim YH, Kim JH, Lee SH, Kim TK. Real-time contrast-enhanced ultrasound-guided biopsy of focal hepatic lesions not localised on B-mode ultrasound. *Eur Radiol* 2010; 20: 2047–2056
- [73] Lackey L 2nd, Peterson C, Barr RG. Contrast-enhanced ultrasound-guided radiofrequency ablation of renal tumors. *Ultrasound Q* 2012; 28: 269–274
- [74] Dietrich CF, Lorentzen T, Appelbaum L, Buscarini E, Cantisani V, Correas JM, Cui XW et al. EFSUMB Guidelines on Interventional Ultrasound (INVUS), Part III - Abdominal Treatment Procedures (Short Version). *Ultraschall Med* 2016; 37: 27–45
- [75] Sanz E, Hevia V, Arias F, Fabuel JJ, Alvarez S, Rodriguez-Patron R, Gomez V et al. Contrast-enhanced ultrasound (CEUS): An excellent tool in the follow-up of small renal masses treated with cryoablation. *Curr Urol Rep* 2015; 16: 469
- [76] Meloni MF, Bertolotto M, Alberzoni C, Lazzaroni S, Filice C, Livraghi T, Ferraioli G. Follow-up after percutaneous radiofrequency ablation of renal cell carcinoma: Contrast-enhanced sonography versus contrast-enhanced CT or MRI. *AJR Am J Roentgenol* 2008; 191: 1233–1238

- [77] Ignee A, Schuessler G, Cui XW. Endocavernous Contrast-Enhanced Ultrasound – Different Applications, Literature Review and Future Perspectives. *Ultraschall Med* 2013; 34: 2–26
- [78] Nylund K, Maconi G, Hollerweger A, Ripolles T, Pallotta N, Higginson A, Serra C et al. EFSUMB Recommendations and Guidelines for Gastrointestinal Ultrasound - Part 1: Examination Techniques and Normal Findings (Long version). *Ultraschall Med* 2016
- [79] Nylund K, Maconi G, Hollerweger A, Ripolles T, Pallotta N, Higginson A, Serra C et al. EFSUMB Recommendations and Guidelines for Gastrointestinal Ultrasound - Part 1: Examination Techniques and Normal Findings (Short version). *Ultraschall Med* 2016
- [80] Cui XW, Ignee A, Maros T, Straub B, Wen JG, Dietrich CF. Feasibility and Usefulness of Intra-Cavitary Contrast-Enhanced Ultrasound in Percutaneous Nephrostomy. *Ultrasound Med Biol* 2016; 42: 2180–2188
- [81] Ignee A, Cui X, Schuessler G, Dietrich CF. Percutaneous transhepatic cholangiography and drainage using extravascular contrast enhanced ultrasound. *Z Gastroenterol* 2015; 53: 385–390
- [82] Ignee A, Jenssen C, Cui XW, Schuessler G, Dietrich CF. Intracavitary contrast-enhanced ultrasound in abscess drainage—feasibility and clinical value. *Scand J Gastroenterol* 2016; 51: 41–47
- [83] Darge K. Voiding urosonography with US contrast agents for the diagnosis of vesicoureteric reflux in children. II. Comparison with radiological examinations. *Pediatr Radiol* 2008; 38: 54–63 quiz 126–127
- [84] Darge K. Voiding urosonography with ultrasound contrast agents for the diagnosis of vesicoureteric reflux in children. I. Procedure. *Pediatr Radiol* 2008; 38: 40–53
- [85] Zengel P, Siedek V, Berghaus A, Clevert DA. Intraductally applied contrast-enhanced ultrasound (IA-CEUS) for improved visualization of obstructive diseases of the salivary glands, primary results. *Clin Hemorheol Microcirc* 2010; 45: 193–205
- [86] Lanzani C, Savasi V, Leone FP, Ratti M, Ferrazzi E. Two-dimensional HyCoSy with contrast tuned imaging technology and a second-generation contrast media for the assessment of tubal patency in an infertility program. *Fertil Steril* 2009; 92: 1158–1161
- [87] Zuber-Jerger I, Endlicher E, Scholmerich J, Klebl F. Endoscopic retrograde cholangiography with contrast ultrasonography. *Endoscopy* 2008; 40: (Suppl 2): E202
- [88] Chew SS, Yang JL, Newstead GL, Douglas PR. Anal fistula: Levovist-enhanced endoanal ultrasound: a pilot study. *Dis Colon Rectum* 2003; 46: 377–384
- [89] Rosch T, Meining A, Fruhmorgen S, Zillinger C, Schusdziarra V, Hellerhoff K, Classen M et al. A prospective comparison of the diagnostic accuracy of ERCP, MRCP, CT, and EUS in biliary strictures. *Gastrointest Endosc* 2002; 55: 870–876
- [90] Hussain S. Welcome to the Journal of Global Radiology. *Journal of Global Radiology* 2015; 1: 1–2
- [91] EFSUMB. Minimum training recommendations for the practice of medical ultrasound (European Federation of Societies for Ultrasound in Medicine Biology Practical Standards Committee). *Ultraschall Med* 2006; 27: 79–105
- [92] Quaiá E, Alaimo V, Baratella E, Pizzolato R, Cester G, Medeot A, Cova MA. Effect of observer experience in the differentiation between benign and malignant liver tumors after ultrasound contrast agent injection. *J Ultrasound Med* 2010; 29: 25–36
- [93] Dong FJ, Xu JF, Du D, Jiao Y, Zhang L, Li M, Liu HY et al. 3D analysis is superior to 2D analysis for contrast-enhanced ultrasound in revealing vascularity in focal liver lesions – A retrospective analysis of 83 cases. *Ultrasonics* 2016; 70: 221–226
- [94] Eisenbrey JR, Sridharan A, Machado P, Zhao H, Halldorsdottir VG, Dave JK, Liu JB et al. Three-dimensional subharmonic ultrasound imaging in vitro and in vivo. *Academic Radiology* 2012; 19: 732–739
- [95] Feingold S, Gessner R, Guracar IM, Dayton PA. Quantitative volumetric perfusion mapping of the microvasculature using contrast ultrasound. *Invest Radiol* 2010; 45: 669–674
- [96] Bamber J, Cosgrove D, Dietrich CF, Fromageau J, Bojunga J, Calliada F, Cantisani V et al. EFSUMB guidelines and recommendations on the clinical use of ultrasound elastography. Part 1: Basic principles and technology. *Ultraschall Med* 2013; 34: 169–184
- [97] Cosgrove D, Piscaglia F, Bamber J, Bojunga J, Correas JM, Gilja OH, Klauser AS et al. EFSUMB guidelines and recommendations on the clinical use of ultrasound elastography. Part 2: Clinical applications. *Ultraschall Med* 2013; 34: 238–253
- [98] Cosgrove D, Barr R, Bojunga J, Cantisani V, Chammas MC, Dighe M, Vinayak S et al. WFUMB Guidelines and Recommendations on the Clinical Use of Ultrasound Elastography: Part 4. Thyroid. *Ultrasound Med Biol* 2017; 43: 4–26
- [99] Barr RG, Cosgrove D, Brock M, Cantisani V, Correas JM, Postema AW, Salomon G et al. WFUMB Guidelines and Recommendations on the Clinical Use of Ultrasound Elastography: Part 5. Prostate. *Ultrasound Med Biol* 2017; 43: 27–48
- [100] Dietrich CF, Muller T, Bojunga J, Dong Y, Mauri G, Radzina M, Dighe M et al. Statement and Recommendations on Interventional Ultrasound as a Thyroid Diagnostic and Treatment Procedure. *Ultrasound Med Biol* 2017
- [101] Dighe M, Barr R, Bojunga J, Cantisani V, Chammas MC, Cosgrove D, Cui XW et al. Thyroid Ultrasound: State of the Art. Part 2 - Focal Thyroid Lesions. *Med Ultrason* 2017; 19: 195–210
- [102] Dighe M, Barr R, Bojunga J, Cantisani V, Chammas MC, Cosgrove D, Cui XW et al. Thyroid Ultrasound: State of the Art Part 1 - Thyroid Ultrasound reporting and Diffuse Thyroid Diseases. *Med Ultrason* 2017; 19: 79–93
- [103] Dietrich CF, Rudd L. The EFSUMB website, a guide for better understanding. *Med Ultrason* 2013; 15: 215–223
- [104] Claudon M, Cosgrove D, Albrecht T, Bolondi L, Bosio M, Calliada F, Correas JM et al. Guidelines and good clinical practice recommendations for contrast enhanced ultrasound (CEUS) – update 2008. *Ultraschall Med* 2008; 29: 28–44
- [105] Fusaroli P, Jenssen C, Hocke M, Burmester E, Buscarini E, Havre RF, Ignee A et al. EFSUMB Guidelines on Interventional Ultrasound (INVUS), Part V - EUS-Guided Therapeutic Interventions (short version). *Ultraschall Med* 2016; 37: 412–420
- [106] Jenssen C, Hocke M, Fusaroli P, Gilja OH, Buscarini E, Havre RF, Ignee A et al. EFSUMB Guidelines on Interventional Ultrasound (INVUS), Part IV - EUS-guided interventions: General Aspects and EUS-guided Sampling (Short Version). *Ultraschall Med* 2016; 37: 157–169
- [107] Fusaroli P, Jenssen C, Hocke M, Burmester E, Buscarini E, Havre RF, Ignee A et al. EFSUMB Guidelines on Interventional Ultrasound (INVUS), Part V. *Ultraschall Med* 2016; 37: 77–99
- [108] Jenssen C, Hocke M, Fusaroli P, Gilja OH, Buscarini E, Havre RF, Ignee A et al. EFSUMB Guidelines on Interventional Ultrasound (INVUS), Part IV - EUS-guided Interventions: General aspects and EUS-guided sampling (Long Version). *Ultraschall Med* 2016; 37: E33–E76
- [109] Lorentzen T, Nolsoe CP, Ewertsen C, Nielsen MB, Leen E, Havre RF, Gritzmann N et al. EFSUMB Guidelines on Interventional Ultrasound (INVUS), Part I. General Aspects (Short Version). *Ultraschall Med* 2015; 36: 464–472
- [110] Lorentzen T, Nolsoe CP, Ewertsen C, Nielsen MB, Leen E, Havre RF, Gritzmann N et al. EFSUMB Guidelines on Interventional Ultrasound (INVUS), Part I. General Aspects (long Version). *Ultraschall Med* 2015; 36: E1–E14
- [111] Jenssen C, Brkljacic B, Hocke M, Ignee A, Piscaglia F, Radzina M, Sidhu PS et al. EFSUMB Guidelines on Interventional Ultrasound (INVUS), Part VI. *Ultraschall Med* 2015

- [112] Fusaroli P, Jenssen C, Hocke M, Burmester E, Buscarini E, Havre RF, Ignee A et al. EFSUMB Guidelines on Interventional Ultrasound (INVUS), Part V. *Ultraschall Med* 2015
- [113] Sidhu PS, Brabrand K, Cantisani V, Correas JM, Cui XW, D'Onofrio M, Essig M et al. EFSUMB Guidelines on Interventional Ultrasound (INVUS), Part II. *Ultraschall Med* 2015; 36: E15–E35
- [114] Sidhu PS, Brabrand K, Cantisani V, Correas JM, Cui XW, D'Onofrio M, Essig M et al. EFSUMB Guidelines on Interventional Ultrasound (INVUS), Part II. Diagnostic Ultrasound-Guided Interventional Procedures (Long Version). *Ultraschall Med* 2015; 36: E15–E35
- [115] Sidhu PS, Brabrand K, Cantisani V, Correas JM, Cui XW, D'Onofrio M, Essig M et al. EFSUMB Guidelines on Interventional Ultrasound (INVUS), Part II. Diagnostic Ultrasound-Guided Interventional Procedures (Short Version). *Ultraschall Med* 2015; 36: 566–580
- [116] Dietrich CF. EFSUMB guidelines 2015 on interventional ultrasound. *Med Ultrason* 2015; 17: 521–527
- [117] Lorentzen T, Nolsoe CP, Ewertsen C, Nielsen MB, Leen E, Havre RF, Gritzmann N et al. EFSUMB Guidelines on Interventional Ultrasound (INVUS), Part I. General Aspects (long Version). *Ultraschall Med* 2015; 36: E1–E14
- [118] Lorentzen T, Nolsoe CP, Ewertsen C, Nielsen MB, Leen E, Havre RF, Gritzmann N et al. EFSUMB Guidelines on Interventional Ultrasound (INVUS), Part I. General Aspects (Short Version). *Ultraschall Med* 2015; 36: 464–472
- [119] Dietrich CF, Lorentzen T, Sidhu PS, Jenssen C, Gilja OH, Piscaglia F. Efsumb. An Introduction to the EFSUMB Guidelines on Interventional Ultrasound (INVUS). *Ultraschall Med* 2015; 36: 460–463
- [120] Piscaglia F, Kudo M, Han KH, Sirlin C. Diagnosis of Hepatocellular Carcinoma with Non-Invasive Imaging: A Plea for Worldwide Adoption of Standard and Precise Terminology for Describing Enhancement Criteria. *Ultraschall Med* 2017; 38: 9–11
- [121] Lyshchik A, Kono Y, Dietrich CF, Jang HJ, Kim TK, Piscaglia F, Vezeridis A et al. Contrast-enhanced ultrasound of the liver: Technical and lexicon recommendations from the ACR CEUS LI-RADS working group. *Abdom Radiol (NY)* 2017
- [122] Kim TK, Noh SY, Wilson SR, Kono Y, Piscaglia F, Jang HJ, Lyshchik A et al. Contrast-enhanced ultrasound (CEUS) liver imaging reporting and data system (LI-RADS) 2017 – a review of important differences compared to the CT/MRI system. *Clin Mol Hepatol* 2017
- [123] Wilson SR, Lyshchik A, Piscaglia F, Cosgrove D, Jang HJ, Sirlin C, Dietrich CF et al. CEUS LI-RADS: Algorithm, implementation, and key differences from CT/MRI. *Abdom Radiol (NY)* 2017
- [124] Piscaglia F, Wilson SR, Lyshchik A, Cosgrove D, Dietrich CF, Jang HJ, Kim TK et al. American College of Radiology Contrast Enhanced Ultrasound Liver Imaging Reporting and Data System (CEUS LI-RADS) for the diagnosis of Hepatocellular Carcinoma: A pictorial essay. *Ultraschall Med* 2017; 38: 320–324
- [125] Rafaelsen SR, Jakobsen A. Contrast-enhanced ultrasound vs multidetector-computed tomography for detecting liver metastases in colorectal cancer: A prospective, blinded, patient-by-patient analysis. *Colorectal Dis* 2011; 13: 420–425
- [126] Bernatik T, Schuler A, Kunze G, Mauch M, Dietrich CF, Dirks K, Pachmann C et al. Benefit of Contrast-Enhanced Ultrasound (CEUS) in the Follow-Up Care of Patients with Colon Cancer: A Prospective Multicenter Study. *Ultraschall Med* 2015; 36: 590–593
- [127] Dietrich CF, Kratzer W, Strobe D, Danse E, Fessl R, Bunk A, Vossas U et al. Assessment of metastatic liver disease in patients with primary extrahepatic tumors by contrast-enhanced sonography versus CT and MRI. *World J Gastroenterol* 2006; 12: 1699–1705

Outcomes of endoscopic biliary drainage in pancreatic cancer patients with an indwelling gastroduodenal stent: a multicenter cohort study in West Japan



Kentaro Yamao, MD, PhD,¹ Masayuki Kitano, MD, PhD,^{1,2} Mamoru Takenaka, MD, PhD,¹ Kosuke Minaga, MD,¹ Toshiharu Sakurai, MD, PhD,¹ Tomohiro Watanabe, MD, PhD,¹ Takahisa Kayahara, MD, PhD,³ Tomoe Yoshikawa, MD,⁴ Yukitaka Yamashita, MD, PhD,⁴ Masanori Asada, MD, PhD,⁵ Yoshihiro Okabe, MD,⁵ Keiji Hanada, MD, PhD,⁶ Yasutaka Chiba, PhD,⁷ Masatoshi Kudo, MD, PhD¹

Osaka-sayama, Wakayama, Kurashiki, Wakayama, Osaka, Onomichi, Japan

Background and Aims: Gastroduodenal and biliary obstruction may occur synchronously or asynchronously in advanced pancreatic cancer, and endoscopic double stent placement may be required. EUS-guided biliary drainage (EUS-BD) often is performed after unsuccessful placement of an endoscopic transpapillary stent (ETS), and EUS-BD may be beneficial in double stent placement. This retrospective multicenter cohort study compared the outcomes of ETS placement and EUS-BD in patients with an indwelling gastroduodenal stent (GDS).

Methods: We recorded the clinical outcomes of patients at 5 tertiary-care medical centers who required biliary drainage after GDS placement between March 2009 and March 2014.

Results: Thirty-nine patients were included in this study. Patients' mean age was 68.5 years; 23 (59.0%) were men. The GDS overlay the papilla in 23 patients (59.0%). The overall technical success rate was significantly higher with EUS-BD (95.2%) than with ETS placement (56.0%; $P < .01$). Furthermore, the technical success rate was significantly higher with EUS-BD (93.3%) than with ETS placement (22.2%; $P < .01$) when the GDS overlies the papilla. The overall clinical success rate of EUS-BD also was significantly higher than for ETS placement (90.5% vs 52.0%, respectively; $P = .01$), and there was no significant difference in the incidence of adverse events (ETS, 32.0% vs EUS-BD, 42.9%; $P = .65$).

Conclusion: Endoscopic double stent placement with EUS-BD is technically and clinically superior to ETS placement in patients with an indwelling GDS. EUS-BD should be considered the first-line treatment option for patients with an indwelling GDS that overlies the papilla. ETS placement remains a reasonable alternative when the papilla is not covered by the GDS. (Gastrointest Endosc 2018;88:66-75.)

Gastroduodenal and biliary obstruction may occur synchronously or asynchronously in advanced pancreatic cancer, and endoscopic double stent placement may

be required. Malignant gastroduodenal obstruction is frequently treated with an endoscopic gastroduodenal stent (GDS),¹ which is considered the least-invasive

Abbreviations: BD, biliary drainage; EUS-BD, EUS-guided biliary drainage; EUS-CDS, EUS-guided choledochoduodenostomy; EUS-GBD, EUS-guided gallbladder drainage; ETS, endoscopic transpapillary stent; GDS, gastroduodenal stent; PTBD, percutaneous transhepatic biliary drainage; SEMS, self-expandable metal stent.

DISCLOSURE: This study was supported by grants from the Japan Society for the Promotion of Science (Masayuki Kitano). All other authors disclosed no financial relationships relevant to this publication.

Copyright © 2018 by the American Society for Gastrointestinal Endoscopy 0016-5107/\$36.00

<https://doi.org/10.1016/j.gie.2018.01.021>

Received June 21, 2017. Accepted January 18, 2018.

Current affiliations: Department of Gastroenterology and Hepatology, Kindai University Faculty of Medicine, Osaka-Sayama (1), Second Department of Internal Medicine, School of Medicine, Wakayama Medical University, Wakayama (2), Department of Gastroenterology and Hepatology, Kurashiki Central Hospital, Okayama (3), Department of Gastroenterology, Japanese Red Cross Wakayama Medical Center, Wakayama (4), Department of Gastroenterology and Hepatology, Osaka Red Cross Hospital, Osaka (5), Department of Gastroenterology, Onomichi General Hospital, Onomichi (6), Division of Biostatistics, Clinical Research Center, Kinki University Faculty of Medicine, Osaka-Sayama, Japan (7).

Reprint requests: Masayuki Kitano, MD, PhD, Second Department of Internal Medicine, School of Medicine, Wakayama Medical University, 811-1 Kimiidera, Wakayama 641-0012 Japan.

option for palliation, given the poor prognosis of the disease.²⁻⁷

Endoscopic transpapillary stent (ETS) placement is a widely used first-line therapy for biliary obstruction, but it is occasionally unsuccessful for a number of reasons. EUS-guided biliary drainage (EUS-BD) was first reported in 2001 by Giovannini et al⁸ and has recently emerged as an effective treatment after unsuccessful placement of an ETS. Although EUS-BD has achieved high technical and clinical success rates, the incidence of adverse events is reportedly higher.⁹

Gastroduodenal obstruction resulting from tumor infiltration of the duodenum poses a challenge during ETS placement, especially in the presence of a GDS covering the papilla. In double stent placement, the biliary stent must be advanced through the papilla between the interstices of the GDS. Although evidence supports the benefits of double stent placement,¹⁰⁻³⁰ the optimum timing of double stent placement in the presence of an indwelling GDS remains undetermined. Also, the clinical features and prognoses of the primary disease causing duodenal and biliary obstruction differed in most previous reports.^{10,11,27,28} The objective of this retrospective multicenter cohort study was to compare the clinical outcomes of ETS placement and EUS-BD in patients with pancreatic cancer requiring biliary drainage in the presence of an indwelling GDS.

PATIENTS, MATERIAL, AND METHODS

This multicenter, retrospective clinical study was approved by the institutional ethics committees of 5 tertiary-care medical centers (Kindai University, Kurashiki Central Hospital, Japanese Red Cross Wakayama Medical Center, Osaka Red Cross Hospital, and Onomichi General Hospital [registration number 29-050]). All patients gave written informed consent.

Patients

All consecutive patients with indwelling GDSs between March 2009 and March 2014 were identified in the medical databases of the 5 centers. Patients were included if they were diagnosed with unresectable pancreatic cancer by either pathology or typical radiologic findings, with compatible clinical presentation and underwent endoscopic biliary drainage after GDS placement. Endoscopic biliary drainage after GDS placement was defined as follows (Fig. 1): First, patients who developed gastroduodenal obstruction before biliary obstruction were treated with GDS placement, and then biliary stent placement was performed on appearance of biliary obstruction. Second, patients who developed synchronous gastroduodenal and biliary obstruction were treated with biliary stent placement followed by placement of a GDS. In patients with

unsuccessful biliary stent placement, GDS placement was performed before the replacement of the biliary stent. Third, patients who developed biliary obstruction before gastroduodenal obstruction were treated with biliary stent placement, and then a GDS was placed on the appearance of gastroduodenal obstruction. In the third group, we evaluated patients with obstructed previous biliary stent placement requiring reintervention. Patients were excluded if their scores on the Eastern Cooperative Oncology Group performance status were higher than 3, or their anatomy had been altered by surgery (eg, Billroth-I or -II and Roux-en-Y reconstruction).

EQUIPMENT AND PROCEDURES

ETS placement

For ETS placement, a duodenal endoscope (TJF-260V, JF-260V; Olympus Medical Systems, Tokyo, Japan), an ERCP catheter (Tandem XL; Boston Scientific, Marlborough, Mass or MTW, MTW Co, Düsseldorf, Germany), a sphincterotome (CleverCut 3V; Olympus Medical Systems), a 0.025-inch wire (VisiGlide; Olympus Medical Systems), and a 0.035-inch wire (Jagwire; Boston Scientific) were used. If the deep cannulation was difficult, a pre-cut technique was performed with a pre-cut needle-knife (NeedleCut3V; Olympus Medical systems). After successful deep cannulation, a self-expandable metal stent (SEMS) (10-mm diameter, 40-80 mm length, fully or partially covered stent; WallFlex, Boston Scientific or 10-mm diameter, 40-80 mm length, Niti-S ComVi, TaeWoong Medical, Seoul, South Korea) or a plastic stent (7F diameter, 70-120 mm length, Flexima; Boston Scientific or 7F diameter, 7-10 cm length, Zimmon Biliary Stent; Cook Medical, Bloomington, Ind) was deployed. We did not widen the GDS interstices with a balloon, trim by using forceps, or use argon plasma coagulation.

Strategy for EUS-BD

The basic procedure for EUS-BD was EUS-guided choledochoduodenostomy (EUS-CDS) or EUS-guided hepaticogastrostomy. The former was performed when there was lower biliary obstruction without an overlying GDS at the puncture site. The latter was performed when there was middle- or upper-biliary obstruction and/or tumor infiltration of the duodenum or the GDS. If EUS-CDS and hepaticogastrostomy were technically difficult, EUS-guided gallbladder drainage (EUS-GBD) was performed as the second-line procedure.

EUS-guided choledochoduodenostomy

For EUS-CDS, an echoendoscope (GF-UCT240, 260; Olympus Medical Systems) was used. Endosonographic images were observed by using an Aloka ProSound SSD α -10 (Hitachi Aloka Medical, Tokyo, Japan). After the

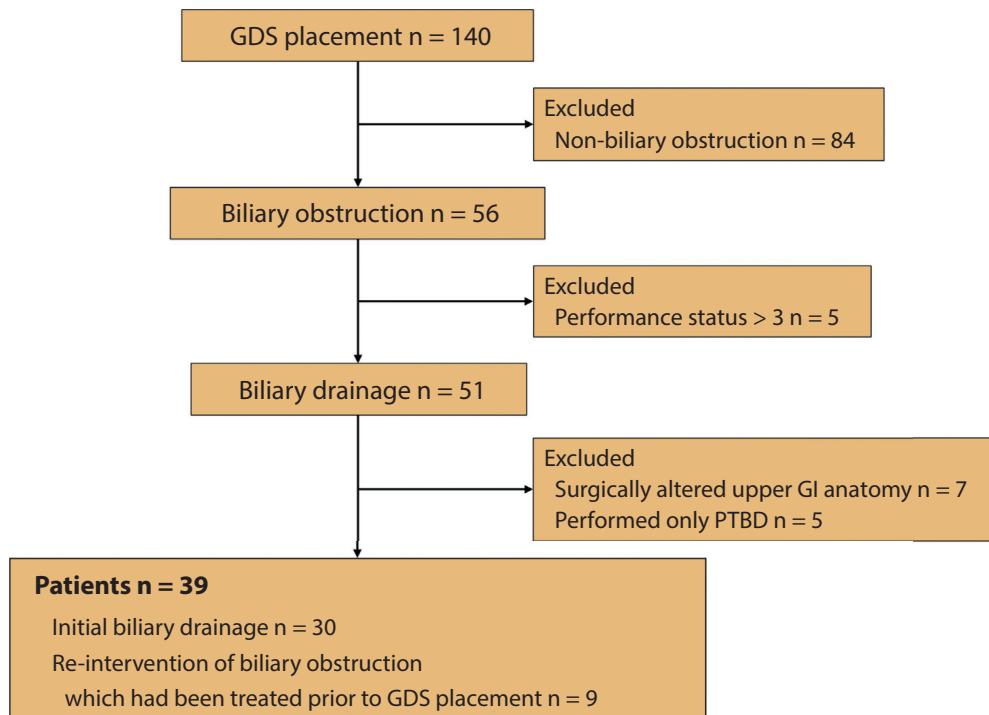


Figure 1. Study flow chart. We enrolled 39 patients on whom we attempted endoscopic biliary drainage after placement of a gastroduodenal stent. *GDS*, gastroduodenal stent; *PTBD*, percutaneous transhepatic biliary drainage.

echoendoscope had been advanced into the duodenal bulb, the dilated extrahepatic bile duct was visualized then punctured with a 19-gauge needle (SonoTip ProControl; Medi-Globe, Rosenheim, Germany or Expect; Boston Scientific) under endosonographic guidance. Contrast medium was injected under fluoroscopic guidance. Thereafter, a 0.025-inch (VisiGlide or Revowave UltraHard; Piolax, Kanagawa, Japan) or 0.035-inch guidewire (Jagwire) was inserted. The fistula tract was serially dilated by using either a 6F or 7F tapered biliary dilation catheter (Soehendra biliary dilation catheter; Cook Medical) over the guidewire. Finally, a covered SEMS (WallFlex; Boston Scientific) was deployed.

EUS-guided hepaticogastrostomy

The dilated left intrahepatic bile duct was visualized with the echoendoscope in the stomach. The duct of the third segment was generally chosen for puncture with a 19-gauge needle (SonoTip) followed by contrast medium injection under fluoroscopic guidance. Thereafter, a guidewire was inserted, the fistula tract was dilated by using biliary dilation catheters (Sohendra; Cook Medical), and a partially covered SEMS (WallFlex) was deployed.

EUS-GBD

We used a previously described method for EUS-GBD³¹ by using a plastic pigtail stent (Zimmon Biliary Stent; Cook Medical).

Outcome measurements and definitions

Our primary objective was to compare the technical success rates of biliary drainage (ETS placement and EUS-BD) at the first attempt and overall after placement of a GDS. The secondary objectives were to compare the clinical success rates, adverse event rates, stent patency, time to stent dysfunction, and survival time of patients who underwent ETS placement and EUS-BD. The technical and clinical success rates of BD were assessed in the following 3 groups, defined by the type of GDS (covered or uncovered) and the relationship between the GDS and the papilla (overlying or not overlying): group A, uncovered GDS overlying the papilla; group B, covered GDS overlying the papilla; and group C, uncovered or covered GDS not overlying the papilla. Technical success was defined as adequate placement of the BD stent. Clinical success was defined as a reduction in serum bilirubin concentration to normal levels or by $\geq 50\%$ within 2 weeks. The incidence of the following adverse events was assessed: pancreatitis, bleeding, perforation, peritonitis, bile leakage, stent migration, and stent dysfunction, according to the criteria reported by Cotton et al.³² Stent patency was defined as *occluded* if liver enzyme levels were elevated, there was BD on imaging, or the patient died. The causes of stent occlusion were determined by endoscopic or imaging findings. Stent dysfunction was defined as a composite endpoint of either occlusion or migration, and the time to stent dysfunction was the duration between

stent placement and recurrence of biliary obstruction. Patient death was treated as a censored case of stent dysfunction. The site of obstruction was classified as follows: type I, the level of the duodenal bulb or upper duodenal genu without involving the major papilla; type II, affecting the second part of the duodenum and involving the papilla; type III, involving the third part of the duodenum distal to the papilla but not involving the papilla¹⁰. All patients were followed-up until death. When a patient could not be followed-up directly, we collected patient data from families or primary care physicians by telephone.

Statistical analysis

Data are presented as numbers and proportions (%) for categorical variables, and as the mean (\pm standard deviation) or the median (range) for continuous variables. Patient survival, stent patency, and stent dysfunction were evaluated by using the Kaplan-Meier method. If stent dysfunction was not evident during a patient's life, the patency time was considered equal to the survival period. Statistical significance was set at $P < .05$. All statistical analyses were performed by using SAS software (version 9.4; SAS Institute Inc, Cary, NC).

RESULTS

Overall patient characteristics and first-line treatment characteristics

GDS placement was performed in 140 patients in this study period. Biliary obstruction developed in 56 patients after placement of a GDS, but BD was attempted in 51 patients; 5 patients could not undergo BD because of a poor general condition and were excluded. Seven patients with surgically altered upper GI anatomy, and 5 patients treated only with percutaneous transhepatic biliary drainage (PTBD) also were excluded. Ultimately, 39 patients formed the study cohort; initial biliary drainage was performed in 30 patients, and reintervention for biliary obstruction that had been treated before GDS placement was performed in 9 (Fig. 1).

The demographic and clinical characteristics of the cohort are shown in Table 1. Their mean age was 68.5 ± 11.3 years. The indwelling GDS was the covered type in 9 patients (23.1%) and the uncovered type in 30 patients (76.9%). The site of obstruction was type I, type II, and type III in 11 (28.2%), 16 (41.0%), and 12 (30.8%) patients, respectively. The papilla was overlain by the GDS in 23 patients (59.0%) but not in 16 patients (41.0%). BD was performed with a median of 7 days (0-243 days) after GDS placement.

Of the 39 included patients, 25 underwent ETS placement, and 14 underwent EUS-BD as first-line treatment. The demographic and clinical characteristics of the patients who underwent ETS placement or EUS-BD as a

TABLE 1. Patient demographic and clinical characteristics (n = 39)

Age, mean \pm SD, y	68.5 \pm 11.3
Sex, no. (%)	
Male	23 (59.0)
Female	16 (41.0)
Gastroduodenal stent, no. (%)	
Covered stent	9 (23.1)
Uncovered stent	30 (76.9)
Site of obstruction, no. (%)	
Type I	11 (28.2)
Type II	16 (41.0)
Type III	12 (30.8)
Relationship with the papilla, no. (%)	
Overlies the gastroduodenal stent	23 (59.0)
Does not overlie the gastroduodenal stent	16 (41.0)
Preceding biliary drainage, no. (%)	
Yes	9 (23.1)
ETS	9 (100)
Metal stent	6 (66.7)
Plastic stent	3 (33.3)
No	30 (76.9)

SD, Standard deviation; ETS, endoscopic transpapillary stent.

first-line treatment are shown in Table 2. There was no significant difference between the groups except for overlying of the papilla by the GDS ($P < .01$).

Technical success of first-line treatment

The technical success rates of first-line procedures are shown in Table 3 and Figure 2. First-line treatment was ETS placement in 25 patients and EUS-BD in 14 patients. ETS placement and EUS-BD were successful in 14 patients for each procedure. Of the 11 patients with unsuccessful ETS placement, deep cannulation could not be achieved in 5 patients, the papilla could not be accessed through the GDS in 4 patients, and the papilla could not be identified within the GDS in 2 patients. The technical success rate was significantly higher in the first-line EUS-BD group than in the first-line ETS group (14/14, 100% vs 14/25, 56.0%, respectively; $P = .01$). In patients with preceding biliary stent placement (n = 9), technical success rates were 83.3% (5/6) and 100% (3/3) for ETS placement and EUS-BD, respectively.

Technical success of overall cumulative procedures

The technical success rates of overall cumulative procedures are shown in Table 4 and Figure 2. ETS procedures were performed in 25 patients as first-line treatments and were successful in 14 patients. Overall, EUS-BD was performed in 21 patients, as first-line treatment in 14 patients, and as second-line treatment in

TABLE 2. Demographic and clinical characteristics of patients undergoing first-line endoscopic transpapillary stent placement or first-line EUS-guided biliary drainage

Variable	First-line ETS group (n = 25)	First-line EUS-BD group (n = 14)	P value
Age, mean ± SD, y	69.7 ± 11.7	66.2 ± 10.6	.18
Sex, no. (%)			
Male	15 (60.0)	8 (57.1)	.87
Female	10 (40.0)	6 (42.8)	
Gastroduodenal stent, no. (%)			
Covered stent	5 (20.0)	4 (28.6)	.83
Uncovered stent	20 (80.0)	10 (71.4)	
Site of obstruction, no. (%)			
Type I	8 (32.0)	3 (21.4)	.09
Type II	7 (28.0)	9 (64.3)	
Type III	10 (40.0)	2 (14.3)	
Relationship with the papilla, no. (%)			
Overlies the GDS	9 (36.0)	14 (100)	< .01
Does not overlie the GDS	16 (64.0)	0 (0)	
Preceding BD, no. (%)			
Yes	6 (24.0)	3 (21.4)	.83
ETS	6 (100)	3 (100)	
Metal stent	4 (66.7)	2 (66.7)	
Plastic stent	2 (33.3)	1 (33.3)	
No	19 (76.0)	11 (78.6)	

ETS, Endoscopic transpapillary stent; BD, biliary drainage; SD, standard deviation; GDS, gastroduodenal stent.

TABLE 3. Clinical outcomes after first-line treatment

Variable	First-line ETS group (n = 25)	First-line EUS-BD group (n = 14)	P value
Technical success, no. (%)	14 (56.0)	14 (100)	.01
Clinical success, no. (%)	13 (52.0)	13 (92.9)	.02
Adverse event, no. (%)			
Pancreatitis	2 (8.0)	0 (0)	
Perforation	1 (4.0)	0 (0)	
Cholangitis and/or recurrent jaundice	5 (20.0)	4 (28.6)	
Stent migration	0 (0)	1 (7.1)	
Peritonitis	0 (0)	2 (14.3)	
Cholecystitis	0 (0)	1 (7.1)	

ETS, Endoscopic transpapillary stent; BD, biliary drainage.

7 patients. EUS-BD was successful in 20 of the 21 patients. In the patient who was a treatment failure, we could not identify the optimal route for EUS-BD because of massive ascites. Collectively, the technical success rate was significantly higher in the EUS-BD group than in the ETS group (95.2% vs 56.0%, respectively; $P < .01$).

Technical success after treatment completion in each group

Group A (n = 19, Supplemental Fig. 1, available online at www.giejournal.org). ETS placement was

performed in 9 patients but was successful in only 2 patients. Fifteen patients underwent EUS-BD, 10 as first-line treatment and 5 as second-line treatment; EUS-BD was successful in 14 of these patients. The technical success rate in group A was significantly higher in the EUS-BD group than in the ETS group (93.3% vs 22.2%, respectively; $P < .01$). Three patients required PTBD, 2 as second-line treatment and 1 as third-line treatment. PTBD was successful in 1 of these patients (33.3%). Two patients in whom PTBD failed were not offered further intervention.

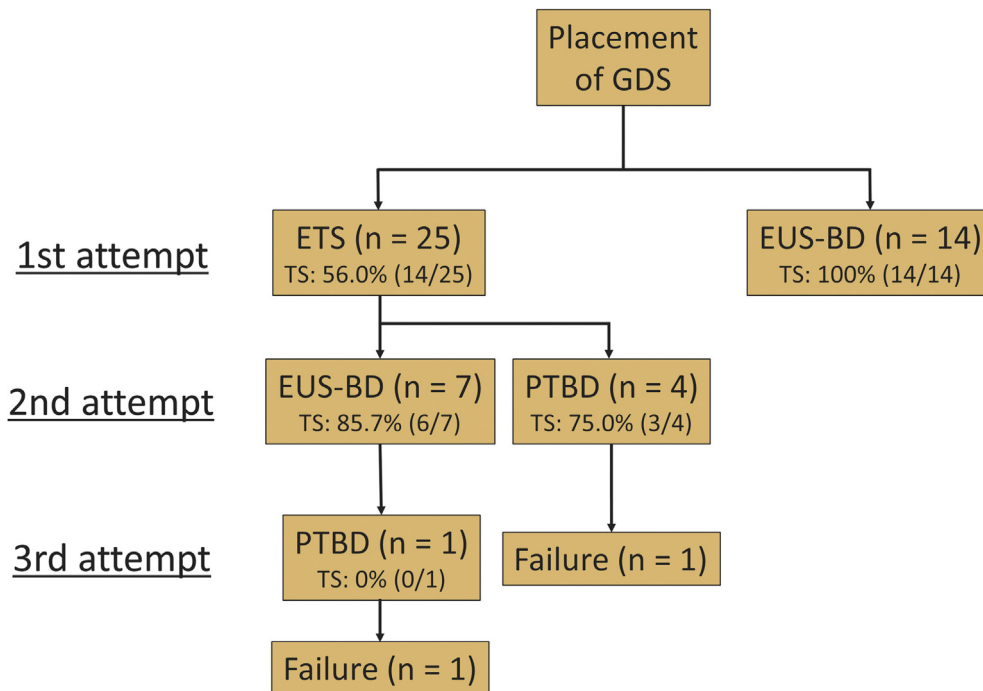


Figure 2. Technical outcomes of biliary drainage in patients with an indwelling gastroduodenal stent (n = 39). *GDS*, gastroduodenal stent; *ETS*, endoscopic transpapillary stent placement; *TS*, technical success; *EUS-BD*, EUS-guided biliary drainage; *PTBD*, percutaneous transhepatic biliary drainage.

TABLE 4. Overall clinical outcomes after treatment

Variable	ETS group (n = 25)*	EUS-BD group (n = 21)*	P value
Technical success, no. (%)	14 (56.0)	20 (95.2)	< .01
Group A	2/9 (22.2)	14/15 (93.3)	< .01
Group B	0/0 (0)	4/4 (100)	NA
Group C	12/16 (75.0)	2/2 (100)	.92
Clinical success, no. (%)	13 (52.0)	19 (90.5)	.01
Adverse event, no. (%)			
Pancreatitis	2 (8.0)	0 (0)	
Perforation	1 (4.0)	0 (0)	
Cholangitis and/or recurrent jaundice	5 (20.0)	5 (23.8)	
Stent migration	0 (0)	2 (9.5)	
Peritonitis	0 (0)	1 (4.8)	
Cholecystitis	0 (0)	1 (4.8)	

ETS, Endoscopic transpapillary stent; *BD*, biliary drainage; *NA*, not applicable.

*Cumulative total number of patients.

Group B (n = 4, Supplemental Fig. 2, available online at www.giejournal.org). None of these patients underwent ETS placement; EUS-BD was performed as the first-line treatment in 4 patients and was successful in all patients (100%).

Group C (n = 16, Supplemental Fig. 3, available online at www.giejournal.org). Sixteen patients underwent ETS placement, which was successful in 12 patients. Two patients underwent EUS-BD, both as second-line treatment. EUS-BD was successful in both patients. We found no significant difference in the technical success

rate in group C between ETS and EUS-BD groups (75.0% vs 100%, respectively; $P = .92$). Two patients required PTBD as second-line treatment, and PTBD was successful in both patients (100%).

Clinical success

First-line and overall cumulative procedures. The clinical success rates after first-line treatment are shown in Table 3. The clinical success rate was significantly higher in the EUS-BD group than in the ETS group

(92.9% vs 52.0%, respectively; $P = .02$) as first-line treatments.

One patient who experienced technical success in the ETS group died on day 3 without clinical success because of rapid disease exacerbation. One patient who experienced technical success in the EUS-BD group (EUS-CDS) developed stent migration on day 13 without clinical success. This patient underwent subsequent EUS-guided hepaticogastrostomy with clinical success.

Clinical success rates of overall cumulative procedures are shown in Table 4. The clinical success rate was significantly higher in the EUS-BD group than in the ETS group (90.5% vs 52.0%, respectively; $P = .01$).

Adverse events

First-line and overall cumulative procedures. The adverse event rates after first-line treatment are shown in Table 3. We found no significant difference in the incidence of adverse events between the ETS and EUS-BD groups (32.0% vs 57.1%, respectively; $P = .23$) as a first-line treatment. Adverse event rates of overall cumulative procedure are shown in Table 4. We found no significant difference in the incidence of adverse events of overall cumulative procedures between the ETS and EUS-BD groups (32.0% vs 42.9%, respectively; $P = .65$).

Patient death, stent patency, and time to stent dysfunction

Patient survival was monitored until December 31, 2016. All patients died during the study period. The Kaplan-Meier plots comparing overall survival time, stent patency, and time to stent dysfunction of the ETS and EUS-BD groups are shown in Figures 3, 4, and 5. There was no significant difference in survival (ETS placement median 79.5 days, EUS-BD median 80 days, $P = .52$), stent patency (ETS placement median 54.5 days, EUS-BD median 57.5 days, $P = .23$), or time to stent dysfunction (ETS placement median 140 days, EUS-BD median 249 days; $P = .45$) between the 2 groups.

DISCUSSION

In this study, we assessed the first-line and overall technical feasibility of EUS-BD in patients with pancreatic cancer and an indwelling GDS. The technical and clinical success rate of EUS-BD was significantly higher than that of ETS placement, especially when the GDS overlay the papilla. However, the incidence of adverse events was comparable between EUS-BD and ETS placement.

The technical success of ETS placement when the GDS did not overlie the papilla was relatively high (75.0% in group C). The technical success of ETS placement in patients with biliopancreatic malignancy is reportedly 75.0% to 95.0%,^{33,34} which is comparable with our findings. However, the technical success of ETS placement when

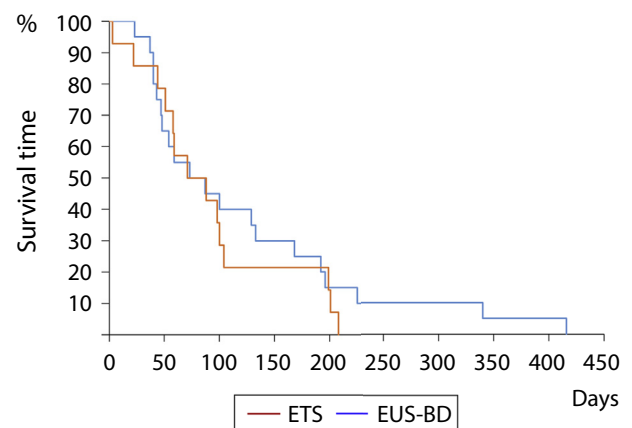


Figure 3. Kaplan-Meier plot of overall survival in the endoscopic transpapillary stent placement group and the EUS-guided biliary drainage group. No statistically significant difference was observed between the groups (ETS median 79.5 days, EUS-BD median 80 days; $P = .52$). ETS, endoscopic transpapillary stent placement; EUS-BD, EUS-guided biliary drainage.

the GDS overlay the papilla was not sufficient (22.2% in group A), because of the inability to achieve deep cannulation, inability to find the papilla, or inability to access the papilla through the interstices of the GDS. Conversely, the technical success of EUS-BD in the presence of the GDS overlying the papilla was excellent (overall technical success in groups A and B was 93.3% and 100%, respectively). Therefore, our results suggest that EUS-BD is superior to ETS placement regarding the technical success rate when the GDS overlies the papilla.

Several reports discussed the technical success rates of ETS placement with an indwelling GDS. Vanbiervliet et al²⁸ reported favorable outcomes (94.4% for ETS placement overall and 91.7% when the GDS overlay the papilla), whereas most of the previous studies report percentages (34.2%-62.5%) of technical success rates of ETS placement in the presence of a GDS.^{10,11,27} Our data are consistent with the latter reports in which cohorts include 33.3% to 40.0% of patients with GDSs overlying the papilla (excluding the rendezvous technique).^{10,27} Several methods have been proposed to improve the technical success rate of ETS placement in patients with a GDS overlying the papilla. GDS trimming with argon plasma coagulation^{35,36} and foreign-body forceps,¹⁰ and balloon dilation within the GDS interstices¹⁰ were reported. Although we did not perform these methods in this cohort study, by using these methods in patients with a GDS overlying the papilla might improve the success rate of ETS placement.

Since Giovannini et al⁸ first described EUS-BD in 2001, much attention has been paid to this novel technique in patients with unsuccessful ETS placement. In a recent systematic analysis of 1192 patients who underwent EUS-BD, the cumulative technical success rate was 94.7%.⁹ EUS-BD enables endoscopists to identify dilated bile ducts by echo

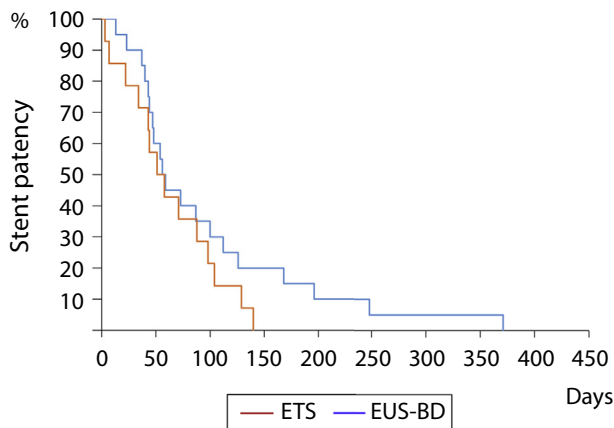


Figure 4. Kaplan-Meier plot of stent patency in the endoscopic transpapillary stent placement group and the EUS-guided biliary drainage group. No statistically significant difference was observed between the groups (ETS median 54.5 days, EUS-BD median 57.5 days; $P = .23$). *ETS*, endoscopic transpapillary stent placement; *EUS-BD*, EUS-guided biliary drainage.

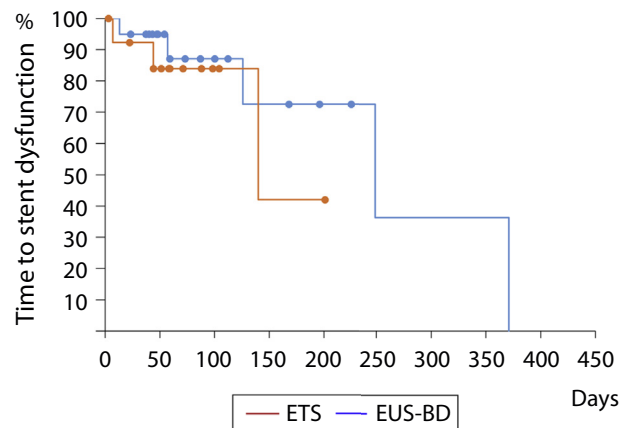


Figure 5. Kaplan-Meier plot of time to stent dysfunction in the endoscopic transpapillary stent placement group and the EUS-guided biliary drainage group. No statistically significant difference was observed between the groups (ETS median 140 days, EUS-BD median 249 days; $P = .45$). *ETS*, endoscopic transpapillary stent placement; *EUS-BD*, EUS-guided biliary drainage.

imaging whether the papilla is visible or approachable or neither. We also obtained very high success rates of EUS-BD in our study.

Gastroduodenal and biliary obstruction may occur synchronously or asynchronously in advanced pancreatic cancer. We assessed endoscopic BD in patients with an indwelling GDS. In patients with synchronous gastroduodenal and biliary obstruction, it is preferable to perform BD before placement of the GDS. In such patients, gastroduodenal obstruction is often type 2, for whom the technical success rate with ETS placement is poor because of the presence of duodenal obstruction. In our study, we compared the success rate of ETS placement and EUS-BD in 39 patients who exhibited concurrent biliary and gastroduodenal obstruction. Consistent with previous studies reporting that the technical success rate of ETS placement was insufficient in the presence of a GDS overlying the papilla,^{10,27} the success rate of ETS placement was relatively low in our study (22.2% with group A). In contrast, the success rate of EUS-BD was very high even in the presence of a GDS overlying the papilla. Therefore, our study highlights the usefulness of EUS-BD, which allows the bile duct to be reached regardless of the presence of an indwelling GDS or tumor infiltration.

Considering these results, the basic strategy for successful ETS placement in double stent placement requires biliary stent placement to be performed first. However, if gastroduodenal obstruction has already developed, ETS placement is made more challenging by the presence of an indwelling GDS. Therefore, performing ETS placement before obstruction in patients in whom biliary and gastroduodenal obstruction are soon expected may be an option to obtain successful double stent placement.

PTBD is variable after unsuccessful ETS placement, and it was performed as a second-line or third-line treatment in

our study. Several studies have compared the clinical outcomes of EUS-BD with PTBD. Although technical success rates of PTBD and EUS-BD were comparable (approximately 90%),³⁷⁻⁴⁰ Sharaiha et al³⁸ reported that the reintervention rate, late adverse event rate, and pain intensity score were higher for PTBD than for EUS-BD. The biggest disadvantage of PTBD was the need for permanent or temporary external drainage, which may necessitate repeated procedures for the patient.

We found no significant difference in the rates of adverse events between the ETS (32.0%) and EUS-BD (42.9%) groups. Cholangitis and/or recurrent jaundice were the most common adverse events in both groups (ETS 20.0%, EUS-BD 23.8%). In the previous reports, the rates of cholangitis were 4.6% to 14.3%⁴¹⁻⁴³ in ETS placement and 2.4% to 11.5%^{9,44} in EUS-BD. In double stent placement, when the GDS was inserted above the papilla, the internal pressure of the digestive tract rose because of the GDS obstruction and developed into retrograde cholangitis. Therefore, cholangitis is more likely to occur in those patients than in patients undergoing only biliary stent placement. In 4 patients in the ETS group, however, the endoscope did not reach the papilla through the GDS. If these patients were excluded, the actual incidence of adverse events with ETS placement was 38.1%, but the difference compared with EUS-BD was still not significant ($P = .75$). Therefore, in contrast to previous studies reporting a high rate of adverse events associated with EUS-BD,⁹ we found no significant difference in terms of adverse events between ETS placement and EUS-BD.

There have been some reports of stent patency after double stent placement.^{12,13,23,30} Hamada et al²³ reported that the time to stent dysfunction after EUS-BD (hepaticogastrostomy in 3 patients and CDS in 4 patients) was significantly longer than with ETS placement. Sato et al¹² have

reported that the time to stent dysfunction was influenced by the positional relationship between the gastroduodenal and biliary stents; the median time to stent dysfunction was significantly longer when stents were separate (mainly EUS-guided hepaticogastrostomy and CDS) than when they overlapped (mainly ETS). We found no significant difference in stent patency between the groups. The discrepancy between our findings and those of Hamada et al²³ can be explained by the difference in the proportion of patients with overlapping gastroduodenal and biliary stents in the ETS group. The GDS overlay the papilla and biliary stent in most patients who underwent ETS placement in the Hamada et al²³ cohort but in a minority of patients in ours (group A). Our findings concur more closely with those of Sato et al.¹²

Our study had several limitations. First, it was a non-randomized retrospective design. Second, different types of GDSs (covered or uncovered) were used. Third, there was no standard biliary drainage protocol: although ETS placement was undertaken as a first-line treatment in many patients, followed by EUS-BD then PTBD, some patients underwent EUS-BD as a first-line procedure and PTBD as second-line. Fourth, EUS-BD was achieved by 3 different techniques (EUS-CDS, hepaticogastrostomy, and GBD). Finally, some plastic stents were used for biliary drainage. Despite these limitations, we were able to establish the technical superiority of EUS-BD in the presence of an indwelling GDS.

In conclusion, we found that endoscopic double stent placement with EUS-BD is technically and clinically superior to ETS placement in patients with an indwelling GDS. EUS-BD needs to be considered as the first-line treatment option in patients with an indwelling GDS that overlies the papilla. ETS placement remains a reasonable alternative when the papilla is not covered by the GDS.

REFERENCES

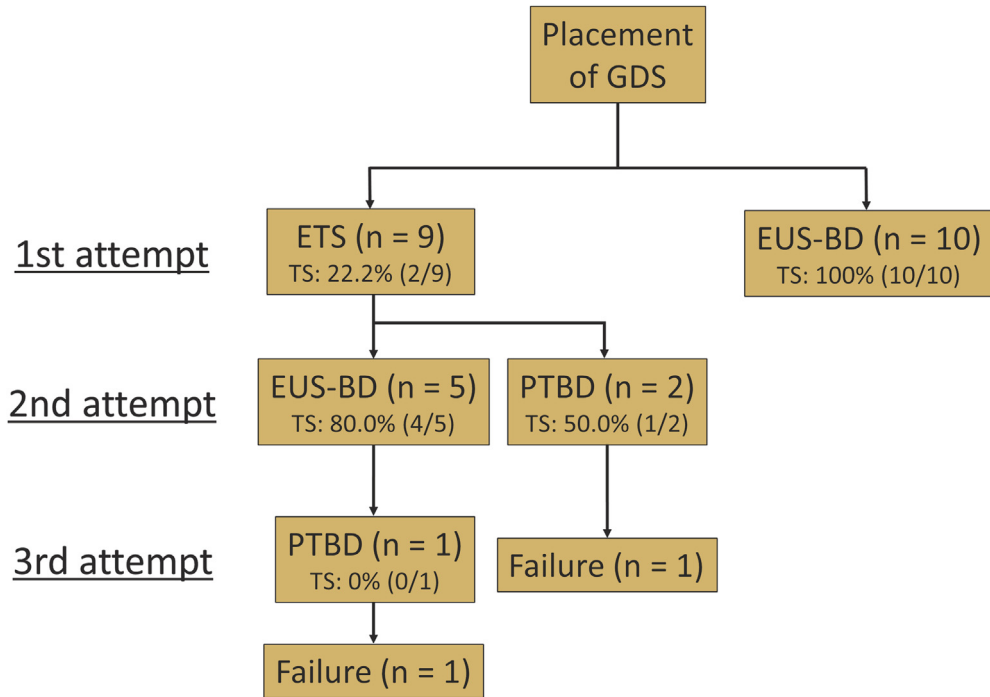
1. Yamao K, Kitano M, Kayahara T, et al. Factors predicting through-the-scope gastroduodenal stenting outcomes in patients with gastric outlet obstruction: a large multicenter retrospective study in West Japan. *Gastrointest Endosc* 2016;84:757-63.e6.
2. Mehta S, Hindmarsh A, Cheong E, et al. Prospective randomized trial of laparoscopic gastrojejunostomy versus duodenal stenting for malignant gastric outflow obstruction. *Surg Endosc* 2006;20:239-42.
3. Jeurnink SM, Steyerberg EW, Hof G, et al. Gastrojejunostomy versus stent placement in patients with malignant gastric outlet obstruction: a comparison in 95 patients. *J Surg Oncol* 2007;96:389-96.
4. Jeurnink SM, Steyerberg EW, van Hooft JE, et al. Surgical gastrojejunostomy or endoscopic stent placement for the palliation of malignant gastric outlet obstruction (SUSTENT study): a multicenter randomized trial. *Gastrointest Endosc* 2010;71:490-9.
5. Rudolph HU, Post S, Schluter M, et al. Malignant gastroduodenal obstruction: retrospective comparison of endoscopic and surgical palliative therapy. *Scand J Gastroenterol* 2011;46:583-90.
6. Chandrasegaram MD, Eslick GD, Mansfield CO, et al. Endoscopic stenting versus operative gastrojejunostomy for malignant gastric outlet obstruction. *Surg Endosc* 2012;26:323-9.
7. Yamaguchi K, Okusaka T, Shimizu K, et al. EBM-based Clinical Guidelines for Pancreatic Cancer (2013) issued by the Japan Pancreas Society: a synopsis. *Jpn J Clin Oncol* 2014;44:883-8.
8. Giovannini M, Moutardier V, Pesenti C, et al. Endoscopic ultrasound-guided bilioduodenal anastomosis: a new technique for biliary drainage. *Endoscopy* 2001;33:898-900.
9. Wang K, Zhu J, Xing L, et al. Assessment of efficacy and safety of EUS-guided biliary drainage: a systematic review. *Gastrointest Endosc* 2016;83:1218-27.
10. Mutignani M, Tringali A, Shah SG, et al. Combined endoscopic stent insertion in malignant biliary and duodenal obstruction. *Endoscopy* 2007;39:440-7.
11. Khashab MA, Valeshabad AK, Leung W, et al. Multicenter experience with performance of ERCP in patients with an indwelling duodenal stent. *Endoscopy* 2014;46:252-5.
12. Sato T, Hara K, Mizuno N, et al. Type of combined endoscopic biliary and gastroduodenal stenting is significant for biliary route maintenance. *Intern Med* 2016;55:2153-61.
13. Ogura T, Chiba Y, Masuda D, et al. Comparison of the clinical impact of endoscopic ultrasound-guided choledochoduodenostomy and hepaticogastrostomy for bile duct obstruction with duodenal obstruction. *Endoscopy*. Epub 2015 Sep 18.
14. Zhao L, Xu H, Zhang Y. Palliation double stenting for malignant biliary and duodenal obstruction. *Exp Ther Med* 2016;11:348-52.
15. Artifon EL, Frazao MS, Wodak S, et al. Endoscopic ultrasound-guided choledochoduodenostomy and duodenal stenting in patients with unresectable periampullary cancer: one-step procedure by using linear echoendoscope. *Scand J Gastroenterol* 2013;48:374-9.
16. Kim KO, Kim TN, Lee HC. Effectiveness of combined biliary and duodenal stenting in patients with malignant biliary and duodenal obstruction. *Scand J Gastroenterol* 2012;47:962-7.
17. Maire F, Hammel P, Ponsot P, et al. Long-term outcome of biliary and duodenal stents in palliative treatment of patients with unresectable adenocarcinoma of the head of pancreas. *Am J Gastroenterol* 2006;101:735-42.
18. Katsinelos P, Kountouras J, Germanidis G, et al. Sequential or simultaneous placement of self-expandable metallic stents for palliation of malignant biliary and duodenal obstruction due to unresectable pancreatic head carcinoma. *Surg Laparosc Endosc Percutan Tech* 2010;20:410-5.
19. Kaw M, Singh S, Gagneja H. Clinical outcome of simultaneous self-expandable metal stents for palliation of malignant biliary and duodenal obstruction. *Surg Endosc* 2003;17:457-61.
20. Akinci D, Akhan O, Ozkan F, et al. Palliation of malignant biliary and duodenal obstruction with combined metallic stenting. *Cardiovasc Intervent Radiol* 2007;30:1173-7.
21. Yu J, Hao J, Wu D, et al. Retrospective evaluation of endoscopic stenting of combined malignant common bile duct and gastric outlet-duodenum obstructions. *Exp Ther Med* 2014;8:1173-7.
22. Itoi T, Itokawa F, Sofuni A, et al. Endoscopic ultrasound-guided double stenting for biliary and duodenal obstruction. *Endosc Ultrasound* 2012;1:36-40.
23. Hamada T, Isayama H, Nakai Y, et al. Transmural biliary drainage can be an alternative to transpapillary drainage in patients with an indwelling duodenal stent. *Dig Dis Sci* 2014;59:1931-8.
24. Tonozuka R, Itoi T, Sofuni A, et al. Endoscopic double stenting for the treatment of malignant biliary and duodenal obstruction due to pancreatic cancer. *Dig Endosc* 2013;25(suppl 2):100-8.
25. Khashab MA, Fujii LL, Baron TH, et al. EUS-guided biliary drainage for patients with malignant biliary obstruction with an indwelling duodenal stent (with videos). *Gastrointest Endosc* 2012;76:209-13.
26. Moon JH, Choi HJ. Endoscopic double-metallic stenting for malignant biliary and duodenal obstructions. *J Hepatobiliary Pancreat Sci* 2011;18:658-63.
27. Moon JH, Choi HJ, Ko BM, et al. Combined endoscopic stent-in-stent placement for malignant biliary and duodenal obstruction by using

- a new duodenal metal stent (with videos). *Gastrointest Endosc* 2009;70:772-7.
28. Vanbiervliet G, Demarquay J-F, Dumas R, et al. Endoscopic insertion of biliary stents in 18 patients with metallic duodenal stents who developed secondary malignant obstructive jaundice. *Gastroenterol Clin Biol* 2004;28:1209-13.
 29. Baron TH. Management of simultaneous biliary and duodenal obstruction: the endoscopic perspective. *Gut Liver* 2010;4(suppl 1):S50-6.
 30. Matsumoto K, Kato H, Tsutsumi K, et al. Long-term outcomes and risk factors of biliary stent dysfunction after endoscopic double stenting for malignant biliary and duodenal obstructions. *Dig Endosc* 2017;29: 617-25.
 31. Imai H, Kitano M, Omoto S, et al. EUS-guided gallbladder drainage for rescue treatment of malignant distal biliary obstruction after unsuccessful ERCP. *Gastrointest Endosc* 2016;84:147-51.
 32. Cotton PB, Eisen GM, Aabakken L, et al. A lexicon for endoscopic adverse events: report of an ASGE workshop. *Gastrointest Endosc* 2010;71:446-54.
 33. Varadarajulu S, Kilgore ML, Wilcox CM, et al. Relationship among hospital ERCP volume, length of stay, and technical outcomes. *Gastrointest Endosc* 2006;64:338-47.
 34. Williams EJ, Taylor S, Fairclough P, et al. Are we meeting the standards set for endoscopy? Results of a large-scale prospective survey of endoscopic retrograde cholangio-pancreatograph practice. *Gut* 2007;56: 821-9.
 35. Kin T, Katanuma A, Takahashi K, et al. Successful reintervention of biliary stent occlusion after biliary and duodenal stenting by using argon plasma coagulation. *Gastrointest Endosc*. Epub 2015 Apr 25.
 36. Topazian M, Baron TH. Endoscopic fenestration of duodenal stents using argon plasma to facilitate ERCP. *Gastrointest Endosc* 2009;69: 166-9.
 37. Khashab MA, Valeshabad AK, Afghani E, et al. A comparative evaluation of EUS-guided biliary drainage and percutaneous drainage in patients with distal malignant biliary obstruction and failed ERCP. *Dig Dis Sci* 2015;60:557-65.
 38. Sharaiha RZ, Kumta NA, Desai AP, et al. Endoscopic ultrasound-guided biliary drainage versus percutaneous transhepatic biliary drainage: predictors of successful outcome in patients who fail endoscopic retrograde cholangiopancreatography. *Surg Endosc* 2016;30:5500-5.
 39. Artifon EL, Aparicio D, Paione JB, et al. Biliary drainage in patients with unresectable, malignant obstruction where ERCP fails: endoscopic ultrasonography-guided choledochoduodenostomy versus percutaneous drainage. *J Clin Gastroenterol* 2012;46:768-74.
 40. Pinol V, Castells A, Bordas JM, et al. Percutaneous self-expanding metal stents versus endoscopic polyethylene endoprotheses for treating malignant biliary obstruction: randomized clinical trial. *Radiology* 2002;225:27-34.
 41. Li F, Wang F, Yang X, et al. Covered stents versus uncovered stents for the palliation of malignant extrahepatic biliary obstruction caused by direct tumor invasion: a cohort comparative study. *Med Oncol* 2012;29:2762-70.
 42. Kullman E, Frozanpor F, Soderlund C, et al. Covered versus uncovered self-expandable nitinol stents in the palliative treatment of malignant distal biliary obstruction: results from a randomized, multicenter study. *Gastrointest Endosc* 2010;72:915-23.
 43. Kawakubo K, Isayama H, Nakai Y, et al. Efficacy and safety of covered self-expandable metal stents for management of distal malignant biliary obstruction due to lymph node metastases. *Surg Endosc* 2011;25:3094-100.
 44. Kawakubo K, Kawakami H, Kuwatani M, et al. Endoscopic ultrasound-guided choledochoduodenostomy vs. transpapillary stenting for distal biliary obstruction. *Endoscopy* 2016;48:164-9.

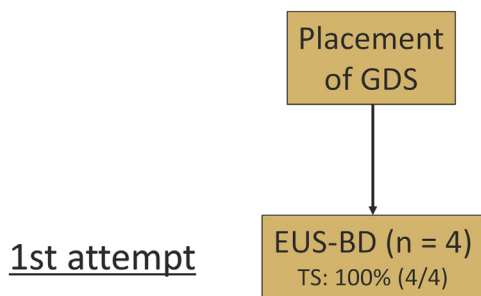
GIE on Facebook

Follow GIE on Facebook to receive the latest news, updates, and links to author interviews, podcasts, articles, and tables of contents. Search on Facebook for "GIE: Gastrointestinal Endoscopy" or use this QR code for quick access to our recent posts.

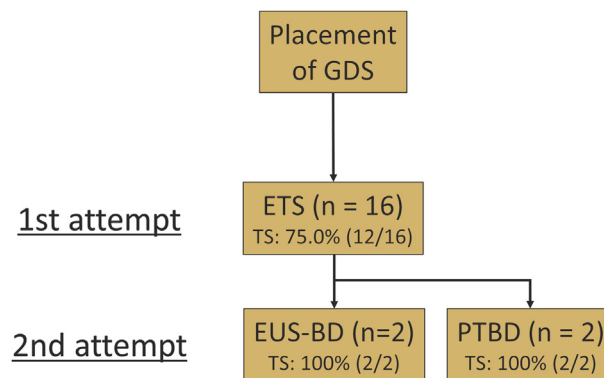




Supplemental Figure 1. Technical outcomes in group A (n = 19). *GDS*, gastroduodenal stent; *ETS*, endoscopic transpapillary stent placement; *TS*, technical success; *EUS-BD*, EUS-guided biliary drainage; *PTBD*, percutaneous transhepatic biliary drainage.



Supplemental Figure 2. Technical outcomes in group B (n = 4). No patients underwent endoscopic transpapillary stent placement. *GDS*, gastroduodenal stent; *EUS-BD*, EUS-guided biliary drainage; *TS*, technical success.



Supplemental Figure 3. Technical outcomes in group C (n = 16). No patients underwent first-line EUS-guided biliary drainage. *GDS*, gastroduodenal stent; *ETS*, endoscopic transpapillary stent placement; *TS*, technical success; *EUS-BD*, EUS-guided biliary drainage; *PTBD*, percutaneous transhepatic biliary drainage.

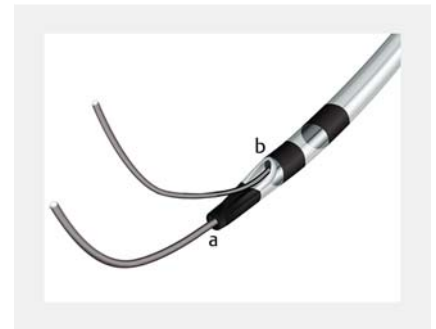
A novel biliary cannulation method for difficult cannulation cases using a unique, uneven, double-lumen cannula (Uneven method)

The utility of pancreatic duct guidewire (P-GW) placement techniques, including the contrast-medium method and the contrast-free wire-guided cannulation method (i.e. the “double-guidewire method” [D-GW]), has been reported for selective biliary cannulation in patients in whom performing cannulation of the bile duct is difficult [1–5]. However, P-GW placement often disturbs the approach to the bile orifice. Moreover, it is sometimes difficult to insert the catheter or guidewire in the direction of the bile duct, which delays biliary cannulation.

Herein, we report a novel biliary cannulation method using a unique, uneven, double-lumen cannula (UDLC; PIOLAX, Tokyo, Japan). The UDLC is a double-lumen catheter, with lumens measuring 0.025 and 0.035 inches in diameter, respectively. The orifice of each lumen is uneven, thereby forming a channel at the tip of the UDLC (► Fig. 1). With such characteristics in mind, we applied the UDLC to develop a new method of selec-

tive biliary cannulation for difficult cannulation cases (UDLC method). We describe a case wherein the UDLC was successfully employed without complications (► Video 1).

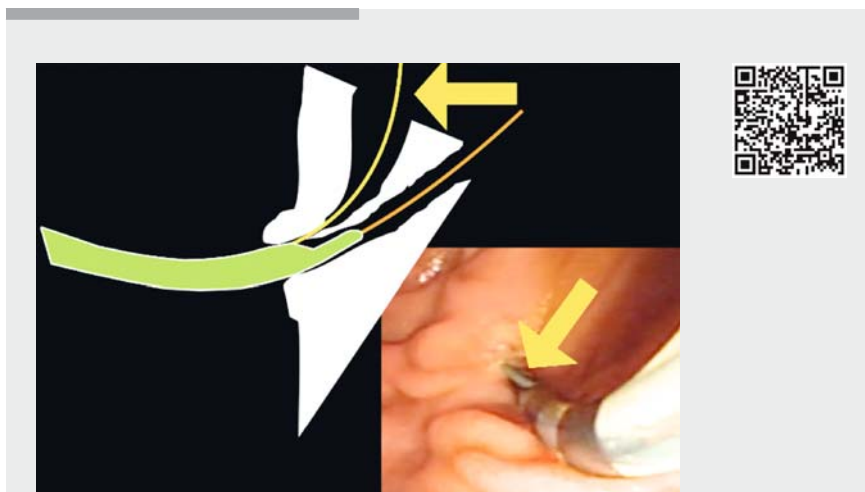
A 75-year-old man presented with pancreatic cancer and was admitted to our hospital for treatment of obstructive cholangitis. It was difficult to perform biliary cannulation as we could insert only the P-GW. Initially, the UDLC was used to intubate the papilla through the P-GW via the distal lumen. This straightened the pancreatic duct and the common channel, thereby effectively stabilizing the papilla (► Fig. 2). Next, we performed biliary cannulation via the proximal lumen, as is done in the D-GW method (► Fig. 3). By using this method, we were able to avoid the time delay in adjusting the catheter axis to comply with the bile duct direction, as required in the P-GW method. Thus, we easily initiated the biliary cannulation approach. Ultimately, we succeeded in performing selective biliary cannulation (► Fig. 4).



► Fig. 1 The uneven double-lumen cannula (UDLC; PIOLAX, Tokyo, Japan) is a double-lumen catheter, with lumens of 0.025 (distal, a) and 0.035 (proximal, b) inches in diameter. The orifice of each lumen is uneven, thereby creating a channel within the tip.

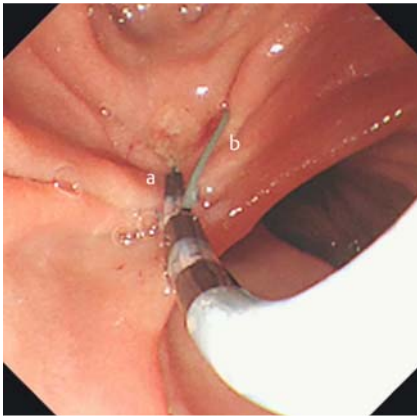


► Fig. 2 A schematic of the uneven double-lumen cannula (UDLC) method. Initially, the UDLC a is intubated to the papilla through the pancreatic guidewire (P-GW) b using the distal lumen. This straightens the pancreatic duct and the common channel, thereby more effectively stabilizing the papilla compared with the use of the P-GW alone. Next, biliary cannulation using the proximal lumen is performed in a manner that is similar to the double-guidewire technique c.

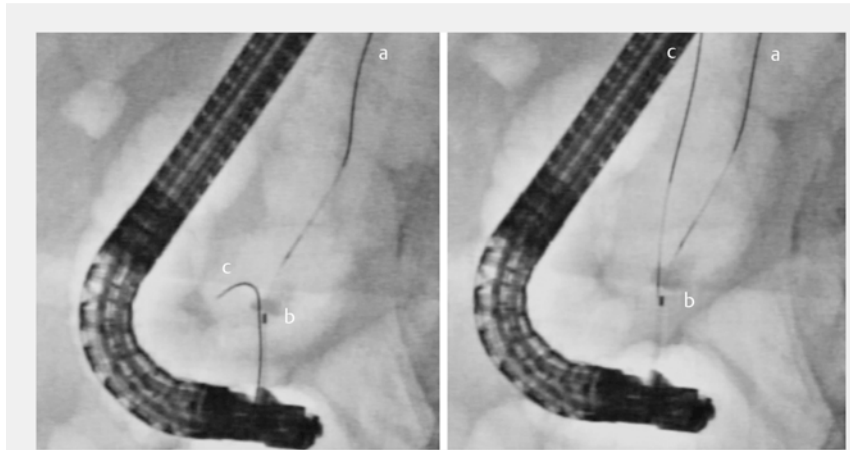


► Video 1 The uneven double-lumen cannula (UDLC) method is used for cases of difficult cannulation. The papilla is intubated using the UDLC, then biliary cannulation via the proximal lumen is quickly performed.





► **Fig. 3** The tip of the uneven double-lumen cannula **a** is intubated to the papilla through the pancreatic guidewire. The guidewire from the proximal lumen **b** is seen.



► **Fig. 4** The uneven double-lumen cannula (UDLC) is intubated to the papilla through the pancreatic guidewire **a**. The fluoroscopic marker of the UDLC **b** is seen. The guidewire from the proximal lumen **c** is used for biliary cannulation, as is done in the double-guidewire method.

In summary, we report a new cannulation method using a UDLC to safely and effectively perform selective biliary cannulation in patients in whom biliary cannulation is otherwise difficult.

Endoscopy_UCTN_Code_CCL_1AZ_2AI

Competing interests

None

The authors

Mamoru Takenaka^{1,2}, **Yoshifumi Arisaka**^{1,3}, **Arata Sakai**¹, **Takashi Kobayashi**¹, **Hideyuki Shiomi**¹, **Atshuhiro Masuda**¹, **Masatoshi Kudo**²

- 1 Department of Gastroenterology, Kobe University Faculty of Medicine, Hyogo, Japan
- 2 Department of Gastroenterology and Hepatology, Kindai University Faculty of Medicine, Osaka-Sayama, Japan
- 3 Department of Gastroenterology, Nissay Hospital, Osaka, Japan

Corresponding author

Mamoru Takenaka, MD, PhD

Department of Gastroenterology and Hepatology, Kindai University Faculty of Medicine, 377-2 Ohno-Higashi, Osaka-Sayama, 589-8511, Japan
Fax: +81-72-3672880
mamoxyo45@gmail.com

References

- [1] Dumonceau JM, Devière J, Cremer M. A new method of achieving deep cannulation of the common bile duct during endoscopic retrograde cholangiopancreatography. *Endoscopy* 1998; 30: S80
- [2] Maeda S, Hayashi H, Hosokawa O et al. Prospective randomized pilot trial of selective biliary cannulation using pancreatic guidewire placement. *Endoscopy* 2003; 35: 721–724
- [3] Ito K, Fujita N, Noda Y et al. Pancreatic guidewire placement for achieving selective biliary cannulation during endoscopic retrograde cholangio-pancreatography. *World J Gastroenterol* 2008; 14: 5595–5600
- [4] Herreros de Tejada A, Calleja JL, Diaz G et al. Double-guidewire technique for difficult bile duct cannulation: a multicenter randomized, controlled trial. *Gastrointest Endosc* 2009; 70: 700–709
- [5] Gronroos JM, Vihervaara H, Gullichsen R et al. Double-guidewire-assisted biliary cannulation: experiences from a single tertiary referral center. *Surg Endosc* 2011; 25: 1599–1602

Bibliography

DOI <https://doi.org/10.1055/a-0624-9317>
Published online: 12.6.2018
Endoscopy 2018; 50: E229–E230
© Georg Thieme Verlag KG
Stuttgart · New York
ISSN 0013-726X

ENDOSCOPY E-VIDEOS <https://eref.thieme.de/e-videos>



Endoscopy E-Videos is a free access online section, reporting on interesting cases and new

techniques in gastroenterological endoscopy. All papers include a high quality video and all contributions are freely accessible online.

This section has its own submission website at

<https://mc.manuscriptcentral.com/e-videos>

DEN Video Article

Novel method of biliary cannulation for patients with Roux-en-Y anastomosis using a unique, uneven, double-lumen cannula (Uneven method)

Mamoru Takenaka,  Kentaro Yamao and Masatoshi Kudo

Department of Gastroenterology and Hepatology, Kindai University, Faculty of Medicine, Osaka, Japan

Efficacy of balloon enteroscopy-assisted endoscopic retrograde cholangiopancreatography (ERCP) for patients with surgically altered gastrointestinal anatomy has previously been reported.^{1–4}

However, although this method allows the endoscope to reach the papilla, successful biliary cannulation is difficult. Unlike normal ERCP, directions in these patients are reversed, and it is difficult to adjust the catheter in the direction of the bile duct. Intubating the cannula to the papilla is therefore time-consuming.

For difficult cannulation cases, a biliary cannulation method using an uneven, double-lumen cannula (UDLC) was reported.⁵ Herein, we report a significant novel method of biliary cannulation for patients with Roux-en-Y anastomosis using a UDLC.

A 75-year-old man who underwent total gastrectomy with Roux-en-Y anastomosis was admitted to our hospital for choledocholithiasis as a result of lymphometastasis. A short-type single-balloon enteroscope (SIF-H290; Olympus Medical Systems, Tokyo, Japan) was inserted into the papilla for biliary drainage. However, selective biliary cannulation was difficult. Only a pancreatic guidewire (P-GW) could be inserted.

The UDLC (PIOLAX, Tokyo, Japan) is a unique catheter with double lumens measuring 0.025 and 0.035 inches in diameter. The orifice of each lumen is uneven.

First, the UDLC was inserted into the papilla using the P-GW in the distal lumen. The tip of the UDLC stabilized

the papilla and could straighten the common channel and the axis of the bile duct. Next, wire-guided biliary cannulation using the GW from the proximal lumen was attempted. In this case, the GW from the proximal lumen could move in the direction of the bile duct, and no effort was needed to adjust the axis of the catheter in the direction of the bile duct (Fig. 1). Consequently, we succeeded in achieving a speedy selective biliary cannulation (Fig. 2). This cannulation method is considered to be a useful option for patients with surgically altered gastrointestinal anatomy (Video S1).

Authors declare no conflicts of interest for this article.

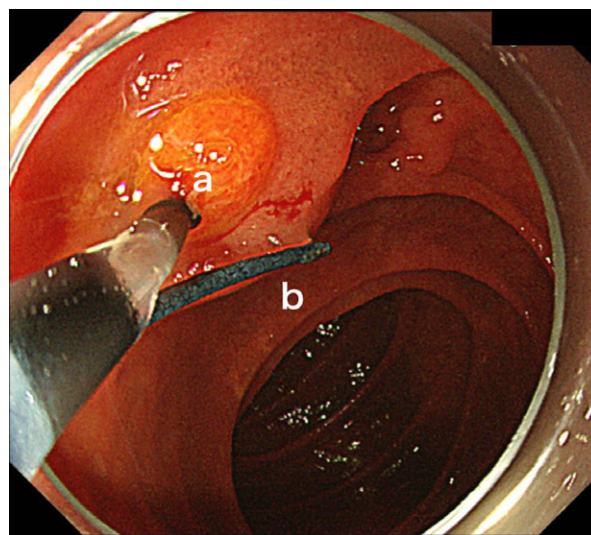


Figure 1 (a) The tip of uneven, double-lumen cannula was inserted into the papilla using the pancreatic guidewire (P-GW) in the distal lumen. (b) In this case, the GW from the proximal lumen could move in the direction of the bile duct.

Corresponding: Mamoru Takenaka, Department of Gastroenterology and Hepatology, Kindai University Faculty of Medicine, 377-2 Ohno-Higashi, Osaka-Sayama 589-8511, Japan. Email: mamoxyo45@gmail.com

Received 20 July 2018; accepted 3 August 2018.

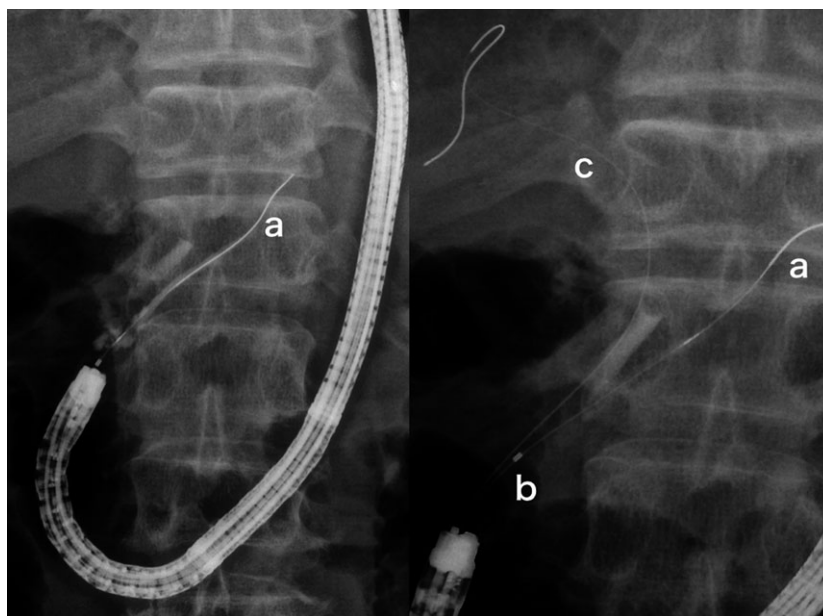


Figure 2 (a) The uneven, double-lumen cannula (UDLC) is intubated to the papilla through the pancreatic guidewire. (b) The fluoroscopic marker of the UDLC is seen. The guidewire from the proximal lumen (c) is used for biliary cannulation, as is done in the wire-guided cannulation (WGC) method. Using this method, no effort was needed to adjust the axis of the catheter in the direction of the bile duct. Consequently, we succeeded in speedy selective biliary cannulation.

REFERENCES

- 1 Ishii K, Itoi T, Tonozuka R *et al.* Balloon enteroscopy-assisted ERCP in patients with Roux-en-Y gastrectomy and intact papillae (with videos). *Gastrointest. Endosc.* 2016; **83**: 377–86.e6.
- 2 Itoi T, Ishii K, Sofuni A *et al.* Single-balloon enteroscopy-assisted ERCP in patients with Billroth II gastrectomy or Roux-en-Y anastomosis (with video). *Am. J. Gastroenterol.* 2010; **105**: 93–9.
- 3 Nakai Y, Kogure H, Yamada A, Isayama H, Koike K. Endoscopic management of bile duct stones in patients with surgically altered anatomy. *Dig. Endosc.* 2018; **30**(Suppl 1): 67–74.
- 4 Yane K, Hayashi T, Katanuma A. Successful emergency endoscopic drainage for afferent limb syndrome-induced severe acute cholangitis in a patient with altered Roux-en Y anatomy. *Dig. Endosc.* 2018. <https://doi.org/10.1111/den.13241>. [Epub ahead of print].
- 5 Takenaka M, Arisaka Y, Sakai A *et al.* A novel biliary cannulation method for difficult cannulation cases using a unique, uneven, double-lumen cannula (Uneven method). *Endoscopy* 2018; **50**: E229–30.

SUPPORTING INFORMATION

ADDITIONAL SUPPORTING INFORMATION may be found in the online version of this article at the publisher's web site.

Video S1 A 75-year-old man who underwent total gastrectomy with Roux-en-Y anastomosis was admitted for choledocholithiasis as a result of lymphometastasis.

[CASE REPORT]

Erythropoietic Protoporphyrin-related Hepatopathy Successfully Treated with Phlebotomy

Akihiro Yoshida¹, Satoru Hagiwara¹, Tomohiro Watanabe¹, Naoshi Nishida¹, Hiroshi Ida¹, Toshiharu Sakurai¹, Yoriaki Komeda¹, Kentaro Yamao¹, Mamoru Takenaka¹, Eisuke Enoki², Masatomo Kimura², Masako Miyake³, Akira Kawada³ and Masatoshi Kudo¹

Abstract:

A 27-year-old man bearing an erythropoietic protoporphyria (EPP)-associated ferrochelatase (FECH) mutation was admitted to our hospital for general malaise and marked elevation of the serum levels of hepatobiliary enzymes and bilirubin. Initial treatment with plasma exchange did not reduce the blood protoporphyrin or serum liver enzyme levels, so phlebotomy was started. Surprisingly, weekly phlebotomy normalized the serum levels of liver enzymes, accompanied by a marked reduction in the blood protoporphyrin levels. The clinical course of this case strongly suggests that phlebotomy may be a suitable treatment option for EPP-related hepatopathy.

Key words: erythrocyte protoporphyrin, plasma exchange, phlebotomy

(Intern Med 57: 2505-2509, 2018)

(DOI: 10.2169/internalmedicine.0673-17)

Introduction

Porphyrias are hereditary disorders in the heme biosynthesis enzymes and are classified into eight types according to genetic abnormalities of the enzymes and the accumulation of biochemical intermediates of the heme biosynthesis pathway (1). Erythropoietic protoporphyria (EPP) is one type of porphyria caused by a reduced activity of ferrochelatase (FECH) and the accumulation of protoporphyrin, a substrate of this enzyme (2). In most cases of EPP, loss of function mutations in FECH result in the massive accumulation of protoporphyrin in erythroid cells residing in the bone marrow due to the disturbance of erythroid heme biosynthesis, subsequently leading to high concentrations of protoporphyrin in the plasma and skin. Such high concentrations of protoporphyrin in the skin are primarily responsible for the immediate photosensitivity in EPP patients who develop erythema and edema in sun-exposed areas. Thus, EPP is a prototypical erythropoietic porphyria associated with skin lesions.

The liver is another target organ of EPP. Plasma protoporphyrin is taken up by hepatocytes, followed by biliary excretion into the feces. A significant proportion of patients with EPP develop hepatobiliary diseases secondary to the massive accumulation of protoporphyrin in the hepatocytes. EPP-associated hepatopathy can be used as a prognostic factor for this disease, since approximately 5% of EPP patients present with life-threatening liver diseases, such as liver cirrhosis. It should be noted, however, that no treatment has been established thus far for EPP-related hepatopathy, although some studies have reported improvement in patients' conditions by ursodeoxycholic acid (3), cimetidine (4-6), cholestyramine (7), adsorption therapy with activated carbon (8), plasmapheresis (9, 10), and exchange blood transfusion (11). Furthermore, a study reported the efficacy of liver transplantation, but its long-term results have not been clarified (12).

We herein report a case of EPP-related hepatopathy successfully treated with phlebotomy.

¹Department of Gastroenterology and Hepatology, Kindai University Faculty of Medicine, Japan, ²Department of Pathology, Kindai University Faculty of Medicine, Japan and ³Department of Dermatology, Kindai University Faculty of Medicine, Japan

Received for publication December 18, 2017; Accepted for publication January 28, 2018

Correspondence to Dr. Satoru Hagiwara, hagi-318@hotmail.co.jp

Case Report

A 27-year-old man was admitted to Kindai University Hospital due to general malaise and jaundice. He had suffered from photodermatitis since childhood. He had been diagnosed with systemic lupus erythematosus (SLE) due to pancytopenia, butterfly rash, and an oral ulcer in May 2015 and was being treated with prednisolone (45 mg). A marked elevation in his hepatobiliary enzymes (aspartate transaminase, AST 130 U/L, alanine aminotransferase, ALT 39 U/L) was seen at this time point, so he was referred to our department. A microscopic examination using liver biopsy specimens revealed an interlobular bile duct and Maltese-cross-positive porphyrin deposition in hepatocytes. Hepatocyte deposition of porphyrin, the marked elevation of serum protoporphyrin level (895 µg/dL, normal range; 30-86 µg/dL), and photosensitivity prompted us to consider a diagno-

sis of EPP-related hepatopathy. A definitive diagnosis of EPP was made since he had a loss of function mutation (IVS3-48T > C) in FECH. The patient was therefore ultimately diagnosed with EPP-related hepatopathy and treated with ursodeoxycholic acid (600 mg/day), cimetidine (800 mg/day), and cholestyramine (27 g/day) along with a reduction in sun exposure to minimize the toxicity of protoporphyrin.

He complained of general malaise in March 2016, and his serum levels of AST (295 U/L), ALT (200 U/L), gamma-glutamyl transpeptidase (GGT, 617 U/L), and total bilirubin (T-bil, 4.0 mg/dL) were again elevated (Table). His serum levels of albumin and prothrombin time levels were normal. In addition, his serum levels of Fe and ferritin were normal and his serum was negative for hepatitis B surface antigen and hepatitis C virus antibody. Since the blood concentration of protoporphyrin remained high (8,500 µg/dL), we considered this to be a case of exacerbation of EPP-related hepato-

Table. Laboratory Data on Admission.

<i>Blood count</i>	WBC (3,300-8,600)	11,400 µL
	Hb (13.7-16.8)	12.3 g/dL
	PLT (15.8-34.8×10 ⁴)	15.8×10 ⁴ µL
<i>Coagulability</i>	PT (70-130)	112.0 %
	PT-INR	0.96
<i>Biochemical values</i>	Na (138-145)	138 mEq/L
	K (3.6-4.8)	4.2 mEq/L
	BUN (8-20)	9 mg/dL
	Cr (0.65-1.07)	0.55 mg/dL
	eGFR	145
	FBS (73-109)	142 mg/dL
	TP (6.6-8.1)	7.0 g/dL
	Alb (4.1-5.1)	4.0 g/dL
	T-bil (0.4-1.5)	4.0 mg/dL
	D-bil (0-0.4)	2.9 mg/dL
	AST (13-30)	295 U/L
	ALT (10-42)	200 U/L
	ALP (106-322)	388 U/L
	GGT (13-64)	617 U/L
	CRP (0-0.14)	0.155 mg/dL
	TC (142-220)	293 mg/dL
	Fe (40-188)	116 µg/dL
Ferritin (25-250)	60 ng/mL	
<i>Porphyrin metabolism</i>	PP (30-86)	8,500 µg/dL RBC
<i>Immunological test</i>	ANA	(-)
	AMA2	(-)
	IgG (870-1,700)	1,227 mg/dL
<i>Viral marker</i>	HBsAg	(-)
	HCVAb	(-)

WBC: white blood cell, Hb: hemoglobin, PLT: platelet, PT: prothrombin time, BUN: blood urea nitrogen, Cr: creatinine, eGFR: estimated glomerular filtration rate, FBS: fasting blood sugar, TP: total protein, Alb: albumin, T-Bil: total bilirubin, D-bil: direct bilirubin, AST: aspartate aminotransferase, ALT: alanine aminotransferase, ALP: alkaline phosphatase, GGT: gamma-glutamyl transpeptidase, CRP: C-reactive protein, TC: total cholesterol, PP: erythrocyte protoporphyrin, ANA: anti-nuclear antibody, AMA2: anti-mitochondrial antibody 2, HBsAg: hepatitis B surface antigen, HCVAb: hepatitis C virus antibody

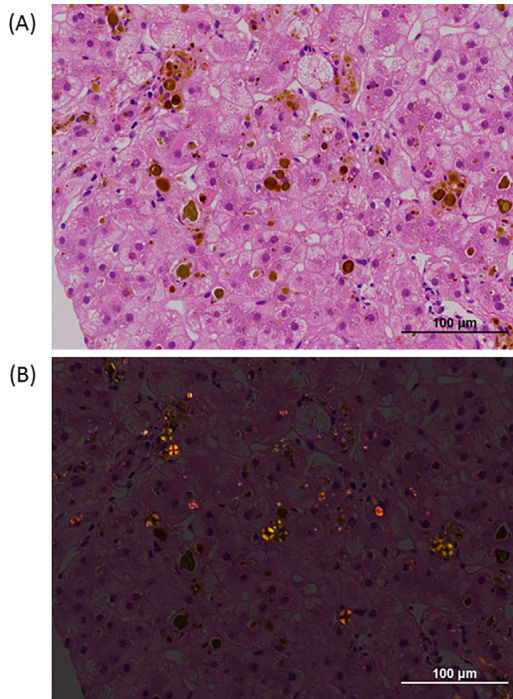


Figure 1. Histology on a liver biopsy at the time of admission. (A) Hematoxylin and Eosin staining shows porphyrin deposition in the liver. Porphyrin deposition was preferentially seen in the hepatocytes rather than in the bile duct. There were no findings suggestive of autoimmune hepatitis, including plasma cell infiltration and rosette formation. (B) Polarizing microscopy confirmed the marked deposition of Maltse-crosc-positive porphyrin.

pathy. Autoimmune-related hepatobiliary disease was unlikely, since the serum levels of anti-nuclear antibody, anti-mitochondrial antibody, and total IgG were normal. Abdominal ultrasonography indicated scattered areas of high brightness, consistent with the deposition of crystalized porphyrin. A liver biopsy was again performed to verify whether or not the abnormalities of hepatobiliary enzymes were due to the exacerbation of EPP-related hepatopathy. Microscopically, the degree of hepatocellular porphyrin deposition was greater than had been noted at the previous biopsy. Although the accumulation of porphyrin is usually observed in the bile duct and hepatocytes (10), porphyrin deposition was preferentially seen in the hepatocytes rather than the bile duct in this case. There were no findings suggestive of autoimmune hepatitis, such as plasma cell infiltration or rosette formation (Fig. 1). Thus, this case was ultimately diagnosed as exacerbation of EPP-related hepatopathy.

Elevated serum levels of total bilirubin in the absence of hemolysis as indicated by normal level of lactate dehydrogenase (LDH) (140 U/L) led us to speculate the presence of severe liver dysfunction despite the normal levels of prothrombin time and albumin. Plasma exchange was selected as the initial treatment, since this treatment is effective not only for the removal of plasma protoporphyrin but also for severe liver dysfunction. Although plasma exchange was repeated for a total of five times, a reduction in the blood levels of AST, ALT, or protoporphyrin was not achieved. Thus, plasmapheresis was not effective for the treatment of EPP-related hepatopathy in this case. We then used phlebotomy to remove red blood cells and plasma protoporphyrin (Fig. 2). Weekly phlebotomy (200-400 mL) was

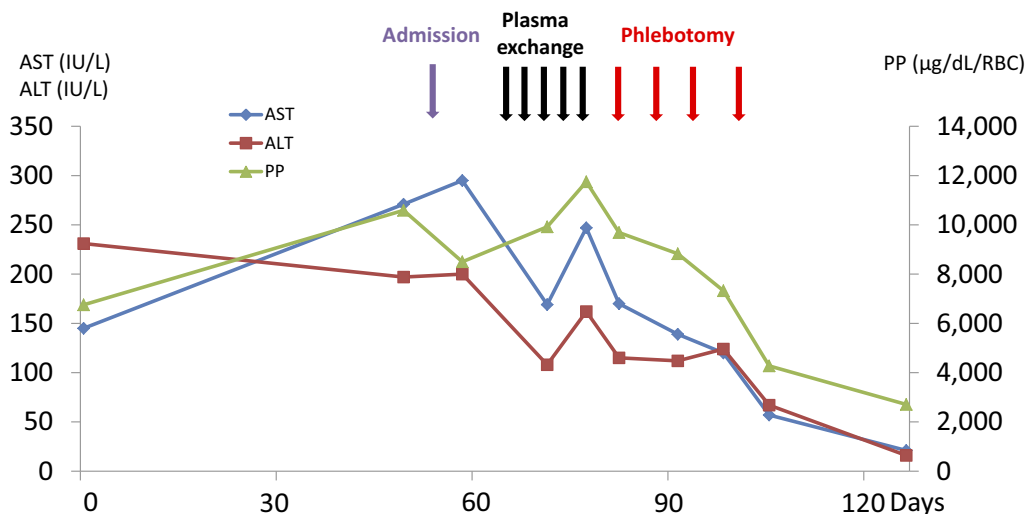


Figure 2. Clinical course before and after admission. After admission, plasma exchange was performed for a total of 5 times, no decrease in the blood protoporphyrin value was observed, and improvement of liver disorder was not observed either. Therefore, when switching to phlebotomy treatment (200 mL ~ 400 mL) once/week, the blood protoporphyrin value was markedly decreased to 2,710 μg/dL, and AST 21 U/L, ALT 16 U/L, T-bil 0.6 mg/dL and liver function also improved.

started, leading to a marked decrease in the serum levels of liver enzymes, AST, and ALT, as well as protoporphyrin. As his serum biochemical markers were decreased, symptom relief was obtained. He was discharged and received follow-up at the outpatient clinic via the oral administration of ursodeoxycholic acid, cimetidine, and cholestyramine.

Discussion

EPP is caused by a loss of mutations in FECH, one of the most critical enzymes in the heme biosynthesis pathway (2). The impaired function of FECH in the presence of EPP-associated FECH mutations causes the massive accumulation of protoporphyrin, a substrate for this enzyme, in erythroid cells. Such an accumulation of erythroid protoporphyrin in the bone marrow results in high concentration of protoporphyrin in the circulating blood and skin. High concentrations of plasma protoporphyrin also cause the hepatic accumulation of protoporphyrin, since protoporphyrin is taken up by hepatocytes. Thus, the accumulation of protoporphyrin in the skin and liver plays a critical role in EPP-associated skin disease and hepatopathy, respectively. A reduction in sun exposure is a well-established aspect of managing EPP-related skin disease caused by photosensitivity, since fluorescent protoporphyrin activated by sunlight promotes subsequent inflammatory responses. However, effective treatments for EPP-related hepatopathy have not yet been established. Given that hepatopathy rather than skin disease is associated with the prognosis of EPP (13, 14), the development of a new treatment for EPP-related hepatopathy is important. We described a case of EPP-related hepatopathy successfully treated with phlebotomy. Our present findings strongly suggest that phlebotomy is a suitable treatment option for EPP-related hepatopathy.

Phlebotomy has been shown to be highly effective in patients with another type of erythropoietic porphyria, porphyria cutanea tarda (PCT), which is caused by a reduced activity of uroporphyrinogen decarboxylase (UROD) (1). PCT, which is classified into sporadic and hereditary types, is also characterized by skin lesions in sun-exposed areas and liver dysfunction, as in EPP. A number of factors, such as alcohol (15), hepatitis C virus infection (16), HIV infection (16, 17), estrogen exposure (18), renal failure (19), and lymphoma (20), have been identified as potential triggers for sporadic PCT. However, in contrast to EPP, PCT is characterized by iron overloading, which partially explains the liver dysfunction in this type of erythropoietic porphyria. Dramatic responses to phlebotomy in our case prompted us to consider the co-occurrence of PCT and EPP. In fact, SLE can trigger the development of PCT (21-23). PCT patients exhibit elevated levels of urinary uroporphyrin or fecal coproporphyrin in addition to elevated levels of serum ferritin (24, 25). It should be noted, however, that there was no significant elevation in these urinary, fecal, or serum biomarkers in the present patient. Thus, we deemed the simultaneous occurrence of EPP and PCT-related hepatopathy

unlikely in this case. Furthermore, the dramatic responses to phlebotomy could not be explained by iron overload, which often accompanies PCT.

Plasma exchange was selected as an initial treatment in this case since this treatment can be effective not only in the removal of blood protoporphyrin but also in the restoration of the liver function. However, plasma exchange did not reduce the blood protoporphyrin or ALT levels. Surprisingly, weekly phlebotomy normalized the blood levels of protoporphyrin as well as AST and ALT. The mechanisms underlying the dramatic responses to phlebotomy but not plasma exchange remain unknown at present. Plasma exchange is generally understood to be more effective in patients with hemolysis than in those without hemolysis. We therefore speculate that the absence of hemolysis might have reduced the sensitivity to plasma exchange in this case. In contrast, phlebotomy is expected to be effective regardless of the presence of hemolysis. Given that exposure to sunlight easily induces hemolysis in EPP patients, the presence or absence of hemolysis might be associated with the sensitivity to plasma exchange in EPP-related hepatopathy. Future studies addressing the therapeutic efficacy of plasma exchange in a larger number of patients with EPP-related hepatopathy will be needed to confirm this hypothesis.

Another question arising from the present case is the optimum schedule of phlebotomy for EPP-related hepatopathy. We selected weekly phlebotomy (200-400 mL/week) in this case, using small-volume phlebotomy since the progression of anemia due to massive phlebotomy may promote the accumulation rather than the removal of protoporphyrin as a result of enhancement of the bone marrow function. Careful monitoring of hemoglobin and the reticulocyte count may be required during phlebotomy for EPP-related hepatopathy. Determining the optimum schedule of phlebotomy is absolutely necessary in order to establish phlebotomy as a treatment option in EPP-related hepatopathy.

The pathogenesis of EPP-related hepatopathy has not been fully elucidated, although bile duct occlusion caused by aggregated protoporphyrin is considered to be involved. It has also been suggested that deposition of protoporphyrin may exert direct toxic effects through the induction of hepatocyte apoptosis. In addition to these mechanism, we previously reported on the possible involvement of ATP-binding cassette transporter G2 (ABCG2) in the development of EPP-related hepatopathy (10). We observed a reduced expression of ABCG2, which functions as an important transporter of not only bile acid but also protoporphyrin. Such a reduced expression of ABCG2 may promote the accumulation of protoporphyrin, subsequently occluding the bile duct. Thus, several mechanisms have been proposed for the pathogenesis of EPP-related hepatopathy. In the present case, the protoporphyrin accumulation in hepatocytes was more marked than that in the bile duct. Furthermore, apoptosis was preferentially seen in hepatocytes rather than in the bile duct. These microscopic findings again support the idea that hepatocyte damage rather than bile duct damage is responsi-

ble for the elevated levels of serum hepatobiliary enzymes in this case.

In conclusion, phlebotomy may be effective in some patients with EPP-related hepatopathy. Future studies addressing the efficacy of phlebotomy in EPP-related hepatopathy are necessary to confirm this idea.

The authors state that they have no Conflict of Interest (COI).

References

- Sassa S, Kappas A. Molecular aspects of the inherited porphyrias. *J Intern Med* **247**: 169-178, 2000.
- Bloomer J, Wang Y, Singhal A, et al. Molecular studies of liver disease in erythropoietic protoporphyria. *J Clin Gastroenterol* **39**: S167-S175, 2005.
- Pirlich M, Lochs H, Schmidt HH. Liver cirrhosis in erythropoietic protoporphyria: improvement of liver function with ursodeoxycholic acid. *Am J Gastroenterol* **96**: 3468-3469, 2001.
- Horie Y, Tanaka K, Okano J, et al. Cimetidine in the treatment of porphyria cutanea tarda. *Intern Med* **35**: 717-719, 1996.
- Tu JH, Sheu SL, Teng JM. Novel treatment using cimetidine for erythropoietic protoporphyria in children. *JAMA Dermatol* **152**: 1258-1261, 2016.
- Fujimori N, Komatsu M, Tanaka N, et al. Cimetidine/lactulose therapy ameliorates erythropoietic protoporphyria-related liver injury. *Clin J Gastroenterol* **10**: 452-458, 2017.
- Bloomer JR. Pathogenesis and therapy of liver disease in protoporphyria. *Yale J Biol Med* **52**: 39-48, 1979.
- Gorchein A, Foster GR. Liver failure in protoporphyria: long-term treatment with oral charcoal. *Hepatology* **29**: 995-996, 1999.
- Do KD, Banner BF, Katz E, et al. Benefits of chronic plasmapheresis and intravenous heme-albumin in erythropoietic protoporphyria after orthotopic liver transplantation. *Transplantation* **73**: 469-472, 2002.
- Hagiwara S, Nishida N, Park AM, et al. Impaired expression of ATP-binding cassette transporter G2 and liver damage in erythropoietic protoporphyria. *Hepatology* **62**: 1638-1639, 2015.
- Eichbaum QG, Dzik WH, Chung RT, et al. Red blood cell exchange transfusion in two patients with advanced erythropoietic protoporphyria. *Transfusion* **45**: 208-213, 2005.
- McGuire BM, Bonkovsky HL, Carithers RL Jr, et al. Liver transplantation for erythropoietic protoporphyria liver disease. *Liver Transpl* **11**: 1590-1596, 2005.
- Doss MO, Frank M. Hepatobiliary implications and complications in protoporphyria, a 20-year study. *Clin Biochem* **22**: 223-229, 1989.
- Meerman L. Erythropoietic protoporphyria. An overview with emphasis on the liver. *Scand J Gastroenterol Suppl* **232**: 79-85, 2000.
- Yang XM, Zhang Y, Wang T, et al. Sporadic porphyria cutanea tarda induced by alcohol abuse. *Chin Med J* **130**: 2011-2012, 2017.
- Quansah R, Cooper CJ, Said S, et al. Hepatitis C- and HIV-induced porphyria cutanea tarda. *Am J Case Rep* **15**: 35-40, 2014.
- Aguilera P, Laguno M, To-Figueras J. Human immunodeficiency virus and risk of porphyria cutanea tarda: a possible association examined in a large hospital. *Photodermatol Photoimmunol Photomed* **32**: 93-97, 2016.
- Modroño Móstoles N, Pavón de Paz I, Guijarro de Armas G, et al. A case of hypopituitarism and porphyria cutanea tarda in relation to estrogen therapy in a patient with empty sella syndrome. *Rev Clin Esp* **215**: e11-e13, 2015.
- Vasconcelos P, Luz-Rodrigues H, Santos C, et al. Desferrioxamine treatment of porphyria cutanea tarda in a patient with HIV and chronic renal failure. *Dermatol Ther* **27**: 16-18, 2014.
- Thawani R, Moghe A, Idhate T, et al. Porphyria cutanea tarda in a child with acute lymphoblastic leukemia. *QJM* **109**: 191-192, 2016.
- Fritsch S, Wojcik AS, Schade L, et al. Increased photosensitivity? Case report of porphyria cutanea tarda associated with systemic lupus erythematosus. *Rev Bras Reumatol* **52**: 968-970, 2012.
- Peitsch WK, Lorentz K, Goebeler M, et al. Subacute cutaneous lupus erythematosus with bullae associated with porphyria cutanea tarda. *J Dtsch Dermatol Ges* **5**: 220-222, 2007.
- Clemmensen O, Thomsen K. Porphyria cutanea tarda and systemic lupus erythematosus. *Arch Dermatol* **118**: 160-162, 1982.
- Dereure O, Jumez N, Bessis D, et al. Measurement of liver iron content by magnetic resonance imaging in 20 patients with overt porphyria cutanea tarda before phlebotomy therapy: a prospective study. *Acta Derm Venereol* **88**: 341-345, 2008.
- Baddams EL, Degg T, Barth JH. Cascade testing of primary care blood samples with hyperferritinaemia identifies subjects with iron overload and porphyria cutanea tarda. *Ann Clin Biochem* **51**: 499-502, 2014.

The Internal Medicine is an Open Access article distributed under the Creative Commons Attribution-NonCommercial-NoDerivatives 4.0 International License. To view the details of this license, please visit (<https://creativecommons.org/licenses/by-nc-nd/4.0/>).

Feature Review

Mechanistic Insights into Autoimmune Pancreatitis and IgG4-Related Disease

Tomohiro Watanabe,^{1,2,*} Kosuke Minaga,¹ Ken Kamata,¹ Masatoshi Kudo,¹ and Warren Strober^{2,*}

Autoimmune pancreatitis (AIP) is a pancreatic manifestation of a recently defined disease form known as IgG4-related disease (AIP/IgG4-RD). AIP/IgG4-RD is characterized by elevated systemic IgG4 antibody concentrations and lesional tissues infiltrated by IgG4-expressing plasmacytes. In addition, recent studies have revealed that, in common with other autoimmune diseases, such as systemic lupus erythematosus (SLE) and psoriasis, AIP/IgG4-RD is associated with increased type I IFN (IFN-I) production by plasmacytoid dendritic cells (pDCs). However, unlike SLE, AIP/IgG4-RD is characterized by elevated IFN-I-dependent IL-33 production, the latter emerging as an important contributor to inflammation and fibrotic responses characterizing this disease. On this basis, we propose that blockade of the IFN-I/IL-33 axis might constitute a successful approach to treating this unique type of autoimmunity.

Autoimmune Pancreatitis/IgG4-Related Disease: A New Kid on the Autoimmunity Block

Chronic fibroinflammatory disorders of the pancreas can be classified into **chronic** (ordinary or generic) **pancreatitis** (CP; see [Glossary](#)) and **autoimmune pancreatitis (AIP)** [1,2]. CP, by far the most common form of pancreatitis, is an inflammation initiated by episodic and/or persistent activation of intrapancreatic digestive enzymes, especially trypsin, and is driven by environmental factors, such as alcohol intake or smoking, and/or genetic factors, such as mutations in genes that regulate trypsin activation [1,3]. Pancreatic inflammation thus initiated is then sustained by innate immune responses of **acinar cells** to ligands associated with gastrointestinal organisms invading the circulation [1]. The latter ultimately leads to progressive destruction of acinar architecture and replacement by fibrotic tissue, which then results in pancreatic exocrine and endocrine insufficiency.

By contrast, AIP is a form of pancreatitis in which a unique type of autoimmunity has a pivotal role in inducing pancreatic inflammation [2]. AIP is, in reality, a pancreatic manifestation of a multiorgan inflammatory condition known as **IgG4-RD** (referred to here as AIP/IgG4-RD), characterized by elevated systemic **IgG4** concentrations and lesions containing IgG4 plasmacytes or other plasmacytes producing autoantibodies (autoAbs) in humans [4,5]. Epidemiological data show that 41% of patients with systemic IgG4-RD (i.e., multiple organ involvement) presented with AIP, whereas 45% of patients with AIP exhibited extrapancreatic lesions [6,7]. Thus, while IgG4-RD can occur as an isolated inflammation of the pancreas, it can also occur as a pancreatitis-associated or independent inflammation involving almost any organ in the body, such as the salivary glands, thyroid gland, and bile ducts [4,5]. Given that AIP/IgG4-RD affects many organs in the body, patients with IgG4-RD manifest a variety of symptoms depending on the organs involved.

Highlights

AIP is a pancreatic manifestation of systemic AIP/IgG4-RD, a newly established disease entity in humans. AIP/IgG4-RD is characterized by enhanced IgG4 antibody responses, multiple organ involvement, and storiform fibrosis.

IFN-I and pDCs have pathogenic roles in AIP/IgG4-RD as in SLE and psoriasis.

In mice, IFN-I-dependent IL-33 production by pDCs mediates fibrosis as well as inflammation in AIP. IFN-I-dependent IL-33 production might have a pathogenic role in other diseases exhibiting both autoimmunity and fibrosis.

The IFN-I/IL-33 axis in pDCs represents a new putative therapeutic target of AIP/IgG4-RD, although further studies in humans are warranted.

¹Department of Gastroenterology and Hepatology, Kindai University Faculty of Medicine, Osaka-Sayama, Osaka 589-8511, Japan

²Mucosal Immunity Section, Laboratory of Host Defenses, National Institute of Allergy and Infectious Diseases, National Institutes of Health, Bethesda, MD 20892, USA

*Correspondence: tomohiro@med.kindai.ac.jp (T. Watanabe) and wstrober@niaid.nih.gov (W. Strober).

Increased awareness and recognition of AIP/IgG4-RD has enabled the establishment of specific pathological and diagnostic criteria for its detection. These include the presence of the aforementioned elevated IgG4 concentrations in the circulation, as well as inflammatory lesions of the affected organs in which IgG4-positive plasma cells and other lymphocytes are embedded in a **'storiform' fibrotic mass**, which comprises a cartwheel or whorled pattern of fibrosis. This inflammatory mass can also be associated with the presence of **obliterative phlebitis** and eosinophilic infiltration, the latter usually in patients with allergic manifestations, such as asthma or **atopy** [5].

In recent years, a great deal of new knowledge concerning the clinical and epidemiological features of AIP/IgG4-RD has come to light, but relatively little is known about its overall immunopathogenesis. Thus, while there is robust literature on immunological findings in these diseases, most studies have been narrowly focused on specific abnormalities. We now seek to correct this deficiency with a review that highlights the more important general points of disease pathogenesis and how these relate to other autoimmune diseases. One overarching theme we emphasize in this respect are recent studies of the etiologic role of IFN-I production by pDCs in this disease, demonstrating that blockade of pDC-mediated IFN-I production can prevent the development of experimental AIP/IgG4-RD [8,9]. Given that pDC-mediated IFN-I responses may also be important events in other autoimmune disorders, such as **SLE**, **psoriasis**, and **type 1 diabetes mellitus** (T1DM) [10], this aspect of AIP/IgG4-RD pathogenesis suggests that the latter is mechanistically linked to general autoimmune processes. However, at least in AIP/IgG4-RD studies in mice, pDC production of IFN-I has been associated with IL-33 secretion, a finding that has not been reported in other autoimmune diseases [9]. These similarities and differences in the role of IFN-I in AIP/IgG4-RD and SLE have led to the view that shared autoimmune pathological mechanisms combined with disease-specific mechanisms may give rise to a unique form of autoimmunity in AIP/IgG4-RD.

We begin our review with a discussion of IFN-I in autoimmune diseases in general to provide a background for a later discussion of how this factor affects the pathogenesis of AIP/IgG4-RD. We next focus on the adaptive T and B cell responses reported to occur in AIP/IgG4-RD, transitioning to the innate immune abnormalities that have been documented. We posit that the latter may constitute the more fundamental factors in disease pathogenesis. We also provide an in-depth look at how IFN-I and IL-33 pathways may contribute to AIP/IgG4-RD in humans and experimental models of disease in mice.

Type I IFN and Autoimmune Diseases

Since abnormal production of IFN-I is a major new finding related to the pathogenesis of AIP/IgG4-RD, we discuss previous studies examining the role of IFN-I in SLE and other autoimmune diseases. This discussion provides background insights into how IFN-I may be driving the immunopathogenesis of AIP/IgG4-RD.

It is now well established that enhanced IFN-I (usually IFN- α or IFN- β) responses are involved in the development of many autoimmune diseases, particularly SLE [11,12]. Evidence for this includes the finding that serum concentrations of IFN-I are sometimes increased in patients with SLE relative to healthy controls and, perhaps more importantly, peripheral blood leukocytes from patients with SLE upregulate genes encoding IFN-I-induced proteins (i.e., IFN-I signatures) [13]. Additional evidence for a role of IFN-I in SLE stems from genome-wide association studies (GWAS) identifying the expression of genetic variants (polymorphisms) of genes associated with IFN-I induction and signaling that confer a heightened susceptibility to the occurrence of SLE and other autoimmune manifestations relative to healthy controls [14].

Glossary

Acinar cells: pancreatic cells lining the acinus that secrete digestive enzymes.

Atopy: the genetic susceptibility to develop allergic diseases, such as atopic dermatitis.

Autoimmune pancreatitis (AIP): fibroinflammatory disease of the pancreas caused by autoimmune responses; most cases of AIP are considered pancreatic manifestations of a multiorgan disease, IgG4-RD.

B cell-activating factor (BAFF): cytokine belonging to the TNF family. BAFF promotes the survival and proliferation of B cells.

CD4⁺ cytotoxic T cells: a cytotoxic subset of CD4⁺ T cells with the ability to target cells in an MHC-class II dependent manner.

Cholecystokinin (CKK): peptide hormone secreted by enteroendocrine cells of the duodenum that binds to the CKK receptor on pancreatic acinar cells to release pancreatic digestive enzymes.

Chronic pancreatitis (CP): a fibroinflammatory disease of the pancreas caused by environmental and genetic factors.

Class switching: molecular process during which the Ig heavy chain switches from one Ig class to another without change in the variable regions.

Complementary determining region 3 (CDR3): part of the variable region of the T cell receptor providing information regarding T cell clonality.

Fab arm change: molecular phenomenon during which IgG4 Abs exchange half-molecules with other IgG4 Abs and become bispecific.

Fc receptor: receptor expressed on the surface of immune cells that interacts with the Fc portion of Ab bound to organisms and autoimmune complexes.

Germinal centers: sites within secondary lymphoid tissues, such as lymph nodes and spleen, in which B cells proliferate and mature.

Group 2 innate lymphoid cells (ILC2): innate counterparts of T cells resembling Th2 cells and producing Th2 cytokines.

IgG4: IgG subtype characterized by poor ability to activate the complement system. It generates

Finally, several agents that downregulate IFN-I responses, such as Abs that block the IFN- α/β receptor (IFNAR), have shown promise in the treatment of SLE, particularly in patients displaying an IFN-I molecular signature [15,16]. Such findings in human SLE are at least partially supported by studies in experimental animal models of SLE, indicating that IFN-I may contribute to the pathogenesis of SLE. Thus, BXSB mice [mice harboring a duplication of the **Toll-like receptor 7** (*Tlr7*) gene] exhibit ameliorated SLE-like disease, as judged by autoAb titers, proteinuria, and survival following administration of a neutralizing Ab against IFNAR relative to that of control Ab [17,18]. Similarly, NZB SLE-prone mice with IFNAR deletion exhibit reduced SLE manifestations, such as autoAb production and kidney diseases, compared with IFNAR-intact NZB mice [19]. However, MRL/lpr mice develop spontaneous SLE in an IFN-I independent fashion and administration of IFN- β or IFN-I protects MRL/lpr mice from autoimmune SLE marked by proteinuria, splenomegaly, and autoAb production [20,21]. These differences among SLE-prone mouse strains remind us that SLE pathogenesis in humans can be influenced by different factors, some of which are independent of IFN-I.

In most ‘humoral’ autoimmune disorders, heightened IFN-I production may be acting as a catalyst for the emergence of pathological autoAbs mediating disease. For instance, IFN-I can have effects on the immune system that favor autoAb development, such as effects on differentiation of disease-associated plasmablasts and **class switching** of IgM B cells into IgG subtype B cells that, in mice, produce **pathogenic autoAbs** [17,22]. In addition, as discussed below, IFN-I in human SLE is implicated in the induction of **neutrophil extracellular traps** (NETs), which can serve as a source of factors that amplify the production of substances eliciting autoAbs as well as IFN-I itself [23,24]. The role of IFN-I as a factor that operates in conjunction with other, more primary (i.e., B cell-related) disease factors may explain the fact that the occurrence of autoAbs may precede clinical symptoms by years and may require the emergence of heightened IFN-I responses to cause disease [11,12]. It should be noted, however, that in the past decade, a class of human SLE-like autoimmune disorders called interferonopathies have been identified as being due to monogenic mutations affecting genes that cause increased IFN-I production [12]. The existence of these diseases supports the view that enhanced IFN-I production can be a primary cause of SLE-like autoimmune responses and that the production of pathological autoAbs could be a secondary effect [12]. In addition, these autoimmune interferonopathies highlight the point that excess IFN-I production could also be causing autoimmune diseases via its effects on cytokine and chemokine production that induce both pathologic T cell and macrophage responses.

While many hematopoietic cells can produce IFN-I, most of this cytokine is produced by pDCs bearing TLR7 and **TLR9** on endosomal membranes [11]. These receptors enable pDCs to sense viral DNA and/or RNA and autoAbs bound to these components [11,25] (Box 1). However, such cells may not be the only source of IFN-I responses in autoimmune diseases because recent studies have shown that neutrophil induction of the aforementioned NETs may induce IFN-I responses by human monocytic cells in response to oxidized mitochondrial DNA in a TLR-independent fashion [26].

The signaling pathways resulting in the production of IFN-I, at least in pDCs, have been intensively studied and proven to be complex. This implies that gene abnormalities affecting any one of a great number of genes can result in increased IFN-I production. Indeed, this is already indicated by the fact that polymorphisms in several such genes can lead to increased susceptibility to autoimmune diseases [14] and frank mutations in several genes can lead to the aforementioned interferonopathies [12]. Finally, since DNA and RNA bound to autoAbs can be taken up by pDCs, increased production of autoAbs could itself be a cause of increased IFN-I

bispecific Ab through the Fab-arm exchange.

IgG4-related disease (IgG4-RD): inflammatory disease characterized by elevated systemic IgG4 Ab responses, infiltration of IgG4-expressing plasmacytes, storiform fibrosis, and multiorgan involvement.

Inflammatory bowel diseases (IBDs): chronic inflammatory diseases of the colon and small bowel, such as Crohn’s disease or ulcerative colitis.

M2 macrophage: subtype of activated macrophage induced by Th2 cytokines and involved in tissue remodeling, fibrosis, and angiogenesis.

Neutrophil extracellular traps

(NETs): web-like extracellular structure comprising double-stranded DNA, histones, and neutrophil-derived proteins.

Nucleotide-binding oligomerization 1 (NOD1) and 2 (NOD2): innate immune receptors

responding to peptidoglycan peptides derived from Gram-negative bacteria, or Gram-positive and -negative bacteria, respectively.

Obliterative phlebitis: blood vessel inflammation characterized by vessel obstruction; one of the characteristic pathological findings in IgG4-RD.

Pathogenic autoantibodies: antibodies directed against self-antigens that frequently form complement-activating immune complexes.

Psoriasis: autoimmune disease of the skin characterized by infiltration of immune cells and hyperproliferation of keratinocytes.

Regulatory T cells (Tregs): T cell subset with the ability to inhibit immune responses; characterized by expression of Foxp3.

Rituximab: chimeric monoclonal Ab against pan B cell marker CD20; used in the treatment of patients with B cell lymphoma or autoimmune diseases.

Sjögren’s syndrome (SS): autoimmune disease characterized by infiltration of immune cells into the salivary and lacrimal glands.

Somatic hypermutation: mechanism of B cell diversification characterized by nongermine (i.e., somatic) mutation of the variable region of immunoglobulins.

Box 1. Type I IFN Signaling Pathways

Signaling pathways resulting in the production of IFN-I in pDCs have been intensively studied and proven to be complex. The main features of these pathways are that ligand binding to TLR7 or TLR9 leads to MyD88 activation, causing the assembly of a complex containing interleukin-1 receptor-associated kinase 1 (IRAK1), IRAK4, TNF receptor-associated factor 6 (TRAF6), and TRAF3 [11,25]. This complex enables the activation of IRF7 and its phosphorylation by I κ B kinase α (IKK α), followed by IRF7 translocation to the nucleus and transactivation of IFN-I [11,25]. A related aspect of IFN-I synthesis is revealed by the fact that impaired function of IFNAR is associated with greatly reduced amounts of IFN-I. This is explained by the fact that IRF7 synthesis is further enhanced by the initial synthesis of IFN-I followed by activation by the latter of IFNAR and induction of IFN-stimulated gene factor 3 (ISGF3), a heterotrimeric complex comprising STAT1, STAT2, and IRF9, which translocates to the nucleus and induces augmented IFN-I transcription. Thus, the induction of ISGF3 constitutes a positive feedback loop of IFN-I responses once small amounts of IFN-I are generated upon TLR encounter with environmental triggers [11,25]. Such enhanced IFN-I responses are useful for antiviral responses, but potentially able to intensify autoimmunity.

A second pathway to IFN-I production involves the interaction of double-stranded RNA (dsRNA) with retinoic acid-inducible gene I (RIG-I) and melanoma differentiation-associated gene 5 (MDA5), which drives activation of IRF3 via TANK-binding kinase 1, or interaction of dsDNA with cGMP-AMP synthase (cGAS) and stimulator of IFN genes (STING), which also drives IRF3 activation [25,86]. Activated IRF3 translocates to the nucleus and *trans*-activates IFN-I. In this case, initial IFN-I induction also becomes magnified, via IFNAR signaling and the formation of ISGF3.

Given the multifaceted signaling pathway involved in IFN-I production, genetic abnormalities affecting any of the molecules involved in IFN-I induction can result in increased IFN-I production. Indeed, polymorphisms associated with several such genes can lead to increased susceptibility to autoimmune diseases [14] and mutations in several genes can lead to interferonopathies [12]. Since DNA and RNA bound to autoAbs can be taken up by pDCs [11], increased production of autoAbs could itself be a cause of increased IFN-I production via an MyD88-IRF7 pathway; this, in turn, could lead to further increases in IFN-I production via microbial stimulation of the alternative pathway, leading to IRF3 generation.

production; this, in turn, could then lead to further increases in IFN-I production via viral stimulation of pDCs. Thus, pathological autoAbs could be caused by several interacting genetic and environmental factors. Further studies are warranted to better elucidate these possibilities.

As alluded to above, neutrophils have emerged as an important source of factors that promote IFN-I production via their generation of NETs [23,24]. In mechanistic studies *in vitro*, neutrophils exposed to IFN-I and anti-DNA Abs (such as those present in the serum of patients with SLE) become susceptible to cell death and, consequently, to the generation of NETs [23,24]. Furthermore, in patients with SLE, the NETs contain self-DNA that, upon formation of complexes with antinuclear Abs, are taken up by **Fc receptors** on the surface of pDCs and transported to endosomal compartments, where they can initiate IFN-I production via TLR7 or TLR9-mediated pathways [27,28]. In addition, in human SLE, NETs contain the LL37 antimicrobial peptide and the nuclear protein, high-mobility group box1 (HMGB1), which can also promote IFN-I production by pDCs via TLRs [23,24].

SLE is not the only autoimmune disease in which IFN-I can have a pathological role. There is evidence that IFN-I also participates in the pathogenesis of psoriasis [29–31], T1DM [32,33], **Sjögren's syndrome** (SS) [34,35], and **systemic sclerosis** (SSc) [36]. For instance, psoriatic plaque lesions are characterized by a massive infiltration of pDCs producing IFN-I [29], and LL37 (related to NETs) can convert inactive self-nucleic acids into IFN-I-inducing forms, through the formation of LL37-self DNA complexes [30,31]. In addition, patients with T1DM exhibit an increased percentage of pDCs in their circulation compared with controls, while, in experimental murine models of T1DM, pDC are stimulated to produce IFN-I by immune complexes comprising NET-derived LL37, self-DNA, and anti-DNA Abs [32,33]. Collectively, these findings support the notion that pDC-mediated IFN-I responses, induced by activation of TLR7 and TLR9, may contribute to the immunopathogenesis of several autoimmune diseases in addition to SLE and, as indicated below, we can now add AIP/IgG4-RD to this list.

Storiform fibrotic mass: matted and irregularly whorled pattern of fibrosis; one of the characteristic pathological features of IgG4-RD.

Systemic lupus erythematosus (SLE): multisystem autoimmune disease caused by immune complex deposition in various organs, particularly the kidney.

Systemic sclerosis (SSc): autoimmune connective tissue disease characterized by fibroinflammatory lesions in the skin, lung, kidney, and heart.

T follicular helper cells (Tfh): CD4⁺ T cell subset that has a major role in the germinal center reaction and Ab production by B cells.

T helper 1 cells (Th1 cells): CD4⁺ T cell subset comprising cells that have undergone IL-12-induced differentiation and produce IFN- γ .

T helper 2 cells (Th2 cells): CD4⁺ T cell subset comprising cells that have undergone IL-4-induced differentiation and produce IL-4, IL-5, and IL-13.

Toll-like receptor 7 (TLR) 7 and TLR 9: receptors expressed by endosomes in DCs and macrophages that detect single-stranded RNA and double-stranded DNA, respectively.

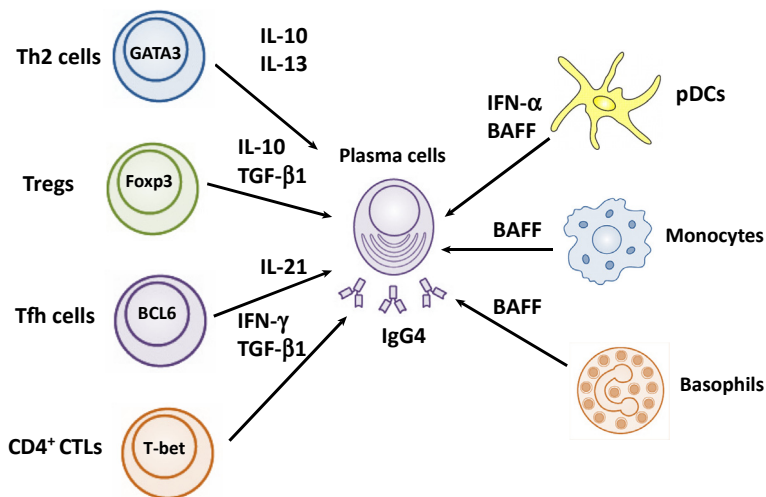
Type 1 diabetes mellitus (T1DM): subtype of diabetes caused by autoimmunity-mediated destruction of pancreas islet tissue.

Adaptive Immunity in AIP/IgG4-RD

The first abnormalities to be investigated in AIP/IgG4-RD were those of adaptive immunity, and they represent the bulk of research focus. Perhaps the most characteristic immunological features of AIP/IgG4-RD are the presence of elevated concentrations of IgG4 in the serum and IgG4 plasmacytes in affected organs [5]. These AIP/IgG4-RD manifestations are indicative of a primary or secondary abnormal adaptive immune response with an important role in the landscape of the disease.

Pathogenic T Cell Subpopulations in AIP/IgG4-RD

In seeking evidence of abnormal adaptive immunity in AIP/IgG4-RD, it was of interest to first define the adaptive T cell responses that contribute to the production of IgG4 Abs. *In vitro* studies using human peripheral blood primary B cells showed that IgG4 production is promoted by **T helper type 2 (Th2)** T cells producing IL-10 and IL-13 as well as by **regulatory T cells (Tregs)** that produce IL-10 (Figure 1) [37–39]. Consistent with this, peripheral blood mononuclear cells (PBMCs) isolated from patients with AIP/IgG4-RD produce a large amount of IL-10 and IgG4 upon stimulation with TLR ligands [40]. Moreover, accumulated cells presumed to be Th2 T cells and Tregs (the latter expressing forkhead box protein p3, Foxp3) are observed in the liver and salivary glands of patients with AIP/IgG4-RD, and are accompanied by enhanced expression of IL-4, IL-10, IL-13, and TGF- β 1 [41,42]. These data suggest that Th2 T cell and/or Treg responses can contribute to IgG4 Ab production in AIP/IgG4-RD, but, as discussed below, cytokines supporting IgG4 induction are also produced by **T follicular helper cells (Tfh cells)** and, in reality, the latter could be the main cells underlying such induction.



Trends in Immunology

Figure 1. Adaptive and Innate Immune Cells Can Lead to IgG4 Antibody Production in IgG4-Related Disease (IgG4-RD). Various kinds of adaptive immune and innate immune cell are involved in enhanced IgG4 antibody (Ab) responses in IgG4-RD. T helper type 2 (Th2) cells expressing GATA binding protein 3 (GATA3) can promote IgG4 secretion by B cells through IL-10 and IL-13 production [37,38,41,42]. Regulatory T cells (Tregs) expressing forkhead box protein p3 (Foxp3) can promote IgG4 secretion by B cells through IL-10 and TGF- β 1 production [41,42]. T follicular helper cells (Tfh) cells expressing B cell lymphoma 6 (BCL6) and secreting IL-21 can induce B cell IgG4 production [43,45,46,47]. The infiltration of CD4⁺ cytotoxic T cells (CD4⁺ CTL) cells expressing T-box transcription factor (T-bet) and producing IFN- γ and TGF- β 1 in the affected organs have correlated to serum levels of IgG4 [48,49,50]. Plasmacytoid dendritic cells (pDCs) secreting IFN-I and B cell-activating factor (BAFF) can induce IgG4 secretion by B cells in a T cell-independent manner [8,9]. Basophils and monocytes producing BAFF can also induce IgG4 secretion by B cells in a T cell-independent manner [70,71].

Studies of ectopic **germinal centers** in salivary gland lesions of patients with AIP/IgG4-RD led to the observation that Tfh cells are another class of T cell associated with AIP/IgG4-RD [43]. These cells are involved in the generation of germinal center reactions through the promotion of long-lived Ab responses by B cells and are characterized by their ability to produce a large amount of IL-21 and to express C-X-C chemokine receptor type 5 (CXCR5), programmed death 1 (PD-1), inducible T cell costimulator (ICOS), and B cell lymphoma 6 protein (BCL6) [44]. Indeed, abundant infiltration of cells expressing these markers and, thus, presumed Tfh cells, has been observed in the submandibular glands of patients with AIP/IgG4-RD and shown to efficiently promote the production of IgG4 and IgG1 upon co-culture with B cells (Figure 1) [45]. Consistent with this, expression of Tfh-associated markers, such as IL-21, BCL6, and CXCR5, is significantly higher in the salivary glands of patients with AIP/IgG4-RD than in patients with SS and healthy controls [43]. In view of these findings, it is not surprising that expansion of Tfh cells has also been observed in the peripheral blood of patients with AIP/IgG4-RD, and the degree of such expansion correlates with IgG4 concentrations and plasmablast numbers [46]. In a recent in-depth analysis of Tfh cells in AIP/IgG4-RD, the percentage of PD-1⁺ cells among CXCR5⁺/ICOS⁺ Tfh cells correlated with serum concentrations of IgG4, the number of organs involved, and the frequency of plasmablasts; in addition, the expression of Blimp-1 and IL-21 was increased in peripheral CD4⁺ T cells; finally, Tfh cells from patients with AIP/IgG4-RD were more efficient in enhancing B cell proliferation and differentiation into plasmablast or plasma cells *in vitro* than comparable cells from healthy controls [47].

Yet another T cell population found in both lesional tissues and the circulation of patients with AIP/IgG4-RD comprises a unique population of **CD4⁺ cytotoxic T cells** often observed in patients with chronic viral infections (Figure 1) [48,49]. These cells have a **T helper 1 cell** (Th1 T cell) signature in that they express T-box transcription factor (T-bet) and produce IFN- γ [48,49]. However, they differ from ordinary Th1 cells in that they produce several cytolytic proteins, such as perforin and granzymes, and express genes usually associated with myeloid cells, such as those encoding CD11b, C-C motif chemokine ligand 4 (CCL4), and IL-1 β [48,49]. The CD4⁺ cytotoxic T cells also express SLAMF7, a molecule expressed on several types of cell, including natural killer (NK) cells and plasmablasts, and involved in the regulation of cell activation [48,49]. Finally, these cells produce TGF- β 1 and, therefore, could be involved in fibrotic reactions characteristic of IgG4-RD, although this remains to be tested [48,49]. While Th2 cells in patients with AIP/IgG4-RD are clonally diverse, CD4⁺ cytotoxic T cells exhibit some degree of oligoclonality [49]. However, the expressed clones differ from patient to patient and shared **complementary determining region 3** (CDR3) sequences are not found; thus, it appears that the expanded clones could represent patient-specific responses to common or diverse antigenic stimuli. These CD4⁺ T cells greatly outnumber GATA binding protein 3 (GATA3)⁺ Th2 cells in lesional tissues and their number declines following glucocorticoid or **rituximab** treatment, which leads to amelioration of inflammation; this suggests that their proinflammatory and profibrotic capabilities allow them to serve as end-stage effector cells [48–50].

From the above discussion, it is evident that several types of potentially pathogenic T cell are expanded in AIP/IgG4-RD lesions. One factor that might explain this diverse assembly of cells is an increase in IFN-I secretion by pDCs, as discussed below. With respect to Tfh cells, there is convincing data showing that IFN-I induces the expression of several factors characteristic of Tfh cells, such as BCL6, CXCR5, and PD-1, via its activation of signal transducer and activator of transcription 1 (Stat1) in murine CD4⁺ T cells [51]. This IFN-I effect can conceivably occur in association with either Th1- or Th2 T cell-inducing factors, leading to expansion of Tfh cells that

exhibit either Th1 or Th2 properties [44]. With respect to cytotoxic CD4⁺ T cells, there is also evidence that IFN-I (IFN- α) (in association with IL-2) can induce the expansion of IgG4-RD-associated CD4⁺ cytotoxic T cells via Stat2-dependent upregulation of T-bet and Blimp-1 expression in a murine model of influenza virus infection [52]. Thus, IFN-I produced by pDCs has the potential to induce two different cell types that could be involved in AIP/IgG4-RD pathogenesis.

B Cell Abnormalities and Autoantibodies in AIP/IgG4-RD

Analyses of cell populations in the circulation and inflamed tissues of patients with AIP/IgG4-RD have disclosed that increased numbers of Tfh cells in these sites are accompanied by increased numbers of either memory B cells or plasmablasts [46,53–55]. Moreover, inasmuch as these B cell increases correlate with assessments of disease activity and IgG4 concentration, they have been considered a putative disease biomarker [53,56].

Studies of the expanded plasmablast subpopulation in AIP/IgG4-RD (defined as CD19⁺CD20⁻CD27⁺CD38^{hi} cells) reveal that this population comprises, for the most part, IgG4-producing cells and contains cells producing IgG4 Abs that react with self-antigens [57]. Of interest, the plasmablasts tend to exhibit extensive **somatic hypermutation** and display considerable oligoclonality [57]. However, the latter is not indicative of a highly specific autoAb response necessary for the development of particular disease manifestations since deletion of these cells with rituximab is eventually followed by reappearance of disease, associated with a different set of oligoclonal plasmablasts [57]. Instead, it may represent a nonpathological response to varying epitopes associated with a limited set of self-antigens [57].

Studies of the specificity of autoAbs in the circulation of patients with AIP/IgG4-RD revealed that these Abs include those specific for several pancreatic antigens, such as lactoferrin, carbonic anhydrase, and pancreatic secretory trypsin inhibitor (reviewed in [58]). However, it is unclear whether these autoAbs are primary disease factors implicated in immune complex-mediated tissue injury (see below) or are secondary nondisease factors that occur as a result of released antigens from necrotic tissue.

Treatment of patients with AIP/IgG4-RD with rituximab to reduce their B cell burden results in at least a temporary reduction in inflammation and associated disease manifestations [54,55]. This suggests that autoAbs have a pathogenic role in AIP/IgG4-RD as they do in SLE, via the formation of complement-fixing immune complexes. Evidence for this comes from immunofluorescence studies of frozen inflamed pancreatic tissues from five patients with AIP/IgG4-RD showing that deposits of IgG4 and IgG associated with complement C3c (but not C1q) were present and colocalized with collagen IV of ductal and acinar basement membranes [59]. However, IgG4 Abs do not have complement-fixing properties [60] and, thus, they might only participate in complement-mediated tissue injury by somehow interacting with other Igs, via an as yet undescribed mechanism. In addition, such antigens that are targeted by circulating autoAbs in AIP/IgG4-RD do not reside in the membranes of pancreatic cells. Thus, the question of whether immune complex-mediated tissue injury in AIP/IgG4-RD occurs remains. Another possible, albeit indirect, pathological mechanism of B cells in AIP/IgG4-RD may be that these act as antigen-presenting cells to pathogenic T cells (possibly the CD4⁺ cytotoxic T cells described above) and thereby upregulate their function. Further studies will be necessary to substantiate this interesting possibility.

Pathogenicity of IgG4 Abs

Having increased IgG4 levels, the hallmark of AIP/IgG4-RD, implies the production of the least common form of IgG, comprising just 5% of total IgG production in normal individuals [60]. This subclass of IgG is said to be produced in response to chronic antigen exposure under the influence of Th2 cytokines as well as IL-10, the latter often produced by Tregs [39]. Studies of IgG4 function have revealed that it is a relatively 'inert' class of Ab, in that it lacks the ability to bind complement via its Fc component and to form immune complexes due to its tendency to exhibit bispecificity caused by **Fab arm exchange** [60]. Nevertheless, it can mediate autoimmune diseases in certain instances via direct binding to, and disabling the functionality of, a critical antigen or receptor [61].

Studies evaluating the pathologic potential of IgG4 in AIP/IgG4-RD were conducted in mouse models in which various forms of IgG were subcutaneously injected into neonatal mice to determine the capacity of these Abs to cause pancreatic injury [62]. In these studies, injection of IgG isolated from patients with AIP/IgG4-RD elicited greater pancreatic injury than injection of IgG isolated from normal individuals. However, this was largely due to the presence of IgG1 in patient sera, as evidenced by the fact that isolated IgG1 had a greater capacity to cause injury than did isolated IgG4 [62]. Furthermore, injection of IgG4 reduced IgG1-mediated injury when co-injected with the latter relative to IgG1 injection alone [62]. In companion studies, the capacity of human IgG4 Ab obtained from patients with AIP/IgG4-RD to block the formation of pathogenic immune complexes (i.e., its 'tolerogenic' capacity) was investigated [63]. In these studies, complexes formed by the binding of IgG1 and IgG4 patient Abs to a shared epitope of annexin A11 were examined because annexin A11 is ubiquitously expressed in a variety of tissues and can therefore serve as a target of (auto) antigen in AIP/IgG4-RD [63]. Both IgG4 and IgG1 Abs from patients with AIP/IgG4-RD bound to the shared epitope of annexin A11 when tested individually, but the IgG4 Ab blocked the binding of IgG1 to annexin a11 when tested together [63]. Since IgG1 Ab can efficiently activate complement whereas IgG4 cannot, this finding suggested that IgG4 in patients with AIP/IgG4-RD could prevent the formation of pathological immune complexes but were themselves unable to form such complexes [60]. Given that elevated concentrations of IgG4 Ab specific to multiple food and animal antigens are present in AIP/IgG4-RD, these data suggest that IgG4 Abs have the capacity to block pathogenic responses mediated by IgG1 Abs to the same antigens present [64]. In this way, the IgG4 Abs in IgG4-RD may not only be inert Igs (as suggested above), but might also be inhibitory of potentially more pathological Igs. If this is the case, the IgG4 Abs in AIP/IgG4-RD could constitute a harmless epiphenomenon of the disease [64].

Innate Immunity in AIP/IgG4-RD

Activation of Innate Immune Receptors in AIP/IgG4-RD

In 2010, mice serially inoculated with heat-killed nonpathogenic *Escherichia coli* were found to develop severe and persistent pancreatic inflammation and fibrosis, as well as subsequent salivary gland inflammation and fibrosis [65]. In addition, because the inoculated mice developed several anti-self-antigen Abs similar to those observed in human AIP/IgG4-RD, investigators postulated that these inoculated mice could be used as a model for AIP/IgG4-RD and that the experimental disease likely resulted from a pathological innate immune response to molecular patterns associated with either pathogenic or nonpathogenic organisms [66]. This idea was reminiscent of the fact that the mucosa of the gastrointestinal tract is constantly exposed to intestinal microflora and that excessive immune responses to such microflora mediated by **nucleotide-binding oligomerization domain** (NOD) receptors and/or TLRs might be implicated in the immunopathogenesis of **inflammatory bowel diseases** (IBDs) [67]. Any possible resemblance of AIP/IgG4-RD pathogenesis to that of IBDs was strengthened by

the fact that IgG4-expressing plasma cells are sometimes found in the lamina propria of the gastrointestinal tracts of patients with AIP/IgG4-RD [40,68]; in addition, in a recent clinicopathological analysis of 91 patients with both AIP and IBD, 72% of patients presented with active IBD at the time of AIP diagnosis [69].

Stimulated in part by these findings, a series of studies were conducted to explore the role of innate immune responses in AIP/IgG4-RD in greater depth [70,71]. Initial *in vitro* studies showed that activation of PBMCs from healthy controls using **NOD2** [an intracellular innate immune receptor recognizing a component of the bacterial cell wall, muramyl dipeptide (MDP)] ligand induced an IgG4 response, and that both TLR2 and TLR4 ligands induced both IgG4 and IgG1 responses [70]. In addition, *in vitro* stimulation of purified monocytes from patients with AIP/IgG4-RD by NOD2 or TLR4 ligands, but not control individuals, induced IgG4 secretion by B cells (from healthy donors) and such responses were dependent on the production of **B cell-activating factor** (BAFF) (Figure 1); the latter, in turn, activated B cell production of IgG4. These responses were T cell independent, as evidenced from the B cell production of IgG4 in the absence of T cells and, in fact, T cells were shown to exert a suppressive effect on these B cell responses, perhaps by their production of IL-10 under these conditions. Various TLR ligands also induced PBMCs to produce IgG4 as well as BAFF, and were similar to MDP in inducing IgG1 production, although not to the same extent as their induction of IgG4 [70].

Previous studies showed that BAFF is a crucial survival factor for B cells [72], as well as a factor that promotes IgG4 class switch DNA recombination in the presence of IL-4 [73]. Thus, the data described above suggest that IgG4 production characteristic of AIP/IgG4-RD is dependent on an innate immune BAFF response, as well as on a Th2 cytokine (IL-4) response. However, this conclusion is at odds with the observation that IgG4 production was T cell independent in these studies; it is possible that T cells (producing Th2 cytokines) are acting at an early stage to induce the differentiation of B cells that can ultimately respond to BAFF in an apparently T cell-independent fashion. While further work is necessary to substantiate this possibility, the importance of BAFF in AIP/IgG4-RD pathogenesis suggested that the *in vitro* studies were consistent with *in vivo* findings that serum BAFF concentrations in patients with AIP/IgG4-RD were higher than those in patients with ordinary (non-autoimmune) pancreatitis [8].

As revealed by immunohistochemical analysis of tissue samples, the types of innate cell that could be responding to NOD and/or TLR ligands in AIP/IgG4-RD include pDCs as well as **M2 macrophages** and basophils (Figure 1) [8,71,74]. With respect to M2 macrophages, one study reported that salivary lesions of patients with AIP/IgG4-RD were characterized by CD163⁺ M2 macrophages producing IL-10 and IL-13 [74]. Both of these cytokines have been shown to be profibrogenic factors [1,74] and, indeed, the numbers of M2 macrophages present in lesional tissues positively correlated with the degree of fibrosis present in these patient tissues; in addition, infiltration of M2 macrophages was seen in the pancreas of patients with AIP/IgG4-RD [75]. With respect to basophils, basophils expressing TLR2 and TLR4 have been found in inflamed pancreas of patients with AIP/IgG4-RD [76]. This is compatible with data showing that peripheral blood basophils isolated and stimulated with either TLR2 or TLR4 ligands from such patients could induce IgG4 Ab production by healthy control B cells via a T cell-independent and BAFF-dependent mechanism [71]. In addition, the basophils secreted IL-13, a cytokine that supports the induction of IgG4-producing B cells [71]. Finally, AIP/IgG4-RD has been noted in many patients exhibiting allergic manifestations, possibly influenced by Th2 responses present in this disease [77]. Therefore, it is possible that this allergic response could contribute to inflammation via the activation of basophils. Further studies will be needed to better elucidate these potential mechanisms.

Overall, the described studies relating to innate responses in AIP/IgG4-RD support the possibility that bacterial cell wall components capable of stimulating cells via NOD2 and/or TLR4, and abundantly expressed in the gut microbiome [67], do indeed have an important role in both the initiation and maintenance of AIP/IgG4-RD; and that BAFF might be an effector molecule in this process.

Type I IFN in AIP/IgG4-RD

Further understanding of the innate immune responses in AIP/IgG4-RD uncovered by studies in patient cells required a murine model to allow detailed identification of the cells and cytokines causing this disease. This need was met by the discovery that MRL/Mp mice develop spontaneous AIP at more than 24 weeks of age and this autoimmune manifestation could be induced at 8 weeks after administration of polyinosinic:polycytidylic acid [poly(I:C)] [78,79]. MRL/Mp mice treated with poly(I:C) exhibited pathological features of pancreatitis akin to human AIP/IgG4-RD, including destruction of pancreas acinar architecture as well as infiltration of pancreas with immune cells and fibrosis [8,9]. Moreover, poly(I:C)-treated mice usually exhibited multiorgan inflammation involving not only the pancreas, but also the salivary glands and kidneys [79]. Aside from the fact that mice lack IgG4 Ab, this experimental model of AIP/IgG4-RD faithfully recapitulates clinical and pathological features of human AIP/IgG4-RD.

Subsequent analysis showed that the development of murine AIP/IgG4-RD was associated with the pancreatic accumulation of PDC antigen-1 (PDCA1)⁺Siglec-H⁺B220^{intermediate} pDCs, accompanied by enhanced production of IFN-I and its downstream ligands CXCL9, CXCL10, and CXCL11 in the serum [8,9]. In addition, when addressing the role of pDCs-derived IFN-I in experimental murine AIP, depletion of pDCs by Ab (120G8 Ab) and neutralization of IFN-I signaling pathways by anti-IFNAR Ab efficiently inhibited the pancreatic accumulation of pDCs and IFN-I responses, respectively, concomitant with abatement of the pancreatitis. Thus, these studies established that experimental AIP/IgG4-RD could result from an innate immune response mediated by pDCs producing IFN-I [8,9]. Of note, this conclusion is seemingly contradicted by the fact that administration of IFN- β protects MRL/*lpr* mice from SLE-like symptoms, as previously mentioned [20]. However, this difference in the effect of IFN-I on the development of autoimmune diseases can be partially explained by the fact that SLE-prone MRL/*lpr* mice develop autoimmune responses due to defective Fas-mediated apoptosis, whereas AIP/IgG4-RD in MRL/Mp mice present intact Fas-mediated apoptosis [20,21].

To establish the relevance of the MRL/Mp model relative to human AIP/IgG4-RD, pancreatic tissue obtained during therapeutic surgery of patients with AIP/IgG4-RD was assessed: inflamed tissue was infiltrated with CD123⁺ blood dendritic cell antigen 2⁺ pDCs expressing both IFN- α and BAFF [8]. By contrast, pancreatic tissue from patients with CP or noncancerous pancreatic tissue from patients with pancreatic cancer did not contain such cells [8]. Consistent with this, serum concentrations of IFN- α were markedly higher in patients with AIP/IgG4-RD compared with those in CP or healthy controls [8].

The above studies were accompanied by those linking increased IFN-I production to B cell IgG4 secretion. An important initial finding was that MRL/Mp mice with experimental AIP, as well as pancreatic tissue from inflamed pancreas of patients with AIP/IgG4-RD, harbored NETs [8]. Subsequent studies investigated if NETs were involved in B cell IgG4 secretion; peripheral blood pDCs isolated from patients with AIP/IgG4-RD co-cultured with NETs induced in normal neutrophils (by anti-lactoferrin Ab or uric acid crystals) produced IFN-I as well as BAFF, leading to an induction of IgG4 production by normal B cells [8]. Of relevance, blockade of IFN-I

signaling with anti-IFNAR Ab resulted in a marked reduction in B cell IgG4 production compared with control Ab [8]. This provided evidence that IFN-I production was an essential element in the IgG4 secretion. Finally, pDCs from patients with AIP/IgG4-RD but not from normal individuals were capable of inducing B cell IgG4 secretion, suggesting that patient pDCs are conditioned *in vivo*, in an as yet unknown way, to mediate IgG4 secretion [8].

The fact that pDCs from patients with AIP/IgG4RD can induce B cell IgG4 production in the presence of NETs expands on previous studies showing that monocytes and basophils from patients activated by microbe-associated molecular patterns (MAMPs) also have this capability [70,71]. Collectively, these studies indicate that pDCs from AIP/IgG4-RD patients, either activated by MAMPs or endogenous factors derived from NETs, can produce factors such as BAFF that support IgG4 B cell differentiation (see Outstanding Questions). Moreover, they also suggest that pDC-mediated IFN-I responses have a pivotal role in AIP/IgG4-RD.

IL-33 in AIP/IgG4-RD

Reports establishing the importance of IFN-I in the pathogenesis of AIP/IgG4-RD are mirrored in studies of CP initiated by an abnormality in the handling of pancreatic digestive enzymes, especially trypsin, and, thus, in the release of active enzymes causing acinar cell injury (reviewed in [1]) (Box 2) [80,81]. Specifically, the recognition of pancreatic inflammation in CP was deemed to depend on the production of IFN-I and IL-33 by pancreatic acinar cells because mice deficient in the IFN-I receptor or those treated with neutralizing Ab against IL-33 receptor (ST2) were protected from the development of CP [80,81]. This prompted an examination of the putative role of IL-33 in AIP/IgG4-RD using the MRL/Mp mouse model of experimental AIP/IgG4-RD, as well as specimens of pancreatic tissue obtained from patients with AIP/IgG4-RD during surgery [9]. IL-33 expression was markedly enhanced in the pancreas of mice with experimental AIP/IgG4-RD compared with those without AIP/IgG4-RD [9] (Figure 2). However, in this case, tissue immunofluorescence showed that pancreatic pDCs, but not acinar cells, were the source of IL-33 [9]. This was consistent with the production of large amounts of IFN-I as well as IL-33, upon stimulation with a TLR9 ligand in pancreatic pDCs isolated from experimental AIP/IgG4-RD mice; in addition, depletion of pDCs in populations of pancreatic mononuclear cells (PMCs) resulted in a marked reduction of these two cytokines compared with PMCs, including pDCs [9]. Furthermore, Ab-mediated depletion of pDCs (with 120G8 Ab) and neutralization of IFN-I signaling pathways via an anti-IFNAR Ab efficiently inhibited chronic inflammation as well as pancreatic fibrosis in these mice [9]. This suggested that chronic pancreatic inflammation as well as pancreatic fibrosis could depend on pDC-mediated IFN-I responses. Finally, blockade of IL-33-mediated signaling pathways via an anti-ST2 Ab resulted in a marked reduction in chronic fibroinflammatory responses *in vivo*, as evidenced by decreased tissue fibrosis and ameliorated pancreatitis pathology scores relative to control Ab-treated mice [9].

With respect to the cellular sources of IFN-I and IL-33 in the pancreas of patients with AIP/IgG4-RD or CP, IFN-I expression was detected (via immunofluorescence) in pDCs in AIP/IgG4-RD and whereas IL-33 expression was present in both pDCs and acinar cells in AIP/IgG4-RD, IL-33 expression was limited to acinar cells in CP [1,8,9,81]. Thus, these data support the hypothesis that activation of the IFN-I/IL-33 axis in pancreatic pDCs and acinar cells is likely to contribute to immunopathogenesis in AIP/IgG4-RD and CP, respectively.

An important question is how IL-33 might induce chronic fibroinflammatory responses that are characteristic of AIP/IgG4-RD (see Outstanding Questions). It is well established that IL-33 activates both Th2 and **group 2 innate lymphoid cells** (ILC2) to promote the production of IL-4, IL-5, and IL-13 [82,83]. Thus, one of the consequences of IL-33 production would be to

Box 2. IFN-I and IL-33 in Conventional Chronic Pancreatitis

The importance of IFN-I in the pathogenesis of AIP/IgG4-RD is mirrored in its involvement in conventional CP pathogenesis. In a well-established murine model of acute pancreatitis induced by administration of high doses of cerulein, an agent that mimics the effect of excess **cholecystokinin** (CCK) signaling, causing active trypsin release, initial cell injury due to active trypsin release led to entry of gut bacteria into the circulation and activation of acinar cell **NOD1**, an intracellular innate immune receptor detecting small peptides derived from the bacterial wall [67,80]. NOD1 signaling initiated an inflammatory response, sustaining pancreatitis initiated by the disturbance in trypsin activation [1].

In a model of acute pancreatitis created by injection of low doses of cerulein and NOD1 ligand (FK156 or FK565), factors resulting from NOD1 activation acted synergistically with factors resulting from cerulein activation of the CCK pathway, causing acinar cell production of an array of proinflammatory chemokines and cytokines, such as C-C motif chemokine ligand 2 (CCL2) and IFN-I (Figure I); these factors were important for inflammation because mice deficient in the receptor for CCL2 (C-C chemokine receptor type 2, CCR2) or deficient in IFNAR were protected from developing acute pancreatitis [80]. This was attributed to the fact that CCL2 promoted the migration of pathological macrophages expressing CCR2 into the pancreas and IFN-I was essential for CCL2 production [80]. Moreover, IFN-I was essential to pancreatic inflammation because this cytokine is necessary for the production of CCL2. Thus, gut commensals enabled acute pancreatic inflammation through NOD1 induction of CCL2 and IFN-I production [1,80,87].

In a chronic model of pancreatitis induced by repeated injection of mice with low-dose cerulein and FK565, pancreatic tissues with CP were characterized by a multifaceted proinflammatory cytokine and chemokine response involving the production of TNF- α , IL-6, CCL2, and IFN-I [81] (Figure I). The importance of IFN-I was shown by the absence of CP in IFNAR-deficient mice and was attributed to both its induction of CCR2 in monocytes and, as in the acute model of pancreatitis, its facilitation of CCL2 effects on the migration of CCR2-expressing monocytes [88]. Thus, IFN-I was necessary for both receptor (CCR2) and ligand (CCL2) components of the chemotactic process allowing pathological infiltration of macrophages into the pancreas [88].

IFN-I in CP also induced macrophage TNF- α production [89], which amplified necroptotic acinar cell death leading to the release of IL-33 [90], an alarmin secreted by dying acinar cells, with a profound effect on the course of pancreatitis [81,82] (Figure I). In this CP model, neutralization of IL-33 signaling (ST2 blocking Ab) resulted in reduced infiltration of immune effector cells in the pancreas and production of proinflammatory mediators, such as CCL2 and TNF- α , as well as profibrogenic factors, such as IL-13 and TGF- β 1, relative to controls [1,81,90]. These models have provided evidence that IL-33 produced by pancreatic acinar cells as a result of IFN-I secretion might have an essential role in CP.

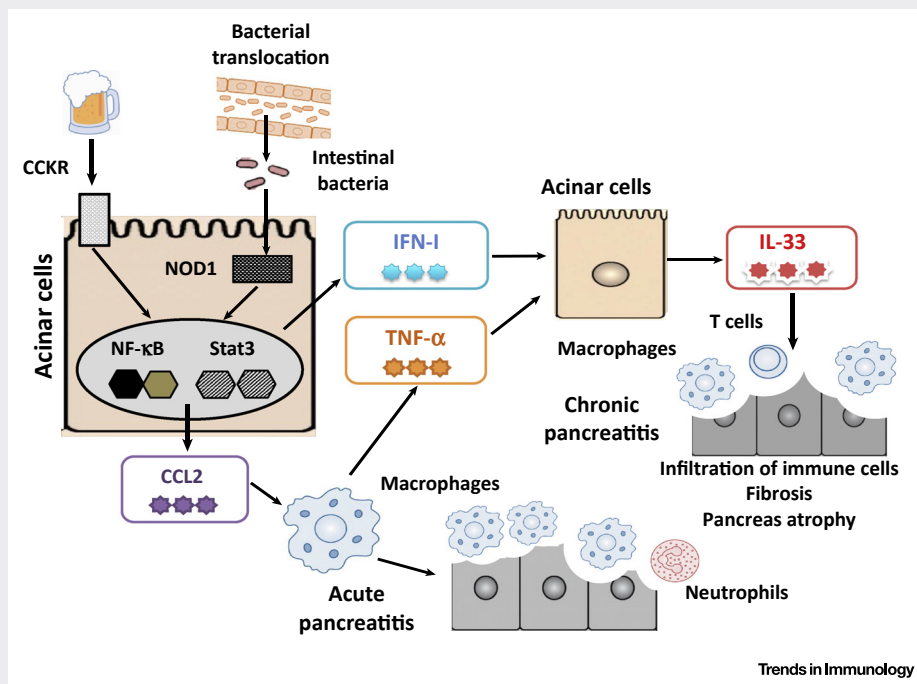
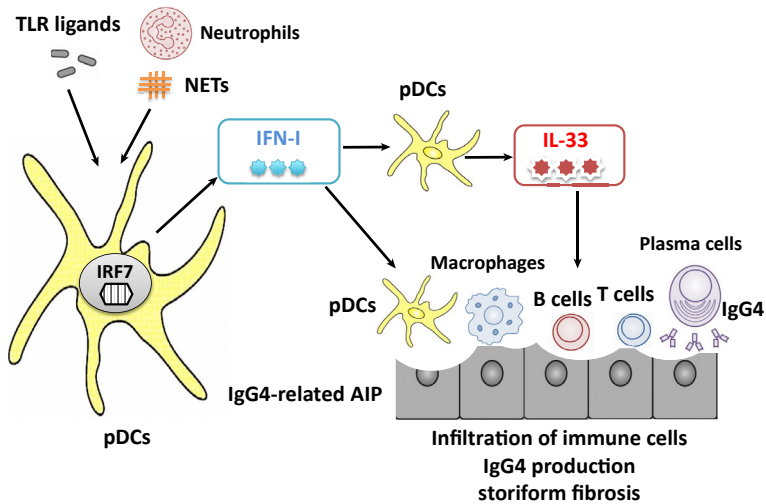


Figure I. Association of Pancreatic Acinar Cell-Derived Type I IFN (IFN-I) and IL-33 with Murine and Human Chronic Pancreatitis (CP). Various environmental factors, such as excessive drinking of alcohol or genetic factors, disturb cholecystokinin receptor (CCKR) signaling and pancreatic enzyme handling in acinar cells and, thus, initiate the non-autoimmune pancreatitis that occurs in CP [1]. In this case, nucleotide-binding oligomerization domain 1 (NOD1) expressed in pancreatic acinar cells is activated by bacterial peptidoglycan derived from intestinal bacteria that are translocated into the pancreas upon initiation of pancreatitis, thereby sustaining inflammation [1]. In acute pancreatitis, NOD1 activation can act synergistically with CCKR activation to induce optimal production of C-C motif chemokine ligand 2 (CCL2) and IFN-I by acinar cells through nuclear translocation of nuclear factor- κ B (NF- κ B) and signal transduction and activator of transcription 3 (Stat3); pathogenic macrophages migrate into the pancreas in response to CCL2 production [80]. In CP due to recurrent acute episodes, activation of CCKR and NOD1 leads to pancreatic accumulation of pathogenic macrophages producing TNF- α . In this setting, pancreatic acinar cells release IL-33 in response to TNF- α and IFN-I derived from macrophages and acinar cells, respectively [81]. IL-33 and IL-13 might then mediate a chronic fibroinflammatory response that is relevant in CP [81].



Trends in Immunology

Figure 2. Plasmacytoid Dendritic Cells (pDCs) Produce Type I IFN (IFN-I) and IL-33 in Murine Autoimmune Pancreatitis (AIP) and Human IgG4-Related Disease (IgG4-RD). AIP and IgG4-RD in a murine model (MRL/Mp mice) and in humans are characterized by the presence of a unique type of pDC capable of producing IFN-I as well as IL-33 (the latter dependent on IFN-I production) in lesional tissues [8,9]. There is strong evidence that such pDCs are activated by substances generated by neutrophil extracellular traps (NETs) and Toll-like receptor (TLR) ligands. In the murine model, both IFN-I and IL-33 are necessary for the development of tissue inflammation and fibrosis and, in humans, pDCs can mediate B cell production of hallmark IgG4 via production of B cell-activating factor (BAFF) [8,9]. IRF7, interferon regulatory factor 7.

support Th2 responses and exert effects on B cell subsets in such a way to contribute to AIP/IgG4-RD pathology. Another consequence might relate to the role of IL-13, known to be a potent profibrogenic factor [84]. For instance, MRL/Mp mice with experimental AIP/IgG4-RD exhibit marked pancreatic expression of IL-13 relative to mice without AIP/IgG4-RD [9]. Moreover, administration of anti-ST2 Ab to neutralize IL-33-mediated signaling pathways resulted in the diminished pancreatic expression of IL-13, as well as diminished pancreatic fibrosis compared with control Ab-treated mice [9]. However, while these data suggest that pDC-derived IL-33 promotes pancreatic fibrosis through IL-13, the cellular sources of IL-13 have yet to be determined, and its putative contribution to pathogenesis further examined [9].

Taken together, robust evidence suggests that pDC-derived IFN-I and IL-33 has an essential role in AIP/IgG4-RD. This is further strengthened by the observation that IL-33 expression has been noted in pDCs and M2 macrophages within the salivary glands of patients with AIP/IgG4-RD [85]. In addition, serum concentrations of IL-33 are reduced upon corticosteroid treatment in patients with AIP/IgG4-RD relative to baseline concentrations, suggesting that IL-33 concentrations correlate with disease activity [85].

Concluding Remarks

The survey of immunological findings in AIP/IgG4-RD in this review teaches us that there is still much to be learned concerning the pathogenesis of this multiorgan disease complex (see Outstanding Questions). Nevertheless, recent discoveries described here have placed us on a new platform of understanding that may inform the way to further research and possible treatment of this disease. Using a reliable murine disease model as well as studies in humans with disease, a chief discovery has been the increased production of IFN-I from pDCs stimulated by MAMPs and/or by factors derived from NETs, as a central mechanism for disease pathogenesis in AIP/IgG4-RD. This IFN-I innate response has two consequences

Outstanding Questions

What are the triggers of pDC activation in AIP/IgG4-RD? Are immune complexes, NETs, or TLR ligands involved in the activation process of pDCs in these autoimmune disorders?

What are the molecular mechanisms accounting for the production of IFN-I and IL-33 by pDCs in AIP/IgG4-RD? Is activation of interferon regulatory factor 3 (IRF3) and IRF7 involved in the production of these cytokines?

How does IL-33 mediate chronic inflammation and fibrosis in AIP/IgG4-RD? Cellular sources of profibrogenic cytokines, such as IL-13 and TGF- β 1, need to be identified.

How do IFN-I and IL-33 preferentially induce IgG4 production by B cells?

Does IL-33 have a role in the immunopathogenesis of other autoimmune disorders driven by IFN-I?

Would blockade of the IFN-I/IL-33 axis be beneficial in AIP and IgG4-RD? Could IFN-I and IL-33 also be useful as putative biomarkers in AIP/IgG4-RD?

Box 3. Similarities and Differences between AIP/IgG4-RD and SLE

Activation of pDCs leading to IFN-I production is a common component in the pathogenesis of SLE and AIP/IgG4-RD. In SLE, such activation arises from immune complexes or NETs containing autoantigens and other factors that facilitate pDC activation via TLR7 and TLR9 [23,24,27,28]. In AIP/IgG4-RD, the mechanism of pDC activation is less clear because the autoAbs present might not form complexes that can access endoplasmic TLR7 and TLR9. In addition, whereas NETs are also involved in the activation of pDCs in AIP/IgG4-RD, it remains unknown whether such activation requires TLR7 and/or TLR9 stimulation. Despite these possible differences in the origin of the IFN-I elevations, the fact that such increases occur in both diseases remains a major commonality between the two autoimmune diseases that is difficult to reconcile with the fact that the clinical manifestations of AIP/IgG4-RD are so different.

In AIP/IgG4-RD, pancreatic inflammation and that of other organs with storiform fibrosis are characteristic features, but it is unlikely that this is related to autoAb deposition because IgG4 autoAbs are relatively inert; in contrast, in SLE, inflammation and organ dysfunction is clearly tied to autoAb deposition or other consequences of immune activation due to autoAbs, including activation of inflammasome release of IL-1 β and IL-18 [91,92]. On the basis of these differences, one might hypothesize that, whereas IFN-I elevations occur in both forms of autoimmunity, these elevations in SLE affect a B cell population that is genetically different from that in AIP/IgG4-RD, with B cells less subject to tolerization by self-antigens and, thus, more likely to produce autoAbs with a pathogenic potential. However, future studies will be required to fully elucidate these differences.

Another important difference between AIP/IgG4-RD and SLE is that, in AIP/IgG4-RD, pDCs producing IFN-I also produce IL-33, the latter depending on IFN-I production. By contrast, in SLE, pDCs are not IL-33 producers, as evidenced by the fact that serum concentrations of IL-33 in SLE are only marginally increased, at best, relative to controls [93,94]. Inasmuch as neutralization of IL-33 signaling prevents not only chronic inflammation, but also fibrosis formation in experimental AIP/IgG4-RD, it appears that the ability of pDCs in AIP/IgG4-RD to produce IL-33 may have profound pathological consequences that could contribute to explaining differences between AIP/IgG4-RD and SLE [8,9]. Aside from B cells, it is possible that pDCs in SLE might behave differently from those in AIP/IgG4-RD, although this remains to be tested.

central to the development of the disease. First, in association with BAFF (also generated by pDCs), IFN-I stimulates B cells (from control individuals) to produce IgG4. Regardless of whether this latter defining disease factor is an important pathological component or an epiphenomenon, IFN-I appears to have a key role in contributing to B cell-mediated autoimmunity in AIP/IgG4-RD. Second, we now understand that IFN-I has, in the context of AIP/IgG4-RD, the unique ability among B cell-associated autoimmune diseases to induce the production of IL-33 (Box 3). This cytokine can induce Th2 cytokines that may support, on the one hand, B cell abnormalities in AIP/IgG4-RD and, on the other hand, cytokines necessary for the induction of the inflammation and fibrosis occurring in this disease. The multifactorial relationship of IFN-I with AIP/IgG4-RD pathogenesis appears to be in contrast to the relationship of IFN-I with SLE and perhaps with other autoimmune diseases that are more dependent on abnormalities intrinsic to B cells. Although many questions remain (see Outstanding Questions), and further research is clearly warranted, the centrality of IFN-I to AIP/IgG4-RD pathogenesis may render this cytokine, or its dependent cytokine, IL-33, compelling putative targets in the treatment of this new disease.

Acknowledgments

This work was supported by the Naito Foundation, SENSHIN Medical Research Foundation, Yakult Bio-Science Foundation, Smoking Research Foundation, Kobayashi Foundation for Cancer Research, Takeda Science Foundation, and Japan Agency for Medical Research and Development (AMED) Grants for Research on Intractable Diseases.

References

1. Watanabe, T. *et al.* (2017) Immunopathogenesis of pancreatitis. *Mucosal Immunol.* 10, 283–298
2. Kamisawa, T. *et al.* (2013) Recent advances in autoimmune pancreatitis: type 1 and type 2. *Gut* 62, 1373–1380
3. Braganza, J.M. *et al.* (2011) Chronic pancreatitis. *Lancet* 377, 1184–1197
4. Kamisawa, T. and Okazaki, K. (2017) Diagnosis and treatment of IgG4-related disease. *Curr. Top. Microbiol. Immunol.* 401, 19–33
5. Stone, J.H. *et al.* (2012) IgG4-related disease. *N. Engl. J. Med.* 366, 539–551
6. Brito-Zeron, P. *et al.* (2014) The clinical spectrum of IgG4-related disease. *Autoimmun. Rev.* 13, 1203–1210

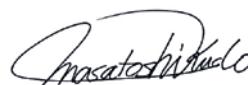
7. Takuma, K. *et al.* (2010) Metachronous extrapancreatic lesions in autoimmune pancreatitis. *Intern. Med.* 49, 529–533
8. Arai, Y. *et al.* (2015) Plasmacytoid dendritic cell activation and IFN- α production are prominent features of murine autoimmune pancreatitis and human IgG4-related autoimmune pancreatitis. *J. Immunol.* 195, 3033–3044
9. Watanabe, T. *et al.* (2017) Chronic fibro-inflammatory responses in autoimmune pancreatitis depend on IFN- α and IL-33 produced by plasmacytoid dendritic cells. *J. Immunol.* 198, 3886–3896
10. Ganguly, D. (2018) Do Type I interferons link systemic autoimmunities and metabolic syndrome in a pathogenetic continuum? *Trends Immunol.* 39, 28–43
11. Swiecki, M. and Colonna, M. (2015) The multifaceted biology of plasmacytoid dendritic cells. *Nat. Rev. Immunol.* 15, 471–485
12. Psarras, A. *et al.* (2017) Type I interferon-mediated autoimmune diseases: pathogenesis, diagnosis and targeted therapy. *Rheumatology (Oxford)* 56, 1662–1675
13. Bennett, L. *et al.* (2003) Interferon and granulopoiesis signatures in systemic lupus erythematosus blood. *J. Exp. Med.* 197, 711–723
14. Deng, Y. and Tsao, B.P. (2010) Genetic susceptibility to systemic lupus erythematosus in the genomic era. *Nat. Rev. Rheumatol.* 6, 683–692
15. Khamashta, M. *et al.* (2016) Sifalimumab, an anti-interferon- α monoclonal antibody, in moderate to severe systemic lupus erythematosus: a randomised, double-blind, placebo-controlled study. *Ann. Rheum. Dis.* 75, 1909–1916
16. Furie, R. *et al.* (2017) Anifrolumab, an anti-interferon- α receptor monoclonal antibody, in moderate-to-severe systemic lupus erythematosus. *Arthritis Rheumatol.* 69, 376–386
17. Baccala, R. *et al.* (2012) Anti-IFN- α /beta receptor antibody treatment ameliorates disease in lupus-predisposed mice. *J. Immunol.* 189, 5976–5984
18. Deane, J.A. *et al.* (2007) Control of toll-like receptor 7 expression is essential to restrict autoimmunity and dendritic cell proliferation. *Immunity* 27, 801–810
19. Santiago-Raber, M.L. *et al.* (2003) Type-I interferon receptor deficiency reduces lupus-like disease in NZB mice. *J. Exp. Med.* 197, 777–788
20. Schwarting, A. *et al.* (2005) Interferon- β : a therapeutic for autoimmune lupus in MRL-Fas lpr mice. *J. Am. Soc. Nephrol.* 16, 3264–3272
21. Hron, J.D. and Peng, S.L. (2004) Type I IFN protects against murine lupus. *J. Immunol.* 173, 2134–2142
22. Sitrin, J. *et al.* (2017) The O $x40$ /O $x40$ ligand pathway promotes pathogenic Th cell responses, plasmablast accumulation, and lupus nephritis in NZB/W F1 mice. *J. Immunol.* 199, 1238–1249
23. Lande, R. *et al.* (2011) Neutrophils activate plasmacytoid dendritic cells by releasing self-DNA-peptide complexes in systemic lupus erythematosus. *Sci. Transl. Med.* 3, 73ra19
24. Garcia-Romo, G.S. *et al.* (2011) Netting neutrophils are major inducers of type I IFN production in pediatric systemic lupus erythematosus. *Sci. Transl. Med.* 3, 73ra20
25. Honda, K. *et al.* (2006) Type I interferon [corrected] gene induction by the interferon regulatory factor family of transcription factors. *Immunity* 25, 349–360
26. Lood, C. *et al.* (2016) Neutrophil extracellular traps enriched in oxidized mitochondrial DNA are interferogenic and contribute to lupus-like disease. *Nat. Med.* 22, 146–153
27. Barrat, F.J. *et al.* (2005) Nucleic acids of mammalian origin can act as endogenous ligands for Toll-like receptors and may promote systemic lupus erythematosus. *J. Exp. Med.* 202, 1131–1139
28. Means, T.K. *et al.* (2005) Human lupus autoantibody-DNA complexes activate DCs through cooperation of CD32 and TLR9. *J. Clin. Invest.* 115, 407–417
29. Nestle, F.O. *et al.* (2005) Plasmacytoid predendritic cells initiate psoriasis through interferon- α production. *J. Exp. Med.* 202, 135–143
30. Lande, R. *et al.* (2007) Plasmacytoid dendritic cells sense self-DNA coupled with antimicrobial peptide. *Nature* 449, 564–569
31. Ganguly, D. *et al.* (2009) Self-RNA-antimicrobial peptide complexes activate human dendritic cells through TLR7 and TLR8. *J. Exp. Med.* 206, 1983–1994
32. Allen, J.S. *et al.* (2009) Plasmacytoid dendritic cells are proportionally expanded at diagnosis of type 1 diabetes and enhance islet autoantigen presentation to T-cells through immune complex capture. *Diabetes* 58, 138–145
33. Diana, J. *et al.* (2013) Crosstalk between neutrophils, B-1a cells and plasmacytoid dendritic cells initiates autoimmune diabetes. *Nat. Med.* 19, 65–73
34. Gottenberg, J.E. *et al.* (2006) Activation of IFN pathways and plasmacytoid dendritic cell recruitment in target organs of primary Sjogren's syndrome. *Proc. Natl. Acad. Sci. U. S. A.* 103, 2770–2775
35. Brkic, Z. *et al.* (2013) Prevalence of interferon type I signature in CD14 monocytes of patients with Sjogren's syndrome and association with disease activity and BAFF gene expression. *Ann. Rheum. Dis.* 72, 728–735
36. Eloranta, M.L. *et al.* (2010) Type I interferon system activation and association with disease manifestations in systemic sclerosis. *Ann. Rheum. Dis.* 69, 1396–1402
37. Punnonen, J. *et al.* (1993) Interleukin 13 induces interleukin 4-independent IgG4 and IgE synthesis and CD23 expression by human B cells. *Proc. Natl. Acad. Sci. U. S. A.* 90, 3730–3734
38. Jeannin, P. *et al.* (1998) IgE versus IgG4 production can be differentially regulated by IL-10. *J. Immunol.* 160, 3555–3561
39. Bynoe, M.S. and Viret, C. (2008) Foxp3+CD4 $^+$ T cell-mediated immunosuppression involves extracellular nucleotide catabolism. *Trends Immunol.* 29, 99–102
40. Akitake, R. *et al.* (2010) Possible involvement of T helper type 2 responses to Toll-like receptor ligands in IgG4-related sclerosing disease. *Gut* 59, 542–545
41. Tanaka, A. *et al.* (2012) Th2 and regulatory immune reactions contribute to IgG4 production and the initiation of Mikulicz disease. *Arthritis Rheum.* 64, 254–263
42. Zen, Y. *et al.* (2007) Th2 and regulatory immune reactions are increased in immunoglobulin G4-related sclerosing pancreatitis and cholangitis. *Hepatology* 45, 1538–1546
43. Maehara, T. *et al.* (2012) Interleukin-21 contributes to germinal centre formation and immunoglobulin G4 production in IgG4-related dacryoadenitis and sialoadenitis, so-called Mikulicz's disease. *Ann. Rheum. Dis.* 71, 2011–2019
44. Yu, D. and Vinuesa, C.G. (2010) The elusive identity of T follicular helper cells. *Trends Immunol.* 31, 377–383
45. Kamekura, R. *et al.* (2017) Cutting edge: a critical role of lesional T follicular helper cells in the pathogenesis of IgG4-related disease. *J. Immunol.* 199, 2624–2629
46. Akiyama, M. *et al.* (2015) Number of circulating follicular helper 2 T cells correlates with IgG4 and interleukin-4 levels and plasmablast numbers in IgG4-related disease. *Arthritis Rheumatol.* 67, 2476–2481
47. Chen, Y. *et al.* (2018) Aberrant expansion and function of T follicular helper cell subsets in IgG4-related disease. *Arthritis Rheumatol.* Published online May 21, 2018. <http://dx.doi.org/10.1002/art.40556>
48. Maehara, T. *et al.* (2017) Lesional CD4 $^+$ IFN- γ cytotoxic T lymphocytes in IgG4-related dacryoadenitis and sialoadenitis. *Ann. Rheum. Dis.* 76, 377–385
49. Mattoo, H. *et al.* (2016) Clonal expansion of CD4(+) cytotoxic T lymphocytes in patients with IgG4-related disease. *J. Allergy Clin. Immunol.* 138, 825–838
50. Della-Torre, E. *et al.* (2018) A CD8 α -subset of CD4 $^+$ SLAMF7+ cytotoxic T cells is expanded in patients with IgG4-related disease and decreases following glucocorticoid treatment. *Arthritis Rheumatol.* 70, 1133–1143
51. Nakayama, S. *et al.* (2014) Type I IFN induces binding of STAT1 to Bcl6: divergent roles of STAT family transcription factors in the

- T follicular helper cell genetic program. *J. Immunol.* 192, 2156–2166
52. Hua, L. *et al.* (2013) Cytokine-dependent induction of CD4⁺ T cells with cytotoxic potential during influenza virus infection. *J. Virol.* 87, 11884–11893
 53. Kubo, S. *et al.* (2018) Correlation of T follicular helper cells and plasmablasts with the development of organ involvement in patients with IgG4-related disease. *Rheumatology (Oxford)* 57, 514–524
 54. Della-Torre, E. *et al.* (2015) B-cell depletion attenuates serological biomarkers of fibrosis and myofibroblast activation in IgG4-related disease. *Ann. Rheum. Dis.* 74, 2236–2243
 55. Khosroshahi, A. *et al.* (2010) Rituximab therapy leads to rapid decline of serum IgG4 levels and prompt clinical improvement in IgG4-related systemic disease. *Arthritis Rheum.* 62, 1755–1762
 56. Wallace, Z.S. *et al.* (2015) Plasmablasts as a biomarker for IgG4-related disease, independent of serum IgG4 concentrations. *Ann. Rheum. Dis.* 74, 190–195
 57. Mattoo, H. *et al.* (2014) De novo oligoclonal expansions of circulating plasmablasts in active and relapsing IgG4-related disease. *J. Allergy Clin. Immunol.* 134, 679–687
 58. Yanagisawa, N. *et al.* (2011) Are dysregulated inflammatory responses to commensal bacteria involved in the pathogenesis of hepatobiliary-pancreatic autoimmune disease? An analysis using mice models of primary biliary cirrhosis and autoimmune pancreatitis. *ISRN Gastroenterol.* 2011, 513514
 59. Detlefsen, S. *et al.* (2010) Deposition of complement C3c, immunoglobulin (Ig)G4 and IgG at the basement membrane of pancreatic ducts and acini in autoimmune pancreatitis. *Histopathology* 57, 825–835
 60. Aalberse, R.C. *et al.* (2009) Immunoglobulin G4: an odd antibody. *Clin. Exp. Allergy* 39, 469–477
 61. Koneczny, I. (2018) A new classification system for IgG4 autoantibodies. *Front. Immunol.* 9, 97
 62. Shiohara, M. *et al.* (2016) Pathogenicity of IgG in patients with IgG4-related disease. *Gut* 65, 1322–1332
 63. Hubers, L.M. *et al.* (2018) Annexin A11 is targeted by IgG4 and IgG1 autoantibodies in IgG4-related disease. *Gut* 67, 728–735
 64. Culver, E.L. *et al.* (2015) Increased IgG4 responses to multiple food and animal antigens indicate a polyclonal expansion and differentiation of pre-existing B cells in IgG4-related disease. *Ann. Rheum. Dis.* 74, 944–947
 65. Haruta, I. *et al.* (2010) A mouse model of autoimmune pancreatitis with salivary gland involvement triggered by innate immunity via persistent exposure to avirulent bacteria. *Lab. Invest.* 90, 1757–1769
 66. Haruta, I. *et al.* (2012) Commensal flora, is it an unwelcomed companion as a triggering factor of autoimmune pancreatitis? *Front. Physiol.* 3, 77
 67. Strober, W. *et al.* (2006) Signalling pathways and molecular interactions of NOD1 and NOD2. *Nat. Rev. Immunol.* 6, 9–20
 68. Notohara, K. *et al.* (2018) Gastrointestinal manifestation of immunoglobulin G4-related disease: clarification through a multicenter survey. *J. Gastroenterol.* 53, 845–853
 69. Lorenzo, D. *et al.* (2018) Features of autoimmune pancreatitis associated with inflammatory bowel diseases. *Clin. Gastroenterol. Hepatol.* 16, 59–67
 70. Watanabe, T. *et al.* (2012) Activation of Toll-like receptors and NOD-like receptors is involved in enhanced IgG4 responses in autoimmune pancreatitis. *Arthritis Rheum.* 64, 914–924
 71. Watanabe, T. *et al.* (2013) Toll-like receptor activation in basophils contributes to the development of IgG4-related disease. *J. Gastroenterol.* 48, 247–253
 72. Mackay, F. and Schneider, P. (2009) Cracking the BAFF code. *Nat. Rev. Immunol.* 9, 491–502
 73. Litinskiy, M.B. *et al.* (2002) DCs induce CD40-independent immunoglobulin class switching through BLyS and APRIL. *Nat. Immunol.* 3, 822–829
 74. Furukawa, S. *et al.* (2015) Preferential M2 macrophages contribute to fibrosis in IgG4-related dacryoadenitis and sialoadenitis, so-called Mikulicz's disease. *Clin. Immunol.* 156, 9–18
 75. Fukui, Y. *et al.* (2015) Possible involvement of Toll-like receptor 7 in the development of type 1 autoimmune pancreatitis. *J. Gastroenterol.* 50, 435–444
 76. Yanagawa, M. *et al.* (2018) Basophils activated via TLR signaling may contribute to pathophysiology of type 1 autoimmune pancreatitis. *J. Gastroenterol.* 53, 449–460
 77. Culver, E.L. *et al.* (2017) Increases in IgE, eosinophils, and mast cells can be used in diagnosis and to predict relapse of IgG4-Related disease. *Clin. Gastroenterol. Hepatol.* 15, 1444–1452 e1446
 78. Kanno, H. *et al.* (1992) Spontaneous development of pancreatitis in the MRL/Mp strain of mice in autoimmune mechanism. *Clin. Exp. Immunol.* 89, 68–73
 79. Qu, W.M. *et al.* (2002) A novel autoimmune pancreatitis model in MRL mice treated with polyinosinic:polycytidylic acid. *Clin. Exp. Immunol.* 129, 27–34
 80. Tsuji, Y. *et al.* (2012) Sensing of commensal organisms by the intracellular sensor NOD1 mediates experimental pancreatitis. *Immunity* 37, 326–338
 81. Watanabe, T. *et al.* (2016) Nucleotide-binding oligomerization domain 1 acts in concert with the cholecystokinin receptor agonist, cerulein, to induce IL-33-dependent chronic pancreatitis. *Mucosal Immunol.* 9, 1234–1249
 82. Cayrol, C. and Girard, J.P. (2014) IL-33: an alarmin cytokine with crucial roles in innate immunity, inflammation and allergy. *Curr. Opin. Immunol.* 31C, 31–37
 83. Vivier, E. *et al.* (2018) Innate lymphoid cells: 10 years on. *Cell* 174, 1054–1066
 84. Fichtner-Feigl, S. *et al.* (2007) Induction of IL-13 triggers TGF-beta1-dependent tissue fibrosis in chronic 2,4,6-trinitrobenzene sulfonic acid colitis. *J. Immunol.* 178, 5859–5870
 85. Furukawa, S. *et al.* (2017) Interleukin-33 produced by M2 macrophages and other immune cells contributes to Th2 immune reaction of IgG4-related disease. *Sci. Rep.* 7, 42413
 86. Ng, K.W. *et al.* (2018) cGAS-STING and cancer: dichotomous roles in tumor immunity and development. *Trends Immunol.* 39, 44–54
 87. Watanabe, T. *et al.* (2017) Nucleotide-binding oligomerization domain 1 and gastrointestinal disorders. *Proc. Jpn. Acad. Ser. B Phys. Biol. Sci.* 93, 578–599
 88. Lee, P.Y. *et al.* (2009) Type I interferon modulates monocyte recruitment and maturation in chronic inflammation. *Am. J. Pathol.* 175, 2023–2033
 89. Mancuso, G. *et al.* (2007) Type I IFN signaling is crucial for host resistance against different species of pathogenic bacteria. *J. Immunol.* 178, 3126–3133
 90. Kempuraj, D. *et al.* (2013) The novel cytokine interleukin-33 activates acinar cell proinflammatory pathways and induces acute pancreatic inflammation in mice. *PLoS One* 8, e56866
 91. Liu, J. *et al.* (2017) Enhanced inflammasome activity in systemic lupus erythematosus is mediated via type I interferon-induced up-regulation of interferon regulatory factor 1. *Arthritis Rheumatol* 69, 1840–1849
 92. Kahlenberg, J.M. *et al.* (2011) Inflammasome activation of IL-18 results in endothelial progenitor cell dysfunction in systemic lupus erythematosus. *J. Immunol.* 187, 6143–6156
 93. Awada, A. *et al.* (2014) Potential involvement of the IL-33-ST2 axis in the pathogenesis of primary Sjogren's syndrome. *Ann. Rheum. Dis.* 73, 1259–1263
 94. Guo, J. *et al.* (2016) The association of novel IL-33 polymorphisms with sIL-33 and risk of systemic lupus erythematosus. *Mol. Immunol.* 77, 1–7

Editorial

Proposal of Primary Endpoints for TACE Combination Trials with Systemic Therapy: Lessons Learned from 5 Negative Trials and the Positive TACTICS Trial

Masatoshi Kudo

Department of Gastroenterology and Hepatology, Kindai University Faculty of
Medicine, Osaka-Sayama, Japan*Prof. M. Kudo*Editor *Liver Cancer*

The multikinase inhibitor sorafenib is the first oral molecular targeted agent to improve survival in patients with unresectable advanced hepatocellular carcinoma (HCC). Various clinical trials have been conducted with the ultimate goal of extending survival not only in advanced HCC patients, but also in intermediate-stage HCC patients. The aim of these trials was to test the hypothesis that combination therapy with transcatheter arterial chemoembolization (TACE) and molecular targeted agents (1) attenuates the release of vascular endothelial growth factor and other angiogenic growth factors in response to hypoxia induced by TACE and (2) prevents a decrease in hepatic functional reserve by extending the interval between TACE sessions through suppression of residual tumor proliferation. Five trials investigating combination therapy with TACE and molecular targeted agents have ended in failure. In the wake of these failures, the recent positive TACTICS trial, which combined TACE and sorafenib and reported extension of the primary endpoint of progression-free survival, was a breakthrough. This editorial interprets the design of the TACTICS trial, provides an in-depth review of factors related to its success by comparison with previous failed trials, and discusses the lessons learned regarding the endpoints to be considered in future trials of combination therapy with TACE.

Masatoshi Kudo
Department of Gastroenterology and Hepatology
Kindai University Faculty of Medicine
377-2 Ohno-Higashi, Osaka-Sayama 589-8511 (Japan)
E-Mail m-kudo@med.kindai.ac.jp

Introduction

The efficacy of the molecular targeted agent sorafenib in patients with unresectable advanced hepatocellular carcinoma (HCC) was demonstrated in the SHARP trial [1] and in a trial conducted in the Asia-Pacific region [2]. Sorafenib is considered a first-line drug for patients with unresectable advanced HCC. The first-line treatment for patients with intermediate-stage HCC is transcatheter arterial chemoembolization (TACE); however, the release of large concentrations of angiogenic factors, such as vascular endothelial growth factor (VEGF), triggered by hypoxia induced by TACE results in tumor progression and recurrence [3–5]. Another disadvantage of TACE is that repeated procedures reduce liver function [6]; therefore, minimizing the number of TACE sessions is a critical challenge in the treatment of intermediate-stage HCC patients. Several clinical trials have attempted to address this problem by combining TACE with molecular targeted agents; however, to date, all have ended in failure [7–11], and the combination of TACE and molecular targeted agents is therefore not recommended in routine practice.

In a subanalysis within the SHARP trial, the hazard ratio (HR) for overall survival (OS) in potential TACE candidates (no vascular invasion or extrahepatic spread) was a very favorable 0.52, clearly demonstrating that sorafenib extended the median OS by a factor of approximately 1.5 [12]. These results suggest that the use of sorafenib in adjuvant, combination, or sequential therapy may extend survival in TACE candidates. The effects of combining sorafenib and TACE go beyond the combination of two different treatment modalities. Sorafenib shows promise for inhibiting recurrence and repeated tumor growth after TACE because it attenuates the acceleration of angiogenesis after the procedure, suggesting it can extend the period during which tumor progression is controllable by TACE. In addition, it may help prevent worsening of hepatic function by reducing the number of TACE sessions required. In summary, sorafenib shows promise for improving survival by extending time to progression (TTP) to advanced-stage HCC in patients with intermediate-stage HCC that are eligible for TACE.

Overview of the TACTICS Trial

Trial Design

The TACTICS trial was a multicenter prospective randomized controlled trial comparing TACE plus sorafenib with TACE alone that was conducted at 33 sites in Japan (Fig. 1). A total of 156 patients with unresectable HCC were assigned to receive sorafenib plus TACE ($n = 80$) or TACE alone ($n = 76$) at a 1:1 ratio. The inclusion criteria were Child-Pugh score ≤ 7 , a maximum of two previous TACE sessions, and ≤ 10 HCCs with none exceeding 10 cm in size. The exclusion criteria were extrahepatic spread and vascular invasion. Patients in the TACE plus sorafenib arm started sorafenib 2–3 weeks before TACE at a dose of 400 mg once daily. The purpose of this sequential pretreatment with sorafenib was to assess tolerability to sorafenib, normalize the tumor vasculature to improve TACE effectiveness, and attenuate VEGF upregulation after the TACE procedure. Sorafenib was temporarily suspended 2 days before and after TACE. In patients showing sorafenib tolerance, the dose was increased to 800 mg daily when possible. TACE was performed on demand, and repeated TACE was generally performed in cases with viable lesions that grew by $\geq 50\%$ over baseline. Response was assessed using computed tomography, magnetic resonance imaging, or other related modalities every 8 weeks. The study had two co-primary endpoints, namely, progression-free survival (PFS) and OS, and adopted a gatekeeping strategy. The secondary endpoints were the time until TACE was no longer feasible or no longer showed any benefit (time to un-TACEable progression: TTUP), TTP, response rate, and safety. As further explained below, the

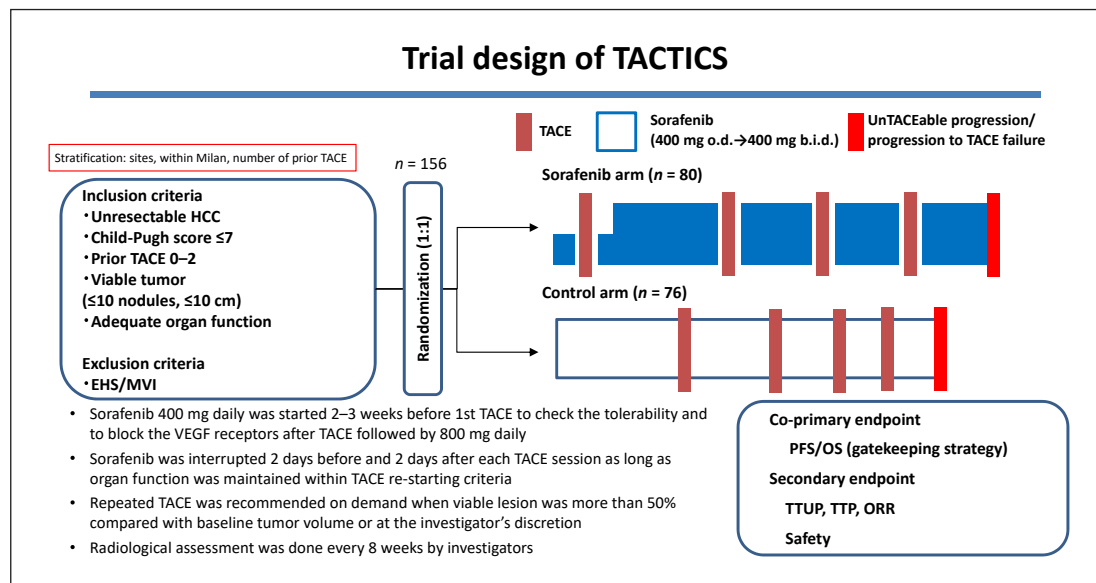


Fig. 1. Trial design of TACTICS.

development of new intrahepatic lesions was not defined as tumor progression. This criterion was introduced to maximize the duration of sorafenib administration and to keep the progression criteria for TACE as consistent as possible with those currently used in clinical practice. Use of the RECIST criteria as response evaluation criteria/a stopping rule is inappropriate because repeated TACE is generally performed after detecting a new intrahepatic lesion, which does not qualify as treatment failure requiring a switch to a next line of treatment. Therefore, the TACE progression criteria were created specifically for the TACTICS trial and were consistent with those used in clinical practice.

The criteria for progression with TACE (unTACEable progression) were (1) $\geq 25\%$ increase in intrahepatic viable lesions, (2) decline in hepatic functional reserve to Child-Pugh class C, (3) appearance of extrahepatic lesions, (4) appearance of vascular invasion, or (5) meeting the Japan Society of Hepatology criteria for TACE-refractory disease [13]. Therefore, PFS was defined as the time to either unTACEable progression or death. The most important feature of the TACTICS trial design is that the RECIST criteria were not used, and consequently the development of new intrahepatic lesions was not considered progression. This enabled long-term administration of sorafenib.

Results of the TACTICS Trial

The results for the primary endpoint of PFS were very favorable, with a median of 25.2 months in the TACE plus sorafenib arm and 13.5 months in the TACE alone arm (HR, 0.59; $p = 0.006$; Table 1) [14]. TTUP results were also favorable, with a median of 26.7 months in the TACE plus sorafenib arm and 20.6 months in the TACE alone arm (HR, 0.57; $p = 0.02$; Table 1). Similarly, TTP results were favorable, with a median of 26.7 months in the TACE plus sorafenib arm and 16.4 months in the TACE alone arm (HR, 0.54; $p = 0.005$). PFS results were also better for the TACE plus sorafenib arm in all subgroup analyses. The response rates after the first TACE session did not differ significantly between the arms. There were no unexpected adverse events. The median duration of sorafenib administration was long at 38.7 months, and the median daily dose was somewhat low at 355.2 mg. The interval between TACE sessions was 21.1 weeks in the TACE plus sorafenib arm, which was significantly longer

Table 1. Results of TACTICS trial

	TACE with sorafenib	TACE alone	HR (95% CI)	p value
PFS	25.2	13.5	0.59 (0.41–0.87)	0.006
TTUP	26.7	20.6	0.57 (0.36–0.92)	0.02
TTP	26.7	16.4	0.54 (0.35–0.83)	0.005
TTVI	31.3	4.0	0.26 (0.09–0.75)	0.005
TTEHS	15.7	6.9	0.21 (0.06–0.70)	0.006
TTSP	22.5	6.3	0.31 (0.15–0.63)	0.001

Data are presented as median values in months. TACE, transcatheter arterial chemoembolization; HR, hazard ratio; PFS, progression-free survival; TTUP, time to unTACEable progression; TTP, time to progression; TTVI, time to vascular invasion; TTEHS, time to extrahepatic spread; TTSP, time to stage progression.

than the interval of 16.9 weeks in the TACE alone arm ($p = 0.018$). Other parameters that were significantly longer in the TACE plus sorafenib arm than in the TACE alone arm were time to detection of vascular invasion (31.3 vs. 4.0 months), time to detection of extrahepatic spread (15.7 vs. 6.9 months), and time to stage progression (22.5 vs. 6.3 months) (Table 1).

Reasons for the Success of the TACTICS Trial

The TACTICS trial, which demonstrated that TACE plus sorafenib extended the primary endpoint of PFS compared with TACE alone, was the world's first positive trial of combination therapy with TACE and a molecular targeted agent. The results of combination therapy were also superior to those of TACE alone for all secondary endpoints except response rate. The key contributing factor to the positive results was the long duration of sorafenib administration (38.7 weeks). The reasons for this long administration period were that (1) the development of new intrahepatic lesions was not considered progression, and (2) new progression criteria optimized for TACE (unTACEable progression) were developed, and TACE-specific PFS was defined according to those criteria.

Reasons for the Failure of Past Negative Trials

Post-TACE Trial

Background

Although TACE is performed as first-line treatment for unresectable HCC, it is rarely curative. Repeated TACE is common; however, this strategy can worsen hepatic function. Post-TACE recurrence is believed to be caused by factors such as increased angiogenesis and high VEGF expression. The trial was designed to test the hypothesis that administration of sorafenib, a tyrosine kinase inhibitor that targets Raf, VEGF receptor, platelet-derived growth factor receptor, and other factors involved in tumor cell proliferation and angiogenesis would delay post-TACE recurrence and consequently extend survival time. The Post-TACE trial was a Phase III placebo-controlled trial conducted in Japan and South Korea [7].

Trial Design

The subjects were patients with unresectable HCC and Child-Pugh A hepatic functional reserve who had responded to TACE as demonstrated by imaging assessment after 1–3 months. Responders were assigned to sorafenib and placebo arms. The primary endpoint was TTP and the secondary endpoint was OS.

Table 2. TACE combination trials with sorafenib

Trial	Ph3 Post-TACE	Ph2 SPACE	Ph3 TACE-2	Ph2 TACTICS
Author	Kudo et al. [7], 2011	Lencioni et al. [9], 2016	Meyer et al. [11], 2017	Kudo M et al. [14], 2018
Child-Pugh class	A	A (no ascites)	A	A5–B7
ECOG-PS	0–1	0	0–1	0–1
Tumor burden	≤7 cm ≤10 tumors	Unresectable multinodular	Not a candidate for resection or transplantation	≤10 cm ≤10 tumors
TACE procedure	cTACE, on demand	DEB-TACE, scheduled	DEB-TACE, on demand	cTACE, on demand
Endpoint	TTP (5.4 months)	TTP (5.6 months)	PFS (8.5 months)	PFS (25.2 months)
Progression criteria	RECICL 2004	mRECIST	RECIST 1.1	UnTACEable progression/TACE failure New lesion: not PD
Sorafenib duration, weeks	17.0	21.0	17.1	38.7
Median follow-up, weeks	NA	38.6	88.6	122.3

cTACE, conventional lipiodol TACE; RECICL, response evaluation criteria in the cancer of liver

Results

The trial enrolled 458 patients (387 from Japan and 71 from South Korea) between April 2006 and July 2009. The primary endpoint of median TTP was 5.4 months in the sorafenib arm and 3.7 months in the placebo arm (HR, 0.87; 95% CI: 0.70–1.09; $p = 0.252$; Table 1). The secondary endpoint of median OS was 29.7 months in the sorafenib arm, but the median value was not reached in the placebo arm (HR, 1.06; 95% CI: 0.69–1.64; $p = 0.790$). In subgroup analysis, the median TTP in Japanese patients was 3.9 months in the sorafenib arm and 3.7 months in the placebo arm, with a HR of 0.94 and no difference between the arms. In Korean patients, however, the HR was 0.38, clearly demonstrating a longer TTP in the sorafenib arm.

Interpretation of the Reasons for Failure

In this trial, the primary endpoint of TTP did not significantly differ between the arms. One reason for this could be the timing of sorafenib administration. Because TACE triggers an increase in VEGF production by inducing ischemic conditions, it may be necessary to inhibit angiogenesis soon after TACE to detect the effect of sorafenib. However, the median delay until administration of sorafenib was 9 weeks because the population included only patients who responded to TACE. This delay may be one reason why sorafenib did not have an additive effect.

Another factor contributing to the trial failure was that although TTP did not differ between arms in Japan, the results of sorafenib treatment were good in South Korea. The longer median treatment period in Korean patients than in Japanese patients (31 vs. 16 weeks) was identified as a possible reason for the significant extension of TTP in Korean patients. Therefore, the short sorafenib administration period of 17 weeks was the main reason for the failure of this trial (Table 2).

SPACE Trial

Background

The SPACE trial was conducted at 85 sites in 13 countries not including Japan. It was a Phase II trial that assessed the safety and efficacy of DEB-TACE with doxorubicin-eluting beads (DEBDOX) plus sorafenib in patients with Barcelona Clinic Liver Cancer (BCLC) stage B unresectable HCC. The trial design incorporated lessons learned from the Post-TACE trial, namely, that sorafenib should be started early to address the increase in VEGF production induced by ischemia after TACE by performing TACE soon after starting sorafenib and then continuing sorafenib after TACE [9].

Trial Design

Patients enrolled at 85 sites in 13 countries were randomly assigned to sorafenib and placebo arms. Sorafenib or placebo was administered 3–7 days before DEB-TACE. Subsequent sessions of DEB-TACE were performed after 3, 7, and 13 months and every 6 months thereafter. The primary endpoint was TTP, and the secondary endpoints were OS, time to extrahepatic spread and vascular invasion, TTUP, and safety. The criteria for unTACEable progression were detection of vascular invasion or extrahepatic spread, persistent ascites, Child-Pugh class B, Eastern Cooperative Oncology Group performance status ≥ 2 , and platelet count $< 60,000/\mu\text{L}$. One-sided significance tests were used for between-arm comparisons with a significance level of 15% ($\alpha = 0.15$).

Results

Of the 307 patients enrolled, 154 were assigned to the sorafenib arm and 153 to the placebo arm. The primary endpoint of median TTP was 169 days in the sorafenib arm and 166 days in the placebo arm (HR, 0.797; 95% CI: 0.588–1.08; $p = 0.072$). Although this trial met the statistical significance requirements for a Phase II trial, the results cannot be considered a clinically significant improvement of TTP. The secondary endpoint of OS did not reach the median value in the sorafenib or placebo arm (HR, 0.898; 95% CI: 0.606–1.33; $p = 0.295$). In addition, time to extrahepatic spread and vascular invasion did not reach median values in the sorafenib or placebo arm (HR, 0.621; 95% CI: 0.321–1.20; $p = 0.076$). In the sorafenib and placebo arms, median TTUP was 95 and 224 days, respectively (HR, 1.586; 95% CI: 1.200–2.096; $p = 0.999$), the number of patients with unTACEable progression was 110 and 96, respectively, and the percentage of patients who only underwent one session of DEB-TACE was 35.9 and 19.2%, respectively.

Comparative analysis between Asian and non-Asian patients showed that the median duration of sorafenib administration was 30 weeks in Asian patients and 17.4 weeks in non-Asian patients. As a result, the HRs for TTP and OS were worse in non-Asian patients (0.865 and 1.062, respectively) than in Asian patients (0.720 and 0.677, respectively).

Interpretation of the Reasons for Failure

The primary endpoint of TTP was met to the extent necessary for a Phase II trial, although the results were not clinically significant. There was no difference in the secondary endpoint of OS. Moreover, there was no difference in TTUP, which was shorter in the sorafenib arm – the opposite of what was predicted.

The TACE method used in this trial was “scheduled TACE” in which DEB-TACE is performed at 1, 3, 7, and 13 months and every 6 months thereafter. Scheduled TACE involves performing TACE at regular intervals, even if intrahepatic lesions respond to TACE. This approach, which could have reduced hepatic function or increased adverse reactions to sorafenib, is different from the Japanese or Asian approach to treatment of “on-demand” TACE performed when necessary.

Many subjects in this trial underwent few TACE sessions, which may be attributable to inappropriate criteria for unTACEable progression. Although factors such as vascular invasion and extrahepatic spread are appropriate criteria for the discontinuation of TACE, other factors such as Child-Pugh B hepatic functional reserve, persistent ascites, and platelet count $<60,000/\mu\text{L}$ do not indicate that TACE is unfeasible. The authors of the Post-TACE trial speculated that long-term administration of sorafenib may improve TTP, and these criteria for discontinuation of TACE may have forced the early termination of sorafenib administration in the SPACE trial. As in the Post-TACE trial, the cumulative duration of sorafenib administration in this trial was short at 21 weeks. Considering that TTP and OS were favorable in Asian patients receiving long-term sorafenib treatment (30 weeks) compared with non-Asian patients (17.4 weeks), the short duration of sorafenib administration can be considered the biggest reason for the failure of this trial. In fact, Lencioni et al. [9] in their SPACE Trial paper state “The duration of sorafenib albeit in combination with TACE may be critical for improved outcome.”

TACE-2 Trial

Background

The TACE-2 trial, which was conducted at 20 sites in England, was designed to test the hypothesis that combination treatment with sorafenib and DEB-TACE would inhibit tumor progression and extend OS [10].

Trial Design

Enrolled patients were assigned to sorafenib or placebo arm, and DEB-TACE was performed within 2–5 weeks of sorafenib administration. After that, on-demand DEB-TACE was performed if additional TACE was deemed necessary based on imaging assessment. The primary endpoint was PFS, and the secondary endpoint was OS.

Results

The 294 enrolled patients were split into two arms, each comprising 147 patients. The primary endpoint of median PFS was 7.8 months in the sorafenib arm and 7.7 months in the placebo arm (HR, 1.03; 95% CI: 0.75–1.42; $p = 0.85$). The secondary endpoint of median OS was 18.8 months in the sorafenib arm and 19.6 months in the placebo arm (HR, 1.03; 95% CI: 0.72–1.49; $p = 0.87$).

Interpretation of the Reasons for Failure

In this trial, there was no difference in PFS or OS, indicating that sorafenib was not effective. The criteria for performing repeated TACE were left to the discretion of individual physicians, and repeated TACE before progressive disease (PD) was not prohibited in both arms. Therefore, some patients underwent repeated TACE before sorafenib had the anticipated effect, which indicates that the results were attributable solely to the effects of TACE. This may account for the lack of differences between the arms.

Previous trials reported an additive effect of molecular targeted agents despite the lack of difference between patients receiving TACE plus a molecular targeted agent and those treated with TACE alone. This trial, however, did not show a difference or an additive effect between arms. The STORM trial, which investigated sorafenib adjuvant to locoregional therapy such as resection or radiofrequency ablation, also failed to show the effect of sorafenib [15]. This suggests that the addition of sorafenib after treatments with more intense necrosis-inducing effects like TACE may not be effective in suppressing the tumor growth after TACE. The short duration of sorafenib administration (17.1 weeks) can be considered the biggest factor in the failure of this study as well.

BRISK-TA and ORIENTAL Trials

These two trials did not investigate sorafenib, but two other molecular targeted agents, brivanib and orantinib. Therefore, the trials failed for different reasons [8, 10]. These reasons will not be discussed in this paper but are discussed elsewhere [16].

Lessons Learned from Negative Trials about Primary Endpoints in the TACE Combination Trials with Systemic Therapy

OS is generally used as the primary endpoint in Phase III studies of cancer treatments and is also recommended as an endpoint for TACE [17, 18]. However, the median OS in clinical trials of TACE is never shorter than 18 months, and can even be as long as 32 months, which is a very long time to conduct a clinical trial. In addition, various treatments can be performed as post-trial treatments in patients that withdraw from the trial because of tumor progression or adverse events. The currently approved or available molecular targeted agents include lenvatinib and sorafenib as first-line drugs, and regorafenib, cabozantinib, and ramucirumab as second-line drugs. Patients in either trial arm can also receive post-trial treatment with an immune checkpoint inhibitor (nivolumab). Therefore, it is currently nearly impossible to use OS as an endpoint in clinical trials of combination systemic therapy with TACE in patients with intermediate-stage HCC.

TTP/PFS is sometimes used instead of OS, although it is not always appropriate as a primary endpoint in trials of TACE. There are no data showing that TTP/PFS is a suitable surrogate endpoint for OS. TTP/PFS is usually defined as the time from randomization or treatment initiation to progression as per RECIST or modified RECIST criteria or death; however, it is common practice to perform repeated TACE for original tumor growth or new intrahepatic lesions. In addition, because patients who undergo TACE often have multiple tumors, the development of new intrahepatic lesions is part of the natural course of HCC, and should not be classified as treatment failure (i.e., PD).

Nevertheless, TTP or PFS was the primary endpoint in past trials of combination therapy with sorafenib and TACE, namely, the Phase III Post-TACE trial, the Phase II SPACE trial, and the Phase III TACE-2 trial. Because trials used the RECIST criteria or modified RECIST criteria for response assessment, new intrahepatic lesions had to be classified as PD, naturally ending the protocol treatment. This ultimately reduced the duration of sorafenib administration. The success of the TACTICS trial can be attributed to alterations to the trial design based on lessons learned from these past negative trials, as well as the establishment of a new TACE-specific definition of progression consistent with current TACE use in clinical practice. The TACTICS trial is planning to evaluate OS benefit as a co-primary endpoint when protocol-specified OS events are obtained. If the trial demonstrates an OS benefit, it will provide clear evidence supporting the use of our proposed TTUP-based “TACE-specific PFS” instead of OS as the endpoint for the registration trial for adding a new indication.

We also proposed time to TACE progression (TTTP) as a new measure of TTP appropriate for TACE [19]. PD is defined as a $\geq 20\%$ increase in the summed diameter of the five largest tumors on post-treatment images relative to baseline images (defined as images from 1 month after treatment) or the detection of extrahepatic spread or vascular invasion, and TTTP is the time from the date of treatment to the date of PD. TTTP is a more clinically appropriate evaluation method for TACE, in addition to correlating well with OS in our validation analysis. As such, we believe that TTTP could be a good surrogate for OS as a primary endpoint in clinical trials of TACE. Izumoto et al. [20] confirmed that TTTP is indeed a good surrogate for OS in trials of TACE.

Conclusion

Many clinical trials to date have investigated combination therapy with TACE and a molecular targeted agent, and all failed to show improvement of OS and even improvement of TTP or PFS. The TACTICS trial emerged after these failures as the world's first positive study showing improvement of PFS and delay of progression to advanced-stage disease. Its success is attributable to the excellent trial design based on lessons learned from past failed trials of combination therapy with TACE and molecular targeted agents. Both the TACE-specific PFS measure we proposed in the TACTICS trial and TTTP are suitable surrogate endpoints for OS. Therefore, either TACE-specific PFS or TTTP may be a useful surrogate endpoint to OS even in registration trials by pharmaceutical companies which combine systemic therapy [21, 22] and TACE.

Disclosure Statement:

Masatoshi Kudo received lecture fees from Bayer, Eisai, MSD, and Ajinomoto, research grants from Chugai, Otsuka, Takeda, Taiho, Sumitomo Dainippon, Daiichi Sankyo, MSD, Eisai, Bayer, AbbVie, Medico's Hirata, Astellas Pharma, and Bristol-Myers Squibb, and advisory consulting fees from Kowa, MSD, Bristol-Myers Squibb, Bayer, Chugai, Taiho, Eisai, and Ono Pharmaceutical.

References

- 1 Llovet JM, Ricci S, Mazzaferro V, Hilgard P, Gane E, Blanc JF, et al.; SHARP Investigators Study Group. Sorafenib in advanced hepatocellular carcinoma. *N Engl J Med*. 2008 Jul;359(4):378–90.
- 2 Cheng AL, Kang YK, Chen Z, Tsao CJ, Qin S, Kim JS, et al. Efficacy and safety of sorafenib in patients in the Asia-Pacific region with advanced hepatocellular carcinoma: a phase III randomised, double-blind, placebo-controlled trial. *Lancet Oncol*. 2009 Jan;10(1):25–34.
- 3 Li X, Feng GS, Zheng CS, Zhuo CK, Liu X. Expression of plasma vascular endothelial growth factor in patients with hepatocellular carcinoma and effect of transcatheter arterial chemoembolization therapy on plasma vascular endothelial growth factor level. *World J Gastroenterol*. 2004 Oct;10(19):2878–82.
- 4 Carmeliet P, Jain RK. Angiogenesis in cancer and other diseases. *Nature*. 2000 Sep;407(6801):249–57.
- 5 Wang B, Xu H, Gao ZQ, Ning HF, Sun YQ, Cao GW. Increased expression of vascular endothelial growth factor in hepatocellular carcinoma after transcatheter arterial chemoembolization. *Acta Radiol*. 2008 Jun;49(5):523–9.
- 6 Hiraoka A, Kumada T, Kudo M, Hirooka M, Koizumi Y, Hiasa Y, et al.; Real-life Practice Experts for HCC (RELPEC) Study Group and HCC 48 Group (hepatocellular carcinoma experts from 48 clinics). Hepatic Function during Repeated TACE Procedures and Prognosis after Introducing Sorafenib in Patients with Unresectable Hepatocellular Carcinoma: multicenter Analysis. *Dig Dis*. 2017;35(6):602–10.
- 7 Kudo M, Imanaka K, Chida N, Nakachi K, Tak WY, Takayama T, et al. Phase III study of sorafenib after transarterial chemoembolisation in Japanese and Korean patients with unresectable hepatocellular carcinoma. *Eur J Cancer*. 2011 Sep;47(14):2117–27.
- 8 Kudo M, Han G, Finn RS, Poon RT, Blanc JF, Yan L, et al. Brivanib as adjuvant therapy to transarterial chemoembolization in patients with hepatocellular carcinoma: A randomized phase III trial. *Hepatology*. 2014 Nov;60(5):1697–707.
- 9 Lencioni R, Llovet JM, Han G, Tak WY, Yang J, Guglielmi A, et al. Sorafenib or placebo plus TACE with doxorubicin-eluting beads for intermediate stage HCC: the SPACE trial. *J Hepatol*. 2016 May;64(5):1090–8.
- 10 Kudo M, Cheng AL, Park JW, Park JH, Liang PC, Hidaka H, et al. Orantinib versus placebo combined with transcatheter arterial chemoembolisation in patients with unresectable hepatocellular carcinoma (ORIENTAL): a randomised, double-blind, placebo-controlled, multicentre, phase 3 study. *Lancet Gastroenterol Hepatol*. 2018 Jan;3(1):37–46.
- 11 Meyer T, Fox R, Ma YT, Ross PJ, James MW, Sturgess R, et al. Sorafenib in combination with transarterial chemoembolisation in patients with unresectable hepatocellular carcinoma (TACE 2): a randomised placebo-controlled, double-blind, phase 3 trial. *Lancet Gastroenterol Hepatol*. 2017 Aug;2(8):565–75.
- 12 Bruix J, Raoul JL, Sherman M, Mazzaferro V, Bolondi L, Craxi A, et al. Efficacy and safety of sorafenib in patients with advanced hepatocellular carcinoma: subanalyses of a phase III trial. *J Hepatol*. 2012 Oct;57(4):821–9.
- 13 Kudo M, Matsui O, Izumi N, Kadoya M, Okusaka T, Miyayama S, et al.; Liver Cancer Study Group of Japan. Transarterial chemoembolization failure/refractoriness: JSH-LCSGJ criteria 2014 update. *Oncology*. 2014;87 Suppl 1:22–31.

- 14 Kudo M, Ueshima K, Torimura T, Tanabe N, Ikeda M, Aikata H, Izumi N, et al. Randomized, open label, multi-center, phase II trial of transcatheter arterial chemoembolization (TACE) therapy in combination with sorafenib as compared with TACE alone in patients with hepatocellular carcinoma: TACTICS trial. *J Clin Oncol* 36 (suppl; abstr 4017), 2018.
- 15 Bruix J, Takayama T, Mazzaferro V, Chau GY, Yang J, Kudo M, et al.; STORM investigators. Adjuvant sorafenib for hepatocellular carcinoma after resection or ablation (STORM): a phase 3, randomised, double-blind, placebo-controlled trial. *Lancet Oncol*. 2015 Oct;16(13):1344–54.
- 16 Kudo M, Arizumi T. Transarterial Chemoembolization in Combination with a Molecular Targeted Agent: Lessons Learned from Negative Trials (Post-TACE, BRISK-TA, SPACE, ORIENTAL, and TACE-2). *Oncology*. 2017;93 Suppl 1:127–34.
- 17 Llovet JM, Di Bisceglie AM, Bruix J, Kramer BS, Lencioni R, Zhu AX, et al.; Panel of Experts in HCC-Design Clinical Trials. Design and endpoints of clinical trials in hepatocellular carcinoma. *J Natl Cancer Inst*. 2008 May; 100(10):698–711.
- 18 Llovet JM, Zucman-Rossi J, Pikarsky E, Sangro B, Schwartz M, Sherman M, et al. Hepatocellular carcinoma. *Nat Rev Dis Primers*. 2016 Apr;2:16018.
- 19 Arizumi T, Ueshima K, Iwanishi M, Minami T, Chishina H, Kono M, et al. The Overall Survival of Patients with Hepatocellular Carcinoma Correlates with the Newly Defined Time to Progression after Transarterial Chemoembolization. *Liver Cancer*. 2017 Jun;6(3):227–35.
- 20 Izumoto H, Hiraoka A, Ishimaru Y, Murakami T, Kitahata S, Ueki H, et al. Validation of Newly Proposed Time to Transarterial Chemoembolization Progression in Intermediate-Stage Hepatocellular Carcinoma Cases. *Oncology*. 2017;93 Suppl 1:120–6.
- 21 Kudo M. Immune checkpoint blockade in hepatocellular carcinoma: 2017 update. *Liver Cancer*. 2016 Nov; 6(1):1–12.
- 22 Kudo M. Molecular Targeted Agents for Hepatocellular Carcinoma: Current Status and Future Perspectives. *Liver Cancer*. 2017 Feb;6(2):101–12.

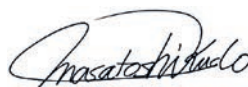
Editorial

Extremely High Objective Response Rate of Lenvatinib: Its Clinical Relevance and Changing the Treatment Paradigm in Hepatocellular Carcinoma

Masatoshi Kudo

Department of Gastroenterology and Hepatology, Kindai University Faculty of Medicine, Osaka-Sayama, Japan

Prof. M. Kudo

Editor *Liver Cancer***Introduction**

The results of a clinical trial of lenvatinib were published in the *Lancet* earlier this year [1]. According to the results, the response rate was higher for lenvatinib than for any other known molecular targeted agents in hepatocellular carcinoma (HCC) patients. The response rates based on independent imaging review and investigator review according to the modified RECIST (mRECIST) assessment were extremely high at 40.6 and 24.1%, respectively. The response rate based on independent imaging review according to RECIST 1.1 was also high (18.8%) (Table 1). The response to locoregional treatment (e.g., transcatheter arterial chemoembolization [TACE] and ablation) is correlated with overall survival (OS). In a meta-analysis of seven studies, Vincenzi et al. [2] showed that the hazard ratio (HR) for OS was 0.39 (95% confidence interval [CI] 0.26–0.61, $p < 0.0001$) when comparing responders and nonresponders among 1,352 patients treated with TACE ($n = 1,236$), cryoablation ($n = 64$), and bland transarterial embolization ($n = 57$). This excellent HR indicated the correlation between response to locoregional therapy and OS benefit (Fig. 1). It is established evidence that OS benefit is more prominent in responders to locoregional therapy than in nonresponders evaluated by mRECIST; thus, the evidence that objective response measured by mRECIST predicts survival in patients receiving locoregional therapies is currently recommended in the EASL guidelines [3]. Regarding molecular targeted agents, most sorafenib-treated patients show stable disease, demonstrating the survival benefit of sorafenib treatment. However, the asso-

Masatoshi Kudo
Department of Gastroenterology and Hepatology
Kindai University Faculty of Medicine
377-2 Ohno-Higashi, Osaka-Sayama 589-8511 (Japan)
E-Mail m-kudo@med.kindai.ac.jp

Table 1. REFLECT study: objective response rate of lenvatinib and sorafenib

	Lenvatinib (n = 478)	Sorafenib (n = 476)	Effect size (95% CI)	p value
<i>Independent imaging review according to mRECIST</i>				
Objective response, n (%), 95% CI	194 (40.6, 36.2–45.0)	59 (12.4, 9.4–15.4)	OR 5.01 (3.59–7.01)	<0.0001
Complete response	10 (2)	4 (1)	–	–
Partial response	184 (38)	55 (12)	–	–
Stable disease	159 (33)	219 (46)	–	–
Durable stable disease lasting ≥23 weeks	84 (18)	90 (19)	–	–
Progressive disease	79 (17)	152 (32)	–	–
Unknown or not evaluable	46 (10)	46 (10)	–	–
Disease control rate, n (%), 95% CI	353 (73.8, 69.9–77.8)	278 (58.4, 54.0–62.8)	–	–
<i>Investigator review according to mRECIST</i>				
Objective response, n (%), 95% CI	115 (24.1, 20.2–27.9)	44 (9.2, 6.6–11.8)	OR 3.13 (2.15–4.56)	<0.0001
Complete response	6 (1)	2 (<1)	–	–
Partial response	109 (23)	42 (9)	–	–
Stable disease	246 (51)	244 (51)	–	–
Durable stable disease lasting ≥23 weeks	167 (35)	139 (29)	–	–
Progressive disease	71 (15)	147 (31)	–	–
Unknown or not evaluable	46 (10)	41 (9)	–	–
Disease control rate, n (%), 95% CI	361 (75.5, 71.7–79.4)	288 (60.5, 56.1–64.9)	–	–
<i>Independent imaging review according to RECIST 1.1</i>				
Objective response, n (%), 95% CI	90 (18.8, 15.3–22.3)	31 (6.5, 4.3–8.7)	OR 3.34 (2.17–5.14)	<0.0001
Complete response	2 (<1)	1 (<1)	–	–
Partial response	88 (18)	30 (6)	–	–
Stable disease	258 (54)	250 (53)	–	–
Durable stable disease lasting ≥23 weeks	163 (34)	118 (25)	–	–
Progressive disease	84 (18)	152 (32)	–	–
Unknown or not evaluable	46 (10)	43 (9)	–	–
Disease control rate, n (%), 95% CI	348 (72.8, 68.8–76.8)	281 (59.0, 54.6–63.5)	–	–

Values are n (%) unless otherwise indicated.

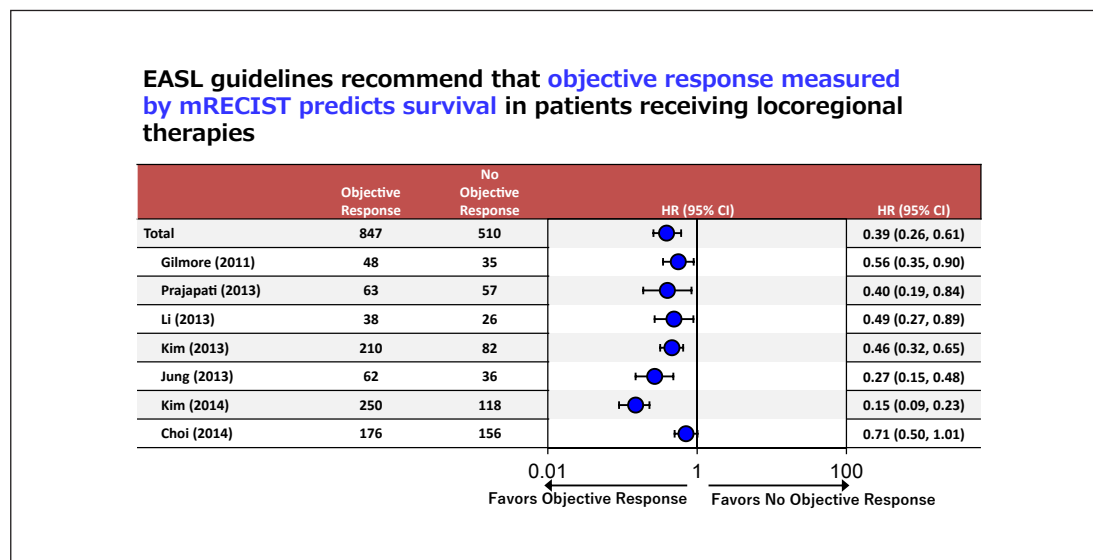


Fig. 1. Correlation between objective response and improved OS in early- or intermediate-stage HCC (from Vincenzi et al. [2]).

ciation between response to molecular targeted agents and improved survival remains unclear. This article reviews recent reports based on retrospective studies and prospective clinical trials of molecular targeted agents with an emphasis on the relationship between response to these agents and improvement of patient survival.

Table 2. Objective response by mRECIST predicts overall survival: retrospective analysis

Study, year	Agents (study design)	ORR (mRECIST), % (n/N)	Median OS, months		HR (95% CI)	p value
			responder (CR + PR)	nonresponder (SD + PD)		
Ronot [4], 2012	sorafenib (retrospective)	28.1 (18/64)	25.5	13.3 (SD) 5.7 (PD)	N/A	<0.001
Arizumi [5], 2014	sorafenib (retrospective)	22.8 (36/158)	25.4	7.3 (PD) 5.7 (short SD)	N/A	<0.0001
Edeline [6], 2014	sorafenib (retrospective)	22.6 (12/53)	18	8	N/A	0.013
Takada [7], 2015	sorafenib (retrospective)	13.1 (25/191)	22.0	10.0	N/A	0.0117

ORR, objective response rate; OS, overall survival; CR, complete response; PR, partial response; SD, stable disease; PD, progressive disease.

Retrospective Studies of Sorafenib

Ronot et al. [4] examined 64 sorafenib-treated HCC patients, and found that the median OS was 25.5 months in 18 patients with objective response (objective response rate [ORR] 28.1%), 13.3 months in 29 patients with stable disease, and 5.7 months in 29 patients with progressive disease, according to the mRECIST criteria; OS was significantly longer in responders than in nonresponders ($p < 0.001$). Arizumi et al. [5] retrospectively analyzed 158 sorafenib-treated patients, and found significantly better OS in responders (patients with complete response or partial response, 25.4 months) than in patients with short stable disease (5.7 months) and progressive disease (7.3 months) ($p < 0.0001$). Edeline et al. [6] analyzed sorafenib-treated patients with unresectable HCC, and reported a median OS of 18 months in 12 responders (response rate, 22.6%), which was significantly longer than the median OS of 8 months in 41 nonresponders ($p = 0.013$). In a retrospective analysis of 191 sorafenib-treated patients, Takada et al. [7] identified 25 responders according to mRECIST, and showed that OS was significantly longer ($p = 0.0117$) in these patients (22 months) than in nonresponders (10 months) (Table 2). However, because these studies were all retrospective analyses, the levels of evidence provided are not high.

Association between Response to Molecular Targeted Agents and Survival Benefit Demonstrated by Prospective Controlled Trials

Lencioni et al. [8] performed a responder analysis using data from a Phase III trial of brivanib as second-line therapy. Among 226 brivanib-treated patients, 26 were responders according to mRECIST (ORR 11.5%); OS was 15.0 months in responders, which was significantly longer than the OS of 9.4 months in nonresponders (HR 0.31, 95% CI 0.16–0.60, $p < 0.001$). Multivariable analysis confirmed that objective response evaluated according to mRECIST was a clear independent predictor of survival. Furthermore, the authors reported that survival becomes more favorable with increasing ORR and longer duration of response.

Meyer et al. [9] analyzed pooled data of the Phase II part of two multicenter open-label Phase I and randomized Phase II studies (nintedanib 200 mg twice daily versus sorafenib 400

Table 3. Objective response by mRECIST predicts overall survival: results of RCT

Study, year	Agents (study design)	ORR (mRECIST), % (n/N)	Median OS, months		HR (95% CI)	p value
			responder (CR + PR)	nonresponder (SD + PD)		
Lencioni [8], 2017	brivanib (Phase III RCT)	11.5 (26/226)	15.0	9.4	0.31 (0.16–0.60)	<0.001
Meyer [9], 2017	nintedanib + sorafenib (Phase II RCT)	15.6 (28/180)	16.7	10.9	0.544 (0.335–0.881)	0.0122
Kudo [10], 2018	sorafenib (Phase III RCT)	18.8 (18/96)	27.2	8.9	N/A	<0.001

RCT, randomized controlled trial; ORR, objective response rate; OS, overall survival; CR, complete response; PR, partial response; SD, stable disease; PD, progressive disease; HR, hazard ratio.

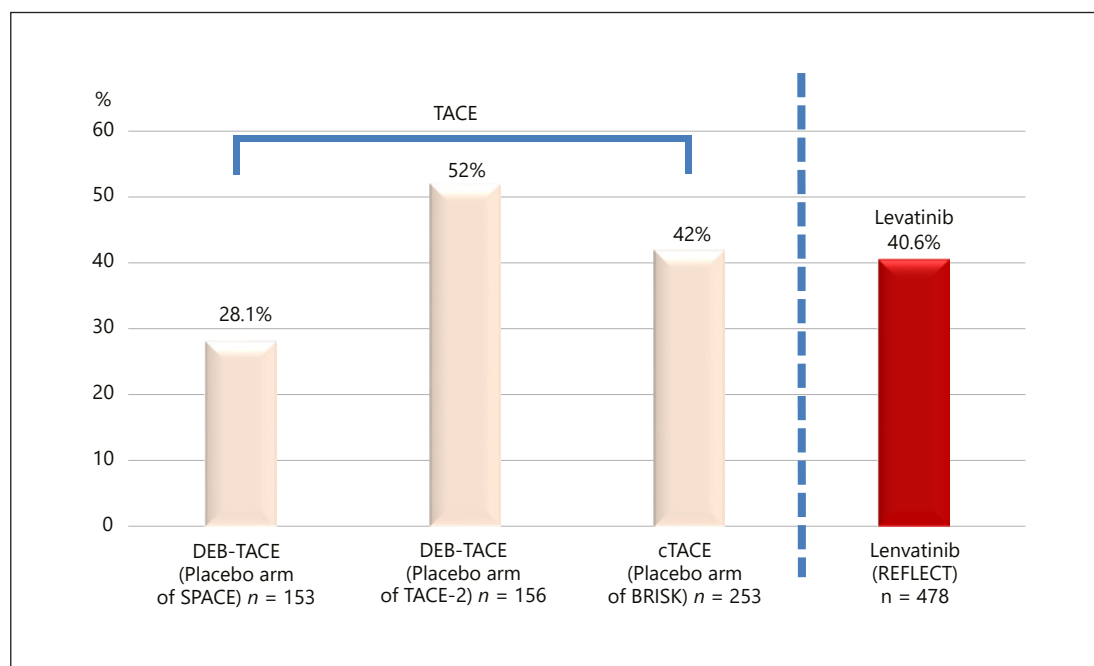


Fig. 2. Objective response rate by mRECIST: TACE and lenvatinib.

mg twice daily) carried out independently in Asia and Europe to examine the association of response (according to RECIST 1.0 or mRECIST) with survival. Of 180 patients, 28 were responders (response rate, 15.6%), with a median OS of 16.7 months, whereas 152 showed no response and had a median OS of 10.9 months; OS was significantly better in responders than in nonresponders (HR 0.544, 95% CI 0.335–0.881, $p = 0.0122$).

Multivariable analysis showed that response according to mRECIST was an independent predictor of survival, albeit only with a trend toward significance (HR 0.62, 95% CI 0.38–1.01, $p = 0.053$), roughly supporting the results of the multivariable analysis reported by Lencioni et al. [8].

Table 4. Response per mRECIST by independent review analysis

	Japan		Overall	
	lenvatinib (n = 81)	sorafenib (n = 87)	lenvatinib (n = 478)	sorafenib (n = 476)
Complete response	2.5	1.1	2.1	0.8
Partial response	44.4	11.5	38.5	11.6
Stable disease	32.1	47.1	33.3	46.0
Durable stable disease	16.0	20.7	17.6	18.9
Progressive disease	16.0	26.4	16.5	31.9
Not evaluable/unknown	4.9	13.8	9.6	9.7
Overall response rate	46.9	12.6	40.6	12.4
95% CI	36.0–57.8	5.7–19.6	36.2–45.0	9.4–15.4
p value*	<0.00001		<0.00001	
Disease control rate	79.0	59.8	73.8	58.4
95% CI	70.1–87.9	49.5–70.1	69.9–77.8	54.0–62.8
p value*	0.00556		<0.00001	

Values are % unless otherwise indicated. * nominal.

Kudo et al. [10] conducted the SILIUS study (a prospective controlled trial), and reported that 18 out of 96 patients who received sorafenib monotherapy were responders (response rate, 18.8%); OS was 27.2 months in these patients, which was significantly longer than the OS of 8.9 months in nonresponders ($p < 0.001$).

The correlation between response and survival suggests that the quality of evidence is high, because this was clearly proven by responder analysis using the database developed from the above three prospective randomized controlled trials (Table 3). This evidence can be applied to the interpretation of a high lenvatinib response rate. Lenvatinib has a high response rate (40.6%), and may therefore offer survival benefit to more than 3-fold as many patients as other agents.

Responder analysis in the SILIUS study showed a response rate of 36% in the sorafenib plus arterial infusion chemotherapy group, which was twice as high as that in the sorafenib only group. In addition, the study indicated that the improvement in survival was comparable between the two groups as long as patients responded to the respective therapies. In other words, the survival benefit is more frequently observed in patients who received sorafenib plus arterial infusion chemotherapy because it has a demonstrably higher response rate. Because lenvatinib has an even higher response rate than sorafenib plus arterial infusion chemotherapy, its survival benefit should apply to a higher proportion of patients, suggesting lenvatinib is a potential alternative to arterial infusion chemotherapy. In addition, the ORR of lenvatinib is similar to the world standard ORR of TACE therapy (Fig. 2) [11–13], indicating that it could replace TACE in certain populations of intermediate-stage HCC patients in the very near future.

ORR of Lenvatinib in the Japanese Subpopulation from the REFLECT Trial

The ORR of lenvatinib in a Japanese subpopulation from the REFLECT trial was reported as 46.9% (sorafenib, ORR = 12.6%), which is considerably higher than the ORR of 40.6% in the overall population of the REFLECT trial (Table 4) [14]. In addition, the ORR in patients with Barcelona Clinic Liver Cancer (BCLC) intermediate stage was markedly higher (61.3%)

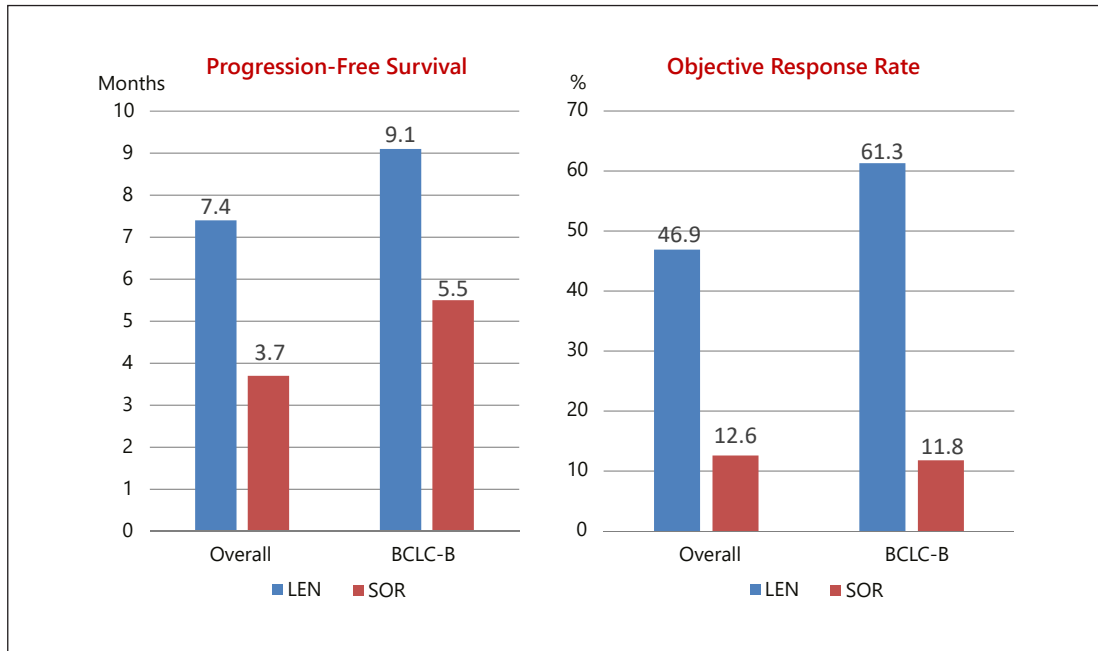


Fig. 3. REFLECT subgroup analysis: Japanese subpopulation showing higher PFS/ORR in BCLC B patients (from Kudo et al. [1]).

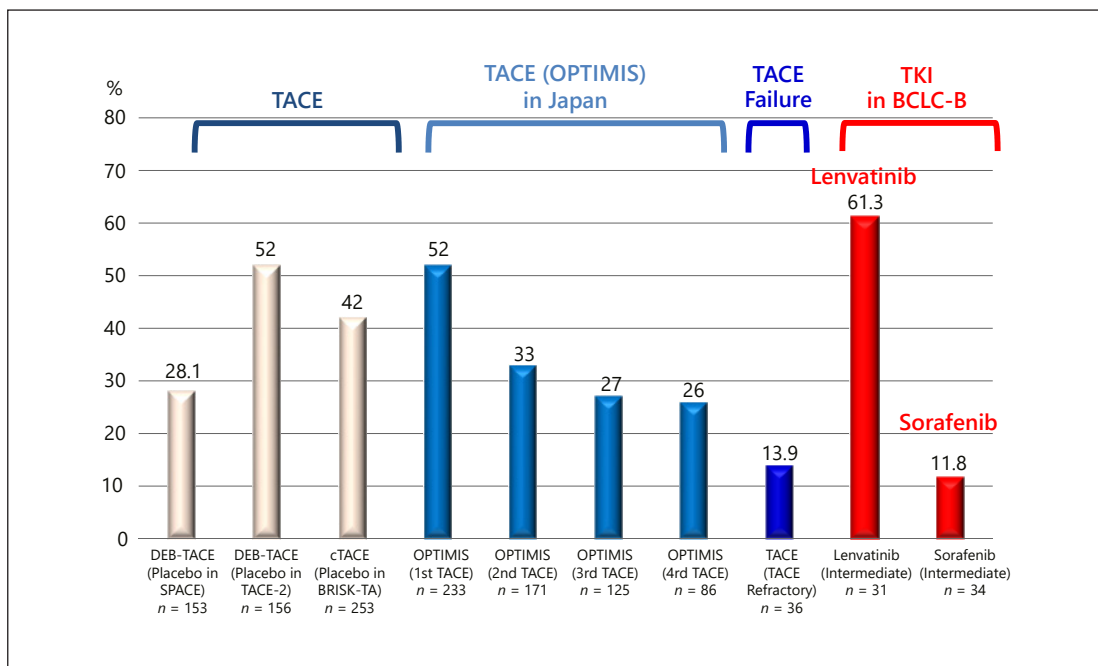


Fig. 4. Objective response rate of TACE and tyrosine kinase inhibitors (TKI).

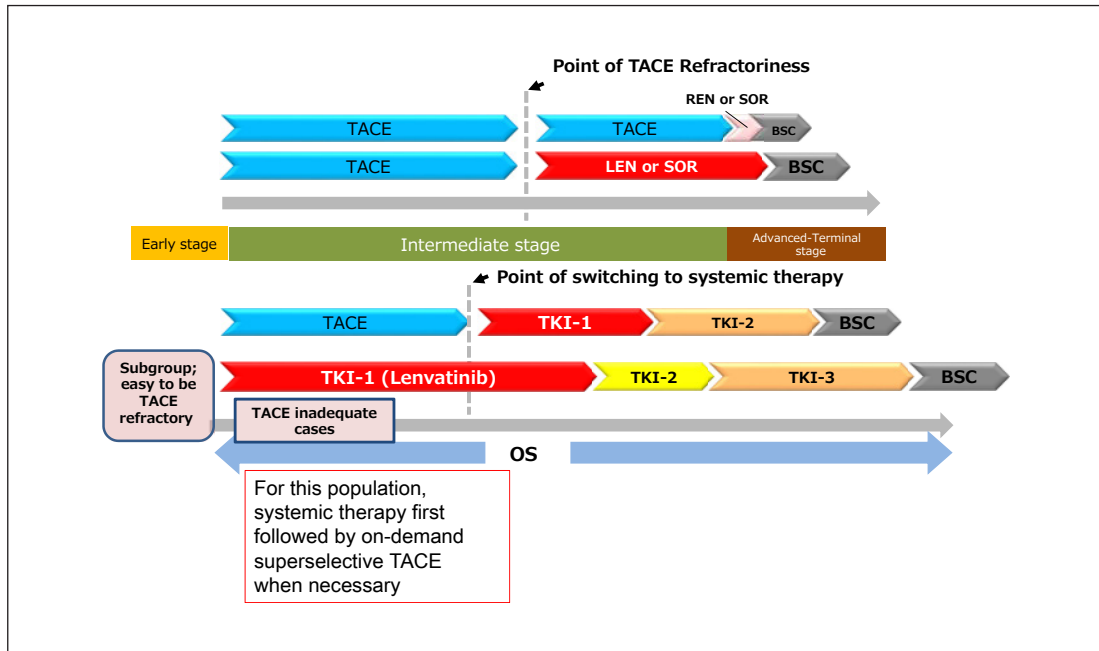


Fig. 5. Treatment strategy of intermediate-stage HCC.

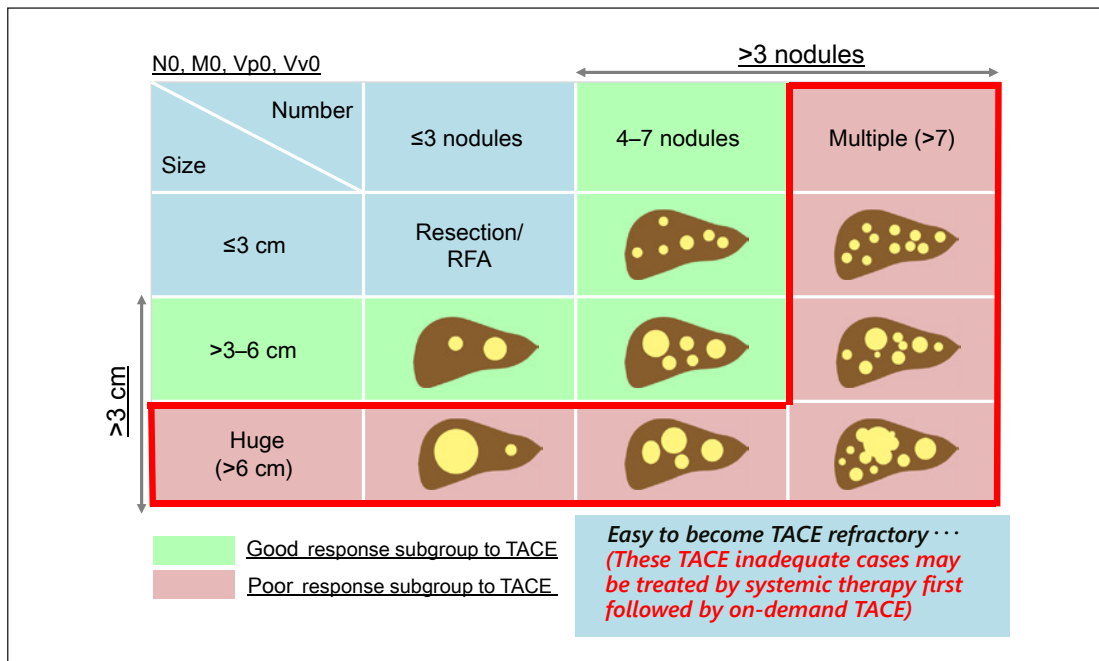


Fig. 6. Heterogeneity of intermediate-stage HCC and response to TACE.

Table 5. New subclassification of intermediate-stage HCC: Kindai criteria (updated version of Kinki criteria)

BCLC substage	B1	B2	B3	
Child-Pugh score	5–7	5–7	8–9	
Beyond Milan and up-to-7 criteria	In	Out	Any In	Out
Sub-substage			B3a	B3b
Concept of treatment strategy	Curative intent	Noncurative Palliative	Curative intent if within up-to-7	Palliative No treatment
Treatment option	Resection Ablation Superselective cTACE	Lenvatinib (Child-Pugh A)	Transplantation Ablation Superselective cTACE	HAIC Selective DEB-TACE BSC
Alternative	DEB-TACE (large, Child-Pugh 7) B-TACE (fewer tumors)	Sorafenib (Child-Pugh A) TACE + sorafenib DEB-TACE (>6 cm) Bland TAE (>6 cm) followed by targeted agents	DEB-TACE B-TACE, HAIC	BSC

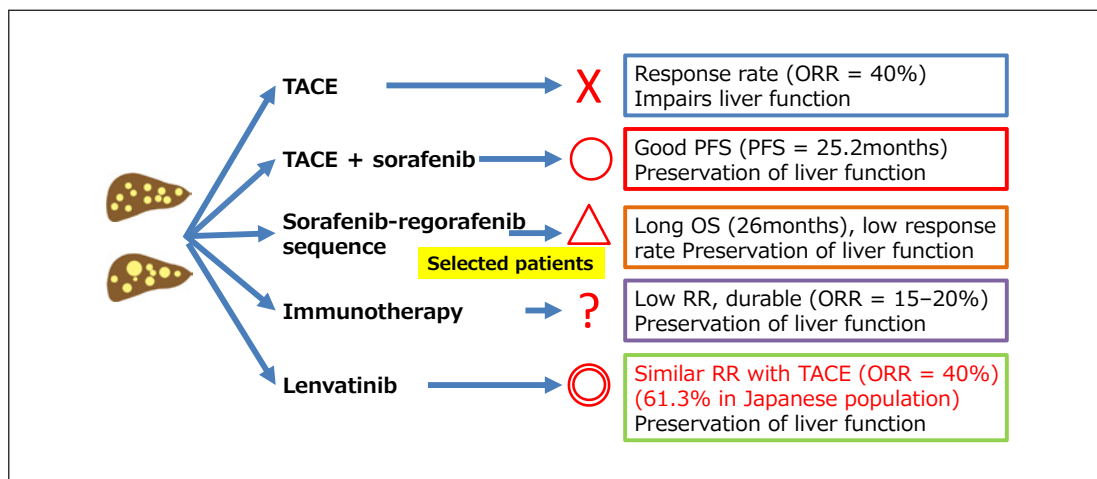


Fig. 7. Treatment strategy of bilobar multifocal intermediate-stage HCC.

(Fig. 2, 3) than the ORR by world standard of TACE, which was 42% in the placebo arm from the BRISK-TA trial or two other trials [11–13], and much higher than the ORR of 52% for the first TACE session in real-world practice in Japan according to the OPTIMIS study (Fig. 4) [14–16]. Furthermore, progression-free survival in the intermediate-stage HCC patients was 9.1 months, which is considerably longer than that of the overall cohort at 7.4 months (Fig. 3).

Therefore, initial treatment with lenvatinib followed by on-demand TACE when necessary may be a good strategy in patients who are likely to become TACE failure in order to preserve liver function and improve OS in BCLC intermediate-stage HCC (Fig. 5, 6; Table 5). The “Kindai criteria,” a new subclassification of BCLC B stage, which recently updated the original version of the Kinki criteria in 2018, is more suitable for treatment decision-making in the intermediate-stage HCC patients than the original version of the Kinki criteria (Table 5). Lenvatinib may be the first treatment option in patients with bilobar multifocal intermediate-stage HCC based on its extremely higher ORR (40.6% in the overall cohort and 61.3% in the Japanese intermediate-stage subpopulation) than that of TACE (Figs. 3, 4, 5, 7).

Clinical Relevance of the High Response Rate

The first important point regarding the clinical relevance of the extremely high lenvatinib response rate is that improvement of survival will be more pronounced in responders (CR + PR), and it will be achieved in a higher proportion of patients (40.6%). The second point is that both physicians and patients are aware of the effect of the therapeutic agent, which should improve compliance and boost motivation to continue therapy. The third point is that lenvatinib is highly effective in reducing tumor size, and achievement of tumor downstaging facilitates the use of more curative treatments (e.g., resection, ablation, and superselective cTACE), which in turn improves survival even further.

Because the response rate to lenvatinib is similar to that of the world standard of TACE (42%) according to international consensus (Fig. 2) [11], the therapeutic effect of the two modalities may be similar. As indicated, the ORR of lenvatinib is better in the Japanese subpopulation. This indicates that lenvatinib could be an alternative to TACE in a subgroup of patients with a high tumor burden of intermediate-stage tumors, such as multiple tumors in both lobes (Fig. 7) [17, 18]. This statement does not mean that TACE should be completely abandoned. TACE can be added after initiation of lenvatinib whenever it is necessary in a superselective and on-demand manner. After progression on lenvatinib, several tyrosine kinase inhibitors such as sorafenib, cabozantinib, or ramucirumab can follow, as suggested by the American Association for the Study of Liver Diseases (AASLD) guidelines [19].

Disclosure Statement:

Masatoshi Kudo received lecture fee from Bayer, Eisai, MSD, Ajinomoto and research grant from Chugai, Otsuka, Takeda, Taiho, Sumitomo Dainippon, Daiichi Sankyo, MSD, Eisai, Bayer, AbbVie, Medico's Hirata, Astellas Pharma, Bristol-Myers Squibb and advisory consulting fee from Kowa, MSD, Bristol-Myers Squibb, Bayer, Chugai, Taiho, Eisai, Ono Pharmaceutical.

References

- 1 Kudo M, Finn RS, Qin S, Han KH, Ikeda K, Piscaglia F, et al. Lenvatinib versus sorafenib in first-line treatment of patients with unresectable hepatocellular carcinoma: a randomised phase 3 non-inferiority trial. *Lancet*. 2018 Mar;391(10126):1163–73.
- 2 Vincenzi B, Di Maio M, Silletta M, D'Onofrio L, Spoto C, Piccirillo MC, et al. Prognostic relevance of objective response according to EASL criteria and mrecist criteria in hepatocellular carcinoma patients treated with loco-regional therapies: A literature-based meta-analysis. *PLoS One*. 2015 Jul;10(7):e0133488.
- 3 Galle PR, Forner A, Llovet JM, Mazzaferro V, Piscaglia F, Raoul JL, et al.; European Association for the Study of the Liver. Electronic address: easloffice@easloffice.eu; European Association for the Study of the Liver. EASL clinical practice guidelines: management of hepatocellular carcinoma. *J Hepatol*. 2018 Jul;69(1):182–236.
- 4 Ronot M, Bouattour M, Wassermann J, Bruno O, Dreyer C, Larroque B, et al. Alternative Response Criteria (Choi, European association for the study of the liver, and modified Response Evaluation Criteria in Solid Tumors [RECIST]) Versus RECIST 1.1 in patients with advanced hepatocellular carcinoma treated with sorafenib. *Oncologist*. 2014 Apr;19(4):394–402.
- 5 Arizumi T, Ueshima K, Chishina H, Kono M, Takita M, Kitai S, et al. Duration of stable disease is associated with overall survival in patients with advanced hepatocellular carcinoma treated with sorafenib. *Dig Dis*. 2014; 32(6):705–10.
- 6 Edeline J, Boucher E, Rolland Y, Vauléon E, Pracht M, Perrin C, et al. Comparison of tumor response by Response Evaluation Criteria in Solid Tumors (RECIST) and modified RECIST in patients treated with sorafenib for hepatocellular carcinoma. *Cancer*. 2012 Jan;118(1):147–56.
- 7 Takada J, Hidaka H, Nakazawa T, Kondo M, Numata K, Tanaka K, et al. Modified response evaluation criteria in solid tumors is superior to response evaluation criteria in solid tumors for assessment of responses to sorafenib in patients with advanced hepatocellular carcinoma. *BMC Res Notes*. 2015 Oct;8:609.
- 8 Lencioni R, Montal R, Torres F, Park JW, Decaens T, Raoul JL, et al. Objective response by mRECIST as a predictor and potential surrogate end-point of overall survival in advanced HCC. *J Hepatol*. 2017 Jun;66(6):1166–72.

- 9 Meyer T, Palmer DH, Cheng AL, Hocke J, Loembé AB, Yen CJ. mRECIST to predict survival in advanced hepatocellular carcinoma: analysis of two randomised phase II trials comparing nintedanib vs sorafenib. *Liver Int.* 2017 Jul;37(7):1047–55.
- 10 Kudo M, Ueshima K, Yokosuka O, Ogasawara S, Obi S, Izumi N, et al.; SILIUS study group. Sorafenib plus low-dose cisplatin and fluorouracil hepatic arterial infusion chemotherapy versus sorafenib alone in patients with advanced hepatocellular carcinoma (SILIUS): a randomised, open label, phase 3 trial. *Lancet Gastroenterol Hepatol.* 2018 Jun;3(6):424–32.
- 11 Kudo M, Han G, Finn RS, Poon RT, Blanc JF, Yan L, et al. Brivanib as adjuvant therapy to transarterial chemoembolization in patients with hepatocellular carcinoma: A randomized phase III trial. *Hepatology.* 2014 Nov;60(5):1697–707.
- 12 Lencioni R, Llovet JM, Han G, Tak WY, Yang J, Guglielmi A, et al. Sorafenib or placebo plus TACE with doxorubicin-eluting beads for intermediate stage HCC: the SPACE trial. *J Hepatol.* 2016 May;64(5):1090–8.
- 13 Meyer T, Fox R, Ma YT, Ross PJ, James MW, Sturgess R, et al. Sorafenib in combination with transarterial chemoembolisation in patients with unresectable hepatocellular carcinoma (TACE 2): a randomised placebo-controlled, double-blind, phase 3 trial. *Lancet Gastroenterol Hepatol.* 2017 Aug;2(8):565–75.
- 14 Yamashita T, Kudo M, Ikeda K, Izumi N, Ikeda M, Okusaka T, et al. Analysis of Japanese subpopulation from reflect trial. The 18th annual meeting of Japan Association of Molecular Targeted Therapy for HCC; 2018 July 14, Tokyo.
- 15 Kudo M. An international observational study to assess the real-world use of transarterial chemoembolization (TACE) in patients with hepatocellular carcinoma (HCC): The final analysis and Japanese subpopulation analysis of OPTIMIS. The 54th annual meeting of Liver Cancer Study Group of Japan; 2018 June 28, Kurume.
- 16 Ogasawara S, Chiba T, Ooka Y, Kanogawa N, Motoyama T, Suzuki E, et al. Efficacy of sorafenib in intermediate-stage hepatocellular carcinoma patients refractory to transarterial chemoembolization. *Oncology.* 2014;87(6):330–41.
- 17 Kudo M. A new era of systemic therapy for hepatocellular carcinoma with regorafenib and lenvatinib. *Liver Cancer.* 2017 Jun;6(3):177–84.
- 18 Kudo M. Lenvatinib in advanced hepatocellular carcinoma. *Liver Cancer.* 2017 Nov;6(4):253–63.
- 19 Marrero JA, Kulik LM, Sirlin C, Zhu AX, Finn RS, Abecassis MM, et al. Diagnosis, Staging, and Management of Hepatocellular Carcinoma: 2018 Practice Guidance by the American Association for the Study of Liver Diseases. *Hepatology.* 2018 Aug;68(2):723–50.

DEN Video Article

Cannulation method for intradiverticular papilla with long oral protrusion using biopsy forceps for axis alignment

Mamoru Takenaka¹, Kosuke Minaga¹ and Masatoshi Kudo¹

Department of Gastroenterology and Hepatology, Kindai University Faculty of Medicine, Osaka-Sayama, Japan

Intradiverticular papilla is considered a difficult anatomical orientation for biliary cannulation.^{1–3} To our knowledge, this is the first report to show the usefulness of biopsy forceps for cannulation not only to expose the ampulla in the case of an intradiverticular papilla but also for axis alignment. An 85-year-old woman underwent endoscopic retrograde cholangiopancreatography for a common bile duct (CBD) stone. A duodenoscope (TJF TYPE 260V; Olympus Medical Systems, Tokyo, Japan) was inserted into Vater's papilla. However, the papilla was hidden within a large diverticulum and could not be everted from the diverticulum. Only a papillary frenulum could be identified. This anatomical orientation prevented cannulation. Initially, an endoclip was used to rotate the papilla and fix it on the external rim of the diverticulum. However, the papilla was not completely exposed because of the long oral protrusion.

Next, biopsy forceps were used to grasp the duodenal mucosa and push it to the side, exposing the ampulla, and oral protrusion. However, the papilla reverted into the diverticulum soon after opening the biopsy forceps. We then used biopsy forceps to expose the ampulla and oral protrusion completely and simultaneously inserted a cannula into the working channel of a duodenoscope.⁴ Retaining the extension force created by the biopsy forceps, the cannula tip was separated from the endoscope tip (Fig. 1).

Next, we inserted the cannula toward the oral protrusion. As a result, pancreatography was successful, but the cannula tip could not be intubated. Thus, we pushed the biopsy forceps further to adjust the axis and successfully inserted the cannula tip into the pancreatic duct (Fig. 2).

Deep cannulation was achieved by guidewire assist, and biliary cannulation using the double-guidewire method was successful (Video S1).⁵

This technique is useful not only for intradiverticular papilla but also for strongly mobile papilla.

Authors declare no conflicts of interest for this article.

Corresponding: Mamoru Takenaka, Department of Gastroenterology and Hepatology, Kindai University Faculty of Medicine, 377-2 Ohno-Higashi, Osaka-Sayama 589-8511, Japan. Email: mamoxyo45@gmail.com

Received 8 June 2018; accepted 19 June 2018.

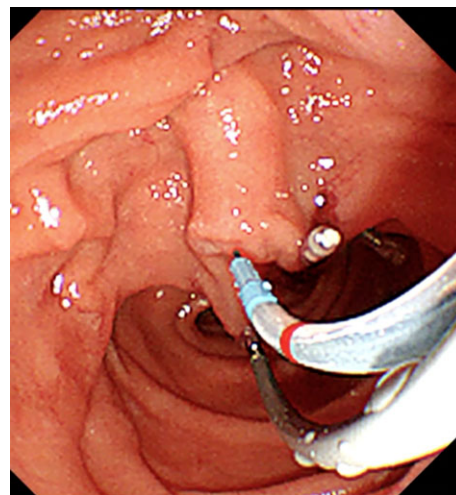


Figure 1 We used biopsy forceps to expose the ampulla and oral protrusion completely and simultaneously inserted a cannula into the working channel of a duodenoscope. Retaining the extension force created by the biopsy forceps, the cannula tip was separated from the endoscope tip. We inserted the cannula toward the oral protrusion.

REFERENCES

- 1 Ahmed AM, Wilcox CM. Endoscopic retrograde cholangiopancreatography cannulation in the difficult duct: which technique should you pull out of your bag? *Dig. Endosc.* 2017; **29**: 149–51.
- 2 Tham TC, Kelly M. Association of periampullary duodenal diverticula with bile duct stones and with technical success of endoscopic retrograde cholangiopancreatography. *Endoscopy* 2004; **36**: 1050–3.
- 3 Suguro M, Yamamoto K, Itoi T. Novel technique using a non-tip and short-wire papillotome for biliary cannulation of intradiverticular papilla in patients with Roux-en-Y anastomosis. *Dig. Endosc.* 2018; **30**: 270–2.
- 4 Fujita N, Noda Y, Kobayashi G, Kimura K, Yago A. ERCP for intradiverticular papilla: two-devices-in-one-channel method. Endoscopic Retrograde Cholangiopancreatography. *Gastrointest. Endosc.* 1998; **48**: 517–20.
- 5 Ito K, Horaguchi J, Fujita N *et al.* Clinical usefulness of double-guidewire technique for difficult biliary cannulation in endoscopic retrograde cholangiopancreatography. *Dig. Endosc.* 2014; **26**: 442–9.

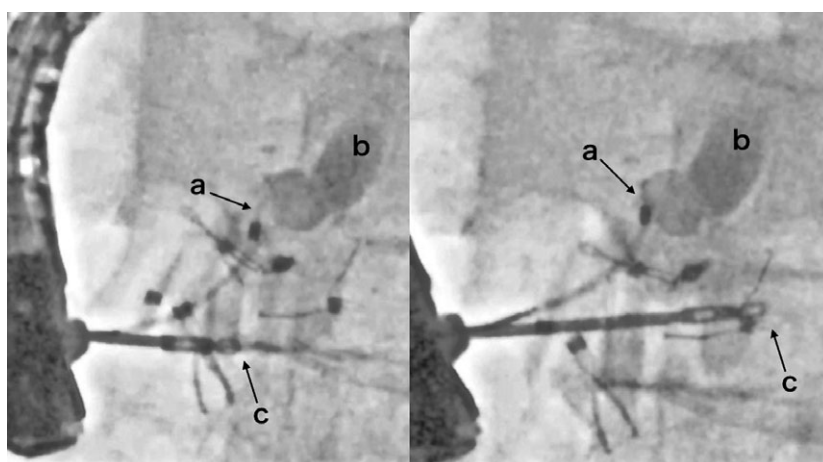


Figure 2 Left image shows fluoroscopic images before pushing the forceps. Right image is after pushing the forceps. Pancreatography was successful, but the cannula tip (a) could not be intubated into the pancreatic duct (b). Thus, we pushed the biopsy forceps (c) further to adjust the axis and successfully inserted the cannula tip (a) into the pancreatic duct (b).

SUPPORTING INFORMATION

ADDITIONAL SUPPORTING INFORMATION may be found in the online version of this article at the publisher's web site.

Video S1 In the case of difficult biliary cannulation because of intradiverticular papilla with long oral protrusion,

we used biopsy forceps to expose the ampulla and oral protrusion completely. Retaining the extension force created by the biopsy forceps, the cannula tip was inserted into the working channel of a duodenoscope simultaneously and separated from the endoscope tip. We inserted the cannula toward the oral protrusion. With axial adjustment by the biopsy forceps, biliary cannulation was successful.

—Images and Videos—

Cystic duct antegrade stenting for cholangitis after the long-term deployment of lumen-apposing metal stents for calculous cholecystitis

Ken Kamata, Mamoru Takenaka, Kosuke Minaga, Atsushi Nakai, Shunsuke Omoto, Takeshi Miyata, Kentaro Yamao, Hajime Imai, Toshiharu Sakurai, Tomohiro Watanabe, Naoshi Nishida, Masatoshi Kudo
Department of Gastroenterology and Hepatology, School of Medicine, Kindai University, Osaka-Sayama, Japan

EUS-guided gallbladder drainage (EUS-GBD) using a metal stent has been reported to be an alternative treatment for patients with cholecystitis at high surgical risk.^[1-3] However, long-term deployment of metal stents may induce late adverse events, such as stent migration and food impaction.^[4] This report describes a fistula created by EUS-GBD using a lumen-apposing metal stent (LAMS) in a patient with calculous cholecystitis to perform biliary drainage for cholangitis due to common bile duct stones induced by long-term LAMS deployment. An 80-year-old man with severe cardiac insufficiency presented with cholangitis due to biliary obstruction by common bile stones. This patient had undergone EUS-GBD using the LAMS for calculous cholecystitis 4 years earlier, along with deployment through the LAMS of a double-pigtail plastic stent between the gallbladder and duodenal bulb to prevent stent migration. After EUS-GBD, there were not any remaining stones in the gallbladder, and a computed tomography scan did not show common bile stones, suggesting that bile turbulence or food impaction due to long-term deployment of the LAMS may have induced stone development [Figure 1]. Biliary drainage using antegrade stenting through a cystic duct from the LAMS

was performed; transpapillary approach was not chosen because this patient had severe cardiac insufficiency and was therefore at risk of possibly fatal pancreatitis. It was the original intention to leave the stent permanently. An endoscope (GIF-HQ290; Olympus, Japan, Tokyo) was introduced into the gallbladder through the LAMS, and a 0.025-inch guidewire (025-inch diameter, angled tip, hydrophilic coating; Olympus, Japan, Tokyo) was deployed within the gallbladder. The gallbladder was collapsed, preventing endoscopic confirmation of the location of the cystic duct opening. Fistulography with the catheter was performed for biliary cannulation, but the contrast medium did not accumulate in the gallbladder because of leakage out of the LAMS without the balloon catheter. Therefore, fistulography was performed using a balloon catheter, of diameter 15 mm (Extractor™ Pro Retrieval Balloon; Boston, USA), inserted into the gallbladder from the LAMS. By this, the contrast medium accumulated in the gallbladder, allowing detection of the cystic duct under fluoroscopic image. Under fluoroscopic guidance, the guidewire was

This is an open access journal, and articles are distributed under the terms of the Creative Commons Attribution-NonCommercial-ShareAlike 4.0 License, which allows others to remix, tweak, and build upon the work non-commercially, as long as appropriate credit is given and the new creations are licensed under the identical terms.

For reprints contact: reprints@medknow.com

How to cite this article: Kamata K, Takenaka M, Minaga K, Nakai A, Omoto S, Miyata T, *et al.* Cystic duct antegrade stenting for cholangitis after the long-term deployment of lumen-apposing metal stents for calculous cholecystitis. *Endosc Ultrasound* 2018;7:349-50.

Access this article online	
Quick Response Code: 	Website: www.eusjournal.com
	DOI: 10.4103/eus.eus_91_17

Address for correspondence

Dr. Mamoru Takenaka, Department of Gastroenterology and Hepatology, Kindai University, Faculty of Medicine, 377-2 Ohno-Higashi, Osaka-Sayama 589-8511, Japan. E-mail: mamoxyo45@gmail.com

Received: 2017-05-03; **Accepted:** 2017-08-29; **Published online:** 2018-05-25

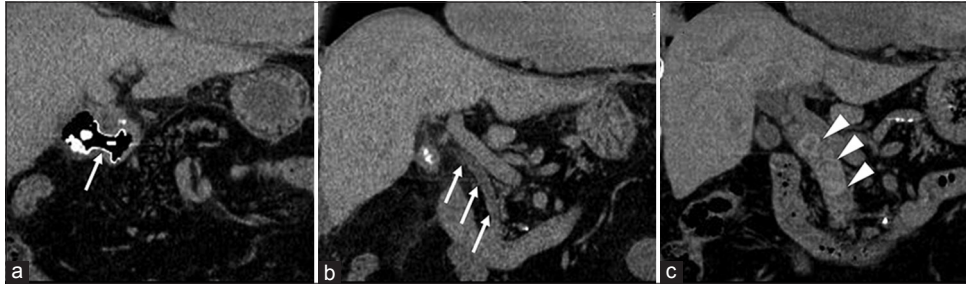


Figure 1. Computed tomography scan at the time of EUS-guided gallbladder drainage the lumen-apposing metal stent (arrow) (a) and no stones in the common bile duct (arrows) (b) computed tomography scan 4 years after EUS-guided gallbladder drainage showing many stones in the common bile duct (arrowheads) (c)

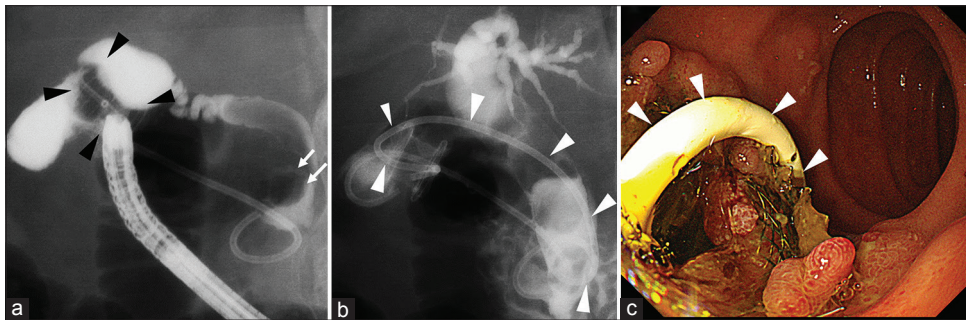


Figure 2. Fistulography under the balloon catheter (arrowheads) inserted into the gallbladder from the lumen-apposing metal stent. Defects in the common bile duct (arrows) were indicative of stones (a). Deployment of a double-pigtail plastic stent (arrowheads) between the common bile duct and duodenal bulb through the lumen-apposing metal stent (b). Endoscopic image after the procedure, showing the stent of the luminal side (arrowheads) (c)

inserted into the common bile duct through the cystic duct, with cholangiography showing the common bile duct stones [Figure 2a]. A 7Fr double-pigtail plastic stent (Through Pass; GADELIUS, Japan, Tokyo), 10 cm in length, was deployed between the common bile duct and duodenal bulb through the LAMS [Figure 2b and c] (Cystic Duct Antegrade Stenting). The following day, the patient's condition had improved and he could resume eating.

Declaration of patient consent

The authors certify that they have obtained all appropriate patient consent forms. In the form the patient has given his consent for his images and other clinical information to be reported in the journal. The patient understands that his name and initial will not be published and due efforts will be made to conceal his identity, but anonymity cannot be guaranteed.

Financial support and sponsorship

Nil.

Conflicts of interest

There are no conflicts of interest.

REFERENCES

1. Kamata K, Kitano M, Komaki T, *et al.* Transgastric endoscopic ultrasound (EUS)-guided gallbladder drainage for acute cholecystitis. *Endoscopy* 2009;41 Suppl 2:E315-6.
2. Walter D, Teoh AY, Itoi T, *et al.* EUS-guided gall bladder drainage with a lumen-apposing metal stent: A prospective long-term evaluation. *Gut* 2016;65:6-8.
3. Kamata K, Takenaka M, Kitano M, *et al.* Endoscopic ultrasound-guided gallbladder drainage for acute cholecystitis: Long-term outcomes after removal of a self-expandable metal stent. *World J Gastroenterol* 2017;23:661-7.
4. Choi JH, Lee SS, Choi JH, *et al.* Long-term outcomes after endoscopic ultrasonography-guided gallbladder drainage for acute cholecystitis. *Endoscopy* 2014;46:656-61.

[PICTURES IN CLINICAL MEDICINE]

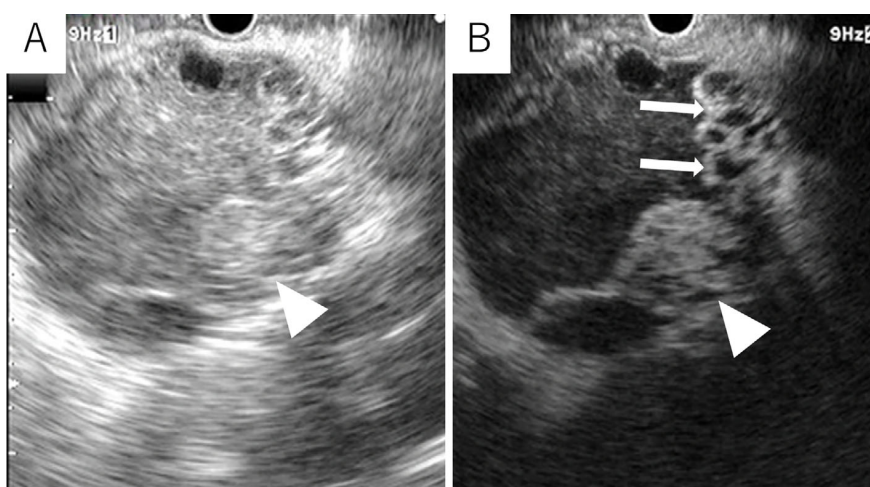
Contrast-enhanced Harmonic EUS Imaging of Pancreatic Mucinous Cystadenocarcinoma

Hidekazu Tanaka, Ken Kamata, Mamoru Takenaka and Masatoshi Kudo

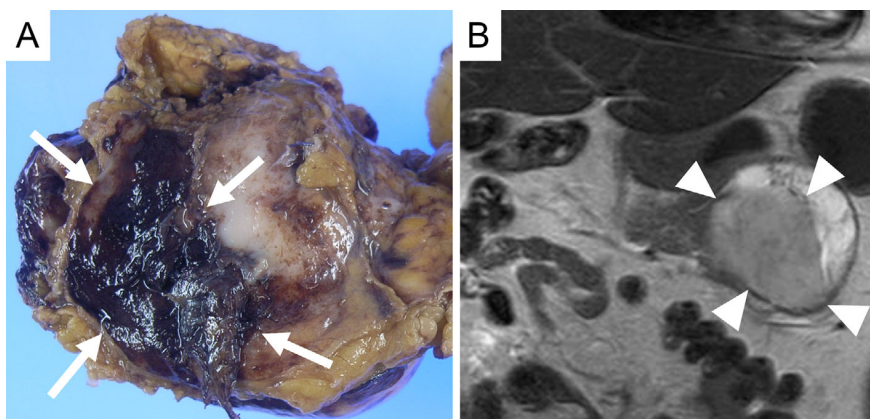
Key words: contrast-enhanced harmonic endoscopic ultrasonography, mucinous cystadenocarcinoma

(Intern Med 57: 3051-3052, 2018)

(DOI: 10.2169/internalmedicine.0846-18)

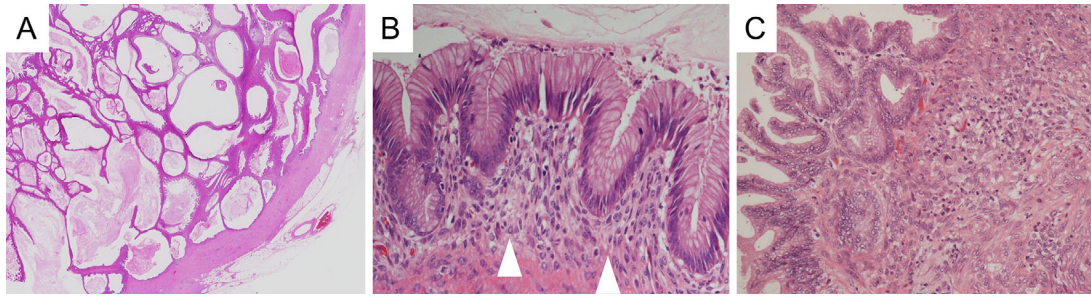


Picture 1.



Picture 2.

Department of Gastroenterology and Hepatology, Kindai University School of Medicine, Japan
Received: January 18, 2018; Accepted: March 1, 2018; Advance Publication by J-STAGE: May 18, 2018
Correspondence to Dr. Ken Kamata, ky11@leto.eonet.ne.jp



Picture 3.

A 52-year-old woman underwent contrast-enhanced harmonic EUS (CH-EUS) for the evaluation of a pancreatic mass. Approval for the performance of CH-EUS was obtained from the Ethics Committee of Kindai University Hospital (25-090). Conventional EUS showed an unclear heterogeneous high-echoic lesion of 8 cm in diameter with a likely solid part in the tail of pancreas (Picture 1A, arrowhead). CH-EUS clearly showed that the mass was composed of multiple cystic lesions with a cyst-in-cyst-like structure (Picture 1B, arrows) and an enhanced solid part (Picture 1B, arrowhead). She underwent distal pancreatectomy. A macroscopic examination revealed massive muddy mucus clots in a cystic tumor (Picture 2A, arrows), which corresponded with an iso-intense area on T1 MRI (Pic-


ture 2B, arrowheads). Hematoxylin and Eosin staining revealed multiple cysts with numerous mucus clots (Picture 3A) and ovarian-type stroma (Picture 3B, arrowheads). Malignant findings, including high-grade nuclear atypia and an irregular ductal structure with an invasive component (<5 mm) were seen (Picture 3C). The postoperative diagnosis was mucinous cystadenocarcinoma with minimal invasion (T1a N0 M0).

The authors state that they have no Conflict of Interest (COI).

The Internal Medicine is an Open Access journal distributed under the Creative Commons Attribution-NonCommercial-NoDerivatives 4.0 International License. To view the details of this license, please visit (<https://creativecommons.org/licenses/by-nc-nd/4.0/>).

Original Article

Novel quantitative assessment system of liver steatosis using a newly developed attenuation measurement method

Nobuharu Tamaki,¹ Yohei Koizumi,² Masashi Hirooka,² Norihisa Yada,³ Hitomi Takada,¹ Osamu Nakashima,⁴ Masatoshi Kudo,³ Yoichi Hiasa²  and Namiki Izumi¹¹Department of Gastroenterology and Hepatology, Musashino Red Cross Hospital, Tokyo, ²Department of Gastroenterology and Hepatology, Kindai University Faculty of Medicine, Osaka, ³Department of Clinical Laboratory Medicine, Kurume University Hospital, Kurume and ⁴Department of Gastroenterology and Metabolism, Ehime University Graduate School of Medicine, Ehime, Japan

Aim: The present study has developed and evaluated the effectiveness of a new echo attenuation measurement function combined with an ultrasonic diagnostic system for the accurate diagnosis of liver steatosis.

Methods: A multicenter prospective study involving patients with chronic hepatitis was carried out. All patients underwent liver biopsy, and attenuation coefficient (ATT) was measured on the same day. The fat area (%) of biopsy specimens was quantitatively evaluated. Correlations between ATT, steatosis grade, and fat area were evaluated.

Results: A total of 351 patients were enrolled in this study. The median values of fat area for steatosis grades S0, S1, S2, and S3 were 0.6%, 3.2%, 6.4%, and 15.5%, respectively. A significant correlation was found between fat area and steatosis grade ($P < 0.001$). Similarly, the median values of ATT for steatosis

grades S0, S1, S2, and S3 were 0.55, 0.63, 0.69, and 0.85 dB/cm/MHz, respectively, and ATT increased with an increase in the steatosis grade ($P < 0.001$). Attenuation coefficient was significantly correlated with fat area ($r = 0.50$, $P < 0.001$). The area under the receiver operating characteristic curve corresponding to $S \geq 1$, $S \geq 2$, and $S \geq 3$ were 0.79, 0.87, and 0.96, respectively. Similarly, the sensitivity and specificity of $S \geq 1$, $S \geq 2$, and $S \geq 3$ were 72%, 82%, and 87% and 72%, 82%, and 89%, respectively.

Conclusions: The newly developed ATT measurement for evaluation of liver steatosis was closely correlated with steatosis grade and automated quantification of fat area, and it provides clinically relevant information.

Key words: attenuation measurement, liver steatosis, NAFLD

INTRODUCTION

THE ASSOCIATION BETWEEN liver steatosis and hepatocellular carcinoma (HCC) has received attention in recent years.¹ Liver steatosis might be a leading factor for liver fibrosis progression and HCC development.^{2,3} Population-based screening suggests that at least 25% of the US population has non-alcoholic fatty liver disease (NAFLD).⁴ The prevalence of NAFLD in Japan ranges from 9% to 30%.⁵ It was reported that the standardized incidence ratio of HCC in patients with NAFLD was 4.4 during 16 years of follow-up.⁶ In Japan, a nationwide survey re-

vealed that 2% of HCC cases are attributable to NAFLD and HCC development rates were 11.3%/5 years in cirrhosis with NAFLD.⁷ However, it is thought that the true prevalence of NAFLD-related HCC is even greater, because HCC associated with cryptogenic cirrhosis was ignored. Therefore, accurate quantitative assessment of liver steatosis is clinically imperative. Although liver biopsy is currently the golden standard method for the diagnosis and grading of liver steatosis,⁸ invasiveness, sampling error, and intra- and inter-observer variability remain significant causes of concern.^{9,10}

Ultrasonography is the most widely used imaging technique for the diagnosis of liver steatosis as a non-invasive alternative to liver biopsy.¹¹ Liver steatosis is diagnosed on the basis of findings such as an increase in echogenicity and deep attenuation due to reflection and scattering of ultrasound. However, it depends on the operator's subjective evaluation and lacks objectivity. Moreover, these findings can only detect steatosis involving approximately 30% of

Correspondence: Dr Namiki Izumi, Department of Gastroenterology and Hepatology, Musashino Red Cross Hospital, 1-26-1 Kyonan-cho, Musashino-shi, Tokyo 180-8610, Japan. Email: izumi012@musashino.jrc.or.jp

Conflict of interest: The authors have no conflict of interest.

Financial support: None declared.

Received 8 February 2018; revision 29 March 2018; accepted 5 April 2018.

fatty infiltration, and its diagnostic accuracy is not adequate.¹² Therefore, a more reliable alternative for quantitative evaluation of liver steatosis is required.

Some studies have been reported to evaluate liver steatosis by focusing attention on echo attenuation due to liver fat.^{13,14} In recent years, controlled attenuation parameter (CAP, Echosens, Paris, France) with transient elastography (FibroScan) has been extensively used as a method for quantitative evaluation of liver steatosis.^{15,16} However, as it has no imaging function, it is indispensable to use it in combination with a general-purpose ultrasonic diagnostic system. Therefore, the present study has developed and evaluated the effectiveness of a novel echo attenuation measurement function combined with an ultrasonic diagnostic system for the accurate diagnosis of liver steatosis.

METHODS

Patients

A MULTICENTER PROSPECTIVE study involving patients with chronic hepatitis was undertaken at Musashino Red Cross Hospital (Tokyo, Japan), Ehime University (Ehime, Japan), and Kinki University (Osaka, Japan) between July 2015 and March 2017. All patients underwent liver biopsy and liver steatosis was evaluated histopathologically. Biological data were obtained on the same day as liver biopsy. Written informed consent was obtained from each patient. The study protocol was approved by the ethics review committees of Musashino Red Cross Hospital and conformed to the ethical guidelines of the Declaration of Helsinki.

Attenuation coefficient measurement

Attenuation coefficient (ATT) was measured on the same day on which liver biopsy was carried out using ultrasound (HI VISION Ascendus; Hitachi, Tokyo, Japan) and an EUP-C715 convex-type probe (5–1 MHz; Hitachi). Ultrasonic waves of different frequencies f_0, f_1 ($f_0 < f_1$) were transmitted to the same beam line, and ATT was determined by calculating the slope of the obtained received signal ratio (f_0/f_1). The probe was applied from the right intercostal space, and the measurement section was determined to avoid the vessel. Attenuation coefficient was determined five times in each case and the median value was taken into consideration.

Histopathological analysis

Laparoscopic liver biopsy was carried out using 13-G needles to obtain liver biopsy specimens; however, in cases with a history of upper abdominal surgery, a percutaneous

ultrasound-guided liver biopsy was carried out using 15-G or 18-G needles. Specimens were fixed using formalin, embedded with paraffin, and stained with hematoxylin–eosin. A biopsy sample with a minimum of five portal tracts was required for diagnosis. All liver biopsy specimens were independently evaluated by a senior pathologist who was blinded to the clinical data. For pathological examination, steatosis grade, fibrosis stage, and activity grade was determined according to the NAFLD activity score.¹⁷

Automated quantification of liver fat area using whole slide imaging

Whole slide imaging of echo specimens was acquired using the NanoZoomer 2.0HT (Hamamatsu Photonics, Hamamatsu, Japan) at a 40× objective lens equivalent to 0.227 $\mu\text{m}/\text{pixel}$ (Fig. 1A). The color image was converted to a grayscale image, and further binarization processing was carried out to create a mask image (Fig. 1B). In addition to fat droplets, mask images included sinusoids, blood vessels, and ballooning cells. In order to remove sinusoids and blood vessels, red blood cells were detected from the color image, masks adjacent to the red blood cells were excluded, and non-circular masks were excluded. Ballooning cells were also removed by excluding masks with high luminance dispersion. In this way, a fat droplet detection image was prepared (Fig. 1C,D) and the fat area was calculated by dividing the total of fat pixels by the total number of pixels. Image processing was prepared automatically using fat ratio calculation software (Hitachi).

Statistical analysis

Correlations between ATT measurement, fat area, and histological findings were analyzed using Spearman's rank correlation analysis. Pearson's correlation test was used for comparison between ATT measurement and fat area. Similarly, correlations between ATT measurement and biological data were analyzed using Pearson's correlation test. The Mann–Whitney *U*-test was used for comparison between the two groups of each steatosis grade and fat area and ATT. Receiver operating characteristic (ROC) curves were constructed, and the area under the ROC curve (AUROC) was calculated. Optimal cut-off values were selected to maximize sensitivity, specificity, and diagnostic accuracy. Sensitivity, specificity, positive predictive value, and negative predictive value were calculated by using cut-off values obtained from the ROC curves. The SPSS software version 18.0 (SPSS, Chicago, IL, USA) was used for analyses. A *P*-value of <0.05 was considered statistically significant.

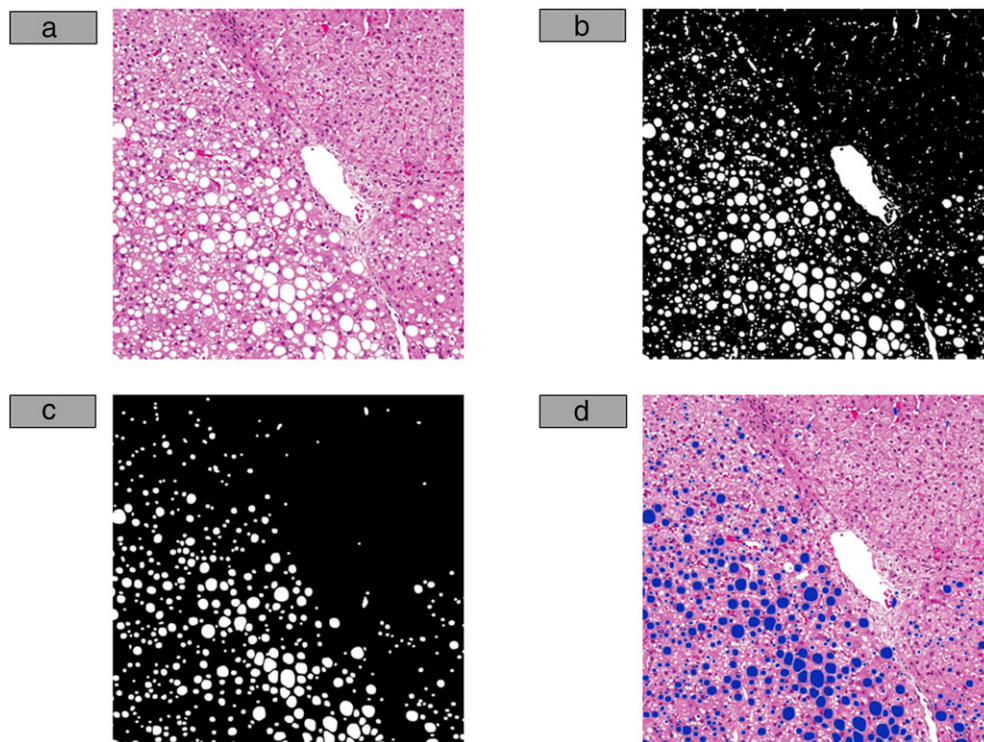


Figure 1 Fat droplet detection images. (A) Hematoxylin–eosin stained image. (B) Binary image. (C) Fat droplet detection image. Sinusoids, blood vessels, and ballooning cells were removed from the binary image. (D) Merged image. Fat droplets are shown in blue and merged with the hematoxylin–eosin image. [Color figure can be viewed at wileyonlinelibrary.com]

RESULTS

Patient characteristics

A TOTAL OF 351 patients were enrolled in this study. Background liver disease was hepatitis C virus (HCV), hepatitis B virus, NAFLD, primary biliary cholangitis, autoimmune hepatitis, alcoholic liver disease, drug-induced liver injury, and others in 182, 18, 33, 16, 21, 15, 7, and 59 cases, respectively. The steatosis grade was S0, S1, S2, and S3 in 285, 38, 13, and 15 cases, respectively (Table 1).

Correlation between ATT, histological steatosis grade, and fat area

Steatosis grade was compared with fat area. The median values of fat area for steatosis grades S0, S1, S2, and S3 were 0.6%, 3.2%, 6.4%, and 15.5%, respectively. Fat area increased with an increase in the steatosis grade (Spearman's $\rho=0.88$, $P<0.001$; Fig. 2A). Similarly, steatosis grade was compared with ATT. The median values of ATT for steatosis grades S0, S1, S2, and S3 were 0.55, 0.63, 0.69, and 0.85 dB/cm/MHz, respectively, and ATT

Table 1 Characteristics and steatosis grade of 351 patients with chronic hepatitis

	S0	S1	S2	S3	Total
HCV	163	14	5	0	182
HBV	15	1	1	1	18
NAFLD	0	13	6	14	33
AIH	13	3	0	0	16
PBC	18	3	0	0	21
ALD	13	2	0	0	15
DILI	6	1	0	0	7
Others	57	1	1	0	59
Total	285	38	13	15	351

AIH, autoimmune hepatitis; ALD, alcoholic liver disease; DILI, drug-induced liver disease; HBV, hepatitis B virus; HCV, hepatitis C virus; NAFLD, non-alcoholic fatty liver disease; PBC, primary biliary cholangitis.

increased with an increase in the steatosis grade (Spearman's $\rho=0.47$, $P<0.001$; Fig. 2B). In the pairwise comparison, the fat area of each steatosis grade significantly differed from each other (S0 vs. S1, $P<0.001$; S1

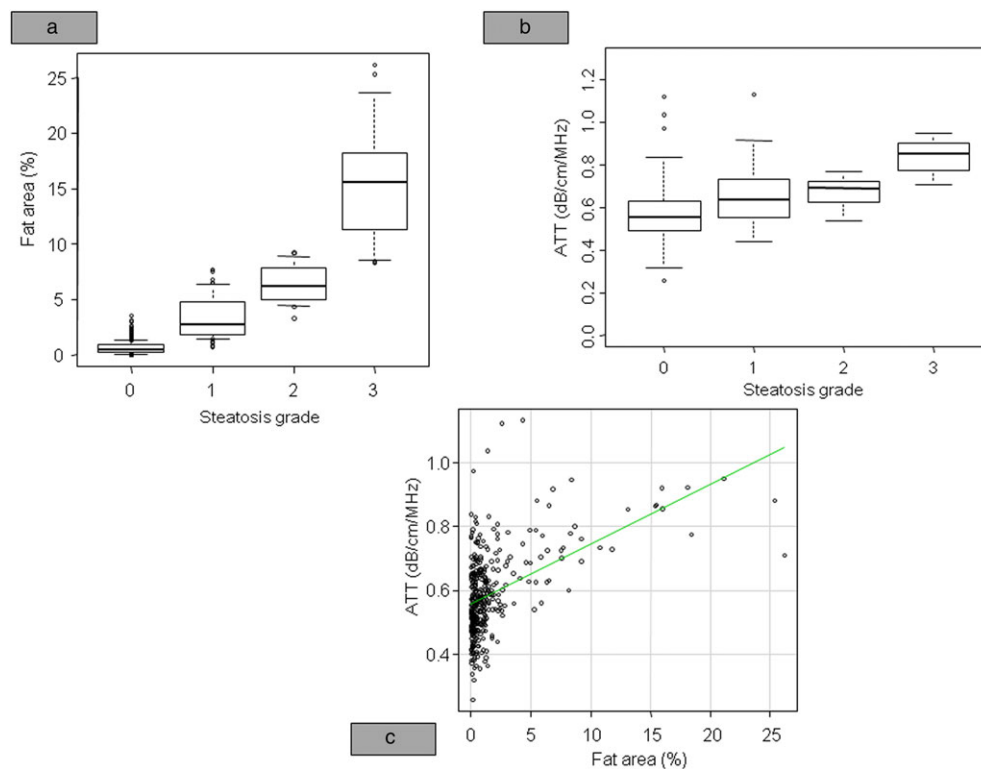


Figure 2 Correlation between steatosis grade, fat area, and attenuation coefficient (ATT) in 351 patients with chronic hepatitis. (A) Correlation between steatosis grade and fat area. (B) Correlation between steatosis grade and ATT. (C) Correlation between fat area and ATT. [Color figure can be viewed at wileyonlinelibrary.com]

vs. S2, $P < 0.001$; S2 vs. S3, $P < 0.001$). In ATT, there was a significant difference between S0/S1 ($P < 0.001$) and S2/S3 ($P < 0.001$), but no significant difference was observed in S1/S2 ($P = 0.44$). Next, the correlation between ATT and fat area was examined. There was a significant correlation between ATT and fat area ($r = 0.50$, $P < 0.001$; Fig. 2C).

Correlation between ATT and histological findings

The median ATT for fibrosis stage (F0, 1, 2, 3, and 4) and activity grade (A0, 1, 2, and 3) were 0.54, 0.57, 0.60, 0.58, and 0.59 and 0.54, 0.57, 0.59, and 0.48 dB/cm/MHz, respectively. There was no correlation between ATT and fibrosis stage and activity grade (Fig. 3).

Diagnostic ability of ATT for steatosis grade

Further, the diagnostic ability of ATT for steatosis grade was examined. The ATT cut-off values of $S \geq 1$, $S \geq 2$, and $S \geq 3$ determined by ROC analysis were 0.62, 0.67, and 0.73 (dB/cm/MHz), respectively. The AUROC calculated

from these cut-off values corresponding to $S \geq 1$, $S \geq 2$, and $S \geq 3$ were 0.79, 0.87, and 0.96, respectively. Similarly, the sensitivity and specificity of $S \geq 1$, $S \geq 2$, and $S \geq 3$ were 72%, 82%, and 87% and 72%, 82%, and 89%, respectively (Table 2).

Correlation between ATT and biological data

Correlation between ATT and biological data was examined. Examination of the correlation between alanine aminotransferase (ALT) and ATT showed no significant correlation ($r = -0.03$, $P = 0.55$; Fig. 4A). Similarly, there was no significant correlation between platelet count and ATT ($r = 0.03$, $P = 0.56$; Fig. 4B). In contrast, a significant correlation was found between triglyceride and ATT ($r = 0.34$, $P < 0.001$; Fig. 4C).

DISCUSSION

NON-INVASIVE EVALUATION OF liver steatosis was efficiently carried out using the newly developed ATT measurement method. Attenuation coefficient correlated with liver steatosis, but did not correlate with fibrosis

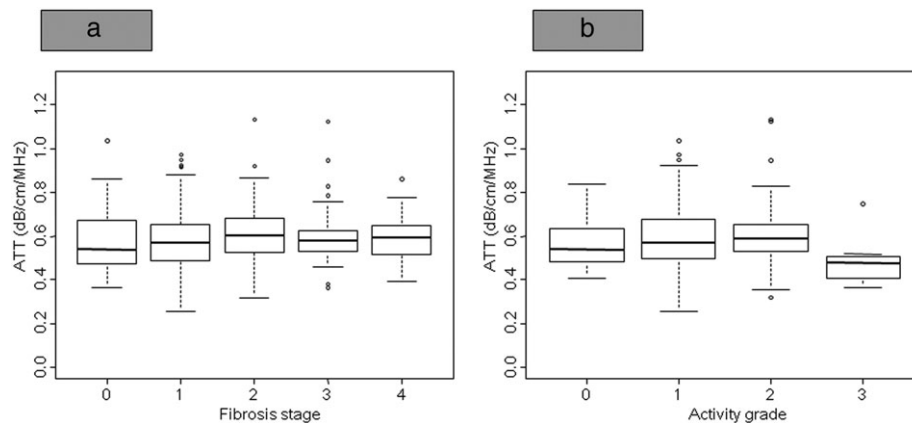


Figure 3 Correlation between attenuation coefficient (ATT) and histological findings in 351 patients with chronic hepatitis. (A) Correlation between ATT and fibrosis stage. (B) Correlation between ATT and activity grade.

Table 2 Diagnostic ability of attenuation coefficient for steatosis grade in patients with chronic hepatitis

	AUROC	Cut-off value	Sensitivity	Specificity	PPV	NPV
S1 \geq	0.79	0.62	0.72	0.72	0.37	0.92
S2 \geq	0.87	0.67	0.82	0.82	0.28	0.98
S3 \geq	0.96	0.73	0.87	0.89	0.26	0.99

NPV, negative predictive value; PPV, positive predictive value.

stage or activity grade. Therefore, it was possible to precisely evaluate liver steatosis by ATT measurement without being affected by liver fibrosis or inflammation, and it showed high diagnostic ability.

In recent years, the number of cases progressing from NAFLD to HCC has significantly increased, and thus, distinguishing patients with liver steatosis is clinically essential.¹ Although liver biopsy is the gold standard for the diagnosis of liver steatosis, it is invasive and cannot be examined repeatedly. It is difficult to evaluate the treatment effect in repeating liver biopsy. Therefore, a non-invasive diagnostic method is important. Ultrasonography is widely used as a non-invasive diagnostic method for fatty liver. However, diagnosis of fatty liver using conventional B-mode echo sonographic imaging was difficult in cases with little fat.^{11,18} Although computed tomography or magnetic resonance imaging are also used as alternative methods, they are costly and cannot be carried out easily. However, ATT can conveniently measure liver steatosis with high accuracy at the same time as the conventional B-mode echo. An important advantage of quantitative evaluation is possible with ATT

measurement. Furthermore, it has been reported that liver fibrosis correlates with the prognosis of chronic hepatitis including NAFLD; thus, assessment of liver fibrosis is also essential.^{19–22} In the present study, we used an ultrasonic system that diagnoses liver fibrosis using a combination of strain and shear wave imaging, and reported the utility of its diagnostic capability for liver fibrosis.^{23,24} Moreover, it is possible to undertake simultaneous diagnosis of B-mode imaging, liver steatosis, and fibrosis using the same device, which is considered to be a unique advantage not established in other equipment.

Controlled attenuation parameter using FibroScan is widely used for the diagnosis of liver steatosis, and its usefulness has been documented. The sensitivity of a diagnosis of steatosis by CAP has been reported as 64–94%, 57–96%, and 64–100% in S1 \geq , S2 \geq , and S3, respectively.²⁵ In another study, the AUROC of CAP for S1, S2, and S3 diagnosis was reported to be 0.79, 0.84, and 0.84, respectively.²⁶ Similarly, it was reported that the AUROC of CAP for S1, S2, and S3 diagnosis in Japanese patients with NAFLD was 0.88, 0.73, and 0.70, respectively.²⁷ The AUROC of ATT in this study for S \geq 1, S \geq 2, and S \geq 3 was 0.79, 0.87, and 0.96, respectively, and its diagnosis accuracy of liver steatosis was comparable to those reported in previous studies using CAP; hence, the ATT measurement method appears clinically useful. Attenuation measurement methods different from ATT and CAP have also been reported.^{28,29} Although we cannot directly compare because the measurement method is different, our study includes more patients, and the prediction accuracy of steatosis grade is high. However, it is necessary to further examine the comparison with these methods.

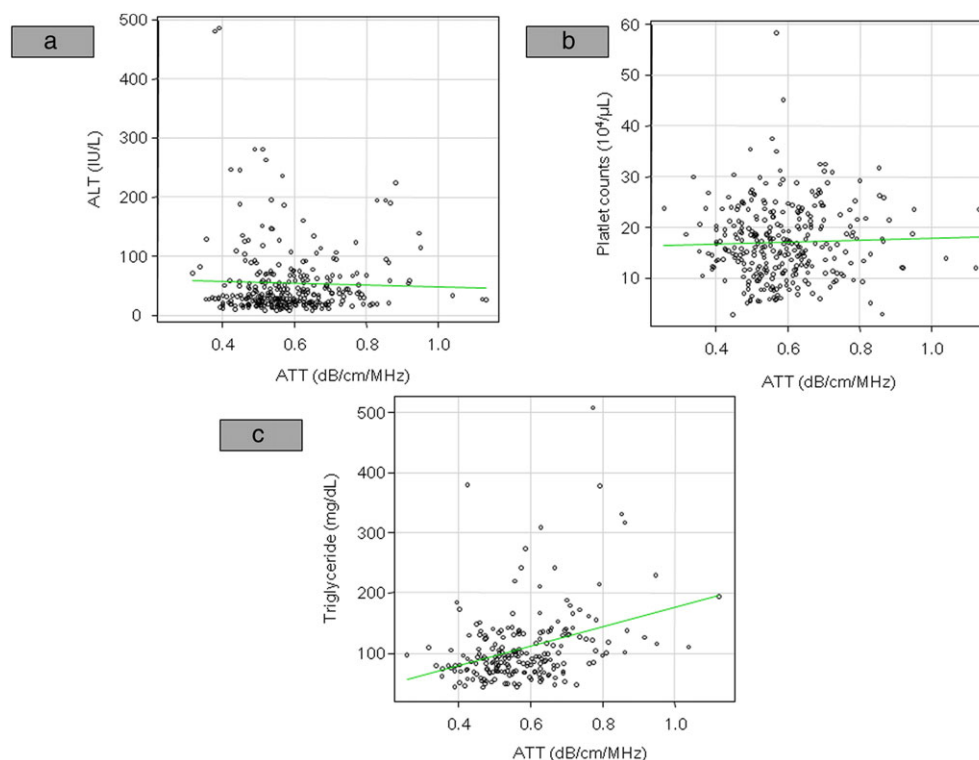


Figure 4 Correlation between attenuation coefficient (ATT) and biological data in 351 patients with chronic hepatitis. (A) Correlation between ATT and alanine aminotransferase (ALT). (B) Correlation between ATT and platelet counts. (C) Correlation between ATT and triglyceride. [Color figure can be viewed at wileyonlinelibrary.com]

One of the features of this study was the quantitative evaluation of fat area. Although liver biopsy is currently the gold-standard method for the diagnosis and grading of liver steatosis, intra- and interobserver variability remain a significant cause of concern. Therefore, methods for quantitatively evaluating pathological images are expanding.^{30,31} In this study, quantitatively evaluated fat area was correlated with steatosis grade and the accuracy of the quantitative method was proved. Furthermore, ATT correlated with fat area, confirming the usefulness of ATT diagnosis of liver steatosis. In recent years, various drugs for liver steatosis have been developed. In the future, such quantitative assessment is extremely important, in view of the therapeutic reactivity to drugs, and is considered to have clinical significance.

It became clear in this study that ATT correlates with liver steatosis. Furthermore, it was also revealed that ATT significantly correlates with serum triglyceride, which is a risk factor of liver steatosis.³² However, ATT was not affected by liver inflammation (activity grade or ALT) or

fibrosis (fibrosis stage or platelet counts). As inflammation and fibrosis are strongly involved in the pathophysiology of NAFLD, it is a great advantage of ATT that it is possible to measure liver steatosis without being affected by these factors.

However, it is necessary to re-evaluate the diagnostic ability of this method on a larger number of advanced cases as there were only a few cases of advanced steatosis in this study. In addition, in the pairwise comparison, there was no significant difference in ATT between S1 and S2, which was a limitation of this study. In this regard, it is also necessary to investigate many cases and to verify diagnostic accuracy. Finally, as we did not directly compare the diagnostic efficiency of this method with that of CAP, such a comparison is recommended in further investigations, which are currently in development.

In conclusion, the newly developed ATT measurement for evaluation of liver steatosis was closely correlated with steatosis grade and automated quantification of fat area and it provides clinically relevant information.





REFERENCES

- 1 Lazo M, Clark JM. The epidemiology of nonalcoholic fatty liver disease: a global perspective. *Semin Liver Dis* 2008; **28**: 339–50.
- 2 Kurosaki M, Hosokawa T, Matsunaga K *et al*. Hepatic steatosis in chronic hepatitis C is a significant risk factor for developing hepatocellular carcinoma independent of age, sex, obesity, fibrosis stage and response to interferon therapy. *Hepatol Res*. 2010; **40**: 870–7.
- 3 Tamaki N, Kurosaki M, Higuchi M *et al*. Genetic polymorphisms of *IL28B* and *PNPLA3* are predictive for HCV related rapid fibrosis progression and identify patients who require urgent antiviral treatment with new regimens. *PLoS One*. 2015; **10**: e0137351.
- 4 Lazo M, Hernaez R, Eberhardt MS *et al*. Prevalence of nonalcoholic fatty liver disease in the United States: the Third National Health and Nutrition Examination Survey, 1988–1994. *Am J Epidemiol* 2013; **178**: 38–45.
- 5 Loomba R, Sanyal AJ. The global NAFLD epidemic. *Nat Rev Gastroenterol Hepatol* 2013; **10**: 686–90.
- 6 Sorensen HT, Mellemkjaer L, Jepsen P *et al*. Risk of cancer in patients hospitalized with fatty liver: a Danish cohort study. *J Clin Gastroenterol* 2003; **36**: 356–9.
- 7 Tokushige K, Hashimoto E, Kodama K. Hepatocarcinogenesis in non-alcoholic fatty liver disease in Japan. *J Gastroenterol Hepatol* 2013; **28**(Suppl 4): 88–92.
- 8 Angulo P. Nonalcoholic fatty liver disease. *N Engl J Med* 2002; **346**: 1221–31.
- 9 Bedossa P, Dargere D, Paradis V. Sampling variability of liver fibrosis in chronic hepatitis C. *Hepatology* 2003; **38**: 1449–57.
- 10 Intraobserver and interobserver variations in liver biopsy interpretation in patients with chronic hepatitis C. The French METAVIR Cooperative Study Group. *Hepatology* 1994; **20**: 15–20.
- 11 Schwenzer NF, Springer F, Schraml C, Stefan N, Machann J, Schick F. Non-invasive assessment and quantification of liver steatosis by ultrasound, computed tomography and magnetic resonance. *J Hepatol* 2009; **51**: 433–45.
- 12 Clark JM, Brancati FL, Diehl AM. Nonalcoholic fatty liver disease. *Gastroenterology* 2002; **122**: 1649–57.
- 13 Fujii Y, Taniguchi N, Itoh K *et al*. A new method for attenuation coefficient measurement in the liver: comparison with the spectral shift central frequency method. *J Ultrasound Med* 2002; **21**: 783–8.
- 14 Lu ZF, Zagzebski JA, Lee FT. Ultrasound backscatter and attenuation in human liver with diffuse disease. *Ultrasound Med Biol* 1999; **25**: 1047–54.
- 15 Sasso M, Beaugrand M, de Ledinghen V *et al*. Controlled attenuation parameter (CAP): a novel VCTE guided ultrasonic attenuation measurement for the evaluation of hepatic steatosis: preliminary study and validation in a cohort of patients with chronic liver disease from various causes. *Ultrasound Med Biol* 2010; **36**: 1825–35.
- 16 Sasso M, Miette V, Sandrin L, Beaugrand M. The controlled attenuation parameter (CAP): a novel tool for the non-invasive evaluation of steatosis using FibroScan. *Clin Res Hepatol Gastroenterol* 2012; **36**: 13–20.
- 17 Kleiner DE, Brunt EM, Van Natta M *et al*. Design and validation of a histological scoring system for nonalcoholic fatty liver disease. *Hepatology* 2005; **41**: 1313–21.
- 18 Ryan CK, Johnson LA, Germin BI, Marcos A. One hundred consecutive hepatic biopsies in the workup of living donors for right lobe liver transplantation. *Liver Transpl* 2002; **8**: 1114–22.
- 19 Angulo P, Kleiner DE, Dam-Larsen S *et al*. Liver fibrosis, but no other histologic features, is associated with long-term outcomes of patients with nonalcoholic fatty liver disease. *Gastroenterology* 2015; **149**: 389389–NaN–97 e10.
- 20 Tamaki N, Kurosaki M, Matsuda S *et al*. Non-invasive prediction of hepatocellular carcinoma development using serum fibrosis marker in chronic hepatitis C patients. *J Gastroenterol* 2014; **49**: 1495–503.
- 21 Tamaki N, Kurosaki M, Kuno A *et al*. *Wisteria floribunda* agglutinin positive human Mac-2-binding protein as a predictor of hepatocellular carcinoma development in chronic hepatitis C patients. *Hepatol Res* 2015; **45**: E82–E88.
- 22 Takahashi Y, Kurosaki M, Tamaki N *et al*. Non-alcoholic fatty liver disease fibrosis score and FIB-4 scoring system could identify patients at risk of systemic complications. *Hepatol Res* 2015; **45**: 667–75.
- 23 Tamaki N, Kurosaki M, Matsuda S *et al*. Prospective comparison of real-time tissue elastography and serum fibrosis markers for the estimation of liver fibrosis in chronic hepatitis C patients. *Hepatol Res* 2014; **44**: 720–7.
- 24 Yada N, Tamaki N, Koizumi Y *et al*. Diagnosis of fibrosis and activity by a combined use of strain and shear wave imaging in patients with liver disease. *Dig Dis* 2017; **35**: 515–20.
- 25 Mikolasevic I, Orlic L, Franjic N, Hauser G, Stimac D, Milic S. Transient elastography (FibroScan) with controlled attenuation parameter in the assessment of liver steatosis and fibrosis in patients with nonalcoholic fatty liver disease – Where do we stand? *World J Gastroenterol* 2016; **22**: 7236–51.
- 26 de Ledinghen V, Vergniol J, Capdepon M *et al*. Controlled attenuation parameter (CAP) for the diagnosis of steatosis: a prospective study of 5323 examinations. *J Hepatol* 2014; **60**: 1026–31.
- 27 Imajo K, Kessoku T, Honda Y *et al*. Magnetic resonance imaging more accurately classifies steatosis and fibrosis in patients with nonalcoholic fatty liver disease than transient elastography. *Gastroenterology* 2016; **150**: 626626–NaN–37 e7.
- 28 Paige JS, Bernstein GS, Heba E *et al*. A pilot comparative study of quantitative ultrasound, conventional ultrasound, and MRI for predicting histology-determined steatosis grade in adult nonalcoholic fatty liver disease. *AJR Am J Roentgenol* 2017; **208**: W168–W177.
- 29 Han A, Andre MP, Deiranieh L *et al*. Repeatability and reproducibility of the ultrasonic attenuation coefficient and backscatter coefficient measured in the right lobe of the liver in adults with known or suspected nonalcoholic fatty liver

- disease. *J Ultrasound Med* 2018. <https://doi.org/10.1002/jum.14537>.
- 30 Abe T, Hashiguchi A, Yamazaki K *et al.* Quantification of collagen and elastic fibers using whole-slide images of liver biopsy specimens. *Pathol Int* 2013; 63: 305–10.
- 31 Yasui Y, Abe T, Kurosaki M *et al.* Elastin fiber accumulation in liver correlates with the development of hepatocellular carcinoma. *PLoS One* 2016; 11: e0154558.
- 32 Chalasani N, Younossi Z, Lavine JE *et al.* The diagnosis and management of non-alcoholic fatty liver disease: practice guideline by the American Gastroenterological Association, American Association for the Study of Liver Diseases, and American College of Gastroenterology. *Gastroenterology* 2012; 142: 1592–609.

Original Article

Value of additional endoscopic ultrasonography for surveillance after surgical removal of intraductal papillary mucinous neoplasms

Ken Kamata,¹ Mamoru Takenaka,¹  Kosuke Minaga,¹  Shunsuke Omoto,¹  Takeshi Miyata,¹ Kentaro Yamao,¹ Hajime Imai,¹ Atsushi Nakai,¹ Hidekazu Tanaka,¹ Yasutaka Chiba,⁴ Tomohiro Watanabe,¹ Toshiharu Sakurai,¹ Naoshi Nishida,¹ Takaaki Chikugo,² Ippei Matsumoto,³ Yoshifumi Takeyama,³ Masayuki Kitano⁵  and Masatoshi Kudo¹

Departments of ¹Gastroenterology and Hepatology, ²Pathology, ³Surgery, Faculty of Medicine, Kindai University, ⁴Clinical Research Center, Kindai University Hospital, Osaka-sayama, and ⁵Second Department of Internal Medicine, Wakayama Medical University, School of Medicine, Wakayama, Japan

Background and Aim: This study evaluated the utility of endoscopic ultrasonography (EUS) combined with contrast-enhanced harmonic EUS (CH-EUS) for surveillance of the remnant pancreas after surgery for intraductal papillary mucinous neoplasm (IPMN).

Methods: This was a single-center, retrospective, descriptive study. A total of 134 consecutive patients who underwent surgical resection for IPMN between April 2009 and March 2015 were evaluated. Rates of recurrence and development of IPMN-concomitant pancreatic ductal adenocarcinoma (PDAC) during follow up were assessed. Clinical findings of patients with recurrence or development of PDAC were also evaluated.

Results: Of 134 resected IPMN 56 (41.8%) and 78 (58.2%) were classified as benign and malignant, respectively. Patients were followed up for a median of 29 months, 33 (24.6%) by both contrast-enhanced computed tomography (CE-CT) and EUS, and 101 (75.4%) by computed tomography (CT) alone. Thirteen

patients (9.7%) showed tumor recurrence, five with intra-pancreatic recurrence and eight with extra-pancreatic metastases. An enhancing mural nodule within the dilated main pancreatic duct was successfully detected by EUS in one patient, but not by CE-CT. Two patients developed IPMN-concomitant PDAC during follow up. EUS combined with CH-EUS successfully detected small IPMN-concomitant PDAC in two patients, whereas these lesions were not detected by CT. CH-EUS was useful for better visualization of the margins of IPMN-concomitant PDAC in one of these two patients.

Conclusion: Endoscopic ultrasonography combined with CH-EUS may improve follow up of patients with resected IPMN.

Key words: contrast-enhanced harmonic endoscopic ultrasonography, endoscopic ultrasonography, intraductal papillary mucinous neoplasm, pancreatic ductal adenocarcinoma, remnant pancreas

INTRODUCTION

INTRADUCTAL PAPILLARY MUCINOUS neoplasms (IPMN) are frequently detected by imaging modalities, such as computed tomography (CT) and magnetic resonance cholangiopancreatography (MRCP). International consensus guidelines (ICG) for the management of IPMN classify CT and MRCP findings into three patterns: high-risk stigmata (HRS), worrisome feature (WF), and others,¹ recommending surgical resection of IPMN classified as HRS. Further

examination by endoscopic ultrasonography (EUS) is recommended for lesions classified as WF, with surgical resection deemed necessary if EUS shows characteristics highly indicative of malignancy. Other lesions, with no indications of malignancy, can be followed up without surgical resection. Thus, EUS is an indispensable diagnostic procedure to determine treatments for IPMN. The ICG also recommend EUS for surveillance of patients with IPMN and cyst size >2 cm. This recommendation, however, was based on insufficient clinical evidence, suggesting that suitable imaging modalities and intervals for follow up of patients with IPMN have not been determined. Furthermore, there is no consensus on the management and follow up of patients with IPMN after surgical resection.

We previously reported that many patients with IPMN develop concomitant pancreatic ductal adenocarcinoma

Corresponding: Ken Kamata, Department of Gastroenterology and Hepatology, Kindai University Faculty of Medicine, 377-2 Ohno-higashi, Osaka-sayama 589-8511, Japan. E-mail: ky11@leto.eonet.ne.jp

Received 20 December 2017; accepted 12 April 2018.

(PDAC) and that EUS was useful for its early detection.² Thus, careful follow up and surveillance are necessary for patients with IPMN, regardless of whether or not surgical resection is carried out. Contrast-enhanced harmonic EUS (CH-EUS) has been shown to be useful for evaluation of pancreatic diseases,^{3–6} including a mural nodule (MN) in IPMN and a small solid pancreatic tumor.^{3,4} A recent review article on the current roles of endoscopy in the management of IPMN also mentioned that EUS and CH-EUS play a crucial role in the surveillance of IPMN, especially for the early detection of pancreatic cancer.⁵ These findings suggested that EUS and CH-EUS may enhance the detection of recurrence after surgical resection of IPMN. To assess the usefulness of EUS and CH-EUS in detecting recurrence and IPMN-concomitant PDAC, patients who underwent surgical resection of IPMN were retrospectively evaluated.

PATIENTS AND METHODS

Study design

THIS WAS A single-center, retrospective, descriptive study. The study protocol was approved by the ethics committee of the Kindai University School of Medicine.

Patients

This study enrolled 134 consecutive patients who underwent surgical resection for IPMN at Kindai University Hospital between April 2009 and March 2015. All patients underwent EUS and CH-EUS examinations at initial diagnosis.

Indications for surgery

All main duct (MD) and branch duct (BD) IPMN showing enhancing MN were surgically resected. IPMN accompanied by symptoms (abdominal pain or pancreatitis) were also surgically resected.

Definitions

As specified by ICG, IPMN were classified as MD type, mixed type, or BD type. Degree of dysplasia was classified as low-grade dysplasia (LGD), high-grade dysplasia (HGD), or invasive carcinoma.⁷ LGD was classified as benign IPMN, and LGD and HGD were considered non-invasive IPMN. MN was defined as a protrusion of the cyst wall into its lumen, as detected by imaging modalities such as CT, MRCP, or EUS. Enhancing MN was defined as cyst wall protrusion with enhancement on contrast-enhanced CT (CE-CT) or CH-EUS.³ PDAC was defined as a solid tumor with hypo-enhancement on CE-CT or CH-EUS.

Recurrence was defined as the development of a MN, a new BD-IPMN in the remnant pancreas, or extra-pancreatic metastasis, as confirmed by surveillance imaging. IPMN-concomitant PDAC were diagnosed based on radiological images and/or pathological findings of the resected specimens.⁸ Secondary IPMN was defined as a cyst (BD-IPMN) other than that which had surgical indications and was resected. Main pancreatic duct (MPD) dilation without MN and enlargement of a secondary IPMN remaining within the remnant pancreas without the development of MN were not considered as recurrences.

Follow-up strategy after resection of IPMN

All patients were followed up by CE-CT after surgical resection. Patients with LGD were evaluated once yearly; patients with HGD were evaluated twice yearly during the first year and once yearly thereafter; and patients with invasive carcinoma were evaluated by CE-CT every 3–4 months during the first 2 years, and twice yearly thereafter. Based on a previous study,² EUS was carried out twice yearly if the patient agreed with the doctor's decision to use EUS in addition to CT for surveillance of the remnant pancreas. If either CE-CT or EUS showed pancreatic tumor recurrence or abnormal changes in the remnant pancreas, such as enlargement of the MPD (>2 mm) or secondary IPMN (>10 mm), patients were evaluated by another modality (CT or EUS) within the following month.

Endoscopic ultrasonography in combination with CH-EUS

An echoendoscope developed specifically for CH-EUS (GF-UCT260; Olympus Medical Systems Co. Ltd, Tokyo, Japan) was used. EUS images were analyzed using an ALOKA ProSound SSD α -10 system (ALOKA Co. Ltd, Tokyo, Japan). Patients showing abnormal changes on conventional EUS, such as intra-pancreatic recurrences, MPD dilation, or enlargement of a secondary IPMN, or an increase in tumor marker concentration during follow up were evaluated by CH-EUS. Each CH-EUS examination lasted 60 s from the time of injection of the contrast agent (Sonazoid; Daiichi-Sankyo, Tokyo, Japan), thus allowing screening of the entire remnant pancreas.

Statistical analysis

Surveillance results are presented as summary statistics. Mean and standard deviation or median and range were used for continuous variables, and the proportion was used for categorical variables. All statistical analyses were carried out

using SAS software version 9.4 (SAS Institute, Cary, NC, USA).

RESULTS

Patient characteristics

CHARACTERISTICS OF THE patients enrolled in the present study are shown in Table 1. Of the 134 patients, 75 (56.0%), 44 (32.8%), and 15 (11.2%) underwent pancreaticoduodenectomy (PD), distal pancreatectomy (DP), and total pancreatectomy (TP), respectively, for IPMN resection. Follow up was by both CE-CT and EUS in 33 (24.6%) patients and by CE-CT alone in 101 (75.4%). Percentages of patients with LGD, HGD, and invasive carcinoma who were followed up by CE-CT and EUS were 33.9%, 22.2%, and 14.3%, respectively. No patient who underwent TP was followed up by EUS. Of the 75 patients who underwent PD, 72 (96.0%) underwent pancreaticogastrostomy and three (4.0%) underwent pancreaticojejunostomy.

Mean cyst size before surgery was 25.1 ± 13.4 mm, as assessed by imaging modalities, and mean MPD diameter

was 6.4 ± 5.1 mm. Enhancing MN was detected before surgery in 107 (80.0%) of the 134 patients who underwent IPMN resection. Of these 134 resected tumors, 56 (41.8%), 36 (26.9%), and 42 (31.3%) were classified as LGD, HGD, and invasive carcinoma, respectively. Percentage of patients with benign IPMN (LGD) was higher in the 33 patients followed up by CT plus EUS than in the 101 followed up by CT alone. Of the 134 patients, 39 (29.1%) were positive for secondary IPMN without MN in the remnant pancreas.

Follow-up outcomes after surgical resection

Median follow-up period after surgery was 29 months (range, 0–99 months). One patient was transferred to another hospital after surgery and was therefore lost to follow up. Thirteen patients (9.7%) were diagnosed with recurrence; their characteristics are shown in Table 2. Mean interval between resection and the diagnosis of recurrence was 30 months. Five patients showed recurrence in the remnant pancreas, including four with BD-IPMN without MN and one with enhancing MN within the MPD. The other

Table 1 Demographic and clinical characteristics of the patient population

	Total <i>n</i> = 134	CT with EUS follow-up group <i>n</i> = 33	CT follow-up group <i>n</i> = 101
Age, mean (SD), y	69.8 (8.61)	69.9 (7.72)	69.7 (8.88)
Sex, <i>n</i> (%)			
Male	69 (51)	16 (48)	53 (52)
Female	65 (49)	17 (52)	48 (48)
Location of resected IPMN, <i>n</i> (%)			
Head	94 (70)	23 (70)	71 (70)
Body	30 (22)	6 (18)	24 (24)
Tail	10 (8)	4 (12)	6 (6)
Type of IPMN, <i>n</i> (%)			
Branch duct type	74 (55)	18 (55)	56 (55)
Main duct	19 (14)	5 (15)	14 (14)
Mixed type	41 (31)	10 (30)	31 (31)
Surgery, <i>n</i> (%)			
Pancreaticoduodenectomy	75 (56)	23 (70)	52 (51)
Distal pancreatectomy	44 (33)	10 (30)	34 (34)
Total pancreatectomy	15 (11)	0 (0)	15 (15)
Diagnosis, <i>n</i> (%)			
Low-grade	56 (42)	19 (58)	37 (37)
High-grade	36 (27)	8 (24)	28 (28)
Invasive	42 (31)	6 (18)	36 (35)
Presence of secondary IPMN [†] , <i>n</i> (%)	39 (29)	13 (39)	26 (26)

[†]A branch duct IPMN other than that which had surgical indications and was resected.

CT, computed tomography; EUS, endoscopic ultrasonography; IPMN, intraductal papillary mucinous neoplasm; SD, standard deviation.

Table 2 Characteristics of the 13 patients with recurrent lesions after surgical resection

No.	Age/sex	Time after surgery (months)	Type of recurrence	Size (mm)	Type of IPMN	Initial surgery	Diagnosis	Secondary IPMN	EUS follow-up	EUS detection	CT detection
1	86/F	24	BD-IPMN without MN	12	BD	PD	Invasive	No	No	Yes	Yes
2	73/M	9	Liver metastasis		BD	PD	Invasive	Yes	No	No	Yes
3	64/F	12	Lung metastasis		Mixed	PD	Invasive	No	No	No	Yes
4	72/M	12	Lung and liver metastasis		Mixed	PD	Invasive	No	No	No	Yes
5	62/M	69	BD-IPMN without MN	17	BD	PD	HGD	No	Yes	Yes	Yes
6	75/M	67	Lung metastasis		BD	PD	Invasive	Yes	No	No	Yes
7	73/M	20	Liver metastasis		MD	TP	Invasive	No	No	No	Yes
8	64/F	18	BD-IPMN without MN	8	BD	DP	LGD	No	Yes	Yes	Yes
9	68/F	6	Peritoneal seeding		Mixed	TP	Invasive	Yes	No	No	Yes
10	84/F	12	Lung metastasis		Mixed	TP	Invasive	Yes	No	No	Yes
11	75/F	12	BD-IPMN without MN	28	Mixed	DP	LGD	No	Yes	Yes	Yes
12	61/F	68	Liver metastasis		BD	DP	HGD	Yes	No	No	Yes
13	78/F	62	MN within a dilated MPD	9	MD	DP	HGD	Yes	Yes	Yes	No

eight patients were diagnosed with distant metastases. Two patients (1.5%) developed IPMN-concomitant PDAC during follow up. Rate of recurrence or the incidence of IPMN-concomitant PDAC was higher in patients with invasive IPMN than in those with non-invasive IPMN (21.4% vs 6.5%). Four of the 36 patients with HGD (11.1%) experienced recurrences (BD-IPMN without MN [$n = 1$], MN within a dilated MPD [$n = 1$], and distant metastasis [$n = 1$] or IPMN-concomitant PDAC ($n = 1$). In contrast, two of the 56 patients with LGD (3.6%) suffered recurrences of BD-IPMN without MN. Thus, the rate of recurrence or the incidence of IPMN-concomitant PDAC was higher in patients with HGD than in those with LGD (11.1% vs 3.6%). The rate of recurrence or the incidence of IPMN-concomitant PDAC was similar in patients with BD type, mixed type, and MD type IPMN (10.8% [8/74] vs 12.2% [5/41] vs 10.5% [2/19]). Lesions not associated with recurrence included enlargement of MPD dilation and secondary IPMN without MN, observed in six and two patients, respectively.

Characteristics of the two patients who developed IPMN-concomitant PDAC after surgical resection of IPMN

The two patients who developed IPMN-concomitant PDAC after surgical resection of IPMN were an 81-year-old man

and a 72-year-old man. The former patient underwent DP for BD-IPMN (invasive carcinoma) whereas the latter patient underwent PD for BD-IPMN with HGD. There was no secondary IPMN in either case. IPMN-concomitant PDAC was detected at 48 and 41 months after surgery during follow up using CT plus EUS in the 81- and 72-year-old patients, respectively.

Detection of recurrence by EUS in combination with CH-EUS

Among 33 patients followed up by CT plus EUS, 17 patients underwent 18 sessions of CH-EUS. EUS in combination with CH-EUS successfully detected enhancing MN within a dilated MPD in one patient (patient no. 13 in Table 2) and IPMN-concomitant PDAC in two patients, whereas CE-CT failed to detect all of these lesions. Although EUS did not clearly visualize the presence of a tumor, CH-EUS successfully detected an IPMN-concomitant PDAC as a hypovascular tumor in one patient (81-year-old man), enabling EUS-guided fine-needle aspiration (EUS-FNA) and leading to a final pathological diagnosis (Figs 1–3). Despite EUS not showing any changes in this patient, CH-EUS was also carried out because of an increase in serum concentration of carbohydrate antigen 19-9 during follow up. In another patient with IPMN-concomitant

PDAC (72-year-old man), both EUS and CH-EUS detected the tumor. Sizes of the two IPMN-concomitant PDAC were 8 mm (Fig. 2) and 13 mm, respectively, and the size of the enhancing MN within the dilated MPD was 9 mm, indicating the sensitivity of EUS in detecting small lesions after surgery. Both EUS and CT successfully detected the four IPMN without MN that developed during follow up.

DISCUSSION

ALTHOUGH NO CONSENSUS has yet been reached on the management of patients with IPMN after surgical resection, studies have assessed their follow-up outcomes.^{9–12} For example, an evaluation of 113 patients with IPMN who underwent surgical resection, with a

median follow up of 37 months, found that the recurrence rates in patients with invasive and non-invasive IPMN were 65.0% (26/40) and 6.8% (5/73), respectively.⁹ In addition, 94.4% (17/18) of distant metastases were observed in patients with invasive IPMN. Another study reported that the recurrence rate in patients with invasive IPMN after a median follow up of 46.4 months was 57.1%, higher than the rates in patients with other grades of IPMN and suggesting that the postoperative follow-up protocol for patients with invasive IPMN should be similar to that for patients with ordinary PDAC.¹⁰ An evaluation of surgical databases from four high-volume centers of 70 patients with IPMN-associated invasive carcinomas, with invasive components measuring ≤ 20 mm, found that the overall recurrence rate after a median 16 months was 24%, and that these

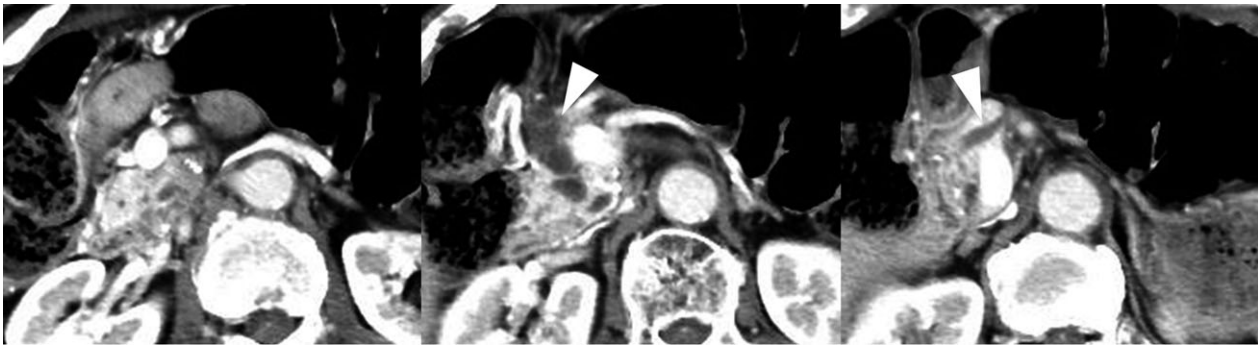


Figure 1 Computed tomography of the remnant pancreas of a patient with an intraductal papillary mucinous neoplasm and concomitant pancreatic adenocarcinoma, showing a dilated pancreatic duct (arrowheads) but no apparent solid tumor in the remnant pancreas.

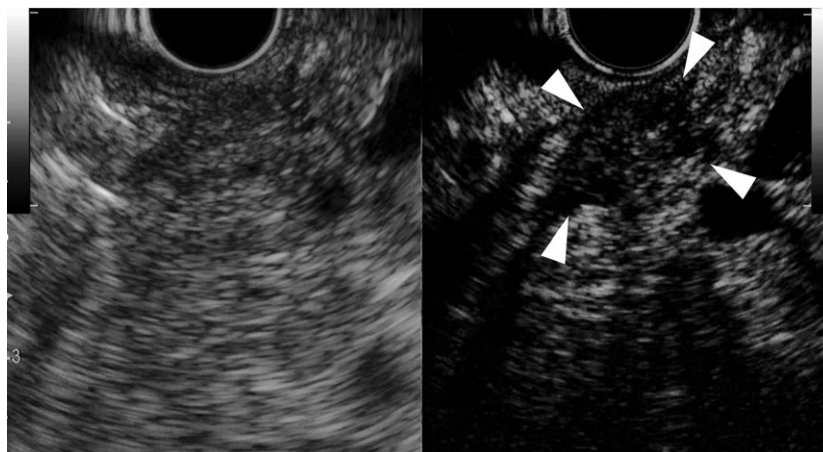


Figure 2 B-mode endoscopic ultrasonography (B-mode endoscopic ultrasonography [EUS], left image) and contrast-EUS (CH-EUS, right image) of a patient with an intraductal papillary mucinous neoplasm and concomitant pancreatic adenocarcinoma. B-mode EUS was unable to detect a solid tumor, whereas CH-EUS detected a hypovascular tumor, 8 mm in diameter (arrowheads).

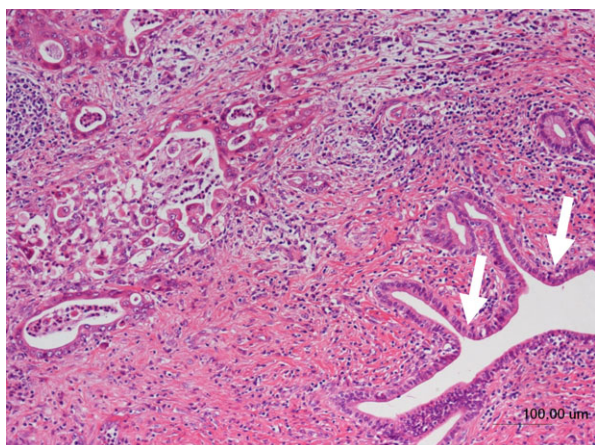


Figure 3 Histology of the tumor (hematoxylin and eosin staining). Pathological examination of the resected specimen showing a pancreatic adenocarcinoma and a normal main pancreatic duct (arrows). An intraductal papillary mucinous neoplasm was not detected close to the tumor.

recurrence patterns varied widely, being local in 35%, distant in 47%, and both in 18% of affected patients.¹¹ In agreement with these previous studies, we found that the recurrence rate was much higher in patients with invasive IPMN than in those with non-invasive IPMN. In the present study, seven of eight patients with distant metastasis were originally diagnosed with invasive IPMN. Taken together, these findings strongly suggest that patients with invasive IPMN are at significant risk of recurrence, even after surgical resection.

Most recurrences of IPMN can be pathologically classified as invasive type, with about half of these patients exhibiting distant metastasis.^{9–11,13,14} It is unclear, however, whether patients with non-invasive IPMN require the strict postoperative surveillance recommended for patients with invasive IPMN. This retrospective study showed that four (11.1%) of the 36 patients with HGD had recurrences or new lesions, ranging from IPMN without MN to IPMN-concomitant PDAC and distant metastasis, suggesting that lesions classified as HGD can give rise to invasive cancer, even after surgical resection. By contrast, the postoperative rate of recurrence or the incidence of IPMN-concomitant PDAC was much lower in patients with lesions classified as LGD than in those classified as HGD or invasive carcinoma (3.6% [2/56] vs 16.7% [13/78]). Collectively, these findings suggest that IPMN patients with HGD require strict surveillance after surgery. Similarly, of 298 patients with non-invasive IPMN, 16 (5.4%) experienced recurrences, including distant metastases, with the 5-year disease-free survival rate being significantly lower in patients with HGD

than in those with LGD.¹⁰ In addition, a recent study suggested that HGD might be a predictor of IPMN recurrence or adenocarcinoma.¹¹

Several studies showed that IPMN were accompanied by concomitant PDAC, both at the initial examination and during follow up.^{2,8,13–17} IPMN-concomitant PDAC can also arise in the remnant pancreas after IPMN resection.^{18–20} In the present study, two patients developed IPMN-concomitant PDAC, 41 and 48 months after initial surgery for BD-IPMN. Interestingly, these patients were diagnosed only by EUS in combination with CH-EUS, despite strict surveillance using both CT and EUS. These findings therefore suggest that IPMN-concomitant PDAC can arise in the remnant pancreas, even after surgical resection of IPMN.

To our knowledge, no previous study has evaluated the utility of EUS for follow up of the remnant pancreas after resection of IPMN. In our institution, pancreaticogastrostomy is routinely carried out in almost all patients undergoing PD. Because the distance between the stomach and the remnant pancreas is short, the remnant pancreas can be satisfactorily evaluated by EUS. We found that the entire remnant pancreas could also be evaluated by EUS in two patients who underwent pancreaticojejunostomy, suggesting the utility of EUS in visualizing the entire remnant pancreas. Of our 134 patients with IPMN, 33 (24.6%) were evaluated by EUS after resection. EUS in combination with CH-EUS, but not CE-CT, detected IPMN-concomitant PDAC in two patients and enhancing MN within the dilated MPD in one patient, suggesting that EUS, which detects small lesions, is a very useful diagnostic modality for surveillance after surgical resection of IPMN. Similarly, CH-EUS was reported to be useful for the diagnosis of small pancreatic tumors not detected by CE-CT.⁴ Another advantage of CH-EUS for the diagnosis of small pancreatic tumors is its efficient visualization of tumor outlines, which are uncertain when evaluated by conventional B-mode EUS.^{6,15} Visualization of pancreatic tumors by CH-EUS enables EUS-FNA, leading to final pathological diagnosis. In the present study, CH-EUS was the only modality that successfully detected an IPMN-concomitant PDAC in one patient. Magnetic resonance imaging (MRI) is advantageous for evaluating the pancreatic duct; however, it has disadvantages for detecting recurrences of distant metastasis or IPMN-concomitant PDAC compared with CT and EUS. Consequently, we did not include MRI in the follow-up surveillance after surgery for IPMN. Figure 4 shows a flow chart of the recommended surveillance of patients after surgery for IPMN based on our results. We recommend that EUS combined with CH-EUS is carried out when CT or conventional EUS shows abnormal changes or a blood test shows an increase in tumor marker concentration during follow up. Further prospective

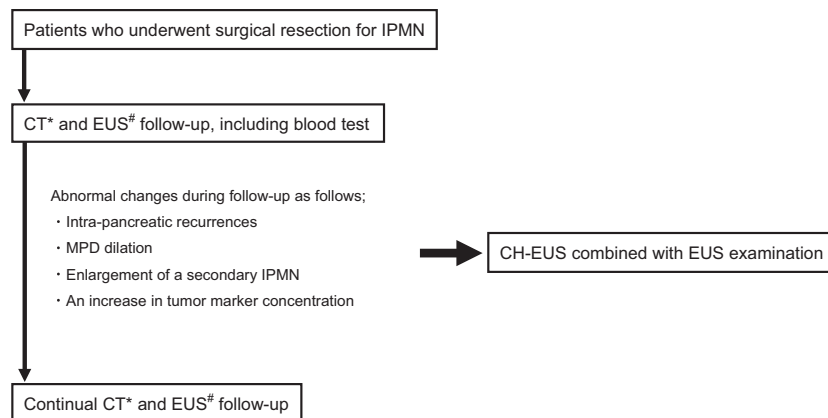


Figure 4 Flow chart of the recommended surveillance of patients after surgery for IPMN. *LGD: once yearly. HGD: twice yearly during the first year and once yearly thereafter. Invasive: every 3–4 months during the first 2 years, and twice yearly thereafter. #All patients except those who underwent total pancreatectomy; twice yearly. CH-EUS, contrast-enhanced harmonic endoscopic ultrasonography; CT, computed tomography; EUS, endoscopic ultrasonography; HGD, high-grade dysplasia; IPMN, intraductal papillary mucinous neoplasm; LGD, low-grade dysplasia; MPD, main pancreatic duct.

randomized studies of large numbers of patients are warranted to determine whether EUS follow up is superior to CT for early detection of recurrence or development of IPMN-concomitant PDAC.

This study had several limitations. First, the study was retrospective in design and all patients were not followed up by both CT plus EUS; therefore, a comparative analysis could not be carried out. Second, the possibility of selection bias cannot be excluded, as there was a significant difference in the degree of dysplasia between patients followed up by CT alone and those followed up by both CT and EUS. Third, it is unclear whether EUS can be used to screen the remnant pancreas in patients who undergo pancreaticojejunostomy, as few of these patients were included in this study. Finally, EUS was not useful for the detection of distant metastasis.

In conclusion, EUS, combined with CH-EUS may improve follow up of patients with resected IPMN, especially in terms of detecting small IPMN-concomitant PDAC or MN that develop during follow up.

CONFLICTS OF INTEREST

AUTHORS DECLARE NO conflicts of interest for this study.

REFERENCES

- 1 Tanaka M, Fernández-del Castillo C, Kamisawa T *et al*. Revisions of international consensus Fukuoka guidelines for the management of IPMN of the pancreas. *Pancreatology* 2017; **17**: 738–53.
- 2 Kamata K, Kitano M, Kudo M *et al*. Value of EUS in early detection of pancreatic ductal adenocarcinomas in patients with intraductal papillary mucinous neoplasms. *Endoscopy* 2014; **46**: 22–9.
- 3 Kamata K, Kitano M, Omoto S *et al*. Contrast-enhanced harmonic endoscopic ultrasonography for differential diagnosis of pancreatic cysts. *Endoscopy* 2016; **48**: 35–41.
- 4 Kitano M, Kudo M, Yamao K *et al*. Characterization of small solid tumors in the pancreas: the value of contrast enhanced harmonic endoscopic ultrasonography. *Am. J. Gastroenterol.* 2012; **107**: 303–10.
- 5 Tanaka M. Current roles of endoscopy in the management of intraductal papillary mucinous neoplasm of the pancreas. *Dig. Endosc.* 2015; **27**: 450–7.
- 6 Adsay NV, Fukushima N, Furukawa T *et al*. Intraductal neoplasms of the pancreas. In: Bosman FT, Hruban RH, Camero F, Theise ND (eds). *WHO Classification of Tumors of the Digestive System. WHO Classification of Tumors*, 4th edn. Lyon: IARC, 2010; 304–13.
- 7 Basturk O, Hong SM, Wood LD *et al*. A revised classification system and recommendations from the Baltimore consensus meeting for neoplastic precursor lesions in the pancreas. *Am. J. Surg. Pathol.* 2015; **39**: 1730–41.
- 8 Yogi T, Hijioka S, Imaoka H *et al*. Risk factors for postoperative recurrence of intraductal papillary mucinous neoplasm of the pancreas based on long-term follow-up study: proposals for follow-up strategies. *J. Hepatobiliary Pancreat. Sci.* 2015; **22**: 757–65.
- 9 Winter JM, Jiang W, Basturk O *et al*. Recurrence and survival after resection of small intraductal papillary mucinous neoplasm-associated carcinomas (≤ 20 -mm Invasive Component): a multi-institutional analysis. *Ann. Surg.* 2016; **263**: 793–801.
- 10 Kang MJ, Jang JY, Lee KB, Chang YR, Kwon W, Kim SW. Long-term prospective cohort study of patients undergoing

- pancreatectomy for intraductal papillary mucinous neoplasm of the pancreas: implications for postoperative surveillance. *Ann. Surg.* 2014; **260**: 356–63.
- 11 Blackham AU, Doepker MP, Centeno BA *et al.* Patterns of recurrence and long-term outcomes in patients who underwent pancreatectomy for intraductal papillary mucinous neoplasms with high grade dysplasia: implications for surveillance and future management guidelines. *HPB (Oxford)* 2017; **19**: 603–10.
 - 12 Otsuka T, Kono H, Tanabe R *et al.* Follow-up study after resection of intraductal papillary mucinous neoplasm of the pancreas; special references to the multifocal lesions and development of ductal carcinoma in the remnant pancreas. *Am. J. Surg.* 2012; **204**: 44–8.
 - 13 Uehara H, Nakaizumi A, Ishikawa O *et al.* Development of ductal carcinoma of the pancreas during follow-up of branch duct intraductal papillary mucinous neoplasm of the pancreas. *Gut* 2008; **57**: 1561–5.
 - 14 Tada M, Kawabe T, Arizumi M *et al.* Pancreatic cancer in patients with pancreatic cystic lesions: a prospective study in 197 patients. *Clin. Gastroenterol. Hepatol.* 2006; **4**: 1265–70.
 - 15 Yamaguchi K, Kanemitsu S, Hatori T *et al.* Pancreatic ductal adenocarcinoma derived from IPMN and pancreatic ductal adenocarcinoma concomitant with IPMN. *Pancreas* 2011; **40**: 571–80.
 - 16 Komori T, Ishikawa O, Ohigashi H *et al.* Invasive ductal adenocarcinoma of the remnant pancreatic body 9 years after resection of an intraductal papillary-mucinous carcinoma of the pancreatic head: a case report and comparison of DNA sequence in K-ras gene mutation. *Jpn. J. Clin. Oncol.* 2002; **32**: 146–51.
 - 17 Marchegiani G, Mino-Kenudson M, Ferrone CR *et al.* Patterns of recurrence after resection of IPMN: who, when, and how? *Ann. Surg.* 2015; **262**: 1108–14.
 - 18 Tamura K, Ohtsuka T, Ideno N *et al.* Treatment strategy for main duct intraductal papillary mucinous neoplasm of the pancreas based on the assessment of recurrence in the remnant pancreas after resection: a retrospective review. *Ann. Surg.* 2014; **259**: 360–8.
 - 19 Fusaroli P, Spada A, Mancino MG. Treatment strategy for main duct intraductal papillary mucinous neoplasm of the pancreas based on the assessment of recurrence in the remnant pancreas after resection: a retrospective review. Contrast harmonic echoscopic ultrasound improves accuracy in diagnosis of solid pancreatic masses. *Clin. Gastroenterol. Hepatol.* 2010; **8**: 629–34.
 - 20 Napoleon B, Alvarez-Sanchez MV, Gincoul R *et al.* Contrast enhanced harmonic endoscopic ultrasound in solid lesions of the pancreas: results of a pilot study. *Endoscopy* 2010; **42**: 564–70.



Endoscopic ultrasound-guided biliary drainage using a newly designed metal stent with a thin delivery system: a preclinical study in phantom and porcine models

Kosuke Minaga¹ · Masayuki Kitano² · Masahiro Itonaga² · Hajime Imai¹ · Takeshi Miyata¹ · Kentaro Yamao¹ · Takashi Tamura² · Junya Nuta² · Kenji Warigaya³ · Masatoshi Kudo¹

Received: 3 September 2017 / Accepted: 7 November 2017 / Published online: 8 December 2017
© The Japan Society of Ultrasonics in Medicine 2017

Abstract

Purpose This study was designed to evaluate the feasibility and safety of a newly designed self-expandable metal stent for endoscopic ultrasound-guided biliary drainage (EUS-BD) when it was delivered via three different stent delivery systems: a 7.5Fr delivery catheter with a bullet-shaped tip (7.5Fr-bullet), a 7Fr catheter with a bullet-shaped tip (7Fr-bullet), or a 7Fr catheter with a tee-shaped tip (7Fr-tee).

Methods This experimental study utilized a porcine model of biliary dilatation involving ten pigs. In the animal study, technical feasibility and clinical outcomes of the stent when placed with each of the delivery systems were examined. In addition, a phantom model was used to measure the resistance of these delivery systems to advancement.

Results Phantom experiments showed that, compared with 7Fr-bullet, 7Fr-tee had less resistance force to the advancement of the stent delivery system. EUS-BD was technically successful in all ten pigs. Fistulous tract dilation was necessary in 100% (2/2), 75% (3/4), and 0% (0/4) of the pigs that underwent EUS-BD using 7.5Fr-bullet, 7Fr-bullet, and 7Fr-tee, respectively. There were no procedure-related complications.

Conclusion Our newly designed metal stent may be feasible and safe for EUS-BD, particularly when delivered by 7Fr-tee, because it eliminates the need for fistulous tract dilation.

Keywords Endoscopic ultrasound · EUS-guided biliary drainage · EUS-BD · EUS-guided choledochoduodenostomy · Stent

Introduction

Endoscopic ultrasound (EUS) is increasingly being used to diagnose and treat pancreaticobiliary diseases. Notably, EUS-guided biliary drainage (EUS-BD), which was first described in 2001 [1], is now frequently used as an alternative in patients with biliary obstruction in whom standard

endoscopic retrograde cholangiopancreatography (ERCP) fails. Its potential and efficacy in this setting have drawn considerable attention in the last decade, and many articles about it have been published. In particular, it is now clear that EUS-BD has an overall technical success rate of more than 90% when performed by operators with expertise in this procedure. However, a recent review also revealed that EUS-BD had a cumulative adverse event rate that ranged from 16.5 to 23.3% [2–4]. This adverse event rate is higher than that for ERCP [5].

This higher adverse event rate of EUS-BD may be due, at least in part, to the fact that there are currently few endoscopic devices that are specifically designed for use in EUS-BD. This can result in device-related difficulties that could cause procedure-related complications. To improve this situation, it is essential to develop new stenting devices that are easy to place in EUS-BD. In particular, it is important to develop a device that eliminates the need to dilate the

✉ Masayuki Kitano
kitano@wakayama-med.ac.jp

¹ Department of Gastroenterology and Hepatology, Kindai University Faculty of Medicine, Osaka-Sayama, Japan

² Second Department of Internal Medicine, Wakayama Medical University, 811-1 Kimiidera, Wakayama 641-8509, Japan

³ Department of Human Pathology, Wakayama Medical University, Wakayama, Japan

fistulous tract. This reflects the fact that this aspect of the EUS-BD procedure is particularly technically challenging and can cause bile leakage and onset of bile peritonitis [6–8].

We hypothesized that the diameter and tip shape of the stent delivery system, along with the stent itself, may affect the technical success of stent deployment without fistulous tract dilation. Several types of covered self-expandable metal stents whose delivery systems have diameters of more than 8Fr are commercially available and used for EUS-BD. Regarding the tip shape of the stent delivery system, a bullet-shaped tip has been conventionally used. We hypothesized that a stent with a more tapered tip and a thin stent delivery system may be advantageous for easy stent placement without fistulous tract dilation. Therefore, we developed newly designed covered self-expandable metal stents with different delivery systems. The diameter of the stent delivery system was reduced to 7.5Fr or 7Fr. Two differently shaped tips were used: a conventional bullet-shaped tip and a newly designed tapered tip, i.e., tee-shaped.

In the present pilot study, we delivered these stents during EUS-BD in a porcine model of biliary dilatation with three different thin pull-back catheters that differed in terms of their diameter and/or tip shape. The feasibility and safety of the stent when placed with each of the delivery systems were examined. In particular, we looked at whether any of the delivery systems obviated the need for fistulous tract dilation. In addition, a phantom model was used to measure the resistance of these delivery systems to advancement.

Materials and methods

Stent structure

The newly designed self-expandable metal stent (Covered BileRush; Piolax Medical Devices, Inc., Yokohama, Japan) has a diameter of 6 mm and a length of 60 mm, and is made of laser-cut nitinol wire that is partially covered by

a silicone membrane to prevent bile leakage (Fig. 1a). The 5 mm proximal end of the stent is uncovered to prevent distal stent migration. The distal end is flared for 10 mm to prevent inward migration. This stent is delivered with three different types of thin pull-back delivery catheters: a 7.5Fr delivery catheter that has a conventional bullet-shaped tip (7.5Fr-bullet), a 7Fr delivery catheter that has a conventional bullet-shaped tip (7Fr-bullet), and a 7Fr delivery catheter that has a newly designed tee-shaped tip (7Fr-tee) (Fig. 1b). The tip of the stent delivery system is made of polyether block amide compounded with 40% barium sulfate. The extent of stent shortening is approximately 2%.

Evaluation of the mechanical properties of the stent delivery systems using a phantom model

We hypothesized that the diameter and tip shape of the stent delivery system may affect the trackability and pushability of the stent. This, in turn, may determine whether fistulous tract dilation is necessary in EUS-BD. To explore whether the tip shape of the delivery system affects the resistance force to advancement of the stent delivery system, we measured the resistance force when the stent delivery tip of the 7Fr-bullet and 7Fr-tee stent delivery systems is inserted by using a phantom experimental study. Briefly, a phantom model was created using a 1-mm-thick silicone plate that was fixed on a metal plate and a force gauge (STROGRAPH EII; Toyo Seiki Seisaku-sho, Ltd., Tokyo, Japan). The silicone plate was punctured with a 19-gauge needle, and a 0.025-inch guidewire (Revowave UltraHard 2; Piolax) was passed through the plate (Fig. 2). The stent delivery system was then inserted into the silicone wall through the guidewire at a speed of 50 mm/min. When the tip of the stent delivery system was advanced over the guidewire to pass the plate, the resistance force was measured. The average resistance force of three replicate measurements was calculated.

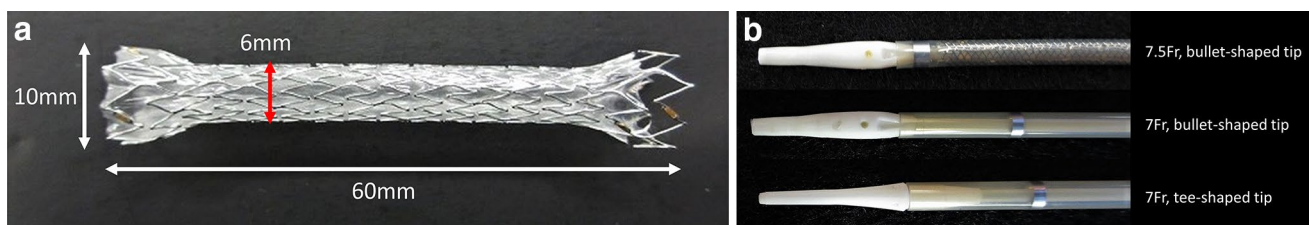


Fig. 1 Illustration of the newly designed self-expandable metal stent. **a** The expanded stent has a diameter of 6 mm and is 60 mm long. It is made from laser-cut nitinol wire and is partially covered by a silicone membrane. The proximal 5 mm of the stent is uncovered to prevent distal stent migration. The distal end is flared for 10 mm to prevent inward migration. **b** Three different types of thin pull-back delivery

catheters are used to deliver the stent: a 7.5Fr delivery catheter with a conventional bullet-shaped tip (7.5Fr-bullet) (upper), a 7Fr delivery catheter with a conventional bullet-shaped tip (7Fr-bullet) (middle), and a 7Fr delivery catheter with a newly designed tee-shaped tip (7Fr-tee) (lower). The stent delivery tip is composed of polyether block amide compounded with 40% barium sulfate

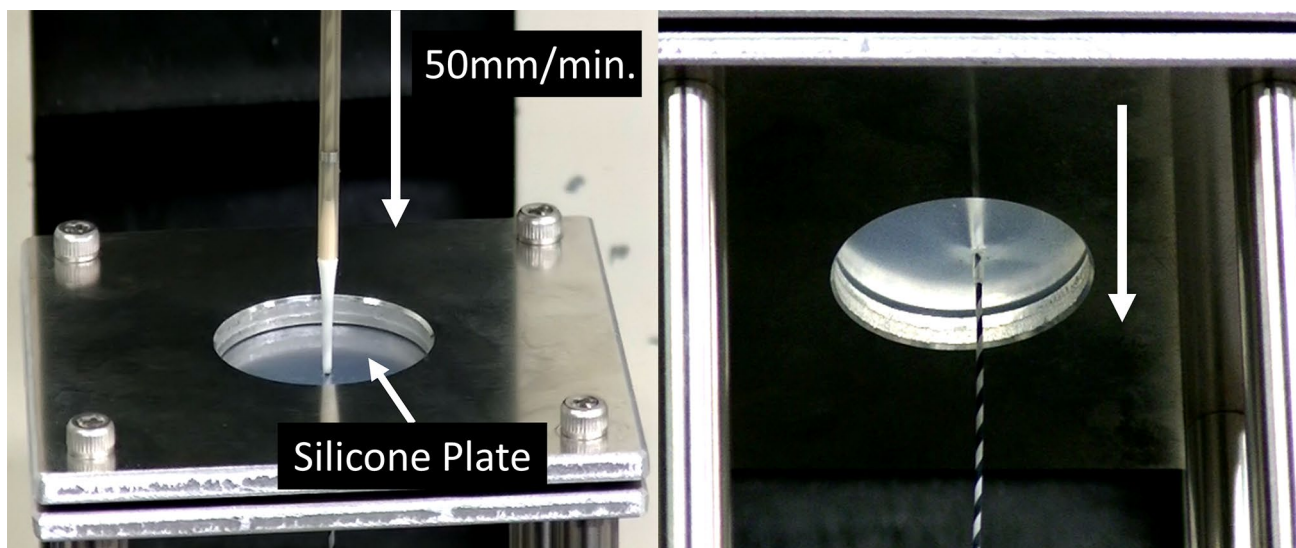


Fig. 2 The phantom machine used to measure the resistance force of the stent delivery system when its tip is inserted. The machine consists of a 1-mm-thick silicone plate that is fixed on a metal plate and a force gauge. The silicone plate is punctured with a 19-gauge needle, and a 0.025-inch guidewire is passed through the plate. Thereafter, the

stent delivery catheter is inserted into the silicone wall through the guidewire at a speed of 50 mm/min. When the tip of the stent delivery catheter is advanced over the guidewire to pass the plate, the resistance force is measured

In vivo experiments

Animal models

Ten pigs (three-way crossbred pigs; mean bodyweight, 30 kg) underwent procedures to induce biliary duct obstruction and then treatment with EUS-BD, where the newly designed stent was delivered by the three delivery systems. Approval from the Institutional Animal Care and Use Committee of our hospitals was obtained before initiating the study. The pigs were fasted from solids and allowed water during the 12 h before the procedure. They were then placed under general anesthesia and intubated endotracheally. Dilatation of the common bile duct (CBD) was followed about 6 h later by EUS-BD with the three stent delivery systems. The procedures were performed with the pigs in the supine position on a fluoroscopy table. Antibiotic agents were not administered before the endoscopic procedure. During the procedure, the heart rate, respiratory rate, oxygen saturation, and body temperature were monitored continuously. The pigs resumed their usual diet on the day after the procedure.

Induction of bile duct dilatation and the EUS-BD procedure

The experimental porcine model of biliary dilatation was created by modifying our previously established model [9]. Thus, on the morning of the endoscopic procedure, a gastroscope was inserted into the duodenal bulb. The ampulla of each pig was then ligated with multiple endoscopic clips

to induce dilatation of the CBD that mimicked obstructive jaundice (Fig. 3a). On the afternoon of the same day (about 6 h after endoscopic ligation of the ampulla), a linear-array EUS endoscope (EG-580UT; Fujifilm, Tokyo, Japan) was inserted per-orally and introduced into the duodenum. After visualizing the dilated CBD adjacent to the duodenum (Fig. 3b), the EUS endoscope was manipulated until an appropriate puncture route that avoided any intervening vessels was identified. In the pigs, the distal bile duct was strongly bent around the ampulla (Fig. 3b). We selected this bending part of the distal bile duct as the optimal puncture site because this allowed the guidewire to be easily directed toward the proximal bile duct (Fig. 3b, c). The distal CBD was punctured with a 19-gauge FNA needle (SonoTip Pro-Control; Medi-Globe, Rosenheim, Germany) under EUS guidance (Fig. 3c, Left). After the bile was aspirated, contrast medium (VISIPAQUE; Daiichi-Sankyo, Tokyo, Japan) was injected (Fig. 3c, Right) and a 0.025-inch angle-tip guidewire (Revowave UltraHard 2, Piolax) was advanced into the CBD (Fig. 3d). Thereafter, we tried to insert the newly designed thin stent delivery system via the fistula without any dilation (Fig. 3e), and the metal stent (Covered BileRush, Piolax) was deployed between the CBD and the duodenum (Fig. 3f). The 7.5Fr-bullet, 7Fr-bullet, and 7Fr-tee stent delivery systems were used in two, four, and four pigs, respectively. If the stent was not advanced via the fistula, the fistulous tract was dilated using a tapered-tip ERCP catheter (Star Tip Cannula, maximum outer sheath diameter of 5.5Fr; Olympus Medical Systems, Tokyo, Japan). The

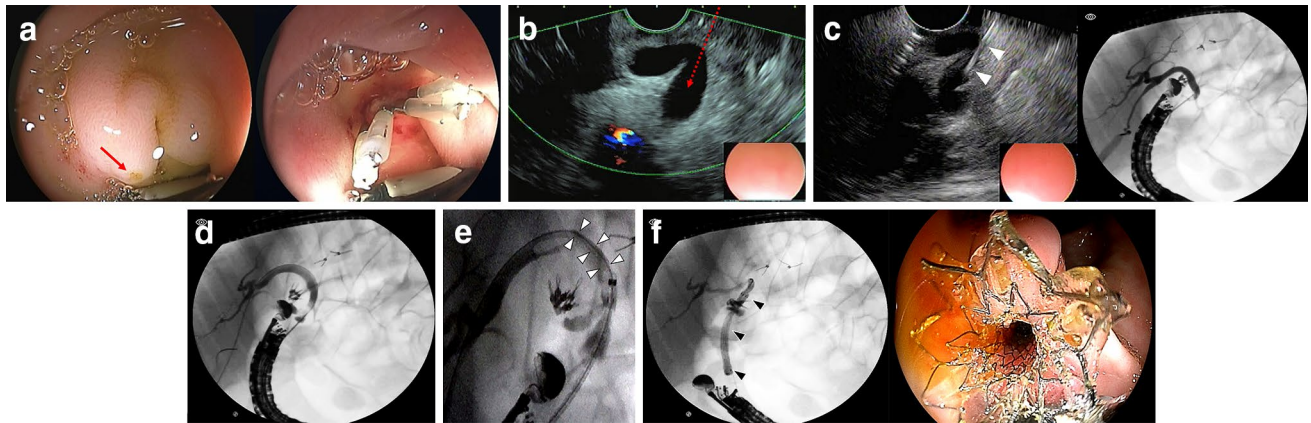


Fig. 3 The endoscopic choledochoduodenostomy procedures used with the newly designed self-expandable metal stent in a porcine model of biliary obstruction. **a** Creation of a porcine model mimicking obstructive jaundice. The ampulla (indicated by the arrow) is ligated with multiple endoscopic clips 6 h before EUS-guided biliary drainage is performed. **b** A linear-array EUS image showing the bending part of the distal common bile duct (CBD). The diameter of the CBD, as measured by EUS, is 9 mm. The red arrow indicates the estimated puncture route. **c** (Left) An EUS image showing a 19-gauge

FNA needle (arrowheads) under EUS. (Right) A fluoroscopic image showing cholangiography after puncturing the CBD. **d** A fluoroscopic image showing insertion of a guidewire. A 0.025-inch angle-tip guidewire is advanced into the CBD. **e** A fluoroscopic image showing insertion of a thin stent delivery system with a newly designed tee-shaped tip (arrow heads) into the CBD without fistulous tract dilation. **f** Fluoroscopic (left) and endoscopic (right) images of stent deployment. The newly designed stent (6 mm wide and 60 mm long) is deployed between the CBD and the duodenum

technical success and complications within 2 weeks after EUS-BD with the three types of stent delivery systems were analyzed. In the present study, all endoscopic procedures were performed by one experienced operator (M. Kitano), who has performed more than 300 EUS-guided interventions in patients. In addition, this operator is familiar with endoscopic procedures in animals [9].

Postprocedural care and autopsy

Two weeks after EUS-BD, a gastroscope was advanced into the duodenum to confirm the stent position. The pigs were then killed and dissected. The peritoneal cavity was studied for evidence of adjacent organ injury, bleeding, or peritonitis. The formation of a fistula between the CBD and the duodenum was also evaluated. Specimens from the fistulous site were collected for macroscopic and histopathological examination. The specimens were examined after being fixed in neutral buffered formalin and stained with hematoxylin and eosin and Masson's trichrome stain.

Statistical analysis

Continuous variables are expressed as mean values with ranges. The Mann–Whitney U test was used to compare continuous variables. Statistical significance was set at a p value of < 0.05 . Analyses were performed using StatMate V statistical software (ATMS, Tokyo, Japan).

Results

The phantom experimental study showed that the mean resistance force of the 7Fr-bullet and 7Fr-tee stent delivery systems to insertion of their tip was 4.3 and 1.8 N, respectively (Fig. 4).

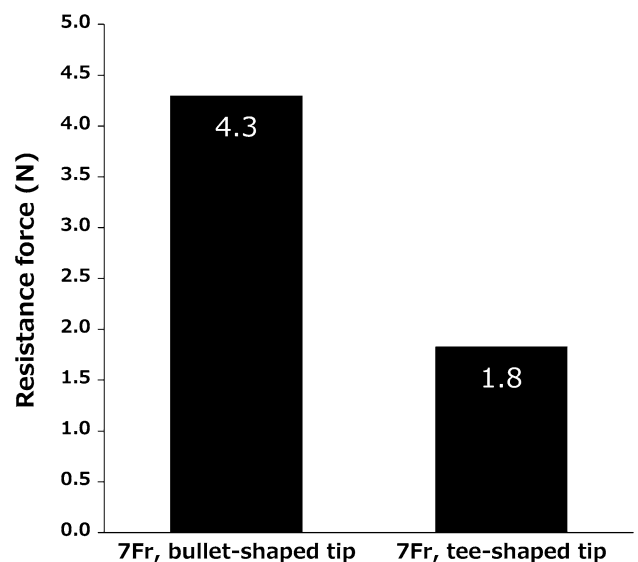


Fig. 4 Resistance force to insertion of the two stent delivery tips. For the 7Fr-bullet stent and the 7Fr-tee stent, the mean resistance force is 4.3 and 1.8 N, respectively

In the animal model, the mean CBD diameter measured on EUS at the time of puncture was 7.7 (range 4.1–9.5) mm. The mean distance and angle between the duodenum wall and the bile duct measured on EUS at the time of puncture were 8.8 (range 8.1–12.2) mm and 73 (range 70–80) degrees, respectively. In all ten pigs, EUS-BD with the newly designed stent was successful regardless of whether it was delivered using the 7.5Fr-bullet, 7Fr-bullet, or 7Fr-tee stent delivery system. The mean procedure time was 29.3 (range 16–47) min. Fistulous tract dilation was necessary in 100% (2/2), 75% (3/4), and 0% (0/4) of the pigs who received stents via the 7.5Fr-bullet, 7Fr-bullet, and 7Fr-tee stent delivery systems, respectively. Nevertheless, in the cases that required fistulous tract dilation, the stent was placed successfully by a tapered-tip thin ERCP catheter only. Bougie dilation catheters or balloon dilation catheters were not required. The mean procedure time was significantly shorter in the five pigs that underwent EUS-BD without fistulous tract dilation (21.8 min) than in the other five pigs who underwent EUS-BD with fistulous tract dilation (36.8 min; $p = 0.028$). There were no procedure-related complications during the procedure or in the 2 weeks after EUS-BD. All 10 pigs survived for 2 weeks after the procedure. They also tolerated the usual quantities of a standard diet within several hours after recovering from anesthesia. Clinically apparent adverse events were not observed during the following week. Gastroscopy performed 2 weeks after the procedure confirmed that all stents were in place

and had not migrated. At autopsy, none of the pigs showed evidence of organ injury, bleeding, or peritonitis. All pigs exhibited strong adhesion with a short band of connective tissue between the duodenum and the CBD (Fig. 5a). Moreover, the microscopic findings showed that mature fibrous tissue that exhibited re-epithelialization had grown around the adhesive sites of the CBD and the duodenum. Abscess formation or perforation was not observed (Fig. 5b).

Discussion

This pilot study showed that, in our porcine model of biliary dilatation, EUS-BD with the newly designed covered metal stent and a thin delivery system was safe and feasible. The endoscopic procedures of EUS-BD consist of three steps: (1) puncture and guidewire insertion, (2) fistulous tract dilation, and (3) stent deployment [8, 10]. The second step, i.e., fistulous tract dilation, is one of the most technically challenging aspects of EUS-BD [6–8]. Graded dilation with bougie dilators is conventionally used for this step because it seems to be safe. However, this procedure is sometimes unsuccessful. Moreover, it can lengthen the procedural time because of the need for multiple accessory changes and difficulties with the advancement of each new bougie dilator. Furthermore, accidental guidewire slipping can occur when a dilator is exchanged for another. Finally, Park et al. showed that one single factor

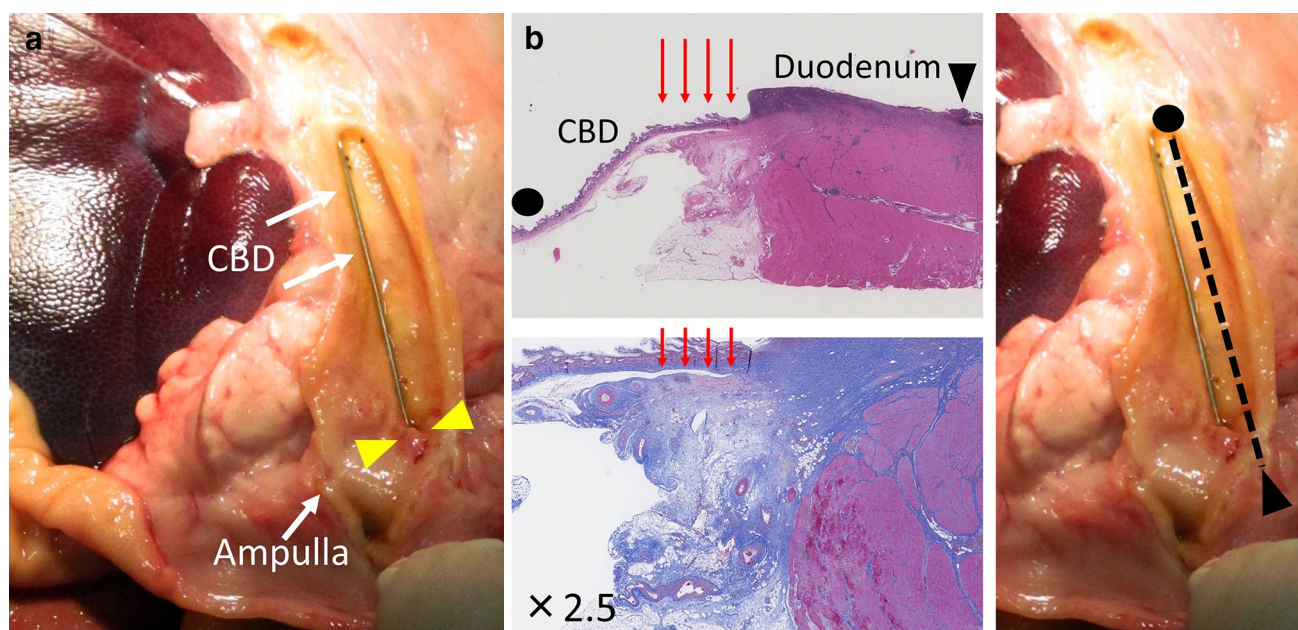


Fig. 5 Autopsy findings. **a** Macroscopic findings. Strong adhesion by a short band of connective tissue between the duodenum and the common bile duct (CBD) is observed. Arrowheads indicate the fistulous site between the lower bile duct and the duodenum. **b** Micro-

scopic findings (upper: hematoxylin and eosin stain; lower: Masson's trichrome stain). Mature fibrous tissue with re-epithelialization grows around the fistulous site of the CBD and the duodenum (red arrows). Right image showing the incision line of the CBD

independently predicted the development of postprocedural adverse events, namely, the use of a needle-knife for fistula dilation [11]. The present animal study revealed that the mean procedure time was significantly shorter in pigs that underwent EUS-BD without fistulous tract dilation than in pigs that underwent EUS-BD with fistulous tract dilation. These observations suggest that omitting the fistulous tract dilation procedure could shorten the EUS-BD procedural time, which in turn could reduce the development of procedure-related complications.

In the present study, we experimentally created three different types of catheters that would deliver the same newly designed covered metal stent. The experimental study using a phantom model showed that, compared with the 7Fr-bullet stent delivery system, the 7Fr-tee stent delivery system had less resistance force to the advancement of the delivery system. Moreover, in the porcine model of biliary dilatation, the 7Fr-tee stent delivery system allowed the stent to be deployed without having to perform fistulous tract dilation in 100% (4/4) of the pigs that were treated with this system. Therefore, this 7Fr-tee stent delivery system combines two steps of the endoscopic procedures of EUS-BD. In other words, this stent delivery system can be used for both fistulous tract dilation (step 2) and stent deployment (step 3). By contrast, the 7.5Fr-bullet and 7Fr-bullet systems required fistulous tract dilation in all (2/2) and nearly all cases (3/4), respectively. These observations suggest that a thin delivery system with a tee-shaped tip can achieve EUS-BD without fistulous dilation, and that this may be due, at least in part, to the lower resistance of the tee-shaped tip during insertion.

Stent migration is most likely to occur during and soon after the procedure and is a serious adverse event [12–14]. A recent systematic analysis of 1192 patients who underwent EUS-BD showed that stent migration occurred in 2.68% of the patients [3]. Moreover, migration of the stent into the abdominal cavity is associated with high mortality rates [15]. In the present study, none of the ten pigs with biliary dilatation that underwent EUS-BD with the newly developed stent exhibited any signs of inward or distal stent migration. These results suggest that both the laser-cut framework of the stent and the flare structure at its distal end effectively prevented stent migration. This is supported by the study of Isayama et al. on their novel covered laser-cut metal stent, which had flare and bank structures: when they used it for biliary stenting under ERCP guidance, they found that the stent had a relatively low rate of migration [16]. Moreover, we previously reported that, compared with the more commonly used braided stents, stents that bear the scaly framework that is left by laser-cutting have greater antimigration properties [17]. One advantage of the laser-cut stent is that it exhibits less shortening on deployment than the braided type. This in turn makes it easy to achieve the expected length and precise placement [16, 18]. These findings suggested that laser-cut

metal stents with a flare structure could reduce the risk of stent migration.

This study had some limitations. First, it was a preclinical study in animals that involved a small sample size and a non-comparative design. In patients with obstructive jaundice or cholangitis, the stiffness or thickness of the bile duct wall may affect the technical success of stent insertion without fistulous tract dilation. A recent study demonstrated the usefulness of EUS elastography for estimating the stiffness of the CBD [19]. Thus, when this newly designed stent is clinically applied in the near future, evaluation of bile duct stiffness via EUS elastography prior to puncture may help to decide whether fistulous tract dilation is required. Second, the follow-up time was only 2 weeks, after which the pigs were killed. This means that the long-term outcomes of stent placement, including stent dysfunction and the emergence of late adverse events, could not be evaluated. These limitations mean that it cannot yet be concluded definitively that the newly designed metal stent with a 7Fr delivery catheter with a tee-shaped end is suitable for EUS-BD. It will be necessary to compare our new stent system with other stents, particularly a novel lumen-apposing metal stent that was recently developed specifically for EUS-guided drainage and is now commercially available [20–22]. This stent allows a sealed transluminal conduit to be created between the drainage lumen and the gastrointestinal tract. Although this approach does require fistulous dilation with cautery, it may reduce the risk of bile leakage and stent migration compared with conventional tubular metal stents.

In conclusion, our newly designed metal stent with a thin delivery system was feasible and safe when used in EUS-BD in an experimental porcine model of biliary obstruction. In particular, delivering this metal stent with a thin delivery system that is equipped with a tee-shaped tip eliminated the need for fistulous tract dilation, which could help to shorten the procedure time and thereby reduce the risk of postprocedural complications. Clinical trials that confirm the feasibility and safety of this promising device are warranted.

Acknowledgements The present study was supported by grants from the Research and Development Committee Program of The Japan Society of Ultrasonics in Medicine, and the Japan Society for the Promotion of Science (Grant No. 16K09410). Piolax Medical Devices, Inc. provided stent samples. The funders did not participate in the study design; the collection, analysis, and interpretation of the data; the writing of the report; or the decision to submit the article for publication. We would also like to thank Jun Sumiya and Kyosuke Shirakawa of Piolax Medical Devices, Inc. (Yokohama, Japan) for their efforts in developing the newly designed metal stent.

Author contributions All authors helped to perform the research; Kosuke Minaga: manuscript writing and performing experiments; Masayuki Kitano: conception and design of the study, performing endoscopic procedures, and data analysis; Masahiro Itonaga, Hajime Imai, Takeshi Miyata, Kentaro Yamao, Takashi Tamura, and Junya Nuta: performing experiments and data analysis; Kenji Warigaya:

pathological assessment; Masatoshi Kudo: conception and design of the study, assistance in writing the manuscript.

Compliance with ethical standards

Conflict of interest The following authors declare no conflicts of interest: K. Minaga, M. Kitano, M. Itonaga, H. Imai, T. Miyata, K. Yamao, T. Tamura, J. Nuta, K. Warigaya, and M. Kudo.

Ethical statements All institutional and national guidelines for the care and use of laboratory animals were followed.

References

- Giovannini M, Moutardier V, Pesenti C, et al. Endoscopic ultrasound-guided bilioduodenal anastomosis: a new technique for biliary drainage. *Endoscopy*. 2001;33:898–900.
- Khan MA, Akbar A, Baron TH, et al. Endoscopic ultrasound-guided biliary drainage: a systematic review and meta-analysis. *Dig Dis Sci*. 2016;61:684–703.
- Wang K, Zhu J, Xing L, et al. Assessment of efficacy and safety of EUS-guided biliary drainage: a systematic review. *Gastrointest Endosc*. 2016;83:1218–27.
- Moole H, Bechtold ML, Forcione D, et al. A meta-analysis and systematic review: success of endoscopic ultrasound guided biliary stenting in patients with inoperable malignant biliary strictures and a failed ERCP. *Medicine*. 2017;96:e5154.
- Wang P, Li ZS, Liu F, et al. Risk factors for ERCP-related complications: a prospective multicenter study. *Am J Gastroenterol*. 2009;104:31–40.
- Kawakubo K, Isayama H, Kato H, et al. Multicenter retrospective study of endoscopic ultrasound-guided biliary drainage for malignant biliary obstruction in Japan. *J Hepatobiliary Pancreat Sci*. 2014;21:328–34.
- Vila JJ, Pérez-Miranda M, Vazquez-Sequeiros E, et al. Initial experience with EUS-guided cholangiopancreatography for biliary and pancreatic duct drainage: a Spanish national survey. *Gastrointest Endosc*. 2012;76:1133–41.
- Hara K, Yamao K, Mizuno N, et al. Endoscopic ultrasonography-guided biliary drainage: who, when, which, and how? *World J Gastroenterol*. 2016;22:1297–303.
- Minaga K, Kitano M, Gon C, et al. Endoscopic ultrasonography-guided choledochoduodenostomy using a newly designed laser-cut metal stent: feasibility study in a porcine model. *Dig Endosc*. 2017;29:211–7.
- Minaga K, Kitano M. Recent advances in endoscopic ultrasound-guided biliary drainage. *Dig Endosc*. 2017. <https://doi.org/10.1111/den.12910>.
- Park DH, Jang JW, Lee SS, et al. EUS-guided biliary drainage with transluminal stenting after failed ERCP: predictors of adverse events and long-term results. *Gastrointest Endosc*. 2011;74:1276–84.
- Martins FP, Rossini LGB, Ferrari AP. Migration of a covered metallic stent following endoscopic ultrasound-guided hepaticogastrostomy. *Endoscopy*. 2010;42:E126–7.
- Okuno N, Hara K, Mizuno N, et al. Stent migration into the peritoneal cavity following endoscopic ultrasound-guided hepaticogastrostomy. *Endoscopy*. 2015;47:E311.
- Minaga K, Kitano M, Yamashita Y, et al. Stent migration into the abdominal cavity after EUS-guided hepaticogastrostomy. *Gastrointest Endosc*. 2017;85:263–4.
- Lakhtakia S. Complications of diagnostic and therapeutic endoscopic ultrasound. *Best Pract Res Clin Gastroenterol*. 2016;30:807–23.
- Isayama H, Kawakubo K, Nakai Y, et al. A novel, fully covered laser-cut nitinol stent with antimigration properties for nonresectable distal malignant biliary obstruction: a multicenter feasibility study. *Gut Liver*. 2013;7:725–30.
- Minaga K, Kitano M, Imai H, et al. Evaluation of anti-migration properties of biliary covered self-expandable metal stents. *World J Gastroenterol*. 2016;22:6917–24.
- Itoi T, Isayama H, Sofuni A, et al. Stent selection and tips on placement technique of EUS-guided biliary drainage: transduodenal and transgastric stenting. *J Hepatobiliary Pancreat Sci*. 2011;18:664–72.
- Rustemovic N, Cukovic-Cavka S, Opacic M, et al. Endoscopic ultrasound elastography as a method for screening the patients with suspected primary sclerosing cholangitis. *Eur J Gastroenterol Hepatol*. 2010;22:748–53.
- Itoi T, Binmoeller KF, Shah J, et al. Clinical evaluation of a novel lumen-apposing metal stent for endosonography-guided pancreatic pseudocyst and gallbladder drainage (with videos). *Gastrointest Endosc*. 2012;75:870–6.
- Walter D, Teoh AY, Itoi T, et al. EUS-guided gall bladder drainage with a lumen-apposing metal stent: a prospective long-term evaluation. *Gut*. 2016;65:6–8.
- Kunda R, Pérez-Miranda M, Will U, et al. EUS-guided choledochoduodenostomy for malignant distal biliary obstruction using a lumen-apposing fully covered metal stent after failed ERCP. *Surg Endosc*. 2016;30:5002–8.

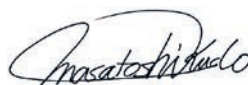
Editorial

Ramucirumab as Second-Line Systemic Therapy in Hepatocellular Carcinoma

Masatoshi Kudo

Department of Gastroenterology and Hepatology, Kindai University Faculty of Medicine, Osaka-Sayama, Japan

Prof. M. Kudo

Editor *Liver Cancer***Introduction**

Ramucirumab, a molecular targeted agent, is a recombinant human IgG1 monoclonal antibody directed against vascular endothelial growth factor receptor 2 (VEGFR-2) that plays an important role in vascular endothelial growth factor (VEGF)-induced tumor angiogenesis. It inhibits VEGFR-2 activation by blocking its binding to VEGF-A, VEGF-C, and VEGF-D, thereby inhibiting endothelial growth, migration, and survival and exerting antitumor effects via inhibition of tumor angiogenesis. Ramucirumab is currently indicated for unresectable advanced/recurrent gastric cancer, colorectal cancer, and non-small-cell lung cancer and is used in routine clinical practice. A randomized phase III trial (REACH-2) investigated ramucirumab as second-line treatment following first-line sorafenib therapy for advanced hepatocellular carcinoma (HCC) in patients with an alpha-fetoprotein (AFP) level ≥ 400 ng/mL, and results demonstrating the superiority of ramucirumab over placebo in overall survival (OS) were reported at the American Society of Clinical Oncology (ASCO) annual meeting in June 2018. This article outlines the results of the REACH-2 trial and previous clinical trials of ramucirumab (REACH).

The REACH Trial*Trial Design of REACH*

Before discussing the REACH-2 trial, a preceding trial (the REACH trial) needs to be described. The REACH trial, like the REACH-2 trial, is a randomized phase III trial investigating ramucirumab as second-line treatment following first-line therapy with sorafenib in

Prof. Masatoshi Kudo
Department of Gastroenterology and Hepatology
Kindai University Faculty of Medicine
377-2 Ohno-Higashi, Osaka-Sayama 589-8511 (Japan)
E-Mail m-kudo@med.kindai.ac.jp

patients with advanced HCC; 146 centers across 26 countries participated in the trial [1]. The inclusion criteria for the REACH trial included history of sorafenib therapy, Barcelona Clinic Liver Cancer (BCLC) stage B/C, Child-Pugh class A, and Eastern Cooperative Oncology Group performance status (ECOG PS) score 0 or 1. Patients were stratified by geographic region (North America, South America, Europe, and Eastern Asia) as well as underlying hepatic disease (infection with hepatitis B virus, hepatitis C virus, and others) and randomly allocated to either the ramucirumab group or the placebo group in a 1:1 ratio. The primary endpoint was OS, and the secondary endpoints were progression-free survival (PFS), time to progression (TTP), objective response rate (ORR), and safety. In the REACH trial, 565 patients were randomly allocated to the ramucirumab group (283 patients) or the placebo group (282 patients) between November 4, 2010 and April 18, 2013; patient characteristics were not markedly different between the two groups. Patients received ramucirumab (8 mg/kg) intravenously on day 1 of a 14-day cycle (ClinicalTrials.gov NCT01140347).

Results of the REACH Trial

The primary endpoint, OS, in the ramucirumab group was 9.2 months (95% CI 8.0–10.6) while that in the placebo group was 7.6 months (95% CI 6.0–9.3); the difference was not significant (HR = 0.87, 95% CI 0.72–1.05, $p = 0.14$). In contrast, when a subgroup of patients with a baseline AFP level ≥ 400 ng/mL ($n = 250$) was analyzed, OS in the ramucirumab group (119 patients) was 7.8 months (95% CI 5.8–9.3) while that in the placebo group (131 patients) was 4.2 months (95% CI 3.7–4.8), showing significant improvement of OS by ramucirumab (HR = 0.67, 95% CI 0.51–0.90, $p = 0.006$). Meanwhile, in a subgroup of patients with a baseline AFP level < 400 ng/mL ($n = 310$), analysis showed that OS in the ramucirumab group (160 patients) was 10.1 months (95% CI 8.7–12.3) while that in the placebo group (150 patients) was 11.8 months (95% CI 9.9–13.1), showing no significant difference between the groups (HR = 1.09, 95% CI 0.84–1.43, $p = 0.51$).

Although the difference in OS was not statistically significant, the difference in PFS was significant between the two groups (HR = 0.63, 95% CI 0.52–0.75, $p < 0.0001$): 2.8 months (95% CI 2.7–3.9) in the ramucirumab group vs. 2.1 months (95% CI 1.6–2.7) in the placebo group. A significant difference in TTP was also found (HR = 0.59, 95% CI 0.49–0.72, $p < 0.0001$): 3.5 months (95% CI 2.8–4.5) in the ramucirumab group vs. 2.6 months (95% CI 1.6–2.8) in the placebo group. ORR was 7% (95% CI 4.6–10.7) in the ramucirumab group, with objective response achieved by 20 patients (1 with complete response [CR] and 19 with partial response [PR]) and $< 1\%$ (95% CI 0.2–2.5) in the placebo group, with 2 patients achieving objective response (none with CR and 2 with PR), with significant intergroup difference ($p < 0.0001$). Grade ≥ 3 severe adverse events occurring in $\geq 5\%$ of patients were ascites (5% in the ramucirumab group vs. 4% in the placebo group), hypertension (12 vs. 4%), asthma (5 vs. 2%), progression of malignant neoplasm (6 vs. 4%), elevated aspartate aminotransferase level (5 vs. 8%), thrombocytopenia (5 vs. 1%), hyperbilirubinemia (1 vs. 5%), and elevated bilirubin level (2 vs. 5%).

Analysis of the REACH Subgroups

The results of the Japanese subgroup analysis of the REACH trial were reported by Kudo et al. [2]. Out of the 565 subjects in the REACH trial, 93 were Japanese, and among this population, OS differed significantly between the ramucirumab group (45 patients, 12.9 months) and the placebo group (48 patients, 8.0 months) (HR = 0.621, 95% CI 0.391–0.986, $p = 0.0416$). PFS was significantly longer in the ramucirumab group (4.1 months) than in the placebo group (1.7 months) (HR = 0.449, 95% CI 0.285–0.706, $p = 0.0004$). ORR was 11% in the ramucirumab group (no patient with CR, 5 with PR), but 2% in the placebo group (no patient with CR, 1 with PR); the difference was not significant ($p = 0.0817$) due to the

small number of cases. Disease control rate (DCR) differed significantly ($p = 0.0462$) between the ramucirumab group (67%; no patient with CR, 5 with PR, and 25 with stable disease [SD]) and the placebo group (46%; no patient with CR, 1 with PR, and 21 with SD). There was no marked difference in therapy received after the REACH trial between the two groups. More adverse events were observed in the ramucirumab group than in the placebo group; grade ≥ 3 severe adverse events occurring in $\geq 5\%$ of patients were ascites (7% in the ramucirumab group vs. 2% in the placebo group), hypertension (7 vs. 2%), and cholangitis (7 vs. 0%), suggesting sufficient tolerability of ramucirumab therapy in the Japanese population.

In Japanese patients with a baseline AFP level ≥ 400 ng/mL (20 and 22 patients in the ramucirumab group and the placebo group, respectively), OS was significantly different between the ramucirumab group (12.9 months) and the placebo group (4.3 months) (HR = 0.464, 95% CI 0.232–0.926, $p = 0.0263$). Ramucirumab therapy prolonged OS by 8.6 months in patients with a baseline AFP level ≥ 400 ng/mL. Meanwhile, in patients with a baseline AFP level < 400 ng/mL (25 and 26 patients in the ramucirumab group and the placebo group, respectively), the difference in OS between the former (12.9 months) and the latter group (12.4 months) was not significant (HR = 0.738, 95% CI 0.391–1.394, $p = 0.3492$).

As mentioned earlier, significant differences in OS between the ramucirumab group and the placebo group were found in the subgroup with an AFP level ≥ 400 ng/mL in the study population of the REACH trial and in the Japanese subgroup with an AFP level ≥ 400 ng/mL. In addition, Park et al. [3] conducted a subgroup analysis of East Asian and non-East Asian populations. OS was prolonged by 3.4 months in the ramucirumab group (7.8 months) compared with the placebo group (4.2 months) in the East Asian population in patients with an AFP level ≥ 400 ng/mL, although the difference was not significant (HR = 0.749, 95% CI 0.519–1.082, $p = 0.1213$). Conversely, in patients with an AFP level ≥ 400 ng/mL, OS was significantly improved in the ramucirumab group (8.2 months) compared with the placebo group (4.5 months) in the non-East Asian population (HR = 0.579, 95% CI 0.371–0.904, $p = 0.0149$). In patients with an AFP level < 400 ng/mL, OS was not significantly different between the two groups, and no elongation of OS by ramucirumab therapy was observed in either population. Chau et al. [4] reported that the percent AFP increase was significantly lower and that decreases in AFP level and the percent tumor reduction were larger in the ramucirumab group than the placebo group: AFP progression and time to radiographic progression, which correlated with each other, were shorter in the ramucirumab group than in the placebo group.

Summary of the REACH Trial

Unfortunately, the REACH trial did not meet the primary endpoint in prolonging OS, although it showed no major safety issues. PFS, TTP, and ORR were significantly better in the ramucirumab group than in the placebo group. In patients with a baseline AFP level ≥ 400 ng/mL, ramucirumab significantly improved OS, and several subgroup analyses confirmed the good outcome in this subgroup of patients. Thus, the REACH-2 trial, focusing on patients with a baseline AFP level ≥ 400 ng/mL, was conducted.

The REACH-2 Trial

Trial Design of REACH-2

The REACH-2 trial, like the REACH trial, is a randomized phase III trial investigating ramucirumab as second-line treatment following first-line sorafenib therapy in patients with advanced HCC; 131 centers across 20 countries participated in the trial. Based on the

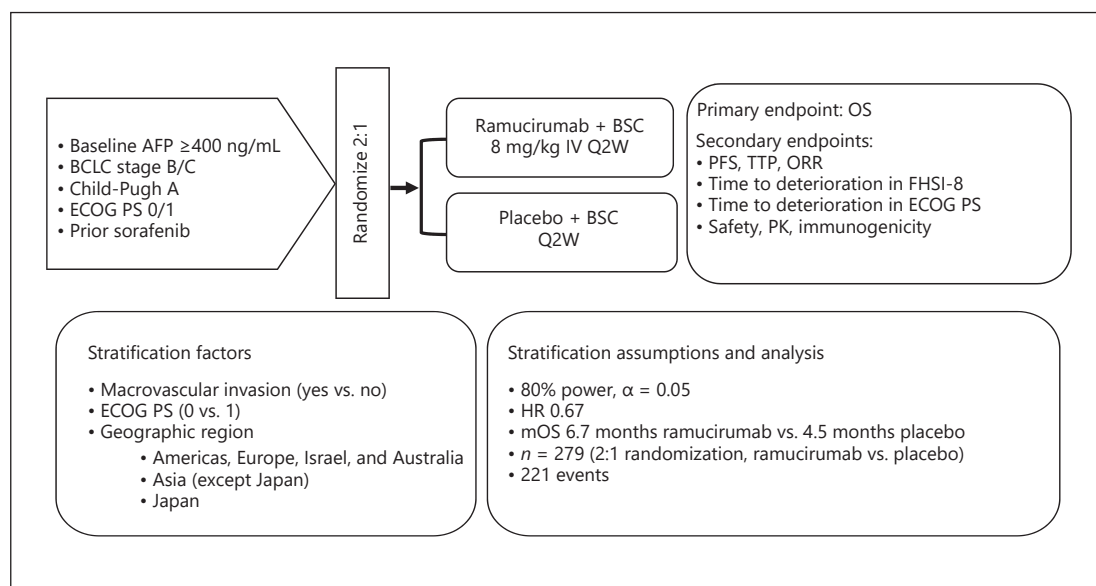


Fig. 1. Study design. ClinicalTrials.gov NCT02435433. Cited and modified from Zhu et al. [5]. AFP, alpha-fetoprotein; BCLC, Barcelona Clinic Liver Cancer; BSC, best supportive care; ECOG PS, Eastern Cooperative Oncology Group performance status; FHSI-8, Functional Assessment of Cancer Therapy Hepatobiliary Symptom Index-8; IV, intravenous; mOS, median overall survival; ORR, objective response rate; OS, overall survival; PFS, progression-free survival; PK, pharmacokinetics; Q2W, every 2 weeks; TTP, time to progression.

findings of the REACH trial, the new criterion of a baseline AFP level ≥ 400 ng/mL was added to the initial inclusion criteria of the REACH trial, including history of sorafenib therapy, BCLC stage B/C, Child-Pugh class A, and ECOG PS score 0 or 1. A new stratification factor, macrovascular invasion, was also added, and patients were also stratified by geographic region (region 1 comprising North America, South America, Europe, Israel, and Australia, region 2 comprising Asian countries except Japan, and region 3 comprising Japan). Patients were stratified by ECOG PS score (0 or 1), but not by underlying liver disease (infection with hepatitis B virus, hepatitis C virus, and others), and were randomly allocated to either the ramucirumab group or the placebo group in a 2:1 ratio. The required number of 279 cases was calculated using the OS of 4.5 months and 6.7 months in the placebo group and the ramucirumab group (HR 0.67), respectively, detection power of 80%, and $\alpha = 0.05$ (two-sided). The primary endpoint was OS, and the secondary endpoints were PFS, TTP, ORR, safety, and pharmacokinetics. A total of 292 patients were randomly allocated to the ramucirumab group (197 patients) or the placebo group (95 patients). There were imbalances in favor of the placebo group: the median baseline AFP level was 3,920 ng/mL in the ramucirumab group and 2,741 ng/mL in the placebo group, and more patients had advanced HCC in the former than in the latter group. As with the REACH trial, patients received ramucirumab (8 mg/kg) intravenously on day 1 of a 14-day cycle (ClinicalTrials.gov NCT02435433) (Fig. 1).

Results of the REACH-2 Trial

The results of the REACH-2 trial were reported at the ASCO annual meeting in June 2018 [5]. OS was 8.5 months in the ramucirumab group and 7.3 months in the placebo group; the difference was significant (HR = 0.710, 95% CI 0.531–0.949, $p = 0.0199$) (Table 1). Ramucirumab therapy decreased the mortality rate by 29%. In all subgroups except for females, OS

Table 1. Results of the REACH-2 trial

	Ramucirumab (n = 197)	Placebo (n = 95)	HR	p value
Median overall survival	8.5 months	7.3 months	0.710	0.0199
Median progression-free survival	2.8 months	1.6 months	0.452	0.0001
Objective response rate	4.6%	1.1%	–	0.1967
Relative dose intensity	97.9%	99.8%	–	–
Discontinuation due to TEAE	10.7%	3.2%	–	–
Dose adjustment due to AE	34.5%	13.7%	–	–

Cited and modified from Zhu et al. [5]. AE, adverse event; TEAE, treatment-emergent adverse event.

was longer in patients who received ramucirumab than in those who received placebo, particularly in men, those with extrahepatic metastases, and those without vascular invasion.

PFS was 2.8 months in the ramucirumab group and 1.6 months in the placebo group; the difference was significant (HR = 0.452, 95% CI 0.339–0.603, $p < 0.0001$). Ramucirumab-treated patients had favorable PFS in all subgroups. ORR was 4.6% (95% CI 1.7–7.5) with no CR case and 9 PR cases in the ramucirumab group, and 1.1% (95% CI 0.0–3.1) with no CR case and 1 PR case in the placebo group; the difference was not significant ($p < 0.1697$) due to the small number of cases. DCR was significantly better in the ramucirumab group than in the placebo group ($p = 0.0006$): 59.9% (118 cases comprising 0 CR, 9 PR, and 109 SD cases) in the former group and 38.9% (37 cases comprising no CR, 1 PR, and 36 SD cases) in the latter group.

The median dose exposure in the ramucirumab group was 6 (range 3–13) cycles, while that in the placebo group was 4 (range 3–6) cycles. The relative dose intensity in the former was 97.7% while that in the latter was 99.8%, indicating that ramucirumab therapy was uninterrupted in almost all cases. Ramucirumab targets a single molecule (VEGFR-2) and is likely to have fewer adverse events and favorable tolerability. The rates of study drug discontinuation due to adverse events were 10.7 and 3.2% in the ramucirumab group and the placebo group, respectively, and those of dose modification were 34.5 and 13.7%, respectively. Grade ≥ 3 adverse events occurring in $\geq 5\%$ of patients were hypertension (12.7% in the ramucirumab group vs. 5.3% in the placebo group), bleeding (5.1 vs. 3.2%), and liver damage (18.3 vs. 15.8%).

Interpretation of REACH-2 Trial Results

REACH-2, which reexamined ramucirumab in patients with a baseline AFP level ≥ 400 ng/mL based on the results of the preceding REACH, was a positive study confirming significantly longer OS in ramucirumab- than in placebo-treated patients. PFS and DCR were also significantly better, indicating the drug's potency. The results regarding adverse events were similar to those shown in ramucirumab monotherapy for other indications, suggesting good tolerability in these patients. REACH-2 is an excellent trial because it is the first prospective randomized controlled biomarker-driven trial with positive outcomes.

Kaplan-Meier survival curves showed a significant difference in survival rate between the ramucirumab group (24.5%) and the placebo group (11.3%) at 18 months ($p = 0.0187$), but not at 12 months. This can be explained by the imbalance between the two groups regarding the baseline AFP level (Table 2) and the proportion of BCLC stage C. Since both were higher in the ramucirumab group than in the placebo group, the effect of ramucirumab was not apparent until the later period. Furthermore, patients with a baseline AFP

Table 2. Comparison between REACH (AFP \geq 400 ng/mL), REACH-2, and pooled REACH-2/REACH (AFP \geq 400 ng/mL)

	REACH (n = 250)		REACH-2 (n = 292)		Pooled REACH-2/REACH (n = 542)	
	ramucirumab	placebo	ramucirumab	placebo	ramucirumab	placebo
mOS, months	7.8	4.2	8.5	7.3	8.1	5.0
HR (95% CI)	0.674 (0.508–0.895)		0.710 (0.531–0.949)		0.694 (0.571–0.842)	
p value	0.0059		0.0199		0.0002	
mAFP, ng/mL	N/A	N/A	3,920	2,741	4,104.6	4,047.5

AFP, alpha-fetoprotein; mAFP, median alpha-fetoprotein; mOS, median overall survival; N/A, not available.

level \geq 400 ng/mL, which is associated with poor prognosis, might have died in the placebo group without having received post-progression treatment. Selection of trial subjects using the level of a biomarker (in this instance, AFP) contributed to the positive outcomes despite an enormously small number of patients ($n = 292$) for a clinical trial of a second-line agent.

Comparison of the results of the placebo group with a baseline AFP level \geq 400 ng/mL showed that OS was 7.3 months in the REACH-2 trial, which was longer than the 4.2 months in patients with an AFP level \geq 400 ng/mL in the REACH trial. This can be explained by the imbalance in patient characteristics regarding baseline AFP level mentioned earlier. The AFP value in the placebo arm (not presented anywhere) in the REACH trial (AFP \geq 400 ng/mL) must have been much higher than that in the placebo arms of REACH-2 (2,741 ng/mL) when considering the pooled data of REACH (\geq 400 ng/mL) plus REACH-2 data (4,047.5 ng/mL) since the AFP value in the placebo arm in REACH-2 was too low as compared with that in the pooled data (Table 2). For the same reason, the HR for OS was slightly lower in the REACH-2 trial (0.67) than in patients with an AFP level \geq 400 ng/mL in the REACH trial (0.71).

Analysis of the REACH-REACH-2 Pooled Population

The results of the analysis of 542 patients comprising 292 subjects of the REACH-2 trial and 250 subjects with an AFP level \geq 400 ng/mL in the REACH trial were also reported at ASCO 2018. More precisely, OS was 3.1 months longer in the ramucirumab group (8.1 months) than in the placebo group (5.0 months); this difference was statistically significant (HR = 0.694, 95% CI 0.571–0.842, $p = 0.0002$) (Table 2). The AFP was well balanced in both arms in these pooled data (4,104.6 ng/mL in the ramucirumab arm and 4,047.5 ng/mL in the placebo arm).

Future Prospects of Ramucirumab in HCC Treatment

Based on the results of REACH-2, ramucirumab will be indicated for advanced HCC as second-line treatment after sorafenib failure when the baseline AFP level is \geq 400 ng/mL. Approval of ramucirumab is awaited as it is likely to be beneficial in HCC patients with elevated AFP level who progressed on sorafenib or even on lenvatinib, and especially in patients intolerant to sorafenib who are not candidates for regorafenib.

Disclosure Statement

Masatoshi Kudo received lecture fees from Bayer, Eisai, MSD, and Ajinomoto, research grants from Chugai, Otsuka, Takeda, Taiho, Sumitomo Dainippon, Daiichi Sankyo, MSD, Eisai, Bayer, AbbVie, Medico's Hirata, Astellas Pharma, and Bristol-Myers Squibb, and advisory consulting fees from Kowa, MSD, Bristol-Myers Squibb, Bayer, Chugai, Taiho, Eisai, and Ono Pharmaceutical.

References

- 1 Zhu AX, Park JO, Ryoo BY, Yen CJ, Poon R, Pastorelli D, et al; REACH Trial Investigators. Ramucirumab versus placebo as second-line treatment in patients with advanced hepatocellular carcinoma following first-line therapy with sorafenib (REACH): a randomised, double-blind, multicentre, phase 3 trial. *Lancet Oncol*. 2015 Jul;16(7):859–70.
- 2 Kudo M, Hatano E, Ohkawa S, Fujii H, Masumoto A, Furuse J, et al. Ramucirumab as second-line treatment in patients with advanced hepatocellular carcinoma: Japanese subgroup analysis of the REACH trial. *J Gastroenterol*. 2017 Apr;52(4):494–503.
- 3 Park JO, Ryoo BY, Yen CJ, Kudo M, Yang L, Abada PB, et al. Second-line ramucirumab therapy for advanced hepatocellular carcinoma (REACH): an East Asian and non-East Asian subgroup analysis. *Oncotarget*. 2016 Nov;7(46):75482–91.
- 4 Chau I, Park JO, Ryoo BY, Yen CJ, Poon R, Pastorelli D, et al. Alpha-fetoprotein kinetics in patients with hepatocellular carcinoma receiving ramucirumab or placebo: an analysis of the phase 3 REACH study. *Br J Cancer*. 2018 Jul;119(1):19–26.
- 5 Zhu AX, Kang YK, Yen CJ, Finn RS, Galle PR, Llovet JM, et al: REACH-2: a randomized, double-blind, placebo-controlled phase 3 study of ramucirumab versus placebo as second-line treatment in patients with advanced hepatocellular carcinoma (HCC) and elevated baseline alpha-fetoprotein (AFP) following first-line sorafenib. *J Clin Oncol*. 2018(suppl):abstract 4003.

Review

Systemic Therapy for Hepatocellular Carcinoma: Latest Advances

Masatoshi Kudo

Department of Gastroenterology and Hepatology, Faculty of Medicine, Kindai University, 337-2 Ohno-Higashi, Osaka-Sayama, Osaka 589-8511, Japan; m-kudo@med.kindai.ac.jp; Tel.: +81-72-366-0221; Fax: +81-72-367-2880

Received: 2 October 2018; Accepted: 25 October 2018; Published: 30 October 2018



Abstract: Systemic therapy for hepatocellular carcinoma (HCC) has changed drastically since the introduction of the molecular targeted agent sorafenib in 2007. Although sorafenib expanded the treatment options for extrahepatic spread (EHS) and vascular invasion, making long-term survival of patients with advanced disease achievable to a certain extent, new molecular-targeted agents are being developed as alternatives to sorafenib due to shortcomings such as its low response rate and high toxicity. Every single one of the many drugs developed during the 10-year period from 2007 to 2016 was a failure. However, during the two-year period from 2017 through 2018, four drugs—regorafenib, lenvatinib, cabozantinib, and ramucirumab—emerged successfully from clinical trials in quick succession and became available for clinical use. The efficacy of combination therapy with transcatheter arterial chemoembolization (TACE) plus sorafenib was also first demonstrated in 2018. Recently, immune checkpoint inhibitors have been applied to HCC treatment and many phase III clinical trials are ongoing, not only on monotherapy with nivolumab, pembrolizumab, and tislelizumab, but also on combination therapy with checkpoint inhibitors, programmed death-1 (PD-1) or PD-ligand 1 (PD-L1) antibody plus a molecular targeted agent (bevacizumab) or the cytotoxic T-lymphocyte-associated antigen 4 (CTLA-4) antibody, tremelimumab. These combination therapies have shown higher response rates than PD-1/PD-L1 monotherapy alone, suggesting a synergistic effect by combination therapy in early phases; therefore, further results are eagerly awaited.

Keywords: hepatocellular carcinoma; systemic therapy; molecular targeted therapy; immune checkpoint inhibitor

1. Introduction

Systemic therapy for hepatocellular carcinoma (HCC) has changed drastically since the introduction of the molecular targeted agent, sorafenib in 2007. Although sorafenib expanded the treatment options for extrahepatic spread (EHS) and vascular invasion, making long-term survival of patients with advanced disease achievable to a certain extent, new molecular targeted agents have been attempted to develop as alternatives to sorafenib due to shortcomings such as its low response rate and high toxicity. Every single one of the many drugs developed during the 10-year period from 2007 to 2016 was a failure [1]. However, during the two-year period from 2017 through 2018, four drugs—regorafenib, lenvatinib, cabozantinib, and ramucirumab—emerged successfully from clinical trials in quick succession and became available for clinical use. The efficacy of combination therapy with transcatheter arterial chemoembolization (TACE) plus sorafenib was also first demonstrated in 2018 [2].

This review describes the current landscape of molecular targeted therapy for HCC, challenges that remain to be solved, and potential future developments.

2. Molecular Targeted Agents

2.1. Sorafenib

Sorafenib is an oral kinase inhibitor that exerts its antitumor effects by suppressing tumor proliferation through inhibition of serine/threonine kinases of *C-Raf*, wild-type *B-Raf*, and mutant *B-Raf*^{V600E}, which are components of the Raf/MEK/ERK pathway (MAP kinase pathway) downstream of vascular endothelial growth factor receptor (VEGFR), platelet-derived growth factor receptor (PDGFR), and epithelial growth factor receptor (EGFR), as well as by suppressing angiogenesis through inhibition of tyrosine kinases such as VEGFR1, VEGFR2, VEGFR3, PDGFR β , RET, and FLT-3 (fms-related tyrosine kinase-3) [3,4]. Sorafenib was shown to significantly prolong overall survival (OS) over placebo in two large trials (the SHARP trial and Asia-Pacific trial) [1,5] and has consequently become the standard therapy for advanced HCC.

2.2. Current Landscape of Molecular Targeted Drug Development for HCC

Several clinical trials of new molecular targeted drugs have been conducted to date [1]. The trials can be broadly classified into four categories: (1) adjuvant therapy after curative therapy, (2) combination therapy with TACE, (3) first-line therapy for advanced HCC, and (4) second-line therapy for advanced HCC. Results of phase III trials are described below.

2.2.1. Prevention of Recurrence After Curative Therapy (Adjuvant Therapy)

Three phase III trials, one comparing vitamin K2 with placebo as adjuvant chemotherapy after radiofrequency ablation or resection [6], one comparing sorafenib with placebo (STORM trial) [7], one comparing peretinoin with placebo (NIK333 trial) [8], and one comparing ablation plus lyso-thermosensitive liposomal doxorubicin [9] have been conducted to date, but all of them failed (Table 1). However, an Asian trial of peretinoin in patients with HCC associated with hepatitis B is currently ongoing in Japan, South Korea, and Taiwan. A phase III trial comparing the anti-programmed death (PD)-1 antibody, nivolumab with placebo after curative therapy is also ongoing (Table 1).

Table 1. Randomized phase II, phase III clinical trials of early/intermediate stage hepatocellular carcinoma (HCC).

Target Population	Design	Trial Name	Result	Presentation	Publication	First Author
Early	1. Vitamin K2 vs. Placebo	NIK-333	Negative	ASCO 2010	<i>Hepatology</i> 2011 [6]	Yoshida H
	2. Peretinoin vs. Placebo	STORM	Negative	ASCO 2014	<i>J Gastroenterol</i> 2014 [8]	Okita K
	3. Sorafenib vs. Placebo	NIK-333/K-333	Ongoing		<i>Lancet Oncology</i> 2015 [7]	Bruix J
	4. Peretinoin vs. Placebo	CheckMate 9DX	Ongoing			
	5. Nivolumab vs. Placebo	HEAT OPTIMA	Negative	ILCA 2013	<i>Clin Cancer Res</i> 2017 [9]	Tak WY
Improvement of RFA	1. RFA +/- LTLD	Post-TACE	Negative	ASCO-GI 2010	<i>Eur J Cancer</i> 2011 [10]	Kudo M
	2. RFA +/- LTLD	SPACE (PhII)	Negative	ASCO-GI 2012	<i>J Hepatol</i> 2016 [11]	Lencioni R
		BRISK-TA	Negative	ILCA 2013	<i>Hepatology</i> 2014 [12]	Kudo M
		ORIENTAL	Negative	EASL 2015	<i>Lancet Gastroenterol Hepatol</i> 2018 [13]	Kudo M
		TACE-2	Negative	ASCO 2016	<i>Lancet Gastroenterol Hepatol</i> 2017 [14]	Meyer T
		6. TACE +/- Sorafenib	TACTICS (Ph III)	Positive	ASCO-GI 2018 [2]	

Red: positive trial; blue: ongoing trial; black: negative trials. LTLD: lipo-thermosensitive liposomal doxorubicin; RFA: radiofrequency ablation; TACE: transcatheter arterial chemoembolization.

2.2.2. Combination Therapy with TACE

Three trials of sorafenib combination therapy with TACE, namely, a phase III trial in Japanese and Korean patients (Post-TACE trial) [10], a phase II trial comparing sorafenib plus TACE with drug-eluting beads (DEB-TACE) to placebo plus DEB-TACE (SPACE trial) [11], and a phase III trial also investigating sorafenib combination with DEB-TACE (TACE 2 trial) [14], have been conducted to date, but all of them failed due to not meeting the primary endpoints of prolonging time to progression (TTP) or progression-free survival (PFS). Phase III trials of the molecular targeted agents, brivanib and orantinib, in combination with TACE, were also conducted, but they also failed due to not meeting the primary endpoint of prolonging OS [12,13].

By learning the lessons from these five negative trials, the definition of “progression” for TACE trials as an endpoint was newly designed, better reflecting how TACE is performed in clinical practice. After application of this newly defined “progression”, results of the first positive trial to demonstrate the clinical efficacy of TACE plus sorafenib (TACTICS trial) were presented at the American Society of Clinical Oncology Gastrointestinal Cancers (ASCO-GI) Symposium in 2018 [2]. In the TACTICS trial, PFS was significantly longer with TACE plus sorafenib than with TACE alone (25.2 months vs. 13.5 months) [2].

2.2.3. First-Line Therapy for Advanced HCC

Overview of First-Line Trials Conducted to Date

Head-to-head trials comparing sorafenib with single-agent sunitinib [15], brivanib [16], and linifanib [17] were conducted, but none of them was able to demonstrate superiority or non-inferiority to sorafenib. Phase III trials assessing the superiority of combination therapy with sorafenib plus erlotinib [18], doxorubicin, or hepatic arterial infusion chemotherapy (HAIC) [19,20] with an implanted reservoir system [21] compared with sorafenib alone all failed as well. Two head-to-head trials comparing radioembolization with Y90 to sorafenib also failed [22,23]. In summary, a total of eight first-line trials have failed to date [24] (Table 2).

Table 2. Phase III clinical trials of advanced-stage HCC.

Target Population	Design	Trial Name	Result	Presentation	Publication	First Author
First line	1. Sorafenib vs. Sunitinib	SUN1170	Negative	ASCO 2011	JCO 2013 [15]	Cheng AL
	2. Sorafenib +/- Erlotinib	SEARCH	Negative	ESMO 2012	JCO 2015 [18]	Zhu AX
	3. Sorafenib vs. Brivanib	BRISK-FL	Negative	AASLD 2012	JCO 2013 [16]	Johnson PJ
	4. Sorafenib vs. Linfanib	LIGHT	Negative	ASCO-GI 2013	JCO 2015 [17]	Cainap C
	5. Sorafenib +/- Doxorubicin	CALGB 80802	Negative	ASCO-GI 2016		
	6. Sorafenib +/- HAIC	SILJUS	Negative	EASL 2016	Lancet GH 2018 [21]	Kudo M
	7. Sorafenib +/- Y90	SARAH	Negative	EASL 2017	Lancet-O 2017 [22]	Vilgrain V
	8. Sorafenib +/- Y90	SIRveNIB	Negative	ASCO 2017	JCO 2018 [23]	Chow P
	9. Sorafenib vs. Lenvatinib	REHELECT	Positive	ASCO 2017	Lancet 2018 [25]	Kudo M
	10. Sorafenib vs. Nivolumab	CheckMate-459	Ongoing			
	11. Sorafenib vs. Durvalumab + Tremelimumab vs. Durva	HIMALAYA	Ongoing			
	12. Sorafenib vs. Atezolizumab + Bevacizumab	IMbrave150	Ongoing			
	13. Sorafenib vs. Tislelizumab		Ongoing			
Advanced	1. Brivanib vs. Placebo	BRISK-PS	Negative	EASL 2012	JCO 2013 [26]	Llovet JM
	2. Everolimus vs. Placebo	EVOLVE-1	Negative	ASCO-GI 2014	JAMA 2014 [27]	Zhu AX
	3. Ramucirumab vs. Placebo	REACH	Negative	ESMO 2014	Lancet-O 2015 [28]	Zhu AX
	4. S-1 vs. Placebo	S-CUBE	Negative	ASCO 2015	Lancet GH 2017 [29]	Kudo M
	5. ADI-PEG 20 vs. Placebo	NA	Negative	ASCO 2016	Ann Oncol 2018 [30]	Abou-Alfa G
	6. Regorafenib vs. Placebo	RESORCE	Positive	WCCG 2016	Lancet 2017 [31]	Bruix J
	7. Tivantinib vs. Placebo	METIV-HCC	Negative	ASCO 2017	Lancet-O 2018 [32]	Rimassa L
	8. Tivantinib vs. Placebo	JET-HCC	Negative	ESMO 2017		
	9. DT vs. Placebo	ReLive	Negative	ILCA 2017		
	10. Cabozantinib vs. Placebo	CELESTIAL	Positive	ASCO-GI 2018	NEJM 2018 [33]	Abou-Alfa G
	11. Ramucirumab vs. Placebo	REACH-2	Positive	ASCO 2018		Zhu AX
	12. Pembrolizumab vs. Placebo	KEYNOTE-240	Ongoing			

Red: positive trials; blue: ongoing trials; black: negative trials. HAIC: hepatic arterial infusion chemotherapy; ADI-PEG 20: arginine deiminase-conjugated with polyethylene glycol; DT: doxorubicin-loaded nanoparticles.

Lenvatinib: Overview of REFLECT Trial Results

The REFLECT trial was the only trial with positive outcomes during this 10-year period of negative trials. Lenvatinib is an oral kinase inhibitor that selectively inhibits receptor tyrosine kinases involved in tumor angiogenesis and tumor growth (e.g., VEGFR1, VEGFR2, VEGFR3, fibroblast growth factor receptor (FGFR)1, FGFR2, FGFR3, FGFR4, PDGFR α , KIT, and RET) [34,35]. A single-arm phase II trial in advanced HCC showed excellent results (TTP: 7.4 months; OS: 18.7 months) [36]. The phase III REFLECT trial comparing sorafenib and lenvatinib was then conducted [25].

The REFLECT trial was a global phase III trial assessing the non-inferiority of lenvatinib to sorafenib. Patients were stratified by race (Asian or non-Asian), vascular invasion and/or EHS (yes or no), Eastern Cooperative Oncology Group performance status (PS) (0 or 1), and body weight (<60 kg or \geq 60 kg). Treatment was continued until disease progression or onset of an intolerable adverse event (AE). Non-inferiority of OS was evaluated as the primary endpoint (non-inferiority margin = 1.08). Secondary endpoints are PFS, TTP, objective response rate (ORR), and safety.

Of the enrolled patients, 478 were assigned to the lenvatinib group and 476 to the sorafenib group. Body weight was less than 60 kg in 32% of patients and 60 kg or higher in 68%. Vascular invasion and/or EHS was present in 69% of patients. The number of patients with HCC due to hepatitis C was favorably imbalanced into the sorafenib group (27% vs. 19% in the lenvatinib group) [37]. Conversely, the number of patients with HCC due to hepatitis B was 53% in the lenvatinib group. An alpha-fetoprotein (AFP) level over 200 ng/mL was seen in the lenvatinib group more frequently than in sorafenib group (46% vs. 39%).

The primary endpoint of OS was 13.6 months in the lenvatinib group and 12.3 months in the sorafenib group, with a hazard ratio of 0.92 (0.79–1.06). The upper limit of the 95% confidence interval (CI) was below the prespecified non-inferiority margin of 1.08, which statistically showed a positive result; the non-inferiority of lenvatinib with respect to OS [25]. PFS (7.4 months in the lenvatinib arm vs. 3.7 months in the sorafenib arm), TTP (8.9 months vs. 3.7 months), and ORR (24.1% vs. 9.2%) per investigator using the modified RECIST criteria (mRECIST) were also better in the lenvatinib arm than the sorafenib arm, thus demonstrating the significantly better antitumor effect of lenvatinib [25]. Another surprising finding was that tumor shrinkage and necrotizing effect were excellent in the lenvatinib group as demonstrated by ORR per independent imaging review using mRECIST (40.6% in the lenvatinib vs. 12.4% in the sorafenib group) [25]. This favorable antitumor effect demonstrated by PFS, TTP, and ORR was also seen in independent imaging review using RECIST 1.1. [38].

Since patients were not stratified by AFP, a higher proportion of patients with AFP over 200 ng/mL were seen in the lenvatinib group than in the sorafenib group. When this AFP imbalance was corrected by covariate analysis, lenvatinib was statistically shown as superior to sorafenib with respect to OS (hazard ratio (HR) = 0.856, 95% CI 0.736–0.995, nominal *p*-value = 0.0342) [25,39]. This result suggests that this global trial could have shown superiority if AFP was included as a stratification factor.

In OS subanalysis, lenvatinib showed longer OS than sorafenib in almost all subgroups. One particularly important finding was that lenvatinib demonstrated longer OS than sorafenib even in patients with a body weight of less than 60 kg receiving a dose of only 8 mg, and the HR was similar to or slightly better than in patients with body weight of 60 kg or more who received 12 mg (<60 kg, HR = 0.85 vs. \geq 60 kg, HR 0.95). This data suggest that weight-based dosing was successful. Longer OS was shown in patients with high baseline AFP (\geq 200 ng/mL), a poor prognostic factor, as revealed by the HR of 0.78 (95% CI, 0.63–0.98). Treatment duration was 5.7 months in the lenvatinib group and 3.7 months in the sorafenib group, indicating that patients were more tolerant to the lenvatinib.

The above results statistically demonstrate the non-inferiority of lenvatinib to sorafenib with respect to OS, and all the secondary endpoints (PFS, TTP, and ORR) showed statistically and clinically significant improvement as well. These findings demonstrated the efficacy of lenvatinib as a first-line agent for unresectable HCC. On 23 March 2018, HCC was aproned in Japan as another indication for lenvatinib along with the previously approved indication of thyroid cancer followed by the United States, Europe, China, and Korea.

2.2.4. Second-Line Therapy for Advanced HCC

Sorafenib is the standard therapy for advanced stage HCC, so placebo-controlled comparative trials were conducted in patients who progressed on sorafenib or were intolerant to sorafenib and could not continue treatment due to adverse reactions.

Overview of Second-Line Trials Conducted to Date

A total of eight placebo-controlled trials of drugs such as brivanib [26], everolimus [27], ramucirumab [28], S-1 [29], arginine deiminase-conjugated with polyethylene glycol (ADI-PEG20) [30], and tivantinib [32] were conducted, but all of them failed (Table 2).

Regorafenib: Overview of the RESORCE Trial

Regorafenib is an oral multikinase inhibitor of protein kinases such as VEGFR1, VEGFR2, VEGFR3, TIE2, PDGFR β , FGFR, KIT, RET, RAF-1, and BRAF [40]. Its molecular structure is nearly identical to that of sorafenib, which gives it a very similar toxicity profile. Unlike other drugs, it was investigated in a phase III placebo-controlled trial in patients refractory to sorafenib but not intolerant to sorafenib. The primary endpoint of OS was significantly better in the regorafenib arm than the placebo arm (10.6 months vs. 7.8 months) [31]. PFS and TTP were also significantly better. Regorafenib became the first drug demonstrated to show efficacy compared with placebo in second-line therapy. After these results were presented, HCC was added as an indication for regorafenib after progression on sorafenib in Japan in May 2017. However, second-line therapy for sorafenib-intolerant patients remains an unmet need because this drug is generally not suitable for use in that population.

The key factor of success of the RESORCE trial can be attributed to the following four factors: (1) patients who discontinued sorafenib due to adverse reactions were excluded from the trial, leaving only patients with progressive disease (PD) on sorafenib, (2) imbalances between the active drug and placebo arms were avoided by including vascular invasion and EHS as separate stratification factors, (3) AFP was also included as a stratification factor, and (4) only patients with adequate tolerance to sorafenib (patients able to take at least 400 mg of sorafenib for at least 20 of the 28 days preceding the PD assessment) were included. This trial design prevented dropouts due to adverse reactions to regorafenib and minimized the effect of post-trial treatment after PD on regorafenib [31]. According to the results of the RESORCE trial, median survival time on regorafenib was 10.6 months (placebo: 7.8 months, HR = 0.63, $p < 0.0001$). Moreover, OS subanalysis showed significantly better results for patients with a Child–Pugh score of 5 on starting sorafenib compared with patients with a score of 6. This is because patients with a score of 5 could quickly be switched from TACE to sorafenib if refractory to TACE, and then could quickly be switched from sorafenib to regorafenib if refractory to sorafenib, which will be an important strategy for improving survival going forward.

The results of the RESORCE trial also showed that sorafenib–regorafenib sequential therapy yielded good OS (26 months from starting sorafenib vs. 19.2 months for placebo) [41,42]. This is an extremely important finding. This long survival time of 26 months nearly rivals conventional TACE outcomes for intermediate-stage HCC [12,42]. The only phase III prospective trial with survival times for the TACE placebo arm presented is the BRISK TA trial, which has the largest enrollment of any such trial in the world. For the above reasons, the outcomes of the placebo arm in this trial could currently be considered the global standard for TACE outcomes with no selection bias whatsoever. The patient population for this trial was 82% early/intermediate-stage (BCLC B: 59%; BCLC A: 23%; BCLC C: 17%), with only 17% of participants in the advanced stage. In contrast, the RESORCE trial enrolled 86% BCLC C advanced-stage patients. When the two cohorts are compared directly, OS is comparable between TACE and sorafenib–regorafenib sequential therapy (26.1 months vs. 26 months). It may not be appropriate to compare individual arms of completely different randomized controlled trials (RCTs), but they are placebo arms of well-designed RCTs, and thus have no selection bias. At the very least, the fact that OS is comparable between the two is very important because sorafenib-regorafenib

sequential therapy was applied to a population with much more advanced disease (i.e., advanced-stage HCC). Undoubtedly the patient population is certainly highly selected, but this means that the same effect obtained with TACE in the population for which TACE is indicated can be obtained with sorafenib-regorafenib sequential therapy in patients with advanced-stage HCC. Now that the potential of sorafenib-regorafenib sequential therapy to greatly improve prognosis is clear, it may be necessary to re-evaluate the appropriate timing for starting sorafenib. The conventional practice has been to switch from TACE to systemic therapy at the point when the patient is found to be refractory to TACE, but one could envision that it may become increasingly important to identify subgroups that tend to be refractory to TACE and start systemic therapy earlier than usual in those groups (while hepatic functional reserve is still Child-Pugh 5 before they are found to be refractory to TACE) [42] (Figure 1). These patient subgroup can be categorized as “TACE unsuitable patient subpopulation”.

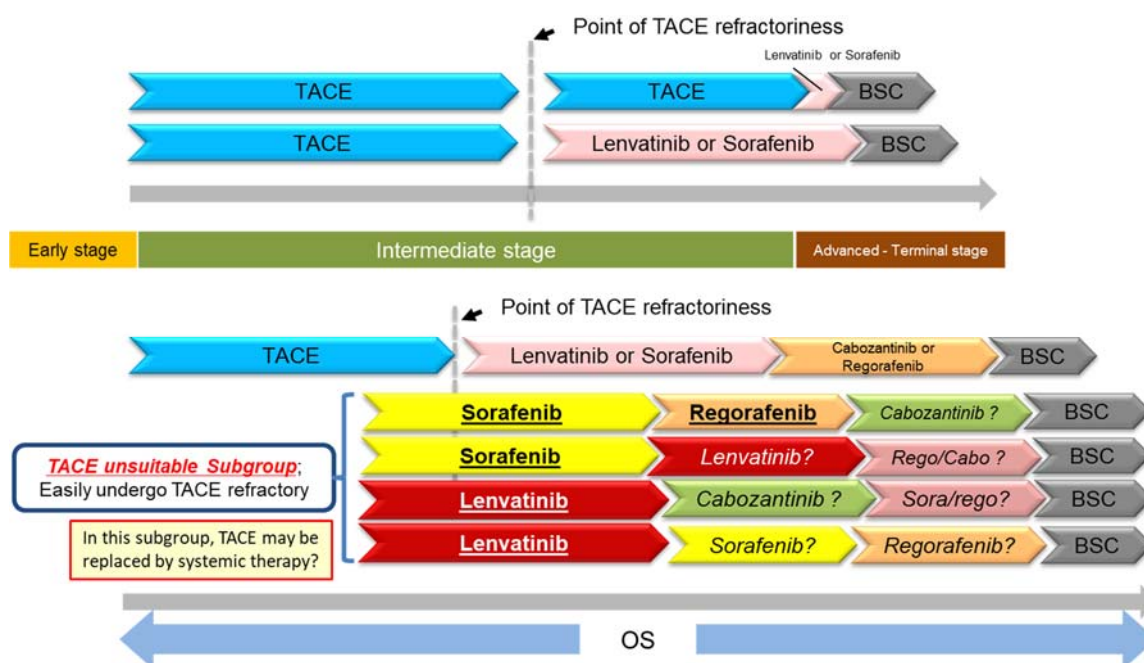


Figure 1. New treatment landscape in HCC. BSC: best supportive care.

Cabozantinib: Overview of the CELESTIAL Trial

The results of this trial were presented at ASCO-GI in 2018 [33]. The study enrolled 773 patients with unresectable HCC that had progressed following at least one prior systemic chemotherapy regimen containing sorafenib from September 2013 to September 2017.

This trial showed significantly better OS in the cabozantinib arm (10.2 months, 95% CI 9.1–12.0) than in the placebo arm (8.0 months, 95% CI 9.1–12.0). The secondary endpoint, PFS, was also better in the cabozantinib arm (5.2 months, 95% CI 4.0–5.5) than the placebo arm (1.9 months, 95% CI 1.9–1.9). In addition, ORR was better in the cabozantinib arm than in the placebo arm (4% vs. 0.4%) ($p = 0.0086$). Post-trial treatment was performed for a comparably low proportion of patients in the cabozantinib and placebo arms (25% vs. 30%).

Cabozantinib and regorafenib had comparable efficacy in terms of OS, ORR, and PFS. Comparable results were obtained for patients who only received prior treatment with sorafenib.

Treatment duration with cabozantinib was 3.8 months, which was similar to that of regorafenib (3.6 months), suggesting good tolerability. Dose reduction and discontinuation due to treatment-related AEs was slightly more common in cabozantinib than in regorafenib. Specific AEs such as hand–foot skin reaction and diarrhea were more common in cabozantinib than in regorafenib, indicating that cabozantinib may be slightly more toxic [43].

Ramucirumab: Overview of the REACH-2 Trial

Results of the REACH-2 trial were reported at the ASCO annual meeting in June 2018 [44]. OS was 8.5 months in the ramucirumab group, and 7.3 months in the placebo group; the difference was significant (HR = 0.710, 95% CI: 0.531–0.949, $p = 0.0199$) (Table 3). Ramucirumab therapy decreased the mortality rate by 29%. In all subgroups, except the female subgroup, OS was longer in patients who received ramucirumab than those placebo, particularly in men, those with extra-hepatic metastases, and those without vascular invasion.

Table 3. Results of the REACH-2 Trial.

Efficacy and Tolerability	Ramucirumab ($n = 197$)	Placebo ($n = 95$)	HR (95% CI)	p -Value
mOS	8.5 m	7.3 m	0.710	0.0199
mPFS	2.8 m	1.6 m	0.452	0.0001
ORR	4.6%	1.1%	-	0.1967
Relative dose intensity	97.9%	99.8%	-	-
Discontinuation due to TEAE	10.7%	3.2%	-	-
Dose adjustment due to AE	34.5%	13.7%	-	-

OS: Overall survival; PFS: progression free survival; TEAE: Treatment-emergent adverse event; ORR: objective response rate; AE: adverse event. Cited and modified from ref. [45].

PFS was 2.8 months in the ramucirumab group, and 1.6 months in the placebo group; the difference was significant (HR = 0.452, 95% CI: 0.339–0.603, $p < 0.0001$). Ramucirumab-treated patients had favorable PFS in all subgroups. ORR was 4.6% (95% CI: 1.7–7.5), with no complete response (CR) cases and nine partial response (PR) cases in the ramucirumab group, and 1.1% (95% CI: 0.0–3.1) with no CR case and one PR case in the placebo group; the difference was not significant ($p < 0.1697$) due to the limited number of cases. Disease control rate (DCR) was significantly better in the ramucirumab group than in the placebo group ($p = 0.0006$); it was 59.9% (118 cases comprising 0 CR, 9 PR, and 109 SD cases) in the former group, with 38.9% (37 cases comprising no CR, 1 PR, and 36 SD cases) in the latter group.

The median dose exposure in the ramucirumab group was six (range, 3–13) cycles, while that in the placebo group was four (range, 3–6) cycles. The relative dose intensity in the former was 97.7% while that in the latter was 99.8%, indicating that ramucirumab therapy was almost uninterrupted in all cases. Ramucirumab targets a single molecule (VEGFR-2) and is likely to have fewer adverse events and favorable tolerability. Rates of study drug discontinuation due to adverse events were 10.7% and 3.2% in the ramucirumab group and the placebo group, respectively, and those of dose modification were 34.5% and 13.7% in the former group and the latter group, respectively. Grade ≥ 3 adverse events that occurred in $\geq 5\%$ of patients were hypertension (12.7% in the ramucirumab group vs. 5.3% in the placebo group), bleeding (5.1% vs. 3.2%), and liver damage (18.3% vs. 15.8%).

REACH-2, which reexamined ramucirumab in patients with baseline AFP level ≥ 400 ng/mL based on the results of the preceding REACH, was a positive study confirming significantly longer OS in ramucirumab- than in placebo-treated patients. PFS and DCR were also significantly better, indicating the drug's potency. Results regarding adverse events were similar to those shown in ramucirumab monotherapy for other indications, suggesting good tolerability in these patients. REACH-2 is an excellent trial because it is the first prospective randomized controlled biomarker-driven trial with positive outcomes.

Kaplan–Meier survival curves showed a significant difference in survival rate between the ramucirumab group (24.5%) and the placebo group (11.3%) at 18 months ($p = 0.0187$), but not at 12 months. This can be explained by the imbalance between the two groups regarding baseline AFP level and the proportion of BCLC C. Because both were higher in the ramucirumab group than in the placebo group, the effect of ramucirumab was not apparent until the late treatment period. Furthermore, patients with baseline AFP level ≥ 400 ng/mL, which is associated with poor prognosis, might have died while on placebo without having post progression treatment. Selection of subjects of the trial

using the level of a biomarker (in this instance, AFP), contributed to the positive outcomes despite a very small number of patients ($n = 292$) for a clinical trial of a second-line agent.

Comparison of the results of the placebo group with baseline AFP level ≥ 400 ng/mL showed that OS was 7.3 months in the REACH-2 trial, which was longer than the 4.2 months in the REACH trial. This can be explained by the imbalance in patient characteristics regarding baseline AFP level, mentioned earlier. The AFP value in the placebo arm (which is not available so far) in the REACH (AFP ≥ 400 ng/mL) trial must have been much higher than that in the placebo arms of REACH-2 (2741) since AFP value in placebo arm in pooled data of REACH (400 \geq ng/mL) and REACH-2 was much higher, 4047.5 ng/mL (Table 4). For the same reason, the HR for OS was slightly lower in the REACH-2 trial (0.67) than in patients with AFP level ≥ 400 ng/mL in the REACH trial (0.71) [45].

Table 4. Comparison between REACH (AFP ≥ 400 ng/mL), REACH-2, and pooled data. OS: overall survival; AFP: alpha-fetoprotein.

Study Name	REACH (AFP ≥ 400 ng/mL) ($n = 250$)		REACH-2 ($n = 292$)		Pooled REACH-2/REACH (AFP ≥ 400 ng/mL) ($n = 542$)	
	Ram	Placebo	Ram	Placebo	Ram	Placebo
Efficacy and AFP						
OS (month) (median)	7.8	4.2	8.5	7.3	8.1	5.0
HR (95% CI)	0.674 (0.508, 0.895)		0.710 (0.531, 0.949)		0.694 (0.571, 0.842)	
<i>p</i> -value	0.0059		0.0199		0.0002	
AFP (ng/mL) (median)	N/A	N/A	3920	2741	4104.6	4047.5

N/A: Not available.

3. Immune Checkpoint Inhibitors

3.1. Immune Checkpoints

The immune checkpoint molecule PD-1 was first discovered in 1992 by Professor Tasuku Honjo and his research team at Kyoto University, Kyoto, Japan. It was named programmed death-1 (PD-1) because the researchers were looking for molecules that induced T lymphocyte apoptosis when they discovered it [46]. It was later discovered to be a receptor that negatively regulates immune responses. The PD-1 ligands PD-L1 and PD-L2 were also discovered in 2000 [47]. It was then discovered that inhibition of this pathway can eliminate tumors by reversing the tumor's immunosuppressive effects and restoring innate immune activity, which prompted the subsequent development of antitumor drugs exploiting that mechanism in 2002 [48]. In 1995, James Allison discovered cytotoxic T-lymphocyte-associated antigen 4 (CTLA-4) [49] and found that inhibition of its function caused tumors to disappear in mice [50]. Such molecules that regulate T lymphocyte activity are called immune checkpoint molecules, and drugs that inhibit these molecules are called immune checkpoint inhibitors. Trials investigating nivolumab and pembrolizumab as anti-PD-1 antibodies, avelumab, durvalumab, and atezolizumab as anti-PD-L1 antibodies, and ipilimumab and tremelimumab as anti-CTLA-4 antibodies for HCC are currently underway [51].

3.2. Nivolumab

Nivolumab is the world's first recombinant human IgG4 monoclonal antibody against human PD-1. In a phase I/II trial in advanced HCC (Checkmate-040 trial), it yielded a response rate of 20%, including two complete responses and a disease control rate of 67%, which are extremely promising results [52] (Table 5). Another unique feature of nivolumab was that its effects persisted in responders [52]. Enrollment for the trial was expanded after that point. The updated results were presented at ASCO 2017, and the OS results of 28.6 months for first-line therapy and 15.6 months for second-line therapy were promising [53]. A phase III head-to-head trial against sorafenib is currently in progress. In light of the above results of the phase I/II trial, nivolumab was designated for priority review by the United States Food and Drug Administration (FDA) and was approved in September 2017.

Table 5. Results of immune checkpoint inhibitors and combination therapy.

Efficacy	Nivolumab [52]	Pembrolizumab [54]	Pembrolizumab Plus Lenvatinib [55]	Atezolizumab Plus Bevacizumab [56]	SHR-1210 Plus Apatinib [57]	Durvalumab Plus Tremelimumab [58]
	(n = 214)	(n = 104)	(n = 30)	(n = 77)	(n = 18)	(n = 40)
ORR (%, 95% CI)	20 (15–26)	17 (11–26)	42.3 (23.4–63.1)	32	38.9	25
DCR (%, 95% CI)	64 (58–71)	62 (52–71)	100	77	83.3	57.5 (>16 week)
PFS (Month, 95% CI)	4.0 (2.9–5.4)	4.9 (3.4–7.2)	9.7 (5.6–NE)	14.9 (0.5–21.5)	7.2 (2.6–NE)	NA
OS (Month, 95% CI)	NR (9M OS, 74%)	12.9 (9.7–15.5)	NR	NR	NR	NA
DOR (Month)	9.9 (8.3–NE)	≤9 (77%)	NE	≥12 (26%)	NE	NA

ORR: objective response rate; DCR: disease control rate; PFS: progression free survival; OS: overall survival; DOR: duration of response; NR: not reached; NE: not estimable; NA: not available.

3.3. Pembrolizumab

Pembrolizumab, like nivolumab, is a recombinant human IgG4 monoclonal antibody against human PD-1. It was investigated for HCC in a phase II trial with a similar result to that of nivolumab [54] (Table 5) and is currently being investigated in a placebo-controlled phase III trial as second-line therapy for patients who have HCC refractory to sorafenib or are intolerant to sorafenib (Table 2).

3.4. Other Immune Checkpoint Inhibitors

Most of PD-L1 antibodies in development have only progressed to phase I or phase II trials so far. Avelumab is being developed in combination with axitinib. Atezolizumab is being developed in combination with bevacizumab. Durvalumab is being developed for combination therapy with the anti-CTLA-4 antibody, tremelimumab [58]. However, recently these 2 latter combination therapies moved forward to phase III trials as mentioned later. Early trials of other drugs, including antibodies that inhibit the immunosuppressive checkpoint molecules TIM3 and Lag3 as well as an antibody that stimulates the immune stimulatory molecule, OX40, are also in progress.

3.5. Combination Therapy with Immune Checkpoint Inhibitors and Molecular Targeted Agents

Results of an open-label phase Ib trial assessing the efficacy and safety of lenvatinib plus pembrolizumab were presented at ESMO 2016. In this trial, which enrolled 13 patients with solid cancers, the therapy yielded a remarkable antitumor effect as demonstrated by the response rate of 69.2% (PR: $n = 9$, SD: $n = 4$) and disease control rate of 100% [59]. Though treatment outcomes for immune checkpoint inhibitors alone have certainly garnered attention, there has been particular interest in the efficacy of combination therapy with molecular targeted drugs. Trials of immune checkpoint therapy with curative treatment for HCC have also been started (Table 1). A phase III head-to-head trial of atezolizumab plus bevacizumab against sorafenib is currently ongoing (Table 2) since very high response rate (61% per RECIST 1.1 by investigator assessment) was shown at ASCO 2018 [30]. However, updated results, presented on 21 October at ESMO 2018 showed a decreased response rate (32%) with this combination therapy [56] (Table 5). Other phase 1b combination therapies, such as pembrolizumab plus lenvatinib [55] or SHR 1210 plus apatinib [57] are ongoing. Also, a phase III head-to-head trial of durvalumab plus tremelimumab against sorafenib is ongoing (Table 2). These combination therapy approaches are extremely promising because combining the two drugs produces not just an additive effect but rather a synergistic effect against the immunosuppressive tumor microenvironment [60,61].

4. Conclusions

This was a review of systemic therapy for HCC. Lenvatinib and regorafenib are now available in addition to sorafenib as molecular targeted agents for the treatment of HCC. Cabozantinib and

ramucirumab may also be approved in 2019. The increase in the number of molecular targeted therapy options for HCC will benefit many patients, but will probably make drug selection and sequences challenging. Combination therapy using targeted treatments with immune checkpoint inhibitors such as atezolizumab and pembrolizumab is expected to yield even better effects when these drugs eventually become available. These new drugs or combination therapy may benefit a wide range of patients from the early, intermediate stage of HCC as an adjuvant use, and advanced stages of HCC, therefore progress in their development is highly anticipated.

Funding: This research received no external funding.

Acknowledgments: I express deep appreciation to the staff members of the Department of Gastroenterology and Hepatology at Kindai University Faculty of Medicine, and give sincere thanks to Tasuku Honjo, the Nobel Prize Winner in Physiology/Medicine 2018, for the discovery of the PD-1 molecule and for teaching me at the Kyoto University Graduate School of Medicine.

Conflicts of Interest: Honoraria from Bayer, Eisai, MSD, Ajinomoto. Consulting or advisory role for Kowa, MSD, BMS, Bayer, Chugai, Taiho. Research funding from Chugai, Otuka, Takeda, Taiho, Sumitomo Dainippon, Daiichi Sankyo, MSD, Eisai, Bayer, Abbvie.

References

- Llovet, J.M.; Ricci, S.; Mazzaferro, V.; Hilgard, P.; Gane, E.; Blanc, J.F.; de Oliveira, A.C.; Santoro, A.; Raoul, J.L.; Forner, A.; et al. Sorafenib in advanced hepatocellular carcinoma. *N. Engl. J. Med.* **2008**, *359*, 378–390. [[CrossRef](#)] [[PubMed](#)]
- Kudo, M.; Ueshima, K.; Torimura, T.; Tanabe, N.; Ikeda, M.; Aikata, H.; Izumi, N.; Yamasaki, T.; Nojiri, S.; Hino, K.; et al. Randomized, open label, multicenter, phase II trial of transcatheter arterial chemoembolization (TACE) therapy in combination with sorafenib as compared with TACE alone in patients with hepatocellular carcinoma: TACTICS trial. *J. Clin. Oncol.* **2018**, *36*, 206. [[CrossRef](#)]
- Wilhelm, S.M.; Carter, C.; Tang, L.; Wilkie, D.; McNabola, A.; Rong, H.; Chen, C.; Zhang, X.; Vincent, P.; McHugh, M.; et al. BAY 43-9006 exhibits broad spectrum oral antitumor activity and targets the RAF/MEK/ERK pathway and receptor tyrosine kinases involved in tumor progression and angiogenesis. *Cancer Res.* **2004**, *64*, 7099–7109. [[CrossRef](#)] [[PubMed](#)]
- Chang, Y.S.; Adnane, J.; Trail, P.A.; Levy, J.; Henderson, A.; Xue, D.; Bortolon, E.; Ichetovkin, M.; Chen, C.; McNabola, A.; et al. Sorafenib (BAY 43-9006) inhibits tumor growth and vascularization and induces tumor apoptosis and hypoxia in RCC xenograft models. *Cancer Chemother. Pharmacol.* **2007**, *59*, 561–574. [[CrossRef](#)] [[PubMed](#)]
- Cheng, A.L.; Kang, Y.K.; Chen, Z.; Tsao, C.J.; Qin, S.; Kim, J.S.; Luo, R.; Feng, J.; Ye, S.; Yang, T.S.; et al. Efficacy and safety of sorafenib in patients in the Asia-Pacific region with advanced hepatocellular carcinoma: A phase III randomised, double-blind, placebo-controlled trial. *Lancet Oncol.* **2009**, *10*, 25–34. [[CrossRef](#)]
- Yoshida, H.; Shiratori, Y.; Kudo, M.; Shiina, S.; Mizuta, T.; Kojiro, M.; Yamamoto, K.; Koike, Y.; Saito, K.; Koyanagi, N.; et al. Effect of vitamin K2 on the recurrence of hepatocellular carcinoma. *Hepatology* **2011**, *54*, 532–540. [[CrossRef](#)] [[PubMed](#)]
- Bruix, J.; Takayama, T.; Mazzaferro, V.; Chau, G.Y.; Yang, J.; Kudo, M.; Cai, J.; Poon, R.T.; Han, K.H.; Tak, W.Y.; et al. Adjuvant sorafenib for hepatocellular carcinoma after resection or ablation (STORM): A phase 3, randomised, double-blind, placebo-controlled trial. *Lancet Oncol.* **2015**, *16*, 1344–1354. [[CrossRef](#)]
- Okita, K.; Izumi, N.; Matsui, O.; Tanaka, K.; Kaneko, S.; Moriwaki, H.; Ikeda, K.; Osaki, Y.; Numata, K.; Nakachi, K.; et al. Peretinoin after curative therapy of hepatitis C-related hepatocellular carcinoma: A randomized double-blind placebo-controlled study. *J. Gastroenterol.* **2015**, *50*, 191–202. [[CrossRef](#)] [[PubMed](#)]
- Tak, W.Y.; Lin, S.M.; Wang, Y.; Zheng, J.; Vecchioione, A.; Park, S.Y.; Chen, M.H.; Wong, S.; Xu, R.; Peng, C.Y.; et al. Phase III heat study adding lyso-thermosensitive liposomal doxorubicin to radiofrequency ablation in patients with unresectable hepatocellular carcinoma lesions. *Clin. Cancer Res.* **2018**, *24*, 73–83. [[CrossRef](#)] [[PubMed](#)]
- Kudo, M.; Imanaka, K.; Chida, N.; Nakachi, K.; Tak, W.Y.; Takayama, T.; Yoon, J.H.; Hori, T.; Kumada, H.; Hayashi, N.; et al. Phase III study of sorafenib after transarterial chemoembolisation in Japanese and Korean patients with unresectable hepatocellular carcinoma. *Eur. J. Cancer* **2011**, *47*, 2117–2127. [[CrossRef](#)] [[PubMed](#)]

11. Lencioni, R.; Llovet, J.M.; Han, G.; Tak, W.Y.; Yang, J.; Guglielmi, A.; Paik, S.W.; Reig, M.; Kim, D.Y.; Chau, G.Y.; et al. Sorafenib or placebo plus TACE with doxorubicin-eluting beads for intermediate stage HCC: The SPACE trial. *J. Hepatol.* **2016**, *64*, 1090–1098. [[CrossRef](#)] [[PubMed](#)]
12. Kudo, M.; Han, G.; Finn, R.S.; Poon, R.T.; Blanc, J.F.; Yan, L.; Yang, J.; Lu, L.; Tak, W.Y.; Yu, X.; et al. Brivanib as adjuvant therapy to transarterial chemoembolization in patients with hepatocellular carcinoma: A randomized phase III trial. *Hepatology* **2014**, *60*, 1697–1707. [[CrossRef](#)] [[PubMed](#)]
13. Kudo, M.; Cheng, A.L.; Park, J.W.; Park, J.H.; Liang, P.C.; Hidaka, H.; Izumi, N.; Heo, J.; Lee, Y.J.; Sheen, I.S.; et al. Orantinib versus placebo combined with transcatheter arterial chemoembolisation in patients with unresectable hepatocellular carcinoma (ORIENTAL): A randomised, double-blind, placebo-controlled, multicentre, phase 3 study. *Lancet Gastroenterol. Hepatol.* **2018**, *3*, 37–46. [[CrossRef](#)]
14. Meyer, T.; Fox, R.; Ma, Y.T.; Ross, P.J.; James, M.W.; Sturgess, R.; Stubbs, C.; Stocken, D.D.; Wall, L.; Watkinson, A.; et al. Sorafenib in combination with transarterial chemoembolisation in patients with unresectable hepatocellular carcinoma (TACE 2): A randomised placebo-controlled, double-blind, phase 3 trial. *Lancet Gastroenterol. Hepatol.* **2017**, *2*, 565–575. [[CrossRef](#)]
15. Cheng, A.L.; Kang, Y.K.; Lin, D.Y.; Park, J.W.; Kudo, M.; Qin, S.; Chung, H.C.; Song, X.; Xu, J.; Poggi, G.; et al. Sunitinib versus sorafenib in advanced hepatocellular cancer: Results of a randomized phase III trial. *J. Clin. Oncol.* **2013**, *31*, 4067–4075. [[CrossRef](#)] [[PubMed](#)]
16. Johnson, P.J.; Qin, S.; Park, J.W.; Poon, R.T.; Raoul, J.L.; Philip, P.A.; Hsu, C.H.; Hu, T.H.; Heo, J.; Xu, J.; et al. Brivanib versus sorafenib as first-line therapy in patients with unresectable, advanced hepatocellular carcinoma: Results from the randomized phase III BRISK-FL study. *J. Clin. Oncol.* **2013**, *31*, 3517–3524. [[CrossRef](#)] [[PubMed](#)]
17. Cainap, C.; Qin, S.; Huang, W.T.; Chung, I.J.; Pan, H.; Cheng, Y.; Kudo, M.; Kang, Y.K.; Chen, P.J.; Toh, H.C.; et al. Linifanib versus Sorafenib in patients with advanced hepatocellular carcinoma: Results of a randomized phase III trial. *J. Clin. Oncol.* **2015**, *33*, 172–179. [[CrossRef](#)] [[PubMed](#)]
18. Zhu, A.X.; Rosmorduc, O.; Evans, T.R.; Ross, P.J.; Santoro, A.; Carrilho, F.J.; Bruix, J.; Qin, S.; Thuluvath, P.J.; Llovet, J.M.; et al. SEARCH: A phase III, randomized, double-blind, placebo-controlled trial of sorafenib plus erlotinib in patients with advanced hepatocellular carcinoma. *J. Clin. Oncol.* **2015**, *33*, 559–566. [[CrossRef](#)] [[PubMed](#)]
19. Moriguchi, M.; Aramaki, T.; Nishiofuku, H.; Sato, R.; Asakura, K.; Yamaguchi, K.; Tanaka, T.; Endo, M.; Itoh, Y. Sorafenib versus Hepatic Arterial Infusion Chemotherapy as Initial Treatment for Hepatocellular Carcinoma with Advanced Portal Vein Tumor Thrombosis. *Liver Cancer* **2017**, *6*, 275–286. [[CrossRef](#)] [[PubMed](#)]
20. Kudo, M.; Trevisani, F.; Abou-Alfa, G.K.; Rimassa, L. Hepatocellular Carcinoma: Therapeutic Guidelines and Medical Treatment. *Liver Cancer* **2017**, *6*, 16–26. [[CrossRef](#)] [[PubMed](#)]
21. Kudo, M.; Ueshima, K.; Yokosuka, O.; Ogasawara, S.; Obi, S.; Izumi, N.; Aikata, H.; Nagano, H.; Hatano, E.; Sasaki, Y.; et al. Sorafenib plus low-dose cisplatin and fluorouracil hepatic arterial infusion chemotherapy versus sorafenib alone in patients with advanced hepatocellular carcinoma (SILIUS): A randomised, open label, phase 3 trial. *Lancet Gastroenterol. Hepatol.* **2018**, *3*, 424–432. [[CrossRef](#)]
22. Vilgrain, V.; Pereira, H.; Assenat, E.; Guiu, B.; Ilonca, A.D.; Pageaux, G.P.; Sibert, A.; Bouattour, M.; Lebtahi, R.; Allaham, W.; et al. Efficacy and safety of selective internal radiotherapy with yttrium-90 resin microspheres compared with sorafenib in locally advanced and inoperable hepatocellular carcinoma (SARAH): An open-label randomised controlled phase 3 trial. *Lancet Oncol.* **2017**, *18*, 1624–1636. [[CrossRef](#)]
23. Chow, P.K.H.; Gandhi, M.; Tan, S.B.; Khin, M.W.; Khasbazar, A.; Ong, J.; Choo, S.P.; Cheow, P.C.; Chotipanich, C.; Lim, K.; et al. SIRveNIB: Selective Internal Radiation Therapy Versus Sorafenib in Asia-Pacific Patients With Hepatocellular Carcinoma. *J. Clin. Oncol.* **2018**, *36*, 1913–1921. [[CrossRef](#)] [[PubMed](#)]
24. Cucchetti, A.; Piscaglia, F.; Pinna, A.D.; Djulbegovic, B.; Mazzotti, F.; Bolondi, L. Efficacy and Safety of Systemic Therapies for Advanced Hepatocellular Carcinoma: A Network Meta-Analysis of Phase III Trials. *Liver Cancer* **2017**, *6*, 337–348. [[CrossRef](#)] [[PubMed](#)]
25. Kudo, M.; Finn, R.S.; Qin, S.; Han, K.H.; Ikeda, K.; Piscaglia, F.; Baron, A.; Park, J.W.; Han, G.; Jassem, J.; et al. A Randomised Phase 3 trial of lenvatinib vs. sorafenib in first-line treatment of patients with unresectable hepatocellular carcinoma. *Lancet* **2018**, *391*, 1163–1173. [[CrossRef](#)]

26. Llovet, J.M.; Decaens, T.; Raoul, J.L.; Boucher, E.; Kudo, M.; Chang, C.; Kang, Y.K.; Assenat, E.; Lim, H.Y.; Boige, V.; et al. Brivanib in patients with advanced hepatocellular carcinoma who were intolerant to sorafenib or for whom sorafenib failed: Results from the randomized phase III BRISK-PS study. *J. Clin. Oncol.* **2013**, *31*, 3509–3516. [[CrossRef](#)] [[PubMed](#)]
27. Zhu, A.X.; Kudo, M.; Assenat, E.; Cattani, S.; Kang, Y.K.; Lim, H.Y.; Poon, R.T.; Blanc, J.F.; Vogel, A.; Chen, C.L.; et al. Effect of everolimus on survival in advanced hepatocellular carcinoma after failure of sorafenib: The EVOLVE-1 randomized clinical trial. *JAMA* **2014**, *312*, 57–67. [[CrossRef](#)] [[PubMed](#)]
28. Zhu, A.X.; Park, J.O.; Ryoo, B.Y.; Yen, C.J.; Poon, R.; Pastorelli, D.; Blanc, J.F.; Chung, H.C.; Baron, A.D.; Pfiffer, T.E.; et al. Ramucirumab versus placebo as second-line treatment in patients with advanced hepatocellular carcinoma following first-line therapy with sorafenib (REACH): A randomised, double-blind, multicentre, phase 3 trial. *Lancet Oncol.* **2015**, *16*, 859–870. [[CrossRef](#)]
29. Kudo, M.; Moriguchi, M.; Numata, K.; Hidaka, H.; Tanaka, H.; Ikeda, M.; Kawazoe, S.; Ohkawa, S.; Sato, Y.; Kaneko, S.; et al. S-1 versus placebo in patients with sorafenib-refractory advanced hepatocellular carcinoma (S-CUBE): A randomised, double-blind, multicentre, phase 3 trial. *Lancet Gastroenterol. Hepatol.* **2017**, *2*, 407–417. [[CrossRef](#)]
30. Abou-Alfa, G.; Qin, S.; Ryoo, B.Y.; Lu, S.N.; Yen, C.J.; Feng, Y.H.; Lim, H.Y.; Izzo, F.; Colombo, M.; Sarker, D.; et al. Phase III randomized study of second line ADI-PEG 20 plus best supportive care versus placebo plus best supportive care in patients with advanced hepatocellular carcinoma. *Ann. Oncol.* **2018**, *29*, 1402–1408. [[CrossRef](#)] [[PubMed](#)]
31. Bruix, J.; Qin, S.; Merle, P.; Granito, A.; Huang, Y.H.; Bodoky, G.; Pracht, M.; Yokosuka, O.; Rosmorduc, O.; Breder, V.; et al. Regorafenib for patients with hepatocellular carcinoma who progressed on sorafenib treatment (RESORCE): A randomised, double-blind, placebo-controlled, phase 3 trial. *Lancet* **2017**, *389*, 56–66. [[CrossRef](#)]
32. Rimassa, L.; Assenat, E.; Peck-Radosavljevic, M.; Pracht, M.; Zagonel, V.; Mathurin, P.; Rota Caremoli, E.; Porta, C.; Daniele, B.; Bolondi, L.; et al. Tivantinib for second-line treatment of MET-high, advanced hepatocellular carcinoma (METIV-HCC): A final analysis of a phase 3, randomised, placebo-controlled study. *Lancet Oncol.* **2018**, *19*, 682–693. [[CrossRef](#)]
33. Abou-Alfa, G.K.; Meyer, T.; Cheng, A.L.; El-Khoueiry, A.B.; Rimassa, L.; Ryoo, B.Y.; Cicin, I.; Merle, P.; Chen, Y.; Park, J.W.; et al. Cabozantinib in patients with advanced and progressing hepatocellular carcinoma. *N. Engl. J. Med.* **2018**, *379*, 54–63. [[CrossRef](#)] [[PubMed](#)]
34. Tohyama, O.; Matsui, J.; Kodama, K.; Hata-Sugi, N.; Kimura, T.; Okamoto, K.; Minoshima, Y.; Iwata, M.; Funahashi, Y. Antitumor activity of lenvatinib (e7080): An angiogenesis inhibitor that targets multiple receptor tyrosine kinases in preclinical human thyroid cancer models. *J. Thyroid Res.* **2014**, *2014*, 638747. [[CrossRef](#)] [[PubMed](#)]
35. Yamamoto, Y.; Matsui, J.; Matsushima, T.; Obaishi, H.; Miyazaki, K.; Nakamura, K.; Tohyama, O.; Semba, T.; Yamaguchi, A.; Hoshi, S.S.; et al. Lenvatinib, an angiogenesis inhibitor targeting VEGFR/FGFR, shows broad antitumor activity in human tumor xenograft models associated with microvessel density and pericyte coverage. *Vasc. Cell* **2014**, *6*, 18. [[CrossRef](#)] [[PubMed](#)]
36. Ikeda, K.; Kudo, M.; Kawazoe, S.; Osaki, Y.; Ikeda, M.; Okusaka, T.; Tamai, T.; Suzuki, T.; Hisai, T.; Hayato, S.; et al. Phase 2 study of lenvatinib in patients with advanced hepatocellular carcinoma. *J. Gastroenterol.* **2017**, *52*, 512–519. [[CrossRef](#)] [[PubMed](#)]
37. Jackson, R.; Psarelli, E.E.; Berhane, S.; Khan, H.; Johnson, P. Impact of Viral Status on Survival in Patients Receiving Sorafenib for Advanced Hepatocellular Cancer: A Meta-Analysis of Randomized Phase III Trials. *J. Clin. Oncol.* **2017**, *35*, 622–628. [[CrossRef](#)] [[PubMed](#)]
38. Kudo, M. Extremely high objective response rate of Lenvatinib: Its clinical relevance and changing the treatment paradigm in hepatocellular carcinoma. *Liver Cancer* **2018**, *7*, 215–224. [[CrossRef](#)] [[PubMed](#)]
39. Kudo, M. Lenvatinib may drastically Change the treatment landscape of hepatocellular carcinoma. *Liver Cancer* **2018**, *7*, 1–19. [[CrossRef](#)] [[PubMed](#)]
40. Wilhelm, S.M.; Dumas, J.; Adnane, L.; Lynch, M.; Carter, C.A.; Schutz, G.; Thierauch, K.H.; Zopf, D. Regorafenib (BAY 73-4506): A new oral multikinase inhibitor of angiogenic, stromal and oncogenic receptor tyrosine kinases with potent preclinical antitumor activity. *Int. J. Cancer* **2011**, *129*, 245–255. [[CrossRef](#)] [[PubMed](#)]

41. Finn, R.S.; Merle, P.; Granito, A.; Huang, Y.H.; Bodoky, G.; Pracht, M.; Yokosuka, O.; Rosmorduc, O.; Gerolami, R.; Caparello, C.; et al. Outcomes of sequential treatment with sorafenib followed by regorafenib for HCC: Additional analyses from the phase III RESORCE trial. *J. Hepatol.* **2018**, *69*, 353–358. [[CrossRef](#)] [[PubMed](#)]
42. Kudo, M. Regorafenib as Second-Line Systemic Therapy May Change the Treatment Strategy and Management Paradigm for Hepatocellular Carcinoma. *Liver Cancer* **2016**, *5*, 235–244. [[CrossRef](#)] [[PubMed](#)]
43. Kudo, M. Cabozantinib as a Second-Line Agent in Advanced Hepatocellular Carcinoma. *Liver Cancer* **2018**, *7*, 123–133. [[CrossRef](#)] [[PubMed](#)]
44. Zhu, A.X.; Kang, Y.K.; Yen, C.J.; Finn, R.S.; Galle, P.R.; Llovet, J.M.; Assenat, E.; Brandi, G.; Lim, H.Y.; Pracht, M.; et al. REACH-2: A randomized, double-blind, placebo-controlled phase 3 study of ramucirumab versus placebo as second-line treatment in patients with advanced hepatocellular carcinoma (HCC) and elevated baseline alpha-fetoprotein (AFP) following first-line sorafenib. *J. Clin. Oncol.* **2018**, *36*, 4003. [[CrossRef](#)]
45. Kudo, M. Ramucirumab as second-line systemic therapy in hepatocellular carcinoma. *Liver Cancer* **2018**, *7*, 305–311. [[CrossRef](#)]
46. Ishida, Y.; Agata, Y.; Shibahara, K.; Honjo, T. Induced expression of PD-1, a novel member of the immunoglobulin gene superfamily, upon programmed cell death. *EMBO J.* **1992**, *11*, 3887–3895. [[CrossRef](#)] [[PubMed](#)]
47. Okazaki, T.; Honjo, T. PD-1 and PD-1 ligands: From discovery to clinical application. *Int. Immunol.* **2007**, *19*, 813–824. [[CrossRef](#)] [[PubMed](#)]
48. Iwai, Y.; Ishida, M.; Tanaka, Y.; Okazaki, T.; Honjo, T.; Minato, N. Involvement of PD-L1 on tumor cells in the escape from host immune system and tumor immunotherapy by PD-L1 blockade. *Proc. Natl. Acad. Sci. USA.* **2002**, *99*, 12293–12297. [[CrossRef](#)] [[PubMed](#)]
49. Krummel, M.F.; Allison, J.P. CD28 and CTLA-4 have opposing effects on the response of T cells to stimulation. *J. Exp. Med.* **1995**, *182*, 459–465. [[CrossRef](#)] [[PubMed](#)]
50. Leach, D.R.; Krummel, M.F.; Allison, J.P. Enhancement of antitumor immunity by CTLA-4 blockade. *Science* **1996**, *271*, 1734–1736. [[CrossRef](#)] [[PubMed](#)]
51. Kudo, M. Immune checkpoint blockade in hepatocellular carcinoma: 2017 update. *Liver Cancer* **2017**, *6*, 1–12. [[CrossRef](#)] [[PubMed](#)]
52. El-Khoueiry, A.B.; Sangro, B.; Yau, T.; Crocenzi, T.S.; Kudo, M.; Hsu, C.; Kim, T.Y.; Choo, S.P.; Trojan, J.; Welling, T.H.R.; et al. Nivolumab in patients with advanced hepatocellular carcinoma (CheckMate 040): An open-label, non-comparative, phase 1/2 dose escalation and expansion trial. *Lancet* **2017**, *389*, 2492–2502. [[CrossRef](#)]
53. Todd, S.C.; El-Khoueiry, A.B.; Yau, T.; Melero, I.; Sangro, B.; Kudo, M.; Hsu, C.; Trojan, J.; Kim, T.-Y.; Choo, S.-P.; et al. Nivolumab (nivo) in sorafenib (sor)-naive and -experienced pts with advanced hepatocellular carcinoma (HCC): CheckMate 040 study. *J. Clin. Oncol.* **2017**, *35*, 4013. [[CrossRef](#)]
54. Zhu, A.X.; Finn, R.S.; Edeline, J.; Cattani, S.; Ogasawara, S.; Palmer, D.; Verslype, C.; Zagonel, V.; Fartoux, L.; Vogel, A.; et al. Pembrolizumab in patients with advanced hepatocellular carcinoma previously treated with sorafenib (KEYNOTE-224): A non-randomised, open-label phase 2 trial. *Lancet Oncol.* **2018**, *19*, 940–952. [[CrossRef](#)]
55. Ikeda, M.; Sung, M.W.; Kudo, M.; Kobayashi, M.; Baron, A.D.; Finn, R.S.; Kaneko, S.; Zhu, A.X.; Kubota, T.; Kraljevic, S. A phase 1b trial of lenvatinib (LEN) plus pembrolizumab (PEM) in patients (pts) with unresectable hepatocellular carcinoma (uHCC). *J. Clin. Oncol.* **2018**, *36*, 4076. [[CrossRef](#)]
56. Pishvaian, M.J.; Lee, M.S.; Ryoo, B.; Stein, S.; Lee, K.; Verret, W.; Spahn, J.; Shao, H.; Liu, B.; Iizuka, K.; et al. *Updated Safety and Clinical Activity Results from a Phase 1b Study of Atezolizumab + Bevacizumab in Hepatocellular Carcinoma (HCC)*; ESMO: Munich, Germany, 2018.
57. Xu, J.M.; Zhang, Y.; Jia, R.; Wang, Y.; Liu, R.; Zhang, G.; Zhao, C.; Zhang, Y.; Zou, J.; Wang, Q. Anti-programmed death-1 antibody SHR-1210 (S) combined with apatinib (A) for advanced hepatocellular carcinoma (HCC), gastric cancer (GC) or esophagogastric junction (EGJ) cancer refractory to standard therapy: A phase 1 trial. *J. Clin. Oncol.* **2018**, *36*, 4075. [[CrossRef](#)]

58. Kelley, R.K.; Abou-Alfa, G.K.; Bendell, J.C.; Kim, T.Y.; Borad, M.J.; Yong, W.P.; Morse, M.; Kang, Y.K.; Rebelatto, M.; Makowsky, M.; et al. Phase I/II study of durvalumab and tremelimumab in patients with unresectable hepatocellular carcinoma (HCC): Phase I safety and efficacy analyses. *J. Clin. Oncol.* **2017**, *35*, 4073. [[CrossRef](#)]
59. Taylor, M.; Dutcus, C.E.; Schmidt, E.; Bagulho, T.; Li, D.; Shumaker, R.; Rasco, D. A phase 1b trial of lenvatinib (LEN) plus pembrolizumab (PEM) in patients with selected solid tumors. *Ann. Oncol.* **2016**, *27*. [[CrossRef](#)]
60. Kudo, M. Immuno-Oncology in Hepatocellular Carcinoma: 2017 Update. *Oncology* **2017**, *93*, 147–159. [[CrossRef](#)] [[PubMed](#)]
61. Kudo, M. Combination Cancer Immunotherapy in Hepatocellular Carcinoma. *Liver Cancer* **2018**, *7*, 20–27. [[CrossRef](#)] [[PubMed](#)]



© 2018 by the author. Licensee MDPI, Basel, Switzerland. This article is an open access article distributed under the terms and conditions of the Creative Commons Attribution (CC BY) license (<http://creativecommons.org/licenses/by/4.0/>).

Cabozantinib for advanced hepatocellular carcinoma

Masatoshi Kudo

Kindai University Faculty of Medicine, Osaka-Sayama, Japan

Correspondence to: Masatoshi Kudo, MD, PhD. Kindai University Faculty of Medicine, Osaka-Sayama, Japan. Email: m-kudo@med.kindai.ac.jp.

Comment on: Abou-Alfa GK, Meyer T, Cheng AL, *et al.* Cabozantinib in Patients with Advanced and Progressing Hepatocellular Carcinoma. *N Engl J Med* 2018;379:54-63.

Submitted Nov 17, 2018. Accepted for publication Nov 22, 2018.

doi: 10.21037/hbsn.2018.11.22

View this article at: <http://dx.doi.org/10.21037/hbsn.2018.11.22>

Introduction

Results of the phase III CELESTIAL trial of cabozantinib were recently reported in the *New England Journal of Medicine* (1). Whereas all preceding clinical trials examining second-line agents ended in failure (2-7), the CELESTIAL trial succeeded, and cabozantinib has become the fourth molecular-targeted agent for hepatocellular carcinoma (HCC). This success was followed by another clinical trial of ramucirumab, the success of which was reported at the American Society of Clinical Oncology meeting in June 2018. As a result, two first-line agents, sorafenib and lenvatinib (8), and three second-line agents, regorafenib, cabozantinib, and ramucirumab, are now available for the treatment of HCC.

Characteristics of cabozantinib

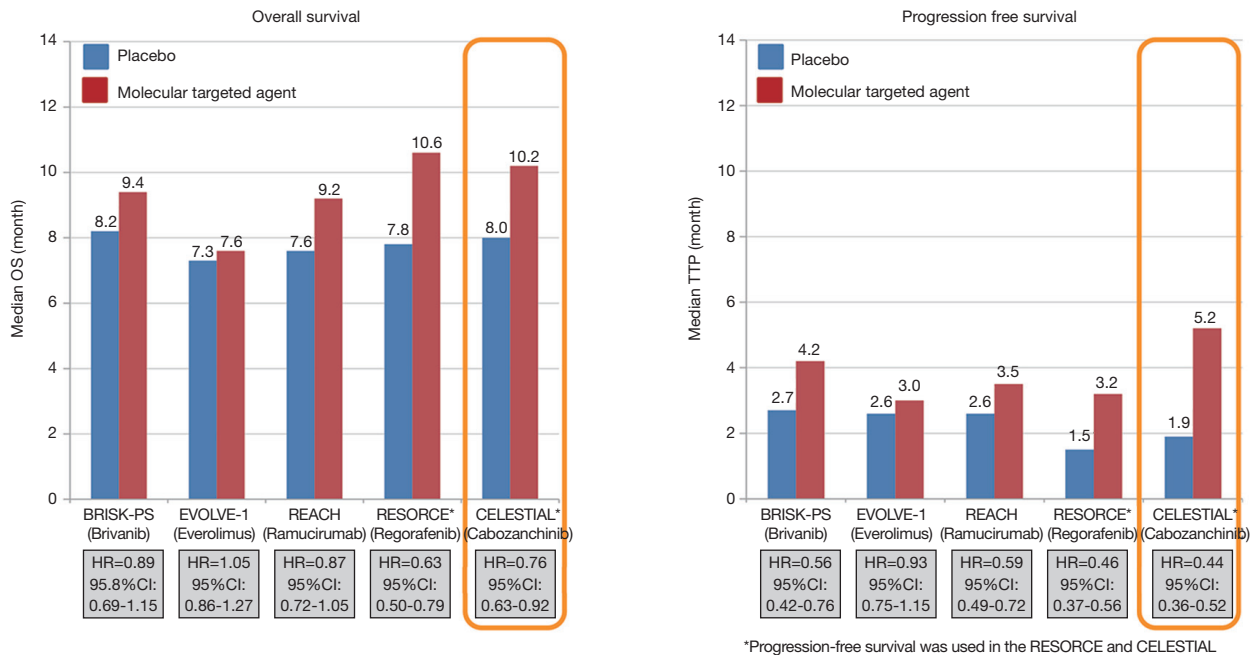
The chemical structure of cabozantinib is relatively similar to that of regorafenib (9,10). However, the kinase inhibitory activity (IC₅₀) of cabozantinib is quite different from that of regorafenib. Although cabozantinib is generally known as a dual inhibitor of VEGFR-2 and c-MET (11,12), compared with regorafenib it is a more potent inhibitor of MET, AXL, and TIE-2. VEGF, MET, and AXL are deeply involved in tumor growth and angiogenesis. MET and AXL are involved in acquisition of resistance to anti-angiogenic agents (11,13). Also, expression of VEGF, MET, and AXL is a known predictor of poor prognosis (14,15).

A waterfall plot from the phase II trial showed tumor reduction in a considerable proportion of patients. Progression-free survival (PFS) was 4.2 months in sorafenib-naïve patients and 5.5 months in sorafenib-treated patients; overall survival (OS) was 11.5 months. Given that some

participants had received first-line therapy, the overall response rate (ORR) of 5%, the disease control rate (DCR) of 81%, and PFS of 5.2 months were not particularly good compared to the results of the phase II trial of regorafenib (16). Also, adverse event (AE) profiles showed that AEs were slightly more common with cabozantinib than with regorafenib (12).

Phase III CELESTIAL trial

In light of these results, cabozantinib proceeded to a phase III CELESTIAL trial. The study design was not as sophisticated or well thought out as the RESORCE trial's (17). For example, use of "vascular invasion and/or extrahepatic spread" as a stratification factor posed a potential risk of a disadvantageous imbalance in vascular invasion. In fact, such a disadvantageous imbalance occurred in the BRISK-PS trial that ended in failure. Further, alpha-fetoprotein (AFP) was not included among the stratification factors, posing a potential risk of a disadvantageous imbalance as actually seen in the REFLECT trial. After the RESORCE trial, use of vascular invasion as an independent stratification factor, along with the use of AFP as a stratification factor, became a standard trial design for second-line agents (18). However, the design of this phase III trial was conventional and lacked the sophistication seen in some other trials. For example, exclusion of sorafenib-intolerant patients, a criterion used in the RESORCE trial, was not applied in this phase III trial. The inclusion criteria related to prior treatment in this trial were (I) prior sorafenib treatment; (II) disease progression following at least one prior systemic treatment for HCC; and (III) up to two prior systemic regimens for advanced HCC. The



*Progression-free survival was used in the RESORCE and CELESTIAL

BRISK-PS: Llovet JM *et al.* J Clin Oncol 2013;31(28):3509–3516. EVOLVE-1: Zhu AX *et al.* JAMA 2014;312(1):57–67
 REACH: Zhu AX *et al.* Lancet Oncol. 2015 Jul;16(7):859–70. RESORCE: J Bruix *et al.* Lancet 2017
 CELESTIAL :Abou Alfa G, *et al.* NEJM 2018

Figure 1 Phase III trial: 2nd line.

proportion of sorafenib-intolerant participants was not reported.

A total of 707 patients with progression of unresectable HCC following at least 1 prior systemic treatment with sorafenib between September 2013 and September 2017 were enrolled in this trial, and the second interim analysis in January 2016 demonstrated superiority in the primary endpoint OS. This successful clinical trial showed significantly longer OS in the cabozantinib group (10.2 months; 95% CI, 9.1–12.0 months) than in the placebo group (8.0 months; 95% CI, 6.8–9.4 months). PFS, a secondary endpoint, was also longer in the cabozantinib group (5.2 months; 95% CI, 4.0–5.5) than in the placebo group (1.9 months; 95% CI, 1.9–1.9). Because neither vascular invasion nor extrahepatic spread (EHS) was used independently for stratification, imbalances in patient characteristics were observed between the two groups. Specifically, there was a favorable imbalance in the proportion of patients with macrovascular invasion (MVI): 27% in the cabozantinib group versus 34% in the placebo group. MVI is a well-known extremely strong predictor of poor prognosis. OS values in patients with and without MVI were 5.3 and 9.7 months, respectively,

in the placebo group, and 7.6 months and 12.4 months, respectively, in the cabozantinib group, suggesting that the above imbalance had some influence on the trial outcomes. Also, HBV was the major etiology of HCC in this trial (38% of participants with HBV versus 24% with HCV), and the hazard ratio (HR) for OS was 0.69 in those with HBV but 1.11 in those with HCV. The HR for PFS was 0.31 in patients with HBV while 0.61 in those with HCV, indicating that cabozantinib may be more effective in those with HBV.

PFS of 1.9 months in the placebo group was quite short, which is the second shortest after the PFS of 1.5 months in the RESORCE trial among previous clinical trials for second-line agents (*Figure 1*). This means that the CELESTIAL trial, like the trial for regorafenib, might have included a small number of sorafenib-intolerant patients, and in those patients, the disease progressed during the sorafenib-treated period, and then progressed further and rapidly during the placebo-treated period. The median length of prior sorafenib treatment was relatively long (5.3 months) in the CELESTIAL trial, suggesting that many patients were with stable disease (SD) for long time. Incidentally, the median duration of prior sorafenib

Table 1 Time to event: CELESTIAL (SOR→CAB) vs. RESORCE

Efficacy	CELESTIAL trial (SOR→CAB)			RESORCE trial (SOR→REG)			
	Cabozantinib (n=331)	Placebo (n=164)	HR	Regorafenib (n=379)	Placebo (n=194)	HR	P
TTP	NA	NA	NA	3.2	1.5	0.44	<0.0001
PFS	5.5	1.9	0.40	3.1	1.5	0.46	<0.0001
OS	11.3	7.2	0.70	10.6	7.8	0.63	<0.0001

TTP, time to progression; PFS, progression-free survival; OS, overall survival.

treatment was 7.8 months in the trial for regorafenib. This suggests the possibility that patients who were more responsive to sorafenib were included in the trial, which in turn resulted in the favorable outcome for patients treated with the testing agent. Also, the percentages of patients who received post-trial treatment was comparable in the cabozantinib group (25%) and in the placebo group (30%), suggesting that conditions were pretty poor in these groups. Thus, although not reported, the proportion of sorafenib-intolerant patients might have been relatively small in this trial, which resulted in the favorable outcome.

Comparison between regorafenib and cabozantinib: efficacy and safety

Comparison of OS, ORR, and FPS indicates that efficacy is roughly similar between cabozantinib and regorafenib. Even in the subgroup of patients who received sorafenib alone during prior treatment, HRs for PFS and OS were comparable between the CELESTIAL trial and the RESORCE trial: 0.40 vs. 0.46 for PFS, and 0.70 vs. 0.63 for OS (Table 1). The CELESTIAL trial showed OS of 8 months in placebo-treated patients, which was roughly same compared to the previous phase III trials for second-line agents, and OS of 10.2 months in the cabozantinib-treated patients, which was similar to the OS in regorafenib-treated patients in the RESORCE trial, the only other positive trial. Compared with these positive trials, three previous unsuccessful trials (BRISK-PS, EVOLVE, and REACH trials) showed shorter OS in patients treated with second-line agents despite similar OS in the placebo group, indicating that the efficacy of cabozantinib is as good as that of regorafenib. Similarly, PFS in the placebo-treated patients was very short, but that in cabozantinib-treated patients was longest (5.2 months), clearly indicating its favorable efficacy (Figure 1).

The treatment durations were comparable between

cabozantinib (3.8 months) and regorafenib (3.6 months), indicating acceptable tolerability of these agents. Dose reduction and treatment discontinuation due to AEs occurred more frequently with cabozantinib than with regorafenib. Palmar-plantar erythrodysesthesia, diarrhea and asthenia were more common with cabozantinib than with regorafenib, indicating that the toxicity may be slightly higher for cabozantinib than for regorafenib. However, given strict exclusion of sorafenib-intolerant patients in the RESORCE trial, cabozantinib and regorafenib may be comparable in terms of AEs.

Key factors contributing to success of CELESTIAL trial

What were the key factors that contributed to the success of the CELESTIAL trial, despite toxicity possibly being slightly higher for cabozantinib and the lack of design sophistication (e.g., different from the RESORCE trial).

There were six main factors:

- (I) The antitumor effect of cabozantinib was sufficiently potent;
- (II) Its toxicity and tolerability were acceptable;
- (III) There was a favorable imbalance of vascular invasion for cabozantinib;
- (IV) Cabozantinib is effective in HBV patients, and the HBV patients were the largest subpopulation (38% of total) in the trial;
- (V) Based on short time to progression and a low proportion of patients who received post-trial treatment, it is possible that a low proportion of sorafenib-intolerant patients were enrolled, thus could not readily received post-trial treatment because of poor general condition;
- (VI) Largest sample size [707] among the previous trials for second-line agents provided adequate power to detect small differences as significant.

Conclusions

The success of the clinical trial for cabozantinib expands the agents available for HCC treatment. Further, it will offer more treatment options, such as sequential therapy involving other molecular targeted agents, and advanced therapy in combination with immune checkpoint inhibitors, thereby considerably contributing to a better prognosis of HCC.

Acknowledgements

None.

Footnote

Conflicts of Interest: The author has no conflicts of interest to declare.

References

1. Ghassan K, Abou-Alfa GK, Meyer T, et al. Cabozantinib (C) versus placebo (P) in patients (pts) with advanced hepatocellular carcinoma (HCC) who have received prior sorafenib: Results from the randomized phase III CELESTIAL trial. *J Clin Oncol* 2018;36:abstr 207.
2. Llovet JM, Decaens T, Raoul JL, et al. Brivanib in patients with advanced hepatocellular carcinoma who were intolerant to sorafenib or for whom sorafenib failed: results from the randomized phase III BRISK-PS study. *J Clin Oncol* 2013;31:3509-16.
3. Zhu AX, Kudo M, Assenat E, et al. Effect of everolimus on survival in advanced hepatocellular carcinoma after failure of sorafenib: the EVOLVE-1 randomized clinical trial. *JAMA* 2014;312:57-67.
4. Zhu AX, Park JO, Ryoo BY, et al. Ramucirumab versus placebo as second-line treatment in patients with advanced hepatocellular carcinoma following first-line therapy with sorafenib (REACH): a randomised, double-blind, multicentre, phase 3 trial. *Lancet Oncol* 2015;16:859-70.
5. Kudo M, Moriguchi M, Numata K, et al. S-1 versus placebo in patients with sorafenib-refractory advanced hepatocellular carcinoma (S-CUBE): a randomised, double-blind, multicentre, phase 3 trial. *Lancet Gastroenterol Hepatol* 2017;2:407-17.
6. Kudo M. Molecular Targeted Agents for Hepatocellular Carcinoma: Current Status and Future Perspectives. *Liver Cancer* 2017;6:101-12.
7. Cucchetti A, Piscaglia F, Pinna AD, et al. Efficacy and Safety of Systemic Therapies for Advanced Hepatocellular Carcinoma: A Network Meta-Analysis of Phase III Trials. *Liver Cancer* 2017;6:337-48.
8. Kudo M, Finn RS, Qin S, et al. Lenvatinib versus sorafenib in first-line treatment of patients with unresectable hepatocellular carcinoma: a randomised phase 3 non-inferiority trial. *Lancet* 2018.
9. Lacy S, Hsu B, Miles D, et al. Metabolism and Disposition of Cabozantinib in Healthy Male Volunteers and Pharmacologic Characterization of Its Major Metabolites. *Drug Metab Dispos* 2015;43:1190-207.
10. Strumberg D, Schultheis B. Regorafenib for cancer. *Expert Opin Investig Drugs* 2012;21:879-89.
11. Yakes FM, Chen J, Tan J, et al. Cabozantinib (XL184), a novel MET and VEGFR2 inhibitor, simultaneously suppresses metastasis, angiogenesis, and tumor growth. *Mol Cancer Ther* 2011;10:2298-308.
12. Kelley RK, Verslype C, Cohn AL, et al. Cabozantinib in hepatocellular carcinoma: results of a phase 2 placebo-controlled randomized discontinuation study. *Ann Oncol* 2017;28:528-34.
13. Gay CM, Balaji K, Byers LA. Giving AXL the axe: targeting AXL in human malignancy. *Br J Cancer* 2017;116:415-23.
14. Zhu AX, Duda DG, Sahani DV, et al. HCC and angiogenesis: possible targets and future directions. *Nat Rev Clin Oncol* 2011;8:292-301.
15. Ueki T, Fujimoto J, Suzuki T, et al. Expression of hepatocyte growth factor and its receptor, the c-met proto-oncogene, in hepatocellular carcinoma. *Hepatology* 1997;25:619-23.
16. Bruix J, Tak WY, Gasbarrini A, et al. Regorafenib as second-line therapy for intermediate or advanced hepatocellular carcinoma: multicentre, open-label, phase II safety study. *Eur J Cancer* 2013;49:3412-9.
17. Kudo M. Regorafenib as Second-Line Systemic Therapy May Change the Treatment Strategy and Management Paradigm for Hepatocellular Carcinoma. *Liver Cancer* 2016;5:235-44.
18. Kudo M. A New Era of Systemic Therapy for Hepatocellular Carcinoma with Regorafenib and Lenvatinib. *Liver Cancer* 2017;6:177-84.

Cite this article as: Kudo M. Cabozantinib for advanced hepatocellular carcinoma. *HepatoBiliary Surg Nutr* 2018. doi: 10.21037/hbsn.2018.11.22

Autoimmune Pancreatitis Mouse Model

UNIT 15.31

Ken Kamata,¹ Tomohiro Watanabe,^{1,2} Kosuke Minaga,¹ Warren Strober,² and Masatoshi Kudo¹

¹Department of Gastroenterology and Hepatology, Kindai University Faculty of Medicine, Osaka-Sayama, Osaka, Japan

²Mucosal Immunity Section, Laboratory of Host Defenses, National Institute of Allergy and Infectious Diseases, National Institutes of Health, Bethesda, Maryland

Autoimmune pancreatitis (AIP) is a chronic fibro-inflammatory disorder of the pancreas. However, extensive clinico-pathological analyses have revealed that AIP is, in reality, a pancreatic manifestation of a newly described systemic disease known as IgG4-related disease (IgG4-RD). IgG4-RD is characterized by enhanced local and systemic IgG4 antibody (Ab) responses as well as inflammation involving multiple organs, including the pancreas, bile ducts, and salivary glands. Although mice lack the IgG4 Ab subtype, autoimmune-prone MRL/Mp mice treated with repeated injection with polyinosinic-polycytidylic acid (poly (I:C)) provide an experimental model of AIP. These mice exhibit massive destruction of pancreatic architecture associated with pancreatic immune cell infiltration and fibrosis. Moreover, this experimental AIP may be accompanied by involvement of multiple organs as well as elevation of serum levels of autoAbs, resembling humans with IgG4-RD. Thus, elucidation of the molecular mechanisms accounting for the development of experimental AIP can potentially provide new insights into the immuno-pathogenesis of human IgG4-related AIP. © 2018 by John Wiley & Sons, Inc.

Keywords: autoimmune pancreatitis • IgG4-related disease • plasmacytoid dendritic cells

How to cite this article:

Kamata, K., Watanabe, T., Minaga, K., Strober, W., & Kudo, M. (2018). Autoimmune pancreatitis mouse model. *Current Protocols in Immunology*, 120, 15.31.1–15.31.10. doi: 10.1002/cpim.41

INTRODUCTION

IgG4-related disease (IgG4-RD) is a newly established disease entity first proposed by Japanese physicians (Kamisawa & Okamoto, 2006). It is a chronic fibro-inflammatory condition characterized by enhanced serum levels of IgG4 antibody (Ab) and by massive infiltration of IgG4-expressing plasma cells into the affected organs (Kamisawa, Zen, Pillai, & Stone, 2015; Stone, Zen, & Deshpande, 2012). Thus, enhanced IgG4 Ab responses are one of the most prominent features of IgG4-RD. Another important feature of this disorder is the presence of inflammation in multiple organs and tissues such as the pancreas, bile duct, salivary glands, periorbital tissues, kidneys, lungs, lymph nodes, and retroperitoneum (Okazaki & Umehara, 2017). IgG-RD has a distinct histopathological signature that is very important for its diagnosis; this includes the presence of three key pathological findings: lymphoplasmacytic infiltration including IgG4-expressing plasma cells, storiform fibrosis, and obliterative phlebitis (Kamisawa et al., 2015; Stone et al., 2012). As physicians' awareness and recognition of IgG4-RD expand rapidly, the numbers of patients diagnosed with IgG4-RD is increasing.

Autoimmune pancreatitis (AIP) is a chronic fibro-inflammatory disease of the pancreas. It is classified into two types, type 1 (lymphoplasmacytic sclerosing pancreatitis, LPSP)

Animal Models for Autoimmune and Inflammatory Disease

15.31.1



Current Protocols in Immunology 15.31.1–15.31.8, February 2018
Published online February 2018 in Wiley Online Library (wileyonlinelibrary.com).
doi: 10.1002/cpim.41
Copyright © 2018 John Wiley & Sons, Inc.

Supplement 120

and type 2 (idiopathic ductcentric pancreatitis, IDCP), based on pathological findings (Kamisawa et al., 2013). Type 1 AIP (also called LPSP) is characterized by dense lymphoplasmacytic infiltration, storiform fibrosis, and obliterative phlebitis. This is accompanied by massive accumulation of IgG4-expressing plasma cells and, in some patients with elevated levels of serum IgG4 and involvement of other organs, including bile ducts, salivary glands, and kidney. In contrast, infiltration of IgG4-expressing plasma cells is absent in the pancreas of type 2 (also called IDCP) AIP. Thus, it is now generally accepted that only type 1 AIP is a pancreatic manifestation of systemic IgG4-RD.

Although clinico-pathological analyses of patients with IgG4-RD have helped to establish diagnostic criteria that establish the presence of this disease, the understanding of its immuno-pathogenesis is very limited. Initial studies of IgG4-RD focused on adaptive immune responses rather than innate immune responses since IgG4-RD is characterized by enhanced adaptive IgG4 Ab responses. These studies established that abnormal T helper type 2 (Th2), regulatory T cell (Treg), and T follicular helper (Tfh) responses as well as the generation of plasmablasts are implicated in the immuno-pathogenesis of this disorder (Akitake et al., 2010; Akiyama et al., 2015; Della-Torre, Lanzillotta, & Doglioni, 2015; Zen et al., 2007). More recently, the pathological role played by abnormal innate immune responses in IgG4-RD have been examined using an experimental model of AIP, consisting of MRL/Mp mice subjected to repeated injections of polyinosinic-polycytidylic, poly (I:C) (Arai et al., 2015; Watanabe et al., 2017). Extensive analyses of this experimental AIP revealed that chronic fibro-inflammatory responses of the pancreas depend upon the activation of plasmacytoid dendritic cells (pDCs) with the ability to produce a large amount of IFN- α and IL-33. pDCs expressing both IFN- α and IL-33 are also present in the pancreas of patients with IgG4-RD and that pDCs isolated from such patients promote IgG4 Ab production by B cells (Arai et al., 2015; Watanabe et al., 2017). Thus, this experimental model of AIP is very useful for the elucidation of immuno-pathogenesis of IgG4-related AIP despite the fact that mice lack the IgG4 Ab subtype. This unit reviews methods to study IgG4-related AIP in mice, using the MRL/Mp model.

BASIC PROTOCOL

INDUCTION OF AUTOIMMUNE PANCREATITIS IN MRL/Mp MICE

Spontaneous development of AIP is seen in female MRL/Mp mice at 34 to 38 weeks old (Kanno, Nose, Itoh, Taniguchi, & Kyogoku, 1992). The incidence of AIP was reported to be ~70%. Nevertheless, male MRL/Mp mice spontaneously develop AIP later, ~45 to 50 weeks and the incidence is <40% (Kanno et al., 1992). Poly (I:C) is a prototypical Toll-like receptor 3 (TLR3) ligand with the ability to induce systemic type I IFN responses. Repeated injection of poly (I:C) accelerates the development of AIP. The pancreas of MRL/Mp mice treated with repeated injection with poly (I:C) exhibits destruction of pancreatic acinar architecture, massive immune cell infiltration, and fibrosis. These histological findings are similar to those of human AIP. Moreover, extra-pancreatic involvement such as the bile duct and salivary glands is seen in this experimental model (Qu et al., 2002; Yamashina et al., 2012). Finally, autoAbs against the pancreatic secretory trypsin inhibitor, carbonic anhydrase II, and lactoferrin, all of which are elevated in patients with human AIP, can also be detected in the serum of MRL/Mp mice treated with repeated injection with poly (I:C) (Asada et al., 2010; Okazaki et al., 2000). The development of AIP in MRL/Mp mice is independent of Fas-Fas ligand interaction since MRL/Mp *lpr/lpr* mice bearing the Fas deletion mutant gene and wild-type MRL/Mp mice exhibit comparable sensitivity to AIP (Qu et al., 2002). Thus, this experimental model of AIP shares important immunological features with human IgG4-related AIP.

Materials

Endotoxin-free physiological water (InvivoGen)
Poly (I:C), high molecular weight (InvivoGen)

Autoimmune Pancreatitis Mouse Model

15.31.2

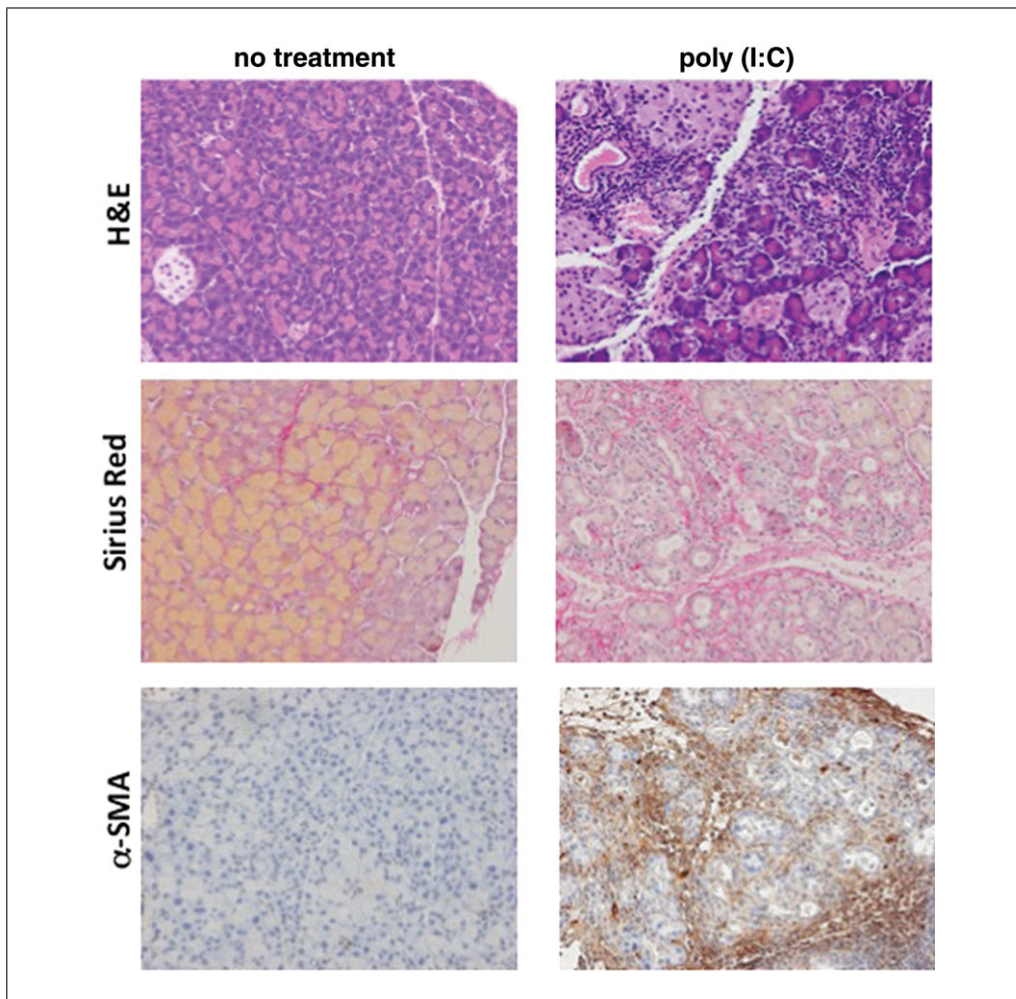


Figure 15.31.1 Pathological findings of experimental autoimmune pancreatitis. MRL/Mp mice received intraperitoneal poly (I:C) injection two times a week for a total of 14 to 16 times. Pancreas tissues were removed and then subjected to H&E, Sirius Red, and α -smooth muscle actin (α -SMA) staining. Massive destruction of acinar architecture, infiltration of immune cells, and fibrosis are seen in the pancreas of MRL/Mp mice treated with poly (I:C). The development of pancreas fibrosis is confirmed by Sirius Red and α -SMA staining.

6- to 8-week-old female MRL/Mp Mice (Japan SLC or Charles River Laboratory)
 10% formalin (Wako Laboratory Chemicals)
 PBS
 Hematoxylin and eosin (H&E)
 Sirius Red staining kit (Polysciences)
 Alpha smooth muscle actin Ab (Abcam)
 65° to 70°C heating block or bath
 27- to 29-G needles
 1-ml syringes
 Surgical instruments

Prepare poly (I:C)

Each mouse receives intra-peritoneal (i.p.) injection of poly (I:C) (100 μ g) two times a week for a total of 14 to 16 times. Each mouse receives a total volume of 100 μ l per i.p. injection.

1. Add 50 ml of endotoxin-free physiological water to the vial of 50 mg poly (I:C).
2. Mix solution by pipetting up and down.

3. Heat mixture 10 min at 65° to 70°C and then allow solution to cool for 1 hr at room temperature to achieve proper annealing.
4. Prepare sterile stock solution of poly (I:C) (1 mg/ml). Store sterile stock solution in 1-ml aliquots 6 months at –20°C.

Inject poly (I:C)

5. Thaw frozen poly (I:C) stock solution at room temperature. Carefully draw up poly (I:C) stock solution into a 1-ml syringe with 27- to 29-G needle attached. Perform i.p. injection of 100 µl of poly (I:C) stock solution.
6. Inject 100 µl of poly (I:C) stock solution i.p. two times a week (e.g., Monday and Thursday *or* Tuesday and Friday) for a total of 14 to 16 times.

Collect pancreas and blood

7. Euthanize mice 3 hr after final i.p. injection and collect blood by cardiac puncture or retro-orbital bleeding.
8. Surgically remove the pancreas.

The pancreas is attached to the spleen; therefore, gently lift the spleen to identify the underlying pancreas. The whole pancreas extends horizontally towards the duodenum.

9. Fix half of the excised pancreas in 10% formalin for pathologic examination and place the other half of the excised pancreas into PBS for the isolation of pancreatic mononuclear cells.
10. Subject the pancreatic tissue fixed in formalin to appropriate slide preparation and stain with hematoxylin and eosin (H&E). Stain slides with Sirius Red or α-smooth muscle actin (α-SMA) for evaluation of pancreatic fibrosis.

Stained slides should reveal AIP, i.e., destruction of acinar architecture, infiltration of immune cells, and fibrosis (Fig. 15.31.1).

**SUPPORT
PROTOCOL**

ISOLATION OF PANCREATIC MONONUCLEAR CELLS

Immunological analyses of pancreatic mononuclear cells (PMNCs) obtained from MRL/Mp mice with experimental AIP allows direct evaluation of the pancreatic immune response and inflammation occurring in the pancreas. Isolation of PMNCs from the inflamed pancreas is described below.

Materials

- Collagenase (Wako Laboratory Chemicals)
- PBS without CaCl₂ or MgCl₂
- DNase I (Roche)
- RPMI1640
- Heat-inactivated FBS
- IM HEPES
- Mouse pancreas
- HBSS without CaCl₂ or MgCl₂
- Percoll (GE-Healthcare)
- FITC-conjugated B220 Ab (eBioscience)
- PE-conjugated PDCA-1 Ab (eBioscience)

- Petri dishes
- 15- and 50-ml centrifuge tubes (Falcon)
- Refrigerated centrifuge
- 37°C shaker

70- μ m cell strainer (BD Falcon)

Centrifuge, room temperature

Prepare collagenase digestion medium

1. Prepare stock solution of collagenase by dissolving 400 mg collagenase in 20 ml PBS (20 mg/ml) and store stock solution at -20°C .
2. Prepare stock solution of DNase I by dissolving 20 mg DNase I in 20 ml PBS (1 mg/ml) and store stock solution at -20°C .
3. Prepare digestion medium as follows:

437.5 ml RPMI1640

50 ml heat-inactivated FBS

12.5 ml IM HEPES (final concentration 25 mM)

Digestion medium can be stored 1 month at 4°C .

4. Prepare collagenase digestion medium as follows:

100 ml digestion medium (from step 3)

5 ml collagenase stock solution

1 ml DNase I stock solution

Isolate PMNCs

5. Remove pancreas and place in a petri dish containing PBS.
6. Cut pancreas into 3-mm pieces and place them into a 50-ml centrifuge tube containing 20 ml PBS.
7. Centrifuge 5 min at $400 \times g$, 4°C , and discard supernatant.
8. Add 10 ml HBSS, centrifuge 5 min at $400 \times g$, 4°C , and discard supernatant.
9. Add 10 ml HBSS, centrifuge 5 min at $400 \times g$, 4°C , and discard supernatant.
10. Add 10 ml collagenase digestion medium containing collagenase and DNase I and shake 30 min at 37°C at 150 rpm.
11. Centrifuge 5 min at $30 \times g$, 4°C , and collect supernatant to remove the debris.

This low-speed centrifugation is necessary to remove the debris. Immune cells should be present in the supernatant.

12. Centrifuge 5 min at $400 \times g$, 4°C , and discard supernatant.
13. Add 10 ml HBSS to pellet and centrifuge 5 min at $400 \times g$, 4°C , and discard supernatant.
14. Add 10 ml HBSS to pellet and filter solution through a 70- μ m filter into a 50-ml centrifuge tube. Transfer solution to a 15-ml centrifuge tube.
15. Centrifuge 5 min at $400 \times g$, 4°C , and discard supernatant.
16. Add 5 ml of 30% Percoll solution to the pellet and centrifuge 30 min at $600 \times g$, room temperature, and discard supernatant.
17. Add 10 ml HBSS to pellet and wash two times by centrifuging 5 min at $400 \times g$, 4°C .
18. Use cell pellet for flow-cytometric analysis or for culture experiments.

Approximately 2×10^6 cells are obtained from the whole pancreas of poly (I:C)-treated MRL/Mp mice.

**Animal Models for
Autoimmune and
Inflammatory
Disease**

15.31.5

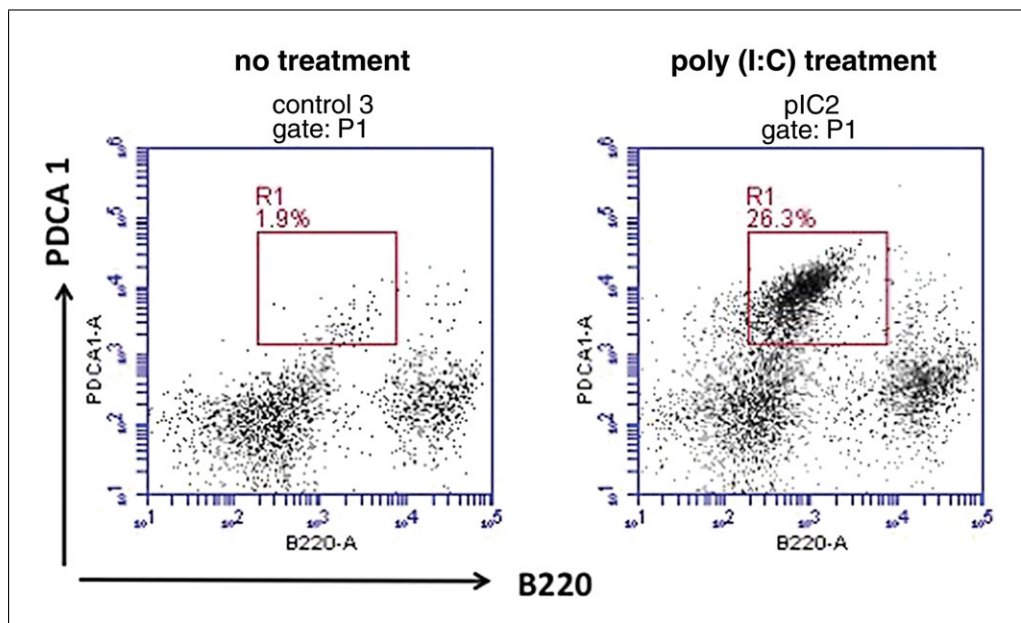


Figure 15.31.2 Accumulation of plasmacytoid dendritic cells into the pancreas. MRL/Mp mice received intraperitoneal poly (I:C) injection two times a week for a total of 14 to 16 times. Pancreas mononuclear cells were isolated and then subjected to flow-cytometric analysis. Massive accumulation of plasmacytoid dendritic cells (pDCs) defined as pDC Ag-1 (PDCA-1)⁺ B220^{low} is seen in the pancreas of MRL/Mp mice treated with poly (I:C).

Accumulation of pDCs into the pancreas can be visualized by flow-cytometric analysis by staining with FITC-conjugated B220 Ab and PE-conjugated PDCA-1 Ab (Fig. 15.31.2).

PMNCs can be isolated by enzymatic digestion of the pancreatic tissue as described above and then subjecting the digested cell mixture to appropriate density gradient centrifugation.

COMMENTARY

Background Information

Repeated i.p. injection of poly (I:C) into MRL/Mp mice results in the development of AIP, a pancreatic inflammation characterized by three key pathological findings, massive destruction of acinar architecture, infiltration of immune cells, and development of fibrosis (Arai et al., 2015; Watanabe et al., 2017). The development of sialoadenitis and cholangitis, which often simultaneously occur in patients with IgG4-related AIP, are also observed in this experimental model of AIP. Thus, repeated i.p. injection of poly (I:C) into MRL/Mp mice causes experimental AIP accompanied by extra-pancreatic lesions (Qu et al., 2002; Yamashina et al., 2012). Other manifestations of human AIP such as elevated serum levels of autoAbs against the pancreatic secretory trypsin inhibitor, carbonic anhydrase II, and lactoferrin, can also be detected in the serum of MRL/Mp mice treated with repeated injection with poly (I:C) (Asada et al., 2010; Okazaki et al., 2000). Thus, collectively, this experimental murine AIP share many immunological

features with human IgG4-related AIP except for the fact that the former lacks IgG4 Ab responses. Extensive analysis of this animal model of murine AIP could provide new insights into the immuno-pathogenesis of human IgG4-related AIP and lead to the identification of novel therapeutic targets of this disorder.

Flow-cytometric analysis of PMNCs obtained from the digested pancreas of mice with AIP identifies the type of immune cell that migrate into the pancreas in this model. These are composed of a wide variety of immune cells such as CD3⁺ T cells, B220⁺ B cells, CD11b⁺ or Gr-1⁺ myeloid cells (Arai et al., 2015; Watanabe et al., 2017). Massive infiltration of the inflamed pancreas by pDCs defined as PDCA-1⁺ B220^{low} is also one of the most prominent features of this model (Fig. 15.31.2). pDCs are unique DCs in that they have been shown to have the ability to produce type I IFNs and marked increases in the levels of type I IFN has been reported in both the pancreas and the serum of mice with experimental AIP in addition to prototypical

pro-inflammatory cytokines such as TNF- α and IFN- γ (Arai et al., 2015; Watanabe et al., 2017). Therefore, this experimental AIP model could be used to elucidate the mechanisms by which activated pDCs mediate autoimmunity.

Critical Parameters and Troubleshooting

In general, the methods described in this section are very straightforward and the chance of experimental failure is very low.

Experimental AIP does not develop or too mild

It is important to use female MRL/Mp mice since male MRL/Mp mice are resistant to the induction of experimental AIP. Ensure female MRL/Mp mice are 6 to 8 weeks old. MRL/Mp mice are available from Japan SLC (Arai et al., 2015; Watanabe et al., 2017) or Charles River Laboratory (Schwaiger et al., 2014). Do not use MRL/Mp *lpr/lpr* mice bearing the Fas deletion mutant gene. Another critical point is the preparation of poly (I:C). Ensure that the poly (I:C) HMW is properly prepared according to the protocol.

Yields of PMNCs are too low

It is important to prepare collagenase digestion medium according to the protocol and digest the pancreas tissue enough at the indicated condition. Another important point is low-speed centrifugation to remove debris. After low-speed centrifugation, collect supernatant, not the pellet.

Anticipated Results

Repeated i.p. injection of poly (I:C) into MRL/Mp mice results in the development of AIP characterized by massive destruction of pancreas acinar architecture, infiltration of immune cells, and fibrosis in hematoxylin and eosin (H&E) staining (Fig. 15.31.1, top panel). Pancreatic fibrosis can be evaluated by Sirius Red or α -smooth muscle actin (α -SMA) staining. Positive areas for Sirius Red or α -SMA is markedly increased in the pancreas of MRL/Mp mice treated with poly (I:C) (Fig. 15.31.1, middle and bottom panels).

A wide variety of immune cells such as CD3⁺ T cells, B220⁺ B cells, CD11b⁺ or Gr-1⁺ myeloid cells accumulate in the pancreas of this experimental AIP (Arai et al., 2015; Watanabe et al., 2017). Massive infiltration of pDCs defined as PDCA-1⁺ B220^{low} is one of the most prominent features of this model (Fig. 15.31.2).

Time Considerations

The development of AIP requires i.p. injection of poly (I:C) two times a week for a total of 14 to 16 times; thus requires 7 to 8 weeks to induce experimental AIP. Isolation of PMNCs will take ~4 to 5 hr after removal of pancreas.

Acknowledgements

This work has been supported in part by grants from the Naito Foundation, Yakult Bio-science Foundation, SENSHIN Medical Research Foundation, Kobayashi Foundation for Cancer Research, Smoking Research Foundation, Takeda Science Foundation, and Japan Agency for Medical Research and Development for Research on Intractable Diseases. W.S. is supported by the Intramural Research Program of the National Institute of Allergy and Infectious Diseases, National Institutes of Health.

Literature Cited

- Akitake, R., Watanabe, T., Zaima, C., Uza, N., Ida, H., Tada, S., . . . Chiba, T. (2010). Possible involvement of T helper type 2 responses to Toll-like receptor ligands in IgG4-related sclerosing disease. *Gut*, *59*, 542–545. doi: 10.1136/gut.2009.200972.
- Akiyama, M., Suzuki, K., Yamaoka, K., Yasuoka, H., Takeshita, M., Kaneko, Y., . . . Takeuchi, T. (2015). Number of circulating follicular helper 2 T cells correlates with IgG4 and interleukin-4 levels and plasmablast numbers in IgG4-related disease. *Arthritis & Rheumatology*, *67*, 2476–2481. doi: 10.1002/art.39209.
- Arai, Y., Yamashita, K., Kuriyama, K., Shiokawa, M., Kodama, Y., Sakurai, T., . . . Watanabe, T. (2015). Plasmacytoid dendritic cell activation and IFN- α production are prominent features of murine autoimmune pancreatitis and human IgG4-related autoimmune pancreatitis. *Journal of Immunology*, *195*, 3033–3044. doi: 10.4049/jimmunol.1500971.
- Asada, M., Nishio, A., Akamatsu, T., Tanaka, J., Saga, K., Kido, M., . . . Chiba, T. (2010). Analysis of humoral immune response in experimental autoimmune pancreatitis in mice. *Pancreas*, *39*, 224–231. doi: 10.1097/MPA.0b013e3181bab5e2.
- Della-Torre, E., Lanzillotta, M., & Doglioni, C. (2015). Immunology of IgG4-related disease. *Clinical and Experimental Immunology*, *181*, 191–206. doi: 10.1111/cei.12641.
- Kamisawa, T., Chari, S. T., Lerch, M. M., Kim, M. H., Gress, T. M., & Shimosegawa, T. (2013). Recent advances in autoimmune pancreatitis: Type 1 and type 2. *Gut*, *62*, 1373–1380. doi: 10.1136/gutjnl-2012-304224.
- Kamisawa, T. & Okamoto, A. (2006). Autoimmune pancreatitis: Proposal of IgG4-related sclerosing disease. *Journal of Gastroenterology*, *41*, 613–625. doi: 10.1007/s00535-006-1862-6.

- Kamisawa, T., Zen, Y., Pillai, S., & Stone, J. H. (2015). IgG4-related disease. *Lancet*, 385, 1460–1471. doi: 10.1016/S0140-6736(14)60720-0.
- Kanno, H., Nose, M., Itoh, J., Taniguchi, Y., & Kyogoku, M. (1992). Spontaneous development of pancreatitis in the MRL/Mp strain of mice in autoimmune mechanism. *Clinical and Experimental Immunology*, 89, 68–73. doi: 10.1111/j.1365-2249.1992.tb06879.x.
- Okazaki, K., Uchida, K., Ohana, M., Nakase, H., Uose, S., Inai, M., . . . Chiba, T. (2000). Autoimmune-related pancreatitis is associated with autoantibodies and a Th1/Th2-type cellular immune response. *Gastroenterology*, 118, 573–581. doi: 10.1016/S0016-5085(00)70264-2.
- Okazaki, K. & Umehara, H. (2017). Current concept of IgG4-related disease. *Current Topics in Microbiology and Immunology*, 401, 1–17. doi: 10.1007/82_2016_47
- Qu, W. M., Miyazaki, T., Terada, M., Okada, K., Mori, S., Kanno, H., & Nose, M. (2002). A novel autoimmune pancreatitis model in MRL mice treated with polyinosinic: POLycytidylic acid. *Clinical and Experimental Immunology*, 129, 27–34. doi: 10.1046/j.1365-2249.2002.01881.x.
- Schwaiger, T., van den Brandt, C., Fitzner, B., Zaatreh, S., Kraatz, F., Dummer, A., . . . Mayerle, J. (2014). Autoimmune pancreatitis in MRL/Mp mice is a T cell-mediated disease responsive to cyclosporine A and rapamycin treatment. *Gut*, 63, 494–505. doi: 10.1136/gutjnl-2012-303635.
- Stone, J. H., Zen, Y., & Deshpande, V. (2012). IgG4-related disease. *The New England Journal of Medicine*, 366, 539–551. doi: 10.1056/NEJMra1104650.
- Watanabe, T., Yamashita, K., Arai, Y., Minaga, K., Kamata, K., Nagai, T., . . . Kudo, M. (2017). Chronic fibro-inflammatory responses in autoimmune pancreatitis depend on IFN-alpha and IL-33 produced by plasmacytoid dendritic cells. *Journal of Immunology*, 198, 3886–3896. doi: 10.4049/jimmunol.1700060.
- Yamashina, M., Nishio, A., Nakayama, S., Okazaki, T., Uchida, K., Fukui, T., & Okazaki, K. (2012). Comparative study on experimental autoimmune pancreatitis and its extrapancreatic involvement in mice. *Pancreas*, 41, 1255–1262. doi: 10.1097/MPA.0b013e31824a0e58.
- Zen, Y., Fujii, T., Harada, K., Kawano, M., Yamada, K., Takahira, M., & Nakanuma, Y. (2007). Th2 and regulatory immune reactions are increased in immunoglobulin G4-related sclerosing pancreatitis and cholangitis. *Hepatology*, 45, 1538–1546. doi: 10.1002/hep.21697.

[CASE REPORT]

Acute Pancreatitis with Disturbed Consciousness Caused by Hyperparathyroidism

Yasuo Otsuka, Ken Kamata, Kosuke Minaga, Mamoru Takenaka,
Tomohiro Watanabe and Masatoshi Kudo

Abstract:

Although hyperparathyroidism has been reported to cause acute pancreatitis, little is known about the mechanism involved. This study describes the case of an 86-year-old woman with acute pancreatitis and consciousness disturbance caused by hyperparathyroidism and hypercalcemia, respectively. The consciousness disturbance caused by severe hypercalcemia probably masked the typical symptoms associated with pancreatitis because she did not report abdominal pain during the clinical course.

Key words: pancreatitis, hyperparathyroidism

(Intern Med 57: 3075-3078, 2018)

(DOI: 10.2169/internalmedicine.0552-17)

Introduction

Acute pancreatitis is an inflammatory disease of the pancreas; acute abdominal pain is the most common symptom. While several causes of acute pancreatitis have been described, including hyperparathyroidism, there have only been a few reports of patients with acute pancreatitis caused by hyperparathyroidism who did not experience abdominal pain. This report describes the case of a patient with acute pancreatitis and consciousness disturbance caused by hyperparathyroidism and hypercalcemia, respectively.

Case Report

An 86-year-old woman was referred to our hospital due to consciousness disturbance. She had a history of acute pancreatitis of unknown etiology. A physical examination at admission revealed the following findings: body temperature, 36.8°C; blood pressure, 129/78 mmHg; heart rate, 119/min; and respiratory rate was 25 breaths/min. A blood test revealed leukocytosis (24,280/ μ L), a normal platelet count (151,000/ mm^3), increased serum concentrations of C-reactive protein (CRP, 25.4 mg/dL) and amylase (273 IU/L), a normal serum level of aspartate aminotransferase (AST, 27 IU/L) and the modest elevation of alanine aminotransferase

(ALT, 77 IU/L) and triglycerides (83 mg/dL). Her serum calcium level was markedly elevated (17.5 mg/dL) relative to her serum albumin level, while her serum phosphorus level was decreased (2.2 mg/dL). Her serum concentrations of blood urea nitrogen (43 mg/dL) and creatinine (1.81 mg/dL) were also elevated. Her serum lactate dehydrogenase level was normal (159 IU/L). A blood gas analysis showed hypoxemia (pO_2 , 60.2 mmHg) and low base excess (BE, -3.7 mEq). A brain computed tomography (CT) scan showed no major abnormalities. She had not been treated with Vitamin D. These findings suggested that her consciousness disturbance was caused by hypercalcemia. Intravenous fluid resuscitation combined with the administration of calcitonin (40 units/day) was initiated.

Although the patient had not reported abdominal pain, abdominal CT was performed to identify any inflammatory foci and to determine the etiology of hyperamylasemia. Unexpectedly, abdominal CT revealed the diffuse enlargement of the pancreatic parenchyma with surrounding fluid collection (Fig. 1), a finding fully consistent with acute pancreatitis (1). She had no history of alcohol consumption, and choledocholithiasis was not detected by abdominal CT or ultrasonography. She was diagnosed with acute pancreatitis secondary to hypercalcemia, since hypercalcemia is known to trigger acute pancreatitis (1, 2). Based on the Japanese criteria, the prognostic factor score in this case was 5

points (3) (BE, <-3 mEq; blood urea nitrogen, >40 mg/dL; CRP, >15 mg/dL; systemic inflammatory response syndrome (SIRS); and age, >70 years). Contrast-enhanced CT was not performed because of renal dysfunction. Plain CT showed that the panniculitis extended to the anterior pararenal space; thus, the CT grade was considered to be 1 or 2. Consequently, she was diagnosed with severe acute pancreatitis (3). These findings suggested that consciousness disturbance caused by severe hypercalcemia masked the typical pancreatitis-related symptoms, including the acute onset of

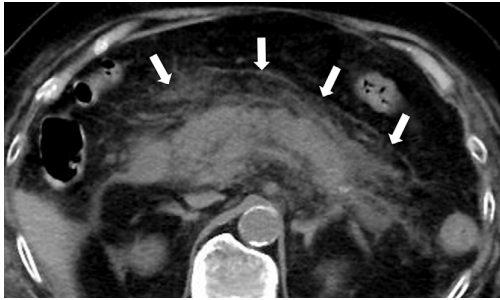


Figure 1. Abdominal computed tomography showed the diffuse enlargement of the pancreatic parenchyma with surrounding fluid collection (arrows).

persistent and severe epigastralgia.

Intravenous fluid resuscitation in combination with the administration of calcitonin and antibiotics (carbapenem) reduced her inflammatory responses, improved her consciousness level and kidney function, and reduced her serum ALT level. At 12 days after her admission, the patient's serum amylase concentration was normal and did not increase again during the remainder of her clinical course (Fig. 2). At 14 days after her admission, her corrected calcium concentration was normal, and calcitonin injection was replaced by zoledronic acid injection as maintenance therapy. At this time, her serum concentration of intact parathyroid hormone (PTH) was extremely high (470 pg/mL; normal range <50 pg/mL), while her PTH-related protein level was normal. The fractional urinary excretion of calcium was high (13%), suggesting primary hyperparathyroidism rather than familial hypocalciuric hypercalcemia, caused by mutations in the parathyroid calcium-sensing receptor gene (4). Parathyroid imaging using ^{99m}Tc -methoxyisobutylisonitrile revealed a marked uptake by the left lobe of her parathyroid gland in the delayed phase (Fig. 3), a finding consistent with primary hyperparathyroidism (4). No apparent neck tumor was detected by ultrasonography or CT. She had no family history of neuroendocrine tumor or hypercalcemia. A further exami-

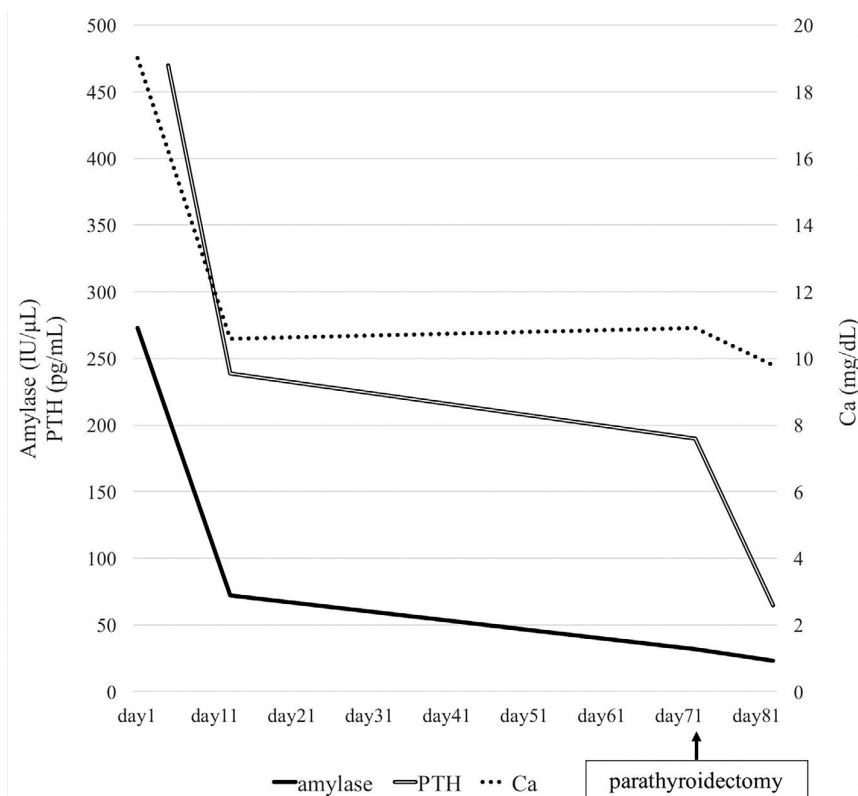


Figure 2. The serum concentrations of amylase (solid line), calcium (dotted line), and intact parathyroid hormone (double line) during the disease course of this patient. The patient's serum amylase and calcium concentrations improved 12 days after admission, whereas the intact parathyroid hormone concentration was markedly reduced after surgery, which was performed 74 days after admission.

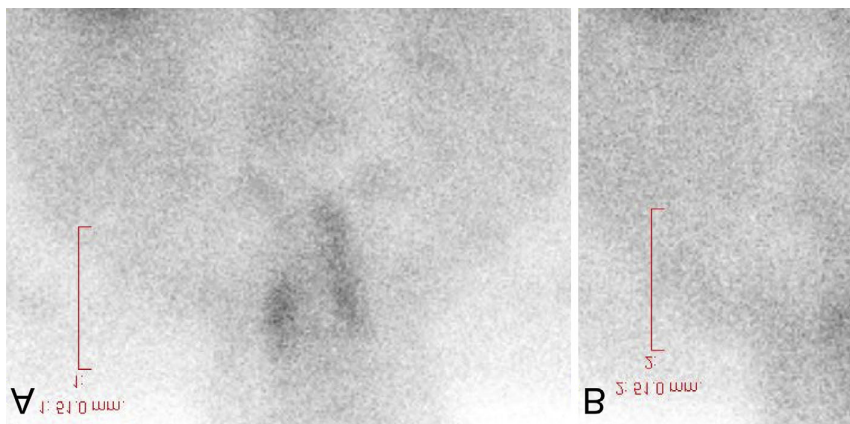
in this system. Second, the fact that the number of bacteria and the number of spores are both high in the same system suggests that the bacteria are not only present but also viable. The fact that the number of bacteria is high in the same system suggests that the bacteria are not only present but also viable. The fact that the number of bacteria is high in the same system suggests that the bacteria are not only present but also viable.

Discussion

... (text continues) ...

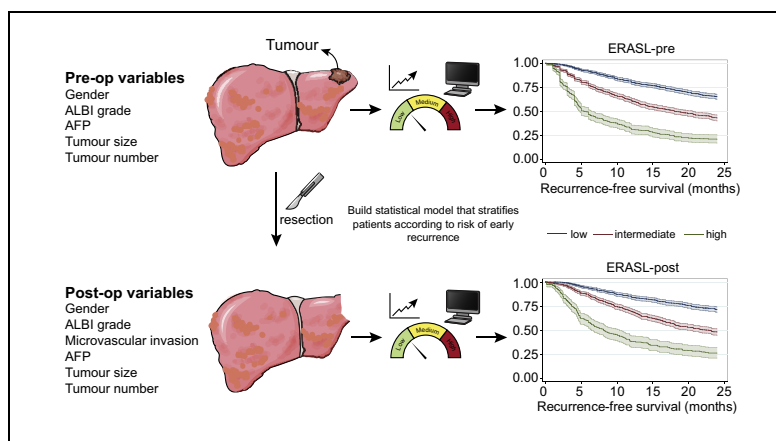
... (text continues) ...

Figure 3: Bacterial growth curves of *S. aureus* in different media. (A) Bacterial growth curve in TSB. (B) Bacterial growth curve in TSB with 10% serum. (C) Bacterial growth curve in TSB with 20% serum.



Development of pre and post-operative models to predict early recurrence of hepatocellular carcinoma after surgical resection

Graphical abstract



Highlights

- Recurrence is frequent within 2 years of surgical resection of hepatocellular carcinoma.
- In this large collaboration, we identify readily available, clinical parameters which influence early recurrence.
- A simple and extensively validated statistical model for estimating early recurrence risk using an online calculator.
- This facility will enhance patient counselling and will help in design of adjuvant clinical trials.

Authors

Anthony W.H. Chan, Jianhong Zhong, Sarah Berhane, ..., Takashi Kumada, Sasan Roayaie, Philip J. Johnson

Correspondence

Philip.Johnson@liverpool.ac.uk
(P.J. Johnson)

Lay summary

The most effective treatment of hepatocellular carcinoma is surgical removal of the tumour but there is often recurrence. In this large international study, we develop a statistical method that allows clinicians to estimate the risk of recurrence in an individual patient. This facility enhances communication with the patient about the likely success of the treatment and will help in designing clinical trials that aim to find drugs that decrease the risk of recurrence.



Development of pre and post-operative models to predict early recurrence of hepatocellular carcinoma after surgical resection[☆]

Anthony W.H. Chan¹, Jianhong Zhong², Sarah Berhane³, Hidenori Toyoda⁴, Alessandro Cucchetti⁵, KeQing Shi⁶, Toshifumi Tada⁴, Charing C.N. Chong¹, Bang-De Xiang², Le-Qun Li², Paul B.S. Lai¹, Vincenzo Mazzaferro⁷, Marta García-Fiñana⁸, Masatoshi Kudo⁹, Takashi Kumada⁴, Sasan Roayaie¹⁰, Philip J. Johnson^{3,*}

¹State Key Laboratory in Oncology in South China, Sir Y. K. Pao Centre for Cancer, Department of Anatomical & Cellular Pathology, and Department of Surgery, The Chinese University of Hong Kong, Hong Kong; ²Department of Hepatobiliary Surgery, Affiliated Tumour Hospital of Guangxi Medical University, Nanning, China; ³Department of Molecular and Clinical Cancer Medicine, University of Liverpool, Liverpool, UK; ⁴Department of Gastroenterology and Hepatology, Ogaki Municipal Hospital, 4-86 Minaminokawa-cho, Ogaki, Gifu 503-8052, Japan; ⁵Department of Medical and Surgical Sciences, Alma Mater Studiorum, University of Bologna, Italy; ⁶Department of Infection and Liver Diseases, Liver Research Center, The First Affiliated Hospital of Wenzhou Medical University, Wenzhou, China; ⁷University of Milan and Gastrointestinal Surgery and Liver Transplantation Unit, Fondazione IRCCS, Istituto Nazionale dei Tumori, Milan, Italy; ⁸Department of Biostatistics, University of Liverpool, Liverpool, UK; ⁹Department of Gastroenterology and Hepatology, Faculty of Medicine, Kindai University, Osaka, Japan; ¹⁰Liver Cancer Program, White Plains Hospital – Montefiore Health System, White Plains, NY, United States

Background & Aims: Resection is the most widely used potentially curative treatment for patients with early hepatocellular carcinoma (HCC). However, recurrence within 2 years occurs in 30–50% of patients, being the major cause of mortality. Herein, we describe 2 models, both based on widely available clinical data, which permit risk of early recurrence to be assessed before and after resection.

Methods: A total of 3,903 patients undergoing surgical resection with curative intent were recruited from 6 different centres. We built 2 models for early recurrence, 1 using preoperative and 1 using pre and post-operative data, which were internally validated in the Hong Kong cohort. The models were then externally validated in European, Chinese and US cohorts. We developed 2 online calculators to permit easy clinical application.

Results: Multivariable analysis identified male gender, large tumour size, multinodular tumour, high albumin-bilirubin (ALBI) grade and high serum alpha-fetoprotein as the key parameters related to early recurrence. Using these variables, a preoperative model (ERASL-pre) gave 3 risk strata for recurrence-free survival (RFS) in the entire cohort – low risk: 2-year RFS 64.8%, intermediate risk: 2-year RFS 42.5% and high risk: 2-year RFS 20.7%. Median survival in each stratum was similar between centres and the discrimination between the 3 strata was enhanced in the post-operative model (ERASL-post) which included ‘microvascular invasion’.

Conclusions: Statistical models that can predict the risk of early HCC recurrence after resection have been developed, exten-

sively validated and shown to be applicable in the international setting. Such models will be valuable in guiding surveillance follow-up and in the design of post-resection adjuvant therapy trials.

Lay summary: The most effective treatment of hepatocellular carcinoma is surgical removal of the tumour but there is often recurrence. In this large international study, we develop a statistical method that allows clinicians to estimate the risk of recurrence in an individual patient. This facility enhances communication with the patient about the likely success of the treatment and will help in designing clinical trials that aim to find drugs that decrease the risk of recurrence.

© 2018 The Authors. Published by Elsevier B.V. on behalf of European Association for the Study of the Liver. This is an open access article under the CC BY license (<http://creativecommons.org/licenses/by/4.0/>).

Introduction

Worldwide, hepatocellular carcinoma (HCC) is the sixth most frequent malignancy and the second most common cause of cancer-related death.¹ There is a wide variety of therapeutic options for patients with HCC, depending on tumour burden, liver function and performance status.² Potentially curative therapy recommended for those patients with very early/early stage tumour (Barcelona Clinic Liver Cancer [BCLC] 0/A) consists of surgical resection, liver transplantation or local ablation. Because of the scarcity of donor organs, surgical resection and ablation are the mainstay of curative treatment options in Asian-Pacific countries, which account for three-quarters of all new patients globally.¹ Surgical resection provides better clinical outcome than local ablation particularly among patients with well-preserved hepatic function.^{3,4}

However, tumour recurrence is a major post-operative complication and is generally classified into early or late recurrence by using 2 years as the cut-off.^{5,6} Early recurrence (i.e. within 2 years of resection) accounts for more than 70% of tumour

Keywords: Hepatocellular carcinoma; Recurrence; Resection; ERASL, modelling, prognosis.

Received 31 January 2018; received in revised form 22 August 2018; accepted 28 August 2018; available online 18 September 2018

[☆] List of where and when the study has been presented in part elsewhere: International Liver Cancer Association meeting, Seoul, South Korea, 2017.

* Corresponding author. Address: Department of Molecular and Clinical Cancer Medicine, University of Liverpool, 2nd floor Sherrington Building, Ashton Street, Liverpool L69 3GE, UK; Tel.: +44 0151 795 8410.

E-mail address: Philip.Johnson@liverpool.ac.uk (P.J. Johnson).



ELSEVIER

recurrence and is assumed to represent ‘true recurrence’ whereas after this period “recurrences” are assumed to be largely accounted for by ‘*de novo*’ tumours.⁷ The 2-year recurrence-free survival (RFS) is about 50% and 30% among those with BCLC 0 or A tumours, respectively.^{7–9} Identification of patients after potentially curative surgery who are at high risk of recurrence allows clinicians to provide appropriate surveillance to detect recurrent HCC at its earliest stage, when curative therapy may still be feasible.

Curative therapy offers much more favourable long-term survival than palliative therapy among patients with recurrent HCC.^{3,10,11} Patients at high risk of early recurrence are potential candidates for clinical trials of adjuvant therapy although there is no standard of care for adjuvant therapy for surgically treated patients with HCC.^{6,12–15}

Currently, there is no consensus regarding the optimal tool for risk stratification, which may partially contribute to failure of clinical trials of adjuvant therapy because of suboptimal patient selection. Except for the American Joint Committee on Cancer (AJCC) tumour-node-metastasis (TNM) system, the majority of HCC staging systems are not derived from surgically managed patients. Their prognostic performances on classifying post-operative early recurrence have not been fully evaluated. A few models including the Singapore Liver Cancer Recurrence (SLICER) score, the Korean model, Surgery-Specific Cancer of the Liver Italian Program (SS-CLIP), have been developed specifically to detect tumour recurrence after surgical resection but none of them have been externally validated.^{8,9,16} Moreover, microvascular invasion is an important component of AJCC TNM, SLICER, SS-CLIP and Korean models, but can only be evaluated pathologically in the resected specimen after operation. A prognostic model that only requires parameters that are available preoperatively may help surgeons to better select surgical candidates.

In this study, we employed large cohorts from different countries to develop and validate prognostic models for surgically treated patients with HCC based on readily accessible clinical and pathological parameters in order to predict early recurrence. Two models were developed: one included parameters available before surgery enabling prediction of early recurrence preoperatively, and a second included parameters available only after resection to give a more accurate prediction.

Patients and methods

This analysis was reported according to the TRIPOD (Transparent reporting of a multivariable prediction model for individual prognosis or diagnosis) guidelines.¹⁷

Patients

In this international retrospective cohort study, a total of 3,903 surgically treated patients with HCC from 6 centres in different countries were accrued. These centres comprise Hong Kong (the Chinese University of Hong Kong), mainland China (the First Affiliated Hospital of Wenzhou Medical University, Wenzhou; Affiliated Tumour Hospital of Guangxi Medical University, Nanning), Italy (S.Orsola-Malpighi Hospital, University of Bologna and Gastrointestinal Surgery, Istituto Nazionale Tumori, Milan), Japan (Ogaki Municipal Hospital), and the United States (personal experience Sasan Roayaie, New York). All centres fulfilled ethical requirements (including informed consent) according to local practice and it is our understanding that such studies do

not require formal protocol approval. Inclusion requirements were that the patients underwent surgical resection of HCC with curative intent. Patients who underwent resection for tumour rupture were excluded. All resections were undertaken after the year 2000 except for the Japanese cohort where patients were recruited between 1990 and 2014. There was no statistically significant difference in survival or recurrence rates between those treated before and after the year 2000. Table 1 summarizes baseline characteristics of the patient cohorts. Patients with missing data were excluded from the analysis.

The preoperative and post-operative Early Recurrence After Surgery for Liver tumour (ERASL) models were built on the Hong Kong dataset (dates 2001–2012) and then internally validated on a similar population from Hong Kong (dates 2013–2015). We then validated the models externally on datasets from mainland China, Italy, Japan and the United States. The criteria for surgical resection in Eastern centres (Hong Kong, mainland China and Japan) included: good liver function indicated by a 15 min ICG retention rate of <30% (Hong Kong and Japan) or Child-Pugh A with presence of appropriate residual liver volume determined by volumetric computed tomography and/or magnetic resonance imaging (mainland China); a single HCC, or not more than 3 HCCs, located in the same segment; less than 85 years of age (<75 years in Wenzhou); and absence of extrahepatic metastasis. In Italy,¹⁸ and the United States, a personalized approach was undertaken based on multidisciplinary discussion.

All clinical and laboratory parameters were collected and reviewed from patients’ records. The albumin-bilirubin (ALBI) score was computed by the formula, $-0.085 \times (\text{albumin g/l}) + 0.66 \times \log (\text{bilirubin } \mu\text{mol/l})$.¹⁹ Patients were stratified into 3 groups according to previously described cut-offs resulting in 3 grades: ALBI grade 1 (≤ -2.60), grade 2 (> -2.60 to -1.39) and grade 3 (> -1.39).¹⁹ Macrovascular invasion was defined as vascular invasion of large vessels detectable radiologically, whereas microvascular invasion was vascular invasion of small vessels only identifiable histologically. There was no microvascular invasion data available in the Nanning cohort, hence this cohort was used for validation of the preoperative model only. Patients in the Hong Kong cohort were classified according to 7th edition of AJCC TNM, Korean model (including 5 parameters: gender, tumour volume, microvascular invasion, serum albumin and platelet count) and SLICER score (using 8 parameters: symptomatic, cirrhotic background, Child-Pugh grade, surgical resection margin distance, tumour size, tumour number, vascular invasion, and preoperative serum alpha-fetoprotein [AFP]).^{8,9} After tumour resection, all patients were followed up according to institutional practice including clinical assessment serum AFP 6-monthly and ultrasound or contrast-enhanced computed tomography every 6 to 12 months. RFS was defined as the time from date of curative surgery to the time of recurrence. Patients with no recurrent disease were censored at the last time at which they were known to be recurrence free. Those dying within 90 days of surgery were not excluded from the analysis. The 90-day mortality rate was 0.6% (Hong Kong derivation cohort), 0.7% (Hong Kong internal validation cohort), 1.5% (Japan), 7.7% (the United States), 0% (Wenzhou, China), 0.9% (Nanning, China) and 2.7% (Italy).

Statistical analyses

All statistical analyses were performed in R version 3.2.5 (R Foundation for Statistical Computing, Vienna, Austria) or

Table 1. Baseline characteristics of patients.

Variables	Derivation cohort			Validation cohorts				
	Hong Kong, n = 451	Hong Kong, n = 130	Japan, n = 615	The United States, n = 661	Wenzhou, China, n = 100	Nanning, China, n = 1,204	Italy, n = 742	
Patient factors/laboratory parameters								
Male gender, n (%)	387 (85.8)	107 (82.3)	469 (76.3)	517 (78.2)	86 (86.0)	1,042 (86.5)	578 (77.9)	
Age [years, mean (SD)]	56 (10.7)	60 (9.2)	66 (9.3)	60 (11.7)	56 (10.9)	49 (11.4)	66 (9.1)	
Etiology								
Hepatitis B	380 (84.3)	107 (82.3)	126 (20.5)	286 (43.3)	89 (89.0)	1,026 (85.2)	154 (20.8)	
Hepatitis C	18 (4.0)	10 (7.7)	362 (59.0)	217 (32.8)	1 (1.0)	12 (1.0)	408 (55.0)	
Other	53 (11.8)	13 (10.0)	126 (20.5)	158 (23.9)	10 (10.0)	166 (13.8)	180 (24.3)	
Child-Pugh grade, n (%)								
A	442 (98.0)	127 (97.7)	577 (94.3)	590 (94.6)	63 (63.0)	1,154 (95.9)	697 (93.9)	
B	9 (2.0)	3 (2.3)	35 (5.7)	34 (5.5)	35 (35.0)	50 (4.2)	45 (6.1)	
C	0 (0)	0 (0)	0 (0)	0 (0)	2 (2.0)	0 (0)	0 (0)	
ALBI grade, n (%)								
1	329 (73.0)	99 (76.2)	356 (58.2)	409 (65.8)	51 (51.0)	829 (68.9)	396 (53.4)	
2	119 (26.4)	30 (23.1)	253 (41.3)	197 (31.7)	45 (45.0)	373 (31.0)	338 (45.6)	
3	3 (0.7)	1 (0.8)	3 (0.5)	16 (2.6)	4 (4.0)	2 (0.2)	8 (1.1)	
Albumin [g/L, mean (SD)]	40 (4.4)	41 (4.5)	40 (4.9), n = 612	40 (5.7), n = 623	39 (5.9)	41 (4.4)	40 (5.2)	
Bilirubin [μ mol/L, median (IQR)]	10 (7, 13)	9 (7, 13)	12.0 (9, 15), n = 613	12 (9, 15), n = 626	14 (10, 18)	12 (9, 16)	15 (12, 22)	
AFP [μ g/L, median (IQR)]	52.1 (5.4, 585.0)	20.0 (4.0, 411.0)	13.0 (5.0, 93.0), n = 607	45.5 (7.1, 756.0), n = 564	175.6 (7.2, 768.8)	139.0 (10.2, 539.7)	12.3 (4.6, 70.0)	
Tumour characteristics								
Tumour size [mm, median (IQR)]	40 (25–60)	30 (20, 55)	28 (18, 44), n = 609	50 (30, 85), n = 651	50 (30, 70)	60 (40, 98)	35 (23, 50)	
Solitary tumour, n (%)	350 (77.6)	95 (73.1)	489 (80.2), n = 610	514 (78.5), n = 655	84 (85.7), n = 98	885 (71.3), n = 1,199	573 (77.2)	
Tumour differentiation								
Well	76 (16.9)	21 (16.2)	146 (24.4)	134 (21.7)	18 (18.0)	n.a	79 (13.6)	
Moderate	318 (70.5)	91 (70.0)	408 (68.1)	318 (51.5)	55 (55.0)	n.a	257 (44.2)	
Poor	57 (12.6)	18 (13.9)	45 (7.5)	166 (26.9)	27 (27.0)	n.a	246 (42.3)	
Microvascular invasion	121 (26.8)	38 (29.3)	166 (27.7), n = 599	476 (73.1), n = 651	48.0 (48.0)	n.a	366 (49.3)	
Macrovascular invasion	38 (8.4)	9 (6.9)	44 (7.4), n = 599	186 (28.6), n = 651	9 (9.0)	205 (17.0), n = 1,203	0 (0)	
Clinical outcome								
Recurrence within 2 years, n (%)	162 (35.9)	43 (33.1)	245 (40.0), n = 613	284 (43.0)	30 (30.0)	511 (42.4)	295 (39.8)	
Recurrence-free survival, months (95% CI)	66.7 (48.0, 83.1)	Not reached	27.6 (24.0, 33.8), n = 611	21.8 (18.2, 27.9), n = 660	Not reached	11.0 (10.0, 13.0)	27.7 (24.1, 32.6)	

Mean (standard deviation) presented for normally distributed continuous variables, while median (interquartile range) was given to those with non-normally distributed continuous variable. Unless otherwise state n is as indicated in the column headings. AFP, alpha-fetoprotein; ALBI, albumin-bilirubin; CI, confidence interval; IQR, interquartile range; n.a., not available; RFS, recurrence-free survival; SD, standard deviation.

Stata/SE 14.2 (StataCorp, Texas, USA). Continuous variables were reported as mean (with standard deviation [SD]) or median (with interquartile range [IQR]), the latter for variables with highly skewed distributions. Categorical variables were presented as percentages. We constructed 2 models to predict early recurrence using the derivation cohort. One model, the preoperative model, was based on clinicopathological parameters available before surgery; the second, the post-operative model, was developed on all available parameters. Clinicopathological parameters that were shown to be potentially relevant (with $p < 0.2$ in the univariable Cox regression) were considered for generating the multivariable Cox model. The multivariable Cox regression model was built by stepwise backward selection of variables significant at the 10% level. A number of potentially clinically plausible interactions were also included in the selection. Model β -estimates were used to compute hazard ratios and calculate the risk score for prediction of early recurrence. The risk score was a weighted sum of those significant parameters, of which the weights were β -estimates from the multivariable Cox regression analysis. The proportional hazards assumption of the models was tested by examining the plots of scaled Schoenfeld residuals against time for each variable in the models. By applying previously reported cut-offs (50th and 85th centile) to the score.²⁰ 3 risk groups (low, intermediate and high) were generated. Kaplan-Meier survival curves according to the risk groups were plotted for each of the derivation and validation sets. Median RFS, hazard ratio, and percentage RFS at 2 years were also calculated for each risk group.

Model discrimination was assessed via the “regression on the prognostic index (PI)” approach,²⁰ also known as the “calibration slope”. The regression coefficient on the risk score in the validation sets was estimated and compared to that of the derivation set, which is by construction exactly 1. If the validation set coefficients equals to 1, < 1 or > 1 , they reflect as good as, poorer or better discrimination respectively in relation to the derivation set.

Model discrimination in the derivation and validation sets was also measured by the Harrell’s c-index, Gönen & Heller’s K, Royston-Sauerbrei’s R^2_D and time-dependent receiver operat-

ing characteristic curve (tdAUC).^{20–22} Cumulative/dynamic tdAUC was evaluated because we aimed to discriminate between individuals experiencing recurrence and those recurrence-free prior to 2 years. Discriminatory performance of our newly established models was also compared to AJCC TNM, the Korean model and the SLICER in the Hong Kong derivation and validation sets.

Models were calibrated using calibration plots and comparing model-predicted vs. observed survival curves.

Calibration plots were applied to the derivation and validation sets. Estimates of predicted vs. observed values were generated via bootstrapping (with 200 resampling). In order to obtain a continuous calibration plot for a specific survival time, regression-spline interpolations^{23,24} were used to generate a continuous observed survival probability. The resulting plot was also “optimism-corrected” by a method described by Harrell *et al.*²⁵

Model-predicted mean survival curves were generated by applying fractional polynomial regression to approximate the log baseline cumulative hazard function as a smooth function of time.²⁰ Model-predicted vs. Kaplan-Meier estimates was then plotted according to each risk group in the derivation and validation sets.

Results

Construction of the model predicting early recurrence

In the derivation cohort, 451 patients receiving curative surgery between 2001 and 2012 were recruited after excluding 44 patients who were complicated by tumour rupture before operation. There were only 2 patients with missing data on at least 1 of the variables. ALBI grade 2 and ALBI grade 3 were group together due to low sample size in the latter. A total of 162 patients (35.9%) developed recurrence within 2 years of surgery. Among 18 clinicopathological parameters analysed, 12 were found to be potentially relevant with $p < 0.2$ in the univariable Cox regression analysis (Table S1). Four of these, namely positive resection margin, alanine aminotransferase, alkaline phosphatase and international normalized ratio, had to be

Table 2. Multivariable Cox regression analyses of prognostic factors in the derivation cohort.

Variable	ERASL-pre			ERASL-post		
	Hazard ratio (95% CI)	β -estimate (95% CI)	<i>p</i> value*	Hazard ratio (95% CI)	β -estimate (95% CI)	<i>p</i> value*
Gender						
Female	ref	ref		ref	ref	
Male	2.265 (1.305, 3.932)	0.818 (0.266, 1.369)	0.004	1.969 (1.128, 3.434)	0.677 (0.121, 1.234)	0.017
ALBI grade						
1	ref	ref		ref	ref	
2 or 3	1.563 (1.128, 2.166)	0.447 (0.121, 0.773)	0.007	1.581 (1.142, 2.190)	0.458 (0.133, 0.784)	0.006
Microvascular invasion						
No	Not applicable	Not applicable	n.a.	ref	ref	
Yes	Not applicable	Not applicable	n.a.	1.938 (1.353, 2.775)	0.661 (0.302, 1.021)	<0.0001
ln(AFP)	1.106 (1.053, 1.161)	0.100 (0.052, 0.149)	<0.0001	1.086 (1.033, 1.141)	0.082 (0.032, 0.132)	0.001
ln(Tumour size)	1.785 (1.374, 2.320)	0.580 (0.318, 0.841)	<0.0001	1.570 (1.202, 2.052)	0.451 (0.184, 0.719)	0.001
Tumour number (1 vs. 2/3 vs. > 3)	1.636 (1.350, 1.983)	0.492 (0.300, 0.685)	<0.0001	1.461 (1.194, 1.789)	0.379 (0.177, 0.582)	<0.0001
ERASL-pre score = 0.818 × Gender (0: Female, 1: Male) + 0.447 × Albumin-Bilirubin (ALBI) grade (0: Grade 1; 1: Grade 2 or 3) + 0.100 × ln(Serum AFP in µg/L) + 0.580 × ln(Tumour size in cm) + 0.492 × Tumour number (0: Single; 1: Two or three; 2: Four or more)						
Cut-offs to generate the risk groups: ≤2.558 (low), >2.558 to ≤3.521 (intermediate), >3.521 (high)						
ERASL-post score = 0.677 × Gender (0: Female, 1: Male) + 0.458 × Albumin-Bilirubin (ALBI) grade (0: Grade 1; 1: Grade 2 or 3) + 0.661 × microvascular invasion (0: no, 1: yes) + 0.082 × ln(Serum AFP in µg/L) + 0.451 × ln(Tumour size in cm) + 0.379 × Tumour number (0: Single; 1: Two or three; 2: Four or more)						
Cut-offs to generate the risk groups: ≤2.332 (low), >2.332 to ≤3.445 (intermediate), >3.445 (high)						

AFP, alpha-fetoprotein; ALBI, albumin-bilirubin; CI, confidence interval; RFS, recurrence-free survival.

*Wald test.

excluded because they were not available in all of the external validation cohorts. Two parameters, namely (intraoperative blood loss and microvascular invasion) were only recorded after the operation and hence excluded in the multivariable analysis for establishing the preoperative model, whereas all 8 parameters were employed for building the post-operative model. By the stepwise multivariable analysis, independent parameters were identified for both models (Table 2). We did not detect any significant violation of the proportional hazard assumption, assessed by scaled Schoenfeld residuals on functions of time.

The preoperative model, the ERASL-pre score, was constructed; its formula shown in Table 2. The RFS of an individual patient with a particular ERASL-pre score can be estimated by applying a previously described formula (Table S2).²⁶ Using 2.558 and 3.521 as the cut-off values of the ERASL-pre score (which correspond to the 50th and 85th centile of the score in the derivation cohort, respectively), 3 prognostically distinct groups were stratified (derivation cohort): low-risk (2-year RFS: 76.3%), intermediate-risk (2-year RFS: 57.4%; $p < 0.001$ in comparison to low-risk) and high-risk (2-year RFS: 29.5%; $p < 0.001$ in comparison to intermediate-risk) (Table 3; Fig. 1A). The ERASL-pre score could identify 15% of patients at particularly high-risk (70.5%) of early recurrence. For routine clinical application a simple online calculator that takes the variables from the model(s) and returns the ERASL scores, the risk group and the RFS likelihood at any time between 1 and 24 months after resection for the individual patient was developed and is available at: <https://jscalc.io/calc/Fu3bREKIInObXCtj>

Similarly, the post-operative model, ERASL-post, was built according to the formula shown in Table 2. As in ERASL-pre, the RFS of an individual patient with a particular ERASL-post score can be estimated (Table S2). Using the 50th and 85th centiles of the ERASL-post scores in the derivation cohort, 2.332 and 3.445 respectively, as cut-off values, 3 prognostically distinct groups were classified (derivation cohort): low-risk (2-year RFS: 80.9%), intermediate-risk (2-year RFS: 50.9%; $p < 0.001$ in

comparison to low-risk) and high-risk (2-year RFS: 30.0%; $p < 0.001$ in comparison to intermediate-risk) (Table 4; Fig. 2A). The ERASL-post score was able to identify 15% of patients at high-risk (70.0%) of early recurrence.

Internal and external validation of the ERASL models

Both ERASL models were first validated in an internal validation cohort, which was composed of 130 patients with HCC receiving curative surgery between 2013 and 2015 in Hong Kong. There was no missing data in the internal validation set. By using the cut-off values established in the derivation cohort (2.558 and 3.521), the ERASL-pre model categorized patients into low-risk (2-year RFS: 77.1%), intermediate-risk (2-year RFS: 67.5%; $p = 0.313$ in comparison to low-risk) and high-risk (2-year RFS: 19.4%; $p < 0.001$ in comparison to intermediate-risk) groups (Table 3; Fig. 1B). Similarly, patients from the independent external validation cohorts from 5 centres (after exclusion of patients with incomplete data on predictor parameters), Japan ($n = 582$), the United States ($n = 548$); Wenzhou, China ($n = 98$); Nanning, China ($n = 1,198$); and Italy ($n = 742$), could be also categorized into 3 separate risk groups by the ERASL-pre model (Fig. 1C-F) (Table 3). Likewise, the ERASL-post model subdivided patients from the internal and external validation cohorts into 3 distinct risk groups (Fig. 2C-F) (Table 4).

Assessing model discrimination

Overall, the regression coefficient on the ERASL-pre and post scores showed good discrimination relative to the derivation set across validation cohorts (coefficient figures ranging from 0.70 to 1.21) although discrimination was less good in the Italian cohort (ERASL-pre: 0.59, ERASL-post: 0.65).

Similarly, the discriminatory performance of the models was compared via Harrell's c-index, Gönen & Heller's K, Royston-Sauerbrei's R^2 and tDAUC as shown in Table 5. Both models showed similar performance in the derivation and internal validation sets. In the external validation cohorts, good discrimina-

Table 3. Median RFS, hazard ratio and 2-year RFS according to each risk group as defined by ERASL-pre model.

Cohort	Group	n	Median recurrence-free survival, months (95% CI)	Hazard ratio (95% CI)	p value*	2-year RFS,% (95% CI)
Hong Kong (derivation set)	Low	226	84.90 (71.00, not reached)	1		76.34 (70.14, 81.42)
	Intermediate	158	68.20 (23.20, 102.90)	2.05 (1.42, 2.96)	<0.0001	57.36 (49.04, 64.82)
	High	67	7.80 (4.90, 11.80)	5.63 (3.78, 8.40)	<0.0001	29.46 (18.95, 40.74)
Hong Kong (validation set)	Low	76	Not reached	1		77.09 (65.70, 85.12)
	Intermediate	35	33.40 (18.40, not reached)	1.48 (0.69, 3.16)	0.313	67.46 (48.95, 80.50)
	High	19	6.20 (4.20, 11.30)	6.51 (3.22, 13.19)	<0.0001	19.74 (5.51, 40.32)
Japan	Low	404	36.00 (31.20, 48.00)	1		62.52 (57.15, 67.42)
	Intermediate	158	18.00 (14.40, 24.00)	2.03 (1.55, 2.67)	<0.0001	39.73 (31.59, 47.74)
	High	34	4.80 (2.40, 14.40)	4.36 (2.79, 6.80)	<0.0001	19.87 (7.44, 36.61)
U.S.	Low	242	41.86 (30.00, 54.86)	1		64.66 (57.65, 70.80)
	Intermediate	214	15.31 (12.42, 20.80)	2.08 (1.54, 2.80)	<0.0001	41.59 (34.17, 48.83)
	High	93	5.45 (4.24, 10.64)	4.20 (2.95, 5.99)	<0.0001	25.66 (15.87, 36.61)
China (Nanning and Wenzhou)	Low	366	41.00 (30.00, 50.00)	1		60.86 (53.26, 67.61)
	Intermediate	687	12.53 (10.00, 15.00)	2.21 (1.72, 2.83)	<0.0001	34.88 (30.06, 39.74)
	High	244	4.00 (4.00, 5.00)	4.43 (3.38, 5.82)	<0.0001	13.55 (8.52, 19.74)
Italy	Low	421	36.15 (30.76, 44.70)	1		60.51 (55.22, 65.37)
	Intermediate	284	23.16 (19.11, 25.59)	1.53 (1.21, 1.93)	<0.0001	47.20 (40.74, 53.38)
	High	37	11.22 (4.51, 18.09)	2.71 (1.68, 4.37)	<0.0001	31.77 (15.47, 49.44)
All	Low	1,735	45.76 (40.79, 49.20)	1		64.82 (62.23, 67.28)
	Intermediate	1,536	18.00 (16.30, 20.60)	2.07 (1.85, 2.33)	<0.0001	42.46 (39.56, 45.33)
	High	494	5.45 (4.80, 6.41)	4.67 (4.05, 5.38)	<0.0001	20.70 (16.67, 25.04)

CI, confidence interval; RFS, recurrence-free survival.

*Wald test.

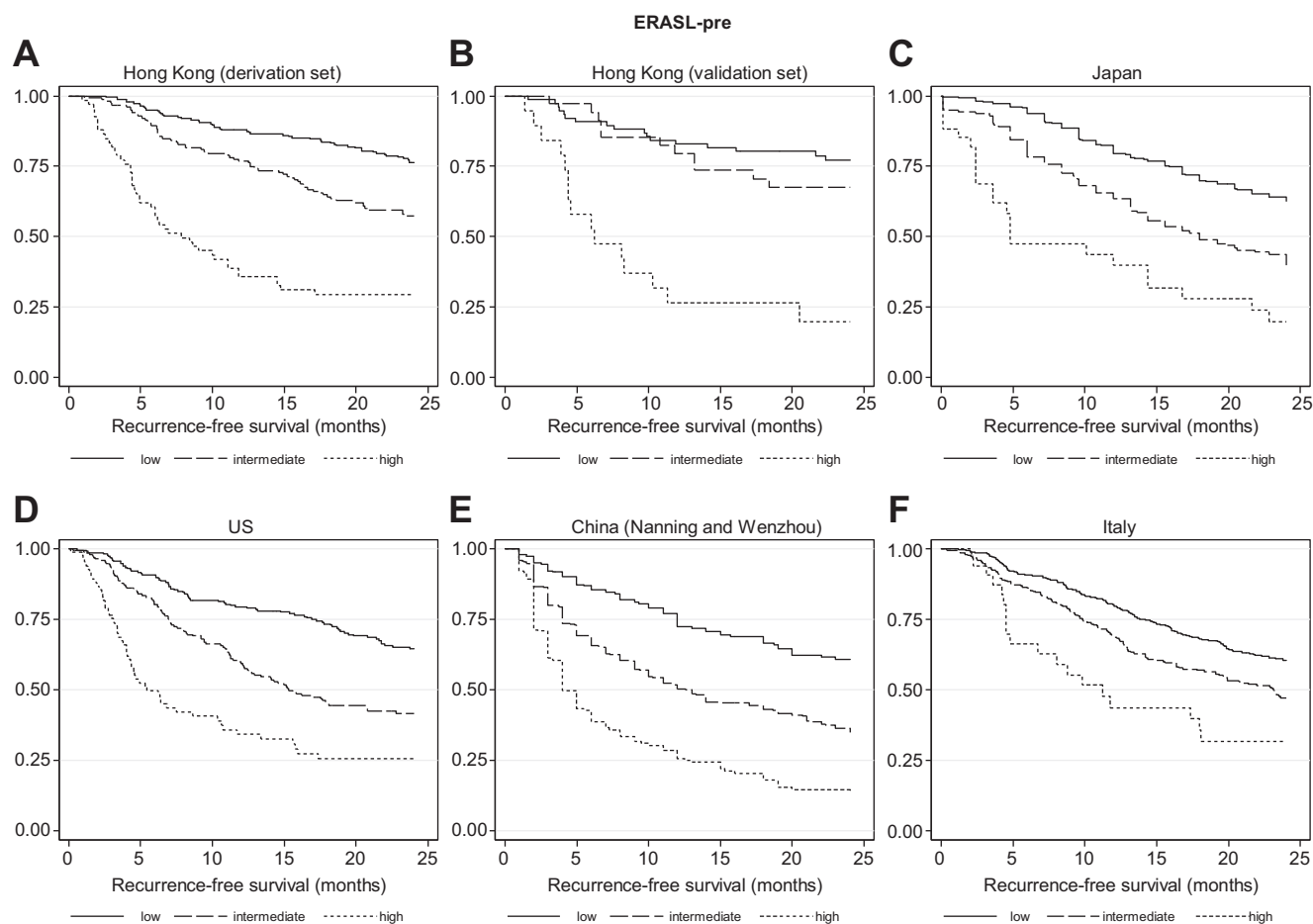


Fig. 1. RFS according to risk groups defined by the ERASL-pre model. Kaplan-Meier plots for RFS in the low, intermediate and high-risk groups of the ERASL-pre model in each of (A) Hong Kong (derivation), (B) Hong Kong (internal validation), (C) Japan, (D) the United States, (E) China and (F) Italy cohorts. Median RFS, hazard ratios (with *p* values) and percentage RFS at 2 years, are reported in Table 3. RFS, recurrence-free survival.

Table 4. Median RFS, hazard ratio and 2-year RFS according to each risk group as defined by ERASL-post model.

Cohort	Group	n	Median recurrence-free survival, months (95% CI)	Hazard ratio (95% CI)	<i>p</i> value*	2-year RFS, % (95% CI)
Hong Kong (derivation set)	Low	226	102.90 (78.90, not reached)	1		80.87 (75.02, 85.49)
	Intermediate	158	25.70 (18.60, 72.50)	3.11 (2.13, 4.55)	<0.0001	50.89 (42.58, 58.61)
	High	67	9.00 (5.70, 12.60)	6.79 (4.47, 10.33)	<0.0001	29.85 (19.44, 40.97)
Hong Kong (validation set)	Low	76	Not reached	1		82.38 (71.55, 89.39)
	Intermediate	36	27.80 (13.20, not reached)	3.00 (1.44, 6.23)	0.003	54.90 (37.16, 69.54)
	High	18	6.20 (4.40, 11.30)	8.45 (3.93, 18.17)	<0.0001	18.52 (3.98, 41.40)
Japan	Low	369	37.20 (31.22, 48.00)	1		63.28 (57.67, 68.35)
	Intermediate	167	20.40 (16.80, 25.20)	1.89 (1.43, 2.49)	<0.0001	42.17 (34.09, 50.01)
	High	46	6.00 (3.60, 14.40)	4.78 (3.24, 7.05)	<0.0001	16.73 (6.89, 30.26)
US	Low	154	70.80 (42.45, 108.62)	1		73.55 (65.21, 80.20)
	Intermediate	275	18.30 (15.31, 25.69)	2.69 (1.86, 3.90)	<0.0001	44.94 (38.31, 51.33)
	High	119	6.37 (4.50, 8.61)	6.09 (4.05, 9.18)	<0.0001	25.91 (16.91, 35.85)
China (Wenzhou only)	Low	31	Not reached	1		87.10 (69.19, 94.95)
	Intermediate	55	60.83 (34.13, not reached)	2.65 (0.89, 7.89)	0.079	68.87 (54.78, 79.37)
	High	12	9.47 (6.77, not reached)	6.91 (2.02, 23.66)	0.002	40.00 (13.52, 65.73)
Italy	Low	325	40.46 (33.35, 46.09)	1		66.32 (60.47, 71.51)
	Intermediate	366	21.88 (17.47, 24.57)	1.86 (1.45, 2.39)	<0.0001	45.98 (40.28, 51.49)
	High	51	11.78 (8.03, 19.11)	3.31 (2.16, 5.07)	<0.0001	29.23 (15.27, 44.71)
All	Low	1,181	54.30 (48.00, 64.50)	1		71.03 (68.18, 73.67)
	Intermediate	1,057	22.57 (19.84, 24.57)	2.18 (1.89, 2.51)	<0.0001	47.51 (44.23, 50.72)
	High	313	8.10 (6.41, 10.30)	4.92 (4.11, 5.90)	<0.0001	26.10 (20.77, 31.72)

CI, confidence interval; RFS, recurrence-free survival.
*Wald test.

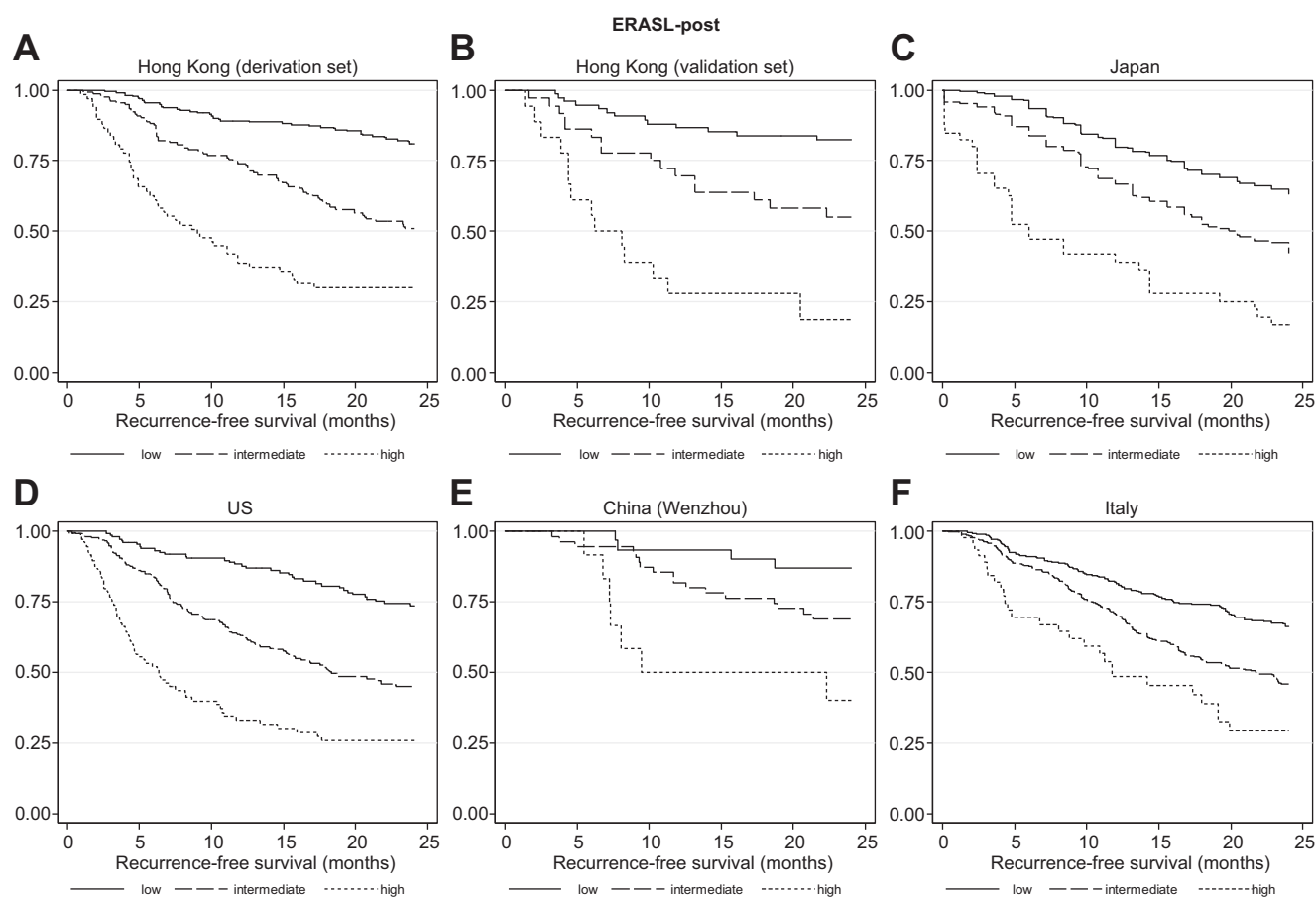


Fig. 2. RFS according to risk groups defined by the ERASL-post model. Kaplan-Meier plots for RFS in the low, intermediate and high-risk groups of the ERASL-post model in each of (A) Hong Kong (derivation), (B) Hong Kong (internal validation), (C) Japan, (D) the United States, (E) China and (F) Italy cohorts. Median RFS, hazard ratios (with *p* values) and percentage RFS at 2 years, are reported in Table 4. RFS, recurrence-free survival.

Table 5. Prognostic performance of the ERASL models.

Measure of discrimination	Cohort	ERASL-pre (SE)	ERASL-post (SE)	AJCC TNM (SE)	Korean (SE)	SLICER (SE)
Harrell's c-index	Hong Kong (Derivation)	0.713 (0.021)	0.735 (0.020)	0.693 (0.018)	0.627 (0.023)	0.716 (0.023)
	Hong Kong (Validation)	0.708 (0.043)	0.723 (0.043)	0.685 (0.039)	0.642 (0.090)	0.717 (0.045)
	Japan	0.656 (0.018)	0.668 (0.018)			
	U.S.	0.669 (0.019)	0.698 (0.018)			
	China	0.672 (0.012)	0.725 (0.056)			
	Italy	0.601 (0.016)	0.616 (0.016)			
Gönen & Heller's K	Hong Kong (Derivation)	0.689 (0.015)	0.695 (0.014)	0.638 (0.012)	0.599 (0.017)	0.667 (0.014)
	Hong Kong (Validation)	0.692 (0.027)	0.693 (0.027)	0.654 (0.025)	0.614 (0.031)	0.695 (0.028)
	Japan	0.631 (0.016)	0.640 (0.016)			
	U.S.	0.645 (0.017)	0.668 (0.017)			
	China	0.645 (0.010)	0.695 (0.047)			
	Italy	0.599 (0.016)	0.616 (0.015)			
Royston-Sauerbrei's R_D^2	Hong Kong (Derivation)	0.316 (0.050)	0.354 (0.050)	0.290 (0.050)	0.093 (0.062)	0.270 (0.051)
	Hong Kong (Validation)	0.365 (0.102)	0.388 (0.102)	0.300 (0.098)	0.138 (0.116)	0.320 (0.092)
	Japan	0.154 (0.034)	0.182 (0.040)			
	U.S.	0.177 (0.040)	0.225 (0.042)			
	China	0.166 (0.025)	0.313 (0.128)			
	Italy	0.076 (0.025)	0.104 (0.029)			
$\hat{t}dAUC$ (2 years)	Hong Kong (Derivation)	0.736 (0.025)	0.763 (0.023)	0.709 (0.023)	0.644 (0.028)	0.740 (0.025)
	Hong Kong (Validation)	0.745 (0.049)	0.755 (0.049)	0.699 (0.050)	0.673 (0.054)	0.726 (0.053)
	Japan	0.661 (0.025)	0.680 (0.024)			
	U.S.	0.682 (0.026)	0.718 (0.025)			
	China	0.692 (0.022)	0.750 (0.058)			
	Italy	0.614 (0.023)	0.653 (0.023)			

Standard errors (SE) were estimated from 200 bootstrap samples* or from the iid-representation of the estimator $\hat{t}dAUC$, areas under time-dependent receiver operating characteristic curve.

AJCC TNM, American Joint Committee on Cancer Tumor-Node-Metastasis; ERASL, Early Recurrence After Surgery for Liver tumour; SLICER, Singapore Liver Cancer Recurrence; $\hat{t}dAUC$, areas under time-dependent receiver operating characteristic curve.

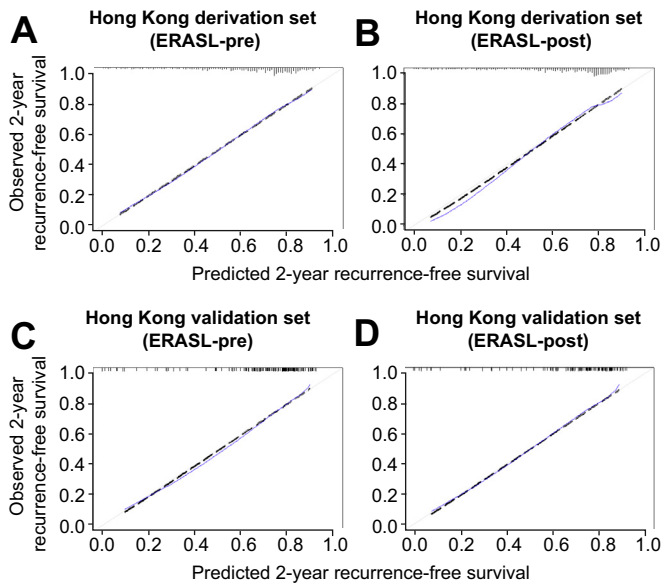


Fig. 3. Calibration plots for the ERASL-pre and ERASL-post models in predicting 2-year RFS. (A, B) Hong Kong (derivation) cohort and (C, D) Hong Kong (internal validation) cohort. Thick dashed line: observed, solid thin line: optimism-corrected. RFS, recurrence-free survival.

tion was also observed, although there was a slight deterioration in the measurement figures, which was most pronounced in the Italian cohort.

The discriminatory performance of both ERASL models exceeded those of AJCC TNM, the Korean model and the SLICER score in predicting early recurrence (Table 5). By including microvascular invasion, ERASL-post showed a better performance than ERASL-pre.

Calibration

The calibration plots showed an overall good agreement between the predictions made by the ERASL-pre and ERASL-post models and observed outcome in the Hong Kong derivation and internal validation sets (Fig. 3A-F). This was also the case for the external validation sets (Fig. S1A-H).

Plots of Kaplan-Meier estimates vs. ERASL-pre predicted survival curves were overall very similar (Fig. S2A-F), with the exception of the Chinese cohort, the lowest risk groups of the Japanese, US and Italian cohorts where the ERASL-pre model overestimated RFS. In the ERASL-post model, there was also an overall agreement between Kaplan-Meier estimates and model-predicted survival probabilities (Fig. S3A-F), with the exception of model overestimation of RFS in the low risk categories of Japan and Italy. Nevertheless, despite some of discrepancies between predicted and Kaplan-Meier estimates in some of the risk groups, the stratification of each of the cohorts into 3 groups according to risk was maintained.

Kaplan-Meier survival plots according for the ERASL-pre and post risk groups involving the entire cohort are shown (Fig. S4).

Discussion

Two models (ERASL-pre and ERASL-post) that enable risk assessment of early recurrence before and after resection have been derived and validated in a large international multicentre

study of surgically treated patients with HCC. Although they were derived from a hepatitis B prevalent region (Hong Kong), their application was generalizable to regions with predominant hepatitis C (Japan and Italy) or mixed aetiologies (the United States). They were capable of stratifying patients into 3 groups with discrete risk profiles. Using the ERASL-pre model, the high-risk group consisted of 13.1% of the patients among the entire cohort but accounted for 79.3% of those who developed early recurrence, whereas the low-risk and intermediate-risk groups comprised of 46.1% and 40.8% of patients but only 35.2% and 57.5% of those who developed early recurrence, respectively (Fig. S4). Correspondingly, the ERASL-post also identified a high-risk group comprising 12.3% of patients among the entire cohort with 73.9% chance of early recurrence (Fig. S4). Both models are clinically relevant because they allow the identification of a small, but potentially manageable, portion of patients at high risk of early recurrence. Although it may not be considered appropriate to exclude those patients at high risk of early recurrence from curative surgery, more intensive surveillance might be offered and they would be candidates for clinical trials of adjuvant therapy. The ERASL models are also reliable as they are the first models designed to predict early recurrence that have been externally validated in different geographic regions and with different aetiological factors. Despite, a minor degree of discrepancy between predicted and Kaplan-Meier estimates (Figs. S2 and S3), the stratification of each of the cohorts into 3 groups according to risk was maintained. Although the ERASL-pre model is the first to be applicable solely on the basis of pretreatment parameters, it still appears to outperform existing models which require additional postoperatively acquired variables. It may also help surgeons to identify those surgical candidates at high risk of early recurrence before operation. Furthermore, the models only require simple, readily available clinicopathological parameters.

Vascular invasion, in particular microvascular invasion, is a well-known independent prognostic factor associated with more advanced tumour stage, tumour progression and poorer clinical outcome.²⁷ Microvascular invasion is the single parameter shared by ERASL-post, SLICER, SS-CLIP and Korean models.^{8,9,16} It is also an essential component in the AJCC TNM system. The incidence of microvascular invasion was 33.1% (26.8–73.1%) in our current cohorts. Assessment of microvascular invasion currently relies on histological examination of surgically resected specimens by pathologists. Subjectivity and sampling error are undoubtedly potential problems in evaluating microvascular invasion. Serum tumour markers, preoperative imaging and gene signatures have been investigated as possible approaches to predict microvascular invasion but none has yet been validated and they are not routinely applicable in daily clinical practice.²⁷ Histological classifications of microvascular invasion have been proposed but none of them are universally accepted and their clinical significance has yet to be validated.^{28–30} Hence, for simplicity and better acceptance, only the presence/absence of microvascular invasion was used in the ERASL-post model. Other parameters that might influence RFS could be added to our models although it is evident that extent of surgical resection, resection margin and degree of blood loss did not emerge as independent prognostic variables. Nonetheless, the models give strikingly clear-cut risk groups and show very similar results within each of the validation sets. Adding more prognostic variables is unlikely to improve our models'

performance significantly other than further narrowing the current confidence intervals.

Liver (dys)function is another independent prognosticator to predict tumour recurrence used in ERASL, SLICER and SS-CLIP models.^{8,16} To evaluate liver dysfunction, our ERASL models used ALBI grade, whereas the latter 2 models used Child-Pugh grade. The ALBI grade is our recently proposed, widely-validated and evidence-based refinement of the Child-Pugh grade.^{19,31} The majority of surgically treated patients with HCC belong to Child-Pugh A, which accounted for more than 95% of patients in our current dataset and SLICER and SS-CLIP and Korean cohorts, respectively.^{8,9,16} We previously demonstrated that Child-Pugh A patients were composed of 2 prognostically distinct subgroups as classified by the ALBI grade.^{4,19} Therefore, ALBI grade rather than Child-Pugh grade was incorporated in our ERASL models to provide better discriminatory power. However, the underlying reason for the association between liver dysfunction and early recurrence remains unclear.

Tumour recurrence may represent either intrahepatic metastases or development of *de novo* tumours. Time of recurrence is 1 of the factors that has been proposed to distinguish these 2 entities,^{32,33} although the exact differentiation requires assessment of recurrence clonality by genetic/genomic analyses.^{34,35} Early recurrence is generally believed to represent pre-existing intrahepatic metastasis, whereas late recurrence is regarded as *de novo* tumour. A cut-off of 2 years has been generally adopted to classify early and late recurrence.⁶ Our findings echo other studies in that early and late tumour recurrence are 2 distinct entities associated with different risk factors.^{7,32,36} Early recurrence is mainly determined by aggressive characteristics of the primary (resected) tumour such as tumour size, tumour multiplicity, vascular invasion and higher serum AFP level. These associations support the contention that early recurrence is likely to result from intrahepatic metastasis disseminated from the primary tumour. In contrast, late relapse is primarily associated with aetiology and cirrhotic background, which are well-established risk factors of hepatocarcinogenesis and provide fertile soil for development of *de novo* tumours.^{2,6,37}

There are limitations to our study. Our models, at first sight, may appear complex and difficult to apply at the bedside, but our simple online calculator overcomes this problem. The online calculators, by providing a quantitative measure of recurrence risk at any post-operative time point, are an important step in our ultimate goal of providing personalized prognostication. Antiviral treatment has not been included in our models because it was not recorded in all of our cohorts. However, although the use of antiviral treatment for hepatitis B-related HCC has been consistently shown to improve overall survival, its effect on post-operative recurrence prevention is still inconclusive.^{38–40} Reduction of tumour recurrence by antiviral agents on hepatitis C-related HCC is also controversial.^{41,42} Third, tumour size and number were measured radiologically or pathologically in different centres. Although there might be some variations in tumour size depending on the method of assessment, the discrepancies are unlikely to be clinically significant.

In summary, tumour recurrence after curative surgery for HCC is a serious and common complication. Our ERASL models are clinically relevant, externally validated and offer powerful tools to predict early recurrence. Further prospective studies are required to explore the clinical applicability of ERASL

models in patient allocation for more frequent follow-up and clinical trials for adjuvant therapy. We are currently developing a more general prognostic model that is applicable to both early and late recurrence, and the performance of the ERASL models is being prospectively evaluated in an adjuvant clinical trial.

Financial support

SB and MGF acknowledges support from the UK EPSRC grant EP/N014499/1.

Conflicts of interest

The authors declare no conflicts of interest that pertain to this work.

Please refer to the accompanying [ICMJE disclosure](#) forms for further details.

Authors' contributions

Concept and design: PJJ, AWHC. Data collection: JZ, HD, AC, KS, TT, CCNC, BDX, LQL, PBSL, VM, MK, TK, SR. Statistical analysis: SB, AWHC, MGF. Writing of article: all authors

Supplementary data

Supplementary data associated with this article can be found, in the online version, at <https://doi.org/10.1016/j.jhep.2018.08.027>.

References

Author names in bold designate shared co-first authorship

- [1] Ferlay J, Soerjomataram I, Ervik M, Dikshit R, Eser S, Mathers C, et al. GLOBOCAN 2012 v1.0, Cancer Incidence and Mortality Worldwide: IARC CancerBase No. 11 [Internet]. [cited 2014 January 20]; Available from: <http://globocan.iarc.fr>.
- [2] Bruix J, Sherman M, American Association for the Study of Liver Diseases. Management of hepatocellular carcinoma: an update. *Hepatology* 2011;53:1020–1022.
- [3] Chan AC, Chan SC, Chok KS, Cheung TT, Chiu DW, Poon RT, et al. Treatment strategy for recurrent hepatocellular carcinoma: salvage transplantation, repeated resection, or radiofrequency ablation? *Liver Transpl* 2013;19:411–419.
- [4] Toyoda H, Lai PB, O'Beirne J, Chong CC, Berhane S, Reeves H, et al. Long-term impact of liver function on curative therapy for hepatocellular carcinoma: application of the ALBI grade. *Br J Cancer* 2016;114:744–750.
- [5] Cucchetti A, Piscaglia F, Caturelli E, Benvegna L, Vivarelli M, Ercolani G, et al. Comparison of recurrence of hepatocellular carcinoma after resection in patients with cirrhosis to its occurrence in a surveilled cirrhotic population. *Ann Surg Oncol* 2009;16:413–422.
- [6] European Association for the Study of the Liver, European Organisation For Research and Treatment of Cancer. EASL-EORTC clinical practice guidelines: management of hepatocellular carcinoma. *J Hepatol* 2012;56:908–943.
- [7] Chan AW, Chan SL, Wong GL, Wong VW, Chong CC, Lai PB, et al. Prognostic nutritional index (PNI) predicts tumor recurrence of very early/early stage hepatocellular carcinoma after surgical resection. *Ann Surg Oncol* 2015;22:4138–4148.
- [8] Ang SF, Ng ES, Li H, Ong YH, Choo SP, Ngeow J, et al. The Singapore Liver Cancer Recurrence (SLICER) Score for relapse prediction in patients with surgically resected hepatocellular carcinoma. *PLoS One* 2015;10:e0118658.
- [9] Shim JH, Jun MJ, Han S, Lee YJ, Lee SG, Kim KM, et al. Prognostic nomograms for prediction of recurrence and survival after curative liver resection for hepatocellular carcinoma. *Ann Surg* 2015;261:939–946.

- [10] Meniconi RL, Komatsu S, Perdigo F, Boelle PY, Soubrane O, Scatton O. Recurrent hepatocellular carcinoma: a Western strategy that emphasizes the impact of pathological profile of the first resection. *Surgery* 2015;157:454–462.
- [11] Tabrizian P, Jibara G, Shrager B, Schwartz M, Roayaie S. Recurrence of hepatocellular cancer after resection: patterns, treatments, and prognosis. *Ann Surg* 2015;261:947–955.
- [12] Bruix J, Takayama T, Mazzaferro V, Chau GY, Yang J, Kudo M, et al. Adjuvant sorafenib for hepatocellular carcinoma after resection or ablation (STORM): a phase 3, randomised, double-blind, placebo-controlled trial. *Lancet Oncol* 2015;16:1344–1354.
- [13] Zhong JH, Li LQ. Postoperative adjuvant transarterial chemoembolization for participants with hepatocellular carcinoma: a meta-analysis. *Hepatol Res* 2010;40:943–953.
- [14] Wang H, Liu A, Bo W, Feng X, Hu Y, Tian L, et al. Adjuvant immunotherapy with autologous cytokine-induced killer cells for hepatocellular carcinoma patients after curative resection, a systematic review and meta-analysis. *Dig Liver Dis* 2016;48:1275–1282.
- [15] Ferrer-Fabrega J, Forner A, Llicioni A, Miquel R, Molina V, Navasa M, et al. Prospective validation of ab initio liver transplantation in hepatocellular carcinoma upon detection of risk factors for recurrence after resection. *Hepatology* 2016;63:839–849.
- [16] Huang S, Huang GQ, Zhu GQ, Liu WY, You J, Shi KQ, et al. Establishment and validation of SSCLIP scoring system to estimate survival in hepatocellular carcinoma patients who received curative liver resection. *PLoS One* 2015;10:e0129000.
- [17] Collins GS, Reitsma JB, Altman DG, Moons KG. Transparent reporting of a multivariable prediction model for individual prognosis or diagnosis (TRIPOD): the TRIPOD statement. *BMJ* 2015;350:g7594.
- [18] Cucchetti A, Mazzaferro V, Pinna AD, Sposito C, Golfieri R, Serra C, et al. Average treatment effect of hepatic resection versus locoregional therapies for hepatocellular carcinoma. *Br J Surg* 2017;104:1704–1712.
- [19] Johnson PJ, Berhane S, Kagebayashi C, Satomura S, Teng M, Reeves HL, et al. Assessment of liver function in patients with hepatocellular carcinoma: a new evidence-based approach—the ALBI grade. *J Clin Oncol* 2015;33:550–558.
- [20] Royston P, Altman DG. External validation of a Cox prognostic model: principles and methods. *BMC Med Res Methodol* 2013;13:33.
- [21] Steyerberg EW, Vickers AJ, Cook NR, Gerds T, Gonen M, Obuchowski N, et al. Assessing the performance of prediction models: a framework for traditional and novel measures. *Epidemiology* 2010;21:128–138.
- [22] Rahman MS, Ambler G, Choodari-Oskooei B, Omar RZ. Review and evaluation of performance measures for survival prediction models in external validation settings. *BMC Med Res Methodol* 2017;17:60.
- [23] Stone CJ. The use of polynomial splines and their tensor products in multivariate function estimation. *Ann Stat* 1994;118–171.
- [24] Kooperberg C, Stone CJ, Truong YK. Hazard regression. *J Am Stat Assoc* 1995;90:78–94.
- [25] Harrell FE, Lee KL, Mark DB. Multivariable prognostic models: issues in developing models, evaluating assumptions and adequacy, and measuring and reducing errors. *Stat Med* 1996;15:361–387.
- [26] Yang JD, Kim WR, Park KW, Chaiteerakij R, Kim B, Sanderson SO, et al. Model to estimate survival in ambulatory patients with hepatocellular carcinoma. *Hepatology* 2012;56:614–621.
- [27] Zhang X, Li J, Shen F, Lau WY. Significance of presence of microvascular invasion in specimens obtained after surgical treatment of hepatocellular carcinoma. *J Gastroenterol Hepatol* 2018;33:347–354.
- [28] Sumie S, Kuromatsu R, Okuda K, Ando E, Takata A, Fukushima N, et al. Microvascular invasion in patients with hepatocellular carcinoma and its predictable clinicopathological factors. *Ann Surg Oncol* 2008;15:1375–1382.
- [29] Roayaie S, Blume IN, Thung SN, Guido M, Fiel MI, Hiotis S, et al. A system of classifying microvascular invasion to predict outcome after resection in patients with hepatocellular carcinoma. *Gastroenterology* 2009;137:850–855.
- [30] Cong WM, Bu H, Chen J, Dong H, Zhu YY, Feng LH, et al. Practice guidelines for the pathological diagnosis of primary liver cancer: 2015 update. *World J Gastroenterol* 2016;22:9279–9287.
- [31] Chan AW, Chan RC, Wong GL, Wong VW, Choi PC, Chan HL, et al. New simple prognostic score for primary biliary cirrhosis: albumin-bilirubin score. *J Gastroenterol Hepatol* 2015;30:1391–1396.
- [32] Poon RT, Fan ST, Ng IO, Lo CM, Liu CL, Wong J. Different risk factors and prognosis for early and late intrahepatic recurrence after resection of hepatocellular carcinoma. *Cancer* 2000;89:500–507.
- [33] Li Q, Wang J, Juzi JT, Sun Y, Zheng H, Cui Y, et al. Clonality analysis for multicentric origin and intrahepatic metastasis in patients with multiple hepatocellular carcinoma. *J Gastrointest Surg* 2008;12:1540–1547.
- [34] Morimoto O, Nagano H, Sakon M, Fujiwara Y, Yamada T, Nakagawa H, et al. Diagnosis of intrahepatic metastasis and multicentric carcinogenesis by microsatellite loss of heterozygosity in patients with multiple and recurrent hepatocellular carcinomas. *J Hepatol* 2003;39:215–221.
- [35] Furuta M, Ueno M, Fujimoto A, Hayami S, Yasukawa S, Kojima F, et al. Whole genome sequencing discriminates hepatocellular carcinoma with intrahepatic metastasis from multi-centric tumors. *J Hepatol* 2017;66:363–373.
- [36] Imamura H, Matsuyama Y, Tanaka E, Ohkubo T, Hasegawa K, Miyagawa S, et al. Risk factors contributing to early and late phase intrahepatic recurrence of hepatocellular carcinoma after hepatectomy. *J Hepatol* 2003;38:200–207.
- [37] Utsunomiya T, Shimada M, Kudo M, Ichida T, Matsui O, Izumi N, et al. A comparison of the surgical outcomes among patients with HBV-positive, HCV-positive, and non-B non-C hepatocellular carcinoma: a nationwide study of 11,950 patients. *Ann Surg* 2015;261:513–520.
- [38] Yin J, Li N, Han Y, Xue J, Deng Y, Shi J, et al. Effect of antiviral treatment with nucleotide/nucleoside analogs on postoperative prognosis of hepatitis B virus-related hepatocellular carcinoma: a two-stage longitudinal clinical study. *J Clin Oncol* 2013;31:3647–3655.
- [39] Chong CC, Wong GL, Wong VW, Ip PC, Cheung YS, Wong J, et al. Antiviral therapy improves post-hepatectomy survival in patients with hepatitis B virus-related hepatocellular carcinoma: a prospective-retrospective study. *Aliment Pharmacol Ther* 2015;41:199–208.
- [40] Sakamoto K, Beppu T, Hayashi H, Nakagawa S, Okabe H, Nitta H, et al. Antiviral therapy and long-term outcome for hepatitis B virus-related hepatocellular carcinoma after curative liver resection in a Japanese cohort. *Anticancer Res* 2015;35:1647–1655.
- [41] Conti F, Buonfiglioli F, Scuteri A, Crespi C, Bolondi L, Caraceni P, et al. Early occurrence and recurrence of hepatocellular carcinoma in HCV-related cirrhosis treated with direct-acting antivirals. *J Hepatol* 2016;65:727–733.
- [42] Petta S, Cabibbo G, Barbara M, Attardo S, Bucci L, Farinati F, et al. Hepatocellular carcinoma recurrence in patients with curative resection or ablation: impact of HCV eradication does not depend on the use of interferon. *Aliment Pharmacol Ther* 2017;45:160–168.